2.01
Alkali Metal Organometallics – Structure and Bonding

K Ruhlandt-Senge, Syracuse University, Syracuse, NY, USA
K W Henderson, University of Notre Dame, Notre Dame, IN, USA
P C Andrews, Monash University, Melbourne, VIC, Australia

2.01.1 Introduction

This article summarizes the chemistry of alkali metals with group 14, 15, and 16 ligands with specific emphasis on structure and bonding. With several excellent, recent review articles in the area, we focus specifically on newer developments, with already reviewed material only mentioned briefly to show trends and connections.

The importance of alkali group 14, 15, and 16 derivatives cannot be overstated, with a host of far reaching applications, as summarized in several review articles on the subject.[1–12] Outstanding coverage on the subject is also provided in Elschenbroich's organometallic text.[13]

The compounds are strong bases with important applications in synthetic chemistry whose reactivity depends critically on their structure. In addition to their value in organic synthesis, these compounds (particularly the lithium and potassium species) have shown enormous utility in the preparation of organometallic compounds throughout the periodic table. The organopotassium derivatives are also discussed as reactive intermediates in superbase chemistry.[14] An understanding of the structure–function relations of the reagents requires detailed insights into the metal–ligand bonding, and extensive investigations have resulted in theory rationalizing metal–ligand binding trends.

This chapter is concerned with structure and bonding in alkali metal centers connected to group 14, 15, and 16 ligands, with a specific section on mixed metal species. The overlying structural theme of these compounds is their strong tendency toward aggregation, which in solution and the solid state critically depends on the nature of the ligand, donor, solvent, temperature, and concentration with occasional striking differences between the two states of matter.

Aggregation of the alkali metal species is very common and well documented with an extensive section in COMC (1995).[7] Aggregates include monomers, dimers (as head-to-tail aggregation products of monomers), trimers (typically in the form of six-membered rings), tetramers (typically in the form of dimers of dimers), and hexamers (as dimers of trimers). There is significant evidence for the formation of higher oligomers, as well as polymers, often consisting of polymeric chains or ladders (Scheme 1).

As documented in detail for organolithium species, ligand and donor play a key role in determining the degree of aggregation. Methyllithium adopts a hexameric structure in hydrocarbon solvents.[13,15] In the presence of monodentate, donors such as THF or diethyl ether tetramers are observed, while the increase in donor denticity to 2 (1,1–Dimethoxyethane (DME), N,N,N′,N′–Tetramethylethylenediamine (TMEDA)) affords monomeric structures. Further documenting the differences between solution and solid states, $[CH_3Li]_4$ adopts a tetrameric structure in the latter.[15,15a–15e]

The size of the ligand is crucial in deciding the degree of association, as shown by the very similar structural features of methyl- and ^{n}butyllithium derivatives. With hexameric structures in cyclohexane, the addition of diethyl ether affords tetramers in both cases. Further demonstrating the importance of the donor, the two-dimensional phenyl ligand also adopts a tetrameric structure in diethyl ether $[Li(OEt_2)Ph]_4$, which upon addition of the bidentate

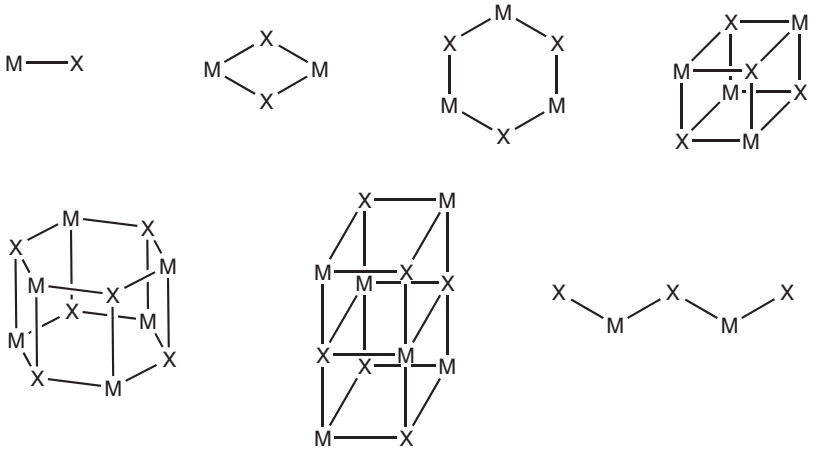

Scheme 1 Graphical representation of various aggregation modes in alkali metal compounds.

TMEDA changes into the dimeric $[PhLi(TMEDA)]_2$. Monomeric phenyllithium PhLi(PMDTA) is observed if the tridentate donor ligand PMDTA (PMDTA = N,N,N′,N′,N″–Pentamethyldiethylenetriamine) is utilized.[13]

The ligand and/or an additional neutral donor may interact with the metal center in various bonding modes, including highly polar σ- or π-bonding. The different metal–ligand binding modes have a significant effect on the structural chemistry of the resulting complexes, and will be discussed in the pertinent sections below.

Information on structure and bonding in alkali metal species with group 14, 15, and 16 ligands has been mainly focused on lithium derivatives; the heavier analogs have been dealt with to a much-reduced extent. As mentioned in a 2004 review article,[11] a search in the Cambridge Structural Database (CSD) revealed 778 structures with an Li–C bond, but only 197 with an Na–C, 235 with a K–C, 57 with an Rb–C, and just 31 with a Cs–C bond.

Interestingly, more structures with a K–C than Na–C bond are known, despite the increasing reactivity of the compounds as descending the group of alkali metals. As frequently observed, K, Rb, and Cs compounds display somewhat similar chemistry, which typically differs from that of the lithium analogs. Sodium, in many instances, adopts a chemistry that resembles more that of lithium than the heavier congeners, most likely a function of the ionic size.

The slow development of heavy alkali organometallic chemistry is due to high reactivity, as rationalized by the increase of polar character of the metal–ligand bond due to the reduced polarizing ability of the metals. The increase in ionic character on descending the group of alkali metals is clearly demonstrated by the increase in ionic radii with Li^+(0.69 Å), Na^+(0.97 Å), K^+(1.33 Å), Rb^+(1.47 Å), and Cs^+(1.67 Å), resulting in a radius of Cs^+ that is more than double of that of Li^+.

The increase in ionicity on descending the group of alkali metals is demonstrated clearly within the group of CH_3M species (M = Na, K, Rb, Cs), with CH_3Na crystallizing in the CH_3Li structure as a cubic body-centered heterocubane consisting of Na_4 tetrahedra with methyl groups capping the faces.[13] Further supporting the similarity of organolithium and sodium compounds, structural information on the solvent-free CH_3M (M = Li, Na) using millimeter and submillimeter spectroscopy revealed very similar structures with Li–C and Na–C distances of 1.959 and 2.299 Å, respectively.[16] The H–C–H angles in both compounds display slightly pyramidal character with 106.2° and 107.2°. These data agree well with *ab initio* calculations.[16] In contrast, the potassium, rubidium, and cesium species adopt the ionic lattice of the NiAs structure type, where the methyl groups are surrounded in trigonal prismatic fashion by the alkali metals, while the metal coordination spheres are comprised of an octahedral environment provided by six methyl groups.[15a–15c]

In addition to the decreased polarizability of the heavier metals, their larger radii require higher metal coordination numbers to achieve steric saturation. As a result, extensive aggregation, frequently coinciding with rather limited solubility in non-donor solvents, and occasionally even in donor solvents, complicates the characterization of these species in solution and the solid state. In fact, several structural characterizations of organoalkali species have relied on recent advances in powder diffraction techniques using synchrotron radiation.[17–19]

A further significant factor slowing the development of the chemistry of the heavy alkali metal derivatives has been the high reactivity of the complexes, with frequent attack of the ethers used to break up the aggregates in hopes to achieve increased solubility. In fact, ether cleavage is a common observation and manipulations at very low temperatures are often required to overcome this issue.[9] Ether cleavage may also be suppressed by the introduction of nitrogen-based donors such as TMEDA and PMDTA.

With solubility as one of the principal problems to obtain structural information, the introduction of lipophilic ligands has been particularly successful, as shown impressively with the silyl substituted $[CH(SiMe_3)_2]^-$ and $[C(SiMe_3)_3]^-$ ligands.[20] Steric bulk has also been applied successfully to reduce the tendency toward aggregation. This has been vividly demonstrated by recent chemistry utilizing terphenyl ligands.[21]

2.01.2 Alkali Metal Chemistry with Carbon-Based Ligands

A major surge in the chemistry of alkali organometallics occurred during the 1980s and the 1990s. Organolithium chemistry was summarized as recently as 2004,[11] while the organometallic chemistry of the heavier metals was reviewed in 1999,[9] with a limited number of new results accumulated since. As a result, we will keep this section brief in order to avoid duplicating information already summarized.

The flow of information on the highly reactive alkali organometallics in the 1990s is certainly closely connected to the wider availability of low temperature crystallography and advanced crystal mounting techniques,[22] allowing the structural characterization of compounds previously deemed too reactive for investigation.

2.01.2.1 Alkyl Derivatives

2.01.2.1.1 Methyl derivatives

Structural information on the alkali metal methyl derivatives is available for all metals (Li–Cs), as mentioned above.[13,15,15a–15c,16] Replacement of the hydrogen atoms in the methyl groups by other substituents to afford more sterically demanding ligands supports the view that kinetic stabilization and the ability for charge delocalization is critical in isolating these highly reactive species. Not only is the isolation of the complexes possible, so are solution studies and the more facile growth of single crystals. While the recent advent of powder diffraction studies using synchrotron radiation may circumvent some of the solubility difficulties, limited reagent solubility is typically met with reduced usefulness in synthetic applications. Some of the developments on substituted methyl derivatives will be discussed below.

2.01.2.1.2 Benzyl, diphenyl, and triphenyl methane derivatives

A unique compound in this category is the alkali metal salt of a benzenoid radical anion $[(\eta^6CH_2C_6H_5)K(18\text{-crown-}6)]$ **1**.[23] In this complex the potassium π-bonds to the aromatic segment of the ligand rather than σ-bonding to the methylene unit. The isolation and subsequent structural characterization of this highly reactive toluene radical anion is possible due to the kinetic stabilization of potassium by 18-crown-6. The radical anion crystallizes as a tight ion pair with the crown encapsulating the potassium which is bound in an approximate η^6-fashion to the planar C_6H_5 ring, with carbon–potassium distances ranging from 3.044(5) Å to 3.311 Å. Not only do the K–C bond lengths vary widely, so do the C–C bonds, as well as the endocyclic angles within the six-membered ring with a range from 117.4(6) to 123.4(6)°.

More classical metal–ligand bonding is observed upon deprotonation of toluene to afford alkali metal benzyl derivatives, with the prototypical example being the lithium chain polymer $[C_7H_7Li(OEt_2)_2]_\infty$ **2**.[23a] The chain is constructed of alternating lithium and benzyl units. The lithium centers exhibit trigonal planar geometry, comprised of two benzyl ligands and one diethyl ether. Structural features in the compound reveal extensive perturbation within the benzyl units. The structural features of this compound resemble that of $[(2\text{-}CH_2C_6H_4)_2Li(TMEDA)_2]$ **3**,[24] with similar interactions between the metal and ligands. Other examples include $[(C_7H_7)Li(DABCO)]_\infty$ **4**[25] and the mixed donor species $[(C_7H_7)Li(THF)(TMEDA)]$ **5**.[26]

Heavier metal analogs include the tetrameric $[(C_7H_7)Na(TMEDA)]_4$ **6**,[27] as well as the polymeric $[(C_7H_7)Na(PMDTA)]_\infty$ **7**,[28] $[(C_7H_7)K(PMDTA)]_\infty \times [0.5CH_3C_6H_5]$ **8**, and $[(C_7H_7)Rb(PMDTA)]_\infty$ **9**.[29] The structures of the PMDTA solvated potassium and rubidium compounds display polymeric zigzag arrangements. In both compounds, η^6-metal ligand arrangements are observed, with rubidium situated slightly asymmetrically over the arene ring. The metals also bind to the CH_2 group, resulting in a planar ligand geometry to allow for maximum charge delocalization. The comparison of benzyl compounds clearly shows that the trend towards π-bonding increases for the heavier alkali metals.

Alkali metal triphenylmethanides have been the subject of structural and calculational investigations, but only a small group of compounds have been well characterized. Examples include $[(CPh_3)Li(TMEDA)]$ **10**,[30] and the charge-separated lithium triphenylmethanide $[Li(12\text{-crown-}4)][CPh_3)]$ **11**.[31] Heavier metal derivatives include the TMEDA and PMDTA adducts $[(CPh_3)Na(TMEDA)]$ **12**[32] and $[(CPh_3)M(PMDTA)]$ [M = K **13**, Rb **14**, Cs **15** (Figure 1)],[33] as well as several other potassium derivatives with various donors.[34] In contrast to the benzyl derivatives, all the triphenylmethane compounds display monomeric structures due to the increased steric demand of the ligand. This observation is further confirmed by studies involving substituted benzyl derivatives, including α-(dimethylamino)benzyllithium **16**,[35] where the increased steric demand of the ligand affords monomeric formulations. NMR studies of this compound in THF reveal a dynamic equilibrium between an η^1- and an η^3-isomer, of which the η^1-derivative is thermodynamically preferred. Substitution of the benzylic system may also suppress π-interactions, as seen with the trimethylsilyl substituted potassium α,α-bis(trimethylsilyl)benzyl derivative **17**.[36] This compound is also polymeric, but potassium is only η^3-coordinated to the benzylic ligand, due to steric repulsion with the large trimethylsilyl substituents. The coordination sphere on potassium is completed by several agostic interactions involving the $SiMe_3$ substituents.

Similar work on diphenylmethanides is almost non-existent, with only the charge-separated $[Li(12\text{-crown-}4)][(HCPh_2)]$ **18**,[37] the polymeric $[(HCPh_2)Na(TMEDA)]_\infty$ **19**, and the monomeric $[(HCPh_2)Na(PMDTA)]$ **20** known.[38] Recently, a pair of crown ether encapsulated rubidium diphenylmethanides with two different metal coordination modes, depending on the temperature of crystallization, was reported.[39] Crystallization at −23 °C led to a η^3-contact rubidium diphenylmethanide **21** (Figure 2), in which the metal assumes a geometry with one face

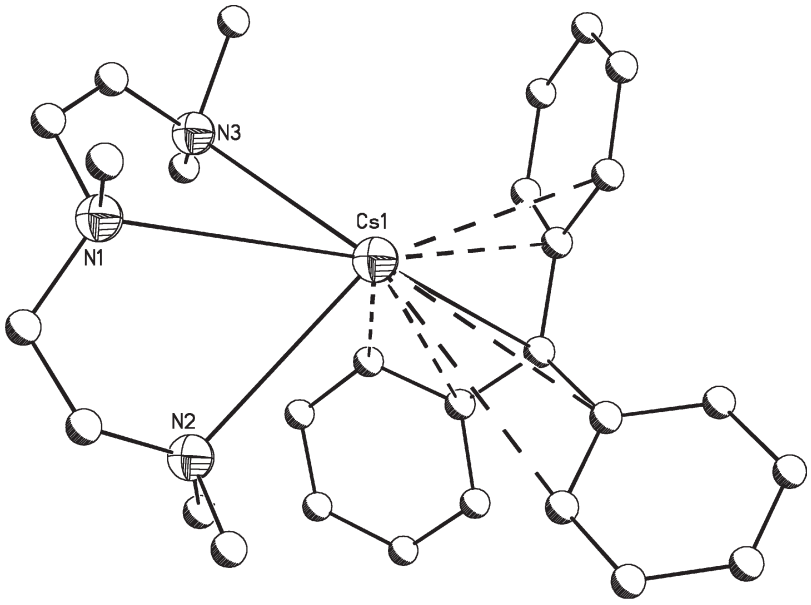

15

Figure 1 The structure of [$(Ph_3C)Cs(PMDTA)$] **15**. Hydrogen atoms have been omitted for clarity.

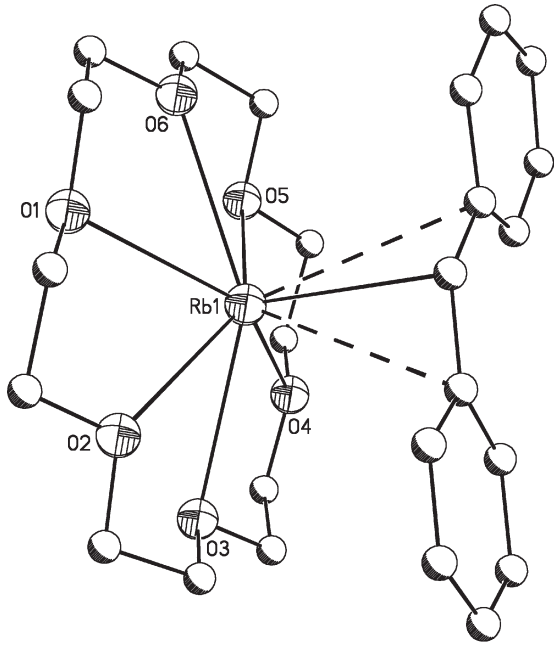

21

Figure 2 The structure of [$\eta^3Ph_2CHRb(18\text{-crown-}6)$] **21**. Hydrogen atoms have been omitted for clarity.

capped by the crown ether and the other occupied by the ligand, resulting in a metal coordination number of 9. The rubidium is directly bonded to the methylene carbon of the ligand at a distance of 3.063(3) Å with two longer interactions to the phenyl rings at 3.311(3) Å and 3.393(3) Å. The C2–C1–C8 angle of 132.6(3)° is consistent with a near planar geometry at the central methine carbon atom. The phenyl rings are slightly twisted (4.4° and 7.6°) relative

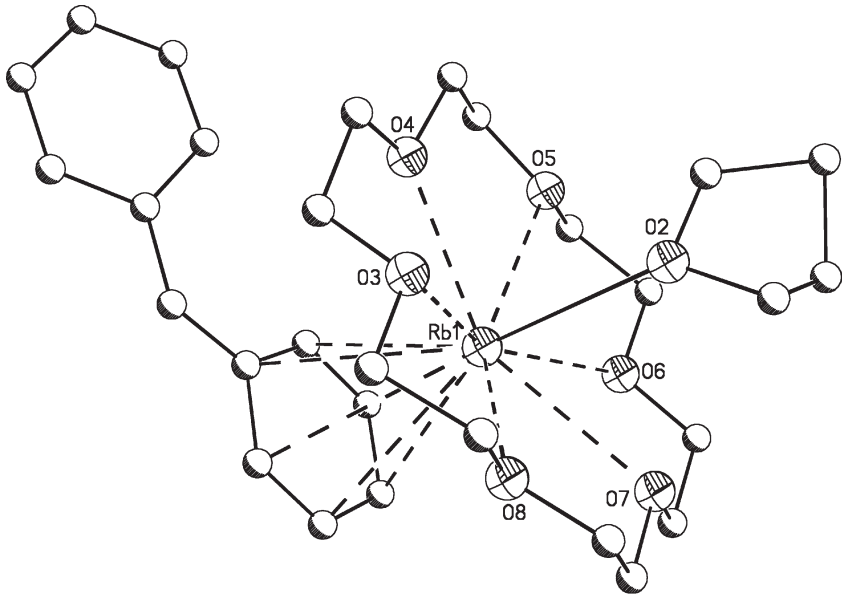

22

Figure 3 The structure of [η^6Ph$_2$CHRb(18-crown-6)] **22**. Hydrogen atoms have been omitted for clarity.

to the plane of the methine, methine hydrogen, and *ipso* carbons. This is in contrast to the alkali metal triphenylmethanides, in which these angles regularly exceed 25°.[30–33]

Crystallization of the reaction mixture at 4 °C leads to the formation of the η^6-coordinated rubidium diphenylmethanide **22** (Figure 3), where the metal is again encapsulated by crown ether. Here, the metal sits slightly below the center of the crown ether with average Rb–O distances of 2.85(5) Å. THF is located at an axial position, while one η^6-coordinated ligand phenyl group occupies the other with a metal–ring (centroid) distance of 3.076(9) Å, resulting in a formal coordination number of 13. On average, the phenyl bond lengths in the bound ring do not deviate significantly from those in the unbound one with values of 1.382–1.412(15) Å. The C2–C1–C8 angle of 133.0(9)° suggests a near planar geometry at the methine carbon atom.

Previous theoretical work focused on the degree of charge localization induced by the cation in the ligand.[40,41] The prevailing theory suggests that the larger, more diffuse alkali cations flatten the potential energy surface and allow for larger flexibility in π-type coordination, explaining in part the isolation of the two different modifications.

Other diphenylmethanides include the charge-separated compounds [K(18-crown-6)(THF)$_2$][HCPh$_2$] **23**, [Cs$_2$(18-crown-6)$_3$] [HCPh$_2$]$_2$ **24**, [Rb(15-crown-5)$_2$][HCPh$_2$] **25**, [K(15-crown-5)$_2$][HCPh$_2$] **26**, [Rb(12-crown-4)$_2$][HCPh$_2$] **27**, [K(2.2.2 crypt)][HCPh$_2$] **28**, [Rb(2.2.2 crypt)][HCPh$_2$] **29**, as well as the contact pair [(HCPh$_2$)Cs(2.2.2 crypt)] **30**.[42] In all species, the anion structure is very similar, based on conformational disorder in the diphenylmethanide anion. Generally, these compounds crystallize as charge-separated ion pairs, although this is greatly influenced by the size of the crown cavity. In the case of cations that fit well in the cavity of the donor, the cation is coordinatively saturated, and the metal–carbon interaction completes the metal coordination sphere. In cases where the cavity size is too small to fully encompass the cation, however, the need for further electrostatic stabilization cannot be filled by the organic ligand, and often a second crown ether will coordinate to the metal affording a sandwich-type complex with separated ions. This arrangement appears to take place regardless of reagent stoichiometry. An example for this trend is given by the contact structures of [(HCPh$_2$)Rb(18-crown-6)], **21**, **22**, whereas utilization of 15-crown-5 leads to the separated ion [Rb(15-crown-5)$_2$][CHPh$_2$] **25**. The tendency to form separated ion pairs is even more exaggerated in solution; all of these complexes display extremely little differentiation in chemical shift in both the ^{1}H and ^{13}C NMR studies. In polar solvents such as THF the contact structures appear to dissociate completely.

Clearly demonstrating the steric difference between a hydrogen atom and a phenyl group, the diphenylmethanide anion adopts a geometry that is approximately planar through the central methylene carbon with C–C–C angles of about 132°. This widening allows for the phenyl rings to be effectively coplanar with only minor ring twisting (ca. 5°).

This is in strong contrast to the ring twisting observed for the triphenylmethanide anions with twist angles in the range of 30°.

While the di- and triphenylmethanide anions are resonance stabilized, there is a tendency for isolating the π-system with a systematic localization of the double bonds; this discrete arrangement of single and double bonds has been observed and studied in detail in alkali bisdipyridylmethanides.[43–45]

Several studies have examined the relationship between di- and triphenylmethanides of the alkali metals and the corresponding pyridylmethanes.[43–45] In the trityl systems, low coordination numbers are favored for the smaller cations with the heavier metals tending toward higher coordination and polymerization, with as many as 20 close contacts to the metal being observed. This trend is explained by noting that the polarizing power of the cation decreases with increasing size of the ion, and subsequently the ability of the metal to localize charge density at one point in the anion is reduced. In the pyridyl analogs for both the diphenyl and trityl systems, the presence of the nitrogen in the ring draws the majority of the charge density into that atom, and coordination is exclusively through that point. Indeed, it was noted that the diphenyl anion might only be called a carbanion in the most formal sense; all indications are that there is very little charge density on the methylene carbon. In addition, it is well established that the potential energy surface for these compounds is very flat, with difficulties in trying to assign minima.[46,47] This critically important observation implies that attempts to explain the structural features of the heavier alkali metal diphenylmethanides using simple electrostatic point charge models may not be entirely adequate.

2.01.2.1.3 Silyl substituted alkanes

The steric demand and high lipophilicity of the $[CH(SiMe_3)_2]^-$ and the $[C(SiMe_3)_3]^-$ ligands have allowed the preparation and structural characterization of a significant number of alkali metal complexes. Examples of such compounds are contained in several comprehensive reviews, the latest published in 2001.[9,20,47–49]

The success of preparing heavy alkali metal complexes with these ligands can be accredited to the large number of methyl groups helping to increase solubility. Trimethylsilyl substitution also increases the size of the ligands helping to kinetically stabilize the metal centers and prevent extensive aggregation. Furthermore, the absence of β-hydrogen atoms helps to suppress unwanted side-reactions. The introduction of the bis(trimethylsilyl)methane and tris(trimethylsilyl)methane ligands affords alkali metal derivatives with reasonable to excellent solubility in hydrocarbon and etheral solvents, providing access to donor-containing and donor-free derivatives.

The structural chemistry of silyl substituted alkali methyl derivatives began to emerge about 30 years ago. Since then, an extended selection of fascinating compounds with a variety of structural features has been published. Work on these ligands was summarized in 1995,[20] 1996,[48] and 2001.[49] We review here some key compounds within the series, and discuss some newer developments obtained by replacing some of the $SiMe_3$ groups by phenyl or methoxy groups to introduce the capacity for π-bonding or intramolecular interaction.

The first structural evidence of an alkali metal derivative bearing a silyl substituted alkane ligand was the unusually stable $[(SiMe_3)_3CLi]$, **31**.[50, 51] The kinetic acidity of the $HC(SiMe_3)_3$ ligand was shown to be greater than the commonly known and used $HCPh_3$ due to the delocalization of negative charge into *d*- and σ^*-orbitals of silicon.[49] As such, synthetic access proved to be straightforward (under strictest inert gas conditions), and the improved solubility properties of the ligand made the isolation of a significant number of complexes possible. Since then, a multitude of compounds, including ionic species such as the elusive lithiate $[Li(THF)_4][\{(SiMe_3)_3C\}_2Li]$ **32** (Figure 4),[52] clearly demonstrate the unique capabilities of the ligand systems.

The two main groups of silyl substituted alkane ligands $HC(SiMe_3)_3$ and $HCH(SiMe_3)_2$ demonstrate significantly different steric demands, and we will discuss the two groups of alkali metal complexes separately. Only select compounds will be discussed.

Sodium complexes of $[CH(SiMe_3)_2]^-$ afford polymeric, donor-free $[(SiMe_3)_2CHNa]_\infty$ chains **33**.[53] Being isostructural to the lithium analog, $[(SiMe_3)_2CHLi]_\infty$, **34**,[54] the polymer displays planar $CHSi_2$ coordination, with C–Na–C angles within the polymer at 143°. This arrangement suggests weak secondary interactions between the $SiMe_3$ groups and the metal. The good solubility of the ligand in hexane suggests an easy breakup of the polymeric chain into monomeric units, further underscoring the significant steric demand of the ligand.

Crystallization of the potassium derivative in THF affords $[(SiMe_3)_2CHK(THF)]_\infty$ **35**, as an infinite polymer, with each metal center ligated to THF and two ligand carbon atoms.[55] Replacement of THF by *tert*-butylmethylether affords an isostructural species, **36**.[56] Demonstrating the importance of metal size and donor denticity, crystallization of the rubidium derivative in the presence of PMDTA affords a dimeric molecule $[(SiMe_3)_2CHRb(PMDTA)]_2$ **37** (Figure 5),[57] while the larger cesium displays polymeric chains with the same donor. $[(SiMe_3)_2CHCs(TMEDA)]_\infty$

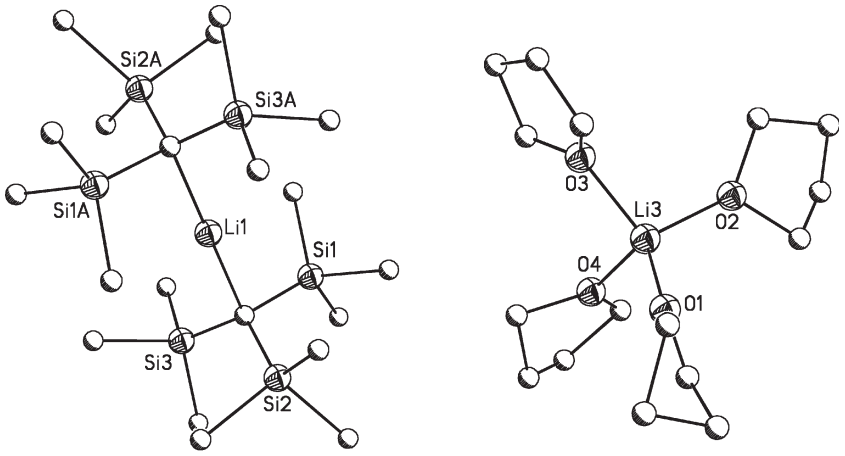

32

Figure 4 The structure of $[Li(THF)_4][\{(Me_3Si)_3C\}_2Li]$ **32**. Hydrogen atoms have been omitted for clarity.

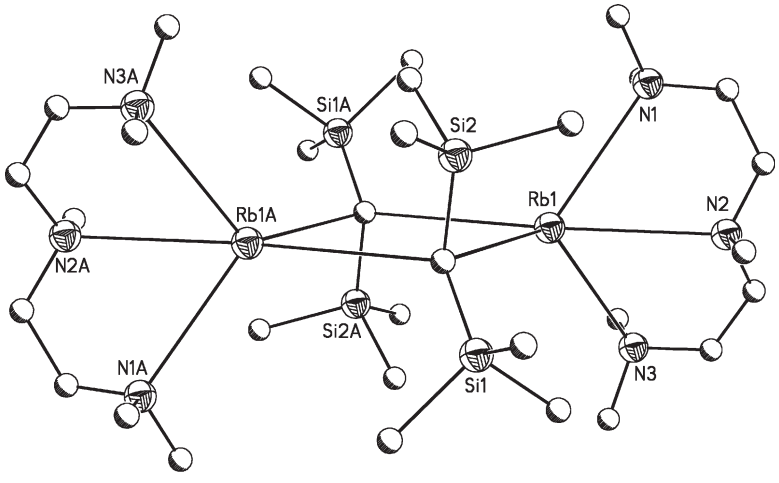

37

Figure 5 The structure of $[(Me_3Si)_2CHRb(PMDTA)]_2$ **37**. Hydrogen atoms have been omitted for clarity.

38 crystallizes with formally five-coordinate metal centers.[56] One of the recurring structural features with these ligands are dimeric units, as observed in the tetrameric $[(\mu\text{-}SiMe_3)_2CHK(PMDTA)K(\mu\text{-}CH(SiMe_3)_2K(\mu\text{-}CH(SiMe_3))_2K(PMDTA)]$ **39** exhibiting a central K_2C_2 four-membered ring flanked by two potassium units coordinated by PMDTA.[56]

Replacement of the hydrogen in $[CH(SiMe_3)_2]^-$ by $SiMe_3$ increases the ligand bulk, the resulting ligand is coined Tsi. Examples of heavy alkali metal derivatives include the donor-free potassium and rubidium compounds $[(SiMe_3)_3CM]_\infty$ (M = K **40**,[58] Rb **41**[59]) obtained from crystallization from ether solution. While the unsolvated sodium derivative $[(SiMe_3)_3CNa]_\infty$ has not been isolated yet, the potassium **42** and rubidium **43** compounds display an infinite chain comprised of alternating metal and C atoms, with several additional contacts between the metal and the $SiMe_3$ groups. Interestingly, the cesium analog crystallizes from benzene solution as the benzene solvate $[(SiMe_3)_3CCs(\eta^6C_6H_6)_3]$ **44** (Figure 6), clearly demonstrating the preference of the large metal toward π-bonding.[60]

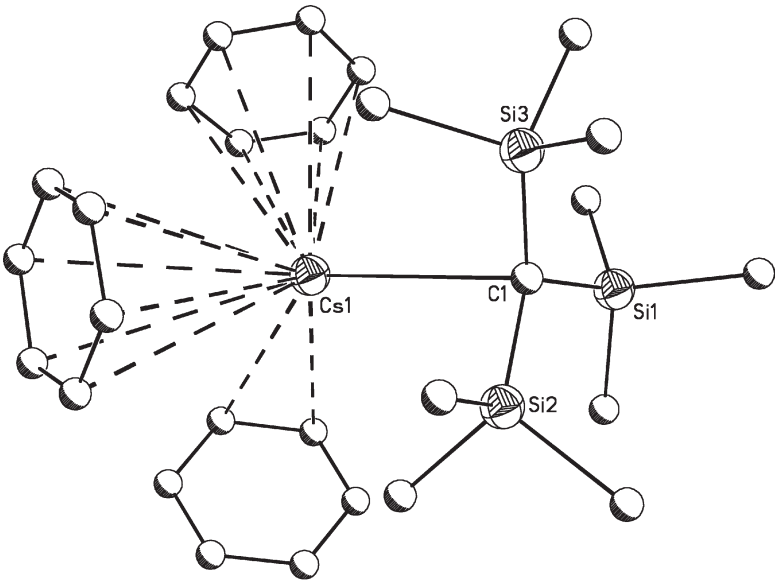

44

Figure 6 The structure of [μ-$(Me_3Si)_3CCs(\eta^6C_6H_6)_3$] **44**. Hydrogen atoms have been omitted for clarity.

Other examples include the donor-containing compounds $[(SiMe_3)_3CK(TMEDA)]$ **45**.[61] Here, the large steric demand of the ligand is demonstrated by a "loose" polymeric arrangement, with molecular units linked into chains by the coordination of potassium to neighboring molecules via agostic interactions, leaving each potassium formally four-coordinate. Not surprisingly, the compound is highly reactive.

The Tsi and the $CH(SiMe_2)_2$ ligands are capable of stabilizing elusive "ate" complexes, as shown initially with the isolation of the lithiate $[Li(THF)_4][Tsi_2Li]$ **46**.[62] Originally postulated by Wittig,[63] the lithiate has since been identified in several other instances.[64,65] The sodium compound $[Na(OEt_2)(TMEDA)_2][Tsi_2Na]$ **47**, together with a sodium cyclopentadienide (see below), is a rare example of a sodiate.[66]

The replacement of one, two, or even three methyl groups in tris(trimethylsilyl)methane by phenyl leads to $[C(SiMe_3)_2(SiMe_2Ph)]^-$, $[C(SiMe_3)(SiMe_2Ph)_2]^-$ as well as the $[C(SiMe_2Ph)_3]^-$ ligand. All possess the capability for metal π-bonding; alkali metal complexes have been prepared for all three. With the exception of the lithium derivative $[(SiMe_2Ph)_3CLi(THF)]$ **48**,[67] the heavier alkali compounds bearing the $[C(SiMe_2Ph)_3]^-$ ligand afford donor-free species in the form of polymeric chains. While the monomeric lithium species displays some π-interactions, the donor-free nature of the heavier analogs can clearly be understood by the increased propensity of the alkali metals toward π-bonding on descending the group. In fact, the chain polymers are held together by π-interactions between neighboring molecules. Further underscoring the strength of the π-interactions, the donor-free compounds were obtained after crystallization from THF for the Na **49**,[66] K **50**,[58] Rb **51**, and Cs **52** derivatives.[61] All display low solubility in benzene or toluene, attributed to the inability of the solid to interact with neutral arenes since the metal centers are already coordinatively saturated by metal–ligand (arene) bonding.

If only one or two of the trimethyl groups in the $[C(SiMe_3)_3]^-$ ligand are replaced by $SiMe_2Ph$, the competition between arene coordination and donation can be nicely demonstrated. With a reduced capability toward π-bonding, donor-containing complexes with good solubility in hexane including $[(SiMe_3)_2(SiMe_2Ph)CNa(TMEDA)]$ **53** are obtained.[61] Phenyl substituted silylalkanes are also capable of stabilizing "ate" complexes, as shown with $[Li(TMEDA)_2][\{(SiMe_3)_2SiMe_2Ph)C\}_2Li]$ **54**.[68]

The introduction of intramolecular coordination sites by placement of donor atoms within the ligand affords the ligand systems $[C(SiMe_3)_2(SiMe_2X)]^-$ (X = NMe_2 or C_5H_4N-2)[68] or $[CH(SiMe_3)\{SiMe_{3-n}(OMe)_n\}]^-$ ($n = 1, 2$).[69] These ligands afford metallacycles with the alkali metals, as demonstrated in $[(SiMe_3)_2(SiMe_2NMe_2)CLi(TMEDA)]$ **55**, where the metal center is coordinated to carbon, two nitrogen atoms from TMEDA, and the NMe_2 ligand group, thus providing an increase in metal coordination number without external donor or aggregation.[68] Examples of alkali metal

complexes carrying a methoxy substituted ligand system include the octamer $[(SiMe_3)(SiMe_2OMe)CHLi]_8$ **56**, the polymers $[(SiMe_3)(SiMe_2OMe)_2CHLi(SiMe_3)_2]_\infty$ **57** and $[(SiMe_2OMe)_2CHLi]_\infty$ **58**.

Examples of heavier alkali metal complexes include [{$CH(SiMe_3)(SiMe_2OMe)$}M] (M = Na **59**, K **60**) as well as the polymeric etherate $[CH(SiMe_3)(SiMe_2OMe)K(OEt_2)]_\infty$ **61**.[69] All these examples demonstrate the potency of intramolecular coordination, since methoxide–metal interactions under formation of metallacycles are observed in all cases.

2.01.2.2 Aryl Derivatives

Aryllithium compounds have been investigated in quite some detail, including NMR and crystallographic studies of donor-containing compounds. An excellent overview of this chemistry has been provided in a 2004 review article.[11]

Donor-containing phenyllithium derivatives display a variety of structural modes, as seen for the tetrameric $[PhLi(OEt_2)]_4$ **62**,[70] the dimeric $[PhLi(TMEDA)]_2$ **63**,[71] and the monomeric [PhLi(PMDTA)] **64**,[72] clearly demonstrating the structure-determining role of the donor.

Only a few examples of base-free organolithium compounds have been structurally characterized, all of them bearing alkyl ligands; examples include $[EtLi]_4$ **65**[73,73a] and $[^nBuLi]_6$ **66**.[74,74a] So far, the low solubility of unsubstituted phenyl derivatives has prevented the growth of suitable crystals. Structural information on Lewis base-free PhLi **67** was accomplished by synchrotron powder diffraction methods,[75] revealing a new structure type in organometallic lithium chemistry. With a Ph_2Li_2 dimer as a fundamental unit, the central C_2Li_2 rings are required to be absolutely planar as the result of a crystallographic inversion center. The phenyl rings are perpendicular to the central C_2Li_2 ring. The individual dimers are arranged in an extended structure by η^6-coordination to neighboring phenyl rings, thus creating a polymeric zigzag ladder arrangement. With this structural information in hand it is now possible to understand why donor-free phenyllithium displays such poor solubility in hydrocarbons. Addition of Lewis bases cleaves the metal–arene interactions, reducing the degree of aggregation.

Substitution of the phenyl rings affords compounds with increased solubility and steric demand, thus displaying a reduced degree of aggregation. Examples include the dimeric $[MesLi(THF)_2]_2$ (Mes = Mesityl, 2,4,6-$Me_3C_6H_2$) **68** (Figure 7)[23,23a] or the donor-free terphenyl dimer $[(2,6\text{-}Mes_2C_6H_3)Li]_2$ **69**.[76] Again, ligand bulk is detrimental;

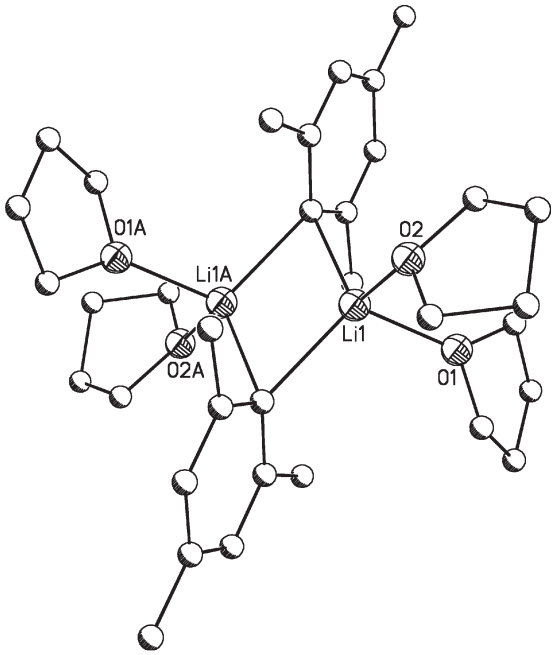

68

Figure 7 The structure of $[MesLi(THF)_2]_2$ **68**. Hydrogen atoms have been omitted for clarity.

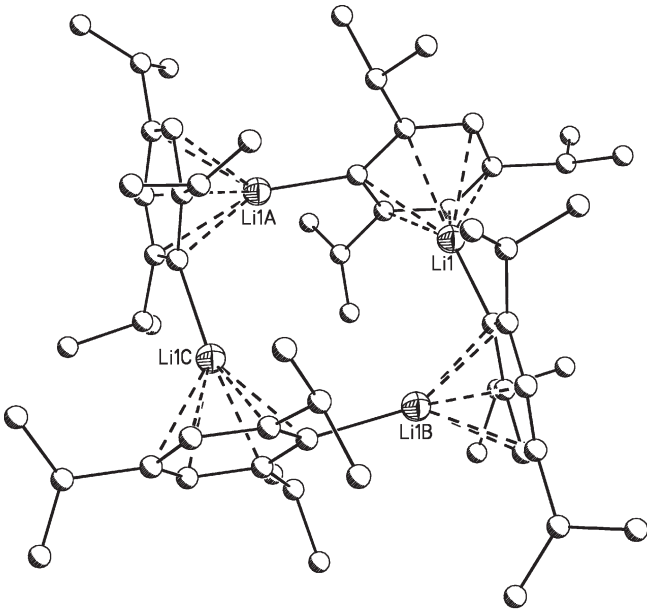

70

Figure 8 The structure of $[TripLi]_4$ **70**. Hydrogen atoms have been omitted for clarity.

replacement of the methyl groups in the *ortho*-positions by isopropyl as seen in the donor-free $[TripLi]_4$ **70** (Figure 8) increases aggregation to 4.[76] In this tetramer, each lithium atom is σ-bonded to one aryl ring, and η^6-coordinated to the aryl system of a neighboring unit resulting in a four-membered ring. Use of the larger *tert*-butyl substituents affords a dimeric molecule, $[Mes^*Li]_2$ **71** ($Mes^* = Supermesityl$, 2,4,6-$^tBu_3C_6H_2$) displaying similar metal–ligand interactions.[76] The even larger 2,6-$^iPr_2C_6H_2$ substituents in the *ortho*-position afford a dimeric molecule with σ- and π-bonding **72**.[77]

The influence of ligand size is further demonstrated in a series of unsolvated aryllithium derivatives, made possible by the introduction of alkyl groups. Not surprisingly, introduction of substituents in the 4 position has no or little effect on steric demand, affording polymeric molecules as displayed in the polymeric species $[4\text{-}^nBuC_6H_4Li]_\infty$ **73**, $[4\text{-}SiMe_2{}^tBuC_6H_4Li]_\infty$ **74**, and $[4\text{-}^tBuC_6H_4Li]_\infty$ **75**.[78] Introduction of two *tert*-butyl groups in the 3 and 5 positions reduces aggregations to the hexameric $[3,5(^tBu)_2C_6H_3Li]_6$ **76** (Figure 9).[78] As observed previously, reduction of association is also displayed in the presence of donors, and indeed, monomeric molecules may be obtained if sterically demanding ligands and donors are used, as seen in $[2,6\text{-}Trip_2C_6H_3Li(OEt_2)_2]$ **77**.[79] Detailed discussions of the effect of phenyl ring substitution on aggregation pattern in the sterically very demanding terphenyl lithium derivatives can be found in Refs: 80–82.

Examples of heavier alkali metals bearing phenyl ligands are scarce; only one example of a terphenylsodium derivative $[(2,6\text{-}Mes_2C_6H_3)Na]_2$ **78** has been structurally characterized (Figure 10).[83] Many structural features of this sodium dimer resemble that of the dimeric lithium analog with σ- and π-bonding motifs.[76] The structural differences between the lithium and sodium structures can be clearly accredited to the larger radius of sodium with its increased tendency toward π-bonding. In the lithium compound the metal centers interact primarily with the *ipso*-carbons of the phenyl rings, and also display fewer interactions with the mesityl *ipso*-carbons in the *ortho*-positions.

Introduction of Lewis donors provides access to a larger library of compounds, including the dimeric $[PhNa(PMDTA)]_2$ **79**[84] and the rare mixed metal "ate" complex $[\{Na(TMEDA)\}_3Ph_4Li]$ **80**.[85] Intramolecular coordination has been used successfully in the trimer $[2,6\text{-}(CH_2NMe_2)_2C_6H_3Na]_3$ **81** (Figure 11),[86] as well as the hexameric 2-β-[N,N-dimethylamino]ethoxyphenylsodium **82**.[87] This hexamer consists of two stacked trimers with a pseudo-threefold inversion axis. The Na_6 polyhedron forms a distorted octahedron, with the bonding resembling that of hexameric $[^nBuLi]_6$.[74,74a]

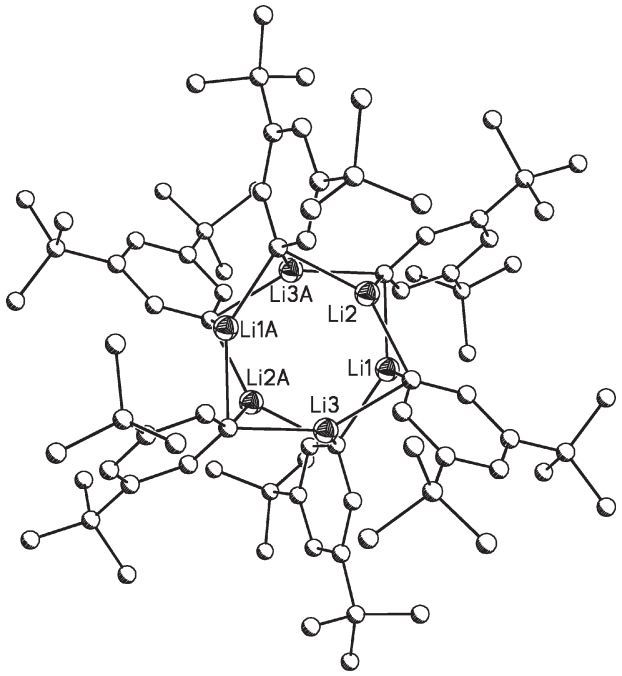

76

Figure 9 The structure of $[3,5\text{-}(^{t}Bu)_2C_6H_3Li]_6$ **76**. Hydrogen atoms have been omitted for clarity.

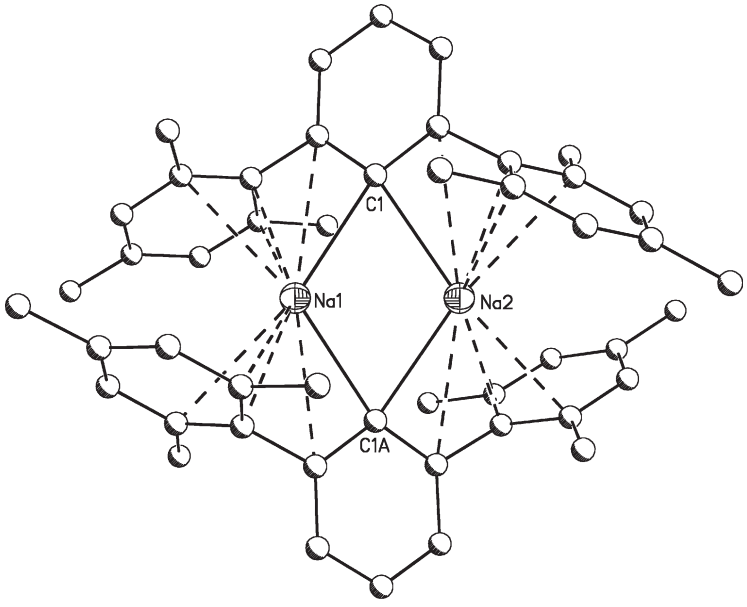

78

Figure 10 The structure of $[2,6\text{-}Mes_2C_6H_3Na]_2$ **78**. Hydrogen atoms have been omitted for clarity.

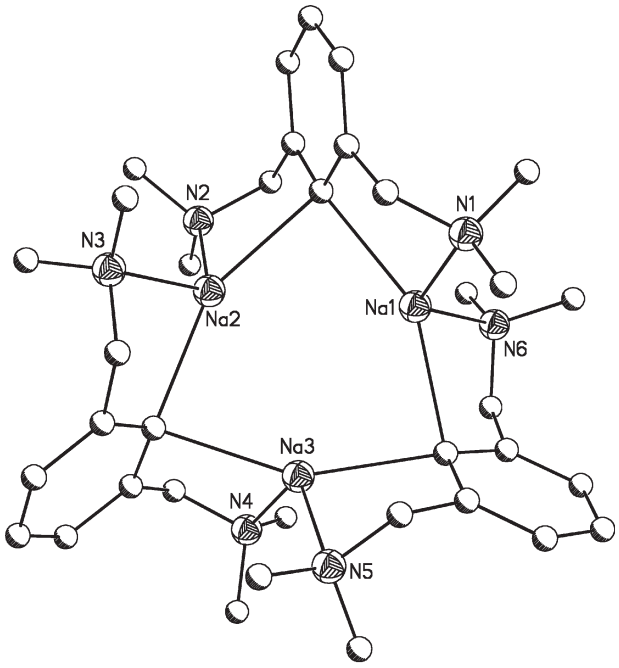

81

Figure 11 The structure of [2,6-$(CH_2NMe_2)_2C_6H_3Na]_3$ **81**. Hydrogen atoms have been omitted for clarity.

2.01.2.3 Cyclopentadienide, Fluorenide, and Indenide Derivatives

The first organometallic compound containing a cyclopentadienide ($Cp = C_5H_5$) ligand was CpNa, prepared in 1900.[88] Only a year later, CpK was reported by the same authors.[89] Several excellent review articles are available on the subject;[90–92] here we review only recent information.

Intense studies in the 1950s focused on the nature of the metal–ligand (Cp, substituted Cp, fluorenide (Fl), and indenide (Ind)) bond establishing a largely ionic bonding model with a smooth increase in polarity of the R_5C_5–M bond as descending the group of alkali metals, but detailed structural information did not become available until 1976.[93–97] Since then, significantly more information has been gathered providing detailed data on substituted, unsubstituted, as well as ionic Cp's, Ind's, and Fl's. The compounds may exist as unsolvated as well as solvated linear polymers, oligomers, and also monomers, with the main structure-determining factor being ring substituent(s), co-ligands, and the metal.

Unsubstituted, unsolvated complexes have been observed for all metals, but their low solubility prevents the growth of quality single crystals. This problem was recently overcome with data collected on a powder sample on a synchrotron X-ray source followed by Rietveld refinement.[17–19] Not surprisingly, the structures display polymeric chains with alternating metal and Cp units.

Vividly demonstrating the influence of ring substitution as well as the effect of donor molecules, monomeric complexes can only be obtained if the substitution pattern on the Cp ring is extensive, thus significantly increasing the ligand's steric bulk, as strikingly demonstrated with 1,2,4-$(Me_3Si)_3$CpLi(THF) **83**.[98]

A family of recently published Cp complexes sheds a more detailed light on the role of the donors on the overall structural pattern. Demonstrated with a group of Cp derivatives in the presence of the crown ethers 15-crown-5 and 18-crown-6, monomeric complexes may be obtained in the form CpNa(15-crown-5) **84**.[99] In a parallel fashion, 18-crown-6 has been shown to be effective in supporting monomeric structures of the heavier alkali metals bound to Cp. Examples include CpM(18-crown-6) (M = K **85**, Rb **86**, Cs **87**).[100,101]

Structural details in CpNa(15-crown-5) **84**[99] show the Cp and the crown ether to be arranged in an almost coplanar manner with the oxygen atoms coordinated in a slightly asymmetric manner to sodium (Na–O 2.42–2.55 Å). The Cp ring displays an asymmetric metal coordination mode with two close (2.67 and 2.71 Å), two medium (2.85 and 2.91 Å), and one longer Na–C distance (2.99 Å). The asymmetric metal coordination may be accredited to the small sodium

radius not being able to support a coordination number of 10. With the 12-crown-4 analog of sodium not being available to support this assumption, a 12-crown-4 derivative has been reported for lithium **88**. Here, much more symmetrical Li–C interactions (2.34–2.42 Å) are observed.[102]

Monomeric 18-crown-6 complexes in the form of contact ion pairs (CIPs) are also known for K **89**, Rb **90**, and Cs **91**. Again, the metal radius is structure determining, with potassium within the plane of the crown ether; the heavier metals are located above the plane of the crown ether oxygens toward the Cp ring. While the potassium **89** and rubidium **90** compounds exhibit an almost coplanar arrangement between Cp and the crown, the cesium analog **91** displays a bent geometry with angles of 154.7° and 160.1° (two independent molecules) between the two planes.[100, 101] It appears reasonable to accredit the distortion to somewhat similar factors as observed in the bent Cp derivatives of the alkaline earth metal derivatives,[103] where facile distortion from ideal geometry due to the largely ionic bond contribution and lack of orbital control is observed.

A significant number of substituted Cp complexes have been prepared and structurally characterized. Substituents frequently consist of alkyl or silyl groups used to enhance the solubility of the resulting complexes, although a small number of arene substituted derivatives are known as well. Pentamethyl substituted Cp, commonly known as Cp^*($Me_5Cp = Cp^*$) is frequently used, although recent work included multiple $SiMe_3$ substituted species as well. Besides increased steric bulk, alkyl substituents on the Cp result in slightly increased metal–ligand bond strength, while silyl substitution has the opposite effect.[91] The influence of methyl substitution can be verified by comparing bond length in a series of lithium compounds with increased methyl substitution on Cp. Indeed, a small but recognizable bond shortening is observed upon Cp substitution, as explained by increased electron density in the ligand. The slight bond weakening in the silyl substituted derivatives is less intuitive, since the substituents also increase the electron density of the σ-system. However, negative hyperconjugation draws electron density from the Cp-π system, slightly overcompensating for the bond-strengthening effect of the σ-electron donation.

Most commonly, structurally characterized potassium pentamethylcyclopentadienides involve strongly coordinating bases, such as Cp^*K(18-crown-6) **92**,[104] $[Cp^*K(pyridine)]_\infty$ **93**,[105] $[Cp^*K(THF)]_\infty$ **94**,[106] and $[\mu\text{-}(C_5Me_4SiMe_2CH_2CH{=}CH_2)K(THF)]_\infty$ **95**.[106] Each of these crystallizes as an extended structure, with alternating Cp and metal moieties. Further increase of ligand size increases the likelihood to obtain monomeric or oligomeric compounds, as demonstrated with the monomeric $[(Ph_4C_5H)Na(DME)_2]$ **96**[107] or $[(benzyl)_5C_5K(THF)_3]$ **97**.[108]

The Ind and Fl ligands can be classified as the benzo and dibenzo analogs of the Cp anion, and may be viewed as closely related Cp analogs. Indeed, many structural parameters closely resemble that of the more intensively studied Cp's. Structural information on heavy alkali metal Fl's and Ind's dates back to the 1990s with the characterization of a series of fluorenyl alkali metal PMTDA adducts as well as IndK(TMEDA) **100**.[110] Since then, the alkali metal chemistry of these ligands has been extended toward the remaining alkali metals, incorporating a variety of donors, including 15-crown-5 and 18-crown-6.[99,101] In analogy to the Cp's, ligation to crown ether affords monomeric, nearly coplanar species with metal-π bonding. Selected examples include [IndNa(15-crown-5)] **101**, and [FlNa(15-crown-5)] **102**,[99] [IndM(18-crown-6)] (M = Rb **103**, Cs **104**)[99] and [FlM(18-crown-6)] (M = Rb **105**, Cs **106**).[101] A series of fluorenyl alkali metal diglyme complexes reveals contact and separated ion pairs including $[Li(diglyme)_2][Fl]$ **107**, $[Na(diglyme)_2][Fl]$ **108**, the trimer $[FlK(diglyme)]_3$ **109**, the nonamers $[FlRb(diglyme)]_9$ **110**, $[FlCs(diglyme)]_9$ **111**, the dimer $[FlNa(diglyme)]_2$ **112**, and the polymer $[FlK)_2diglyme]_\infty$ **113**.[111] Complementing this series of fluorenyl complexes bearing tridentate donors are [FlNa(TMEDA)] **114**[112] as well as [FlM(PMDTA)] (M = Na **115**, Rb **116**, Cs **117**).[112, 113] An interesting dimeric molecule, bis-μ^2-diglyme bis-fluorenyl disodium **118**, has been reported. Here, diglyme bridges the sodium centers with fluorenyl in terminal positions (Figure 12).[111]

The significant structural differences between the tridentate PMDTA and diglyme complexes indicate the importance of small differences affecting the structural features of the resulting compounds. The slightly more sterically demanding PMDTA donor (two methyl groups on the nitrogen as compared to one methyl group on oxygen in diglyme) affords monomeric species, whereas additional coordination is needed to saturate the metal center for the smaller diglyme, resulting in the formation of higher aggregates. This demonstrates nicely the ongoing problem of predicting the structural chemistry of alkali metal compounds: very small differences may have a profound effect on the ion association, aggregation, and overall geometry of the resulting complexes.

Studies of CpLi solutions showed high conductivity, suggesting ionic particles in solution.[91] Ionic particles could consist of the free ions, but anionic cyclopentadienides MCp_2^- particles isoelectronic to the well-known alkaline earth cyclopentadienides Cp_2M (M = alkaline earth metal),[103] could also be envisioned. Moreover, the structural motif of a sandwich complex where two Cp ligands bind to a metal center is well established throughout the periodic table. Indeed, the Cp_2^-Li anion was suggested based on NMR techniques,[114–116] and

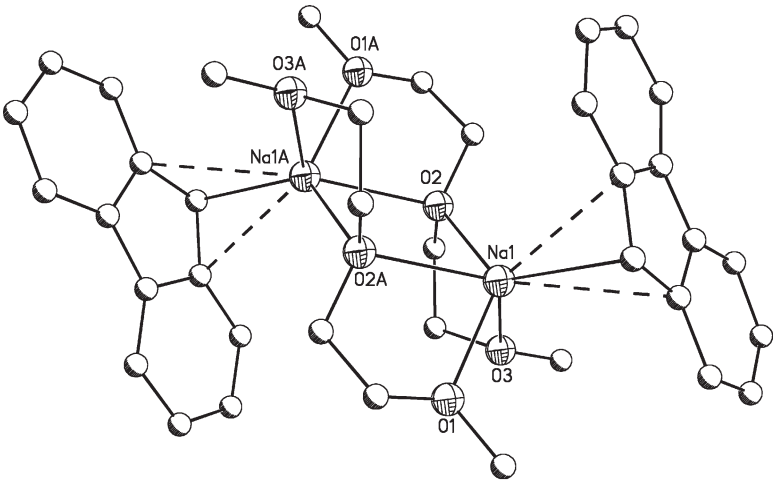

118

Figure 12 The structure of [FlNa(diglyme)]$_2$ **118**. Hydrogen atoms have been omitted for clarity.

structural proof for the lithocene anion [PPh_4][Cp_2Li] **119** was first provided in 1994 by Harder and Prosenc.[117,117a] Since then, several other examples have been isolated including [$(Me_2N)_3S$][Cp_2Li] **120**,[118,118a] [PPh_4][Cp_2Na] **121**,[119] [$(Me_2N)_3S$][Cp_2Na] **122**,[118,118a] [PPh_4][Cp_3Cs_2] **123**,[120,120a] the fused ring system [Li(12-crown-4)$_2$][(CpC_5H_8)Li)] **124**,[121] in addition to the *tert*-butyl substituted [Ph_2PMe_2][(^{t}BuCp$_2$)Li] **125**.[122] Other examples of substituted lithiocenes include di(isodicyclopentadienide)lithium **126**.[121] The lithiocene complexes typically display a staggered configuration with approximate D_5-symmetry. The coordination of two Cp rings to lithium results in significant bond lengthening as compared to LiCp, likely due to steric repulsion between the two Cp rings. Since the alkali metal–Cp bond increases in polarity as descending group 1, two competing factors determine the strength of the metal–ligand interaction. Apparently, steric arguments prevail, as calculations showed the association of a second Cp to be more exothermic for sodium than for lithium.[91] A very unusual example of an anionic complex is the dianion [$(Fl)_3Na]^{2-}$ **127**.[122a] Here, the three Fl anions adopt a paddle wheel conformation around sodium.

Several examples of *ansa*-alkali metallocene sandwiches exist, in which the two Cp rings in a [$Cp_2M]^-$ arrangement are bridged and the molecular geometry underlies geometrical restraints. Examples include [PPh_4][(Me_4C_2)Cp_2Na],[119] [PPh_4][($allyl)_2SiCp_2Na$] **128**,[123] and [$Li(THF)_4$][$Me_2Si(Fl)_2Li$] **129**.[124] In some of the molecules the Cp tilt angles are as small as 100°.

Another group of charged Cp derivatives needs to be mentioned, a group of "inverse" sandwich complexes of the type [$CpM_2]^+$. Here, a Cp unit is flanked by two alkali metals. Examples include the triple cation [(MeCp)Li_2(TMEDA)$_2$] **130**,[125] in addition to the [$CpNa_2(THF)_6$] **131**[126] and [^{t}BuCpK_2(18-crown-6)] **132**[127] cations.

2.01.2.4 Alkali Metal Interaction With π-Systems

The deprotonation of alkenes by organometallic reagents affords allyl species. As the simplest example of delocalized organometallic systems, the alkali metal allyl system has been studied in solution and the solid state in quite some detail;[128] this work has been further supported by theoretical studies.[129] Allyl species are usually very reactive undergoing complex rearrangement reactions, and often, the reaction products cannot be directly characterized. Instead, they are often identified by their reaction products.

Two main structural types have been identified for allyl alkali metal species: solvated ions in the form of CIPs where a delocalized anion with metal coordination is perpendicular to the ligand plane,[130–134] or unsolvated allylic lithium compounds displaying localized ligand systems with NMR spectra closely resembling those of alkenes.[135–138]

The study of solvated alkali metal allyl species remains a complex topic due to a variety of reorganization processes. Structural data on alkali metal allyl derivatives include [C_3H_5Li(TMEDA)] **133**,[139] where solvated lithium ions act as

bridges between the terminal CH_2 groups of the allyl ions. In contrast, Li is coordinated to the allyl π-system if the tridentate donor PMDTA is utilized. For example, [$\eta^2C_3H_5Li$(PMDTA)] **134** crystallizes as a monomeric molecule.[140] The unexpected η^2-coordination appears to be the result of the large steric shielding by PMDTA. The argument of steric shielding is further supported by the crystal structure of [1,3-diphenylallylLi(TMEDA)] **135**, where η^3-metal coordination is confirmed for the first time in the solid state.[141] This observation is further confirmed with structural data on [$C_3H_3(SiMe_3)_2$Li(TMEDA)] **136**, where essentially symmetrical geometry, slightly perturbed by lithium–TMEDA coordination, is observed.[142]

Calculations of alkali metal allyl derivatives involving all alkali metals (Li–Cs) indicate a preferred geometry with the metal symmetrically bound in a predominantly electrostatic manner to all three carbon atoms.[143] Solution studies of allyllithium in ether indicate the compounds to be highly aggregated; in THF complex dynamic behavior is observed.

To further study the preferred coordination of the alkali metal ions and its potential toward synthetic applications, recent studies focused on the preparation of compounds by encapsulating the metal in an allylic lithium compound by coordinating it to an attached ligand, resulting in the first structural characterization of an internally solvated pair by NMR methods.[144] The attachment of pendant arms to the center carbon of the allylic moiety afforded an extended family of compounds that were investigated by NMR and crystallographic methods.[145–148] These compounds display structures (by NMR) that lie between the two expected structural types: solvated ions in the form of CIPs or an unsolvated allylic lithium compound with a localized ligand system. This work established that the role of the tether is critical in determining the geometry of the metal. If the tether is too short, it may not be possible for lithium to position itself on the center of the allylic plane; rather coordination closer to one of the terminal allylcarbon is observed, thus affording a compound with a partially localized π-system.

Heavy alkali metal allyl systems include [1-phenylallylNa(PMDTA)] **137** with the expected η^3-metal coordination;[149] the η^3-coordination is in stark contrast to that of the corresponding η^2-lithium derivative.[140] The metallation of 1-phenylcyclohexene with sodium in the presence of PMDTA also affords an allyl system **138**.[149,149a] Interestingly, the solvated sodium cation does not coordinate to the allyl moiety but is η^6-centered over the phenyl ring. The rationale for phenyl rather than allyl metal binding lies in the strong shielding of sodium by PMDTA preventing its close approach.

In contrast to the allyl system, where the reduction of an isolated double bond is investigated, the reduction of extensively delocalized aromatic systems has been in the focus of interest for some time. Reduction of the systems with alkali metals in aprotic solvents under addition of effective cation-solvation agents affords initially radical anions that have found extensive use as reducing agents in synthetic chemistry. Further reduction is possible under formation of dianions, etc. Like many of the compounds mentioned in this article, the anions are extremely reactive, and their intensive studies were made possible by the advancement of low temperature X-ray crystallographic methods (including crystal mounting techniques) and advanced synthetic capabilities.

Compounds of this type may only be isolated in the presence of suitable donor molecules, among those, diglyme has been used frequently, but other examples include TMEDA or 2,2,1-crypt for sodium.[150] The reduction of naphthalene or anthracene with sodium in diglyme affords separated ions with the radical anion [Na(diglyme)$_2$][naphthalene/anthracene]$^{\cdot}$ **139**, **140**.[151]

Numerous other examples of alkali metals in conjunction with extended π-systems have been reported; we present only a very brief overview. In many cases, extensive distortion upon reduction is observed, especially when the second electron is added. This is shown in the cesium contact "multiples" containing bis-diglyme salts of the tetraphenylethanediyl ligand **141**, where extensive association between neighboring molecules through π-bonding is observed. In the dianion, the [Cs(C_6H_5)$_2$] halves are twisted by 76° around the single C–C bond, and the C–C bond is elongated from 1.36 Å in the neutral precursor to 1.51 Å.[152] These changes in geometry upon deprotonation are in agreement with the analogous disodium salt **142**.[153,153a]

Other selected examples include tris(tetramethylethylene diamine–sodium)-9,9-dianthryl **143**,[154] alkali metal salts of 9,10-bis(diisopropylsilyl)anthracene **144**,[155] as well as the closely related "naked" 9,10-bis(trimethylsilyl)anthracene radical anion **145**.[156] This chemistry is further extended to the solvent-shared and solvent-separated alkali metal salts of perylene radical anions and dianions **146**, **147**,[156] while other examples focus on alkali metal salts of 1,2-diphenylbenzene and tetraphenylethylene derivatives, where reduction with potassium in diglyme afforded contact molecules with extensive π-bonding, [1,2-$Ph_2C_6H_4$K(diglyme)] **148**.[157] Extensive π-coordination is also observed in (1,1,4,4 tetraphenylbutadiene-2,3-diyl)tetracesiumbis(diglyme)bis(methoxyethanolate) **149**.[158]

2.01.2.5 Alkynyl Alkali Metal Derivatives

The simplest (and smallest) alkali metal alkynyl derivative, ethynyllithium, can only be obtained in the form of single crystals as a base adduct. In the presence of ethylenediamine (en), a polymeric compound as double strands connected by the en donors is obtained, **150**.[159]

The strong tendency toward aggregation, a commonly observed structural motif within organoalkali metal derivatives, is widely observed in alkali metal alkynyl chemistry, likely due to the small size of the ligand.

Demonstrating the strong tendency toward aggregation, and the importance of the donor molecule, phenylethynyllithium crystallizes either as a dimer **151** or a cubane-like tetramer **152**: the dimer is obtained in the presence of N,N,N′N′-tetramethyl(1,3-propanediamine),[160] whereas the longer chain donor N,N,N′N′-tetramethyl-1,6-hexanediamine affords a polymeric structure with cubane-like C_4Li_4 units.[161,161a] Providing a strong argument for parallel solid-state and solution studies, ^{13}C NMR studies in D_8-THF indicated a smaller degree of aggregation in the form of a dimeric phenylethynyllithium,[162] a result also confirmed by cryoscopic measurements.[163] Aggregates are also observed in *tert*-butylethynyllithium derivatives, where both a dimer [^{t}BuCCLi(THF)]$_2$ **153** (Figure 13) and a dodecamer [^{t}BuCCLi(THF)$_4$] **154** were obtained from identical THF solutions.[164] The compounds display heterocubanes – a common structural motif in organolithium chemistry. In the tetramer, each lithium is also coordinated by a THF, whereas the dodecamer is comprised of fused cubanes with THF located only at the endpoints of the oligomer.

The larger radii of the heavier alkali metals, and the pronounced aggregation tendencies of the alkynyl ligands, even observed for the small lithium, indicate extensive aggregation chemistry for the heavier metals. Indeed, only sparsely soluble compounds were obtained for a series of $[CH_3CCM]_n$ (Na **154**, K **155**, Rb **156**, Cs **157**). Structural data were obtained from powders using synchrotron radiation.[165,165a,166] In contrast to the lithium compounds, the heavier metal analogs prefer a doubly bridged π-structure, with each metal symmetrically located over a face.

The tendency toward aggregation may be suppressed by application of large, multidentate donors, as shown with the monomeric [PhCCK(18-crown-6)] **158**.[167]

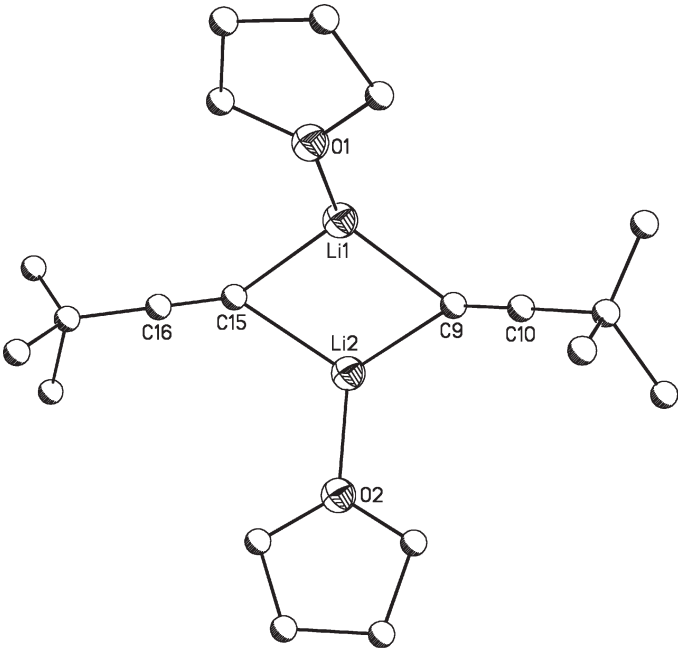

153

Figure 13 The structure of [^{t}BuCCLi(THF)]$_2$ **153**. Hydrogen atoms have been omitted for clarity.

2.01.3 Alkali Metal Derivatives with Heavy Group 14 Ligands

2.01.3.1 Alkali Metal Silanides

Over the past decade alkali metal silanides have gained importance due to their application as reagents in synthetic chemistry, resulting in an upsurge of detailed information available on such compounds. Several review articles summarize recent developments.[168,168a–168e]

Alkali metal silanides were first intensively studied in the 1950s by Gilman *et al.*[169, 170] Later work by Wiberg *et al.* focused on $MSiPh_3$, available by the cleavage of the Si–Si bond in $Ph_3SiSiPh_3$ with alkali metals. However, the amount of undesired byproducts was very high.[171]

Since then, several different alkali metal silanide systems have been reported. One of them, the hypersilyl $[Si(SiMe_3)_3]^-$ ligand, was first prepared by Gilman and Smith.[172, 173] Another ligand includes supersilyl $[Si^tBu_3]^-$ prepared in 1975.[174–176] Several other variations of the ligand systems are known with the recent addition of $[Si^tBu_2Ph]^-$, for which several alkali metal derivatives have been prepared and characterized.[177,178]

Amongst the different silanide ligands, the hypersilanides $[Si(SiMe_3)_3]^-$ have received most attention. The advantages of this ligand are its ease of preparation, the high solubility in a variety of solvent systems, and large steric demand resulting in effective kinetic stabilization of the metal centers. Moreover, the alkali metal derivatives may be prepared with ease using several different synthetic routes.

$[(Me_3Si)_3SiLi(THF)_n]$ **159** was first prepared by Gilman and Smith in 1967,[179, 180] with structural data becoming first available about 15 years later with $[(Me_3Si)_3SiLi(DME)_{1.5}]$ **160**[181] followed by $[(Me_3Si)_3SiLi(THF)_3]$ **161**.[182,182a]

Heavy alkali metal hypersilanides were first prepared by Klinkhammer, who reported on a series of donor-free dimers of the form $[(Me_3Si)_3SiM]_2$ (M = Li **162**, Na **163**, K **164**, Rb **165**, $Cs{\cdot}1.5C_6H_5CH_3$ **166**) (Figure 14) from crystallization of aromatic solvents.[183, 184] A rare example of an ether-solvated product is $[\{(Me_3Si)_3SiCs\}_2THF]$ **167**, with the THF bridging the two metal centers.[185]

The use of crown ether or multidentate donors with alkali metal tris(trimethyl)silyl silanides affords both contact molecules and separated ion pairs, depending on the coordinative saturation provided by the ligand.[186] As an example, $[(Me_3Si)_3SiK(18\text{-crown-}6)]$ **168** (Figure 15) crystallizes as a contact molecule, whereas use of the smaller crown ether, 12-crown-4, affords separated ions with two crown ethers coordinating to the cation in a sandwich-type fashion as seen in $[K(12\text{-crown-}4)_2][Si(SiMe_3)_3]$ **169** or for the larger metal with 18-crown-6 in

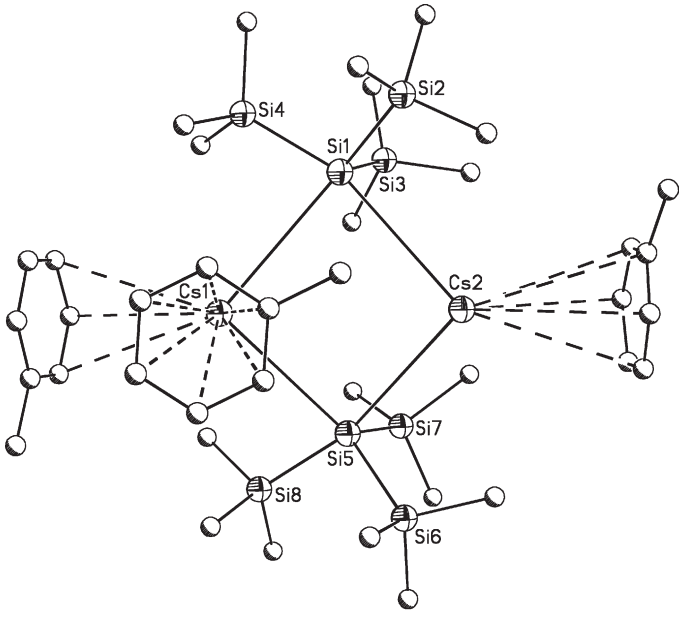

166

Figure 14 The structure of $[(Me_3Si)_3SiCs(C_6H_5CH_3)_{1.5}]_2$ **166**. Hydrogen atoms have been omitted for clarity.

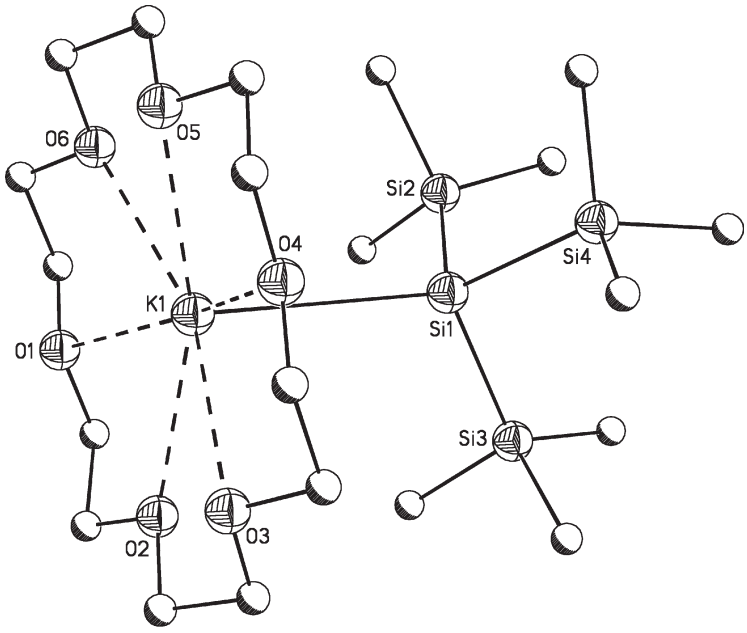

168

Figure 15 The structure of $[(Me_3Si)_3SiK(18\text{-crown-}6)]$ **168**. Hydrogen atoms have been omitted for clarity.

$[Cs(18\text{-crown-}6)_2][Si(SiMe_3)_3]$ **170**. An interesting example, rubidium hypersilanide with 18-crown-6, crystallizes with two contact molecules and one separated ion in the form $[Rb(18\text{-crown-}6)Si(SiMe_3)_3]_2$ $[Rb(18\text{-crown-}6)_2][Si(SiMe_3)_3]$ **171**, indicating energetic similarities between solvation and ligation. The presence of two contact molecules and one separated ion pair in one asymmetric unit is independent of reagent stoichiometry. Underscoring the subtle, but distinctive differences between silicon and germanium, the addition of 1.5 equiv. of 18-crown-6 to rubidium hypergermanide afforded only the contact molecule $[(Me_3Si)_3GeRb(18\text{-crown-}6)]$ **172**.[187]

The alkali metal tris(trimethylsilyl)silanides dissociate in solution into separated ion pairs, as indicated by very similar chemical NMR shifts in aromatic solvents.[186] The dissociation into separated ions supports the view of highly polarized alkali metal–silicon bonds. The ease of dissociation into separated ion pairs can also be rationalized when analyzing the structural parameters of MSi^tBu_2Ph (M = Na **173**, K **174**).[177,178] While the sodium derivative displays a polymeric chain held together by π-interactions involving the phenyl rings and the sodium centers, the potassium analog displays a dimeric structure based on π-interactions between the alkali metal and the ligand. The propensity for π-bonding provides a rationale for the formation of separated ions as observed in NMR studies of hypersilanides. The isolation of the benzene solvate $[(Me_3Si)_3SiK(C_6H_6)_3]$ **175** (Figure 16)[184] further underscores the propensity for heavy alkali metal–aryl interactions.

All alkali metal hypersilanides display highly pyramidal central silicon centers with Si–Si–Si angles around 100°. Remarkably, these angles do not differ in the contact or separated ion pairs, further indicating the large degree of charge transfer from the alkali metal cation to the silanide anion. The pyramidalization is also an expression of the increased *p*-character of the Si–Si bond, and consequent increase in the alkali metal–silicon bond.

The tris(trimethylsilyl)silyl ligands can be easily modified by reactions with silyl chlorides, as shown with a series of phenylated species $Me_{3-n}Ph_nSiCl$ ($n = 0$–3).[188] Furthermore, triisopropyl, thexyldimethylsilyl, [189] or *tert*-butyldimethylsilyl substitution are all easily possible.[190] The crystallographic characterization of some of the alkali metal derivatives indicates a direct correlation between ligand size and resulting structural parameters.

The chemistry of the supersilyl $Si(^tBu)_3$ ligands was established about 20 years ago with the report of a straightforward ligand synthesis.[191] Since then, several examples of alkali metal derivatives have been disseminated, including a series of supersilyl derivatives $[(^tBu)_3SiM]$ (M = Na, K, Rb, Cs), prepared by treating silyl halides with the appropriate alkali metals.[192] The supersilyl derivatives exist in a number of structural motifs depending on the presence of donor molecules during the preparation and the solvent of crystallization, as shown for the contact molecules $[(^tBu)_3SiNa(THF)_2]$ **176** or $[(^tBu)_3SiNa(PMDTA)]$ **177** (Figure 17).[192] Underscoring the high affinity of potassium

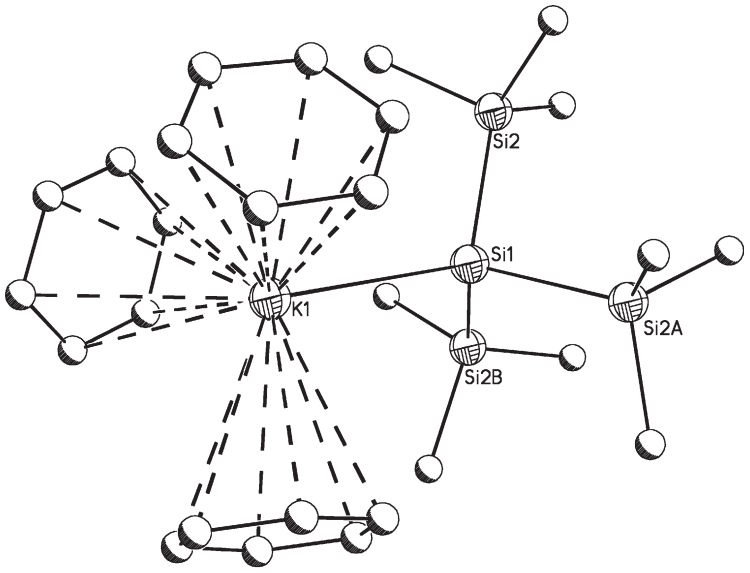

175

Figure 16 The structure of $[(Me_3Si)_3SiK(C_6H_6)_3]$ **175**. Hydrogen atoms have been omitted for clarity.

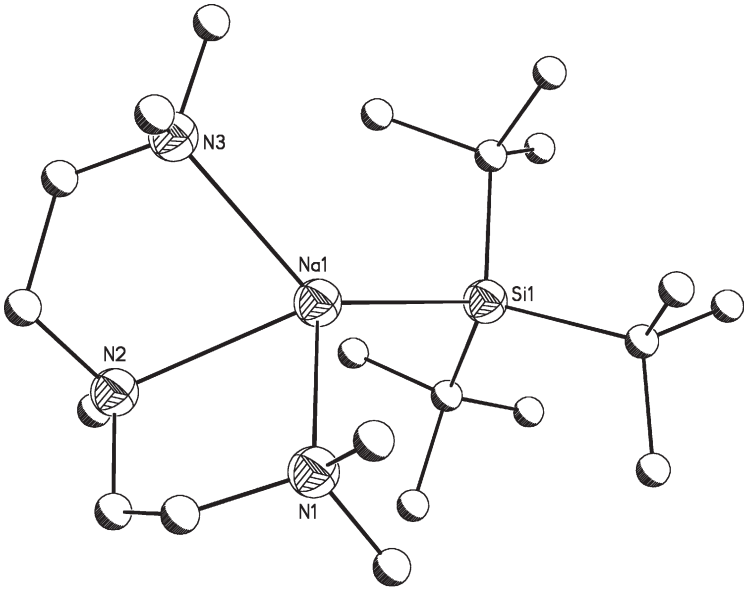

177

Figure 17 The structure of $[^tBu_3SiNa(PMDTA)]$ **177**. Hydrogen atoms have been omitted for clarity.

toward aromatic solvents, crystallization of the lithium and sodium derivatives in hydrocarbon solvents affords a dimeric species, whereas crystallization of the potassium derivative from benzene yields $[(^tBu)_3SiK(C_6H_6)_3]$ **178**. Simple ethers may be exchanged by stronger donors such as PMDTA, crown ether, or cryptand-2,2,2.[192]

It is instructive to compare the geometry of the supersilyl with the hypersilyl ligands. The geometry at the supersilyl ligands is clearly less pyramidal with C–Si–C angles frequently in the range of 106–107°. In contrast,

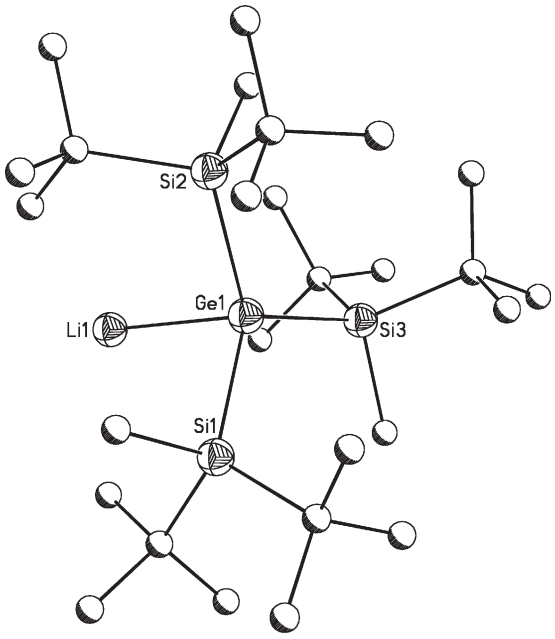

180

Figure 18 The structure of $[(^tBu_2Me)_3GeLi]$ **180**. Hydrogen atoms have been omitted for clarity.

Si–Si–Si angles in the hypersilanides range around 100°, an expression of reduced ligand bulk due to the longer Si–Si as compared to the Si–C bonds. However, not all silanides display a pyramidal environment at the central silicon atom, as shown with a donor-free silyl and germyllithium derivative $[(^tBu_2Me)_3ELi]$ (E = Si **179**, Ge **180** (Figure 18)).[193] In contrast to the above results, the environment at the central silicon atom is trigonal planar with Si–Si–Si angles close to 120°. The planar geometry at silicon and germanium is made possible by secondary metal–ligand interactions in the form of CH–Li agostic interactions.

The degree of pyramidicity of alkali metal derivatives bearing heavy group 14 ligands increases on descending group 14, as evident upon comparing triphenyl silanides, germanides, stannides, and plumbides. The C–E–C angles in the compounds compress smoothly with 101.3°(avg.) for $[Ph_3SiLi(THF)_3]$ **181**,[194] 98.3°(avg.) for $[Ph_3GeLi(OEt_2)_3]$ **182**,[195] 96.1° (avg.) for $[Ph_3SnLi(PMDTA)]$ **183** [196], and 94.3° (avg.) for $[Ph_3PbLi(PMDTA)]$ **184**.[197]

The silole and germole anions have been a topic of interest for quite some time, with initial theoretical studies of the silole anion dating back to 1983.[198] The following narrative provides a brief glimpse into this area.

In 1993, Boudjouk proposed the aromaticity of these systems based on NMR data.[199] Since then, several studies have been attempted to provide detailed insights into the bonding in these systems. Interestingly, localized and delocalized systems have since been prepared, including the lithium salt of the germole anion $[(MeC)_4GeSi(SiMe_3)_3]^-$ **185** as a highly localized structure with significant variations in C–C ring bond lengths.[200,200a] Further investigations provided the dilithium salt of the tetraphenylgermole anion, which was crystallized from dioxane. Depending on the temperature, two different compound modifications are observed. Crystals obtained at −20 °C display a reverse sandwich structure with two lithium atoms above and below the five-membered ring **186**. In contrast, in crystals obtained at 25 °C, one of the lithium atoms is coordinated η^1 to the ring system while the other coordinates in an η^5-fashion to the five-membered ring **187**. In both compounds the electrons in the ring are highly delocalized with nearly equal C–C bond lengths.[201] The structure of the product crystallized at room temperature is closely related to the silicon analog $[(PhC)_4SiLi_2]\cdot 5THF$ **188**, which also contains η^1- and η^5-coordinated lithium centers, with nearly identical C–C bond lengths.[202] Theoretical investigations showed only a small aromatic stabilization energy of 5.3 kcal mol^{-1} for the compound reported by Tilley *et al.*, while theoretical studies for a hypothetical $[H_4C_4Ge]^{2-}$ anion indicate the high likelihood for identical C–C distances with an aromatic stabilization energy of 13.0 kcal mol^{-1}.[201] These studies also indicate the η^5-coordination as energetically preferred over the η^1-coordination by 25 kcal mol^{-1}. Further theoretical work by Schleyer *et al.* also indicates that the free silole dianion would be highly aromatic and form dilithium, sodium, and potassium with the metals bound to both sides of the ring.[203]

Several closely related systems have since been described, with more recent examples of dilithio and disodio salts of aromatic benzannulated silole **189**[204] and germole dianion **190**.[205] In analogy to some of the compounds mentioned above, the X-ray structure of the lithiumsilole shows two differently coordinated lithium atoms, one η^1, also coordinated to three dioxane molecules, while the other is η^5 with coordination to two dioxane molecules. The dilithium salt of the germole dianion displays η^5-bonding to the lithium centers, and nearly equal C–C bond lengths suggest a significant degree of aromaticity. Demonstrating the timeliness of this work, a recent example includes 1,2-disila-3-germacyclopentadienide, **191**, a 6π aromatic system, where lithium is situated in an η^5-fashion above the five-membered system.[206]

Over the last few years, structural data on rare examples of dilithiosilanides and germanides have been reported. This group of compounds has not received extensive attention due to synthetic difficulties. Dialkali metal derivatives were initially reported only for siloles and germoles as mentioned above. Lagow *et al*. reported the generation of the 1,1-dilithio derivative 2,2-dilithio-1,1,13,3,3-hexamethyltrisilane **192** by pyrolysis of $[(Me_3Si)_3SiLi(THF)_n]$ at 140–150 °C in low yields.[207] Other attempts included the preparation of the bulky aryl substituted [(Dipp)TbtSiLi$_2$] **193** (Dipp = 2,6–^{i}Pr$_2$C$_6$H$_3$; Tbt = 2,4,6-tris[bis(trimethylsilyl)methyl]phenyl); however, no structural or spectroscopic data have been reported.[208] $[(^iPr_3Si)_3Li(THF)_2]$ **194** has a monomeric structure, with each lithium coordinated to two THF donors and the central silicon.[209] The central silicon has nearly tetrahedral geometry with somewhat expanded bond angles (112–114°) due to the bulkiness of the two ligands. Recently, the same group has reported on two dilithiogermanes, the first of their class.[209] The two compounds bear the sterically demanding bis(triisopropylsilyl) **195** or the bis(di-*tert*-butyl(methyl)silyl) ligands **196**. The crystal structure of the bis(di-*tert*-butyl(methyl)silyl)dilithiogermane was determined to reveal dimeric molecules. Containing a central Ge_2Li_2 ring, each germanium is bound to three lithiums, two bridging and one terminal. Each of the lithium atoms (bridging and terminal) is bound to a THF donor.

2.01.3.2 Alkali Metal Germanides

Despite a significant number of reports on the synthesis of germyl anions[210], relatively little is known about the structural chemistry of alkali metal germanides; among those, the tri(trimethylsilyl) germanide ligand ($[Ge(SiMe_3)_3]^-$ ligand) is most prominent. A rare example of a lithium germanide with a different ligand system is $[Ph_3GeLi(OEt_2)_2]$ **182**.[195]

While the parent compound for $[Ge(SiMe_3)_3]^-$, $Ge(SiMe_3)_4$ was reported decades ago,[212,212a] metal derivatives remain scarce and examples are mainly limited to a few lithium derivatives. Examples include $[Ge(SiMe_3)_3Li(THF)_3]$ **197**, $[(Me_3Si)_3GeLi(PMDTA)]$ **198**,[213] and $[Li(12\text{-crown-}4)_2][Ge(SiMe_3)_3]$ **199**.[214] Germanides involving the heavier alkali metals had been limited to $[Ge(SiMe_3)_3Cs]_2$ **200**,[185] until very recently, when two studies provided detailed information on the structural chemistry of the heavy alkali metal germanides.

The combination of heavy tris(trimethyl)silylgermanides with crown ethers or multidentate donors afforded families of contact molecules and separated ions.[215] Examples include the contact molecules $[(Me_3Si)_3GeK(18\text{-crown-}6)]$ **201**, $[(Me_3Si)_3GeRb(18\text{-crown-}6)]$ **202**, and $[(Me_3Si)_3GeK(TMEDA)_2]$ **203**. The list of separated ions includes $[K(15\text{-crown-}5)_2][Ge(SiMe_3)_3]$ **204**, $[K(12\text{-crown-}4)_2][Ge(SiMe_3)_3]$ **205**, and $[Cs(18\text{-crown-}6)_2][Ge(SiMe_3)_3]$ **206** (Figure 19). In analogy to the silanide structural chemistry reported above, contact molecules are obtained if the crown cavity and cation diameter match, as is the case for 18-crown-6 and potassium or rubidium. Separated ions are observed if the crown is too small to fully encapsulate the metal center. In these cases, the metal will coordinate to two crown ether macrocycles under the formation of sandwich complexes. The drive toward cation coordinative saturation is so strong that the formation of sandwich complexes is also observed if only 1 equiv. of crown ether is present. The separated ions resulting from this arrangement are observed for a potassium cation coordinated to two 15-crown-5 or 12-crown-4 macrocycles, as well as the coordination of cesium to two 18-crown-6 donors.

In the presence of multidentate nitrogen donors (TMEDA, PMDTA), essentially analogous trends as seen for the silanides are observed, and again the ability of a donor to sterically saturate a metal center is key. The degree of cation steric saturation is also the main determining factor in regard to reactivity. Rather than observing increased reactivity on descending the group of alkali metals as one may expect, the coordinative saturation of the alkali metal is essential. As such, it comes as no surprise that the five-coordinate $[(Me_3Si)_3GeK(TMEDA)_2]$ **203** is significantly more reactive than the related crown ether complexes, while the THF adducts are too reactive to be isolated and fully characterized.

The comparison of metal–ligand bond lengths in the closely related silanides[187] and germanides[215] reveals shorter M–Ge bond lengths than M–Si, despite the "larger" ionic radius for germanium. As an example, [(Me$_3$Si)$_3$Ge K (18-crown-6)] **201** displays K–Ge distance of 3.399(8) Å with the corresponding K–Si distances in **168**, 3.447(8) Å.[186] This initially curious result, considering the larger germanium radius (ionic radius Ge^{4+} (CN = 4) = 0.53 Å; Si^{4+}

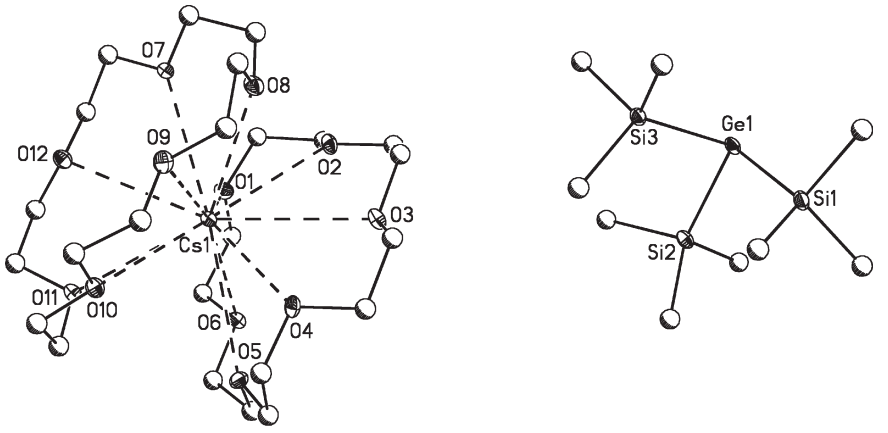

206

Figure 19 The structure of $[Cs(18\text{-crown-}6)_2][Ge(SiMe_3)_3]$ **206**. Hydrogen atoms have been omitted for clarity.

(CN = 4) = 0.40 Å)[216] may be explained by the increased polarity in the metal–germanium bond due to larger differences in electronegativity (Allred Rochow electronegativity Si = 1.74, Ge = 2.02).[217]

Similar trends are observed for other members of the series, such as lithium silanides and germanides where consistently shorter Li–Ge bonds than Li–Si are observed.[213] Similarly, heavy alkaline earth metal silanides and germanides display the same trend – slightly shorter M–Ge bonds than M–Si distances.[218–220]

The geometry in the $[Ge(SiMe_3)_3]^-$ anions is very consistent, with Ge–Si bond lengths ranging from 2.34 to 2.40 Å and significant pyramidal geometry with the Si–Ge–Si angles of about 100°. These values are very similar to those of the hypersilanides, further underscoring the close chemical relationship between silicon and germanium. The pyramidicity of the Si compounds has been discussed above and similar arguments may be applied to the heavier congeners. With very similar geometries for contact molecules and separated ions, the charge transfer between cation and anion must be substantial in all cases, supporting the view that the metal–ligand bond is highly polar. This view is further supported by spectroscopic studies where the formation of separated ions is observed upon dissolution in D_6-benzene, again in complete agreement with the silicon analogs.

A group of oligosilyl potassium germanide derivatives has recently been reported.[221] The geometry at the alkali metal closely resembles those reported by Teng *et al.* where crown ethers were used to stabilize the metal center. With the structural characterization of two dianions, $[\{(Me_3Si)_2(Me_2Si)_2Ge\}_2\{K(18\text{-crown-}6)\}_2]$ **207** and $[\{(Me_3Si)_2\}_2Ge\{K(18\text{-crown-}6)\}_2]$ **208**, Fischer *et al.* confirmed that the coordination of 18-crown-6 to potassium tends to produce contact molecules.[221] Geometrical data for the germanides bound to the alkali metals are very similar to those reported above, with a distinctly pyramidal character and angles of about 100°.

A recent addition to the structural variety of alkali metal germanides is a trimeric, donor-free $[(Me_3Si)_3GeLi]_3$ **209**.[222] This trimeric molecule is the first such example among all structurally characterized heavy group 14 element-centered anionic species. The molecule displays an equilateral triangle with Li···Li distances of 3.3 Å, which is somewhat longer than in trimeric aryllithiums (2.96–3.17 Å).[223,223a,223b] The planar Li_3Ge_3 core displays formally two-coordinate Li centers with several additional CH_3···Li interactions. The geometry of germanium is a distorted trigonal bipyramid.

2.01.3.3 Alkali Metal Stannides

Alkali metal stannides date back to 1922 with the preparation of $[Me_3SnNa]$ **210** by the reduction of Me_3SnBr with sodium in liquid ammonia.[224] Since then, the alkali metal stannides $[R_3SnM]$ have been used extensively in organic chemistry, most prominently in Sn element coupling reactions.[13] Almost exclusively, the reagents have been used *in situ* with little or no information on their structural chemistry. This is now changing with an increasing number of well-characterized alkali metal stannides. A review article summarizing the chemistry of heavy group 14 ligands appeared in 1995.[225,225a]

Examples of alkali metal stannides are mainly limited to tris(trimethylsilyl)- and triphenylstannides. NMR studies of trimethyl- and tributylstannide in ether, THF, and hexamethylphosphoramide (HMPA, $OP(NMe_2)_3$) reveal the compounds to be monomeric in solution, as indicated by the large Li–Sn coupling. The addition of HMPA produces an

unusual dimeric structure $[Bu_3SnLi(HMPA)_3]_2$ **211**, in which each tin is coordinated by one lithium, and the two lithiums are bridged by three molecules of HMPA. In ether and THF solutions, the addition of more than 2 equiv. of HMPA affords separated ions.[226] The facile formation of separated ions in polar solvents was already mentioned in 1987.[227]

Structural data on lithium triphenylstannides were first disseminated in 1991 with $[Ph_3SnLi(PMDTA)]$ **183**.[228] Another example involving the triphenylstannide anion is the monomeric $[Ph_3SnK(18\text{-crown-}6)]$ **212**.[229] Both compounds display pyramidal geometries at Sn, with a C–Sn–C angle of 96.1° for the lithium species, and with almost similar values for the potassium compound (sum of angles at Sn: 290.3°). An unusual variation of triphenylstannide is obtained when one phenyl group is replaced by a very bulky terphenyl ligand.[230] The donor-free dimer $[(2,6\text{-}Trip_2C_6H_3)Ph_2SnLi]_2$ **213** has a symmetrical structure without a Sn–Sn bond, and is associated through Li–aryl interactions.

Triphenylstannide anions are also observed as separated ions, a common occurrence as the alkali metal group 14 bond strength decreases upon descending group 14. Competition between solvation by strong donors such as HMPA or multidentate donors such as PMDTA and ligation often results in the separation of cation and anion, illustrating the polarity of the alkali metal group 14 element bond. Examples include $[Li_2(HMPA)_5]^{2+}$ $[SnPh_3]_2$ **214**,[231] as well as $[Li(TMEDA)_2][SnPh_3]$ **215**.[232] The facile formation of separated ions further underscores the high polar character of the alkali metal–Sn bond.

Several examples of alkali metal stannides carrying the $Sn(SiMe_3)_3$ ligand have been reported, including $[(Me_3Si)_3SnLi(THF)_3]$ **216**, published in 1999.[233] The closely related TMEDA adduct $[(Me_3Si)_3SnLi(TMEDA)_2]$ **217** was mentioned in an overview article.[225a] An unusual dimeric stannyllithium derivative, $[\{(Me_3Si)_3Sn\}_2(\mu\text{-}Li(THF))(\mu\text{-}Li)]$ **218**, with one solvated and one donor-free lithium has recently been disseminated.[222] The central Sn_2Li_2 ring is bent with a dihedral angle of 21° between the Sn1–Li(1)–Li(2) and Sn(2)–Li(1)–Li(2) planes. Angles within the ring are quite narrow with 57° and 58° for Sn(1) and Sn(2). In analogy with geometrical values in the monomeric complexes, the environment at Sn is quite pyramidal with angles of about 303°. It is important to note that the coordination environment on the non-solvated lithium is completed through several Li···CH_3 interactions. Other examples involving the tris(trimethylsilyl)stannane ligand are the recent $[(Me_3Si)_3SnLi(12\text{-crown-}4)]$ **219**, $[(Me_3Si)_3SnM(18\text{-crown-}6)]$, (M = Na **220**, K **221**, Rb **222**, Cs **223**), as well as $[(Me_3Si)_3SnCs(2,2,2\text{-crypt})]$ **224**. However, structural data are only available for the sodium derivative **220**,[234] which can be compared to the previous $[(Me_3Si)_3SnNa(\eta^6\text{-}C_6H_5CH_3)]$ **225**.[184]

In analogy to the corresponding silanides $Si(SiMe_3)_3^-$ and germanides $Ge(SiMe_3)_3^-$, the lithium and sodium stannides display either separated ion pairs or almost exclusively monomeric contact molecules as a result of the sterically demanding ligand and the coordination of either 3 THF or a TMEDA to lithium, or one crown ether to the larger alkali metal centers. The presence of 18-crown-6 in conjunction with sodium or potassium supports the formation of a monomeric contact molecule. For the heavier alkali metal, structural predictions are less straightforward as the larger metal centers are situated above the plane of the 18-crown-6 cavity. As such, for the rubidium and cesium derivatives, sandwich-type complexes $[M(18\text{-crown-}6)_2][E(SiMe_3)_3]$ (M = Rb, Cs; E = Si, Ge) with separated ions may be observed, but this assumption will need to be verified experimentally.

Other alkali metal stannides include the toluene-solvated potassium derivative $[(CH_2{}^tBu)_3SnK(\eta^6\text{-}C_6H_5Me)_3]$ **226**.[235] This compound displays contact molecules with pronounced pyramidicity as expressed by average C–Sn–C angles of 91.7°. Structural data also exist for the tripodal triamido $[\{(4\text{-}MeC_6H_4)NSiMe_2\}_3CHSnLi(THF)_3]$ **227**,[236] the cyclosiloxy derivative $[(OSiPh_2O)_2Cl_2Sn\mu\text{-}Li(THF)_2]$ **228**,[237] as well as a 1,2-oxastannetanide as an intermediate in the tin-Peterson reaction, in the form of separated ion pairs $[K(18\text{-crown-}6)(H_2O)_n][SnPh_2\{OC(CF_3)_2SPh\}]$ **229**.[238]

Several tri(cyclopentadienyl)tin(II) and lead(II) complexes have been prepared with alkali metal cations. The arrangement of Cp rings around the metal is in a paddle wheel configuration; the alkali cation is bound to Cp and not Sn or Pb, further supporting the view of a weak alkali metal group 14 bond. Representative examples of these compounds include $(\eta^5\text{-Cp})_2E(\mu\text{-Cp})\text{-Na(PMDTA)}$ (E = Sn **230**, Pb **231**).[239,240]

2.01.3.4 Alkali Metal Group 14 Zintl Clusters

Numerous alkali metal cations with heavy group 14 anions have been observed as Zintl phases in the form of homoatomic clusters.[241,241a] The following is a brief glimpse of this emerging area of Zintl chemistry. Among the homoatomic clusters involving group 14 anions, the E_9M_4 (M = alkali metal; E = Si, Ge, Sn, Pb) clusters are most prominent; selected examples include $Ge_{17}K_{12}$ **232**,[242] $Si_{17}Rb_{12}$ **233**,[243] Ge_9M_4 (M = K **234**, Cs **235**),[244,244a] as well as Pb_9K_4 **236**.[245] The listing of the 17:12 clusters as examples for E_9M_4 geometry is not a mistake, since E_9M_4 clusters coordinate with additional E_4^{4-} units.

Use of sequestering agents such as crown ethers or cryptands to dissolve the alkali metals led to the isolation of a larger variety of discrete E_n clusters, an example being Ge_9^{2-} **237**.[246,246a–246c] Other selected examples include [2,2,2-crypt-K]$_3$[KSn$_9$] **238**,[247] the dicationic [Ge$_9$enK(18-crown-6)$_2$] **239**,[248] or the tin analogs [K(18-crown-6)]$_3$[KSn$_9$(en)] **240** and [Sn$_9$[K(18-crown-6)]$_4$] **241**.[249] In all species, alkali metal group 14 contacts are present.

2.01.3.5 Anionic Group 14 Element Alkyne Derivatives

Stable group 14 alkyne derivatives may be reduced by alkali metals to form singly and doubly reduced congeners $[ArEEAr]^-$ and $[ArEEAr]^{2-}$ (E = Ge, Sn, Pb; Ar, Ar* = terphenyl).[250,250a,250b] Prepared by the reduction of a terphenyl halide Ar*ECl (E = Ge, Sn) with an alkali metal, several species with alkali metal group 14 contacts have been isolated, including [Ar′GeGeAr′K] **241**, [Ar′GeGeArLi] **242**, [K(THF)$_6$][Ar′SnSnAr′] **243**, and [Ar′SnSnAr′K$_2$] **244** (Ar′ = C$_6$H$_3$-2,6-Dipp$_2$).[251] In many of these compounds the alkali metal cations are complexed by the π-cloud of the arene rings, providing η^6-metal–arene coordination. In several instances, interactions between the group 14 elements and the alkali metals are evident as well, as seen in [{Ge(2,6Trip$_2$C$_6$H$_3$)$_2$}$_2$K$_2$] **245** and [{Sn(2,6Trip$_2$C$_6$H$_3$)$_2$}$_2$K$_2$] **246**.[252] Here, the alkali metals are π-coordinated to the aryl rings, while displaying Na–Ge contacts of 3.1 Å and K–Sn bonds of 3.6 Å. The alkali metal group 14 element contacts are rather weak, since the contacts are longer than the predicted single bond distance for Na–Ge (2.86 Å) or the Na–Ge distance in [Na(15-crown-5)][C$_4$Me$_4$GeMes] **247**, (3.0 Å).[253] In a similar manner, K–Sn bonds (3.579(2) and 3.591(2) Å) are slightly longer than those previously determined. The sum of covalent radii is 3.36 Å, and the K–Sn bond length in [(CH$_2$^{t}Bu)$_3$SnK(η^6C$_6$H$_5$CH$_3$)$_3$] **226** is observed at 3.548(3) Å.[236] Other examples of alkali metal group 14 contacts in this group of compounds include [Ar*GeGeAr*Na$_2$] **247** or [Ar*SnSnAr*K$_2$] **248** (Ar* = 2,6DippC$_6$H$_3$).[251] Alkali metal group 14 bonds are also observed in a singly reduced compound [(2,6Trip$_2$)$_2$C$_6$H$_3$Na(THF)$_3$] **249**, obtained by the reduction of Sn(Cl)(2,6Trip$_2$)$_2$C$_6$H$_3$ with sodium and anthracene in THF.[254] The compound crystallizes as a CIP with an Na–Sn distance of 3.240(7) Å. This value is considerably longer than that in (η^6C$_6$H$_5$CH$_3$)NaSn(SiMe$_3$)$_3$ **226** (3.070(5) Å[184] or [(Me$_3$Si)$_3$SnNa(15-crown-5)] (3.075(2) Å) **220**.[234]

2.01.3.6 Alkali Metal Plumbides

As discussed above, the strength of the alkali metal group 14 bond decreases as descending group of alkali metals and 14, as such; only a small number of compounds displaying alkali metal lead bonds are known, with first structural data appearing in 1992 with [Ph$_3$PbLi(PMDTA)], **184**.[197] As discussed above, the lead center is highly pyramidal, with narrow C–Pb–C angles. This compound is stable for only about 12 h, upon which it decomposes. This observation may explain the scarcity of other compounds in this group, another example being [Pb(2-Py)$_3$Li(THF)] **250**.[255] The increased stability of the pyridyl compound may be due to its cage structure resulting in a symmetrical coordination of the lithium center by the pyridyl N-centers of the $[Pb(2\text{-}Py)_3]^-$ ligand.

2.01.4 Group 15 Alkali Metal Bonded Complexes

2.01.4.1 N–M Bonded Complexes

One of the most intensively studied classes of alkali metal complexes are the N-bonded species. In particular, the utility of secondary amidolithium compounds (R^1R^2NLi) as selective Brönsted bases in organic synthesis has led to detailed investigations regarding their reaction and aggregation behavior.[256,257] The structures adopted by secondary amidolithium complexes, and also by iminolithium complexes ($R^1R^2C{=}NLi$), were reviewed in detail by Beswick and Wright in COMC (1995).[7] These complexes also played an important role in the development of the now well-established ring-laddering and ring-stacking principles in alkali metal structural chemistry.[258,258a,258b] (For early reviews on ring-laddering and ring-stacking, see Refs: 259 and 259a.) These concepts remain central in rationalizing the aggregation patterns of various alkali metal complexes and updated reviews by both Mulvey and Chivers are available.[260,261] Indeed, these ideas have also been successfully applied to classify the solid-state structures adopted by other main group complexes and even organic ammonium halides.[262,262a] Over the last decade many enlightening contributions have been made through the application of NMR spectroscopic techniques to determine the behavior of alkali metal N-bonded complexes in solution. Of particular note to ring laddering is a study of lithium diethylamide solvated by oxetane, THF or Et$_2$O, which revealed that four-, five-, and six-rung ladders, as well as the more commonly encountered cyclic dimers and

trimers, exist in solution.[263] Collum has reviewed the use of ^{6}Li–^{15}N double labeling NMR studies to determine the solution structures of lithium amides,[264] and a detailed account of the solvation of lithium hexamethyldisilazide (LHMDS) is also available.[265]

Since the COMC (1995) review, there have been significant developments in the characterization of a broad range of N–M bonded complexes. One of the highlights in this area has been the synthesis and structural studies of metallated ligands composed of imido (NR) units that are bonded to a central *p*-block element. Separate articles by Chivers and Russell review the imido analogs of the widely studied isoelectronic oxo anions.[266,267] Wright has also reviewed an emerging class of nitrogen-containing inorganic macrocycles, many of which contain alkali metal counteractions, and Stalke published an article specific to sulfur polyimido anions.[268, 269] The chemistry of imino-aza-P(v) species has been reviewed by Steiner, and an article by Gade detailing tripodal triamidometallates has been published.[270,271] Lappert has also contributed an extensive review covering the coordination chemistry of the popular β-diketiminate ligands.[272] Pauer and Power have written an extensive article on lithium complexes of the main group elements excluding carbon.[6] This section of the present review will concentrate on the characterization, primarily in the solid state, of specific classes of N-bonded alkali metal complexes that have been significantly developed since 1993 and which have not been reviewed in detail elsewhere. Specifically, the chemistry of primary amides [RN(H)M], hydrazides [$R^1(R^2)N$–$N(R^3)M$], and five-membered anionic heterocycles containing at least one N–N unit (pyrazolates, triazolates, and tetrazolates) will be detailed as representative classes of ligands that have received attention. This section of the review will be restricted mainly to homometallic, homoleptic complexes in order to illustrate any emerging trends.

2.01.4.1.1 Primary amide complexes

Only a handful of structural reports of primary amidolithium complexes were available prior to 1993. Their investigation as an independent class of ligands was undoubtedly overshadowed by their secondary amidolithium counterparts. However, primary amidolithium compounds have found use in polymerizations,[273] epoxide cleavages,[274] metallations,[275] and in asymmetric organic synthesis.[276,276a,276b] In turn, this interest has led to the coordination chemistry of these species being studied in more detail. The early characterizations of monomeric [2,4,6-$^{t}Bu_3C_6H_2N(H)Li$ (TMEDA)] **251** and N(H)-bridged dimeric [2,4,6-$^{t}Bu_3C_6H_2N(H)Li(OEt_2)]_2$ **252** did not suggest any unusual aggregation chemistry for this class of ligand.[277,278] However, as detailed in Table 1, the structural characterization of primary amidolithium complexes has revealed an unexpected degree of complexity.

This can be demonstrated on comparing the structures formed by various solvated forms of lithium anilide, [PhN(H)Li·L_n]. As shown in Scheme 2, lithium anilide has been characterized in dimeric, trimeric, tetrameric, pentameric (as part of a polymer), and hexameric forms. This remarkable set of compounds displays several unexpected structural aspects. First, as is commonly encountered for *s*-block complexes, altering the amount of Lewis base present can dramatically affect the structure adopted. The dimeric complex **261** was prepared by lithiating aniline in neat THF, whereas the highly unusual distorted hexameric ladder complex **271** crystallizes from hexane solutions of lithium anilide on the addition of 1.5 molar equiv. of THF.[286,294] The positions adopted by the neutral Lewis bases are also of note in **267** and **271**, where the ligands bridge between a pair of metal centers.[283,294] This type of bridging is also seen in polymeric complex **273**.[296] Application of the tridentate donor PMDTA (2 molar equiv.) results in the formation of trimer **264**, instead of a tetracoordinate monomer as may have been expected.[288] Another unusual aspect of trimer **264** is that three-, four-, and five-coordinate lithium centers coexist in a single aggregate. All of these anilide complexes retain Li_2N_2 ring cores as components of their structures.

A significant development in general for lithium amide structural chemistry came with the characterization of the ladder polymers **273**, **274**, and **275**.[296–298] It has been long assumed that many insoluble secondary amides, as well as many other classes of ligands, adopt infinite ladders, and the structural elucidation of these primary amidolithium derivatives supports this view.[259,259a] In these instances, solubility is achieved either through the use of a chelating group on the ligand backbone or alternatively through the use of a weak Lewis base that is unable to deaggregate the polymer on crystallization.

Interestingly, in addition to the ladder-type structures, which can be considered comparable to their secondary amide counterparts, primary amidolithium complexes have also been found to adopt tetrameric cubane **266**,[290] prismatic hexameric **270**,[293] and also prismatic octameric **272**[295] structures in the solid state. Such prismatic structures are unusual for sterically demanding secondary amidolithium complexes but are commonly encountered for lithium alkoxides and alkyllithium complexes.[259,259a] ^{13}C, ^{6}Li, and ^{15}N solution NMR spectroscopic studies of the primary amidolithium compounds $^{t}BuN(H)Li$ and $Me_2NCH_2CH_2N(H)Li$ confirm the presence of prismatic structures in solution, although their exact identity has not been fully established.[299] Solid-state, solution NMR spectroscopic and computational studies have also been conducted on the competitive lithiation of primary and secondary amine mixtures.[293,300] Generally, addition of a simple monoalkylamine such as $^{t}BuNH_2$ to a sterically encumbered

Table 1 Crystallographically characterized primary amidolithium compounds

Compound	*Structure*	*References*
[2,4,6-$^{t}Bu_3C_6H_2N(H)Li(TMEDA)$] **251**	Monomer	277
[2,4,6-$^{t}Bu_3C_6H_2N(H)Li(OEt_2)]_2$ **252**	Li_2N_2 ring dimer	278
[2-Me_2As-$C_6H_4N(H)Li(THF)_2]_2$ **253**	Li_2N_2 ring dimer	279
[{$^{i}Pr(Me_3Si)N\}_2Si(F)OSi^{t}Bu_2N(H)Li]_2$ **254**	Li_2N_2 ring dimer	280
[(2,4,6-Me_3-$C_6H_2)_2BN(H)Li(OEt_2)]_2$ **255**	Li_2N_2 ring dimer	281
[$^{t}Bu_2(F)SiN(H)Li(TMEDA)]_2$ **256**	Li_2N_2 ring dimer	282
[PhN(H)Li(Pyr)$_2]_2$ **257**	Li_2N_2 ring dimer	283
[PhN(H)Li(4-Me-$C_5H_4N)_2]_2$ **258**	Li_2N_2 ring dimer	283
[$EtCH_2C(H)$═$C(^{t}Bu)N(H)Li(HMPA)]_2$ **259**	Li_2N_2 ring dimer	284
[1-LiN(H)-3-(2-Me-C_6H_4)-isoquinoline(HTriMEDA)$]_2$ **260**	Li_2N_2 ring dimer	285
[PhN(H)Li(THF)$_2]_2$ **261**	Li_2N_2 ring dimer	286
[$C_6F_5N(H)Li(THF)_2]_2$ **262**	Li_2N_2 ring dimer	286
[NCC(H)═C(Me)N(H)Li(Pyr)$_2]_2$ **263**	Li_2N_2 ring dimer	287
[{PhN(H)Li}$_3$(PMEDTA)$_2$] **264**	Distorted trimer	288
[$(Me_2N)_3SiN(H)Li]_4$ **265**	Tetrameric ladder	289,289a
[$^{t}Bu_2(Me)SiN(H)Li]_4$ **266**	Tetrameric cubane	290
[{PhN(H)Li}$_4$(4-^{t}Bu-pyr)$_6$] **267**	Distorted tetrameric ladder	283
[(8-quinolylamidoLi)$_4(OEt_2)_2$] **268**	Tetrameric ladder	291
[(PhN(H)Li)$_5$(DMP)$_2]_\infty$ **269**	Pentameric distorted ladder	292
[$Me_2NCH_2C(Me)_2CH_2N(H)Li]_6$ **270**	Prismatic hexamer	293
[{PhN(H)Li}$_6$(THF)$_8$] **271**	Distorted ladder	294
[$^{t}BuN(H)Li]_8$ **272**	Prismatic octamer	295
[{$PhCH_2N(H)Li\}_2(THF)]_\infty$ **273**	Distorted ladder polymer	296
[$PhCH_2N(H)Li{\cdot}N(H)_2CH_2Ph]_\infty$ **274**	Ladder polymer	297
[$H_2NCH_2CH_2N(H)Li]_\infty$ **275**	Ladder polymer	298

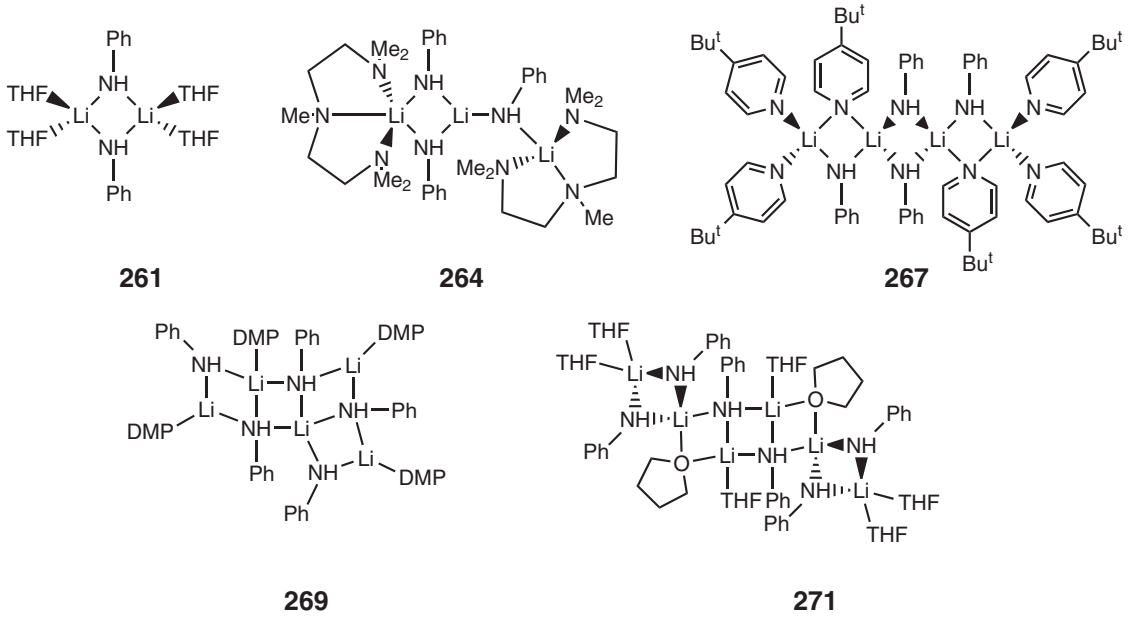

Scheme 2 Aggregated forms of variously solvated lithium anilides.

dialkylamidolithium such as $^{i}Pr_2NLi$ results in transamination. The key element in this process is the ability of the primary amide to form prismatic aggregates, which increases the local electron density at the metal centers and is therefore preferred on electrostatic grounds. In addition, examples of primary amines acting as Lewis bases to secondary amidolithiums have been characterized, as have mixed anion aggregates containing both lithiated primary and secondary amides.[293] More specifically, monoalkylamines tend to solvate the relatively weak base $(Me_3Si)_2NLi$

rather than undergoing transamination. However, addition of a chelating primary amine such as $Me_2NCH_2CH_2NH_2$ to $(Me_3Si)_2NLi$ results in the establishment of a highly complex series of solvates and mixed anion aggregates, demonstrating the importance of the chelate effect.[301]

Overall, the ability of primary amidolithium complexes to form such a wide range of architectures can be considered as a consequence of the relatively small steric demands of the N(H) unit. These complexes therefore possess a combination of characteristics of secondary amidolithium complexes and the sterically less encumbered imidolithium species previously reviewed in COMC (1995).[7]

The geminally dilithiated primary amides, $[(ArNLi_2)_{10}(L)_n]$, where Ar = 1-$C_{10}H_7$, L = Et_2O, $n = 6$ **276**; Ar = C_6H_4-4-CPh_3, L = Et_2O, $n = 6$ **277**; and Ar = C_6H_4-4-Me, L = THF, $n = 10$ **278**, have been prepared by the direct metallation of the aromatic primary amines with 2 molar equiv. of BuLi in the appropriate donor solvent.[302,303] These three compounds possess isostructural $(Li_{14}N_{10})^{6-}$ cores, consisting of two fused rhombic dodecahedra (Figure 20). Molecular orbital calculations of these systems indicate that the donor solvent plays a critical role in the stabilization of the geminal dimetallated complexes. Direct dilithiation appears to be limited to aromatic amines due to their ability to delocalize the large charge buildup on the nitrogen center. However, dilithiated primary amides have been reported to be prepared via the transmetallation of distannylamines, $RN(SnMe_3)_2$, with 2 molar equiv. of an alkyllithium reagent.[304] The dilithiated amides can subsequently be converted into diborylamines or disilylamines, which are difficult to access by other means. A mixed anion cage aggregate that contains dilithiated biphenylamide, $[(2\text{-biphenyl-NLi}_2)_5(MeLi)_2(Et_2O)_5]$ **279**, has also been structurally characterized.[304]

Only a small number of heavier group 1 metal primary amides has been structurally characterized. Table 2 lists six compounds, three containing sodium and three containing cesium. The structures characterized contain the well-established M_2N_2 ring motif to build dimers **280** and **281**, a tetrameric cubane **282**, and polymers **283–285**. The

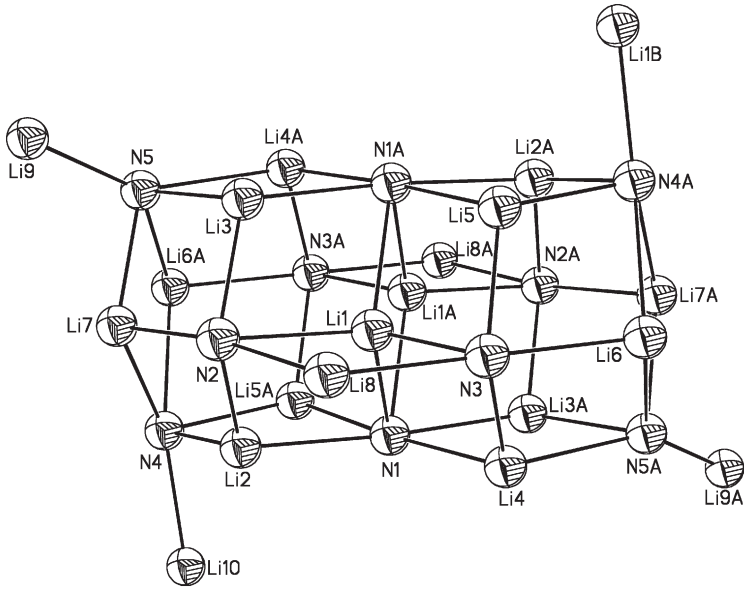

276

Figure 20 Core of the molecular structure of the dilithiated amide **276**.

Table 2 Crystallographically characterized heavy alkali metal primary amides

Compound	*Structure*	*References*
$[(2\text{-PhO-}C_6H_4)N(H)Na{\cdot}PMDTA]_2$ **280**	Na_2N_2 ring dimer	305
$[PhN(H)Na{\cdot}PMEDTA]_2$ **281**	Na_2N_2 ring dimer	288
$[Me_3SiN(H)Cs]_4$ **282**	Tetrameric cubane	306
$[\{^tBuN(H)Na\}_2N(H)^tBu]_\infty$ **283**	Polymeric ladder	307
$[\{2\text{-N(H)}C_5H_4N\}Cs(12\text{-crown-4})]_\infty$ **284**	Polymer of tetramers	308
$[\{(2\text{-N(H)}C_5H_4N)Cs\}_2(18\text{-crown-6})]_\infty$ **285**	Polymer of dimers	309

structural diversity found from this handful of complexes suggests that further studies will reveal rich coordination chemistry for primary amides of the heavier alkali metals.

2.01.4.1.2 Hydrazide complexes

Alkali metal hydrazides, $(R^1R^2NNR^3)M$, are useful intermediates in the preparation of a wide range of metal and non-metal hydrazides.[310,311,311a,311b] As expected, lithium hydrazides are the most intensely studied systems from group 1, and Table 3 lists the monolithiated hydrazides that have been structurally characterized. The most commonly used strategy for the synthesis of lithium hydrazides is by the deprotonation of the requisite hydrazine with an alkyllithium base. However, a complication for the hydrazides is that the attached functional group may migrate during the metallation (Scheme 3). (For early studies of anionic hydrazide rearrangements see Refs: 312 and 312a.) For example, the *N*,*N*′-dibenzylated hydrazide **291** was unexpectedly obtained during the deprotonation of the *N*,*N*-dibenzyl derivative.[317] An NMR study of this system suggests that both the *N*,*N*′- and *N*,*N*-dibenzylated species are present in solution but that interchange between them is slow after the metallation is complete. Reduction of the hydrazine unit may also occur upon metallation, resulting in fragmentation of the N–N backbone. This fragmentation process becomes more common upon dimetallation of hydrazines due to the increase in charge on the ligand backbone.

Overall, the structures adopted by these complexes are reminiscent of their secondary amidolithium counterparts but with some additional features due to the donor properties of the N–N linkage. A recurring motif in many of the structures in Table 3 is Li_2N_2 central rings formed between the anionic nitrogen centers and the metals. However, in some instances, the tertiary nitrogen is employed as a chelating group, resulting in side-on coordination of the hydrazide to the metal centers and formation of LiN_2 three-membered rings. It is noteworthy that this coordination mode was predicted in advance of the structural studies by computational methods.[324] The Li–N(dative) bond lengths are normally in the order of 0.1–0.2 Å longer than those to the anionic nitrogen. LiN_2 rings are seen for all of the structures of **290–296**.[316–321] In contrast, chelation of the hydrazide does not occur in complex **297** but rather the metals form close contacts to the aromatic π-systems of the attached phenyl groups.[318] The stabilizing effect of Li–Ph π-interactions allows for the construction of trimeric $(LiN)_3$ rings for **298** and also for the assembly of the unusual tetrameric $(LiNPh)_4$ ring structure of **299**.[318] Chelation of the hydrazides is also absent in the monomers **286** and **287**,[313,314] and in polymer **301**,[323] presumably due to filling of the metal's coordination sphere by the neutral Lewis bases. It is however worth noting that

Table 3 Crystallographically characterized monolithiated hydrazides

Compound	*Structure*	*References*
$[Me_2NN(Ph)Li{\cdot}PMDTA]$ **286**	Monomer	313
$[(Me_3Si(Ph)NN(Ph)Li(OEt_2)_2]$ **287**	Monomer	314
$[\{^tBuN(H)N(SiMe_3)Li\}(GaMe_3)]_2$ **288**	$(LiN_2)_2$ ring dimer	315
$[\{^tBuN(H)N(SiMe_3)Li\}(InMe_3)]_2$ **289**	$(LiN_2)_2$ ring dimer	315
$[(Me_3Si)_2NN(SiMe_3)Li]_2$ **290**	$(LiN)_2$ ring dimer	316,316a
$[Me_3Si(PhCH_2)NN(CH_2Ph)Li]_2$ **291**	$(LiN)_2$ ring dimer	317
$[PhCH_2(SiMe_3)NN(SiMe_3)Li]_2$ **292**	Li_2N_2 ring dimer	318
$[(Me_2(Ph)Si)_2NN(H)Li]_2$ **293**	Li_2N_2 ring dimer	319
$[\{Me_2(^tBu)Si\}(H)NNSiMe_2(^tBu)Li(THF)]_2$ **294**	Li_2N_2 ring dimer	320
$[^tBu(H)NN(SiMe_3)Li(THF)]_2$ **295**	Li_2N_2 ring dimer	320
$[Me_2NN(Si(^tBu)_2F)Li(THF)]_2$ **296**	Li_2N_2 ring dimer	321
$[Me_3Si(H)NN(Ph)Li(OEt_2)]_2$ **297**	Li_2N_2 ring dimer	318
$[Ph_2NN(SiMe_3)Li]_3$ **298**	$(LiN)_3$ ring trimer	318
$[(Me_3Si)_2NN(Ph)Li]_4$ **299**	$(LiNPh)_4$ ring tetramer	318
$[Et(H)NN(Et)Li]_6$ **300**	Prismatic hexamer	322
$[Me_2NN(Ph)Li(THF)]_\infty$ **301**	1D chain polymer	323

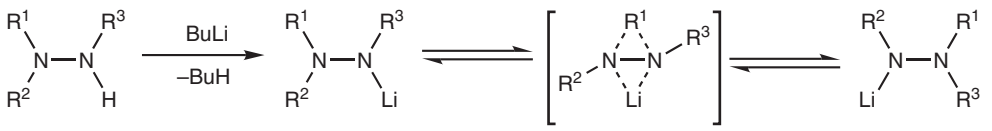

Scheme 3 Migration of hydrazine substituents upon metallation.

chelation of the dimeric hydrazides is retained in complexes **294–297** despite the presence of external donor solvents.[318,320,321] This demonstrates that the bonding within the aggregates is relatively strong.

An alternative structural arrangement is found in complexes **288** and **289**, where the lithium hydrazides act as Lewis base donors.[315] These complexes are isostructural and contain a central $(LiN_2)_2$ six-membered ring with either Me_3Ga or Me_3In bound in a terminal fashion to an anionic hydrazide nitrogen center. In these instances, the N–N backbones of the hydrazide units act as "end-on" bridging units between the metal centers instead of chelating. Only one example of a hexameric lithium hydrazide aggregate has been characterized.[322] Complex **300** again contains chelated hydrazide units, but in this case the relatively small size of the groups attached to the ligand (hydrogen and ethyl) allows for cage formation. Scheme 4 shows the molecular structures adopted by a representative set of monolithiated hydrazide complexes.

Solution studies of the complexes outlined in Table 3 are in general agreement that they remain aggregated in solution, with the most common form being dimers.[325] Solution studies of **300** in arene solvent indicate that at least two independent aggregates coexist.[322] The most likely scenario from the data available is that a dimer–hexamer equilibrium is present in solution. Gas-phase studies of the hydrazides have proved to be problematic due to decomposition of the complexes on volatilization.

A highly interesting series of dilithiated hydrazide complexes has also been structurally characterized, as outlined in Table 4. A common structural motif is double side-on coordination of the N–N linkage by a pair of metal centers to form Li_2N_2 bicyclic rings. These Li_2N_2 units may remain monomeric if sterically encumbered hydrazides are used and the coordination sphere of the metals can be satisfied by binding to donor solvent molecules, e.g. **302** and **303**. Otherwise, the complexes aggregate to form cage dimers **304**, **305**, trimers **306**, **307**, and tetramers **308–311**. Figure 21 shows the molecular structures of three representative compounds.

Both **302** and **303** adopt very similar monomeric structures wherein each metal binds to both nitrogen centers of the hydrazide, to a terminal THF molecule, and also to one bridging THF molecule.[326,327] The metal centers in **302** and **303** are clearly in a *cis*-position with respect to the N–N linkage to give the overall arrangement of a "butterfly" shape. Indeed, the Li_2N_2 bicyclic unit is the building block for the construction of the dimers **304** and **305**,[328] trimers **306** and **307**,[316,319] and tetramers **308–310**.[322,329] The tetramers **308–310** are isostructural, whereas complex **311** adopts a unique structure composed of an Li_6N_8 core and with the remaining two lithium centers η^6-bound to a pair of phenyl rings on the periphery of the structure.[322] It is also worth noting that **308** and **309** have essentially identical molecular cores despite the presence of THF in the latter compound.[322,329] Again, as with the monolithiated hydrazides, this illustrates that the bonding within these complexes is relatively strong.

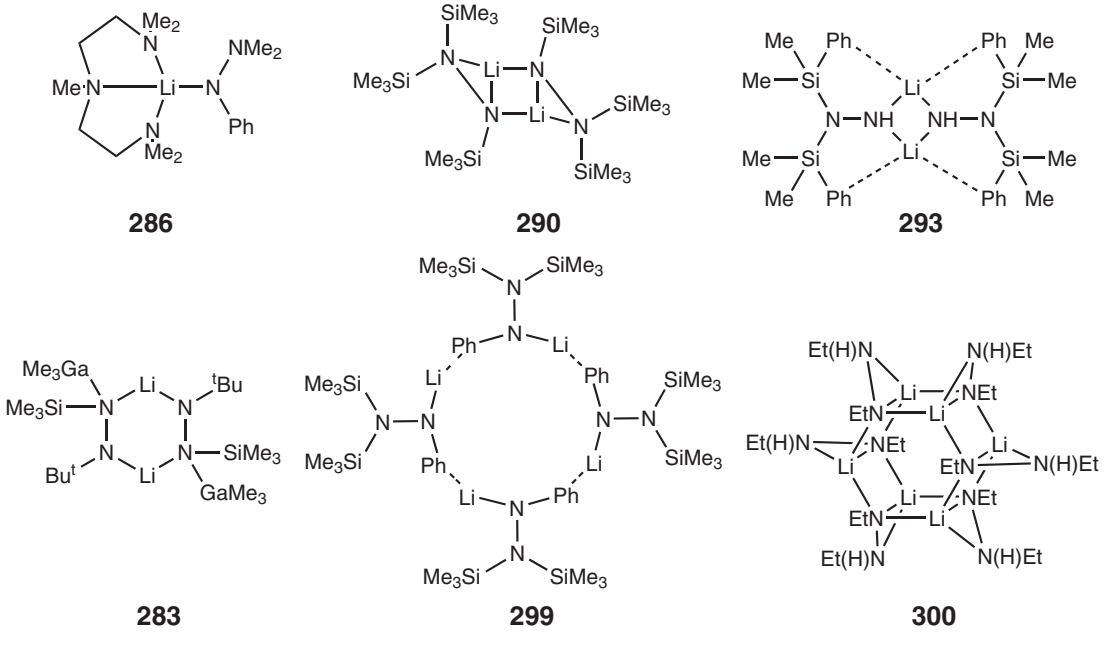

Scheme 4 Representative structural arrangements for monolithiated hydrazides.

Table 4 Crystallographically characterized dilithiated hydrazides

Compound	*Structure*	*References*
$[(Ph_2(^tBu)Si)_2N_2Li_2(THF)_3]$ **302**	Monomer	326
$[(^tBu_2(Me)Si)_2N_2Li_2(THF)_3]$ **303**	Monomer	327
$[(Ph_2(^tBu)Si)_2N_2Li_2]_2$ **304**	Dimer	328
$[(^tBu_2(H)Si)_2N_2Li_2]_2$ **305**	Dimer	328
$[(Me_2(^tBu)Si)_2N_2Li_2]_3$ **306**	Cyclic trimer	316
$[(Me_2(Ph)Si)_2N_2Li_2]_3$ **307**	Cyclic trimer	319
$[(Me_3Si)_2N_2Li_2]_4$ **308**	Cage tetramer	322
$[\{(Me_3Si)_2N_2Li_2\}_4(THF)_2]$ **309**	Cage tetramer	329
$[Me_3SiNN(^tBu)Li_2]_4$ **310**	Cage tetramer	322
$[(Me_3Si)NN(Ph)Li_2]_4$ **311**	Cage tetramer	322

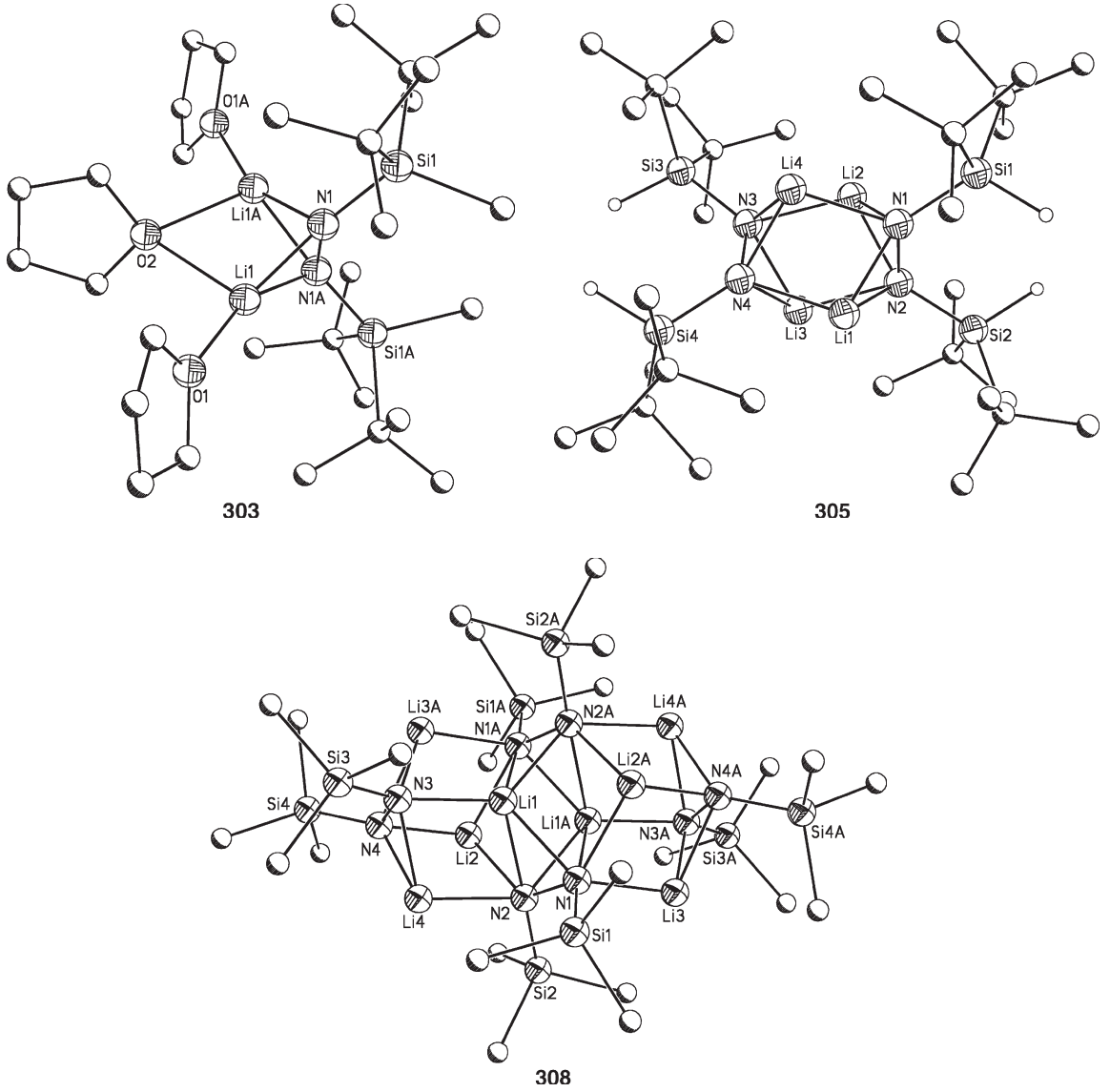

Figure 21 Examples of the molecular structures of monomeric **303**, dimeric **305**, and tetrameric **308** dilithiated hydrazides. Hydrogen atoms have been omitted for clarity (except for the Si–H centers).

A small number of mixed anion complexes containing lithiated hydrazides have also been identified.[330, 330a, 318, 322] These include complexes containing both mono- and dilithiated hydrazides, as well as products resulting from the fragmentation of the N–N backbone.

Investigations of heavy group 1 metal hydrazides are very limited, with no reports of structurally characterized potassium or rubidium complexes (Table 5 and Figure 22). The sodium hydrazides **312–316** were prepared by the reaction of either $NaNH_2$ or $NaN(SiMe_3)_2$ with appropriate protonated hydrazine ligand.[314,318] In contrast, reaction of $NaN(SiMe_3)_2$ with $Ph(H)NN(Ph)SiMe_3$ or of $NaNH_2$ with $Me_3Si(H)NNPh_2$ results in desilylation to form complexes **317** and **318**, respectively.[314] Monomer **312** contains tetracoordinate sodium centers without chelation of the N–N linkage similar to the lithium complex **286**.[314] This end-on coordination of hydrazide is also found in complexes **314–316**, which utilize Na–Ph π-interactions to form 1D chain polymers. Chelation of the hydrazide is however present in the dimer **313** (similar to lithium complex **290**), the face-shared double cube **317**, and the mixed anion complex **318**.[314,318] It is interesting to note that hexamer **317** adopts a face-shared double cubane rather than a prismatic hexamer as was found for lithium derivative **300** (Figure 5).[314,322] This is likely due to the larger size of the cation allowing additional transannular interactions. The mixed anion complex **318** is included in Table 5 as it is the only report of a structurally characterized disodiated species.[314] The central dimetallated Na_2N_2 unit in **318** does not adopt the *cis*-"butterfly" arrangement noted for the dilithiated derivatives (Figure 22). Instead, the structure is composed of a central N–N dianion which binds to two Na centers in an end-on fashion. In turn, this group connects with a pair of NaN_2 triangular units. Complex **319** was prepared by the direct reaction of metallic cesium with $Ph(H)NN(SiMe_3)_2$.[318] The structure of this compound is similar to that of the sodium counterparts **314–316**, as it forms monomeric, end-on coordinated hydrazide, which are further associated into polymeric chains via Cs–Ph π-interactions.

Table 5 Crystallographically characterized heavy alkali metal hydrazides

Compound	*Structure*	*References*
$[(Me_3Si)_2NN(Ph)Na(THF)_3]$ **312**	Monomer	314
$[Me_3Si(Ph)NN(Ph)Na(NH_3)]_2$ **313**	Na_2N_2 ring dimer	318
$[(Me_3Si)_2NN(Ph)Na(THF)]$ **314**	1D chain polymer	314
$[(Me_3Si)_2NN(Ph)Na\{O(^tBu)Me\}]$ **315**	1D chain polymer	314
$[(Me_3Si)_2NN(Ph)Na(OEt_2)]$ **316**	1D chain polymer	314
$[Ph_2NN(H)Na]_6$ **317**	Face-shared double, cube	314
$[\{Ph(H)NN(Ph)Na\}\{Ph_2N_2Na_2\}(DME)_4]$ **318**	Distorted ladder	314
$[(Me_3Si)_2NN(Ph)Cs]_2$ **319**	1D chain polymer	318

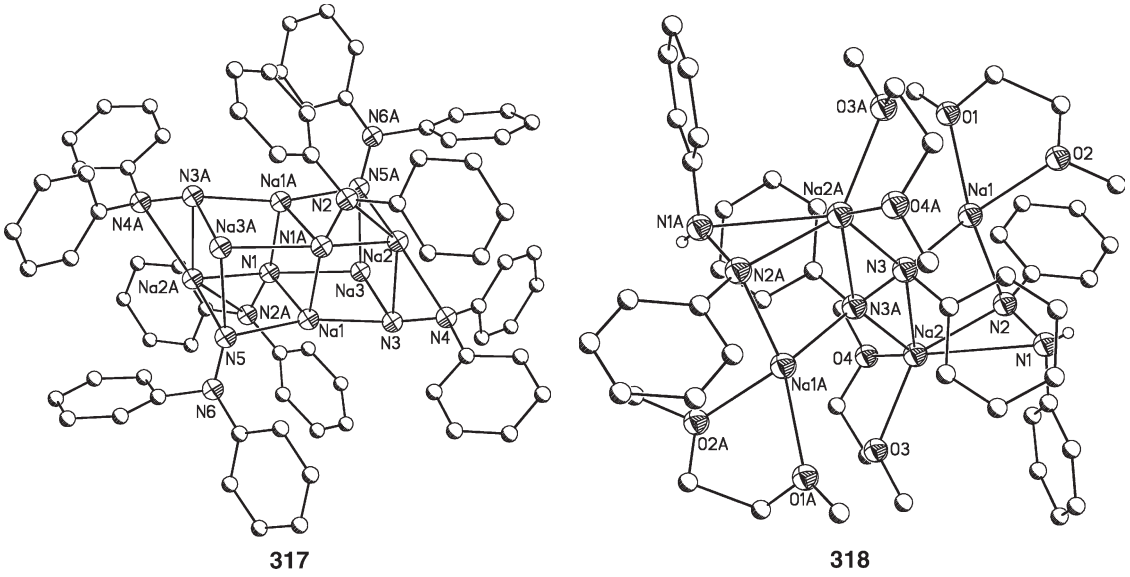

Figure 22 Structures of the hexameric sodium hydrazide **317** and the mixed mono- and dianionic complex **318**. Hydrogen atoms have been omitted for clarity.

2.01.4.1.3 Pyrazolato, triazolato, and tetrazolato complexes

Another area of recent activity has been the synthesis and structural characterization of anionic five-membered ring heterocycles containing N–N bonded units (Scheme 5). (For reviews on pyrazolates, see Refs: 331, 331a, and 331b.) Nitrogen-rich heterocycles are a remarkable set of compounds which have found a wide variety of uses including corrosion inhibitors, components of pharmaceuticals, high energy materials, sweeteners, and photographic processing chemicals.[332] These heterocyclic anions are also interesting ligands in organometallic chemistry as they have the ability to bond to metals in a number of ways and can be considered as analogs to cyclopentadienyl ligands. Scheme 6 outlines some of the known binding modes that the ligands adopt on bonding to alkali metal, and Table 6 lists a series of crystallographically characterized complexes.

A clear pattern emerging from Table 6 is that these ligands have a strong tendency to bridge between metal centers, resulting in the formation of coordination polymers. Compounds **326** and **332** are useful examples to illustrate the trends within this class of complex, and Figure 23 shows sections of their crystal structures.[338] Both complexes contain six-membered $(LiN_2)_2$ dimeric rings. In triazole **326**, these dimers associate in a lateral fashion (end-on) to form 1D extended ladders. In **332**, bridging between the dimers is achieved via a nitrogen on the tetrazole ring, leading to the formation of the 2D sheet assembly instead of a chain. In both instances, tetracoordination of the lithium centers is completed by solvation of one DMSO ligand per metal. The presence of a very strong donor solvent in these instances, as well as many of the other examples in Table 6, is due to the poor solubility of these complexes in hydrocarbon or ethereal solvents. This is presumably due to the formation of polymers in these solvents. However, cryoscopic measurements of **326** and **332** in DMSO solution indicate that they exist mainly as charge-separated species in this highly polar solvent.[338] It is also of note that the metals prefer to bond in the σ-plane of the heterocycles rather than forming π-interactions, as is found in the alkali metal cyclopentadienyl derivatives.[91] This point is reinforced by examination of the binding modes shown in Scheme 6. The majority of structurally characterized alkali metal amides adopt oligomeric structures as a consequence of steric interactions inhibiting further association. In the pyrazolates, triazolates, and tetrazolates, the negative charge is

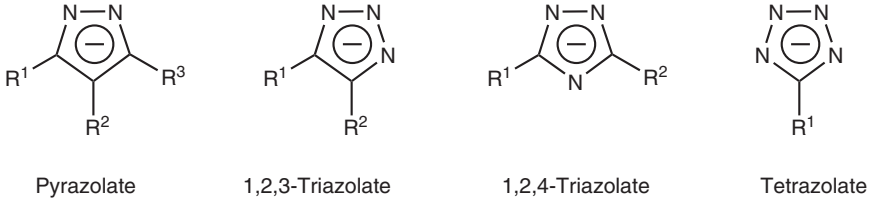

Scheme 5

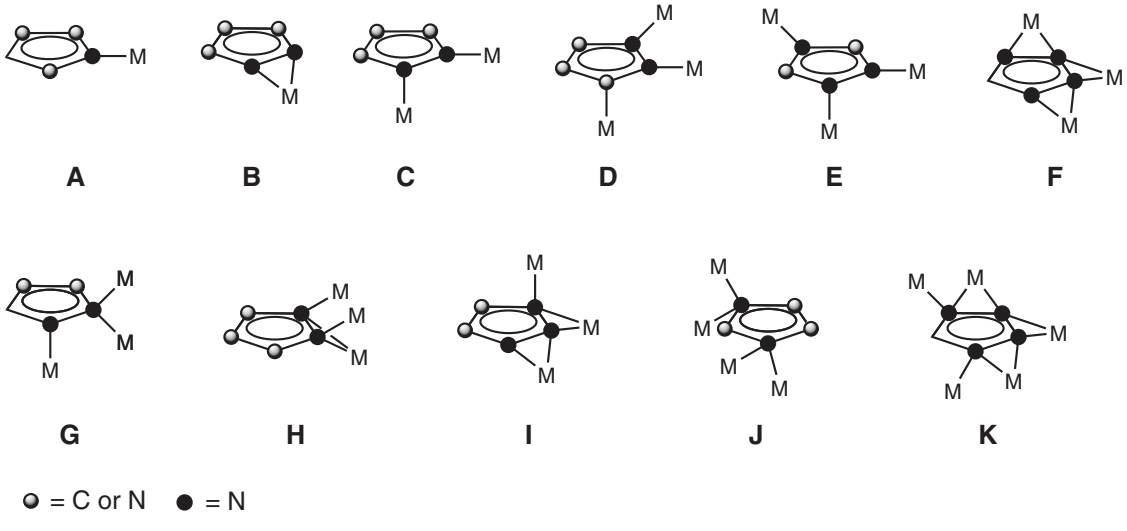

Scheme 6 Known binding modes for $[(RC)_xN_y]^-$ (where $x+y=5$) to alkali metal cations.

Table 6 Crystallographically characterized alkali metal pyrazolato, triazolato, and tetrazolato complexes

Compound	*Structure*	*Coord Mode*	*References*
Pyrazolates **(pz)**			
[(3,5-Ph_2-pz)K(18-crown-6)] **320**	Monomer	B	333
[(3,5-Me_2-pz)K(18-crown-6)(H_2O)] **321**	Monomer	B	333
[(3,5-Me_2-pz)Na(THF)]$_4$ **322**	Tetrameric cubane	H	334
[(3,5-Ph_2-pz)K(THF)]$_6$ **323**	Prismatic hexamer	H	335
[(2-pyr-pz)Li(DMF)]$_\infty$]**324**	1D chain polymer	C	336
Triazolates			
[(3,5-$^i Pr_2$-triazolato)K(18-crown-6)] **325**	Monomer	B	337
[(benztriazolato)Li(DMSO)]$_\infty$ **326**	1D ladder polymer	D	338
[(benztriazolato)K(HMPA)]$_\infty$ **327**	1D ladder polymer	I	339
Tetrazolates			
[(5-Ph-tetrazolato)K(18-crown-6)] **328**	Monomer	B	337
[(5,5′-azotetrazolato)$Li_2(H_2O)_6$]$_2$ **329**	Dimer	A	340
[(5,5′-azotetrazolato)$Na_2(H_2O)_5$]$_\infty$ **330**	1D chain polymer	A/C	340
[(1,4-ditetrazolylethylene)$Na_2(H_2O)_5$]$_\infty$ **331**	1D chain polymer	A/C	341
[(tetrazolato)Li(DMSO)]$_\infty$ **332**	2D sheet polymer	E	338
[(tetrazolato)Na(H_2O)]$_\infty$ **333**	2D sheet polymer	J	342
[losartan potassium]$_\infty$ **334**	3D network polymer	F	343
[(5,5′-azotetrazolato)$Rb_2(H_2O)$]$_\infty$ **335**	3D network polymer	G	340
[(5-nitraminotetrazolato)Cs]$_\infty$ **336**	3D network polymer	C	344
[(5-CN-tetrazolato)Cs]$_\infty$ **337**	3D network polymer	K	345

delocalized and the metal centers may bind to two or more nitrogen centers of a given ring. In turn, this leads to the preferred coordination mode of in-plane bonding to the nitrogen lone pairs to form extended networks instead of molecular species.

Monomeric complexes **320**, **325**, and **328** are useful in illustrating the preferred bonding of these aromatic amides since the ligands bind to single metal centers.[333,337] In each case, the rings adopt an η^2-coordination mode as exemplified in Figure 24. Whereas the η^2-coordination is almost ideal in **320**, the ligands adopt distinctly "slipped" η^2-bonding in both **325** and **328** (with one K–N distance being 0.36–0.60 Å longer than the other). This distortion was attributed to the decreased basicity of the tetrazolato ligands leading to competitive binding of the out-of-plane π-orbitals. These results have led to the speculation that the $[K(18\text{-crown-6})]^+$ fragment may be useful in stabilizing the recently discovered N_5^- anion.[346]

As Table 6 shows, there are only a few examples of molecular derivatives of alkali metal pyrazolates, triazolates, or tetrazolates. Molecular forms of the potassium complexes **320**, **321**, **325**, and **328** are attained using 18-crown-6 as complexing agent, which reduces the number of possible metal coordination sites.[333,337] A molecular species is also formed by tetrazolate **329** but in this instance each lithium center is almost completely solvated by water, with only a single Li–N interaction present.[340] The pyrazolates are more likely to form stable molecular species as they have only two adjacent nitrogen centers within the rings available for metal binding. This is seen in the characterization of **322** and **323**, which form molecular tetramers and hexamers, respectively (Figure 25).[334,335] Both complexes are similar to the tetrameric cubanes and prismatic hexamers found for many alkali metal complexes.[259,259a] The difference in these instances is that the cubane and hexamer are "enlarged" through bridging the metals via the N–N linkage. Again this is due to delocalization of the anionic charge within the ligand frameworks leading to the metals bridging between two adjacent nitrogens on aromatic rings. The structures can therefore be considered as being composed of MN_2 triangles that aggregate to form cyclic ladders.

2.01.4.2 P–M, As–M, Sb–M, and Bi–M Bonded Complexes

Alkali metal complexes of the heavier group 15 elements are important transfer reagents in organometallic synthesis. The structural and aggregation chemistry of alkali metal phosphanides has received the most attention, with several hundred crystal structures reported in the literature over the past decade alone. In turn, this has led to numerous excellent reviews.[347–352] The patterns that have emerged from this extensive structural database are generally consistent with the ring-laddering and ring-stacking principles developed for the N–Li bonded species.[259] To summarize, the majority of the simple phosphanide complexes adopt one of the aggregation patterns that are

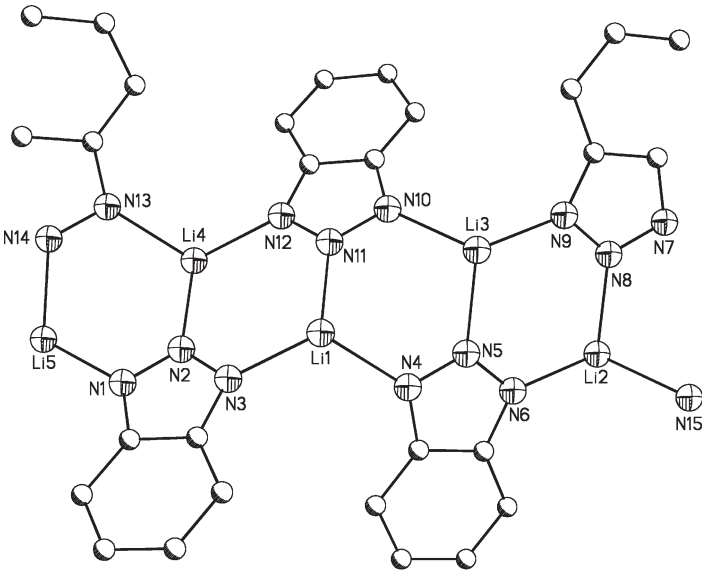

326

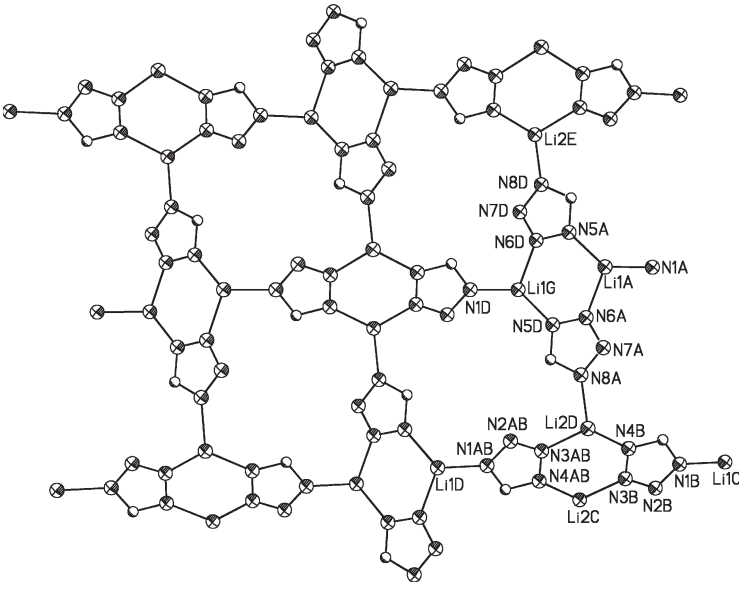

332

Figure 23 Sections of the solid-state polymeric structures of **326** and **332**. DMSO ligands and hydrogen atoms have been omitted for clarity.

characteristic of many group 1 metal complexes. Specifically, M_2P_2 rings are the fundamental building blocks of the majority of structures, leading to the formation of dimers, ladders of various lengths, cubanes, hexamers, and other prismatic oligomers. As expected, the particular structure adopted is dependent on the nature of the cation, the steric demands of the phosphanide, and also on the influence of any donor solvent present. In solution, phosphanides may undergo complex dynamic exchange between aggregated species similar to that of their amide analogs. However, the generally weaker bonding present leads to more facile dissociation compared to the amides.

A recent development that has gained attention is the characterization of a remarkable series of complexes resulting from the multiple metallation of primary phosphanes, and also a smaller number of the heavier group 15

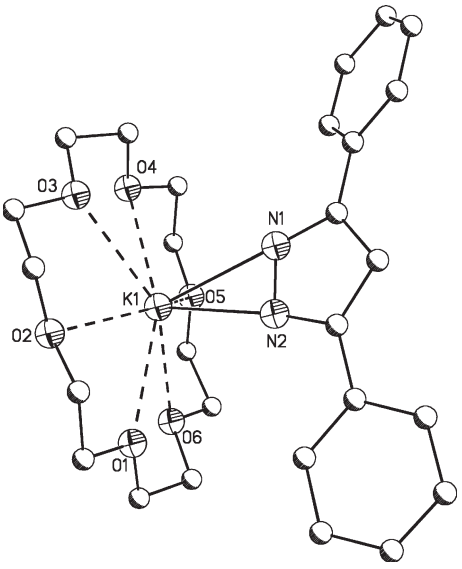

320

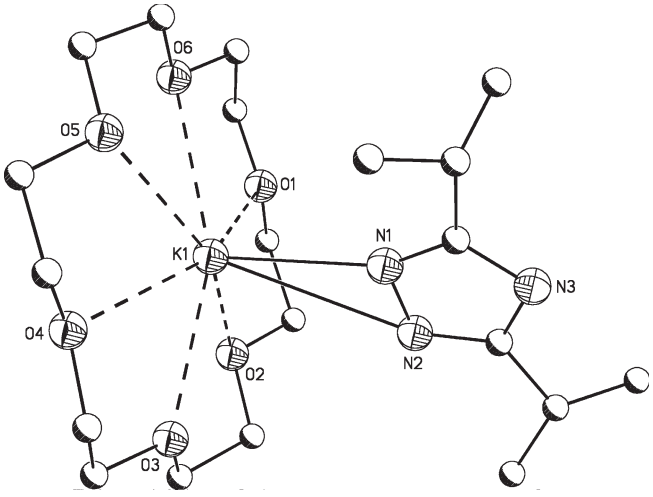

325

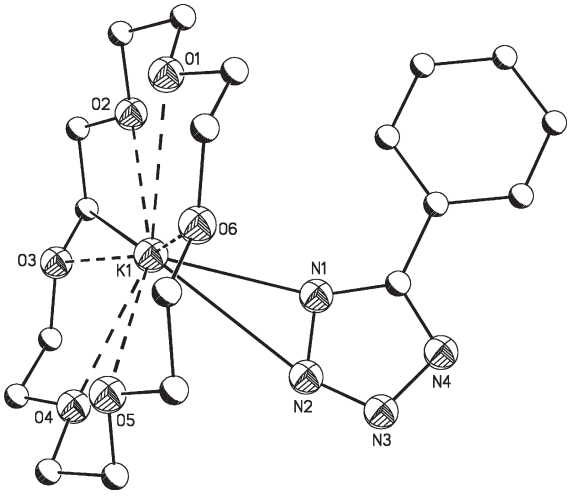

328

Figure 24 Structures of the monomeric pyrazolate **320**, triazolate **325**, and tetrazolate **328**. Hydrogen atoms have been omitted for clarity.

element derivatives.[349,351,352] These are generally prepared through the direct double deprotonation of primary phosphanes by a suitable alkali metal base (alkyl or amide). The increased acidity of the E–H bonds in comparison to their amide analogs facilitates the double deprotonation process. Although dilithium organophosphandiides were first prepared nearly half a century ago, it was only in 1996 that such a species was unambiguously characterized.[353,354,354a] A long-standing problem in the characterization of multimetallated complexes in general is their insolubility or amorphous nature. However, the attachment of sterically encumbered silyl groups to the central group 15 element allows the isolation of relatively stable crystalline materials that prove amenable to X-ray characterization. The first dilithiated phosphandiide to be structurally characterized was the unusual dimeric fluorosilane complex $[RPLi_2(RF)]_2$ **338**, where $R = {}^{i}Pr_2(2,4,6\text{-}{}^{i}Pr_3C_6H_2)Si$, as shown in Figure 26.[353] Dilithiation of the parent primary silyl phosphane resulted in the formation of a hexane-soluble complex that

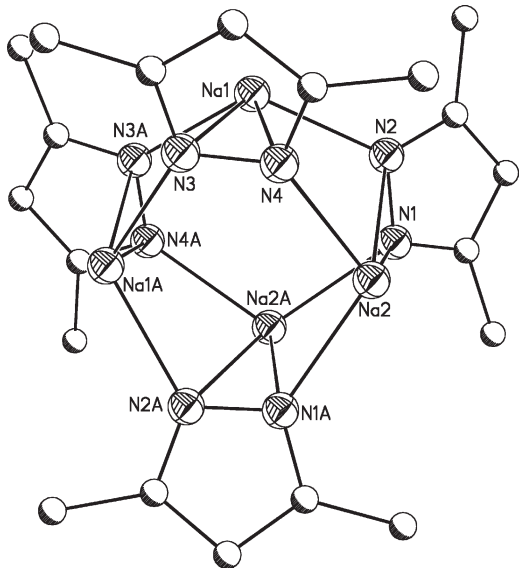

322

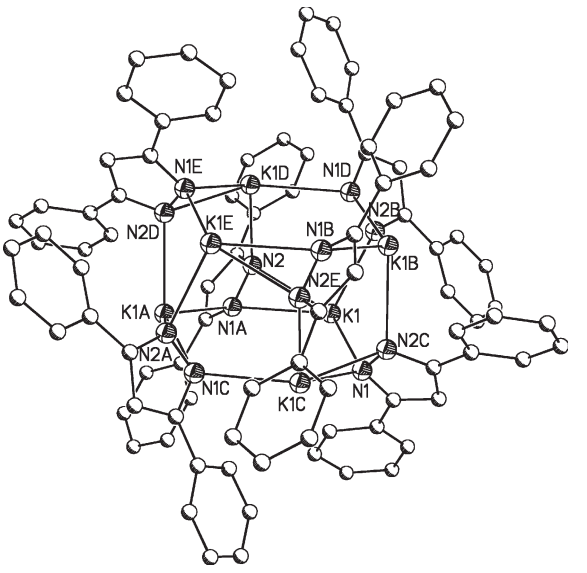

323

Figure 25 Structures of tetramer **322** and hexamer **323**. Hydrogen atoms have been omitted for clarity.

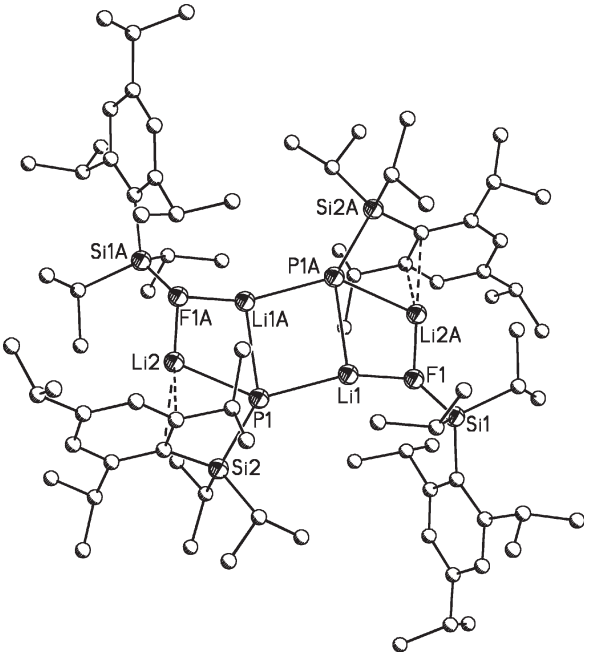

338

Figure 26 Structure of the dilithiated phosphandiide **338**. Hydrogen atoms have been omitted for clarity.

was found to be dimeric in benzene solution but could not be crystallized. Reaction of this compound with the fluorosilane $^{i}Pr_2(2,4,6\text{-}^{i}Pr_3C_6H_2)SiF$ did not result in the expected nucleophilic substitution but rather in the formation of **338**, where the fluorine center is incorporated as bridging Lewis base. The overall structure of **338** can be described as a four-rung heteroladder.

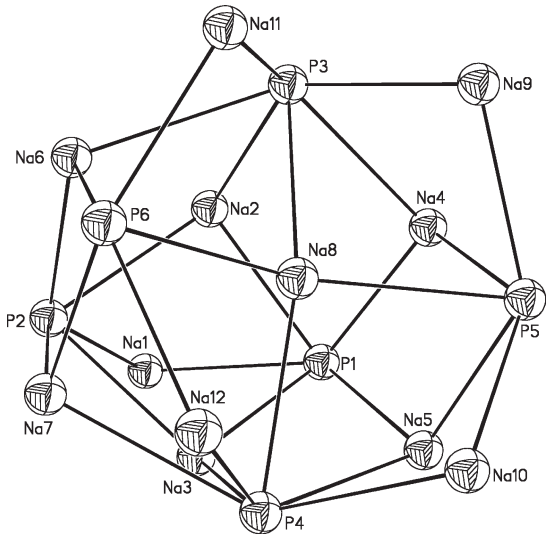

339

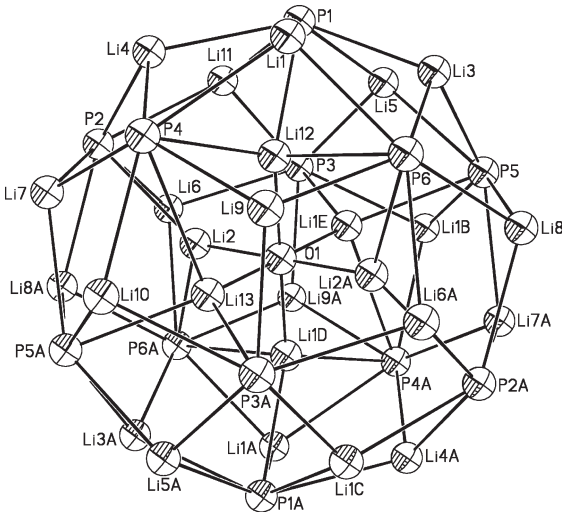

340

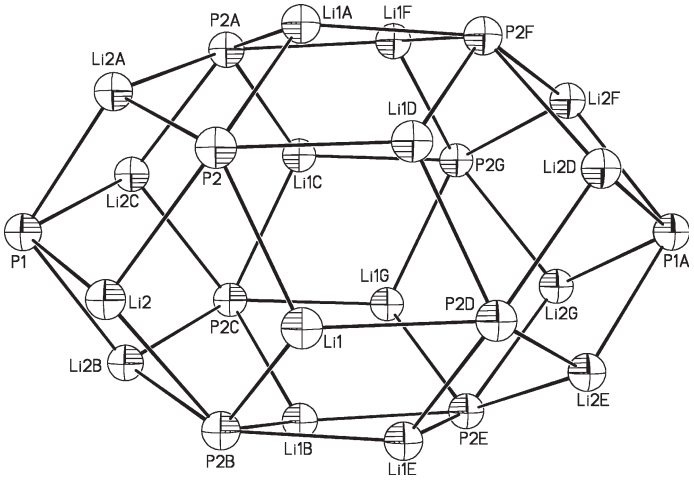

341

Figure 27 Molecular cores of the representative dimetallated organophosphandiides **339–341**.

Further studies on dimetallating the heavy group 15 elements have produced a series of globular cluster molecules that can be categorized with the general formula $[M_nO_m(REH)_x(RE)_y]$, where M = Li or Na, and E = P, As, or Bi.[352] These include "pure" dimetallated clusters, mono- and dimetallated mixed anion complexes, M_2O-encapsulated species, and electron-deficient clusters.[355,355a,355b,356,356a,356b] In general, the structures adopted can be considered as group 15 element polyhedra which have their faces capped by alkali metals. Three representative molecular structures of complexes $[(^tBu_3SiP)_6Na_{12}(THF)_2]$ **339**,[356] $[\{Me_2(^iPrMe_2C)SiP\}_{12}Li_{24}(Li_2O)]$[355] **340**, and $[(^iPr_3SiP)_{10}Li_{16}]$[355a] **341** are shown in Figure 27, and a detailed review by Driess is available for further information.[351,352]

In comparison to N- or P-bound species, there are far fewer reports involved with alkali metal complexes containing As–M, Sb–M, or Bi–M bonds. Nevertheless, their chemistry has continued to develop over the past decade and Tables 7–9 detail examples of structurally characterized complexes.

A highly productive area of study has been the development of the trisamide group 15 reagents $E(NMe_2)_3$ (E = As, Sb, Bi).[380] Whereas these reagents react with metallated primary amides [RN(H)M] (M = Li–Cs) to form stable imido anions, their reaction with primary phosphides [RP(H)M] (M = Li–Cs) results in the facile generation of Zintl compounds and $(PN)_n$ rings.[381] For example, reaction of $Sb(NMe_2)_3$ with 3 molar equiv. of CyN(H)Li

Table 7 Crystallographically characterized As–alkali metal complexes

Compound	*Structure*	*References*
$[H_2AsLi(DME)_2]$ **342**	Monomer	357
$[Ph_2AsLi(dioxane)_3]$ **343**	Monomer	358
[(2,3,4,5-tetramethyl-1-arsolide)Li(TMEDA)] **344**	Monomer	359
$[(^tBuP)_3AsLi(TMEDA)(THF)]$ **345**	Monomer	360
$[(^tBuP)_3AsLi(DABCO)_3]$ **346**	Monomer	362
$[(1\text{-}AdP)_3AsLi(TMEDA)(THF)]$ **347**	Monomer	361
$[(CyP)_4AsLi(Me_2NH)_3]$ **348**	Monomer	361
$[(CyP)_4AsLi(TMEDA)(THF)]$ **349**	Monomer	362
$[\{(^tBuP)_3AsLi\}_2(TMEDA)_3]$ **350**	Monomer	362
$[\{^iPr_3Si\}\{(2,4,6\text{-}^iPr_3C_6H_4)_2Si(F)\}AsLi(THF)_2]$ **351**	Monomer	363
$[^tBu_2AsAs(^tBu)Li(THF)]_2$ **352**	Li_2As_2 ring dimer	364
$[Ph_2AsLi(OEt_2)]_2$ **353**	Li_2As_2 ring dimer	358
$[(Me_3Si)_2AsLi(DME)]_2$ **354**	Li_2As_2 ring dimer	365
$[(Me_3Si)_2AsLi(THF)_2]_2$ **355**	Li_2As_2 ring dimer	367
$[(CyP)_4AsNa(TMEDA)]_2$ **356**	Na_2As_2 ring dimer	361
[(2,3,4,5-tetraethyl-1-arsolide)Na(TMEDA)]$_2$ **357**	Expanded dimer	377
$[((Me_3Si)_2CH)_2AsLi]_3$ **358**	$(LiAs)_3$ ring trimer	366
$[(Me_2AsLi)_4(THF)_2]$ **359**	Four-rung ladder	367
$[Ph_2AsLi(dioxane)]_\infty$ **360**	1D chain polymer	368
$[Ph(H)AsLi(THF)_2]_\infty$ **361**	1D chain polymer	369
$[\{(Me_2N)_2AsN(Cy)K\}_2]_\infty$ **362**	1D chain polymer	370
[(2,3,4,5-tetraethyl-1-arsolide)K(DME)]$_\infty$ **363**	1D chain polymer	377
[(2,3,4,5-tetraethyl-1-arsolide)Rb(DME)]$\}_\infty$ **364**	1D chain polymer	377
[(2,3,4,5-tetraethyl-1-arsolide)Cs(DME)]$_\infty$ **365**	1D chain polymer	377

Table 8 Crystallographically characterized Sb–alkali metal complexes

Compound	*Structure*	*References*
$[(Me_3Si)_2C(H)Sb\{(2\text{-}Me_2NCH_2)C_6H_4\}Li(THF)_2]$ **366**	Monomer	371
$[(^tBu_4Sb_3)Na(PMDTA)]$ **367**	Monomer	372
$[(Me_3Si)_2C(H)Sb\{(2\text{-}Me_2NCH_2)C_6H_4\}Na(TMEDA)]$ **368**	Monomer	371
$[\{(CyP)_4Sb\}Na(Me_2NH)(TMEDA)]_2$ **369**	Na_2Sb_2 ring dimer	360
$[(^tBu_3Sb_2)K(PMDTA)]_\infty$ **370**	1D chain polymer	372
$[(Me_3Si)_2SbLi(DME)]_\infty$ **371**	1D chain polymer	373
$[(^tBu_4Sb_3)K(PMDTA)]_\infty$ **372**	1D chain polymer	372
$[(2\text{-}\{3',5'\text{-}Me_2C_6H_3\}\text{-}5,7\text{-}Me_2stibindolyl)K(PMDTA)]_\infty$ **373**	1D chain polymer	374
$[(1,4,2\text{-}P_2SbC_2{}^tBu_2)K(DME)]_\infty$ **374**	1D chain polymer	375
$[(2,3,4,5\text{-tetraethyl-1-stibolide})_2K_2(THF)]$ **375**	1D ribbon polymer	376
[(2,3,4,5-tetraethyl-1-stibolide)Na(DME)]$_\infty$ **376**	1D chain polymer	377
[(2,3,4,5-tetraethyl-1-stibolide)Rb(DME)]$_\infty$ **377**	1D chain polymer	377
[(2,3,4,5-tetraethyl-1-stibolide)Cs(DME)]$_\infty$ **378**	1D chain polymer	377

Table 9 Crystallographically characterized Bi–alkali metal complexes

Compound	*Structure*	*References*
$[(^tBu_3Si)_2BiNa(THF)_3]$ **379**	Monomer	355c
$[Bi_2\{Cs(18\text{-crown-}6)\}_2(NH_3)_7]$ **380**	Monomer	378
$[\{(^tBu_3SiBi)_{12}Na_{21}\}Na_3(THF)_{14}]$ **381**	Na-capped Bi_{12} icosahedron	356c
$[(Me_3Si)_2BiLi(DME)]_\infty$ **382**	1D chain polymer	379

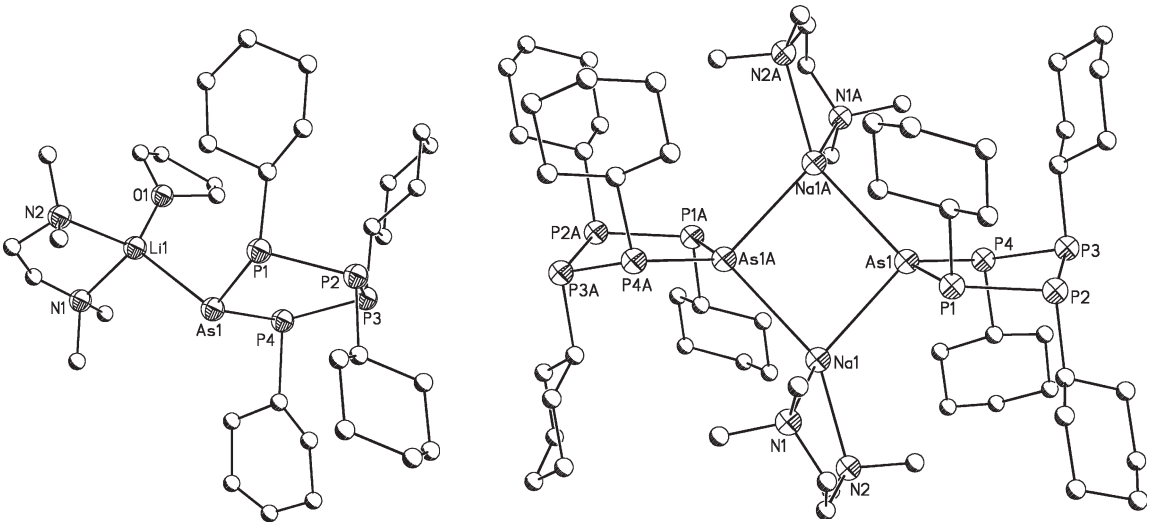

349 **356**

Figure 28 Structures of heterocycles **349** and **356**. Hydrogen atoms have been omitted for clarity.

(Cy = cyclohexyl, C_6H_{11}) leads to the formation of $[\{(CyP)_3Sb\}_2Li_6(Me_2NH)_6]$ **383**, which decomposes at 30 °C to the Zintl compound $[Sb_7Li_3(Me_2NH)_6]$ **384** and $(CyP)_4$.[382,383] It was determined that the formation of thermodynamically favorable P–P bonds was the driving force for such reactions.[360,363] Several heterocyclic intermediates of the type $[(RP)_nEM]$ which contain M–E bonds have been identified on the pathway to Zintl anion formation (E = As: **345–350** and **356**; E = Sb: **369**). The size of the heterocycle was found to be primarily dependent on the nature of the organic unit as opposed to the particular group 15 element employed.[361] Further details can be found in review articles by Wright, and typical heterocyclic complexes **349** and **356** are shown in Figure 28.[380,381]

Another area of rapid development is the synthesis and identification of alkali metal phospholides, arsolides, and stibolides. (For work on alkali metal complexes of phospholides, see Refs: 384, 384a–384d.) These are generally prepared via reduction of the neutral phosphole, arsole, or stibole with an alkali metal. However, alternative syntheses have been reported including the reaction of trimesitylstibane with potassium metal in the presence of PMDTA, which produced compound **373**.[374] The mechanism for this transformation is yet to be established. Overall, the most common arrangement for the solid-state structures of these complexes is η^5-coordination of the delocalized system to the alkali metal center. This may result in the formation of simple monomers if sufficient Lewis base is present,[384d] molecular dimers which aggregate through η^5-bonded anions and E–M σ-bonds, and 1D chains that may use a combination of σ- and π-bonding interactions. Figure 29 shows representative structures of the three complexes $[(Me_4C_4P)Li(TMEDA)]$ **385**,[384d] **357**, and **377**. For a particular cyclic ligand system, the structures adopted can be rationalized by considering the respective radii of the alkali metal and the pnictogen atom. Linear stacking of alternating cations and anions is preferred if the heterocyclic rings are sufficiently separated by the metal ions. Many of the 1D chains, such as **377**, deviate from linearity and adopt zigzag orientations in order to accommodate additional Lewis bases into their structures.

Finally, the number of structurally characterized complexes containing a Bi-alkali metal bond still remains small due to their prevalence to form charge-separated species. The Bi_{12} icosahedral cage arrangement found for the bismuthanediide **381** is of note as the remaining complexes in Table 9 are simple monomers **379**, **380** or a 1D chain of monomers **382**. Indeed, the structure of **381** is consistent with the findings from the lighter phosphandiides and arsanediides.[351] Also of note is the dibismuthide **380**, which was prepared by solvating Cs_5Bi_4 with 18-crown-6 and ammonia. The compound contains a Bi_2^{2-} unit that coordinates side-on to a pair of Cs centers, with a Bi–Bi distance of 2.8635(4) Å (Figure 30). This distance is significantly shorter than single Bi–Bi bonds (2.990(2) Å in Ph_4Bi_2)[385] and can be considered as a double bond. Naked Bi_2^{2-} complexes without additional interactions to alkali metal centers have also been prepared and contain even shorter Bi–Bi bonds (2.8377(7) Å in $(K\text{-crypt})_2Bi_2$).[386,386a,386b]

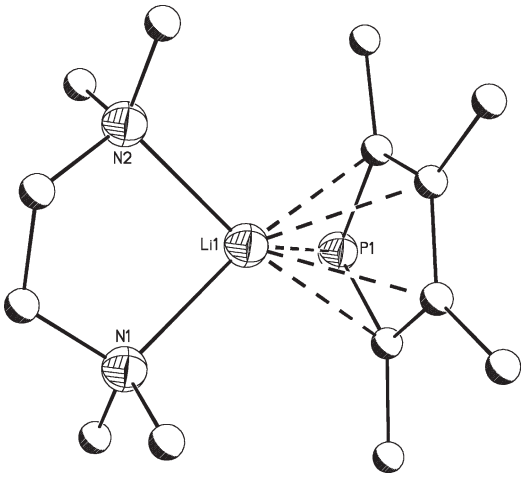

385

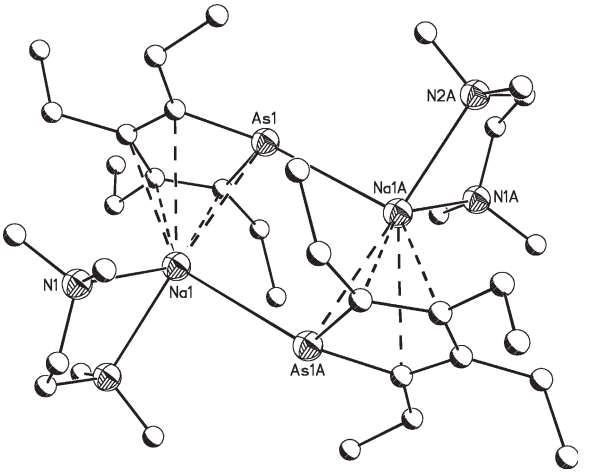

357

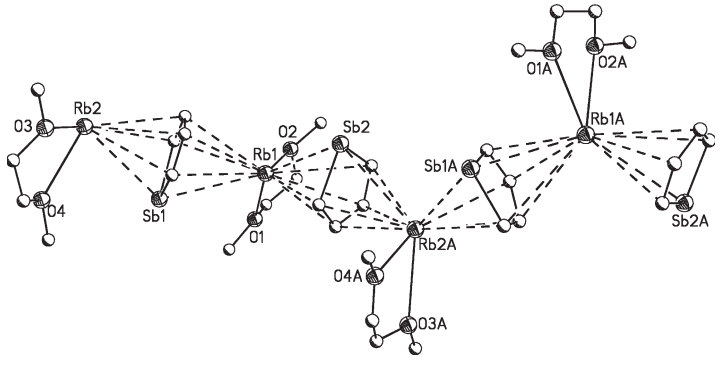

377

Figure 29 Structures of complexes **385**, **357**, and **377** illustrating the possible bonding modes of $(R_4C_4E)^-$ units to alkali metal centers. Hydrogen atoms have been omitted for clarity.

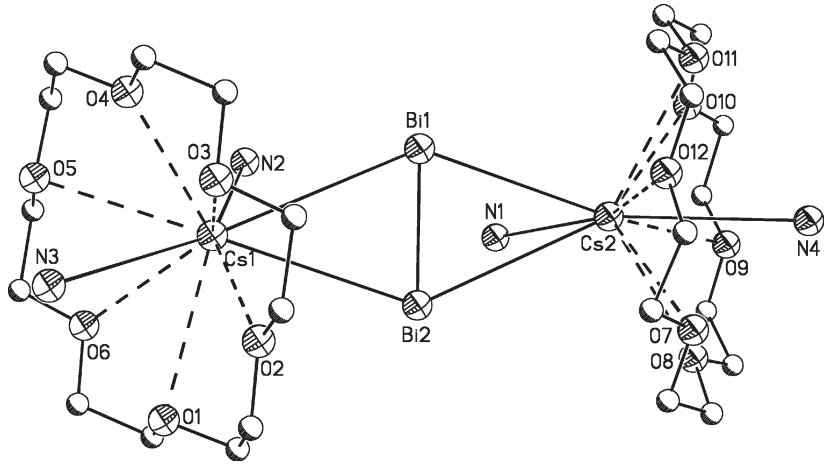

380

Figure 30 Structure of **380** showing the Cs-bound Bi_2^{2-} unit. Hydrogen atoms have been omitted for clarity.

2.01.5 Group 16 Alkali Metal Bonded Complexes

2.01.5.1 O–M Bonded Complexes

In COMC (1995), it was stated that there were comparatively few reports of structurally characterized alkali metal alkoxides, although the synthetically important enolates had been extensively studied.[7] Since that time, there have been a very large number of complexes containing O–M bonds that have been characterized,[6] although the majority are either heterometallic systems and/or are mixed anion complexes. This is mostly a consequence of the uses of these complexes, which include molecular precursors for ceramics and other materials.[387] A recent review article by Fromm covering a wide range of *s*-block complexes containing O–M bonds is available.[388] This section of the present review therefore provides an update on recent notable developments regarding simple homometallic, homoleptic O–M species.

The relatively high acidity of most alcohols and phenols allows numerous methods for the preparation of their metallated forms.[389,389a,389b] The most widely applicable methods are direct reaction of the metal with the alcohol, and deprotonation of the alcohol with a suitable metallating reagent (hydride, hydroxide, alkyl, amide, etc.). The unsolvated methoxides, MeOM (M = Li–Cs), have been known for a considerable time to form infinite layer-type structures.[390,390a–390f] In contrast, the sterically more encumbered *tert*-butoxides of K, Rb, and Cs form molecular M_4O_4 tetrameric cubanes, whereas the Na analog crystallizes containing both prismatic hexamers and nonamers.[391,391a–391c] Remarkably, due to crystallographic issues, it was only in 2002 that the first detailed report of the crystal structure of lithium *tert*-butoxide was reported.[392,392a,392b] The structure was determined to be a prismatic hexamer, $[^tBuOLi]_6$ **386a**, consistent with the expectations from complementary measurements of the compound.[393,393a] Subsequently, an unexpected prismatic octameric form of this compound, $[^tBuOLi]_8$ **386b**, was discovered (Figure 31).[394] The octameric structure adopted is distinct from the cyclic ladder arrangement found for the primary amide octamer $[^tBuN(H)Li]_8$ **272**.[295] Apparently, the method of preparation of the alkoxide is critical in determining the aggregation state. Deprotonation of the alcohol resulted in the formation of hexamer **386a**, whereas controlled oxidation of ^{t}BuLi yielded octamer **386b**. Experimental and theoretical studies indicated that the hexamer is the thermodynamically favored aggregate and **386b** could be converted into **386a** on heating. Although the prismatic octameric aggregation state is unusual for alkali metal complexes, some other examples have recently appeared including the lithium alkoxides $[Me_2N(CH_2)_2OLi]_8$ **387**,[395] and $[^tBuCH_2OLi]_8$ **388**.[396]

A particularly revealing series of aggregates has been discovered for the variously substituted lithiated aryloxides. (For early solution studies on lithium aryloxide aggregation, see Refs: 397 and 397a.) The aggregation state of these

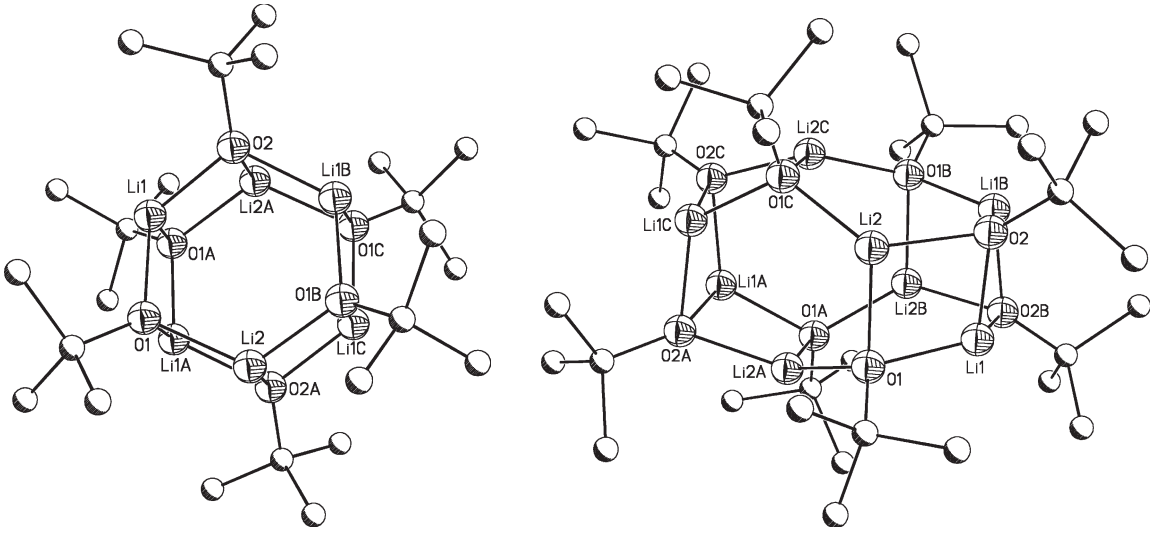

386(a) **386(b)**

Figure 31 Structures of the hexameric **386a** and octameric **386b** forms of ^{t}BuOLi. Hydrogen atoms have been omitted for clarity.

complexes is dictated by the steric bulk of the substituents at the 2,6-positions of the aryloxy ring. This is conveniently demonstrated for a series of THF-solvated lithiated aryloxides (ArOLi), which form stable ring dimers $[2,6\text{-}^{t}Bu_2C_6H_3OLi(THF)]_2$ **389**,[398] ring trimers $[2,6\text{-}^{i}Pr_2C_6H_3OLi(THF)]_3$ **390**,[399] tetrameric cubanes $[2,6\text{-}Me_2C_6H_3OLi(THF)]_4$ **391**,[399] and prismatic hexamers $[C_6H_5OLi(THF)]_6$ **392a**.[400] Interestingly, simple lithium phenolate solvated by THF has also been found to adopt an alternative tetrameric cubane structure $[C_6H_5OLi(THF)]_4$ **392b**.[399]

Lithiated aryloxides have been utilized as molecular secondary building units in the controlled assembly of metal–organic frameworks.[401] Although there are many examples of coordination polymers composed of *s*-block metals, these have normally been prepared inadvertently or in order to study the localized metrical parameters of a complex. Also, these polymers most commonly consist of isolated metal centers rather than linked aggregates. It was shown that pre-assembled tetrameric Li_4O_4 cubanes could be linked through the divergent didentate Lewis base 1,4-dioxane to generate a series of closely related 1D zigzag chains, 2D hexagonal sheets, and 3D diamondoid networks, with the general formula $[(ArOLi)_4(dioxane)_x]_\infty$ (where $x = 3$, 2.5, or 2). The Li_4O_4 cubanes act as either V-shaped, trigonal, or tetrahedral nodes depending on the number of bridging dioxane molecules present. It was found that the substitution pattern on the aromatic ring was critical in determining the dimensionality adopted by the polymer as a consequence of space-filling considerations. Similarly, sodium aryloxides that adopt molecular hexameric face-shared double cubane aggregates have been employed in network assembly.[402] In these instances, networks with the general formula $[(ArONa)_6(dioxane)_x]_\infty$ (where $x = 5$, 4, or 3) are formed where the aggregates act as linear nodes to form 1D chains, square-planar nodes to form 2D square nets, or octahedral nodes to form 3D primitive cubic networks.[402,403] As with their lithium counterparts, the substitution pattern on the aromatic ring is critical in determining the dimensionality of the resulting polymer.

Overall, the alkali metal alkoxide and aryloxide systems are excellent examples in demonstrating the effects of steric influences on both molecular aggregation and also on the nature of any extended network architecture adopted. The large database of O–M complexes that have now been identified has led to a good deal of predictability regarding the coordination chemistry of these species.

2.01.5.2 S–M, Se–M, and Te–M Bonded Complexes

Investigations into the alkali metal complexes of the heavier group 16 elements are not nearly as extensive as those concerned with O–M bound species. Nevertheless, structural investigations of S–M, Se–M, and Te–M complexes have grown rapidly over the past decade and an extensive review of the thiolates, selenolates, and tellurolates of the *s*-block elements by Ruhlandt–Senge is available.[404] Reviews specific to thiolates and tellurolates by van Koten and Arnold, respectively have also appeared.[8,405] A review on bis(amido)cyclodiphosphazane chalcogenides by Chivers includes details of complexes prepared using group 1 metals.[406]

Some notable contributions have appeared in this area since the COMC (1995) article and a selection of these will be put in context and briefly summarized. The S–M bonded complexes are the most studied of the heavier group 16 systems, with the first structural characterizations of thiolates appearing for the series MeSM (where M = Li, Na, and K) using powder diffraction methods in 1972.[407] This was followed by the first report of a single crystal structure in 1985 for the lithiated dimeric complex $[(Me_3Si)_2C(H)SLi(THF)_2]_2$ **393**.[408] However, it was as recently as 1991 that the first single crystal analyses of sodium and potassium thiolates appeared, namely $[2,4,6\text{-}(F_3C)_3C_6H_2SNa(THF)_2]_\infty$ **393** and $[2,4,6\text{-}(F_3C)_3C_6H_2SK(THF)]_\infty$ **394**.[409] Both complexes were found to be polymers; but whereas **393** adopts a 1D chain structure, complex **394** crystallizes as a polymeric ladder. The first single crystal analyses of rubidium and cesium thiolates were reported in 1996 as part of the homologous series of complexes $[2,6\text{-}(Trip)_2C_6H_3SM]_2$, where M = Li **395**, Na **396**, K **397**, Rb **398**, and Cs **399**.[410] This is a notable set of compounds as the entire alkali metal series of this ligand form isostructural M_2S_2 ring dimers. In these instances, the dimeric arrangements are stabilized due to the steric bulk of the ligand and also as a consequence of interactions between the metal centers and the aryl rings. Indeed, solvated monomers and M_2S_2 ring dimers are the most commonly encountered aggregation states in the solid state for alkali metal thiolates.[404] However, examples of M_3S_3 ring trimers,[410,411] M_6S_6 hexamers (double cubanes and cyclized ladders),[412,412a,412b,413,413a,413b] as well as various types of polymers[414,414a] are also known.

Far fewer structural studies have been conducted for the alkali metal chalcogenolates Se–M and Te–M. Nevertheless, the general aggregation patterns emerging are similar to those for S–M complexes, with solvated monomers and ring dimers being the dominant aggregation states for the reported structures.[404]

2.01.6 Mixed Metal Complexes

2.01.6.1 Introduction

This section surveys the rapid development which has occurred in the synthesis and structural analyses of mixed metal complexes in the 12 years since the publication of COMC (1995). The limited information which was available then on "ate" complexes has expanded into a more sophisticated understanding of how different metals gathered in a single complex influence the adopted structure and observed reactivity.

The basis for these developments lies not only in a natural scientific inquisitiveness for extending our knowledge of analogous unimetallic and homometallic systems, as discussed above, but derives from the increasing application of mixed metal systems in organic syntheses where highly unusual reactivities and selectivities are observed. These unusual properties can only be rationalized through a thorough investigation of the structural properties of the mixed metal complexes. Heterobimetallic complexes which contain one or more of the alkali metals are widely used in catalysis, as bases in deprotonation reactions, in conjugate addition reactions, and as ligand-transfer agents. It is known that the properties they exhibit in these roles can differ substantially from that observed for their component unimetallic parts. These complexes can be broadly placed in three categories. The first is traditional "superbase" mixtures, which have been developed and described by Lochmann and Schlosser.[415,416] Historically, these have been composed of two different anions, a carbanion in conjunction with an alkoxide, and two different metals, normally Li and K. However, this has since been extended to include other heteroatom and metal permutations including amides and group 2 metals. The second group are traditional "ate" complexes, such as aluminates and cuprates, which can exist as CIPs and solvent-separated ion pairs (SSIPs). New growth areas in this field include magnesates and zincates. Perhaps the most significant development in the last decade has come from Mulvey and co-workers who have developed and described the structural chemistry of a family of "inverse crown" complexes.[417] These were originally derived from group 1 and 2 heterobimetallic amides but have evolved to include alkyls and aryls, and thus become, in composition and structure, related to traditional superbases. These complexes have demonstrated some remarkable reactivity and selectivity toward aromatic substrates arising from a "synergistic" relationship between the metals themselves, and with the accompanying anions. One further structural breakdown which can be made is the difference between composite complexes which arise when each metal brings its own accompanying anion(s) into the newly formed heterobimetallic complex, and those where a single organic substrate is doubly metallated to provide a heterobimetallic dianion where each metal bonds with a different heteroatom.

In surveying the structural information available, several factors have become apparent which are important in explaining the structures which heterobimetallic complexes adopt. These include: (i) the lighter group 2 metals and those of groups 11–15 will preferentially form short, strong σ-bonds, while the alkali metals will balance σ- and π-bonding in forming longer weaker bonds; (ii) the structures of aggregates and clusters are primarily determined by the shorter, stronger, more covalent metal–carbon (heteroatom) bonds; and (iii) the atoms involved in these bonds are more likely to be found in the center of any clusters, while the heavier alkali metal cations are located in peripheral positions engaging in extensive π-bonding (where possible) and agostic bonding.

This section is limited to complexes which have a group 1 metal in conjunction with another, different main group metal, but also includes Cu and Cd since they exhibit properties akin to their main group analogs. It is also limited mainly to those complexes in which the metals find themselves attached to different atoms and there is a particular emphasis on compounds with alkali metal–carbon bonds of various types, except where the evolution of "inverse crown" complexes is discussed. There are many more heterobimetallic–heteroatom complexes (e.g., mixed metal amides), but these lie outside the scope of this current review though references may be found to them in the references for the complexes described herein.

2.01.6.2 Group 1

Though Wittig had reported the formation of diphenyllithiumsodium in 1958, structural confirmation of a mixed metal carbanionic species did not occur until 1988 when Weiss reported the structure of $[\{Na(TMEDA)\}_3\{LiPh_4\}]$ **400**, which crystallized from a 2.2 : 1 reaction mixture of PhNa/PhLi in hexane and TMEDA.[85,418] Attempts at preparing a 1 : 1 complex led to $[PhLi(TMEDA)]_2$ crystallizing preferentially. The Li cation is located in the center of the "ate" complex in a pseudo-tetrahedral environment coordinated by the four Ph anions with the three Na cations, coordinated by the TMEDA, forming an equatorial triangle around it. The mixed Na/Li benzyl complex, $[(PhCH_2)_4Li_{2-x}Na_{2+x}(TMEDA)_4]$ ($x = 0.33$) **401**, was described 6 years later and is formed from the metallation of an excess of toluene by ^{n}BuNa and ^{n}BuLi in the presence of TMEDA.[419] The structure has an eight-membered M_4C_4 ring, based on C_2-crystallographic symmetry, in which the Li and Na cationic sites are interchangeable in the crystal and are complexed by TMEDA. The

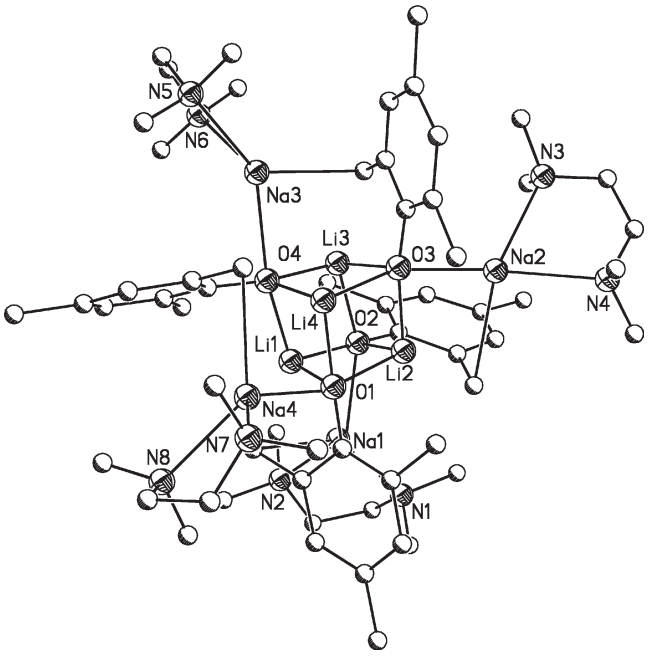

402

Figure 32 The structure of $[2,4\text{-}(Me)_2C_6H_3(CH_2)Na\}OLi(TMEDA)]_4$ **402**. Hydrogen atoms and arene contacts have been omitted for clarity.

first structure of a mixed Li/Na complex which had the "superbase" characteristic of two different metals being attached to different atoms (C–Na, O–Li), $[\{2,4\text{-}Me_2C_6H_3(CH_2)Na\}OLi(TMEDA)]_4$ **402** was achieved in 1993.[420] The tetrameric complex (Figure 32) established a breakthrough in that earlier attempts at mixing organolithium compounds with heavier metal alkoxides had invariably led to precipitation of the pure organosodium or potassium compounds. A fact which still plagues efforts today.

The complex, obtained from the reaction of sodium 2,4,6-trimethylphenoxide with butyllithium, crystallizes with S4 symmetry having a cubic core of eight Li–O bonds. These eight long and short bonds, familiar in ring stacking, dominate the structure with the Na^+ cations, coordinated by TMEDA, bridging the O^- and CH_2^- groups perpendicular to the aryl ring. Extensive *ab initio* calculations into the structure and stability of mixed alkali metal dimers, which could be implicated in "superbases," were described by Schleyer in 1996 indicating that the mixed aggaregates should be thermodynamically stable species.[421] Models for the mixed carbanion/alkoxide motif have been successfully extended to mixed metal carbanion/amide complexes. Based on *ab initio* calculations, which indicated that the formation of such mixed metal aggregates was only slightly less favorable than transmetallation, sodium methyl(4-methylbenzyl)amide was reacted with ^{n}BuLi in the presence of TMEDA to produce the intramolecular heterobimetallic complex $[\{Me(C_6H_3)CH_2N(Me)\}Na{\cdot}Li(TMEDA)]_4$ **403** (Figure 33).[422] Crystallizing as a tetramer, the structure has an aggregate core with Li cations arranged at the corners of a planar centrosymmetric arrangement with the triangular faces bridged by C^- ions. The Na cations lie external to the core and are only weakly bonded. Each Na bridges one amide and two aryl functionalities, almost perpendicular to the rings, and is coordinated by one TMEDA molecule.

Further intramolecular Li/Na and Li/K carbanion/amide clusters were formed on dimetallation of the chiral amine (S)-α-(methylbenzyl)allylamine with ^{n}BuLi and ^{n}BuNa(K) in hexane and THF, producing, respectively, the tetrameric chiral complexes $[\{(S)\text{-}\alpha\text{-}(PhC(H)Me)(CH_2CH{=}CHM)N\}Li(THF)]_4$ (M = Na, K) **404**, **405** (Figure 34).[423,424] The basic core structure of both the Li/Na and Li/K complexes is similar, being characterized by an inner distorted cubane core of C–Li bonds with the heavier alkali metals forming an eight-membered N_4M_4 outer chain. Analysis of the N–Li bond lengths (range 1.896(6)–1.937(6) Å) indicates that the complexes retain the bonding features of lithium amides. The Na cations sit on either side of the vinylic moieties interacting with the π-electron density. In the K complex, the K cations move further toward the amido N bonding with all available electron density in the allyl group. In the Na complex, each Na cation is complexed by a single THF molecule, while in the K complex there is competitive bonding between the π-(arene)-electrons and THF such that there are three different coordination

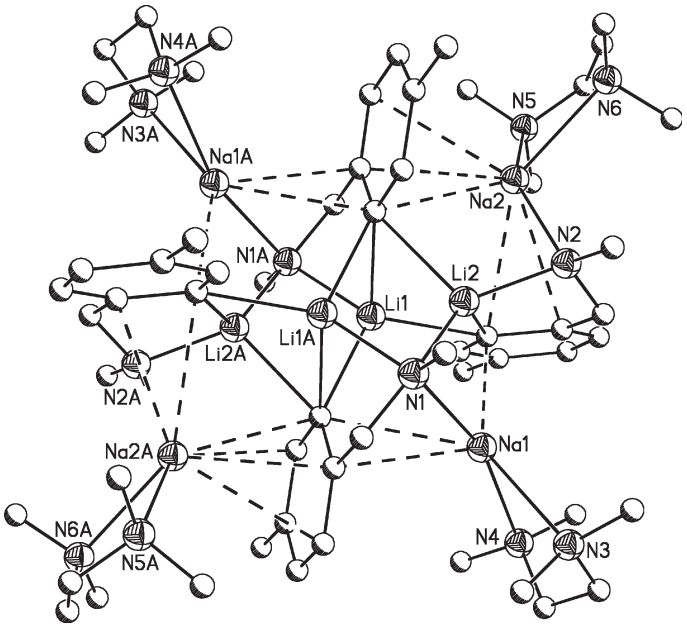

403

Figure 33 The structure of [{Me(C_6H_3)CH_2N(Me)}Na•Li(TMEDA)]$_4$ **403**. Hydrogen atoms have been omitted for clarity.

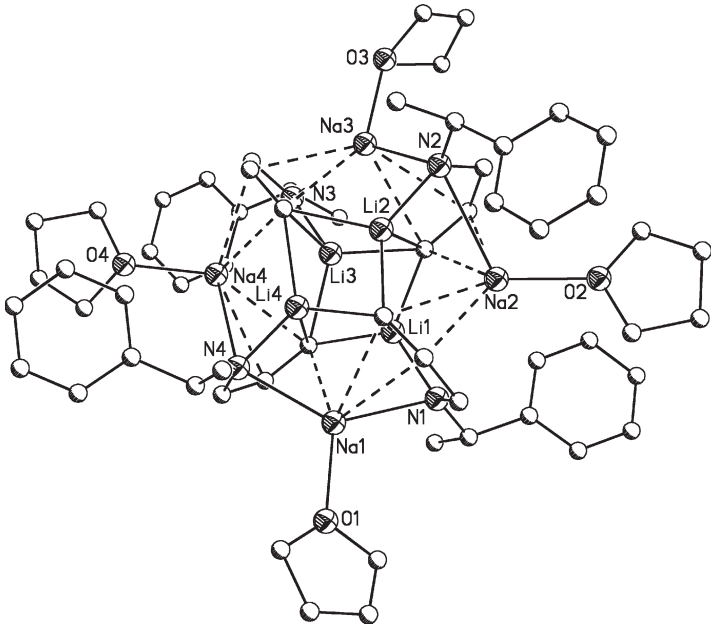

404

Figure 34 The structure of [{(S)-α-(PhC(H)Me)(CH_2CH═CHNa)N}Li(THF)]$_4$ **404**. Hydrogen atoms have been omitted for clarity.

environments for the four K centers: one is sandwiched between two aryl groups with no THF coordination, one has two coordinated THF molecules, while the third only has one.

The family of complexes which contain amide/alkoxide functionalities constitute the largest group. The reaction of lithium anilide with ^{t}BuONa, ^{t}BuOK, and TMEDA in a 2 : 1 : 1 : 2 ratio produced the remarkable trimetallic complex

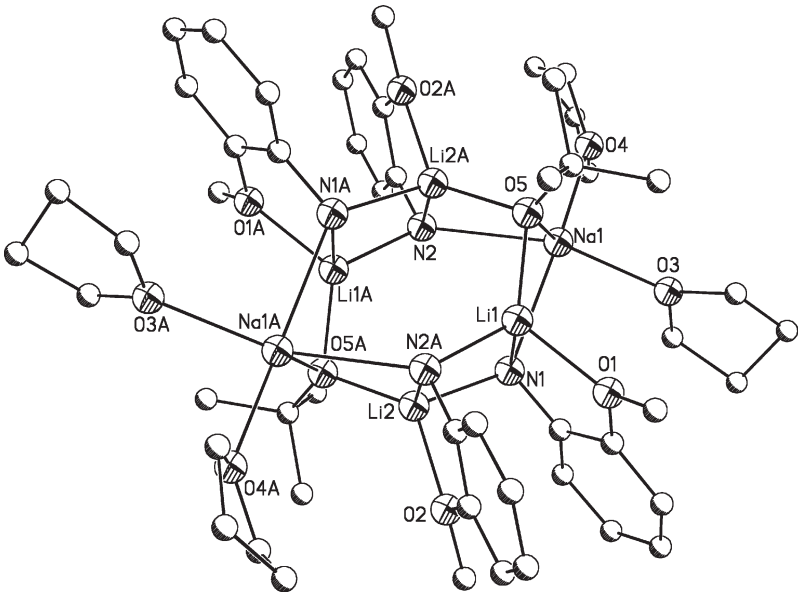

407

Figure 35 The structure of $[\{MeO(C_6H_4)N\}_2\{^tBuO\}NaLi_2]_2$ **407**. Hydrogen atoms have been omitted for clarity.

$[(PhN(H))_2(^tBuO)LiNaK(TMEDA)_2]_2$ **406**.[425] The centrosymmetric structure is composed of a 12-vertex cage in which two Li and two Na cations are four-coordinate in a distorted tetrahedron, while the K cations are six coordinate and octahedral. While Na binds only to N, the Li and K cations bond with 2N/2O and 4N/2O, respectively. In a now familiar pattern, the Li cations occupy the core while the structure periphery is comprised of a (K···N···Na···N···K···N···Na···N) cycle of atoms, though an alternative description is of a $(KO)_2$ ring sandwiched between two heterometallic (LiNNaN) rings.

The first structurally characterized hetero-bis-*s*-block amide/alkoxide complex, $[\{MeO(C_6H_4)N\}_2\{^tBuO\}NaLi_2]_2$ **407** (Figure 35), can be formed from the reaction of 2-methoxyanalidolithium with sodium *tert*-butoxide in THF.[426] The cyclic ladder structure arises from the fusing of four LiNNaO heterobimetallic rings and two Li_2N_2 rings. This provides for a CIP formed around a hexagonal prismatic core. The methoxyanalide molecules provide intramolecular bonding to only the Li cations. As such, each Li is four coordinate forming bonds with two amido groups, one alkoxide and one methoxy, while Na is five coordinate bonding with two amido groups, one alkoxide, and two THF molecules. The pentasodium–tetralithium mixed alkoxide/amide complex, $[\{PhN(H)\}_4(^tBuO)_4(OH)Li_4Na_5(4\text{-Me-Py})]$ **408**, was isolated and characterized through investigations into metal exchange reactions between *t*-BuONa and PhN(H)Li and with ^{t}BuOLi and PhN(H)Na.[427] The structure is of a 17-vertex dome comprised of three stages: a basal $(NaN)_4$ ring, a central smaller $(LiO)_4$ ring, and an apical Na. The OH^- anion from the adventitious NaOH occupies a central position. The sodium coordination sphere comprises one ^{t}BuO, two anilides, and one datively bound 4-Me-Py ligand, while that of Li comprises two ^{t}BuO, one anilide, and OH^-. The apical Na bonds to four ^{t}BuO (mean 2.557 Å) and the OH (2.349(5) Å). The Na cations in the base are situated orthogonal to the aryl rings implying significant π-bonding, while the Li cations are in plane and predominantly σ-bonded. A major step forward for this class of mixed metal, mixed anion, complexes was achieved when Mulvey *et al.* demonstrated that $[(^tBuN(H))_4(^tBuO)_4Li_4K_4]\cdot 3(C_6H_6)$ **409** (Figure 36) provides for a significant increase in basicity in the deprotonation/potassiation of toluene in comparison with the lithium amide alone.[428]

The formulation of this complex, based on the dissolution in benzene of the lithium amide and the potassium *tert*-butoxide, was provided from early observations by Lochmann on the atypical behavior of this mixture.[429] The centrosymmetric structure is constructed around four metal–heteroatom dimeric rings arranged in two pairs. The symmetry in the molecule places 2 equiv. $(LiN)_2$ rings parallel to each other in the center and perpendicular to two terminal $(KO)_2$ rings. All these rings bisect a ring plane defined by Li_4O_4. One benzene molecule binds η^6 to one K center in a terminal manner, while another is sandwiched between two K cations in an η^3 fashion providing for polymer formation by linking the discrete heterobimetallic clusters. As with the majority of clusters discussed, the structure is organized around the more covalent Li–O bonds.

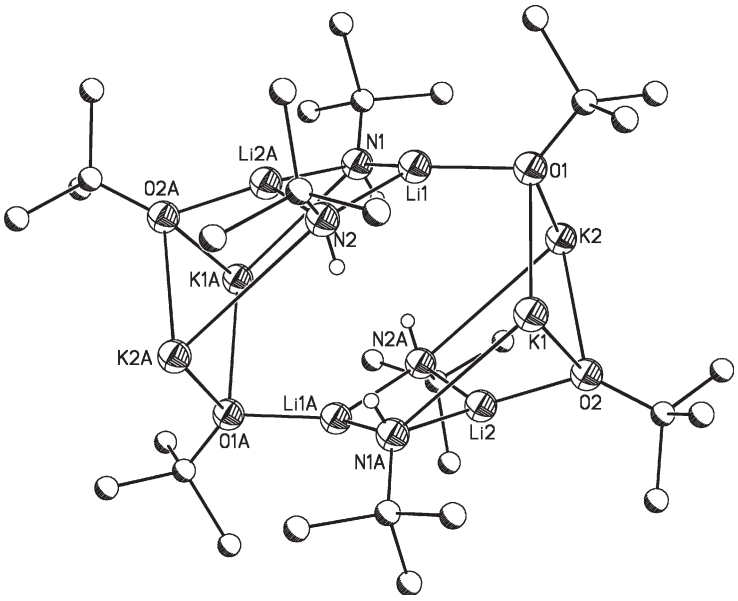

409

Figure 36 The structure of $[(^tBuN(H))_4(^tBuO)_4Li_4K_4]\cdot 3(C_6H_6)$ **409**. Benzene molecules and hydrogen atoms, except N–H have been omitted for clarity. Agostic interactions between potassium and ^{t}BuO are not shown.

2.01.6.3 Group 1/Group 2

In extending the development of "inverse crown" mixed metal amides beyond simple oxo and peroxo encapsulation, Mulvey and co-workers discovered that benzene and toluene can be dimetallated by a compound derived from the 1 : 1 : 3 reaction of ^{n}BuNa, Bu_2Mg, and TMPH in hydrocarbon media.[430] The two new hexanuclear "guest–host" complexes produced, $[(TMP)_6Na_4Mg_2(L)]$ (TMP = 2,2,6,6–tetramethylpiperidide; L = C_6H_3(Me) **410**, C_6H_4, **411**), are isostructural (if the Me on tolyl is ignored). The arene group sits perpendicular to, and in the center of, a 12-membered severely puckered $Na_4Mg_2N_6$ ring. In a remarkable result, the toluene dianion rather than being stabilized in the most thermodynamically stable benzylic form, is metallated at the *o*- and *m*-positions. Geometry-optimized *ab initio* calculations hinted at the unusual metallating power of the mixed metal amide in that the observed dianion is 14 kcal mol^{-1} less favorable than that of a benzylic dianion. Mg forms two σ Mg–C bonds with the arenes, while the Na cations are π-bonded. The replacement of Na with K produced two expanded, and unprecedented, 24-membered hexapotassium, hexamagnesium ring complexes $[(TMP)_{12}K_6Mg_6(L)_6](L')_n$ (L = C_6H_5, L′ = C_6H_6, n = 5.07; L = C_6H_4(Me), L′ = C_6H_5(Me), n = 2.15) **412**, **413**.[431] While reaction with benzene and toluene again led to smooth deprotonation, this produced isostructural complexes but with only monoanionic arenes. Rather than being host molecules the phenyl and tolyl anions are attached around the heterobimetallic puckered ring by *ipso* C–Mg σ-bonds and C–K π-interactions (μ-η3 : η2, bond range 3.009–3.354 Å). A series of *d*–block metallocenes were the next target molecules for reaction with the mixed metal bases resulting firstly in the isolation of $[\{Fe(C_5H_4)_2\}_3\{(TMP)_2(TMPH)_2\}Na_2Mg_3]$ **414** from the reaction of $[(TMP)_6Na_4Mg_2\{C_6H_3(Me)\}]$ with ferrocene, TMPH being available for coordination through metallation of the ferrocene molecules.[432] The three distorted tetrahedral Mg centers glue together the three 1,1′-ferrocenediyl units. The coordination sphere of the central Mg is fully occupied through bridging with all three ferrocene dianions, while the two "terminal" Mg ions are three coordinate with respect to the ferrocene units with the fourth coordination site being engaged with two almost planar {C–Mg–N(TMP)–M} (M = Na or Li) rings. Lithium forms an analogous structure, though with pyridine replacing TMPH as the coordinating base **415**. Replacement of TMPH with $(^iPr)_2NH$ in the initial formation of "$[\{(^iPr)_2N\}_3NaMg]$" resulted in the tetradeprotonation of ferrocene at the 1,1′,3,3′ positions to give $[\{Fe(C_5H_3)_2\}\{(^iPr)_2N\}_8Na_4Mg_4]$ **416**.[433] The 16-membered host of alternating N–M–N–M′ (M = Li, M′ = Mg) atoms surrounds the out-of-plane ferrocenyl tetraanion which is tethered in place by Na–C and Mg–C bonds. Two of the Na cations sit above the two opposing arene rings bonding with the π-electron density, while the other two form an η^2-bridging arrangement (mean 2.67 Å). The short, strong Mg–C bonds (mean 2.153 Å) are no longer in plane with the aromatic rings

but tilt away due to steric requirements imposed by the large ferrocenyl guest, still suggesting though, that it is Mg rather than Na which acts to deprotonate the ferrocene. This reaction protocol was subsequently applied to the analogous metallocenes of Ru and Os with similar results **417**, **418**.[434]

Searching for further "inverse crown" complexes, the same group investigated variations in the amide bases and the metals, and produced a series of "ate" complexes, all of which are CIPs involving substantial agostic bonding (Si–Me···M) which, in the absence of traditional Lewis donors, is mediated by the strength of competing solvation of the alkali metal centers by typical arene solvents.[435] The complexes correspond to the general formulas $[(Ar)_2K][ML_3]$ (L = $(SiMe_3)_2N$; M = Mg, Ar = benzene **419**, toluene **420**, or *p*-xylene **421**; M = Zn, Ar = *o*-xylene **422**), $[(toluene)_3Rb][ML_3]$ (L = $(SiMe_3)_2N$, M = Mg **423** or Zn **424**), $[(Cp)K_2][ZnL_3]$ **425**. It was inferred that the low basicity and steric bulk of the trimethylsilylamido anion favors distinct triamidometallate anion formation rather than bridging [M(amide)$_2$X] fragments. However, this was not observed in the formation of the unsolvated Li/Ca complex, $[\{(Me_3Si)_2N\}\{\mu\text{-}N(SiMe_3)\}_2CaLi]$ **426**,[436] a heterobimetallic monomer which contains a four-membered Ca–N–Li–N ring and significant SiMe···M agostic bonding. These interactions arise only from various Me groups on the bridging amides (Me···Li 2.368(4) and 2.413(4) Å; Me···Ca 2.831(2) and 2.859(2) Å) and not from the terminal one attached solely to Ca, and it is thought that these interactions hinder the formation of an "inverse crown" structure. Analogous solvent-free and TMEDA complexes were isolated from further reactions of ^{n}BuM (M = Na or K) and Bu_2Mg with $(^{i}Pr)_2NH$.[437] $[\{(^{i}Pr)_2N\}_3MMg(TMEDA)]$ **427**, **428** are isostructural monomeric dinuclear complexes with TMEDA bonding to the alkali metal center. In contrast, the solvent-free complex, $[\{(^{i}Pr)_2N\}_3KMg]_\infty$ **429** (Figure 37), is polymeric; the monomers being linked through the terminal amide on the Mg by K···N···Mg bridges. The K cations in both complexes engage in agostic bonding; K···C range in the TMEDA complex is 3.277(2)–3.475(2)Å, while in the polymer there are a greater number of these bonds and they are on average shorter, 3.126(2)–3.285(2) Å.

"Inverse crown" complexes, though being heterobimetallic, are usually formed with only one type of amide. Introducing two different amines by reacting BuLi, HMDSH, Bu_2Mg, and TMPH resulted in the mixed metal, mixed amide, carbanion/amide complex, $[(Me_3Si)N(Me_2SiCH_2)(TMP)LiMg]_2$ **430**.[438] This could also be synthesized from $(TMP)_2Mg$ and LiHMDS. The dimeric structure is formed from two dinuclear (LiNMgN) fragments with pendant Me_2SiCH_2 arms. The TMP moieties bridge the Li and Mg centers while the anionic CH_2^- groups bind to Mg acting to bridge the heterobimetallic "monomeric" units. It is assumed, as in previous analogous reactions, that deprotonation occurs via the Mg base (in this case $Mg(HMDS)_2$). The distorted tetrahedral environment of the Mg is comprised therefore of 2N and 2C atoms while Li raises its formal two-coordinate environment by forming agostic bonds with Me groups on TMP. Deprotonation of an Me_3Si group was also observed in the formation of the first mixed Li, Mg, K *N*-metallated/*N*,*C*-metallated amide, $[\{^{t}Bu(Me_3Si)N\}_4\{^{t}Bu(Me_2SiCH_2)N\}_4Li_2K_2Mg_2]$ **431**,[439] which is described as an "inverse crown" complex with a vacant cavity. Li inclusion was initially fortuitous arising from incomplete ^{n}BuK synthesis though the complex could be reproduced by deliberate inclusion of ^{t}BuOLi and using $PhCH_2K$ as a weaker potassium base. The 16-membered primary crown-like ring of $(N_4Mg_2LiK)_2$ has four appended six-membered (MgCSiNLiN) secondary rings. These are arranged in two transannular sets of two. In contrast to the previous structure where the $SiCH_2^-$ units act to bridge two Mg atoms, in this it is the K cations which play this role.

In a deliberate attempt to trap the carbanion/amide intermediates formed en route to the homoamido inverse crown complexes, $[\{(TMP)(\mu\text{-}Bu)(\mu\text{-}TMP)NaMg(TMEDA)\}]$ **432** (Figure 38) was isolated and characterized.[440] This complex spans the "superbase" and "inverse crown" structural modalities.

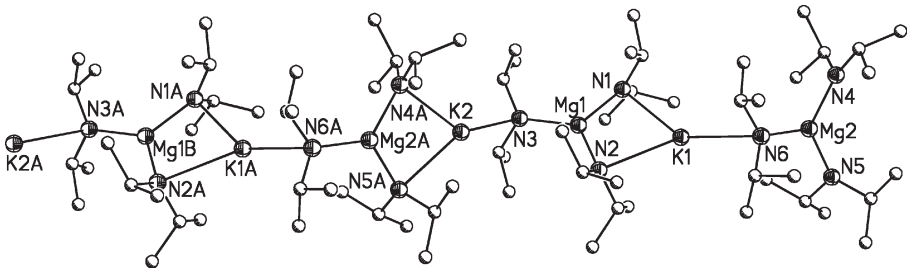

429

Figure 37 The structure of $[(^{i}Pr)_2N_3KMg]_\infty$ **429**. Hydrogen atoms have been omitted for clarity. Agostic interactions between potassium and methyl groups are not shown.

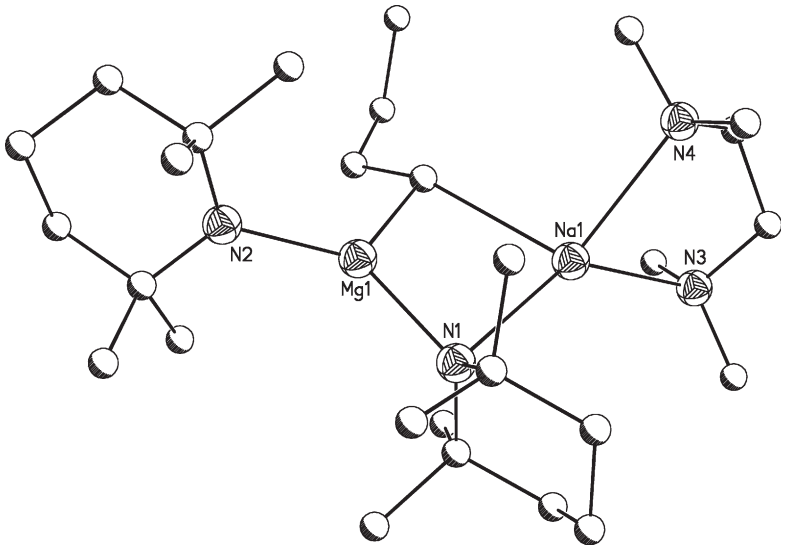

432

Figure 38 The structure of [{(TMP)(μ-Bu)(μ-TMP)NaMg(TMEDA)}] **432**. Hydrogen atoms have been omitted for clarity.

The gross structural features are typical of the dinuclear puckered ring complexes described above, though one of the bridging amides is replaced by the bridging carbanion; however, it can also be described as having a highly covalent trigonal planar framework around the Mg center with Na^+ then bonding electrostatically to one triangular edge. The terminal amide resides on Mg while Na is complexed by TMEDA. Reaction of the complex with benzene allowed for replacement of the Bu^- anion and formation of [(TMP)(μ-TMP)(μ-C_6H_5)NaMg(TMEDA)] **433**.[440]

The mixed K/Ca amide complex, [$(HMDS)_3$KCa(THF)] **434**, which is structurally analogous to the dinuclear amide complexes described above, was reacted with the ketone Mes(Me)C═O resulting in the 2:2 and 2:1 enolate complexes, [{Mes(H_2C=)CO}$_6$$K_2$$Ca_2$$(THF)_2$] **435** and [{Mes($H_2$C=)CO}$_4$$K_2Ca(THF)_4$] **436**, respectively.[441] The 2:2 THF-deficient structure **435** is comparable with the family of "inverse crowns". The Ca centers are pentacoordinate bonding with four enolate anions and a THF molecule, while in the 2:1 complex **436** the Ca centers raise their coordination number by binding with an additional THF. Surprisingly, the K cations in both complexes bond only very weakly with the O atoms of the anions though this is most pronounced in the 2:1 complex where the K–O(enolate) distances are 2.762(3)–2.852(3) Å. The bonding distance to THF is shorter at 2.697 Å. However, all the K cations also engage in additional π-interactions with surrounding alkenes and arenes with K···C distances of approximately 3.5 Å.

Mixed carbanion/alkoxide complexes were formed from combining $^{n,s}Bu_2Mg$, ^{t}BuOM (M = Na or K), and TMEDA to form the dimeric CIPs $[(Bu)_2(^tBuO)MMg(TMEDA)]_2$ (M = Na and K) **437**, **438**.[442] While the two structures are identical in their atom connectivity, they are not precisely isostructural in that K shows a bias toward C-coordination while Na is inclined toward N. The alkali metal cations are both formally five-coordinate bonding with two α-C(Bu) atoms, two N(TMEDA) atoms, and a single O(^{t}Bu) atom. The dominant feature in both structures though is the $[(Bu)_2Mg(\mu\text{-}^tBuO)_2MgBu_2]^{2-}$ dianion.

2.01.6.4 Group 1/Group 11

Due to their synthetic importance, substantial effort has been directed at both the synthesis and structural characterization of alkali metal cuprates. Formed from the reaction of organolithium compounds with Cu(I) salts, these complexes can exist as either CIPs or SSIPs dependent, as Boche has demonstrated,[443] on the strength of the solvating ligands which attach to the lithium cations. They showed that while [{Li$(DME)_3$}{Me_2Cu}] **439** (Figure 39a) and [{Li$(DME)_3$}{$(Me_3Si)CH_2)_2$Cu] **440** exist as SSIPs, the presence of weaker donors such as Et_2O and Me_2S provides for CIP structures: [{{$(Me_3Si)CH_2)_2$CuLi}$_2$$(Et_2O)_3$] **441** (Figure 39b) and polymeric [{$(Me_3Si)CH_2)_4Cu_2Li_2(Me_2S)_2]_\infty$ **442**.[443] The Li cations in the DME complexes are hexacoordinated, which is very unusual for Li, with the shortest separation between Li and C being 5.8 and 6.0 Å. The anions contain essentially linear C–Cu–C bonds. The diethyl

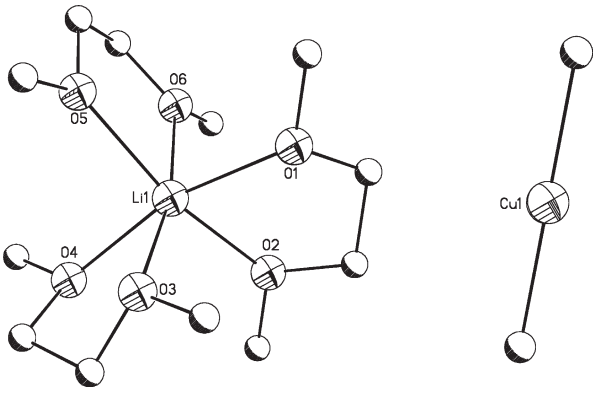

439

Figure 39a The structure of [{Li(DME)$_3$}{Me$_2$Cu}] **439**. Hydrogen atoms have been omitted for clarity.

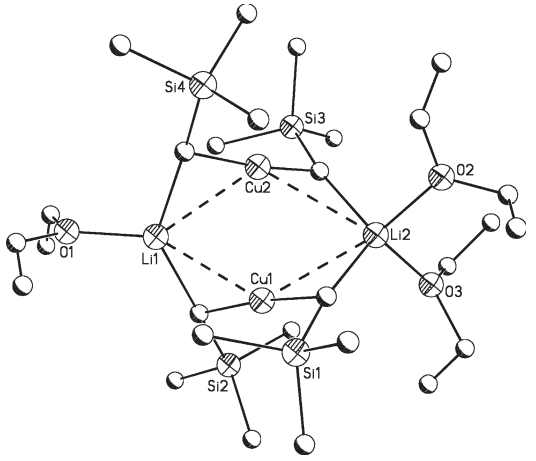

441

Figure 39b The structure of [{{(Me$_3$Si)CH$_2$}$_2$CuLi}$_2$(Et$_2$O)$_3$] **441**. Hydrogen atoms have been omitted for clarity.

ether complex is a dimer with the cuprate anions being held together by the Li cations (Li–C bond range 2.199–2.312 Å). Though one of the Li cations is bonded to one Et_2O and the other to two Et_2O molecules, they prefer to include the α-$C^{\delta-}$ atoms in their coordination sphere rather than becoming saturated with Et_2O molecules. A similar arrangement is found in the dimethylsulfide complex where the Li ions contribute to a six-membered {Li–C–Cu–C–Li–C–Cu} rings; however, the DMS molecules bridge the Li cations binding separate ring together into a polymeric CIP structure. Weiss reported the first structure of a lithium alkynylcuprate in 1993, $[(PhCC)_{10}Cu_4Li_6(Et_2O)_3]$ **443**.[444] The tetracuprate is composed of two units, the first involves a tetrahedral tetracoordinated Cu center in a $[(PhCC)_4Cu]^-$ anion, which sits above a basal 11-membered heterobimetallic ring ($Li_3Cu_3C_5$) resembling a crown on a threefold axis. The Li cations are also tetrahedral, each coordinated by an Et_2O molecule and three α-C atoms: two from the basal ring and a third from the second unit. This second unit also sits on a threefold axis comprised of a six-membered puckered Li_3Cu_3 ring in which the three Li cations bridge the three [PhCC-Cu-CCPh]$^-$ anions through all the α-C atoms. van Koten has used achiral and chiral aryl ligands with pendant amines to structurally characterize CIPs of general form [{L_2Cu}{Li_2Br}] (L = $C_6H_4(CH_2N(Me)CH_2CH_2NMe_2)$ **444**, 1-$C_{10}H_6(CH_2N(Me)CH_2CH_2NMe_2)$ **445**, (*R*)-$C_6H_4(CH(Me)N(Me)CH_2CH_2NMe_2)$ **446**, *rac*-$C_6H_4(CH(Me)N(Me)CH_2CH_2NMe_2)$ **447**, which are composed of six-membered central (Li_2CuC_2Br) rings in which the coordination environment of each Li cation is formed by two intramolecularly bonding amine N's, one i*pso*-C, and Br.[445] The chiral analogs were only observed in solution but were determined to provide excellent examples of highly specific enantioselective recognition in the aggregation of the lithium

cuprates. This ligand-type (specifically $C_6H_4(CH_2N(Me)CH_2CH_2NMe_2)$) was also successfully incorporated into the first structurally characterized mixed anion (aryl/alkynyl) lithium cuprates formed on reaction of LLi with $(RCC)_2Cu$ in toluene (R = *p*-C_6H_4Me **448**, *p*-$C_6H_4SiMe_3$ **449**).[446] In fact, each structure of $[L_2(RCC)_2Cu_2Li_2]$ contains two different organic homocuprate moieties, $[L\text{-}Cu\text{-}L]^-$ and $[(RCC)\text{-}Cu\text{-}(CCR)]^-$, which are orthogonal to each other and bound together by the Li cations bridging the C_{ipso} of the aryl and the α-C of the alkynyl. The tetrahedral coordination environment of each Li is completed by two intramolecular N atoms. Analysis of the bond lengths suggested little or no interaction of Li with the π-electron density of the alkynyl and that the heterobimetallic interaction with the α-C could be described as 3c–2e μ_2–η^1. However, ^{13}C NMR revealed significant interaction of lithium with the β-C suggesting that the best description is intermediate between μ_2-η^2 and μ_1-η^2.

The importance of alkali metal binding with available π-electron density in the formation of CIPs was also demonstrated by Niemeyer in the structural elucidation of the first monomeric non-solvated lithium cuprate, [(2,6-$Mes_2C_6H_3)_2CuLi$] **450**, formed from the reaction of 2 equiv. of (2,6-$Mes_2C_6H_3$)Li with *t*-BuOCu in pentane.[447] The complex crystallizes as two different independent molecules in which the C–Cu–C angles differ (171.1° and 173.8°) as does the mode of coordination to the Li cations; C_{ipso} and η^6 to one pendant Ph in molecule 1, with an additional η^3 interaction to a second Ph group in molecule 2. In the second molecule, the Li site is 10% occupied by a Cu ion.

2.01.6.5 Group 1/Group 12

Reaction of $ZnCl_2$ with a series of 1,4-dilithiated butane derivatives, with various substitutions of the four backbone carbons, produced a plethora of metallocyclic CIP lithium zincate complexes of which $[\{CH_2CH(Me)CH_2CH_2\}_2ZnLi_2(TMEDA)_2]$ **451** was structurally determined by single crystal X-ray diffraction.[448] Two independent molecules exist in the crystal differing only in the twist of the butyl chains. The tetrahedral Zn center is σ-bonded with the four terminal carbons of the two butyl groups (Zn–C range 2.098(5)–2.141(4) Å), while each Li cation bonds with two α-carbons (Li–α-C range 2.279(8)–2.316(8) Å) and one bidentate TMEDA molecule. Thus, the core of the complex can be considered as four fused rings: two (C_4Zn) and two (C_2LiZn). The same author later reacted 2 equiv. of $ClCH_2Si(Me_2)Si(Me_2)CH_2Cl$ with 8 equiv. of Li metal (with 1% Na) and $ZnCl_2$ in a one-pot reaction to produce an isostructural complex, $[(CH_2Si(Me_2)Si(Me_2)CH_2)_2ZnLi_2(TMEDA)_2]$ **452**, though the inclusion of the two silyl groups substantially raised the thermal stability of the complex over its butyl analogs.[449] van Koten also successfully prepared and described the homoleptic intramolecularly stabilized 1:1 and 1:2 lithium zincates $[(C_6H_4CH_2NMe_2)_3ZnLi(THF)]$ **453** and $[(C_6H_4CH_2NMe_2)_4ZnLi_2]$ **454**.[450] The 1:1 THF-solvated monomeric CIP complex **453** contains a tetrahedral Zn center with a coordination environment comprised of three σ-Zn–C_{ipso} bonds (mean 2.049 Å) and a dative Zn–N bond. The tetrahedral Li cation is joined with the anionic unit through one of the C_{ipso} atoms (Li–C 2.414(6) Å), the two remaining Me_2N groups, and, finally, one THF molecule. The non-solvated 2:2 complex, **454**, is a monomeric dilithium tetraarylzincate. All four aryl ligands are bound to the tetrahedral Zn center by four similar η^1–μ^2–C_{ipso} bonds. Each Li cation bonds to two of the bridging C_{ipso} atoms and two of the pendant Me_2N atoms. The Zn center adopts an in-plane arrangement relative to all the aryl rings highlighting the strong σ-bonding while the Li cations approach a perpendicular orientation to the rings (range 71.5–72.9 Å) establishing more π-bonded character.

Wheatley and co-workers had established that lithium aluminates formed from N-2-pyridylaniline could act to trap an H^- anion in the center of a cationic lithium amide cage (See the next section).[451] On replacing the anilide with the non-aromatic amine bicyclic 1,3,4,6,7,8-hexahydro-2*H*-pyrimido[1,2-*a*] pyrimidine (hppH) they were able to generate the ion pair $[\{(hpp)_6Li_8(H)\}^+\{^tBu_3Zn\}^-]$.(0.5 toluene) **455** from the reaction with Me_2Zn followed by 1.5 ^{t}BuLi.[452] The cationic cluster contains a cubic array of Li atoms which bond η^8 to a central H^- (mean 2.16 Å; cf. LiH, 2.04 Å). Each of the cubic faces is bridged by the hpp^- anions which delocalize the negative charge over all three N's. The three-coordinate Zn atom in the counter anion adopts a trigonal planar arrangement.

Extending their work on inverse crown complexes to Zn, Mulvey *et al.* discovered the exceptional reactive synergism which can be achieved from mixed metal complexes when they showed that the potassium zincate "$[(HMDS)_3ZnK]$" deprotonates toluene, *m*-xylene, and mesitylene when neither KHMDS nor $Zn(HMDS)_2$ is able to achieve this.[453] The resulting polymeric complex from the reaction with toluene, $[(HMDS)_2(PhCH_2)ZnK]_\infty$ **456**, is comprised of four-membered rhomboidal heterobimetallic amide rings (N_2KZn) joined through K···π(arene) bonds (range 3.02–3.43 Å). K also forms two short agostic interactions with SiMe (3.082 and 3.089 Å) and completes its coordination environment with two bridging amide N's. In studying whether mixed anion alkali metal zincates behave as carbanion or amide bases, the same group synthesized and structurally characterized the first sodium zincate $[(^tBu)(\mu\text{-}^tBu)(\mu\text{-TMP})ZnNa(TMEDA)]$ **457** from the reaction of $^tBu_2Zn$ and TMPNa in the presence of TMEDA.[454] The complex contains an unusual five-membered central ring resulting from Na···H_3C–$C(Me)_2$ bridging interactions from one of the ^{t}Bu groups (Na–C

agostic, 2.750(10) Å). The closest analogous complexes are $[(Me_3SiCH_2)_2\{\mu\text{-}(Me_3Si)_2N\}ZnLi(tmta)]$ **458** and $[(^nC_5H_{11})_3ZnNa]_2$ **459**; however, these adopt different open- and bicyclic structures, respectively.[455,456] Reaction of the mixed carbanion/amide zincate with benzene resulted in $[(^tBu)(C_6H_5)(\mu\text{-TMP})ZnNa(TMEDA)]$ **460**, which adopts the more common structural motif of a four-membered ($NaC_{ipso}ZnN$) ring, though this complex contains three different anionic ligands since deprotonation has displaced a $^tBu^-$ rather than the expected TMP^-. The remaining ^{t}Bu sits terminal on Zn which in turn displays the usual σ-bonded in-plane arrangement with the Ph group. The Na–π(Ph) bond distance of 2.706(3) Å is only marginally shorter than that to the *t*-butyl Me group that it replaced.

The homoleptic sodium zincate $[\{2,6\text{-}(Ph)_2C_6H_3O\}_3ZnNa(H_2O)]$ **461** was obtained from combining the Na and Zn salts of the phenoxide in diethyl ether.[457] The Zn center has distorted tetrahedral geometry from three phenoxide ligands and one water molecule. In addition the Na cation bonds with the three phenoxide O atoms as well as π-bonds with one of the pendant Ph substituents on each of the three phenoxide ligands, allowing it to become six coordinate. A different reaction protocol involving the phenol, $ZnCl_2$, and NaHMDS resulted in the 2 : 1 complex $[\{2,6\text{-}(Ph_2)C_6H_3O\}_4(Cl)Zn_2Na(THF)_3]$ **462**. There are two different pseudo-tetrahedral environments for the Zn centers. While the coordination environments of both are defined by one terminal and two bridging phenoxides they differ in having a single THF molecule bound to one and Cl to the other. The Na cation bonds with the Cl anion and also coordinates to one Ph group in a η^6 manner and two THF molecules.

A series of heteroleptic carbanion/alkoxide alkali metal zincates and siloxides have been prepared from the reaction of Me_2Zn with MOR (M = Li, Na, K; R = ^{t}BuO, Me_3Si).[458] All the structures of $[(^tBuO)_2(Me)ZnLi(THF)]_2$ **463**, $[(^tBuO)_2(Me)ZnNa(THF)]_2$ **464**, $[(Me_3SiO)_2(Me)ZnK(THF)_2]_2$ **465**, and $[(Me_3SiO)_3ZnK(TMEDA)]_2(THF)$ **466** (Figure 40) contain distorted cubic heterobimetallic alkoxide cores, though complete removal of the Me groups from the Zn atoms in the final complex causes an extension of the cube to include an additional $[(Me_3SiO)_2K(TMEDA)]$ fragment. The Lewis donor molecules THF and TMEDA bind only to the alkali metal centers. The solvent-free potassium complex $[(^tBuO)_4(Me)_3Zn_3K]_\infty$ **467**, formed from refluxing in toluene, has the distorted cubic bimetallic alkoxide "monomeric" cores linked through agostic K···MeZn interactions (2.9–3.1 Å).

Crystals of the cadmate $[\{HMDS\}_2\{PhN)_3C\}CdLi_2(THF)_3]$ **468** were characterized on isolation from combining $Cd(HMDS)_2$ with 1,2,3-dilithio triphenylguanidine in THF.[459] The complex contains three different metal coordination environments. The Cd center is trigonal planar attached to two HMDS groups, and the N atom of the guanidine group, which causes an elongation of this N–C bond in the guanidine. One of the Li cations is coordinated by two THF molecules and achieves a five-coordination environment through additional bonding to one of the

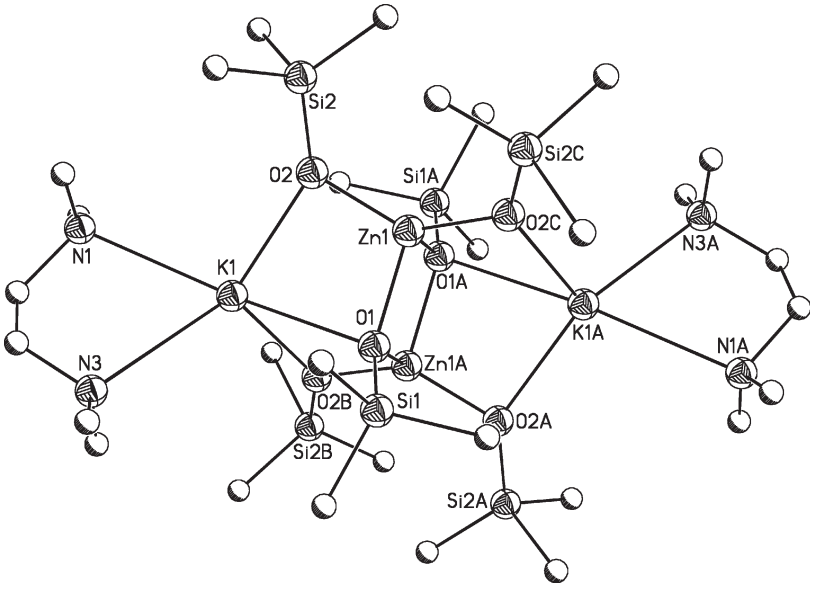

466

Figure 40 The structure of $[(Me_3SiO)_3ZnK(TMEDA)]_2(THF)$ **466**. Hydrogen atoms have been omitted for clarity.

guanidine N′s and the C_{ipso} and *o*-C of one of the Ph groups. The second Li cation bonds to three N atoms, two from guanidine and one from HMDS. Its fourth coordination site is occupied by a single THF molecule.

2.01.6.6 Group 1/Group 13

This constitutes perhaps the largest and most established group of heterobimetallic main group complexes and is structurally dominated by CIP "ate" species. The complexes which are described in this section provide insight into the development of this area over the past decade focusing on the formation of new types of compounds and/or bonding motifs. While this does not provide an exhaustive catalog it does establish lead reference points for more routine structural analogs. From an organometallic viewpoint, by far the most studied are those with mixed C and N ligand bonding to the metals.

In developing comparisons with the bulky $(Me_3Si)_3C^-$ anionic ligand Power and co-workers investigated the complicated behavior of the isoelectronic analogs $[(Me_3M)(Me_3Si)_2N]^-$ (M = Al **469**, Ga **470**).[460] Me_3M was reacted with LiHMDS in toluene to produce the isostructural CIP complexes $[(Me_3M)(Me_3Si)_2NLi]_\infty$ as polymers in which the "monomers" are linked through the Li^+ cations forming bridging agostic bonds with the one Me group in each of the datively bound Me_3M moieties (M = Al; Li–C, 2.252(8), 2.157(8) Å; M = Ga, Li–C 2.233(13), 2.205 (Å)). The fact that the M–N bond is dative, in comparison with the traditional covalent C–Si bond in the analogous carbanion complex allows more flexibility for the ligands to maximize their interactions with the Li centers. The reaction of $LiAlMe_4$ with $\{(^iPr)_2CH_2Me_2Si\}_2NLi$ or 4MeLi with $\{(^iPr)_2CH_2Me_2Si\}_2NAlCl_2$ produced the C_2-symmetric 2:2 dimer $[\{(^iPr)_2CH_2Me_2Si\}_2NLi.LiAlMe_4]_2$ **471**.[461] The cationic Li centers are in distorted tetrahedral environments with one being coordinated by two phosphine ligands, one amide (N–Li 2.075(8) Å), and forming additional agostic interactions with one Me group in an $[Me_4Al]^-$ unit, whereas the second Li center bonds to the amide group (N–Li 1.988 Å) and with three of the Me groups on a second more closely bound $[Me_4Al]^-$ unit.

Wheatley has produced a series of papers on the inclusion of mixed organic ions in heterobimetallic Li/Al systems which can act to encapsulate small ions or molecules in cage structures. The reaction of dimethyl-2-pyridylanilidoaluminum with 1.5 equiv. of ^tBuLi in toluene resulted in the ion pair $[\{(2\text{-pyr})(Ph)\}_6(H)Li_8][\{(^tBu)_2Me_2Al\}_2Li]$ **472** (Figure 41) in which an H^- anion is trapped in the center of an octameric lithium amide cage.[462] The Li cations form a distorted cube whose six faces are straddled by the N–C–N backbone of the amide. The presence of the hydride was deduced from the difference map and from charge balance; however, it was later confirmed by using the very intense vertical-axis neutron Laue diffractometer at 1.5 K.[463] The Li···H bonding is asymmetric, with a range of distances of 1.92–2.07 Å for the seven bonding Li cations and 2.86 Å for one which is non-bonding. The mixed metal counter anionic unit $[\{(^tBu)_2Me_2Al\}_2Li]$ typically has two four-membered (C_2AlLi) rings joined by the four-coordinate central Li ion. The Me moieties bridge the metal centers while the ^tBu groups are terminal on the Al. Reaction of the starting aluminum amide with ^{n} or ^{s}BuLi in THF resulted in the lithium amide $[(Ph(2\text{-pyr})N)_6(H)Li_7]$ **473** alongside $[Li(THF)_4][\{(R)_2Me_2Al\}_2Li]$ (R = ^{n}Bu **474**, ^{s}Bu **475**), while with MeLi it gave [(Ph(2-pyr)N)Me_3AlLi] **476**.[462] The reaction with LiHMDS in toluene produced the CIP lithium aluminate polymer $[\{Ph(2\text{-pyr})N\}(HMDS)Me_2AlLi]_\infty$ **477** whose monomeric units contain Li and Al bridged by HMDS and by the Ph(2-pyr) unit which uses its amido N to bind with Al and the pyridyl N to bond with Li, thus forming a five-membered ring.[464] These monomers are then linked through the intermolecular agostic interaction of Li^+ with Me groups on the aluminum. This complex, though stable in toluene,

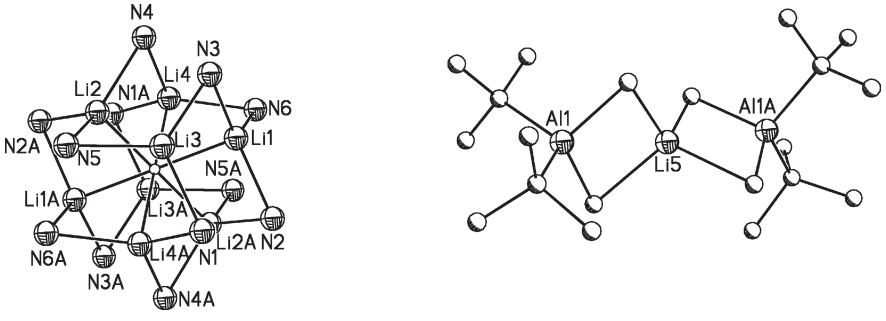

472

Figure 41 The structure of the anionic fragment $[\{(2\text{-pyr})(Ph)\}_6(H)Li_8][\{(^tBu)_2Me_2Al\}_2Li]$ **472**. Hydrogen atoms have been omitted for clarity. Only the core structure of $[\{(2\text{-pyr})(Ph)\}_6(H)Li_8]$ has been shown.

oxygenates in THF to produce $[\{(Ph(2\text{-}pyr)N)Me_2\}_2(O)Al_2Li_2(THF)_2]_\infty$ **478** which has a central heterobimetallic butterfly-shaped Al_2Li_2 core with 2 equiv. of the starting amide, $(Ph(2\text{-}pyr)N)Me_2Al$, stabilizing a discrete molecule of Li_2O. These Li cations interact with both pyridyl nitrogens and one THF molecule each. An extension of this work saw the introduction of an amidinate ligand to form $[(PhN\text{–}C(Ph)\text{–}NPh)_3Li_4][\{(^tBu)Me_3Al\}_2Li]$ **479**, a mixed aggregate in which the cationic fragment is a smaller version of the H^- capturing Li_8N_6 cluster described above, necessitated by the larger amide ligand.[465] The anionic fragment has a familiar four-membered central (C_2LiAl) ring incorporating bridging methyls while polymer formation is achieved through agostic interaction of the terminal Me groups with the Li cations to form a planar four-membered ring composed of (···Li···C-Al-C···).

Weidlein has reported the synthesis of a series of hypersilanides, $(Me_3Si)_3Si^-$, incorporating Me_3M (M—Al, Ga, In) in the anion of a CIP with various alkali metal counterions.[466] The only heterobimetallic complex for which the crystal structure was reported was that of $[\{(Me_3Si)_3SiGaMe_3\}Na(toluene)]$ **480**. Analysis revealed four-coordinate tetrahedral Si centers, which are glued together by the Na^+ cations bonding agostically with the two Me groups of one Me_3Ga moiety (2.549(7), 2.571(7) Å) and a single methyl group of the next moiety in the chain (2.866(7) Å). Thus, every Me_3Ga unit is bound to two Na^+. These sodium cations also form an η^6 interaction with a single toluene molecule.

Reaction of $LiAlH_4$ with the triamine ligand, tacnH (1,4,diisopropyl-1,4,7-triazacyclononane) produced the first unsolvated lithium trihydroaluminate dimer, which upon reaction with the acetylenes RCCH (R = Ph **481**, Me_3Si **482**) in toluene, led to the monomeric trialkynylaluminates $[(RCC)_3(tacn)AlLi]$, of which only the Ph complex was crystallographically characterized.[467] The CIP is established through the formation of a four-membered (AlNLiC) ring with a bridging tacn amide N and alkynyl α-C (Li–C 2.230(5) Å). The distance of Li^+ to the β-C in the alkynyl of 2.718(5) Å appears to preclude any significant π-interaction.

In seeking to form new imido ligands, Chivers and co-workers reacted $[\{^tBu(H)N\}_3M]$ (M = Al, Ga) with either MeLi or ^{t}BuLi in varying stoichiometries.[468] While a number of heterobimetallic complexes were formed, the only crystal structures of $[\{^tBu(H)N\}_2\{^tBuN\}AlLi][^tBuLi]$ **483**, $[\{^tBu(H)N\}_2\{^tBuN\}MLi][^tBu(H)NLi]$ (M = Al **484**, Ga **485**) were obtained. The first complex contains a 12-membered ($Li_3Al_2N_6C$) open framework quaternary cluster which is comprised of six fused four-membered rings of which five have (N_2AlLi) and one has (NAlCLi). This latter ring incorporates a trapped molecule of ^{t}BuLi in an apical position though it cannot be established from a simple bond distance analysis which Li cation is directly associated with this. The two latter complexes **484** and **485** are isostructural with the first though they have ^{t}Bu(H)NLi included rather than ^{t}BuLi. An earlier example of this phenomenon had shown that two ^{n}BuLi molecules could also be captured in the formation of $[\{^tBu(H)N\}_3\{^tBuN\}_3Al_2Li_2][(^nBuLi)_2]$ **486**.[469] This forms when the aluminum amide : ^{n}BuLi ratio is varied anywhere between 1 : 4 and 1 : 8 though the optimum is 1 : 5. The structure is trilithiated $\{^tBu(H)N\}_3Al$ with an additional bound butterfly-shaped C_2Li_2 ring relative to which the two butyl groups adopt a *cis*-arrangement and extend away from the cluster.

Related alkyltriimido aluminate cages which contain the tetraanion $[R\{(2\text{-}MeOC_6H_4)N\}_3Al]^{4-}$ (R = ^{n}Bu, Et), were formed in the reaction of $\{R(H)N\}_3Al$ with 3 equiv. of ^{n}BuLi.[470] Each N–H was deprotonated in the reaction along with nucleophilic addition of an $^nBu^-$ moiety to produce $[Li(THF)]_2[\{(2\text{-}MeOC_6H_4N)_3BuAl\}_2Li_6]$ **487**. This ion separated complex has an anionic component similar to that observed in the analogous complex $[Li(THF)]_2[\{(2\text{-}MeOC_6H_4N)_3EtAl\}_2Li_6]$ **488** which is a 14-membered $Al_2N_6Li_6$ rhombododecahedral cluster which contains within it the hexagonal prismatic (stacked trimer) structure which is common for lithium amides. Alternatively, the six Li cations are sandwiched between two $[R\{(2\text{-}MeOC_6H_4)N\}_3Al]^{4-}$ anions.

The extensive and highly effective use of metallated binol complexes in asymmetric catalysis means that a structural investigation of the alkali metal "ate" complexes will yield valuable activity information. The 1 : 1 reaction of $PhCH_2InCl_2$ with dilithiated (S)-binolate in THF followed by DME produced crystals of $[(DME)Li]_3[\{(S)\text{-binolate}\}_3In](DME)_2$ **489** while the analogous complex $[(DME)Li]_3[\{(S)\text{-binolate}\}_3In](THF)_{0.75}$ **490** which has THF molecules in the lattice rather than DME was prepared from the direct reaction of the dilithiated (*S*)-binolate with $InCl_3$ in a 3 : 1 ratio. These complexes contain a tetranuclear InO_6Li_3 framework in which the central In is surrounded and coordinated by the six O atoms of the three binol dianions and the three Li cations situate themselves between the binolate molecules spanning the O centers. Their coordination number is increased to 4 by the addition of a DME molecule on each. The analogous K complex is formed by a similar reaction methodology in toluene producing $[(toluene)_2Li]_3[\{(S)\text{-binolate}\}_3In](toluene)_2$ **491**. The core is isostructural with that of the lithium complexes, though in a familiar motif each K cation bonds in an η^6 manner to two toluene molecules.

2.01.6.7 Group 1/Group 14

Very few mixed heterobimetallic complexes which contain an alkali metal and a group 14 which are metal not directly bonded to one another have been structurally characterized. Wright and co-workers, in developing a series

of imido and phosphinidene complexes, extended their study to Sb (see the next section) and Sn, and from the reaction of the polynuclear dimethylamido Sn(II) complex $[\{(MesN)_2Sn\}(\mu\text{-}NMe_2)Sn\}_2]$ with $[\{(2\text{-}MeO)C_6H_4\}N(H)Li]$ produced the heterobimetallic complex $[\{(MesNH)(\mu\text{-}(2\text{-}MeO)C_6H_4N\}_2SnLi(THF)_4]$ **492** from $(Me_2N)_2Sn$ elimination.[471] The structure of the complex is that of a four-runged ladder in which the central $(SnN)_2$ ring and $(LiN)_2$ ring are fused at either side. The mesitylamide moieties provide terminal N bridges for Li and Sn centers while the methoxyanilide ligands are central and coordinated by three metals: two Sn and one Li. The influence of the stereochemically active lone pair on Sn is highlighted by its pseudo-pyramidal geometry. The structure is dominated the covalent Sn–N bonding with the Li cations forming longer, more ionic bonds and coordinated by two THF molecules each.

2.01.6.8 Group 1/Group 15

A series of heterobimetallic (imido)Sb/Li cage complexes containing $[(RN)_3Sb]^{3-}$ trianions have been structurally characterized and contain 14-membered polyhedral cages formed through association of the two imido–antimony trianions with six lithium cations.[472] The complexes $[\{(PhCH_2CH_2N)_3Sb\}_2Li_6(THF)_2]$ **493**, $[\{(CyN)_3Sb\}_2Li_6(Me_2NH)_2]$ **494**, $[\{(2,4\text{-}(MeO)_2C_6H_3N)_3Sb\}_2Li_6(THF)_2(toluene)_2]$ **495**, and $[\{(^tBuN)_3Sb\}_2Li_6]$ **496** are formed in the reaction of the appropriate primary lithium amide with $[(Me_2N)_3Sb]$ in a 3 : 1 ratio in toluene/THF solutions. The cores of the clusters can be viewed as two stacked N_3Li_3 trimeric rings, typical of lithium imides, capped on each open face by Sb(III) centers. The Li cations have varied and complex coordination environments dependent on the nature of the amide and the solvating ligands. The complexes **493** and **494** both display intramolecular bonding from the amide to four of the six Li cations through π(Ph) agostic interactions and internal MeO coordination, respectively. The remaining two Li centers are coordinated by THF molecules. In the unsolvated complex the Li cations form short compensatory agostic interactions with CH_3 groups on the ^{t}Bu moieties (avg. Li···C 2.65 Å).

The reaction of $[\{(CyN)_3Sb\}_2Li_6]$ with ^{t}BuOK results in the co-complex $[\{(CyN)_3Sb\}_2Li_6\{^tBuOK\}_3]$ **497**. The complexes $[(CyN)_4Sb_2Na_2]$ **498** and $[(CyNH)(\mu\text{-}CyN)_2Sb_2M(THF)_2]$ (M = K **499**, Rb **500**), formed on reaction of the alkali metal benzyl derivative with cyclohexylamine and $[(Me_2N)_3Sb]$, were structurally characterized to investigate how the dianion, $[(CyN)_4Sb_2]^{2-}$, and the monoanion, $[(CyNH)(\mu\text{-}CyN)_2Sb_2]^-$, adjust to accommodate differing alkali metals.[473] They were directly compared with their Li analogs. The change from Li to Na in the unsolvated complexes causes a change in the geometry of the central cage from one which is constructed from two cubane halves and a tetrahedral arrangement of Li cations (also similar with the Bi analog) to one in which the Na cations adopt a central planar rhombic arrangement and the cubic framework becomes completely distorted. The complexes with the dianionic CyN^{2-} bridged fragments have a common structural motif in which two fused Sb_2N_2 rings share a central four-coordinate square-based Sb atom. The alkali metal cations all display the same coordination pattern of bonding with the terminal amide ligands of the Sb(III) monoanions and two of the μ–NCy groups within the $[Sb_3N_4]$ cores. The K and Rb cations each have additional two THF molecules increasing their coordination environment (distorted octahedral) over that observed for tetrahedral Li. While overall it is the Sb–N bonds which dominate the structures of all these complexes, it is the Li centers though which provoke the greatest degree of distortion in the SbN cages due to the Li–N bonds being shorter, stronger, more covalent in comparison to those of K or Rb.

Acknowledgments

The authors thank Dr Weijie Teng for the preparation of most of the artwork in this article. K. Ruhlandt-Senge and K. W. Henderson are indebted to the National Science Foundation for generous support of their work. The authors would also like to thank many talented researchers in this field for their contributions.

References

1. Schleyer, P. v. R. *Pure Appl. Chem.* **1984**, *56*, 151.
2. Setzer, W. N.; Schleyer, P. v. R. *Adv. Organomet. Chem.* **1985**, *24*, 353.
3. Schade, C.; Schleyer, P. v. R. *Adv. Organomet. Chem.* **1987**, *27*, 169.
4. Weiss, E. *Angew. Chem., Int. Ed. Engl.* **1993**, *32*, 1501.
5. Lukehart, C. M., Ed., In *Encyclopedia of Inorganic Chemistry*; 1st ed.; Wiley: Chichester, 1994, p 54.
6. Pauer, F.; Power, P. P. In *Lithium Chemistry: Theoretical and Experimental Overview*; Sapse, A. M., Schleyer, P. v. R., Eds.; Wiley: New York, 1995, p 295.
7. Beswick, M. A.; Wright, D. S. Alkali metals. In *Comprehensive Organometallic Chemistry II*; Abel, E. W., Stone, F. G. A., Wilkinson, G., Eds.; Elsevier: Oxford, 1995; Vol. 1.

8. Janssen, M. D.; Grove, D. M.; Koten, G. v. *Prog. Inorg. Chem.* **1997**, *46*, 97.
9. Smith, J. D. *Adv. Organomet. Chem.* **1999**, *43*, 267.
10. Englich, U.; Ruhlandt-Senge, K. *Coord. Chem. Rev.* **2000**, *210*, 135.
11. Stey, T.; Stalke, D. In *The Chemistry of Organolithium Compounds*; Rappoport, Z., Marek, I., Eds.; Wiley: New York, 2004.
12. Harvey, M.; Lukehart, C. M. In *Encyclopedia of Inorganic Chemistry*, 2nd Ed.; Wiley: Chichester (in press)
13. For the latest edition please see: Elschenbroich, C. *Organometallchemie,* 4te Auflage, Teubner: Wiesbaden, 2003 (a revised English edition is forthcoming).
14. Schlosser, M. *Pure Appl. Chem.* **1988**, *60*, 1627.
15. Weiss, E.; Hencken, G. *J. Organomet. Chem.* **1970**, *21*, 265.

15a. Weiss, E.; Sauermann, G. *Angew. Chem., Int. Ed. Engl.* **1968**, *7*, 133.

15b. Weiss, E.; Sauermann, G. *Chem. Ber.* **1970**, *103*, 265.

15c. Weiss, E.; Köster, H. *Chem. Ber.* **1977**, *110*, 717.

16. Grotjahn, D. B.; Pesch, T. C.; Xin, J.; Ziurys, L. M. *J. Am. Chem. Soc.* **1997**, *119*, 12368.
17. Dinnebier, R. E.; Behrens, U.; Olbrich, F. *Organometallics* **1997**, *16*, 3855.
18. Dinnebier, R. E.; Olbrich, F.; Smaalen, S. v.; Stephens, P. W. *Acta Cryst. B* **1997**, *53*, 153.
19. Dinnebier, R. E.; Olbrich, F.; Bendele, G. M. *Acta Cryst. C* **1997**, *53*, 699.
20. Eaborn, C.; Izod, K.; Smith, J. D. *J. Organomet. Chem.* **1995**, *500*, 89.
21. Niemeyer, M.; Power, P. P. *Organometallics* **1997**, *16*, 3258.
22. Hope, H. *Prog. Inorg. Chem.* **1994**, *41*, 1.
23. Hitchcock, P. B.; Lapert, M. F.; Protchenko, A. V. *J. Am. Chem. Soc.* **2001**, *123*, 189.

23a. Beno, M. A.; Hope, H.; Olmstead, M.; Power, P. P. *Organometallics* **1985**, *4*, 2117.

24. Engelhardt, L. M.; Leung, W.-P.; Raston, C. L.; Twiss, P.; White, A. H. *J. Chem. Soc., Dalton Trans.* **1984**, 321.
25. Patterman, S. P.; Karle, I. L.; Stucky, G. D. *J. Am. Chem.Soc.* **1970**, *92*, 1150.
26. Zarges, W.; Marsch, M.; Harms, K.; Boche, G. *Chem. Ber.* **1989**, *122*, 2303.
27. Schade, C.; Schleyer, P. v. R.; Dietrich, H.; Mahdi, W. *J. Am. Chem. Soc.* **1986**, *108*, 2484.
28. Corbelin, S.; Lorenzen, N. P.; Kopf, J.; Weiss, E. *J. Organomet. Chem.* **1991**, *415*, 293.
29. Schleyer, P. v. R.; Bauer, W.; Hampel, F.; Eikema Hommes, N. J. R. v.; Otto, P.; Pieper, U.; Stalke, D.; Wright, D. S.; Snaith, R. *J. Am. Chem. Soc.* **1994**, *116*, 528.
30. Brooks, J. J.; Stucky, D. G. *J. Am. Chem. Soc.* **1972**, *94*, 7333.
31. Power, P. P.; Olmstead, M. *J. Am. Chem. Soc.* **1985**, *107*, 2174.
32. Weiss, E.; Köster, H. *J. Organomet. Chem.* **1979**, *168*, 273.
33. Schleyer, P. v. R.; Stalke, D.; Pieper, U.; Bauer, W.; Hoffman, D. *Organometallics* **1993**, *12*, 1193.
34. Weiss, E.; Behrens, U.; Panther, T.; Viebrock, H. *J. Organomet. Chem.* **1995**, *491*, 19.
35. Ahlbrecht, H.; Harbach, J.; Hauck, T.; Kalinowski, H. O. *Chem. Ber.* **1992**, *125*, 1753.
36. Feil, F.; Harder, S. *Organometallics* **2000**, *19*, 5010.
37. Power, P. P.; Olmstead, M. *J. Am. Chem. Soc.* **1985**, *107*, 2174.
38. Weiss, E.; Kopf, J.; Lorenzen, N. P.; Corbelin, S. *J. Organomet. Chem.* **1991**, *415*, 293.
39. Alexander, J. S.; Allis, D. G.; Hudson, B. S.; Ruhlandt-Senge, K. *J. Am. Chem. Soc.* , *125*(49), 15002.
40. Schleyer, P. v. R.; Schade, C. *Adv. Organomet. Chem.* **1991**, *27*, 169.
41. Schleyer, P. v. R. *Pure Appl. Chem.* **1983**, *55*, 355.
42. Alexander, J. S.; Allis, D. G.; Ruhlandt-Senge, K. (in preparation)
43. Stalke, D.; Gornitzka, H. *Organometallics* **1994**, *13*, 4398.
44. Stalke, D.; Pfeiffer, M.; Bertrand, G.; Hemmert, C.; Gornitzka, H. *Organometallics* **2000**, *19*, 112.
45. Stalke, D.; Pieper, U. *Organometallics* **1993**, *12*, 1201.
46. Schleyer, P. v. R.; Stalke, D.; Pieper, U.; Bauer, W.; Hoffman, D. *Organometallics* **1993**, *12*, 1193.
47. Bushby, R. J.; Steel, H. L.; Tytko, M. P. *J. Chem. Soc., Perkin Trans. 2* **1990**, *7*, 1155.
48. Eaborn, C.; Smith, J. D. *Coord. Chem. Rev.* **1996**, *154*, 125.
49. Eaborn, C.; Smith, J. D. *J. Chem. Soc., Dalton Trans.* **2001**, 1541.
50. Cook, M. A.; Eaborn, C.; Jukes, A. E.; Walton, D. R. M. *J. Organomet. Chem.* **1970**, *24*, 529.
51. Aiube, Z. H.; Eaborn, C. *J. Organomet. Chem.* **1984**, *269*, 217.
52. Eaborn, C.; Hitchcock, P. B.; Smith, J. D.; Sullivan, A. C. *J. Chem. Soc., Chem. Commun.* **1983**, 827.
53. Hitchcock, P. B.; Lappert, M. F.; Leung, W.-P.; Liu, S.-S.; Shun, T. *J. Chem. Soc., Chem. Commun.* **1993**, 1386.
54. Atwood, J. L.; Fjeldberg, T.; Lappert, M. F.; Luong-Thi, N. T.; Shakir, R.; Thorne, A. J. *J. Chem. Soc., Chem. Commun.* **1984**, 1163.
55. Hitchcock, P. B.; Khostov, A. V.; Lappert, M. F. *J. Organomet. Chem.* **2002**, *663*, 263.
56. Boesfeld, W. M.; Hitchcock, P. B.; Lappert, M. F.; Liu, D.-S.; Tian, S. *Organometallics* **2000**, *19*, 4030.
57. Hitchcock, P. B.; Lappert, M. F.; Leung, W.-P.; Diansheng, L.; Shun, T. *J. Chem. Soc., Chem. Commun.* **1993**, 1386.
58. Eaborn, C.; Hitchcock, P. B.; Izod, K.; Jaggar, A. J.; Smith, J. D. *Organometallics* **1994**, *13*, 753.
59. Eaborn, C.; Hitchcock, P. B.; Izod, K.; Smith, J. D. *Angew. Chem., Int. Ed. Engl.* **1995**, *34*, 687 and 2697.
60. Eaborn, C.; Hitchcock, P. B.; Izod, K.; Smith, J. D. *Angew. Chem., Int. Engl.* **1995**, *34*, 687.
61. Eaborn, C.; Clegg, W.; Hitchcock, P. B.; Hopmann, M.; Izod, K.; O'Shaughnessy, P.; Smith, J. D. *Organometallics* **1997**, *16*, 4728.
62. Eaborn, C.; Hitchcock, P. B.; Smith, J. D.; Sullivan, A. C. *J. Chem. Soc., Chem. Commun.* **1983**, 827.
63. Wittig, G.; Meyer, F. J.; Lange, G. *Liebigs Ann. Chem.* **1951**, *571*, 167.
64. Avent, A. G.; Eaborn, C.; Hitchcock, P. B.; Lawless, G. A.; Lickiss, P. D.; Mallien, M.; Smith, J. D.; Webb, A. D.; Wrackmeyer, B. *J. Chem. Soc., Dalton Trans.* **1993**, 3259.
65. Boese, R.; Paetzold, P.; Tapper, A. *Chem. Ber.* **1987**, *120*, 1069.
66. Al-Juaid, S. S.; Eaborn, C.; Hitchcock, P. B.; Izod, K.; Mallien, M.; Smith, J. D. *Angew. Chem., Int. Ed. Engl.* **1994**, *33*, 1268.
67. Eaborn, C.; Hitchcock, P. B.; Sullivan, A. C. *J. Chem. Soc., Chem. Commun.* **1983**, 1390.
68. Al-Juaid, S. S.; Avent, A. G.; Eaborn, C.; El-Hamruni, S. M.; Hawkes, S. A.; Hill, M. S.; Hopmann, M.; Hitchcock, P. B.; Smith, J. D. *J. Organomet. Chem.* **2001**, *631*, 76.
69. Antolini, F.; Hitchcock, P. B.; Lappert, M. F.; Wei, X.-H. *Organometallics* **2003**, *22*, 2505.

70. Hope, H.; Power, P. P. *J. Am. Chem. Soc.* **1983**, *105*, 5320.
71. Thönnes, D.; Weiss, E. *Chem. Ber.* **1978**, *111*, 3157.
72. Schumann, U.; Kopf, J.; Weiss, E. *Angew. Chem., Int. Ed.,Engl.* **1985**, *24*, 215.
73. Dietrich, H. *Acta Cryst.* **1963**, *16*, 681.
73a. Dietrich, H. *J. Organomet. Chem.* **1981**, *205*, 291.
74. Kottke, T.; Stalke, D. *Angew. Chem.* **1993**, *105*, 619.
74a. Kottke, T.; Stalke, D. *Angew. Chem., Int. Ed. Engl.* **1993**, *32*, 580.
75. Dinnebier, R. E.; Behrens, U.; Olbrich, F. *J. Am. Chem. Soc.* **1998**, *120*, 1430.
76. Ruhlandt-Senge, K.; Ellison, J. J.; Wehmschulte, R. J.; Pauer, F.; Power, P. P. *J. Am. Chem. Soc.* **1993**, *115*, 11353.
77. Schiemenz, B.; Power, P. P. *Angew. Chem., Int. Ed. Engl.* **1996**, *35*, 2150.
78. Wehmschulte, R. J.; Power, P. P. *J. Am. Chem. Soc.* **1997**, *119*, 2847.
79. Schiemenz, B.; Power, P. P. *Organometallics* **1996**, *15*, 958.
80. Rabe, G. W.; Sommer, R. D.; Rheingold, A. L. *Organometallics* **2000**, *19*, 5537.
81. Hardman, N. J.; Twamley, B.; Stender, M.; Baldwin, R.; Hino, S.; Schiemenz, B.; Kauzlarich, S. M.; Power, P. P. *J. Organomet. Chem.* **2002**, *643*, 461.
82. Hino, S.; Olmstead, M. M.; Fettinger, J. C.; Power, P. P. *J. Organomet. Chem.* **2005**, *690*, 1638.
83. Niemeyer, M.; Power, P. P. *Organometallics* **1997**, *16*, 3258.
84. Schürmann, U.; Behrens, U.; Weiss, E. *Angew. Chem., Int. Ed. Engl.* **1989**, *28*, 476.
85. Schürmann, U.; Weiss, E. *Angew. Chem., Int. Ed. Engl.* **1988**, *27*, 584.
86. Besten, R. d.; Brandsma, L.; Spek, A. L.; Kanters, J. A.; Veldman, N. *J. Organomet. Chem.* **1995**, *498*, C6.
87. Besten, R. d.; Lankin, M. T.; Veldman, N.; Spek, A. L.; Brandsma, L. *J. Organomet. Chem.* **1996**, *514*, 191.
88. Thiele, J. *Ber. Dtsch. Chem. Ges.* **1900**, *33*, 666.
89. Thiele, J. *Ber. Dtsch. Chem. Ges.* **1901**, *34*, 68.
90. Stalke, D. *Angew. Chem., Int. Ed. Engl.* **1994**, *33*, 2168.
91. Harder, S. *Coord. Chem. Rev.* **1998**, *176*, 17.
92. Jutzi, P.; Burford, N. *Chem. Rev.* **1999**, *99*, 969.
93. Aoyagi, T.; Shearer, H. M. M.; Wade, K.; Whitehead, G. *J. Chem. Soc., Chem. Commun.* **1976**, 164.
94. Ayoyagi, T.; Shearer, H. M. M.; Wade, K.; Whitehead, G. *J. Organomet. Chem.* **1979**, *175*, 21.
95. Jutzi, P.; Schlüter, E.; Krüger, C.; Pohl, S. *Angew. Chem.* **1983**, *95*, 1015.
95a. Jutzi, P.; Schlüter, E.; Krüger, C.; Pohl, S. *Angew. Chem., Int. Ed. Engl.* **1983**, *22*, 994.
96. Jutzi, P.; Schlüter, E.; Pohl, S.; Saak, W. *Chem. Ber.* **1985**, *118*, 1959.
97. Lappert, M. F.; Singh, A.; Engelhard, L. M.; White, A. H. *J. Organomet. Chem.* **1984**, *262*, 271.
98. Jutzi, P.; Laffers, W.; Pohl, S.; Saak, W. *Chem. Ber.* **1989**, *122*, 1449.
99. Kähler, T.; Behrens, U.; Neander, S.; Olbrich, F. *J. Organomet. Chem.* **2002**, *649*, 50.
100. Neander, S.; Tio, F. E.; Buschman, R.; Behrens, U.; Olbrich, F. *J. Organomet. Chem.* **1999**, *582*, 58.
101. Neander, S.; Behrens, U.; Olbrich, F. *J. Organomet. Chem.* **2000**, *604*, 59.
102. Chen, H.; Jutzi, P.; Leffers, W.; Olmstead, M. M.; Power, P. P. *Organometallics* **1991**, *10*, 1787.
103. Hanusa, T. P. *Organometallics* **2002**, *21*, 2559.
104. Neander, S.; Tio, F. E.; Buschman, R.; Behrens, U.; Olbrich, F. *J. Organomet. Chem.* **1999**, *582*, 58.
105. Rabe, G.; Roesky, H. W.; Talke, D.; Pauer, F.; Sheldrick, G. M. *J. Organomet. Chem.* **1991**, *403*, 11.
106. Evans, W. J.; Brady, J. C.; Fujimoto, C. H.; Giarikos, D. G.; Ziller, J. W. *J. Organomet. Chem.* **2002**, *649*, 252.
107. Näther, C.; Hauck, T.; Bock, H. *Acta Cryst. C* **1996**, *52*, 570.
108. Lorberth, J.; Shin, S.-H.; Wocadlo, S.; Massa, W. *Angew. Chem., Int. Ed. Engl.* **1989**, *28*, 735.
109. Hoffmann, D.; Hampel, F.; Schleyer, P. v. R. *J. Organomet. Chem.* **1993**, *456*, 13.
110. Jordan, V.; Behrens, U.; Olbrich, F.; Weiss, E. *J. Organomet. Chem.* **1996**, *517*, 81.
111. Neander, S.; Körnich, J.; Olbrich, F. *J. Organomet. Chem.* **2002**, *656*, 89.
112. Corbelin, S.; Kopf, J.; Weiss, W. *Chem. Ber.* **1991**, *124*, 2417.
113. Hoffmann, D.; Hampel, F.; Schleyer, P. v. R. *J. Organomet. Chem.* **1993**, *456*, 13.
114. Paquette, L. A.; Bauer, W.; Sivik, M. R.; Bühl, M.; Feigl, M.; Schleyer, P. v. R. *J. Am. Chem. Soc.* **1990**, *112*, 8776.
115. Eiermann, M.; Hafner, K. *J. Am. Chem. Soc.* **1992**, *114*, 135.
116. Mink, C.; Hafner, K. *Tetrahedron Lett.* **1994**, *35*, 4087.
117. Harder, S.; Prosenc, H. M. *Angew. Chem.* **1994**, *106*, 1830.
117a. Harder, S.; Prosenc, H. M. *Angew. Chem., Int. Ed. Engl.* **1994**, *33*, 1744.
118. Wessel, J.; Behrens, U.; Lork, E.; Mews, R. *Angew. Chem.* **1995**, *107*, 516.
118a. Wessel, J.; Behrens, U.; Lork, E.; Mews, R. *Angew. Chem., Int. Ed. Engl.* **1995**, *34*, 443.
119. Harder, S.; Prosenc, H. M.; Rief, U. *Organometallics* **1996**, *15*, 118.
120. Harder, S.; Prosenc, H. M. *Angew. Chem.* **1996**, *108*, 101.
120a. Harder, S.; Prosenc, H. M. *Angew. Chem., Int. Ed. Engl.* **1996**, *35*, 97.
121. Zaegel, F.; Gallucci, J. C.; Meunier, P.; Gautheron, B.; Sivik, M. R.; Paquette, L. A. *J. Am. Chem. Soc.* **1994**, *116*, 6466.
122. Wong, W.-K.; Zhang, L.; Wong, W.-T.; Xue, F.; Mak, T. C. W. *Polyhedron* **1996**, *15*, 4593.
122a. Dinnebier, R. E.; Neander, S.; Behrens, U.; Olbrich, F. *Organometallics* **1999**, *18*, 2915.
123. Harder, S.; Lutz, M.; Olbert, S. J. *Organometallics* **1999**, *18*, 1808.
124. Harder, S.; Lutz, M.; Straub, A. W. C. *Organometallics* **1997**, *16*, 107.
125. Stults, S. D.; Andersen, R. A.; Zalkin, A. *J. Am. Chem. Soc.* **1989**, *111*, 4507.
126. Evans, W. J.; Sollberger, M. S.; Shreeve, J. L.; Olofson, J. M.; Hain, J. H. Jr.; Ziller, J. W. *Inorg. Chem.* **1992**, *31*, 2492.
127. Berthet, J.-C.; Villiers, C.; Le Maréchal, J.-F.; Delavaux-Nicot, B.; Lance, M.; Nierlich, M.; Vigner, J.; Ephritikhine, M. *J. Organomet. Chem.* **1992**, *440*, 53.
128. Fraenkel, G.; Chow, A.; Fleischer, R.; Liu, H. *J. Am. Chem. Soc.* **2004**, *126*, 3983.
129. van Eikema Hommes, N. J. R.; Bühl, M.; Schleyer, P. v. R.; Wu, Y.-D. *J. Organomet. Chem.* **1991**, *409*, 307.
130. Köster, H.; Weiss, E. *Chem. Ber.* **1982**, *115*, 4322.

131. Schumann, U.; Weiss, E.; Dietrich, H.; Mahdi, W. *J. Organomet. Chem.* **1987**, *322*, 299.
132. Sebastian, J. F.; Grunwell, J. R.; Hsu, B. *J. Organomet. Chem.* **1974**, *78*, C1.
133. Boche, G.; Etzrodt, H.; Marsch, M.; Massa, W.; Baum, G.; Dietrich, H.; Mahdi, W. *Angew. Chem.* **1986**, *98*, 84.
134. Boche, G.; Fraenkel, G.; Cabral, J.; Harms, K.; van Eikema Hommes, N. J. R.; Lorenz, J.; Marsch, M.; Schleyer, P. v. R. *J. Am. Chem. Soc.* **1992**, *114*, 1562.
135. Fraenkel, G.; Halasa, A. F.; Mochel, V.; Stumpe, R.; Tate, D. *Org. Chem.* **1985**, *50*, 4563.
136. Glaze, W. H.; Jones, P. C. *J. Chem. Soc.* **1969**, 1434.
137. Glaze, W. H.; Hanicac, J. E.; Moore, M. L.; Chadpuri, J. *J. Organomet. Chem.* **1972**, *44*, 39.
138. Glaze, W. H.; Hanicac, J. E.; Chandpuri, J.; Moore, M. L.; Duncan, D. P. *J. Organomet. Chem.* **1973**, *51*, 13.
139. Köster, H.; Weiss, E. *Chem. Ber.* **1982**, *115*, 3422.
140. Schümann, U.; Weiss, E.; Dietrich, H.; Mahdi, W. *J. Organomet. Chem.* **1987**, *322*, 299.
141. Boche, G.; Etzrodt, H.; Marsch, M.; Massa, W.; Baum, G.; Dietrich, H.; Mahdi, W. *Angew. Chem., Int. Ed. Engl.* **1986**, *25*, 104.
142. Boche, G.; Fraenkel, G.; Cabral, J.; Harms, K.; van Eikema Hommes, N. J. R.; Schleyer, P. v. R. *J. Am. Chem. Soc.* **1992**, *114*, 1562.
143. Bauer, W.; Feigl, M.; Müller, G.; Schleyer, P. v. R. *J. Am. Chem. Soc.* **1988**, *110*, 6033.
144. Fraenkel, G.; Cabral, J. A. *J. Am. Chem. Soc.* **1993**, *115*, 1551.
145. Fraenkel, G.; Qiu, F. *J. Am. Chem. Soc.* **1997**, *119*, 3571.
146. Fraenkel, G.; Qiu, F. *J. Am. Chem. Soc.* **1996**, *118*, 5828.
147. Fraenkel, G.; Duncan, J. H.; Wang, J. *J. Am. Chem. Soc.* **1999**, *121*, 432.
148. Fraenkel, G.; Martin, K. *J. Am. Chem. Soc.* **1995**, *117*, 10336.
149. Corbelin, S.; Kopf, J.; Lorenzen, N. P.; Weiss, E. *Angew. Chem.* **1991**, *103*, 875.
149a. Corbelin, S.; Kopf, J.; Lorenzen, N. P.; Weiss, E. *Angew. Chem., Int. Ed. Engl.* **1991**, *30*, 825.
150. Hu, N.; Gong, L.; Jin, Z.; Chen, W. *J. Organomet. Chem.* **1988**, *352*, 61.
151. Bock, H.; Arad, C.; Näther, C.; Havlas, Z. *J. Chem. Soc., Chem. Commun.* **1995**, 2393.
152. Bock, H.; Hauck, T.; Näther, N. *Organometallics* **1996**, *15*, 1527.
153. Bock, H.; Ruppert, K.; Näther, C.; Havlas, Z.; Hermann, H. F.; Arad, C.; Göbel, I.; John, A.; Meuret, J., Nick, S., *et al. Angew. Chem.* **1992**, *104*, 565.
153a. Bock, H.; Ruppert, K.; Näther, C.; Havlas, Z.; Hermann, H. F.; Arad, C.; Göbel, I.; John, A.; Meuret, J., Nick, S., *et al. Angew. Chem., Int. Ed. Engl.* **1992**, *31*, 550.
154. Bock, H.; Havlas, Z.; Hess, D.; Näther, C. *Angew. Chem., Int. Ed. Engl.* **1998**, *37*, 502.
155. Bock, H.; Ansari, M.; Nagel, N.; Claridge, R. F. C. *J. Organomet. Chem.* **1996**, *521*, 51.
156. Bock, H.; Ansari, M.; Nagel, N.; Claridge, R. F. C. *J. Organomet. Chem.* **1995**, *501*, 53.
156. Näther, C.; Bock, H.; Havlas, Z.; Hauck, T. *Organometallics* **1998**, *17*, 4707.
157. Bock, H.; Havlas, Z.; Gharagozloo-Hubmann, K.; Holl, S.; Sievert, M. *Angew. Chem., Int. Ed. Engl.* **2003**, *42*, 4385.
158. Bock, H.; Hauck, T.; Näther, N. *Organometallics* **1996**, *15*, 1527.
159. Geissler, M., Diplomarbeit, Hamburg, 1984.
160. Schubert, B.; Weiss, E. *Chem. Ber.* **1983**, *116*, 3212.
161. Schubert, B.; Weiss, E. *Angew. Chem.* **1983**, *95*, 499.
161a. Schubert, B.; Weiss, E. *Angew. Chem., Int. Ed. Engl.* **1983**, *22*, 496.
162. Hässig, R.; Seebach, D. *Helv. Chim. Acta* **1983**, *66*, 2268.
163. Bauer, W.; Seebach, D. *Helv. Chim. Acta* **1984**, *67*, 703.
164. Geissler, M.; Kopf, J.; Schubert, B.; Weiss, E.; Neugebauer, W.; Schleyer, P. v. R. *Angew. Chem., Int. Ed. Engl.* **1987**, *26*, 587.
165. Pulham, R. J.; Weston, D. P.; Salvesen, T. A.; Thatcher, J. J. *J. Chem. Res. (S)* **1995**, 254.
165a. Pulham, R. J.; Weston, D. P. *J. Chem. Res. (S)* **1995**, 406.
166. Weiss, E.; Plass, H. *Chem. Ber.* **1968**, *101*, 2947.
167. Kähler, T.; Olbrich, F. Private Communication to the Cambridge Structural Database, 2001.
168. Belzner, J.; Dehnert, U. In *The Chemistry of Organic Silicon Compounds*; Rappoport, Z., Apeloig, Y., Eds.; Wiley: Chichester, 1998; Vol. 2, 779.
168a. Tamao, K.; Kawachi, A. *Adv. Organomet. Chem.* **1995**, *38*, 1.
168b. Lickiss, P.; Smith, C. *Coord. Chem. Rev.* **1995**, *145*, 75.
168c. Sekiguchi, A.; Ya Lee, V.; Nanjo, M. *Coord. Chem. Rev.* **2000**, *210*, 11.
168d. Riviere, P.; Castel, A.; Riviere-Baudet, M. In *The Chemistry of Organic Germanium, Tin and Lead compounds*; Rappoport, Z., Ed.; Wiley, 2002; Vol. 2, Chapter 11, p 653.
168e. Lerner, H. W. *Coord. Chem. Rev.* **2005**, *249*, 781.
169. Gilman, H.; Wu, T. C.; Hartzfeld, H. A.; Guter, G. A.; Smith, A. G.; Goodman, J. J.; Eidt, S. H. *J. Am. Chem. Soc.* **1952**, *74*, 561.
170. Wittenberg, D.; Gilman, H. *Chem. Ind.* **1958**, 390.
171. Wiberg, E.; Stecher, O.; Andrascheck, H. J.; Kreuzbichler, L.; Staude, E. *Angew. Chem.* **1963**, *75*, 516.
172. Gilman, H.; Smith, C. L. *J. Organomet. Chem.* **1967**, *8*, 245.
173. Gilman, H.; Smith, C. L. *J. Organomet. Chem.* **1968**, *14*, 91.
174. Weidenbruch, M.; Peter, W. *Angew. Chem., Int. Ed. Engl.* **1975**, *14*, 642.
175. Doyle, M. P.; West, C. T. *J. Am. Chem. Soc.* **1975**, *97*, 3777.
176. Dexheimer, E. M.; Spialter, L. *Tetrahedron Lett.* **1975**, 1771.
177. Lerner, H.-W.; Scholz, S.; Bolte, M. *Z. Anorg. Allg. Chem.* **2001**, *627*, 1638.
178. Lerner, H.-W.; Scholz, S.; Wagner, M.; Bolte, M. *Z. Anorg. Allg. Chem.* **2004**, *630*, 443.
179. Gilman, H.; Smith, C. L. *J. Organomet. Chem.* **1967**, *8*, 245.
180. Gilman, H.; Smith, C. L. *J. Organomet. Chem.* **1968**, *14*, 91.
181. Becker, G.; Hartmann, H.-M.; Münch, A.; Riffel, H. *Z. Anorg. Allg. Chem.* **1985**, *580*, 29.
182. Dias, H. V. R.; Olmstead, M. M.; Ruhlandt-Senge, K.; Power, P. P. *J. Organomet. Chem.* **1993**, *462*, 1.
182a. Heine, A.; Herbst-Irmer, R.; Sheldrick, G. M.; Stalke, D. *Inorg. Chem.* **1993**, *32*, 2694–2698.
183. Klinkhammer, K. W.; Schwarz, W. *Z. Anorg. Allg. Chem.* **1993**, *619*, 1777.
184. Klinkhammer, K. W. *Chem. Eur. J.* **1997**, *3*, 1418.
185. Klinkhammer, K. W. Ph.D. Thesis, Universität Stuttgart, Germany, 1988.

186. Jenkins, D. M.; Teng, W.; Englich, U.; Stone, D.; Ruhlandt-Senge, K. *Organometallics* **2001**, *20*, 4600.
187. Teng, W.; Ruhlandt-Senge, K. *Chem. Eur. J.* **2005**, *11*, 2462.
188. Marschner, C. *Eur. J. Inorg. Chem.* **1998**, 221.
189. Kayser, C.; Fischer, R.; Baumgartner, J.; Marschner, C. *Organometallics* **2002**, *21*, 1023.
190. Apeloig, Y.; Bendikov, M.; Yuzefovich, M.; Nakash, M.; Bravo-Zhivotoskii, D.; Blaser, D.; Boese, R. *J. Am. Chem. Soc.* **1996**, *118*, 12228.
191. Wiberg, N.; Fischer, G.; Karampatses, P. *Angew. Chem., Int. Ed. Engl.* **1984**, *23*, 59.
192. Wiberg, N.; Amelunxen, K.; Lerner, H.-W.; Schuster, H.; Nöth, H.; Krossing, I.; Schmidt-Amelunxen, M.; Seifert, T. *J. Organomet. Chem.* **1997**, *542*, 1.
193. Nakamoto, M.; Fukawa, T.; Ya Lee, V.; Sekiguchi, A. *J. Am. Chem. Soc.* **2002**, *124*, 15160.
194. Dias, H. V. R.; Olmstead, M. M.; Ruhlandt-Senge, K.; Power, P. P. *J. Organomet. Chem.* **1993**, *462*, 1.
195. Habereder, T.; Nöth, H. *Z. Anorg. Allg. Chem.* **2001**, *627*, 1003.
196. Reed, D.; Stalke, D.; Wright, D. S. *Angew. Chem., Int. Ed. Engl.* **1991**, *30*, 1459.
197. Armstrong, D. R.; Davidson, M. G.; Moncrieff, D.; Stalke, D.; Wright, D. S. *J. Chem. Soc., Chem. Commun.* **1992**, 1413.
198. Gordon, M.; Boudjouk, P.; Anwari, F. *J. Am. Chem. Soc.* **1983**, *105*, 4972.
199. Hong, J.-H.; Boudjouk, P. *J. Am. Chem. Soc.* **1993**, *115*, 5883.
200. Freeman, W. P.; Tilley, T. D.; Arnold, F. P.; Rheingold, A. L.; Gantzel, P. K. *Angew. Chem.* **1995**, *107*, 2029.
200a. Freeman, W. P.; Tilley, T. D.; Arnold, F. P.; Rheingold, A. L.; Gantzel, P. K. *Angew. Chem., Int. Ed. Engl.* **1995**, *34*, 1887.
201. West, R.; Sohn, H.; Powell, D. R.; Müller, T.; Apeloig, Y. *Angew. Chem., Int. Ed. Engl.* **1996**, *35*, 1003.
202. West, R.; Sohn, H.; Bankwitz, U.; Calabrese, J.; Apeloig, Y.; Müller, T. *J. Am. Chem. Soc.* **1995**, *117*, 11608.
203. Goldfuss, B.; Schleyer, P. v. R. *Organometallics* **1995**, *14*, 1553.
204. Choi, S.-B.; Boudjouk, P.; Wei, P. *J. Am. Chem. Soc.* **1998**, *120*, 5814.
205. Choi, S.-B.; Boudjouk, P.; Qin, K. *Organometallics* **2000**, *19*, 1806.
206. Ya Lee, V.; Kato, R.; Ichinohe, M.; Sekiguchi, A. *J. Am. Chem. Soc* **2005**.
207. Mehotra, S. K.; Kawa, H.; Baran, J. R.; Ludvig, M. M., Jr.; Lagow, R. *J. Am. Chem. Soc.* **1990**, *112*, 9003.
208. Tokitoh, N.; Hatano, K.; Sadahiro, T.; Okazaki, R. *Chem. Lett.* **1999**, 931.
209. Sekiguchi, A.; Ichinohe, M.; Yamaguchi, S. *J. Am. Chem. Soc.* **1999**, *121*, 10231.
210. Riviere, P.; Riviere-Baudet, M.; Satge, J. In *Comprehensive Organometallic Chemistry II*; Abel, E. W., Stone, F. G. A., Wilkinson, G., Eds.; Elsevier: Oxford, 1995; Vol. 2, Chapter 5.
211. Sekiguchi, A.; Izumi, R.; Ihara, S.; Ichinohe, M.; Ya Lee, V. *Angew. Chem., Int. Ed. Engl.* **2002**, *41*, 1598.
212. Bürger, H.; Goetze, U. *Angew. Chem., Int. Ed.* **1968**, 7, 212.
212a. Brook, A. G.; Abdesaken, F.; Sollradl, H. *J. Organomet. Chem.* **1986**, *299*, 9.
213. Freitag, S.; Herbst-Irmer, R.; Lameyer, L.; Stalke, D. *Organometallics* **1996**, *15*, 2839.
214. Heine, A.; Stalke, D. *Angew. Chem., Int. Ed. Engl.* **1994**, *33*, 113.
215. Teng, W.; Ruhlandt-Senge, K. *Chem. Eur J.* **2005**, *11*, 2462.
216. Shannon, R. D. *Acta Cryst. A* **1976**, *32*, 751.
217. Allred, A. L.; Rochow, E. G. *J. Inorg. Nucl. Chem.* **1958**, *5*, 264.
218. Teng, W.; Ruhlandt-Senge, K. *Angew. Chem., Int. Ed. Engl.* **2003**, *42*, 3661.
219. Teng, W.; Ruhlandt-Senge, K. *Organometallics* **2004**, *23*, 952.
220. Teng, W.; Ruhlandt-Senge, K. *Organometallics* **2004**, *23*, 2694.
221. Fischer, J.; Baumgartner, J.; Marscher, C. *Organometallics* **2005**, *24*, 1263.
222. Nanjo, M.; Nanjo, E.; Mochida, K. *Eur. J. Inorg. Chem.* **2004**, 2961.
223. Harder, S.; Boersma, J.; Brandsma, L.; Kanters, J. A.; Bauer, W.; Schleyer, P. v. R. *Organometallics* **1989**, *8*, 1696.
223a. Harder, S.; Boersma, J.; Brandsma, L.; Kanters, J. A.; Duisenberg, A. J. M.; van Lenthe, J. H. *Organometallics* **1991**, *10*, 1623.
223b. Harder, S.; Ekhart, P. F.; Brandsma, L.; Kanters, J. A.; Duisenberg, A. J. M.; Schleyer, P. v. R. *Organometallics* **1992**, *11*, 2623.
224. Kraus, C. A.; Greer, W. N. *J. Am. Chem. Soc.* **1922**, *44*, 2629.
225. Paver, M. A.; Russell, C. A.; Wright, D. S. *Angew. Chem., Int. Ed. Engl.* **1995**, *34*, 1545.
225a. Becker, G.; Gekeler, M.; Hartmann, H.-M.; Mundt, O.; Westerhausen, M. In *Synthetic Methods in Organometallic and Inorganic Chemistry*; (series editor: W. A. Herrmann; volume editors: N. Auner, U. Klingebiel,); Thieme: Stuttgart, **1996**; Vol. 2, pp 186–192.
226. Reich, H. J.; Borst, J. P.; Dykstra, R. R. *Organometallics* **1994**, *13*, 1.
227. Edlund, U.; Lejon, T.; Pyykkö, P.; Nemkatachalam, T. K.; Buncel, E. *J. Am. Chem. Soc.* **1987**, *109*, 5982.
228. Reed, D.; Stalke, D.; Wright, D. S. *Angew. Chem., Int. Ed. Engl.* **1991**, *30*, 1459.
229. Birchall, T.; Ventrone, J. A. *J. Chem. Soc., Chem. Commun.* **1988**, 77.
230. Eichler, B. E.; Philipps, A. D.; Power, P. P. *Organometallics* **2003**, *22*, 5423.
231. Crow, L.; Endwards, A. J.; Paver, M. A.; Raithby, P. R.; Rennie, A.-A.; Stalke, D.; Wright, D. S. (unpublished)
232. Armstrong, D. R.; Moncrieff, D.; Paver, M. A.; Stalke, D.; Wright, D. S. (unpublished).
233. Cardin, C. J.; Cardin, D. J.; Clegg, W.; Coles, S. J.; Constantine, S. P.; Rowe, J. R.; Treat, S. J. *J. Organomet. Chem.* **1999**, *573*, 96.
234. Fischer, R.; Baumgartner, J.; Marschner, C.; Uhlig, F. *Inorg. Chim. Acta* **2005**, *358*, 3174.
235. Hitchcock, P. B.; Lappert, M. F.; Lawless, G. A.; Rojo, B. *J. Chem. Soc., Chem. Commun.* **1993**, 554.
236. Hellmann, K. W.; Gade, L. H.; Gevert, O.; Steinert, P.; Lauer, J. W. *Inorg. Chem.* **1995**, *34*, 4069.
237. Abrahams, I.; Montevalli, M.; Shah, S. A. A.; Sullivan, A. C. *J. Organomet. Chem.* **1995**, *492*, 99.
238. Kawashima, T.; Iwama, N.; Okazaki, R. *J. Am. Chem. Soc.* **1993**, *115*, 2507.
239. Davidson, M. G.; Stalke, D.; Wright, D. S. *Angew. Chem., Int. Ed. Engl.* **1992**, *31*, 1226.
240. Armstrong, D. R.; Duer, M. J.; Davidson, M. G.; Moncrieff, D.; Russell, C. A.; Stourton, C.; Steiner, A.; Stalke, D.; Wright, D. S. *Organometallics* **1997**, *16*, 3340.
241. von Schnering, H.-G. *Angew. Chem., Int. Ed.* **1981**, *20*, 33.
241a. Corbett, J. D. *Struct. Bond.* **1997**, *87*, 157.
242. Quéneau, V.; Sevov, S. C. *Angew. Chem., Int Ed. Engl.* **1997**, *36*, 1754.
243. Quéneau, V.; Todrov, E.; Sevov, S. C. *J. Am. Chem. Soc.* **1998**, *120*, 3263.
244. Quéneau, V.; Sevov, S. C. *Angew. Chem., Int. Ed. Engl.* **1997**, *36*, 1754.

244a. von Schnering, H. G.; Baitinger, M.; Bolle, U.; Carillo-Cabrera, W.; Curda, J.; Grin, Y.; Heinemann, F.; Llanos, J.; Peters, K., Schmeding, A., *et al. Z. Anorg. Allg. Chem.* **1997**, *623*, 1037.
245. Quéneau, V.; Sevov, S. C. *Inorg. Chem.* **1998**, *37*, 1358.
246. Belin, C. H. E.; Corbett, J. D.; Cisar, A. *J. Am. Chem. Soc* **1977**, *99*, 7163.
246a. Belin, C.; Mercier, H.; Angilella, V. *New J. Chem.* **1991**, *15*, 931.
246b. Fässler, T. F.; Hunziker, M. *Inorg. Chem.* **1994**, *33*, 5380.
246c. Belin, C. E.; Corbett, J. D.; Cisar, A. *J. Am. Chem. Soc.* **1977**, *99*, 716.
247. Burns, R. C.; Corbett, J. D. *Inorg. Chem.* **1985**, *24*, 1489.
248. Downie, C.; Tang, Z.; Gulroy, A. M. *Angew. Chem., Int. Ed. Engl.* **2000**, *39*, 338.
249. Fässler, T. F.; Hoffmann, R. *Angew. Chem., Int. Ed. Engl.* **1999**, *38*, 543.
250. Stender, M.; Philipps, A. D.; Wright, R. J.; Power, P. P. *Angew. Chem., Int. Ed. Engl.* **2002**, *41*, 1785.
250a. Philipps, A. D.; Wright, R. J.; Olmstead, M. M.; Power, P. P. *J. Am. Chem. Soc.* **2002**, *124*, 5930.
250b. Pu, L.; Twamley, B.; Power, P. P. *J. Am. Chem. Soc.* **2000**, *122*, 3523.
251. Pu, L.; Philipps, A. D.; Richards, A. F.; Stender, M.; Simon, R. S.; Olmstead, M. M.; Power, P. P. *J. Am. Chem. Soc.* **2003**, *125*, 11626.
252. Pu, L.; Senge, M. O.; Olmstead, M. M.; Power, P. P. *J. Am. Chem. Soc.* **1998**, *120*, 12682.
253. Freeman, W. P.; Tilley, T. D.; Liable-Sands, L. M.; Rheingold, A. L. *J. Am. Chem. Soc.* **1996**, *118*, 10457.
254. Pu, L.; Haubrich, S. T.; Power, P. P. *J. Organomet. Chem.* **1999**, *582*, 100.
255. Beswick, M. A.; Davies, M. K.; Raithby, P. R.; Steiner, A.; Wright, D. S. *Organometallics* **1997**, *16*, 1109.
256. Heathcock, C. H. The Aldol Reaction: Group 1 and 2 Enolates. In *Comprehensive Organic Synthesis*; Trost, B. M., Fleming, I., Eds.; Pergamon: New York, 1991; Vol. 2, Chapter 1.6.
257. Majewski, M.; Gleave, D. M. *J. Organomet. Chem.* **1994**, *470*, 1.
258. Barr, D.; Clegg, W.; Mulvey, R. E.; Snaith, R.; Wade, K. *J. Chem. Soc., Chem. Commun.* **1986**, 295.
258a. Armstrong, D. R.; Barr, D.; Clegg, W.; Mulvey, R. E.; Reed, D.; Snaith, R.; Wade, K. *J. Chem. Soc., Chem. Commun.* **1986**, 869.
258b. Armstrong, D. R.; Barr, D.; Clegg, W.; Hodgson, S. M.; Mulvey, R. E.; Reed, D.; Snaith, R.; Wright, D. S. *J. Am. Chem. Soc.* **1989**, *111*, 4719.
259. Mulvey, R. E. *Chem. Soc. Rev.* **1991**, *20*, 167.
259a. Gregory, K.; Schleyer, P. v. R.; Snaith, R. *Adv. Inorg. Chem.* **1988**, *27*, 1624.
260. Mulvey, R. E. *Chem. Soc. Rev.* **1998**, 339.
261. Downard, A.; Chivers, T. *Eur. J. Inorg. Chem.* **2001**, 2193.
262. Bond, A. D. *Chem. Eur. J.* **2004**, *10*, 1885.
262a. Bond, A. D. *Cryst. Growth Des.* **2005**, *5*, 755.
263. Rutherford, J. L.; Collum, D. B. *J. Am. Chem. Soc.* **1999**, *121*, 10198.
264. Collum, D. B. *Acc. Chem. Res.* **1993**, *26*, 227.
265. Lucht, B. L.; Collum, D. B. *Acc. Chem. Res.* **1999**, *32*, 1035.
266. Brask, J. K.; Chivers, T. *Angew. Chem., Int. Ed.* **2001**, *40*, 3960.
267. Aspinall, G. M.; Copsey, M. C.; Leedham, A. P.; Russell, C. A. *Coord. Chem. Rev.* **2002**, *227*, 217.
268. Doyle, E. L.; Riera, L.; Wright, D. S. *Eur. J. Inorg. Chem.* **2003**, 3279.
269. Fleischer, R.; Stalke, D. *Coord. Chem. Rev.* **1998**, *176*, 431.
270. Steiner, A.; Zacchini, S.; Richards, P. I. *Coord. Chem. Rev.* **2002**, *227*, 193.
271. Gade, L. H. *Eur. J. Inorg. Chem.* **2002**, 1257.
272. Bourget-Merle, L.; Lappert, M. F.; Severn, J. R. *Chem. Rev.* **2002**, *102*, 3031.
273. Okamoto, Y.; Nakano, T. *Chem. Rev.* **1994**, *94*, 349.
274. Crandall, J. K.; Apparu, M. *Org. React.* **1983**, *29*, 345.
275. Caubère, P. *Chem. Rev.* **1993**, *93*, 2317.
276. Myers, A. G.; Yoon, T.; Gleason, J. *Tetrahedron Lett.* **1995**, *36*, 4555.
276a. Imai, M.; Hagihara, A.; Kawakasi, H.; Manabe, K.; Koga, K. *J. Am. Chem. Soc.* **1994**, *116*, 8829.
276b. Yasukata, T.; Koga, K. *Tetrahedron: Asymmetry* **1993**, *4*, 35.
277. Fjeldberg, T.; Hitchcock, P. B.; Lappert, M. F.; Thorne, A. J. *Chem. Commun.* **1984**, 822.
278. Cetinkaya, B.; Hitchcock, P. B.; Lappert, M. F.; Misra, M. C.; Thorne, A. J. *Chem. Commun.* **1984**, 148.
279. Cole, M. L.; Jones, C.; Junk, P. C. *New J. Chem.* **2002**, *26*, 89.
280. Reiche, C.; Kliem, S.; Klingebiel, U.; Noltemeyer, M.; Voit, C.; Herbst-Irmer, R.; Schmatz, S. *J. Organomet. Chem.* **2003**, *667*, 24.
281. Bartlett, R. A.; Chen, H.; Dias, H. V. R.; Olmstead, M. M.; Power, P. P. *J. Am. Chem. Soc.* **1988**, *110*, 446.
282. Kottke, T.; Klingebiel, U.; Noltemeyer, M.; Pieper, U.; Walter, S.; Stalke, D. *Chem. Ber.* **1991**, *124*, 1941.
283. Clegg, W.; Horsburgh, L.; Liddle, S. T.; Mackenzie, F. M.; Mulvey, R. E.; Robertson, A. *J. Chem. Soc., Dalton Trans.* **2000**, 1225.
284. Armstrong, D. R.; Clegg, W.; Dunbar, L.; Liddle, S. T.; MacGregor, M.; Mulvey, R. E.; Rees, D.; Quinn, S. A. *J. Chem. Soc., Dalton Trans.* **1998**, 3431.
285. Feeder, N.; Snaith, R.; Wheatley, A. E. H. *Eur. J. Inorg. Chem.* **1998**, 879.
286. Bulow, R. v.; Gornitzka, H.; Kottke, T.; Stalke, D. *Chem. Commun.* **1996**, 1639.
287. Avent, A. G.; Frankland, A. D.; Hitchcock, P. B.; Lappert, M. F. *Chem. Commun.* **1996**, 2433.
288. Barr, D.; Clegg, W.; Cowton, L.; Horsburgh, L.; Mackenzie, F. M.; Mulvey, R. E. *Chem. Commun.* **1995**, 891.
289. Walther, D.; Schramm, F.; Theyssen, N.; Beckert, R.; Gorls, H. *Z. Anorg. Allg. Chem.* **2002**, *628*, 1938.
289a. Bradley, J. S.; Cheng, F.; Archibald, S. J.; Supplit, R.; Rovai, R.; Lehmann, C. W.; Kruger, C.; Lefebvre, F. *Dalton Trans.* **2003**, 1846.
290. Ruwisch, L.; Klingebiel, U.; Rudolph, S.; Herbst-Irmer, R.; Noltemeyer, M. *Chem. Ber.* **1996**, *129*, 823.
291. Jones, C.; Junk, P. C.; Smithies, N. A. *J. Organomet. Chem.* **2000**, *607*, 105.
292. Clegg, W.; Liddle, S. T.; Mulvey, R. E.; Robertson, A. *Chem. Commun.* **2000**, 223.
293. Henderson, K. W.; Williard, P. G. *Organometallics* **1999**, *18*, 5620.
294. Clegg, W.; Horsburgh, L.; Mackenzie, F. M.; Mulvey, R. E. *Chem. Commun.* **1995**, 2011.
295. Barnett, N. D. R.; Clegg, W.; Horsburgh, L.; Lindsay, D. M.; Liu, Q.-Y.; Mackenzie, F. M.; Mulvey, R. E.; Williard, P. G. *Chem. Commun.* **1996**, 2321.
296. Clegg, W.; Liddle, S. T.; Mulvey, R. E.; Robertson, A. *Chem. Commun.* **1999**, 511.
297. Kennedy, A. R.; Mulvey, R. E.; Robertson, A. *Chem. Comun.* **1998**, 89.

298. Kowach, G. R.; Warren, C. W.; Haushalter, R. C.; DiSalvo, F. J *Inorg. Chem.* **1998**, *37*, 156.
299. Aubrecht, K. B.; Lucht, B. L.; Collum, D. B. *Organometallics* **1999**, *18*, 2981.
300. Armstrong, D. R.; Carstairs, A.; Henderson, K. W. *Organometallics* **1999**, *18*, 3589.
301. Lucht, B. L.; Collum, D. B. *J. Am. Chem. Soc.* **1996**, *118*, 3529.
302. Armstrong, D. R.; Barr, D.; Clegg, W.; Drake, S. R.; Singer, R. J.; Snaith, R.; Stalke, D.; Wright, D. S. *Angew. Chem., Int. Ed.* **1991**, *30*, 1707.
303. Armstrong, D. R.; Ball, S. C.; Barr, D.; Clegg, W.; Linton, D. J.; Kerr, L. C.; Moncrieff, D.; Raithby, P. R.; Singer, R. J., Snaith, R., *et al. J. Chem. Soc., Dalton Trans.* **2002**, 2505.
304. Neumann, C.; Schulz, A.; Seifert, T.; Storch, W.; Vosteen, M. *Eur. J. Inorg. Chem.* **2002**, 1040.
305. Cragg-Hine, I.; Davidson, M. G.; Edwards, A. J.; Raithby, P. R.; Snaith, R. *J. Chem. Soc., Dalton Trans.* **1994**, 2901.
306. Tesh, K. F.; Jones, D. B.; Hanusa, T. P.; Huffman, J. C. *J. Am. Chem. Soc.* **1992**, *114*, 6590.
307. Clegg, W.; Henderson, K. W.; Horsburgh, L.; Mackenzie, F. M.; Mulvey, R. E. *Chem. Eur. J.* **1998**, *4*, 53.
308. Liddle, S. T.; Clegg, W. *J. Chem. Soc., Dalton Trans.* **2001**, 402.
309. Liddle, S. T.; Clegg, W. *Acta Crystallogr., Sect. E* **2003**, *59*, m1062.
310. For a review on silylhydrazines see: Bode, K.; Klingebiel, U. *Adv. Organomet. Chem.* **1996**, *40*, 1.
311. Uhl, W.; Molter, J.; Saak, W. *Z. Anorg. Allg. Chem.* **1999**, *625*, 231.
311a. Drost, C.; Klingebiel, U. *Chem. Ber.* **1993**, *126*, 1413.
311b. Neumayer, D. A.; Cowley, A. H.; Decken, A.; Jones, R. A.; Lakhotia, V.; Ekerdt, J. G. *Inorg. Chem.* **1995**, *34*, 4698.
312. Bailey, R. E.; West, R. *J. Am. Chem. Soc.* **1964**, *86*, 5389.
312a. West, R.; Ishikava, M.; Bailey, R. E. *J. Am. Chem. Soc.* **1966**, *88*, 4648.
313. Bosold, F.; Marsch, M.; Harms, K.; Boche, G. *Z. Kristallogr.* **1998**, *213*, 619.
314. Knizek, J.; Krossing, I.; Nöth, H.; Schwenk, H.; Seifert, T. *Chem. Ber.* **1997**, *130*, 1053.
315. Nöth, H.; Seifert, T. *Eur. J. Inorg. Chem.* **2002**, 602.
316. Metzler, N.; Nöth, H.; Sachdev, H. *Angew. Chem., Int. Ed.* **1994**, *33*, 1746.
316a. Bode, K.; Klingebiel, U.; Noltemeyer, M.; Witte-Abel, H. *Z. Anorg. Allg. Chem.* **1995**, *621*, 500.
317. Sachdev, H.; Preis, C. *Eur. J. Inorg. Chem.* **2002**, 1495.
318. Gemund, B.; Nöth, H.; Sachdev, H.; Schmidt, M. *Chem. Ber.* **1996**, *129*, 1335.
319. Witte-Abel, H.; Klingebiel, U.; Schafer, M. *Z. Anorg. Allg. Chem.* **1998**, *624*, 271.
320. Bode, K.; Klingebiel, U.; Witte-Abel, H.; Gluth, M.; Noltemeyer, M.; Herbst-Irmer, R.; Schafer, M.; Shomaly, W. *Phosphorus, Sulfur, Silicon, Relat. Elem.* **1996**, *108*, 121.
321. Drost, C.; Jager, C.; Klingebiel, U.; Freire-Erdbrugger, C.; Herbst-Irmer, R.; Schafer, M. *Z. Naturforsch., B.* **1995**, *50*, 76.
322. Nöth, H.; Sachdev, H.; Schmidt, M.; Schwenk, H. *Chem. Ber.* **1995**, *128*, 105.
323. Bosold, F.; Marsch, M.; Harms, K.; Boche, G. *Z. Kristallogr.* **1998**, *213*, 621.
324. Dillworth, D. J.; Rodriguez, A.; Leigh, G. L.; Murrell, J. N. *J. Chem. Soc., Dalton Trans.* **1983**, *2*, 455.
325. For early solution studies see: Wiberg, N.; Weinberg, E.; Joo, W. C. *Chem. Ber.* **1974**, *107*, 1664.
326. Gellermann, E.; Klingebiel, U.; Schafer, M. *Z. Anorg. Allg. Chem.* **2000**, *626*, 1131.
327. Witte-Abel, H.; Klingebiel, U.; Noltemeyer, M. *Chem. Commun.* **1997**, 771.
328. Gellermann, E.; Klingebiel, U.; Pape, T.; Antonia, F. D.; Schneider, T. R.; Schmatz, S. *Z. Anorg. Allg. Chem.* **2001**, *627*, 2581.
329. Drost, C.; Jager, C.; Freitag, S.; Klingebiel, U.; Noltemeyer, M.; Sheldrick, G. M. *Chem. Ber.* **1994**, *127*, 845.
330. Bosold, F.; Marsch, M.; Harms, K.; Boche, G. *Z. Kristallogr.* **1998**, *213*, 623.
330a. Bode, K.; Drost, C.; Jager, C.; Klingebiel, U.; Noltemeyer, M.; Zak, Z. *J. Organomet. Chem.* **1994**, *482*, 285.
331. Sadimenko, A. P.; Basson, S. S. *Coord. Chem. Rev.* **1996**, *147*, 247.
331a. Cosgriff, J. E.; Deacon, G. B. *Angew. Chem., Int. Ed.* **1998**, *37*, 286.
331b. Neif, F. *Eur. J. Inorg. Chem.* **2001**, 891.
332. Butler, R. N. *Comprehensive Heterocyclic Chemistry*, 1st ed., Pergamon: Oxford, 1984; Vol. 5, p 791, and references therein.
333. Zheng, W.; Heeg, M. J.; Winter, C. H. *Eur. J. Inorg. Chem.* **2004**, 2652.
334. Cortes-Llamas, S.; Velázquez-Carmona, M. A.; Muñoz-Hernámdez, M. A. *Inorg. Chem. Commun.* **2005**, *8*, 155.
335. Yélamos, C.; Heeg, M. J.; Winter, C. H. *Inorg. Chem.* **1998**, *37*, 3892.
336. Singh, K.; Long, J. R.; Stavropoulos, P. *J. Am. Chem. Soc.* **1997**, *119*, 2942.
337. Zheng, W.; Heeg, M. J.; Winter, C. H. *Angew. Chem., Int. Ed.* **2003**, *42*, 2761.
338. Lambert, C.; Hampel, F.; Schleyer, P. v. R. *J. Organomet. Chem.* **1993**, *445*, 29.
339. Andrews, P. C.; Clegg, W.; Mulvey, R. E.; O'Neil, P. A.; Wilson, H. M. *Chem. Commun.* **1993**, 1142.
340. Hammer, A.; Holl, G.; Klapötke, T. M.; Mayer, P.; Nöth, H.; Piotrowski, H.; Warchhold, M. *Eur. J. Inorg. Chem.* **2002**, 834.
341. Huang, X. F.; Song, Y. M.; Wu, Q.; Ye, Q.; Chen, X. B.; Xiong, R. G.; You, X. Z. *Inorg. Chem. Commun.* **2005**, *8*, 58.
342. Palenik, G. J. *Acta Crystallogr.* **1963**, *16*, 596.
343. Fernández, D.; Vega, D.; Ellena, J. A.; Echeverría, G. *Acta Cryst., Sect. C.* **2002**, *58*, m418.
344. Tappan, B. C.; Incarvito, C. C.; Rheingold, A. L.; Brill, T. B. *Thermochim. Acta* **2002**, *384*, 113.
345. Arp, H. P. H.; Decken, A.; Passmore, J.; Wood, D. J. *Inorg. Chem.* **2000**, *39*, 1840.
346. Vij, A.; Pavlovich, J. G.; Wilson, W. W.; Vij, V.; Christie, K. O. *Angew. Chem., Int. Ed.* **2002**, *41*, 3051.
347. Chivers, T. *Top. Curr. Chem.* **2003**, *229*, 143.
348. Izod, K. *Adv. Inorg. Chem.* **2000**, *50*, 33.
349. Driess, M. *Adv. Inorg. Chem.* **2000**, *50*, 235.
350. Fritz, G.; Scheer, P. *Chem. Rev.* **2000**, *100*, 3341.
351. Driess, M. *Acc. Chem. Res.* **1999**, *32*, 1017.
352. Driess, M.; Mulvey, R. E.; Westerhausen, M. In *Molecular Clusters of the Main Group Elements*; Driess, M., Nöth, H., Eds.; Wiley: New York, 2004, p 391.
353. Driess, M.; Rell, S.; Pritzkow, H.; Janoschek, R. *Chem. Commun.* **1996**, 305.
354. Isslieb, K.; Tzschach, A. *Chem. Ber.* **1959**, *92*, 1118.
354a. Parshall, G. W.; Lindsey, R. V., Jr., *J. Am. Chem. Soc.* **1959**, *81*, 6273.
355. Driess, M.; Pritzkow, H.; Martin, S.; Rell, S.; Fenske, D.; Baum, G. *Angew. Chem., Int. Ed.* **1996**, *35*, 986.
355a. Driess, M.; Hoffmanns, U.; Martin, S.; Merz, K.; Pritzkow, H. *Angew. Chem., Int. Ed.* **1999**, *38*, 2733.

355b. Driess, M.; Schaller, T.; Sebald, A. *Solid State Nucl. Magn. Reson.* **1997**, *9*, 219.
356. Wiberg, N.; Wörner, A.; Fenske, D.; Nöth, H.; Kinizek, J.; Polborn, K. *Angew. Chem., Int. Ed.* **2000**, *39*, 1838.
356a. Westerhausen, M.; Weinreich, S.; Schmid, B.; Schneiderbauer, M.; Suter, M.; Nöth, H.; Piotrowski, H. *Z. Anorg. Allg. Chem.* **2003**, *629*, 625.
356b. Linti, G.; Kostler, W.; Pritzkow, H. *Eur. J. Inorg. Chem.* **2002**, 2643.
357. Becker, G.; Eschbach, B.; Mundt, O.; Reti, M.; Niecke, E.; Issberner, K.; Nieger, M.; Thelen, V.; Nöth, H., Waldhor, H., *et al. Z. Anorg. Allg. Chem.* **1998**, *624*, 469.
358. Bartlett, R. A.; Dias, H. V. R.; Hope, H.; Murray, B. D.; Olmstead, M. M.; Power, P. P. *J. Am. Chem. Soc.* **1986**, *108*, 6921.
359. Sendlinger, S. C.; Haggerty, B. S.; Rheingold, A. L.; Theopold, K. H. *Chem. Ber.* **1991**, *124*, 2453.
360. Beswick, M. A.; Choi, N.; Hopkins, A. D.; McPartlin, M.; Mosquera, M. E. G.; Raithby, P. R.; Rothenberger, A.; Stalke, D.; Wheatley, A. E. H.; Wright, D. S. *Chem. Commun.* **1998**, 2485.
361. Bashall, A.; Garcia, F.; Hopkins, A. D.; Wood, J. A.; McPartlin, M.; Woods, A. D.; Wright, D. S. *Dalton Trans.* **2003**, 1143.
362. Bashall, A.; Beswick, M. A.; Choi, N.; Hopkins, A. D.; Kidd, S. J.; Lawson, Y. G.; Mosquera, M. E. G.; McPartlin, M.; Raithby, P. R., Wheatley, A. E. H., *et al. J. Chem. Soc., Dalton Trans.* **2000**, 479.
363. Driess, M.; Pritzkow, H. *Angew. Chem., Int. Ed.* **1992**, *31*, 316.
364. Arif, A. M.; Jones, R. A.; Kidd, K. B. *Chem. Commun.* **1986**, 1440.
365. Becker, G.; Witthauer, C. *Z. Anorg. Allg. Chem.* **1982**, *492*, 28.
366. Hitchcock, P. B.; Lappert, M. F.; Smith, S. J. *J. Organomet. Chem.* **1987**, *320*, C27.
367. Jones, L. J.; McPhail, A. T.; Wells, R. L. *J. Coord. Chem.* **1995**, *34*, 119.
368. Belforte, A.; Calderazzo, F.; Morvillo, A.; Pelizzi, G.; Vitali, D. *Inorg. Chem.* **1984**, *23*, 1504.
369. Beswick, M. A.; Lawson, Y. G.; Raithby, P. R.; Wood, J. A.; Wright, D. S. *J. Chem. Soc., Dalton Trans.* **1999**, 1921.
370. Beswick, M. A.; Bashall, A.; Hopkins, A. D.; Kidd, S. J.; Lawson, Y. G.; McPartlin, M.; Raithby, P. R.; Rothenberger, A.; Stalke, D.; Wright, D. S. *Chem. Commun.* **1999**, 739.
371. Breunig, H. J.; Ghesner, I.; Ghesner, M. E.; Lork, E. *Inorg. Chem.* **2003**, *42*, 1751.
372. Breunig, H. J.; Ghesner, M. E.; Lork, E. *J. Organomet. Chem.* **2002**, *660*, 167.
373. Becker, G.; Munch, A.; Witthauer, C. *Z. Anorg. Allg. Chem.* **1982**, *492*, 15.
374. Breunig, H. J.; Ghesner, M. E.; Lork, E. *Chem. Commun.* **2003**, 274.
375. Jones, C.; Thomas, R. C. *J. Organomet. Chem.* **2001**, *622*, 61.
376. Westerhausen, M.; Guckel, C.; Warchhold, M.; Nöth, H. *Organometallics* **2000**, *19*, 2393.
377. Westerhausen, M.; Ossberger, M. W.; Mayer, P.; Piotrowski, H.; Nöth, H. *Organometallics* **2004**, *23*, 3417.
378. Hanauer, T.; Korber, N. *Z. Anorg. Allg. Chem.* **2004**, *630*, 2432.
379. Mundt, O.; Becker, G.; Rossler, M.; Witthauer, C. *Z. Anorg. Allg. Chem.* **1983**, *506*, 42.
380. Beswick, M. A.; Wright, D. S. *Coord. Chem. Rev.* **1998**, *176*, 373.
381. Hopkins, A. D.; Wood, J. A.; Wright, D. S. *Coord. Chem. Rev.* **2001**, *216–217*, 155.
382. Beswick, M. A.; Goodman, J. M.; Harmer, C. N.; Hopkins, A. D.; Paver, M. A.; Raithby, P. R.; Wheatley, A. E. H.; Wright, D. S. *Chem. Commun.* **1997**, 1897.
383. Beswick, M. A.; Harmer, C. N.; Hopkins, A. D.; McPartlin, M.; Wright, D. S. *Science* **1998**, *281*, 1500.
384. Westerhausen, M.; Ossberger, M. W.; Keilbach, A.; Gückel, C.; Piotrowski, H.; Suter, M. *Z. Anorg. Allg. Chem.* **2003**, *629*, 2398.
384a. Nief, F.; Ricard, L. *J. Organomet. Chem.* **2002**, *642*, 208.
384b. Paul, F.; Carmichael, D.; Ricard, L.; Mathey, F. *Angew. Chem., Int. Ed.* **1996**, *35*, 1125.
384c. Niecke, E.; Nieger, M.; Wenderoth, P. *Angew. Chem., Int. Ed.* **1994**, *33*, 353.
384d. Douglas, T.; Theopold, K. H. *Angew. Chem., Int. Ed.* **1989**, *28*, 1367.
385. Whitmire, K. H.; Cassidy, J. M. *Acta Crystallogr. C* **1992**, *48*, 917.
386. Xu, L; Bobev, S.; El-Bahraoui, J.; Sevov, S. C. *J. Am. Chem. Soc.* **2000**, *122*, 1838.
386a. Gascoin, F.; Sevov, S. C. *J. Am. Chem. Soc.* **2000**, *122*, 10251.
386b. Gascoin, F.; Sevov, S. C. *Inorg. Chem.* **2001**, *40*, 5177.
387. Chandler, C. D.; Roger, C.; Hapden-Smith, M. J. *Chem. Rev.* **1993**, *93*, 1205.
388. Fromm, K.; Gueneau, E. D. *Polyhedron* **2004**, *23*, 1479.
389. Bradley, D. C. *Chem. Rev.* **1989**, *89*, 1317.
389a. Veith, M. *Chem. Rev.* **1990**, *90*, 3.
389b. Caulton, K. G.; Hubert-Pfalzgraf, L. G. *Chem. Rev.* **1990**, *90*, 696.
390. Wheatley, P. J. *J. Chem. Soc.* **1960**, 4270.
390a. Dunken, H.; Krausse, J. *Z. Chem.* **1961**, *1*, 27.
390b. Weiss, E. *Z. Anorg. Allg. Chem.* **1964**, *332*, 197.
390c. Weiss, E.; Büchner, W. *Angew. Chem., Int. Ed. Engl.* **1964**, *3*, 152.
390d. Weiss, E. *Helv. Chim. Acta* **1963**, *46*, 2051.
390e. Weiss, E.; Alsdorf, H. *Z. Anorg. Allg. Chem.* **1970**, *372*, 206.
390f. Greiser, T.; Weiss, E. *Chem. Ber.* **1979**, *112*, 844.
391. Greiser, T.; Weiss, E. *Chem. Ber.* **1977**, *110*, 3388.
391a. Davies, J. E.; Kopf, J.; Weiss, E. *Acta Crystallogr., Sect B* **1982**, *38*, 2251.
391b. Weiss, E.; Alsdorf, H.; Kühr, H. *Angew. Chem., Int. Ed. Engl.* **1967**, *6*, 801.
391c. Weiss, E.; Alsdorf, H.; Kühr, H.; Grützmacher, H.-F. *Chem. Ber.* **1968**, *101*, 3777.
392. Nekola, H.; Olbrich, F.; Behrens, U. *Z. Anorg. Allg. Chem.* **2002**, *628*, 2067.
392a. Fromm, K. M.; Gueneau, E. D.; Bernardinelli, G.; Goesmann, H.; Weber, J.; Mayor-López, M.-J.; Boulet, P.; Chermette, H. *J. Am. Chem. Soc.* **2003**, *12*, 125.
392b. Thomas, R. D.; Bott, S. G.; Gravelle, P. W.; Nguyen, H. D. *Abstracts of Papers*, 215th ACS National Meeting, Dallas, 1998, Part 1, INOR 291.
393. Huml, K. *Czech J. Phys.* **1965**, *15*, 699.
393a. Chisholm, M. H.; Drake, S. R.; Naiini, A. A.; Streib, W. E. *Polyhedron* **1991**, *10*, 337.
394. Allan, J. F.; Nassar, R.; Specht, E.; Beatty, A.; Calin, N.; Henderson, K. W. *J. Am. Chem. Soc.* **2004**, *126*, 484.
395. Andrews, P. C.; MacLellan, J. G.; Mulvey, R. E.; Nichols, P. J. *J. Chem. Soc., Dalton Trans.* **2002**, *8*, 1651.
396. Boyle, T. J.; Alam, T. M.; Peters, K. P.; Rodriguez, M. A. *Inorg. Chem.* **2001**, *40*, 6281.

397. Jackman, L. M.; Cizmeciyan, D.; Williard, P. G.; Nichols, M. A. *J. Am. Chem. Soc.* **1993**, *115*, 6262.
397a. Jackman, L. M.; Smith, B. D. *J. Am. Chem. Soc.* **1988**, *110*, 3829.
398. Huffman, J. C.; Geerts, R. L.; Caulton, K. G. *J. Crystallogr. Spectrosc. Res.* **1984**, *14*, 541.
399. Boyle, T. J.; Pedrotty, D. M.; Alam, T. M.; Vick, S. C.; Rodriguez, M. A. *Inorg. Chem.* **2000**, *39*, 5133.
400. Jackman, L. M.; Cizmeciyan, D.; Williard, P. G.; Nichols, M. A. *J. Am. Chem. Soc.* **1993**, *115*, 6262.
401. MacDougall, D. J.; Morris, J. J.; Noll, B. C.; Henderson, K. W. *Chem. Commun.* **2005**, 456.
402. MacDougall, D. J.; Noll, B. C.; Henderson, K. W. *Inorg. Chem.* **2005**, *44*, 1181.
403. Also see: Morris, J. J.; Noll, B. C.; Henderson, K. W. *Cryst. Growth Des.* **2006** DOI: 10.1021/cg0600187.
404. Englich, U.; Ruhlandt-Senge, K. *Coord. Chem. Rev.* **2000**, *210*, 135.
405. Arnold, J. *Prog. Inorg. Chem.* **1995**, *43*, 353.
406. Briand, G. G.; Chivers, T.; Krahn, M. *Coord. Chem. Rev.* **2002**, *233–234*, 237.
407. Weiss, E.; Joergens, U. *Chem. Ber.* **1972**, *105*, 481.
408. Aslam, M.; Bartlett, R. A.; Block, E.; Olmstead, M. M.; Power, P. P.; Sigel, G. E. *Chem. Commun.* **1985**, 1674.
409. Brooker, S.; Edelmann, F. T.; Kottke, T.; Roesky, H. W.; Sheldrick, G. M.; Stalke, D.; Whitmire, K. H. *Chem. Commun.* **1991**, 144.
410. Niemeyer, M.; Power, P. P. *Inorg. Chem.* **1996**, *35*, 7264.
411. Ruhlandt-Senge, K.; Englich, U.; Senge, M. O.; Chadwick, S. **1996**, *35*, 5820
412. Englich, U.; Chadwick, S.; Ruhlandt-Senge, K. *Inorg. Chem.* **1998**, *37*, 283.
412a. Chadwick, S.; Englich, U.; Ruhlandt-Senge, K. *Organometallics* **1997**, *16*, 5792.
412b. Ruhlandt-Senge, K.; Englich, U. *Chem. Commun.* **1996**, 147.
413. Chivers, T.; Downard, A.; Yap, G. P. A. *Inorg. Chem.* **1998**, *37*, 5708.
413a. Janssen, M. D.; Rijnberg, E.; de Wolf, C. A.; Hogerheide, M. P.; Kruis, D.; Kooijman, H.; Spek, A. L.; Grove, D. M.; van Koten, G. *Inorg. Chem.* **1996**, *35*, 6735.
413b. Rose, D. J.; Chang, Y. D.; Chen, Q.; Kettler, P. B.; Zubieta, J. *Inorg. Chem.* **1995**, *34*, 3973.
414. Hernandez-Arganis, M.; Toscano, R. A.; Moya-Cabrera, M.; Garcia-Montalvo, V.; Cea-Olivares, R. *Z. Anorg. Allg. Chem.* **2004**, *630*, 1627.
414a. Heigel, E.; Bock, H.; Krenzel, V.; Sievert, M. *Acta Crystallogr., Sect. C* **2001**, *57*, 154.
415. Lochmann, L. *Eur. J. Inorg Chem.* **2000**, 1115.
416. Schlosser, M. Organoalkali Chemistry. In *Organometallics in Synthesis – A Manual*; Schlosser, M., Ed.; Wiley: Chicester, **2002**; Chapter 1.
417. Mulvey, R. E. *Chem. Commun.* **2001**, 1049.
418. Wittig, G.; Bickelhaupt, F. *Chem. Ber.* **1958**, *91*, 865.
419. Baker, D. R.; Clegg, W.; Horsburgh, L.; Mulvey, R. E. *Organometallics* **1994**, *13*, 4170.
420. Harder, S.; Streitwieser, A. *Angew. Chem., Int. Ed.* **1993**, *32*, 1068.
421. Kremer, T.; Harder, S.; Junge, M.; Schleyer, P. v. R. *Organometallics* **1996**, *15*, 585.
422. Harder, S.; Lutz, M.; Kremer, T. *Organometallics* **1995**, *14*, 2133.
423. Andrews, P. C.; Calleja, S. M.; Maguire, M. *Dalton Trans.* **2002**, 3640.
424. Andrews, P. C.; Calleja, S. M.; Maguire, M. *J. Organomet. Chem.* **2005**, *690*, 4343.
425. Clegg, W.; Horsburgh, L.; Mackenzie, F. M.; Mulvey, R. E. *J. Am. Chem. Soc.* **1996**, *118*, 4721.
426. Holland, R.; Jeffrey, J. C.; Russell, C. A. *Dalton Trans.* **1999**, 3331.
427. Kennedy, A. R.; MacLellan, J. G.; Mulvey, R. E.; Roberston, A. *Dalton Trans.* **2000**, 4112.
428. Kennedy, A. R.; MacLellan, J. G.; Mulvey, R. E. *Angew. Chem., Int. Ed.* **2001**, *40*, 3245.
429. Lochmann, L.; Trevokal, J. *J. Organomet. Chem.* **1979**, *179*, 123.
430. Armstrong, D. R.; Kennedy, A. R.; Mulvey, R. E.; Rowlings, R. B. *Angew. Chem., Int. Ed.* **1999**, *38*, 131.
431. Andrews, P. C.; Kennedy, A. R.; Mulvey, R. E.; Raston, C. L.; Roberts, B. A.; Rowlings, R. B. *Angew. Chem., Int. Ed.* **2000**, *39*, 1960.
432. Henderson, K. W.; Kennedy, A. R.; Mulvey, R. E.; O'Hara, C. T.; Rowlings, R. B. *Chem. Commun.* **2001**, 1678.
433. Clegg, W.; Henderson, K. W.; Kennedy, A. R.; Mulvey, R. E.; O'Hara, C. T.; Rowlings, R. B.; Tooke, D. M. *Angew. Chem., Int. Ed.* **2001**, *40*, 3902.
434. Andrikopoulos, P. C.; Armstrong, D. R.; Clegg, W.; Gilfillan, C. J.; Hevia, E.; Kennedy, A. R.; Mulvey, R. E.; O'Hara, C. T.; Parkinson, J. A.; Tooke, D. M. *J. Am. Chem. Soc.* **2004**, *126*, 11612.
435. Forbes, G. C.; Kennedy, A. R.; Mulvey, R. E.; Roberts, B. A.; Rowlings, R. B. *Organometallics* **2002**, *21*, 5115.
436. Kennedy, A. R.; Mulvey, R. E.; Rowlings, R. B. *J. Organomet. Chem.* **2002**, *648*, 288.
437. Hevia, E.; Kenley, F. R.; Kennedy, A. R.; Mulvey, R. E.; Rowlings, R. B. *Eur. J. Inorg. Chem.* **2003**, 3347.
438. Barr, L.; Kennedy, A. R.; MacLellan, J. G.; Moir, J. H.; Mulvey, R. E.; Rodger, P. J. A. *Chem. Commun.* **2000**, 1757.
439. Forbes, G. C.; Kenley, F. R.; Kennedy, A. R.; Mulvey, R. E.; O'Hara, C. T.; Parkinson, J. A. *Chem. Commun.* **2003**, 1140.
440. Hevia, E.; Gallagher, D. J.; Kennedy, A. R.; Mulvey, R. E.; O'Hara, C. T.; Talmard, C. *Chem. Commun.* **2004**, 2422.
441. He, X.; Noll, B. C.; Beatty, A.; Mulvey, R. E.; Henderson, K. W. *J. Am. Chem. Soc.* **2004**, *126*, 7444.
442. Barnett, N. D. R.; Clegg, W.; Kennedy, A. R.; Mulvey, R. E.; Weatherstone, S. *Chem. Commun.* **2005**, 375.
443. John, M.; Auel, C.; Behrens, C.; Marsch, M.; Harms, K.; Bosold, F.; Geschwind, R. M.; Rajamohanan, P. R.; Boche, B. *Chem. Eur. J.* **2000**, *6*, 3060.
444. Olbrich, F.; Kopf, J.; Weiss, E. *Angew. Chem., Int. Ed.* **1993**, *32*, 1077.
445. Kronenburg, C. M.; Amijs, C. H. M.; Jastrzebski, J. T. B. H.; Lutz, M.; Spek, A. L.; van Koten, G. *Organometallics* **2002**, *21*, 4662.
446. Kronenburg, C. M.; Jastrzebski, J. T. B. H.; Lutz, M.; Spek, A. L.; van Koten, G. *Organometallics* **2003**, *22*, 2312.
447. Niemeyer, M. *Organometallics* **1998**, *17*, 4649.
448. Fröhlich, H.-O; Kosan, B.; Undeutsch, B. *J. Organomet. Chem.* **1994**, *472*, 1.
449. Wyrwa, R.; Fröhlich, H.-O.; Görls, H. *Organometallics* **1996**, *15*, 2833.
450. Rijnburg, E.; Jastrzebski, J. T. B. H.; Boersma, J.; Kooijman, H.; Veldman, N.; Spek, A. L.; van Koten, G. *Organometallics* **1997**, *16*, 2239.
451. Armstrong, D. R.; Clegg, W.; Davies, R. P.; Liddle, S. T.; Linton, D. J.; Raithby, P. R.; Snaith, R.; Wheatley, A. H. *Angew. Chem., Int. Ed.* **1999**, *38*, 3367.
452. Boss, S. R.; Coles, M. P.; Haigh, R.; Hitchcock, P. B.; Snaith, R.; Wheatley, A. H. *Angew. Chem., Int. Ed.* **2003**, *42*, 5593.
453. Clegg, W.; Forbes, G. C.; Kennedy, A. R.; Mulvey, R. E.; Liddle, S. T. *Chem. Commun.* **2003**, 406.
454. Andrikopoulos, P. C.; Armstrong, D. R.; Barley, H. R. L.; Clegg, W.; Dale, S. H.; Hevia, E.; Honeyman, G. W.; Kennedy, A. R.; Mulvey, R. E. *J. Am. Chem. Soc.* **2005**, *127*, 6184.
455. Westerhausen, M.; Rademacher, B.; Schwarz, W. *Z. Naturforsch.* **1994**, *496*, 199.

456. Purdy, A. P.; George, C. F. **1992**, *11*, 1955
457. Darensbourg, D. J.; Yoder, J. C.; Stuck, G. E.; Holtcamp, M. W.; Draper, J. C.; Reibenspies, J. H. *Inorg. Chem. Acta*. **1998**, *274*, 115.
458. Merz, K.; Block, S.; Schoenen, R.; Driess, M. *Dalton Trans*. **2003**, 3365.
459. Bailey, P. J.; Mitchell, L. A.; Raithby, P. R.; Rennie, M.-A.; Verhorevoort, K.; Wright, D. S. *Chem. Commun*. **1996**, 1351.
460. Niemeyer, M.; Power, P. P. *Organometallics* **1995**, *14*, 5488.
461. Fryzuk, M. D.; Giesbrecht, G. R.; Rettig, S. J. *Organometallics* **1997**, *16*, 725.
462. Armstrong, D. R.; Clegg, W.; Davies, R. P.; Liddle, S. T.; Linton, D. J.; Raithby, P. R.; Snaith, R.; Wheatley, A. H. *Angew. Chem., Int. Ed*. **1999**, *38*, 3367.
463. Boss, S. R.; Cole, J. M.; Haigh, R.; Snaith, R.; Wheatley, A. H. *Organometallics* **2004**, *23*, 4527.
464. Armstrong, D. R.; Davies, R. P.; Linton, D. J.; Snaith, R.; Schooler, P.; Wheatley, A. H. *Dalton Trans*. **2001**, 2838.
465. Davies, R. P.; Linton, D. J.; Schooler, P.; Snaith, R.; Wheatley, A. E. H. *Eur. J. Inorg. Chem*. **2001**, 619.
466. Wochele, R.; Schwarz, W.; Klinkhammer, K. W.; Locke, K.; Weidlein, J. *Z. Anor. Allg. Chem*. **2000**, *626*, 1963.
467. Cui, C.; Schmidt, J. A. R.; Arnold, J. *Dalton Trans*. **2002**, 2992.
468. Brask, J. K.; Chivers, T.; Schatte, G.; Yap, G. P. A. *Organometallics* **2000**, *19*, 5683.
469. Brask, J. K.; Chivers, T.; Yap, G. P. A. *Chem. Commun*. **1998**, 2543.
470. Copsey, M. C.; Jeffrey, J. C.; Russell, C. A.; Slattery, J. M.; Straughan, J. A. *Chem. Commun*. **2003**, 2356.
471. Allen, R. E.; Beswick, M. A.; Feeder, N.; Kranz, M.; Mosquera, M. E. G.; Raithby, P. R.; Wheatley, A. E.; Wright, D. S. *Inorg. Chem*. **1998**, *37*, 2602.
472. Beswick, M. A.; Choi, N.; Harmer, C. N.; Hopkins, A. D.; McPartlin, M.; Paver, M. A.; Raithby, P. R.; Steiner, A.; Tombul, M.; Wright, D. S. *Inorg. Chem*. **1998**, *37*, 2177.
473. Bashall, A.; Beswick, M. A.; Harmer, C. N.; Hopkins, A. D.; McPartlin, M.; Paver, M. A.; Raithby, P. R.; Wright, D. S. *Dalton Trans*. **1998**, 1389.

2.02
Alkaline Earth Organometallics

T P Hanusa, Vanderbilt University, Nashville, TN, USA

2.02.1 Introduction

Not long after the publication of COMC (1995), the centenary of the first use of organomagnesium compounds in organic synthesis (1898) was passed.[1] Since the days of Barbier's pioneering work, the subsequently developed family of Grignard reagents has remained the most intensively used class of organoalkaline earth complexes. Study of the other members of group 2, however, varies considerably from element to element. Experimental beryllium chemistry is restricted by concerns over toxicity, although there has been a recent surge of activity with beryllocenes (Section 2.02.2.3) that has partially reversed a mutiple decade-long decline in synthetic research. The revival of interest in calcium, strontium, and barium compounds that was started in the 1980s has continued, and it has expanded from the original emphasis on metallocenes to include many varieties of non-cyclopentadienyl derivatives. Applications in material science (e.g., chemical-vapor deposition (CVD) reagents[2,3]) and catalysis[4] have helped to sustain research with these elements.

As noted in COMC (1995), low-oxidation state group 2 species have been known for some time, but are not readily isolable. Organoalkaline earth gas-phase radicals MR containing the monovalent metals (M = Mg–Sr; R = Me, CCH, η-Cp, η-pyrrolate, C≡CCH$_3$[5]) continue to be studied with both experimental and theoretical methods.[6–8] The gas-phase RaC_2^- ion, which could be considered a radium(I) acetylide (and the only known organoradium species), has been produced with a Cs sputter-ion source.[9] An IR study of the reaction of laser-ablated beryllium and magnesium atoms with acetylene in argon at 10 K indicates that BeCCH and MgCCH are products;[10] under similar conditions in a methane/argon matrix, $BeCH_3$ has been identified.[11] Various low oxidation state aggregates with magnesium–magnesium bonds (e.g., $MeMg_2F$,[12] $MeMg_n$,[13] and $(MeCl)Mg_{(4–21)}$[14]) have been examined computationally as models of Grignard reagent formation, and cluster Grignard reagents $PhMg_4X$ (X = F, Cl, Br) have been prepared by metal-vapor synthesis.[15] None of these compounds is covered further in this chapter; a review of the chemistry of the gas-phase radical species is available.[16]

Even when the metals are in the usual +2 oxidation state, the determination of what constitutes an energetically significant metal–carbon bonding interaction, and hence whether a given compound should be considered an organometallic species, is not always unequivocal. Following the conventions of COMC (1982) and COMC (1995), metal cyanides (i.e., $M(CN)_2$) and salt-like carbides containing the methanide (C^{4-}), acetylide (C_2^{2-}), or allylenide (C_3^{4-}) ions (e.g., Be_2C, CaC_2, Mg_2C_3) are not detailed here; the formation, structures, and spectroscopy of carbides have been reviewed elsewhere.[17]

A more subtle bonding issue in alkaline earth compounds stems from their largely electrostatic metal–ligand interactions, which diminish only slowly with distance (i.e., as $1/r$). As a result, distinctions between bonding and non-bonding contacts cannot always be made from simple distance criteria alone. The magnesium complex $(Me_2NMe_2Si)_3CMgI$ **1**, for example, reacts as a typical Grignard reagent (e.g., $(Me_2NMe_2Si)_3CSnMe_3$ is produced on treatment of **1** with Me_3SnCl).[18] The solid-state structure of **1** indicates that all three N atoms are coordinated to Mg, and that the Mg···C(1) distance is 2.418(6) Å, which is not substantially longer than the 2.10–2.30 Å distances found in typical Grignard reagents (Figure 1).[19] Nevertheless, the carbanionic center is essentially planar (sum of angles = 358.6°), suggesting extensive charge delocalization, and the angles around Mg are typical for a four- rather than five-coordinate metal center. The totality of evidence suggests that there is no direct ionic or covalent Mg···C bonding. Precisely the opposite conclusion about Mg–C bonding was reached in the case of the magnesium bis(phosphoranimine) $CH(Ph_2PNSiMe_3)_2MgI(THF)$ **2**. Despite a magnesium–carbon separation of up to 2.638(6) Å, the geometry about the magnesium is best described as a five-coordinate square-based pyramid (Figure 2). Distortions in the MgN_2P_2C ring also indicate that there is an energetically significant HC···Mg interaction.[20]

A complication in the analysis of structural data is the growing recognition that the involvement of metal cations with a ligand's π-electrons (often in aromatic rings) can give rise to various structural distortions. Such cation–π

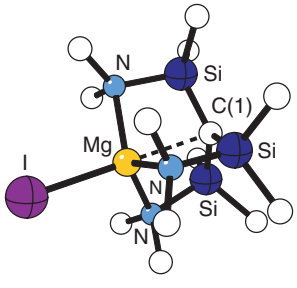

Figure 1 The structure of the magnesium halide $(Me_2NMe_2Si)_3CMgI$ **1**.

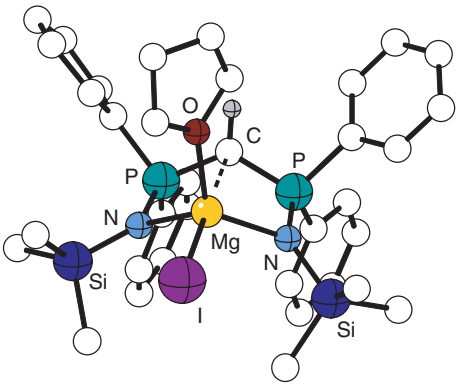

Figure 2 The structure of the magnesium bis(phosphoranimine) $CH(Ph_2PNSiMe_3)_2MgI(THF)$ **2**, with a long Mg···C interaction.

interactions may be surprisingly strong (e.g., the gas-phase binding energy of benzene to the 'hard' K^+ ion (19.2 kcal mol^{-1}) is slightly greater than to water itself),[21] and are increasingly well-documented in many organoalkaline earth compounds. In the solid state, structural perturbations can be imposed on a compound because of packing effects, however, and hence precise discrimination between intra- and intermolecular forces on the geometry of a compound is not always possible. In such cases, assignment of a formal coordination number to a metal center, for example, may not be meaningful.

Molecules in which the only metal–carbon interactions are of the cation–π-type straddle the border between organometallic and coordination chemistry. The organic ligand may be a pendant substituent,[22] or it may be supplied by the solvent; for example, when $BaSn_3[\mu\text{-}PSiBu^t_3]_4$ is synthesized in toluene, the resulting complex **3** displays a neutral arene coordinated in an η^6-fashion to the barium (Figure 3).[23] Not surprisingly, the Ba–C contacts of 3.36–3.48 Å are considerably longer than are typical of distances to charged cyclopentadienyl rings (ca. 3.0 Å),[24] and the toluene is more weakly held. For the purposes of this review, complexes in which the only M–C contacts are from coordinated solvent will not generally be included. Similarly, most complexes containing only macrocyclic ligands, although they may display secondary M···C contacts, are more reasonably considered coordination complexes, and details for them can be found in *Comprehensive Coordination Chemistry* (*CCC*, 2004) or *Comprehensive Supramolecular Chemistry*.

Owing to the common divalent oxidation state of the metals, compounds with similar formulas are frequently found for the entire set of group 2 elements. Nevertheless, the large change in ionic radii (e.g., from four-coordinate Be^{2+} (0.27 Å) to 12-coordinate Ba^{2+} (1.61 Å)[25]) and the variation in covalency associated with it give rise to many differences in structure and reactivity. Complexes of beryllium and magnesium have their own distinctive chemistries, and are covered in separate sections (Sections 2.02.2 and 2.02.3, respectively). Compounds of the metals Ca–Ba are often more similar to each other than they are to the lighter metals, and are discussed as a group (Section 2.02.5).

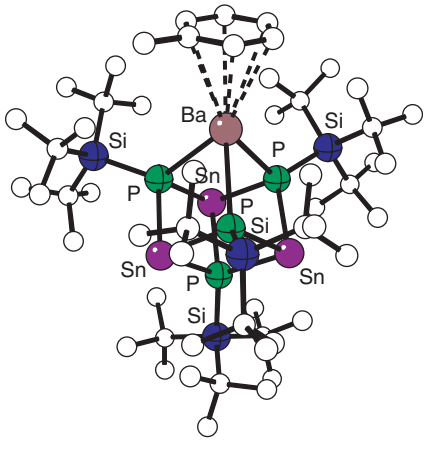

Figure 3 The structure of the solvated barium–tin aggregate, $(\eta^6\text{-toluene})BaSn_3[\mu\text{-}PSiBu^t_3]_4$ **3**.

2.02.2 Beryllium

The revitalization of interest in the organometallic chemistry of the heavy group 2 elements (Ca–Ba) since the 1980s has included the use of ligands that are sterically bulky and/or contain internally chelating groups.[26] The resulting compounds are often monomers or low oligomers (dimers, trimers) with well-defined stoichiometries and reproducible reactivity. A notable development since COMC (1995) is the use of such large ligands with beryllium and magnesium, for which coordination numbers as low as two are now known in several classes of complexes.

2.02.2.1 Alkyl and Aryl Compounds

Although dimethylberyllium is a coordination polymer in the solid state,[27] it has long been known to be monomeric in the gas phase.[28] It has also been found to be monomeric when synthesized from the co-condensation of laser-ablated beryllium atoms and a methane/argon mixture at 10 K.[11] Formed in conjunction with several other species, including hydrides (see Section 2.02.2.4), $(CH_3)_2Be$ was identified from its infrared absorption bands, which were compared to DFT-calculated frequencies (DFT = density functional theory).

The bulky terphenyl substituent $–C_6H_3–2,6\text{-(mesityl)}_2$ (Ar^*) has been used to generate arylberyllium complexes with coordination numbers less than 4. For example, reaction of 1 equiv. of Li[Ar^*] with $BeCl_2(OEt_2)_2$ or $BeBr_2(OEt_2)_2$ gives the monomeric complexes $Ar^*BeX(OEt)_2$ (X = Cl **4** or Br), which possess three-coordinate beryllium atoms.[29] Attempts to use the Ar^* ligand to stabilize a Be–Mo bond were unsuccessful, as addition of 1 equiv. of **4** to $NaMo(\eta^5\text{-}C_5H_5)(CO)_3$ gives the isocarbonyl complex $Ar^*(THF)_2Be(OC)_3Mo(\eta^5\text{-}C_5H_5)$ **5**, which features four-coordinate Be bound to Ar, two THF ligands, and an O from one of the Mo-bound carbonyls (Figure 4). Amino and thio beryllium derivatives containing the Ar^* ligand are described elsewhere (see Section 2.02.2.2). Organometallic *m*-terphenyl derivatives of beryllium have been reviewed.[30]

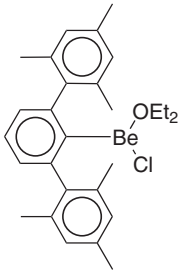

4

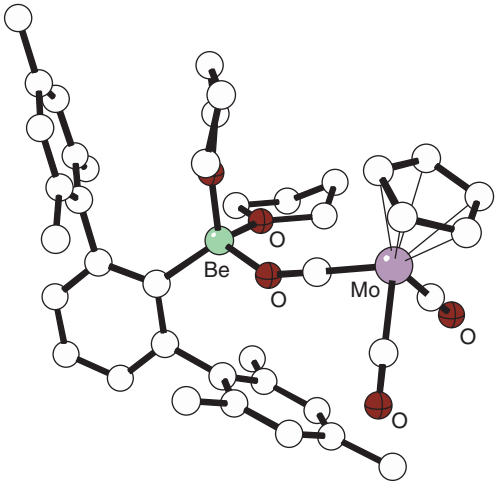

Figure 4 The structure of the isocarbonyl complex $Ar^*(THF)_2Be(OC)_3Mo(\eta^5\text{-}C_5H_5)$ **5**.

2.02.2.2 Derivatives with Group 15 and 16 Donors

The reaction of 4 with LiNHPh affords the thermally unstable dimer $(Ar^*BeNHPh)_2$, which decomposes at room temperature to yield HAr^* and the imide $(MeNPh)_x$.[29] When 4 is allowed to react with $LiNHSiPh_3$ or $LiN(SiMe_3)_2$, the crystallographically characterized monomers $Ar^*BeNHSiPh_3(OEt_2)$ and $Ar^*BeN(SiMe_3)_2$ **6** can be isolated. The latter is a rare example of a compound with a two-coordinate Be center in the solid state (Be–C = 1.519(4); Be–N = 1.519(4) Å) (Figure 5).

The diorganoarsenide derivative $(\eta^5\text{-}Cp^*)BeAsBu^t_2$ **7** was prepared from the reaction of Cp^*BeCl[31] with $LiAs(t\text{-}Bu)_2$ in Et_2O at 0 °C. The structure of the moderately air- and moisture-sensitive compound (mp = 75–76 °C) has been determined with X-ray crystallography.[32] Two nearly identical monomeric molecules are found in the asymmetric unit; for one of them, As–Be = 2.174(14), Be–C = 1.90(3) (av.), and Be–As–CBu^t = 102.3(3)°; the $AsBu^t_2$ ligand behaves as a one-electron donor (Figure 6). The ^{9}Be NMR shift of +14.16 ppm is highly unusual for Cp–Be–X complexes, which are usually in the −27 to −16 ppm range. A DFT study of beryllium NMR shifts predicted that $Cp^*BeAsBu^t_2$ would have a ^{9}Be resonance at −22.30 ppm if the Cp^* ligand were strictly η^5, but that lower ring hapticity in solution (either a static η^3 or an average between η^1 and η^5) would explain the observed downfield NMR shift.[33]

Treatment of 4 with 1 equiv. of Li[SMes*] (Mes* = –C_6H_2–2,4,6-Bu^t_3) produces the colorless three-coordinate thiolate derivative, $Ar^*BeSMes^*(OEt_2)$ 8, which has been crystallographically characterized.[29] Although the Be–S distance of 1.984(3) Å is similar to the 1.989(9) Å bond length observed in $Be(SMes^*)_2(THF)$,[34] the C–Be–S angle of 120.5° angle in 8 is some 10° wider than the comparable values in the bis(thiolate), which suggests that steric crowding is affecting the geometry of 8.

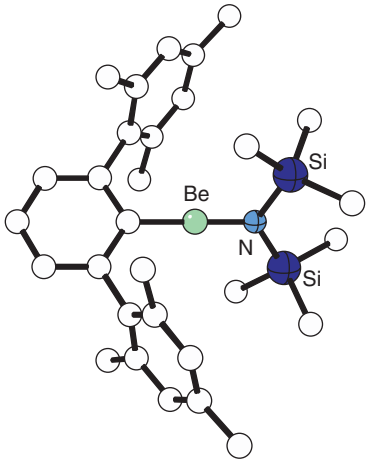

Figure 5 The structure of monomeric $Ar^*BeN(SiMe_3)_2$ **6**, with two-coordinate beryllium.

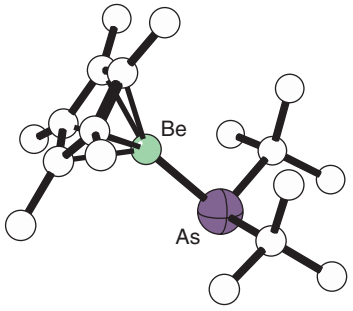

Figure 6 The diorganoarsenide derivative $(\eta^5\text{-}Cp^*)BeAsBu^t_2$ **7**.

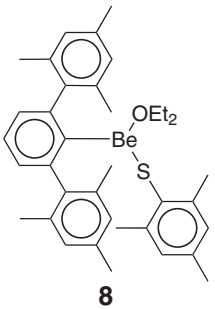

8

2.02.2.3 Cyclopentadienylberyllium Compounds

Cyclopentadienyl derivatives of beryllium are described in reviews that include main-group,[35,36] and specifically group 2, metallocenes.[4,37]

2.02.2.3.1 Dicyclopentadienylberyllium (beryllocene) and related compounds

For four decades after the report of the volatile, hydrocarbon-soluble dicyclopentadienylberyllium **9** by Fischer and Hofmann in 1959,[38] it remained the only crystallographically characterized beryllocene (the mixed-ring complex $(C_5Me_5)Be(C_5H_5)$ was reported in 1990,[39] but not structurally authenticated). The difficulty of establishing and understanding the non-classical structure of **9** has made it one of the most intensively studied main group metallocenes. In 2000, Carmona and co-workers reported the first structures of substituted beryllocenes, $(C_5Me_4H)_2Be$ and $(C_5Me_5)_2Be$,[40] which not only displayed unanticipated geometries, but also provided insight into the bonding of the parent molecule.

9

The many attempts to determine the structure of Cp_2Be have been reviewed,[37] but from the beginning, a ferrocene-like structure with D_{5h} or D_{5d} symmetry was ruled out from dipole-moment measurements (2.24 D in cyclohexane at 25 °C).[38] The results of electron-diffraction data,[41,42] Raman spectroscopy,[43] and X-ray diffraction results[44–46] were not always consistent with one another, but the consensus in recent years, bolstered by molecular dynamics[47,48] and OFT calculations,[49] is that **9** adopts an η^5/η^1-slip-sandwich structure in solution and the solid state. DFT calculations have been used to determine that the η^5/η^1-C_s structure is indeed the global minimum on the potential energy surface.[49] With some density functionals (BP86, B3P86), this conclusion is basis-set dependent, and the use of a relatively large basis set (6-311G(*d*,*p*)) is required to establish that the C_s structure is in fact the lowest-energy conformer. A redetermination of the X-ray structure of **9** at −100 and 20 °C confirmed the η^5/η^1-structure at the lower temperature but at 20 °C, there is somewhat less slippage of the rings, which can be described as η^5/η^2-coordination.[50] Beryllocene is thought to adopt its easily distorted structure because of a balance between Be–C bond strength, favored by σ-bonding, and Cp delocalization energy, which is favored by π-bonding.[51]

Beryllocene has long been known to be fluxional in solution (down to −125 °C),[52] but a more recent study has found it to be fluxional in the solid state as well.[50] The nature of the fluxional process has been studied with a combination of DFT, the Car–Parrinello projector augmented wave method, and Car–Parrinello molecular dynamics calculations. Two facile rearrangements have been recognized. One of them is a 1,5-sigmatropic shift of the Be(η^5-C_5H_5) unit around the periphery of the η^1-C_5H_5 ring, proposed to occur through a η^5/η^2-transition state, with an activation barrier of 5 kJ mol^{-1}. The second rearrangement involves a molecular inversion process that interchanges the η^5- and η^1-ligands through an η^3/η^3-transition state with an activation energy of 8 kJ mol^{-1} (Scheme 1). The rate of hapticity change in vacuum at 400 K is on the order of $1–5 \times 10^{12}$ s^{-1}.[53] In the solid state, ^{13}C VT CP/MAS NMR spectra of **9** have been used to demonstrate that the hapticities of the rings are exchanged by the motion of the beryllium atom between crystallographically equivalent sites; the activation energy of the inversion process is experimentally found to be 36.9 kJ mol^{-1}.

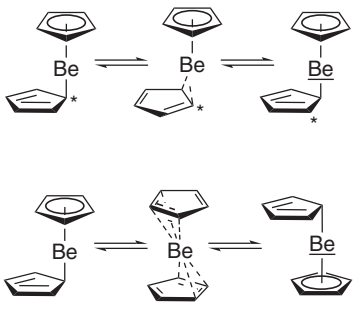

Scheme 1

The gas-phase decomposition of beryllocenes has been examined for the doping of semiconductor materials and in the preparation of thin metal films. Molecular-beam expitaxy has been used with $(MeC_5H_4)_2Be$ to dope InP semiconductors; only a small amount of carbon is found in the doped films.[54] Beryllocene **9** has been explored as a precursor for coating capsules with beryllium metal for use as targets in experiments with inertial confinement fusion.[55]

The failure of attempts[31,39] to prepare the permethylated derivative of **9**, $(C_5Me_5)_2Be$ **10**, was at one point rationalized by arguing that "steric oversaturation" of the metal center would be present in a sandwich compound containing the small Be^{2+} cation and such sterically bulky rings.[26] Nevertheless, the beryllocenes $(C_5Me_4H)_2Be$ **11**, **10**, and $(C_5Me_5)Be(C_5Me_4H)$ **12** can be prepared from $BeCl_2$ and the appropriate KCp′ reagent in Et_2O or toluene/Et_2O mixtures. The synthesis of **11** proceeds in 70% yield under mild conditions (12 h at 20 °C in Et_2O), but generation of **10** requires prolonged reaction times (3–4 days) and higher temperatures (115 °C reflux). The product is isolated in only 50% yield and is always contaminated with $(C_5Me_5)BeCl$, which can be removed by sublimation. Clearly, the exchange reaction of $(C_5Me_5)BeCl$, which evidently is an intermediate in the formation of **10**, is slow.

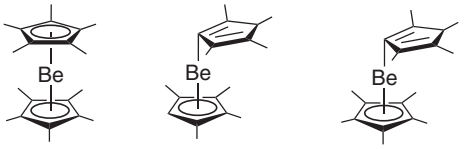

10 **11** **12**

Kinetics appears to play a strong role in the formation of cyclopentadienylberyllium compounds, and the identity of the Cp′ ring is critical to the outcome of synthetic reactions. In the case of Cp′ = C_5Me_4H, reaction of equal equivalents of $K[C_5Me_4H]$ and $BeCl_2$ leads exclusively to **11**, and not $(C_5Me_4H)BeCl$ (Equation (1)):

$$2K[C_5Me_4H] + 2BeCl_2 \longrightarrow (C_5Me_4H)_2Be + 2KCl + BeCl_2 \quad (1)$$

When Cp′ = 1,2,4-$(SiMe_3)_3C_5H_2$, reaction of 2 equiv. of its potassium salt with $BeCl_2$ under the forcing conditions that produced **10** generates only decomposition products. As the calculated ground-state structure of [1,2,4-$(SiMe_3)_3C_5H_2]_2Be$ possesses the η^5/η^1-geometry observed in other beryllocenes, steric crowding does not appear to be the reason for its failure to form.[56]

Like the parent Cp_2Be, the beryllocenes **10**, **11**, and **12** are sublimable, air- and oxygen-sensitive solids. They do not react with pyridine, CO, or 1,3,4,5-tetramethylimidazol-2-ylidene, but do react with $CNC_6H_3Me_2$-2,6 to give half-sandwich iminoacyl products via insertion into the Be–C σ-bond, described in Section 2.02.2.3.2.

The structures of the three metallocenes have been determined with low-temperature X-ray studies. Both **11** and **12** possess η^5/η^1-geometries of the slip-sandwich type. The distances between the Be atoms and the η^5-ring centroids are the same (av. 1.47 Å) and are close to those in **9** (1.505 Å).[46] The Be–CH bond lengths are also indistinguishable within experimental error (1.77 Å) and are only slightly shorter than the analogous distance in Cp_2Be (1.826(6) Å).[46] The two rings in each complex are planar and only slightly canted, with interplanar angles of 6.6(1)° for **11** and 4.9(1)° for **12**. The substitution of the ring H by CH_3 does not cause overt changes in the molecular geometry.

Unlike the slipped octa- or non-methyl derivatives, however, **10** exhibits a ferrocene-like η^5/η^5-parallel-sandwich structure. The Be–C_5Me_5 centroid distance (1.655(1) Å) and the Be–C distance (av. 2.049 Å) are noticeably longer than in **9** (by 0.12 Å). There is some spread in the Be–C bond lengths in **10** ($\Delta = 0.15$ Å), and there are inter-ring Me–Me′ contacts as close as 3.63 Å (cf. the sum of the van der Waals radii of 4.0 Å[57]).

Solution and solid-state NMR variable-temperature NMR studies have revealed the bonding and conformational changes in the methylated beryllocenes **10–12**. The molecules are fluxional in solution, and are believed to undergo the same types of 1,5-sigmatropic shifts and molecular inversion around the metal center that are associated with the parent beryllocene. The rings of **11** are equivalent in their ^{1}H and ^{13}C NMR spectra from −90 to +80 °C. Similarly, **10** displays a singlet in its ^{1}H NMR spectrum at $\delta = 1.9$–2.0 between −90 and +80 °C and a single ^{13}C resonance for the ring carbons even at low temperature ($\delta = 109.7$ at −90 °C). It is assumed that η^5/η^5- and η^5/η^1-conformers are in equilibrium in solution, a supposition supported by the isolation of iminoacyl isomers (see Section 2.02.2.3.2). The tetramethyl-substituted ring of **12** displays more variability with temperature (a shift in the ^{13}C resonance of the CH position resonance from $\delta = 67.0$ to 59.3 ppm during the temperature change from +95 to −90 °C). A well-resolved coupling of 10 Hz is observed between the ^{13}CH and quadrupolar ($I = 3/2$) ^{9}Be nuclei at +95 °C; this NMR evidence supports the assumption that the (η^5-C_5Me_5)Be(η^1-C_5Me_4H) structure observed in the solid state also contributes to the solution structure.

Solid-state ^{9}Be and ^{13}C NMR studies have been used to characterize the structure and dynamics of the methyl-substituted beryllocenes. The isotropic ^{9}Be chemical shift has been found to vary with the coordination of the Cp′ rings, from −19.8 ppm in **11** (η^5/η^1) to −24.4 ppm in **10** (η^5/η^5). The Cp′ rings of **11** display comparatively little motion from −100 to 80 °C, whereas the rate of reorientation of the C_5Me_5 rings decreases substantially at low temperatures in **10**.[50]

Calculations at various levels of theory have been used to analyze the bonding in **10** and **12** and how it differs from that in **9**.[58] DFT calculations using the B3LYP functional place a η^5/η^1 C_s symmetric conformation 3 kcal mol^{-1} lower in energy than a ferrocene-like η^5/η^5 D_{5d} form, although the difference shrinks to only 1 kcal mol^{-1} with the PW91 functional. It is possible that the η^5-rings of **10** observed in the solid state are an artifact of crystal packing. The electrostatic contribution to the bonding in **9** and **10** is estimated at roughly 65% and 58%, respectively, highlighting the considerable covalent contribution to the bonding.

2.02.2.3.2 Beryllium monocyclopentadienyls

The monocyclopentadienyl complexes (C_5Me_5)BeX (X = Cl **13**, Br) are versatile stating materials for other half-sandwich complexes. The chloride derivative **13** can be prepared in 20% yield from the reaction of $(C_5Me_5)_2Mg$ with $BeCl_2(OEt_2)_2$ in Et_2O; the yield rises to 55% in refluxing toluene/diethyl ether.[59] The reaction of M[C_5Me_5] (M = Na, K) with $BeX_2(OEt_2)_2$ (X = Cl, Br) generates both halide derivatives in high yield. Subsequent reaction with alkyllithium reagents LiR in Et_2O (R = Me, CMe_3, CH_2CMe_3, CH_2Ph) produces the monomeric (η^5-C_5Me_5)BeR derivatives. Although the halide derivatives can be sublimed under vacuum (60 °C, 0.05 mm), the alkyl derivatives are more volatile; for example, (η^5-C_5Me_5)BeMe **14** sublimes at 60 °C at atmospheric pressure or at 0.1 mm at ambient temperature. The ^{13}C NMR resonance of the methyl group in **14** appears as a 1 : 1 : 1 : 1 pattern from coupling to ^{9}Be ($^1J_{(Be–C)} = 30$ Hz); quadrupolar relaxation by beryllium ($I = 3/2$) may be the reason that the resonance is not observed with the other alkyl derivatives. The alkyl derivatives are stable toward ligand rearrangement, and although they are decomposed by water, the Be–R bond does not undergo hydrogenolysis.

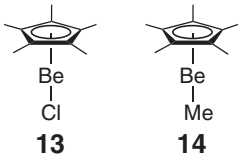

13 **14**

Direct reaction of the substituted beryllocenes **10–12** with the isonitrile CNXyl (Xyl = C_6H_3–2,6-Me_2) forms the iminoacylberyllium compounds Cp′BeC(=NXyl)Cp″, in which the isonitrile has inserted into a Be–C bond.[60] The process is reversible with **10** ($\Delta H° = 18 \pm 0.4$ kcal mol^{-1}; $\Delta S° = 35 \pm 1$ cal mol^{-1} K^{-1}), and the insertion product **15** obtained at 25 °C was characterized with X-ray diffraction (Figure 7).[60] With **11**, three iminoacyl isomers are possible; two of them have been isolated, which differ by the carbon of the Cp′ ring to which the isonitrile carbon has coupled (either at the CH unit of the Cp′ ring or β to it). The formation of the iminoacyl complexes is proposed to occur by direct attack of the CNXyl on a Be–η^1-Cp′ bond. A migratory insertion reaction, involving precoordination of the

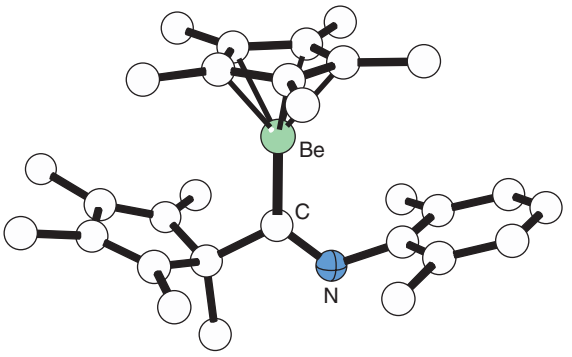

Figure 7 The structure of the iminoacylberyllium complex $(C_5Me_5)BeC(=NXyl)(C_5Me_5)$ **15**.

isonitrile unit, is probably unlikely, given the steric crowding around the metal center and the lack of available orbitals on the metal center. The isolation of the iminoacyl provides direct support for the existence of η^5/η^1-conformers in solution.

The reaction of CNXyl with the nonamethyl complex **12** generates an insertion product **16**. It has four possible isomers if both the η^5/η^1- and the "molecular inversion" rearrangements that are proposed to occur in Cp_2Be are operative (Scheme 2, **A–D**). Three isomers have been isolated;[59] at −78 °C, isomer C is formed exclusively and reversibly, suggesting that it has the lowest barrier to C–C coupling reactions. At room temperature, the "inverted" isomer D forms, which has been crystallographically authenticated, and which substantiates the existence of the inverted beryllocene structure in solution.[61] Only by heating to 80–100 °C is the isomer **A** generated, suggesting that the Be–η^1-C_5Me_4H bond is the strongest and most resistant to coupling.

In a search for CVD precursors for beryllium, the air sensitive, volatile solid $CpBe(SiMe_3)$ **17** was prepared from the reaction of $Li[SiMe_3]$ with CpBeCl in pentane.[62] Characterized with single crystal X-ray diffraction, multinuclear NMR, and mass spectra, the compound displays a Be–Si bond length of 2.185(2) Å that is somewhat longer than the sum of covalent radii (2.01 Å). The lengthening is similar to that observed in the related $Be(Si(t\text{-}Bu)_3)_2$ (Be–Si = 2.193(1) Å),[63] so there is not a pronounced effect from the Cp ligand on the Be–Si interaction.

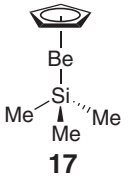

17

DFT calculations were used to optimize the geometry and to derive charges on the molecular fragments in **17**, and the values for Cp (−0.79 e$^-$), Be (+1.26 e$^-$), Si (+0.81 e$^-$), and Me_3 (−1.28 e$^-$) indicate that the interaction between the cyclopentadienyl ring and beryllium is largely ionic, and that the Be–Si bond is polarized toward Si. The ^{9}Be and ^{29}Si NMR spectra exhibit a substantial J(Be–Si) of 51 Hz and a large upfield ^{9}Be shift of $\delta = -27.7$ ppm (see Section 2.02.2.5). Thermal decomposition of **17** produces $C(SiMe_3)_4$, CpBeMe, and $CpBe(SiMe_2SiMe_3)$ **18** as principle products; the latter was independently synthesized from the reaction of CpBeCl and $Li[SiMe_2SiMe_3]$; its ^{9}Be shift of $\delta = -27.2$ ppm is similar to that of **17**.[62]

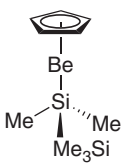

18

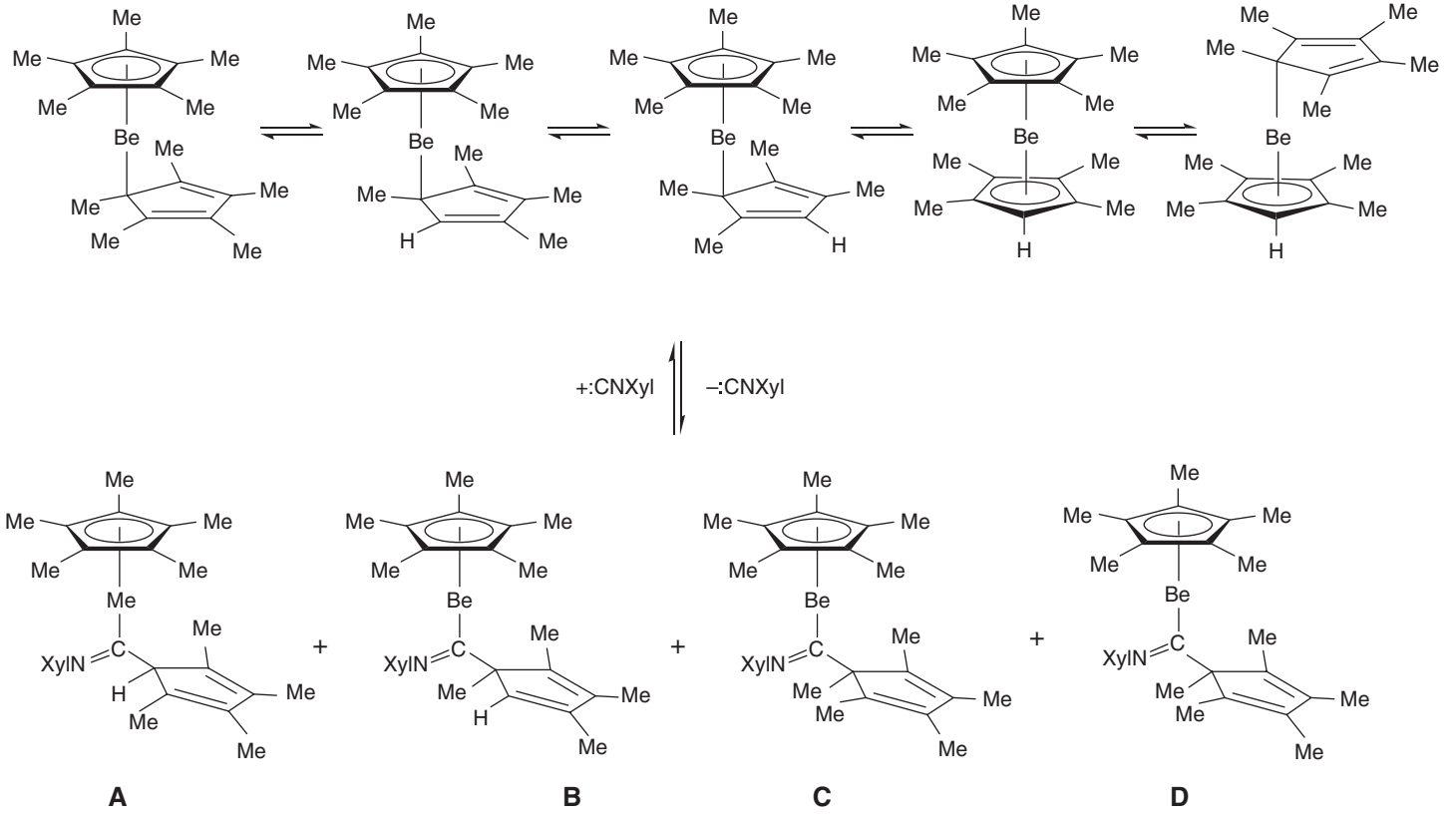

Scheme 2

2.02.2.4 Hydrides

When beryllium atoms produced by laser ablation are co-condensed with methane/argon mixtures onto a substrate at 10 K, a variety of products are formed, including organoberyllium hydrides. In conjunction with DFT calculations, infrared spectroscopy using ^{2}H and ^{13}C substitution experiments have been used to identify the species CH_3BeH ($\nu_{(Be-H)} = 2{,}062/2{,}059\,cm^{-1}$ (site-split)), H_2CBeH ($\nu_{(Be-H)} = 2{,}072\,cm^{-1}$), and HCBeH ($\nu_{(Be-H)} = 2{,}072\,cm^{-1}$).[11] It is likely that all of these are generated from an initial insertion of a Be atom in the C—H bond of methane, followed by H or H_2 loss (Scheme 3).

Beryllium atoms generated under similar conditions react in an acetylene/argon matrix at 10 K to produce HBeCCH ($\nu_{(Be-H)} = 2{,}119\,cm^{-1}$).[10] The observation of BeH, BeH_2, ·CCH, and HCC–CCH as co-products indicates that some fraction of the beryllium atoms abstracts hydrogen from HCCH (Equation (2)):

$$Be^{*} + HCCH \longrightarrow BeH + {\bullet}CCH \qquad (2)$$

An attempt to generate the hydride $(C_5Me_5)BeH$ from the reaction of $(C_5Me_5)BeBr$ with $LiAlH_4$ produced a white solid with an IR absorption variably observed at 1950–1985 cm^{-1} that is in the region for Be–H stretches.[59] No hydride resonance could be found in the ^{1}H NMR spectrum, however, and ^{1}H, ^{9}Be, and $^{13}C\{^{1}H\}$ NMR indicated that the only products were a mixture of **10** and unreacted $(C_5Me_5)BeBr$. It is possible that $(C_5Me_5)BeH$ forms but decomposes at room temperature to form **10** and undetected, insoluble BeH_2.

2.02.2.5 Miscellaneous Reactions and Data

Pulsed laser-evaporated Be atoms and CO react during condensation in an argon matrix at 10 K to produce several beryllium carbonyls. Identification was based on the further reactions that occurred on warming to 30 K, changes in relative Be/CO concentration, ^{13}CO and $C^{18}O$ isotopic substitution, and *ab initio* calculations. The simplest possible beryllium carbonyl, the triplet BeCO molecule, does not form on annealing in solid argon; it is calculated to be less stable than the energy of just Be + CO alone. The primary products formed during condensation are identified as BeBeCO ($\nu_{CO} = 1{,}943.6\,cm^{-1}$) and OCBeBeCO ($\nu_{CO} = 1{,}906.4,\ 1{,}903.4\,cm^{-1}$), whose IR bands decrease on broad-band photolysis but are regenerated on annealing the matrix. Secondary product bands assigned to higher carbonyls grow strongly on annealing and are identified as the stable $Be(CO)_2$, $Be(CO)_3$, $BeBe(CO)_2$, $(OC)BeBe(CO)_2$, and $(OC)_2BeBe(CO)_2$ molecules. It was proposed that clustering of Be atoms and CO molecules leads to product formation in these experiments; for example, BeBeCO is thought to form on reaction of CO with the initially formed Be_2 dimer.[64]

Under conditions similar to that used with CO, laser-evaporated Be atoms and CO_2 react during condensation in excess argon to form CO, ArBeO, BeOBe, and two new molecules in a 29 : 1 ratio that display CO and BeO stretching absorptions, identified as OC–BeO and the isocarbonyl CO–BeO (Equation (3)).

$$Be + CO_2 \longrightarrow BeO + CO \longrightarrow OC{-}BeO + CO{-}BeO \qquad (3)$$

The characterization of the species was accomplished with the aid of isotopic labeling studies and *ab initio* calculations. The Be–CO stretching frequency of 2,189.5 cm^{-1}, above that of CO itself in solid argon (2,138.4 cm^{-1}) indicates the considerable strength of BeO as a Lewis acid.[65]

Three or more equivalents of the nucleophilic Wanzlick-type carbene[66] 1,3-dimethylimidazolin-2-ylidene react with $BeCl_2$ to cleave its bridging Be–Cl–Be bonds, forming the stable pale yellow ionic coordination compound $[(1,3\text{-}Me_2\text{-}C_3N_2H_2)_3BeCl]^{+}Cl^{-}$ **19**.[67] There is a large upfield shift in the ^{13}C NMR resonances of the carbene atom

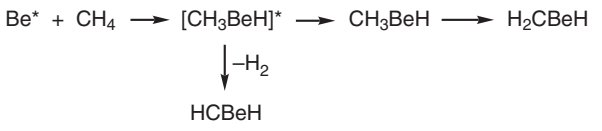

Scheme 3

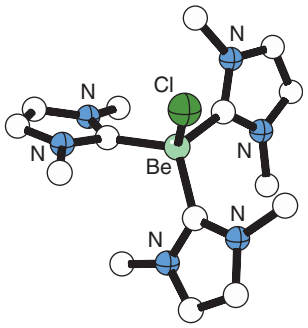

Figure 8 The structure of the beryllium carbene complex $[(1,3\text{-}Me_2\text{-}C_3N_2H_2)_3BeCl]^+Cl^-$ **19**.

from 213 to 174.8 ppm on complexation. The solid-state structure reveals a Be–Cl distance (av. 2.08 Å) that is unusually long for four-coordinate beryllium, but the Be–C length of 2.08 Å (av.) is comparable to the bond distance in $(CH_3)_2Be$ (1.85(3) Å) (Figure 8).

The stability of the coordination complex **19**, despite the obvious lack of $R_2C \leftarrow ML_n$ backdonation such as that occurs in transition metal–carbene complexes, prompted an extensive quantum chemical *ab initio* study of the beryllium–carbene complexes $Be(CX_2)_n^{2+}$ (X = H, F; n = 1–4), $ClBe(CX_2)_n^+$ (X = H, F; n = 1–3), $Cl_2Be(CX_2)_n$ (X = H, F; n = 1, 2), and $ClBe(C(NH_2)_2)_3^+$. The carbene ligands were found to be pure donors in the complexes. The dications $Be(CX_2)_n^{2+}$ (X = H, F; n = 1–4) have strong Be^{2+}–C donor–acceptor bonds. The bond strengths decrease when the number of carbene ligands increases, and the CH_2 complexes have stronger Be–C bonds than the CF_2 complexes. Yet the methylene complexes are chemically less stable than the CF_2 complexes, because the carbon $p(\pi)$-orbital of CH_2 stays nearly empty in the complexes, which makes them prone to nucleophilic attack. The chief determinant of the chemical stability of carbenes and carbene complexes is the population of the carbon $p(\pi)$-orbital. In the case of pure acceptor metals such as beryllium, this is accomplished by enhanced π-donation from the substituents to the carbene.[68]

An extensive survey and computational analysis of solution ^{9}Be NMR has been published; the organometallic species, with several additions, are listed in Table 1.[33] Interestingly, organoberyllium species mark both extremes of the known chemical shift range (−27.7 ppm for $CpBeSiMe_3$; +20.8 ppm for Me_2BeOEt_2). Cyclopentadienyl complexes are found from −28 to −15 ppm; the high-field chemical shifts of Be nuclei are ascribed to ring-current effects, assisted by increased electron density on the Cp ring.[62] Beryllium complexes with coordination numbers of two and three tend to have values below 8 ppm. In general, calculated chemical shifts using the B3LYP/6-311 + G(2*d*,*p*) combination in conjunction with the GIAO method produced chemical-shift values with an average discrepancy from experimentally determined values of 0.5 ppm (maximum 1.6 ppm). The accuracy of the predictions was used as evidence that the previously reported value for $(\eta^5\text{-}Cp^*)BeAsBu^t_2$ was in error (see Section 2.02.2.2).

2.02.3 Magnesium

2.02.3.1 Organomagnesium Halides

As in COMC (1995), Grignard reagents will normally be represented in this chapter by the simple formula RMgX (R = organic group, X = halogen), although solvation, dismutation (often called "disproportionation," but erroneously so, as no oxidation state changes are involved), aggregation, and deviations from this stoichiometry are common. Despite extensive work in the area, as documented in the previous review,[72–75] the mechanisms of Grignard reagent formation still require further study. The many variables involved, including the identity of the substrates, the nature of the solvents used, and the physical form of the magnesium, greatly complicate the research. For example, analysis of byproducts suggests that the formation of a Grignard reagent from magnesium and an aliphatic halide in ether proceeds via a radical mechanism. In contrast, Grignard reactions of aryl halides appear to proceed largely through a pathway along which R· is not an intermediate. This is probably a dianion pathway, one along which RX^{2-} is an intermediate or transition state.[76] Several books and reviews on Grignard reagents, stressing applications in organic synthesis,[77–79] and the chemistry of highly functionalized organomagnesium reagents[80] have been published.

Table 1 Organometallic ^{9}Be NMR chemical shift values[a]

Compound	*δ*	*Solvent/lock* (°C)	$W_{1/2}$ (Hz)	*Formal C.N.*	*References*
$CpBeSi(CH_3)_3$	−27.7	C_6D_6 (20)	8	η^5+1	62
$CpBeSi(CH_3)_2Si(CH_3)_3$	−27.2	C_6D_6 (20)		η^5+1	62
$CpBeBH_4$	−22.1	C_6F_6 (20)	31	η^5+2	69
$CpBeB_5H_8$	−21.0	C_5H_{12}/F_3Br (20)	28	η^5+2	69
$CpBeCH_3$	−20.5	$C_6H_5CH_3$ (20)	10	η^5+1	70
$CpBeCH_3$	−20.5	C_6D_6 (20)		η^5+1	62
$CpBeCH_3$	−20.4	C_5H_{12}/F_3Br (20)	8	η^5+1	69
$CpBeCH_3$	−20.1	C_6H_{12} (20)	7	η^5+1	70
CpBeCl	−19.5	C_6H_6 (20)		η^5+1	69
CpBeBr	−19.5	C_6H_6 (20)	4	η^5+1	70
CpBeCl	−19.1	C_6F_6 (20)	3	η^5+1	69
Cp_2Be	−18.5	$C_6H_5CH_3$ (20)		$\eta^5+\eta^1$	69
Cp_2Be	−18.3	$C_6H_{11}CH_3$ (20)		$\eta^5+\eta^1$	70
$Cp^*Be(CH_3)$	−16.7	C_6D_6 (25)	16	4	59
Cp^*BeBr	−15.2	C_6D_6 (25)	3.5	4	59
$Ar^*(THF)_2Be(OC)_3MoCp$[b]	2.7	C_6D_6 (70)	150	4	29
$[(CH_3)_2Be{\cdot}\{P(CH_3)_3\}_2]$	3.6	$P(CH_3)_3$ (20)		4	69
$CH_3BeCl{\cdot}[S(CH_3)_2]_2$	4.2	$(CH_3)_2S$ (20)		4	69
$(B_3H_8BeCH_3)_2$	6.6	CH_2Cl_2/CF_3Br (20)	19	4	69
$(B_3H_8BeCH_3)_2$	7.6	C_6F_6 (20)	18	4	69
$Bu^t(CH_3)_3SiNBeOEt$	9.12	C_6D_6 (20)	85	3	71
$(CH_3)_2Be{\cdot}S(CH_3)_2$	11.6	$S(CH_3)_2$ (20)			69
$Bu^t(CH_3)_3SiNBeCl$	11.60	C_6D_6 (20)	90	3	71
$(CH_3BeBH_4)_2$	11.7	C_5H_{12}/CF_3Br (20)	7	4	69
$[(TMP)BeBu^t]_2$[c]	11.9	C_6D_6 (20)	140	3	71
$(CH_3)_2Be{\cdot}[N(CH_3)_3]_2$	12.0	$N(CH_3)_3$ (20)			69
$(CH_3BeBH_4)_2$	12.2	C_6F_6 (20)	12		69
$Ar^*BeNHSiPh_3{\cdot}OEt_2$[b]	12.6	C_6D_6 (70)	285	3	29
$Ar^*BeCl(OEt_2)$[b]	12.8	C_6D_6 (20)	315	3	29
$ArBeBr(OEt_2)$[b]	13.4	C_6D_6 (20)	245	3	29
$Cp^*BeAsBu^t_2$	14.16	C_6D_6 (20)		η^5+1	32
$Ar^*BeN(Si(CH_3)_3)_2$[b]	15.6	C_6D_6 (20)	580	2	29
$[Pr^i_2NBeBu]_2$	16.60	C_6D_6 (20)	180	3	71
$Ar^*BeSMes{\cdot}OEt_2$[b]	17.4	C_6D_6 (20)	540	3	29
$[Pr^i_2NBe(t\text{-}Bu)]_2$	19.10	C_6D_6 (20)	190	3	71
$(CH_3)_2Be{\cdot}N(CH_3)_2$	19.9	C_6H_{12} (20)			69
$(CH_3)_2Be{\cdot}OEt_2$	20.8	OEt_2 (20)			69

[a]Relative to $Be(H_2O)_4^{2+}$, defined as 0.0 ppm.
[b]Ar* = C_6H_3-2,6-(mesityl)$_2$.
[c]TMP = 2,2,6,6-tetramethyl-1-piperidinyl.

2.02.3.1.1 Preparation

2.02.3.1.1.(i) Direct reaction in organic solution

By "direct reaction," interaction of elemental magnesium with an organic halide is meant, although this can occur in solution or the solid state (Equation (4)). Various methods of activating Grignard formation are broadly effective, such as the use of finely divided Rieke metal[81] or the application of ultrasound.[82–84] Schlenk equilibrium[85] (Equation (5)) occurs normally with many Grignard reagents, especially in ethereal solvents, but deliberate manipulation of the equilibrium can affect the progress of reactions and the product distribution. Grignard formation is found to be dramatically affected by the presence of $MgBr_2$, which catalyzes reactions of magnesium with organic bromides.[86] For example, the addition of $MgBr_2$ eliminates an autocatalytic induction period in the reaction of magnesium with bromocyclopropane. Furthermore, magnesium does not react with either 1-bromo-2,2,3,3-tetramethylcyclopropane or bromopentamethylbenzene in pure Et_2O, but both substrates react with magnesium in the presence of 2.6 M $MgBr_2$. The same is true for $(Me_3Si)_3CBr$, which does not react with Mg that is purified from $MgBr_2$, but does react with $BrCH_2CH_2Br$-activated Mg; such activation generates $MgBr_2$ as a byproduct.[87] The kinetics of the reaction of

acetylene with phenylmagnesium bromide reagents of different $MgBr_2$ contents (Br/Mg = 1.08 and 1.27) in Et_2O in the presence of various amounts of NEt_3 has also been studied. The reagent of average stoichiometry $PhMgBr{\cdot}2NEt_3$ reacts approximately 20,000 times faster than in the absence of the amine. Although the results were complicated by the reaction of MgBrCCH with the Grignard reagent,[88] elevated content of $MgBr_2$ bromide in the reagent enhances the accelerating effect of the amine, through the formation of species such as $PhMgBr{\cdot}nMgBr_2{\cdot}mNEt_3$.[89]

$$Mg + RX \longrightarrow RMgX \quad (4)$$

$$2RMgX \rightleftharpoons MgR_2 + MgBr_2 \quad (5)$$

The polarity of the reaction mixtures can strongly affect the course of Grignard reagent formation. Ratios of the yields of addition to reduction products for reactions of $MgBu^nX$ (X = Cl or Br) with $Pr^i{}_2CO$ in toluene have been determined at different concentrations of diethyl ether, *tert*-butyl methyl ether, and THF. The solvation of the species in the reaction mixture is critical; the ratio of addition to reduction products is higher for partially solvated reagents than for conventional Grignard reagents.[90] Similar studies of solvation effects have been conducted with $MgBu^tCl$ and $Pr^i{}_2CO$, methyl 2-methylpropanoate, and isopropyl 2-methylpropanoate in toluene in the presence of diethyl ether, THF, or Bu^tOMe.[91] Grignard reagents have been prepared from RCl ($R = Pr^i$, Bu^n, Bu^s or Bu^t) in toluene in the presence of $\leq$1 equiv. of various organic bases (ethers, NEt_3). Diethyl ether was most effective; stronger solvation favored the dismutation reaction to dialkylmagnesium. Increasing bulkiness of the alkyl group in the Grignard reagent hinders the complexation with the donor and shifts the equilibrium to the formation of unsymmetrical species.[83]

In toluene, primary (Bu^n) and secondary (Bu^i, Pr^i) alkyl chlorides can be converted into Grignard reagents in good yields if a small amount of ether is present (less than one mole per mole of halide). Tertiary chlorides (Bu^t) form only monosolvated organomagnesium compounds. Although the reagents so obtained are not homogeneous, the solubilities of the partially solvated complexes in toluene are fairly high, and roughly 20% of the Grignard reagent is available in solution.[82]

The thiomethylmercury chlorides $Hg(CH_2SMe)Cl{\cdot}HgCl_2$ and $Hg(CH_2SPh)Cl$ react with magnesium in THF to give the Grignard reagents $Mg(CH_2SR)Cl$ (R = Me or Ph). The phenyl compound crystallizes from THF–hexane as a 1 : 1 adduct $[Mg(CH_2SPh)_2(THF)_3][MgCl_2(THF)_4]$. In THF at room temperature, Schlenk equilibrium gives a mixture of $Mg(CH_2SPh)Cl$ (89%) and $Mg(CH_2SPh)_2$ (11%).[92]

Transition metal-catalyzed preparations of Grignard reagents from inactive chloro arene compounds have been described. For example, $FeCl_2$-catalyzed and $MgCl_2$-co-catalyzed Grignard reaction of 1-chloronaphthalene with magnesium in THF gave 82.3% 1-naphthylmagnesium chloride.[93]

Di- or polyfunctionalized Grignard reagents remain comparatively rare, although they can offer enhanced reactivity relative to their monofunctional counterparts RMgX.[94] The regioselective synthesis of 1,4-$Bu^t{}_2$-2,5-bis(chloromagnesio)benzene **20** was conducted by treating 1,5-bis(chloromercurio)-1,4-di-*tert*-butylbenzene with methylmagnesium chloride (Equation (6)). The characterization of **20** included hydrolysis, halogenation (Br_2, I_2), and treatment with allyl bromide. NMR spectra suggest that **20** exists in equilibrium with oligomers of low solubility.[95]

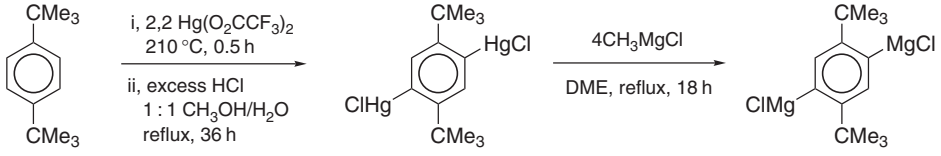

(6)

20

2.02.3.1.1.(ii) Direct reaction in aqueous media

For over a century, it has been taken as axiomatic that, owing to the high reactivity of the magnesium–carbon bond, successful Grignard chemistry requires the use of anhydrous experimental conditions. This assumption was disproved in the case of Barbier–Grignard allylation of aldehydes (Equation (7)).[96] In dry THF, the reaction between benzaldehyde, allyl bromide, and Mg proceeds quantitatively, but when the water content in THF reaches 7%, the reaction stops, presumably reflecting complete surface coverage of magnesium by water molecules. When pure water is the solvent, however, the allyl halide is apparently confined to the magnesium surface because of hydrophobic interactions, shielding the metal from the water. The allylation reaction then proceeds, but with low (16%) conversion, probably because of the formation of $Mg(OH)_2$ on the magnesium. Reaction of allyl bromide or iodide

with benzaldehyde and Mg in 0.1 N aqueous HCl or NH_4Cl once again produces quantitative conversion of the aldehyde to allylation and pinacol-coupling products.

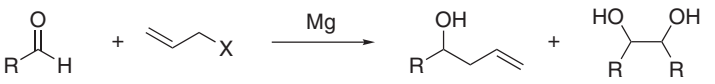

(7)

Further investigations of this system[97] revealed that halogenated (X = F, Cl, or Br) or hydroxylated aldehydes undergo allylation without difficulty, and that aldehydes react chemoselectively in the presence of aliphatic aldehydes (Table 2). An exclusive selectivity is also observed when both aliphatic and aromatic aldehyde functionalities are present in the same molecule. In the absence of allyl halides, aldehydes and ketones react with magnesium in aqueous 0.1 N NH_4Cl to form the corresponding pinacol-coupling products in high yields. The effectiveness of the pinacol reaction is strongly influenced by the steric environment surrounding the carbonyl group, that is, *ortho*-substituents (F, Cl) increase the amount of benzyl alcohol product, whereas the same substituents in the *meta*- or *para*-positions have little effect. Two *ortho*-substituents (i.e., as in 2,6-dichlorobenzaldehyde) suppress pinacol coupling entirely. Aliphatic aldehydes and simple alkyl halides are inert under the reaction conditions for either alkylation or the pinacol-coupling reaction.[97]

The research has inspired related investigation into the coupling reaction between aromatic aldehydes and benzyl bromide or chloride in water. The yields are slightly higher than the results for allylation despite the fact that aqueous benzylation is intrinsically more difficult than allylation. It is also found that the coupling reaction is chemoselective for aromatic aldehydes over aliphatic aldehydes, and also for aromatic aldehydes over aromatic ketones.[98] Aqueous Grignard chemistry is attractive for its use of an environmentally benign solvent, and has been the subject of several reviews.[99–103]

2.02.3.1.1.(iii) Direct reaction in the solid state

Reactions of magnesium with halogenonaphthalenes in a ball mill in the absence of solvent provide the corresponding Grignard reagents in good yield. When quenched with aromatic ketones, however, the use of excess metal to obtain a solid product gives rise to McMurry coupling in addition to alcohol formation by the quenching process.[104]

Excited state (^{3}P) magnesium atoms generated by laser ablation react with methyl halides diluted in an argon matrix. Infrared spectra (supported by ^{13}C, D, and ^{26}Mg isotopic substitution and DFT frequency calculations) have been used to identify the Grignard molecules CH_3MgX, including the fluoride Grignard species, CH_3MgF.[105] The secondary reaction products CH_3MgCH_3, $XMgCH_2$, $HMgCH_3$, and $HMgCH_2X$ are also formed. If methane is present in addition to the methyl halides, metal–carbene species $MgCH_2$, are observed. DFT calculations indicate that there is no significant metal–carbon π-bonding in the carbene and carbenoid radicals ($XMgCH_2$) species, but rather a polar one-electron σ-bond resulting from electron donation from metal to carbon.[106]

2.02.3.1.1.(iv) Indirect syntheses

A general route to highly functionalized arylmagnesium halides, which involves the use of a polymer support and proceeds via I–Mg exchange, has been described.[107] As an example of the technique, Wang resin was charged with 4-iodobenzoic acid, and the mixture was subsequently treated with Pr^iMgBr to give a Grignard reagent. Quenching of the latter with tosyl cyanide and removal of the resin support gave 4-cyanobenzoic acid.[107] Reactions of polystyrene-supported magnesium anthracene, which contains radical anion and dianion sites, with benzylic chlorides or bromides afford Grignard reagents in THF at −10 °C to 20 °C.[108] Benzylic-type Grignard reagents prepared this way include those of 2,6-(dichloromethyl)pyridine, 2,6-(dibromomethyl)pyridine, 2,2′,2′-trispyridylmethyl chloride, 2-methoxy-3-methyl-1-benzyl chloride, 2,4-dimethoxy-5-methyl-1-benzyl chloride, 3,5-dimethoxy-4-methyl-1-benzyl chloride, 2,4,6-trimethoxy-3-methyl-1-benzyl chloride, and 2,5-dimethoxybenzyl chloride. Silica is also effective as a support material; hydroxyl-depleted SiO_2 surfaces derived from treating chloropropylsilyl- (or chloropropylsilyl/trimethylsilyl-) functionalized SiO_2 with $H_3Al{\cdot}NMe_3$ afford the corresponding organolithium reagent when treated with $Li^+(biphenyl)^{\cdot-}$.[109] Successive treatment with 9-(chlorodimethylsilyl)anthracene and Mg(anthracene)$(THF)_3$ generates anthracene- and SiO_2-supported Mg–anthracene (Figure 9), which gives Grignard reagents of benzylic halides in THF in high yield. The spent SiO_2-supported anthracene can be recycled.

Magnesium complexes of bis(phosphoranimine)methane and -methanide ligands have been isolated from the reaction of $CH_2(Ph_2PNSiMe_3)_2$ with MeMgI and MeMgCl, which gave the crystalline products $CH_2(Ph_2PNSiMe_3)_2MgI_2$ and $[HC(Ph_2PNSiMe_3)_2Mg(\mu\text{-}Cl)]_2$, respectively.[20] The crystalline compound **21**, in which the $[CH(SiMe_3)(SiMe_2Ph)]^-$ ligand is bound to Mg in a terminal fashion, was prepared from $CH(Br)(SiMe_3)(SiMe_2Ph)$

Table 2 Allylation reactions in aqueous media[a]

Substrate	*Yields*		
	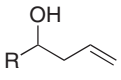	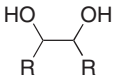	RCH_2OH
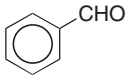	58	34	8
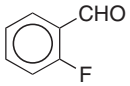	57	36	7
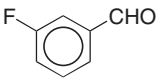	52	36	12
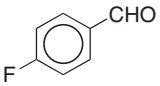	53	35	12
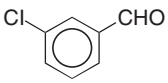	42	37	21
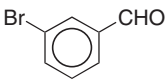	39	54	1
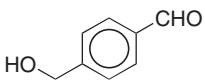	53	33	14
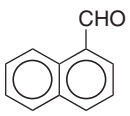	47	38	5
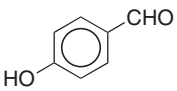	30	54	16
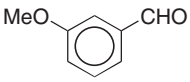	45	37	18
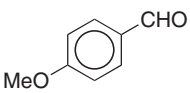	27	52	21

(*Continued*)

Table 2 (Continued)

Substrate	*Yields*		
	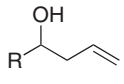	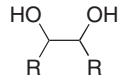	RCH_2OH
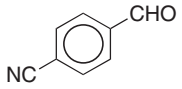	3	2	95
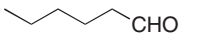	0	0	0
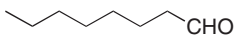	0	0	0

[a]Data from Ref. 97. Yields of the products (%) were determined with ^{1}H NMR; those of the pinacol coupling product are the sum of *erythro*- and *threo*-isomers.

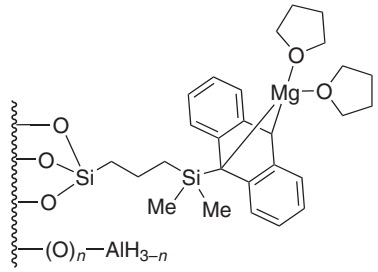

Figure 9 A cartoon of SiO_2-supported Mg–anthracene.

in Et_2O and Li followed by treatment with magnesium metal.[110] The regio- and stereoselective addition of a series of Grignard reagents across $Bu^tC{\equiv}P$ yields 2-phospha-1-vinylmagnesium halide species, $[MgX(RP{=}C(Bu^t)(OEt_2)]_2$ (R = Et, Mes, Cy, cyclopentyl;[111] R = Pr^i or Bu^t;[112] X = Cl or Br), in high yield (Equation (8)).

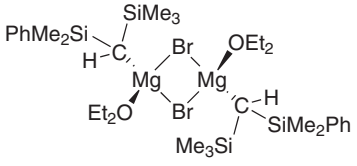

21

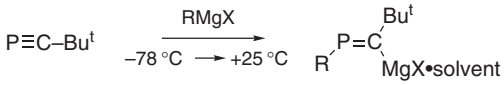

(8)

2.02.3.1.1.(v) Chiral Grignard reagents

Grignard reagents that are chiral at the metal should give strong asymmetric induction, and if their chirality is controlled, they could have great potential in stereoselective syntheses. There are also possibilities for studying single-electron transfer (SET) in the reaction of Grignard reagents, in which the metal-bearing carbon is the only

stereogenic center. In order to avoid the free-radical reactions that would thwart the synthesis of such species, the α-chloro- and α-bromoalkyl Grignard reagents (R)-BrMgCHXCH$_2$Ph (X = Cl, Br), with >97% ee were generated by a sulfoxide Mg exchange reaction from the enantiomerically and diastereomerically pure sulfoxides, *p*-ClC$_6$H$_4$S(O)CHCXCH$_2$Ph. These Grignard reagents are configurationally stable at −78 °C, but racemization occurs ≥−60 °C, especially when the solution contains bromide ions. In the absence of halide ions, the configurational stability extends to −20 °C.[113] A review[114] document shows the asymmetric synthesis of the related Grignard reagent ((*S*)-1-benzylpropylmagnesium chloride) (Equation (9)) was used as a probe to examine the extent to which SET is involved in reactions of organomagnesium reagents, including amination,[115] allylation,[116,117] oxidation,[118] and transmetallation.[119]

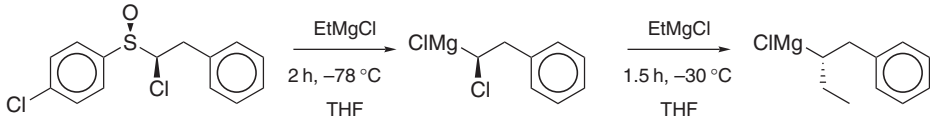

97% ee

(9)

The Grignard reagent (*S*)-PhCH$_2$CH(MgCl)CH$_2$CH$_3$, in which the magnesium-bearing carbon atom is the sole stereogenic center, adds to CO$_2$, PhNCO, PhNCS, and certain aldehydes with full retention of configuration. In contrast, reaction with benzophenone, electron-deficient aldehydes, and several allyl halides proceeds with partial or complete racemization. The findings reflect a competition between concerted polar and stepwise SET reaction pathways.[116] 3-Iodoenoates are converted into the corresponding alkenylmagnesium species with complete retention of configuration of the double bond; both direct reaction and copper(I)-mediated reactions (via CuCN·2LiCl) with various electrophiles (e.g., PhCOCl, Me$_3$SnCl, ethyl 2-(bromomethyl)prop-2-enoate) provide polyfunctional enoates.[120]

The majority of Grignard reagents are four coordinate, but the *cis*-isomers of octahedral complexes would be useful in the study of stereoselective synthesis. Six-coordinate octahedral Grignard reagents, (thienyl)MgBr(dme)$_2$ and (vinyl)MgBr(dme)$_2$, were prepared as racemic mixtures of D- and L-*cis*-isomers and characterized with X-ray crystallography. They are stereochemically rigid in toluene solution, but were not enantiomerically resolved.[121] The absolute asymmetric syntheses of the D and L enantiomers for both *cis*-[MgBr(4-MeC$_6$H$_4$)(dme)$_2$] and *cis*-[MgMe(dme)$_2$(THF)]I have been accomplished. Subsequent reaction with RCHO (R = Pr^i or Ph) yields the corresponding alcohol in up to 22% ee. The enantiomeric Grignard reagents crystallize separately but racemize in solution; at −60 °C, the racemic species crystallize.[122] Three chiral species *cis*-[MgBr(R)(dme)$_2$] (R = Pr^n, Pr^i, allyl) have been prepared and characterized with X-ray diffraction; all are racemic. The isolation of *trans*-[MgBr$_2$(tmen)$_2$] and *cis*-[MgBr$_2$(dme)$_2$] indicates that bidentate tertiary amine bases are less suitable for the preparation of *cis*-octahedral compounds, but the structures of *cis*-[MgBr$_2$(triglyme)] and [Mg$_2$(μ-Br)$_2$(triglyme)$_2$][Mg$_2$(μ-Me)$_2$Br$_4$] suggest that triglyme may be well suited for this purpose.[123]

Optical activity retention is observed in the course of the formation of the Grignard reagent from optically active (+)-*R*-1-chloro-1-phenylethane and Mg in Et$_2$O.[124] Treatment of the latter with Mg in Et$_2$O and then with Me$_3$COD gives 88% (+)-S-PhCHDMe in 6.2% optical yield.[124]

After quenching with D$_2$O or Bu^{t}OD, analysis of the products from the Grignard reagents formed from PhCHXMe (X = Cl, Br, I) in the optically active solvent –(*R*)-2-methoxypentane leads to the conclusion that Grignard reagent formation occurs on the Mg surface within a solvent cage by a one-electron transfer mechanism.[125]

2.02.3.1.2 Structures and physical properties

Determination of the structures of Grignard reagents continues to be of interest, and reviews on this subject have appeared.[126,127] Most of the structure authentications are done on crystalline materials, although solution studies performed with extended X-ray absorption fine structure (EXAFS) spectroscopy are also available. The Grignard compounds MeMgBr and EtMgBr in Bu$^n_2$O were studied at room temperature and −85 °C with EXAFS. At both temperatures, dimers are observed (Mg–(μ-Br) = 2.5 Å; Mg–O = 2.0 Å).[128]

The Grignard reagents [Mg{C(SiMe$_3$)$_3$}I(OEt$_2$)]$_2$ and [Mg{C(SiMe$_3$)$_2$(SiMe$_2$Ph)}I(OEt$_2$)]$_2$ were obtained from the reactions between (Me$_3$Si)$_3$CI and (Me$_2$Ph)(Me$_3$Si)CI, respectively, with magnesium metal, and shown to have halide-bridged structures.[129] The bulky bidentate ligand HC(SiMe$_3$)$_2$(SiMe$_2$C$_5$H$_4$N-2) reacts with MeLi in THF to yield the lithium derivative Li[C(SiMe$_3$)$_2$(SiMe$_2$C$_5$H$_4$N-2)], which in turn reacts with MgBr$_2$ to give the Grignard reagent **22**, with Mg–C = 2.189(9) Å.[130]

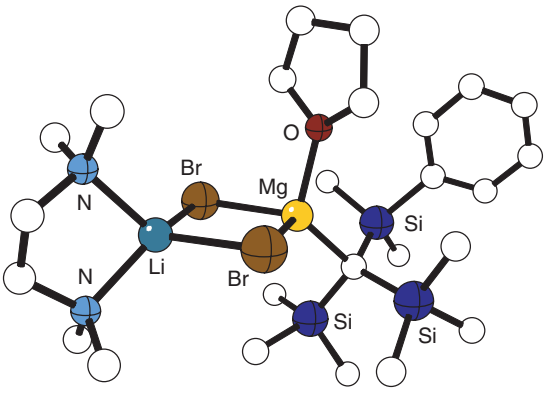

Figure 10 The structure of the lithium–magnesium complex [Li(tmeda)(μ-Br)$_2$Mg{C(SiMe$_3$)$_2$(SiMe$_2$Ph)}(THF)] **23**.

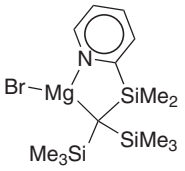

22

The reaction of the dialkyl lithiated compound [Li(tmeda)$_2$][Li{C(SiMe$_3$)$_2$(SiMe$_2$Ph)}$_2$] with MgBr$_2$ gave the doubly bromide-bridged lithium–magnesium complex [Li(tmeda)(μ-Br)$_2$Mg{C(SiMe$_3$)$_2$(SiMe$_2$Ph)}(THF)] **23** (Figure 10), and MgBr$_2$ and [Li(THF){C(SiMe$_3$)$_2$(SiMe$_2$C$_5$H$_4$N-2)}] yielded the singly bridged compound [Li(THF)$_3$(μ-Br)MgBr{C(SiMe$_3$)$_2$(SiMe$_2$C$_5$H$_4$N-2)}] **24**,[129] which differs from **23** primarily by the addition of a solvated LiBr moiety.

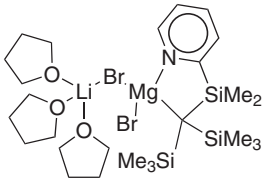

24

Another halide-bridged species, the only product isolated from the reaction of (Me$_3$Si)$_3$CBr with BrCH$_2$CH$_2$Br-activated Mg in THF, was (Me$_3$Si)$_3$CMg(μ-Br)$_3$Mg(THF)$_3$ **25**, which contains one four-coordinate and one six-coordinate Mg atom (Figure 11). A similar product, (Me$_3$Si)$_3$CMg(μ-Br)$_3$Mg(Et$_2$O)$_x$, appears to be formed in the reaction in ether.[87] Despite the bulk of the organic ligands, both the di-*n*-butyl ether adduct of anthracenyl magnesium bromide[131] and MgBr(C$_6$H$_3$-Mes-2,6)(THF) **26** (Figure 12) crystallize as dimers.[132]

The Grignard reagent Mg(C$_6$H$_3$Et$_2$-2,6)I(THF)$_n$ undergoes rapid aryl exchange in THF solution at room temperature to afford the sparingly soluble salt MgI$_2$(THF)$_6$ and the diorganomagnesium compound Mg(C$_6$H$_3$Et$_2$-2,6)$_2$(THF)$_n$. Removal of the coordinated THF from the latter under reduced pressure and elevated temperature affords the unsolvated complex **25**, which possesses three-coordinate metal centers, an unusually low number for magnesium. At room temperature, **25** is fluxional in benzene or toluene solution and dissociates into monomeric Mg(C$_6$H$_3$Et$_2$-2,6)$_2$ near 115 °C.[133]

The crystallographically characterized cyclic Grignard reagent **28** was isolated from the reaction between the iodide R$_2$C(SiMe$_2$OMe)I and Mg in toluene.[134] The reaction of LiCH(Ph$_2$PNSiMe$_3$)$_2$ with MeMgI affords CH(Ph$_2$PNSiMe$_3$)$_2$MgI(THF) **2**. Crystallographic data confirm that significant Mg···C interactions, at about 2.6 Å exist in this and the related CH$_2$(Ph$_2$PNSiMe$_3$)$_2$MgI$_2$ and [HC(Ph$_2$PNSiMe$_3$)$_2$Mg(μ-Cl)]$_2$ bis(phosphoranimine)methanides.[20] The phosphavinyl Grignard [MgCl((*c*-C$_5$H$_9$)P═C(Bu^t)(OEt$_2$)] **29** has Mg–C = 2.118 Å (Figure 13).[111]

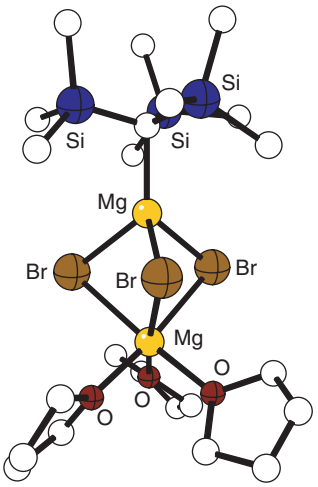

Figure 11 The structure of the bimetallic complex $(Me_3Si)_3CMg(\mu\text{-}Br)_3Mg(THF)_3$ **25**.

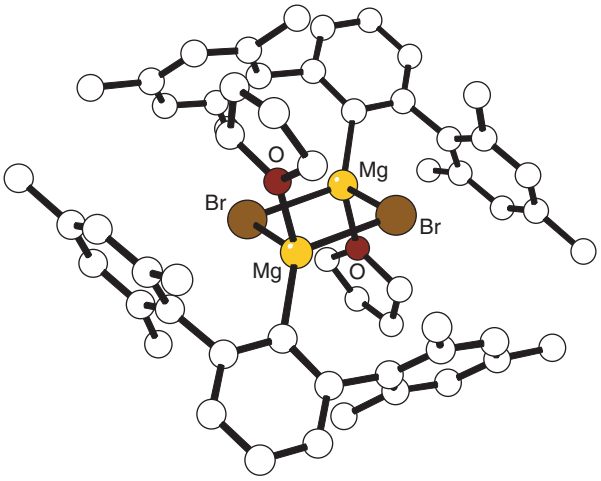

Figure 12 The structure of the dimeric complex $[MgBr(C_6H_3\text{-Mes-2,6})(THF)]_2$ **26**.

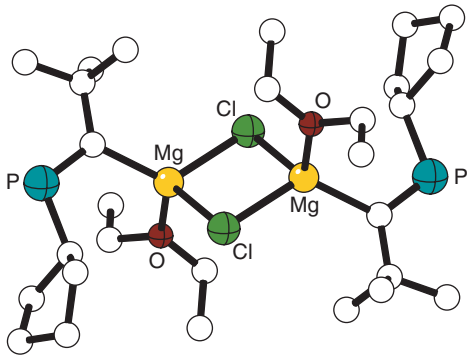

Figure 13 The phosphavinyl species $[MgCl((c\text{-}C_5H_9)P{=}C(Bu^t)(OEt_2)]_2$ **29**.

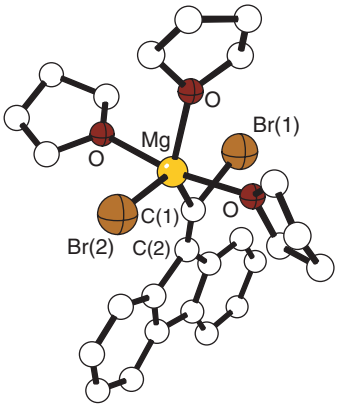

Figure 14 The structure of 9-bromo-9-[(bromomagnesium)methylene]fluorene **30**.

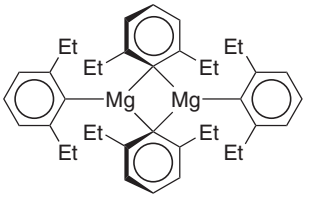

27

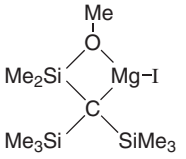

28

The reaction of 9-(dibromomethylene)fluorene in THF and *n*-octylmagnesium bromide in Et_2O yielded crystals of 9-bromo-9-[(bromomagnesium)methylene]fluorene **30** as a solvate with three-coordinated THF molecules (Figure 14). The magnesium is five-coordinate, and the molecule has structural features characteristic of a carbenoid. The C(1)–Br(1) bond of 2.006(10) Å is ca. 0.10 Å longer than is typical for C_{sp^2}–Br bonds, and the C(2)–C(1)–Mg angle of 147.3(8)° is unusually wide for the formally sp^2-hybridized C(1) atom. Together with the slightly lengthened C(1)–Mg bond (2.190(10) Å; cf. typical values near 2.13 Å), the geometric features suggest that the molecule is primed for α-elimination of $MgBr_2$.[135]

Spectroscopic studies of the structure and dynamics of allylic magnesium compounds indicate that the IR spectra of allyl- and methallyl-d_2-Mg bromides have two double bond stretching bands, corresponding to C═CH_2 and C═CD_2 groups in equilibrating allylic isomers (Equation (10)). The methylene resonances in the ^{13}C NMR spectra of allylmagnesium bromide and chloride and methylallylmagnesium bromide are broadened at low temperature by an exchange process, presumably involving interconversion between the unsymmetrical allylic structures. Analogous changes are seen in the spectrum of 1,3-dimethylallylmagnesium chloride and in the ^1H NMR spectrum of allylmagnesium bromide. Rate constants and activation parameters for the exchange were determined from the line broadenings (e.g., at 298 K, $k = 28 \times 10^6$ and $7.7 \times 10^6\ s^{-1}$ for (allyl)MgCl (0.2 M) and (allyl)MgBr (0.6–1.1 M), respectively). Unlike the Grignard reagents, the methylene resonances of diallylmagnesium in THF are not significantly broadened at reduced temperature, and the deuterated reagent does not have two distinct double bond stretching bands in the IR spectrum, suggestive of more extensive delocalized bonding in the ligands.[136]

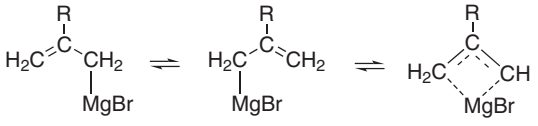

(10)

2.02.3.1.3 Miscellaneous reactions

The traditional uses of Grignard reagents in organic synthesis are documented in many references outside this review.[77–79] There are numerous cases in which a Grignard reagent is used as a source of magnesium or as a ligand-transfer reagent. In many reactions, the products are not organometallic species, and are not detailed here.

Examples include the formation of oxalic amidine compounds,[137] diethylamino-bridging and bromo-bridging Hauser bases,[138] phosphoranes,[139] alkoxides,[140] carboxylato or carbamato complexes,[141] iminophosphoranes,[142] adamantyl aluminates and gallates,[143] a novel silsesquioxane complex $[MgCl_2(THF)_2\{(c\text{-}C_5H_9)_7Si_7O_{12}\}_2]\cdot 4THF$,[144] a long-lived iodine "-ate" complex $[I_2CH\text{–}I\text{–}CHI_2]^-$,[145] diketiminates,[146,147] a diarylbromoarsine and a bromoarsenate,[148] the polymeric coordination complex $[(ImN)MgI]_n$,[149] the dinuclear isothiocyanate insertion product $Mg_2(SCEtNPh)_4(OEt_2)_2$,[150] and the phosphoraniminato complex $[MgBr(NPMe_3)]_4$.[142] Sometimes unexpected halogen exchange can occur, as in the isolation of $[Mg_3Cl_5(Et_2O)_6]^+[Me_2SbI_2]^-$ from the reaction of Grignard reagent MeMgI with $SbCl_3$ in Et_2O.[151] *S*-functionalized methyltin compounds $Bu_3SnCH_2S(O)_nR$ ($n = 0$, 1, 2; R = Me, Ph) undergo transmetallation with MgR^1X (R^1 = Me, Bu, Ph; X = Cl, Br, I) to provide $SnBu_3R$ and $Mg[CH_2S(O)_nR]X$.[152] Analogously, the reaction of $Bu_3SnCH_2P(O)Ph_2$ with MgBuBr generates $Mg[CH_2P(O)Ph_2]Br$ and $SnBu_4$.[152]

Reaction of the silylated phosphinimine $Me_3SiNPMe_3$ with the Grignard reagents EtMgBr or MeMgI gives the corresponding carbanionic phosphoraniminato derivatives $[XMg(CH_2PMe_2NSiMe_3)]_n$ (X = Br, I) as main products. The byproducts of these reactions, $[MgBr_{1.25}I_{0.75}(Me_3SiNPMe_3)(OEt_2)]$, $[MgI_2(Me_3SiNPMe_3)_2]$, and $[Mg_2I_2(CH_2PMe_2NSiMe_3)(OCHMeCH_2PMe_2NSiMe_3)(OEt_2)]$ **31** were identified with crystal-structure determinations.[142] The preparations of $[MgCH_2S(O)_nR]X$ ($n = 0$, 1, or 2; R = Me or Ph; X = Cl, Br, I, Me, or Bu) and $[MgCH_2P(O)Ph_2]Br$ were accomplished via Sn–Mg transmetallation with the *S*-functionalized methyltin compounds $Bu_3SnCH_2S(O)_nR$ ($n = 0$, 1, 2; R = Me, Ph).[152]

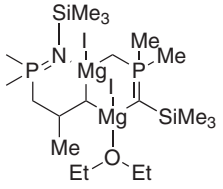

31

The possibilities provided by the synthesis of permagnesiated aromatic rings have been demonstrated by the preparation of ruthenocenes bearing pentamagnesiated cyclopentadienyl ligands have been reported.[153] Treatment of pentakis(chloromercurio)(pentamethyl)ruthenocene with MeMgCl in THF gives the pentamagnesiated ruthenocene **32** (Equation (11)), whereas similar reaction of decakis(chloromercurio)ruthenocene with MeMgCl in THF yields decamagnesiated ruthenocene **33** (Equation (12)). Reaction of **32** with H_2O, Br_2, and CH_3I produces $(C_5Me_5)Ru(C_5H_5)$, $(C_5Me_5)Ru(C_5Br_5)$, and $(C_5Me_5)Ru(C_5Me_5H_{5-n})$ ($n = 0$–5), respectively. The same reagents react with **33** to produce $(C_5H_5)_2Ru$, $(C_5Br_5)_2Ru$, and $(C_5Me_5H_{5-n})_2Ru$ ($n = 0$–5), respectively.

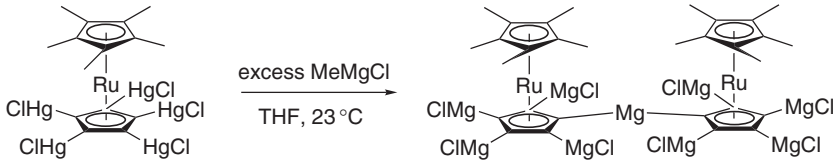

(11)

32

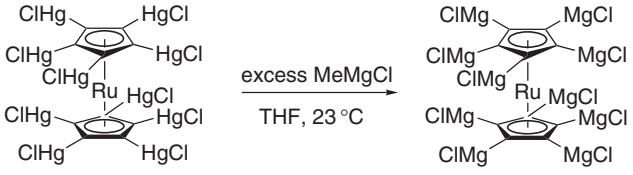

(12)

33

2.02.3.2 Diorganylmagnesium Compounds with σ-Bonded Ligands

Sterically bulky ligands have been used increasingly to enforce low coordination numbers (as low as two) in σ-bonded compounds. A review on the chemistry of compounds containing the tris(trimethylsilyl)methyl and related bulky groups is available.[154]

2.02.3.2.1 Preparation

Heating the lithium magnesate $Li(THF)_2(\mu\text{-}Br)_2Mg(Tsi)(THF)$ ($Tsi = (Me_3Si)_3C$) under vacuum gives the dialkylmagnesium compound $Mg(Tsi)_2$, a two-coordinate magnesium derivative. The compound displays remarkable stability up to 350 °C.[155] A high-yield synthesis (>70%) of $(PhCH_2)_2Mg(THF)_2$ and $\{(PhCH_2)(CH_3)Mg(THF)\}_2$ is possible from the reaction of benzylpotassium and $PhCH_2MgCl$ or MeMgCl, respectively, in THF. This procedure sidesteps problems with shifting the Schlenk equilibrium of benzylmagnesium chloride or in transmetallating dibenzylmercury. Reaction of $(PhCH_2)_2Mg(THF)_2$ with various nitrogen bases (tmeda, teeda, pmdeta) displaces the coordinated THF and generates the corresponding base adducts.[156] The reaction between the iodide $R_2C(SiMe_2OMe)I$ and Mg in Et_2O produces the chelated dialkylmagnesium $Mg\{C(SiMe_3)_2(SiMe_2OMe)\}_2$ **34** and $MgI_2(OEt_2)_2$, presumably via the intermediacy of the Grignard reagent **28**.[134] The tmeda adducts of phosphinomethyllithium compounds $[LiCH_2PR_2(tmeda)]_2$ (R = Me, Ph) react with $MgCl_2$ in THF/Et_2O to yield $Mg(CH_2PMe_2)_2{\cdot}2LiCl$ and $Mg(CH_2PPh_2)_2(tmeda){\cdot}2Et_2O$. The Et_2O is rapidly lost under vacuum.[157] The unsymmetrical dialkylmagnesium $MgBu\{C(SiMe_3)_2(SiMe_2NMe_2)\}(THF)$ **35** was prepared from a mixture of LiBu, $Li(tmeda)\{C(SiMe_3)_2SiMe_2NMe_2\}$, and $[MgBr_2(OEt_2)_2]$.[129]

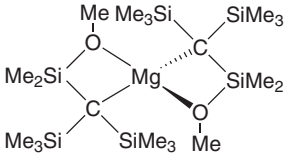

34

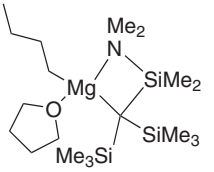

35

Magnesium alkyls with S–C–Mg linkages are rare. The trigonal-bipyramidal molecules $Mg(CHSR)_2(THF)_3$ **36** (R = Me, Ph) are prepared from the reaction of activated magnesium with $Hg(CH_2SR)_2$ (R = Me, Ph).[158] $Mg(CHSMe)_2(THF)_3$ loses THF *in vacuo* to give the solvate-free complex $Mg(CH_2SMe)_2$. X-ray structure analysis of **36** (R = Ph) reveals that the S atoms are not coordinated to Mg. Racemic mixtures of the unsymmetrical substituted Mg alkyl $Mg(Bu)\{CH[SPh][SiPh_2(CH_2NR_2)]\}$ (NR_2 = 1-piperidyl, 1-pyrrolidyl) **37**, which possesses a stereogenic metallated C atom, is obtained by deprotonation of an (aminomethyl)[(phenylthio)methyl]silane with $MgBu^nBu^s$ (Equation (13)). Only the $MgBu^n$ moiety is transferred to the (aminomethyl)silanes, and detectable amounts of the substituted alkyl are not obtained when the reaction is conducted in THF, presumably because of the blockage of coordination sites by the solvent.[159]

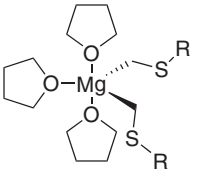

36

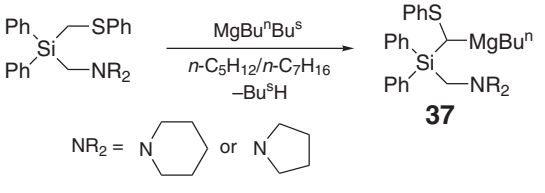

37

(13)

2.02.3.2.2 Structures and physical properties

Low coordination numbers are associated with the increasingly common use of sterically bulky ligands. The dialkyl $Mg(Tsi)_2$ has a linear structure, with Mg–C = 2.116(2) Å.[155] The X-ray crystal structure of $MgMes^*_2$ is an example of an almost linear two-coordinate diaryl. The average Mg–C distance and C–Mg–C angle are 2.116(3) Å and 158.2(1)°, respectively. There are also close (ca. 2.2–2.3 Å) contacts involving the metal and hydrogens from the *o*-Bu^t groups.[160]

Intramolecular coordination in organomagnesium compounds is a common feature of their structures, and the subject has been reviewed.[161] The diorganomagnesium adducts, $MgR_2(L)$ (R = methyl, ethyl; L = tmeda, pmdta),

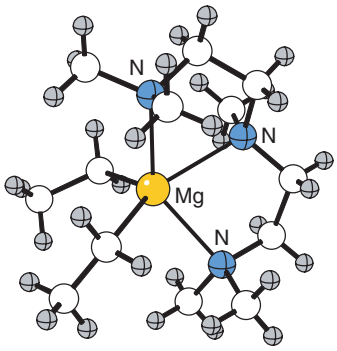

Figure 15 The structure of chelated $MgEt_2$(pmdta) **38**.

have been prepared from $MgMe_2$ and $MgEt_2$, and tmeda or pmdta, respectively. Crystal structures of $MgEt_2$(tmeda), $MgMe_2(pmdta)_2$, and $MgEt_2$(pmdta) **38** (Figure 15) have been determined with X-ray crystallography. The structure of $MgEt_2$(tmeda) is similar to that of $MgMe_2$(tmeda)[162] with the Mg atom being fourfold coordinated by the Et groups and the chelate ligand. In $MgMe_2(pmdta)_2$ and **38**, the magnesium atoms are five coordinate. Steric crowding of the magnesium coordination sphere is apparent from the bond lengths and angles; in **38**, the C–Mg–C angle is 116.5°, substantially compressed from the analogous angle 127.7° in $MgEt_2$(tmeda).[163]

Crystals obtained from a solution of commercial $MgBu^i(Bu^n)$ and tmeda were shown to be $MgBu^i_2$·tmen **39** with X-ray crystallography.[164] The complex is mononuclear in the solid state and displays a large C–Mg–C bond angle of 133.6(2)°, attributable to the branched nature of the alkyl substituents (Figure 16). The angular distortion may encourage the partial loss of tmeda from Mg centers that is observed in solution. X-ray crystallography and NMR spectra have indicated that $MgBu^t_2$ **40** (Figure 17) is a dimer with a folded $CMg(\mu\text{-}C)_2MgC$ skeleton (C(1)–Mg(2)–Mg(1)–C(2) = 140.45(4)°) The crystal structure reveals that intra- (2.49–2.54 Å) and intermolecular (2.67 Å) $Mg\cdots CH_3$ agostic interactions support the assembly (cf. 2.30 Å for Mg–(μ-C) bonds).[165]

Treatment of the (*Z*)-1,4-dilithio-1,4-bis(trimethylsilyl)but-2-ene adduct of tmeda, $(CH(Me_3Si)CH)_2\{Li(tmeda)\}_2$, with either $MgCl_2$ or Pr^iMgCl in Et_2O gave the tmeda adduct of the magnesacyclopent-3-ene, spectroscopically and crystallographically characterized as {*meso*-$(CH(Me_3Si)CH)_2Mg$}(tmeda) **41** (Figure 18).[166] Interestingly, the six-coordinate octahedral *trans*-[Mg(thienyl)$_2$(THF)$_4$] is stable despite the lack of chelating ligands, and has Mg–C = 2.290(6) Å.[121] The MgR_2 reagent $Mg(THF)_2(viph)_2$ **42** crystallizes as a monomer from a THF solution.[167]

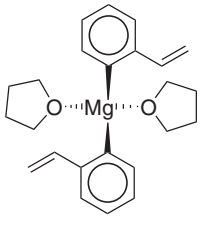

42

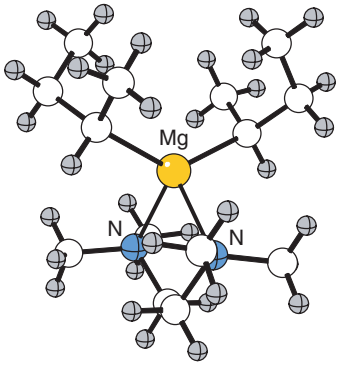

Figure 16 The structure of $MgBu^i_2$·tmen **39**.

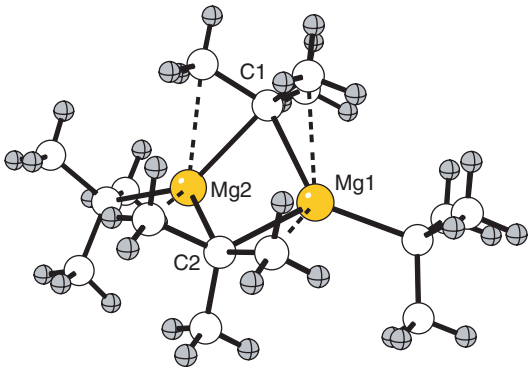

Figure 17 The structure of dimeric $[MgBu^t_2]_2$ **40**.

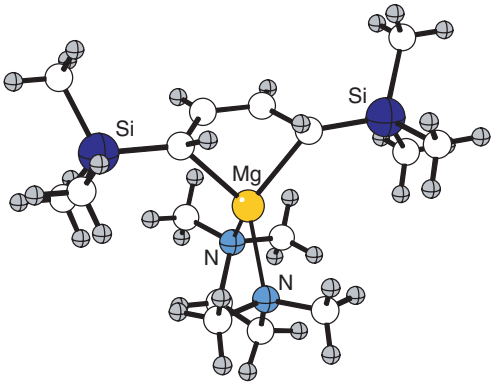

Figure 18 The structure of {*meso*-$(CH(Me_3Si)CH)_2Mg$}(tmeda) **41**.

Reaction of $MgMe_2$ with *N,N′,N″*-trimethyl-1,4,7-triazaacyclononane (tacn) in C_6H_6 gave the charge-separated ion pair $[(tacn)Mg(\mu\text{-}Me)_3Mg(tacn)]^{2+}[Mg_3Me_8]^{2-}$ **43** (Figure 19) in 46% yield. The triple-decker cations have Mg–C distances of 2.35 Å (av.).[168]

The reaction of [*C,N*-$[Fe(\eta^5\text{-}C_5H_5)(\eta^5\text{-}C_5H_3(CH_2NMe_2)\text{-}2)]$]Li, (FcN)Li, with magnesium bromide affords the magnesate complex $Li_2Mg(FcN)_2Br_2(OEt_2)_2$ **44** (Figure 20).[169] Extraction of **44** with Et_2O yields $(FcN)_2Mg(OEt_2)$. The reaction of (FcN)Li with magnesium halides and THF directly affords $(FcN)_2Mg(THF)$ **45** (Figure 21). In solution, the compounds appear as a mixture of diastereomers, whereas in the solid state, they crystallize as a single *rac*-diastereomer. The ratio of *rac*-/*meso*-diastereomers in solution is solvent and temperature dependent, consistent

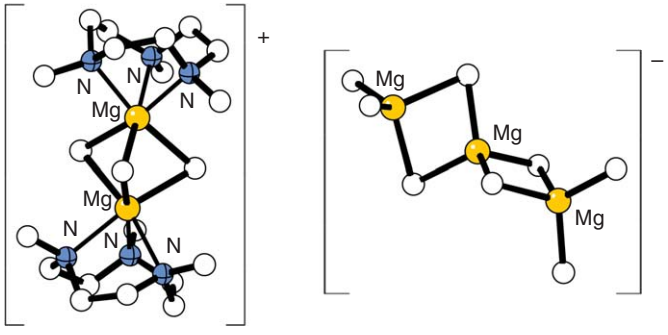

Figure 19 Structure of the charge-separated ion pair $[(tacn)Mg(\mu\text{-}Me)_3Mg(tacn)]^{2+}[Mg_3Me_8]^{2-}$ **43**.

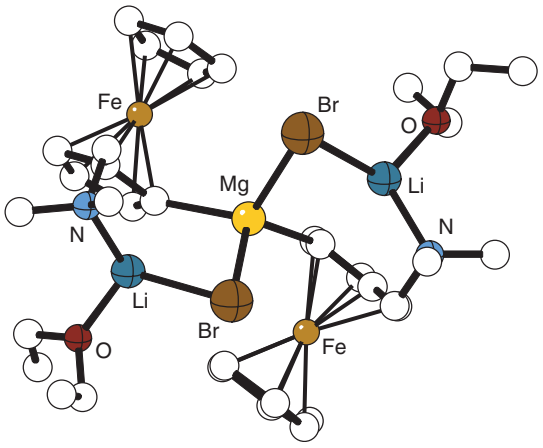

Figure 20 Structure of the magnesate complex $Li_2Mg(FcN)_2Br_2(OEt_2)_2$ **44**.

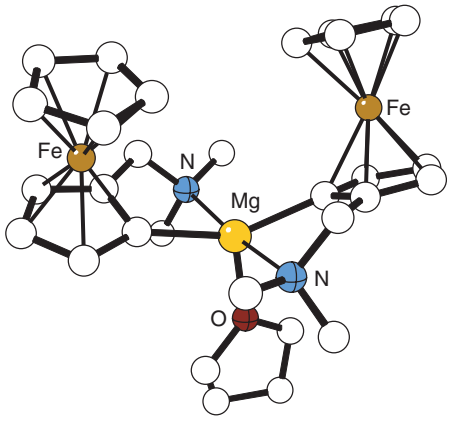

Figure 21 Structure of $(FcN)_2Mg(THF)$ **45**.

with an intermolecular exchange between the diastereomers. An intramolecular dynamic phenomenon involving dissociation and recoordination of Mg–N bonds is also operative.[169]

The amine adduct $Et_2Mg(tmeda)$ (R = Me, Et) reacts with phenylacetylene to produce $[Mg_2Et(phenylethynyl)_3(tmeda)]_2$·benzene **46** (Figure 22).[170] Related to that of alkali metal alkynyl magnesates, the structure of **46** is

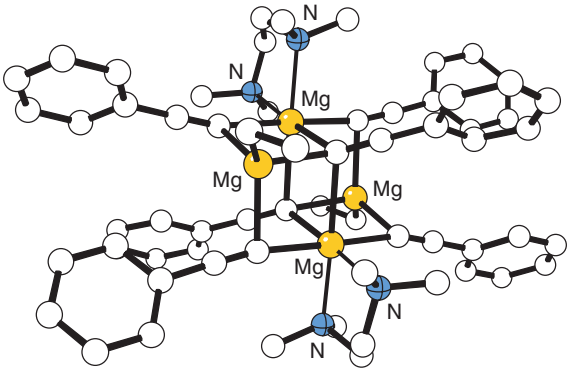

Figure 22 Structure of the trinuclear Mg compound $(Bu^tC{\equiv}C)(THF)Mg(\mu\text{-}C{\equiv}CBu^t)(\mu\text{-}NPr^i_2)Mg(\mu\text{-}C{\equiv}CBu^t)(\mu\text{-}NPr^i_2)Mg(THF)(C{\equiv}CBu^t)$ **46**.

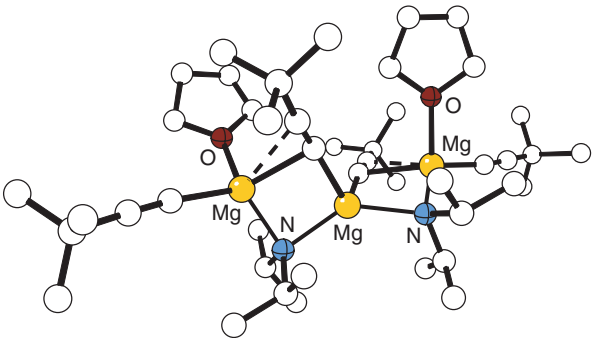

Figure 23 Structure of the trinuclear Mg compound ($Bu^tC{\equiv}C$)(THF)Mg(μ-$C{\equiv}CBu^t$)(μ-NPr^i_2)Mg(μ-$C{\equiv}CBu^t$)(μ-NPr^i_2)Mg(THF)($C{\equiv}CBu^t$) **47**.

constructed from two partial cubes, fused on a face. The equimolar reaction of $Bu^tC{\equiv}CH$ and $Mg(NPr^i_2)_2$ leads to the trinuclear Mg compound, ($Bu^tC{\equiv}C$)(THF)Mg(μ-$C{\equiv}CBu^t$)(μ-NPr^i_2)Mg(μ-$C{\equiv}CBu^t$)(μ-NPr^i_2)Mg(THF)($C{\equiv}CBu^t$) **47** (Figure 23), exhibits both an electron-rich bridging ligand $-NPr^i_2$ and electron-deficient bridging ligand $-C{\equiv}CBu^t$.[138]

In a remarkable transformation, the crystallographically characterized cyclic hexanuclear species {HC[C(Bu^t)-NAr′]$_2$Mg(C_3H_5)}$_6$ (Ar′ = 2,6-diisoprophylphenyl) **48** (Figure 24) is formed on thermal treatment under vacuum of the β-diketiminiate [HC{C(Bu^t)NAr′}$_2$Mg(C_3H_5)(THF)] (Equation (14)). The allyl groups in **48** exhibit μ-η^1:η^1 bonding, an unprecedented arrangement for an organoalkaline earth species.[171]

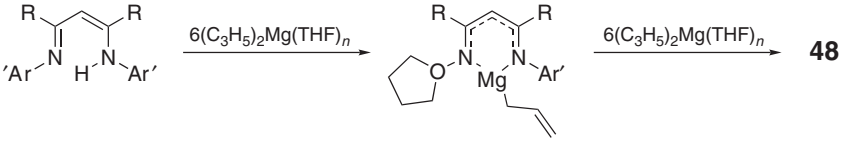

(14)

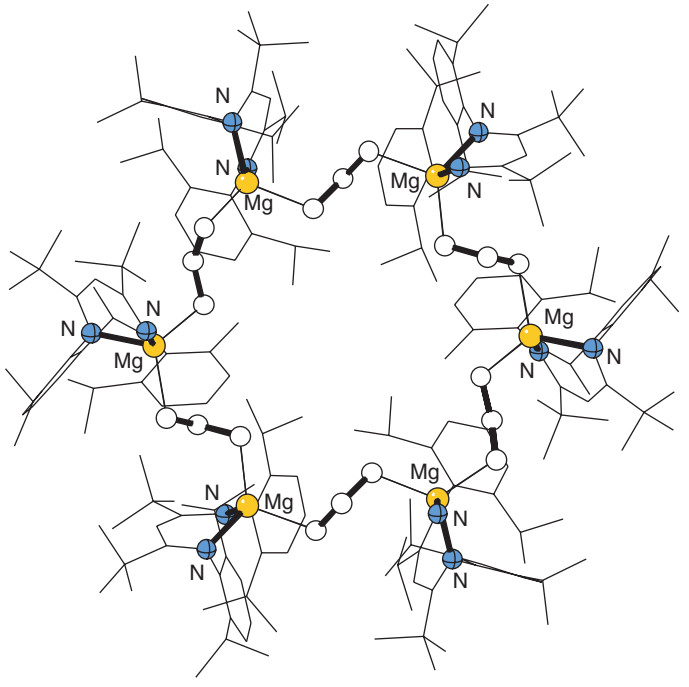

Figure 24 Structure of the cyclic hexanuclear species {HC[C(Bu^t)NAr′]$_2$Mg(C_3H_5)}$_6$ (Ar′ = 2,6-diisoprophylphenyl) **48**.

2.02.3.2.3 Reactions

The steric bulky ligands that are increasingly used to impose low coordination numbers on compounds can also limit their reactivity. For example, although $Mg(Tsi)_2$ was originally anticipated to serve as a TSi-transfer reagent, it has low reactivity, failing to react in toluene with CO_2, Me_3SiCl, Me_2SiHCl, MeI, BCl_3, or CH_3COCl. It reacts only slowly with I_2 in toluene to give TsiI, and more rapidly with Br_2 to give TsiBr, and with an excess of $PhSO_2Cl$ in toluene at 100 °C to give TsiCl. It decomposes quickly in the air, however, and reacts readily with MeOH or O_2 in toluene forming TsiH.[155] Dismutation of a THF solution of Mes^*MgBr with 1,4-dioxane affords $MgMes^*_2$.[172] The steric bulk of the mesityl ligand blocks reactions between $MgMes^*_2$ and THF, pyridine, or MeCN, unlike the case with the less bulky $Mg(2,4,6\text{-}R_3C_6H_2)_2$ (R = Me or Pr^i).[160]

Reaction rates of ketones with organomagnesium compounds can be highly sensitive to the identity and quantity of the ketone. For example, the initial rate of formation of the addition product from reactions of $MgNp_2$ (Np = neopentyl) and $Ph(Bu^t)CO$ or *o*-methylphenyl(Bu^t)CO in benzene is proportional to $[MgNp_2]^0[\text{ketone}]^1$ when $MgNp_2$ is in excess, and to $[MgNp_2]^1[\text{ketone}]^0$ when the ketone is excess. For either ketone, the rate is ca. 15-fold greater when the ketone is in excess than when $MgNp_2$ is in excess; in any case, reactions of $Ph(Bu^t)CO$ are ca. 600 times faster than reactions of *o*-methylphenyl(Bu^t)CO.[173] The rates of formation of the addition products from *o*-methylphenyl(Bu^t)CO and $Np_3Mg\text{–}NpMg(14N4)^+$ (14N4 = 1,4,8,11-tetramethyl-1,4,8,11-tetraazacyclotetradecane) or $Np_3Mg(THF)\text{–}NpMg(14N4)^+$ have been reported.[173]

In addition to participation in the classic Schlenk equilibrium (Equation (5)), MgR_2 complexes also interact with other potentially coordinating species, including the solvent. These can produce coordinated MgR^+ cations and organomagnesate anions. For example, benzene solutions of $MgNp_2$ and HMPA exhibit NMR absorptions attributed to $[NpMg(HMPA)]^{+2}$ and to $[MgNp_3]^-$ (equilibrating with $(MgNp_2)$). Absorptions for these ions are observed only for preparations having $0.5 < HMPA : Np_2Mg < 2$.[174] Competition experiments have been used to evaluate the coordinating ability of potential donors (Scheme 4). Addition of a second ligand L^2 (L^2 = various cryptands or azacrowns) to a solution of $[Mg(R)L^1Cp']$ (R = Et or CH_2Bu^t; Cp′ = 1,2,3,4-tetraphenylcyclopentadienyl) provides an equilibrium mixture of L^1 (generally pmedta or 2,5,8,11-tetramethyl-2,5,8,11-tetraazadodecane) and $[Mg(R)L^2Cp']$. The exchange with $[Mg(R)L^1]^+$, monitored with ^1H NMR spectroscopy, requires the addition of a small amount of MgR_2, apparently by generating some organomagnesate anion (MgR_3^-). The equilibrium constants give information about the relative abilities of different ligands to coordinate to MgR^+. Cryptands with multiple *O*- and *N*-binding sites have *K* values far higher than cyclic or acyclic *N*-donors, by as much as 6.6×10^7 for crypt 2.1.1 relative to pmdeta. Reactions of $[Mg(R^1)L^1]^+$ with MgR^2_2 (R^1 = Et, $R^2 = CH_2Bu^t$; $R^1 = CH_2Bu^t$, R^2 = Et) give equilibrium mixtures of these components, $[Mg(R^2)L^1]^+$ and MgR^1_2. The equilibrium constants indicate that there is little difference between the R groups regarding $[Mg(R)L^1]^+$ stability.[175]

The stoichiometric, position-selective deprotonation of cyclopropanecarboxamides and other weak CH acids (as encountered, for example, in the synthesis of the antidepressant Milnacipran) is hindered by the problems of high nucleophilicity and slow reaction times involved with lithium and magnesium alkyl compounds and side-reactions involving liberated amines with pK_a values similar to the CH acids. Alkylmagnesium amides, in particular, $Mg(Bu)NPr^i_2$, have been studied as new bases to address this issue. When the Bu_2Mg : diisopropylamine (DAH) ratio is 1 : 1, *cis*-*β*-metallation is favored, but at 2 : 1, *α*-metallation predominates, indicating that excess Bu_2Mg scavenges the DAH formed in the initial *α*-deprotonation, preventing equilibration.[176]

Diorganyl magnesium complexes are used in many syntheses as either a source of magnesium or as a ligand-transfer reagents. A full listing of individual compounds would be prohibitively long, and as many of the products are not organometallic species, they are often discussed in other places, such as COMC (1995). Among the more commonly used reagents is the commercially available "$MgBu_2$," which is a statistical mixture of $MgBu^n_2$ and $MgBu^s_2$. It has been used to produce magnesium thiolates,[177–179] amides[180–185] (sometimes with heteroleptic alkyl/amide species),[181,186] carboxylato or carbamato complexes,[187] furfurylamides,[188] isothiocyanate and carbodiimide insertion products,[150] phosphides,[186,189–191] hydrazides,[192,193] phosphanediides,[194,195] arsandiides,[196] arsinoanilides,[197] aryloxides,[198–200] siloxides,[200] molecular hydrides,[201] inverse crown complexes,[202,203] the polymeric coordination

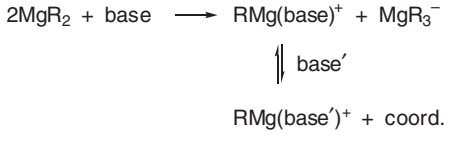

Scheme 4

complex $[(ImN)_2Mg]_n$,[149] the heteroleptic amide/alkoxide complex $\{(Me_3Si)_2NMg\text{-}[\mu\text{-}OC(H)Ph_2]\cdot(O{=}CPh_2)\}_2$,[204] the Mn(II) and Fe(II) diaryls $MnMes^*_2$ and $FeMes^*_2$,[160] the cage compound $Mg_n(O_2CC{\equiv}CSiMe_3)_{2n}(THF)_m$ and the trimeric $Mg_3(O_2CC{\equiv}CSiMe_3)_6(HMPA)_4$.[205]

S-functionalized methyltin compounds $Bu_3SnCH_2S(O)_nR$ ($n = 0$, 1, 2; R = Me, Ph) undergo transmetallation with diorganomagnesium compounds MgR′R″ (R′/R″ = Me/Me, Bu^n/Bu^s) to provide $SnBu_3R'$ and $Mg[CH_2S(O)_nR]R''$.[152] Transmetallations between $Bu_3SnCH_2YMe_2$ (Y = N, P) and $MgMe_2$ proceeded only in the presence of catalytic amounts (10–20 mol%) of LiBu, yielding $Mg(CH_2YMe_2)Me$ and $SnBu_3Me/SnBu_4$.[152]

The mechanism of chelation-controlled addition reactions of α- and β-alkoxy carbonyl compounds (methoxyacetone, methoxyacetaldehyde, 3-methoxy-2-butanone, 2-methoxypropanal, 4-methoxy-2-butanone, 3-methoxypropanal, and 3-methoxybutanal) with $MgMe_2$ has been investigated with *ab initio* calculations. The calculations suggest that the carbonyl substrate and $MgMe_2$ initially form a stable chelate complex with $>20\,kcal\,mol^{-1}$ exothermicity. Stereochemically determining C–C bond formation then ensues via 1,3-migration of the nucleophilic Me group to the carbonyl C with a 6–9 $kcal\,mol^{-1}$ activation energy, which then gives rise to a product chelate. The β-chelation-controlled reaction may proceed via either a stereoselective chair or nonselective boat transition state, the latter being energetically favored.[206]

2.02.3.2.4 Catalysis

Several neodymium alkoxides derived from simple and functionalized tertiary monoalcohols, in particular, $[Nd_3(\mu_3\text{-}OR)_2(\mu_2\text{-}OR)_3(OR)_4(THF)_2]$, form an active catalyst system for ethylene polymerization with dialkylmagnesiums (MgBuEt, $Mg(CH_2TMS)_2$, $Mg(n\text{-hex})_2$). Under mild conditions (0 °C, 1 bar), the catalyst system exhibits moderate activity (5–10 $kg\,mol^{-1}\,h^{-1}\,bar^{-1}$), and renewal/improvement of activity occurs upon addition of extra dialkylmagnesium. Diblock polyethylene–PMMA co-polymers could also be prepared with high diblock efficiency and high molecular weights ($M_n > 200{,}000$). A transmetallation product, $[RMg(OAr)]_2$ (R = hexyl; Ar = 2,6-Bu^t_2-4-MeC_6H_2), was isolated from an Nd alkoxide/MgR_2 combination; its formation suggests that an unisolated and presumably unstable $\{(ArO)_2Nd(n\text{-hex})\}_n$ species is generated in the catalytic cycle.[207]

Dialkylmagnesium compounds with alkyl groups of 4–200 carbons can be prepared by ethylene living-transfer polymerization initiated with MgEtBu in the presence of the lanthanocene catalyst $[Li(OEt_2)][(C_5Me_5)_2SmCl_2]$.[208] Reactions of organomagnesium compounds in the presence of zirconium catalysts (for cyclometallation of alkenes, synthesis of alkenyl organomagnesium compounds from α-olefins and MgR_2, and transformation of cyclopentanes with Cp_2ZrCl_2) have been reviewed.[209]

2.02.3.3 Cyclopentadienylmagnesium Compounds

2.02.3.3.1 Dicyclopentadienylmagnesium (magnesocene) and related compounds

2.02.3.3.1.(i) Magnesocene

Magnesocene, Cp_2Mg **49**, was the first of the group 2 metallocenes to be synthesized,[210] and its ferrocene-like structure (Mg–C = 2.304(8) Å (solid state)[211]; 2.339(4) Å (gas phase)[212]) and usefulness as a cyclopentadienyl-transfer reagent for transition metal complexes has long been known.[213–216] The lability of the rings of **49** is displayed in other ways. Reaction of **49** with DMSO affords the ionic compound $[Mg(DMSO)_6]^{2+}[C_5H_5]_2^-$ with uncoordinated cyclopentadienyl rings.[217] The reaction of **49** with the less strongly donating THF leads to the neutral complex $Cp_2Mg(THF)_2$ **50** with differently ligated cyclopentadienyl rings: one with η^1-coordination (Mg–C = 2.282(3) Å) and the other with η^5-(Mg–C = 2.417–2.479(3) Å) (Figure 25). Steric crowding presumably leads to the change in bonding arrangment.[217] A displaced ring is also found in $(\eta^5\text{-Cp})(\eta^1\text{-Cp})MgNHBu^t$, the product of the reaction of **49** with Bu^tNH_2; the average Mg–C(η^5) distance of 2.46 Å and the Mg–C(η^1) distance of 2.370 Å reflect the stronger donor properties of the amine relative to THF.[185]

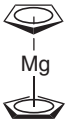

49

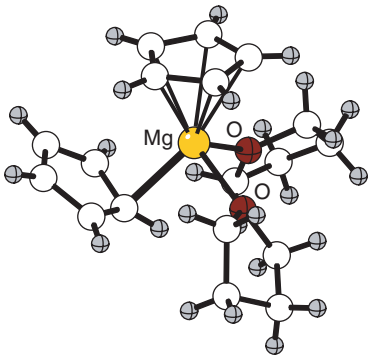

Figure 25 The structure of the differently ligated $(\eta^5\text{-Cp})(\eta^1\text{-Cp})_2Mg(THF)_2$ **50**.

2.02.3.3.1.(ii) Applications in CVD

Various techniques of thin film deposition, including CVD (also abbreviated as MOCVD, metalloorganic chemical-vapor deposition) have been under intensive development for the *s*-block elements, and particularly the alkaline earth metals, since the late 1980s.[3,218–221] The lability of the Cp rings of **49** has also made it a useful source of the Mg^{2+} ion. **49** has been used to deposit MgO by atomic layer epitaxy,[222] and is commonly employed as a *p*-type dopant for semiconductors, particularly GaAs,[223] GaN,[224,225] and AlGaN.[226] In GaN, Mg doping induces a blue 2.8 eV photoluminescence band arising from donor–acceptor (D–A) pair recombination.[227] It is likely that isolated Mg ions serve as the acceptors, while Mg/nitrogen vacancy complexes are the donors.[228,229]

The reaction of **49** with alkylamines has been examined in the context of $Cp_2Mg–MR_3–NH_3$ (M = group 13 metal) mixtures as CVD precursors. Addition of primary and secondary amines to **49** at ambient temperature in toluene affords stable amine adducts in good yield (Table 3).[230,231] Most adducts can be sublimed at under 100 °C/0.05 torr in good yields (72–95%) without decomposition and with less than 1% residue; the exception is $Cp_2Mg(NH_2CH_2Ph)$, which decomposes to **49** and $Cp_2Mg(NH_2CH_2Ph)_2$. The solid-state structures of $Cp_2Mg(NH_2R)$ ($R = CH(CHMe_2)_2$ **51** (Figure 26), C_6H_{11}, CH_2Ph) contain one η^5- and one η^2-coordinated cyclopentadienyl ring. IR spectroscopy suggests that the adducts are stabilized by $N–H\cdots C_5H_5^-$ hydrogen bonding, an interpretation supported by MO calculations on the model complex $Cp_2Mg(NH_2Me)$.[231] The $N–H\cdots C_5H_5^-$ hydrogen bond strength is estimated at 4.2 ± 1.4 kcal mol^{-1}; the amine hydrogen atoms are calculated to undergo site exchange by a low-energy (2.3 ± 0.5 kcal mol^{-1}) intramolecular rotational process that interconverts the η^2- and η^5-Cp ligands.[230,231]

2.02.3.3.1.(iii) Substituted magnesocenes and related compounds

Although it was the earliest known group 2 decamethylmetallocene,[232] bis(pentamethylcyclopentadienyl)magnesium **52**, was the last of the group 2 decamethylmetallocenes to be structurally authenticated with X-ray or electron diffraction. Unlike its counterparts with the heavier group 2 metals, **52** is linear, with Mg–C = 2.302 Å.[233] The stable carbene 1,3,4,5-tetramethylimidazol-2-ylidene reacts with $(C_5Me_5)_2Mg$ to generate the $(C_5Me_5)_2Mg(1,3,4,5\text{-}Me_4\text{-}C_3N_2)$ adduct.[234] The

Table 3 Primary and secondary amine adducts of Cp_2Mg[a]

Adduct	*Yield* (%)	*Cp ring binding*[b]
$Cp_2Mg(NH_2CH(CHMe_2)_2)$ **51**	91	$\eta^5 + \eta^2$
$Cp_2Mg(NH_2Pr^i)$	80	
$Cp_2Mg(NH_2Bu^t)$	67	
$Cp_2Mg(NH_2CH_2Ph)$	80	$\eta^5 + \eta^2$
$Cp_2Mg(NH(CH_2Ph)_2)$	86	
$Cp_2Mg(NH_2(C_6H_{11}))$	93	$\eta^5 + \eta^2$
$Cp_2Mg(NH(C_6H_{11})_2)$	84	
$Cp_2Mg(NHEt_2)$	84	
$Cp_2Mg(NH(Pr^i)(CH_2Ph))$	91	$\eta^5 + \eta^5$ (distorted)

[a]From Ref. 230,231.
[b]Listed ring binding modes are crystallographically verified.

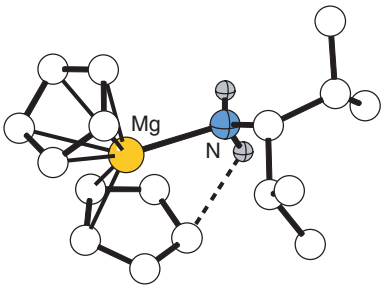

Figure 26 The structure of $(\eta^5\text{-Cp})(\eta^2\text{-Cp})Mg(NH_2CH(CHMe_2)_2)$ **51**.

rings in the complex are differently bound (η^5/η^3; Mg–C(ring centroid) = 2.17, 2.24 Å; Mg–C(carbene) = 2.194(2) Å), probably the result of steric crowding. Both **52** and other magnesocenes react with the related 1,3-di-isopropyl-4,5-dimethylimidazol-2-ylidene carbene to form adducts.[235] The chlorogallate $[Mg_3Cl_5(Et_2O)_6][GaCl_4]$ is isolated from the reaction of **52** with Ga_2Cl_4 in Et_2O.[236] The structure of the latter comprises a Mg_3Cl_3 ring with one μ_3-Cl above and below the ring; each metal is also coordinated by two ether molecules.

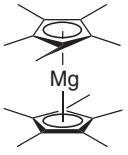

52

A magnesocene with pendant 3-butenyl substituents, $[C_5Me_4(CH_2CH_2CH{=}CH_2)]_2Mg$, was prepared by deprotonation of (3-butenyl)tetramethyl-1,3-cyclopentadiene followed by transmetallation with MgI_2. Unlike counterparts containing the heavier alkaline earth metals, the butenyl groups remain uncoordinated in the solid state.[237] The base-free metallocene $[1,2,4\text{-}Bu^t{}_3C_5H_2]_2Mg$ was prepared from the cyclopentadiene, $1,2,4\text{-}Bu^t{}_3C_5H_3$, and dibutylmagnesium. The magnesocene is slightly bent in the solid state with centroid–Mg–centroid angles of 171°.[238]

Various fulvenes have been used as precursors to magnesium–cyclopentadienyl complexes. Some of this research has been motivated by the potential use of these compounds as synthons for chiral *ansa*-metallocene complexes. Reactions with a minimally substituted fulvene such as dimethylfulvene may yield an inseparable mixtures of products (Equation (15)).[239] In contrast, the reaction of $MgBu^nBu^s$ with 6-methyl-6-phenylfulvene (Scheme 5) and 6,6-dicyclopropylfulvene gives the β-hydride transfer products **53** and 1,1′-bis-(dicyclopropylmethyl)magnesocene, respectively; both have been crystallographically characterized. $MgMe_2$ deprotonates the two fulvenes to form the readily decomposed 1,1′-bis(1-phenylethenyl)magnesocene **54** (Scheme 5), and the cyclopentadienyl derivative

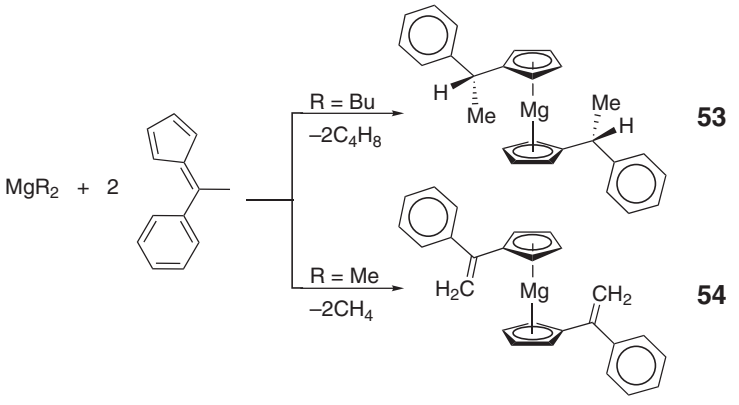

Scheme 5

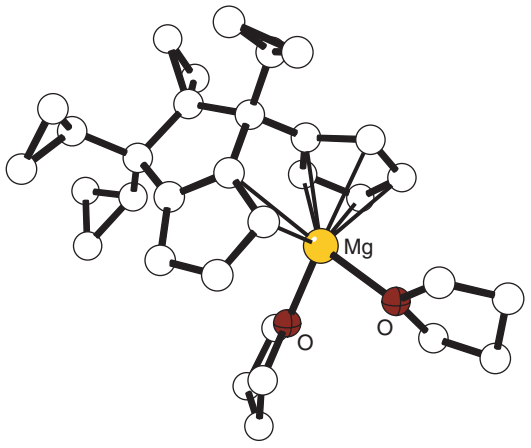

Figure 27 The structure of cyclopentadienyl–magnesium complex **55**.

55 (Figure 27), respectively. In the absence of β-H atoms, only the addition reaction is possible, and one Mg–C bond of $MgMe_2$ adds to tetramethylfulvene to give dimeric $[(EtMe_4C_5)Mg(\mu\text{-}Me)]_2$, in which the bridging Me groups are sterically shielded against further attack of the fulvene.[240]

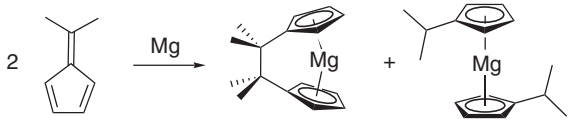

(15)

Treatment of *N,N′*-dicyclohexyl-6-aminofulvene-2-aldimine (HCy_2AFA) **56** with MeLi followed by MeMgBr gives the *N,N′*-coordinated complex [1,2-$(CyN{=}CH)_2C_5H_3$-*N,N′*]MgMe(THF), in which the cyclopentadienyl ring is uncoordinated. In contrast, the direct reaction of HCy_2AFA with MeMgBr liberates methane and affords the binuclear bromide-bridged complex $(Cy_2AFA)_2MgBr_2$ **57** (Figure 28), in which one of the magnesium centers is ligated both to the η^5-cyclopentadienyl ring of one of the ligands and to both nitrogen donors of the other ligand.[241]

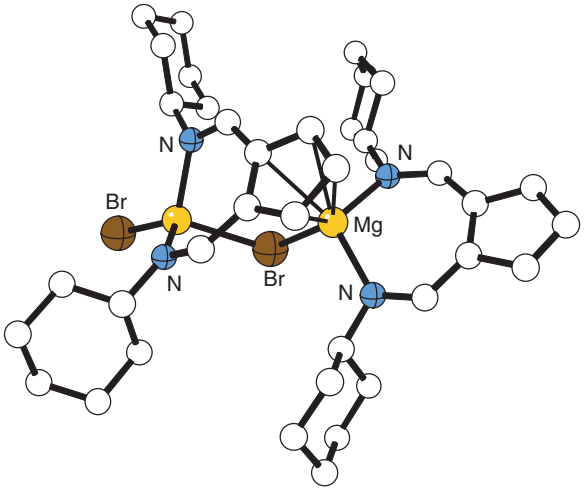

Figure 28 The structure of the binuclear bromide-bridged complex $(Cy_2AFA)_2MgBr_2$ **57**.

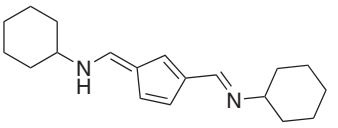

56

A series of chiral *ansa*-magnesocene complexes (**58–61**) with dimethylsilanediyl- or ethanediyl-bridged, substituted cyclopentadienyl or indenyl ligands, prepared in the form of their THF adducts, has been structurally characterized with X-ray crystallography and with NMR studies in solution.[242] The hapticities of the ring ligands vary between one and five, depending on the nature of the interannular bridge and the C ring substituents. A racemic configuration is preferred by Mg bis-indenyl complexes with either Me_2Si or C_2H_4 bridges in the solid state (**58** (Figure 29), **59** (Figure 30)) and in solution, while *meso* isomers predominate for Bu^t-substituted ansa-magnesocenes (**60** (Figure 31), **61** (Figure 32)).

2.02.3.3.2 Magnesium monocyclopentadienyls

2.02.3.3.2.(i) Complexes with carbocylic rings

The gas-phase coordination chemistry of the monocyclopentadienyl $[CpMg]^+$ cation with small inorganic ligands (NH_3, H_2, H_2O, CO, NO, O_2, CO_2, N_2O, NO_2, N_2) and saturated hydrocarbons (C_nH_{2n+2}; $n = 1–7$) has been measured with the selected-ion flow-tube technique.[243–245] Relative binding energies and standard enthalpies of formation have been estimated with DFT calculations, and single-point energy calculations have been completed with large basis sets at both the DFT and MP4 levels of theory. It it typically observed that ligation of one Cp to the

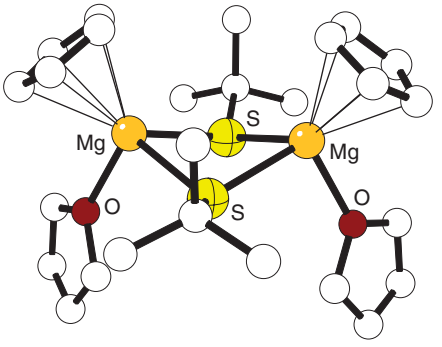

Figure 29 The structure of the *ansa*-magnesocene $C_2H_4(indenyl)_2Mg(THF)$ **58**.

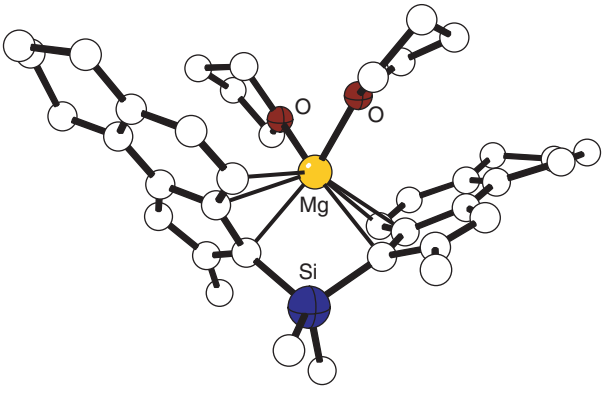

Figure 30 The structure of the *ansa*-magnesocene $Me_2Si(2\text{-}Me\text{-}tetrahydrobenz[e]inden\text{-}3\text{-}yl)Mg(THF)_2$ **59**.

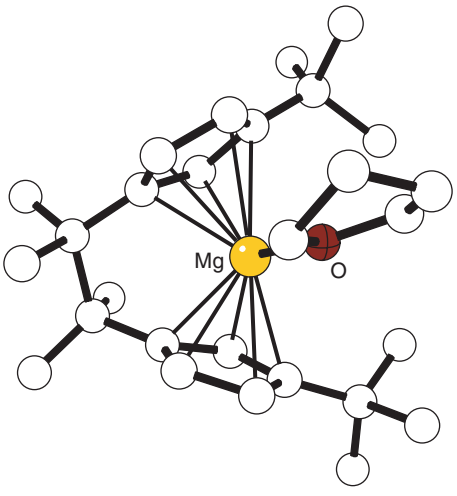

Figure 31 The structure of the *ansa*-magnesocene $(CH_3)_4C_2(3\text{-}Bu^t\text{–}C_5H_5)Mg(THF)$ **60**.

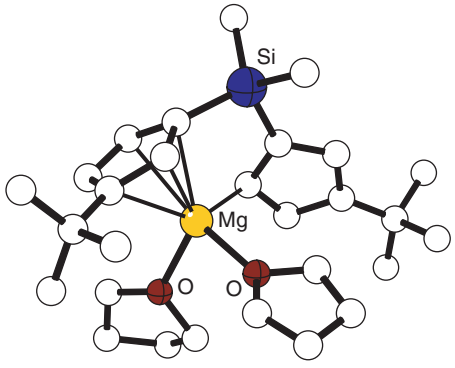

Figure 32 The structure of the *ansa*-magnesocene $Me_2Si(3\text{-}Bu^t\text{–}C_5H_3)Mg(THF)_2$ **61**.

Mg metal center enhances the efficiency of coordination of most small molecules, but ligation of a second Cp dramatically reduces it; no coordination of any type is seen to $[Cp_2Mg]^+$.

For ammonia, the initial addition of NH_3 to the $[CpMg]^+$ cation is three orders of magnitude faster ($k > 5 \times 10^{-11}$ cm^3 molecule^{-1} s^{-1}) than to the Mg^+ cation itself ($k = 4 \times 10^{-12}$ cm^3 molecule^{-1} s^{-1}). Ammonia does not form an adduct with the $[Cp_2Mg]^+$ cation, but rather displaces a Cp ring.[244] Similar behavior is observed with H_2O, but not with H_2, N_2, other gaseous oxides, or saturated hydrocarbons. Among the structures proposed for the adducts is a *C*-bound carbonyl species, $[CpMg(CO)_2]^+$; its formulation is based on analogy with the $[Mg\text{–}CO]^+$ system, for which calculations indicate that *C*-bound CO is preferred over the *O*-bound variety by >3 kcal mol^{-1}.[246] In the solution phase, treatment of **49** with $DippNH_2$ (dipp = 2,6-$Pr^i{}_2C_6H_3$) protonates a Cp ring, leading to the amide (η^5-Cp)Mg(NHdipp)THF.[185]

$[CpMgMe(Et_2O)]_2$, a versatile reagent for monocyclopentadienyl–magnesium chemistry, is prepared by dissolving **49** and dimethylmagnesium in Et_2O.[247] It reacts readily with a variety of amines and 2,5-bis(dimethylaminomethyl)-pyrrole to substitution products (Table 4). The solid-state structures of the dimers, for example, **62** (Figure 33), are constructed around nearly square Mg_2N_2 cores. The pyrrolate complex **63** (Figure 34) is monomeric, with one η^2-2,5-bis(dimethylaminomethyl)pyrrolato ligand.[248] The monomeric amidinate complexes $CpMg[\eta^2\text{-}Bu^tC(Ndipp)_2]$ **64** (Figure 35) and $CpMg(\eta^2\text{-}Bu^tC(Nmes)_2)(THF)$ were similarly prepared; **64** sublimes unchanged with 80% recovery at (180 °C/0.05 torr), whereas the latter decomposes to **49** and $Mg[\eta^2\text{-}Bu^tC(N(2,4,6\text{-}Me_3C_6H_2))]_2$ on heating. The bis(amidinate) was prepared independently through treatment of $MgBu_2$ with 2 equiv. of *N*,*N*′-bis(2,4,6-trimethyl-phenyl)(*tert*-butyl)amidine in toluene.[249]

Table 4 Monocyclopentadienyl derivatives of $[CpMgMe(Et_2O)]_2$

Complex	*Yield (%)*	*Mg–C*	*References*
$[CpMg(NPh_2)]_2$	83	η^5-Cp	248
$[CpMg(NHCH(CHMe_2)_2)]_2$	75	η^5-Cp	248
$[CpMg(NHPr^i{}_2C_6H_3)]_2$	61	η^5-Cp	248
$[CpMg(NPr^i(CH_2Ph))]_2$	62	η^5-Cp	248
$[CpMg(MeNCH_2CH_2NMe_2)]_2$ **61**	76	η^5-Cp	248
$CpMg(Et_2O)(\eta^2\text{-}Me_2NCH_2(C_4H_2N)CH_2NMe_2)$	84	η^5-Cp	248
$CpMg[\eta^2\text{-}Bu^tC(Ndipp)_2]$	87	η^5-Cp	249
$CpMg[\eta^2\text{-}Bu^tC(Nmes)_2](THF)$	76	η^5-Cp	249

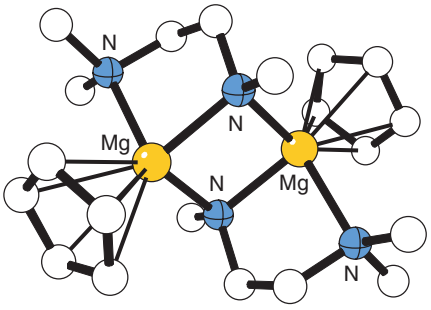

Figure 33 The structure of the dimeric monocyclopentadienyl $[CpMg(MeNCH_2CH_2NMe_2)]_2$ **62**.

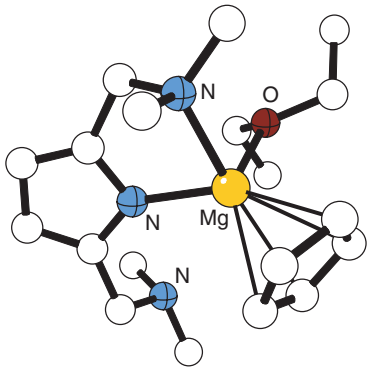

Figure 34 The structure of the pyrrolate complex $CpMg(Et_2O)(\eta^2\text{-}Me_2NCH_2(C_4H_2N)CH_2NMe_2)$ **63**.

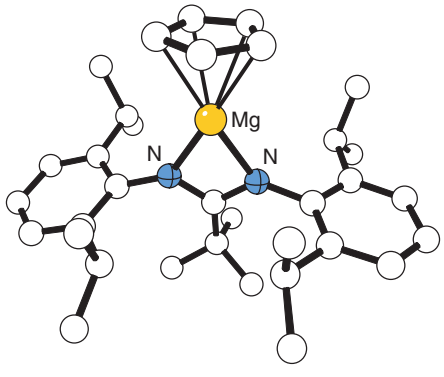

Figure 35 The structure of the amidinate complex $CpMg[\eta^2\text{–}Bu^tC(Ndipp)_2]$ **64**.

Monocyclopentadienyl complexes containing the β-diketiminato ligand can display either η^2- or π-coordination to a magnesium center. Reaction of $[CpMgMe(Et_2O)]_2$ with the diketimine N-Bu^t-4-(Bu^t-imino)-2-penten-2-amine in Et_2O (Equation (16)) produces $CpMg(HC(C(Me)N(Bu^t))_2)$ **65**. In the solid state, **65** contains a π-coordinated β-diketiminato ligand (Mg–N = 2.006(4), 2.021(3) Å; the Mg–C_α distances of 2.689(3) and 2.729(3) Å represent weak bonding interactions). Treatment of **65** with 4-*tert*-butylpyridine generates **66**, which possesses a η^2-β-diketiminato ligand. A related complex **67** is isolated from *N*-Pr^i-4-(Pr^{i}imino)-2-penten-2-amine and 4-*tert*-butylpyridine in Et_2O. Without the 4-*tert*-butylpyridine, an unstable Et_2O adduct is formed, which decomposes to a mixture of **49** and the bis(β-diketiminato)complex $Mg[HC(C(Me)N(Pr^i))_2]_2$ **68**. Both **68** and **69** were separately prepared independently through treatment of $MgBu_2$ with 2 equiv. of the appropriate diketimines.[250] Complexes **65**, **68**, and **69** sublime without decomposition on heating under vacuum, although they are not as volatile as **49**.

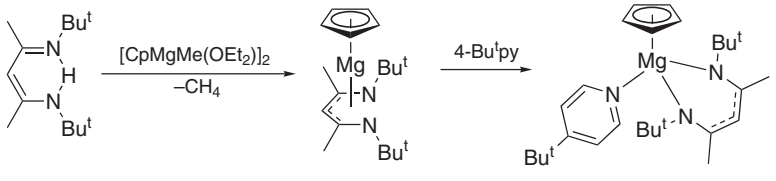

65 **66**

(16)

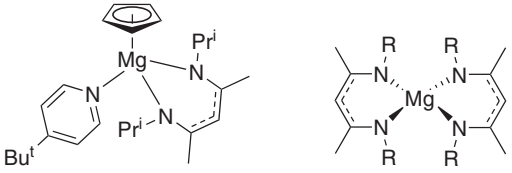

67 **68**: R = Pr^i
69: R = Bu^t

$[CpMgMe(Et_2O)]_2$ also reacts with phenylacetylene and ferrocenylacetylene in Et_2O to yield the tetrameric acetylide complexes $[CpMg(\mu_3\text{-}C{\equiv}CPh)]_4$ **70** (Figure 36) and $[CpMg(\mu_3\text{-}C{\equiv}CC_5H_4FeCp)]_4$, respectively.[251] Both complexes have C_4Mg_4 cubic cores and are rare examples of organomagnesium compounds with isostructural lithium analogs.[252,253–256] Treatment of **70** with THF afforded the dimeric acetylide complex $[CpMg(\mu_2\text{-}C{\equiv}CPh)(THF)]_2$ with a 1,3-dimagnesiacyclobutane core.[251]

Related sulfur-containing derivatives are formed from the reaction of **49** with 2-methyl–2-propanethiol, cyclohexanethiol, and 2-propanethiol in toluene at ambient temperature. The resulting tetrameric cyclopentadienyl thiolato complexes $[(\eta^5\text{-}Cp)Mg(\mu_3\text{-}SR)]_4$ (R = Bu^t, C_6H_{11}, Pr^i) are colorless crystalline solids. Treatment of

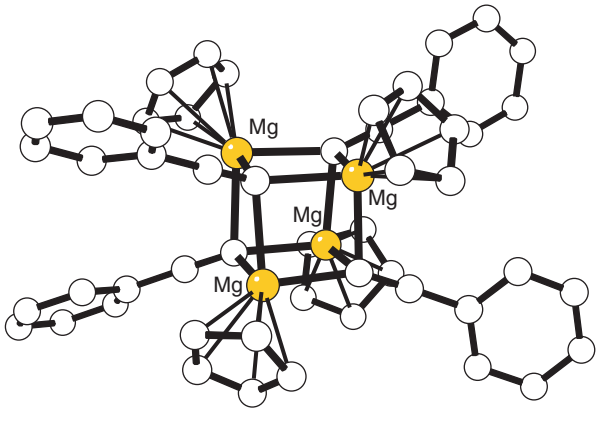

Figure 36 The structure of the tetrameric acetylide complex $[CpMg(\mu_3\text{-}C{\equiv}CPh)]_4$ **70**.

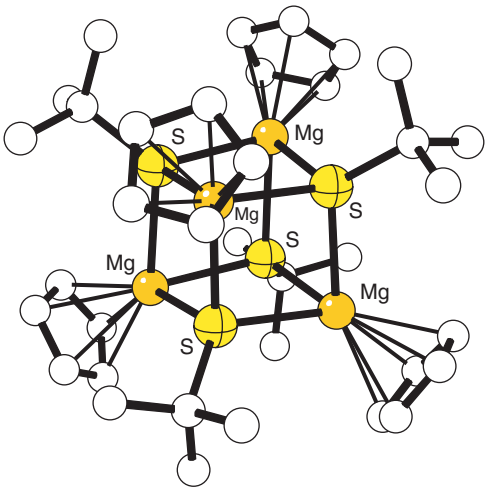

Figure 37 The structure of the tetrameric $[(\eta^5\text{-Cp})Mg(\mu_3\text{-SBu}^t)]_4$ **71**.

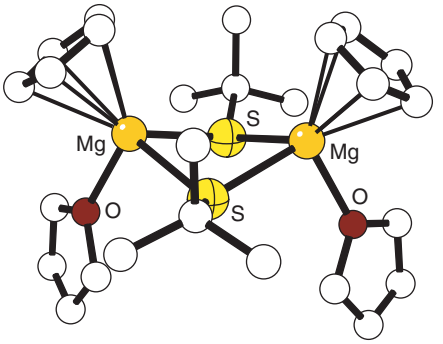

Figure 38 The structure of the dimeric solvated complex $[(\eta^5\text{-Cp})Mg(\mu_2\text{-SBu}^t)(THF)]_2$ **72**.

$[(\eta^5\text{-Cp})Mg(\mu_3\text{-SBu}^t)]_4$ **71** with THF and *tert*-butylpyridine in dichloromethane/hexane affords the colorless dimeric solvated complexes $[(\eta^5\text{-Cp})Mg(\mu_2\text{-SBu}^t)(L)]_2$ (L = THF **72**, Bu^tpy). In the solid state, **71** (Figure 37) is constructed around a Mg_4S_4 cubic core; the solvated derivative **72** (Figure 38) contains a bent Mg_2S_2 core (Mg–S–Mg′–S′ = 29.8°); the similar core in $[(\eta^5\text{-Cp})Mg(\mu_2\text{-SBu}^t)(Bu^t\text{py})]_2$ is planar.[257]

A procatalyst for ethylene and propene polymerization has been developed from CpMgCl.[258] The mono(ring) complex can be treated directly with $TiCl_4$ or it can be allowed first to react with $LiBu^n$, followed by $TiCl_4$. In either case, subsequent activation with MAO or $Al(C_2H_5)_3$ generates catalytically active species. There is little evidence for ligand exchange between CpMgCl and $TiCl_4$ (the use of $CpTiCl_3$, which would form if ring exchange had occurred, does not produce an active catalyst), and the CpMgCl/$TiCl_4$/MAO combination shows more than 70% greater reactivity in ethylene polymerization than does a standard mixture of $MgCl_2/TiCl_3/Al(C_2H_5)_3$. Isotactic indices of the polymer obtained from the CpMgCl-supported systems appear to be similar to those from the magnesium halide mixtures.

Asymmetric substituted derivatives $MgRR^1(L)$ are available by substituting one organic group by a different carbanion via acid–base reactions (Equation (17)), with HR^1 being stronger a CH-acid than HR. From the amine adducts $Me_2Mg(tmeda)$ (L = tmeda, pmdta) and the carbon acids, cyclopentadiene, indene, and fluorene, $MgMe(\eta^3\text{-Cp})(tmeda)$, $MgMe(\eta^3\text{-indenyl})(tmeda)$, and $MgMe(\eta^1\text{-fluorenyl})(tmeda)$ have been synthesized and crystallographically characterized. The Cp, indenyl, and fluorenyl ligands have a hapticity lower than η^5, evidently a result of steric repulsion by the other ligands. When the highly coordinated $Me_2Mg(pmdta)$ reacts with fluorene, the solvent-separated ion pair $[Mg_2Me_2(pmdta)_2]^{2+}[fluorenyl]^{2-}$ **73** (Figure 39) is isolated; there is no direct interaction between the fluorenide anion and magnesium.[170]

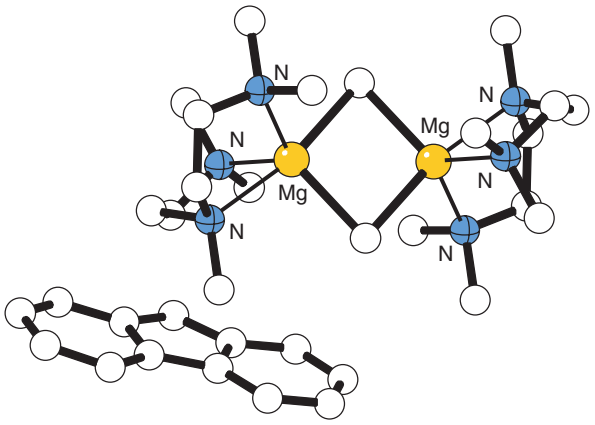

Figure 39 The structure of the solvent-separated ion pair $[Mg_2Me_2(pmdta)_2]^{2+}[fluorenyl]^{2-}$ **73**.

$$R_2Mg(L) + HR^1 \longrightarrow RR^1Mg(L) + HR \quad (17)$$

The *exo*,*exo*-bis(isodicyclopentadienyl)magnesium sandwich and the monomeric *exo*-(isodicyclopentadienyl)butylmagnesium tmeda complex **74** (Figure 40) have been synthesized and characterized by ^1H and ^{13}C NMR spectroscopy and X-ray crystallography. When treated with $TiCl_3 \cdot 3THF$ and $ZrCl_4$, ligand transfer to the transition metals occurs to form mixtures of all three possible isomers (*exo*,*exo*;*endo*,*endo*; and *exo*,*endo*).[259]

2.02.3.3.2.(ii) Heterocyclic derivatives

Heterocyclic derivatives of the cyclopentadienyl ligand have been incorporated in organomagnesium species. The reaction of bis(cyclopentadienyl)–1-zircona–2,3,4,5-tetraethylcyclopenta–2,4-diene with ECl_3 (E = P, As, Sb) yields 1-chloro-tetraethylphosphole, -arsole, and -stibole. The reduction of these pentoles initially gives the corresponding octaethyldiphospholyl, -diarsolyl, and -distibolyl. Further reduction of these dipentolyls with Mg in the presence of $MgCl_2$ generates $[Mg(\mu\text{-}Cl)(\eta^5\text{-}C_4Et_4E)(THF)]_2$ (E = P, As, or Sb); no reaction is observed without the dichloride.[260] The phospholide derivative **75** has been structurally characterized (Figure 41).

The donor-free boratobenzene derivatives $Mg(\eta^6\text{-}C_5H_5BMe)_2$ **76** and $Mg(\eta^6\text{-}3,5\text{-}Me_2C_5H_3BNMe_2)_2$ **77** were synthesized in good yields by the reactions of $MgMe_2$ with the (trimethylstannyl)dihydroborinines 2-$(Me_3Sn)C_5H_5BMe$ and 2-$(Me_3Sn)(3,5\text{-}Me_2C_5H_3BNMe_2)$, respectively.[261] In the solid state, both **76** and **77** display crystallographic centrosymmetry; Mg–C distances average 2.403 Å in **76**, 2.391 Å in **77**. **76** reacts with 2,2-bipyridine to give the adduct $Mg(\eta^6\text{-}C5H5BMe)(\eta^1\text{-}C_5H_5BMe)(bipy)$ **78** (Figure 42), with Mg–C_5 = 2.618 Å (av.); Mg–$C(\eta^1)$ = 2.313(7) Å. Crystallization of **77** from THF produces the solvate $Mg(\eta^1\text{-}3,5\text{-}Me_2C_5H_3BNMe_2)_2(THF)_2$, which exhibits a distorted tetrahedral N_2O_2 coordination environment around the Mg atom (Mg–N = 2.141(3) Å

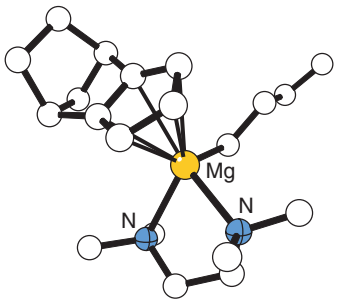

Figure 40 The structure of the *exo*-(isodicyclopentadienyl)butylmagnesium tmeda complex **74**.

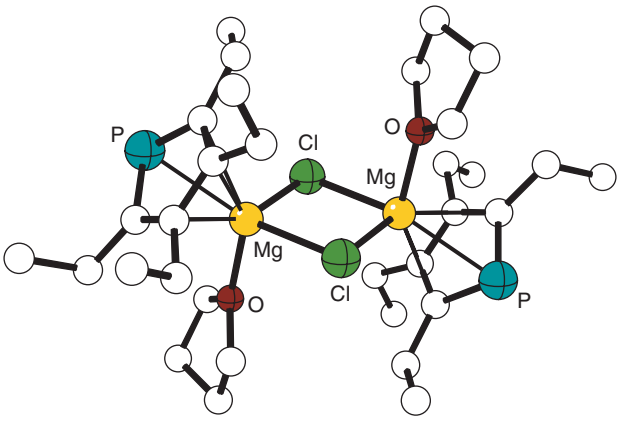

Figure 41 The structure of the phospholide $[Mg(\mu\text{-}Cl)(\eta^5\text{-}C_4Et_4P)(THF)]_2$ **75**.

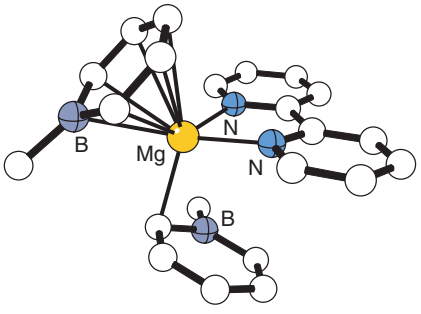

Figure 42 The structure of the adduct $Mg(\eta^6\text{-}C_5H_5BMe)(\eta^1\text{-}C_5H_5BMe)(bipy)$ **78**.

(av.); N–Mg–N, 148.0(1)°) with a σ-bonded aminoboratabenzene ligand.[261] All the structures are consistent with predominantly ionic bonding between the magnesium and the boratabenzene ligands (whether η^6- or η^1-bonded).

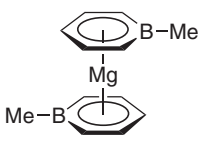

76

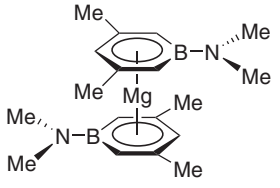

77

2.02.3.4 Addition Compounds of Magnesium with Unsaturated Organic Molecules

Ligand exchange of the *Mg*-bound butadiene in $[Mg(C_4H_6)(THF)_2]_n$ **79**[262] has been studied with 1,4-diphenyl-1,3-butadiene or 1,6-diphenyl-1,3,5-hexatriene.[263] In addition to butadiene, the reaction affords Mg(*s-cis*-1,4-diphenyl-1,3-butadiene)$(THF)_3$ **80** or Mg(1,6-diphenyl-1,3,5-hexatriene)$(THF)_3$ **81**, respectively (Scheme 6). Similarly, treatment of **79** with 1,3,5,7-cyclooctatetraene and anthracene yields the corresponding Mg adducts Mg(cot)$(THF)_{2.5}$ **82** Mg(anthracene)$(THF)_3$ **83**, respectively (Scheme 3). Reaction of **79** with diphenylacetylene in THF also induces a ligand exchange reaction, giving the diphenylacetylene adduct $[Mg_2(PhC_2Ph)_2(THF)]_2$.[263]

Ab initio calculations at the MP2/3-21G* level of theory were performed for the Mg–anthracene complexes 9,10-magnesium–anthracene·$3H_2O$ **84** and the 9-Me-, 9,10-dimethyl-, and 9,10-bis(methylsilyl)-substituted

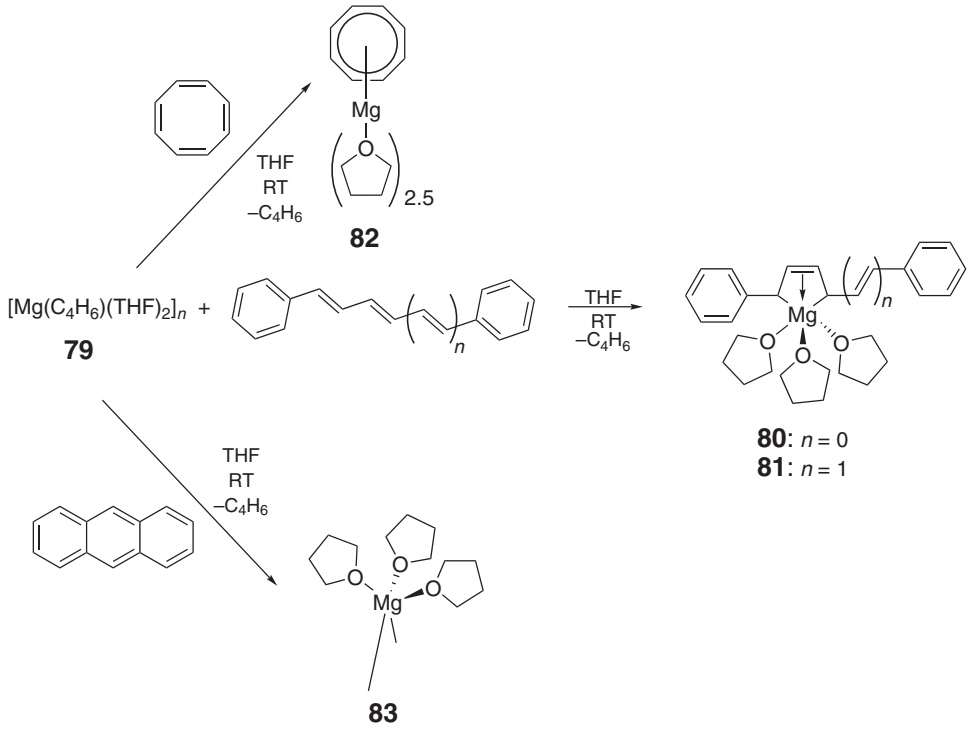

Scheme 6

derivatives.[264] The calculated geometries are in good agreement with experimental values for the corresponding THF complexes. The anthracene ligands are folded by approximately 40° along the C9–C10 line in the complexes. Topological and NBO analysis of the electronic structure shows clearly that the Mg–C9,10 bonds should be considered highly ionic. The predicted NMR chemical shifts using the GIAO method give ^{13}C resonances for **84** that are in good agreement with experimental values for **83**.[264]

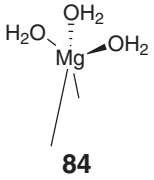

2.02.3.5 Organomagnesium Amides, Alkoxides, and Related Compounds

2.02.3.5.1 Organomagnesium amides and related compounds with group 15-bonded ligands

Reaction of $[K\{N(SiMe_3)C(Bu^t)C(H)R\}]_n$ $\{[K(LL')]_n\}$ or $[Li(\{N(SiMe_3)C(Ph)\}_2CH)]_2\{\equiv [Li(LL)]_2\}$ with Mg bromide yields the monomeric, crystalline complexes $[Mg(LL')_2]$ or $[Mg(LL)_2]_2$ **85** (Figure 43). In **85**, the Mg atom lies in an unusual planar environment (Mg–C = 2.284(4) Å; Mg–N = 2.084(3) Å), an arrangement apparently promoted by intermolecular steric interactions.[265] *s*-Block azaallyl chemistry has been reviewed.[266]

On reaction with MeMgCl, the lithium triazine $Li(THF)_2\{N[C(Ph)=N]_2\}CBu^t(Bu^n)$ yields the methylmagnesiodihydrotriazine **86** (Equation (18)). An X-ray crystal structure determination revealed that the compound closely resembled its lithio precursor; the formal substitution of $MeMg^+$ (Mg–C = 2.164(3) Å) for Li^+ did not produce the substantial structural differences often observed between isoleptic organolithium and organomagnesium systems.[267]

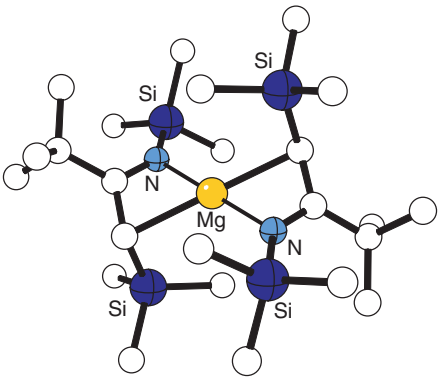

Figure 43 The structure of the 1-azaallyl complex **85**, with a planar Mg environment.

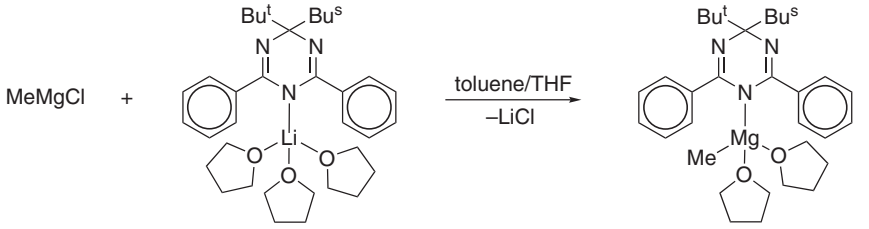

(18)

86

The structure of some heteroleptic magnesium amides, of potential use in organic synthesis (including Hauser bases, R_2NMgBr), depends on the Lewis acidity and steric bulk of the amido groups. For example, the 1 : 1 stoichiometric reaction between MgR_2 and diphenylamine produces the monomeric heteroleptic alkylmagnesium amides $RMgNPh_2(THF)_2$ (R = Et, Pr^i).[138] Adding the stronger donor solvent HMPA to $EtMgNPh_2(THF)_2$ initiates rearrangement to produce the bis(amido)magnesium compound $Mg(NPh_2)_2(HMPA)_2$. The stoichiometric reaction between $Mg(NPr^i_2)_2$ and different substituted acetylenes HC≡CR in THF solution produces dimeric amidomagnesium acetylide compounds $[(RC{\equiv}C)Mg(\mu\text{-}NPr^i_2)(THF)]_2$ (R = Ph, $SiMe_3$). Unexpectedly, the reaction of $MgEt_2$ and $HN(SiMe_3)_2$ in refluxing THF produced $[(Me_3Si)_2NMg(\mu\text{-}OEt)(THF)]_2$.[138]

Reaction of dpp–bian with Mg in THF for 30 min reflux gives complex **87** (Ar = 2,6-diisopropylphenyl) which undergoes oxidative addition via σ-bond metathesis with PhC≡CH to give the black alkynyl amido complex **88**. The insertion reaction of **88** with Ph_2CO in Et_2O yields complex **89**. Unexpectedly, hydrogen abstraction to give the radical anion occurs simultaneously with ketone insertion.[268]

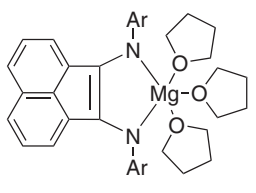

87

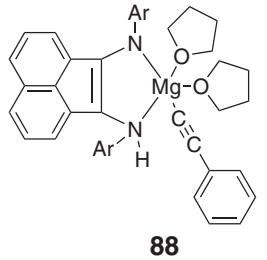

88

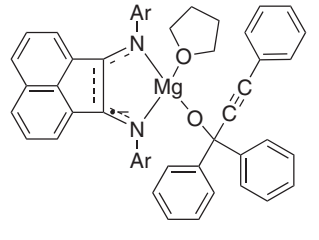

89

Reaction between MgR_2 (R = Bu^t or $Bu^{n/s}$) and Bu^tNH_2 gives the dimeric amide species $[RMg(\mu\text{-}NHBu^t)THF]_2$. A unique product with a rare dodecameric ring structure, $(EtMgNHdipp)_{12}$ **90** (Figure 44), is obtained when $MgEt_2$ reacts with $dippNH_2$.[185] Partial alkyl elimination from $MgBu_2$ occurs on reaction with $HNDiip(SiMe_3)$ in a 1 : 1 hexane : THF mixture to give the alkyl amido complex $BuMg[Ndiip(SiMe_3)](THF)_2$.The same reaction conducted in hexanes only yields the bis(amide) $Mg[Ndiip(SiMe_3)](THF)_2]_2$.[186]

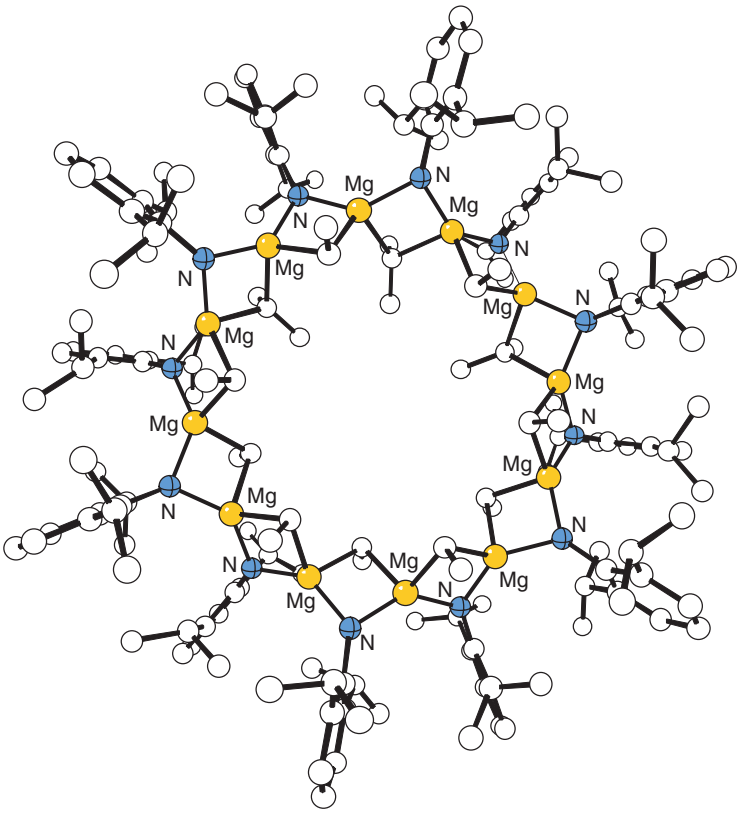

Figure 44 The structure of the dodecameric complex $(EtMgNHdipp)_{12}$ **90**.

2.02.3.5.1.(i) β-Diketiminate and related complexes

The synthesis of some bis(β-diketiminate) complexes, which are not formally organometallic species, has been discussed above (Section 2.02.3.1.2). Several alkylmagnesium complexes stabilized by a bulky β-diketiminate ligand illustrate the sensitivity of the reactions to the identity of the solvent. Thus, reaction of $MgMe_2$ with the sterically bulky β-diketimine ligand **91** in Et_2O gives the monoalkyl derivative $MeMg[N_2C_3HMe_2(2,6\text{-}Pr^i{}_2C_6H_3)_2]OEt_2$ **92** in 68% yield.[269] The same complex with THF replacing Et_2O (**92**·THF) is obtained from the reaction of MgMeCl with $Li[C(Me)=Ndipp]_2CH$ in THF.[270] The methyl-bridged dimeric complex $[Mg(\mu\text{-}Me)\{HC[C(Me)NAr']\}_2]_2$ **93** is obtained by removal of THF from **92**·THF under vacuum at 150 °C or by treatment of **91** with $MgMe_2$ in toluene with elimination of methane. The reaction of **91** in toluene with $MgBu^t{}_2$ in place of $MgMe_2$ generates the base-free species $Bu^tMg[N_2C_3HMe_2(2,6\text{-}Pr^i{}_2C_6H_3)_2]$ **94** (Figure 45) in 57% yield.[269]

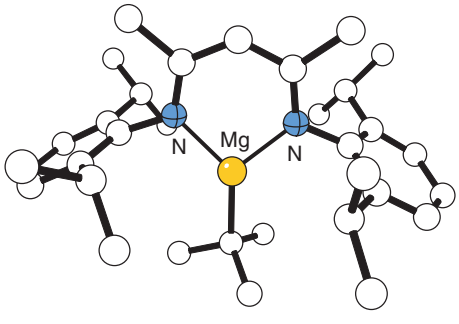

Figure 45 The structure of the base-free β-diketiminate species **94**.

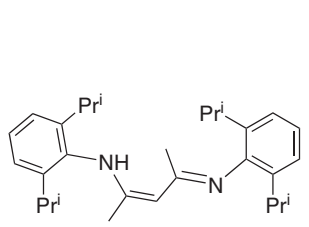

91

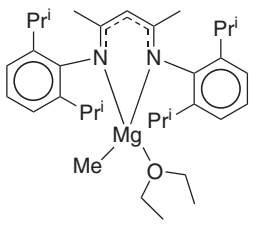

92

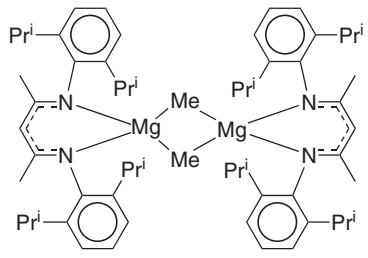

93

Treatment of MgMeCl with the lithium *N*,*N*′-diisopropylaminotroponiminate (LiL) in THF gives the four-coordinate methylmagnesium complex Mg(η^2-L)Me(THF).[270] Both the latter and **92**·THF readily react with oxygen to provide methoxide-bridged dimeric complexes [Mg(μ-OMe)(η^2-L-X)]$_2$. In contrast, treatment of $MgMe_2$ with the aminotriponimine H[(Pr$^i_2$)ATI] provides only the bis-chelate complex [Mg{(Pr$^i_2$)ATI}$_2$]. The methyl-bridged dimer [Mg(μ-Me){η^2-(Pr$^i_2$)ATI}]$_2$ is formed by removal of THF from MgMe{η^2-(Pr$^i_2$)ATI}(THF) at 110 °C under vacuum.[270]

2.02.3.5.1.(ii) Inverse crowns

A particularly interesting development in heterometallic amido complexes are the so-called "inverse crown ether" complexes. Most commonly these are eight-membered (M–N–Mg–N)$_2$ rings (M = Li, Na, K)[271–273] that act as polymetallic hosts to anionic species (e.g., O^{2-}, O_2^{2-}, H^-[274]). In a typical preparation of an inverse crown, the reaction of LiBu^n with dibutylmagnesium and oxygenated 2,2,6,6-tetramethylpiperidine (LH) affords the complex [$L_4Li_2Mg_2O$]. The same reaction with NaBu^n in place of LiBu^n and HN(SiMe$_3$)$_2$ in place of tetramethylpiperidine yields [(Me$_3$Si)$_2$N]$_4$Na$_2$Mg$_2$(O$_2$)$_x$(O)$_{1-x}$.[272] A review of metal inverse crown chemistry is available.[275]

The inverse crown [NaMg(NPr$^i_2$)$_3$]$_n$ has been prepared and found to react with ferrocene in a regioselective fourfold deprotonation at the 1,1′,3,3′ positions. The product [Na$_4$Mg$_4$(NPr$^i_2$)$_8$Fe(C$_5$H$_3$)$_2$] **95** (Figure 46) contains a 16-membered, centrosymmetric $Na_4Mg_4N_8$ ring. As with the known crowns, the deprotonation positions are dictated by the positions of magnesium in the ring. The ring is severely flexed in order to anchor the dideprotonated edge of each Cp ring.[276] A series of inverse crowns with multiple deprotonated ferrocenes and the general formula

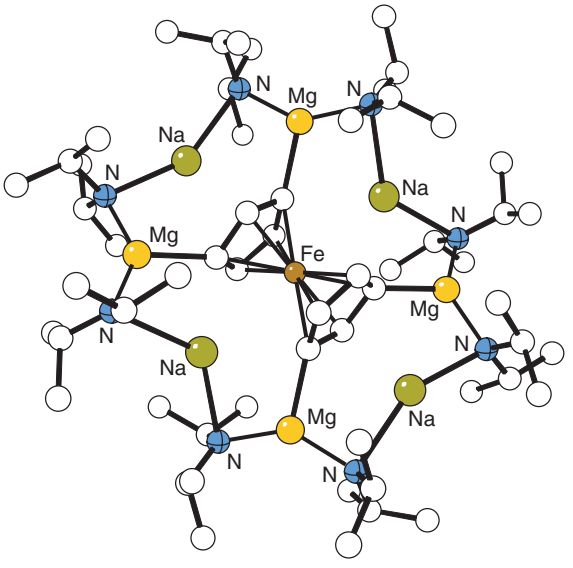

Figure 46 The structure of the inverse crown derivative, [Na$_4$Mg$_4$(NPr$^i_2$)$_8$Fe(C$_5$H$_3$)$_2$] **95**.

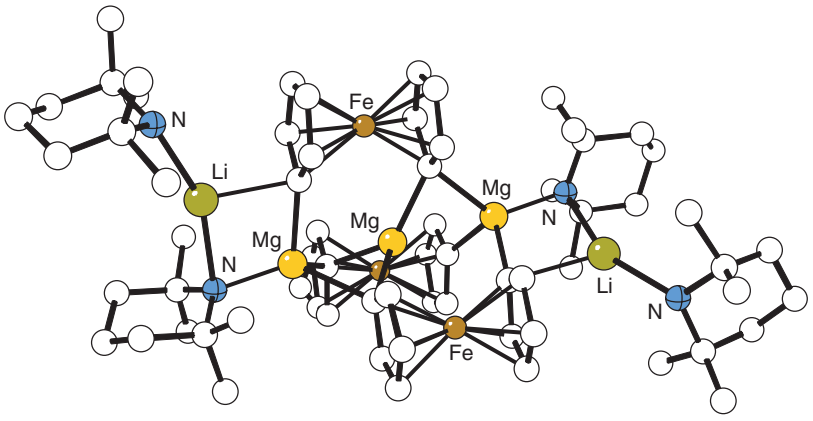

Figure 47 The structure of a inverse crown with multiple deprotonated ferrocenes **96**.

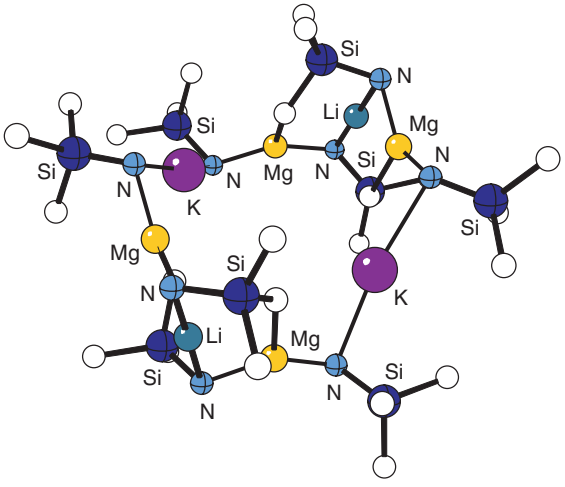

Figure 48 The structure of the heterotrimetallic inverse crown **97** (for clarity, Bu^t groups attached to nitrogen atoms are not shown).

$[\{Fe(C_5H_4)_2\}_3\{M_2Mg_3(tmp)_2L_2\}]$ (M = Li, L = tmpH or py; M = Na, L = tmpH; tmpH = 2,2,6,6-tetramethylpiperidine) **96** (Figure 47) has also been prepared.[277]

An unusual heterotrimetallic inverse crown $Li_2K_2Mg_4\{Bu^t(Me_3Si)N\}_4\{Bu^t[Me_2(H_2C)Si]N\}_4(hexane)_x$ **97** (Figure 48) has been prepared from the reaction of $Mg[N(SiMe_3)Bu^t]_2$ with $Me_3Si(Bu^t)NH$, followed by sequential treatment with BuLi and KCH_2Ph. The molecule can be viewed as a 16-membered $(KNMgNLiNMgN)_2$ primary ring with four six-membered (MgCSiNLiN) appendant secondary rings; the usual anionic core in inverse crowns is here part of the ring structure.[278]

2.02.3.5.2 Organomagnesium compounds with phosphorus-bonded ligands

Reviews covering the chemistry of group 2 metal complexes with phosphorus-stabilized carbanions,[279] and of molecular clusters of magnesium dimetallated primary phosphanes, are available.[280] Magnesium phosphanes remain rare compounds.[281] Lithiation of bromide **98** with BuLi in the presence of tmeda in pentane produces a lithium phosphine dimer; subsequent treatment with $MgCl_2$ in Et_2O gives the phosphane **99** in 69% overall yield (Equation (19)). The centrosymmetric **99** has Mg–C = 2.217 Å; Mg–P = 2.77 Å (av.).[282]

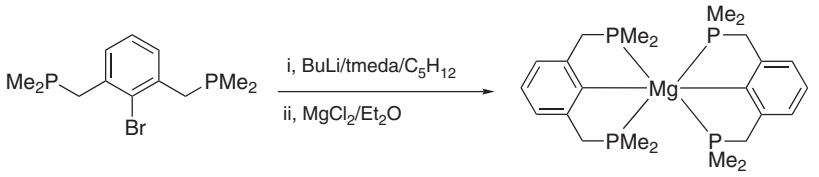

98 **99** (19)

The reaction of $Mg[N(SiMe_3)_2]_2$ with diphenylbutadiyne in toluene at room temperature produces the dimeric addition product **100** (Figure 49), which crystallizes from toluene with a centrosymmetric Mg_2P_2 core (Mg–C = 2.157(3) Å; Mg–P = 2.708(3) Å).[283] Addition of RMgX (R = Pr^i or Bu^t; X = Cl or Br) to $Bu^tC{\equiv}P$ at −78 °C in ether or THF results in a regio- and stereoselective 1,2-addition process to give the corresponding 2-phospha-1-vinylmagnesium halides in high yields (Equation (20)). At higher temperature (50 °C), the phosphavinylmagnesium chloride reacts with 2 more equiv. of $Bu^tC{\equiv}P$ to afford the magnesium–phosphorus cage compound **101** (Mg–C = 2.247(3)–2.284(3) Å) (Figure 50).[112]

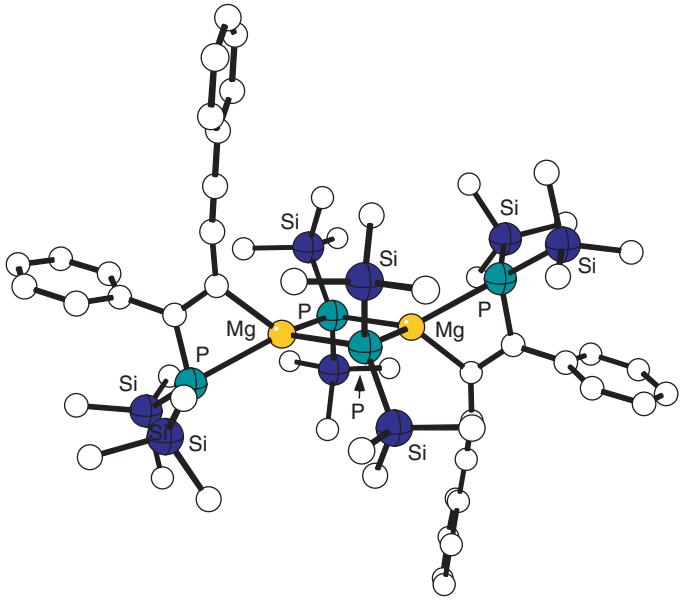

Figure 49 The structure of the dimeric magnesium phosphane **100**.

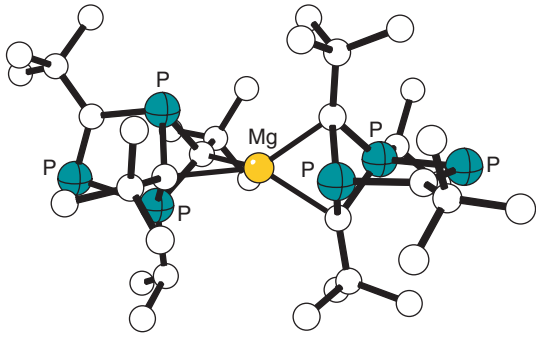

Figure 50 The structure of the magnesium–phosphorus cage compound **101**.

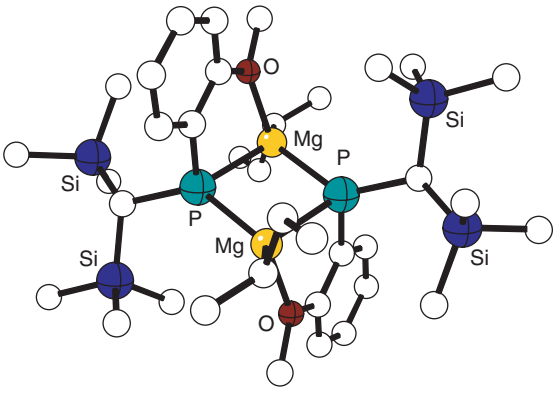

Figure 51 The structure of $[Bu^{s}Mg\{P[CH(SiMe_3)_2](C_6H_3\text{–}2\text{-}OMe\text{–}3\text{-}H)\}]_2$ **102**.

$$P{\equiv}C{-}Bu^{t} \xrightarrow[-78 \text{ to } 25\,^{\circ}C]{RMgX} \underset{R}{P{=}C}\!\!<^{Bu^{t}}_{MgX\bullet solvent} \qquad (20)$$

The reaction between either 1 or 2 equiv. of the secondary phosphine $\{(Me_3Si)_2CH\}PH(C_6H_3\text{–}2\text{-}OMe\text{–}3\text{-}R)$ (R = H, Me) and $MgBu^{n}Bu^{s}$ yields the heteroleptic complexes $[BuMg\{P[CH(SiMe_3)_2](C_6H_3\text{-}2\text{-}OMe\text{-}3\text{-}R^{1})\}]_2$ (R = H, Me). The dimers contain a central, nearly square Mg_2P_2 core (for R = H, Mg–P = 2.5760(8), 2.5978(8) Å) **102** (Figure 51). Dissolution of the complexes in THF results in degradation and formation of the tertiary phosphines $\{(Me_3Si)_2CH\}P(Me)(C_6H_3\text{–}2\text{-}OMe\text{–}3\text{-}R)$ and unidentified magnesium-containing products.[284]

2.02.3.5.3 Organomagnesium aryloxides

The use of Grignard reagents to synthesize aryloxide complexes, which are not formally organometallic species, has been mentioned above (Section 2.02.3.2.3). The heteroleptic magnesium complexes $[ArOMgBu]_2$ **103** and $[ArOMgN(Pr^{i})_2]_2$ (ArO = 2,6-di-tert-butylphenoxy) were prepared from $MgBu_2$ (Equation (21)) and are dimeric in the solid state, with tricoordinate metal centers. Interestingly, **103** uses the aryloxide anions as bridging groups (Mg–C = 2.126(3), 2.133(5); Mg–O = 1.967(1), 1.971(1) Å), whereas in the amido complex, anions connect the metals in the amide. Solution NMR spectroscopic studies of both complexes reveal that rearrangement to the homoleptic solvated bis(aryloxide) is promoted in THF-d_8, but that the main component (≥95%) still appears to be the heteroleptic species.[285]

$$2MgBu_2 + 2ArOH \xrightarrow[-2BuH]{\text{hexane}} \underset{\textbf{103}}{\overset{Ar}{\underset{Ar}{O}}\!\!<^{Bu\text{–}Mg}_{Mg\text{–}Bu}\!\!>O} \qquad (21)$$

2.02.3.6 Aluminum compounds

A review of magnesium organodiamides and mixed magnesium–aluminum bridged oligomers, with a focus on heterocumulene reactivity, is available.[286]

Reaction of $\{[(Me_3Si)_2N]_2Mg\}_2$(1,4-dioxane) with trimethylaluminum produces the dialuminum–tetramagnesium complex $[\{(R_2N)Mg(Me)\}_2\{Mg(NR_2)(NR_2AlMe_3)\}_2]$ (R = $SiMe_3$) **104** with near-linear (178.6(6)°) Mg–Me–Mg

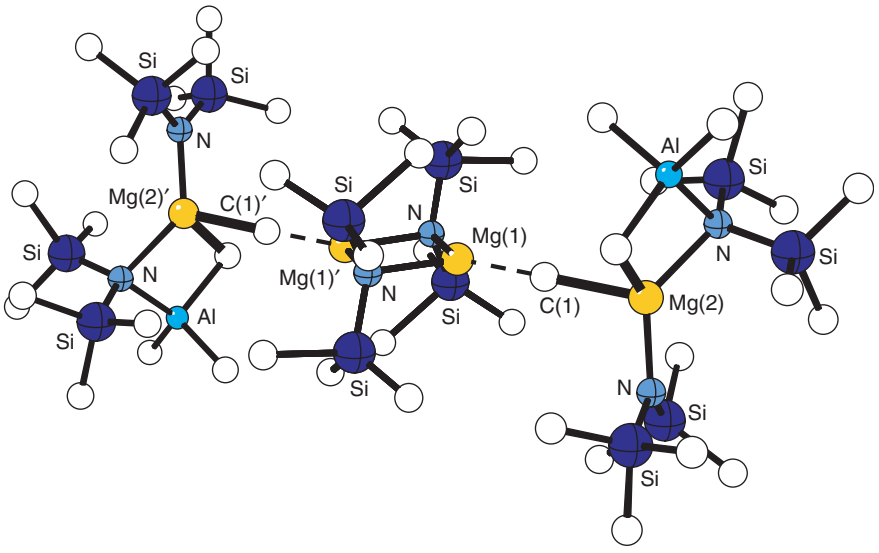

Figure 52 The structure of the centrosymmetric dialuminum–tetramagnesium complex **104**.

bridging groups (Figure 52). The Mg–C(1) distance of 2.16(1) Å is normal for a Mg–C σ-bond, but the Mg–C(2) distance of 2.43(1) Å suggests a weak interaction. Curiously, the reaction of $Mg(NPr^i_2)_2$ with $AlEt_3$ or of $Mg(NBu^i_2)_2$ with $AlMe_3$ also affords Al–Mg complexes, but that of $Mg(NPr^i_2)_2$ with $AlMe_3$ or of $Mg(NEt_2)_2$ with $AlBu^i_3$ produces only dialuminum complexes. The thermal instability of reaction intermediates may be responsible for the differences, as the heterometallic complex $\{Me_2Al(\mu\text{-}NEt_2)_2Mg(\mu\text{-}Me)\}_2$ decomposes on heating to form the dialuminum complex $[Me_2Al(\mu\text{-}NEt_2)]_2$ and possibly $\{Me_2Mg(NEt_2)\}\infty$). Insertion of O_2 into the Mg–R bond of the Al–Mg complexes results in the formation of magnesium alkoxide derivatives $[R^1{}_2Al(\mu\text{-}NR^2{}_2)_2Mg(\mu\text{-}OR^1)]_2$ ($R^1 = Me$, $R^2 = Pr^i$; $R^1 = Et$, $R^2 = Et$; $R^1 = Me$, $R^2 = Et$; $R^1 = Me$, $R^2 = Bu^i$).[287]

The nucleophilic attack of amines (Et_2NH and $Pr^i{}_2NH$) alcohols (MeOH, EtOH, and Bu^tOH) and iodine on the magnesium atoms of $[Me_2Al(\mu\text{-}NPr^i{}_2)_2MgMe]_4$ and $[Me_2Al(\mu\text{-}NEt_2)_2MgMe]_2$ has been investigated.[288] The former Mg–Al complex undergoes metathesis with the amines to give $[Me_2Al(\mu\text{-}NPr^i{}_2)_2Mg(\mu\text{-}NR_2)]_2$ ($R = Et$ **105** or Pr^i) and with iodine to give $[Me_2Al(\mu\text{-}NPr^i{}_2)_2Mg(\mu\text{-}I)]_2$. Partial degradation of the complex with the alcohols occurs only at the Mg–C bonds. The intermediate in the reaction of both Mg–Al comlexes with Bu^tOH is a mixed alkyl alkoxide, $Me_2Al(\mu\text{-}NR_2)_2Mg(\mu\text{-}Me)(\mu\text{-}OBu^t)Mg(\mu\text{-}NR_2)_2AlMe_2$.[288]

Ethynyl-bridged polynuclear aluminum–magnesium complexes, $[Me_2Al(\mu\text{-}R^1N)_2Mg(\mu\text{-}C{\equiv}CR)]_2$ ($R = C_6H_5$, C_6H_4-*p*-CH_3, Bu^t, $SiMe_3$, $R^1 = Pr^i$; $R = C_6H_5$, C_6H_4-*p*-CH_3, $R^1 = Et$), are prepared by reaction of the aluminum–magnesium tetramer $[Me_2Al(\mu\text{-}Pr^i{}_2N)_2Mg(\mu\text{-}Me)]_4$ and the dimer $[Me_2Al(\mu\text{-}Et_2N)_2Mg(\mu\text{-}Me)]_2$ with various substituted acetylenes.[289] In the ^{13}C NMR spectra of the complexes, the acetylide carbon atoms display resonances at a lower field than for the corresponding free acetylenes, suggesting that there is some π-interaction with the Mg atoms. In the solid state, however, the bridging ethynyl groups are almost perpendicular to the Mg–Mg vector (**106**, Figure 53), and there is no clear evidence for the π-interactions indicated by the NMR spectra. Subsequent reaction of the Mg–Al complexes ($R = Pr^i$, $R^1 = C_6H_5$, C_6H_4-*p*-CH_3) with CO_2 gives selective insertion products, that is, $\{Me_2Al(\mu\text{-}Pr^i{}_2N)_2Mg[\mu\text{-}OOC(C{\equiv}CR)]\}_2$ **107** ($R = C_6H_5$, C_6H_4-*p*-CH_3), in which the insertion has occurred at the Mg–C bond rather than at the Al–N center. In contrast, reaction of the dimeric $[Me_2Al(\mu\text{-}Et_2N)_2Mg(\mu\text{-}Me)]_2$ with CO_2 produces an aluminum–magnesium carbamato complex that is the result of insertion of CO_2 into the metal–N bond at the bridging amido ligands. It decomposes on sublimation to yield an aluminum-only carbamato complex. Reaction of the tetrameric $[Me_2Al(\mu\text{-}Pr^i{}_2N)_2Mg(\mu\text{-}Me)]_4$ with CO_2 produces both aluminum–magnesium and dialuminum carbamato complexes.[289]

Various isothiocyanates (RNCS; $R = Bu^t$, Ph) and CS react with exclusively with the Mg–C bonds of dinuclear Al–Mg compounds to give dinuclear insertion products (Scheme 7). In the case of the reaction of $\{Me_2Al(\mu\text{-}Et_2N)_2Mg(CH_3)\}_2$ with PhNCO, a tetranuclear insertion product is formed.[290]

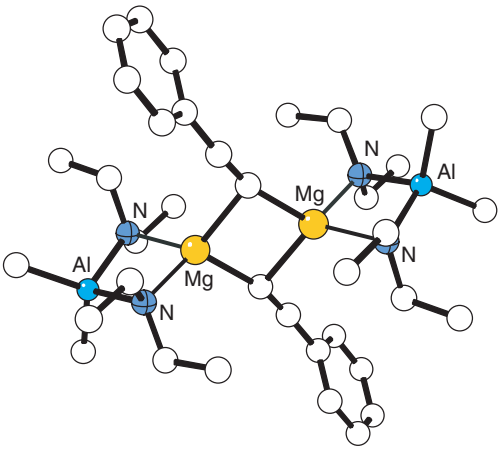

Figure 53 The structure of the ethynyl-bridged aluminum–magnesium complex $[Me_2Al(\mu\text{-EtN})_2Mg(\mu\text{-C}{\equiv}\text{CPh})]_2$ **106**.

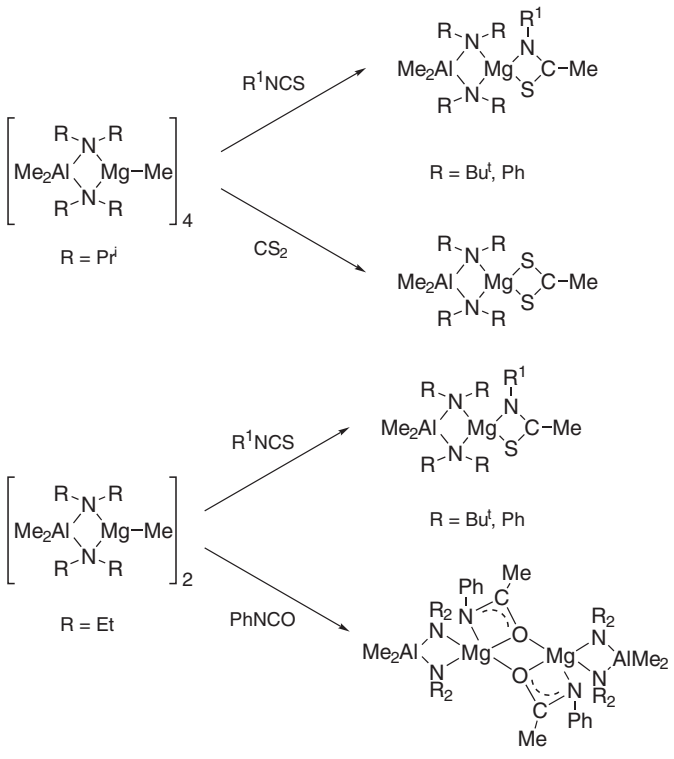

Scheme 7

2.02.4 Calcium, Strontium, and Barium

2.02.4.1 Organometal Halides

2.02.4.1.1 Aryl derivatives

Although the first report of an organometallic compound of the heavier alkaline earth metals appeared near the beginning of the twentieth century,[291] the RMX Grignard analogs of Ca, Sr, and Ba never fulfilled their promise as general-purpose synthetic reagents. More difficult to form, less thermally stable, and less selective in their reactions than their Mg counterparts, the literature data of the compounds was often contradictory, and many syntheses were irreproducible (see *Calcium, Strontium, and Barium* in COMC (1982)).

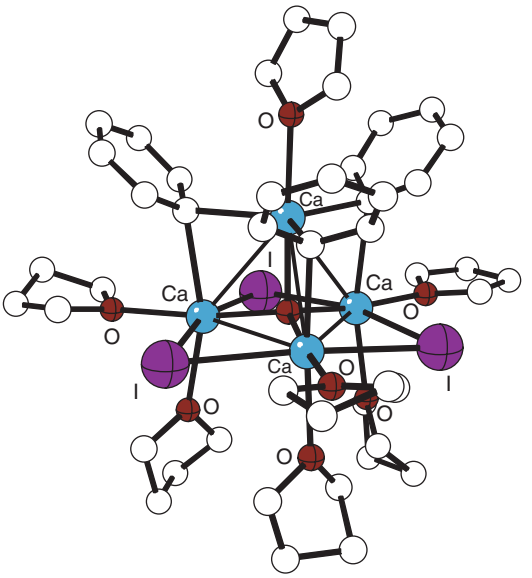

Figure 54 The structure of the tetrametallic complex $[(THF)_2CaPhI]_3{\cdot}(THF)CaO$ **107**.

A reinvestigation of the chemistry of PhCaX found that in the reaction of aryl halides with activated calcium, only iodobenzene in THF at low temperature gives good yields of $PhCaX(THF)_n$. The use of chloro- or bromobenzene generates large amounts of biphenyl from Wurtz coupling reactions, and reaction in Et_2O is much slower. Ether cleavage reactions are apparent even at −20 °C, and colorless crystals of the oxo-centered tetrametallic complex **107** (Figure 54) can be isolated from a cooled solution. The distorted Ca_4O core displays Ca–C contacts of 2.57–2.62 Å, and the average Ca–μ-I distance of 3.22 Å, longer than typical bridging lengths.[292] Reaction of activated calcium with mesityliodide, followed by a D_2O quench, resulted in deuterium incorporation into a methyl group. The mechanism may involve a 1,3-H shift and the formation of 3,5-dimethylbenzylcalcium iodide.[292]

The reaction of phenylcalcium iodide with nitrous oxide in diethyl ether was reported to yield a mixture of products presumably arising from insertion of N_2O into the phenyl–calcium bond, including azobenzene (15%), benzidene, and *N*-phenylbenzidene.[293] Subsequent examination of this reaction with various $(C_6Me_nH_{5-n})CaI$ reagents and solvent combinations[294] found that the distribution and yield of products are strongly dependent on the solvent and on the ring substitution; the yield of azobenzene, for example, rises to 61% in dimethoxyethane, but no insertion occurs with $(2,6\text{-}Me_2C_6H_3)CaI$, probably for steric reasons.

2.02.4.1.2 Monocyclopentadienyl derivatives

2.02.4.1.2.(i) Preparation

Compounds of the general form $Cp'MX(L)_n$ (M = Ca,Sr,Ba; X = a monoanionic ligand; L = optional neutral Lewis base(s)) can be derivatized by exchanging X, and the addition or removal of ligands L (ethers, amines) allows adjustment of the coordination environment. Nevertheless, persistent challenge with studying monocyclopentadienyl and other heteroleptic alkaline earth compounds is the operation of Schlenk-type equilibria (Equation (5)), which leads to the rearrangement of unsymmetrical species into their symmetrical counterparts. Examples are known of kinetically stabilized complexes in which exchange reactions are blocked.

The mono[(tetraisopropyl)cyclopentadienyl]calcium halide $(C_5Pr^i{}_4H)CaI(THF)_2$ is isolated in high yield (>90%) from the 1 : 1 reaction of $K[C_5Pr^i{}_4H]$ and CaI_2 in THF or by the redistribution of $(C_5Pr^i{}_4H)_2Ca$ and CaI_2 in THF.[295] One THF ligand in $(C_5Pr^i{}_4H)CaI(THF)_2$ is easily removed by recrystallization from toluene to generate the monosolvated derivative $(C_5Pr^i{}_4H)CaI(THF)$; allowing $K[C_5Pr^i{}_4H]$ and CaI_2 (1 : 1) to react in a toluene/THF solvent mixture produces $(C_5Pr^i{}_4H)CaI(THF)$ directly. $[(C_5Pr^i{}_4H)SrI(THF)_2]_2$ has been obtained both from SrI_2 and $Na[C_5Pr^i{}_4H]$ or by ligand redistribution between octaisopropylstrontocene and SrI_2.[296] The mono(ring) complexes $\{[C_5(Bu^t{}_3\text{-}1,2,4)H_2]BaI(THF)_2\}_\infty$ and $[(C_5Pr^i{}_4H)BaI(THF)_2]_2$ have been synthesized from BaI_2 and the corresponding sodium cyclopentadienides. The heavier metal compounds are more susceptible to loss of donor solvent and ring redistribution than their calcium counterparts.

The mono(tri-*t*-butyl) compound $[C_5(Bu^t_3\text{-}1,2,4)H_2]CaI(THF)_n$ ($n = 1, 2$) can be isolated from the 1 : 1 reaction of $K[C_5(Bu^t_3\text{-}1,2,4)H_2]$ and CaI_2 in THF.[297] The complex can be isolated from THF solution as a monomer with two THFs, or from THF/toluene as a dimer with only one THF per calcium atom. The chloro-bridged calcium complex $\{[C_5(Bu^t_3\text{-}1,2,4)H_2]CaCl(dme)\}_2$ is available from $CaCl_2$ and $Na[C_5(Bu^t_3\text{-}1,2,4)H_2]$.[296] The related mono(ring) complexes $[C_5((SiMe_3)_3\text{-}1,2,4)H_2]MI(THF)_n$ can be prepared as crystalline solids by halide-displacement reactions between $K[C_5(SiMe_3)_3\text{-}1,2,4)H_2]$ and the metal diiodides.[298]

2.02.4.1.2.(ii) Structures, properties, and reactivity

$[C_5Pr^i_4H]CaI(THF)$ crystallizes from toluene as the iodide-bridged dimer **108** with a pentahapto $(C_5Pr^i_4H)^-$ ligand and a terminal THF on each calcium atom (Figure 55).[295] The Ca–I and Ca–I′ distances are nearly equal at 3.101(4) Å and 3.110(4) Å. No rearrangement of $(C_5Pr^i_4H)CaI(THF)_{(1,2)}$ into $(C_5Pr^i_4H)_2Ca$ and $CaI_2(THF)_n$ is observed in either THF or aromatic solvents at room temperature. This stability is ascribed to the inability of THF to dissociate completely from the oxophilic calcium center in the mono(cyclopentadienyl) complexes, which consequently blocks the formation of the base-free $(C_5Pr^i_4H)_2Ca$.[299]

Under reflux, a toluene solution of $(C_5Pr^i_4H)CaI(THF)_{(1,2)}$ is converted nearly quantitatively (93%) into $(C_5Pr^i_4H)_2Ca$ and $CaI_2(THF)_n$. Redistribution is also observed after adding 1,4-dioxane to a THF solution of $(C_5Pr^i_4H)CaI(THF)_{(1,2)}$. Heating $(C_5Pr^i_4H)CaI(THF)_{(1,2)}$ at 110 °C and 10^{-6} torr for 4 h removes all coordinated THF without causing rearrangement, leaving unsolvated $\{(C_5Pr^i_4H)CaI\}_n$. In aromatic solution, $\{(C_5Pr^i_4H)CaI\}_n$ slowly redistributes into $(C_5Pr^i_4H)_2Ca$ and CaI_2; coordinated THF is evidently important to the stability of $(C_5Pr^i_4H)CaI(THF)_{(1,2)}$. Heating solid $\{(C_5Pr^i_4H)CaI\}_n$ at 215–220 °C and 10^{-6} torr produces $(C_5Pr^i_4H)_2Ca$ as a white sublimate.[295]

The calcium and strontium iodide complexes $\{[C_5((SiMe_3)_3\text{-}1,2,4)H_2]M(\mu\text{-}I)(THF)_n\}_2$ ($n = 1$ for M = Ca; $n = 2$ for M = Sr) are dimers with bridging iodide ligands,[298] as are the $(C_5Pr^i_4H)$ analogs with strontium and barium.[296] The organobarium complex $\{[C_5((SiMe_3)_3\text{-}1,2,4)H_2]BaI(THF)_2\}_\infty$ **109** crystallizes from THF/toluene as a coordination polymer with both linear and near-linear (177.8°) Ba–I–Ba′ links in a zigzag arrangement **Ba1** (Figure 56).[298] The polymeric structure of the mono(ring) complex $[C_5(Bu^t_3\text{-}1,2,4)H_2]BaI(THF)_2$ is similar to that of **109**.[296]

The cationic complex $[(C_5Me_5)Ca(OPPh_3)_3]^+I^-$ **110** is obtained by the displacement of an iodide from $(C_5Me_5)CaI(THF)_2$ with triphenylphosphine oxide.[300] The latter's ability to substitute for I^- and THF but not $(C_5Me_5)^-$ on calcium follows the approximate pK_b of the bases (i.e., −12 ($[C_5Me_5]^-$) ~8 ($OPPh_3$) < ~12 (THF) < ~24 (I^-)). The piano-stool geometry of **110** (Figure 57) is coupled with a longer than average Ca–C distance of 2.684(4) Å.[24] DFT calculations on the model compound $[(C_5H_5)Ca(OPMe_3)_3]^+$ indicate that the increased Ca–C distance reflects the strong electron donor properties of the $OPPh_3$ ligands.

2.02.4.1.2.(iii) Heterocyclic mono(ring) complexes

Various organometallic complexes containing heterocyclic group 15 rings are known. These are often formed in complex reactions. For example, a mixture of the phosphacyclopentadienes **111** and **112** reacts slowly with distilled calcium metal to yield the tetranuclear **113** (Figure 58).[301] The centrosymmetric Ca_2Cl_2 core is nearly square, with

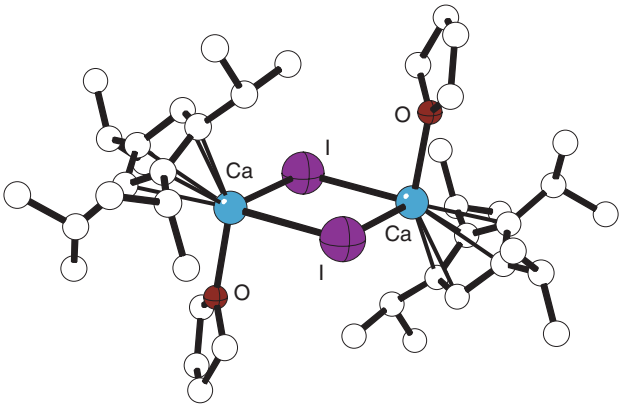

Figure 55 The structure of the iodide-bridged dimer $\{[C_5Pr^i_4H]CaI(THF)\}_2$ **108**.

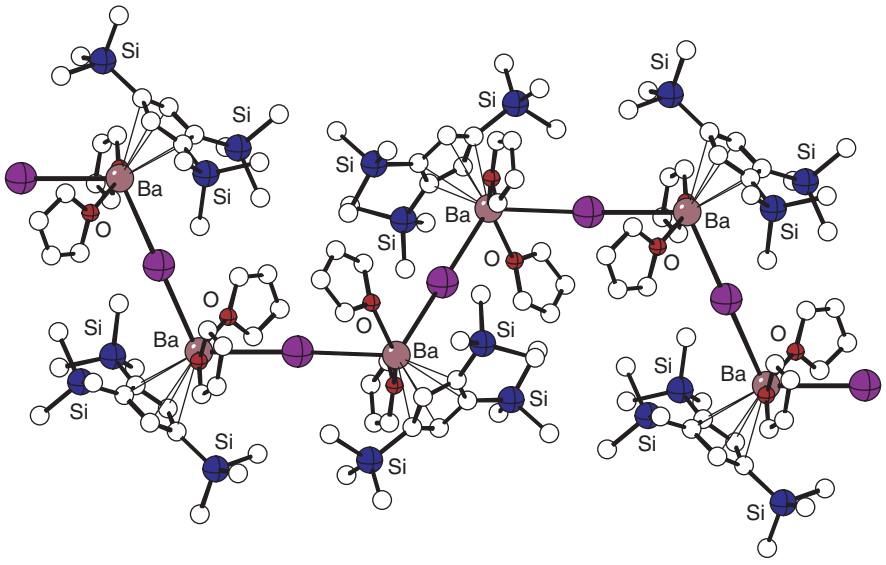

Figure 56 The structure of the polymeric organobarium complex $\{[C_5((SiMe_3)_3\text{-}1,2,4)H_2]BaI(THF)_2\}_\infty$ **109**.

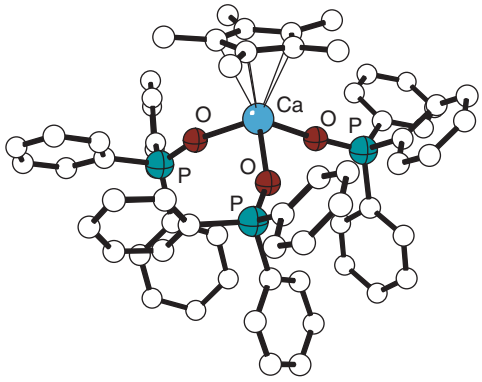

Figure 57 The structure of the cationic complex $[(C_5Me_5)Ca(OPPh_3)_3]^+ I^-$ **110**.

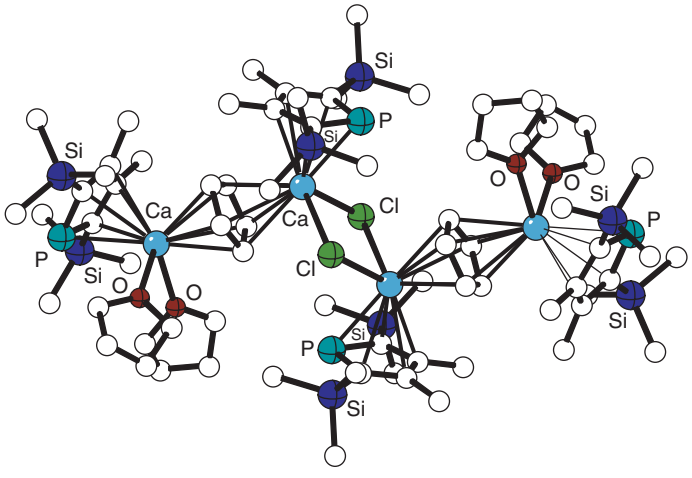

Figure 58 The structure of the tetranuclear complex **113**.

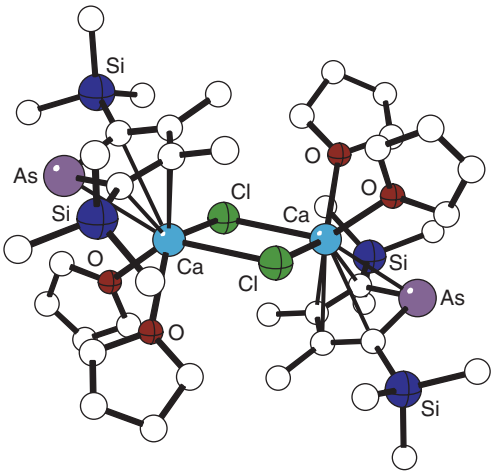

Figure 59 The structure of the dimeric arsolide complex $\{(\eta^5\text{-}AsC_4(2,5\text{-}SiMe_3)_2(3,4\text{-}Me)_2)Ca(\mu\text{-}Cl)(THF)_2\}_2$ **114**.

Ca–Cl distances of 2.826(5) and 2.813(6) Å. Ca–phospholide distances range from Ca1–P at 2.933(2) Å and Ca2–P at 2.912(2) Å, to an average of 2.805 Å for Ca1–C and 2.845 Å for Ca2–C.

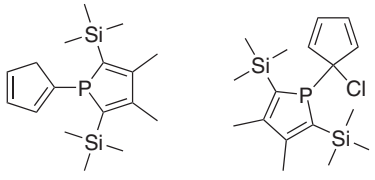

111 **112**

Reduction of the arsole $ClAsC_4(2,5\text{-}SiMe_3)_2(3,4\text{-}Me)_2$ with distilled calcium metal produces the dimeric **114** (Figure 59).[301] The centrosymmetric Ca_2Cl_2 core has nearly equal Ca–Cl distances of 2.714(1) and 2.724(1) Å, and a Cl–Ca–Cl′ angle of 79.25(3)°. The Ca–arsolide distances range from Ca–As of 3.0737(8) Å, to 2.832(3) and 2.903(4) Å for the trimethylsilyl-substituted carbons, to 2.770(3) and 2.817(3) Å for the methyl-substituted carbons. In a reaction paralleled with magnesium (see Section 2.02.3.3.2.(ii)), the reduction of octaethyldiphospholyl, -diarsolyl, and -distibolyl with Ca in the presence of $CaCl_2$ generates $[Ca(\mu\text{-}Cl)(\eta^5\text{-}C_4Et_4E)(THF)_2]_2$ (E = P, As, or Sb); no reaction is observed without the dichloride.[260]

2.02.4.2 Diorganylmetal Compounds

The use of sterically bulky ligands to provide kinetic stability to compounds of the heavier group 2 elements has become widely practiced, and has facilitated the synthesis of diorganyl complexes of various types. Advances in the organometallic chemistry of σ-bonded compounds of calcium, strontium, and barium have been reviewed.[302]

2.02.4.2.1 Dialkyl and diaryl metal compounds

A general review that contains material on *s*-block compounds containing the tris(trimethylsilyl)methyl groups is available.[154] Bis(tris(trimethylsilyl)methyl)calcium, $[C(SiMe_3)_3]_2Ca$ **115**, is made from the reaction of $K[C(SiMe_3)_3]$ and CaI_2 in benzene and crystallizes from a heptane/benzene solution.[303] In the solid state, **115** is bent, with Ca–C = 2.459(9) Å and C–Ca–C = 149.7(7)°, and displays several close intramolecular contacts that could influence the bending angle (e.g., Ca···C(Me) distances of ca. 3.0 Å with Ca···H distances of 2.5 Å). It reacts with ethers ROEt to produce RH, ethylene, and $Ca(OEt)_2$, behavior that adds to the doubt about claims in the earlier literature that sigma-bonded heavy alkaline earth alkyl species were synthesized using ethers as solvents.

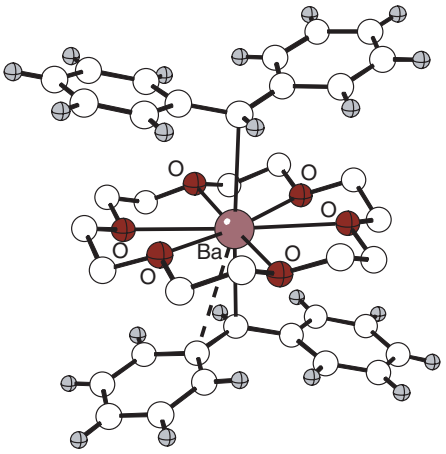

Figure 60 The structure of the crown ether complex of barium diphenylmethanide **116** (the dashed line is to a contact at 3.39 Å).

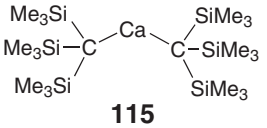

115

The reaction of diphenylmethane with dibenzylbarium in THF, or barium *t*-butoxide with trimethylsilyldiphenylmethane, $Ph_2CH(SiMe_3)$, in the presence of Bu^nLi forms barium diphenylmethanide by hydrocarbon elimination and desilylation mechanisms, respectively.[304] Crystallized in the form of its 18-crown-6 ether derivative **116** (Figure 60), the complex displays direct Ba–C bonds of 3.065(3) and 3.097(3) Å, and a longer contact at 3.39 Å.

Metathesis between either SrI_2 or BaI_2 and 2 equiv. of $K[(Me_3Si)_2(MeOMe_2Si)C]$ in THF yields the dialkyls $\{(Me_3Si)_2(MeOMe_2Si)C\}_2M(L)$ (M(L) = Sr(THF) **117**, Ba(dme) **118**).[305] The metals are bonded to the ligand C and O atoms in four-membered chelate rings, with Sr–C = 2.786(3) and 2.849(3) Å, and Ba–C = 3.049(2) and 3.0363(18) Å. The geometry around barium in **118** is a distorted trigonal antiprism.

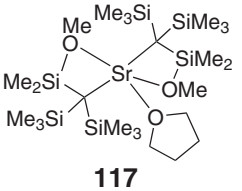

117

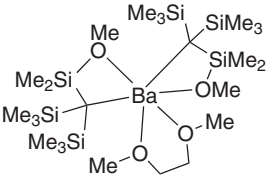

118

Lithiation of the multidentate *O*-substituted phosphine 2-$MeOC_6H_4CH(P(tolyl\text{-}p)_2)$ with $LiBu^n$ produces the dimeric salt **119**.[306] Transmetallation of **119** with $NaOBu^t$ in ether generates the sodium derivative, which reacts with CaI_2 in ether to produce the sodium trialkyl calcate $[Na(OEt_2)][Ca(MeOC_6H_4CH(P(tolyl\text{-}p)_2)_3]$ **120**. Containing a formally six-coordinate Ca^{2+} center (Ca–C = 2.55 Å), **120** displays agostic Ca···H contacts (2.41 Å av.); the sodium ion bridges the phosphorus atoms (Na–P = 2.885 Å) (Figure 61).

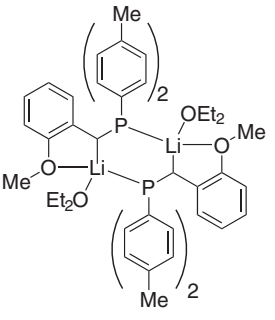

119

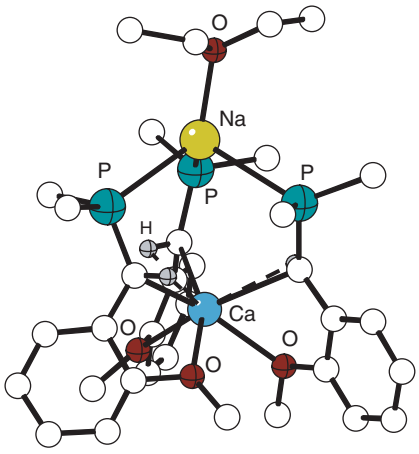

Figure 61 The structure of the trialkyl calcate $[Na(OEt_2)][Ca(MeOC_6H_4CH(P(tolyl\text{-}p)_2)_3]$ **120**, with only C_{ipso} atoms of the *p*-tolyl groups displayed.

2.02.4.2.2 Dibenzyl, dialkynyl, and dialkenyl metal compounds

Sigma-bonded structures. A variety of benzyl complexes containing calcium, strontium, or barium is now known. The bis(benzyl) complexes of calcium and strontium are synthesized by transmetallation of the appropriate potassium salts with CaI_2[307–311] or SrI_2,[312] respectively; a barium derivative forms from $LiCH_2Ph{\cdot}tmen$ with $Ba[N(SiMe_3)_2]_2(THF)_2$ or $Ba[O(Mes^*)]_2$.[313] As expected, the complexes are quite basic: dibenzylcalcium will deprotonate triphenylmethane ($pK_a = 31.5$), leading to the solvent-separated ion pair $[Ph_3C^-]_2[Ca^{2+}(THF)_6]$,[307] and dibenzylbarium reacts with diphenylmethane ($pK_a = 33.5$) in THF to yield bis(diphenylmethyl)barium in 90% yield and with 1,1-diphenylethene in THF to form bis(1,1,3-triphenylpropyl)barium in near-quantitative yield.[313] The latter is soluble in hydrocarbon solvents, while dibenzylbarium and bis(diphenylmethyl)barium are soluble only in THF.

The calculated energy differences between *cis*- and *trans*-geometries of $(p\text{-Bu}^tBz)_2Ca(THF)_4$ **121** (Figure 62), $(p\text{-}Me_3SiBz)_2Ca(THF)_4$, and $(Bz)_2Ca(THF)_4$ are very small ($<2\,kcal\,mol^{-1}$), and crystal-packing effects are likely responsible for the different geometries observed in the solid state.[307]

A derivative of $[(Me_3Si)_2CPh]_2Ca(THF)_2$ in which one $SiMe_3$ group was replaced by hydrogen and an NMe_2 group was introduced at the 2-position on the ring (bis(2-Me_2N-α-$SiMe_3$-benzyl)calcium·$(THF)_2$ **122** (Figure 63)) is an initiator for the living, although primarily atactic, polymerization of styrene.[309] The related strontium complex is more active.[312]

In α-methyl–benzylcalcium and α-Me_3Si–benzylcalcium complexes, energy barriers for inversion of the chiral benzylic carbon (17–19 kcal mol^{-1}) are concentration independent, suggesting that a dissociative mechanism is involved that involves Ca–C_α bond breakage. The α-methyl–benzylcalcium compounds are less stable and show a

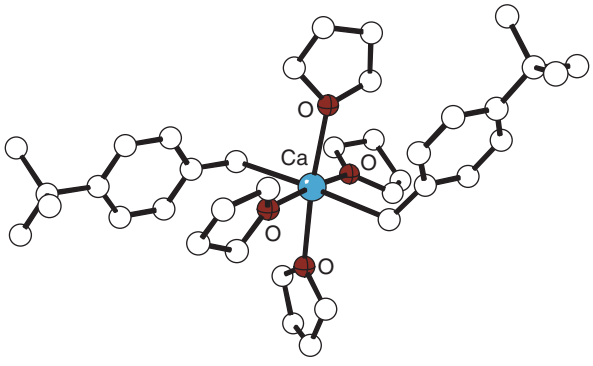

Figure 62 The structure of the benzyl complex *trans*-$[(p\text{-Bu}^tBz)_2Ca(THF)_4]$ **121**.

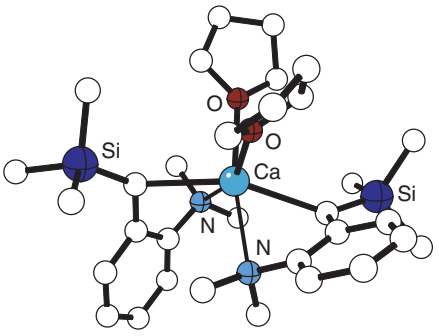

Figure 63 The structure of bis(2-Me_2N-α-$SiMe_3$-benzyl)calcium·$(THF)_2$ **122**.

higher reactivity and faster initiation of styrene polymerization than the analogous α-Me_3Si–benzylcalcium complexes. Even so, the initiation step in styrene polymerization is still slower than chain propagation.[310]

Reaction of the α-methylated alkylated benzylcalcium polymerization initiator **123** with 9-$Si(SiMe_3)_3$–fluorene generated **125**, presumably via the intermediate of **124**, which undergoes an intramolecular C–H activation (or cyclometallation).[310] Steric shielding of the $SiCH_2^-$ site may be reason that **125** is not active as a styrene polymerization initiator.[310] The THF-free dimeric benzylcalcium complex **126** initiates the living polymerization of styrene. Polymers enriched in syndiotactic sequences are obtained (ca. 85% *r*-diads). An insertion step that proceeds with a high degree of syndiotactic selectivity and an inversion mechanism that racemizes the chiral chain ends may be involved. Excess THF increases the rates of inversion of the chiral carbanionic chain ends, destroying the stereoregularity in the polymer chain.[311]

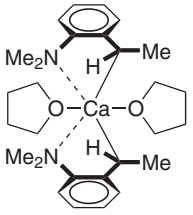

123

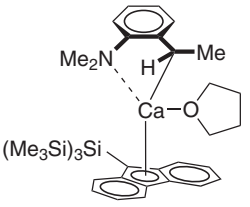

124

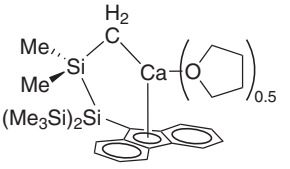

125

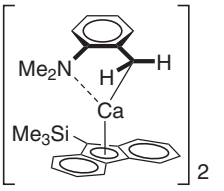

126

An attempt was made to improve the syndioselectivity of the benzylcalcium complex **127** by replacing the fluorenyl ligand with the nacnac ligand (dippNC(Me)CHC(Me)Ndipp) (Scheme 8). Although NMR evidence indicated the presence of **129**, **127**, and **128** in the mixture, **129** could not be isolated, and the deprotonation of a methyl group in the backbone of the nacnac ligand by the benzyl anion generates dimeric **130**.[314]

A comparison of the crystal structures, NMR and IR spectra of various Yb(II) and calcium complexes demonstrated that they were strikingly similar, a reflection of the nearly identical radii of Yb^{2+} and Ca^{2+}.[25] Nevertheless, the dibenzylytterbium(II) analog of **127** produces polystyrene of high syndiotacticity ($r = 94.9\%$, $rr = 90.0\%$), whereas **127** itself yields only atactic or slightly syndiotactic polymer. A difference in Yb–L and Ca–L bond strengths, despite their similar lengths, has been proposed as the source of the difference.[315]

The reaction of the amido complexes $M[N(SiMe_3)_2]_2$ (M = Ca, Sr, Ba) with triphenylsilylethyne in the presence of 18-crown-6 leads to the formation of the bis(acetylide) compounds $M(C{\equiv}CSiPh_3)_2$(18-crown-6).[316] The compounds are monomers, with terminal acetylides (Ca–C = 2.523(7), 2.558(7) Å; Sr–C = 2.692(4), 2.723(4) Å; Ba–C = 2.852(3), 2.853(2) Å). All three compounds display bent C–M–C′ and M–C≡C angles. The C–M–C′ angles slightly decrease with increasing size of the metal (168.7(2)° (Ca); 166.0(1)° (Sr); 162.7(1)° Ba). The M–C≡C angles change more dramatically, from near 160° for M = Ca and Sr, to 126.6(3)° and 141.3(3)° in the barium compound **131** (Figure 64).

The reaction of $Ba[P(SiMe_3)_2]_2(THF)_2$ with diphenylbutadiyne in toluene for 12 days induces a *cis*-addition of the diyne to the phosphide, followed by a 1,3-silyl group shift and ring closure. The dinuclear complex **132** is then isolated in good yield.[283] Its complex structure contains Ba–C σ bonds (2.881(5), 2.899(5) Å), side-on Ba–alkyne (3.003(6), 3.363(6) Å) and arene interactions, and Ba–phospholide bonds (Ba–P = 3.487(2) Å) (Figure 65).

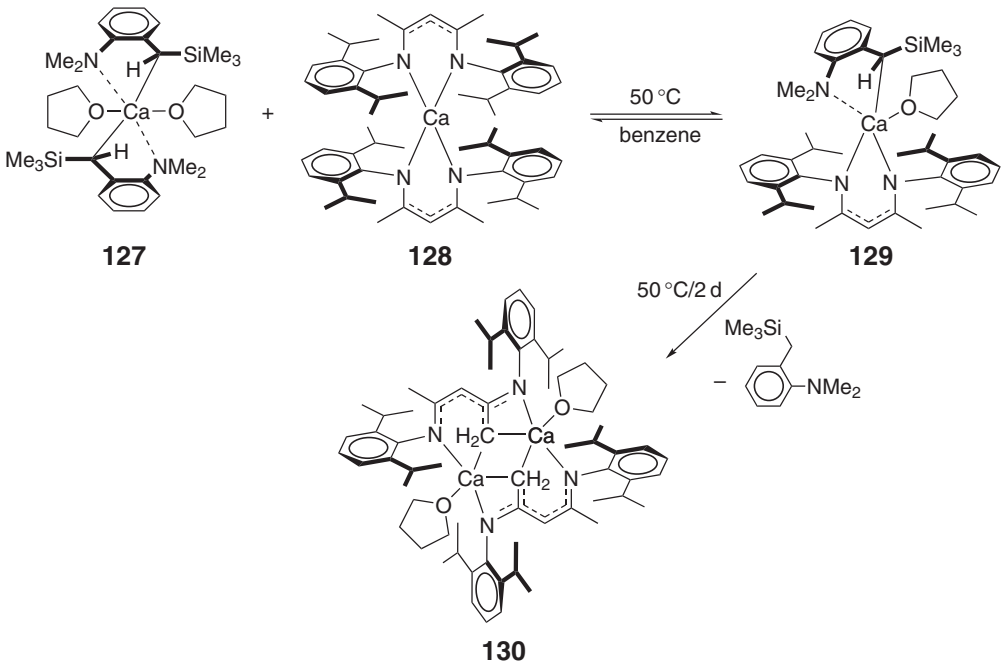

127 **128** **129** **130**

Scheme 8

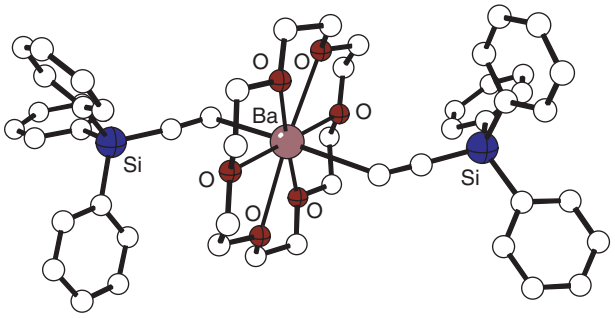

Figure 64 The structure of the barium acetylide complex M(C≡CSiPh$_3$)$_2$(18-crown-6) **131**.

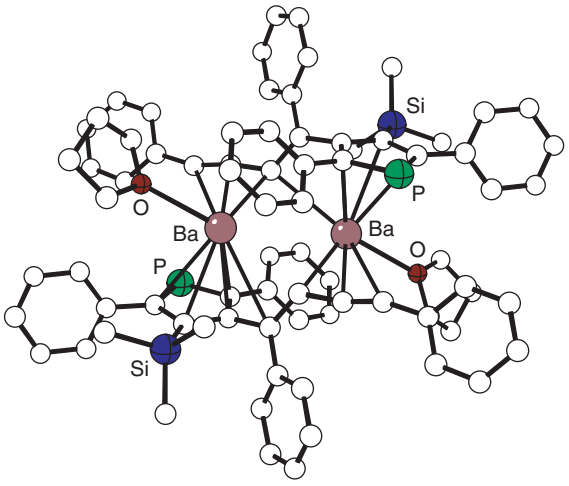

Figure 65 The structure of the barium phospholide complex **132**.

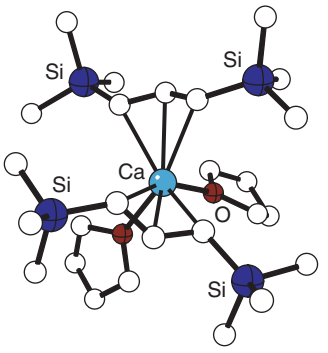

Figure 66 The structure of allyl complex $[C_3(SiMe_3)_2H_3]_2Ca(THF)_2$ **133**.

Pi-bonded structures. Reaction of slightly more than 2 equiv. of $K[C_3(SiMe_3)_2H_3]$ with CaI_2 in THF produces the colorless bis(allyl) complex $[C_3(SiMe_3)_2H_3]_2Ca(THF)_2$ **133** in high yield.[317] The ^1H NMR spectrum of the complex is invariant from room temperature to 172(2) K, suggesting that the molecule is either non-fluxional or the rearrangements are of low energy. The complex crystallizes with two η^3-allyl ligands in an *anti*-configuration (av. Ca–C = 2.654(5) Å) (Figure 66).

Solutions containing allylbarium compounds are highly regio- and stereospecific allylation agents for carbonyl compounds.[318,319] Stereochemically homogeneous (*E*)- and (*Z*)-β,γ-unsaturated carboxylic acids are prepared in good yields by highly α-selective carboxylation of allylic barium reagents with carbon dioxide (Scheme 9). It is possible that the long Ba–C bonds in the allylbarium reagents prevent the generation of six-membered cyclic transition structures that could react at the γ-carbons. Selective 1,4-michael addition reactions with α,β-unsaturated cycloalkanones are also achieved using allylbarium reagents (Equation (22)).

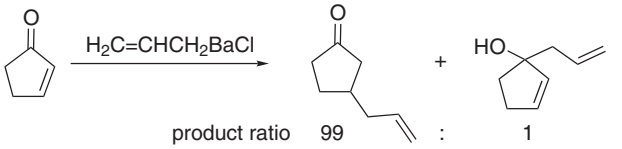

(22)

Regioselective coupling of allylbarium species with epoxides also displays high α selectivity (Equation (23)),[320] and allylbarium reagents cross-couple to allylic alcohol derivatives using bis(2,2,2-trifluoroethyl)phosphate as a leaving group to yield 1,5-dienes with high α,α'-selectivity.[321] Under similar conditions, Grignard reagents produce $\alpha:\gamma$ coupled products.

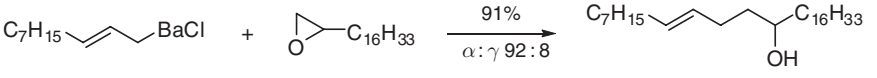

(23)

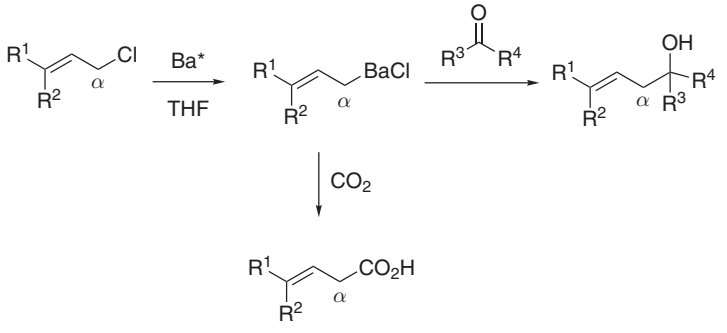

Scheme 9

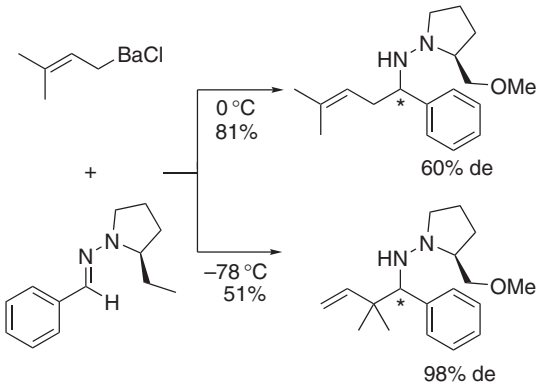

Scheme 10

An unusual temperature dependence on the regioselective behavior of an allylbarium species has been demonstrated in asymmetric allylation with the optically active imine SAMP-hydrazone [SAMP = (*S*)-(−)-1-amino-2-methoxymethylpyrrolidine] (Scheme 10).[322] Its reaction with prenylbarium chloride at 0 °C produced an α-allylated hydrazine in 60% diastereotopic excess, but at −78 °C, the γ-adduct was generated with 98% diastereotopic excess. The temperature dependence of the α/γ ratio may reflect competition between a kinetically favored γ-adduct at low temperature and a thermodynamically preferred α-form at higher temperatures.

The structurally characterized pentadienyl complex $(C_5Bu^t{}_2H_5)_2Ca(THF)$ **134** is prepared from $K[C_5(Bu^t)_2H_5]$ and CaI_2 in THF. It crystallizes with two planar η^5-pentadienyl ligands (Ca–C distances range from 2.74(1)–2.81(2) Å) and a coordinated THF molecule (Figure 67).[323] The pentahapto coordination of the dienyl ligands distinguishes this open calcocene from other structurally characterized main- group pentadienyl complexes, which have σ-bonded, monohapto ligands.[324]

Although the calcium derivative of 1,4-diphenyl-1,3-butadiene is believed to be oligomeric, the addition of two methyl groups causes the deep red 2,3-dimethyl-1,4-diphenyl-1,3-butadiene complex to be monomeric.[325] The structures of the calcium- and strontium-butadienyl complexes are intermediate between those of "face-on" η^4-dienes and "side-on" (η^2-coordinated) metallacyclo-3-pentenes. In the strontium complex **135** (Figure 68), the Sr is coordinated in a distorted octahedral environment by four THF molecules and the butadiene moiety. The Sr–C bond distances range from 2.73(2) to 2.95(2) Å in one of the two crystallographically independent molecules. The two phenyl rings bend toward the metal, leading to Sr···C(phenyl) contacts as close as 3.16 Å these probably represent weak σ-type interactions.

Miscellaneous compounds. Metallation of 2-pyridylphenylmethane and barium in liquid ammonia in the presence of diglyme and THF affords the red $Ba[\eta^5\text{-}PhCH(C_5H_4N\text{-}2)]_2(diglyme)(THF)$ **136**.[326] The barium is coordinated by two 2-pyridylphenylmethyl groups in an η^5-manner, the trihapto diglyme ligand, and a THF molecule (Figure 69).

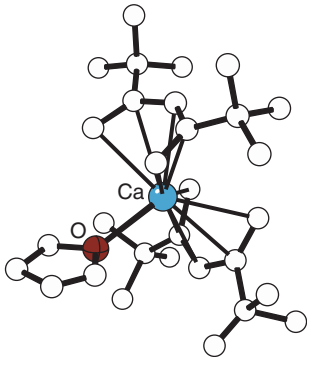

Figure 67 The structure of the pentadienyl complex $(C_5Bu^t{}_2H_5)_2Ca(THF)$ **134**.

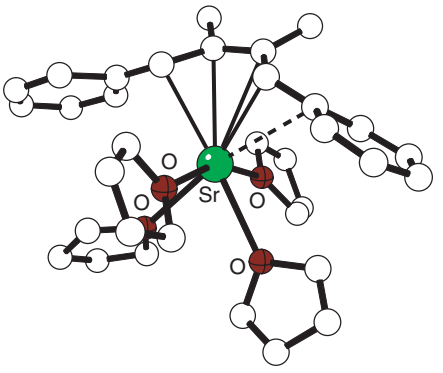

Figure 68 The structure of the butadiene strontium complex **135**.

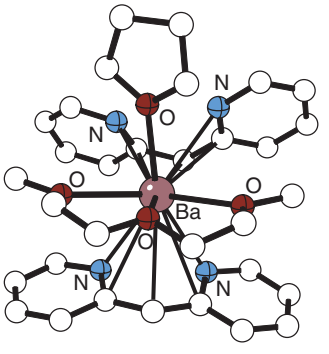

Figure 69 The structure of the barium complex [η^5-PhCH(C_5H_4N-2)]$_2$Ba(diglyme)(THF) **136**.

Within each anionic ligand, the Ba–C/N distances are the shortest (2.983(6), 3.156(6) Å), followed by the central *ipso*-carbons (3.146(7), 3.138(7) Å), and then the intermediate carbons (3.245(6), 3.223(7); 3.215(6), 3.303(6) Å).

The phosphonium bromide [Ph_2P(4-Me$C_6H_5CH_2$)$_2$]Br is deprotonated with KN($SiMe_3$)$_2$ in THF to form the corresponding neutral ylide, Ph_2P(4-MeC_6H_5CH)(4-Me$C_6H_5CH_2$). The latter reacts with the amido complex Ba[N($SiMe_3$)$_2$]$_2$ in THF to yield the orange Ba[Ph_2P(4-MeC_6H_5CH)]$_2$ **137**.[327] The barium center is coordinated by four benzyl ligands, each in a roughly η^3-fashion (Figure 70); the carbon atoms adjacent to the ylidic carbons have the shortest contacts (2.981(6)–3.031(6) Å), but the barium–ylidic carbon distances that are considered bonding range from 3.106(7) to 3.454(6) Å. Rotation of the benzylide rings and possible disruption of the Ba–ylide interaction occurs in solution.

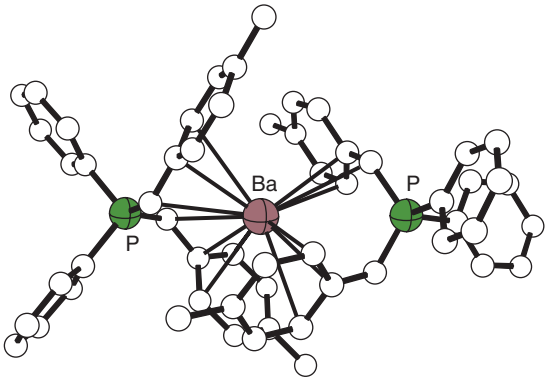

Figure 70 The structure of the barium complex Ba[Ph_2P(4-MeC_6H_5CH)]$_2$ **137**.

2.02.4.2.2.(i) Metallocenes and related compounds

(i) *Complexes with unsubstituted cyclopentadienyl rings*. The structure of unsolvated Cp_2Ca was described in 1974,[328] but attempts to crystallize the strontium and barium analogs for characterization with X-ray crystallography were frustrated by their insolubility in common solvents. Reaction of C_5H_6 with $Ba[N(SiMe_3)_2]_2{\cdot}(THF)_2$ gives Cp_2Ba, which can be recrystallized from DMSO to give $Cp_2Ba{\cdot}DMSO$ **138**. The latter forms an extended structure with four Cp^- Ba groups surrounding the central Ba^{2+} ion (Ba–C = 3.138(6)–3.164(5) Å) (Figure 71). Reaction of Cp_2Ba with 18-crown-6 affords monomeric Cp_2Ba(18-crown-6) **139** with two axial Cp^- rings (Ba–C = 3.180(6)–3.257(7) Å (Figure 72).[329]

The organobarate complex, $[Cp_3Ba]^-$ **140**, is formed in the reaction of Cp_2Ba with a free Cp^- anion generated *in situ* from NaCp in refluxing THF/pyridine (Equation (24)).[330] The same product is obtained from the reaction of 3 equiv. of Cp_2Ba with $[Bu^n{}_4P]^+Cl^-$, and consists of a linear coordination polymer of Cp^- anions tetrahedrally surrounding each barium cation (Figure 73). All Cp rings are bound η^5 to the Ba and the Ba–Cp distances are surprisingly similar for both the terminal (3.047(7)–3.184(6) Å) and bridging ligands (3.123(7)–3.220(7) Å).

$$NaCp + [Bu^n{}_4P]^+Cl^- + Cp_2Ba \longrightarrow [Bu^n{}_4P]^+[Cp_3Ba]^- + NaCl \qquad (24)$$

Metallocenes with substituted cyclopentadienyl rings. Metallocenes with methylated rings were among the first heavy alkaline earth metallocenes to be structurally characterized, but many other substituents have been incorporated into bis(cyclopentadienyl) complexes. Under this classification are included compounds with indenyl ligands, which in

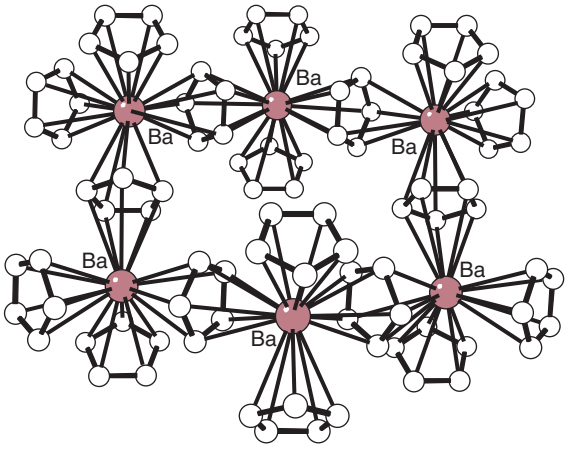

Figure 71 The structure of the polymeric complex $Cp_2Ba{\cdot}DMSO$ **138**.

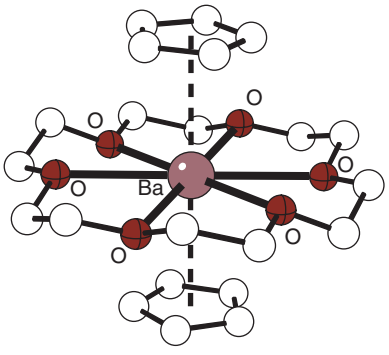

Figure 72 The structure of the monomeric Cp_2Ba(18-crown-6) **139**.

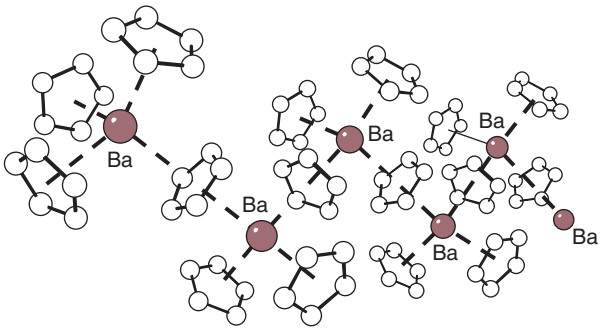

Figure 73 Portion of the coordination polymer of the non-hydrogen atoms of $[Bu^n{}_4P]^+$ $[Cp_3Ba]^-$ **140**.

group 2 compounds function as benzo-Cp groups, without the slippage that is observed in many transition metal complexes. The metal sources can take a variety of forms, including the elements themselves (as metal vapor,[331,332] in the form of finely divided powders,[333,334] or dissolved in liquid ammonia[235]), the metal hydrides,[335] metal alkyls,[235] the anhydrous metal halides, and the toluene-soluble bis(trimethylsilyl)amides, $M[N(SiMe_3)_2]_2(THF)_n$ (M = Ca, Sr, Ba).[336] The latter are useful in preparing base-free metallocenes, as the bulky hexamethyldisilazane byproduct does not bind to the metallocenes.[337] A representative selection of metallocenes is given in Table 5; more comprehensive compilations are available.[4,35]

Fulvenes or analogs have been used as precursors to bis(cyclopentadienyl) complexes, both unbriged and *ansa*-bridged; some of latter are chiral. The reaction of $Ca[N(SiMe_3)_2]_2(THF)_2$ with 6-alkyl-6-methylfulvenes (R = Me, Bu^i) or 6-methyl-6-phenylfulvene yields the corresponding calcocenes $[C_5(RC{=}CH_2)H_4]_2Ca{\cdot}(THF)_2$ (R = Me, Ph **141**, Bu^i).[338] Similar compounds are formed from $M[N(SiMe_3)_2]_2(THF)_2$ (M = Sr, Ba) and 6-methyl-6-phenylfulvene.[339] The reaction of $Sr[N(SiMe_3)_2]_2(THF)_2$ with equimolar amounts of 6-methyl-6-phenylfulvene and acetophenone leads to the formation of the bimetallic complex **142**, which contains a planar $(SrO)_2$ ring (Figure 74).[339]

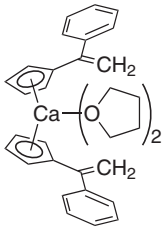

141

Photolysis of 1,1′-dicyclopentellylcalcocene **143**, which is formed in the reaction between cyclopentylidenefulvene and activated calcium, leads to [2+2]-cyclization of the cyclopentenyl substituents to form **144** (Equation (25)).[340]

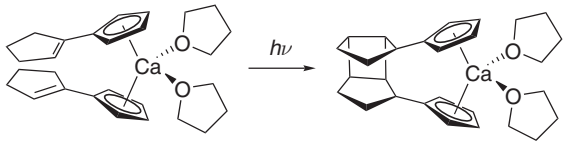

143 **144** (25)

Substituents on fulvenes affect whether bridged or unbridged calcocenes are formed preferentially.[340] Hydrogen atom or proton transfer between dialkyl fulvenes and their radical anions is responsible for the formation of unbridged calcocenes. The tendency to form unbridged calcocenes instead of *ansa*-calcocenes is higher for 6,6-diethylfulvene and 6-cyclopentylidenefulvene than for 6,6-dimethylfulvene. Reductive coupling of several 6-R-fulvenes (R = Bu^t, phenyl, mesityl, 3,5-$Bu^t{}_2$phenyl, 1-naphthyl) with $HgCl_2$-activated calcium has demonstrated that increasing the steric bulk of the 6-substituent does not enhance selectivity for the *rac ansa*-calcocene product over the

Table 5 Metallocenes of calcium, strontium, and barium and their Lewis base adducts

Compound	*NMR*	*M–C(centroid)*[c] (Å)	*References*
$[C_5(1,2,4\text{-}Pr^i)_3H_2]_2Ca(X)$, $[C_5(1,2,4\text{-}Pr^i)_3H_2]_2Ca\cdot THF$	^1H, ^{13}C	2.33	354,355
$[C_5(1,2,4\text{-}Bu^t)_3H_2]_2Ca(X)$	^1H, ^{13}C	2.35	238
$[C_5(1,2,4\text{-}(SiMe_3)_3)H_2]_2Ca(X)$	^1H, ^{13}C	2.35	56
$(C_5Me_5)_2Ca(Me\text{–}carbene)$[a](X)	^1H, ^{13}C	2.38	234
$[(S)\text{-}\eta^5\text{:}\eta^1\text{-}C_5(CH_2CH(Me)OMe)H_4]_2Ca(X)$, $[(S)\text{-}\eta^5\text{:}\eta^1\text{-}C_5(CH_2(Ph)CH_2NMe_2)H_4]_2Ca(X)$	^1H, ^{13}C	2.38, 2.40	345
$[C_5H_4(CH_2CH_2NMe_2)]_2Ca$, $[C_5H_4(CH_2CH_2OMe)]_2Ca(X)$	^1H, ^{13}C	(2.39, 2.40)	344,356
$(C_5Me_4H)_2Ca(NH_3)_2(X)$, $(C_5Me_4H)_2Ca(NH_3)(THF)$, $(C_5Me_4H)_2Ca(THF)$	^1H, ^{13}C	2.44	235
$(C_9H_7)_2Ca(THF)_2(X)$	^1H	2.45	357
$[C_9(1,3\text{-}Pr^i_2)H_5]_2Ca(THF)(X)$	^1H, ^{13}C	2.41	357
$(C_5Me_4Pr^i)_2Ca(THF)(X)$	^1H, ^{13}C	2.40	235
$(C_5Me_4H)_2Ca(Pr^i\text{–carbene})(X)$	^1H, ^{13}C	(2.45, 2.43)	235
$(C_5Me_4Pr^i)_2Ca(Pr^i\text{–carbene})(X)$	^1H, ^{13}C	2.43, 2.44 (mol. 1) 2.43, 2.43 (mol. 2)	235
$(C_5Me_5)_2Sr(Me\text{–carbene})$[a], $(C_5Me_5)_2Sr(Me\text{–carbene})_2$[a](X)	^1H, ^{13}C	(2.66, 2.67)	234
$(C_5Me_5)_2Sr(Pr^i\text{–carbene})$[b](X)	^1H, ^{13}C	(2.58, 2.59)	235
$[C_5(1,2,4\text{-}(SiMe_3)_3)H_2]_2Sr$	^1H, ^{13}C	2.54	56
$\{C_5[CH_2CMe_2(2\text{-}C_5H_4N)]H_4\}_2Sr(X)$, $[C_5(CH_2CH_2OMe)H_4]_2Sr$	^1H, ^{13}C	2.58	344
$[C_5(1,2,4\text{-}Pr^i)_3H_2]_2Sr(THF)(X)$	^1H, ^{13}C	2.57	358
$[C_5(1,2,4\text{-}Bu^t)_3H_2]_2Sr$, $[C_5(1,2,4\text{-}Bu^t)_3H_2]_2Sr(THF)(X)$	^1H, ^{13}C	2.61	238
$[(C_9H_7)_2Sr(THF)]_\infty(X)$, $[(1,3\text{-}Pr^i_2)C_9H_5]_2Sr(THF)_2$	^1H, ^{13}C	2.69 (terminal) 2.84 (bridging)	357
$(C_5Me_5)_2Ba(Me\text{-}carbene)$[a](X), $(C_5Me_5)_2Ba(Me\text{-}carbene)_2$[a]	^1H, ^{13}C	2.74	234
$[C_5(1,2,4\text{-}Bu^t)_3H_2]_2Ba$, $[C_5(1,2,4\text{-}Bu^t)_3H_2]_2Ba\cdot NC(2,6\text{-}Me_2C_6H_3)$ (adduct)	^1H, ^{13}C		238
$(C_5Me_4Bu^t)_2Ba(THF)_2(X)$, $(C_5Me_4Bu^t)_2Ba(pyridine)_2$	^1H, ^{13}C	(2.79, 2.80)	235
$(C_5Me_4Bu^t)_2Ba(Pr^i\text{–carbene})(X)$	^1H, ^{13}C	(2.79, 2.76)	235
$[C_5(1,2,4\text{-}(SiMe_3)_3)H_2]_2Ba\}_2(X)$	^1H, ^{13}C	2.75	56
$[C_5(1,2,4\text{-}Bu^t_3)H_2]_2Ba(THF)(X)$	^1H, ^{13}C	2.77	359
$[C_5(1,2,3,4\text{-}C_6H_5)_4H]_2Ba(THF)$	^1H, ^{13}C		360
$\{C_5[CH_2CMe_2(2\text{-}C_5H_4N)]H_4\}_2Ba$, $[C_5(CH_2CH_2OMe)H_4]_2Ba$, $[C_5(CH_2CH_2OEt)H_4]_2Ba(X)$	^1H, ^{13}C	2.71	344,359
$[C_5(CH_2CH_2OCH_2CH_2OMe)H_4]_2Ba$	^1H, ^{13}C		361
$(C_9H_7)_2Ba(THF)_2$, $[(1,3\text{-}Pr^i_2)C_9H_5]_2Ba(THF)_2(X)$	^1H, ^{13}C	2.78	357

[a]Me-carbene = 1,3,4,5-tetramethylimidazol-2-ylidene.
[b]Pr^i-carbene = 1,3-diisopropyl-4,5-dimethylimidazol-2-ylidene.
[c]Metal-ring centroid values in parentheses indicate distinct values in the same molecule.

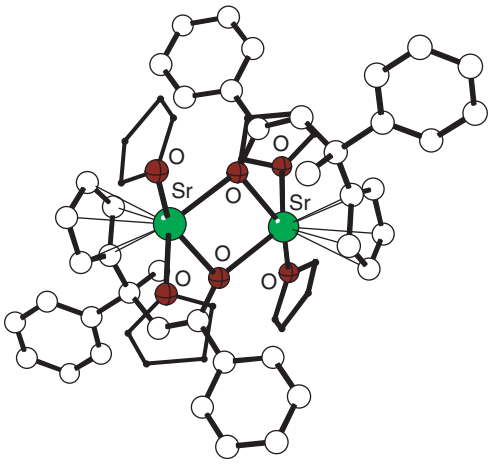

Figure 74 The structure of the bimetallic strontium complex **142**.

meso-isomer.[341] 6-Mesitylfulvene is not coupled by calcium, but on formation readily dimerizes by a Diels–Alder cyclization to form the fulvene **145**, which does not react with activated calcium. A variable temperature ^{1}H NMR study of *meso*-[1,1′-(1,2-Bu^{t}C$_2$H$_2$)(η^5-C$_5$H$_5$)]$_2$Ca **146** identified two concurrent dynamic processes in the molecule; one process involves a rearrangement of the chelating ligand framework between *l* and *d* conformations, while the other involves restricted rotations of the Bu^t groups in the ethylene bridge.[341]

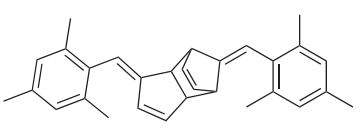

145

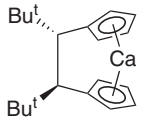

146

The reductive coupling of guaiazulene, a fulvalene analog, with activated calcium in THF affords a 60 : 40 mixture of two isomers, 8,8′-**147** (Figure 75) and 8,6′-(diguaiazulenide)bis(tetrahydrofuran)calcium, respectively. Thermolyses of each isomer revealed that the 8,8′-isomer is the thermodynamically preferred isomer, and it forms preferentially when the coupling is performed at 67 °C.[342]

The reaction of Me$_2$Si(Fl–H)$_2$ (Fl = fluorenyl) with M[N(SiMe$_3$)$_2$] (M = Ca, Ba) lead to the yellow (Ca) or orange (Ba) bis(fluorenyl) complexes.[343] The structure of Me$_2$SiFl$_2$Ca·(THF)$_3$ shows distorted exocylic η^3-bonding of both fluorenyl rings to Ca (Ca–C = 2.668(2)–3.189(2) Å). The analogous Ba compound crystallizes as a tetrakis(THF) solvate, Me$_2$SiFl$_2$Ba·(THF)$_4$ **148** (Figure 76); the unit cell contains two independent molecules with different Ba coordination geometries (η^5, η^3) in one (Ba–C = 3.007(4)–3.441(4) Å) and (η^3, η^3) in the other (Ba–C = 3.067(4)–3.359(4) Å). The fluorenyl rings tilt away from the metal to allow more solvation of the cation by THF.

The donor atoms of pendant substituents on cyclopentadienyl ligands can occupy specific metal coordination sites (e.g., [C$_5$H$_4$(CH$_2$CH$_2$OMe)]$_2$Ca, {C$_5$H$_4$[CH$_2$CMe$_2$(2-C$_5$H$_4$N)]}$_2$Sr[344]). Weaker cation–π binding is observed in metallocenes with pendant 3-butenyl substituents (i.e., [C$_5$Me$_4$(CH$_2$CH$_2$CH=CH$_2$)]$_2$M; M = Ca, Sr, Ba); with M = Mg, the butentyl groups are uncoordinated.[237] In the case of the barocene **149** (Figure 77),[313] the coordination

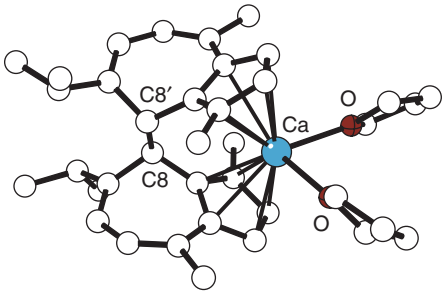

Figure 75 The structure of 8,8′-(diguaiazulenide)bis(tetrahydrofuran)calcium **147**.

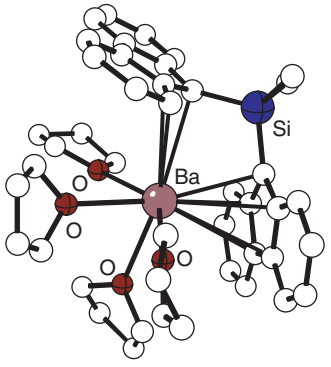

Figure 76 One of two molecules (with η^5-, η^3-coordination) found in the unit cell of Me$_2$SiFl$_2$Ba·(THF)$_4$ **148**.

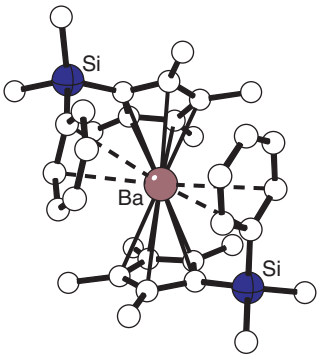

Figure 77 The structure of the barocene $(C_5Me_4SiMe_2C_6H_5)_2Ba$ **149**.

number is indeterminate; the directly bonded Ba–Cp′ distances range from 2.934(4) to 3.096(4) Å, but the barium–aromatic ring carbon contacts range from 3.29 to 4.22 Å. Only the shorter of these (~3.5 Å) are probably energetically significant. In some cases, pendant groups can be used to generate chiral complexes, such as the calcocene **150**.[345]

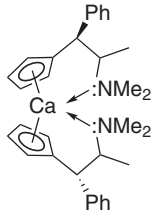

150

Phosphonium-bridged species (i.e., the diylides $[R_2PCp'_2]^-$)[346] are attractive ligands for group 2 elements, as they provide a metallocene-like framework but only a uninegative charge. Reaction of the ylide $Me_2P(2\text{-}Me\text{–}4\text{-}Bu^t\text{–}C_5H_2)(2'\text{-}Me\text{–}4'\text{-}Bu^t\text{–}C_5H_3)$ with 1 equiv. of $Ba[N(SiMe_3)_2]_2$ in toluene at room temperature yields $Me_2P(2\text{-}Me\text{–}4\text{-}Bu^t\text{–}C_5H_2)_2BaN(SiMe_3)_2$. When the same starting reagents are used in a 2 : 1 ratio, $[Me_2P(2\text{-}Me\text{–}4\text{-}Bu^t\text{–}C_5H_2)_2]_2Ba$ is formed. When the protonated ligand salt $R_2P(2\text{-}Me\text{–}4\text{-}Bu^t\text{–}C_5H_3)_2{}^+X^-$ (R = Me, X = I^-, BPh_4^-; R = Bu^n, X = I^-) is treated with 1 equiv. of $Ba[N(SiMe_3)_2]_2$, the cationic barocene derivatives $R_2P(2\text{-}Me\text{–}4\text{-}Bu^t\text{–}C_5H_2)_2Ba^+X^-$ are isolated. The phosphonium-bridged $[Me_2P(2\text{-}Me\text{–}4\text{-}Bu^t\text{–}C_5H_2)_2Ba(THF)_3]^+$ **151** (Figure 78)[347] displays an average Ba–C distance (3.06 Å) that is expected for a complex containing a formally nine-coordinate Ba^{2+} center;[24] the *ansa*-bridge appears to place no geometric constraint on the metal–ligand distances.[347]

As discussed in more detail in Section 2.02.4.2.2.(iii), almost all the metallocenes of calcium, strontium, or barium are bent, even when unsolvated. The only exception to this so far is the sterically crowded $(C_5Pr^i_5)_2Ba$ **152** (Figure 79),[348] whose X-ray crystal structure reveals a linear geometry with Ba–C = 2.997(4) Å. All three

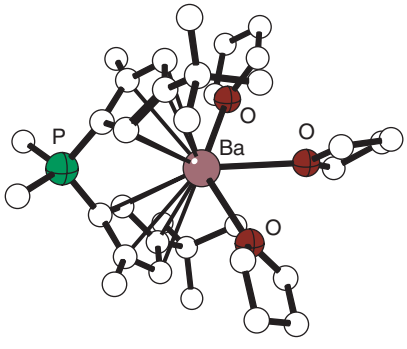

Figure 78 The structure of the phosphonium-bridged complex $[Me_2P(2\text{-}Me\text{–}4\text{-}Bu^t\text{–}C_5H_2)_2Ba(THF)_3]^+$ **151**.

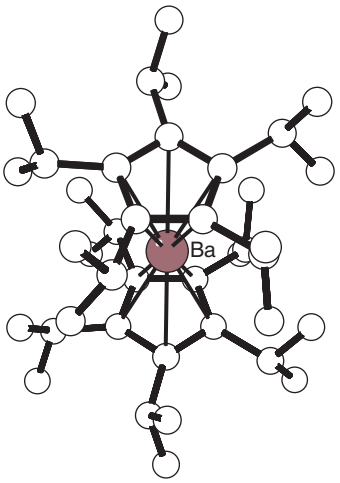

Figure 79 The structure of the linear barocene $(C_5Pr^i_5)_2Ba$ **152**.

$(C_5Pr^i_4H)_2M$ (M = Ca, Sr, Ba) species display exceptional levels of air stability (weeks for the calcium and strontium derivatives), undoubtedly a result of the complete enclosure of the metal centers. Reaction of $[(C_5Pr^i_5)BaI(THF)_2]_2$ with Na_2COT (COT = cyclooctatetraene) in THF/hexane produces the triple-decker sandwich complex $(C_5Pr^i_5)Ba(COT)Ba(C_5Pr^i_5)$ **153** (Figure 80). It crystallizes as a slightly bent stack (Cp′centroid–Ba–COT centroid angle = 169.5°). Short distances (ca. 3.6 Å) below the sum of the van der Waals radii between two of the Me groups of each $(C_5Pr^i_5)$ ligand indicate a $Ba\cdots CH_3$ interaction.[349]

Among the less common adducts of group 2 metallocenes are those with carbon donor ligands. The Wanzlick-type carbenes isolated by Arduengo[66] form robust adducts with many main group element compounds[350] and organolanthanide species.[351] Several alkaline earth metallocenes complexed to 1,3,4,5-tetramethylimidazol-2-ylidene **154**[234] and 1,3-diisopropyl-4,5-dimethylimidazol-2-ylidene[235] have also been isolated and structurally characterized (Table 6). In some cases, close contacts between the metal centers and isopropyl groups of the coordinated carbene are observed. When this occurs, the carbene carbon resonances in the ^{13}C NMR spectra shift upfield (ca. 7–17 ppm), indicating that the close approaches are not simply a consequence of crystal packing. The nucleophilicity of the carbenes toward the metallocenes is remarkable, in that ammonia, Et_2O, and THF can be displaced from the metal centers in favor of the carbon donor ligand. This is noteworthy in the case of calcium species, which usually bind THF strongly.

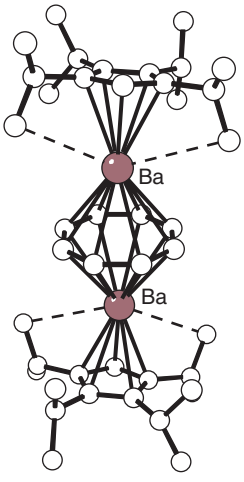

Figure 80 The structure of the triple-decker sandwich complex $(C_5Pr^i_5)Ba(COT)Ba(C_5Pr^i_5)$ **153**.

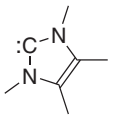

154

The reaction of CO with $(C_5Me_5)_2M$ (M = Mg–Ba) has been studied in toluene or methylcyclohexane solution in a high-pressure IR cell.[352,353] Only with the calcium and strontium complexes carbonyl stretches are observed that could be interpreted as the formation of monocarbonyl complexes $(C_5Me_5)_2MCO$ (for $(C_5Me_5)_2CaCO$, 2158 cm^{-1}; $(C_5Me_5)_2SrCO$, 2159 cm^{-1}). These are greater than that of free CO in toluene or methylcyclohexane (2134 cm^{-1}). Equilibrium constant measurements indicate that the M–CO binding is weak; the CO appears to function as a pure σ-donor to the metals.

Heterocyclic complexes. A straightforward preparation of heterocyclic metallocenes involves halide metathesis. Treatment of SrI_2 with 2 equiv. of $K[P_3C_2Bu^t_2]$ in THF affords the pale yellow hexaphosphastrontocene $(\eta^5\text{-}P_3C_2Bu^t_2)_2Sr$ **155** in 50% yield.[362] It is a polymer in which each strontium atom is coordinated by a terminal η^5-bound triphosphyl ligand and a bridging ring (η^5-bound to one strontium, η^1-bond to an adjacent ring (Figure 81)). The Sr–η^1-P distance of 3.22 Å is only slighty longer than the Sr–η^5-P distance of 3.18 Å. Treatment of **155** with an excess of pyrazine in refluxing toluene converts it quantitatively into the orange Lewis base adduct $(\eta^5\text{-}P_3C_2Bu^t_2)_2Sr(\mu\text{-}C_4H_4N_2)$ **156**, which is also polymeric in the solid state.[362] The pyrazines link the metallocenes togethes in a zigzag arrangment (Sr–N = 2.78 Å (av.), Figure 82).

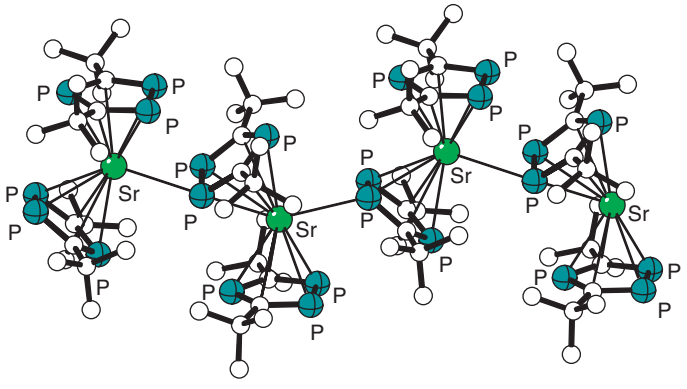

Figure 81 The structure of the hexaphosphastrontocene $(\eta^5\text{-}P_3C_2Bu^t_2)_2Sr$ **155**.

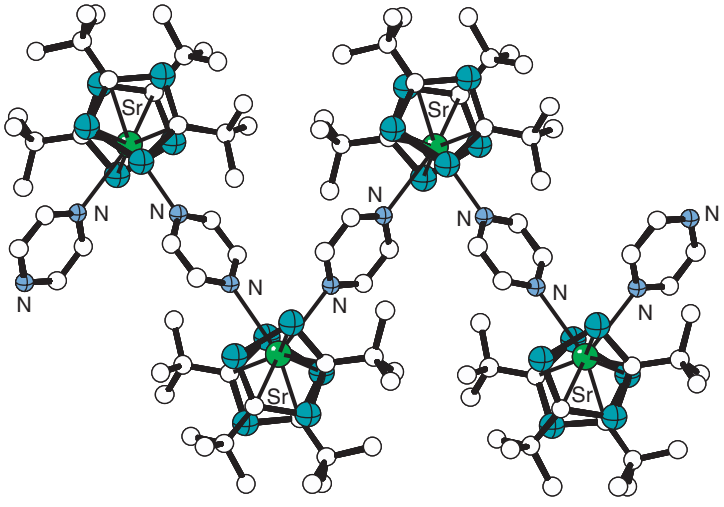

Figure 82 The structure of the coordination polymer $\{(\eta^5\text{-}P_3C_2Bu^t_2)_2Sr(\mu\text{-}C_4H_4N_2)\}_\infty$ **156**.

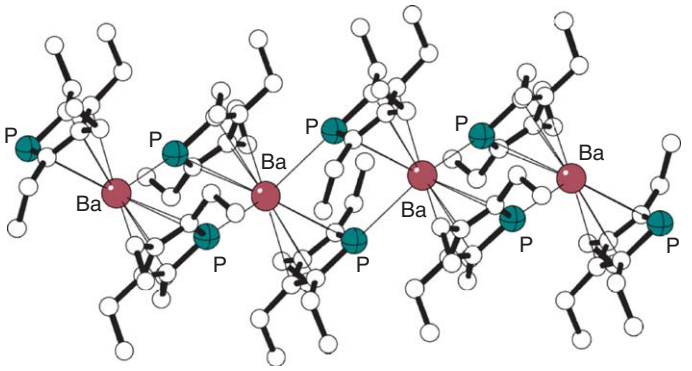

Figure 83 The structure of the coordination polymer $\{(PC_5Et_4H)_2Ba\}_\infty$ **157**.

The reduction of octaethyl–1,1′-biphosphole, -biarsole, and –bistibole with strontium and barium in THF yields the 1,1′-dipentelaoctaethylstrontocenes and -barocenes $(EC_5Et_4H)_2M$ (E = P **157**, As, Sb). The strontocene crystallizes as a THF adduct whereas the barocene **157** precipitates co-ligand-free but as a coordination polymer (Figure 83).[260]

Reaction of $AsH_2(SiPr^i_3)$ with $[N(SiMe_3)_2]_2M(THF)_2$ (M = Ca or Sr) yields $[As(H)SiPr^i_3]_2M(THF)_4$ in equilibrium with $M[As(H)SiPr^i_3][\mu\text{-}As(H)SiPr^i_3]_3M(THF)_3$.[363] Subsequent reaction with diphenylbutadiyne in toluene/THF gives the metal bis(THF)bis(2,5-diphenylarsolide) species. A mechanism based on intermolecular $H/SiPr^i_3$ exchange has been suggested that rationalizes the generation of the $(Pr^i_3Si)_2As^-$ and 2,5-diphenyl-3,4-bis(phenylethynyl)arsolide anions (Scheme 11). The latter was isolated with a binuclear cation as the solvent-separated ion pair $[(THF)_3Ca\{\mu\text{-}As(H)SiPr^i_3\}_3Ca(THF)_3]^+$, and characterized with X-ray crystallography. The arsolide ligands in the calcocene are η^5-bonded to the metal center (Ca–As = 3.0904(9), 3.0750(9) Å; Ca–C = 2.789(4)–2.879(3) Å). NMR evidence suggests that the strontocene is isostructural. Cyclization of diphenylbutadiyne also occurs on reaction with $[P(SiMe_3)_2]_2M(THF)_4$ (M = Ca or Sr) in toluene. The products are the coordination complexes **158**, in which the carbon atoms of the PC_4 rings are not coordinated to the metals (Ca–P = 3.07 Å; Sr–P = 3.14 Å).[364]

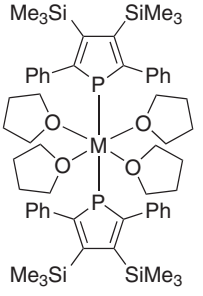

158

The weak interactions that may exist between group 2 cations and anionic hydrocabyl ligands are demonstrated in the "metal-in-a-box" compounds such as $[M(THF)_6][Me_3Si(fluorenyl)]_2$ (M = Ca **159** or Mg), which are formed by the addition of THF to solutions of the bis(fluorenyl) complexes in non-polar solvents. The box may be completed by the presence of aromatic molecules, as in **159** (Figure 84). The disruption of the metal–carbon bonds is thought to stem from a combination of robust M–THF interaction, the stability of the free $[Me_3Si(fluorenyl)]^-$ ion, and the formation of numerous C–H$\cdots\pi$ interactions between THF and the anions. These and related examples are reviewed elsewhere.[365]

2.02.4.2.2.(ii) Monocyclopentadienyl and related compounds

Derivatization of some mono(cyclopentadienyl) complexes to yield new monosubstituted species can often be accomplished by metathetical exchange (Equation (26)) or protonation reaction.[295] Protonolysis of $(C_5Pr^i_4H)Ca[N(SiMe_3)_2](THF)$ with several terminal alkynes HC≡CR in either toluene or hexanes produces the

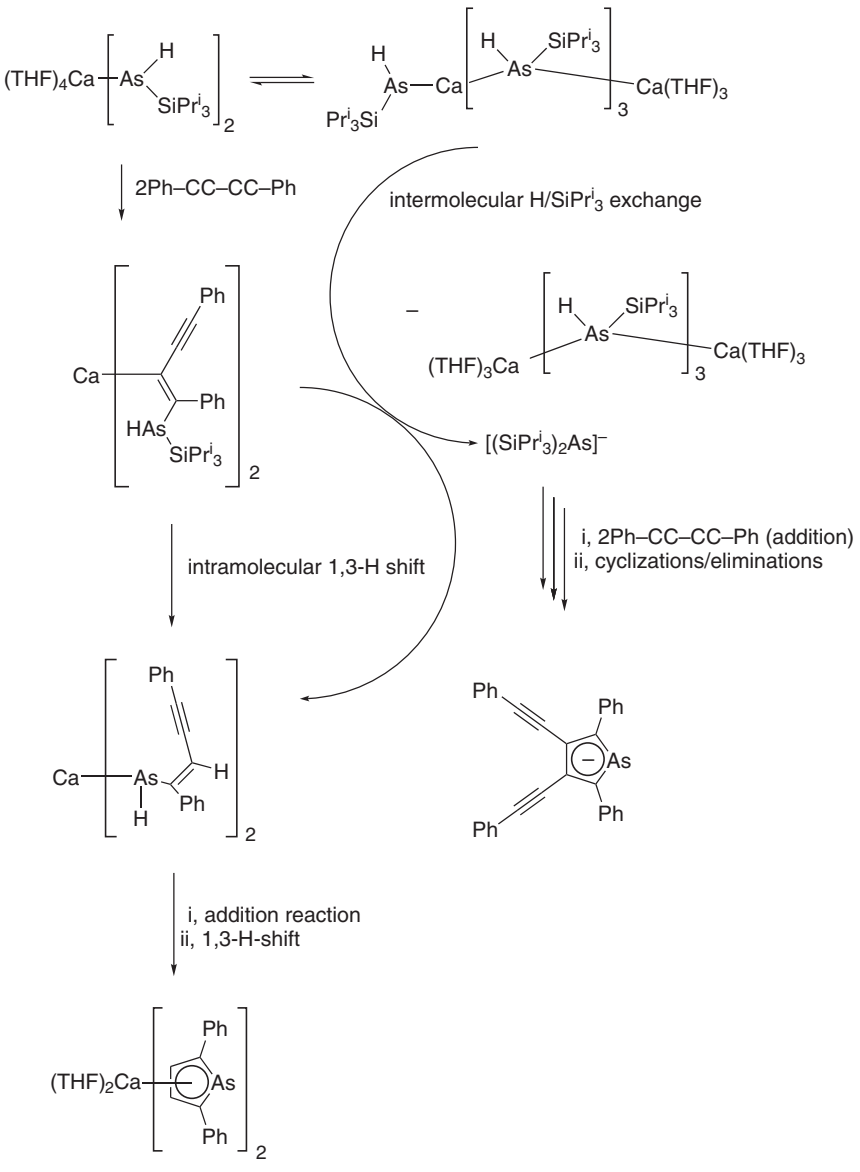

Scheme 11

corresponding calcium acetylide complexes $(C_5Pr^i_4H)Ca[C{\equiv}CR](THF)$ (R = Ph, ferrocenyl, $SiMe_3$, $SiPr^i_3$, $SiPh_3$) in good yield.[366] $(C_5Pr^i_4H)Ca[C{\equiv}CPh](THF)$ **160** (Figure 85) crystallizes from toluene as an acetylide-bridged dimer, with Ca–C(acetylide) distances of 2.551(8) and 2.521(7) Å.

$$\mathrm{Cp'CaI(THF)}_n + \mathrm{ME} \longrightarrow \mathrm{Cp'CaE(THF)}_n + \mathrm{MI} \qquad \mathrm{M = Li, K;\ E = N(SiMe_3)_2,\ BHT} \tag{26}$$

2.02.4.2.2.(iii) Applications

Applications involving ring transfer or loss. The kinetic lability, volatility, and Lewis acidity of heavy alkaline earth metallocenes have been the properties most important to their applications. The gas-phase decomposition of volatile metallocenes is useful in the preparation of thin films of alkaline earth-containing materials and in doping semiconductors. Reviews are available on the use of group 2 organometallic compounds as precursors for chemical-vapour deposition (CVD).[2,3]

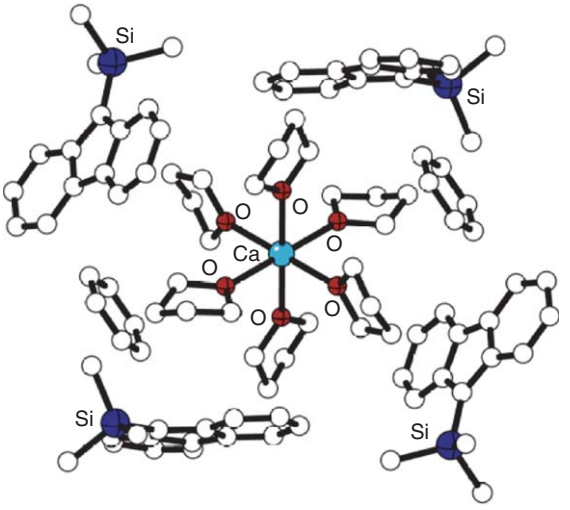

Figure 84 The structure of the ''metal-in-a-box'' complex **159**.

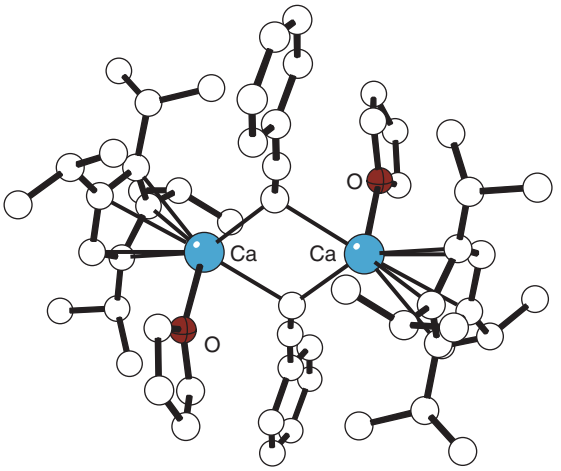

Figure 85 The structure of the dimeric complex $\{(C_5Pr^i{}_4H)Ca[C{\equiv}CPh](THF)\}_2$ **160**.

Atomic layer epitaxy has been used to form films of the dielectric heterometallic oxides $SrTiO_3$ and $BaTiO_3$ from organoalkaline earth precursors.[367] Titanium isoproxide, water, and either $(C_5Pr^i{}_3H_2)_2Sr$ or $(C_5Me_5)_2Ba$ can be used to form films of the oxides at temperatures of 325 °C (for $SrTiO_3$) or 275 °C (for $BaTiO_3$). Annealing in the air at 500 °C leaves polycrystalline films that display excellent conformal coverage of patterned silicon surfaces and have relative permittivities of 180 and 165 for the Sr and Ba oxides, respectively.[368,369] Experiments using D_2O demonstrated that the principle volatile decomposition product during the deposition of SrO or $SrTiO_3$ was $C_5Pr^i{}_3H_2D$;[370] the $SrTiO_3$ films contained low amounts of residual carbon.[369] The use of $[C_5(1,2,4\text{-}Bu^t)_3H_2]_2Ba(THF)$ and $Ti(OPr^i)_4$ provides (100)-oriented tetragonal $BaTiO_3$ at 350 °C without post-deposition processing.[359]

The lability of calcocenes can be used to generate mixed-ring organolanthanide compounds, which are otherwise not available via general routes.[337] Hydrocarbon soluble $(C_5Me_5)_2Ca$ undergoes cyclopentadienyl ring-metathesis reactions with Cp_3Ln to yield $(C_5Me_5)_2LnCp$ complexes (Equation (27)). Adjustments to the reaction stoichiometry with solvated precursors lead to $(C_5Me_5)LnCp_2(THF)_x$ complexes instead.[371] Precipitation of the toluene-insoluble $(Cp_2Ca)_x$ drives the reactions.

$$(C_5Me_5)_2Ca + Cp_3Ln \longrightarrow (C_5Me_5)_2LnCp + Cp_2Ca \quad (Ln = La, Nd, Sm) \tag{27}$$

Ring transfer from **141** occurs with YCl_3, $SnCl_2$, and $FeCl_2$ to yield the corresponding yttrocene chloride,[339] stannocene,[339] amd ferrocene.[338] Reductive coupling of phenylfulvene with activated calcium in THF gives nearly quantitative yields of a mixture of *cis*- and *trans*-diphenylethanediyl-bridged *ansa*-calcocenes **161**. The *cis*-isomer can be removed by recrystallization, yielding the C_2-symmetric *trans*-$Ph_2C_2H_2(\eta^5\text{-}C_5H_4)_2Ca(THF)_2$. Subsequent reaction with $FeCl_2$ and $ZrCl_4$ gives the C_2-symmetric transition metal *ansa*-metallocene complexes.[239] In contrast, reductive coupling of 1-*E*-benzylidene-4,7-dimethylindene with activated calcium forms the two isomers, *trans*-$Ph_2C_2H_2$-*rac*-$(\eta^5\text{-}4,7\text{-Me-2-}C_9H_4)_2Ca(THF)_2$ **162** and *cis*- $Ph_2C_2H_2$-*meso*-$(\eta^5\text{-}4,7\text{-Me-2-}C_9H_4)_2Ca(THF)_2$ **163** in approximately equal amounts. Reaction of the calcium compounds with $FeCl_2$ produces a mixture of the corresponding *trans*-*rac*- and *cis*-*meso*-ferrocenophanes along with another ferrocenophane isomer that is apparently either the *trans*-*meso*- or *cis*-*rac*-isomer. Partial loss of stereochemical integrity occurs during ligand transfer to iron; complete loss occurs on formation of zirconium complexes from the reaction of the calcium metallocenes with $ZrCl_4(SMe_2)_2$ or $ZrCl_4(THF)_2$.[372]

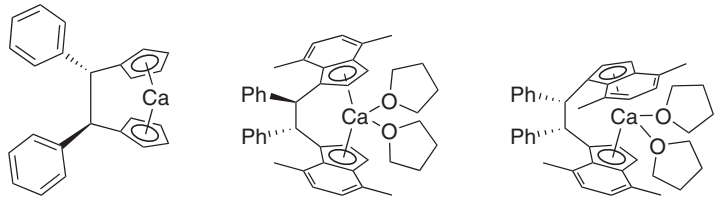

161 **162** **163**

ansa-Calcocene compounds have been used to synthesize *ansa*-chromocene complexes from $CrCl_2$ in the presence of trapping ligands such as CO or RNC. A variety of carbonyl and *tert*-butyl isocyanide complexes have been prepared in this manner.[373]

Applications in catalysis. An early report describing the formation of poly(methylmethacrylate) using Cp_2Ca[374] has been reinvestigated using both Cp_2Ca and the more soluble $(C_5Me_5)_2Ca$.[375] The original claim of high syndiotacticity (*rr* = 94% at 0 °C) could not be reproduced in the new experiments. Problems with the conversion rates and the broad polydispersity of the polymer make Cp_2Ca unattractive as a catalyst for this system. The use of $(C_5Me_5)_2Ca$ produces higher conversions, but even lower syndiotacticity than does Cp_2Ca.

Attempts to control the coordination sphere around calcium so that stereocontrolled polymerization could be realized have had mixed success. The fluorenyl calcium benzyl complex (2-Me_2N–α-Me_3Si–benzyl)(9-Me_3Si–fluorenyl)$Ca(THF)_2$ does not display Schlenk equilibrium with its symmetrical counterparts (bis(fluorenyl)calcium and bis(benzyl)calcium), and living polymerization is observed with this compound at room temperature (10% styrene in cyclohexane or benzene), but the resulting material is largely atactic.[376] The stereoerrors apparently arise from configurational rearrangements of the anionic chain end: inversion of the chain end involving rotation around the *ipso*–C_α bond is possible without breaking the cation–anion bond (Scheme 12). Polymerization in pure styrene produces highly syndiotactic polymer, with less than 2% of the isotatic material. The higher concentration of styrene increases the rate of insertion, which is highly stereospecific. Loss of stereochemical control occurs after the insertion step. The use of the bulky $(SiMe_3)_3Si$–fluorenyl ligand in place of $(SiMe_3)_3Si$–fluorenyl does not improve the syndiotacticity, and in all cases, the large hypersilyl substituent retards the chain growth step.[377]

Reaction of the bis-chelate complex **149** and various bis(arylalkyl)barium complexes generates heteroleptic barium complexes with one chelate and one reactive arylalkyl ligand **164**. The homoleptic and heteroleptic barium complexes both induce living polymerization of styrene to atactic polystyrene in cyclohexane solution. The fact that no stereocontrol is observed during polymerization despite the presence of the chiral carbanionic ligands is

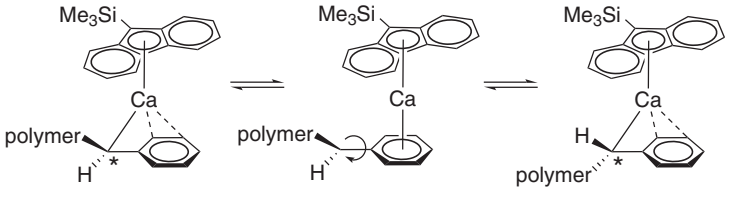

Scheme 12

attributed to the rapid exchange of arylalkyl groups and the growing polymer chains between Ba^{2+} centers, accompanized by epimerization of the chiral carbanion.[313]

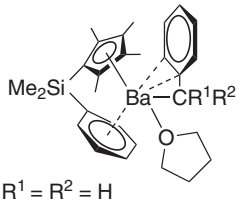

$R^1 = R^2 = H$
$R^1 = Ph; R^2 = H$
$R^1 = Ph; R^2 = CH_2CH_2Ph$

164

Computational Considerations. Reports of organoalkaline earth chemistry increasingly include computational studies as complements to experimental work. Lacking metal valence orbitals to influence the orientation of ligands, ML_2 compounds have linear geometries, as this arrangement serves to minimize intramolecular steric interactions. However, various group 2 dihalides have long been known to be bent in the gas phase or when isolated in matrices (i.e., CaF_2, SrX_2 (X = F, Cl, Br), BaX_2 (X = F–I)).[378] With exception of the sterically congested complex $(C_5Pr^i_5)_2Ba$,[348] the metallocenes Cp'_2M (M = Ca–Ba) possess non-parallel cyclopentadienyl rings, and as noted in Section 2.02.4.2.1, the dialkyl complex **115** is bent.[303] A reverse (core) polarization of the metal cation by the ligands has been suggested as a source of bent alkaline earth ML_2 structures.[379,380] A related explanation of the bending involves an analysis of Laplacian of the electron density in the core metal electrons.[381,382] In the latter analysis, the presence of appropriate ligands induces localization of electron pair density, and MX_2 molecules are then bent owing to a tetrahedrally distorted M^{2+} core.

Other explanations of the bending have also been suggested; for example, attractive van der Waals forces between the substituents on the ligands have been proposed as the primary stabilizing force for the bent metallocene geometries.[383,384] The description of interligand interactions in these molecules has also been investigated with a "through-space coupling" approach, which recasts van der Waals forces in terms of molecular orbitals.[385]

Group 2 complexes are formally electron deficient and conformationally "floppy"; only small energies (often only 1–2 kcal mol^{-1}) are required to alter their geometries by large amounts (e.g., bond angles by 20° or more). In such cases, the inclusion of electron-correlation effects becomes critical to an accurate description of the molecules' structures. Both HF/MP2 and density functional theory (DFT) methods have been applied to organoalkaline earth compounds. DFT approaches, which implicitly incorporate electron correlation in a computationally efficient form, are generally the more widely used.[382,386,387] Molecular orbital calculations that successfully reproduce bent geometries and explicitly include valence *d*-orbitals in the basis sets do not, however, prove that the "reverse polarization" approach to interpreting the bonding in these compounds is invalid, as the *d*-orbitals that are used are usually highly contracted, and in practice act as polarizing functions for the metal cores.

Reviews of quantum chemical calculations on main group metallocenes that include group 2 species are available.[388,389]

2.02.4.3 Addition Compounds with Unsaturated Organic Molecules

Reductive coupling of acenaphthylene with activated calcium forms the yellow complex $(C_{12}H_8)_2Ca(THF)_2$ **165** in high yield; its NMR spectrum is consistent with the presence of η^5-$C_{12}H_8$ rings.[390] On reaction with $ZrCl_4$ in THF, the *ansa*-biacenyl ligand is decoupled, generating dark green $(C_{12}H_8)ZrCl_2(THF)_3$. Alternatively, reaction of $(C_{12}H_8)_2Ca(THF)_2$ with Me_3SiCl in THF generates the 1,2-bis(trimethylsilyl)-substituted acenaphthene **166**. Both these reactions (which also occur with Yb(II)) apparently originate from an equilibrium between the *ansa*-metallocene, decoupled acenyl radical anions, and metal dications (Scheme 13). Subsequent disproportion of $[C_{12}H_8]^{\cdot-}$ to the acenyl dianion and neutral acenaphthylene then leads to addition of $ZrCl_4$ or Me_3SiCl and elimination of the metal dichloride.

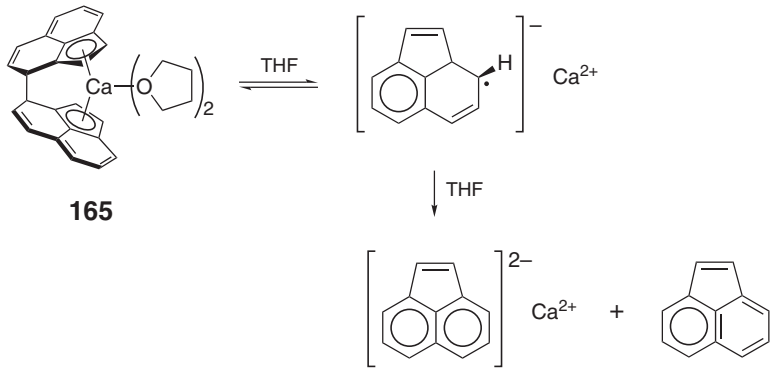

165

Scheme 13

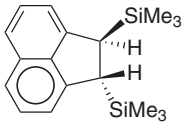

166

2.02.4.4 Organometal Hydrides, Oxides, and Amides

In principle, halide metathesis could be a reliable source of organometallic derivatives containing cyclopentadienyl ligands (Equation (28)). In practice, the product of exchange reactions can depend on the identity of the alkali metal cations present. When Cp′ = C_5(1,2,4-($SiMe_3$)$_3$$H_2$), M = Ca, and M′ = K, reactions such as those in Equation (29) occur largely as expected, but when M = Li (e.g., LiI, CH_3Li, Li[$N(SiMe_3)_2$]), reactions yield mainly the lithium cyclopentadienide, that is, ring transfer occurs from Ca^{2+} to Li^+ (Equation (29)).[298] DFT calculations on base-free model compounds (Cp′ = C_5H_5; E = iodide) suggest that such ring transfer on unsolvated species would in fact be slightly endoergic. When THF-solvated species are used, however, the calculated reaction becomes strongly exoergic; solvation of $CaI_2(THF)_n$ was identified as the principle driving force for the reaction.

$$Cp'MX(THF)_n + M'E \longrightarrow Cp'ME(THF)_n + M'X \quad (M' = Li, Na, K;\ E = \text{hydrocarbyl, alkoxy, amido}) \tag{28}$$

$$[C_5(1,2,4\text{-}(SiMe_3)_3)H_2]CaI(THF)_n + Li[E] \xrightarrow[\text{toluene}]{\text{THF or}} Li[C_5(1,2,4\text{-}(SiMe_3)_3)H_2] + CaIE(THF)_n \tag{29}$$

2.02.4.4.1 Organocalcium hydrides

Calcium atoms react with methyl-substituted benzene derivatives under co-condensation conditions to yield arylcalcium hydrides.[391] With $C_6H_5CH_3$, $C_6H_5Bu^t$, and $C_6H_5Si(CH_3)_3$, the reaction displays no selectivity for C–H activation, giving the *ortho*-, *meta*-, and *para*-isomers of each arylcalcium hydride. With *m*-$C_6H_4(CH_3)_2$, the reaction selectively activates the bond *meta* to the CH_3 groups. The reaction between $HCaC_6H_5Bu^t$ and Bu^t-substituted phenols (2,6-$Bu^t{}_2C_6H_3OH$, 4-Me–2,6-$Bu^t{}_2C_6H_2OH$, 2,4,6-$Bu^t{}_3C_6H_2OH$) produces the corresponding aryloxides in high yields.

A DFT study was performed in order to determine the structures of phenylcalcium hydride and its magnesium analog in donor solvents.[391] A dimeric phenylcalcium hydride was found to be the most stable species in solution, but monomers or tetramers cannot be excluded at very low or very high concentrations. Hydride bridging is favored over phenyl bridging, and a coordination number of six is predicted to be dominant in solution.

An attempt to convert the organocalcium iodide [C_5(1,2,4-($SiMe_3$)$_3$$H_2$]CaI(THF) to a hydride complex by reaction with $NaBEt_3H$ lead instead to the triethyl borohydride complex **167**.[392] Spectroscopic data indicate that the

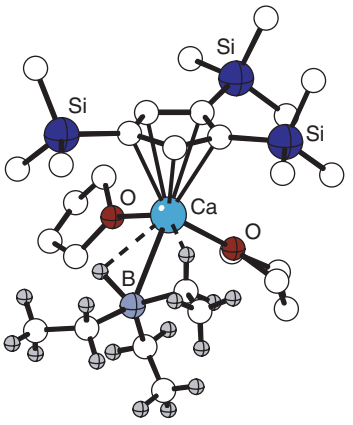

Figure 86 The structure of the calcium triethyl borohydride complex **167**.

$[HBEt_3]^-$ anion is involved in a bridging interaction (IR: $\nu_{BH} = 1935\,cm^{-1}$; ^{11}B NMR: $J_{B-H} = 50\,Hz$), a conclusion supported by a single crystal X-ray structure of the complex (Ca–H = 2.21(4) Å (Figure 86)). The BEt_3 moiety resists removal from the calcium center; no reaction is observed with PMe_3, and refluxing a solution in toluene leads to decomposition and the formation of the metallocene $[C_5(1,2,4\text{-}(SiMe_3)_3)H_2]_2Ca$.

2.02.4.4.2 Organometal oxides

The monocyclopentadienyl halide $(C_5Pr^i{}_4H)CaI(THF)_{(1,2)}$ can be derivatized in a metathetical reaction with K[BHT] (HBHT = HOC_6H_2–$Bu^t{}_2$-2,6–Me-4) to yield the aryloxide derivative $(C_5Pr^i{}_4H)Ca(BHT)(THF)$ in high yield.[295] The aryloxide can also be prepared by the reaction of $(C_5Pr^i{}_4H)Ca[N(SiMe_3)_2](THF)$ with HBHT in toluene.

When the dimeric salt **119** is treated with CaI_2 in THF, cleavage of the methoxy methyl group occurs, and a tetramer **168** containing a Ca_4O_4 cuboidal core is isolated in low yield (12%) (Figure 87).[306] The molecule has crystallographic S_4-symmetry, and each calcium center is coordinated by the oxygen and phospanyl phosphorous atoms on one ligand, the oxygen and anionic carbon of a second ligand (Ca–C = 2.591(5) Å), and the oxygen atom of a third ligand. Ca–O distances in the cube range from 2.346(4)–2.430(3) Å.

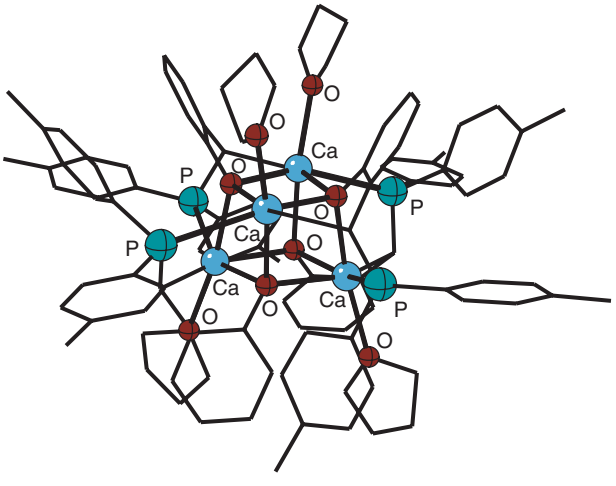

Figure 87 The structure of the cuboidal complex $[Ca(THF)\{CH[P(C_6H_4Me\text{-}4)_2]C_6H_4O\text{-}2\}]_4$ **168**.

2.02.4.4.3 Organometal amides

The halide complex $(C_5Pr^i{}_4H)CaI(THF)_{(1,2)}$ can be derivatized by an exchange reaction with $K[N(SiMe_3)_2]$ to yield the organometallic amide **169** in high yield.[295] In the solid state, **169** is monomeric with a pseudo-trigonal-planar arrangement of the ligands around the calcium (Figure 88). Two crystallographically independent enantiomers are present in the asymmetric unit, with Ca–N bond distances of 2.29(1) and 2.30(1) Å. An agostic interaction exists between the calcium and one of the trimethylsilyl groups of the amido ligand (Ca···C(Me) = 2.99(2) and 2.95(2) Å). At 120 °C and 10^{-6} torr, **169** sublimes to give waxy materials containing **169**, $(C_5Pr^i{}_4H)_2Ca$ and $Ca[N(SiMe_3)_2]_2(THF)_n$.

Two equiv. of 6,6-di(cyclopropyl)fulvene react at 60 °C over a period of a week with $Ca[N(SiMe_3)_2]_2{\cdot}(THF)_2$ bis in THF to yield the metallocene **170**. The heteroleptic amido complex **171** is detected as an intermediate with ^1H and $^{13}C\{1H\}$ NMR spectroscopy. A 1 : 1 reaction of the calcium amide and **170** also produces **171**; in solution, an equilibrium involving these three derivatives exists (Equation (30)). The calcocene **170** crystallizes at −20 °C from THF as colorless cuboids. The metal center is surrounded by the four ligands in a distorted tetrahedral manner, and the cyclopentadienyl group and the propylidene fragment are coplanar with each other.[393]

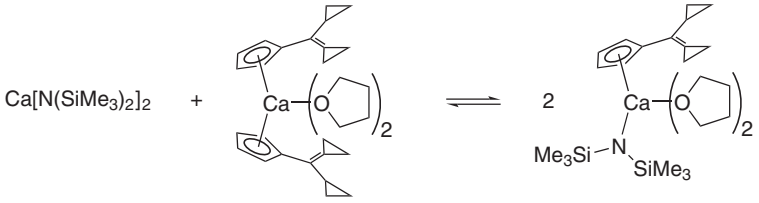

170 **171** (30)

The reaction of $Ba[N(SiMe_3)_2]_2(THF)_2$ with $(C_6H_{11})NHCMeCHCMeN(C_6H_{11})$ in petroleum ether yields the diazapentadienyl (DAP) compound **172**.[394] The dimeric complex retains a bis(trimethylsilyl)amido group from the starting barium amide, and contains three DAP ligands that display different coordination modes (Figure 89). One of these is bonded in a terminal mode to Ba2 (Ba–C ~ 3.2 Å), although the primary interaction is with N6 and N7 at 2.689(4) and 2.635(4) Å, respectively. A second DAP ligand spans Ba1 and Ba2 and adopts a "W" conformation. The principal bonding is again through the nitrogen atoms (Ba1–N2 = 2.613(4), Ba2–N3 = 2.873(4) Å); there are long Ba–C contacts of 3.1–3.2 Å (to C13, C15). A third DAP ligand is turned perpendicularly to the Ba1–Ba2 vector, and adopts a π-bonded orientation to Ba2.

Treatment of the amine **173** (LBu^tH) in a 2 : 1 ratio with $M[N(SiMe_3)_2]_2(THF)_2$ (M = Ca, Sr, Ba) in toluene at ambient temperatures affords $(\eta^5\text{-}LBu^t)_2M$ **174** in ≥93% yields.[395] All three compounds possess bent-sandwich structures with η^5-coordinated β-diketiminato ligands. Similar treatment of the Pr^i analog of **173** (i.e., LPr^iH) yields the corresponding calcium and strontium complexes $(\eta^2\text{-}LPr^i)_2Ca$ **175** and $(\eta^5\text{-}LPr^i)_2Sr$, respectively, in high yield. The reaction of $Ba[N(SiMe_3)_2]_2(THF)_2$ with LPr^iH yield the C_2-symmetric dinuclear complex **176** (Figure 90). The

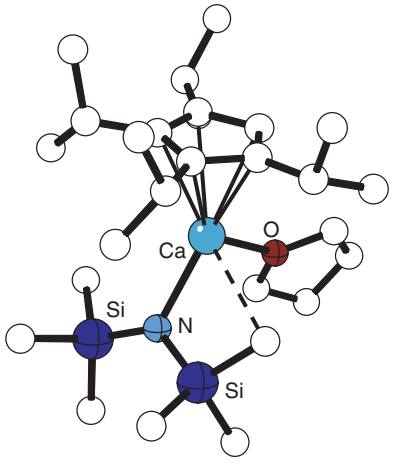

Figure 88 The structure of the organometallic amide **169**.

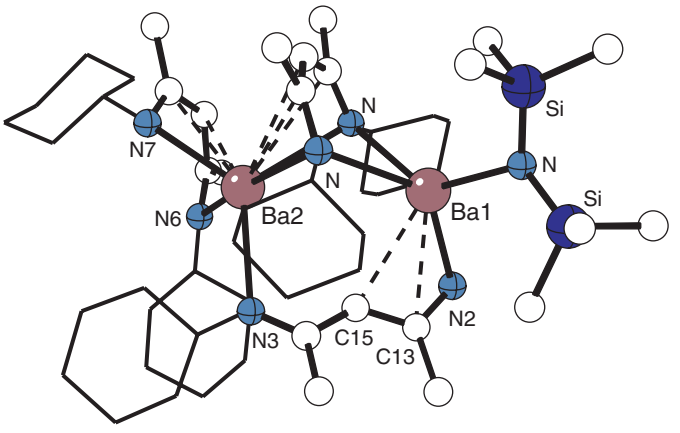

Figure 89 The structure of the diazapentadienyl (DAP) compound **172**.

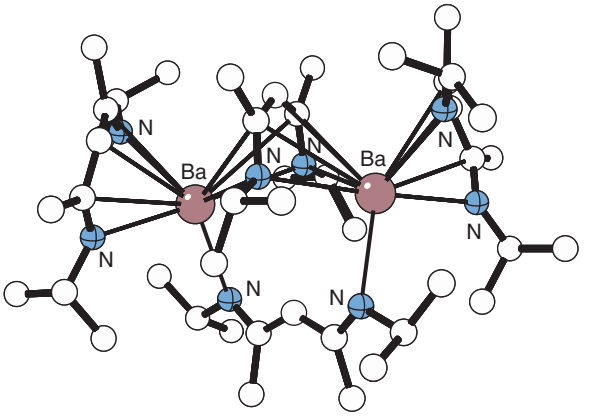

Figure 90 The structure of the dinuclear β-diketiminato complex **176**.

latter exhibits three different bonding modes for the β-diketiminato ligands, including η^5 (Ba–N = 2.685, 2.722 Å), μ-η^1:η^1(Ba–N = 2.790 Å), and μ-η^5:η^5(Ba–N = 2.814, 2.927 Å). NMR evidence indicates that the dinuclear structure of **176** remains intact in solution.[395]

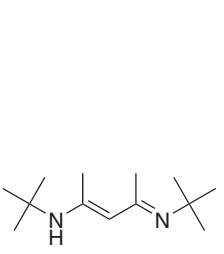

173

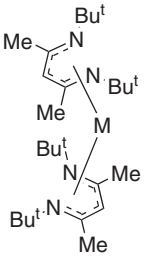

174

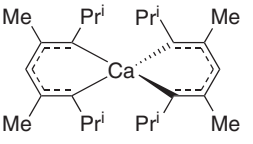

175

Calcium and strontium diiodide react with 2,5-Bu$^t_2$-pyrrolylsodium in THF, yielding $(NC_4H_2Bu^t_2\text{-}2,5)_2M(THF)$ (M = Ca, Sr **177**), for which NMR spectra and the X-ray structures confirm the η^5-bonding character of the ligands (Figure 91).[396] Reaction of barium metal with pyrazole in boiling THF generates the hexanuclear complex $[Ba_6(THF)_6(dmpz)_8\{(OSiMe_2)_2O\}]$ **178**, whose formation apparently involves the cleavage of *cyclo*-$(Me_2SiO)_4$ in

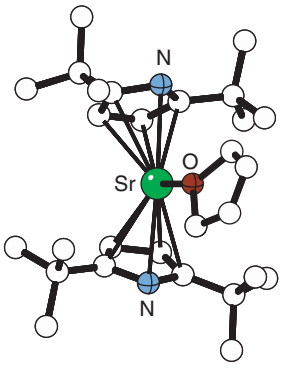

Figure 91 The structure of the bis(pyrrolyl)strontium complex **177**.

silone joint grease.[397] The structure is centered on a rhomboid layer of six barium cations in four adjacent equilateral triangles (Figure 92); three types of σ/π-coordinated pyrazolates are present with long (>3.15 Å) Ba–C contacts. If 3,5-Bu^t_2-pyrazole is heated with calcium, strontium, and barium at 250 °C, the polynuclear complexes $Ca_3(Bu^t_2pz)_6$ **179** (Figure 93), $Sr_4(Bu^t_2pz)_8$, and $Ba_6(Bu^t_2pz)_{12}$ are isolated, respectively.[398] All three compounds display various binding modes to the pyrazolates, including terminal η^2 (Ca, Sr, Ba); μ-η^2:η^2 (Ca, Ba); μ-η^2:η^3 (Sr); μ-η^2:η^4 (Ba); and μ-η^2:η^5 (Sr, Ba).

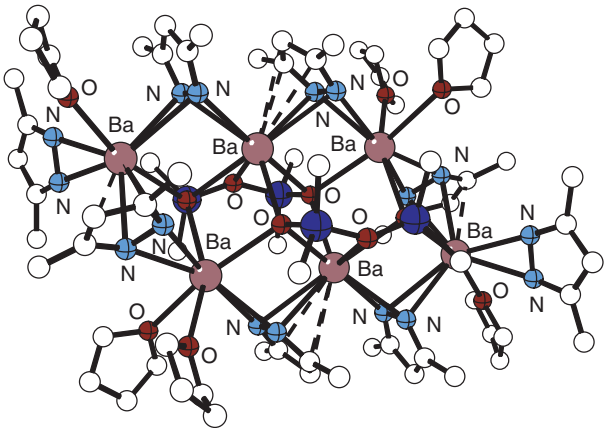

Figure 92 The structure of the hexanuclear barium complex **178**.

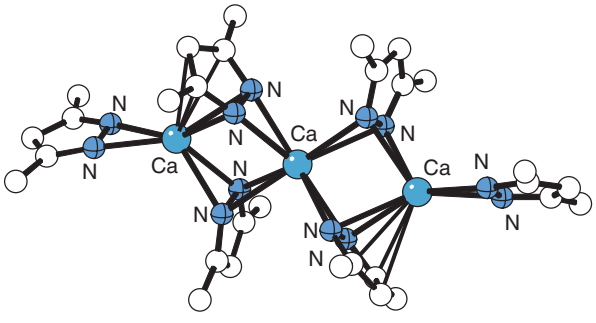

Figure 93 The structure of the trinuclear complex **179** (Bu^t groups are not shown for clarity).

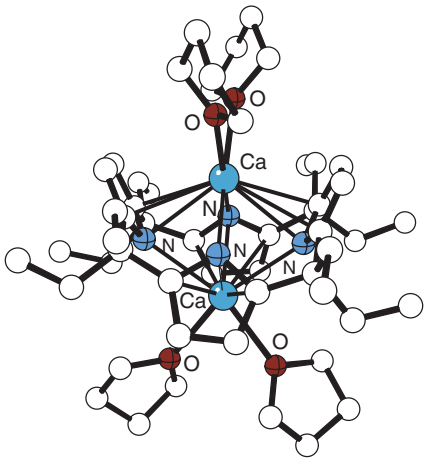

Figure 94 The structure of the dimetallic complex $Ca_2(oepg)(THF)_4$ **180**.

Porphyrins have been incorporated into several varieties of organometallic complexes that display cation–π interactions. A suspension of calcium metal ions added to a THF solution of *meso*-octaethylporphyrinogen (*meso*-oepg) at room temperature produces dimetallic complex $Ca_2(oepg)(THF)_4$ **180** in 73% yield. In the solid state, the pyrrolyl anions display η^3/η^1-bonding and bridge the two calcium cations (Figure 94).[399] A solution of $Et_8N_4Li_4(THF)_4$ and **180** in THF heated under reflux forms the calcium–lithium complex $CaLi_3(oepg)(THF)_3$ **181** in 85% yield. The calcium is η^5-bonded to *trans*-anions and η^1-bonded to the other pair of anions which are also η^3-bonded to lithium (Figure 95).[399]

The metallation of *meso*-octaalkylporphyrinogens $R_8N_4H_4$ (R = Et; Bu^n) with the alkaline earth metals (M = Ca, Sr, Ba) leads to dinuclear compounds $R_8N_4M_2$ (R = Et, M = Ca, Sr, Ba; R = Bu^n, M = Ba), in which both metals inside the cavity are $\eta^1{:}\eta^3{:}\eta^1{:}\eta^3$ (Ca) and $\eta^1{:}\eta^5{:}\eta^1{:}\eta^5$ (Sr and Ba) bonded to the porphyrinogen tetraanion.[400] The coordination sphere of each metal ion is completed by two THF molecules, which, in the barium complex, are easily replaced by various arene rings to form $Bu_8N_4Ba_2(\eta^6\text{-arene})_2$ **182** (Figure 96). Complexes with a single group 2 metal are formed when the dinuclear compounds are treated with the lithium porphyrinogen $Et_8N_8Li_4(THF)_4$; one alkaline

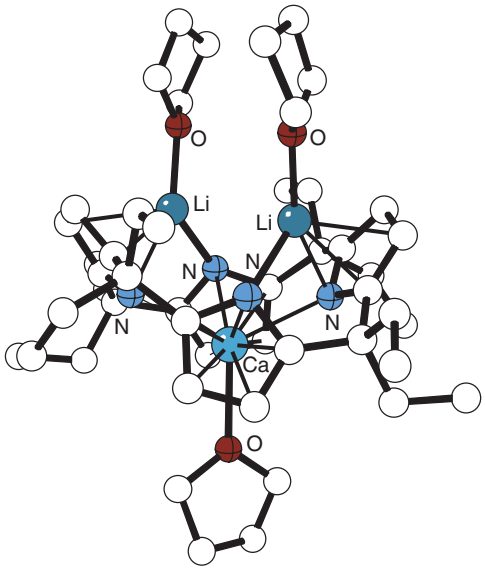

Figure 95 The structure of the the calcium–lithium complex $CaLi_3(oepg)(THF)_3$ **181**.

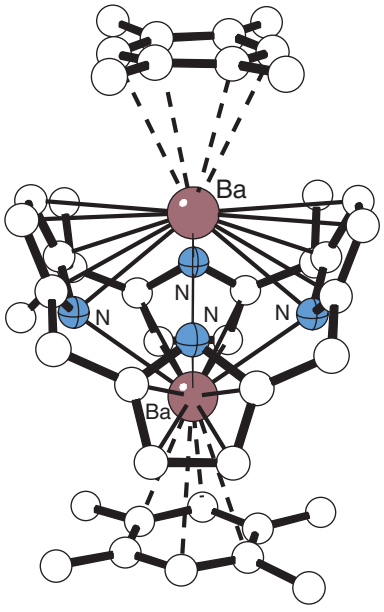

Figure 96 The structure of the porphyrinogen complex $Bu_8N_4Ba_2(\eta^6\text{-durene})_2$ **182** (butyl groups have been removed for clarity).

earth cation is replaced by two lithium cations. Analysis of the ^1H NMR spectra of the complexes indicates that the solid-state structures are retained in solution.[400]

Monomeric bis(phosphinimino)methyl derivatives of calcium, strontium, and barium have been obtained by addition of 2 molar equiv. of $K[N(SiMe_3)_2]$ to a mixture of $CH_2(Ph_2PNC_6H2\text{–}Me_3\text{-}2,4,6)_2$ and MI_2 (M = Ca, Sr, Ba) in THF.[401] The calcium and strontium **183** complexes both contain a five-coordinate metal center as part of a five-membered MNPCPN metallocycle (Figure 97). The bis(phosphinoimino)methyl ligand functions as a tridentate donor through the phosphinimino nitrogens and the C(1) carbon (Ca–C = 2.713(7); Sr–C = 2.861(2) Å). Both complexes are effective initiators for the ring-opening polymerization of *rac*-lactide in THF. The barium analog is not isostructural, and has no close Ba–C contacts.

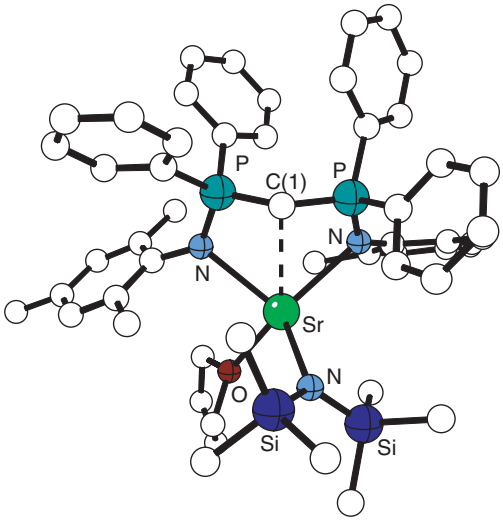

Figure 97 The structure of the strontium bis(phosphinimino)methyl complex **183**.

2.02.4.5 Heterobimetallic Compounds

$Ba[(\mu\text{-}CH_2SiMe_3)_2ZnCH_2SiMe_3]_2$, synthesized from $Zn(CH_2SiMe_3)_2$ and distilled barium, undergoes transmetallation with additional barium in heptane under application of ultrasound to give $Ba_4[Me_3SiCHZn(CH(SiMe_3)Zn(CH_2SiMe_3)_2)_2]_2$ **184**.[402] The central $Ba_4Zn_2C_6$ core can be regarded as a distorted double cube with a common Ba_2C_2 face (Figure 98). Several of the carbon atoms show an unusual high coordination number with distorted octahedral coordination spheres. The Ba–C bond lengths within the $Ba_4Zn_2C_6$ cage vary between 2.84 and 3.20 Å; the coordination spheres of the barium atoms are completed by agostic bonds to methylene groups.

The reaction of $Ca[N(SiMe_3)_2]_2$ or $Sr[N(SiMe_3)_2]_2$ with Et_3Ga produces the aminogallates $[CH_2(Me)GaEt_2N(SiMe_3)_2]_2Ca$ **185** (Figure 99)[403] and $[CH_2(Me)GaEt_2N(SiMe_3)_2]_2Sr$,[404] respectively. In the solid state, the group 2 atoms are coordinated by two nitrogen atoms and two ethyl groups, and display M–C–Ga two-electron three-center bonds (mean distances: Ca–N = 2.43, Ca–C = 2.68, Sr–N = 2.59, Sr–C = 2.82 Å). In solution, fast exchange of the bridging and terminal ethyl groups is observed on the NMR time scale for both compounds.

The poly(pyrazolyl) complex $Ba(3,5\text{-dimethylpyrazol-1-yl})_2$ is formed from the reaction of barium metal and 3,5-dimethylpyrazole in refluxing THF. Subsequent reaction of the barium complex with $GeCl_2$·dioxane in THF produces $Ba[(3,5\text{-dimethylpyrazol-1-yl})_3Ge]_2(dioxane)_{0.5}$ **186**.[405] Four of the anionic ligands are coordinated via their nitrogen atoms in a σ-fashion (av. Ba–N = 2.80(3) Å), but two of the pyrazolyl groups are bound η^2 to the barium (Figure 100). There is a large spread in the ring–barium contact distances; the η^2 Ba–N lengths are longer than the σ-coordinated nitrogens, with the Ba–C distances ranging up to 3.28 Å. The energetic significance of the long-range Ba–C interactions is difficult to access, but both η^2-coordinated pyrazolyl rings are located *cis* with respect to the barium, even though a *trans*-arrangement would minimize steric interactions.

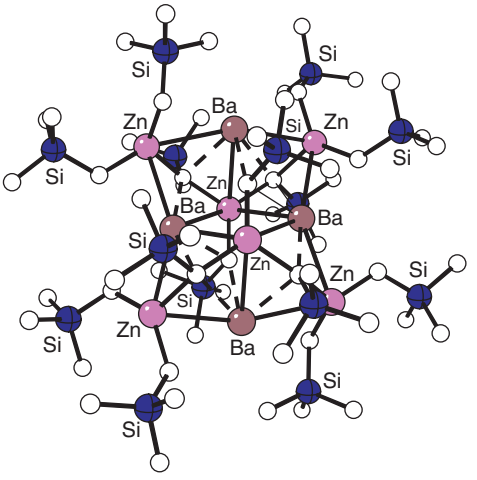

Figure 98 The structure of the bimetallic barium–zinc complex **184**.

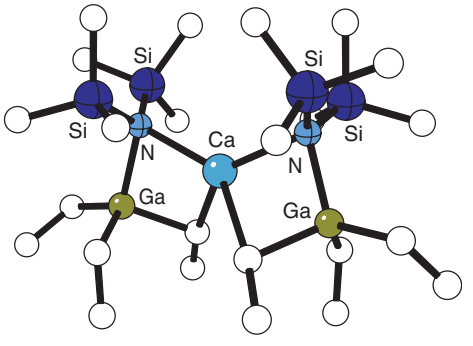

Figure 99 The structure of the aminogallate $[CH_2(Me)GaEt_2N(SiMe_3)_2]_2Ca$ **185**.

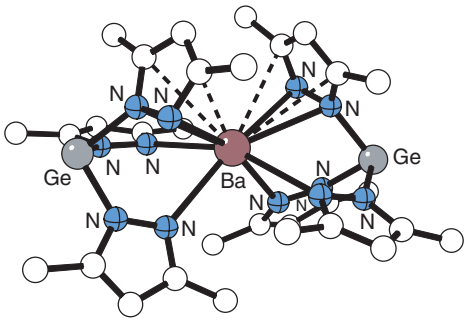

Figure 100 The structure of the dimeric complex Ba[(3,5-dimethylpyrazol-1-yl)$_3$Ge]$_2$(dioxane)$_{0.5}$ **186**.

References

1. Barbier, P. *Compt. Rend.* **1898**, *128*, 110.
2. Matthews, J. S.; Rees, W. S., Jr. *Adv. Inorg. Chem.* **2000**, *50*, 173–192.
3. Wojtczak, W. A.; Fleig, P. F.; Hampden-Smith, M. J. *Adv. Organomet. Chem.* **1996**, *40*, 215–340.
4. Hanusa, T. P. *Organometallics* **2002**, *21*, 2559–2571.
5. Corlett, G. K.; Patel, K.; Wheeler, M. D.; Ellis, A. M. *Phys. Chem. Chem. Phys.* **2003**, *5*, 36–40.
6. Chan, W.-T.; Hamilton, I. P. *Chem. Phys. Lett.* **1998**, *297*, 217–224.
7. Chan, W. T.; Hamilton, I. P. *Chem. Phys. Lett* **2000**, *316*, 171–175.
8. Ketvirtis, A. E.; Simons, J. *J. Am. Chem. Soc.* **2000**, *122*, 369–377.
9. Zhao, X. L.; Nadeau, M. J.; Garwan, M. A.; Kilius, L. R.; Litherland, A. E. *Nucl. Instrum. Methods Phys. Res., Sect. B* **1994**, *92*, 258–264.
10. Thompson, C. A.; Andrews, L. *J. Am. Chem. Soc.* **1996**, *118*, 10242–10249.
11. Greene, T. M.; Lanzisera, D. V.; Andrews, L.; Downs, A. J. *J. Am. Chem. Soc.* **1998**, *120*, 6097–6104.
12. Nemukhin, A. V.; Topol, I. A.; Weinhold, F. *Inorg. Chem.* **1995**, *34*, 2980–2983.
13. Peralez, E.; Negrel, J. C.; Goursot, A.; Chanon, M. *Main Group Met. Chem.* **1999**, *22*, 201–207.
14. Jasien, P. G.; Abbondondola, J. A. *Theochem* **2004**, *671*, 111–118.
15. Tjurina, L. A.; Smirnov, V. V.; Barkovskii, G. B.; Nikolaev, E. N.; Esipov, S. E.; Beletskaya, I. P. *Organometallics* **2001**, *20*, 2449–2450.
16. Bernath, P. F. *Adv. Photochem.* **1997**, *23*, 1–62.
17. Ruschewitz, U. *Coord. Chem. Rev.* **2003**, *244*, 115–136.
18. Eaborn, C.; Farook, A.; Hitchcock, P. B.; Smith, J. D. *Organometallics* **1997**, *16*, 503–504.
19. Holloway, C. E.; Melnik, M. *J. Organomet. Chem.* **1994**, *465*, 1–63.
20. Wei, P.; Stephan, D. W. *Organometallics* **2003**, *22*, 601–604.
21. Ma, J. C.; Dougherty, D. A. *Chem. Rev.* **1997**, *97*, 1303–1324.
22. Deacon, G. B.; Forsyth, C. M.; Junk, P. C. *J. Organomet. Chem.* **2000**, *607*, 112–119.
23. Westerhausen, M.; Krofta, M.; Wiberg, N.; Knizek, J.; Nöth, H.; Pfitzner, A. *Z. Naturforsch., B: Chem. Sci.* **1998**, *53*, 1489–1493.
24. Sockwell, S. C.; Hanusa, T. P. *Inorg. Chem.* **1990**, *29*, 76–80.
25. Shannon, R. D. *Acta Crystallogr., Sect A.* **1976**, *32*, 751–767.
26. Hanusa, T. P. *Chem. Rev.* **1993**, *93*, 1023–1036.
27. Snow, A. I.; Rundle, R. E. *Acta Cryst.* **1951**, *4*, 348–352.
28. Kovar, R. A.; Morgan, G. L. *Inorg. Chem.* **1969**, *8*, 1099–1103.
29. Niemeyer, M.; Power, P. P. *Inorg. Chem.* **1997**, *36*, 4688–4696.
30. Clyburne, J. A. C.; McMullen, N. *Coord. Chem. Rev.* **2000**, *210*, 73–99.
31. Burns, C. J.; Andersen, R. A. *J. Organomet. Chem.* **1987**, *325*, 31–37.
32. Battle, S. L.; Cowley, A. H.; Decken, A.; Jones, R. A.; Koschmieder, S. U. *J. Organomet. Chem.* **1999**, *582*, 66–69.
33. Plieger, P. G.; John, K. D.; Keizer, T. S.; McCleskey, T. M.; Burrell, A. K.; Martin, R. L. *J. Am. Chem. Soc.* **2004**, *126*, 14651–14658.
34. Ruhlandt-Senge, K.; Bartlett, R. A.; Olmstead, M. M.; Power, P. P. *Inorg. Chem.* **1993**, *32*, 1724–1728.
35. Jutzi, P.; Burford, N. *Chem. Rev.* **1999**, *99*, 969–990.
36. Jutzi, P. *Chem. Unserer Zeit* **1999**, *33*, 343–353.
37. Burkey, D. J.; Hanusa, T. P. *Comments Inorg. Chem.* **1995**, *17*, 41–77.
38. Fischer, E. O.; Hofmann, H. P. *Chem. Ber.* **1959**, *92*, 482–486.
39. Pratten, S. J.; Cooper, M. K.; Aroney, M. J. *J. Organomet. Chem.* **1990**, *381*, 147–153.
40. del Mar Conejo, M.; Fernandez, R.; Gutierrez-Puebla, E.; Monge, A.; Ruiz, C.; Carmona, E. *Angew. Chem., Int. Ed.* **2000**, *39*, 1949–1951.
41. Almenningen, A.; Bastiansen, O.; Haaland, A. *J. Chem. Phys.* **1964**, *40*, 3434–3437.
42. Almenningen, A.; Haaland, A.; Lusztyk, J. *J. Organomet. Chem.* **1979**, *170*, 271–284.
43. Lustyk, J.; Starowieyski, K. B. *J. Organomet. Chem.* **1979**, *170*, 293–297.
44. Wong, C. H.; Lee, T. Y.; Lee, T. J.; Chang, T. W.; Liu, C. S. *Acta Crystallogr. Sect. B* **1972**, *28*, 1662–1665.
45. Wong, C.; Lee, T. Y.; Lee, T. J.; Chang, T. W.; Liu, C. S. *Inorg. Nucl. Chem. Lett.* **1973**, *9*, 667–673.
46. Nugent, K. W.; Beattie, J. K.; Hambley, T. W.; Snow, M. R. *Aust. J. Chem.* **1984**, *37*, 1601–1606.
47. Margl, P.; Schwarz, K.; Blochl, P. E. *J. Chem. Phys.* **1995**, *103*, 683–690.
48. Margl, P.; Schwarz, K.; Bloechl, P. E. *J. Am. Chem. Soc.* **1994**, *116*, 11177–11178.
49. Mire, L. W.; Wheeler, S. D.; Wagenseller, E.; Marynick, D. S. *Inorg. Chem.* **1998**, *37*, 3099–3106.
50. Hung, I.; Macdonald, C. L. B.; Schurko, R. W. *Chem. —Eur. J.* **2004**, *10*, 5923–5935.

51. Beattie, J. K.; Nugent, K. W. *Inorg. Chim. Acta* **1992**, *198–200*, 309–318.
52. Nugent, K. W.; Beattie, J. K.; Field, L. D. *J. Phys. Chem.* **1989**, *93*, 5371–5377.
53. Margl, P.; Schwarz, K.; Blöchl, P. E. *J. Am. Chem. Soc.* **1994**, *116*, 11177–11178.
54. Mitsuhara, M.; Ogasawara, M.; Sugiura, H. *J. Cryst. Growth* **1998**, *183*, 38–42.
55. Salazar, K. V.; Pattillo, S. G.; Trkula, M. *Fusion Technol.* **2000**, *38*, 69–73.
56. Harvey, M. J.; Quisenberry, K. T.; Hanusa, T. P.; Young, V. G., Jr. *Eur. J. Inorg. Chem.* **2003**, 3383–3390.
57. Pauling, L. *The Nature of the Chemical Bond*, 3rd ed.; Cornell University Press: Ithaca, 1960.
58. del Mar Conejo, M.; Fernandez, R.; del Rio, D.; Carmona, E.; Monge, A.; Ruiz, C.; Marquez, A. M.; Sanz, F. J. *Chem. —Eur. J.* **2003**, *9*, 4452–4461.
59. del Mar Conejo, M.; Fernandez, R.; Carmona, E.; Andersen, R. A.; Gutierrez-Puebla, E.; Monge, M. A. *Chem. —Eur. J.* **2003**, *9*, 4462–4471.
60. del Mar Conejo, M.; Fernandez, R.; Carmona, E.; Gutierrez-Puebla, E.; Monge, A. *Organometallics* **2001**, *20*, 2434–2436.
61. Conejo, M. M.; Fernandez, R.; del Rio, D.; Carmona, E.; Monge, A.; Ruiz, C. *Chem. Commun.* **2002**, 2916–2917.
62. Saulys, D. A.; Powell, D. R. *Organometallics* **2003**, *22*, 407–413.
63. Lerner, H.-W.; Scholz, S.; Bolte, M.; Wiberg, N.; Noth, H.; Krossing, I. *Eur. J. Inorg. Chem.* **2003**, 666–670.
64. Andrews, L.; Tague, T. J., Jr.; Kushto, G. P.; Davy, R. D. *Inorg. Chem.* **1995**, *34*, 2952–2961.
65. Andrews, L.; Tague, T. J., Jr. *J. Am. Chem. Soc.* **1994**, *116*, 6856–6859.
66. Arduengo, A. J.; Dias, H. V. R.; Harlow, R. L.; Kline, M. *J. Am. Chem. Soc.* **1992**, *114*, 5530–5534.
67. Herrmann, W. A.; Runte, O.; Artus, G. *J. Organomet. Chem.* **1995**, *501*, C1–C4.
68. Fröhlich, N.; Pidun, U.; Stahl, M.; Frenking, G. *Organometallics* **1997**, *16*, 442–448.
69. Gaines, D. F.; Coleson, K. M.; Hillenbrand, D. F. *J. Magn. Reson.* **1981**, *44*, 84–88.
70. Drew, D. A.; Morgan, G. L. *Inorg. Chem.* **1977**, *16*, 1704–1708.
71. Naeth, H.; Schlosser, D. *Eur. J. Inorg. Chem.* **2003**, 2245–2254.
72. Lawrence, L. M.; Whitesides, G. M. *J. Am. Chem. Soc.* **1980**, *102*, 2493–2494.
73. Walborsky, H. M. *Acc. Chem. Res.* **1990**, *23*, 286–293.
74. Walling, C. *Acc. Chem. Res.* **1991**, *24*, 255–256.
75. Walborsky, H. M.; Zimmermann, C. *J. Am. Chem. Soc.* **1992**, *114*, 4996–5000.
76. Garst, J. F.; Ronald, B. J.; Webb, L.; Easton, L. K.; Baxter, J. T.; Ungvary, F. *Inorg. Chim. Acta* **1999**, *296*, 52–66.
77. Wakefield, B. J. In *Organomagnesium Methods in Organic Synthesis*; Katritzky, A. R., Meth-Cohn, O., Best Synthetic Methods Series. Rees, C. W., Eds.; Academic Press: San Diego, 1995.
78. Silverman, G. S., Rakita, P. E., Eds.; *Handbook of Grignard Reagents*; Dekker: Monticello, 1996.
79. Richey, H. G., Jr., Ed.; *Grignard Reagents: New Developments*; Wiley: Chicester, 2000.
80. Knochel, P.; Dohle, W.; Gommermann, N.; Kneisel, F. F.; Kopp, F.; Korn, T.; Sapountzis, I.; Vu, V. A. *Angew. Chem., Int. Ed.* **2003**, *42*, 4302–4320.
81. Rieke, R. D.; Burns, T. P.; Wehmeyer, R. M.; Kahn, B. E. *ACS Symp. Ser.* **1987**, *333*, 223–245.
82. Tuulmets, A.; Mikk, M.; Panov, D. *J. Organomet. Chem.* **1996**, *523*, 133–138.
83. Tuulmets, A.; Panov, D. *J. Organomet. Chem.* **1999**, *575*, 182–186.
84. Tuulmets, A.; Raik, P. *Ultrason. Sonochem.* **1999**, *6*, 85–87.
85. Tidwell, T. T. *Angew. Chem., Int. Ed.* **2001**, *40*, 331–337.
86. Garst, J. F.; Lawrence, K. E.; Batlaw, R.; Boone, J. R.; Ungvary, F. *Inorg. Chim. Acta* **1994**, *222*, 365–275.
87. Al-Juaid, S. S.; Eaborn, C.; Hitchcock, P. B.; Jaggar, A. J.; Smith, J. D. *J. Organomet. Chem.* **1994**, *469*, 129–133.
88. Pällin, V.; Otsa, E.; Tuulmets, A. *J. Organomet. Chem.* **1999**, *590*, 149–152.
89. Pallin, V.; Tuulmets, A. *J. Organomet. Chem.* **1999**, *584*, 185–189.
90. Tuulmets, A.; Sassian, M. *J. Organomet. Chem.* **1999**, *586*, 145–149.
91. Sassian, M.; Tuulmets, A. *Helv. Chim. Acta* **2003**, *86*, 82–90.
92. Rueffer, T.; Bruhn, C.; Steinborn, D. *Z. Anorg. Allg. Chem.* **2001**, *627*, 2408–2412.
93. Bogdanovic, B.; Schwickardi, M. *Angew. Chem., Int. Ed.* **2000**, *39*, 4610–4612.
94. Bickelhaupt, F. *Chem. Soc. Rev.* **1999**, *28*, 17–23.
95. Reck, C. E.; Winter, C. H. *Organometallics* **1997**, *16*, 4493–4496.
96. Li, C.-J.; Zhang, W.-C. *J. Am. Chem. Soc.* **1998**, *120*, 9102–9103.
97. Zhang, W.-C.; Li, C.-J. *J. Org. Chem.* **1999**, *64*, 3230–3236.
98. Deng, W.; Tan, X.-H.; Liu, L.; Guo, Q.-X. *Chin. J. Chem.* **2004**, *22*, 747–750.
99. Zhang, W.-C.; Hua, X.-G.; Meng, Y.; Venkatraman, S.; Keh, C. C. K.; Li, C.-J. *Recent Res. Dev. Org. Chem.* **2000**, *4*, 397–411.
100. Li, C.-J. *Green Chem.* **2002**, *4*, 1–4.
101. Lindstroem, U. M. *Chem. Rev.* **2002**, *102*, 2751–2771.
102. Li, C.-J.; Haberman, J. X.; Keh, C. C. K.; Yi, X.-H.; Meng, Y.; Hua, X.-G.; Venkatraman, S.; Zhang, W.-C.; Nguyen, T., Wang, D., *et al. ACS Symp. Ser.* **2002**, *819*, 178–190.
103. Li, C.-J.; Wang, D. *Chemtracts* **2003**, *16*, 59–78.
104. Harrowfield, J. M.; Hart, R. J.; Whitaker, C. R. *Aust. J. Chem.* **2001**, *54*, 423–425.
105. Bare, W. D.; Andrews, L. *J. Am. Chem. Soc.* **1998**, *120*, 7293–7301.
106. Bare, W. D.; Citra, A.; Trindle, C.; Andrews, L. *Inorg. Chem.* **2000**, *39*, 1204–1215.
107. Boymond, L.; Rottlander, M.; Cahiez, G.; Knochel, P. *Angew. Chem., Int. Ed.* **1998**, *37*, 1701–1703.
108. van den Ancker, T. R.; Harvey, S.; Raston, C. L. *J. Organomet. Chem.* **1995**, *502*, 35–46.
109. van den Ancker, T. R.; Raston, C. L. *Organometallics* **1995**, *14*, 584–585.
110. Antolini, F.; Hitchcock, P. B.; Lappert, M. F.; Wei, X.-H. *Organometallics* **2003**, *22*, 2505–2516.
111. Hibbs, D. E.; Jones, C.; Richards, A. F. *J. Chem. Soc., Dalton Trans.* **1999**, 3531–3532.
112. Renner, J.; Bergstrasser, U.; Binger, P.; Regitz, M. *Eur. J. Inorg. Chem.* **2000**, 2337–2340.
113. Hoffmann, R. W.; Nell, P. G.; Leo, R.; Harms, K. *Chem. —Eur. J.* **2000**, *6*, 3359–3365.
114. Hoffmann, R. W. *Chem. Soc. Rev.* **2003**, *32*, 225–230.
115. Hoffmann, R. W.; Hoelzer, B.; Knopff, O. *Org. Lett.* **2001**, *3*, 1945–1948.
116. Hoffmann, R. W.; Holzer, B. *Chem. Commun.* **2001**, 491–492.

117. Hoelzer, B.; Hoffmann, R. W. *Chem. Commun.* **2003**, 732–733.
118. Hoffmann, R. W.; Holzer, B.; Knopff, O.; Harms, K. *Angew. Chem., Int. Ed.* **2000**, *39*, 3072–3074.
119. Hoffmann, R. W.; Hoelzer, B. *J. Am. Chem. Soc.* **2002**, *124*, 4204–4205.
120. Sapountzis, I.; Dohle, W.; Knochel, P. *Chem. Commun.* **2001**, 2068–2069.
121. Vestergren, M.; Gustafsson, B.; Davidsson, O.; Hakansson, M. *Angew. Chem., Int. Ed.* **2000**, *39*, 3435–3437.
122. Vestergren, M.; Eriksson, J.; Hakansson, M. *Chem. —Eur. J.* **2003**, *9*, 4678–4686.
123. Vestergren, M.; Eriksson, J.; Hakansson, M. *J. Organomet. Chem.* **2003**, *681*, 215–224.
124. Egorov, A. M.; Anisimov, A. V. *J. Organomet. Chem.* **1994**, *479*, 197–198.
125. Egorov, A. M.; Anisimov, A. V. *J. Organomet. Chem.* **1995**, *495*, 131–134.
126. Holloway, C. E.; Melnik, M. *Coord. Chem. Rev.* **1994**, *135–136*, 287–301.
127. Bickelhaupt, F. *J. Organomet. Chem.* **1994**, *475*, 1–14.
128. Abraham, I.; Hoerner, W.; Ertel, T. S.; Bertagnolli, H. *Polyhedron* **1996**, *15*, 3993–4001.
129. Al-Juaid, S. S.; Avent, A. G.; Eaborn, C.; El-Hamruni, S. M.; Hawkes, S. A.; Hill, M. S.; Hopman, M.; Hitchcock, P. B.; Smith, J. D. *J. Organomet. Chem.* **2001**, *631*, 76–86.
130. Al-Juaid, S. S.; Eaborn, C.; Hitchcock, P. B.; Hill, M. S.; Smith, J. D. *Organometallics* **2000**, *19*, 3224–3231.
131. Bock, H.; Ziemer, K.; Naether, C. *J. Organomet. Chem.* **1996**, *511*, 29–35.
132. Ellison, J. J.; Power, P. P. *J. Organomet. Chem.* **1996**, *526*, 263–267.
133. Wehmschulte, R. J.; Twamley, B.; Khan, M. A. *Inorg. Chem.* **2001**, *40*, 6004–6008.
134. Eaborn, C.; Hitchcock, P. B.; Kowalewska, A.; Lu, Z.-R.; Smith, J. D.; Stanczyk, W. A. *J. Organomet. Chem.* **1996**, *521*, 113–120.
135. Boche, G.; Harms, K.; Marsch, M.; Mueller, A. *J. Chem. Soc., Chem. Commun.* **1994**, 1393–1394.
136. Hill, E. A.; Boyd, W. A.; Desai, H.; Darki, A.; Bivens, L. *J. Organomet. Chem.* **1996**, *514*, 1–11.
137. Chen, C.-T.; Huang, C.-A.; Tzeng, Y.-R.; Huang, B.-H. *Dalton Trans.* **2003**, 2585–2590.
138. Yang, K.-C.; Chang, C.-C.; Huang, J.-Y.; Lin, C.-C.; Lee, G.-H.; Wang, Y.; Chiang, M. Y. *J. Organomet. Chem.* **2002**, *648*, 176–187.
139. Batsanov, A. S.; Bolton, P. D.; Copley, R. C. B.; Davidson, M. G.; Howard, J. A. K.; Lustig, C.; Price, R. D. *J. Organomet. Chem.* **1998**, *550*, 445–448.
140. Chisholm, M. H.; Huffman, J. C.; Phomphrai, K. *J. Chem. Soc., Dalton Trans.* **2001**, *222–224*.
141. Ruben, M.; Walther, D.; Knake, R.; Gorls, H.; Beckert, R. *Eur. J. Inorg. Chem.* **2000**, 1055–1060.
142. Muller, A.; Krieger, M.; Neumuller, B.; Dehnicke, K.; Magull, J. *Z. Anorg. Allg. Chem.* **1997**, *623*, 1081–1087.
143. Vohs, J. K.; Ellen Downs, L.; Barfield, M. E.; Latibeaudiere, K.; Robinson, G. H. *J. Organomet. Chem.* **2003**, *666*, 7–13.
144. Hanssen, R. W.; Meetsma, A.; van Santen, R. A.; Abbenhuis, H. C. *Inorg. Chem.* **2001**, *40*, 4049–4052.
145. Hoffmann, R. W.; Mueller, M.; Menzel, K.; Gschwind, R.; Schwerdtfeger, P.; Malkina, O. L.; Malkin, V. G. *Organometallics* **2001**, *20*, 5310–5313.
146. Charette, A. B.; Gagnon, A.; Belanger-Gariepy, F. *Acta Crystallogr., Sect. C* **2000**, *C56*, 538–540.
147. Prust, J.; Most, K.; Muller, I.; Alexopoulos, E.; Stasch, A.; Uson, I.; Roesky, H. W. *Z. Anorg. Allg. Chem.* **2001**, *627*, 2032–2037.
148. Nöth, H.; Waldhor, R. *Z. Naturforsch., B: Chem. Sci.* **1999**, *54*, 603–608.
149. Kuhn, N.; Fawzi, R.; Steimann, M.; Wiethoff, J. *Z. Anorg. Allg. Chem.* **1997**, *623*, 554–560.
150. Srinivas, B.; Chang, C.-C.; Chen, C.-H.; Chiang, M. Y.; Chen, I. T.; Wang, Y.; Lee, G.-H. *J. Chem. Soc., Dalton Trans.* **1997**, 957–963.
151. Zhang, W.; Hu, J.-P.; Ding, X.-F.; Wu, Y.-J.; Ye, Z.-W. *Inorg. Chem. Commun.* **2003**, *6*, 1185–1187.
152. Yousef, R. I.; Ruffer, T.; Schmidt, H.; Steinborn, D. *J. Organomet. Chem.* **2002**, *655*, 111–114.
153. Seneviratne, K. N.; Bretschneider-Hurley, A.; Winter, C. H. *J. Am. Chem. Soc.* **1996**, *118*, 5506–5507.
154. Eaborn, C.; Smith, J. D. *J. Chem. Soc., Dalton Trans.* **2001**, 1541–1552.
155. Al-Juaid, S. S.; Eaborn, C.; Hitchcock, P. B.; Kundu, K.; McGeary, C. A.; Smith, J. D. *J. Organomet. Chem.* **1994**, *480*, 199–203.
156. Bailey, P. J.; Coxall, R. A.; Dick, C. M.; Fabre, S.; Henderson, L. C.; Herber, C.; Liddle, S. T.; Lorono-Gonzalez, D.; Parkin, A.; Parsons, S. *Chem. —Eur. J.* **2003**, *9*, 4820–4828.
157. Ruffer, T.; Bruhn, C.; Steinborn, D. *Main Group Met. Chem.* **2001**, *24*, 369–372.
158. Steinborn, D.; Ruffer, T.; Bruhn, C.; Heinemann, F. W. *Polyhedron* **1998**, *17*, 3275–3280.
159. Strohmann, C.; Abele, B. C.; Schildbach, D.; Strohfeldt, K. *Chem. Commun.* **2000**, 865–866.
160. Waggoner, K. M.; Power, P. P. *Organometallics* **1992**, *11*, 3209–3214.
161. Gruter, G.-J. M.; van Klink, G. P. M.; Akkerman, O. S.; Bickelhaupt, F. *Chem. Rev.* **1995**, *95*, 2405–2456.
162. Thönnes, D.; Weiss, E. *Chem. Ber.* **1978**, *111*, 3381–3384.
163. Viebrock, H.; Weiss, E. *J. Organomet. Chem.* **1994**, *464*, 121–126.
164. Barnett, N. D. R.; Clegg, W.; Mulvey, R. E.; O'Neil, P. A.; Reed, D. *J. Organomet. Chem.* **1996**, *510*, 297–300.
165. Starowieyski, K. B.; Lewinski, J.; Wozniak, R.; Lipkowski, J.; Chrost, A. *Organometallics* **2003**, *22*, 2458–2463.
166. Gardiner, M. G.; Raston, C. L.; Cloke, F. G. N.; Hitchcock, P. B. *Organometallics* **1995**, *14*, 1339–1353.
167. Eriksson, H.; Oertendahl, M.; Haakansson, M. *Organometallics* **1996**, *15*, 4823–4831.
168. Viebrock, H.; Behrens, U.; Weiss, E. *Angew. Chem., Int. Ed. Engl.* **1994**, *33*, 1257–1259.
169. Seidel, N.; Jacob, K.; Fischer, A. K.; Pietzsch, C.; Zanello, P.; Fontani, M. *Eur. J. Inorg. Chem.* **2001**, 145–151.
170. Viebrock, H.; Abeln, D.; Weiss, E. *Z. Naturforsch., B: Chem. Sci.* **1994**, *49*, 89–99.
171. Bailey, P. J.; Liddle, S. T.; Morrison, C. A.; Parsons, S. *Angew. Chem., Int. Ed.* **2001**, *40*, 4463–4466.
172. Wehmschulte, R. J.; Power, P. P. *Organometallics* **1995**, *14*, 3264–3267.
173. Chubb, J. E.; Richey, H. G., Jr. *Organometallics* **2002**, *21*, 3661–3666.
174. Chubb, J. E.; Richey, H. G., Jr. *Organometallics* **2003**, *22*, 5141–5143.
175. Tang, H.; Parvez, M.; Richey, H. G., Jr. *Organometallics* **2000**, *19*, 4810–4819.
176. Zhang, M.-X.; Eaton, P. E. *Angew. Chem., Int. Ed.* **2002**, *41*, 2169–2171.
177. Chadwick, S.; Englich, U.; Senge, M. O.; Noll, B. C.; Ruhlandt-Senge, K. *Organometallics* **1998**, *17*, 3077–3086.
178. Chadwick, S.; Englich, U.; Ruhlandt-Senge, K. *Inorg. Chem.* **1999**, *38*, 6289–6293.
179. Pedrares, A. S.; Teng, W.; Ruhlandt-Senge, K. *Chem. —Eur. J.* **2003**, *9*, 2019–2024.
180. Clegg, W.; Horsburgh, L.; Mulvey, R. E.; Ross, M. J.; Rowlings, R. B.; Wilson, V. *Polyhedron* **1998**, *17*, 1923–1930.
181. Forbes, G. C.; Kennedy, A. R.; Mulvey, R. E.; Rodger, P. J. A.; Rowlings, R. B. *J. Chem. Soc., Dalton Trans.* **2001**, 1477–1484.
182. Kennedy, A. R.; Mulvey, R. E.; Schulte, J. H. *Acta Crystallogr., Sect. C* **2001**, *57*, 1288–1289.

183. Drummond, A. M.; Gibson, L. T.; Kennedy, A. R.; Mulvey, R. E.; O'Hara, C. T.; Rowlings, R. B.; Weightman, T. *Angew. Chem., Int. Ed.* **2002**, *41*, 2382–2384.
184. Hevia, E.; Kenley, F. R.; Kennedy, A. R.; Mulvey, R. E.; Rowlings, R. B. *Eur. J. Inorg. Chem.* **2003**, 3347–3353.
185. Olmstead, M. M.; Grigsby, W. J.; Chacon, D. R.; Hascall, T.; Power, P. P. *Inorg. Chim. Acta* **1996**, *251*, 273–284.
186. Vargas, W.; Englich, U.; Ruhlandt-Senge, K. *Inorg. Chem.* **2002**, *41*, 5602–5608.
187. Yang, K.-C.; Chang, C.-C.; Yeh, C.-S.; Lee, G.-H.; Peng, S.-M. *Organometallics* **2001**, *20*, 126–137.
188. Sachdev, H.; Wagner, C.; Preis, C.; Huch, V.; Veith, M. *J. Chem. Soc., Dalton Trans.* **2002**, 4709–4713.
189. Westerhausen, M.; Digeser, M. H.; Wieneke, B.; Nöth, H.; Knizek, J. *Eur. J. Inorg. Chem.* **1998**, 517–521.
190. Westerhausen, M.; Schneiderbauer, S.; Knizek, J.; Nöth, H.; Pfitzner, A. *Eur. J. Inorg. Chem.* **1999**, 2215–2220.
191. Blair, S.; Izod, K.; Clegg, W. *Inorg. Chem.* **2002**, *41*, 3886–3893.
192. Sachdev, H.; Preis, C. *Eur. J. Inorg. Chem.* **2002**, 1495–1501.
193. Sachdev, H. *Eur. J. Inorg. Chem.* **2002**, 2681–2685.
194. Westerhausen, M.; Krofta, M.; Pfitzner, A. *Inorg. Chem.* **1999**, *38*, 598–599.
195. Westerhausen, M.; Krofta, M.; Mayer, P.; Warchhold, M.; Nöth, H. *Inorg. Chem.* **2000**, *39*, 4721–4724.
196. Westerhausen, M.; Makropoulos, N.; Piotrowski, H.; Warchhold, M.; Nöth, H. *J. Organomet. Chem.* **2000**, *614–615*, 70–73.
197. Cole, M. L.; Jones, C.; Junk, P. C. *New J. Chem.* **2002**, *26*, 89–93.
198. Zechmann, C. A.; Boyle, T. J.; Rodriguez, M. A.; Kemp, R. A. *Polyhedron* **2000**, *19*, 2557–2564.
199. Sobota, P.; Utko, J.; Sztajnowska, K.; Ejfler, J.; Jerzykiewicz, L. B. *Inorg. Chem.* **2000**, *39*, 235–239.
200. Zechmann, C. A.; Boyle, T. J.; Rodriguez, M. A.; Kemp, R. A. *Inorg. Chim. Acta* **2001**, *319*, 137–146.
201. Andrikopoulos, P. C.; Armstrong, D. R.; Kennedy, A. R.; Mulvey, R. E.; O'Hara, C. T.; Rowlings, R. B. *Eur. J. Inorg. Chem.* **2003**, 3354–3362.
202. Drewette, K. J.; Henderson, K. W.; Kennedy, A. R.; Mulvey, R. E.; O'Hara, C. T.; Rowlings, R. B. *Chem. Commun.* **2002**, 1176–1177.
203. Kennedy, A. R.; MacLellan, J. G.; Mulvey, R. E. *Acta Crystallogr., Sect. C* **2003**, *C59*, m302–m303.
204. Henderson, K. W.; Allan, J. F.; Kennedy, A. R. *Chem. Commun.* **1997**, 1149–1150.
205. Yang, K.-C.; Chang, C.-C.; Yeh, C.-S.; Lee, G.-H.; Wang, Y. *Organometallics* **2002**, *21*, 1296–1299.
206. Mori, S.; Nakamura, M.; Nakamura, E.; Koga, N.; Morokuma, K. *J. Am. Chem. Soc.* **1995**, *117*, 5055–5065.
207. Gromada, J.; Mortreux, A.; Chenal, T.; Ziller, J. W.; Leising, F.; Carpentier, J.-F. *Chem. —Eur. J.* **2002**, *8*, 3773–3788.
208. Pelletier, J.-F.; Mortreux, A.; Olonde, X.; Bujadoux, K. *Angew. Chem., Int. Ed. Engl.* **1996**, *35*, 1854–1856.
209. Dzhemilev, U. M.; Sultanov, R. M.; Gaimaldinov, R. G. *J. Organomet. Chem.* **1995**, *491*, 1–10.
210. Weiss, E.; Fischer, E. O. *Z. Anorg. Allg. Chem.* **1955**, *278*, 219–224.
211. Bünder, W.; Weiss, E. *J. Organomet. Chem.* **1975**, *92*, 1–6.
212. Haaland, A.; Lusztyk, J.; Brunvoll, J.; Starowieyski, K. B. *J. Organomet. Chem.* **1975**, *85*, 279–285.
213. Abis, L.; Calderazzo, F.; Maichle-Mossmer, C.; Pampaloni, G.; Strahle, J.; Tripepi, G. *J. Chem. Soc., Dalton Trans.* **1998**, 841–845.
214. Dohmeier, C.; Robl, C.; Tacke, M.; Schnoeckel, H. *Angew. Chem.* **1991**, *103*, 594–595.
215. Bond, A. D.; Layfield, R. A.; MacAllister, J. A.; McPartlin, M.; Rawson, J. M.; Wright, D. S. *Chem. Commun.* **2001**, 1956–1957.
216. Smith, M. E.; Andersen, R. A. *J. Am. Chem. Soc.* **1996**, *118*, 11119–11128.
217. Jaenschke, A.; Paap, J.; Behrens, U. *Organometallics* **2003**, *22*, 1167–1169.
218. Stringfellow, G. B. *Organometallic Vapor Phase Epitaxy: Theory and Practice*; Academic Press: San Diego, 1989.
219. Hitchman, M. L., Jensen, K. F., Eds.; *Chemical Vapour Deposition*; Academic: New York, 1993.
220. Rees, W. S. Jr., Ed.; *CVD of Nonmetals*, VCH Publishers: New York, 1996.
221. Pierson, H. O. In *Handbook of Chemical Vapor Deposition: Principles, Technology, and Applications*, 2nd ed.; Noyes: Norwich, 1999.
222. Putkonen, M.; Sajavaara, T.; Niinisto, L. *J. Mater. Chem.* **2000**, *10*, 1857–1861.
223. Kuech, T. F.; Wang, P. J.; Tischler, M. A.; Potemski, R.; Scilla, G. J.; Cardone, F. *J. Cryst. Growth* **1988**, *93*, 624–630.
224. Leem, J.-Y.; Lee, C.-R.; Lee, J.-I.; Noh, S. K.; Kwon, Y.-S.; Ryu, Y.-H.; Son, S.-J. *J. Cryst. Growth* **1998**, *193*, 491–495.
225. Hacke, P.; Nakayama, H.; Detchprohm, T.; Hiramatsu, K.; Sawaki, N. *Appl. Phys. Lett.* **1996**, *68*, 1362–1364.
226. Suzuki, M.; Nishio, J.; Onomura, M.; Hongo, C. *J. Cryst. Growth* **1998**, *189–190*, 511–515.
227. Lim, P. H.; Schineller, B.; Schon, O.; Heime, K.; Heuken, M. *J. Cryst. Growth* **1999**, *205*, 1–10.
228. Kwon, Y.-H.; Shee, S. K.; Gainer, G. H.; Park, G. H.; Hwang, S. J.; Song, J. J. *Appl. Phys. Lett.* **2000**, *76*, 840–842.
229. Kaufmann, U.; Kunzer, M.; Maier, M.; Obloh, H.; Ramakrishnan, A.; Santic, B.; Schlotter, P. *Appl. Phys. Lett.* **1998**, *72*, 1326–1328.
230. Xia, A.; Heeg, M. J.; Winter, C. H. *J. Am. Chem. Soc.* **2002**, *124*, 11264–11265.
231. Xia, A.; Knox, J. E.; Heeg, M. J.; Schlegel, H. B.; Winter, C. H. *Organometallics* **2003**, *22*, 4060–4069.
232. Cauletti, C.; Green, J. C.; Kelly, M. R.; Powell, P.; Van Tilborg, J.; Robbins, J.; Smart, J. *J. Electron Spectrosc. Relat. Phenom.* **1980**, *19*, 327–353.
233. Vollet, J.; Baum, E.; Schnoeckel, H. *Organometallics* **2003**, *22*, 2525–2527.
234. Arduengo, A. J.; Davidson, F.; Krafczyk, R.; Marshall, W. J.; Tamm, M. *Organometallics* **1998**, *17*, 3375–3382.
235. Schumann, H.; Gottfriedsen, J.; Glanz, M.; Dechert, S.; Demtschuk, J. *J. Organomet. Chem.* **2001**, *617–618*, 588–600.
236. Loos, D.; Eichkorn, K.; Magull, J.; Ahlrichs, R.; Schnoeckel, H. *Z. Anorg. Allg. Chem.* **1995**, *621*, 1582–1588.
237. Schumann, H.; Schutte, S.; Kroth, H.-J.; Lentz, D. *Angew. Chem., Int. Ed.* **2004**, *43*, 6208–6211.
238. Weber, F.; Sitzmann, H.; Schultz, M.; Sofield, C. D.; Andersen, R. A. *Organometallics* **2002**, *21*, 3139–3146.
239. Kane, K. M.; Shapiro, P. J.; Vij, A.; Cubbon, R.; Rheingold, A. L. *Organometallics* **1997**, *16*, 4567–4571.
240. Westerhausen, M.; Makropoulos, N.; Wieneke, B.; Karaghiosoff, K.; Noeth, H.; Schwenk-Kircher, H.; Knizek, J.; Seifert, T. *Eur. J. Inorg. Chem.* **1998**, 965–971.
241. Bailey, P. J.; Lorono-Gonzalez, D.; Parsons, S. *Chem. Commun.* **2003**, 1426–1427.
242. Damrau, H. R. H.; Geyer, A.; Prosenc, M. H.; Weeber, A.; Schaper, F.; Brintzinger, H. H. *J. Organomet. Chem.* **1998**, *553*, 331–343.
243. Milburn, R. K.; Baranov, V. I.; Hopkinson, A. C.; Bohme, D. K. *J. Phys. Chem. A* **1998**, *102*, 9803–9810.
244. Milburn, R. K.; Baranov, V. I.; Hopkinson, A. C.; Bohme, D. K. *J. Phys. Chem. A.* **1999**, *103*, 6373–6382.
245. Milburn, R. K.; Baranov, V. I.; Hopkinson, A. C.; Bohme, D. K. *J. Phys. Chem. A.* **2000**, *104*, 3926–3932.
246. Bauschlicher, C. W., Jr.; Partridge, H. *Chem. Phys. Lett.* **1991**, *181*, 129–133.
247. Parris, G. E.; Ashby, E. C. *J. Organomet. Chem.* **1974**, *72*, 1–10.
248. Xia, A.; Heeg, M. J.; Winter, C. H. *Organometallics* **2002**, *21*, 4718–4725.
249. Xia, A.; El-Kaderi, H. M.; Heeg, M. J.; Winter, C. H. *J. Organomet. Chem.* **2003**, *682*, 224–232.

250. El-Kaderi, H. M.; Xia, A.; Heeg, M. J.; Winter, C. H. *Organometallics* **2004**, *23*, 3488–3495.
251. Xia, A.; Heeg, M. J.; Winter, C. H. *Organometallics* **2003**, *22*, 1793–1795.
252. Geissler, M.; Kopf, J.; Schubert, B.; Weiss, E.; Neugebauer, W.; Schleyer, P. V. R. *Angew. Chem. Int. Ed. Engl.* **1987**, *26*, 587–588.
253. Schubert, B.; Weiss, E. *Angew. Chem., Int. Ed. Engl.* **1983**, *22*, 496–497.
254. Fraenkel, G.; Pramanik, P. *J. Chem. Soc., Chem. Commun.* **1983**, 1527–1529.
255. Bauer, W.; Seebach, D. *Helv. Chim. Acta* **1984**, *67*, 1972–1988.
256. Schubert, B.; Weiss, E. *Chem. Ber.* **1983**, *116*, 3212–3215.
257. Xia, A.; Heeg, M. J.; Winter, C. H. *J. Organomet. Chem.* **2003**, *669*, 37–43.
258. Mortara, S.; Fregonese, D.; Bresadola, S. *Macromol. Chem. Phys.* **2001**, *202*, 2630–2633.
259. Gobley, O.; Gentil, S.; Schloss, J. D.; Rogers, R. D.; Gallucci, J. C.; Meunier, P.; Gautheron, B.; Paquette, L. A. *Organometallics* **1999**, *18*, 2531–2535.
260. Westerhausen, M.; Giuckel, C.; Piotrowski, H.; Mayer, P.; Warchhold, M.; Noth, H. *Z. Anorg. Allg. Chem.* **2001**, *627*, 1741–1750.
261. Zheng, X.; Englert, U.; Herberich, G. E.; Rosenplaenter, J. *Inorg. Chem.* **2000**, *39*, 5579–5585.
262. Bogdanovic, B.; Janke, N.; Kinzelmann, H. G.; Westeppe, U. *Chem. Ber.* **1988**, *121*, 33–37.
263. Mashima, K.; Matsuo, Y.; Fukumoto, H.; Tani, K.; Yasuda, H.; Nakamura, A. *J. Organomet. Chem.* **1997**, *545–546*, 549–552.
264. Stegmann, R.; Frenking, G. *Can. J. Chem.* **1996**, *74*, 801–809.
265. Caro, C. F.; Hitchcock, P. B.; Lappert, M. F. *Chem. Commun.* **1999**, 1433–1434.
266. Caro, C. F.; Lappert, M. F.; Merle, P. G. *Coord. Chem. Rev.* **2001**, *219–221*, 605–663.
267. Armstrong, D. R.; Henderson, K. W.; MacGregor, M.; Mulvey, R. E.; Ross, M. J.; Clegg, W.; O'Neil, P. A. *J. Organomet. Chem.* **1995**, *486*, 79–93.
268. Fedushkin, I. L.; Khvoinova, N. M.; Skatova, A. A.; Fukin, G. K. *Angew. Chem., Int. Ed.* **2003**, *42*, 5223–5226.
269. Gibson, V. C.; Segal, J. A.; White, A. J. P.; Williams, D. J. *J. Am. Chem. Soc.* **2000**, *122*, 7120–7121.
270. Bailey, P. J.; Dick, C. M. E.; Fabre, S.; Parsons, S. *Dalton Trans.* **2000**, 1655–1661.
271. Kennedy, A. R.; Mulvey, R. E.; Rowlings, R. B. *J. Am. Chem. Soc.* **1998**, *120*, 7816–7824.
272. Kennedy, A. R.; Mulvey, R. E.; Rowlings, R. B. *Angew. Chem., Int. Ed.* **1998**, *37*, 3180–3183.
273. Kennedy, A. R.; Mulvey, R. E.; Roberts, B. A.; Rowlings, R. B.; Raston, C. L. *Chem. Commun.* **1999**, 353–354.
274. Gallagher, D. J.; Henderson, K. W.; Kennedy, A. R.; O'Hara, C. T.; Mulvey, R. E.; Rowlings, R. B. *Chem. Commun.* **2002**, 376–377.
275. Mulvey, R. E. *Chem. Commun.* **2001**, 1049–1056.
276. Clegg, W.; Henderson, K. W.; Kennedy, A. R.; Mulvey, R. E.; O'Hara, C. T.; Rowlings, R. B.; Tooke, D. M. *Angew. Chem., Int. Ed.* **2001**, *40*, 3902–3905.
277. Henderson, K. W.; Kennedy, A. R.; Mulvey, R. E.; O'Hara, C. T.; Rowlings, R. B. *Chem. Commun.* **2001**, 1678–1679.
278. Forbes, G. C.; Kenley, F. R.; Kennedy, A. R.; Mulvey, R. E.; O'Hara, C. T.; Parkinson, J. A. *Chem. Commun.* **2003**, 1140–1141.
279. Izod, K. *Coord. Chem. Rev.* **2002**, *227*, 153–173.
280. Driess, M. *Adv. Inorg. Chem.* **2000**, *50*, 235–284.
281. Lehmkuhl, H.; Mehler, K.; Benn, R.; Rufinska, A.; Krueger, C. *Chem. Ber.* **1986**, *119*, 1054–1069.
282. Pape, A.; Lutz, M.; Mueller, G. *Angew. Chem., Int. Ed. Engl.* **1994**, *33*, 2281–2284.
283. Westerhausen, M.; Digeser, M. H.; Noth, H.; Seifert, T.; Pfitzner, A. *J. Am. Chem. Soc.* **1998**, *120*, 6722–6725.
284. Blair, S.; Izod, K.; Clegg, W.; Harrington, R. W. *Eur. J. Inorg. Chem.* **2003**, 3319–3324.
285. Henderson, K. W.; Honeyman, G. W.; Kennedy, A. R.; Mulvey, R. E.; Parkinson, J. A.; Sherrington, D. C. *Dalton Trans.* **2003**, 1365–1372.
286. Chang, C. C.; Ameerunisha, M. S. *Coord. Chem. Rev.* **1999**, *189*, 199–278.
287. Her, T. Y.; Chang, C. C.; Lee, G. H.; Peng, S. M.; Wang, Y. *Inorg. Chem.* **1994**, *33*, 99–104.
288. Chang, C. C.; Lee, W. H.; Her, T. Y.; Lee, G. H.; Peng, S. M.; Wang, Y. *J. Chem. Soc., Dalton Trans.* **1994**, 315–322.
289. Chang, C.-C.; Srinivas, B.; Mung-Liang, W.; Wen-Ho, C.; Chiang, M. Y.; Chung-Sheng, H. *Organometallics* **1995**, *14*, 5150–5159.
290. Chang, C.-C.; Chen, J.-H.; Srinivas, B.; Chiang, M. Y.; Lee, G.-H. *Organometallics* **1997**, *16*, 4980–4984.
291. Beckman, E. *Chem. Ber.* **1905**, *38*, 904–906.
292. Fischer, R.; Görls, H.; Westerhausen, M. *Angew. Chem. Int. Ed.* **2005**, *44*, 8185–8187.
293. Meier, R.; Rappold, K. *Angew. Chem.* **1953**, *65*, 560–561.
294. Hays, M. L.; Hanusa, T. P. *Tetrahedron Lett.* **1995**, *36*, 2435–2436.
295. Burkey, D. J.; Alexander, E. K.; Hanusa, T. P. *Organometallics* **1994**, *13*, 2773–2786.
296. Sitzmann, H.; Weber, F.; Walter, M. D.; Wolmershaeuser, G. *Organometallics* **2003**, *22*, 1931–1936.
297. Harvey, M. J.; Hanusa, T. P.; Young, V. G., Jr. *J. Organomet. Chem.* **2001**, *626*, 43–48.
298. Harvey, M. J.; Hanusa, T. P. *Organometallics* **2000**, *19*, 1556–1566.
299. Williams, R. A.; Tesh, K. F.; Hanusa, T. P. *J. Am. Chem. Soc.* **1991**, *113*, 4843–4851.
300. Jayaratne, K. C.; Fitts, L. S.; Hanusa, T. P.; Young, V. G., Jr. *Organometallics* **2001**, *20*, 3638–3640.
301. Westerhausen, M.; Digeser, M. H.; Gückel, C.; Noth, H.; Knizek, J.; Ponikwar, W. *Organometallics* **1999**, *18*, 2491–2496.
302. Alexander, J. S.; Ruhlandt-Senge, K. *Eur. J. Inorg. Chem.* **2002**, 2761–2774.
303. Eaborn, C.; Hawkes, S. A.; Hitchcock, P. B.; Smith, J. D. *Chem. Commun.* **1997**, 1961–1962.
304. Alexander, J. S.; Ruhlandt-Senge, K. *Chem.—Eur. J.* **2004**, *10*, 1274–1280.
305. Izod, K.; Liddle, S. T.; Clegg, W. *J. Am. Chem. Soc.* **2003**, *125*, 7534–7535.
306. Knapp, V.; Muller, G. *Angew. Chem., Int. Ed.* **2001**, *40*, 183–186.
307. Harder, S.; Mueller, S.; Huebner, E. *Organometallics* **2004**, *23*, 178–183.
308. Feil, F.; Harder, S. *Organometallics* **2000**, *19*, 5010–5015.
309. Harder, S.; Feil, F.; Weeber, A. *Organometallics* **2001**, *20*, 1044–1046.
310. Feil, F.; Muller, C.; Harder, S. *J. Organomet. Chem.* **2003**, *683*, 56–63.
311. Harder, S.; Feil, F. *Organometallics* **2002**, *21*, 2268–2274.
312. Feil, F.; Harder, S. *Organometallics* **2001**, *20*, 4616–4622.
313. Weeber, A.; Harder, S.; Brintzinger, H. H.; Knoll, K. *Organometallics* **2000**, *19*, 1325–1332.
314. Harder, S. *Angew. Chem., Int. Ed.* **2003**, *42*, 3430–3434.
315. Harder, S. *Angew. Chem., Int. Ed.* **2004**, *43*, 2714–2718.
316. Green, D. C.; Englich, U.; Ruhlandt-Senge, K. *Angew. Chem. Int. Ed.* **1999**, *38*, 354–357.

317. Harvey, M. J.; Hanusa, T. P.; Young, V. G., Jr., *Angew. Chem. Int. Ed.* **1999**, *38*, 217–219.
318. Yanagisawa, A.; Habaue, S.; Yamamoto, H. *J. Am. Chem. Soc.* **1991**, *113*, 8955–8956.
319. Yanagisawa, A.; Habaue, S.; Yasue, K.; Yamamoto, H. *J. Am. Chem. Soc.* **1994**, *116*, 6130–6141.
320. Yasue, K.; Yanagisawa, A.; Yamamoto, H. *Bull. Chem. Soc.* **1997**, *70*, 493–497.
321. Yanagisawa, A.; Yasue, K.; Yamamoto, H. *Synlett* **1996**, *9*, 842–843.
322. Yanagisawa, A.; Ogasawara, K.; Yasue, K.; Yamamoto, H. *Chem. Commun.* **1996**, 367–368.
323. Overby, J. S.; Hanusa, T. P. *Angew. Chem. Int. Ed. Engl.* **1994**, *33*, 2191–2193.
324. Yasuda, H.; Ohnuma, Y.; Nakamura, A.; Kai, Y.; Yasuoka, N.; Kasai, N. *Bull. Chem. Soc. Jpn.* **1980**, *53*, 1101–1111.
325. Mashima, K.; Sugiyama, H.; Kanehisa, N.; Kai, Y.; Yasuda, H.; Nakamura, A. *J. Am. Chem. Soc* **1994**, *116*, 6977–6978.
326. Gardiner, M. G.; Raston, C. L.; Viebrock, H. *Chem. Commun.* **1996**, 1795–1796.
327. Harder, S.; Lutz, M. *Organometallics* **1997**, *16*, 225–230.
328. Zerger, R.; Stucky, G. *J. Organomet. Chem.* **1974**, *80*, 7–17.
329. Fichtel, K.; Hofmann, K.; Behrens, U. *Organometallics* **2004**, *23*, 4166–4168.
330. Harder, S. *Angew. Chem. Int. Ed.* **1998**, *37*, 1239–1241.
331. Gowenlock, B. G.; Lindsell, W. E.; Singh, B. *J. Chem. Soc., Dalton Trans.* **1978**, 657–664.
332. Engelhardt, L. M.; Junk, P. C.; Raston, C. L.; White, A. H. *J. Chem. Soc., Chem. Commun.* **1988**, 1500–1501.
333. McCormick, M. J.; Moon, K. B.; Jones, S. R.; Hanusa, T. P. *J. Chem. Soc., Chem. Commun.* **1990**, 778–779.
334. Wu, T. C.; Xiong, H.; Rieke, R. D. *J. Org. Chem.* **1990**, *55*, 5045–5051.
335. Fischer, E. O.; Stölzle, G. *Chem. Ber.* **1961**, *94*, 2187–2193.
336. Westerhausen, M. *Coord. Chem. Rev.* **1998**, *176*, 157–210.
337. Tanner, P. S.; Burkey, D. J.; Hanusa, T. P. *Polyhedron* **1995**, *14*, 331–333.
338. Westerhausen, M.; Hartmann, M.; Schwarz, W. *J. Organomet. Chem.* **1995**, *501*, 359–367.
339. Westerhausen, M.; Hartmann, M.; Makropoulos, N.; Wieneke, B.; Wieneke, M.; Schwarz, W.; Stalke, D. *Z. Naturforsch.* **1998**, *53b*, 117–125.
340. Sinnema, P.-J.; Shapiro, P. J.; B., H.; Bitterwolf, T. E.; Twamley, B. *Organometallics* **2001**, *20*, 2883–2888.
341. Sinnema, P.-J.; Hoehn, B.; Hubbard, R. L.; Shapiro, P. J.; Twamley, B.; Blumenfeld, A.; Vij, A. *Organometallics* **2002**, *21*, 182–191.
342. Sinnema, P.-J.; Shapiro, P. J.; Hohn, B.; Twamley, B. *J. Organomet. Chem.* **2003**, *676*, 73–79.
343. Harder, S.; Lutz, M.; Straub, A. W. G. *Organometallics* **1997**, *16*, 107–113.
344. Hays, M. L.; Hanusa, T. P.; Nile, T. A. *J. Organomet. Chem.* **1996**, *514*, 73–79.
345. Molander, G. A.; Schumann, H.; Demtschuk, J. *Organometallics* **1996**, *15*, 3817–3824.
346. Cristau, H.-J. *Chem. Rev.* **1994**, *94*, 1299–1313.
347. Leyser, N.; Schmidt, K.; Brintzinger, H.-H. *Organometallics* **1998**, *17*, 2155–2161.
348. Sitzmann, H.; Dezember, T.; Ruck, M. *Angew. Chem. Int. Ed.* **1998**, *37*, 3114–3115.
349. Sitzmann, H.; Walter, M. D.; Wolmershauser, G. *Angew. Chem., Int. Ed.* **2002**, *41*, 2315–2316.
350. Kuhn, N.; Kratz, T.; Blaeser, D.; Boese, R. *Chem. Ber.* **1995**, *128*, 245–250.
351. Arduengo, A. J., III; Tamm, M.; McLain, S. J.; Calabrese, J. C.; Davidson, F.; Marshall, W. J. *J. Am. Chem. Soc.* **1994**, *116*, 7927–7928.
352. Selg, P.; Brintzinger, H. H.; Andersen, R. A.; Horváth, I. T. *Angew. Chem., Int. Ed. Engl.* **1995**, *34*, 791–793.
353. Selg, P.; Brintzinger, H. H.; Schultz, M.; Andersen, R. A. *Organometallics* **2002**, *21*, 3100–3107.
354. Burkey, D. J.; Williams, R. A.; Hanusa, T. P. *Organometallics* **1993**, *12*, 1331–1337.
355. Burkey, D. J.; Hanusa, T. P.; Huffman, J. C. *Adv. Mater. Opt. Electron.* **1994**, *4*, 1–8.
356. Jutzi, P.; Dahlhaus, J.; Kristen, M. O. *J. Organomet. Chem.* **1993**, *450*, C1–C3.
357. Overby, J. S.; Hanusa, T. P. *Organometallics* **1996**, *15*, 2205–2212.
358. Burkey, D. J.; Hanusa, T. P. *Acta Crystallogr., Sect. C* **1996**, *52*, 2452–2454.
359. Hatanpää, T.; Vehkamaki, M.; Mutikainen, I.; Kansikas, J.; Ritala, M.; Leskela, M. *Dalton Trans.* **2004**, 1181–1188.
360. Tanner, P. S.; Hanusa, T. P. *Polyhedron* **1994**, *13*, 2417–2420.
361. Rees, W. S., Jr.; Lay, U. W.; Dippel, K. A. *J. Organomet. Chem.* **1994**, *483*, 27–31.
362. Francis, M. D.; Hitchcock, P. B.; Nixon, J. F. *Chem. Commun.* **2000**, 2027–2028.
363. Westerhausen, M.; Birg, C.; Piotrowski, H. *Eur. J. Inorg. Chem.* **2000**, 2173–2178.
364. Westerhausen, M.; Digeser, M. H.; Nöth, H.; Ponikwar, W.; Seifert, T.; Polborn, K. *Inorg. Chem.* **1999**, *38*, 3207–3214.
365. Harder, S.; Feil, F.; Repo, T. *Chem. —Eur. J.* **2002**, *8*, 1991–1999.
366. Burkey, D. J.; Hanusa, T. P. *Organometallics* **1996**, *15*, 4971–4976.
367. Ritala, M.; Kukli, K.; Vehkamaki, M.; Hanninen, T.; Hatanpaa, T.; Raisanen, P. I.; Leskela, M. *Proc.–Electrochem. Soc.* **2000**, *2000–13*, 597–604.
368. Vehkamaki, M.; Hatanpaa, T.; Hanninen, T.; Ritala, M.; Leskela, M. *Electrochem. Solid-State Lett.* **1999**, *2*, 504–506.
369. Vehkamaki, M.; Hanninen, T.; Ritala, M.; Leskela, M.; Sajavaara, T.; Rauhala, E.; Keinonen, J. *Chem. Vap. Deposition* **2001**, *7*, 75–80.
370. Rahtu, A.; Hanninen, T.; Ritala, M. *J. Phys. IV* **2001**, *11*, 923–930.
371. Tanner, P. S.; Overby, J. S.; Henein, M. M.; Hanusa, T. P. *Chem. Ber./Recueil* **1997**, *130*, 155–159.
372. Shapiro, P. J.; Kane, K. M.; Vij, A.; Stelck, D.; Matare, G. J.; Hubbard, R. L.; Caron, B. *Organometallics* **1999**, *18*, 3468–3473.
373. Matare, C. J.; Foo, D. M.; Kane, K. M.; Zehnder, R.; Wagener, M.; Shapiro, P. J.; Concolino, T.; Rheingold, A. L. *Organometallics* **2000**, *19*, 1534–1539.
374. Allen, K. A.; Gowenlock, B. G.; Lindsell, W. E. *J. Polym. Sci.* **1974**, *12*, 1131–1133.
375. Li, Y.; Deng, H.; Brittain, W.; Chisholm, M. S. *Polym. Bull. (Berlin)* **1999**, *42*, 635–639.
376. Harder, S.; Feil, F.; Knoll, K. *Angew. Chem. Int. Ed.* **2001**, *40*, 4261–4264.
377. Feil, F.; Harder, S. *Eur. J. Inorg. Chem.* **2003**, 3401–3408.
378. Hargittai, M. *Chem. Rev.* **2000**, *100*, 2233–2301.
379. Madden, P. A.; Wilson, M. *Chem. Soc. Rev.* **1996**, *25*, 339–350.
380. Sugarman, R.; Wilson, M.; Madden, P. A. *Chem. Phys. Lett.* **1999**, *308*, 509–515.
381. Bytheway, I.; Gillespie, R. J.; Tang, T. H.; Bader, R. F. W. *Inorg. Chem.* **1995**, *34*, 2407–2414.
382. Bytheway, I.; Popelier, P. L. A.; Gillespie, R. J. *Can. J. Chem.* **1996**, *74*, 1059–1071.
383. Hollis, T. K.; Burdett, J. K.; Bosnich, B. *Organometallics* **1993**, *12*, 3385–3386.
384. Timofeeva, T. V.; Lii, J.-H.; Allinger, N. L. *J. Am. Chem. Soc.* **1995**, *117*, 7452–7459.

385. Sapunov, V. N.; Kirchner, K.; Schmid, R. *J. Organomet. Chem.* **2001**, *214*, 143–185.
386. Bridgeman, A. J. *J. Chem. Soc. Dalton. Trans.* **1997**, *17*, 2887–2893.
387. Milman, V.; Lee, M. H. *J. Phys. Chem.* **1996**, 6093–6096.
388. Kwon, O.; McKee, M. L. In *Computational Organometallic Chemistry*; Cundari, T. R., Ed.; Dekker: New York, 2001.
389. Rayón, V. M.; Frenking, G. *Chem. —Eur. J.* **2002**, *8*, 4693–4707.
390. Fedushkin, I. L.; Petrovskaya, T. V.; Bochkarev, M. N.; Dechert, S.; Schumann, H. *Angew. Chem., Int. Ed.* **2001**, *40*, 2474–2477.
391. Dunne, J. P.; Tacke, M.; Selinka, C.; Stalke, D. *Eur. J. Inorg. Chem.* **2003**, 1416–1425.
392. Harvey, M. J.; Hanusa, T. P.; Pink, M. *Chem. Commun.* **2000**, 489–490.
393. Westerhausen, M.; Hartmann, M.; Heckmann, G.; Schwarz, W. *J. Organomet. Chem.* **1997**, *541*, 261–268.
394. Clegg, W.; Coles, S. J.; Cope, E. K.; Mair, F. S. *Angew. Chem. Int. Ed.* **1998**, *37*, 796–798.
395. El-Kaderi, H. M.; Heeg, M. J.; Winter, C. H. *Organometallics* **2004**, *23*, 4995–5002.
396. Schumann, H.; Gottfriedsen, J.; Demtschuk, J. *Chem. Commun.* **1999**, 2091–2092.
397. Steiner, A.; Lawson, G. T.; Walfort, B.; Leusser, D.; Stalke, D. *J. Chem. Soc., Dalton Trans.* **2001**, 219–221.
398. Hitzbleck, J.; Deacon, G. B.; Ruhlandt-Senge, K. *Angew. Chem., Int. Ed.* **2004**, *43*, 5218–5220.
399. Bonomo, L.; Dandin, O.; Solari, E.; Floriani, C.; Scopelliti, R. *Angew. Chem., Int. Ed.* **1999**, *38*, 914–915.
400. Bonomo, L.; Solari, E.; Scopelliti, R.; Floriani, C. *Chemistry (Weinheim)* **2001**, *7*, 1322–1332.
401. Hill, M. S.; Hitchcock, P. B. *Chem. Commun.* **2003**, 1758–1759.
402. Westerhausen, M.; Gueckel, C.; Mayer, P. *Angew. Chem., Int. Ed.* **2001**, *40*, 2666–2668.
403. Westerhausen, M.; Weinrich, S.; Ossberger, M.; Mitzel, N. W. *Z. Anorg. Allg. Chem.* **2003**, *629*, 575–577.
404. Westerhausen, M.; Weinrich, S.; Ossberger, M.; Mitzel, N. *Inorg. Chem. Commun.* **2003**, *6*, 23–25.
405. Steiner, A.; Stalke, D. *Inorg. Chem.* **1995**, *34*, 4846–4853.

2.03
Copper Organometallics

P J Pérez and M M Díaz-Requejo, Universidad de Huelva, Huelva, Spain

2.03.1 Introduction

As in most areas of chemistry, the number of contributions related to organometallic complexes of copper has considerably increased in the last decade. The use of organocopper reagents in organic synthesis, the catalytic properties of certain copper compounds, and its importance in many biological processes have impelled a large number of researchers to focus on this metal, leading to the mentioned impressive scientific production. A survey of the crystallographic databases has shown that in the period 1994–2004, nearly 800 structures containing at least one copper–carbon bond, the *sensus strictus* definition of an organometallic compound, have been found. In addition, a large number of non-structurally characterized but well-defined compounds has also been reported. Because of this, it is obvious that this chapter cannot provide in full the copper organometallic chemistry in the referred decade. However, it has been constructed so as to provide the reader access to a few, relevant, and recent references of nearly most of the different aspects of this area of copper chemistry.

After the excellent chapters in COMC (1982) and COMC (1995), the reader should first refer to them at the beginning of his/her survey, particularly for the organocopper complexes in which the organo group is bonded to copper as a monoanionic ligand. In this edition, a wider, but obviously less precise range of compounds has been included. In addition to those, alkenes, arenes, alkynes, carbonyls, cyanocuprates, and isocyanides have been revised and included. These, along with the alkyls, aryls, alkenyls, and alkynyls, contain the overall different organometallic compounds known for copper. The sections within this chapter contain some relevant information about the type of compounds, and some of the different variations that have been described, illustrated with their X-ray structures. At variance with previous editions, there is not a specific chapter for the preparation of the compounds: most of them have been prepared by the methods already reported there, or, if new, are briefly described in the corresponding section.

2.03.2 Monohapto σ-Ligands

2.03.2.1 Alkyl and Aryl Complexes

Organocopper complexes (alkyl and aryl) constitute a class of reagents with synthetic applications, specially for 1,4-addition reactions.[1,1a] This feature was first presented by Karash and Tawney more than 50 years ago.[2] However, the knowledge of organocopper species appeared 100 years before that finding, when Buckton reported[3] the reaction of $ZnEt_2$ and CuCl. The preparation of phenylcopper, although as impure samples, was described by Reich in 1923,[4] whereas the first synthesis of pure alkylcoppers was carried out by Gilman and co-workers[5] in the 1950s. Solid

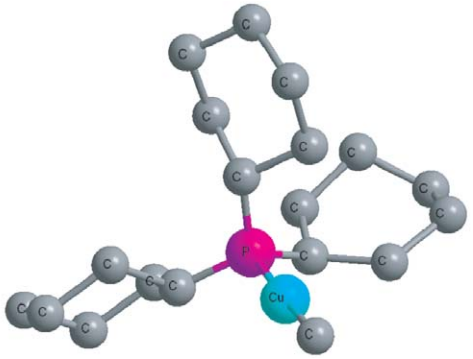

1

Figure 1 Geometry of the molecules of $(PCy_3)Cu(CH_3)$ **1** and the equilibrium observed in solution.

alkylcoppers often display an explosive nature, although they could be somewhat stabilized with the aid of several ligands, but in the absence of solvents or ligands, methylcopper or other alkylcopper are quite difficult to characterize due to their instability. Only the use of gas-phase synthesis has allowed the detection and characterization of methylcopper in the absence of any solvent.[6] The vast majority of organocoppers RCu display an oligomeric nature, whereas this trend is lower in the case of the organocuprates R_2Cu^-.[7] Theoretical studies[8,8a–8f] have focused on the calculation of the structures of simple derivatives, such as methylcopper or the dimethylcuprate ion.

The main synthetic route for alkylcoppers corresponds to the direct reaction of a copper halide and an organolithium reagent (Equation (1)). Excess of the latter leads to organocuprate compounds (Equation (2)), the CuX : LiR ratio being crucial for the composition of the resulting products. The complex $(PCy_3)CuCH_3$ **1**[9] constitutes an example of the group of mononuclear, monoalkyl copper complexes. The presence of PCy_3 provides the aforementioned stability, that has supposed the elucidation of the X-ray structure. In solution, NMR studies revealed that this complex exhibits an equilibrium with a dimeric form, a tight ion pair of composition $[Cu(PCy_3)_2][CuMe_2]$ (Figure 1).

$$CuX + LiR \longrightarrow CuR + LiX \quad (1)$$

$$CuX + 2LiR \longrightarrow LiCuR_2 + LiX \quad (2)$$

The existence of two different species in solution has also been proposed for lithium cuprates R_2CuLi. Two forms (Equation (3)), named contact ion pair (CIP) and solvent-separated ion pair (SSIP),[10] have been detected in solution for a series of lithium diorganocuprates, and in some cases both structures have been characterized by X-ray studies. The compounds $[Li(dme)_3]^+[Me_2Cu]^-$ **2** and $[Li(dme)_3]^+[\{(Me_3Si)CH_2\}_2Cu]^-$ **3** present SSIP structures, whereas the CIP case is exemplified by the structure of $\{[(Me_3Si)CH_2]_2CuLi\}_2(Et_2O)_3$ **4**. The position of the equilibrium is strongly influenced by the salt effect as well as by the solvent (Figure 2).

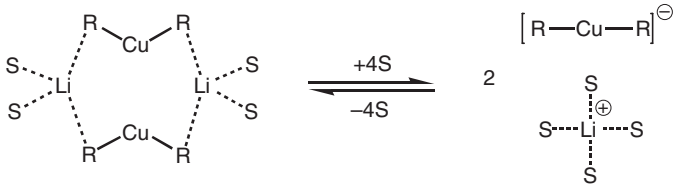

(3)

Other monoalkylcopper complexes have dimeric structures in the solid state. This feature is favored when bulky bridging ligands are employed with no β-hydrogens available to undergo elimination reactions. Otherwise, the resulting complexes decompose thermally and/or photochemically. Figure 3 shows the structure of two compounds containing 1-azaallyl[11] or pyridyl[12] functionalized alkyl ligands. Their stabilities have been attributed to the steric protection of the ^{t}Bu or the $SiMe_2$ groups, respectively. Compounds with Me_3Si-substituted alkyls are less prone to thermal decomposition when compared with simple alkyl compounds.

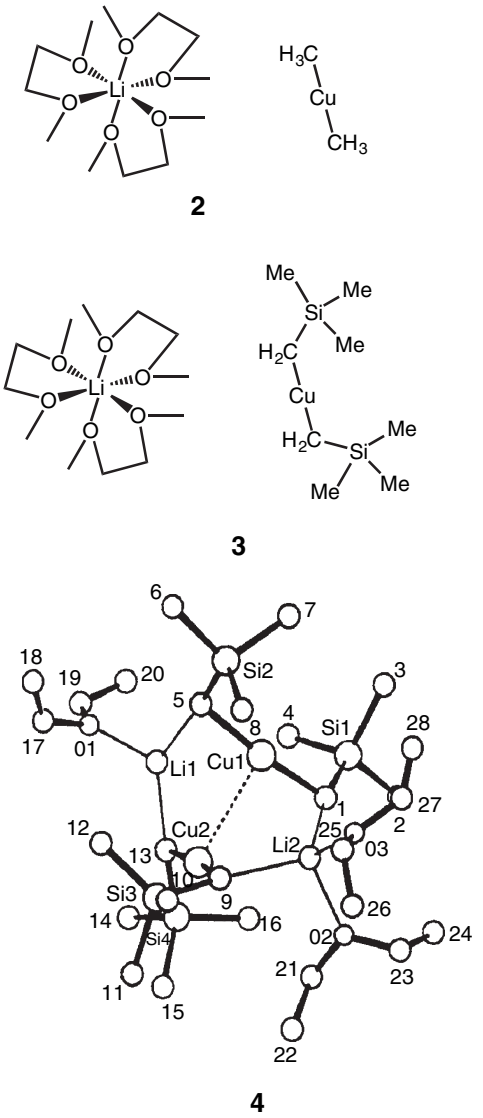

Figure 2 X-ray structures of $[Li(dme)_3]^+[Me_2Cu]^-$ **2**, $[Li(dme)_3]^+[\{(Me_3Si)CH_2\}_2Cu]^-$ **3**, and $\{[(Me_3Si)CH_2]_2CuLi\}_2(Et_2O)_3$ **4**.

The complex $Cu_3(Ph_2PCHPPh_2)_3$ is known to display a Cu–C interaction with the methyne carbon displaying a geometry nearly tetrahedral, suggesting sp^3-hybridation.[13] Several related complexes have been reported, where the copper center is bonded to the carbon atom of the group X–C–X (X = C, P, Si, S). For instance, the copper–antimonium cluster $Cu_{17}Sb_8(dppm)(Ph_2PCHPh_2)$[14] **7** (Figure 4) contains a Cu–C interaction similar to that of $Cu_3(Ph_2PCHPPh_2)_3$. A mixed Mn–Cu complex **8** (Figure 4) also presents a P–C–P linkage to copper,[15] with the assistance of a dithiocarbamyl group. In the case of β-diketoiminate ligands, dimeric structures[16] are supported by halide bridges, as shown in the structure of compound **9** (Figure 5). The formation of mononuclear species can be enforced by increasing the number of donor atoms in a given ligand: that is the case of the tris(2-pyridilthio)methane (TPTM), that occupies four coordination sites around the copper center in the complex $[Cu(TPTM)(CH_3CN)]PF_6$ **10** (Figure 5).[17]

Monomeric, dialkylcopper complexes have been prepared and structurally characterized. The reaction of $CpCuPPh_3$ with lithium fluorenyl[18] provided the complex $[(fluorenyl)_2CuPPh_3]^-[Li(THF)_4]^+$ **11**. The use of the anionic ligand $CH(Me)PEt_2NSiMe_3$[19] afforded the mononuclear complex **12** in which the ligand acts as a bridge

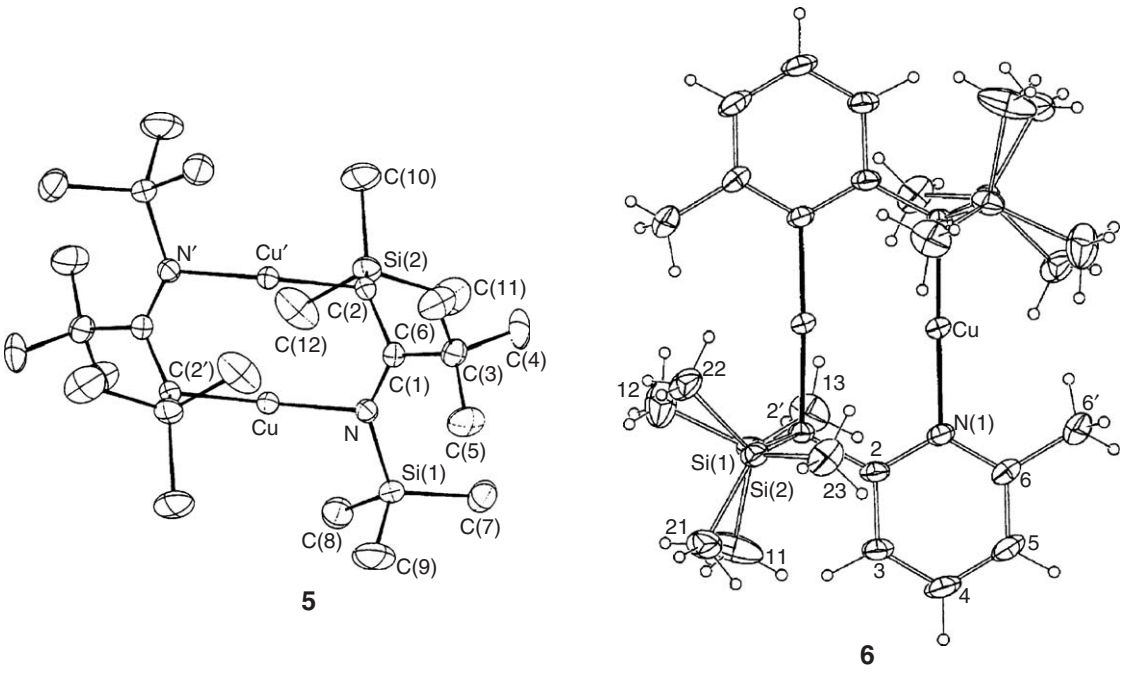

Figure 3 Dimeric monoalkyl copper complexes, Cu[μ-NRC^{t}BuC(H)R]$_2$ **5** (R=SiMe$_3$) and Cu$_2$(2-C(SiMe$_3$)$_2$-6-MePy)$_2$ **6**. Compound **5**: Hitchcock, P. B.; Lappert, M. F.; Layh, M. *Dalton Trans.* **1998**, 1619 – reproduced by permission of The Royal Society of Chemistry. Compound **6**: Van den Anckor, T. R.; Bhangava, S. K.; Mohr, F.; Papadopoulos, S.; Raston, C. L.; Skelton, B. W.; White, A. H. *Dalton Trans.* **2001**, 3069 – reproduced by permission of The Royal Society of Chemistry.

between the copper and the lithium atoms, the copper atom being dicoordinate (Figure 6). Fluorinated alkylcopper(III) complexes are also known.[20,20a,20b] The bisalkyls (dtc)Cu(R)$_2$ (where R = CF_3 or CF_2CF_3; dtc = dithiocarbamate) are neutral complexes, in contrast with the anionic $Cu(CF_3)_4^-$ and $Cu(CHF_2)_4^-$. Tetrahedral geometries were found in all cases (Figure 7).

Similarly to the alkyl derivatives, the most common route for arylcopper compounds is the reaction of a copper halide and aryllithium compounds (Equation (4)). Organocuprates with aryl groups are obtained by using an appropriate excess of the lithium reagent. Magnesium aryls have also been employed in transmetallation reactions with Cu(I) salts to yield both arylcopper compounds and arylcuprates (Equations (5) and (6)).

$$LiAr + CuBr \longrightarrow ArCu + LiBr \quad (4)$$

$$MgAr_2 + 2CuBr \longrightarrow \text{“}Cu_2Ar_2\text{”} + MgBr_2 \quad (5)$$

$$5MgArX + 5CuX \longrightarrow Cu_5Ar_5 + 5MgX_2 \quad (6)$$

Most of the reported organocopper compounds are polynuclear in nature, in which the copper center is bonded to the C atom either in a classical two-center two-electron (2c-2e) fashion or by means of an electron-deficient linkage, that is, a 3c-2e bond. The latter case is very common in the case of arylcopper compounds, the “Cu_2Ar” fragments being responsible for the aggregation of the monomeric, usually unisolable “CuAr” monomers. The electron-deficient case has been explained in terms of the orbital interaction depicted in Figure 8.[21] **A** (Figure 8) represents the interaction that is bonding for both the Cu–C–Cu bridge and for the two Cu atoms. The **B** interaction is bonding

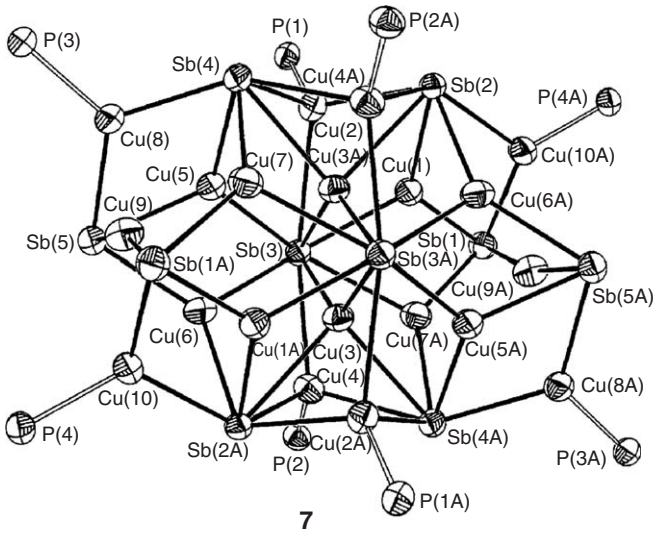

7

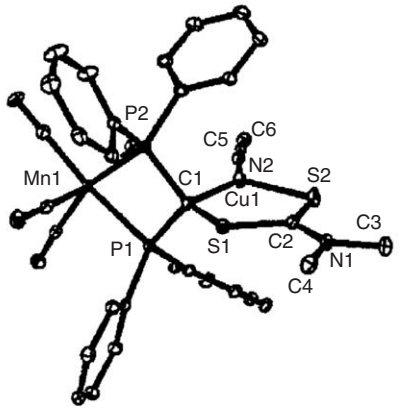

8

Figure 4 Monoalkyl copper complexes **7** and **8** containing an X–C(Cu)–X linkage. **7** reproduced with permission from wiley. **8** reproduced with permission from the Royal society of chemistry.

for the bridge but antibonding for the metal–metal case. The contributions of **A** and **B** in each structure should account for the observance, or absence, of any Cu–Cu bond.

A representative example of a polynuclear, homoleptic arylcopper complex is mesitylcopper, $[Cu(Mes)]_n$, a well-known reagent for the synthesis of copper(I) compounds. It has been reported, in the solid state, as a pentamer, although further studies revealed the existence of a tetrameric form.[22] The degree of aggregation depends on the solvent employed in the crystallization (toluene for pentamers, ethers for tetramers). As shown in Figure 9, the tetramer **17** shows a square-planar geometry for the four Cu atoms. The mean value of 2.42 Å for the Cu–Cu distances clearly indicates the existence of a bonding interaction. A particular feature of **17** is the co-planarity of the C_{ipso} atoms with the Cu_4 unit; this has also been observed in the pentamethylphenyl copper **18**.[23] This is at variance with the related compounds (2,4,6-trisopropylphenylcopper)[24] and *o*-vinylphenylcopper[25] **19**, that in spite of the existence of the planar Cu_4 fragment, the C_{ipso} atoms alternate above and below the plane containing the Cu atoms. It is worth mentioning that the vinyl groups in the molecules of **19** are not coordinated to the copper atom. The presence of donor ligands such as nitrogen in the *ortho*-position usually stabilizes the arylcopper compounds; however, the alkene and alkyne fragments coordinate more weakly than nitrogen, explaining the absence of vinyl–copper bonds in **19**. Such an interaction has been enforced in the case of heteroleptic compounds containing bromide ions. The reaction of the Grignard reagent (viph)MgBr with CuCl yields a mixture of two compounds $[Mg(THF)_6][Cu_5(viph)_2Br_4]$ **20** and $[Mg(THF)_5Cl][Cu_5(viph)_2Br_2]$ **21**. In both cases, vinyl coordination, bromide bridges, and Cu–aryl–Cu linkages are present in the copper-containing anionic complexes.[25]

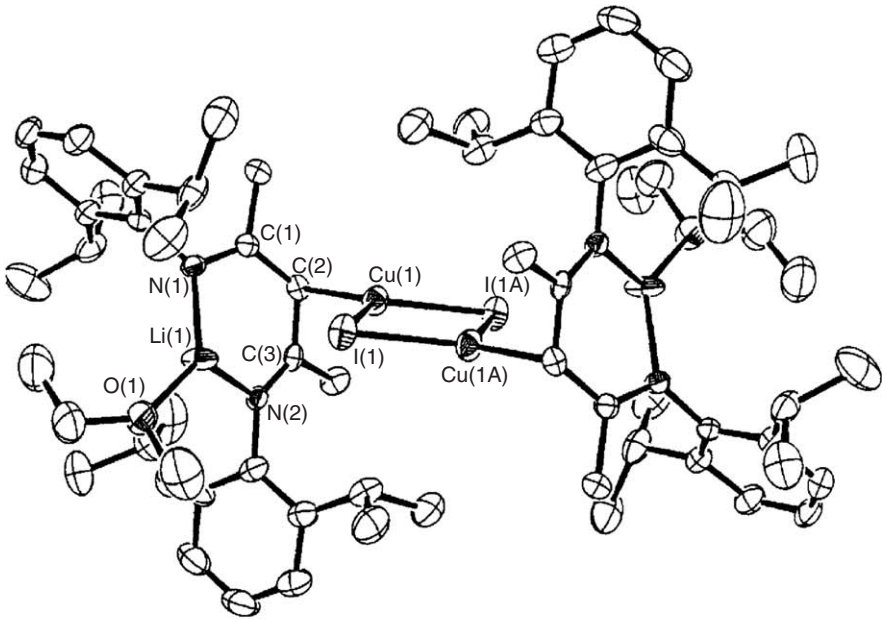

9

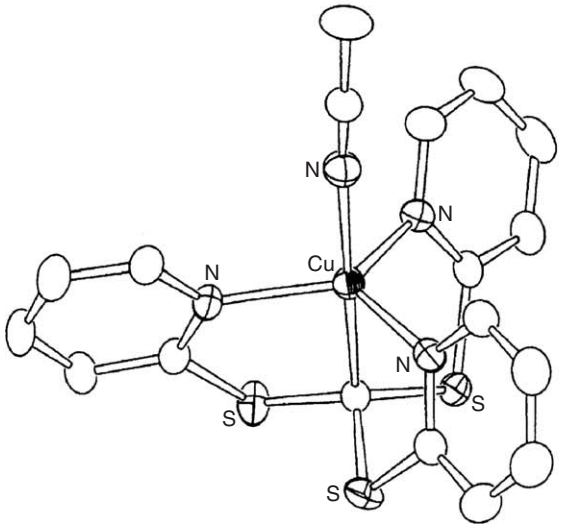

10

Figure 5 Monoalkyl copper complexes **9** and **10** containing a X–C(Cu)–X linkage. **9** reproduced with permission from wiley. **10** reproduced with permission from the Royal society of chemistry.

The existence of fluoro substituents in the aryl rings provides some differences to the related unsubstituted arylcopper compounds. The homoleptic $[Cu(C_6F_5)_4]$, similar to mesitylcopper, is obtained in a crystalline form on cooling cyclohexane or 1,2-dichloroethane solutions, whereas the π-complex $Cu_4(C_6F_5)_4(\eta^2\text{-toluene})_2$ **22** is obtained from toluene solutions.[26] The structural parameters for **22** are quite distinct, compared to those of mesitylcopper, since the four copper atoms in the square-planar geometry in the tetrameric compound form a butterfly structure in the toluene adduct. The molecules of **22** could be described as an ion pair consisting of two $(C_6F_5)_2Cu^-$ cuprate anions that are assembled with two copper cations bonded to toluene. The trinuclear complex $[Cu(C_6H_3Ph_2)]_3$ **23** obtained from the reaction of CuO^tBu and $LiC_6H_3Ph_2$[27] displays three copper centers linked by two 3c-2d interactions (Figure 10).

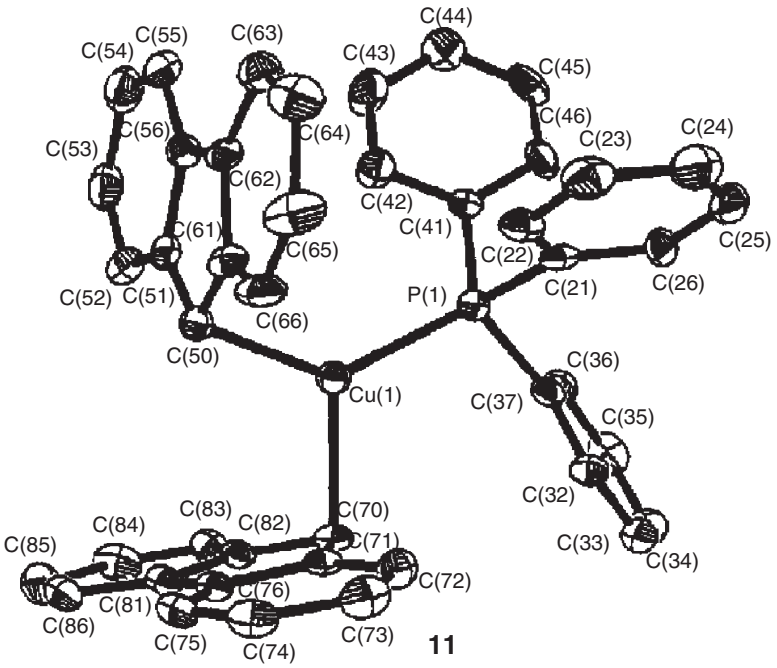

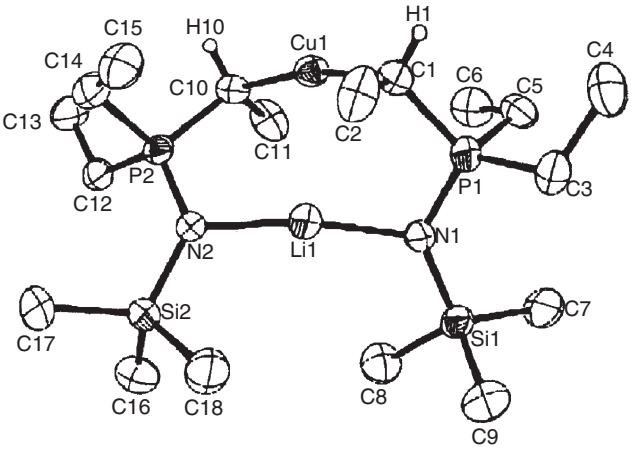

Figure 6 Structures of the bis-alkyl complexes[(fluorenyl)$_2$CuPPh$_3$]$^-$ **11** and [CH(Me)PEt$_2$NSiMe$_3$]$_2$CuLi **12**. **11** reproduced with permission from ACS publications. **12** reproduced with permission from Wiley.

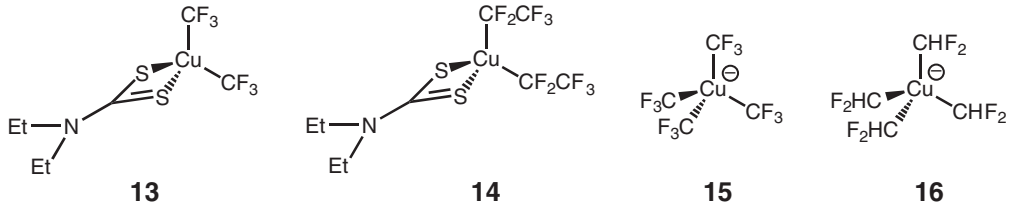

Figure 7 Geometries found for bis- and tetrafluoroalkyls copper complexes **13–16**.

The aforementioned effect of nitrogen donors can be exemplified by the use of amine functionalities in the *ortho*-position.[21] The reaction of $Li_2\{C_6H_4\text{-}(CH_2N(Me)CH_2CH_2NMe_2)\text{-}2\}_2$ with copper bromide afforded two different products depending on the ratio of reagents (Scheme 1). The trinuclear compound **24** $Cu_3Br\{C_6H_4\text{-}(CH_2N(Me)CH_2CH_2NMe_2)\text{-}2\}_2$ was obtained with a 2 : 3 ratio (lithium reagent : CuBr), whereas the tetranuclear

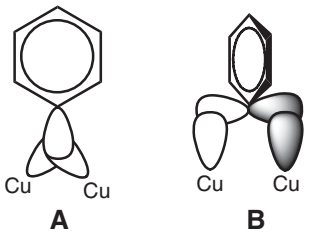

Figure 8 The 3c-2e interaction for the Cu_2C(aryl) bond.

complex **25** $Cu_4Br_2\{C_6H_4\text{-}(CH_2N(Me)CH_2CH_2NMe_2)\text{-}2\}_2$ was the main isolated product when a 2 : 4 ratio was employed (Figure 11). These compounds can be described as mixed 2 : 1 and 2 : 2 organocopper–copper bromide aggregates, respectively. The related compounds with naphthyl fragments have also been prepared. Heating of the benzene solutions of **23** induces the coupling of both aryl rings to give, in addition to CuBr and metallic copper, the biaryl derivative. This feature has also been observed for the naphthyl analogs. The use of equimolar amounts of the lithium reagent and copper bromide leads to neutral aggregates of formula $CuLi_2BrAryl_2$.[28] These compounds have a stable configuration, and serve as the starting material to obtain higher aggregates with a given stereochemistry.

The complex $CuMes^*$ $\{Cu_2Br_2(SMe_2)_3\}$ **26** ($Mes^* = C_6H_2{}^tBu_3\text{-}2,4,6$) exemplifies the rare 1 : 2 organocopper : copper halide case, where SMe_2 coordinates to the Cu center.[29] The importance of the steric hindrance of the aryl groups in the degree of aggregation can be envisaged in the reaction of CuI with $LiC_6H_3\text{-}2,6\text{-}Mes_2$ ($Mes = C_6H_2\text{-}2,4,6\text{-}Me_3$) and $LiC_6H_3\text{-}2,6\text{-}Trip_2$ ($Trip = C_6H_2\text{-}2,4,6\text{-}iPr_3$).[30] The Mes-containing reagent leads to the formation of the aggregate $[Li(THF)_4][2,6\text{-}Mes_2C_6H_3Cu_2I_2]$ **27**, whereas in the case of Trip, the bulkiness of the aryl group drives the reaction toward the formation of $(Et_2O)Li\{ICuC_6H_3\text{-}2,6\text{-}Trip_2\}$ **28** (Figure 12).

The use of very bulky groups in the *ortho*-position is usually incompatible with the formation of polynuclear structures with 3c-2e bonds. In contrast, mononuclear compounds with classical 2c-2e accounting for the Cu–C(aryl) bonds have been described. The reaction of the sterically encumbered terphenyl ligand $(Et_2O)LiC_6H_3\text{-}2,6\text{-}Trip_2$ with CuBr in the presence of SMe_2 gives the mononuclear $(Me_2S)Cu(C_6H_3\text{-}2,6\text{-}Trip_2)$ **29**.[31] The strategy of bulky groups in the *ortho*-position is therefore complemented with the addition of good donor ligands, as has been also proved for the synthesis of the complexes (2,6-dimesitylphenyl)triphenylphosphine–copper(I)[32] and (2,4,6-trimethylphenylamido)-(2-(triphenylphosphino)-phenyl)copper(II).[33] The existence of a multidentate ligand also enforces the formation of monocopper complexes. This is the case of the Cu(III)–aryl complex **30**,[34] generated by means of a carbon–hydrogen bond-activation process. The geometry around the metal center is nearly planar, due to the conformation of the macrocyclic ligand. It is worth mentioning that the absence of 3c-2e bonds and the sole formation of 2c-2e bonds do not support the unique observation of mononuclear compounds. For example, the compound $[Cu(2\text{-}py)]_3$ **31**[35] shows a trimeric structure in the solid state that forms chains due to Cu–Cu interactions. In other cases, the presence of certain donor ligands in the *ortho*-positions favors the formation of dinuclear species, although the Cu–aryl bonds must be considered as a classical σ-2c-2e interaction, as in the structure of compound **32** (Figure 13).[36]

2.03.2.2 Alkenyl and Alkynyl Complexes

The addition of organocopper reagents to triple bonds usually generates alkenylcopper intermediates with practical uses in the stereospecific formation of functionalized olefins (Equation (7)).[37,37a] This characteristic is usually controlled by the nature of the substituents of the initial alkyne and/or by the presence of certain additives.[38,38a] There are a number of examples of the use of this methodology that proposes the formation of carbon–carbon bonds. For instance, fullerene C_{60} has been modified with this procedure,[39] where the penta-addition of 1-alkenylcopper reagents gave a pentaalkenyl Fp ligand (Scheme 2). Fluorinated alkenes have also been synthesized by a similar method.[40]

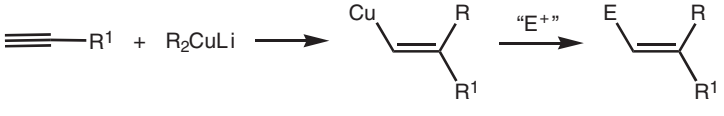

(7)

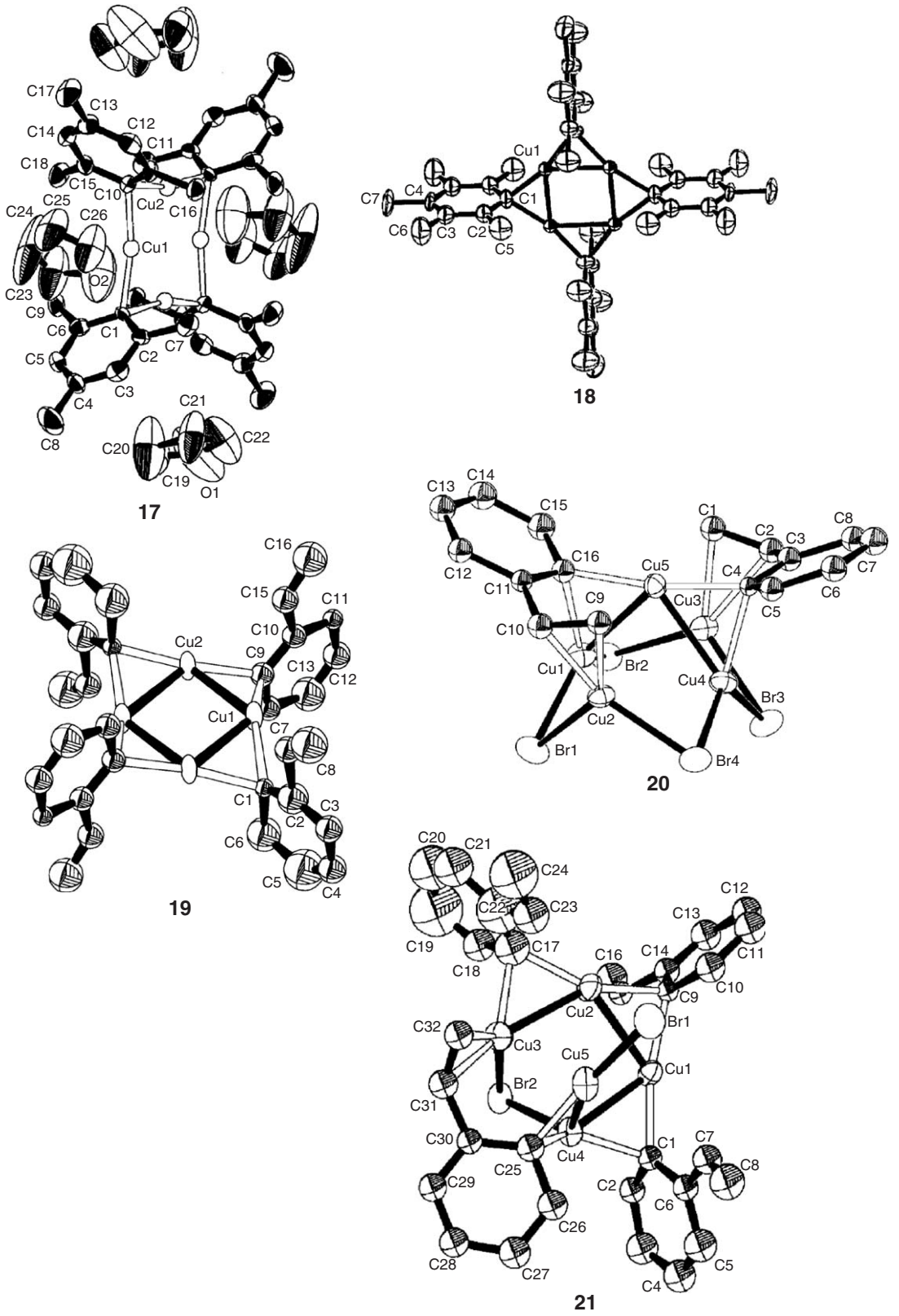

Figure 9 X-Ray sturctures of the arylcopper complexes **17**–**21**. Reproduced with permission from ACS publications, except for **18**: reproduced with permission from Elsevier.

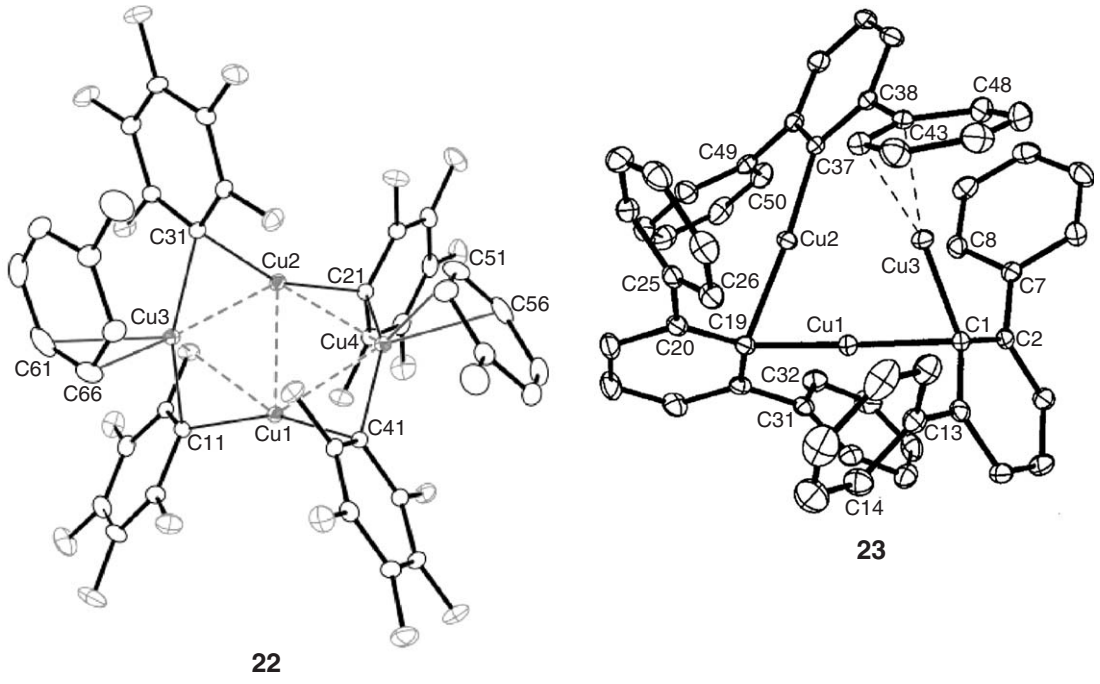

Figure 10 X-ray structures of the arylcopper complexes **22** and **23**. Reproduced with permission from ACS publications.

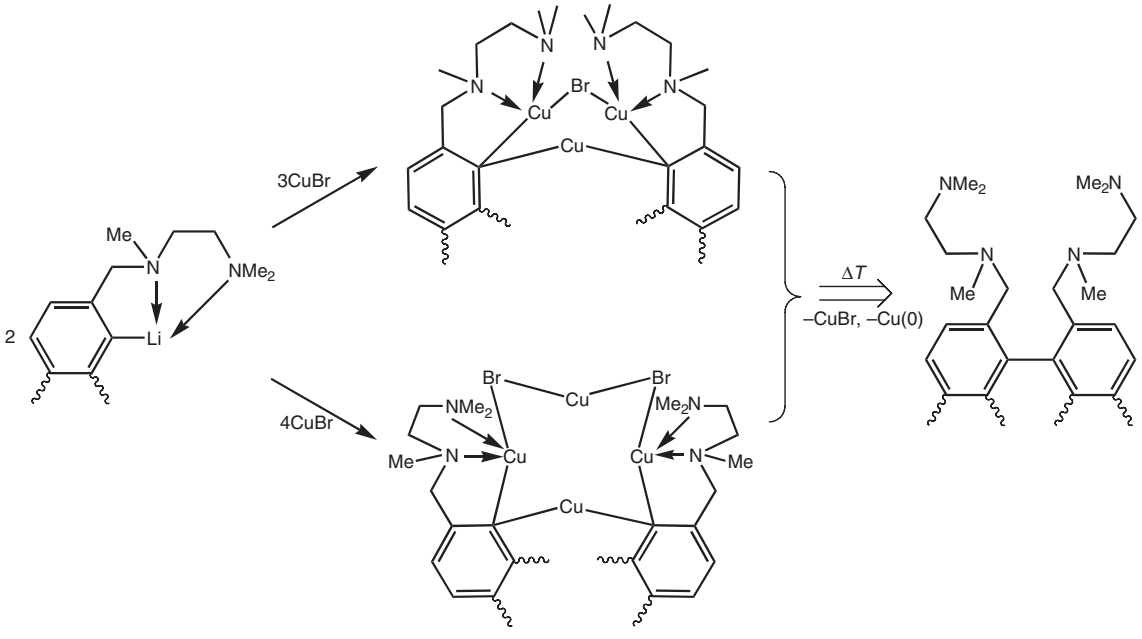

Scheme 1 Arylcopper–copper bromide aggregates and biaryl formation.

The high reactivity of alkenylcopper compounds has precluded their synthesis and subsequent isolation and characterization in such a way that prior to 1994 only two structurally characterized compounds of this class had been reported, a number that has not been substantially incremented. The 1,1-bismetallaalkenyl complex $[\eta^5\text{-}(C_5H_4SiMe_3)_2Ti(C{\equiv}CSiMe_3)\{\mu\text{-}C{=}C(SiMe_3)(R)\}Cu]$ **33** (Figure 14) was obtained from the reaction of the arylcopper $[Cu_4Br_2R_2]$ ($R = C_6H_3(CH_2NMe_2)$ and $\eta^5\text{-}(C_5H_4SiMe_3)_2Ti(C{\equiv}CSiMe_3)_2$) which yielded the first example of a mononuclear alkenyl copper complex.[41]

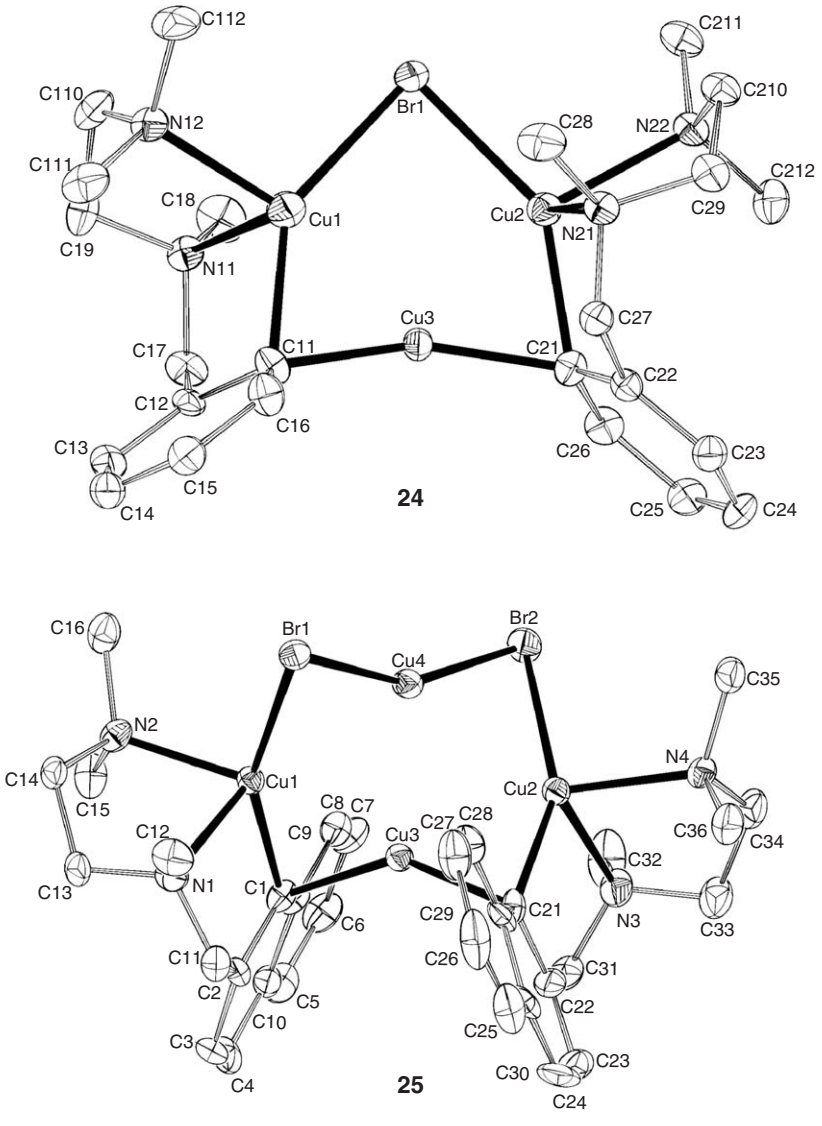

Figure 11 X-ray structures of the complexes **24** and **25**. Reproduced with permission from ACS publications.

A family of alkenylcopper compounds has also been reported with a common feature: the use of porphyrin-like skeletons surrounding the copper center. The existence of one or two pyrrole rings in a "confused" conformation (α–βinstead of the α–α) has allowed the isolation of several Cu(II) and Cu(III) organometallic complexes containing an alkenylcopper moiety. These are the cases of compounds NCPCu^{II} **34**,[42] *trans*-N_2CPCu^{III} **35**,[43] and *cis*- N_2CPCu^{III} **36**,[44] and the related copper complex with an *N*-confused calix[4]phyrin **37** (see Figure 15).[45] In all cases, the distances Cu–C were found within the range for a covalent interaction, whereas those of the C_α–C_β compared well with what is expected for a double bond. An easy protonation–deprotonation process of the peripheral nitrogen in **35** has improved the control of the exchange between the Cu(II) and Cu(III) oxidation states.[46]

Alkynylcoppers constitute a class of compounds relevant to several synthetic organic reactions,[47] where they have been proposed as key intermediates. The interest in this area has supposed that the number of structurally characterized alkynylcopper complexes has considerably expanded in the last few years. The most common route toward alkynylcoppers is based on the reaction of a terminal alkyne with a copper source, either a salt or an organocopper compound (Equations (8) and (9)).

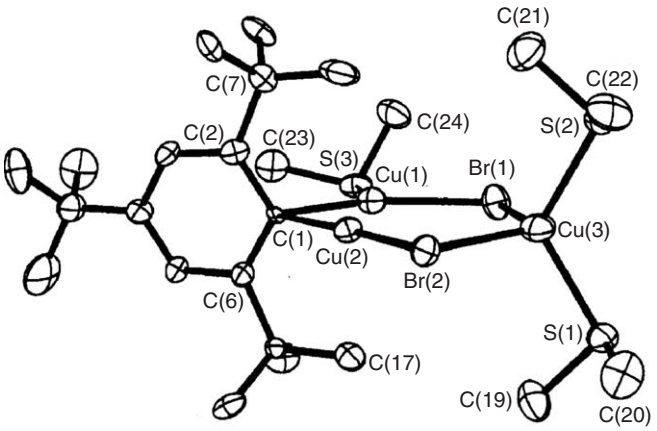

26

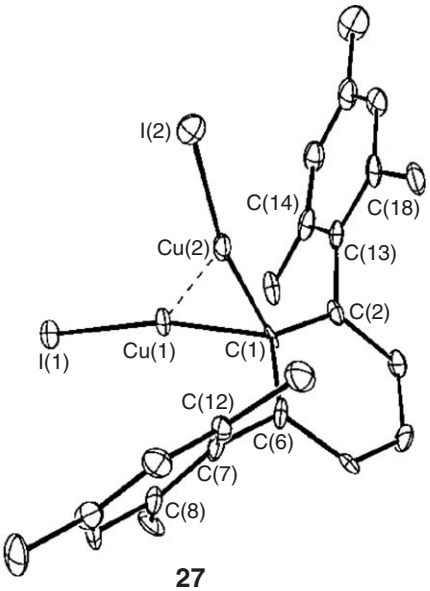

27

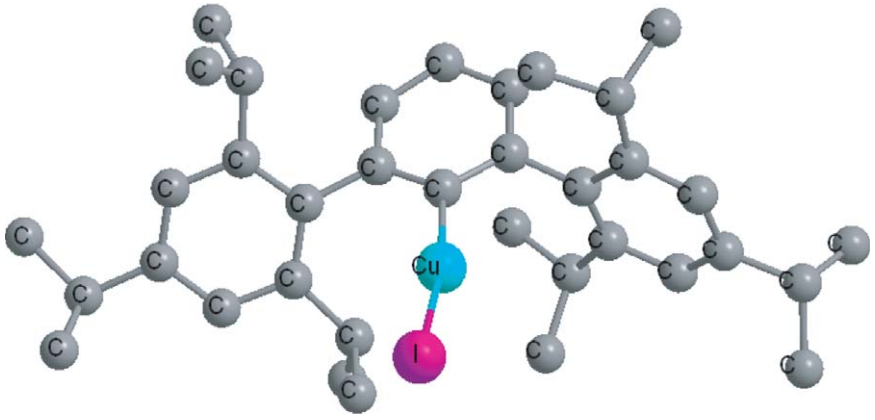

28

Figure 12 X-ray structures of the complexes **26** and **27** and geometry of the molecules of **28**. **26** reproduced with permission from the Royal society of chemistry. **27** reproduced with permission from ACS publications.

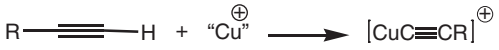

(8)

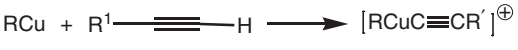

(9)

Several coordination modes for an alkynyl group to a metal center are known (Scheme 3). In the case of copper, there is a propensity to give multinuclear structures supported by bridging alkynyl groups. Therefore, mononuclear alkynylcopper(I) compounds are difficult to prepare and isolate. A strategy to confer additional stability consists of the use of bisalkynyltitanocenes as chelating ligands that led to the isolation and structural characterization of $[(\eta^5\text{-}C_5H_4SiMe_3)_2Ti(C{\equiv}CSiMe_3)_2]Cu(C{\equiv}CSiMe_3)$[48] **38** or $[(\eta^5\text{-}C_5H_4SiMe_3)_2Ti(C{\equiv}C^tBu)_2]Cu(C{\equiv}C\text{–}C{\equiv}C\text{–}Et)$ (Figure 16).[49]

The reaction of **38** with nucleophiles gave a dinuclear species **39** in which each copper center is bonded to three C≡C units, in contrast with the usual two-alkynyl-based bridge observed in many dinuclear alkynylcoppers.[18] This

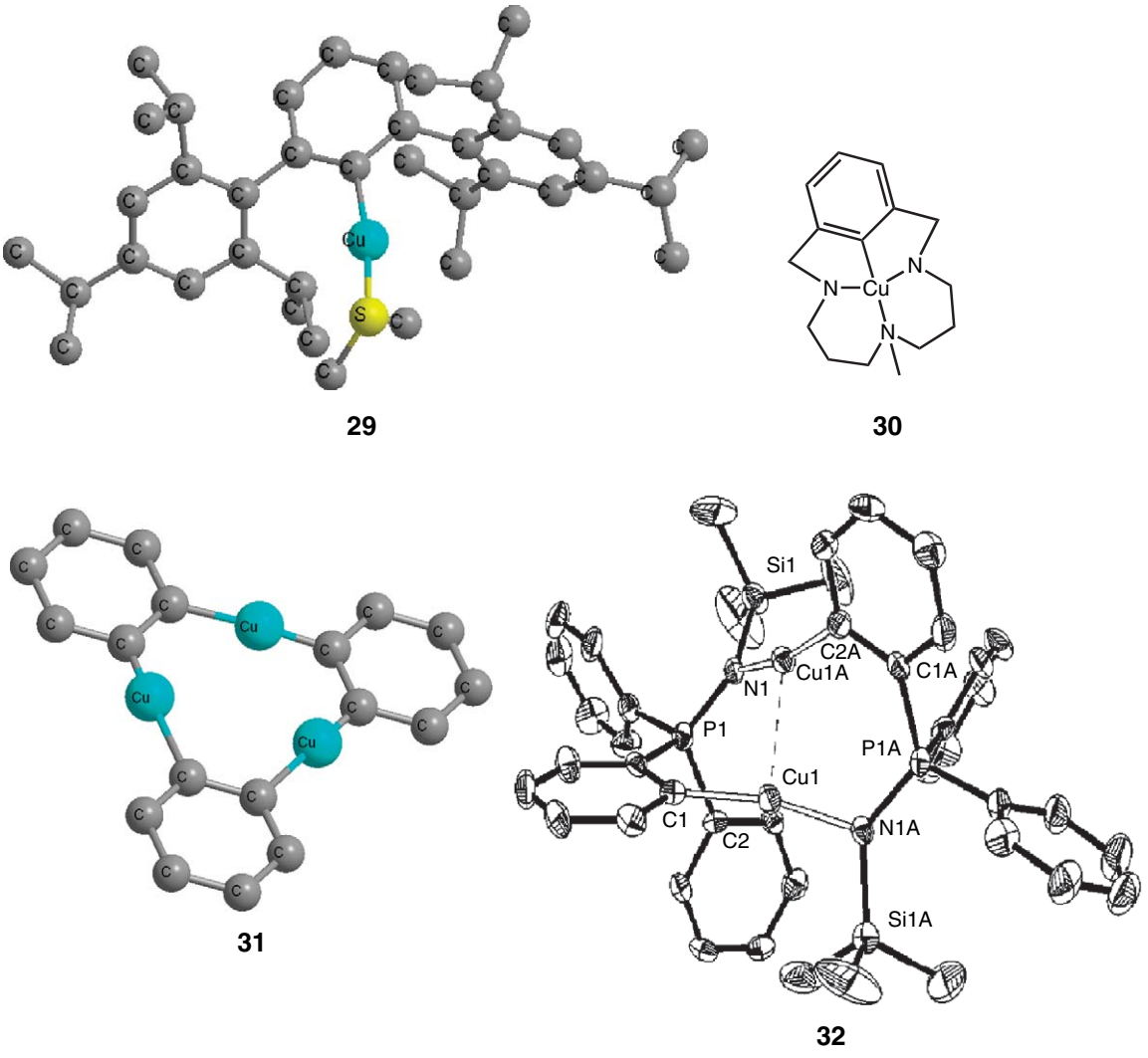

Figure 13 X-ray structures of the complexes **30** and **32** and geometry of the molecules of **29** and **31**. **32** reproduced with permission from Wiley.

is the case of the Cu(I) complex containing 1,1-bis(diphenylphosphino)ferrocene as bridging and chelating ligand in $Cu_2(\mu\text{-}\eta^1\text{-}C{\equiv}CC_6H_4CH_3\text{-}4)_2(\mu\text{-dppf})_2$ **40** (Figure 17).[50] Another example is given by $Cu_2(\mu\text{-}\eta^1C{\equiv}CPh)_2(PPh_2Me)_4$[51] **41** prepared by direct reaction of $[Cu(C{\equiv}CPh)]_n$ and the phosphine. The $\mu\text{-}\eta^1$ coordination mode has also been found in the cationic complex $[Cu_2(\mu\text{-}L^1)_2(\mu\text{-}\eta^1C{\equiv}CPh)]^+$ **42**,[52] with two nitrogen donors being coordinated, in addition to one phosphine group, to each copper center (Figure 17).

Trinuclear alkynylcopper complexes have been reported to contain $Cu_3C{\equiv}CR$ or $RC{\equiv}CCu_3C{\equiv}CR$ units, in which the structure is based on the existence of one (monocapped, Scheme 3) or two (bicapped) 4c-2e bonds. Chelating bis(phosphines) usually occupy the coordination sites in the equatorial positions of the Cu_3 core. These compounds exhibit photophysic properties related to luminescence. The structure of the diynyl complex $[Cu_3(\mu\text{-dppm})_3(\mu_3\text{-}\eta^1\text{-}C{\equiv}C\text{–}C{\equiv}CPh)_2]PF_6$ **43**,[53] prepared by the direct reaction of $[Cu_2(\mu\text{-dppm})_3(MeCN)_2](PF_6)_2$ and H–C≡C–C≡C–Ph, exemplifies this class of compounds.[54,54a,55] The same starting material was used in the synthesis of the monocapped compound $[Cu_3(\mu\text{-dppm})_3(\mu_3\text{-}\eta^1\text{-}C{\equiv}CBu^t)]PF_6$ **44**,[56] the alkyne group being introduced by means of ^{t}BuC≡CLi. A related hexanuclear acetylide **45** complex has been reported when 1,4-diethynylbenzene was employed as the alkyne source (Figure 18).[57]

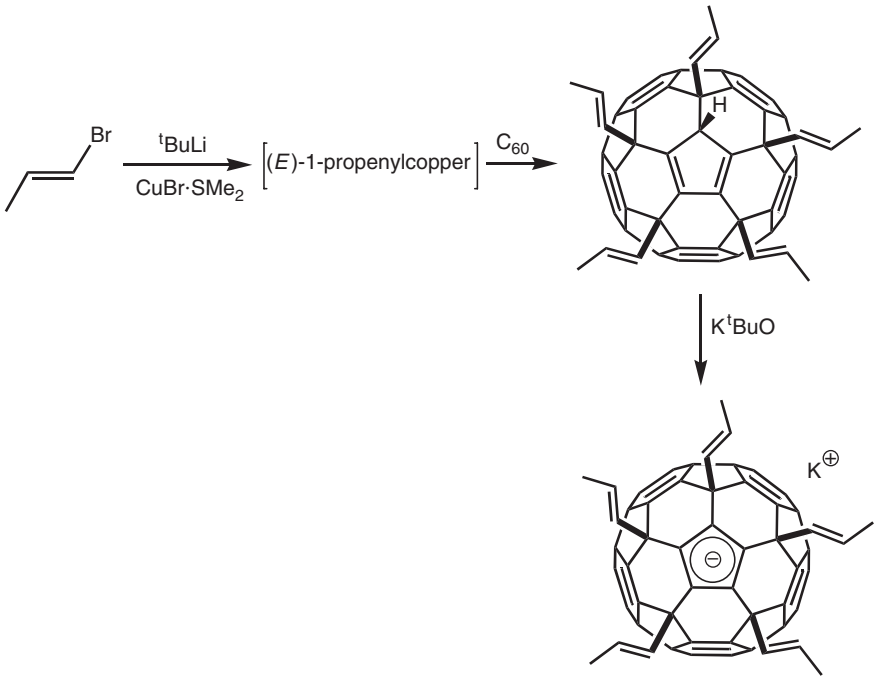

Scheme 2 Functionalization of C_{60} using an alkenylcopper reagent.

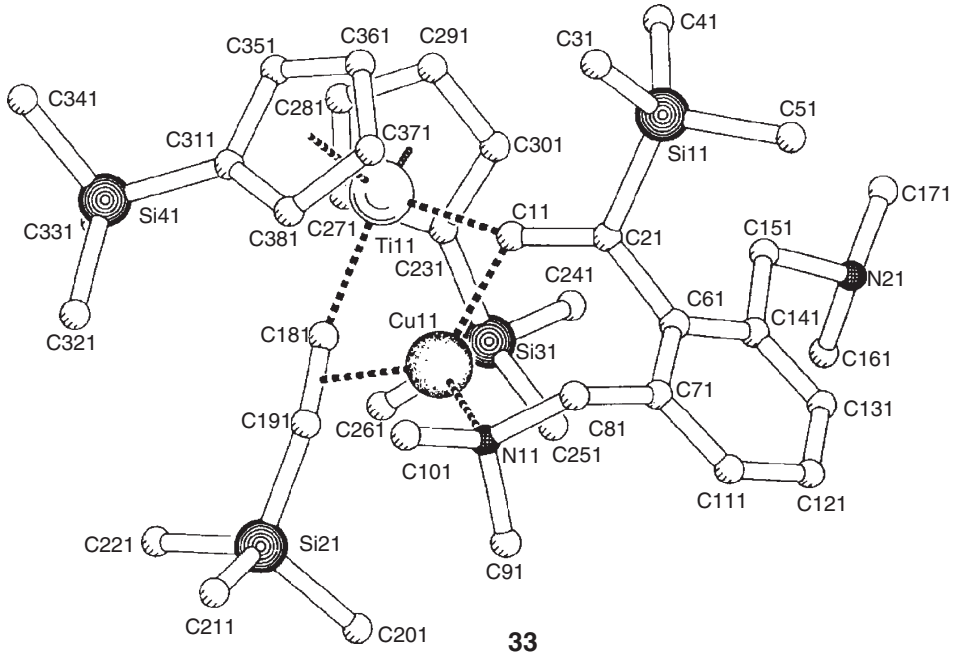

Figure 14 X-ray structure of the complex **33**. Reproduced with permission from Elsevier.

The tetranuclear copper(I) acetylides are also of interest due to their luminescence properties. Two types of general structures are known,[58] named "cubane-like" and "step-like". Figure 19 shows the structure of the complexes $[Cu(C{\equiv}CSiMe_3)(PPh_3)]_4$[58] (**46**, cubane-like)[59,60,61] and $Cu_4(C{\equiv}CPh)_4L_2$ (**47**, step-like, $L = Ph_2PCH_2(CH_2OCH_2)_2CH_2PPh_2$).[62] A tetranuclear, butterfly-shaped Cu(I) complex has also been characterized.[63] A number of examples of higher nuclearity C_5,[64] C_{16},[65] C_{18},[66] C_{20},[65] and C_{26}[67,68] have also been described.

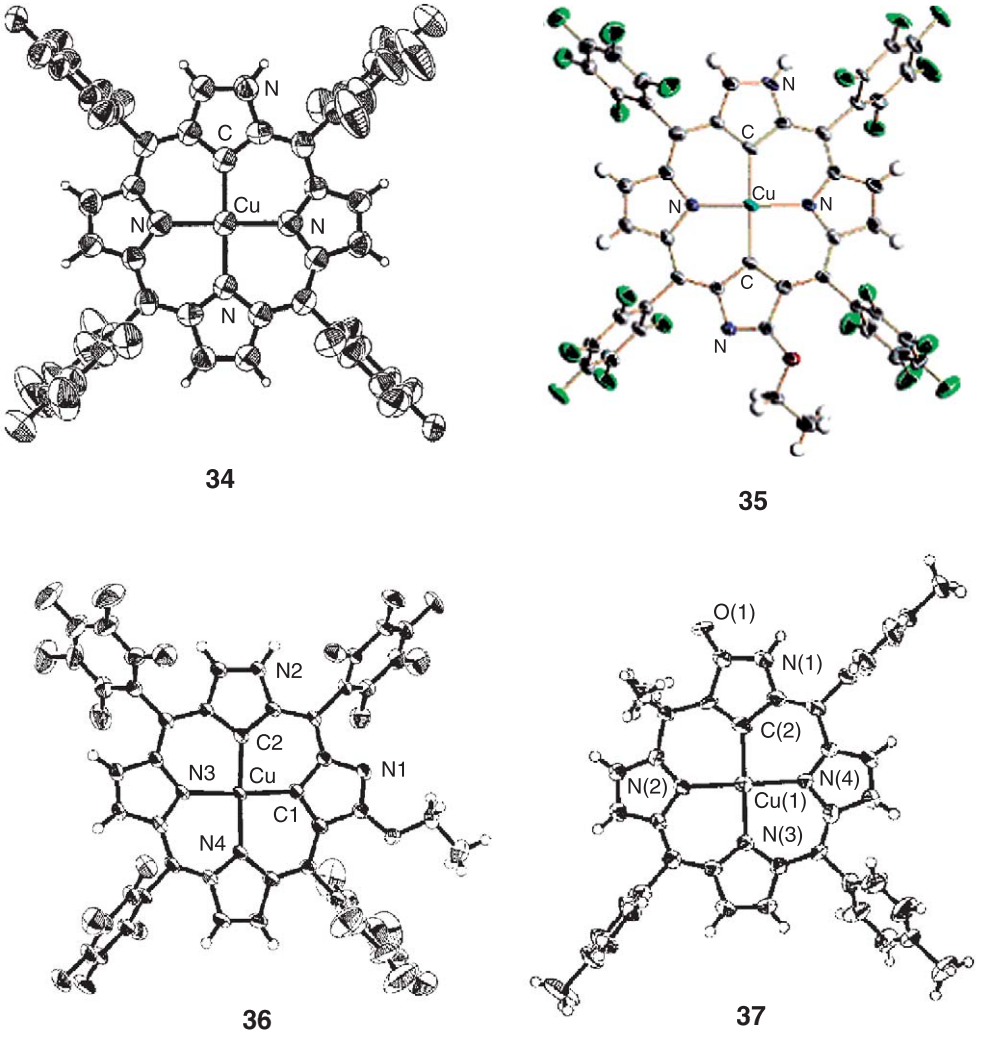

Figure 15 X-ray structures of complexes **34–37**. Reproduced with permission from ACS publications.

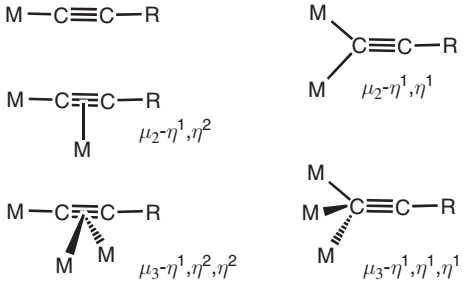

Scheme 3 Coordination modes of an alkynyl ligand to transition metals.

Heteronuclear alkynyl complexes in which the alkynyl fragment is bonded both to copper and to other transition metals have been prepared.[47] In addition to the aforementioned Ti–Cu compounds, others with ytterbium or europium with the general formula $\{[PhC{\equiv}C)_3Cu][M(Py)(THF)_2]\}_2$ (M = Eu, Yb) **48** (Figure 20) have been reported.[69] The bicapped geometry commented on for homonuclear copper complexes has also been found in Re–Cu heteronuclear compounds,[70,71] as in $[Cu_3(\mu\text{-dppm})_3\{\mu_3\text{-}\eta^1\text{-}C{\equiv}C\text{–}C{\equiv}C\text{–Re-}(Me_2bpy)(CO)_3\}_2]PF_6$ **49** (Figure 20).[70]

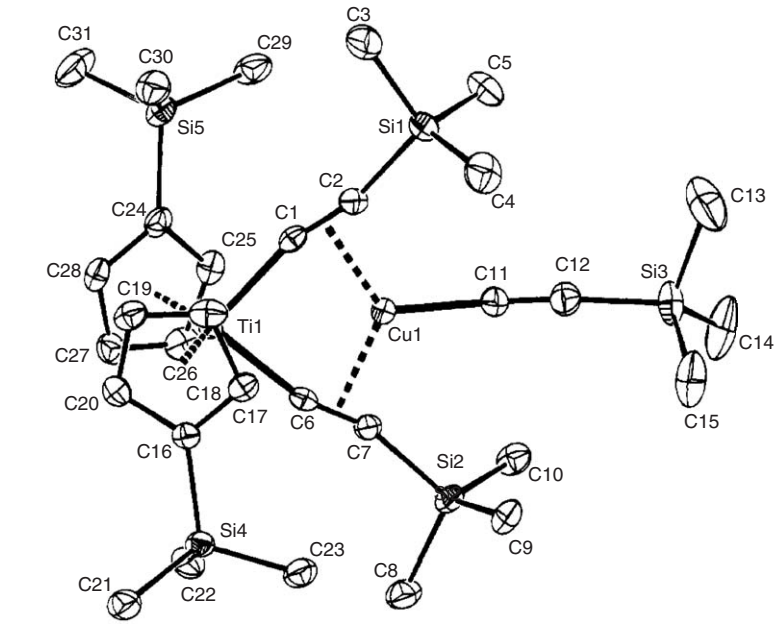

38

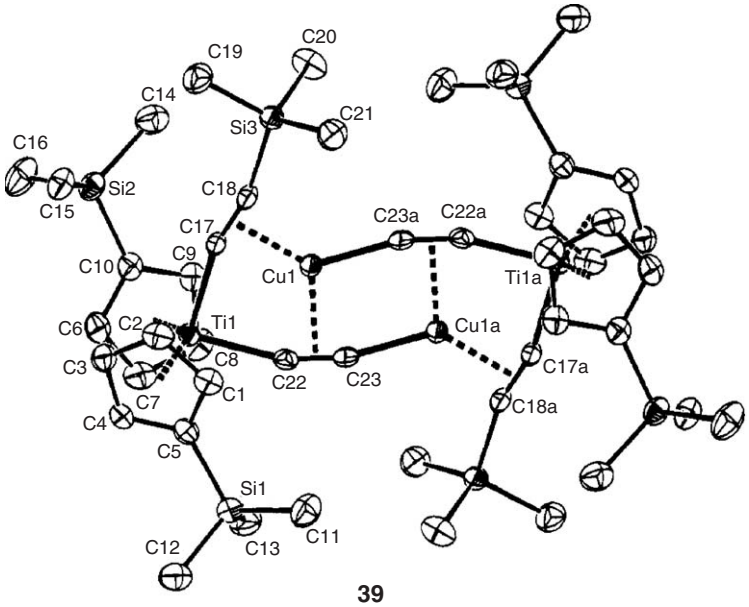

39

Figure 16 X-ray structures of complexes **38** and **39**. Reproduced with permission from ACS publications.

Heterobi-, tri-, tetra-, and pentametallic transition metal complexes have been obtained from the reaction of *cis*-[Pt](C≡CPh)$_2$ ([Pt] = Pt(bipy)) and different copper salts.[72] Hexanuclear platinum–copper acetylide complexes[73,74] display an additional interest in view of their luminescence properties. For instance, the complex [$Pt_2Cu_4(C_6F_5)_4$-(C≡C^{t}Bu)$_4$(acetone)$_2$] **50** (Figure 21)[73] shows a hexametallic core in which three alkynyl groups are π-bonded to the copper atoms, and the fourth forms a 4c-2e bond for the $PtCu_2C{\equiv}CR$ unit. A series of heteronuclear, luminescence Ag–Cu complexes was prepared and structurally characterized with distinct nuclearity.[75] The heterohexanuclear complex [Ag_4Cu_2(μ-$Ph_2PNHPPh_2$)$_4$(C≡CC_6H_4R-4)$_4$](ClO_4)$_2$ **51** (Figure 21) displays a bicapped cubic skeleton formed by four silver atoms, four copper atoms, and four acetylides. Gold has also been incorporated with a bicapped Cu_3 core, in the complex {Cu_3(μ-dppm)$_3$}(μ_3-I)(μ_3-η^1-C≡CC≡CAuC≡CC≡CH) **52**.[76]

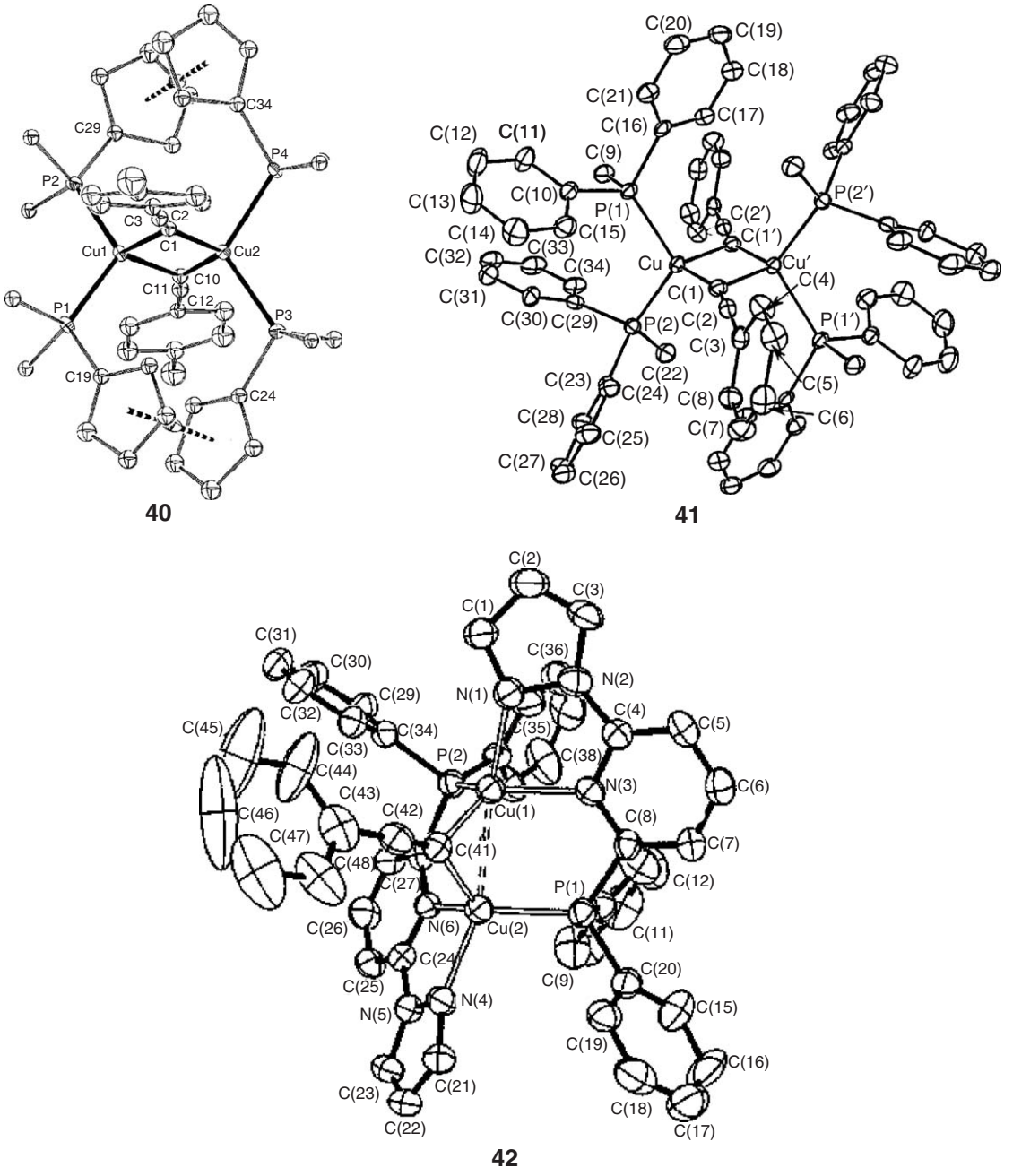

Figure 17 X-ray structures of complexes **40**–**42**. **40** reproduced with permission from ACS publications. **41** and **42** reproduced with permission from the Royal society of chemistry.

2.03.2.3 Carbene Complexes

The decomposition of diazo compounds in the presence of copper complexes constitutes a powerful tool in organic synthesis.[77,77a] This methodology is based on the formation of transient copper–carbene species that have been spectroscopically elusive for decades, until the observation by NMR of the species (NPN)Cu=C(Ph)CO_2Et (NPN = imidophosphanamide ligand) in the reaction of the ethylene complex (NPN)Cu(C_2H_4) with methyl 2-phenyl-2diazoacetate (Figure 22).[78] The extremely reactive nature of these copper–carbene compounds (Figure 23) precluded their isolation, although a few examples have been reported in which X-ray studies have

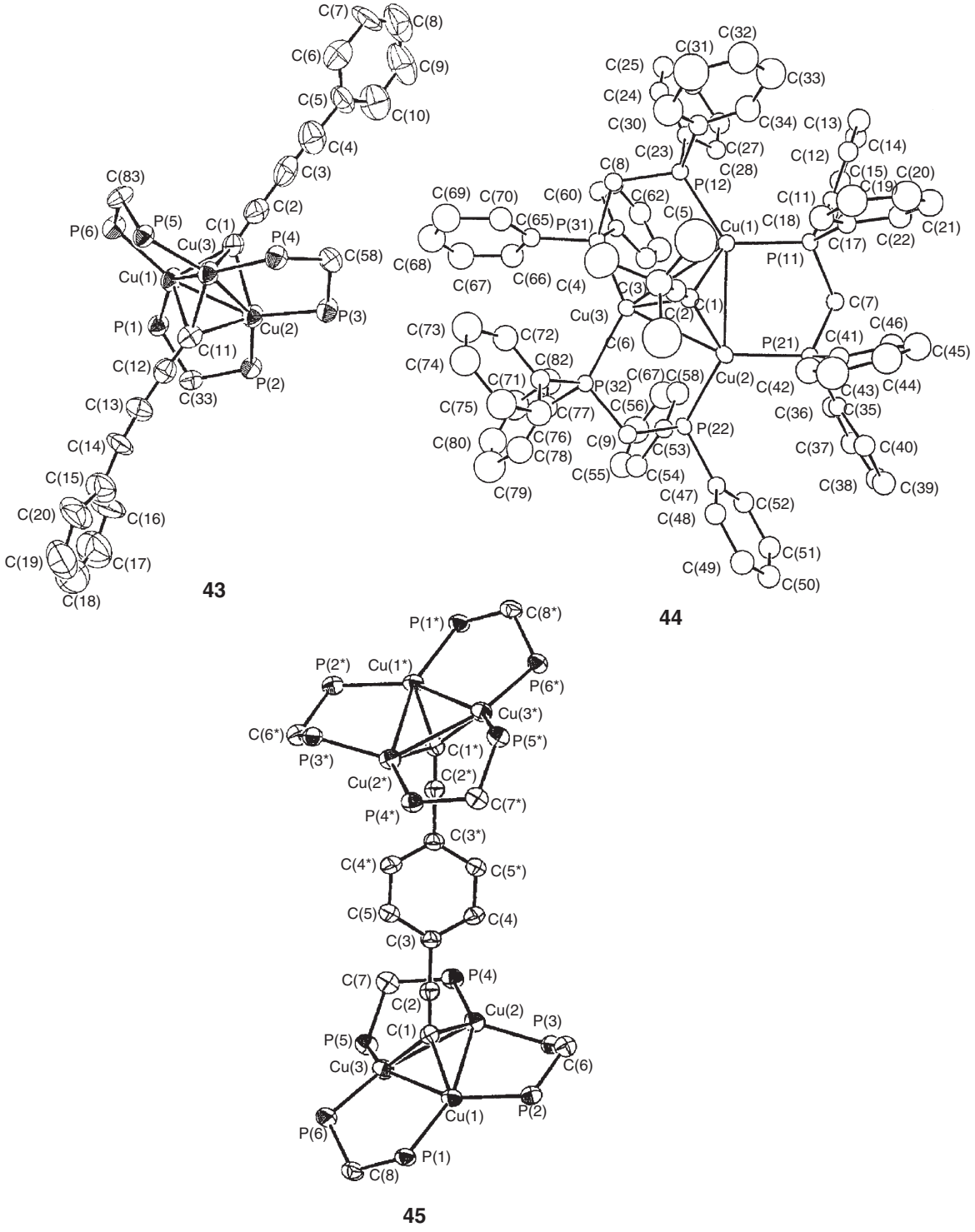

Figure 18 X-ray structures of complexes **43**–**45**. **43** reproduced with permission from ACS publications. **44** and **45** reproduced with permission from the Royal society of chemistry.

confirmed the existence of the metallocarbene fragment. It is the case of the complex $[Cu\{=CR^1(OR^2)\}(MeCN)(Et_2O)][PF_6]$ **53**,[79] obtained from the transfer of the carbene group from $(CO)_5Cr(=CR^1(OR^2))$ to $[Cu(NCMe)_4]PF_6$. A dicopper–carbene **54**[80] complex formed from the direct reaction of a Cu(I) source and a diazo compound has also been isolated and structurally characterized from the reaction of $[Me_2NN]Cu(C_2H_4)$ and

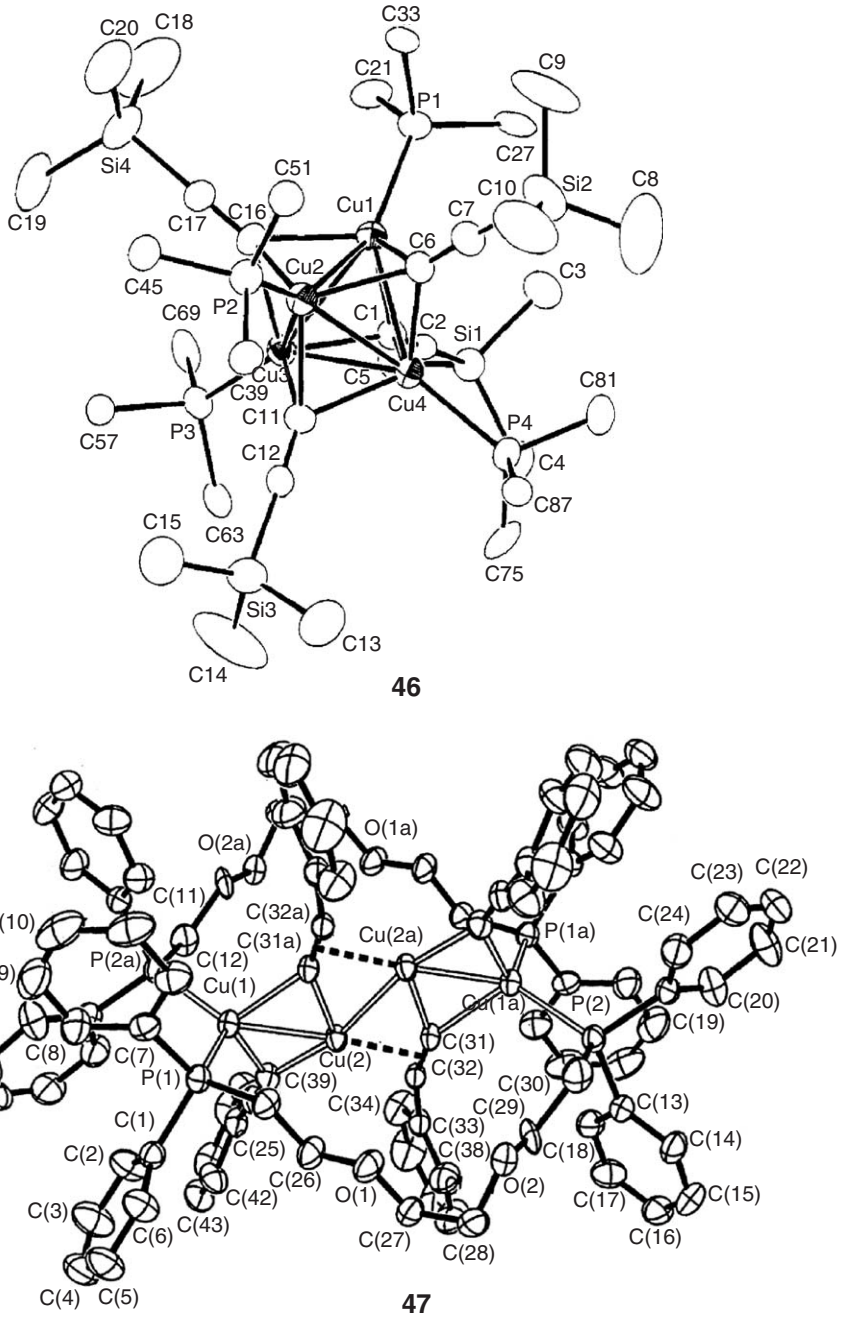

Figure 19 X-ray structures of complexes **46** and **47**. **46** reproduced with permission from ACS publications. **47** reproduced with permission from Elsevier.

diphenyldiazomethane (Me_2NN = β-diketiminate ligand). This complex dissociates an $[Me_2NN]Cu$ unit to yield the copper–carbene $[Me_2NN]Cu{=}CPh_2$ **55**.[80]

Stable copper–carbene compounds can be prepared and isolated with *N*-heterocyclic carbene (NHC) ligands.[81] These are robust ligands in which the donor carbon atom binds to the metal exclusively by a σ-interaction. The first example of a copper complex with these carbene ligands was the homoleptic $[(IPr)_2Cu]CF_3CO_3^-$ (IPr = bis-(1,3-dimesitylimidazol-2-ylidene),[82] obtained upon reacting the free carbene ligand and a copper salt (Equation (10)). The two-coordinated copper(I) thiazol-2-ylidene chloride **56** was later prepared and structurally characterized.[83] A general procedure for the preparation of compounds of general formula (NHC)CuCl consists of the direct reaction

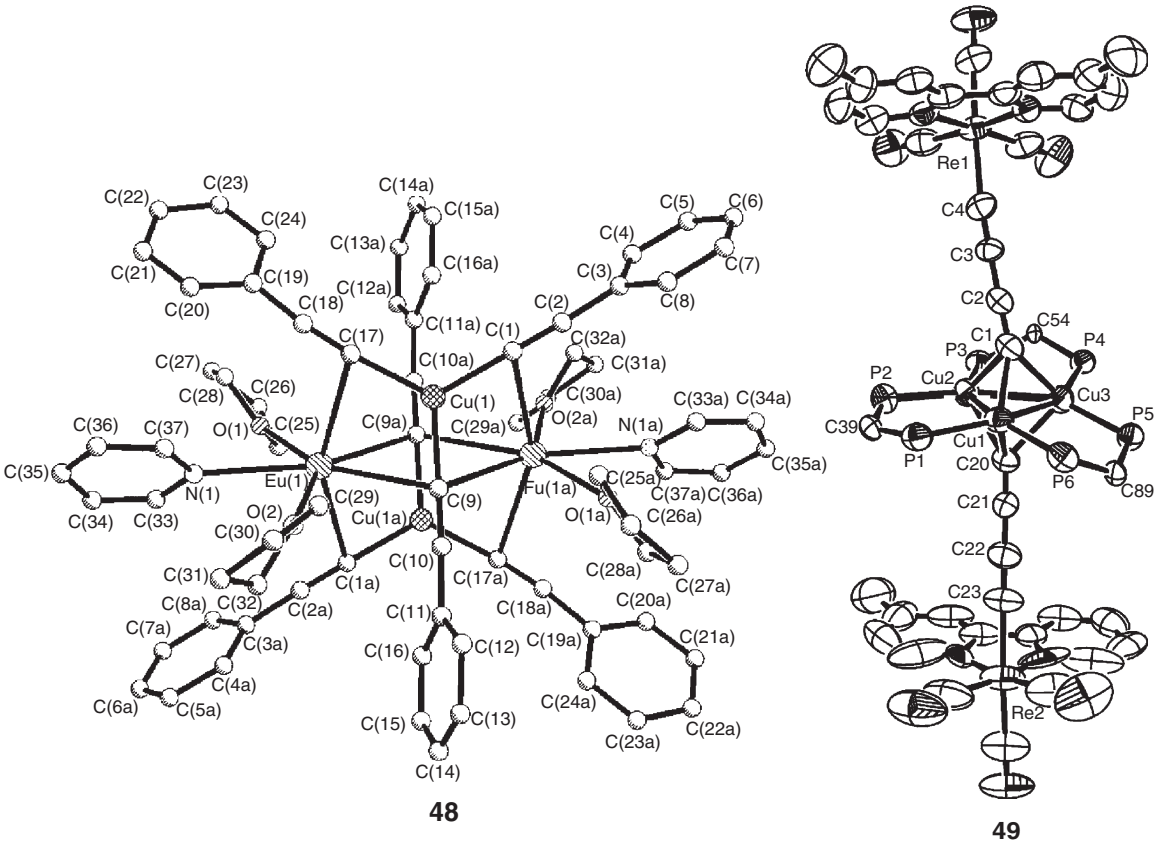

Figure 20 X-ray structures of complexes **48** and **49**. **48** reproduced with permission from ACS publications. **49** reproduced with permission from Elsevier.

of CuCl and the free carbene, isolated or generated *in situ*. Figure 24 shows the structure of a representative example of this class, IPrCuCl **57**,[84,84a,85] where the mutually *trans*-disposition of the chloride and the NHC-carbon atom is clearly observable. Other (NHC)CuL compounds have been prepared, with L = CH_3 **58**,[85] aryl,[32] OCOMe,[85] or O^{t}Bu,[86] the methyl derivative being similar to the PCy_3 complex **1**.[9] The alkenyl complex IPrCu(C(Et)=CHEt) **59** was obtained upon treating the *t*-butoxi derivative with 3-hexyne and triethoxysilane.[85] The reported dynamic equilibrium shown in solution by **1** (Figure 1) has not been observed for **58**. A series of (NHC)CuCl complexes, varying the NHC ligand, is also available.[87] Most of the reported complexes of this composition have been reported to promote catalytic transformations. [84,84a,87,88–90a]

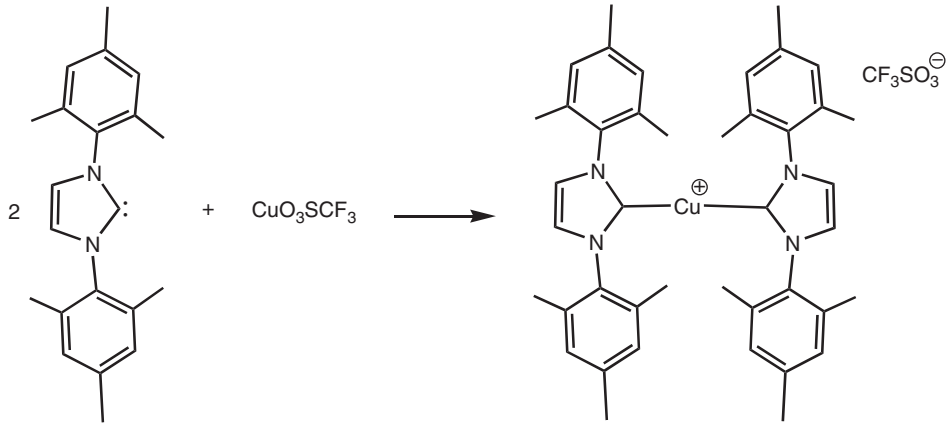

(10)

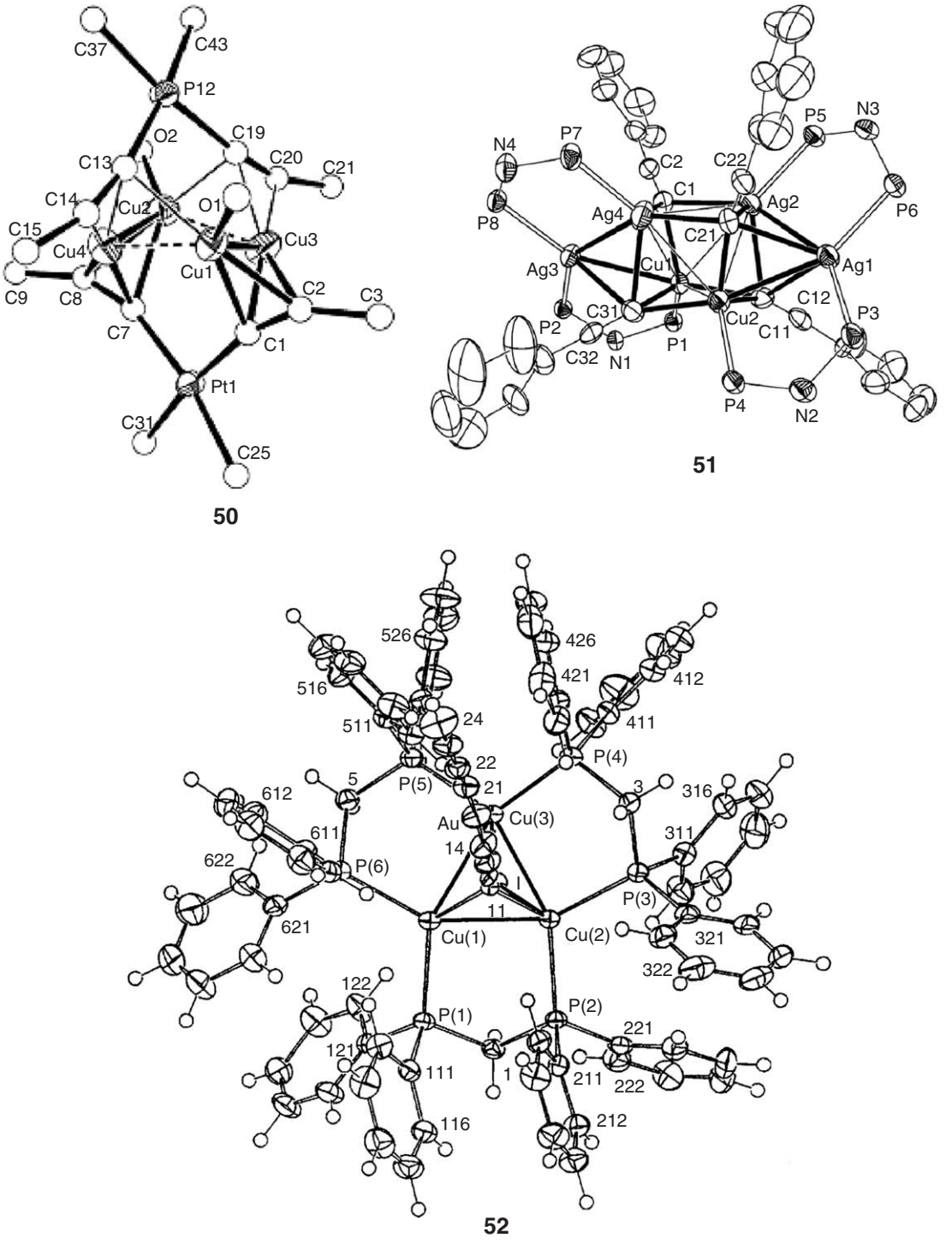

Figure 21 X-ray structures of complexes **50**–**52**. **50** reproduced with permission from Elsevier. **51** reproduced with permission from ACS publications. **52** reproduced with permission from the Royal society of chemistry.

NHC ligands with a pendant group that enforces chelation have also been coordinated to copper centers. The reaction of Cu_2O with pyridine *N*-functionalized carbene ligand led to the formation of several compounds.[91] In the case of mesityl derivatives, a dinuclear complex with a weak metal–metal interaction was isolated **60**,[91] whereas for the bulkier 2,6-diisopropylphenyl group, a monomeric complex was formed and characterized **61** (Figure 25).[91]

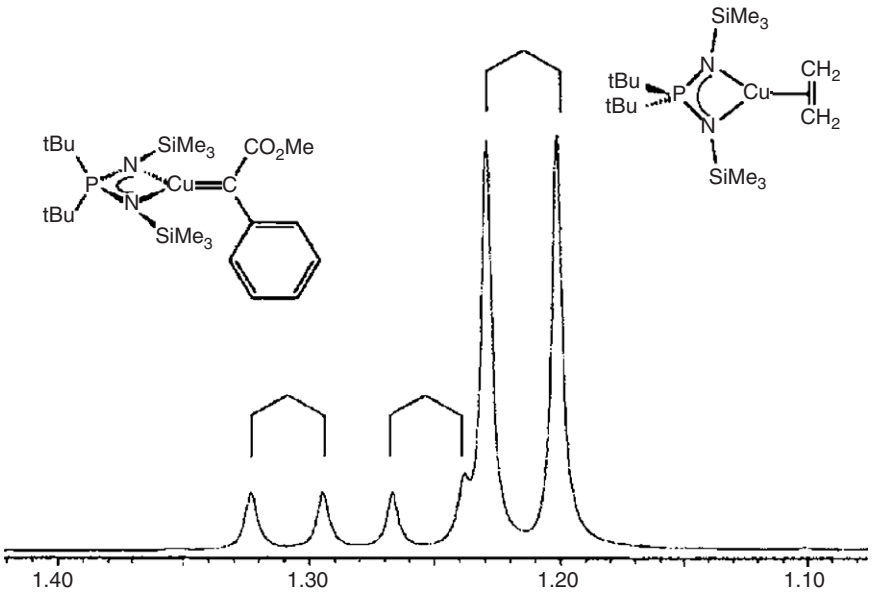

Figure 22 *In situ* NMR observation of the copper carbene (NPN)Cu═C(ph)co$_2$Et. Reproduced with permission from Wiley.

The facile exchange of the NHC ligand from Ag complexes to copper salts constitutes a common methodology in this area.[81] In the case of alkoxide-containing carbene ligands, transmetallation from a silver compound is required to yield a copper complex in which two oxo-bridges sustained a dimeric structure.[92,92a] This has also been applied for the preparation of a dinuclear Cu(II) chiral complex with carbene and aryloxi groups binding the copper centers.[93] Another example of chiral, dinuclear compound is that of complex **62**, in which the carbene ligand appears as a bridge between both copper atoms (Figure 25).[94]

The new triscarbene ligands TIME^R (Figure 26) have been synthesized, and several Cu(I) complexes containing this ligand have been prepared and structurally characterized.[95–97] The nature of the R substituent in the *N*-imidazolyl atom influences the structure of the resulting organometallic compound. Thus, for the methyl derivative (TIME^{Me}), a trinuclear complex of composition [(TIME^{Me})$_2$Cu$_3$](PF$_6$)$_3$ **63** (Figure 27)[95] was obtained, where each copper center is bonded to two carbene groups. However, the use of TIME^{tBu} yielded the formation of the complex [(TIME^{tBu})$_2$Cu$_2$](PF$_6$)$_2$ **64** that displays tricoordinated copper atoms.[96] Only two of the three coordination sites are occupied by carbene atoms; the third one consists of an alkenyl group, as the result of the activation of one of the C–H bonds of the NHC ring. The incorporation of a nitrogen functionality led to the discovery of a new type of tetradentate triscarbene ligand TIMEN^R.[97] The use of the methyl derivative provided the trinuclear complex [(TIMEN^{Me})$_2$Cu$_3$](PF$_6$)$_3$ **65** similar to **63** but with each copper bonded to two carbene and the nitrogen atoms. The increase of the steric hindrance (R = ^{t}Bu) allowed the isolation of the mononuclear complex [(TIMEN^{tBu})Cu](PF$_6$) **66**, where the three carbenoids atoms are bonded to copper. The nearly trigonal-planar geometry of the CuC$_3$ unit suggested that the Cu–N distance is electronically non-significant, although it has a certain effect in terms of the structural stabilization.

2.03.3 Dihapto π-Ligands

2.03.3.1 Alkene and Arene Complexes

Copper olefin complexes are usually generated by the direct reaction of a Cu(I) source, the ligand, and the corresponding olefin. Copper ethylene complexes are of interest in view of their biochemical importance,[98,98a–98e] their applications in organic chemistry,[99,99a,99b] and industrial applications.[100,100a] Because of this, many copper alkene complexes have been reported, with different nuclearity, in compounds with one, two, or even three C═C units coordinated to a given copper center.

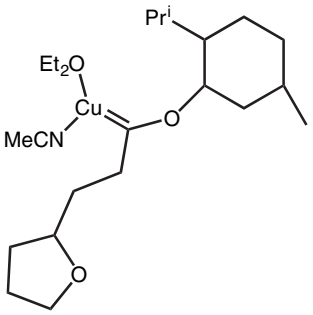

53

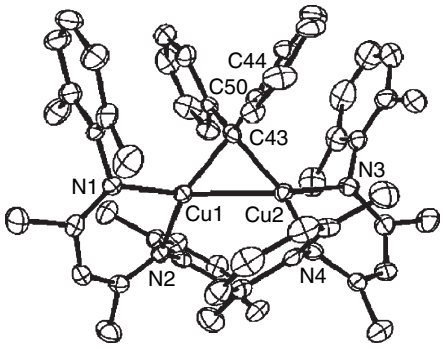

54

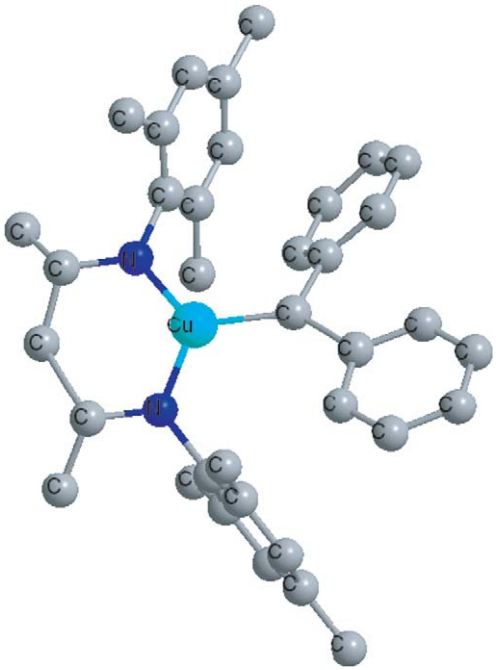

55

Figure 23 X-ray structures of the copper carbene complexes **53** and **54** and geometry of the molecules of **55**. **54** reproduced with permission from ACS publications.

Mononuclear monoalkene complexes usually consist of ethylene or styrene adducts. Trispyrazolylborate ligands[101] have provided a family of compounds of the general formula Tp^{x}Cu(C_2H_4), with catalytic applications.[98,98a–98e,102] As mentioned above, the β-diketiminato Cu(I) ethylene adduct [Me_2NN]Cu(C_2H_4)[103] **67** (Figure 28) allowed the isolation of the copper carbene complexes **54** and **55**. Similarly, the ethylene complex (NPN)Cu(C_2H_4)[104,104a,104b] **68** (NPN = imidophosphanamide) also served as the precursor for the detection of the (NPN)Cu=C(Ph)CO_2Et copper carbene. Both structures revealed a coplanar geometry of the C–C double bond and the co-ligand with neglectable backbonding. Styrene adducts have also been reported, usually with regard to the use of those (or related) compounds in asymmetric, copper-catalyzed cyclopropanation[105,106,106a,107] and/or aziridination[105,107] reactions. The diimine complex **69**[105] and the bis-azaferrocene derivative **70**[106,106a] could be considered as representative examples of this class of compounds (Figure 29). In addition to ethylene and styrene, other olefin adducts have been prepared with norbornene,[108] norbornadiene,[109] allylic alcohols,[110] or 2-vinylpyridines,[111] among others.[112,113] In some cases, alkene copper species

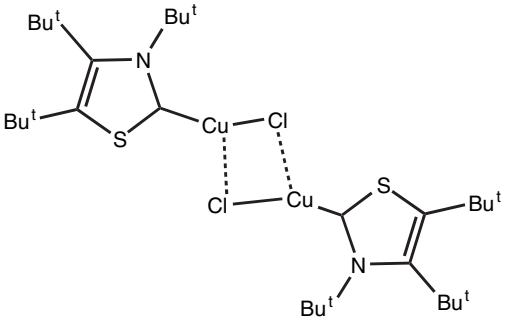

56

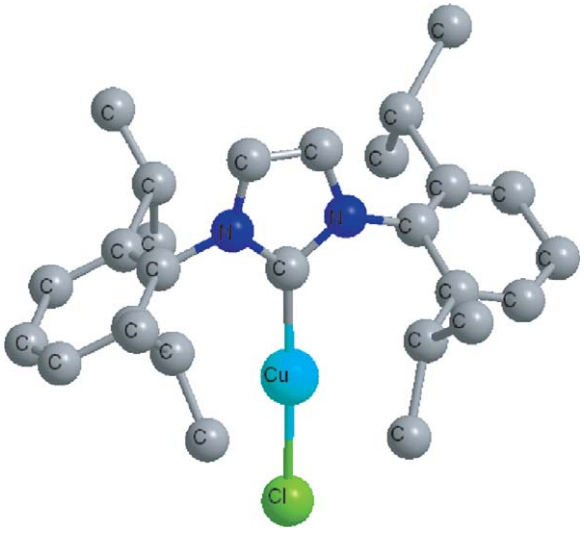

57

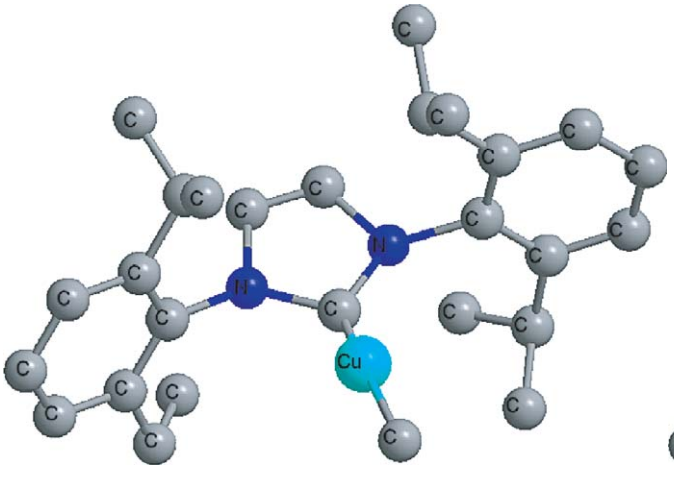

58

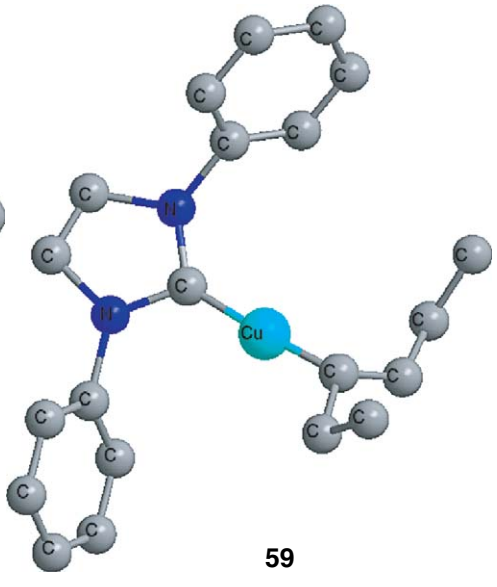

59

Figure 24 X-ray structure of **56** and geometry of the molecules of the complexes **57**–**59**.

have been proposed as intermediates in catalytic cycles, for example, amidocupration or carbonyl allylation processes.[114–117] Bis- and tris(alkene) mononuclear copper compounds are also known. It has been shown that ethylene reversibly binds $CuAl_4$, forming the bis(adduct) $(C_2H_4)_2CuAl_4$ **71**.[118] The stable Cu(I) complex **72**[119] with *all-Z*-tribenzo[12]annulene was obtained upon reaction with the macrocycle and copper triflate, showing three C═C units bonded to the metal center.

Dinuclear alkene copper compounds with different bridging units have been described. In some cases, two halide groups are responsible for the dinuclear structure, with the alkene ligand being bonded to each copper atom.[112,120–123] On the other hand, a given bis(alkene) ligand can exert the role of the bridge, giving two different Cu(C═C) units.[124–126] The compounds **73**[121] and **74**[125] (Figure 30) represent both types of dinuclear copper alkene compounds, respectively. The interaction of a copper source with tetravinylsilane[127] constitutes a nice example for the synthesis of mono-, di-, tri-, and tetranuclear adducts (Scheme 4). Other tetranuclear copper alkene complexes display the already-mentioned cubane-like structure of the Cu_4O_4 core, with one C═C unit bonded separately to each copper center.[128–129]

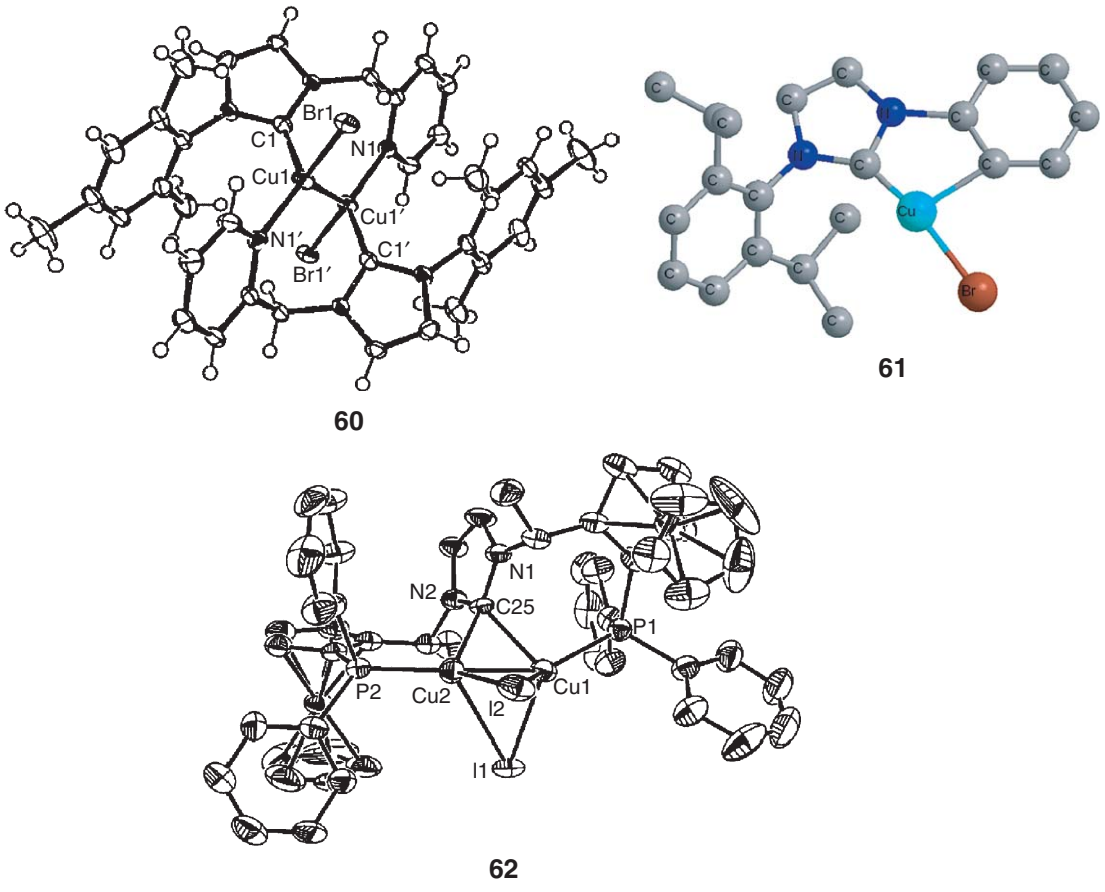

Figure 25 X-ray structures of the copper carbene complexes **60** and **62** and geometry of the molecules of **61**. **60** and **62** reproduced with permission from ACS publications.

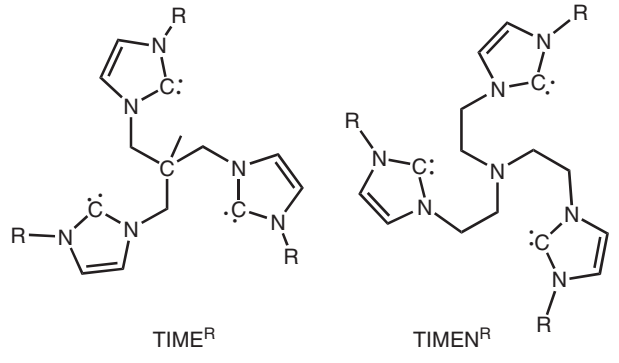

Figure 26 TIME^R and TIMEN^R ligands.

The reaction of copper(I) chloride or bromide with 4-vinylpyridine produces a two-dimensional (2-D) copper(I)–olefin luminescence coordination polymer.[130] This is a common methodology to obtain layered Cu(I) coordination polymers that display exceptional thermal stability. Following this strategy, the use of other olefin-containing substrates such as 2- or 3-pyridylacrylic acid[131] and 4-pyridylacrylic acid in combination with bipyridines[132,133] has led to the assembly of layered solids. Figure 31 shows the monomeric unit as well as the extended 2-D chain representation of {(phen)(4-HPYA)Cu](BF$_4$)}$_n$ **75** in which the π–π stacking is clearly observable.[133] The use of

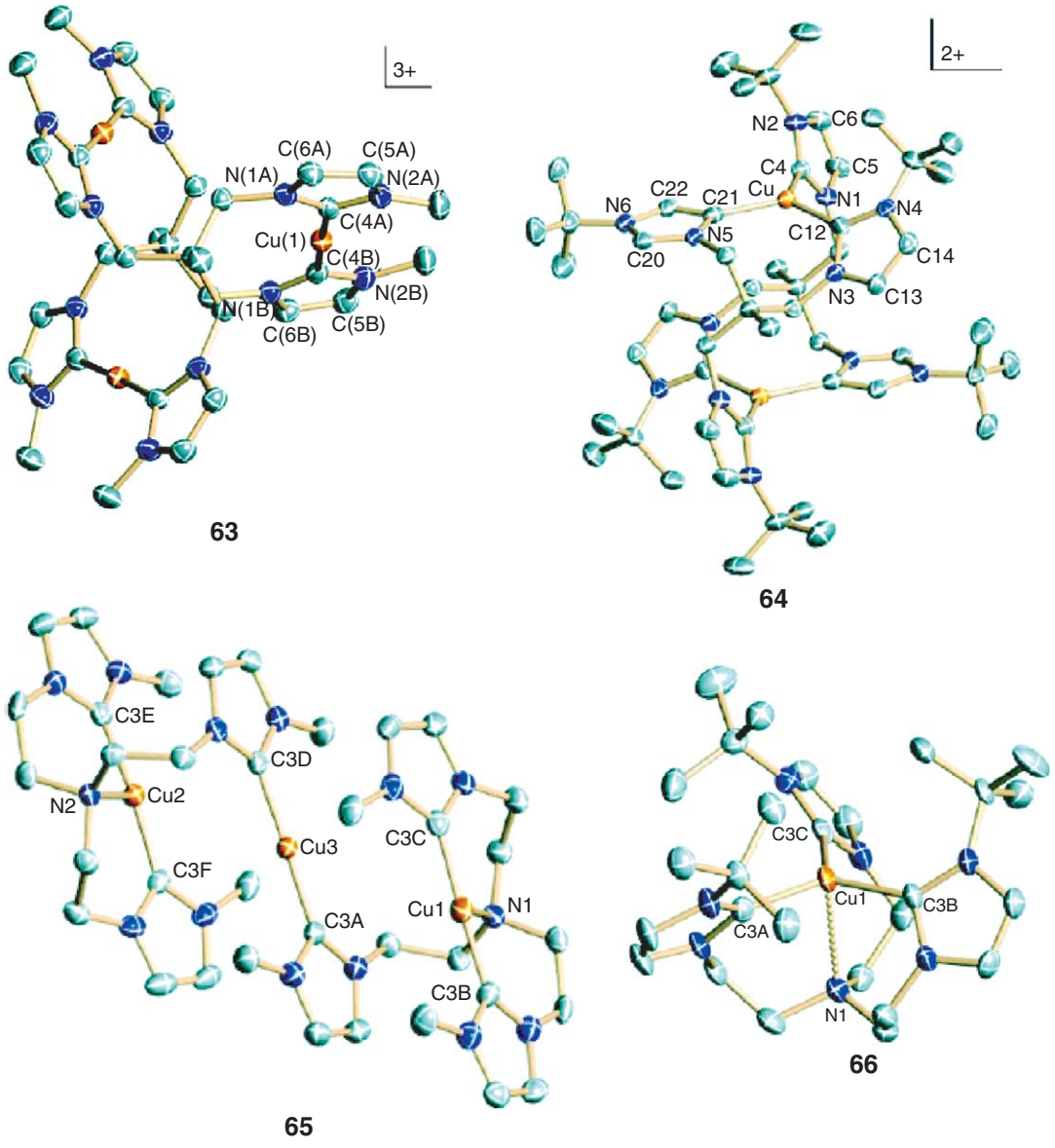

Figure 27 X-ray structures of the copper carbene complexes **63–66**. Reproduced with permission from ACS publications.

the appropriate chiral groups attached to the olefin-containing ligand has allowed the formation of related homochiral coordination polymers.[134,135] A variation of this methodology supposed the formation of a 2-D polymer with clusters as connecting nodes.[136] A different approach consisted of the reaction of copper(II) acetate and hydroquinone, that led to a Cu(I) dinuclear complex which in the presence of the appropriate co-ligand forms ordered 1-D or 2-D coordination polymers.[137,138] The use of fumaric acid instead of the quinone also led to layered materials.[139]

Previous to 1994, the number of structurally characterized copper arene complexes was quite small,[140,140a–140d] although it has increased in the last decade. Some of the arylcopper compounds already commented on in previous sections also displayed π-coordination of the aromatic rings.[26,27] The classical example of a benzene adduct, very common for many metals, has also been found in copper compounds. This is the case of the β-diketiminato-containing complexes **76**[141,141a] and **77**[142] (Figure 32), where the benzene ring is bonded to the metal center in a dihapto fashion. However, in most of the copper arene complexes developed to date, the arene ring is included in the ligands bonded to the metal center. The use of triamine ligands with the skeleton bis[2-(2-pyridyl)ethyl]amine has

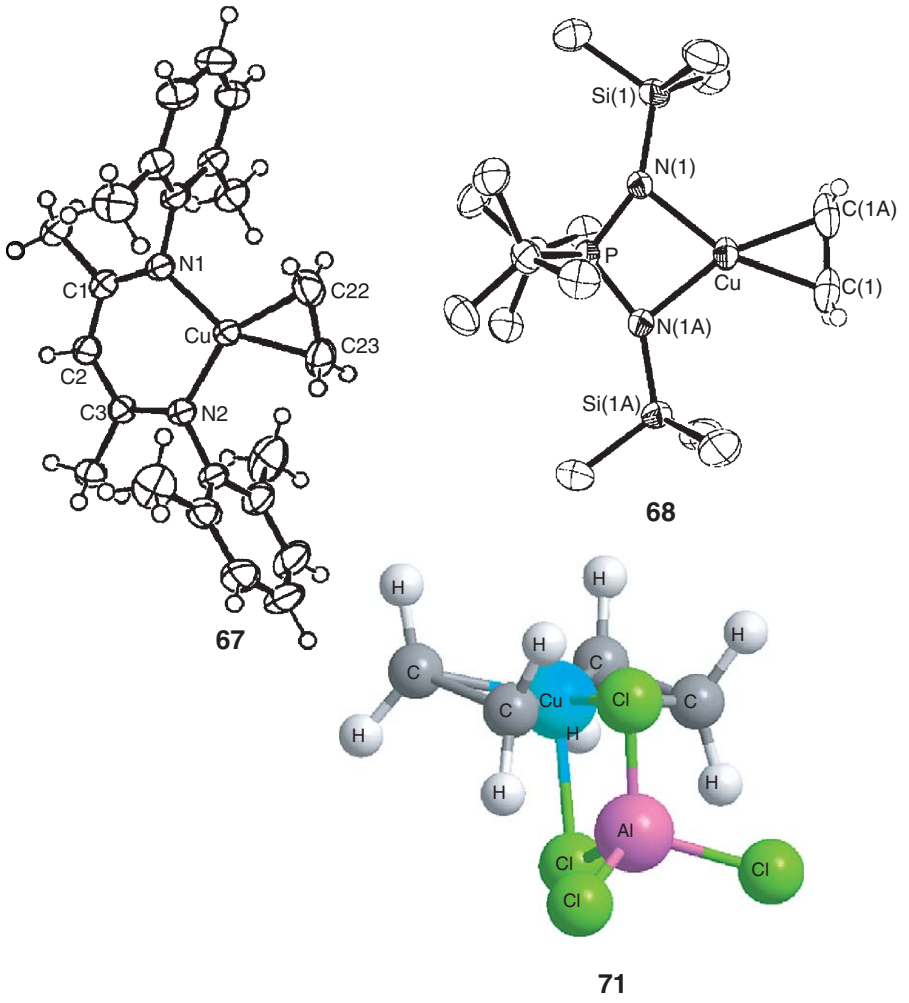

Figure 28 X-ray structures of the copper–alkene complexes **67** and **68**, and geometry of the molecules of **71**. **67** and **68** reproduced with permission from the Royal society of chemistry.

led to the formation of a series of η^2-arene complexes such as **78**,[143] where the copper atom is located in a distorted tetrahedral geometry. The *d*–π-interaction in this and related compounds has been explained as the result of the overlapping of the copper d_z^2-orbital and a π-orbital of the arene ring. The effect of the ligand affected the structures and redox properties of these compounds, with special emphasis on the nature of the alkyl linker between the central nitrogen and the aryl groups.[144,145] Anthracene-[146] and naphthalene-containing[147,147a,147b] ligands have also been coordinated to copper(I). The naphthalene group is included in the macrocycle *N*-[2-(1-naphtyl)ethyl]1-aza-4,8-dithiacyclodecane, that gave complex **79**[147,147a] upon reacting it with $[Cu(NCMe)_4](PF_6)$. The latter case exemplifies the arene coordination–decoordination process that takes place in the presence of donor ligands such as acetonitrile. The more elaborated macrobicycle *S*-cylindrophane afforded a bis-arene with the "coppercene" structure **80**[148,148a] (Figure 33), in which each ring is assumed to be η^6-bonded to the copper center. Other examples where the copper atom is bonded to phenyl rings of boron-containing ligands[149,150] or in heterobimetallic[151,152] complexes are also known.

Similar to arene copper compounds, not many π-bound Cu–Cp complexes are known (for structurally characterized, previous examples see Refs: 153,153a–153e), probably because the common η^5-bonding mode in many metals is not strong enough for this metal, in such a way that loss of the Cp ligand has been observed in some cases. The use of certain Cp-substituted ligands conferred additional stability to these compounds, as in the pentaphenylcyclopentadienyl complex $(Ph_5Cp)Cu(PPh_3)$ **81** (Figure 34).[155] A slipped-sandwich structure was found for the complex $[PPh_4][CuCp_2]$ **82**,[156] in which an η^2-coordination mode was observed for each ring. *N*- and *P*-containing five-membered rings bonded to a copper center in a π-interaction are also known.[157–159] A novel copper–indole bonding

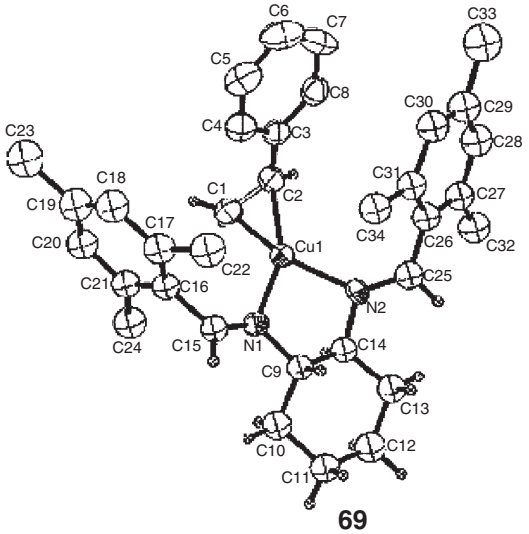

69

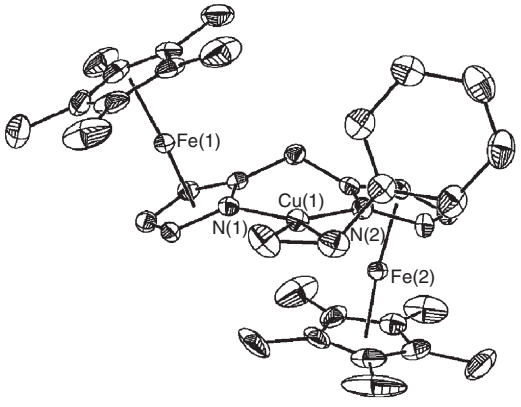

70

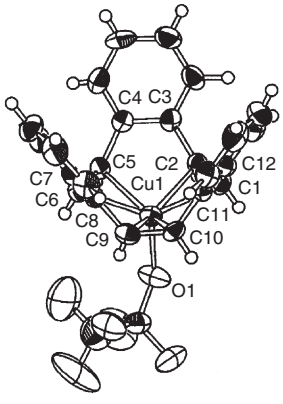

72

Figure 29 X-ray structures of the copper–alkene complexes **69**, **70**, and **72**. **69** and **70** reproduced with permission from ACS publications. **72** reproduced with permission from Elsevier.

was observed in the complex [Cu(Me_2IMP)(CH_3CN)](PF_6) **83**,[157] with an η^2-coordination of the double C–C bond of the five-membered ring to the copper atom. A π-complex **84**[158] was formed with a phosphaarene, although in this case the structure showed the existence of a bonding interaction between Cu and the P–C double bond.

2.03.3.2 Alkyne Complexes

There has been an increasing interest in recent years in copper alkyne complexes since they can be used as precursors for chemical vapor deposition (CVD) processes.[126] The generation of pure copper films from Cu(I) compounds under thermal conditions has been achieved in a general manner using the commercially available (hfac)Cu(VTMS) (hfac: hexafluoroacetylacetonate; VTMS: vinyltrimethylsilane).[160] The related [(hfac)Cu]$_2$-(MHY) **85** (Figure 35)[126,161] (MHY: 2-methyl-1-hexen-3-yne) has also been employed for such purposes. This complex contains two copper centers, each of them bonded in an η^2-fashion to an unsaturated C–C bond, a triple and a double. Dinuclear, heteroatom bridges, bisalkyne complexes, such as {Cu(acac)}$_2$(S(C$\equiv$C^{t}Bu)$_2$) **86**[162] also display the volatility required for their use in CVD. Cu(I) complexes with a chelating, monoanionic ligand and one alkyne group side-on bonded to the metal center have been described.[104a,163,164,164a] It is worth mentioning the use of the strained alkyne 3,3,6,6-tetramethyl-1-thiacyclohept-4-yne (tmch) that led to both mono- and dinuclear complexes.[165–168] The compound (acac)Cu(tmch)[165] **87** constitutes an example of this family of

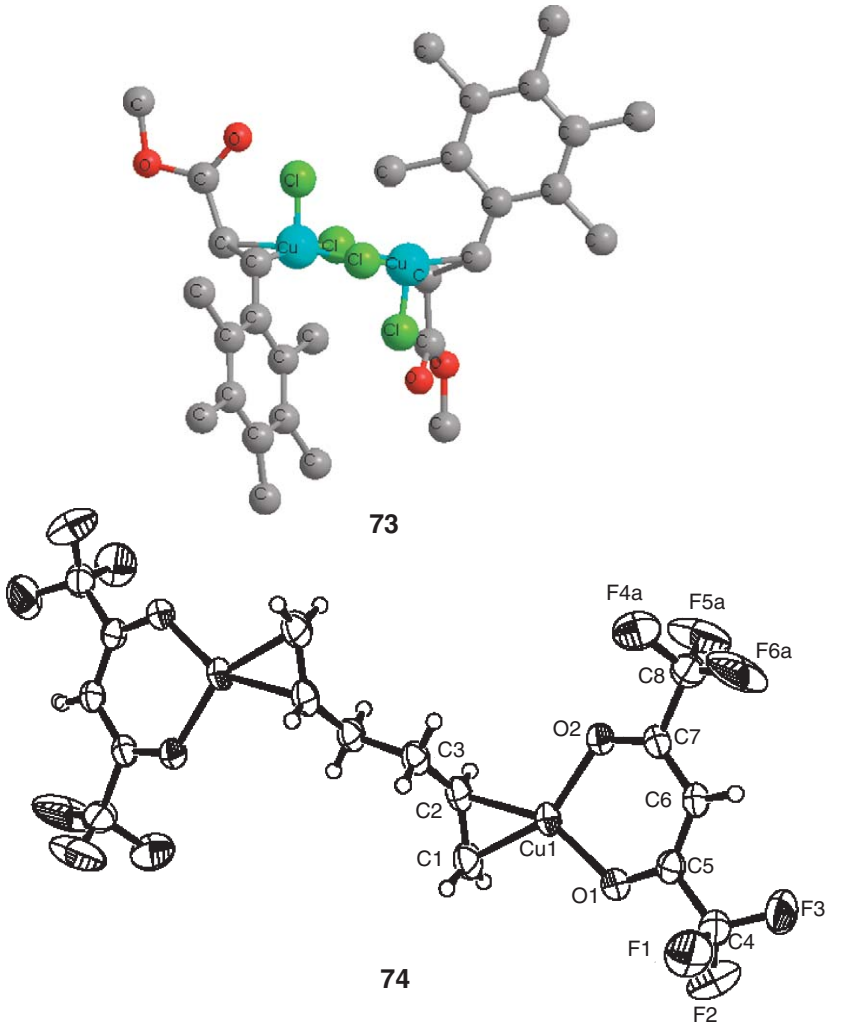

Figure 30 X-ray structures of the copper–alkene complexes **73** and **74**.

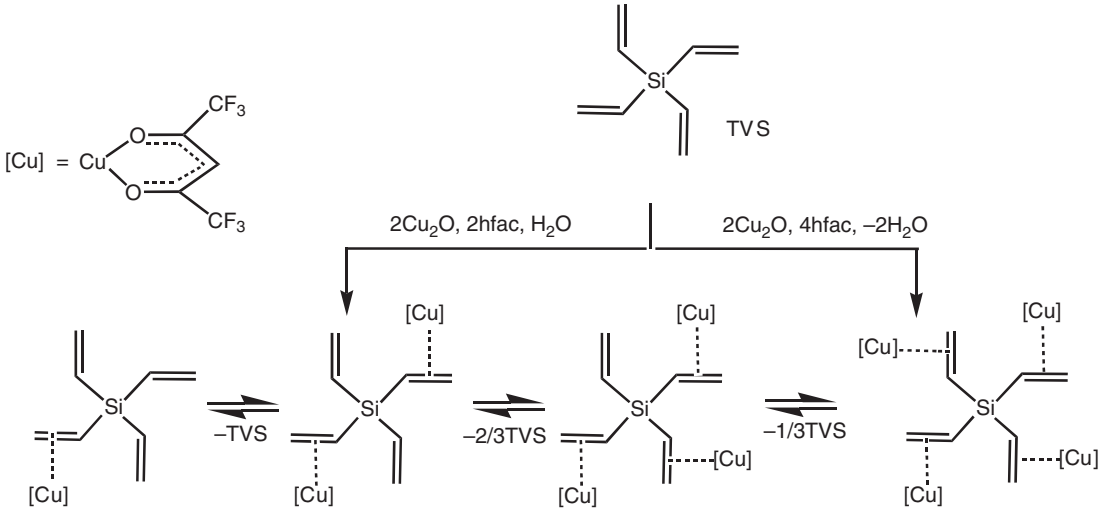

Scheme 4 Formation of mono-, di-, tri-, and tetranuclear olefin–copper complexes.

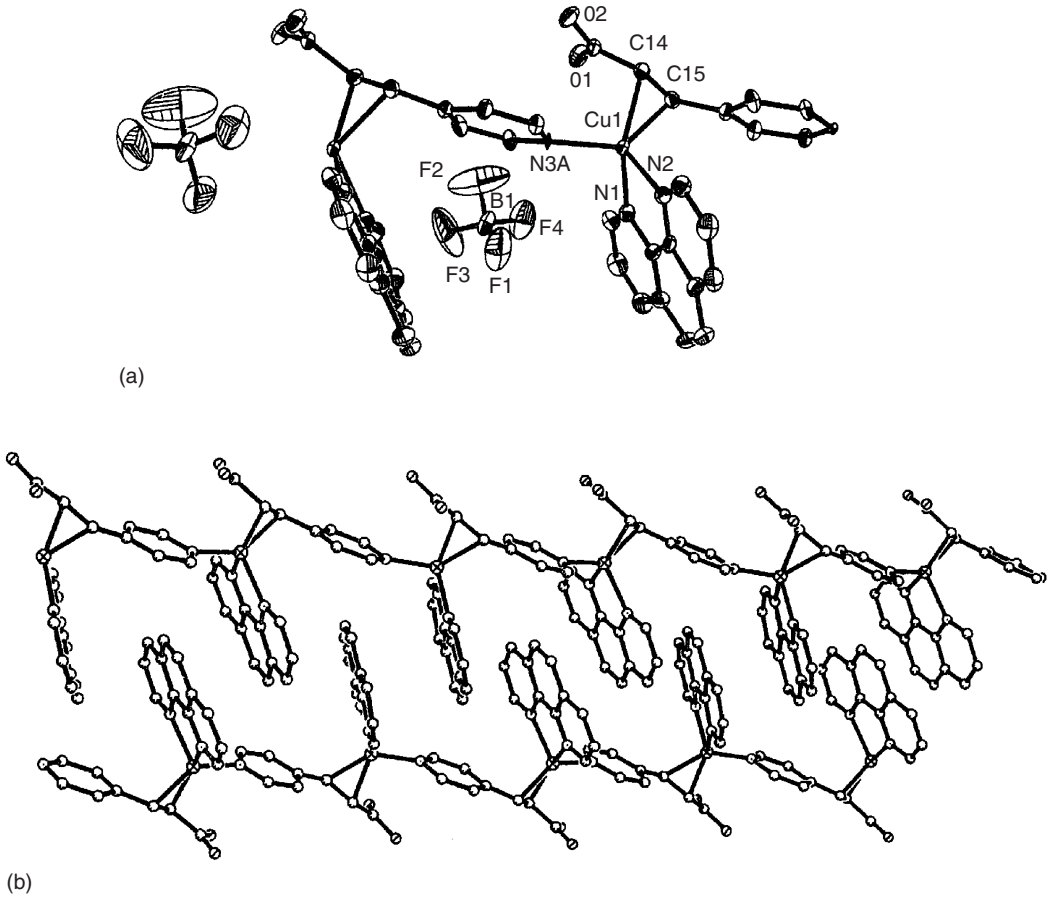

75

Figure 31 Structure of (a) the monomeric unit and (b) the 2-D polymer {(phen)(4-HPYA)Cu](BF$_4$)}$_n$**75**. Reproduced with permission from the Royal society of chemistry.

compounds, and it has also been employed as a CVD precursor. The hfac group can be replaced by a halide and a neutral, 2e-donor (phosphine, amine).[166–168]

The general synthetic route for Cu(I) alkyne-containing complexes is the reaction of a Cu(I) source (CuX, X = halide, acac, or similar) and the alkyne in the presence of an additional donor. In the absence of the latter, dinuclear species have been obtained, where two halides usually sustain the bridge between both copper atoms.[169,170] The structure of the complex [CuCl(tmch)]$_2$[169] **88** (Figure 36) shows the halide-bridging unit, where the copper center displays a trigonal-planar coordination and the alkyne ligand appears in the coordination plane. Some of these compounds reacted further with Na^{t}OBu to exchange the halide with the O^{t}Bu group as the bridge unit. In addition, Cu–Cu bonding interaction was also observed.[171,172] Analogous compounds to **88** have also been prepared with cyclooctyne to give [CuX(cyclooctyne)]$_2$,[173] which in the presence of an excess of the alkyne afforded the mononuclear bisalkyne CuX(cycloctyne)$_2$ **89**,[173] for which low stability had been proposed from theoretical studies with simplified models.[174] Tetranuclear compounds in which only one chloride ion forms the bridge between two adjacent copper atoms are also known, with one alkyne group bonded to each metal center.[175,176] It is interesting to note that in some cases, polymeric materials are formed due to the existence of donor atoms that can bind two different metal centers. In the case of the sulfur-containing, strained alkynes, this is a very common feature.[170,171,173,177,178] The alkyne ligand can also act as the bridge between two copper centers,[163,177] as shown in the structure of Cu(hfac)$_2$(Me$_3$SiCCSiMe$_3$) **90**.[163]

A number of stable heterobimetallic copper alkyne complexes have been reported, based on the strategy of using another metal bis(alkynyl) complex as a "chelating" ligand for copper. The 1,4-diyne [(η^5-C$_5$H$_4$SiMe$_3$)$_2$Ti-(C≡CSiMe$_3$)$_2$][180] (or related complex) was found to stabilize the copper units CuX, with X = alkyl,[180,181] vinyl,[180]

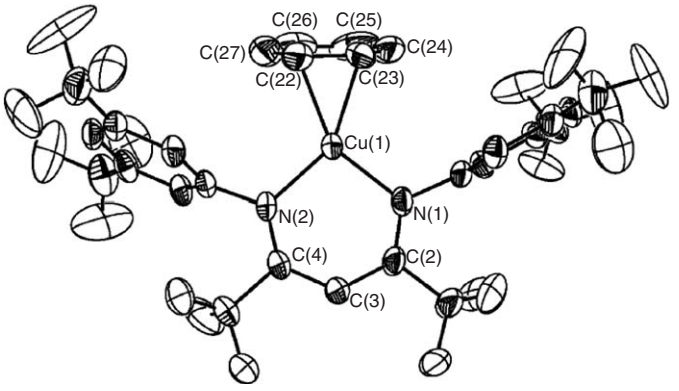

76

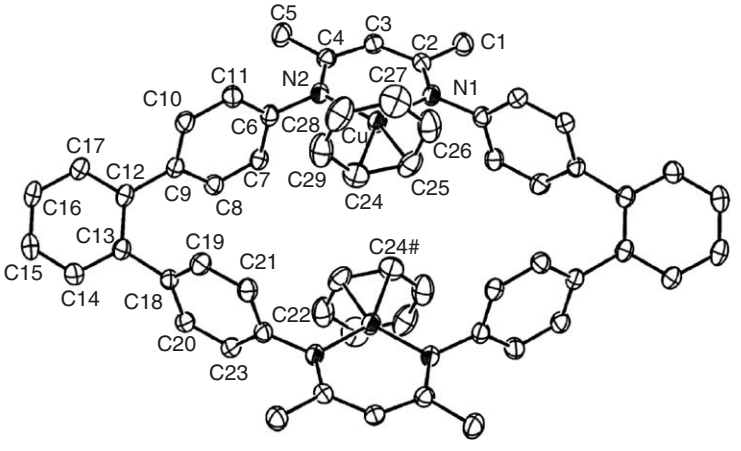

77

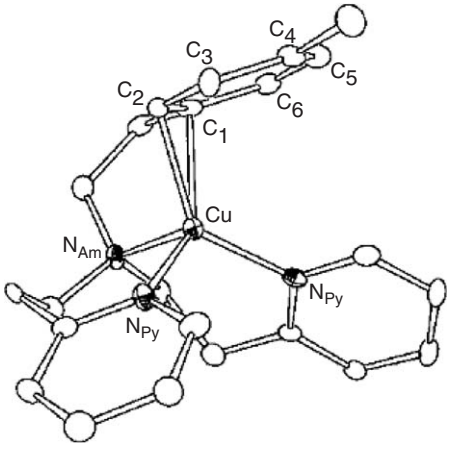

78

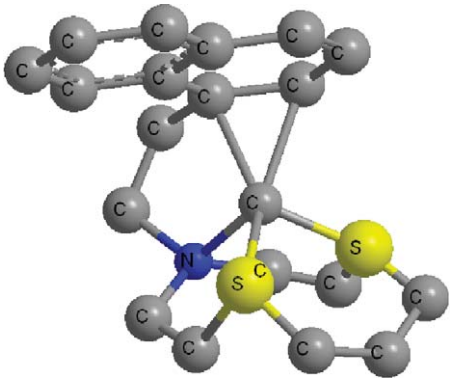

79

Figure 32 X-ray structures of the arene complexes **76**–**78** and geometry of the molecules of **79**. **76** and **77** reproduced with permission from ACS publications. **78** reproduced with permission from Wiley.

aryl,[180,182] alkynyl,[183–187] halide,[188,189] arenethiolate,[190,191] among others.[192] As representative examples, the structures of the methyl **91**[180] and mesityl **92**[180] derivatives are shown in Figure 37. Platinum bisalkynyl complexes have also been employed with the same purpose, leading to several types of mixed compounds, some of them with luminescence properties. The (^{t}Bu$_2$bipy)Pt(C≡CR)$_2$Cu(SCN) complex **93**[193] displays a *cis*-geometry of the alkynyl

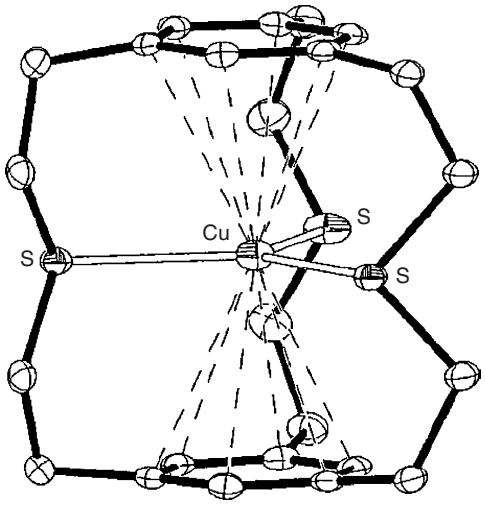

80

Figure 33 The bisarene copper complex with *S*-cylindrophane **80**. Reproduced with permission from Wiley.

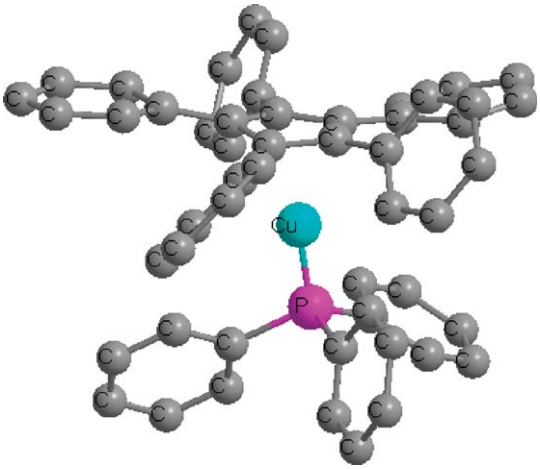

81

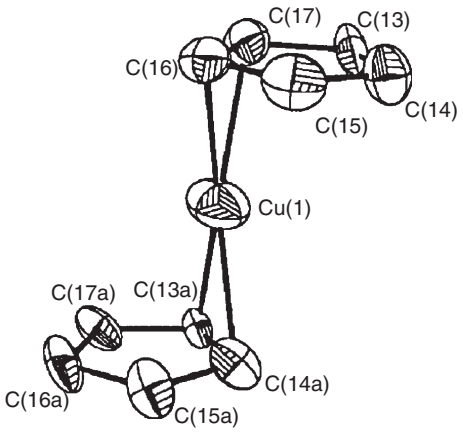

82

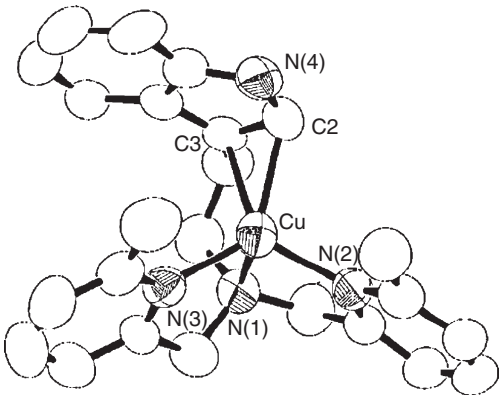

83

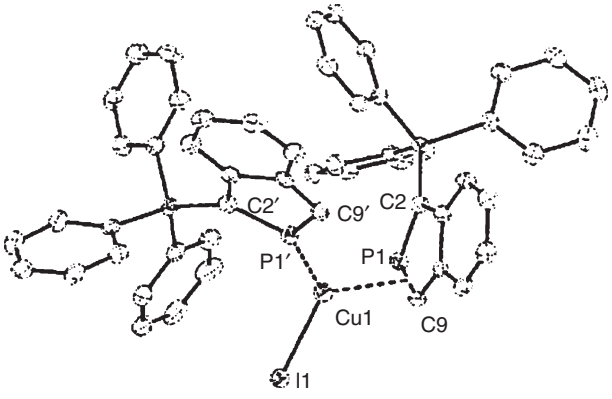

84

Figure 34 Geometry of the molecules of **81** and the X-ray structure of the complexes **81**–**83** containing Cp and Cp-like ligands. **82** reproduced with permission from Elsevier. **83** reproduced with permission from Wiley. **84** reproduced with permission from the Royal society of chemistry.

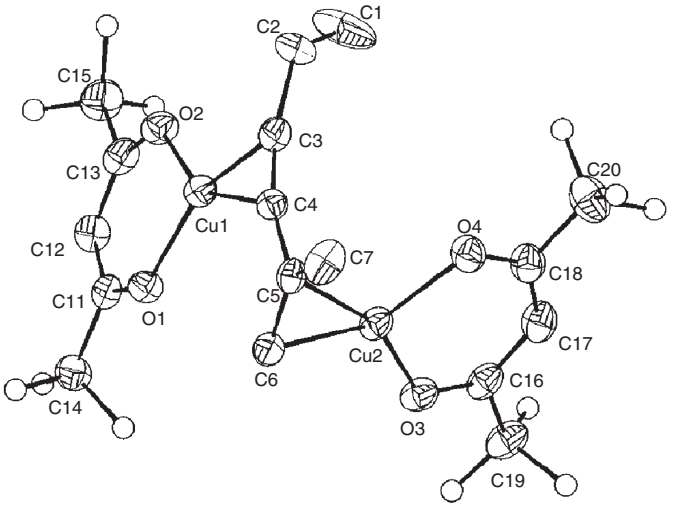

85

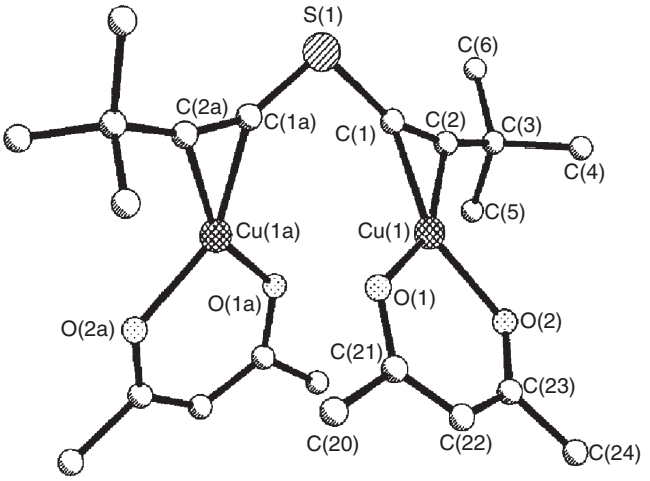

86

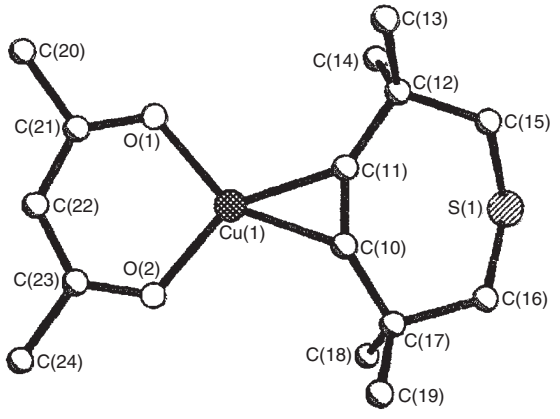

87

Figure 35 X-ray structures of the copper alkyne compounds 85–87. 85 reproduced with permission from ACS publications. 85 and 87 reproduced with permission from Elsevier.

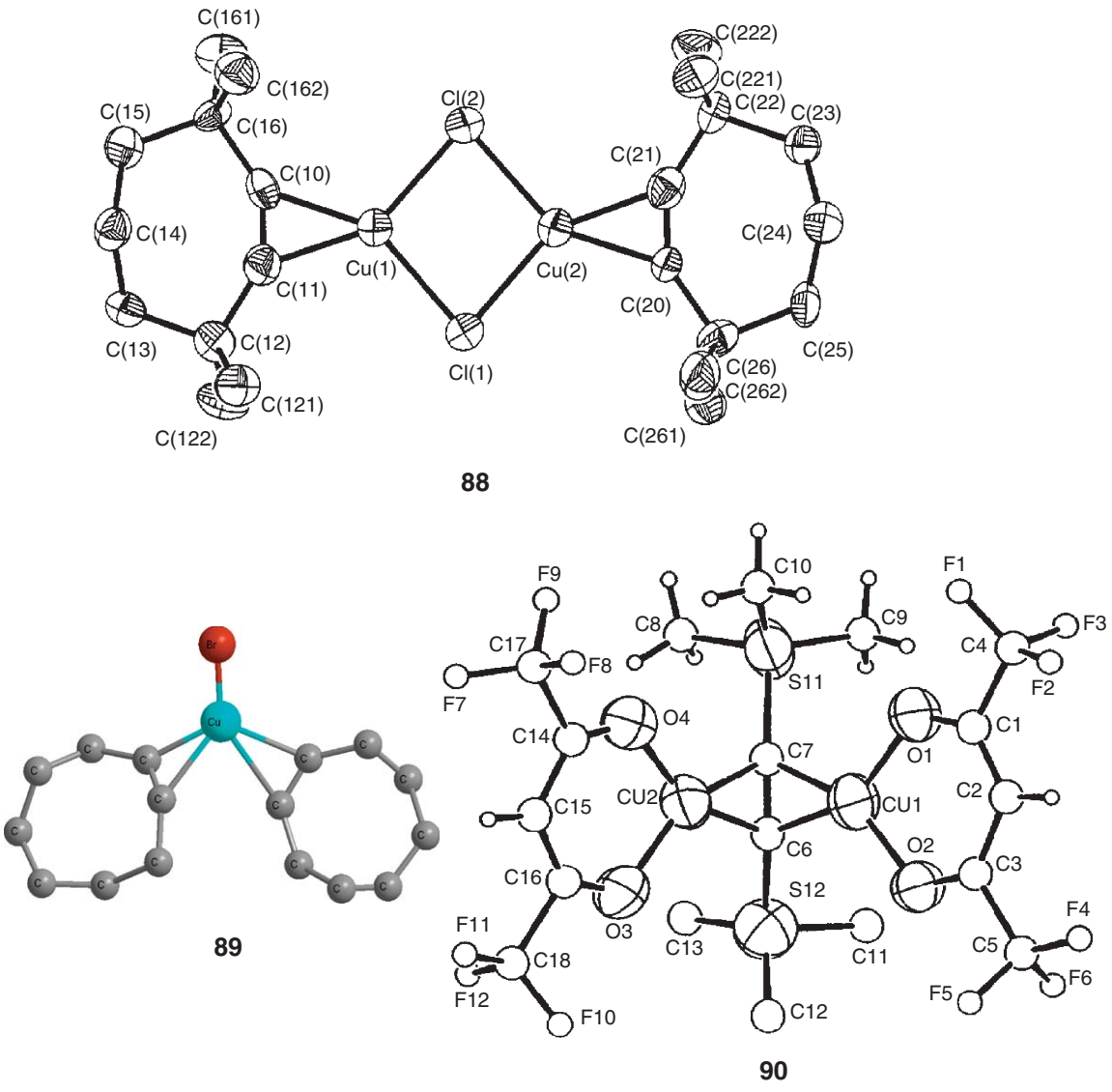

Figure 36 XX-ray structures of the copper alkyne compounds **88** and **90** geometry of the molecules of **89**. Reproduced with permission from Elsevier.

groups with respect to the platinum center, the copper atom being located in a trigonal-planar environment. This structure has been found for other compounds with halides[194–196] or *N*-donor ligands[73,197,198] bonded to copper. In some cases, homoleptic compounds have been reported, in which the copper is exclusively coordinated by a number of the Pt bisalkynyl groups.[199,200] In addition, copper-containing fragments have been coordinated to the *trans*-Pt(C≡CR)$_2$ unit,[201,202] as in compound **94**. Other metals such as ruthenium,[203] rhenium,[204,205] rhodium,[206] iridium,[206] gold,[207] or mercury[207a] containing alkynyl ligands have been reported to behave in a similar manner, with the copper center binding the unsaturated carbon–carbon bond in a dihapto fashion.

2.03.4 Carbonyl, Cyanocuprates, and Isocyanide Complexes

Although some copper carbonyls were known before, the first crystallographic characterization of one of these compounds was carried out in 1973 with TpCu(CO).[208] Similar complexes have been reported to date,[209–215] particularly in the last decade, since the CO ligand can be used as a probe to estimate electronic and also, to some extent, steric effects of the Tp^x ligand. The related trispyrazolylmethane group has also been employed to yield the

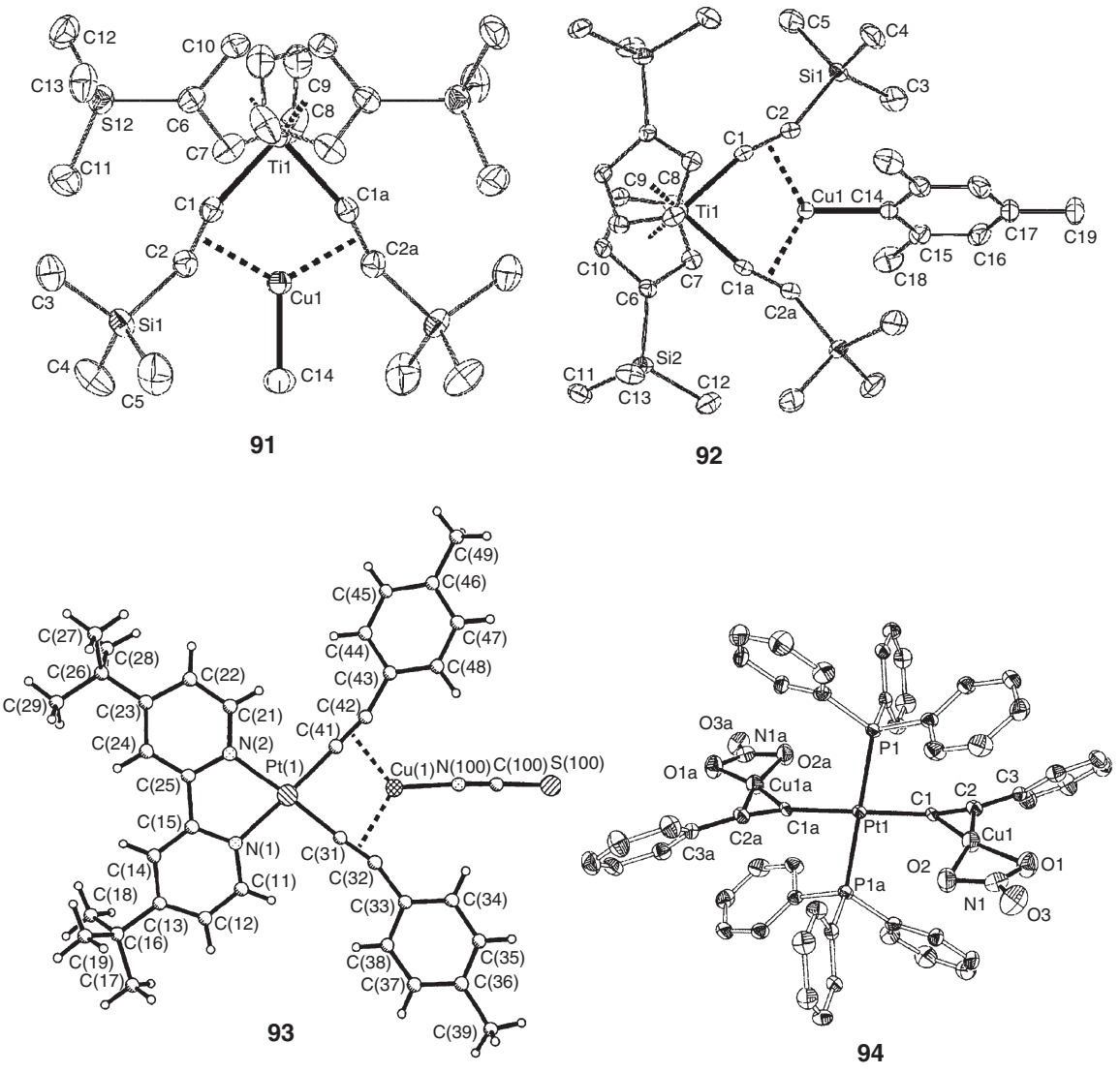

Figure 37 X-ray structures of the heterobimetallic copper alkyne compounds **91**–**94**. **91** and **92** reproduced with permission from ACS publications. **91** and **94** reproduced with permission from Elsevier.

corresponding $(HCpz^{x}_{3})Cu(CO)$ complexes.[216] In this family of compounds, the copper center is located in a distorted tetrahedral environment, as shown in the structure of $Tp^{(CF_3)_2}Cu(CO)$ **95** (Figure 38).[215] An interesting correlation between the ^{63}Cu chemical shift and the CO stretching vibrations has been found:[211] when the $\nu(CO)$ value increases, the corresponding ^{63}Cu NMR signal shifts toward lower field. Other nitrogen-containing ligands such as triazapentadienyl[217] or the triamine Me-imp[218] (*N*-(3-indolylmethyl)-*N*-(6-methyl-2-pyridylmethyl)-*N*-(2-pyridylmethyl)amine) also led to the formation, isolation, and characterization of monocarbonyl complexes, as is the case of the cationic $[Cu(Me\text{-}imp)(CO)]^+$ **96**.

The use of triazacyclononanyl[219] or hexaaza[220] macrocyclic ligands has allowed the synthesis of dinuclear carbonyl compounds. The carbonylation of aryloxocopper[221] compounds also affords dinuclear complexes. A different case is that of the compound $[Cu(CO)(H(CF_3CO_2)_2)]_2$, for which two trifluoroacetates act as the bridging ligands.[222] A trinuclear complex, although with a 1 : 1 Cu : CO ratio, has been characterized, with the mixed pyridine–pyrazol ligand 2-(3(5)-pyrazolyl),6-methylpyridine.[223] It is also worth mentioning the first structurally characterized copper dicarbonyl $Cu(CO)_2(N(SO_2CF_3)_2)$ **97**,[224] prepared from mesitylcopper and $HN(SO_2CF_3)_2$. Also, the homoleptic tetracarbonyl $Cu(CO)_4^+$ has been structurally characterized, as the cation of the complex $[Cu(CO)_4][1\text{-}Et\text{-}CB_{11}F_{11}]$

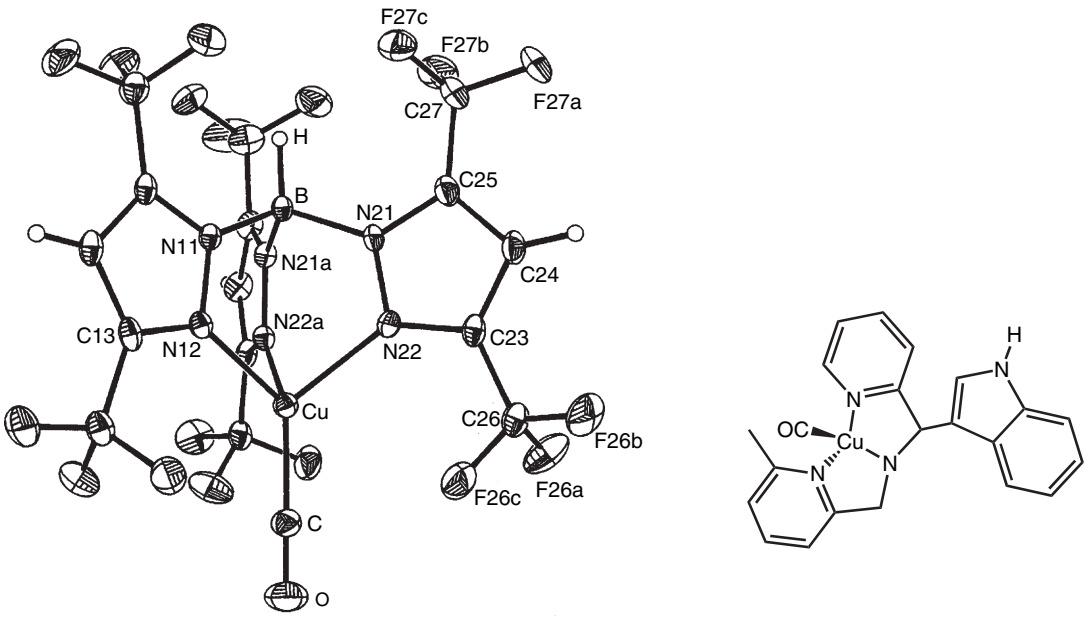

Figure 38 X-ray structures of the copper carbonyls **95** and **96**. **95** reproduced with permission from ACS publications.

98.[150] Although evidences for $Cu(CO)_2^+$ and $Cu(CO)_3^+$ have been collected, only in this case has it been possible to elucidate the solid structure. In the absence of the above chelating ligands, copper carbonyls are somewhat unstable. The simple copper carbonyl chloride Cu(CO)Cl has been prepared in solid argon under extreme conditions.[225] At room temperature, polynuclear carbonyl copper materials have been obtained when using trihalogenoacetates[226] or hydrogensulfate[227] in addition to carbon monoxide and a Cu(I) source.

In some heterometallic compounds of copper with other metal, carbonyl groups bonded to the latter have been found to weakly bond the copper atom, therefore acting as a bridging ligand. This is a rare and weak interaction, as inferred from the slight to zero deviation from linearity of the M–C–O group. Structurally characterized examples have been reported with Nb,[228] Fe, or Ru, and proposed for others. The structure of the niobium complex $[\{Nb(C_5H_4SiMe_3)_2(CO)\}_2(\mu\text{-}H)_2]^+$ **99** shown in Figure 39 shows this feature, in which the Cu–Nb moiety is linked by a hydride and by the referred weak interaction with the carbonyl group. The mentioned linearity is clearly observable, although the Cu–C distance of 2.351(13) and 2.510(13) fall in the range of bonding interaction.

Cyanocuprates constitute a class of organocopper compounds that finds applications in organic synthesis.[234] They are prepared by the direct reaction of an organolithium reagent and CuCN, with two different types of compounds being prepared depending on the stoichiometry employed: the 1 : 1 ratio leads to RCu(CN)Li compounds whereas the 2 : 1 mixture affords $R_2Cu(CN)Li_2$. The lower- order[235–237] or 1 : 1 cyanocuprates usually display the Cu–C–N–Li fragment, with the R group bonded to the copper atom, with several aggregation degrees (monomeric to oligomeric). Figure 40 contains the X-ray structure of $[Li(THF)_2\{Cu(CN)C_6H_3\text{-}2,6\text{-}Trip_2\}]_2$ **100**,[234] where the N_2Li_2 core is responsible for the dimeric nature. In contrast with this, the 2 : 1 higher-order cyanocuprates have been the object of many studies, and only very recently the structures of some members of the family have been elucidated. For a compound of composition $R_2Cu(CN)Li_2$, a rather "ionic" formulation $[R_2Cu]^-[LiCNLi]^+$ is more appropriate, lacking the above CuCNLi moiety. The compounds $[^tBuCu^tBu\{Li(THF)(pmdeta)\}_2CN]$ **101**[237] and $[Ar_2Cu(CN)Li_2(THF)_4]_\infty$ **102**[238] correspond to this case, with the difference of a discrete ionic structure in the former compared with the chain observed for the latter.

Copper isocyanides have been reported with many co-ligands and different nuclearity. The isocyanide analog to the carbonyl **95**, the complex $Tp^xCu(CNR)$,[239] exemplifies a series of copper isocyanides in which several nitrogen donors are also bonded to the copper center, in addition to the isocyanide. This is the case of imido,[240] hexaaza,[220] pyrazolato,[241,241a] or $MePY_2$ ligands,[242] among others, that led to complexes containing the Cu–CNR group. The

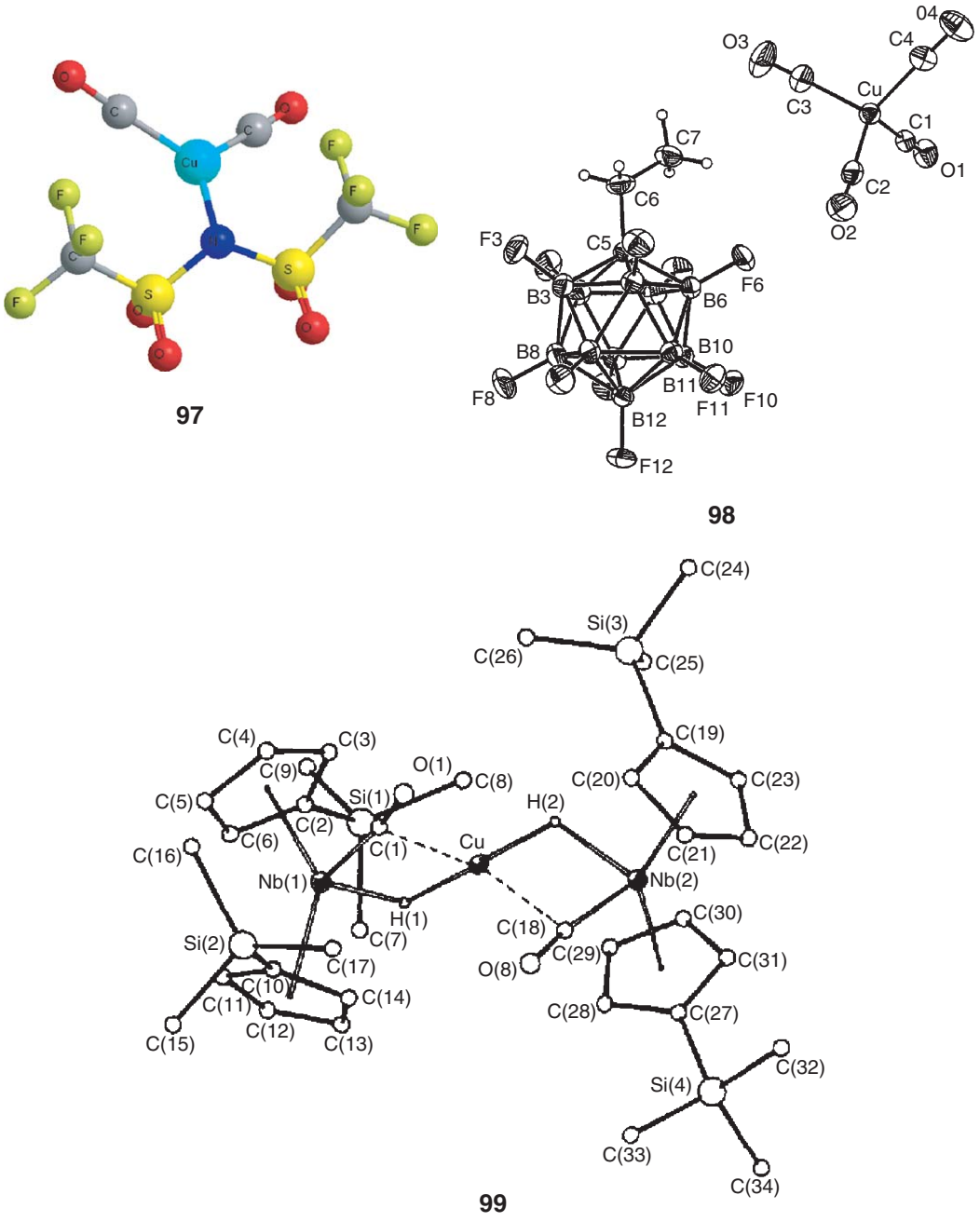

Figure 39 Copper carbonyls: geometry of the molecules of **97** and X-ray structures of **98** and **99**. **98** and **99** reproduced with permission from ACS publications.

structure of the complex $L^{iPr}Cu(CNC_6H_3\text{-}Me_2\text{-}3,5)$[240] **103** ($L^{iPr}$ = 2,6-((diisopropylphenyl)imido)pentane) shows the copper–isocyanide group with the typical Cu–C–N–R quasi-linear geometry (Figure 41). The existence of more than one CNR ligand bonded to the same copper atom,[241a,243–245] using chelating phosphines[243,244] or carboxylates[245] as the co-ligand, has also been described. However, the CNR group may also act as a bridge between two copper centers, with a bonding mode similar to that observed in alkynyl derivatives: the carbon atom is bonded to both Cu atoms by means of a 3c-2e linkage, as can be seen in the structure of $[Cu_3(\mu_3\text{-}\eta^1\text{-}C{\equiv}CC_6H_4CH_3\text{-}4)(\mu\text{-}\eta^1\text{-}C{\equiv}NC_6H_4CH_3\text{-}4)(\mu\text{-dppm})_3]^{2+}$ **104**.[246]

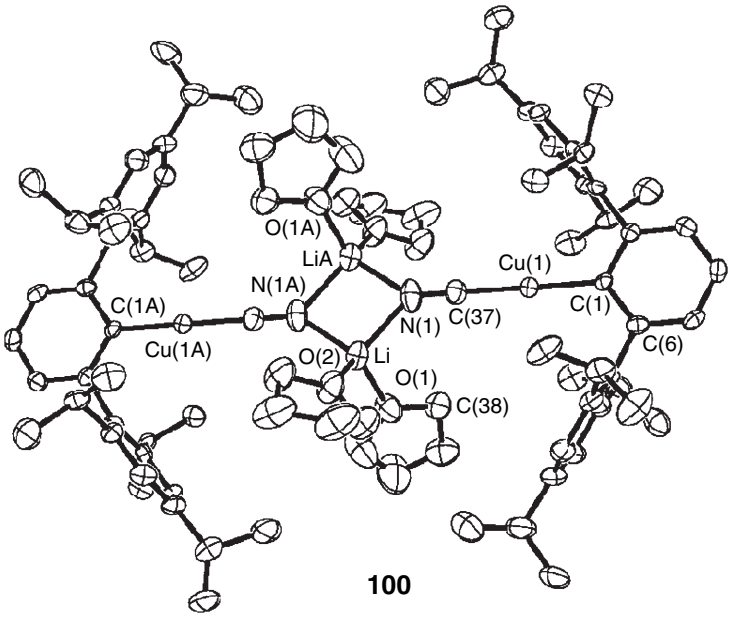

100

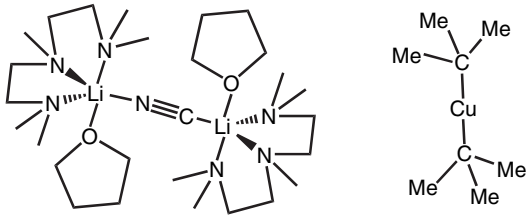

101

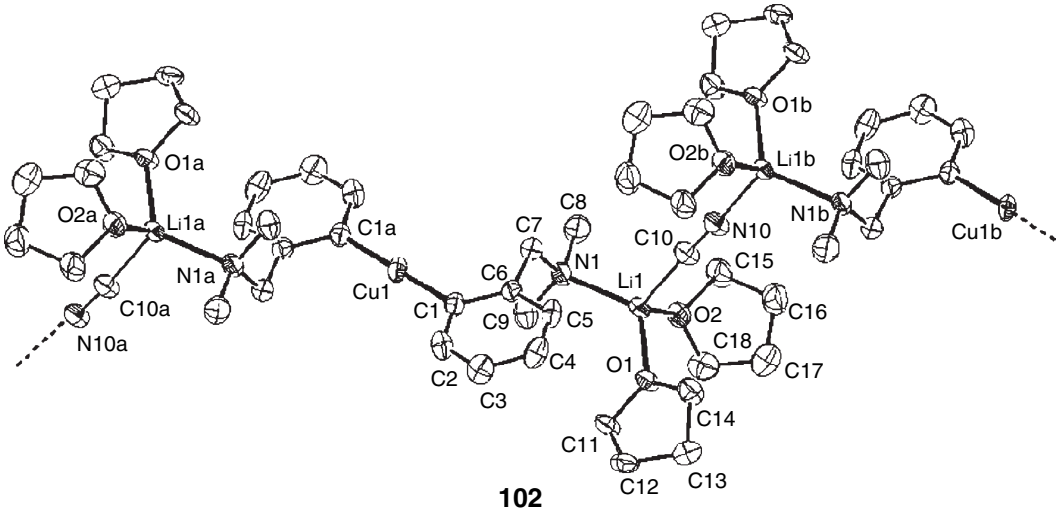

102

Figure 40 X-ray structures of the cyanocoppers **100**–**102**. **100** reproduced with permission from ACS publications. **102** reproduced with permission from Wiley.

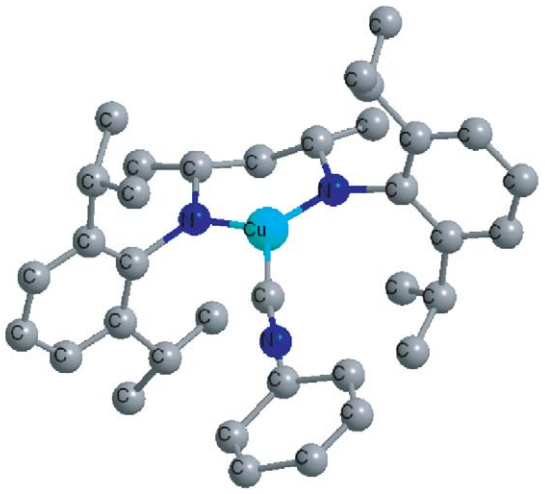

103

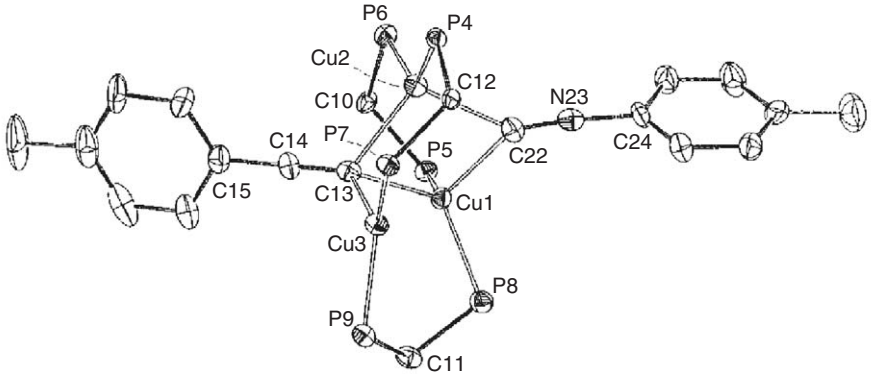

104

Figure 41 The copper isocyanide complexes **103** and **104**. **104** reproduced with permission from ACS publications.

References

1. Krause, N., Ed. *Modern Organocopper Chemistry*; Wiley-VCH: Weinheim, 2002.
1a. Lipshutz, B. H. In *Organometallic in Synthesis: A Manual*; Schlosser, M., Ed.; Wiley: Chichester and New York, 2002; pp 665–815.
2. Kharash, M. S.; Tawney, P. O. *J. Am. Chem. Soc.* **1941**, *63*, 2308.
3. Buckton, G. B. *Ann. Chem. Pharm.* **1859**, *109*, 218.
4. Reich, M. R. *C. R. Acad. Sci.* **1923**, *177*, 322.
5. Gilman, H.; Jones, R. G.; Woods, L. A. *J. Org. Chem.* **1952**, *17*, 1630.
6. Grotjhan, D. B.; Halfen, D. T.; Ziurys, L. M.; Cooksy, A. L. *J. Am. Chem. Soc.* **2004**, *126*, 12621.
7. Lang, H.; Köhler, K.; Blau, S. *Coord. Chem. Rev.* **1995**, *143*, 113.
8. Mori, S.; Nakamura, E. *J. Mol. Struct. (THEOCHEM)* **1999**, 461–462, 167.
8a. Böhme, M.; Frenking, G.; Reetz, M. T. *Organometallics* **1994**, *13*, 4237.
8b. Antes, I.; Frenking, G. *Organometallics* **1995**, *14*, 4263.
8c. Snyder, J. P.; Bertz, S. H. *J. Org. Chem.* **1995**, *60*, 4312.
8d. Barone, V.; Adamo, C. *J. Phys. Chem.* **1996**, *100*, 2094.
8e. Hermann, H. L.; Boche, G.; Schwerdtfeger, P. *Chem. Eur. J.* **2001**, 7, 5333.
8f. Suresh, C. H.; Koga, N. *J. Am. Chem. Soc.* **2002**, *124*, 1790.
9. Schaper, F.; Foley, S. R.; Jordan, R. F. *J. Am. Chem. Soc.* **2004**, *126*, 2114.
10. John, M.; Auel, C.; Behrens, C.; Marsch, M.; Harmas, K.; Bsold, F.; Gschwind, R. M.; Rajamohanan, P. R.; Boche, G. *Chem. Eur. J.* **2000**, *6*, 3060.
11. Hitchcock, P. B.; Lappert, M. F.; Layh, M. *Dalton Trans.* **1998**, 1619.
12. Van den Ancker, T. R.; Bhargava, S. K.; Mohr, F.; Papadopoulos, S.; Raston, C. L.; Skelton, B. W.; White, A. H. *Dalton Trans.* **2001**, 3069.
13. Meyer, E. M.; Gambarotta, S.; Floriani, C.; Chiesi-Villa, A.; Guastini, C. *Organometallics* **1989**, *8*, 1067.
14. Ahlrichs, R.; Anson, C. E.; Clerac, R.; Fenske, D.; Rothenberger, A.; Sierka, M.; Wieber, S. *Eur. J. Inorg. Chem.* **2004**, 2933.

15. Ruiz, J.; Quesada, R.; Riera, V.; García-Granda, S.; Díaz, M. R. *Chem. Commun.* **2003**, 2028.
16. Prust, J.; Hohmeister, H.; Stasch, A.; Roesky, H. W.; Magull, J.; Alexopoulos, E.; Usón, I.; Schmidt, H.-G.; Noltemeyer, M. *Eur. J. Inorg. Chem.* **2002**, 2156.
17. Kinoshita, I.; Wright, J.; Kubo, S.; Kimura, K.; Sakata, A.; Yano, T.; Miyamoto, R.; Nishioka, T.; Isobe, K. *Dalton Trans.* **2003**, 1993.
18. Edwards, A. J.; Paver, M. A.; Raithby, P. R.; Rennie, M.-A.; Russell, C. A.; Wright, D. S. *Organometallics* **1994**, *13*, 4967.
19. Muller, A.; Neumuller, B.; Dehnicke, K. *Angew. Chem., Int. Ed.* **1997**, *36*, 2350.
20. Schlueter, J. A.; Geiser, U.; Williams, J. M.; Hau Wang, H.; Kwok, W.-K.; Fendrich, J. A.; Carlson, K. D.; Achenback, C. A.; Dudek, J. D., Naumann, D., *et al. Chem. Commun.* **1994**, 1599.

20a. Eujen, R.; Hoge, B.; Brauer, D. J. *J. Organomet. Chem.* **1996**, *519*, 7.

20b. Naumann, D.; Roy, T.; Caeners, B.; Hutten, D.; Tebbe, K.-F.; Gilles, T. *Z. Anorg. Allg. Chem.* **2000**, *626*, 999.

21. Janssen, M. D.; Cornsten, M. A.; Spek, A. L.; Grove, D. M.; van Koten, G. *Organometallics* **1996**, *15*, 2810.
22. Eriksson, H.; Hakansson, M. *Organometallics* **1997**, *16*, 4243.
23. Eriksson, H.; Hakansson, M.; Jagner, S. *Inorg. Chim. Acta* **1998**, *277*, 233.
24. Nobel, D.; van Koten, G.; Spek, A. L. *Angew. Chem., Int. Ed. Engl.* **1989**, *28*, 208.
25. Eriksson, H.; Ortendahl, M.; Hakansson, M. *Organometallics* **1996**, *15*, 4823.
26. Sundararaman, A.; Lalancette, R. A.; Zakharov, L. N.; Rheingold, A. L.; Jäkle, F. *Organometallics* **2003**, *22*, 3526.
27. Niemeyer, M. *Organometallics* **1998**, *17*, 4649.
28. Kronenburg, C. M. P.; Amijs, C. H. M.; Jastrzebski, J. T. B. H.; Lutz, M.; Spek, A. L.; van Koten, G. *Organometallics* **2002**, *21*, 4662.
29. Hwang, C.-S.; Olmstead, M. M.; He, X.; Power, P. P. *J. Chem. Soc. Dalton. Trans.* **1998**, 2599.
30. Hwang, C.-S.; Power, P. P. *Organometallics* **1999**, *18*, 697.
31. Schiemenz, B.; Power, P. P. *Organometallics* **1996**, *15*, 958.
32. Niemeyer, M. *Z. Anorg. Allg. Chem.* **2003**, *629*, 1535.
33. Reiss, P.; Fenske, D. *Z. Anorg. Allg. Chem.* **2000**, *626*, 1317.
34. Ribas, X.; Jackson, D. A.; Donnadieu, B.; Mahía, J.; Parella, T.; Xifra, R.; Hedman, B.; Hodgson, K. O.; Llobet, A.; Stack, D. P. *Angew. Chem., Int. Ed.* **2002**, *41*, 2991.
35. García, F.; Hopkins, A. D.; Koweniki, R. A.; McPartlin, M.; Rogers, M. C.; Wright, D. S. *Organometallics* **2004**, *23*, 3884.
36. Wingerter, S.; Gornitzka, H.; Bertrand, G.; Stalke, D. *Eur. J. Inorg. Chem.* **1999**, 173.
37. Taguchi, H.; Ghoroku, K.; Tadaki, M.; Tsubouchi, A.; Takeda, T. *J. Org. Chem.* **2002**, *67*, 8450.

37a. Takahashi, T.; Sun, W.-H.; Liu, Y.; Nakajima, K.; Kotora, M. *Organometallics* **1988**, *17*, 3841.

38. Zhu, N.; Hall, D. G. *J. Org. Chem.* **2003**, *68*, 6066.

38a. Nilsson, K.; Andersson, T.; Ullenius, C.; Gerold, A.; Krause, N. *Chem. Eur. J.* **1998**, *4*, 2051.

39. Sawamura, M.; Nagahama, N.; Toganoh, M.; Nakamura, E. *J. Organomet. Chem.* **2002**, *652*, 31.
40. Guneratne, R. D.; Burton, D. J. *J. Fluorine Chem.* **1999**, *98*, 11.
41. Janssen, M. D.; Smeets, W. J. J.; Spek, A. L.; Grove, D. M.; Lang, H.; van Koten, G. *J. Organomet. Chem.* **1995**, *505*, 123.
42. Maeda, H.; Osuka, A.; Ishikawa, Y.; Aritome, I.; Hisaeda, Y.; Furuta, H. *Org. Lett.* **2003**, *5*, 1293.
43. Maeda, H.; Osuka, A.; Furuta, H. *J. Am. Chem. Soc.* **2003**, *125*, 15690.
44. Furuta, H.; Maeda, H.; Osuka, A. *J. Am. Chem. Soc.* **2000**, *122*, 803.
45. Furuta, H.; Ishizuka, T.; Osuka, A.; Uwatoko, Y.; Ishikawa, Y. *Angew. Chem. Int. Ed.* **2001**, *40*, 2323.
46. Maeda, H.; Ishikawa, Y.; Matsuda, T.; Osuka, A.; Furuta, H. *J. Am. Chem. Soc.* **2003**, *125*, 11822.
47. Osakada, K.; Yamamoto, T. *Trends Organomet. Chem.* **1999**, *3*, 219.
48. Janssen, S. D.; Herres, M.; Zsolnai, L.; Grove, D. M.; Spek, A. L.; Lang, H.; van Koten, G. *Organometallics* **1995**, *14*, 1098.
49. Frosch, W.; Back, S.; Müller, H.; Köhler, K.; Driess, A.; Schiemenz, B.; Huttner, G.; Lang, H. *J. Organomet. Chem.* **2001**, *619*, 99.
50. Díez, J.; Gamasa, M. P.; Gimeno, J.; Aguirre, A.; García-Granda, S. *Organometallics* **1999**, *18*, 662.
51. Yam, V. W.-W.; Lee, W.-K.; Cheung, K. K.; Lee, H.-K.; Leung, W.-P. *J. Chem. Soc. Dalton. Trans.* **1996**, 2889.
52. Kuang, S.-M.; Zhang, Z.-Z.; Wang, Q.-G.; Mak, T. C. W. *J. Chem. Soc. Dalton. Trans.* **1998**, 1115.
53. Lo, W.-Y.; Lam, C.-H.; Yam, V. W.-W.; Zhu, N.; Cheung, K.-K.; Fathallah, S.; Messaoudi, S.; Le Guennic, B.; Kahlal, S.; Halet, J.-F. *J. Am. Chem. Soc.* **2004**, *126*, 7300.
54. Yip, J. H. K.; Wu, J.; Wong, K. Y.; Yeung, K.-W.; Vittal, J. J. *Organometallics* **2002**, *21*, 1612.

54a. Yam, V. W.-W.; Lam, C.-H.; Cheung, K. K. *Inorg. Chim. Acta.* **2001**, *316*, 19.

55. Yam, V. W.-W.; Fung, W. K.-M.; Cheung, K. K. *Organometallics* **1998**, *17*, 3293.
56. Yam, V. W.-W.; Lee, W.-K.; Cheung, K. K.; Crystall, B.; Phillips, D. *J. Chem. Soc. Dalton. Trans.* **1996**, 3283.
57. Yam, V. W.-W.; Fung, W. K.-M.; Cheung, K. K. *Chem. Commun.* **1997**, 963.
58. Osakada, K.; Tazikawa, T.; Yamamoto, T. *Organometallics* **1995**, *14*, 3531.
59. Yam, V. W.-W.; Lee, W.-K.; Cheung, K. K. *J. Chem. Soc. Dalton. Trans.* **1996**, 2335.
60. Yam, V. W.-W.; Lam, C.-H.; Zhu, N. *Inorg. Chim. Acta.* **2002**, *331*, 239.
61. Yam, V. W.-W.; Choi, S. W.-K.; Chan, C.-L.; Cheung, K. K. *Chem. Commun.* **1996**, 2067.
62. Chan, W.-H.; Zhang, Z.-Z.; Mak, T. C. W.; Che, C.-M. *J. Organomet. Chem.* **1998**, *556*, 169.
63. Song, H.-B.; Wang, Q.-M.; Zhang, Z.-Z.; Mak, T. C. W. *Chem. Commun.* **2001**, 1658.
64. Reger, D. L.; Collins, J. E.; Huff, M. F.; Rheingold, A. L.; Yap, G. P. A. *Organometallics* **1995**, *14*, 5475.
65. Baxter, C. W.; Higgs, T. C.; Jones, A. C.; Parsons, S.; Bailey, P. J.; Tasker, P. A. *J. Chem. Soc. Dalton. Trans.* **2002**, 4395.
66. Higgs, T. C.; Parsons, S.; Jones, A. C.; Bailey, P. J.; Tasker, P. A. *J. Chem. Soc. Dalton. Trans.* **2002**, 3427.
67. Higgs, T. C.; Bailey, P. J.; Parsons, S.; Tasker, P. A. *Angew. Chem., Int. Ed.* **2002**, *41*, 3038.
68. Higgs, T. C.; Parsons, S.; Bailey, P. J.; Jones, A. C.; McLachlan, F.; PArkin, A.; Dawson, A.; Tasker, P. A. *Organometallics* **2002**, *21*, 5692.
69. Bochkarev, L.; Druzhkova, O. N.; Zhiltsov, S. F.; Zakharov, L. N.; Fukin, G. K.; Khorshev, S. Y.; Yanovsky, A. I.; Struchkov, Y. T. *Organometallics* **1997**, *16*, 500.
70. Yam, V. W.-W.; Lo, W.-Y.; Lam, C.-H.; Fung, W. K.-M.; Wong, K. M.-C.; Lau, V. C.-Y.; Zhu, N. *Coord. Chem. Rev.* **2003**, *245*, 39.
71. Yam, V. W.-W.; Fung, W. K.-M.; Wong, K. M.-C.; Lau, V. C.-Y.; Cheung, K. K. *Chem. Commun.* **1998**, 777.
72. Lang, H.; del Villar, A. *J. Organomet. Chem.* **2003**, *670*, 45.
73. Ara, I.; Berenguer, J. R.; Eguizábal, E.; Forniés, J.; Gómez, J.; Lalinde, E. *J. Organomet. Chem.* **2003**, *670*, 221.
74. Yam, V. W.-W.; Yu, K.-L.; Cheung, K.-K. *J. Chem. Soc. Dalton. Trans.* **1999**, 2913.

75. Wei, Q.-H.; Yin, G.-Q.; Zhang, L.-Y.; Shi, L.-X.; Mao, Z.-W.; Chen, Z.-N. *Inorg. Chem.* **2004**, *43*, 3484.
76. Bruce, M. I.; Hall, B. C.; Skelton, B. W.; Smith, M. E.; White, A. H. *J. Chem. Soc. Dalton. Trans.* **2002**, 995.
77. Doyle, M. P.; McKervey, M. A.; Ye, T. *Modern Catalytic Methods for Organic Synthesis with Diazo Compounds*; Wiley: New York, 1998.
77a. Kirmse, W. *Angew. Chem., Int. Ed.* **2003**, *42*, 1088.
78. Straub, B. F.; Hofmann, P. *Angew. Chem., Int. Ed.* **2001**, *40*, 1288.
79. Barluenga, J.; López, L. A.; Löber, O.; Tomás, M.; García-Granda, S.; Alvarez-Rúa, C.; Borge, J. *Angew. Chem., Int. Ed.* **2001**, *40*, 3392.
80. Dai, X.; Warren, T. H. *J. Am. Chem. Soc.* **2004**, *126*, 10085.
81. Arnold, P. L. *Heteroatom Chem.* **2002**, *13*, 534.
82. Arduengo, A. J.; Rasika Dias, R. V.; Calabrese, J. C.; Davidson, F. *Organometallics* **1993**, *12*, 3405.
83. Raubenheimer, H. G.; Cronje, S.; van Rooyen, P. H.; Olivier, P. J.; Toerien, J. G. *Angew. Chem., Int. Ed.* **1994**, *33*, 672.
84. Jurkauskas, V.; Sadighi, J. P.; Buchwald, S. L. *Org. Lett.* **2003**, *5*, 2417.
84a. Haur, H.; Zinn, F. K.; Stevens, E.; Nolan, S. P. *Organometallics* **2004**, *23*, 1157.
85. Mankad, N. P.; Gray, T. G.; Laitar, D. S.; Sadighi, J. P. *Organometallics* **2004**, *23*, 1191.
86. Mankad, N. P.; Laitar, D. S.; Sadighi, J. P. *Organometallics* **2004**, *23*, 3369.
87. Díez-González, S.; Haur, H.; Zinn, F. K.; Stevens, E.; Nolan, S. P. *J. Org. Chem.* **2005**, *70*, 4784.
87a. Haur, H.; Zinn, F. K.; Stevens, E.; Nolan, S. P. *Organometallics* **2004**, *23*, 1157.
88. Fructos, M. R.; Belderrain, T. R.; Nicasio, M. C.; Nolan, S. P.; Kaur, H.; Díaz-Requejo, M. M.; Pérez, P. J. *J. Am. Chem. Soc.* **2004**, *126*, 10846.
89. Tominaga, S.; Oi, Y.; Kato, T.; An, D. K.; Okamoto, S. *Tetrahedron. Lett.* **2004**, *45*, 5585.
90. Alexakis, A.; Winn, C. L.; Guillen, F.; Pytkowicz, J.; Roland, S.; Mangeney, P. *Adv. Synth. Catal.* **2003**, 345.
90a. Clavier, H.; Coutable, L.; Guillemin, J.-C.; Mauduit, M. *Tetrahedron Asymmetry* **2005**, *16*, 921.
91. Tulloch, A. A. D.; Danapoulos, A. A.; Kleinhenz, S.; Light, M. E.; Hursthouse, M. B.; Eastham, G. *Organometallics* **2001**, *20*, 2027.
92. Arnold, P. L.; Scarisbrick, A. C.; Blake, A. J.; Wilson, C. *Chem. Commun.* **2001**, 2340.
92a. Arnold, P. L.; Rodden, M.; Davis, K. M.; Scarisbrick, A. C.; Blake, A. J.; Wilson, C. *Chem. Commun.* **2004**, 1612.
93. Larsen, A. O.; Leu, W.; Nieto Oberheuber, C.; Campbell, J. E.; Hoveyda, A. H. *J. Am. Chem. Soc.* **2004**, *126*, 11131.
94. Gishig, S.; Togni, A. *Organometallics* **2005**, *24*, 203.
95. Hu, X.; Castro-Rodríguez, I.; Olsen, K.; Meyer, K. *Organometallics* **2004**, *23*, 755.
96. Hu, X.; Castro-Rodríguez, I.; Meyer, K. *Organometallics* **2003**, *22*, 3016.
97. Hu, X.; Castro-Rodríguez, I.; Meyer, K. *J. Am. Chem. Soc.* **2003**, *125*, 12237.
98. Schaller, G. E.; Bleecker, A. B. *Science* **1995**, *270*, 1809.
98a. Rodriguez, F. I.; Esch, J. J.; Hall, A. E.; Binder, B. M.; Schaller, G. E.; Bleeckert, A. B. *Science* **1999**, *283*, 996.
98b. Ecker, J. R. *Science* **1995**, *268*, 667.
98c. Beyer, E. M.; Blomstrom, D. C. In *Plant Growth Substances 1979*; Skoog, F., Ed.; Springer-Verlag: New York, 1980; pp 208.
98d. Thompson, J. S.; Harlow, R. L.; Whitney, J. F. *J. Am. Chem. Soc.* **1983**, *105*, 3522.
98e. Munakata, M.; Kitagawa, S.; Kosome, S.; Asahara, A. *Inorg. Chem.* **1986**, *25*, 2622.
99. Pérez, P. J.; Brookhart, M.; Templeton, J. L. *Organometallics* **1993**, *12*, 261.
99a. Díaz-Requejo, M. M.; Pérez, P. J.; Brookhart, M.; Templeton, J. L. *Organometallics* **1997**, *16*, 4399.
99b. Hallnemo, G.; Olsson, T.; Ullenius, C. *J. Organomet. Chem.* **1985**, *282*, 133.
100. Parshall, G. W.; Ittel, S. D. *Homogeneous Catalysis: The Applications and Chemistry of Catalysis by Soluble Transition Metal Complexes*, 2nd ed.; Wiley: New York, 1992.
100a. Weissermel, K.; Arpe, H.-J. *Industrial Organic Chemistry*, 3rd ed.; VCH: New York, 1997.
101. Trofimenko, S., *Scorpionates: The Coordination Chemistry of Polypyrazolylborate Ligands*; Imperial College: London, 1999.
102. Rasika Dias, H. V.; Lu, H.-L.; Kim, H.-J.; Polach, S. A.; Goh, T. K. H. H.; Browning, G.; Lovely, C. J. *Organometallics* **2002**, *21*, 1466.
103. Dai, X.; Warren, T. H. *Chem. Commun.* **1998**, 1998.
104. Straub, B. F.; Eisenträger, F.; Hofmann, P. *Chem. Commun.* **1999**, 2507.
104a. Straub, B. F.; Gruber, I.; Rominger, F.; Hofmann, P. *J. Organomet. Chem.* **2003**, *684*, 124.
104b. Straub, B. F.; Rominger, F.; Hofmann, P. *Organometallics* **2000**, *19*, 4305.
105. Quan, R. W.; Li, Z.; Jacobsen, E. N. *J. Am. Chem. Soc.* **1996**, *118*, 8156.
106. Lo, M. M.-C.; Fu, G. C. *J. Am. Chem. Soc.* **1998**, *120*, 10270.
106a. Rios, R.; Liang, J.; Lo, M. M.-C.; Fu, G. C. *Chem. Commun.* **2000**, 377.
107. Lewelling, D. B.; Adamson, D.; Arndtsen, B. A. *Org. Let.* **2000**, *2*, 4165.
108. LeCloux, D. D.; Davydov, R.; Lippard, S. J. *Inorg. Chem.* **1998**, *37*, 6814.
109. Chi, K.-M.; Hou, H.-C.; Hung, P.-T.; Peng, S.-M.; Lee, G.-H. *Organometallics* **1995**, *14*, 2641.
110. Cavallo, L.; Cucciolito, M. E.; De Martino, A.; Giordano, F.; Orabona, I.; Vitagliano, A. *Chem. Eur. J.* **2000**, *6*, 1127.
111. Kuzelka, J.; Mukhopadkyay, S.; Spingler, B.; Lippard, S. J. *Inorg. Chem.* **2004**, *43*, 1751.
112. Goreshnik, E. A.; Schollmeyer, D.; Myskiv, M. G. Z. *Anorg. Allg. Chem.* **2002**, *628*, 2118.
113. Chen, T. Y.; Omnés, L.; Vaisserman, J.; Doppelt, P. *Inorg. Chim. Acta* **2004**, *357*, 1299.
114. Snyder, J. P. *J. Am. Chem. Soc.* **1995**, *117*, 11025.
115. Eriksson, J.; Davidsson, Ö. *Organometallics* **2001**, *20*, 4763.
116. Tan, X.-H.; Shen, B.; Liu, L.; Guo, Q.-X. *Tetrahedron Lett.* **2002**, *43*, 9373.
117. Kundu, A.; Prabhakar, S.; Vairamani, M.; Roy, S. *Organometallics* **1997**, *16*, 4796.
118. Sullivan, R. M.; Liu, H.; Smith, D. S.; Hanson, J. C.; Osterhout, D.; Ciraolo, M.; Grey, C. P.; Martin, J. P. *J. Am. Chem. Soc.* **2003**, *125*, 11065.
119. Yoshida, T.; Kuwatani, Y.; Hara, K.; Yoshida, M.; Matsuyama, H.; Iyoda, M.; Nagase, S. *Tetrahedron Lett.* **2001**, *42*, 53.
120. Miyaji, T.; Xi, Z.; Nakajima, K.; Takahashi, T. *Organometallics* **2001**, *20*, 2859.
121. Li, Y.-H.; Wang, X.-S.; Zhao, H.; Yuan, R.-X.; Zhang, J.; Xiong, R.-G.; You, X.-Z.; Ju, H.-X.; Xue, Z.-L. *Inorg. Chem.* **2004**, *43*, 712.
122. Goreshnik, E. A.; Schollmeyer, D.; Myskiv, M. G. Z. *Anorg. Allg. Chem.* **2003**, *629*, 2040.
123. Alyea, E. C.; Meechan, P. R.; Ferguson, G.; Kannan, S. *Polyhedron* **1997**, *16*, 3479.
124. Franceshi, F.; Guardigli, M.; Solari, E.; Floriani, C.; Chiesi-Villa, A.; Rizzoli, C. *Inorg. Chem.* **1997**, *36*, 4099.
125. Krisyuk, V. V.; Turgambaeva, A. E.; Rhee, S.-W. *Polyhedron* **2004**, *23*, 809.
126. Chen, T. Y.; Vaisserman, J.; Doppelt, P. *Inorg. Chem.* **2001**, *40*, 6167.
127. Rozenberg, G. G.; Steinke, J. H. G.; Gelbrich, T.; Hursthouse, M. B. *Organometallics* **2001**, *20*, 4001.

128. Hakansson, M.; Lopes, C.; Jagner, S. *Organometallics* **1998**, *17*, 210.
129. Gustafsson, B.; Hakansson, M.; Westman, G.; Jagner, S. *J. Organomet. Chem.* **2002**, *649*, 204.
130. Zhang, J.; Xiong, R.-G.; Chen, X.-T.; Xue, Z.; Peng, S.-M.; You, X.-Z. *Organometallics*. **2002**, *21*, 235.
131. Zhang, J.; Xiong, R.-G.; Chen, X.-T.; Che, C.-M.; Xue, Z.; You, X.-Z. *Organometallics* **2001**, *20*, 4118.
132. Zhang, J.; Xiong, R.-G.; Zuo, J.-L.; You, X.-Z. *Chem. Commun.* **2000**, 1495.
133. Zhang, J.; Xiong, R.-G.; Zuo, J.-L.; Che, C.-M.; You, X.-Z. *J. Chem. Soc. Dalton. Trans.* **2000**, 2898.
134. Qu, Z.-R.; Chen, Z.-F.; Zhang, J.; Xiong, R.-G.; Abrahams, B. F.; Xue, Z. L. *Organometallics* **2003**, *22*, 2814.
135. Xie, Y.-R.; Wang, X.-S.; Zhao, H.; Zhang, J.; Weng, L.-H.; Duan, C.-Y.; Xiong, R.-G.; You, X.-Z.; Xue, Z. L. *Organometallics* **2003**, *22*, 4396.
136. Xue, X.; Wang, X.-S.; Xiong, R.-G.; You, X.-Z.; Abrahams, B. F.; Che, C.-M.; Ju, H.-X. *Angew. Chem., Int. Ed.* **2002**, *41*, 2944.
137. Masaoka, S.; Akiyama, G.; Horike, S.; Kitakawa, S.; Ida, T.; Endo, K. *J. Am. Chem. Soc.* **2003**, *125*, 1152.
138. Masaoka, S.; Tanaka, D.; Nakanishi, Y.; Kitakawa, S. *Angew. Chem., Int. Ed.* **2004**, *43*, 2530.
139. Young, D. M.; Geiser, U.; Schultz, A. J.; Wang, H. H. *J. Am. Chem. Soc.* **1998**, *120*, 1331.
140. Turner, R. W.; Amma, E. L. *J. Am. Chem. Soc.* **1966**, *88*, 1877.
140a. Dines, M. B.; Bird, P. H. *J. Chem. Soc. Chem. Commun.* **1973**, 12.
140b. Rodesiler, P. F.; Amma, E. L. *J. Chem. Soc. Chem. Commun.* **1974**, 599.
140c. Pasquali, M.; Floriani, C.; Gaetani-Manfredotti, A. *Inorg. Chem.* **1980**, *19*, 1191.
140d. Schmidbaur, H.; Bublak, W.; Huber, B.; Reber, G.; Müller, G. *Angew. Chem., Int. Ed. Engl.* **1986**, *25*, 1089.
141. Laitar, D. S.; Mathison, C. J. N.; Davis, W. M.; Sadighi, J. P. *Inorg. Chem.* **2003**, *42*, 7354.
141a. Hamilton, C. W.; Laitar, D. S.; Sadighi, J. P. *Chem. Commun.* **2004**, 1628.
142. Lee, S. Y.; Na, S. J.; Kwon, H. Y.; Lee, B. Y.; Kang, S. O. *Organometallics* **2004**, *23*, 5382.
143. Osako, T.; Tachi, Y.; Doe, M.; Shiro, M.; Ohkubo, K.; Fukuzumi, S.; Itoh, S. *Chem. Eur. J.* **2004**, *10*, 237.
144. Osako, T.; Ueno, Y.; Tachi, Y.; Itoh, S. *Inorg. Chem.* **2003**, *42*, 8087.
145. Osako, T.; Tachi, Y.; Taki, M.; Fukuzumi, S.; Itoh, S. *Inorg. Chem.* **2001**, *40*, 6604.
146. Xu, F.-B.; Li, Q.-S.; Wu, L.-Z.; Leng, X.-B.; Li, Z.-C.; Zeng, X.-S.; Chow, Y. L.; Zhang, Z.-Z. *Organometallics* **2003**, *22*, 633.
147. Conry, R. R.; Striejewske, W. S.; Tipton, A. A. *Inorg. Chem.* **1999**, *38*, 2833.
147a. Conry, R. R.; Striejewske, W. S. *Chem. Commun.* **1998**, 555.
147b. Conry, R. R.; Striejewske, W. S. *Organometallics* **1998**, *17*, 3146.
148. Mascal, M.; Kerdelhué, J.-L.; Blake, A. J.; Cooke, P. A. *Angew. Chem., Int. Ed.* **1999**, *38*, 1968.
148a. Mascal, M.; Hansen, J.; Blake, A. J.; Li, W.-S. *Chem., Commun.* **1998**, 355.
149. Ohrenberg, C.; Liable-Sands, L.; Rheingold, A. L.; Riordan, C. G. *Inorg. Chem.* **2001**, *40*, 4276.
150. Ivanova, S. I.; Ivanov, S. V.; Miller, S. M.; Anderson, O. P.; Solntsev, K. A.; Strauss, S. H. *Inorg. Chem.* **1999**, *38*, 3756.
151. Karshted, D.; Bell, A. T.; Tilley, T. D. *Organometallics* **2003**, *22*, 2855.
152. Dattelbaum, A. M.; Martin, J. D. *Inorg. Chem.* **1999**, *38*, 6200.
153. Cotton, F. A.; Takats, J. *J. Am. Chem. Soc.* **1970**, *92*, 2353.
153a. Delbaere, L. T. J.; McBride, D. W.; Ferguson, R. B. *Acta Crystallogr., Sect. B* **1970**, *26*, 515.
153b. Carriedo, G. A.; Howard, J. A. K.; Stone, F. G. A. *J. Chem. Soc., Dalton Trans.* **1984**, 1555.
153c. Carriedo, G. A.; Howard, J. A. K.; Stone, F. G. A. *J. Organomet. Chem.* **1983**, *250*, C28.
153d. Hanusa, T. P.; Ulibarri, T. A.; Evans, W. J. *Acta Crystallogr., Sect. C* **1985**, *41*, 1036.
153e. Zybill, Chr.; Müller, G. *Organometallics* **1987**, *6*, 2489.
154. Lettko, L.; Rausch, M. D. *Organometallics* **2000**, *19*, 4060.
155. Anderson, Q. T.; Erkizia, E.; Conry, R. R. *Organometallics* **1998**, *17*, 4917.
156. Jutzi, P.; Wieland, W.; Neumann, B.; Stammler, H.-G. *J. Organomet. Chem.* **1995**, *501*, 369.
157. Shimazaki, Y.; Yokoyama, H.; Yamauchi, O. *Angew. Chem., Int. Ed.* **1999**, *38*, 2401.
158. Gudat, D.; Nieger, M.; Schmitz, K.; Szarvas, L. *Chem. Commun.* **2002**, 1820.
159. Heinemann, F. W.; Zeller, M.; Zenneck, U. *Organometallics* **2004**, *23*, 1689.
160. Norman, J. A. T.; Muratore, B. A.; Dyer, P. N.; Roberts, D. A.; Hochberg, A. K. *J. Phys. IV* **1991**, *C2*, 271.
161. Combellas, C.; Doppelt, P.; Kanoufi, F.; Chen, T.-Y.; Thiebault, A. *Chem. Vap. Deposition* **1999**, *5*, 185.
162. Schmidt, G.; Behrens, U. *J. Organomet. Chem.* **1995**, *503*, 101.
163. Doppelt, P.; Baum, T. H. *J. Organomet. Chem.* **1996**, *517*, 53.
164. Baker, M. V.; Brown, D. H.; Somers, N.; White, A. H. *Organometallics* **2001**, *20*, 2161.
164a. Köhler, K.; Eichhorn, J.; Meyer, F.; Vidovic, D. *Organometallics* **2003**, *22*, 4426.
165. Schmidt, G.; Behrens, U. *J. Organomet. Chem.* **1996**, *509*, 49.
166. Gröger, G.; Olbrich, F.; Schulte, P.; Behrens, U. *J. Organomet. Chem.* **1998**, *557*, 251.
167. Schulte, P.; Gröger, G.; Behrens, U. *Z. Anorg. Allg. Chem.* **2000**, *626*, 679.
168. Schulte, P.; Gröger, G.; Behrens, U. *Z. Anorg. Allg. Chem.* **1999**, *625*, 1447.
169. Schulte, P.; Schmidt, G.; Kramer, C.-P.; Krebs, A.; Behrens, U. *J. Organomet. Chem.* **1997**, *530*, 95.
170. Schulte, P.; Gröger, G.; Behrens, U. *J. Organomet. Chem.* **1999**, *584*, 1.
171. Brussaard, Y.; Olbrich, F.; Behrens, U. *J. Organomet. Chem.* **1996**, *519*, 115.
172. Gröger, G.; Olbrich, F.; Weiss, E.; Behrens, U. *J. Organomet. Chem.* **1996**, *514*, 81.
173. Gröger, G.; Behrens, U.; Olbrich, F. *Organometallics* **2000**, *19*, 3354.
174. Kovács, A.; Frenking, G. *Organometallics* **1999**, *18*, 887.
175. Schmidt, G.; Schittenhelm, N.; Behrens, U. *J. Organomet. Chem.* **1995**, *496*, 49.
176. Lorber, C. Y.; Youinou, M.-T.; Kress, J.; Osborn, J. A. *Polyhedron* **2000**, *19*, 1693.
177. Schulte, P.; Behrens, U. *J. Organomet. Chem.* **1998**, *563*, 235.
178. Schulte, P.; Behrens, U.; Olbrich, F. *Z. Anorg. Allg. Chem.* **2000**, *626*, 1692.
179. Yam, V. W.-W.; Fung, W. K.-M.; Cheung, K.-K. *Angew. Chem., Int. Ed.* **1996**, *35*, 1100.
180. Janssen, M. D.; Köhler, K.; Herres, M.; Dedieu, A.; Smeets, W. J. J.; Spek, A. L.; Grove, D. M.; Lang, H.; van Koten, G. *J. Am. Chem. Soc.* **1996**, *118*, 4817.
181. Stein, T.; Lang, H. *J. Organomet. Chem.* **2002**, *664*, 142.
182. Lang, H.; Kohler, K.; Rheinwald, G.; Zsoinai, L.; Buchner, M.; Driess, A.; Huttner, G.; Strahle, J. *Organometallics* **1999**, *18*, 598.

183. Lang, H.; Frosch, W.; Wu, I. Y.; Blau, S.; Nuber, B. *Inorg. Chem.* **1996**, *35*, 6266.
184. Kohler, K.; Pritzkow, H.; Lang, H. *J. Organomet. Chem.* **1998**, *553*, 31.
185. Frosch, W.; Back, S.; Rheinwald, G.; Kohler, K.; Pritzkow, H.; Lang, H. *Organometallics* **2000**, *19*, 4016.
186. Lang, H.; Blau, S.; Pritzkow, H.; Zsolnai, L. *Organometallics* **1995**, *14*, 1850.
187. Lang, H.; Herres, M.; Köhler, K.; Blau, S.; Weinmann, S.; Weinmann, M.; Rheinwald, G.; Imhof, W. *J. Organomet. Chem.* **1995**, *505*, 85.
188. Delgado, E.; Hernández, E.; Mansilla, N.; Moreno, M. T.; Sabat, M. *J. Chem. Soc. Dalton. Trans.* **1999**, 533.
189. Back, S.; Reinwald, G.; Lang, H. J. *J. Organomet. Chem.* **2000**, *601*, 93.
190. Janssen, M. D.; Herres, M.; Zsolnai, L.; Spek, A. L.; Grove, D. M.; Lang, H.; van Koten, G. *Inorg. Chem.* **1996**, *35*, 2476.
191. Enders, M.; Köhler, K.; Frosch, W.; Pritzkow, H.; Lang, H. *J. Organomet. Chem.* **1997**, *538*, 163.
192. Frosch, W.; Back, S.; Rheinwald, G.; Kohler, K.; Zsolnai, L.; Huttner, G.; Lang, H. *Organometallics* **2000**, *19*, 5769.
193. Adams, C. J.; Raithby, P. R. *J. Organomet. Chem.* **1999**, *578*, 178.
194. Lang, H.; del Villar, A.; Rheinwald, G. *J. Organomet. Chem.* **1999**, *587*, 284.
195. Yamazaki, S.; Deeming, A. J.; Hursthouse, M. B.; Abdul Malik, K. M. *Inorg. Chim. Acta* **1995**, *235*, 147.
196. Forniés, J.; Lalinde, E.; Martín, A.; Moreno, M. T. *J. Organomet. Chem.* **1995**, *490*, 179.
197. Wong, W.-Y.; Lu, G.-L.; Choi, K.-H. *J. Organomet. Chem.* **2002**, *659*, 107.
198. Yam, V. W.-W.; Yu, K.-L.; Wong, K. M.-C.; Cheung, K.-K. *Organometallics* **2001**, *20*, 721.
199. Charmant, J. P. H.; Forniés, J.; Gómez, J.; Lalinde, E.; Merino, R. I.; Moreno, M. T.; Orpen, A. G. *Organometallics* **1999**, *18*, 3353.
200. Ara, I.; Berenguer, J. R.; Eguizabal, E.; Forniés, J.; Lalinde, E.; Martín, A. *Eur. J. Inorg. Chem.* **2001**, 1631.
201. Lang, H.; del Villar, A.; Walfort, B.; Rheinwald, G. *J. Organomet. Chem.* **2004**, *689*, 1464.
202. Li, Q.-S.; Xu, F.-B.; Cui, D.-J.; Yu, K.; Zeng, X.-S.; Leng, X.-B.; Song, H.-B.; Zhang, Z.-Z. *Dalton Trans* **2003**, 1551.
203. Zhu, Y.; Clot, O.; Wolf, M. O.; Yap, G. P. A. *J. Am. Chem. Soc.* **1998**, *120*, 1812.
204. Yam, V. W.-W.; Chong, S. H.-F.; Wong, K. M.-C.; Cheung, K.-K. *Chem. Commun.* **1999**, 1013.
205. Mihan, S.; Sünkel, K.; Beck, W. *Chem. Eur. J.* **1999**, *5*, 745.
206. Bruce, M. I.; Zaitseva, N. N.; Skelton, B. W.; Somers, N.; White, A. H. *Aust. J. Chem.* **2003**, *56*, 509.
207. Lang, H.; Köcher, S.; Back, S.; Rheinwald, G.; van Koten, G. *Organometallics* **2001**, *20*, 1968.
207a. Rais, D.; Mingos, D. M. P.; Vilar, R.; White, A. J. P.; Williams, D. J. *Organometallics* **2000**, *19*, 5209.
208. Churchill, M. R.; DeBoer, B. G.; Rotella, F. J.; Abu Salah, O. M.; Bruce, M. I. *Inorg. Chem.* **1975**, *14*, 2051.
209. Dias, H. V. R.; Goh, K. H. H. *Polyhedron* **2004**, *23*, 273.
210. Conry, R. R.; Ji, G.; Tipton, A. A. *Inorg. Chem.* **1999**, *38*, 906.
211. Imai, S.; Fujisawa, K.; Kobayashi, T.; Shirasawa, N.; Fujii, H.; Yoshimura, T.; Kitajima, N.; Moro-oka, Y. *Inorg. Chem.* **1998**, *37*, 3066.
212. Kiani, S.; Long, J. R.; Stavropoulos, P. *Inorg. Chim. Acta* **1997**, *263*, 357.
213. Dias, H. V. R.; Kim, H.-J.; Lu, H.-L.; Rajeshwar, K.; de Tacconi, N. R.; Derecskei-Kovacs, A.; Marynick, D. S. *Organometallics* **1996**, *15*, 2994.
214. Dias, H. V. R.; Kim, H.-J. *Organometallics* **1996**, *15*, 5374.
215. Dias, H. V. R.; Lu, H.-L. *Inorg. Chem.* **1995**, *34*, 5380.
216. Reger, D. L.; Collins, J. E.; Rheingold, A. L.; Liable-Sands, L. M. *Organometallics* **1996**, *15*, 2029.
217. Dias, H. V. R.; Singh, S. *Inorg. Chem.* **2004**, *43*, 5786.
218. Shimazaki, Y.; Nogami, T.; Tani, F.; Odani, A.; Yamauchi, O. *Angew. Chem., Int. Ed.* **2001**, *40*, 3859.
219. Mahapatra, S.; Kaderli, S.; Llobet, A.; Neuhold, Y.-M.; Palanché, T.; Halfen, J. A.; Young, V. G., Jr.; Kaden, T. A.; Que, L. Jr.; Zuberbühler, A. D.; Toman, W. B. *Inorg. Chem.* **1997**, *36*, 6343.
220. Costas, M.; Xifra, R.; Llobet, A.; Solá, M.; Robles, J.; Parella, T.; Stoeckli-Evans, H.; Neuburger, M. *Inorg. Chem.* **2003**, *42*, 4456.
221. Lopes, C.; Hakansson, M.; Jagner, S. *Inorg. Chem.* **1997**, *36*, 3232.
222. Polyakov, O. G.; Nolan, B. G.; Fauber, B. P.; Miller, S. M.; Anderson, O. P.; Strauss, S. H. *Inorg. Chem.* **2000**, *39*, 1735.
223. Singh, K.; Log, J. R.; Stavropoulos, P. *Inorg. Chem.* **1998**, *37*, 1073.
224. Polyakov, O. G.; Ivanova, S. M.; Gaudinski, C. M.; Miller, S. M.; Anderson, O. P.; Strauss, S. H. *Organometallics* **1999**, *18*, 3769.
225. Shao, L.; Zhang, L.; Zhou, M.; Qin, Q. *Organometallics* **2001**, *20*, 1137.
226. Dell'Amico, D. B.; Alessio, R.; Calderazzo, F.; Della Pina, F.; Englert, U.; Pampaloni, G.; Passarelli, V. *J. Chem. Soc. Dalton Trans.* **2000**, 2067.
227. Dell'Amico, D. B.; Calderazzo, F.; Labella, L.; Lorenzini, F.; Marchetti, F. *Z. Anorg. Allg. Chem.* **2002**, *628*, 1868.
228. Antiñolo, A.; Carrillo, F.; Chaudret, B.; Fajardo, M.; García-Yuste, S.; LAhoz, F. J.; Lanfranchi, M.; López, J. A.; Otero, A.; Pellinghelli, M. A. *Organometallics* **1995**, *14*, 1297.
229. Cui, D.-J.; Li, Q.-S.; Xu, F.-B.; Leng, X.-B.; Zhang, Z.-Z. *Organometallics* **2001**, *20*, 4126.
230. Bachman, R. E.; Whitmire, K. H.; van Hai, J. *Organometallics* **1995**, *14*, 1792.
231. Housecoft, C. E.; Draper, S. M.; Hattersley, A. D.; Rheingold, A. L. *J. Organomet. Chem.* **2000**, *614–615*, 202.
232. Anderson, S.; Hill, A. F.; Nasir, B. A. *Organometallics* **1995**, *14*, 2987.
233. Krause, N.; Gerold, A. *Angew. Chem., Int. Ed.* **1997**, *36*, 186.
234. Hwang, C.-S.; Power, P. P. *J. Am. Chem. Soc.* **1998**, *120*, 6409.
235. Eaborn, C.; Hill, M. S.; Hitchcock, P. B.; Smith, J. D. *Organometallics* **2000**, *19*, 5780.
236. Eaborn, C.; El-Hamruni, S. M.; Hill, M. S.; Hitchcock, P. B.; Smith, J. D. *J. Chem. Soc. Dalton Trans.* **2002**, 3975.
237. Boche, G.; Bosold, F.; Marsch, M.; Harms, K. *Angew. Chem., Int. Ed.* **1998**, *37*, 1684.
238. Kronenburg, C. M. P.; Jastrzebski, J. B. T. H.; Spek, A. L.; van Koten, G. *J. Am. Chem. Soc.* **1998**, *120*, 9688.
239. Dias, H. V. R; Lu, H.-L.; Gorden, J. D.; Jin, W. *Inorg. Chem.* **1996**, *35*, 2149.
240. Jazdzewski, B. A.; Holland, P. L.; Pink, M.; Young, V. G., Jr.; Spencer, D. J. E.; Tolman, W. B. *Inorg. Chem.* **2001**, *40*, 6097.
241. Ardizzoia, G. A.; La Monica, G.; Maspero, A.; Masciocchi, N.; Moret, M. *Eur. J. Inorg. Chem.* **1999**, 1301.
241a. Ardizzoia, G. A.; Cenini, S.; La Monica, G.; Masciocchi, N.; Maspero, A.; Moret, M. *Inorg. Chem.* **1998**, *37*, 4284, 1301.
242. Reedy, B. J.; Murthy, N. N.; Karlin, K. D.; Blackburn, N. J. *J. Am. Chem. Soc.* **1995**, *117*, 9826.
243. Domínguez-Vera, J. M.; Moreno, J. M.; Colacio, E. *Inorg. Chim. Acta* **2004**, *357*, 611.
244. Díez, J.; Gamasa, M. P.; Gimeno, J.; Lanfranchi, M.; Tiripicchio, A. *J. Organomet. Chem.* **2001**, *637*, 677.
245. LeCloux, D. D.; Lippard, S. J. *Inorg. Chem.* **1997**, *36*, 4035.
246. Díez, J.; Gamasa, M. P.; Gimeno, J.; Aguirre, J.; García-Granda, S. *Organometallics* **1997**, *16*, 3684.
247. Fournier, E.; Lebrun, F.; Drouin, M.; Decken, A.; Harvey, P. D. **2004**, *43*, 3127.

2.04
Silver Organometallics

V W W Yam and E C C Cheng, The University of Hong Kong, Hong Kong, People's Republic of China

2.04.1 Introduction

Organometallic compounds of silver are relatively unexplored compared with those of its congeners, copper and gold. The major reason for this phenomenon is attributed to the general thermal instability and light sensitivity of organosilver compounds under ambient conditions. Nevertheless, there has been a growing attention to the study of organosilver complexes, particularly their synthesis and structural properties. Examples of organosilver complexes are known and have been reviewed,[1–3] and typical examples reported prior to 1994 have been comprehensively reviewed in COMC (1995).[4,5] Continuing the tradition of COMC (1995), this chapter presents an overview of reports on organometallic silver complexes since 1994, with emphasis given to σ-bonded organosilver systems. We hope this will provide readers and researchers in this field a quick and easy glance at the burgeoning field of organosilver chemistry.

2.04.2 Silver(I) Organometallics

2.04.2.1 Synthesis and Properties of Alkyl, Alkenyl, Aryl, and Related Complexes of Silver

Examples of silver(I) alkyl and alkenyl (including aryl) complexes have been known from as early as 1941;[6–9] however, the number of examples is fairly limited with respect to that of the heavier congeners, copper(I) and gold(I). Such a phenomenon can readily be attributed to the relatively low stability of this class of complexes, both photochemically and thermally. Simple homoleptic alkyl and alkenyl complexes of silver(I) are known to be very unstable under ambient temperature and light, and successful isolation of this class is fairly limited and mainly confined to those involving perfluoroorganics.[10] The structures and the metal–carbon bond-dissociation energies for

the methyl and phenyl complexes of group 11 and 12 metals have been investigated using quantum mechanical calculations employing relativistic pseudopotentials with large valence basis sets.[11] It has been estimated that the metal–carbon bond strength for silver is the weakest of the group 11 triad (Cu, Ag, and Au).

In general, the syntheses of these complexes are achieved through: (i) nucleophilic addition/substitution reactions of silver(I) fluoride or (ii) transmetallation reactions with other metal alkyl, alkenyl, and aryl complexes.

Girolami reported the crystal structure of a tetranuclear silver(I) alkenyl complex, [*trans*-{$CF_3CF{=}C(CF_3)Ag$}]$_4$ **1**, prepared from the nucleophilic addition of silver(I) fluoride to perfluoro-but-2-yne in acetonitrile.[12–14] The tetranuclear complex consisted of four silver(I) centers arranged in a square, with each edge bridged by a *trans*-perfluoro-1-methyl-1-propenyl ligand. Examples with such a tetrameric square structure were also reported for the related aryl silver(I) complexes.[15,16] The Ag–C distance and C–Ag–C and Ag–C–Ag angles of 2.19 Å, 166.7° and 78.3°, respectively, in conjunction with the presence of short Ag–Ag contacts of 2.761 Å, are not uncommon for this type of complexes. This complex was shown to act as a precursor for the fabrication of silver-metal film by both thermal and plasma-enhanced metalorganic chemical vapor deposition (MOCVD).[14] Substitution reactions between AgF and Me_3SiCF_3 yield $AgCF_3$ selectively and quantitatively at room temperature in *N*-donor solvents such as alkyl nitrile, which is in contrast to that observed in *O*-donor solvents, where a decomposition to a silver(III) salt is the only reaction observed.[17] Although $AgCF_3$ could not be isolated, segregation of the complex adduct (ppn)[Ag(CF_3)Cl] was possible upon reaction with excess (ppn)Cl, and was structurally characterized with an Ag–C bond length of 2.072 Å and a Cl–Ag–C bond angle of 176.7°. It has also been demonstrated that $AgCF_3$ and Ag(C_6F_5) can function as versatile precursors for the preparation of other perfluoroalkylsilver(I) complexes.[17] In addition, substitution reactions of $AgCF_3$ with a wide variety of elements in group 12–16 were shown to be feasible for the synthesis of the respective CF_3-substituted compounds, without the need of using the respective group 12–16 halide or alkyl.[17] Related studies were also reported on the widely utilized analog, AgC_6F_5, together with the structural characterization of [AgC_6F_5·EtCN]$_n$ **2** (Figure 1).[18] An infinite zigzag chain structure was determined with the presence of two crystallographically differing silver(I) centers alternating with respect to one another. One silver(I) center was linearly coordinated with two C_6F_5 groups and had an Ag–C bond distance of 2.13 Å, while the other was bound to two C_6F_5 groups and two *N*-coordinating EtCN in a distorted tetrahedral configuration with a significantly longer Ag–C bond distance of 2.39 Å. All the C_6F_5 units were coordinated to the two different silver centers in a μ-bridging fashion. Short Ag–Ag contacts of 2.82 Å were also observed.

Reactions of lithiated reagents with a silver salt represent a common and important means for the synthesis of silver(I) alkyl and aryl complexes. For instance, in 1973, Leusink *et al.* reported the reaction of Li($C_6H_4CH_2NMe_2$-2) with AgBr in diethyl ether at −78 °C to afford [Ag($C_6H_4CH_2NMe_2$-2)] **3** (Figure 2), while Mulloy demonstrated its tetrameric nature crystallographically in 1997.[19,20] This structure featured a planar Ag_4 rhomboidal core with adjacent silver atoms bridged by aryl ligands at their *ipso*-carbons. Two of the four silver(I) centers were further coordinated by the CH_2NMe_2 pendants, giving rise to two distinct silver(I) coordination environments. The Ag–C bond distances for the four-coordinated silver(I) centers (2.351(11)–2.410(12) Å) were significantly longer than those for the two-coordinated silver(I) centers (2.134(12)–2.166(13) Å). The observed short Ag–Ag contacts (2.729(2)–2.748(2) Å) were typical of electron-deficient closed-shell organometallic compounds and might be indicative of the presence of weak

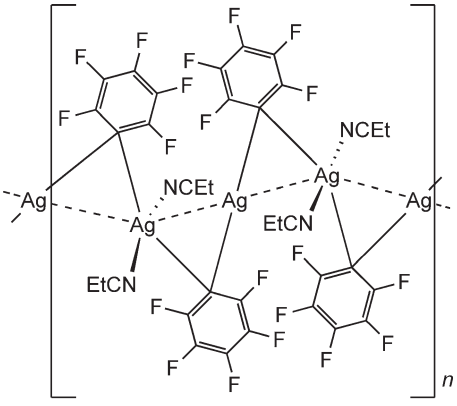

2

Figure 1 Structure of [AgC_6F_5·EtCN]$_2$ **2**.

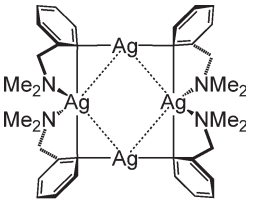

3

Figure 2 Tetrameric structure of [Ag($C_6H_4CH_2NMe_2$-2] **3**.

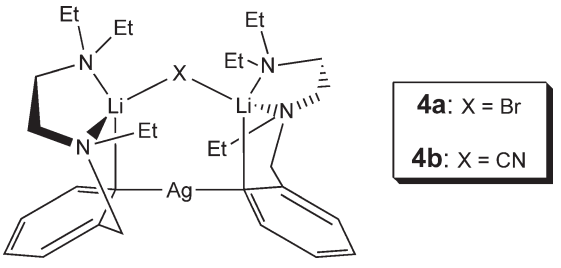

Figure 3 Structure of **4a** and **4b**.

metal–metal interactions. Complexes with extended *N*-donor pendants, **4a** and **4b** (Figure 3), were synthesized by van Koten and co-workers by the reaction of AgBr or AgCN with the corresponding aryllithium.[21] Single crystal structure analysis of **4a** revealed its trinuclear nature, with one Ag(I) and two Li centers. Nonetheless, the positions of the two lithium atoms were found to be occupied by silver in 2.3% and 2.9% of the cases, indicative of the possibility of obtaining a small degree of isomorphic Ag_3 complex.

Power reported the synthesis and crystal structures of two homoleptic diarylargentate(I) complexes with bulky aryls, [Li(thf)$_4$][Ag($C_6H_2Ph_3$-2,4,6)$_2$]·(thf) **5a** and [Li(thf)$_4$][Ag($C_6H_3mes_2$-2,6)$_2$]·1/8(Et_2O) **5b**.[22] Their synthesis involved the reaction of the respective aryllithium reagents with silver(I) cyanate (AgOCN), which is more soluble than the commonly employed silver halides. The complex anions in **5a** and **5b** possessed similar structures with linear, two-coordinate silver(I) centers bonded to the *ipso*-carbons of the two aryl ligands. The Ag–C_{ipso} distances (**5a**: 2.091(9), 2.103(9) Å; **5b**: 2.048(15)–2.112(19) Å) and the close-to-ideal C_{ipso}–Ag–C_{ipso} bond angles (**5a**: 176.7(4)°; **5b**: 176.0(7), 177.4(6)°) in both complexes were as expected; however, the dihedral angles between the two silver-coordinated aryl rings for **5a** (56.5°) and **5b** (83.4°) were quite different.

A series of binuclear silver(I) complexes with pyridyl substituted alkyl ligands, **6a** and **6b** (Figure 4), was reported, as well as their copper(I) and gold(I) analogs.[23–25] These binuclear silver(I) complexes were found to be very light and air sensitive and would readily decompose at room temperature in solution. Even when stored under argon in unlit conditions, decomposition would occur within several days.

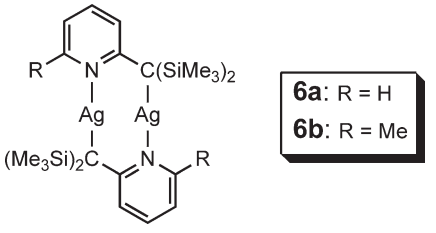

Figure 4 Structure of **6a** and **6b**.

In addition to the widely utilized lithiated reagents, other organometallic reagents have been used as precursors for making organosilver(I) complexes. For example, Naumann reported the synthesis of a series of perfluoroalkylsilver(I) compounds by the ligand exchange reaction of the corresponding perfluoroalkylcadmium(II) complexes with $AgNO_3$ in polar aprotic solvents such as dmf.[26] An equilibrium between the neutral [AgR(solv)] (solv = donor solvent; R = CF_3, C_2F_5, $C_3F_7^n$, $C_3F_7^i$, $C_4F_9^n$) (Equation (1)) and the anionic $[AgR_2]^-$ was investigated using NMR spectroscopy.

$$2[AgR(solv)] \rightleftharpoons [Ag(solv)_2]^+ + [AgR_2]^- \quad (1)$$

A tetranuclear silver(I) complex, **7a** (Figure 5), was formed unexpectedly from the reaction of the corresponding diaryllead(II) and $AgAsF_6$ in liquid SO_2 in 64% yield.[27] Crystal structure determination revealed a close-to-planar Ag_4 core with short Ag–Ag contacts of 2.726(1) and 2.754(1) Å, and the Ag–C bond distances ranged from 2.191(5) to 2.275(4) Å. In addition, density functional theory (DFT) calculations were performed on a previously reported analog, $[Ag(mes)]_4$ **7b** (Figure 5), to study the electronic structures and bonding interactions, and these results were compared to the pentanuclear star-shaped complex, $[Ag(mes)]_5$, as well as the isostructural $[M(mes)]_5$ (M = Cu, Au).[28] Metal–metal bonding was found to exist in these complexes, and the stability of **7b** was found to be similar to that of $[Ag(mes)]_5$.[28] Relativistic effects – essential in considering gold(I) systems – were found to be unremarkable for these silver(I) and copper(I) systems.

Rather than utilizing complete transmetallation reactions, mixed metal silver(I) aryl complexes **8–11** were obtained from the reaction of soluble silver salts with arylgold(I) complexes possessing ancillary phosphine or arsine ligands, as shown in Scheme 1.[29,30]

The solid-state structures of **8b** and **9c** were confirmed crystallographically, with the former being unimolecular in nature and the latter crystallized as a polymeric chain through intermolecular Au–Au interactions (Au–Au distance = 3.132 Å). Relatively long Ag–C bond distances of 2.326(3) Å (in **8b**) and 2.27(2) Å (in **9c**) were observed. These are in the range typical for a three-center two-electron bonding mode in μ-bridging d^{10}-metal aryl complexes. The Ag–Au bond distances were fairly short **8b**: 2.8245(6) Å; **9c**: 2.7758(8) Å), and were shorter than the sum of van der Waals radii for silver and gold.[31] An interesting feature worth mentioning was that the mesityl bridge was not symmetrically disposed among the gold(I) and silver(I) centers. Complex **9c** displayed a planar coordination geometry at the silver(I) center with the Au–Ag–C and C–Au–C angles of 180°, in contrast to the non-planar geometry found in complex **8b**. The crystal structure of a previously reported complex, $[Au_2(C_6F_5)_4Ag_2(OCMe_2)_2]$ **12** (Figure 6), was also determined, and shown to have structural similarities to that of **9c**.[32]

Unlike **9c**, in which alternating Au(mes)L units were bridged by one silver(I) atom, the $Au(C_6F_5)_2$ units in **12** were bridged by Ag_2 units. The Ag–C, Ag–Au, Ag–Ag, and Au–Au distances showed values of 2.440(8)–2.506(8), 2.7829(9)–2.7903(9), 3.1810(13), and 3.1674(11) Å, respectively. The optical and luminescence properties of **12** were studied in the solid state and as acetone solution, with concentration dependence observed in the latter due to self aggregation.[32] The spectroscopic and photophysical origins of these species were assigned and supported by ground-state and TD-DFT calculations.[32]

Apart from the gold(I) system, bis(mesityl)mercury(II), which also possesses a heavy metal center with strong relativistic effects, has been used for the synthesis of the mixed metal silver(I) aryl complexes, $[HgAg_2(mes)X_2]_2$ (X = OTf **13a** (Figure 7), ClO_4 **13b**).[33] X-ray crystal structure analysis of **13a** revealed its hexanuclear nature with the

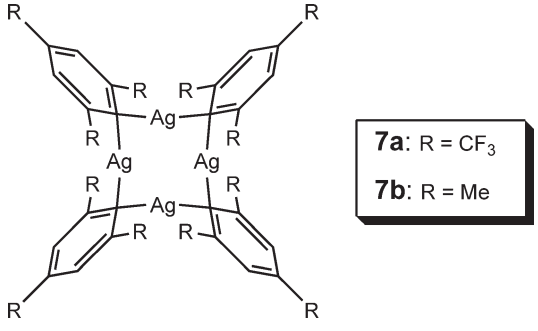

Figure 5 Structure of **7a** and **7b**.

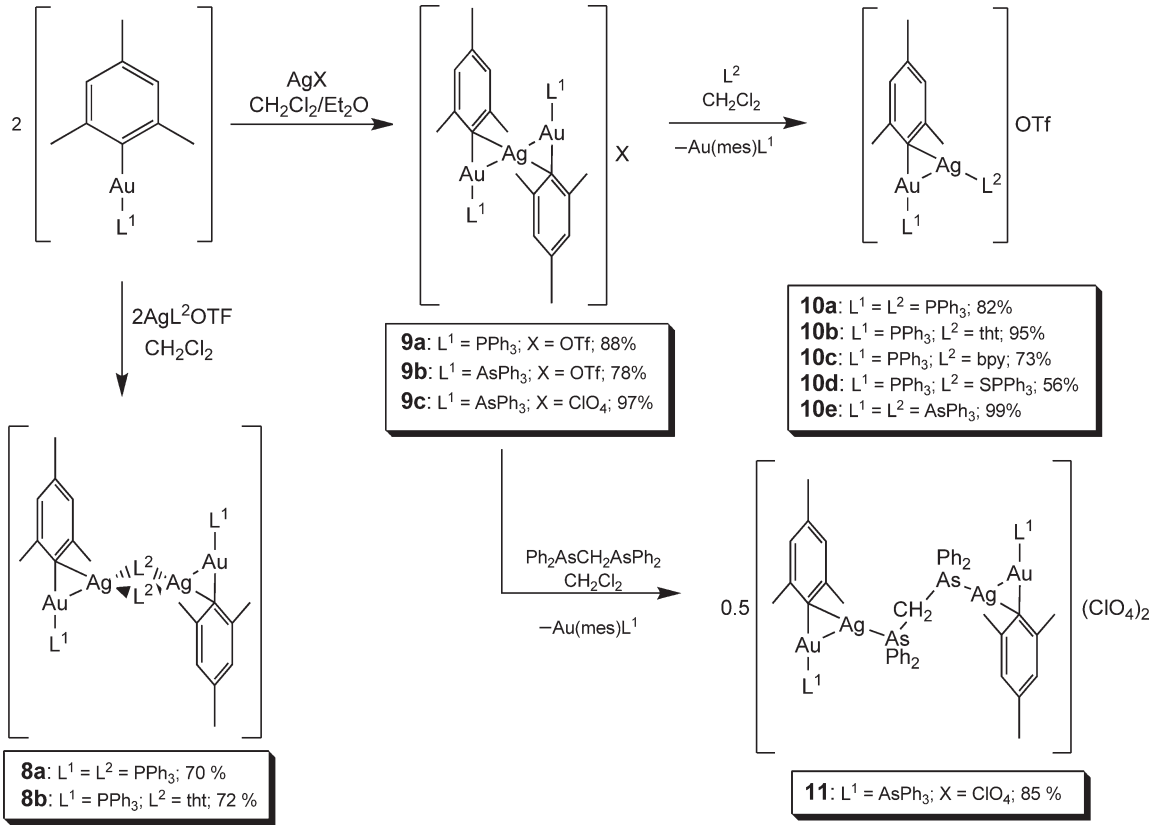

9a: $L^1 = PPh_3$; X = OTf; 88%
9b: $L^1 = AsPh_3$; X = OTf; 78%
9c: $L^1 = AsPh_3$; $X = ClO_4$; 97%

10a: $L^1 = L^2 = PPh_3$; 82%
10b: $L^1 = PPh_3$; L^2 = tht; 95%
10c: $L^1 = PPh_3$; L^2 = bpy; 73%
10d: $L^1 = PPh_3$; $L^2 = SPPh_3$; 56%
10e: $L^1 = L^2 = AsPh_3$; 99%

8a: $L^1 = L^2 = PPh_3$; 70 %
8b: $L^1 = PPh_3$; L^2 = tht; 72 %

11: $L^1 = AsPh_3$; $X = ClO_4$; 85 %

Scheme 1

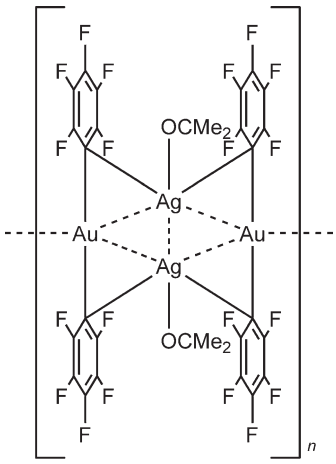

12

Figure 6 Structure of **12**.

two $Hg(mes)_2$ units bridged by an $Ag_4(OTf)_4$ core through Ag–C and Ag–Hg bonding interactions.[33] The Ag–C and Ag–Hg bond distances were 2.284(10)–2.368(10) and 3.101(1)–3.386(1) Å, respectively. Rather than a three-center two-electron bond as in the cases of **8b** and **9c**, the aromatic *ipso*-carbons in **13a** were believed to be σ-bonded to the mercury(II) centers but π-bonded to the silver(I).

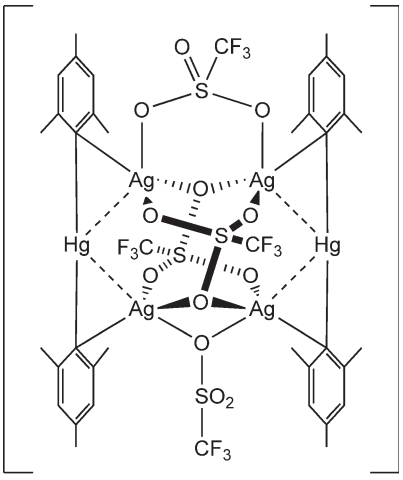

13a

Figure 7 Structure of **13a**.

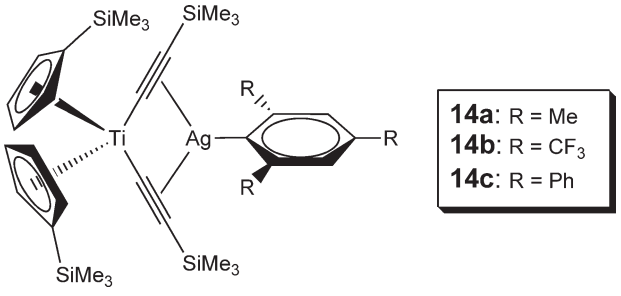

Figure 8 Structure of **14a–c**.

Lang and van Koten reported the isolation of a titanium(IV)–silver(I) mixed metal complex **14a** (Figure 8) using mesitylsilver(I).[34,35] The crystal structure revealed a tweezer-type π-coordination of the [Ti](C≡CSiMe$_3$)$_2$ moiety to Ag(mes), with the silver(I) center possessing a trigonal-planar tricoordinate geometry. The Ag–C$_{ipso\text{-mes}}$, Ag–C$_{\alpha\text{-alkynyl}}$, and Ag–C$_{\beta\text{-alkynyl}}$ bond distances were 2.099(5), 2.270(9), and 2.305(9) Å, respectively. Subsequent works by Lang extended the variety of aryl groups attached to the silver centers by a modified reaction pathway, through the transmetallation reaction of [(Me$_3$SiC$_5$H$_4$)$_2$Ti(C≡CSiMe$_3$)$_2$Ag(OAc)] with the lithiated aryl or aryl Grignard's reagents to afford **14b** and **14c** (Figure 8), respectively.[36] The crystal structure of **14c** was also determined.

Laguna reported the synthesis and crystal structures of **15** and **16** (Scheme 2). The reaction proceeded via the *in situ* deprotonation of phosphine–phosphonium salts by the acac ligand on the silver(I) precursor complex, followed by subsequent coordination of the ylide ligands to the silver(I) center.[37] The silver(I) center in **15** was found to assume a highly distorted tetrahedral coordination geometry, in contrast to **16** where distorted trigonal-planar geometries were observed for the two different silver(I) centers. The Ag–C bond distance in **15** was found to be 2.414(6) Å, which is fairly long and could be due to the four-coordinate geometry of the silver(I) center. In **16**, the Ag–C bonds had distances of 2.289(11) and 2.231(10) Å, which are not unusual for a three-coordinate silver(I) center.

Although there are relatively fewer reports dealing with the synthesis and structural characterization of silver(I) alkyl and aryl complexes in the literature when compared to other transition metals, this class of compounds is still considered an important source of precursors for synthesizing (fluorine-rich) alkyl, alkenyl, and aryl complexes of other transition metals, including gold(I),[38] rhodium(III),[39] iridium(III),[39] molybdenum(0),[40] nickel(II),[41] palladium(II),[42,43] platinum(II),[44] thallium(III),[45] tellurium(IV),[46] as well as silver(I) itself.[47] For example, Bu$_4$N[Ag(C$_6$F$_5$)$_2$] was used in the synthesis of [Ag(C$_6$F$_5$){N(H)=CPh$_2$}] **17** (Figure 9), which crystallized as a chain of dimers with the presence of both intermolecular Ag–Ag interactions within the dimer and interdimer H–F

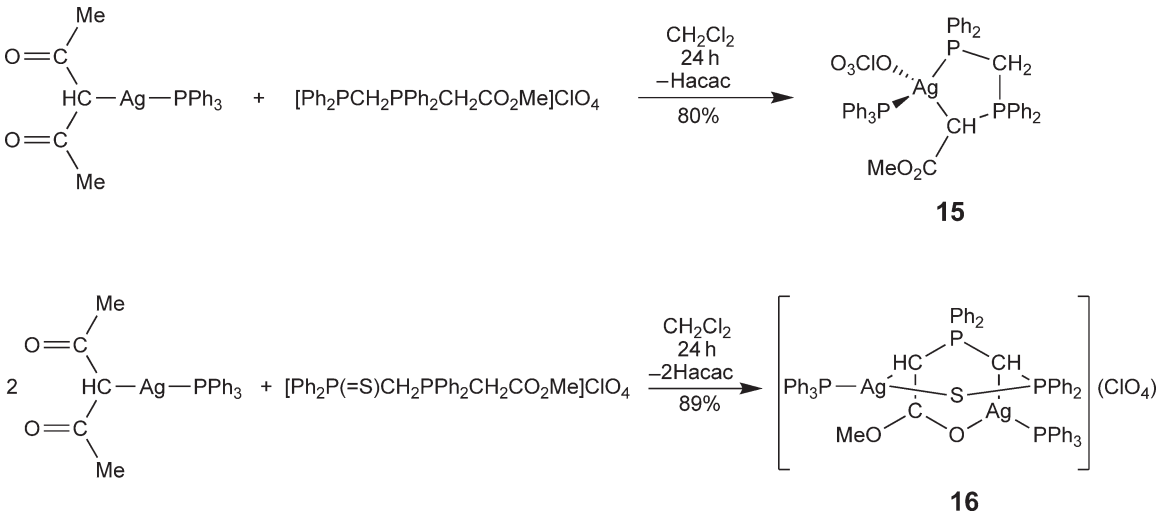

Scheme 2

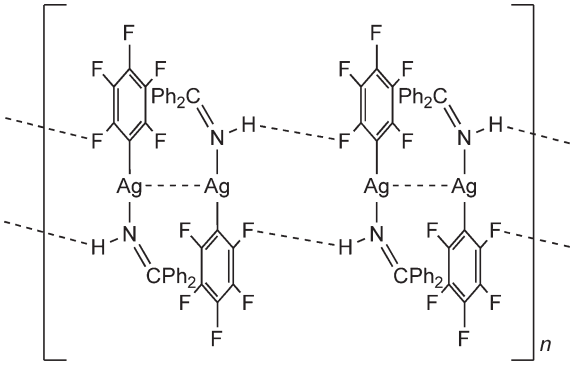

Figure 9 Structure of **17**.

hydrogen bonding within the chain.[47] *Ab initio* calculations based on several possible bonding modes were made at the HF and MP2 levels, and comparison studies with the gold(I) analogs have also been made.[47]

It was demonstrated that a series of perfluoroalkyl and -phenyl silver(I) compounds could also be used as a perfluoroorgano-transfer reagent in organic synthesis, where the reaction of tetraethylthiuram disulfide, $Et_2NC(=S)S\text{-}SC(=S)NEt_2$ (or alternatively, $[Et_2NC(=S)S]_2$), with AgR_F ($R_F = CF_3$, C_2F_5, *iso*-C_3F_7, *n*-C_4F_9, C_6F_5) afforded the corresponding perfluoroorgano esters of diethyldithiocarbamic acid, $Et_2NC(=S)SR_F$.[48] Coinage metal mesityls, including $[Ag(mes)]_4$ **7b**, were also used as precursors toward the synthesis of the respective oxide-free metal nanoparticles by thermolysis.[49] Uniform, well-defined spherical nanosilver particles with an average diameter of 8.5 ± 1.1 nm were obtained.

2.04.2.2 Synthesis, Properties, and Reactions of Carbene Complexes of Silver

2.04.2.2.1 Introduction

Carbene ligands, especially the *N*-heterocyclic carbenes, are regarded as universal ligands in coordination and organometallic chemistry. They are able to bind to a wide variety of metal centers in various oxidation states, as well as to both stabilize and activate metal centers of key intermediates in the catalytic cycles of various organic

reactions. The corresponding organometallic and/or coordination compounds have great catalytic potential, and indeed, it has been a recent trend to explore this class of complexes as a new generation or as a supplement (or in some cases as a replacement) to the currently well-known transition metal phosphine-containing catalysts.

Reports on the coordination chemistry of *N*-heterocyclic carbene-containing metal complexes started to appear as long ago as 1968,[50,51] while metal-free carbenes have only been isolated very recently.[52] In view of the fact that the general chemistry and applications of organic carbenes and related metal complexes in chemical synthesis have been reviewed several times recently,[53–57] examples limited only to those carbene complexes with silver(I) have been discussed. Nevertheless, it is worth mentioning that the developments in silver(I) *N*-heterocyclic carbenes have also been reviewed recently by Lin.[58]

2.04.2.2.2 Synthesis via the reaction of AgX salt with free carbene ligand

The silver(I) carbene chemistry was pioneered by Arduengo and co-workers, who made the first report on the isolation of stable homoleptic silver(I) *N*-heterocyclic carbene complexes in 1993.[59] The synthesis involved the direct reaction of 1,3-dimesitylimidazol-2-ylidene with silver(I) trifluoromethanesulfonate (triflate) in thf to afford **18** as high-melting (m.p. 274–275 °C) colorless crystals in 80% yield (Scheme 3).[59] Complex **18** was structurally characterized, and the silver(I) center was found to possess a linear two-coordinate geometry with Ag–C bond distances of 2.067(4) and 2.078(4) Å and C–Ag–C angles of 176.3(2)°.[59] Interestingly, the two imidazole rings were twisted 39.7° with respect to each other, a phenomenon attributed to the steric bulk introduced by the mesityl groups and crystal packing forces. ^{1}H, ^{13}C, ^{15}N, and ^{109}Ag NMR studies indicated that the degree of delocalization of the imidazole rings in **18** was enhanced as compared to that of the free carbene but not as strong as in imidazolium ions.[59] NMR studies further revealed the absence of a rapid ligand exchange, even in the presence of nucleophilic solvent.[59]

Although this synthetic method provides a direct reaction pathway for yielding silver(I) carbene complexes, reports based on this approach are rather limited. This is mainly because of the sensitivity and stability of the free carbene ligands, in general, toward air, moisture, temperature, and strong bases. Nevertheless, Bertrand made use of this simple strategy and extended the chemistry to polymeric silver(I) carbenes.[60,61] Complex **19** could be obtained from the reaction of 2 equiv. of silver(I) acetate with 1 equiv. of the cationic triazole, and its crystallographic structure indicated the existence of co-planarity across the silver(I)–triazolium chain (Scheme 4). Crystals of **19** were found to be totally insoluble, but addition of a small amount of silver(I) triflate to a suspension of **19** in MeCN gave a

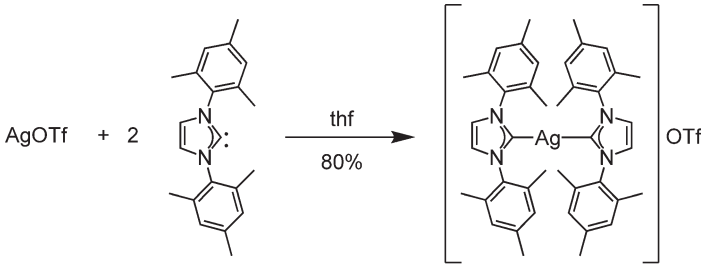

18

Scheme 3

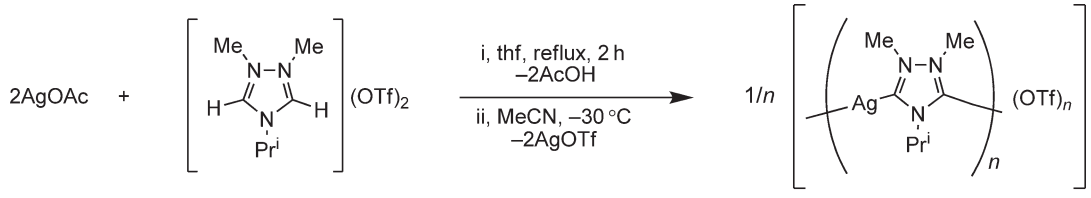

19

Scheme 4

homogeneous solution. Results from NMR studies supported the observation of a rapid metal–ligand exchange process, which could be slowed down in the presence of coordinating anions such as Cl^-.

In view of the interesting structural features and the low coordinating properties of carborane monoanion and its related derivatives, together with the potential of silver(I) carbene complexes as highly active catalysts, Weller and co-workers reported the preparation of an interesting white crystalline silver(I) complex **20** that contained a bis(carbene)silver(I) cation and a tetrakis(carborane)diargentate(I) anion from the reaction of the corresponding free carbene with Ag[*closo*-$CB_{11}H_{12}$] salt (Scheme 5).[62] The crystal structure of **20** revealed Ag–C bond distances of 2.069(6) and 2.070(5) Å and C–Ag–C bond angles of 174.3(2)° in the bis(carbene)silver(I) cation, comparable to those observed in **18**. However, an interplanar angle of 59.1° between the two imidazole planes was obviously different from that in **18** (39.7°), which could be readily attributed to the difference in crystal packing forces imposed by the anions. The Ag–H and Ag–B distances observed in the anion were in the ranges of 1.96–2.52 and 2.586(8)–2.94(2) Å, respectively. On the other hand, Chung reported the use of silver(I) salts with coordinating 1,3-diphenyl-1,3-propanedionate and benzoate anion for the synthesis of the respective neutrally charged silver(I) monocarbene complexes, **21a**[63] and **21b**[64] (Scheme 6).

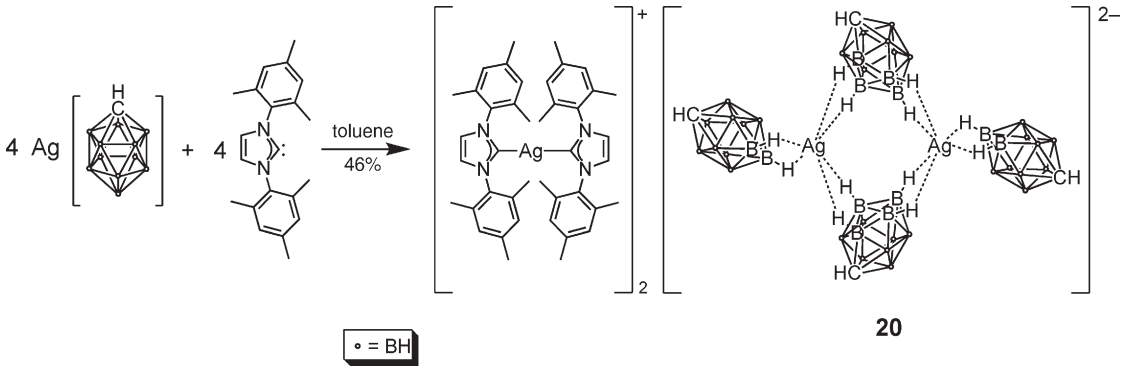

Scheme 5

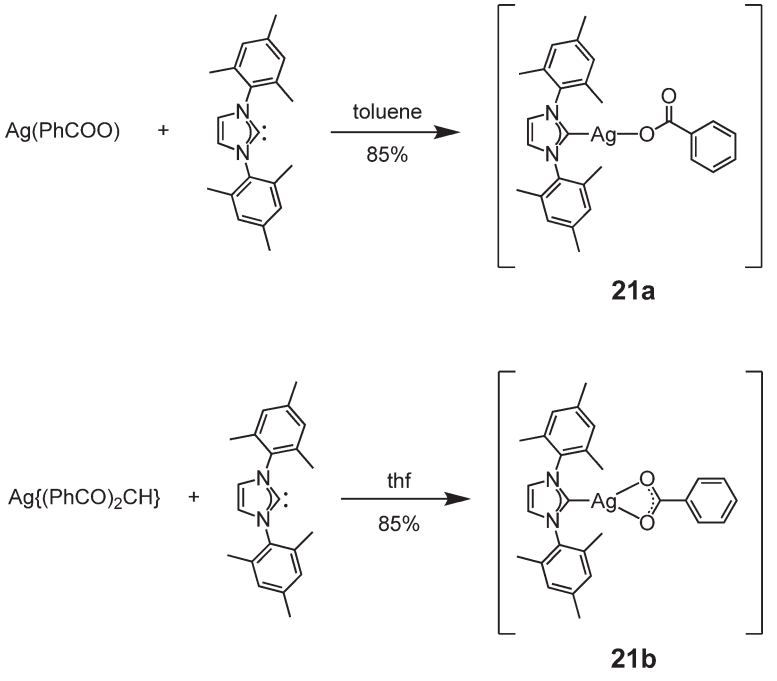

Scheme 6

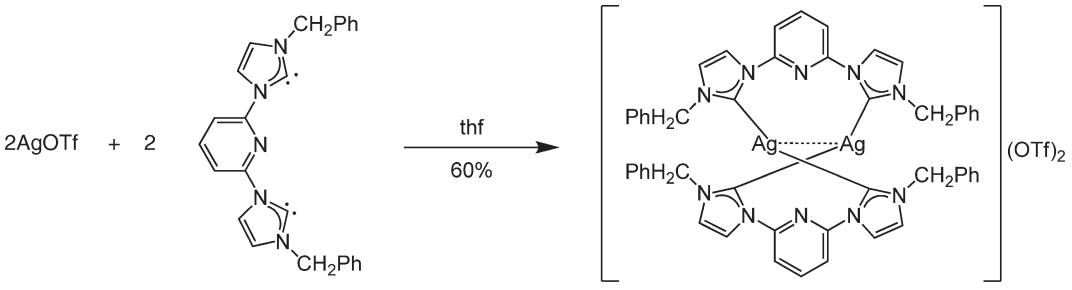

22

Scheme 7

It was found that the 1,3-diphenyl-1,3-propanedionate anion behaved as a bidentate ligand whereas the benzoate acted as a monodentate ligand. The Ag–C bonds in **21a** and **21b** were more or less similar to that found in **18** (**21a**: 2.064(6) Å, **21b**: 2.085(10) Å). It is interesting to note that **21b** crystallizes as dimers with the presence of short intermolecular Ag–Ag distance of 3.000(10) Å, in contrast to the monomeric nature of **21a** with a longer Ag–Ag distance of 3.2177(13) Å.

A dinuclear silver(I) carbene complex, **22**, was also isolated using a pyridyl-bridged biscarbene ligand (Scheme 7).[65a,65b] Complex **22** possessed a double helical structure with Ag–C bond distances of 2.080(4) and 2.087(4) Å and a C–Ag–C angle of 165.5(2)°.[65a] Weak Ag–Ag interaction could also be observed with an Ag–Ag distance of 3.158 Å.[65a]

2.04.2.2.3 Synthesis via *in situ* deprotonation of imidazolium salts using silver(I) oxide

Since the successful exploration of silver(I) oxide usage as a multifunctional precursor for the synthesis of silver(I) *N*-heterocyclic carbene complexes, there has been an increasing number of reports related to silver(I) *N*-heterocyclic carbene chemistry. Silver(I) oxide can act as a weak base to deprotonate imidazolium salts, generating the free *N*-heterocyclic carbene ligands *in situ*, which then forms the silver(I) carbene complexes readily. This reaction can take place in the presence of air and moisture, and as a result, no special treatment in regard to the solvents has to be undertaken. More importantly, its basicity is rather specific toward the deprotonation at the C2 position of the imidazole moiety. Exploration of using silver(I) carbonate as a milder precursor in place of silver(I) oxide has also been pursued, but longer reaction times are usually required.

2.04.2.2.3.(i) Silver(I) complexes with monodentate *N*-heterocyclic carbene ligands

There has been a tremendous growth in the number of reports on silver(I) *N*-heterocyclic carbene chemistry since the publication of the first report on the facile synthesis of silver(I) carbenes using silver(I) oxide and imidazolium salts by Lin's research group in 1998.[66] Complex **23a** was synthesized in 89% yield by the reaction of silver(I) oxide with diethylbenzimidazolium bromide in dichloromethane at room temperature (Scheme 8). The crystal structure of **23a** revealed the linear two-coordinate geometry of the silver(I) centers in both the cation and anion, with C–Ag–C and Br–Ag–Br angles of 175.6(11) and 175.1(2)°, respectively. Short Ag–Ag contact of 2.954(4) Å could be observed. The Ag–C bonds have distances of 2.052(26) and 2.073(26) Å. The bromo-free silver(I) carbene complex, **23b**, was synthesized in a similar fashion using the same starting materials, but in the presence of aqueous NaOH and $Bu^n_4NPF_6$, the latter of which functioned as a phase-transfer catalyst. Both complexes have been demonstrated to act as efficient carbene transfer reagents for the synthesis of palladium(II) and gold(I) carbene complexes. Later, Crabtree reported the synthesis of **23c** and **23d** (Figure 10) in 95% and 94% yield, respectively, and used them as precursors for the preparation of related iridium(I) and rhodium(I) carbene complexes.[67]

In spite of the isolation of the bis(carbene)silver(I) complex **18** from the reaction of silver(I) triflate and the free carbene ligand as discussed in Section 2.04.2.2.2, the mono(carbene)silver(I) counterpart, [chloro(1,3-dimesitylimidazolium)silver(I)] **24**, was isolated as a chloro complex in 73% yield using silver(I) oxide and 1,3-dimesitylimidazolium chloride as precursors.[68] Crystal structure determination of **24** (Figure 11) revealed an idealized linear two-coordinate geometry at the silver(I) center, with an Ag–C bond distance of 2.056(7) Å and C–Ag–Cl bond angle of 180.00(11)°. Interestingly, weak intermolecular head-to-tail H···Cl hydrogen bonds were observed between the imidazolium protons and the Cl ligand.

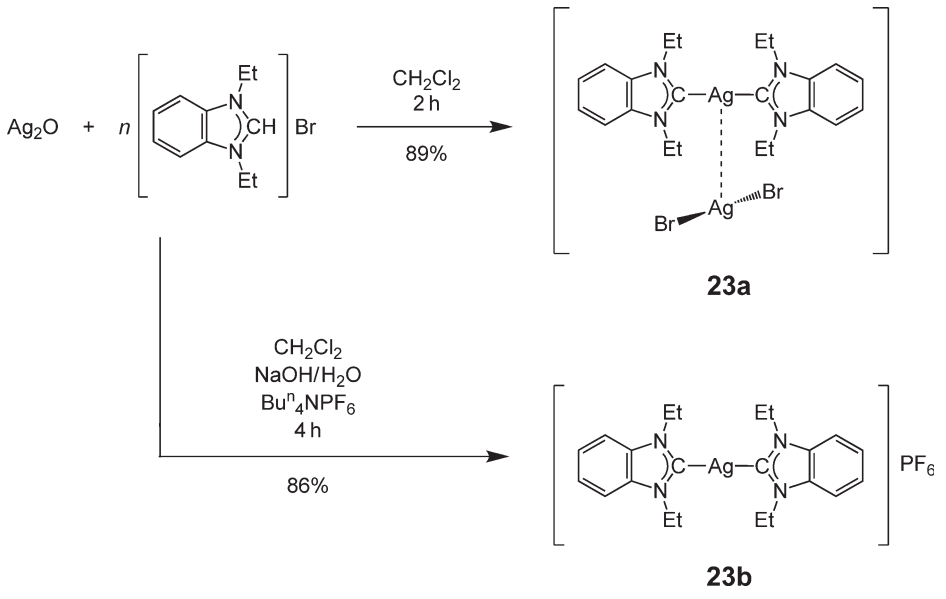

Scheme 8

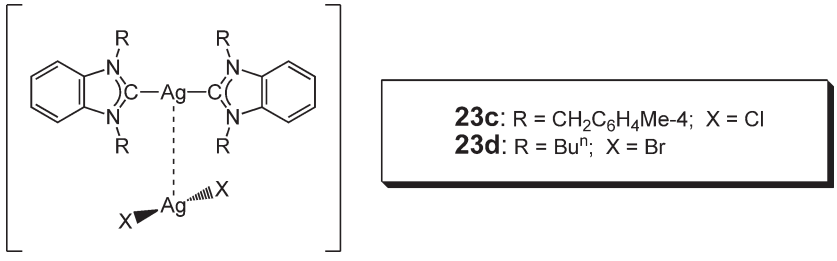

Figure 10 Structure of **23c** and **23d**.

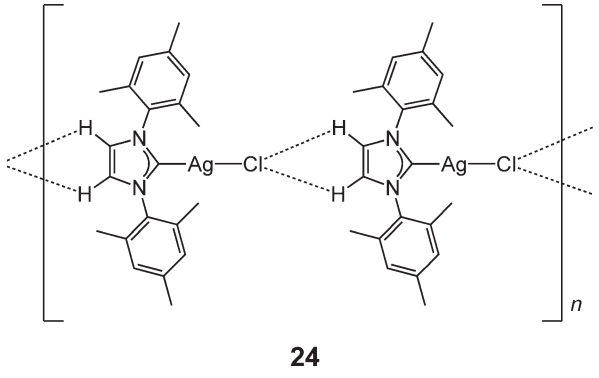

Figure 11 Structure of **24**.

$[Ag(carbene)_2][AgCl_2]$ (carbene = 1,3-dimesitylimidazol-2-ylidene) was also reported for use as a pre-catalyst for the polymerization of L-lactide with low PDI and in the absence of monomer racemization.[69]

Lin investigated the structural effects of changing the anion in a series of bis(1,3-dimethylimidazolylidenyl)silver(I) complexes.[70] For **25a** and **25b** (Figure 12), having the $AgCl_2^-$ or $AgBr_2^-$ as anion, the crystal structures displayed

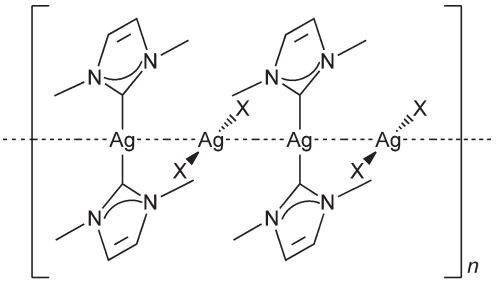

25a: X = Cl
25b: X = Br

Figure 12 Structure of **25a** and **25b**.

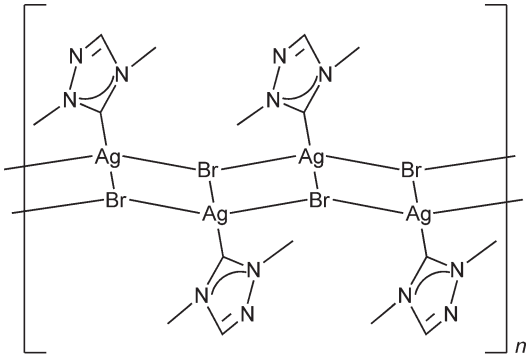

26

Figure 13 Structure of **26**.

linearly aligned chains of alternating bis(carbene)silver(I) cations and AgX_2^- anions with weak Ag–Ag contacts of 3.189(4) (for **25a**) and 3.2082(4) Å (for **25b**). The silver centers have a close-to-perfect linear two-coordinate geometry, and the Ag–C bond distances of 2.096(6) (for **25a**) and 2.084(5) Å (for **25b**) are not unusual. However, when triazolium salt was used in place of imidazolium salt, **26** (Figure 13) was isolated which crystallized as an infinite [Ag(carbene)Br] polymeric chain that stemmed from the bridging AgBr staircase structure. The Ag–C bond of 2.131(5) Å was slightly longer than that observed in **25a** or **25b**. Discrete silver(I) complexes with the triazolylidene ligand, $[Ag(carbene)_2]^+$, were obtained as a nitrate salt. Interestingly, intermolecular π–π stacking of ~3.42 Å was observed between the triazolylidene rings in a head-to-tail fashion. Related studies on the iodo counterparts of silver(I) 1,3-dimethylimidazol-2-ylidene complexes resulted in a polynuclear complex that contained discrete $[Ag(carbene)_2]^+$ cations and the infinite polymeric anionic $\{[Ag_4I_6]^{2-}\}_n$.[71] Detailed quantum chemical calculations on a series of halo(imidazolylidene) and di(imidazolylidene) complexes of copper(I), silver(I), and gold(I) were reported by Frenking, where the nature and strength of the metal–carbene bonds were discussed. [72,73]

With the long alkyl chain substitutions on the *N*-heterocyclic carbenes, lamella-structured silver(I) carbene complexes **27a** and **27b** (Figure 14) were isolated.[74] It is interesting to note that the synthetic procedures for the two complexes are the same except for the use of different solvents of crystallization. The dinuclear **27a** was obtained from recrystallization in dichloromethane–*n*-hexane while the tetranuclear **27b** was obtained from acetone. The structure of **27a** could be interpreted as the dimeric form of [Ag(carbene)Br] bridged by intermolecular Ag–Br interactions. The Ag–C bond has a distance of 2.094(5) Å. The tetranuclear **27b**, on the other hand, could be regarded as two monocationic bis(carbene)silver(I) bridged by an $[Ag_2Br_4]^{2-}$ anion, with the presence of short Ag(cationic)–Ag(anionic) contact (3.0038(18) Å) and comparable Ag–C bond distances (2.0945(5), 2.138(13) Å). A related

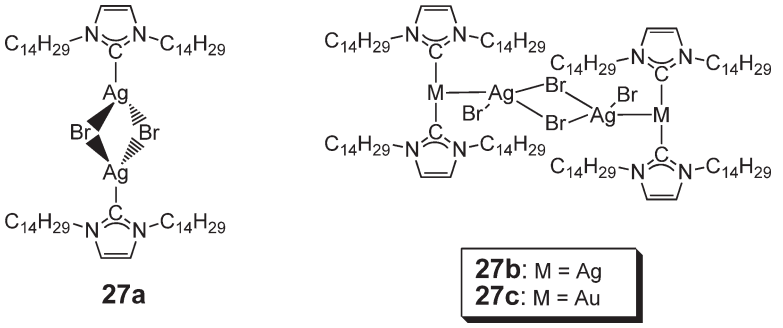

Figure 14 Structures of **27a–c**.

tetranuclear mixed metal complex **27c** was also isolated using the silver–carbene-transfer strategy, and a short Au(cationic)–Ag(anionic) distance of 2.988(3) Å was observed in its crystal structure.

Examples of silver(I) carbene complexes with unsymmetrically disubstituted *N*-heterocyclic carbene ligands have also been prepared using this synthetic strategy. For instance, $[Ag(carbene)_2][AgBr_2]$ **28a** (carbene = 1-ethyl-3-methylimidazol-2-ylidenyl) was made in 87% yield and used as precursor for the synthesis of *trans*-$[PdCl_2(carbene)_2]$.[75] The chloro counterpart, $[Ag(carbene)_2][AgCl_2]$ **28b**, was reported as an ionic liquid and as a pre-catalyst which underwent thermal decomposition to generate the free carbene *in situ*, which could then be used as a *trans*-esterification catalyst, as well as for the polymerization of L-lactide with low PDI and in the absence of monomer racemization.[69] Treatment of 1-allyl-3-methylimidazolium iodide with silver(I) oxide in dichloromethane afforded a tetranuclear complex of the type $[Ag(carbene)_2]_2[Ag_4I_6]$ **29a**.[71] Recrystallization from hot dmso yielded the insoluble polymeric $[Ag(carbene)I{\cdot}Ag_2I_2{\cdot}Ag(carbene)I]_n$ **29b**.

The reaction of 1-(9-anthracenylmethyl)-3-ethylimidazolium iodide with silver(I) oxide in refluxing dichloromethane for 2 days afforded a moderately light sensitive iodosilver(I) carbene polymer **30** (Figure 15) in 50% yield.[76] The crystal structure of **30** stems from a polymeric $[AgI]_n$ staircase, and each silver(I) center is additionally coordinated to the 1-(9-anthracenylmethyl)-3-ethylimidazol-2-ylidene ligand. A relatively long Ag–C distance of 2.182(7) Å was observed. The Ag–Ag distances of 3.473 and 4.063 Å indicate the absence of Ag–Ag interactions, while the center-to-center distance of the anthracenyl rings of 3.572 Å clearly demonstrates the presence of π–π stacking interactions. The carbene ligands in **30** could readily be replaced by refluxing in pyridine, forming the corresponding $[Ag(py)I]_n$ staircase polymer. The ease of such substitution is in accordance with the fairly weak Ag–C bonding, as reflected by the relatively long Ag–C bond distance.

Apart from common organic groups, a silver(I) carbene complex, **31**, with the organometallic ferrocenyl groups attached to the *N*-heterocyclic carbene ligands was isolated and structurally characterized (Scheme 9).[77]The Ag–C bond distances, C–Ag–C bond angle, and the interplanar angle of the two imidazolium rings were found to be

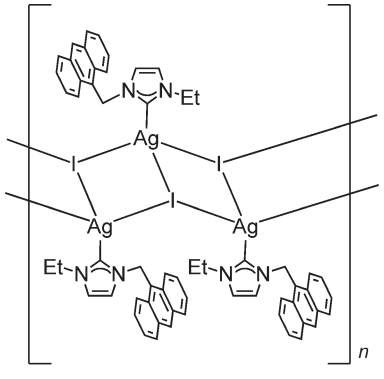

Figure 15 Structure of **30**.

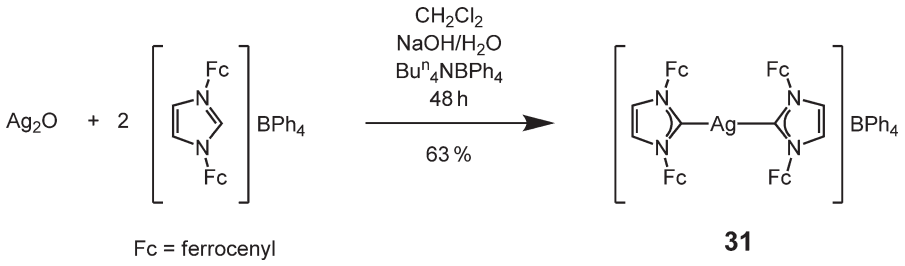

Scheme 9

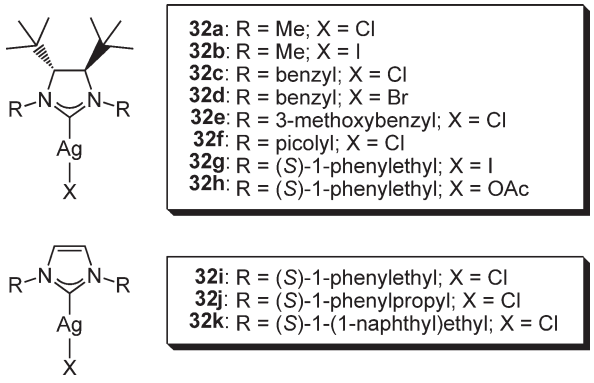

Figure 16 Mononuclear silver(I) monocarbene complexes **32a–k**.

2.082(4)–2.092(4) Å, 176.8(2)°, and 38.4(2)°, respectively, and were comparable to those observed for **18**. Analogous silver(I) complexes with the bis(ferrocenyl)imidazolium ligands modified to the more saturated bis(ferrocenyl)imidazolinium counterparts could not be prepared due to the reduced acidity of the bis(ferrocenyl)imidazolinium salts and the weakly basic nature of silver(I) oxide. Nevertheless, chiral-center-containing organic imidazolinium (and imidazolium) silver(I) halides, **32a–32k** (Figure 16), have been prepared and used as carbene-transfer reagents for the copper-catalyzed enantioselective conjugate addition of dialkylzinc reagents to various Michael acceptors. The synthesis of chiral palladium(II) imidazolinium complexes and their use as catalysts in the Mizoroki–Heck reactions were also reported.[78–81] Among these complexes, the crystal structures of **32b** and **32d** were determined.[78] The former has a dimeric structure with a relatively long Ag–C bond of 2.120(8) Å and a weak Ag–Ag contact of 3.0196(14) Å, whereas the latter is monomeric in nature with Ag–C bond distance of 2.089(17) Å.

Silver(I) complexes with a six-membered *N*-heterocyclic carbene ligand were reported by Herrmann.[82] Under the previously employed carbene-transfer conditions, the reaction of **33** with $[Pd(MeCN)_2Cl_2]$ in dichloromethane did not give the corresponding bis(carbene)dichloropalladium(II) complex but, instead, afforded the bis(carbene)silver(I) hexachlorodipalladate, **34**, in 82% yield (Scheme 10). The crystal structures of **33** and **34** were determined, both of which displayed a monomeric structure with linear, two-coordinate silver(I) centers. The Ag–C bond distances of 2.095(3) Å in **33** and 2.097(3) and 2.101(3) Å in **34** are comparably longer than that for the well-known example **18**, probably as a result of the steric bulk introduced by the six-membered ring ligand(s).

2.04.2.2.3.(ii) Silver(I) complexes with Lewis base-functionalized mono(*N*-heterocyclic carbene) ligands

In addition to the enormous attention given to silver(I) *N*-heterocyclic carbene complexes as effective carbene-transfer reagents toward the synthesis of new transition metal carbene complexes, the study of their coordination chemistry is also an active area of research owing to the findings that *N*-heterocyclic carbene ligands are considered to be better σ-donor ligands than the well-known phosphines, with the additional advantages of the ease of synthesis and relative stability in air. In contrast to the great interest in the metal–metal interactions present between transition

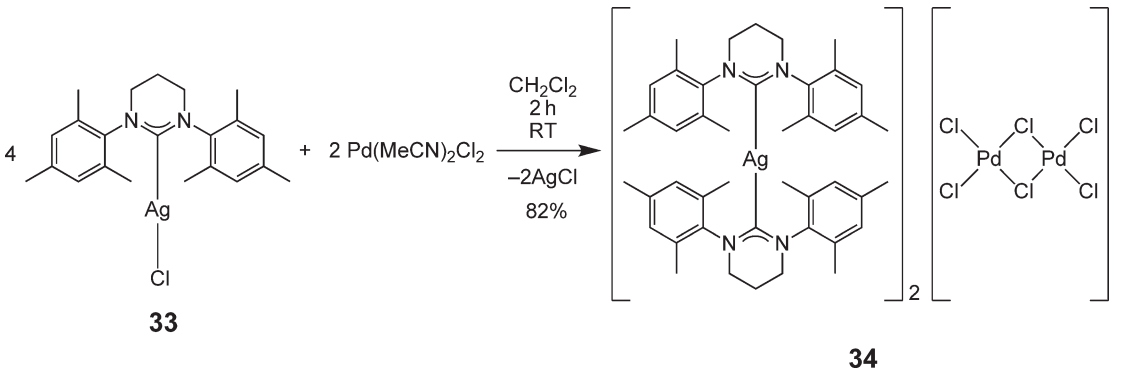

Scheme 10

metal centers of closed-shell configuration in the last two decades – of which phosphines have been commonly employed as ancillary and supporting ligands – corresponding research using the *N*-heterocyclic carbene ligands has been reported only recently.[83,84] To introduce the capability of carbene ligands for bridging metal centers in close proximity, additional donor groups as substituents were incorporated on the ligand. For instance, the reaction of 1,3-bis(2-pyridinylmethyl)-1*H*-imizazolium or 1,3-bis(2-quinolylmethyl)-1*H*-imizazolium salts with silver(I) oxide, sodium hydroxide and catalytic amounts of tetra-*n*-butylammonium tetrafluoroborate afforded the mononuclear bis(carbene)silver(I) complexes (Scheme 11) **35a–c**.[85,86]

Subsequent reactions of **35a** and **35b** with silver(I) tetetrafluoroborate in acetonitrile yielded the trinuclear silver complexes **36a** and **36b**, respectively. Alternatively, **36a** and **36b** could be obtained from the direct reaction of the imidazolium salts with an excess of silver(I) oxide in acetonitrile. The X-ray crystal structures of **35a**, **35c**, and the analogous chloride salt of **35a** were determined and found to possess similar molecular structures that are typical of $[Ag(carbene)_2]^+$-type complexes, with Ag–C bond distances of 2.093(4), 2.106(6)–2.117(5), and 2.082(6)–2.083(6) Å, respectively. Among these three crystal structures, it is noteworthy to mention that only the chloride counterpart of **35a** displays weak intermolecular Ag–Ag interactions with Ag–Ag contacts of 3.650 Å, whereas **35a** and **35c**, with Ag–Ag distance of 8.545 and 7.786 Å, respectively, show no intermolecular Ag–Ag interactions. This further demonstrates the effect of counteranion on the extent of metal–metal closed-shell interactions in the solid state. Moreover, **36a** was structurally characterized, which showed the complex cation consisted of three silver(I) centers arranged in an almost equilateral triangular array with exceptionally short Ag–Ag contacts that ranged from 2.7249(10) to 2.7718(9) Å. The carbene C atom was bonded to two silver centers on each side of the Ag_3 triangle in a novel bridging mode, with Ag–C bond distances of 2.223(8)–2.266(7) Å. The imidazolium rings were found to be

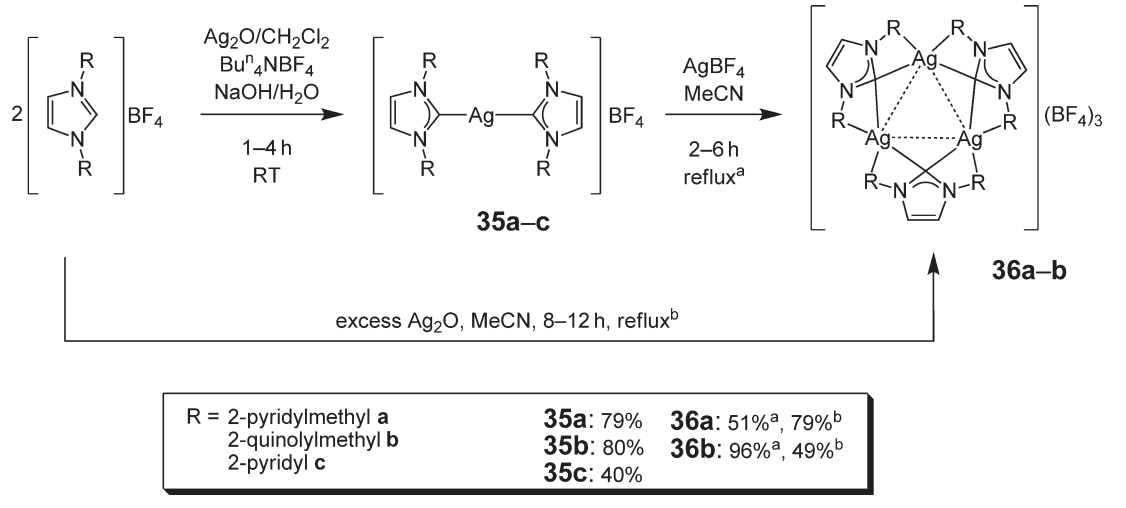

Scheme 11

perpendicular to the Ag_3 plane and the coordinating pyridyl side-arms were arranged in an alternating up- and-down fashion to give an overall D_3-symmetry. Complexes **35a–c** were also used as precursors for a series of gold(I) and mercury(II) carbene complexes, some of which contained pyridyls further coordinated to silver(I) centers to form bimetallic complexes.

A silver(I) complex having the heterosubstituted 3-methyl-1-(2-pyridylmethyl)imidazol-2-ylidene ligand, $[Ag(carbene)_2][I/AgI_2]$ **37**, was reported, which was further reacted to give a series of palladium(II) carbene complexes that were demonstrated to be active catalysts toward Heck, Suzuki, and Sonogashira coupling reactions.[87]

Complexes **38–40** (Figure 17) were also synthesized and structurally characterized, exemplifying the various types of possible molecular structures for this class of complexes.[88]

Imine-functionalized mono-*N*-heterocyclic carbene ligands were complexed to the silver(I) center to form the corresponding $[Ag(carbene)_2][AgX_2]$ complexes **41–43** (Figure 18).[88–90]

The employment of silver(I) complexes having a chiral carbene ligand **L** (Figure 19) and the empirical formula [AgBr**L**] has been reported for use as both carbene-transfer reagents to the corresponding dichloropalladium(II)

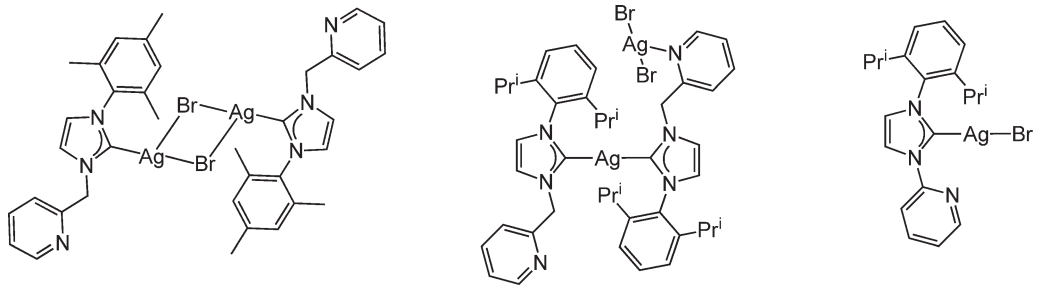

38 **39** **40**

Figure 17 Structure of **38–40**.

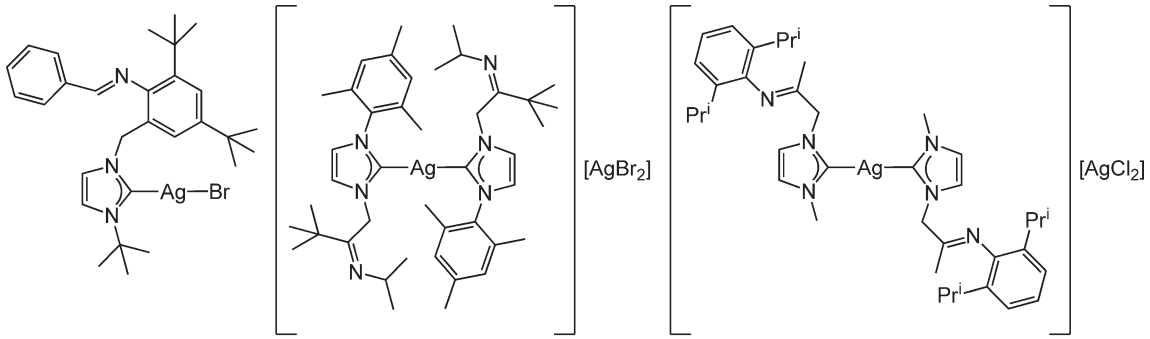

41 **42** **43**

Figure 18 Structure of **41–43**.

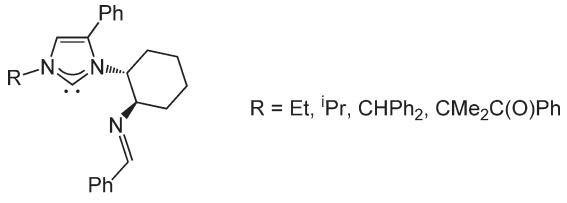

L

Figure 19 Structure of the chiral carbene ligand L.

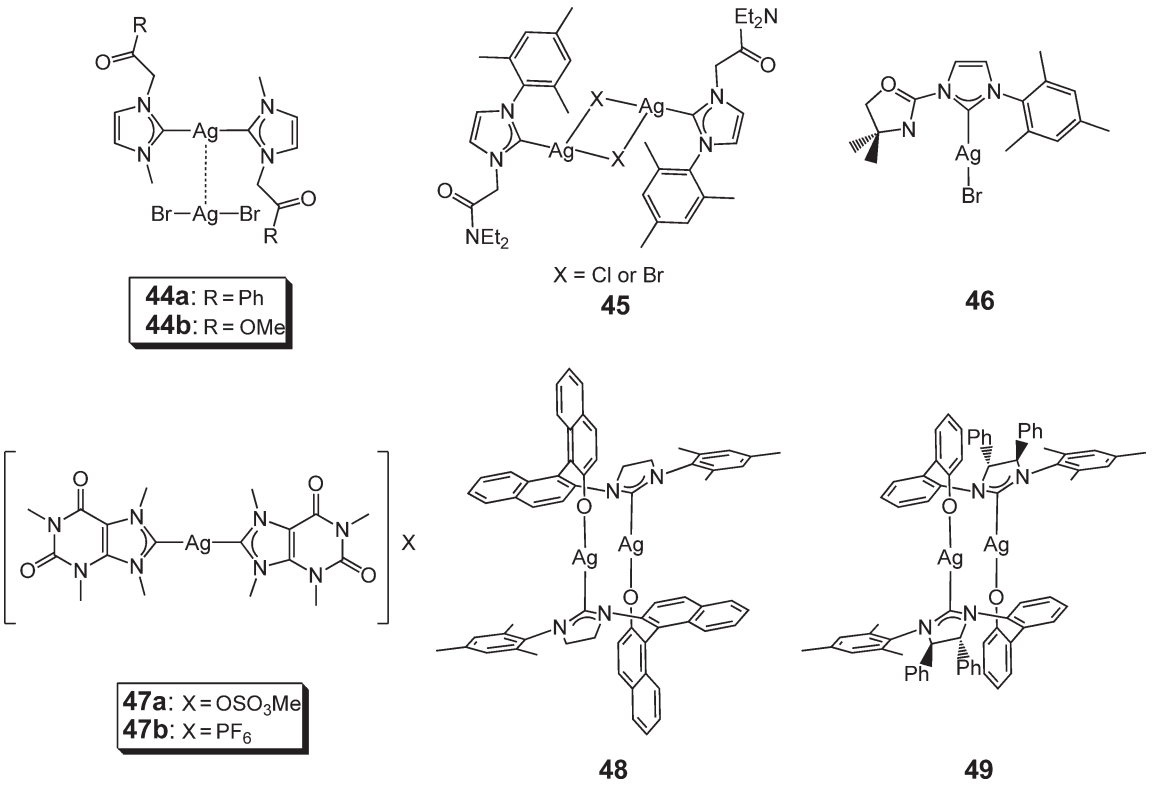

Figure 20 Structure of **44–49**.

complex and as catalysts themselves for the asymmetric allylic alkylation reactions.[91] Despite a failure to obtain crystals suitable for X-ray diffraction studies, imine-functionalized carbene complexes of palladium(II) were isolated and their structures determined.[89–91]

Owing to the responsibility of nitrogen donors for the semi-labileness of *N*-heterocyclic carbene ligands, related research on oxygen donor silver(I) complexes – such as **44–49** (Figure 20) – has also been reported.[87,88,92–95] With the exception of **44a** and **44b**, all of these complexes were structurally characterized. The Ag–C bond distances in **45** (2.099(3) Å)[88] and **46** (2.093(4) Å)[92] are relatively longer than in the well-known example **18**, whereas the distance in **47b** (2.068(4) Å)[93] is comparable to that of **18**. However, none of these complexes has the structural evidence for any metal center coordination through the oxygen donor atoms in this class of ligands. The findings in **45** and **46** also conveyed an important message on the structural characterization of silver(I) *N*-heterocyclic carbene complexes. Their X-ray crystal structures revealed a general formulation of neutral $[Ag(carbene)X]_n$, whereas the molecular ion of the type $[Ag(carbene)_2]^+$ was observed in the ESI or FAB mass spectra of their corresponding acetonitrile solutions, indicating structural differences in the solid state and in solution, hence the low diagnostic value of ESI-MS and FAB-MS on the structural identification of this class of complexes. It is also noteworthy to mention that the carbene ligand in **47a** and **47b** was derived from the methylation of caffeine that is generally used in medicine, which underscores the potential application of using this class of xanthines as carbene ligands.[93] Nevertheless, these complexes were shown to be effective carbene-transfer reagents for making the corresponding palladium(II) and rhodium(I) carbene complexes. Complexes **48** and **49** were used for the *in situ* preparation of effective chiral ruthenium(II) and copper(II) carbene complexes that promoted enantioselective olefin metathesis and allylic alkylations.[94,95]

An extension of the research on silver(I) complexes with Lewis base-functionalized mono(*N*-heterocyclic carbene) ligands has been made toward the better-studied and stronger coordinating phosphine systems. The reaction of a diphenylphosphine-functionalized imidazolium salt with silver(I) oxide in dichloromethane affords a trinuclear silver(I) carbene complex **50**, as confirmed by electrospray-ionization mass spectrometry.[96,97] Metathesis reaction of **50** in methanol using silver(I) nitrate gives **51** in 33% yield. The crystal structures of **51** were found to be different when different solvents were used during crystallization (Scheme 12).[97] One NO_3^- anion was found to be chelated to

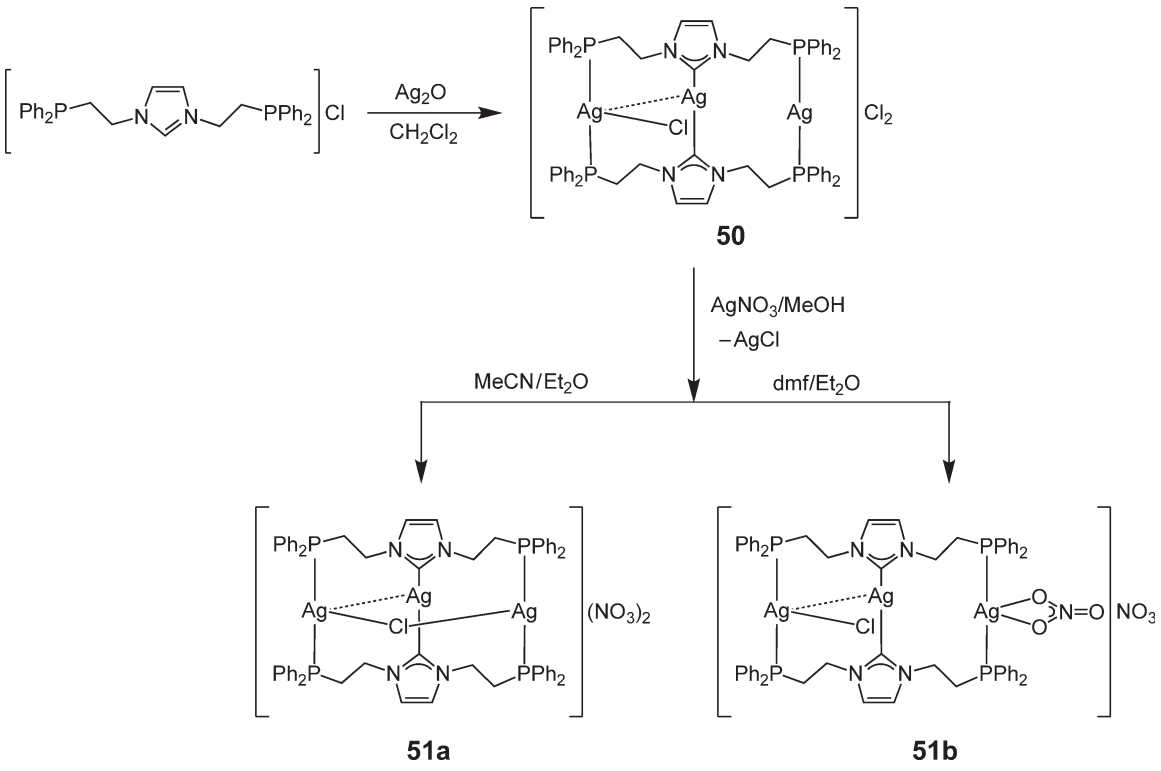

Scheme 12

one of the silver(I) centers, and one chloride anion was coordinated to another silver(I) center when the crystallization process proceeded in dimethylformamide–diethyl ether mixture, whereas only a bridging chloride instead of a chelating nitrate was observed to be coordinated to the complex cation in crystals grown from acetonitrile–diethyl ether. The Ag–C distances in **51a** (2.095(14), 2.117(14) Å) and **51b** (2.110(5) Å) were more or less the same, and short Ag–Ag contacts were observed in both complexes, with values of 2.9281(14) Å for **51a** and 3.0585(15) Å for **51b**. ^{31}P NMR studies of the trinuclear silver(I) nitrate complex indicated the existence of a rapid equilibrium between **51a** and **51b** in solution.

2.04.2.2.3.(iii) Silver(I) complexes with bis- and poly(*N*-heterocyclic carbene) ligands

In view of the versatility of *N*-heterocyclic carbenes as ligands and their structural diversity in silver(I) coordination chemistry, an extension of the work to ligands with two or more carbene moieties was reported. A dinuclear silver(I) complex **52** (Figure 21) with an *o*-phenylenedimethylene-bridged bis(carbene) ligand has been synthesized in 66% yield from silver(I) oxide and the bis(imidazolium) salt.[88] The reaction to synthesize **52** has to be carried out in

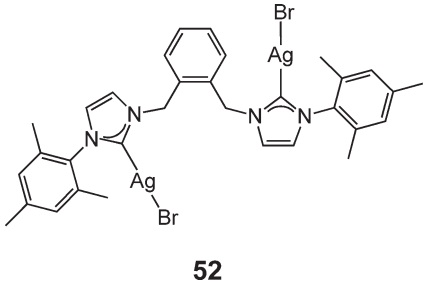

52

Figure 21 Structure of **52**.

refluxing 1,2-dichloroethane, that is, in a reaction medium of higher temperature compared with the usual case of using dichloromethane at room temperature, probably due to the bulky nature of the carbene substituents. The solid-state structure of **52**, in which each silver(I) center adopts a linear geometry and coordinates to one carbene moiety and one chloro ligand, was determined crystallographically. The Ag–C bond distances were found to be 2.061(7) and 2.092(8) Å, and the two Cl–Ag–carbene moieties were arranged in an *anti*-configuration.

Later, a less sterically substituted *m*-phenylenedimethylene-bridged dinuclear silver(I) complex, **53** (Figure 22), was made in about 95% yield by stirring in dichloromethane at room temperature.[98] Complex **53** was structurally characterized and was found to adopt a chair-like conformation, with an Ag–C bond distance of 2.068(3) Å, a value very close to that of **18**. The intermolecular Ag–Ag distances of 4.054 and 4.377 Å were suggestive of the absence of weak Ag–Ag interactions. Polymeric structured halosilver(I) complexes, **54a–54g** (Figure 23), with ethylene-bridged bis(carbene) ligands were reported by Lin, and later by Lee.[70,99] Crystal structures of **54a** and **54c** were obtained with the Ag–C bond distances of 2.1113(1) Å for **54a**[70] and 2.093(8) Å for **54c**[99] The two carbene moieties in each ligand were arranged in an *anti*-conformation, and each ligand was connected through an Ag_2X_2 unit.

A homoleptic methylene-bridged bis(carbene) dinuclear silver(I) complex, **55**, was isolated in 81% yield from a two-step reaction, as shown in Scheme 13.[100] The structure of **55** reveals a boat conformation with the two methylene groups protruding away from the Ag_2 core in one direction. The Ag–C distances of 2.081(2)–2.095(2) Å were in the normal range for silver(I) *N*-heterocyclic carbene complexes, while an uncommonly short intramolecular Ag–Ag contact of 3.2039(3) Å was observed in the homoleptic silver(I) carbene complexes.

Meyer reported the synthesis and isolation of the trinuclear silver(I) carbene complexes, **56a** and **56b**, having bridging tripodal tris(carbene) ligands (Scheme 14).[101,102] The crystal structure of **56b** revealed a local D_3-symmetry with the threefold axis passing through the two carbons that anchored the three pendants of the ligands, with the Ag–C distance and C–Ag–C bond angle of 2.082(2) Å and 178.56(13)°, respectively.[101] The analogous trinuclear copper(I) and gold(I) complexes were prepared from the reaction of **56b** with copper(I) bromide and [Au(SMe_2)Cl], respectively, and both were also structurally characterized.[102] Electronic structures of these trinuclear complexes were elucidated by DFT calculations, which suggested that the *N*-heterocyclic carbene ligands did not act solely as

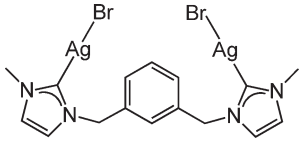

53

Figure 22 Structure of **53**.

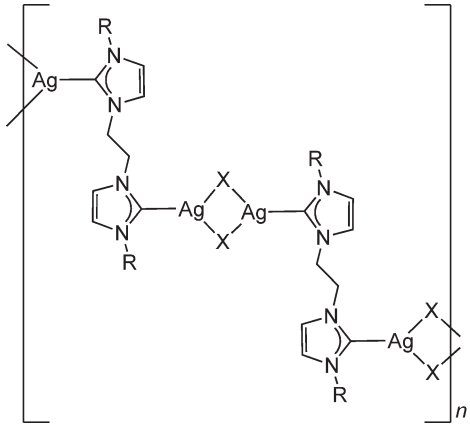

54a: X = Cl; R = Me
54b: X = Br; R = Me
54c: X = Br; R = CH_2Ph
54d: X = Br; R = $CH_2C_6H_4OMe$-4
54e: X = Br; R = $CH_2C_6H_4OMe$-3
54f : X = Br; R = $CH_2C_6H_4F$-4
54g: X = Br; R = CH_2Np-1

Figure 23 Structure of **54a–g**.

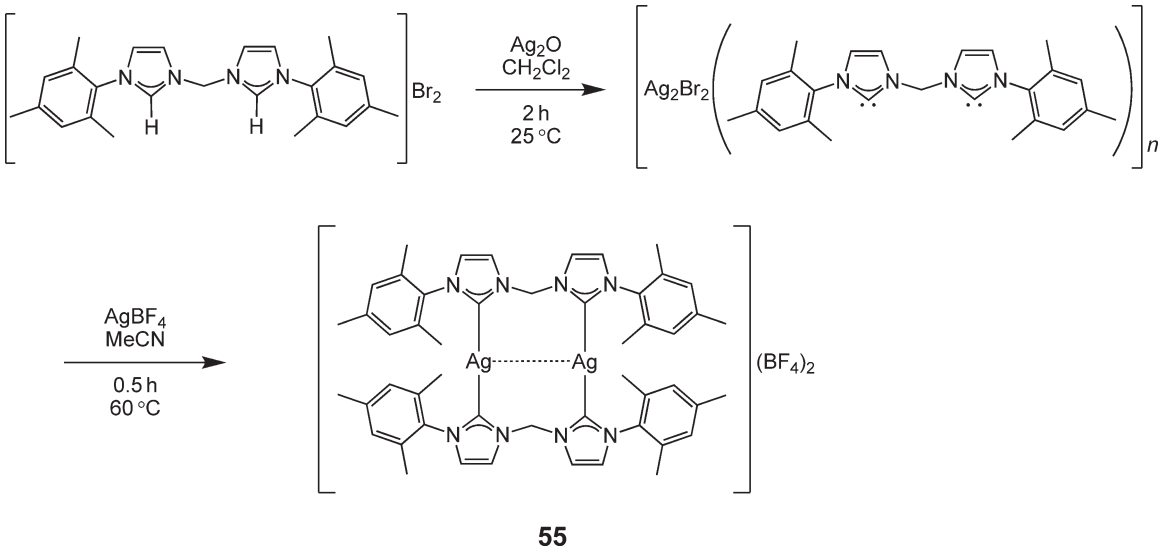

55

Scheme 13

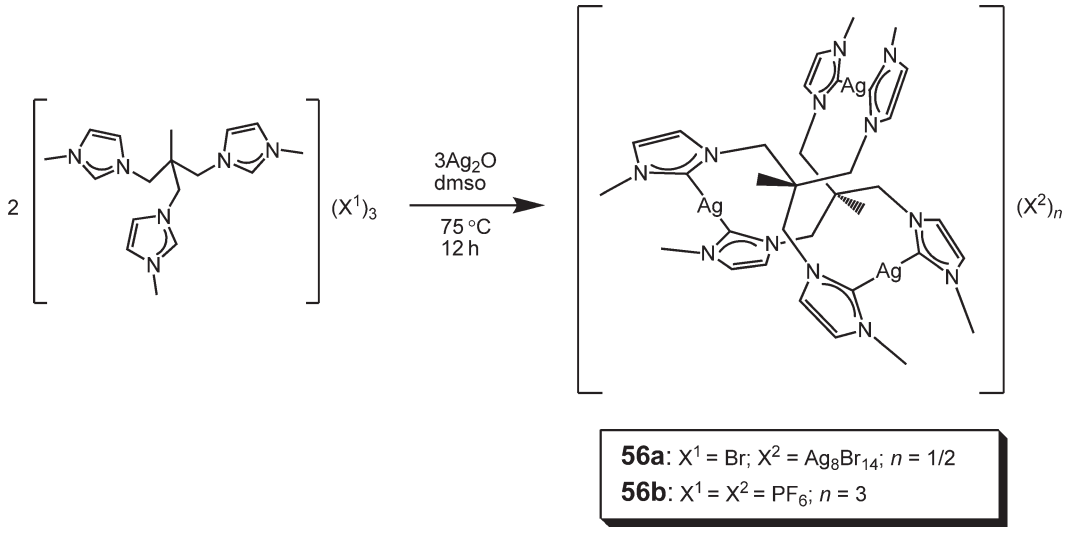

56a: X^1 = Br; X^2 = Ag_8Br_{14}; n = 1/2
56b: X^1 = X^2 = PF_6; n = 3

Scheme 14

σ-donors but also as π-acceptors. The π-backbonding interactions were found to contribute about 15–30% of the overall orbital interaction energies. Cyclophanes, with two imidazolium moieties bridged by *ortho*-, *meta*-, and mixed *ortho*/*meta*-substituted aromatic rings, were used as ligand precursors for a variety of interesting dinuclear silver(I) carbene complexes.[103]

The structure of the complexes was found to be dependent on the nature of the bridges in the cyclophane and the anion present in the imidazolium precursors. For instance, complexes **57–59** (Figure 24) were obtained from the reaction of 1 equiv. of the bis(imidazolium)cyclophane with more than 1 equiv. of silver(I) oxide, while **60** (Figure 24) was obtained from recrystallization after the reactions using precursors in a 1 : 1 molar ratio. The Ag–C distances in **57–59** of 2.095(3), 2.095(4), and 2.088(4) Å, respectively, were in the usual range, while those for **60** (2.14(2), 2.15(2) Å) were significantly longer. This also accounts for their relative stability and/or rigidity in solution, where only **60** exhibits structural equilibrium with its monomeric forms, in line with the much more labile nature of its Ag–C bond. Short intramolecular Ag–Ag contacts were present in **57** (2.9620(6) Å), **59** (3.2908(4) Å), and **60** (2.996(2)-3.003(3) Å)

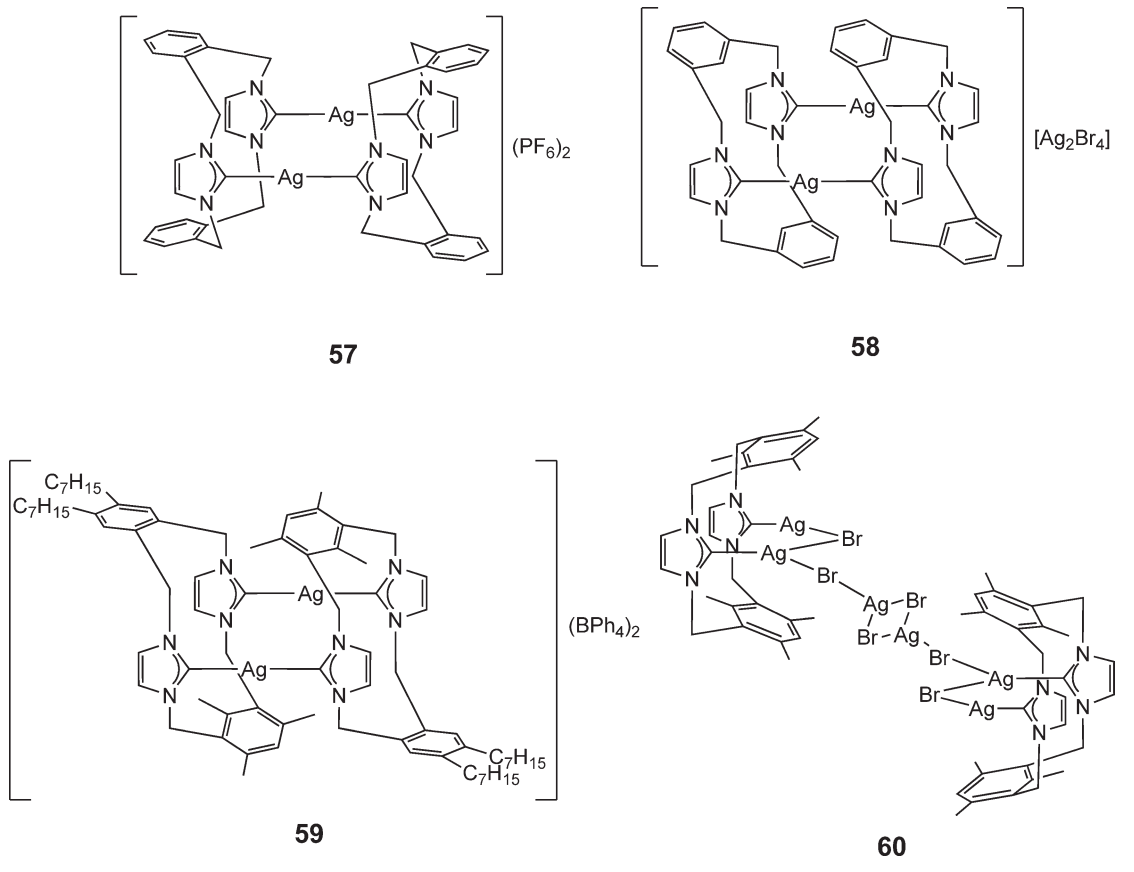

Figure 24 Structure of **57–60**.

but not in **58**, in which a short intermolecular Ag(cation)–Ag(anion) contact of 2.8999(4) Å was observed instead. It is interesting to note the unusual stability of **57–59** and the neutral monomeric form of **60**, [cyclophane($AgBr)_2$], in dmso, in which no sign of decomposition was observed after 8 days of exposure toward light and moisture, or after heating at 100 °C in the presence of air.

2.04.2.2.3.(iv) Silver(I) complexes with Lewis base-functionalized bis- and poly(*N*-heterocyclic carbene) ligands

The variety of silver(I) carbene complexes has been further diversified with the use of polydentate ligands with more than one carbene moiety in addition to the ancillary donor groups. The most studied class, albeit still fairly limited, is that having two *N*-heterocyclic carbenes bridged by a pyridyl group. For example, the reaction of the pyridylbis-(imidazolium) salt with silver(I) oxide at room temperature afforded the intermediate of the type $[Ag(C\hat{}N\hat{}C)]_n{\cdot}n(AgBr_2)$, and subsequent reactions with silver(I) tetrafluoroborate in refluxing acetonitrile gave **61** in an overall yield of 57% (Scheme 15).[104] The structure of **61** was identified crystallographically as a centrosymmetric

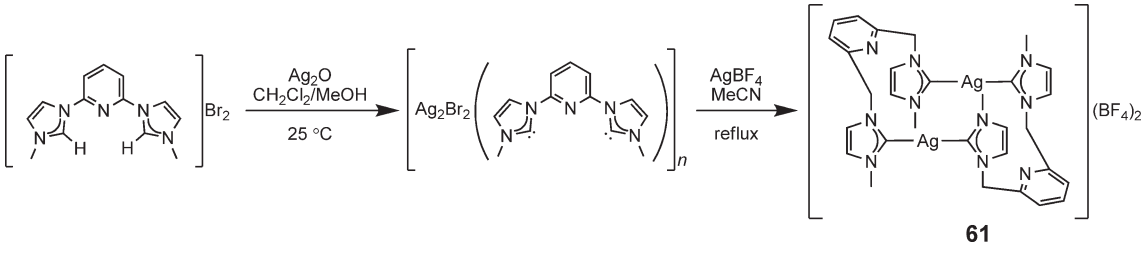

Scheme 15

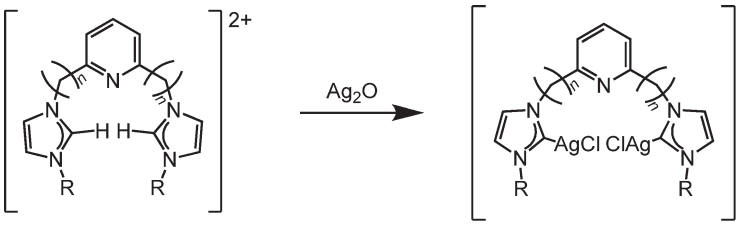

62a: n = 0; R = 2,6-$Pr^i_2C_6H_3$; solv = $ClCH_2CH_2Cl$; 16 h, reflux; 75%
62b: n = 0; R = 2,4,6-$Me_3C_6H_2$; solv = $ClCH_2CH_2Cl$; 16 h, reflux; 72%
62c: n = 1; R = 2,6-$Pr^i_2C_6H_3$; solv = $ClCH_2CH_2Cl$; 16 h, reflux; 85%
62d: n = 1; R = 2,4,6-$Me_3C_6H_2$; solv = $ClCH_2CH_2Cl$; 16 h, reflux; 60%
62e: n = 1; R = Bu^n; solv = CH_2Cl_2; 2 h; RT; 70 %

Scheme 16

dinuclear complex with two Ag(I) centers bridged by two bis(carbene) ligands. The Ag–C bond distances of 2.088(4) and 2.093(4) Å are in the normal range of this class of complexes, but no short Ag–Ag contacts could be observed. The pyridyl nitrogens were not coordinated to the silver(I) centers. Nevertheless, a series of cationic palladium(II) complexes bearing the C^N^C ligands were prepared from **61**, and were shown to exhibit good activities in the Heck coupling reactions of aryl halides and alkyl acrylates.

Neutral dinuclear silver(I) complexes, **62a–62e**, bearing one pyridylbis(carbene) ligand, were reported independently by Danopouluos and Youngs, with **62e** being structurally characterized (Scheme 16).[105,106] The comparably more rigorous synthetic conditions for **62a–62d**[105] compared to **62e**[106] may be attributed to the more steric demanding nature of the substituent pendants on the imidazolylidene rings. The solid-state structure of **62e** revealed a monomeric nature,[106] fairly similar to that reported for **53**. A comparably short Ag–C bond with distances of 2.064(13) Å and an intramolecular Ag–Ag contact of 3.269(2) Å could be observed.[106] However, the absence of any intermolecular Ag–Ag interactions may be attributed to the bulky nature of the substituents attached to the imidazolylidene rings. These dinuclear neutral silver(I) carbene complexes were shown to display good carbene-transfer behavior for the synthesis of the corresponding "pincer" type bis(carbene)palladium(II) and rhodium(I) complexes. A related dinuclear silver(I) complex with a secondary amine-bridged bis(carbene) ligand was also reported and used for making palladium(II) bis(carbene)amino and amido complexes.[107] Prior to the report of using of phenylene-bridged bis(carbene) cyclophanes as ligands for the synthesis of silver(I) carbene complexes, examples of pyridyl-bridged bis(carbene) cyclophanes containing silver(I) complexes were reported by Tessier and Youngs.[108–110] The Ag–C bond distances of 2.084(9) and 2.096(9) Å in **63a**[108] were consistent with the commonly observed values, while those of 2.133(6) and 2.350(6) Å in **64**[109] and 2.148(6)–2.516(6) in **65**[110] were significantly longer and possibly a result of the weaker Ag_2C three-center two-electron bond in the latter. Interestingly, short Ag–Ag contacts of 2.8512(8) and 3.3460(17) Å in **64**[109] and 2.7680(9)–2.9712(11) Å in **65**[110] were observed in the unusual centrosymmetric Ag_4 core. The C–Ag–C angles for the bridging silver centers in **64**[109] and **65**[110] were 179.8(4) and 176.2(2)°, respectively, indicating the essentially linear two-coordinate geometry (see Figure 25).

Besides nitrogen donors, bis(carbene) ligands with oxygen donors were reported by Arnold. A dinuclear silver(I) carbene complex, **66** (Figure 26), was prepared in 61% yield from the reaction of the corresponding imidazolium chloride with silver(I) oxide in dichloromethane.[111] Although no crystal structure was reported for **66**, the analogous dinuclear copper(I) complex was synthesized using **66** as a carbene-transfer reagent and its identity was confirmed crystallographically.[111] Related *p*-cymene ruthenium(II) carbene complexes were prepared similarly.[112] On the other hand, there were also dinuclear silver(I) carbene complexes with additional oxygen donor atoms that did not coordinate to the silver centers. Complex **67** (Figure 27) was synthesized from the reaction of its parent imidazolium salts with silver(I) oxide, forming intermediates of the type $[Ag(carbene)_2][AgX_2]$ *in situ*, and subsequent reactions with silver(I) tetrafluoroborate afforded the target complex.[113] The B–F bond in **67** was activated using $ZrCl_4$, and a bis(carbene:BF_3) adduct was isolated that demonstrated for the first time the use of metal carbene complexes as both a source of BF_3 and carbenes in the synthesis of this type of adduct, rather than using the metal-free carbene with $BF_3{\cdot}Et_2O$ as in the usual practice.

Youngs and co-workers extended the chemistry toward synthesizing water-soluble silver(I) carbene complexes **68a–68c** (Figure 28) by using hydroxyl-containing pincer-type *N*-heterocyclic carbenes as ligands.[114] It is interesting

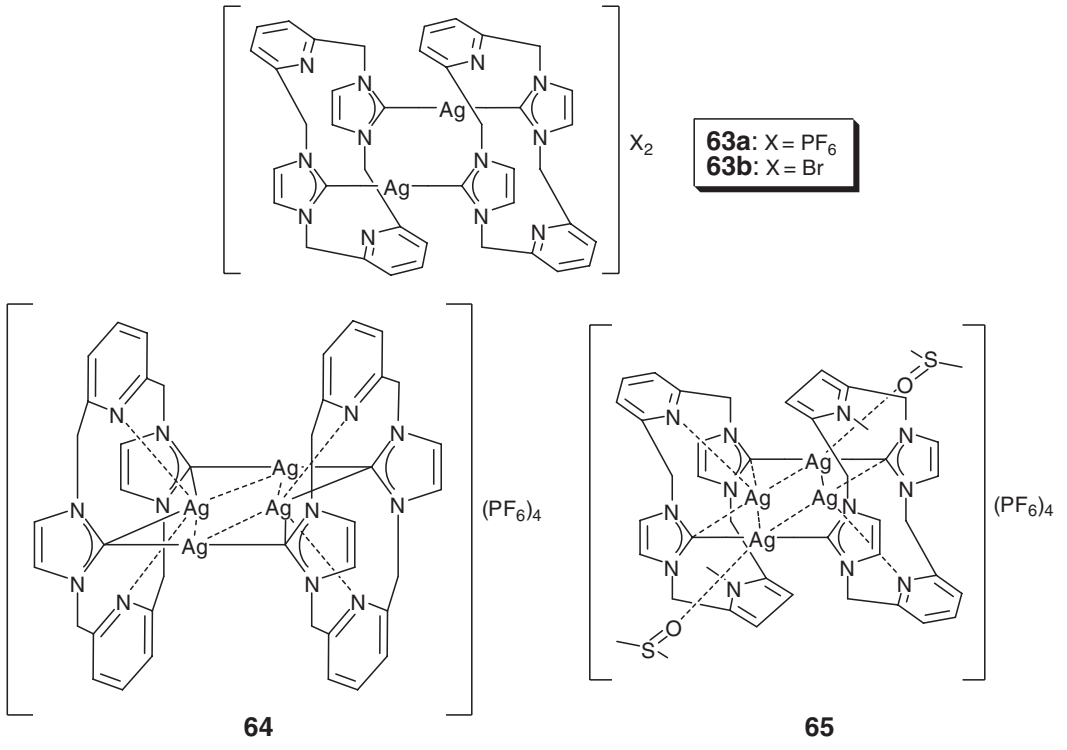

Figure 25 Structure of **63a, 63b, 64** and **65**.

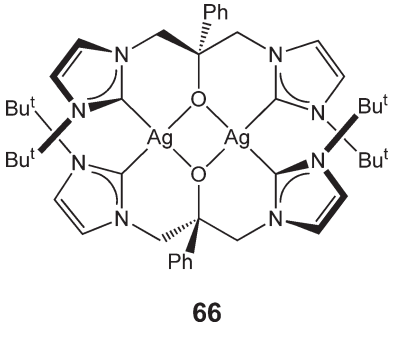

66

Figure 26 Structure of **66**.

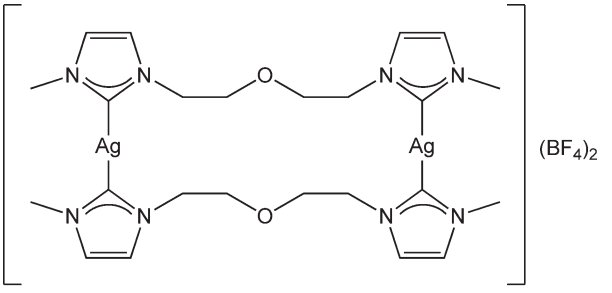

67

Figure 27 Structure of **67**.

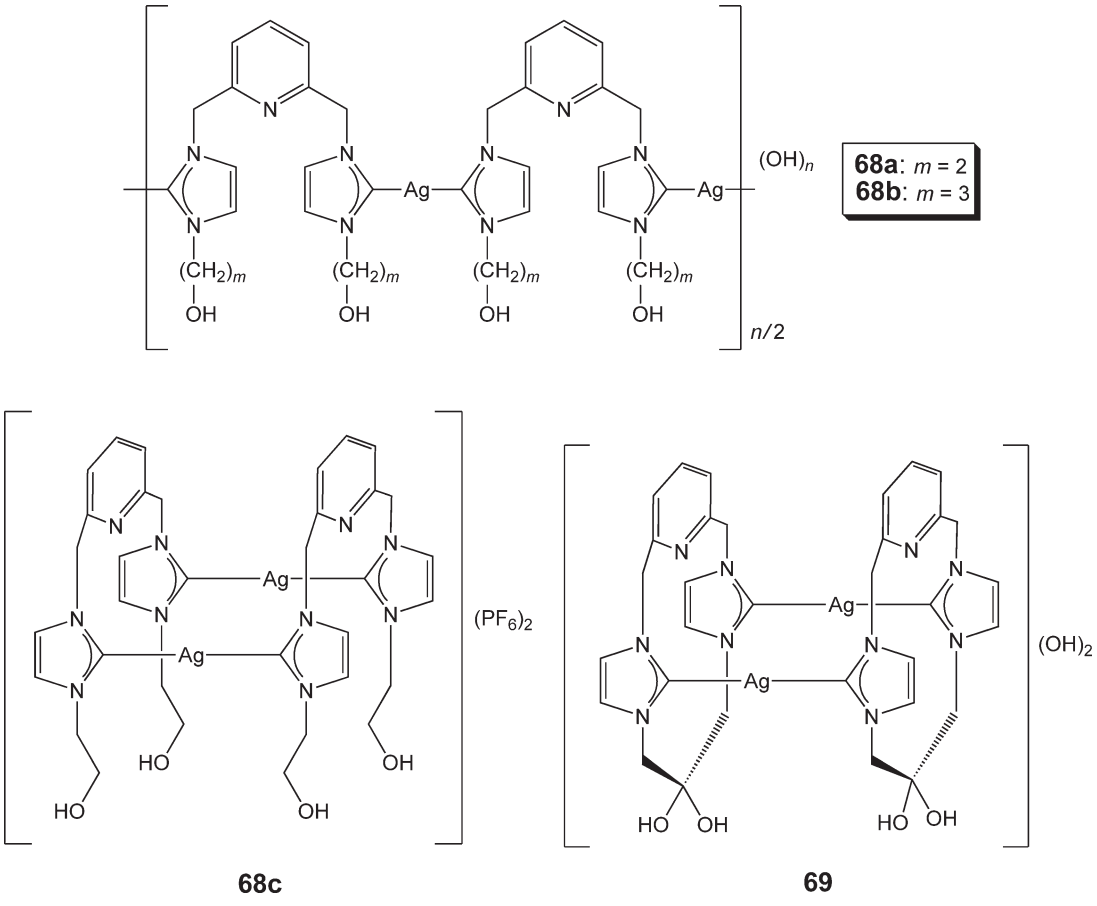

Figure 28 Structure of **68a–c** and **69**.

to note that the crystal structure of **68a** appeared as a polymer, while **68c**, obtained from the anion exchange of **68a**, crystallized as a dimer. A dinuclear silver(I) complex **69** (Figure 28) with an imidazole cyclophane *gem*-diol was also synthesized and structurally characterized.[115]

Their antimicrobial activities were found to be improved compared with those of silver(I) nitrate. Encapsulation of **69** by electrospun tecophilic nanofibres for the formation of antimicrobial nanosilver particles was also achieved.

Burgess reported the synthesis of a series of silver(I) carbene complexes bearing chiral diamide bis(carbene) ligands, **70a–70f**, (Figure 29) and their application in making the *trans*-chelating palladium(II) carbene complexes, using typical synthetic methodology.[57,116]

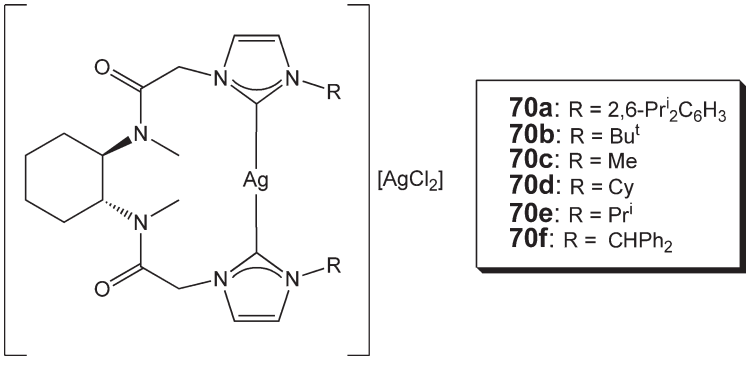

Figure 29 Structure of **70a–f**.

2.04.2.2.4 Miscellaneous

In spite of the fact that silver(I) *N*-heterocyclic carbene complexes were widely employed as carbene-transfer reagents for the synthesis of other transition metal carbene complexes, their synthesis could also be achieved by the reaction of silver salts with relatively more labile carbene metal complexes, albeit rare. Complexes **71a–71c** were reported to be synthesized from the reaction of the corresponding pentacarbonyl(carbene)chromium(I) complexes with silver(I) hexafluorophosphate in $CDCl_3$ under inert atmosphere (Scheme 17).[117]

Apart from the widely studied silver(I) *N*-heterocyclic carbenes, Stoltz and Beauchamp made the first report on the gas-phase synthesis of silver(I) Fischer carbenes from the loss of N_2 in various diazo malonates upon electrospray ionization and subsequent collisional activation.[118] The carbenes generated were capable of undergoing multiple Wolff rearrangements and loss of CO (Scheme 18).

2.04.2.3 Synthesis and Properties of Isocyanide and Carbonyl Complexes of Silver

2.04.2.3.1 Silver(I) isocyanide complexes

A series of air- and light-stable one-dimensional polymeric silver(I) diisocyanide complexes, **72a–72e** (Figure 30), was reported by Harvey, with their structural, spectroscopic, and photophysical properties described in detail.[119,120]

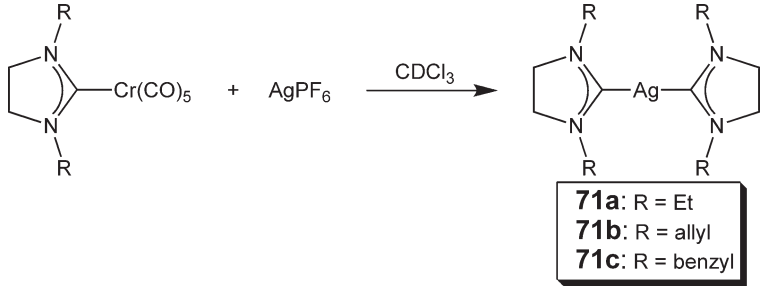

Scheme 17

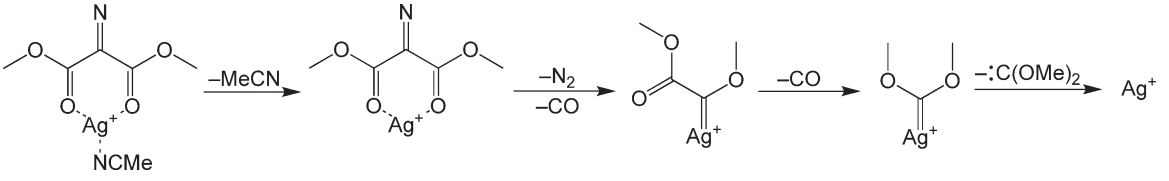

Scheme 18

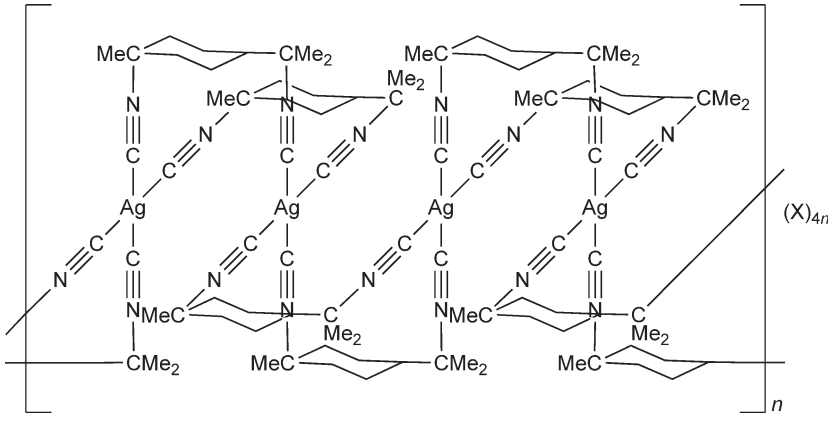

	X	*M*· · ·*M*(Å)
72a	PF_6	4.964(1)
72b	BF_4	4.9557(9)
72c	NO_3	5.1884(6)
72d	OAc	- - -
72e	ClO_4	4.9496(1)

Figure 30 Structure of **72a–e**.

Except for **72a**, all the polymers exhibited low glass transition temperatures in the range of 37–58 °C, even if the materials were highly crystalline. Complexes **72a–d** also gave intense luminescence, with emission maxima in the blue-green range (435–510 nm) at 77 K which decayed poly-exponentially. Comparison with the monomeric counterpart, $[Ag(C{\equiv}NBu^t)_4](BF_4)$, showed that the emission decay traces in the higher-energy region were attributed to states localized at one silver center within the polymer. Components in the lower-energy region with poly-exponential decays, which were only present in the polymers, were associated with a metal-to-metal delocalized energy transfer along the metal chain, somewhat similar to the exciton phenomenon known in organic solids. According to the DFT calculations on the model compound $[Ag(C{\equiv}NH)_4]^+$, the lowest energy excited state has been assigned to a metal-to-ligand charge transfer (MLCT) origin, in which the HOMO was dominated by the 4*d*(Ag) orbitals while the LUMO was mostly of the π^*(C≡NH) character.[119,120] Complexes **72b**, **72c**, and **72e** were found to dissociate readily in solution, and the corresponding polymeric nature in solution could not be probed using the conventional molecular weight determination methods such as light scattering, osmometric, and intrinsic viscosity measurements.[120] ^{13}C NMR T_1 (spin lattice relaxation time) and nuclear Overhauser effect (NOE) measurements have provided alternative means to estimate the degree of oligomerization of these complexes in solution, of which the average number of silver(I) units in acetonitrile of 7–9(±1) was determined.[121] Discrete binuclear complexes such as **72f–j** (Figure 31) could be obtained instead of infinite polymer chains in which the two silver centers were doubly bridged by two coordinating anions.[122,123]

A relationship between the intramolecular metal–metal separation and metal–metal force constants (estimated from the metal–metal stretching frequencies) was also determined for the halo complexes as:

$$d(\text{Ag–Ag}) = -0.284(\ln F(\text{Ag–Ag}) + 2.53)$$

where *d*(Ag–Ag) and *F*(Ag–Ag) refer to the intramolecular Ag–Ag separation and force constant, respectively.[122]

Subsequent work using the $tcnq^-$ (tcnq = 7,7,8,8-tetracyano-*p*-quinodimethane) as counteranion afforded $[Ag(dmb)_2(tcnq)]_n$ (dmb = 1,8-diisocyano-*p*-menthane) which was also crystallographically characterized.[124] $[Ag(dmb)_2(tcnq)]_n$ crystallized as linear, staircase, and ladder-like polymers based on the two rotameric forms of the dmb ligand, and in all three cases the $tcnq^-$ anions were found to crystallize as dimers with short interplanar separation of 3.312(6)–3.436(6) Å. Paramagnetic tetranuclear and thermoplastic polymeric semiconducting silver(I) complexes with dmb and mixed-valent $tcnq^{0/-}$ moieties were also reported.[123,125] In addition to the homoleptic polymeric silver(I) diisocyanide systems, reports were also made on the heteroleptic polymeric silver(I) complexes with both dmb and diphosphinoalkane ligands. A series of silver(I) polymers having the general formula of $[Ag\{Ph_2(CH_2)_xPPh_2\}(dmb)]_n(X)_n$ (x = 1–6; X = BF_4, ClO_4) was synthesized.[126,127] Discrete mono- and binuclear complexes, $[Ag\{Ph_2(CH_2)_2PPh_2\}(C{\equiv}NBu^t)_2](BF_4)$ and $[Ag_2(Ph_2CH_2PPh_2)(C{\equiv}NBu^t)_2](X)_2$ (X = BF_4, ClO_4), as well as the polymeric monoisocyanide counterparts, $[Ag\{Ph_2(CH_2)_xPPh_2\}(C{\equiv}NBu^t)_y]_n(X)_n$ (x = 1, 4–6; y = 1–2; X = BF_4, ClO_4), were also synthesized for comparison purposes.[126,127]

Cheung and Mayr reported the synthesis and isolation of mononuclear two-coordinate silver(I) complexes having a mixed cyano/isocyano ligand.[128] Complexes **73a** and **73b** (Figure 32) were isolated from the reaction of silver(I) salts with 4-isocyano-3,5-diisopropylbenzonitrile. From the X-ray crystal structural analysis on complex **73a**, preferential coordination of the isocyanide over the cyano group toward the silver(I) center was found with Ag–C distances of 2.092(5) and 2.098(5) Å and a C–Ag–C angle of 156.1(2)°, the latter of which was found to deviate significantly from the usual and ideal two-coordinate geometry due to the presence of Ag–F interactions with the tetrafluoroborate

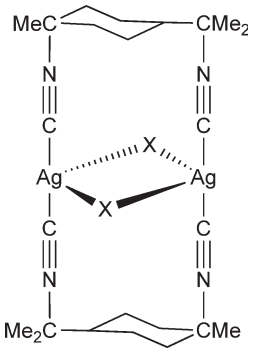

	X	M···M (Å)	$\bar{\nu}$[M···M] (cm^{-1})
72f	Cl	3.451(2)	42
72g	Br	3.345(1)	42
72h	I	3.378(2)	33
72i	NO_3	3.9075(14)	–
72j	OAc	3.6832(7)	–

Figure 31 Structure of **72f–j**.

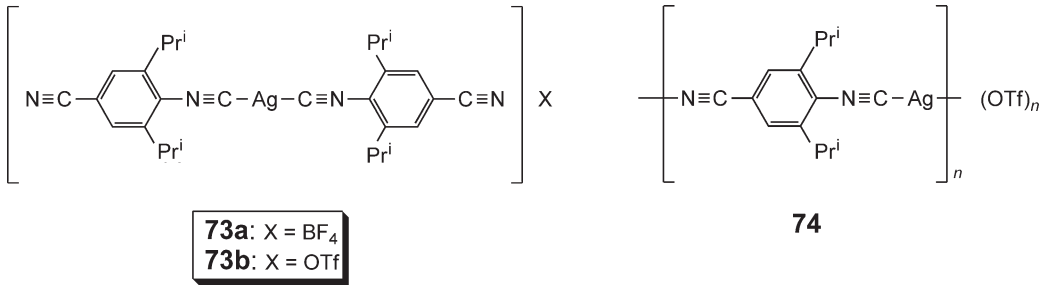

Figure 32 Structure of **73a, 73b** and **74**.

anion. Subsequent reactions of **73b** with 2 equiv. of AgOTf resulted in the formation of **74** (Figure 32), which has a linear chain structure with each silver(I) center coordinated with one nitrile and one isocyano group of consecutive cyanoisocyanoarene ligands, in addition to the presence of weak Ag–O interactions to the triflate anion. The Ag–C and Ag–N distances were 2.076(3) and 2.194(3) Å, respectively.

A series of mononuclear homoleptic silver(I) isocyanide complexes with various alkoxyaryl groups, [RN≡C–Ag–C≡NR]X (R = $C_6H_4OC_nH_{2n+1}$-4, $C_6H_4C_6H_4OC_nH_{2n+1}$-4, $C_6H_2(OC_nH_{2n+1})$-3,4,5; n = 4, 8, 12; X = BF_4, NO_3), was reported by Espinet, all of which exhibited interesting liquid crystalline behavior.[129] The phenyl and biphenyl derivatives displayed Sm_A and Sm_C mesophases, whereas the 3,4,5-trialkoxyphenyl compounds showed hexagonal columnar mesophases, with the absence of such behavior in the free ligand state.

Stable monoisocyanide complexes with ancillary tripodal tripyrazolyl ligands were synthesized and structurally characterized. For example, mononuclear monoisocyanide complexes **75a** and **75b** that contained the tris(pyrazolyl)borate and tris(pyrazolyl)methane ligands, respectively, were synthesized from the tris(pyrazolyl)silver(I) precursors with weakly coordinating solvent and anion.[130–133] (Scheme 19). Complexes **75a–j** possessed similar structures, with a pseudo-tetrahedral-coordinated silver(I) center. The observed Ag–C bond distances are not uncommon, and the Ag–C–NR bond angles are slightly deviated from the ideal linear geometry. It is also worth mentioning that the ν(C≡N) values for these complexes are higher than those for the corresponding free ligands $CNBu^t$ (2138 cm^{-1}) and CNCy (2140 cm^{-1}), indicative of the predominantly σ-bonding nature of the Ag–CNR bond. In general, relatively higher ν(C≡N) values were observed for complexes with the enhanced Lewis acidity at the silver(I) center attached with less electron-rich tris(pyrazolyl)borate ligands. Isostructural congeners of **75a** were also reported, with the ν(C≡N) values in the order: Au (2248 cm^{-1})[134] > Ag (**75a**, 2214 cm^{-1}) > Cu (2196 cm^{-1}).[135] Later, a sterically demanding fluoroalkyl-substituted triazapentadienyl ligand was used as a monodentate ligand for the synthesis of a related thermally stable mononuclear silver(I) monoisocyanide complex, **76** (Scheme 20).[136] Again, the ν(C≡N) value of 2219 cm^{-1} for **76** was found to be higher than that of the free ligand and its isostructural copper analog (2176 cm^{-1}).[137] X-ray crystal structural analysis revealed that the triazapentadienyl ligand coordinated to the silver(I) center via the central nitrogen atom in a κ^1-mode. The Ag–C bond distances showed values of 2.046(5) and 2.026(5) Å, and the Ag–C–N angles were essentially linear with angles of 175.7(4) and 177.5(4)°, all of which were typical of this class of complexes. Interestingly, the silver(I) center was further encapsulated weakly by the two aryl rings on the triazapentadienyl ligand with the closest Ag–C_{aryl} distances of ~2.80 Å. Very recently, Schmidbaur reported the synthesis and isolation of a binuclear silver(I) isocyanide complex using bridging trifluoroacetate ligands.[138] The silver(I) centers in **77** (Figure 33) were planar three coordinate, with Ag–C bonds of 2.056(5) and 2.080(4) Å and Ag–C–N angles of 171.89(36)° and 174.49(36)°. A short intramolecular Ag–Ag contact of 3.0213(4) Å was also observed.

2.04.2.3.2 Silver(I) carbonyl complexes

In contrast to the silver(I) isocyanide chemistry, examples of isolatable silver(I) carbonyl complexes are extremely limited. The carbonyl ligand is regarded as an extremely weak base, with its gas-phase proton affinity of 141 kcal mol^{-1} being much lower than that of NH_3 (207 kcal mol^{-1}) or H_2O (173 kcal mol^{-1}).[139] Strauss reported the synthesis, isolation, and crystal structure determination of the first silver(I) carbonyl complexes in 1991.[140–143] The key strategy in this synthesis involved the use of weakly coordinating anions, showing the silver(I) center (already a poor π-donor) to be a stronger Lewis acid than that for usual anions. So the extremely hygroscopic Ag{$B(OTeF_5)_4$} salt was found to reversibly absorb CO gas in 1 atm of CO at 25 °C, and single crystals of

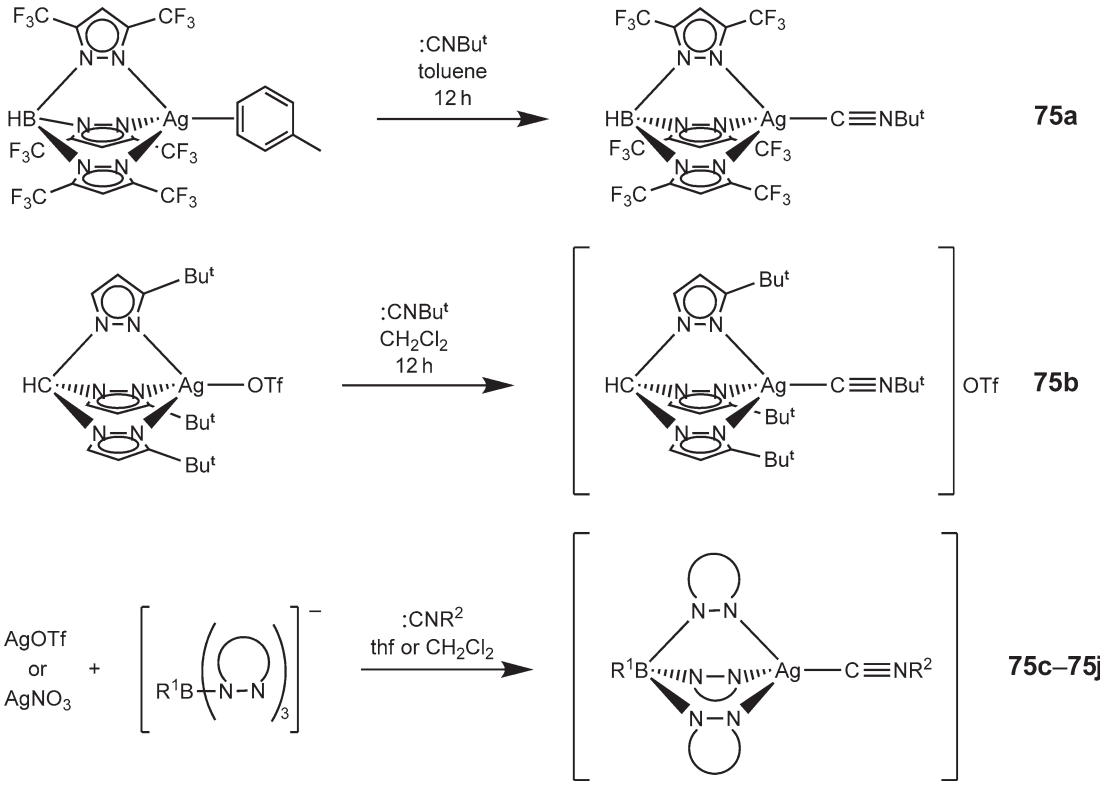

	R^1	N-N	R^2	$\tilde{\nu}$ (C≡N) (cm^{-1})	Ag–C (Å)	∠Ag–C-N (°)
75a				2214	2.059(4)	173.7(4)
75b				2202	2.053(7)	168.2(6)
75c	H	3,5-Me_2pz	Bu^t	2178	2.05(1)	172(1)
75d	H	3,5-Me_2pz	Cy	2191	2.063(5)	179.8(5)
75e	H	3,5-Ph_2pz	Bu^t	2185	2.08(1)	177.7(9)
75f	H	3,5-Ph_2pz	Cy	2187		
75g	pz	pz	Cy	2215		
75h	pz	pz	Bu^t	2207		
75i	3-Mepz	3-Mepz	Bu^t	2206		
75j	3-Mepz	3-Mepz	Cy	2183		

Scheme 19

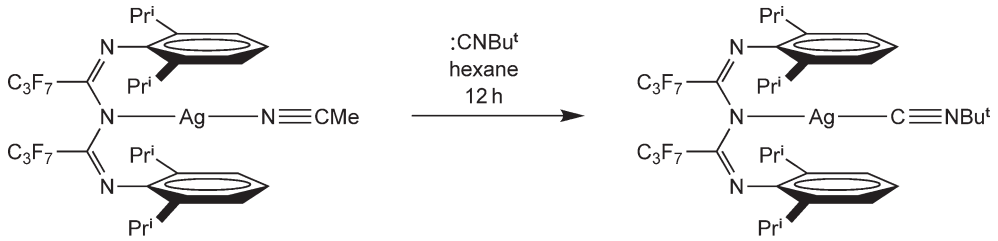

Scheme 20

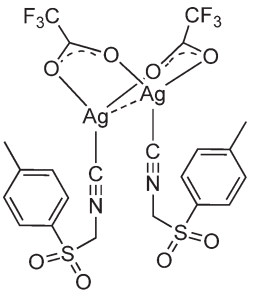

77

Figure 33 Structure of **77**.

$[Ag(CO)]\{B(OTeF_5)_4\}$ **78** and $[Ag(CO)_2]\{B(OTeF_5)_4\}$ **79** suitable for X-ray crystallography were obtained. The structure of **78** was composed of a silver(I) center coordinated with a CO ligand and two oxygen atoms from the anion. The Ag–C and $C–O_{carbonyl}$ distances were 2.10(1) and 1.077(16) Å, respectively, and the $Ag–C–O_{carbonyl}$ angle was found to be 175.7(1)°. In addition, there were four Ag–F contacts of ~3.0 Å. For **79**, the O–C–Ag–C–O geometry was essentially linear with slight deviation. The Ag–C and $C–O_{carbonyl}$ bonds have ranges of 2.06(5)–2.20(4) and 1.07(5)–1.09(6) Å, respectively. The $\nu(C{\equiv}O)$ values of 2204 and 2211 cm^{-1} for the mono- and dicarbonyl complexes, respectively, were found to be higher than that for the free CO (2143 cm^{-1}) and were suggestive of a predominantly CO σ-donation to the silver(I) centers with almost no $Ag \rightarrow CO$ π-backbonding. Complexes with $OTeF_5^-$ anion as well as other weakly coordinating anions such as $Zn(OTeF_5)_4^{2-}$, $Nb(OTeF_5)_6^-$, and $Ti(OTeF_5)_6^{2-}$ were also prepared. In view of the absence of the well-known classical CO π-backbonding in these complexes, they are often classified as the "non-classical" metal carbonyls. Quantum chemical calculations on the bonding nature of these non-classical metal carbonyls were also performed.[144]

In addition to the silver(I) isocyanide complex **75a** as discussed previously, the analogous carbonyl complex, **80**, was also synthesized by bubbling CO at 1 atm pressure to the toluene adduct precursor in hexane (Scheme 21).[130,131] The coordinated CO ligand in **80** could readily be lost under reduced pressure, or replaced in the presence of weakly coordinating solvents such as benzene. Structural characterization of **80** revealed Ag–C and C–O distances of 2.037(5) and 1.116(7) Å, respectively, and an Ag–C–O bond angle of 175.6(6)°, which was close to the ideal value of 180°. The $\nu(C{\equiv}O)$ at 2178 cm^{-1} was observed for pure crystals of **80**, a value higher than that in the free ligand, and hence suggestive of the absence of any $Ag \rightarrow CO$ π-backbonding interaction.

Xu reported the IR, Raman, and NMR spectroscopic characterization of $[Ag(CO)_n]^+$ ($n = 1–3$) over a range of temperature and in various acids.[145,146] The cations $[Ag(CO)]^+$, linear $[Ag(CO)_2]^+$, and trigonal-planar $[Ag(CO)_3]^+$ were formed in HSO_3F and $HSO_3F{\cdot}SBF_5$, while only $[Ag(CO)]^+$ was formed in 96% H_2SO_4. Comparative studies on the copper(I) and gold(I) analogs have also been described.[145,146] The silver and copper carbonyls prepared by this method were found to function as catalysts in the high-yield carboxylation of olefins, alcohols, dienes, diols, aldehydes, and saturated hydrocarbons under atmospheric pressure and temperature.[147] Silver carbonyls formed in silver-supported solid superacids such as Nafion and others were also used to catalyze the carbonylation of hydrocarbons and alcohols, in which the $\nu(CO)$ stretch of the silver carbonyl was observed at 2173 cm^{-1} by Souma.[148]

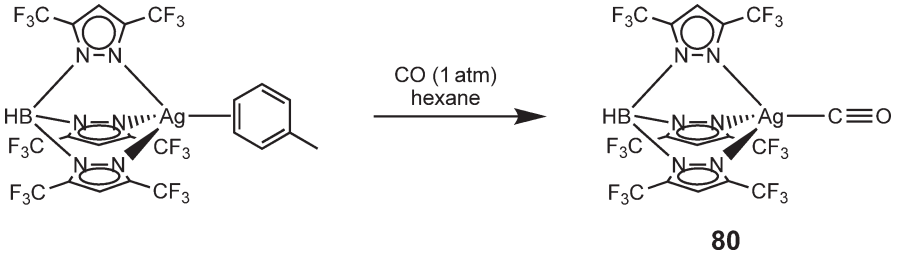

80

Scheme 21

2.04.2.4 Synthesis and Properties of Alkynyl and Related Complexes of Silver

Although reports on silver(I) σ-alkynyl complexes have appeared for more than a century, the number of examples was still very limited prior to the past decade, and many of them were referred to as insoluble homoleptic polymeric $[Ag(C{\equiv}CR)]_{\infty}$. Molecular alkynylsilver(I) complexes were often heteroleptic in nature and were achieved commonly through the stabilization by an extra coordination with strong σ-donor ligands such as amines, phosphines, and arsines.

Despite the ready formation of the well-studied polymeric homoleptic alkynylsilver(I) complexes $[Ag(C{\equiv}CR)]_{\infty}$, examples of the molecular counterparts were also reported. For instance, Abu-Salah reported the crystal structure of pentanuclear trigonal-bipyramidal silver(I) complexes with "disordered copper" composition, that is, (ppn)$[Ag_{4.46}Cu_{0.54}(C{\equiv}CPh)_6]$ **81** (Figure 34).[149] The three linear PhC≡C–Ag–C≡CPh moieties were aligned together in a parallel fashion, with another two silver(I) centers further coordinated to the alkynyl units to form a triangular barrel structure. The silver(I) centers at the equatorial positions were found to be disordered with copper(I) occupancy. The Ag–C_{σ}, Ag–$C_{\pi\text{-}\alpha}$, and Ag–$C_{\pi\text{-}\beta}$ bond distances were found to be 2.027(5)–2.037(5), 2.274(4)–2.362(4), and 2.665(4)–2.905(4) Å, respectively, and short Ag_{axial}–$Ag_{equatorial}$ contacts of 2.903(1)–3.024(1) Å were also observed. Mingos and Vilar reported the synthesis of a novel series of anion-encapsulated tetradecanuclear silver(I) alkynyl cages, $[Ag_{14}(C{\equiv}CBu^t)_{12}X]BF_4$ (X = F **82a**, Cl **82b**, Br **82c**) (Figure 35) from the reaction of $AgBF_4$, $HC{\equiv}CBu^t$, triethylamine, and the corresponding tetrabutylammonium halide in thf.[150,151] Structural characterization of **82a–c** revealed their isostructural relationship, with 14 silver(I) centers being held together by a combination of bridging alkynyl ligands (both σ- and π-bonded) and argentophilic interactions, forming a rhombohedral cage structure with the halide anion encapsulated inside the cage.

It is interesting to note that the size of the cluster cage, as reflected by their Ag–Ag and Ag–X distances, follows a trend with **82a** < **82b** < **82c**, which is in line with the increasing size of the halide ion and demonstrates clearly the template effect of the halide ion in the cluster formation process. Analogous reactions using AgOTs or $AgNO_3$ as

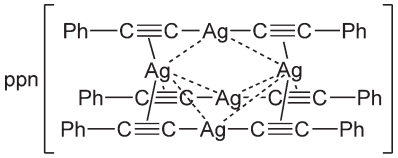

81

Figure 34 Structure of **81**.

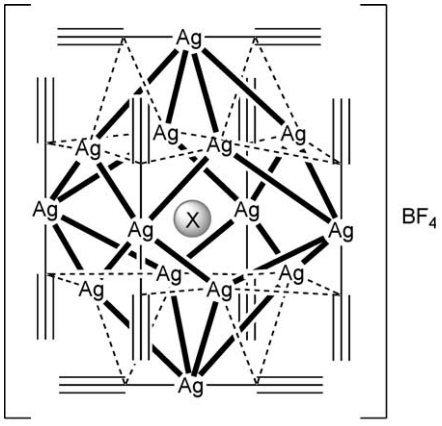

Figure 35 Structure of **82a–c**.

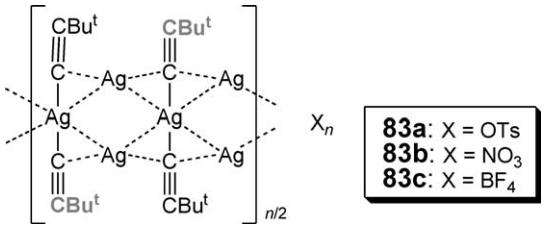

Figure 36 Structure of **83a–c**.

precursor, that is, in the absence of the template halide ion but in the presence of a coordinating anion, resulted in the polymeric alkynylsilver(I) complexes $[Ag_3(C{\equiv}CBu^t)_2X]_\infty$ (X = OTs **83a**, NO_3 **83b**) (Figure 36).[151] Crystal structure determination of **83a** revealed a ladder-like structure with the tosylate being *O*-bonded to one of the three unique silver centers and the presence of weak Ag–Ag interactions (Ag–Ag, 2.901(1)–3.035(1) Å). Al-Farhan also isolated a similar complex **83c** (Figure 36) at an earlier time from the reaction of $[Ag(C{\equiv}CBu^t)]_\infty$ with 2 equiv. of $AgBF_4$ in acetone, of which the BF_4^- anions were found to be non-coordinating and the extent of Ag–Ag interactions was found to be comparable (Ag–Ag: 2.979(1)–3.002(1) Å).[152] Che recently investigated the solid-state structure of a well-known complex, $[Ag(C{\equiv}CPh)]_\infty$ **84**, by X-ray powder diffraction.[153] It has been known since its discovery for its intractable polymeric nature, which hinders the possibility of yielding single crystals suitable for X-ray crystallographic studies. The use of X-ray powder diffraction opens up a new avenue for the structural determination of this class of complexes, in spite of the fact that a successful structure determination has to be facilitated by the well-defined and rigid geometry of the alkynyl ligands, the availability of the involving bond distance and bonding mode data in the literature, as well as a small and simple crystallographic unit cell. The solid-state structure of **84** revealed an infinite Ag–Ag ladder-like chain structure with zigzag folding of the phenylethynyl units. The Ag–C and C≡C distances were in the range of 2.12(1)–2.71(1) and 1.19(5) Å, respectively. The Ag–Ag contacts of 3.11(1)–3.15(1) Å were shorter than the sum of van der Waals radii for two Ag atoms (3.4 Å),[31] and might be suggestive of the presence of weak metal–metal interactions. Complex **84** was also found to undergo pyrolysis to give metallic silver above 185 °C, and was emissive in the yellow-green region at both 298 and 77 K.

In addition to homoleptic complexes, strong σ-donating ligands such as phosphines are often employed in making heteroleptic silver(I) alkynyl complexes. In 1966, Corfield reported the first crystal structure of the silver alkynyl complex, $[Me_3PAg(C{\equiv}CPh)]$ **85** (Figure 37), which consisted of consecutive packing of alternating $[Ag(PMe_3)_2]^+$ and $[Ag(C{\equiv}CPh)_2]^-$ through weak argentophilic interactions, with the alkynyl units in the anionic $[Ag(C{\equiv}CPh)_2]^-$ being further coordinated to the cationic silver(I) center in $[Ag(PMe_3)_2]^+$.[154] Its bonding picture was also discussed by King.[155] Nonetheless, it was only after 30 years that the second example was reported. Russell and Wright reported the synthesis of $[Me_3PAg(C{\equiv}CSiMe_3)]$ **86** and $[Ph_3PAg(C{\equiv}CPh)]_4$ **87** (Figure 37), starting from the reaction of the

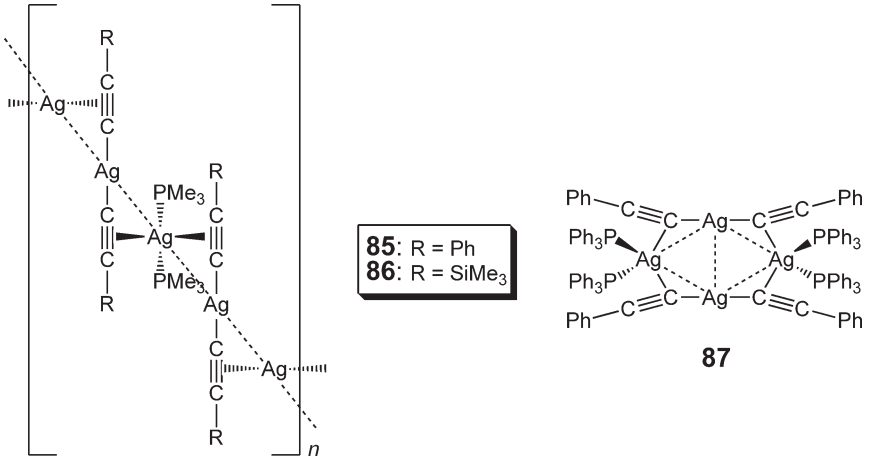

Figure 37 Structure of **85–87**.

respective [R_3PAgCp] with lithiated alkynyls.[156] Their crystal structures were also determined, in which **85** was shown to possess a similar structure to that of **86**. Complex **87**, having the bulkier PPh_3 ligands, adopted a tetranuclear diamond structure with the alkynyl moieties in two anionic $[Ag(C{\equiv}CPh)_2]^-$ units coordinated to two cationic $[Ag(PMe_3)_2]^+$ units in a face-to-face fashion through π-bonding interactions. The Ag–C_σ, C≡C and Ag–Ag distances in **85–87** (**85**: 2.040, 1.208, 3.033 Å; **86**: 2.053(8)–2.065(8), 1.194(10)–1.216(9), 3.0339(10)–3.170(10) Å; **87**: 2.044(9)–2.065(11), 1.202(13)–1.230(12), 2.921(1)–3.084(1) Å, respectively) were fairly similar. The Ag–$C_{\pi\alpha}$ distances in the polymeric chain-structured **85** (2.552 Å) and **86** (2.450(7)-2.521(7) Å) were comparatively longer than those found in the less open tetranuclear diamond-structured **87** (2.399(9)–2.4868 Å). The work was further extended by Lai and Che using the aromatic-free PCy_3 ligand, and a series of luminescent tetranuclear silver(I) alkynyl complexes, $[Ag_4(C{\equiv}CC_6H_4R\text{-}p)_4(PCy_3)_2]$ (R = H **88a**, Me **88b**, OMe **88c**, C≡CPh **88d**) (Figure 38) was reported.[157] Structural characterization of **88a–d** revealed some structural similarities with **87**, except for the observation that each silver(I) center being π-coordinated to the alkynyl moieties was coordinated with one PCy_3 ligand in an out-of-plane arrangement, rather than having two PPh_3 ligands as in the latter.

Complexes **88a–d** possessed comparable Ag–C_σ and Ag–Ag distances in the range of 2.048(3)–2.083(3) and 2.8670(4)–3.0707(5) Å, respectively, whereas the Ag–$C_{\pi\alpha}$ distances of 2.285(3)–2.414(3) Å were relatively shorter, compared to that of **87**. Besides, a tetranuclear closed-cuboidal complex, $[Ag_4(C{\equiv}CC{\equiv}CPh)_4(PCy_3)_4]$ **89** (Figure 38), was obtained when the phenylbutadiynyl ligand was used. Asymmetric Ag–C contacts of 2.151(3)–2.194(3) and 2.421(3)–2.559(3) Å as well as the Ag–Ag contacts of 2.9295(6)–3.2067(5) Å are generally longer than the Ag–C_σ, Ag–$C_{\pi\alpha}$, and Ag–Ag distances, respectively, observed in **88a–d**. The average C≡C bond distance of 1.20 Å in **88a–d** and **89** is typical for a C≡C bond. The photophysical properties of **88a–d** and **89** were studied, and the origins of the electronic absorption (with $\lambda > 250$ nm) as well as photoluminescence were suggested to be derived from the $^1(\pi\text{–}\pi^*)$ and $^3(\pi\text{–}\pi^*)$ excited states of the alkynyl ligands, respectively. The use of the aromatic-free PCy_3 ligand could eliminate possible interference by the $\pi\text{–}\pi^*$ transition present in the commonly encountered PAr_3 ligands during spectroscopic origin(s) assignment.

Bridging diphosphines with small bite angles have the propensity to bring metal centers into close proximity and have been employed in the design and synthesis of silver(I) alkynyls. The first report of this kind involved the depolymerization of **84** with the well-known dppm ligand that resulted in a trinuclear silver(I) complex $[Ag_3(dppm)_3(C{\equiv}CPh)_2]Cl$ **90** (Figure 39).[158] The molecular structure of **90** in the solid state consisted of a triangular $Ag_3(dppm)_3$ motif and bicapped by two phenylethynyl ligands in an asymmetric coordination mode. Ag–Ag contacts of 2.866(2)–2.983(1) were obtained. Complex **90** was also found to be emissive upon UV irradiation. The luminescence origin in the solid state was suggested to be derived from metal–metal $[d\text{-}\sigma^*(Ag\cdots Ag)]$ to ligand $[\pi^*(PhC{\equiv}C^-)]$ charge transfer, whereas in solution, it was dominated by the $^3[\pi\text{–}\pi^*(PhC{\equiv}C^-/dppm)]$ character. Yam reported the systematic synthesis of a series of monocapped trinuclear silver(I) arylalkynyls with bridging dppm and bis(diphenylphosphino)amines, $[Ag_3(dppm)_3(C{\equiv}CR)](BF_4)_2$ (R = Ph **91a**, C_6H_4OMe-4 **91b**, $C_6H_4NO_2$-4 **91c**) and $[Ag_3\{Ph_2PN(Pr^n)PPh_2\}_3(C{\equiv}CPh)](BF_4)_2$ **91d** (Figure 39), starting from the respective $[Ag_2(diphosphine)_2]^{2+}$ precursor and LiC≡CR in a ratio of 3 : 2.[159] The bicapped trinuclear silver(I) complexes, $[Ag_3(dppm)_3(C{\equiv}CR)_2]PF_6$ (R = $C_6H_4NO_2$-*p* **92a**, C≡CPh **92b**, C≡CC_6H_4OMe-*p* **92c**)) Figure 39), were also made from the reaction of the disilver(I) precursor with the alkynyl ligand deprotonated *in situ* using KOH, in a ratio of 3 : 4 (**92a**)[159] or 3 : 8 (**92b** and **92c**).[160] All these complexes bore the triangular $\{Ag_3(P\text{^}P)_3\}$ skeleton, and structural characterization of **91c** and **92a** revealed Ag–Ag contacts of 2.9850(6)–3.4030(6) and 2.8946(8)–3.1948(9) Å, respectively, which might be suggestive

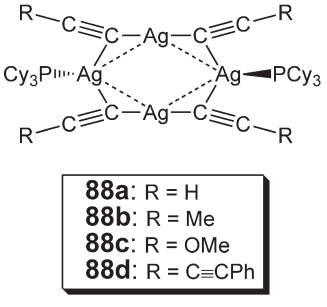

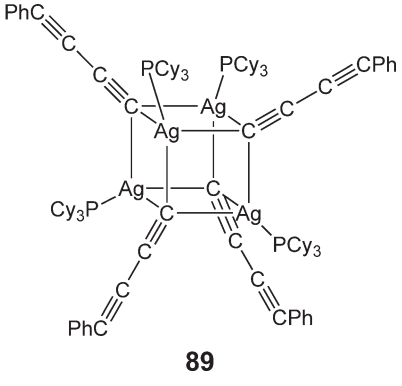

Figure 38 Structure of **88a–d** and **89**.

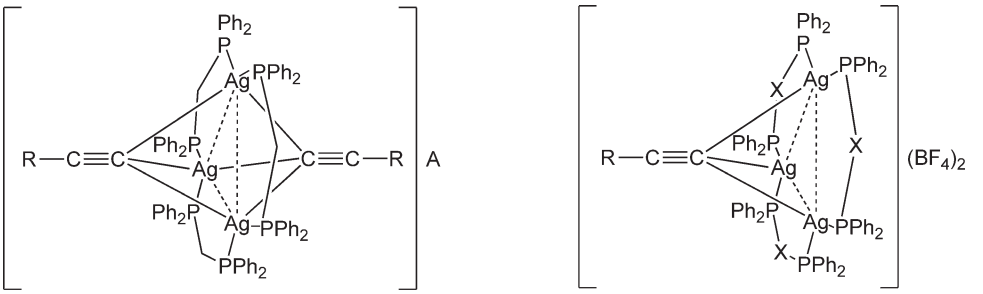

90: A = Cl; R = Ph
92a: A = PF_6; R = $C_6H_4NO_2$-4
92b: A = PF_6; R = C≡CPh
92c: A = PF_6; R = $C{\equiv}CC_6H_4OMe$-4

91a: X = CH_2; R = Ph
91b: X = CH_2; R = C_6H_4OMe-4
91c: X = CH_2; R = $C_6H_4NO_2$-4
91d: X = NPr^n; R = Ph

Figure 39 Trinuclear silver(I) alkynyl complexes.

of very weak or no Ag–Ag bonding interactions. It is interesting to note that the 4-nitrophenylethynyl ligands in **92a** were coordinated to the Ag_3 core in a highly unsymmetrical mode, and such an asymmetric coordination mode has also been observed in the related trinuclear copper(I) system bearing alkynyl ligands with electron-deficient substituents.[161,162] The photophysical properties of **91a–d** and **92a–c** were studied and the corresponding emission spectra were found to be vibronically structured with progressional spacings of ca. 1450–1600 and 1800–2200 cm^{-1}, typical of the ν(C≡C) and ν(C≡C) modes in the ground state, respectively, and were suggestive of the involvement of the alkynyl ligands in the excited states. Comparison studies among these complexes together with those of the isostructural copper(I) analogs provided the basis for the assignment of their photoluminescence origin, which was derived from triplet states of a ligand-to-metal charge-transfer (LMCT, $RC{\equiv}C^- \rightarrow Ag_3$) character that mixed with the metal-centered *d*–*s* states, in the cases of **91a**, **91b**, and **91d**. For complexes **91c** and **92a–c**, that bore either the electron-deficient 4-nitrophenylethynyl ligands or the more conjugated arylbutadiynyl ligands, significant contributions of the ligand-centered triplet excited states in the lowest energy emissive state were observed. Similar observations and assignments of ligand-centered phosphorescence were also reported in the related trinuclear copper(I) systems.[161,163,164] Yam also increased the nuclearity of this class of complexes by bridging two monocapped $\{Ag_3(P\text{^}P)_3\}$ skeletal moieties with a 1,4-diethynylbenzene ligand, and reported a luminescent hexanuclear silver(I) complex, $[Ag_3(dppm)_3(C{\equiv}CC_6H_4C{\equiv}C\text{-}p)Ag_3(dppm)_3](BF_4)_4$ **93** (Figure 40).[165] Structural characterization revealed its dumbbell-shaped structure with Ag–Ag distances of 3.079(1)–3.338(1) Å, comparable to the trinuclear monocapped **91c**.

Through the metalloligand approach, Yam reported the isolation of a luminescent pentanuclear silver(I)–rhenium(I) alkynyl rigid-rod complex, $[Ag_3(dppm)_3\{C{\equiv}CC{\equiv}CRe(bpy)\text{-}(CO)_3\}_2]PF_6$ **94** (Figure 41), using $[Re(bpy)(CO)_3C{\equiv}CC{\equiv}CH]$ in place of organic alkynes.[166] The well-known luminescence behavior of rhenium(I) diimine alkynyls and their generally lower excited state energies compared to the homometallic trinuclear silver(I)

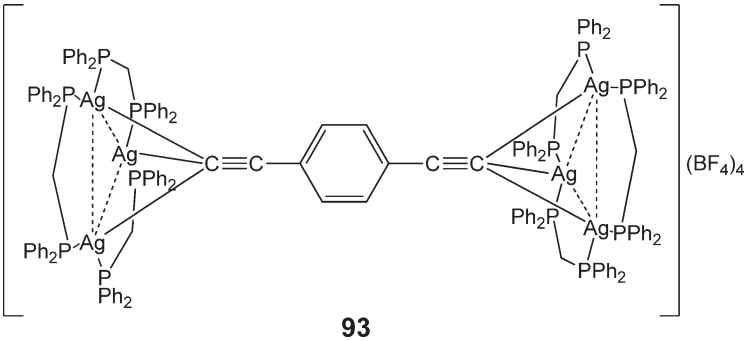

93

Figure 40 Structure of **93**.

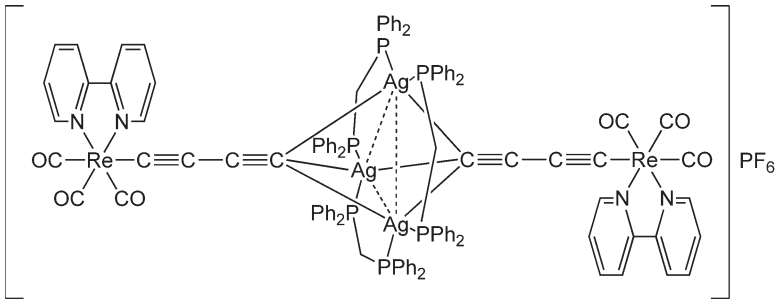

94

Figure 41 Structure of **94**.

counterparts allowed the luminescence properties of **94** to be dominated by excited state character of a ^{3}MLCT [dπ(Re) $\rightarrow \pi^*$(bpy)] origin. Interestingly, rather than the predicted rigid-rod structure, a series of luminescent decanuclear silver(I)–rhenium(I) complexes, $[Ag_6(dppm)_4\{C{\equiv}CC{\equiv}CRe(N\text{^}N)\text{-}(CO)_3\}_4](PF_6)_2$ (N^N = Bu^t_2bpy **95a**, Me_2bpy **95b**, phen **95c**, Br_2phen **95d**) (Figure 42), was obtained when diimine ligands other than bpy were employed.[167] The formulation of these decanuclear complexes could easily be differentiated from that of **94** using ^{1}H NMR spectroscopy, which showed that the dppm : N^N ratio was 1 : 1 rather than 3 : 2. Crystal structures of **95b** and **95d** confirmed their decanuclear nature, with a hexanuclear $\{Ag_6(dppm)_4\}$ core decorated by four peripheral rhenium(I) diimine alkynyl pendants. Such an unusual $\{Ag_6(dppm)_4\}$ core was first reported in a series of related hexanuclear silver(I) chalcogenolate complexes, $[Ag_6(dppm)_4(ER)_4](PF_6)_2$ (E = S, Se) in 2002 by the same group.[168] The Ag–Ag contacts (**95b**: 2.940(3)–3.007(3) Å; **95d**: 3.0206(11)–3.0415(10) Å) were shorter than the sum of van der Waals radii for silver (3.4 Å)[31] and were suggestive of the presence of weak Ag–Ag interactions. Short metal–metal contacts were also observed in $[Ag_6(dppm)_4(ER)_4](PF_6)_2$ (E = S, Se) but not in the isostructural copper(I) counterpart, $[Cu_6(dppm)_4(SePh)_4](BF_4)_2$.[169] Complexes **95a–d** also exhibited interesting fluxional behavior in solution, as indicated by the broad signals in their ^{31}P NMR spectra. Again, similar fluxional behavior was also observed in $[Ag_6(dppm)_4(ER)_4](PF_6)_2$ (E = S, Se) but not in $[Cu_6(dppm)_4(SePh)_4](BF_4)_2$. It was suggested that the presence of weak metal–metal interactions played an important role in governing the rigidity of the structure, and hence the fluxional properties of these complexes.

In addition to the well-known luminescent $\{Re(N\text{^}N)(CO)_3\}$ moieties, the electrochemically active ferrocenyl groups were employed as building blocks for the construction of polynuclear silver(I) alkynyl complexes. Yip reported the synthesis, structural characterization, and electrochemistry of a tetranuclear complex, $[Ag_3(dppm)_3(C{\equiv}CFc)(OTf)]OTf$ **96** (Figure 43), with the $\{Ag_3(dppm)_3\}$ skeletal unit being capped by a ferrocenylethynyl ligand on one side and an OTf^- anion on the other, all in a μ_3-η^1-bonding mode.[170]

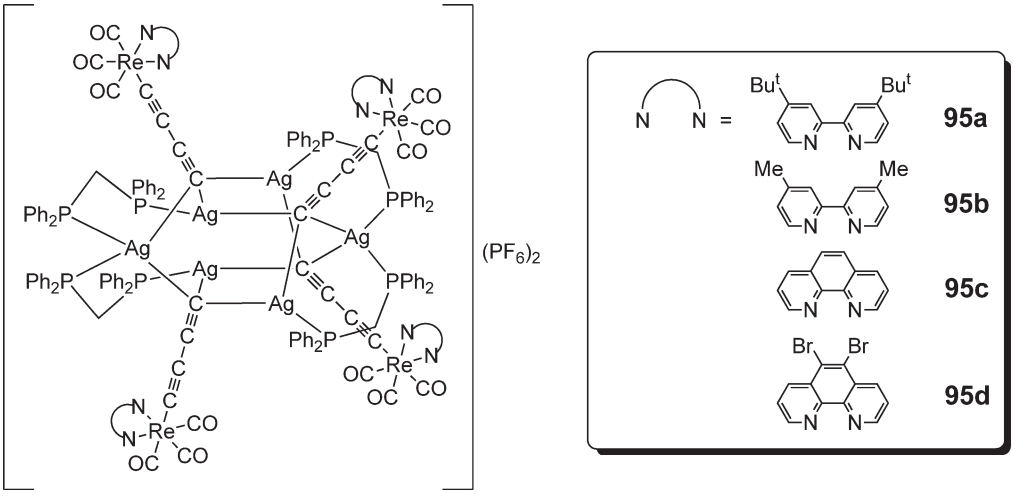

Figure 42 Decanuclear silver(I)–rhenium(I) alkynyl complexes **95a–d**.

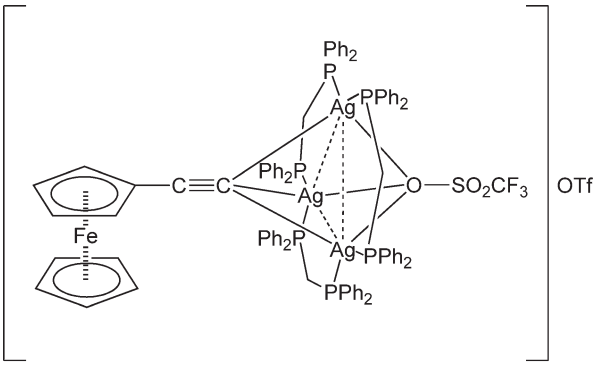

96

Figure 43 Structure of **96**.

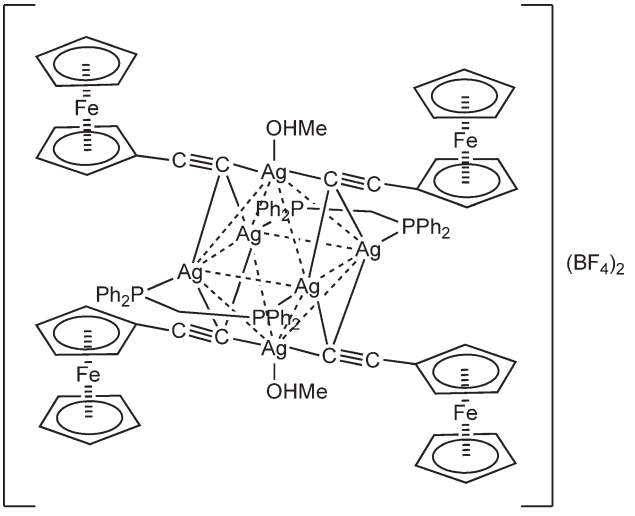

97

Figure 44 Structure of **97**.

Similar studies on a decanuclear complex, $[Ag_6(dppm)_2(C{\equiv}CFc)_4(MeOH)_2](BF_4)_2$ **97** (Figure 44), were also reported by Chen.[171] The Ag–Ag distances in **96** (3.2416(6)–3.2527(6) Å) and **97** (2.8977(10)–3.2463(10) Å) were unremarkable and were comparable to those in related examples discussed previously. The six Ag centers in **97** assembled in an octahedron, with two dppm ligands bridging the four silver(I) centers at the equatorial positions and the ferrocenylethynyl ligands coordinated to the octahedron in a μ_3-η^1-bonding fashion. It is noteworthy mentioning that **97** did not possess any fluxional behavior in solution, which was in contrast to that found in the more dppm-rich **95a–d**. There was also no appreciable wave splitting observed during cyclic and differential pulse voltammetric scans, indicative of the insignificance or absence of electronic communication between the ferrocenyl moieties across the Ag_6 cluster core.

$[Ag_4Cu_2(Ph_2NHPPh_2)_4(C{\equiv}CR)_4](ClO_4)_2$ (R = Ph **98a**, Tol-4 **98b**), having a mixed metal $\{M_6(P\text{^}P)_4\}$ core isostructural to that of **95a–d**, was isolated from the reaction of $[Cu_2(Ph_2NHPPh_2)_2(MeCN)_2](ClO_4)_2$ and $[Ag(C{\equiv}CR)]_\infty$ in MeCN.[172] Noticeable metal–metal contacts were observed for **98a** and **98b**, with the Cu–Cu, Ag–Cu, and Ag–Ag distances in the ranges of 2.5733(18)–2.5315(12), 2.7514(15)–3.1071(17), and 2.9783(13)–3.2652(15) Å, respectively. When dppm was employed in place of Ph_2NHPPh_2, a series of octanuclear silver(I)–copper(I) mixed metal complexes was isolated, having the formulation of $[Ag_6Cu_2(dppm)_3(C{\equiv}CC_6H_4R\text{-}p)_6(MeCN)](ClO_4)_2$ (R = Ph **99a**, C_6H_4Me-4 **99b**, C_6H_4OMe-4 **99c**, $C_6H_4NO_2$-4 **99d**) (Figure 45).[172] The molecular

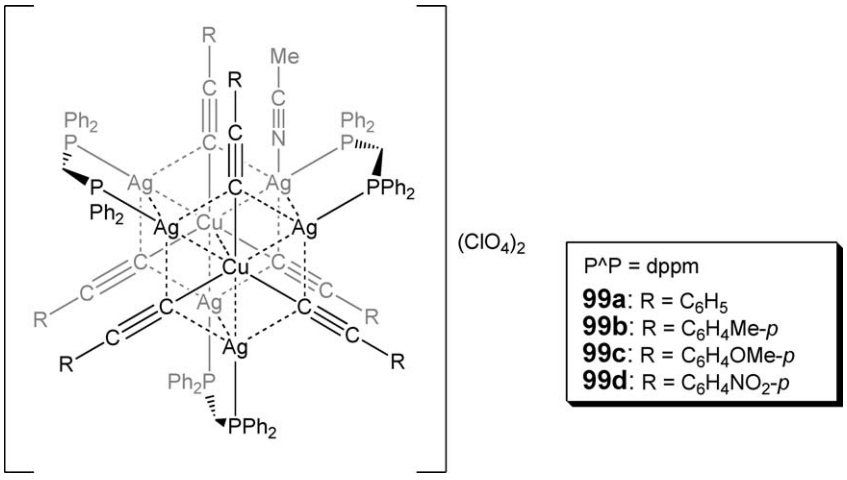

Figure 45 Structure of **99a–d**.

structures of **99a–d** could be considered as two slightly distorted trigonal-planar $\{Cu(AgC{\equiv}CC_6H_4R\text{-}p)_3\}$ units connected by three dppm ligands at the silver centers, giving a threefold paddlewheel structure. With 4-acetylphenylethynyl as ligand, a dimeric form of the octanuclear complex was isolated, that is, $[(Ag_6Cu_2(dppm)_3\{C{\equiv}CC_6H_4C(=O)Me\text{-}p\}_6)_2](ClO_4)_4$ **99e**. Instead of having a coordinated MeCN as is the case for **99a–d**, the two octanuclear units in **99e** were linked to each other by two 4-acetylphenylethynyl units as a result of the replacement of the MeCN group by the acetyl end of the 4-acetylphenylethynyl. Metal–metal separations in **99a–e**, including Cu–Cu, Ag–Cu, and Ag–Ag, were in the ranges of 2.960(2)–3.424(2), 2.5916(12)–2.8317(18), and 2.9826(14)–3.0689(17) Å, respectively. The photophysical behavior of these silver(I)–copper(I) mixed metal alkynyl aggregates was also studied, with the emissive states in **98a** and **98b** and **99a–c** similarly assigned as the assignments proposed by Yam,[159–165] that is, derived from a ^{3}LMCT ($C{\equiv}CC_6H_4R \rightarrow Ag_4Cu_2/Au_6Cu_2$) state that mixed with metal-centered ($d \rightarrow s$) excited states. The lowest-energy excited states in **99d** and **99e**, on the other hand, are dominated by the ^{3}IL ($\pi \rightarrow \pi^*$) character due to the presence of strongly electron-withdrawing substituents on the alkynyl ligands, similar to that observed by Yam[159–161,163–165] and others.[162]

Reactions of $[Ag(C{\equiv}CR)]_\infty$ with the related binuclear gold(I) precursor afforded a novel series of tridecanuclear silver(I)–gold(I) mixed metal alkynyl complexes, $[Au_5Ag_8(dppm)_4\{C_6R_3\text{-}1,2,3\}(C{\equiv}CR)_7](SbF_6/PF_6)_2$ (R = Ph **100a**, C_6H_4Me-4 **100b**, $C_6H_4Bu^t$-4 **100c**), with the 1,2,3-trisubstituted aryl ligand being formed in an alkynyl cyclotrimerization reaction coordinated to three gold(I) and two silver(I) centers.[173] The Ag–C_{aryl}, Ag–Ag, and Ag–Au distances of 2.672(15), 3.1674(18), and 2.7434(14)–3.1490(15) Å, respectively, were observed in the crystal structure of **100a** (with PF_6 anions). Of the seven phenylethynyl ligands, three were μ_3-η^1-coordinated to one gold(I) and two silver(I) centers, whereas the other four exhibited a μ-η^1,η^2-bonding mode σ-bonded to a gold(I) and π-bonded to a silver(I) center. The Ag–$C_{alkynyl}$ bond lengths were in the range of 2.318–2.576 Å.

The third-order non-linear optical properties of $[Ag(C{\equiv}CPh)]_\infty$ **84**, the related double salt $[Ag(C{\equiv}CPh){\cdot}Ag(SBu^t)]_\infty$ **101**, organic poly(phenylacetylene), and $[(Ph_3P)Ag(C{\equiv}CPh)]_4$ **102** were determined via ultrafast heterodyned optical Kerr effect measurements, with the third-order optical non-linear response being enhanced by the incorporation of silver *d*-electrons into the delocalized conjugated organic π-system.[174] The relative magnitudes have been found to follow the order: **84** > **101** > poly(phenylacetylene) > **102**, which was in line with and possibly attributed to the decreasing length of π-conjugation.

Although it has been a common perception that organosilver(I) compounds are generally unstable and as a result their applications in organic synthesis are not well studied, silver(I) alkynyls represent an exceptional subclass and have been utilized quite often in organic alkynylation reactions.[175,176] For example, the synthesis of a series of silver(I) alkynyls with polycycloaliphatic,[177,178] hydroxypolycycloaliphatic,[177,178] and 2-naphthyl groups, starting from $[Ag(NH_3)_2]NO_3$ and the terminal alkynes, was reported.[179] Subsequent reactions of the silver(I) alkynyls with iodine afforded the corresponding iodoalkynes.[177–179]

A wide variety of organoalkynyl derivatives of cotarnine hydrochloride, a cyclic iminium salt with rich biological activity, were prepared from the direct alkynylation of cotarnine hydrochloride using silver(I) alkynyls.[180] Substituted enynes were prepared from the coupling reactions of silver alkynyls with the palladium allyl intermediates, which was

formed *in situ* from the palladium catalyst $Pd(PPh_3)_4$ and the corresponding alkenyltriflates.[181] Koide reported a versatile synthesis of γ-hydroxy-α,β-acetylenic esters by the coupling reaction of [Ag{C≡CC(=O)OMe}] with a series of aldehydes and ketones in the presence of the $[Cp_2ZrCl_2]$ catalyst, of which the use of air sensitive lithiated alkynylating reagents and base could be avoided, and the reaction was found to be compatible with the presence of base sensitive functional groups.[182] Alkynyl-substituted adamantanes were reported to be synthesized by the one-step alkynylation of iodoadamantane with silver(I) alkynyls in the presence of *N*-methylmorpholine.[176]

The silver(I) alkynyl chemistry was also employed in the fabrication and formation of rigid polychelate monolayer. Armand reported the interconnection of cobalt(II) ethynyl-containing porphyrin complex in Langmuir-Blodgett (LB) and self-assembled monolayer films by silver(I) alkynyl bridges, in which dissolution of the surfactant fillings was possible without destroying the monolayers or disturbing the macrocycle orientation inside the LB film.[183]

Apart from the growing interest in silver(I) "organo"-alkynyl chemistry in the past few years, Mak and co-workers revisited the synthesis and structural characterization of silver(I) multiple salts containing acetylenediide ($C{\equiv}C^{2-}$) in 1998, starting with the report of the isolation of a double salt $[Ag_2(C{\equiv}C){\cdot}8AgF]$ **103**.[184] Simple silver(I) acetylenediide $[Ag_2(C{\equiv}C)]$ (also known as silver carbide), which is an insoluble amorphous light sensitive yellow precipitate and is explosive when dry, was prepared early in 1858 (a time even earlier than the identification of acetylene itself!),[185,186] albeit its composition was completely solved almost a century later.[187] Its structural features were determined when a crystalline sample of a double salt $[Ag_2(C{\equiv}C){\cdot}6AgNO_3]$ **104** was first obtained and analyzed crystallographically by Österlöf in 1954, and further refinements were subsequently made and data improved by Tang in 1990 and Mak in 1999.[188,189–190] Complex **104** (Figure 46) possessed a naked $C{\equiv}C^{2-}$ being disordered in three possible orientations but fully encapsulated in a rhombohedral Ag_8 cage.

Complex **103** possessed a structure with the capped square antiprism Ag_9 cluster core encapsulating a naked $C{\equiv}C^{2-}$ unit, and further attached to an AgF_4 moiety at the apex exohedrally. Thereafter, the wide structural diversity of these $[Ag_x(C{\equiv}C)_y]$ cage-type clusters as building blocks in the crystal structures of the silver(I) multiple salts were exemplified in subsequent reports (Table 1), where various approaches such as the use of different silver salts, solvents (during reaction and crystallization), mixing ratio of precursors, and synthetic methods (conventional and hydrothermal, etc.) have been employed. Some of the examples prior to 2002 have also been reviewed very recently.[191] A general overview of these crystal structures provides an indication that the basic structural motifs involved are $[Ag_n(C{\equiv}C)]^{(n-2)}$ cage-type clusters with n spanning from 6 to 9, and fusion of these cages by sharing of common vertices to form multiple cages of higher nuclearities is also possible and not uncommon. Supramolecular architectures have also been achieved through the use of coordinating anions and solvents, and additional (bridging) ligands.[192–210]

In general, the $[Ag_6(C{\equiv}C)]$ cage appeared as an octahedral array **105** and **106** (Figure 47).[190,192] The $C{\equiv}C^{2-}$ unit was encapsulated inside the octahedral Ag_6 cage, σ- and π-bonded to two and four Ag vertices, respectively, in **105**, or four and two Ag vertices, respectively, in **106**. A significant lengthening of the C≡C bond in **105** relative to **106** and free acetylene was observed and was further revealed by a red shift in its Raman C≡C stretch (2,069 cm^{-1}), indicative of the presence of metal-to-ligand π-backbonding. On the other hand, $[Ag_7(C{\equiv}C)]$ cage appeared as pentagonal-bipyramidal **107–109** (Figure 48), (distorted/slanted) monocapped trigonal-prismatic **111–116** (Figure 48), monocapped octahedral **117** and **118** (Figure 48), crown-like **119**, and basket-like **120** and **121** arrangements upon subtle changes in the conditions and slight variations in the nature of the counteranions. For example, the slow release of fluoride anions during the crystallization of **112** and **113** played a crucial role in their formation and was achieved by the slow hydrolysis of BF_4^- in $AgBF_4$ to F^- and species such as $BF_3(OH)^-$ and $BF_2(OH)_2^-$,[196] while a direct addition of AgF would result in the direct formation of the relatively more stable **103**

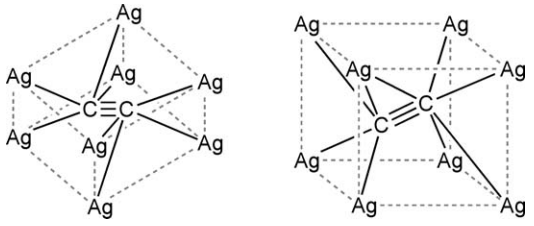

Figure 46 Selected rhombohedral $[Ag_8(C{=}C)]$ cages in **104**.

Table 1 Structural features of silver(I) acetylenediide complexes

Complex	*Bond distances*			*Cluster-core geometry*	*References*
	Ag–Ag/Å	*Ag–C*/Å	*C≡C*/Å		
$[Ag_2(C{\equiv}C)\cdot 8AgF]$ **103**	2.8441(4)–3.0863(5)	2.110(4)–2.311(4)	1.175(7)	$Ag_9(C{\equiv}C)$ monocapped square antiprism	184
$[Ag_2(C{\equiv}C)\cdot 6AgNO_3]$ **104**	2.9546(5)–3.0521(6)	2.089(9)–2.488(8)	1.22(2)	$Ag_8(C{\equiv}C)$ rhombohedron	188–190
$[Ag_2(C{\equiv}C)\cdot 2AgClO_4\cdot 2H_2O]$ **105**	NA	2.087(3), 2.108(6)(σ); 2.382(6), 2.554(4) (π)	1.212(7)	$Ag_6(C{\equiv}C)$ octahedron	192
$[Ag_2(C{\equiv}C)\cdot AgNO_3]$ **106**	2.9253(9)	2.163(3) (σ), 2.432(1) (π)	1.225(7)	$Ag_6(C{\equiv}C)$ octahedron	190
$[Ag_2(C{\equiv}C)\cdot 5AgCF_3CO_2\cdot 2([15]$-crown-5)$\cdot H_2O]\cdot 3H_2O$ **107**	2.954(1) (shortest)	2.13–2.62	1.13(1)–1.26(1)	$Ag_7(C{\equiv}C)$ pentagonal bipyramid	193
$[Ag_2(C{\equiv}C)\cdot 6AgCF_3CO_2\cdot 2([15]crown\text{-}5)\cdot H_2O]\cdot$ 0.5 H_2O **108**	2.830(1) (shortest)	2.118–2.555	1.13(1)–1.26(1)	$Ag_7(C{\equiv}C)$ pentagonal bipyramid	193
$[Ag_2(C{\equiv}C)\cdot 6AgC_2F_5CO_2\cdot 2([15]crown\text{-}5)]_2$ **109**	NA	NA	NA	$Ag_7(C{\equiv}C)$ pentagonal bipyramid	194
$[Ag_2(C{\equiv}C)\cdot 4AgCF_3CO_2\cdot 2(PyCN\text{-}p)]$ **110**	2.844(2)–3.335(2)	2.07(2)–2.70(2)	1.18(2), 1.20(2)	$Ag_7(C{\equiv}C)$ distorted pentagonal bipyramid	195
$[Ag_2(C{\equiv}C)\cdot 5AgNO_3]$ **111**	2.712(2)–3.361(2)	2.051(5)–2.416(6)	1.224(10)	$Ag_7(C{\equiv}C)$ monocapped trigonal prism	190
$[Ag_2(C{\equiv}C)\cdot AgF\cdot 4AgOTf\cdot MeCN]$ **112**	2.878(1)–3.003(1)	2.14(1)–2.319(9)	1.21(1)	$Ag_7(C{\equiv}C)$ monocapped trigonal prism	196
$[Ag_2(C{\equiv}C)\cdot AgF\cdot 4AgOTf\cdot EtCN]$ **113**	NA	NA	NA	$Ag_7(C{\equiv}C)$ monocapped trigonal prism	196
$[Ag_2(C{\equiv}C)\cdot 8AgCF_3CO_2\cdot 2EtCN\cdot 3H_2O]$ **114**	2.853(1)–3.298(2)	2.153(9)–2.69(1)	1.18(1)	$Ag_7(C{\equiv}C)$ slanted monocapped trigonal prism	197
$[Ag_6(C{\equiv}C)(CF_3CO_2)_5$-$(HPyCH_2CH_2CH_2Py\text{-}4,4')]_n$ **115**	2.860(2)–3.399(2)	2.122(5)–2.640(5)	1.217(7)	$Ag_7(C{\equiv}C)$ distorted monocapped trigonal prism	198
$[Ag_6(C{\equiv}C)(C_2F_5CO_2)_5$-$(PyCH_2CH_2CH_2Py\text{-}4,4')]_n$ **116**	NA	NA	NA	$Ag_7(C{\equiv}C)$ distorted monocapped trigonal prism	198
$[Ag_2(C{\equiv}C)\cdot 5.5AgNO_3\cdot 0.5H_2O]$ **117**	2.9073(5)–3.3604(5)	2.108(3)–2.437(3)	1.180(4)	$Ag_7(C{\equiv}C)$ monocapped octahedron	190
$[Ag_2(C{\equiv}C)\cdot 5AgCF_3CO_2\cdot 2MeCN\cdot 2H_2O]$ **118**	2.938(1)–3.332(1)	2.12(1)–2.607(9)	1.17(1)	$Ag_7(C{\equiv}C)$ monocapped octahedron	197
$[Ag_2(C{\equiv}C)\cdot 3AgO_2CCF_2CF_2CO_2Ag\cdot 7H_2O]$ **119**	2.8848(8)–2.9526(8)	2.111(6)–2.521(6)	1.21(1)	$Ag_7(C{\equiv}C)$ crown-like cage	199
$[Ag_2(C{\equiv}C)\cdot 6AgCHF_2CO_2]$ **120**	2.8133(9)–3.2041(8)	2.155(7)–2.497(7)	1.24(1)	$Ag_7(C{\equiv}C)$ basket-like cage	197
$[2\{Ag_2(C{\equiv}C)\}\cdot 12AgCF_3CO_2\cdot 5H_2O]$ **121**	2.739(2)–3.185(2)	2.15(1)–2.46(2)	1.19(2)	$Ag_7(C{\equiv}C)$ square-based basket	200
$[2\{Ag_2(C{\equiv}C)\}\cdot 6AgO_2C(CF_2)_2CO_2$-$Ag\cdot AgNO_3\cdot 12H_2O]$ **122**	2.901(1)–3.354(1) 2.849(1)–3.379(2)	2.11(1)–2.63(2) 2.16(1)–2.49(2)	1.21(1) 1.22(1)	$Ag_7(C{\equiv}C)$ pentagonal bipyramid + $Ag_8(C{\equiv}C)$ monocapped pentagonal bipyramid	199
$[2\{Ag_2(C{\equiv}C)\}\cdot AgF\cdot 9AgNO_3\cdot H_2O]$ **123**	2.769(3)–3.177(4)	2.15(2)–2.54(2)	1.18(2),1.22(2)	$Ag_7(C{\equiv}C)$ monocapped (on triangular face) trigonal prism + $Ag_7(C{\equiv}C)$ monocapped (on rectangular face) trigonal prism	201

[4{$Ag_2(C{\equiv}C)$}·23$AgCF_3CO_2$·7EtCN·2.5H_2O] **124**	2.756(1)–3.368(1)	2.120(13)–2.774(11)	1.14(1)–1.21(1)	2 × $Ag_7(C{\equiv}C)$ distorted monocapped trigonal prisms + $Ag_7(C{\equiv}C)$ distorted square-based basket + $Ag_7(C{\equiv}C)$ distorted pentagonal bipyramid	200
[(Ag^{II})(tmc)(BF_4)][$Ag^{I}_6(C{\equiv}C)(CF_3CO_2)_5$-($H_2O$)]$_n$·$H_2O$ **125**	2.818–3.366(1)	2.172(8)–2.497(9)	1.17(1)	$Ag_8(C{\equiv}C)$ triangulated dodecahedron	202
[$Ag_2(C{\equiv}C)$·6$AgCF_3CO_2$·3MeCN] **126**	2.738(1)–3.350(1)	2.20(1)–2.31(1) (σ); 2.35(1), 2.67(1) (π)	1.24(1)	$Ag_8(C{\equiv}C)$ distorted triangulated dodecahedron	200
[$Ag_2(C{\equiv}C)$·4$AgCF_3CO_2$·(PyCONH_2-*p*)·H_2O]·H_2O **127**	2.7520(7)–3.3609(7)	2.158(5), 2.305(4) (σ); 2.369(5), 2.666(54) (π)	NA	$Ag_8(C{\equiv}C)$ distorted triangulated dodecahedron	195
[$Ag_2(C{\equiv}C)$·6$AgCF_3CO_2$·2(PyCN-*m*)] **128**	2.928(2)–3.333(2)	2.169(14)–2.672(16)	1.197(16)	$Ag_8(C{\equiv}C)$ distorted triangulated dodecahedron	195
[$Ag_6(C{\equiv}C)(CF_3CO_2)_4$(Py$CH_2CH_2CH_2$Py-4,4′)] **129**	2.799(1)–3.383(1)	2.122(5)–2.640(5)	1.217(7)	$Ag_8(C{\equiv}C)$ distorted triangulated dodecahedron	198
[Ag([12]crown-4)$_2$][$Ag_{10}(C{\equiv}C)(CF_3CO_2)_9$-([12]crown-4)$_2(H_2O)_3$]·$H_2O$ **130**	2.854(1)–3.320(1)	2.18(1)–2.673(4)	1.18(1)	$Ag_8(C{\equiv}C)$ triangulated dodecahedron	194
[$Ag_2(C{\equiv}C)$·6$AgCF_3CO_2$·2(PyCONH_2-*m*)] **131**	2.814(1)–3.333(1)	2.150(7)–2.589(7)	1.183(9)–1.235(9)	$Ag_8(C{\equiv}C)$ distorted bicapped trigonal prism	195
[$Ag_2(C{\equiv}C)$·4$AgO_2C(CF_2)_3CO_2Ag$·17.5H_2O] **132**	2.909(1)–3.338(2)	2.12(1)–2.61(2)	1.23(2)	$Ag_8(C{\equiv}C)$ square antiprism	199
[$Ag_2(C{\equiv}C)$·8$AgCF_3CO_2$·2(PyCONH_2-*m*)·4H_2O] **133**	2.826(2)–3.165(1)	2.22(1)–2.23(1) (σ); 2.37(1)–2.616(5) (π)	1.24(2)	$Ag_8(C{\equiv}C)$ square antiprism	195
[$Ag_7(C{\equiv}C)(BzNMe_3)$] **134**	2.8076(9)–3.2835(8)	2.100(6)–2.729(5)	1.203(8)	$Ag_8(C{\equiv}C)$·Ag infinite column of square antiprism cages with an additional exohedral Ag	203
[2{$Ag_2(C{\equiv}C)$}·9($AgCF_3CO_2$)·($Me_3NCH_2CO_2)_3$)] **135**	NA	2.143(8)–2.700(9)	1.18(1), 1.23(1)	$Ag_8(C{\equiv}C)$ bicapped trigonal prism + $Ag_8(C{\equiv}C)$ triangulated dodecahedron	204
[Ag^{II}(tmc)][Ag^{II}(tmc)(H_2O)]$_2$[$Ag^{I}_{11}(C{\equiv}C)$-($CF_3CO_2)_{12}(H_2O)_4$]$_2$ **136**	2.8693(7)–3.3236(7)	2.138(6)–2.563(6)	1.212(8)	$Ag_8(C{\equiv}C)$·Ag bicapped trigonal prism with an additional exohedral Ag	205
[$Ag_2(C{\equiv}C)$·7$AgCF_3CO_2$·2($Et_3NCH_2CO_2$)·H_2O] **137**	NA	2.21(2)–2.58(2)	1.10(3)	$Ag_9(C{\equiv}C)$ distorted monocapped cube	204
[$Ag_2(C{\equiv}C)$·7$AgC_2F_5CO_2$·3($Me_3NCH_2CO_2$)·H_2O] **138**	NA	2.2053(8)–2.5752(8)	1.199(1)	$Ag_9(C{\equiv}C)$ distorted monocapped square prism	204
[$Ag_2(C{\equiv}C)$·7$AgCF_3CO_2$·3(Me_3NCH_2-CO_2)·H_2O]·2H_2O **139**	NA	2.10(2)–2.64(2)	1.29(3)	$Ag_9(C{\equiv}C)$ distorted monocapped square antiprism	204
[$Ag_2(C{\equiv}C)$·5$AgCF_3CO_2$·(benzo-15-crown-5)·2H_2O]·0.5H_2O **140**	NA	2.157(6)–3.530(6)	1.221(9)	$Ag_{12}(C{\equiv}C)_2$ double cage, or 2 × $Ag_7(C{\equiv}C)$ monocapped trigonal prisms	194

Table 1 (Continued)

Complex	*Bond distances*			*Cluster-core geometry*	*References*
	Ag–Ag/Å	*Ag–C*/Å	*C≡C*/Å		
$[Ag_2(C{\equiv}C){\cdot}4AgCF_3CO_2{\cdot}(N\text{-}PyCH_2\text{-}CO_2\text{-}p){\cdot}H_2O]{\cdot}0.75H_2O$ **141**	NA	2.077(9)–2.491(8)	1.23(1)	$Ag_{12}(C{\equiv}C)_2$ double cage, or $2 \times Ag_7(C{\equiv}C)$ monocapped trigonal prism	204
$[2\{Ag_2(C{\equiv}C)\}{\cdot}9AgCF_3CO_2{\cdot}2([15]\text{-crown-5}){\cdot}2H_2O]_n$ **142**	2.847(1) (shortest)	2.12–2.70	1.13(1)–1.26(1)	$Ag_{13}(C{\equiv}C)_2$ double cage, or $2 \times Ag_8(C{\equiv}C)$ distorted square antiprisms	193
$[2\{Ag_2(C{\equiv}C)\}{\cdot}3AgCN{\cdot}15AgCF_3\text{-}CO_2{\cdot}2AgBF_4{\cdot}9H_2O]$ **143**	2.879(1)–3.316(1)	2.145(9)–2.59(1)	1.16(1)	$Ag_{13}(C{\equiv}C)_2$ double cage, or $2 \times Ag_8(C{\equiv}C)$ bicapped trigonal prisms	206
$[2\{Ag_2(C{\equiv}C)\}{\cdot}9AgC_2F_5CO_2{\cdot}2([18]\text{-crown-6}){\cdot}3.5H_2O]{\cdot}H_2O$ **144**	NA	2.122(9)–2.66(1)	1.12(1), 1.16(1)	$Ag_{13}(C{\equiv}C)_2$ double cage, or $Ag_7(C{\equiv}C)$ monocapped trigonal prism + $Ag_8(C{\equiv}C)$ bicapped trigonal antiprism	194
$[2\{Ag_2(C{\equiv}C)\}{\cdot}12AgC_2F_5CO_2{\cdot}(N\text{-}PyCH_2\text{-}CH_2CO_2\text{-}p)_2{\cdot}4H_2O]{\cdot}H_2O$ **145**	NA	2.12(2)–2.69(2)	1.09(2), 1.16(2)	$Ag_{14}(C{\equiv}C)_2$ double cage, or $2 \times Ag_7(C{\equiv}C)$ monocapped trigonal prisms	204
$[Ag_2(C{\equiv}C){\cdot}6AgCF_3CO_2{\cdot}2(N\text{-}PyCH_2CH_2CO_2\text{-}p){\cdot}H_2O)]{\cdot}H_2O$ **146**	NA	2.121(9)–2.701(9)	1.22(1)	$Ag_{14}(C{\equiv}C)_2$ double cage, or $2 \times Ag_8(C{\equiv}C)$ triangulated dodecahedron	204
$[Ag_2(C{\equiv}C){\cdot}10AgC_2F_5CO_2{\cdot}9.5H_2O]$ **147**	2.811(1)–3.265(1)	2.167(9)–2.560(9)	1.16(1)	$Ag_{14}(C{\equiv}C)_2$ double cage, or $2 \times Ag_8(C{\equiv}C)$ square antiprism	200
$[Ag_2(C{\equiv}C){\cdot}6AgC_2F_5CO_2{\cdot}2EtCN]$ **148**	2.798(1)–3.311(1)	2.171(9)–2.633(9)	1.19(1)	$Ag_{14}(C{\equiv}C)_2$ double cage, or $2 \times Ag_8(C{\equiv}C)$ distorted dodecahedra	200
$[Ag_9(C{\equiv}C)(CF_3CO_2)_9(HPyCH_2OH)\text{-}(H_2O)][HPyCH_2OH]$ **149**	2.8522(9)–3.379(1)	2.123(7)–2.648(8)	1.25(1)	$Ag_{14}(C{\equiv}C)_2$ centrosymmetric double cage, or $2 \times Ag_8(C{\equiv}C)$ triangulated dodecahedra	197
$(Et_4N)_3[2\{Ag_2(C{\equiv}C)\}{\cdot}AgCN{\cdot}11AgCF_3\text{-}CO_2{\cdot}3CF_3CO_2{\cdot}6H_2O]$ **150**	NA	2.106(6)–2.592(6)	1.221(9)	$Ag_{14}(C{\equiv}C)_2{\cdot}Ag_2$ double cage, or $2 \times Ag_8(C{\equiv}C)$ triangulated dodecahedron	207
$[Ag_{17}(C{\equiv}C)_2(CF_3CO_2)_{16}(NO_3)(H_2O)_4]\text{-}(BzNMe_3)_4$ **151**	2.827(1)–3.386(2)	2.189(7)–2.649(7)	1.212(9), 1.235(9)	$Ag_{15}(C{\equiv}C)_2$ double cage, or $Ag_8(C{\equiv}C)$ triangulated dodecahedron + $Ag_9(C{\equiv}C)$ monocapped square antiprism	208
$[2\{Ag_2(C{\equiv}C)\}{\cdot}10AgCF_3CO_2{\cdot}3(Me_3NCH_2CH_2\text{-}CO_2\text{-}p)]{\cdot}H_2O$ **152**	NA	2.131(9)–2.70(1)	1.15(1), 1.17(1)	$Ag_{15}(C{\equiv}C)_2$ double cage, or $Ag_8(C{\equiv}C)$ square antiprism + $Ag_8(C{\equiv}C)$ distorted bicapped trigonal prism	204
$[1.5\{Ag_2(C{\equiv}C)\}{\cdot}7AgCF_3CO_2{\cdot}2(N\text{-}PyCH_2\text{-}CH_2CO_2\text{-}p)]$ **153**	NA	2.157(7)–3.505	1.174(9), 1.21(1)	$Ag_{15}(C{\equiv}C)_2$ double cage, or $Ag_8(C{\equiv}C)$ distorted triangulated dodecahedron + $Ag_8(C{\equiv}C)$ distorted cube	204
$[Ag_{18}(C{\equiv}C)_2(C_2F_5CO_2)_{18}(HPyPy\text{-}4,4')_4\text{-}(H_2O)_3]$ **154**	2.780(2)–3.372(2)	2.20(1)–2.69(1)	1.18(1), 1.22(1)	$Ag_{16}(C{\equiv}C)_2$ double cage, or $2 \times Ag_9(C{\equiv}C)$ distorted monocapped square antiprisms	198
$[Ag_2(C{\equiv}C){\cdot}9AgC_2F_5CO_2{\cdot}3MeCN{\cdot}H_2O$ **155**	2.845(1)–3.332(1)	2.167(8)–2.596(8)	1.19(1)	$Ag_{16}(C{\equiv}C)_2$ double cage, or $2 \times Ag_9(C{\equiv}C)$ monocapped square antiprism	200

$[Ag_2(C{\equiv}C)\cdot 6(AgC_2F_5CO_2\cdot 2(N\text{-}PyCH_2CO_2\text{-}p))]$ **156**	NA	2.19(1)–2.64(1)	1.21(2)	$Ag_{16}(C{\equiv}C)_2$ double cage, or $2 \times Ag_7(C{\equiv}C)$ irregular monocapped trigonal prism	204
$[Ag_4([18]crown\text{-}6)_4(H_2O)_3][Ag_{18}(C{\equiv}C)_3\text{-}(CF_3CO_2)_{16}(H_2O)_{2.5}]$ **157**	2.759(1)–3.319(1)	2.12(1)–2.635(9)	1.16(1)–1.20(1)	$Ag_{20}(C{\equiv}C)_3$, or $2 \times Ag_8(C{\equiv}C)$ triangulated dodecahedra + $Ag_8(C{\equiv}C)$ bicapped trigonal prism	194
$[Ag_{13}(C{\equiv}C)_2(CF_3CO_2)_9(PyPy\text{-}4,4')_4(H_2O)_3]$ **158**	2.816(3)–3.371(11)	2.098(9)–2.627(8)	1.20(1), 1.23(1)	$Ag_{24}(C{\equiv}C)_4$, or $2 \times Ag_8(C{\equiv}C)$ distorted pentagonal bipyramids + $2 \times Ag_8(C{\equiv}C)$ irregular bicapped trigonal prisms	198
$(Et_4N)_6[2\{Ag_2(C{\equiv}C)\}\cdot 8AgCF_3CO_2\cdot 3CF_3\text{-}CO_2\cdot 2H_2O]$ **159**	NA	2.11(2)–2.59(1)	1.18(1), 1.21(2)	$Ag_{24}(C{\equiv}C)_4$ quadruple cage, or $2 \times Ag_8(C{\equiv}C)$ bicapped trigonal prism and $2 \times Ag_8(C{\equiv}C)$ triangulated dodecahedron	207
$[Ag_{23}(C{\equiv}C)_4(CF_3CO_2)_{15}(PyCH_2CH_2CH_2Py\text{-}4,4')_6]\cdot H_2O$ **160**	2.818(2)–3.351(2)	2.073(14)–2.476(13)	1.158(20)–1.210(18)	$Ag_{25}(C{\equiv}C)_4$ column, or $Ag_7(C{\equiv}C)$ distorted monocapped trigonal prism + $Ag_7(C{\equiv}C)$irregular monocapped trigonal antiprism + $2 \times Ag_8(C{\equiv}C)$ distorted triangular dodecahedra	198
$[AgLi(C{\equiv}C)]$ **161**	NA	2.025(3)	1.278(6) (see text)	Ag–C≡C–Ag	209
$[AgK(C{\equiv}C)]$ **162**	NA	2.032(3)	1.223(6)	Ag–C≡C–Ag	209
$[AgCs(C{\equiv}C)]$ **163**	NA	2.015(4)	1.217(7)	Ag–C≡C–Ag	209
$[Ag_2(C{\equiv}CC{\equiv}C)\cdot 6AgNO_3\cdot 2H_2O]$ **164**	2.880(1)–3.069(1)	2.161(8)–2.338(8) (σ) 2.633(8) (π)	1.216(11)	$Ag_4(C{\equiv}CC{\equiv}C)Ag_4$ dumbbell structure	210
$[Ag_2(C{\equiv}CC{\equiv}C)\cdot 6AgNO_3\cdot 3H_2O]$ **165**	2.854(1)–3.317(1)	2.124(8)–2.419(10) (σ) 2.425(8)–2.503(9) (π)	1.236(11)–1.238(11)	$Ag_4(C{\equiv}CC{\equiv}C)Ag_4$ dumbbell structure	210

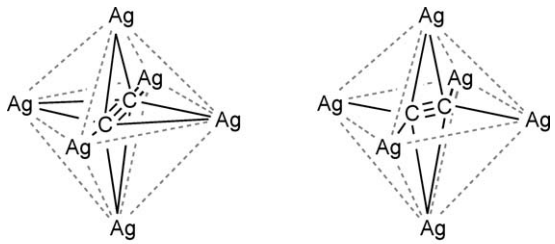

Figure 47 Structure of the $[Ag_6(C{=}C)]$ cages.

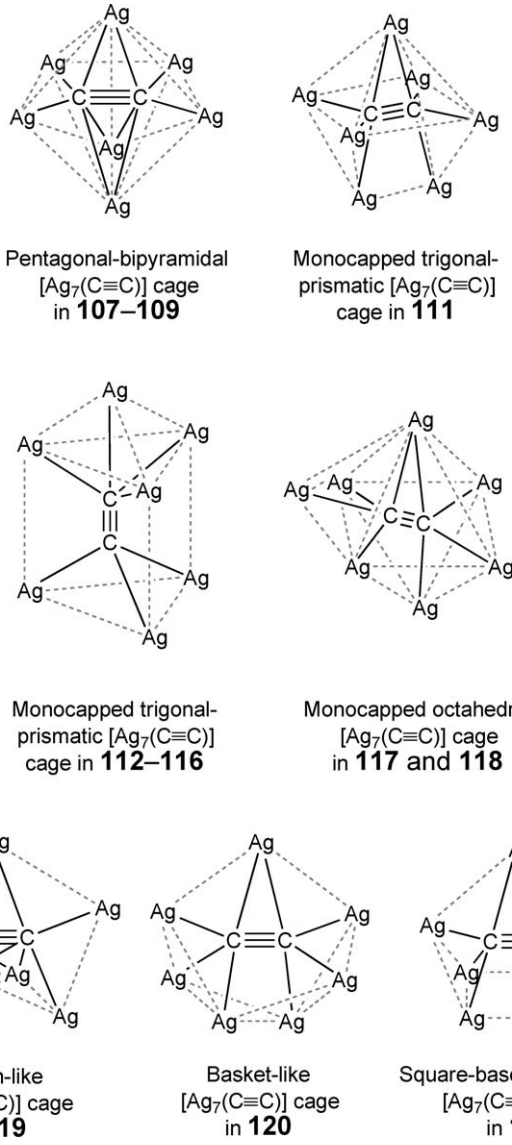

Figure 48 Structure of the $[Ag_7(C{=}C)]$ cages.

instead. A wide structural diversity has also been observed in $[Ag_8(C{\equiv}C)]$ cages, which could appear as rhombohedron **104**, triangulated dodecahedron **125–130**, bicapped trigonal prism **131** (Figure 49), **136**, and square antiprism **132–134**, and cubic cage has also been observed to constitute part of the $[Ag_{15}(C{\equiv}C)_2]$ double cage in **153**. $[Ag_9(C{\equiv}C)]$ cages appeared as monocapped cube **137**, monocapped square prism **138**, and monocapped square antiprism **139** (see Figure 50). For example, the distorted monocapped cubic $[Ag_9(C{\equiv}C)]$ cage in **137** stabilized the $C{\equiv}C^{2-}$ unit by six σ-type and one π-type interactions, with the relatively short C≡C bond distance indicative of a low degree of metal-to-ligand π-backbonding in such a silver-rich environment.[204] The cages were further connected via the anionic $CF_3CO_2^-$ and zwitterionic $Et_3N^+CH_2CO_2^-$ ligands to form a beadlike infinite chain. On the contrary, **139** consisted of distorted monocapped square-antiprismatic $[Ag_9(C{\equiv}C)]$ cages, surrounded by the anionic $CF_3CO_2^-$ ligands, as the basic building block, with the zwitterionic $Me_3N^+CH_2CO_2^-$ ligands as the linkers to connect the cages to form the overall beadlike structure.[204] The $C{\equiv}C^{2-}$ unit was encapsulated inside the cage by six σ-type and two π-type interactions. In addition, many of these salts possessed double or multiple cages as the basic building blocks. These double and multiple cages can mostly be visualized as fusion of the fundamental hexanuclear to nonanuclear cages via the sharing of common vertices and/or edges.[193,194,197,198,200,204,206–208]

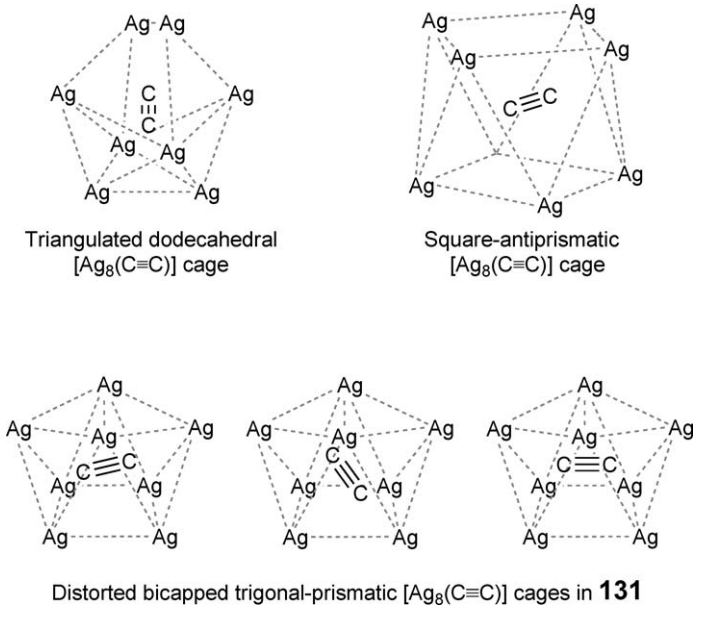

Figure 49 Structure of the $[Ag_8(C{=}C)]$ cages.

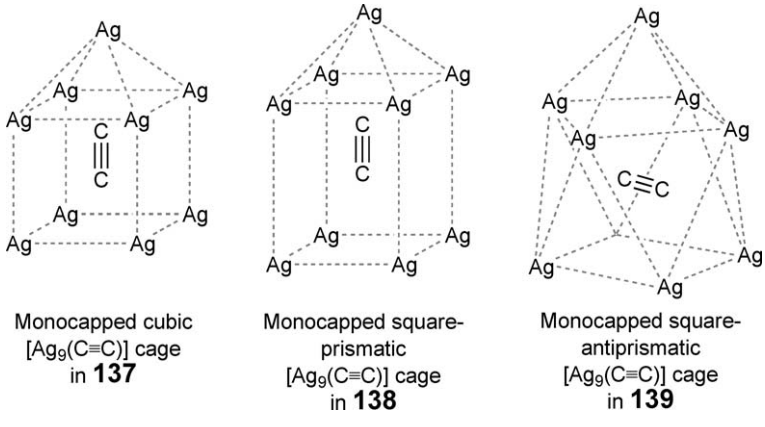

Figure 50 Structure of the $[Ag_9(C{=}C)]$ cages.

Very recently, ligand-induced disruption of polyhedral $[Ag_6(C{\equiv}C)]$ and $[Ag_{13}(C{\equiv}C)_2]$ cages has been achieved and reported.[211]

It is interesting to note that the C–C triple bond character for the acetylenediide inside the silver(I) cages is retained in most of the examples due to the close resemblance of their C≡C bond lengths (~1.09–1.28 Å) with that observed in free acetylene (1.205 Å).[212] The Ag–C bond distances, on the other hand, span a fairly wide range (~2.01–3.53 Å) due to the presence of both σ- and π-bonding interactions in these systems. The observation of short Ag–Ag contacts of ~2.71–3.37 Å, compared to that in silver metal (2.89 Å)[213] and the sum of van der Waals radii for silver (~3.4 Å),[31] was suggestive of weak argentophilic interactions associated with these complexes.

The crystal lattices of a series of ternary alkali metal–silver acetylenediide $[M^IAg(C{\equiv}C)]$ (M^I = Li **161**, Na, K **162**, Rb, Cs **163**) have been analyzed by Ruschewitz and co-workers using X-ray powder diffraction.[209] Neutron powder diffraction experiments have also been performed on **161–163** for obtaining precise bond lengths. It has been found that for **161** and **162**, the $[Ag(C{\equiv}C)]_n$ chains were packed parallel to each other, whereas for **163**, they were aligned in layers that were rotated by 90° with respect to each other (see Figure 51).

The Li^+ ions in **161** were coordinated by three AgC≡CAg dumbbells in a side-on fashion, giving rise to the basic structural motif of a distorted trigonal-bipyramidal Li_3Ag_2 cage encapsulating the $C{\equiv}C^{2-}$ unit. $[M^IAg(C{\equiv}C)]$ complexes with the larger alkali metal ions (Na, K, Rb, and Cs) have the alkali metal ions side-on coordinated by four AgC≡CAg dumbbells, affording the $C{\equiv}C^{2-}$ encapsulated $M^I_4Ag_2$ cage in the form of a distorted octahedron. The frequency of the Raman C≡C stretching vibration for $[M^IAg(C{\equiv}C)]$ (M^I = Li **161**, Na, K **162**, Rb, Cs **163**) was found to show little variation (1961–1965 cm^{-1}). Such findings supported the close similarity of the C≡C distances in these compounds. The exceptionally long C≡C bond distance observed for **161** (1.278(6) Å) was believed to be an artifact of the structural refinement due to the contamination of the sample with $[Li_2(C{\equiv}C)]_n$ and strong anisotropic reflection broadening. Related studies on the isoelectronic copper(I)[214] and gold(I)[215] systems were also reported.

Structural studies of the silver(I) acetylenediide multiple salt complexes were extended recently to the longer carbon chain counterpart, silver(I) 1,3-butadiynediide ($C{\equiv}CC{\equiv}C^{2-}$). Mak reported the synthesis of $[Ag_2(C{\equiv}CC{\equiv}C)]$ from the reaction of $[Li_2(C{\equiv}CC{\equiv}C)]$ (generated *in situ* from hexachloro-1,3-butadiene and Bu^nLi)[216] with 2 equiv. of $AgNO_3$ in thf under nitrogen at room temperature, followed by subsequent washing with saturated aqueous ammonia. The crude product, which was contaminated with 25% metallic silver, was a light grey amorphous powder with a melting temperature of 130 °C (with decomposition). It was insoluble in most solvents, and highly explosive when dried, heated, or shocked. Weak Raman C≡C stretches of 2153 and 1982 cm^{-1} were reported, corresponding to the ν_{sym} and ν_{asym} modes. Employing the crude $[Ag_2(C{\equiv}CC{\equiv}C)]$ as precursor, two silver(I) 1,3-butadiynediide double salts **164** and **165** (Figure 52) have been isolated.[210] The fundamental skeletons of the two salts were similar, with the C_4 chain being capped on both ends each with an Ag_4 butterfly-shaped basket, giving rise to an overall dumbbell structure.

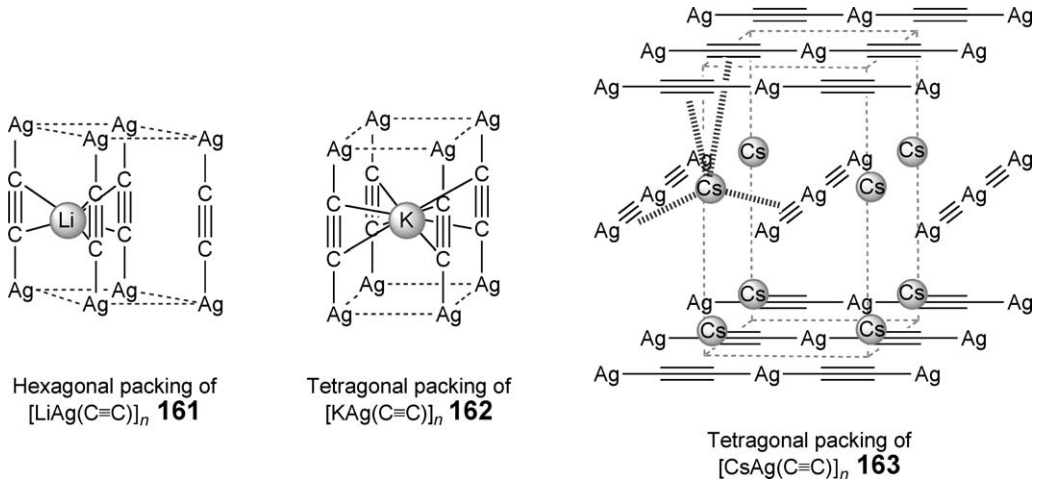

Figure 51 Ternary alkali metal–silver(I) acetylenediides.

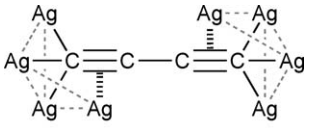

$[Ag_4C{\equiv}CC{\equiv}CAg_4]$
dumbbell structure
in **164** and **165**

Figure 52 Dumbbell structure of $[Ag_4C{\equiv}CC{\equiv}CAg_4]$ in **164** and **165**.

2.04.3 Silver(III) Organometallics

The chemistry of silver has been almost entirely dominated by those with oxidation state +1, and such a phenomenon could be attributed to the high relative stability of silver(I) over silver centers of higher oxidation numbers.[217] Silver(III) has an electronic configuration of $[Kr]4d^8$, and hence prefers a square-planar coordination geometry similar to the well-studied isoelectronic palladium(II), platinum(II), and gold(III) systems. In general, silver(III) compounds are fairly unstable when isolated. Silver(III) complexes are strongly oxidizing in nature. The high charge density of the small silver(III) metal center would in general possess a low-lying unoccupied $d_{x^2-y^2}$ orbital, which is susceptible to electrons or nucleophilic attack and makes the silver(III) center readily reducible. Successful synthesis and isolation of stable organometallic silver(III) compounds have been accomplished since the late 1990s by disproportionation reactions from silver(I) precursors, through the employment of perfluoroalkyl ligands, or polydentate ligands with hard donor groups arranged in a pre-organized and well-defined geometrical arrangement such as carbaporphyrinoids.[218] The relative superior stability of these silver(III) organometallics is often attributed to the use of strong field ligands that raise the energy level of the $d_{x^2-y^2}$ orbital of silver, and hence renders it relatively less accessible to donors. On the other hand, the use of perfluoroorganics could render all the bonding orbitals more low-lying in energy, so as to further enhance the overall stability.[219,220]

2.04.3.1 Silver(III) Complexes with Alkyl, Alkynyl, and Cyano Ligands

In 1986, Dukat and Naumann reported a surprisingly stable silver(III) ion, $[Ag(CF_3)_4]^-$, in the form of a mixed silver(I)–silver(III) salt $Ag^I[Ag^{III}(CF_3)_4]$ **166**.[221] It was formed upon the facile disproportionation reaction of the silver(I) complex, $[Ag(CF_3)_2]^-$, prepared *in situ* from the treatment of silver(I) salts like silver(I) nitrate or silver(I) acetate with $[Cd(CF_3)_2]$, according to Equations (2) and (3).

$$[Cd(CF_3)_2] + Ag^+ \xrightarrow[30\,^\circ C]{\text{glyme/dmf}} [Ag(CF_3)_2]^- + Cd^{2+} \quad (2)$$

$$2[Ag(CF_3)_2]^- + Ag^+ \longrightarrow [Ag(CF_3)_4]^- + 2Ag(0) \quad (3)$$

Complex **166** has unusually high thermal and photolytic stability, with a thermal degradation temperature close to 100 °C. It is also stable in the presence of air and water. The solid-state structure of this tetrakis(trifluoromethyl)-argentate(III) ion, coupled with the semiconducting tetrathiafulvalenes, was determined crystallographically in 1995.[222,223] The silver(III) center possessed a square-planar geometry and was bonded to four trifluoromethyl groups with average Ag–C bond distances of 2.09–2.11 Å, and C–Ag–C angles of 87.3–89.8° and 173.0(5)–180°.

Stable organosilver(III) complexes having a general formula $[Ag(CF_3)_nX_{(4-n)}]^-$ with organic groups such as cyano, halo, methyl, alkynyl, difluoromethyl, and perfluoroethyl, replacing the trifluoromethyl groups in the $[Ag(CF_3)_4]^-$ anion, as well as $[Ag(CF_3)_3(NCMe)]$, were prepared.[219,224,225] For instance, the air and moisture sensitive silver(I) complex $[Ag(CF_3)(CN)]^-$, obtained from trifluoromethylation of $[Ag(CN)_2]^-$ with $[Cd(CF_3)_2{\cdot}glyme]$, was readily oxidized by bromine to yield $[Ag(CF_3)_n(CN)_{4-n}]^-$ ($n = 1$–4), which was isolated in the form of PPh_4^+ salts. Halogenation of these complexes with acetyl chloride or bromine to afford $[Ag(CF_3)_nX_{4-n}]^-$ (X = Cl, Br; $n = 1$–4) was also accomplished, albeit the products were stable only when $n = 3$. Subsequent dehalogenation with $AgNO_3$ in a donor solvent (solv) gave the solvento complex, $[Ag(CF_3)_n(solv)_{4-n}]^{3-n}$ ($n = 2$, 3) (see Equations (4) and (5)).

$$2[Ag(CN)_2]^- \xrightarrow[-[Cd(CN)_2]]{+[Cd(CF_3)_2]} 2[Ag(CF_3)(CN)]^- \xrightarrow[-AgBr\ -Br]{+Br_2} 2[Ag(CF_3)_n(CN)_{4-n}]^- \quad (n = 1-4) \tag{4}$$

$$[Ag(CF_3)_3(CN)]^- \xrightarrow[-CH_3C(O)CN]{+CH_3C(O)Cl} [Ag(CF_3)_3Cl]^- \xrightarrow[+solv\ -AgCl]{+Ag^+} [Ag(CF_3)_3(solv)] \quad (solv = dmf, dmso, MeCN, glyme, py) \tag{5}$$

The synthesis of $[Ag(CF_3)_nR_{4-n}]^-$ (R = Me, C≡CCy; $n = 2$, 3) was accomplished by the reaction of the related $[Ag(CF_3)_n(CN)_{4-n}]$ with MeMgCl and LiC≡CCy, respectively. In general, the stability of all these complexes decreases significantly with an increasing number of less fluorinated groups and/or a decrease in the degree of fluorination within the groups. The solid-state crystal structures of *trans*-$(Ph_4P)[Ag(CF_3)_2(CN)_2]$ **167**, $(Ph_4P)[Ag(CF_3)_3Me]$ **168**, and (ppn)$[Ag(CF_2H)_4]$ **169** further supported the almost ideal square-planar geometry about the silver(III) centers in this class of complexes. The Ag–C(alkyl) bonds have values of 2.105(4) Å for **167**, 2.097(5)–2.127(5) Å for **168**, and 2.07(1)–2.10(2) Å for **169**, and are comparable to those observed in the $[Ag(CF_3)_4]^-$ anion.[222,223] The Ag–C(cyano) bond of 2.013(3) Å in **167** is significantly shorter than the σ(Ag–C) bonds (ca. 2.05 Å) observed in other isolated anionic complexes.[219]

2.04.3.2 *N*-confused Porphyrin System

N-confused porphyrins refer to the isomeric forms of porphyrin-type ligands, with at least one of the pyrrole units being inverted. This class of ligands possesses at least one carbon and at most three nitrogen donor atoms, giving a total of four donor atoms that provide a pre-organized square-planar coordination environment for transition metal centers, and has been found to be able to stabilize transition metals in the unusually high oxidation states. Compared to the usual porphyrin-type ligands, the replacement of nitrogen by the less electronegative carbon donor atoms would enhance the σ-donating ability of the ligand, and hence would be capable of stabilizing metal centers in the high oxidation states to a better extent. This effect of stabilization has been demonstrated in the examples with silver metal centers. The first report on the isolation of porphyrin-type organometallic silver(III) complexes appeared in 1999. Based on prior developments in silver(II/III) porphyrin and palladium(II) *N*-confused porphyrin systems, Furuta reported a silver(III) *N*-confused porphyrin complex, [Ag(NCTPP)] **170**, which was synthesized by the reaction of silver(I) trifluoroacetate with the free base ligand H_3NCTPP in dichloromethane/methanol at room temperature (Scheme 22).[226]

The complex has been structurally characterized, and the silver(III) center was found to adopt a slightly distorted square-planar geometry, tetra-coordinated with one carbon and three nitrogen atoms of the *N*-confused porphyrin ring forming one Ag–C and three Ag–N bonds, respectively. The Ag–C bond distance was found to be 2.04(2) Å. The complex was found to be essentially planar in structure with the N–Ag–N angles of 89.7(8), 89.6(9), and 179(1)° and N–Ag–C angle of 90.3(9), 90.9(1), and 179(1)°, very close to the ideal values of 90 and 180°. No counterion was detected in the structure, suggesting that the complex has a neutral charge. The diamagnetic nature of the complex was confirmed by magnetic susceptibility and NMR studies, which were used to exclude the possibility of the complex bearing a silver(II) center. Unlike the usual porphyrin system, in which silver(II) porphyrin complexes were first isolated and subsequent chemical oxidation produced the silver(III) porphyrins, isolation of the silver(II) *N*-confused porphyrins has not been achieved, but instead the silver(III) *N*-confused porphyrins were obtained spontaneously.

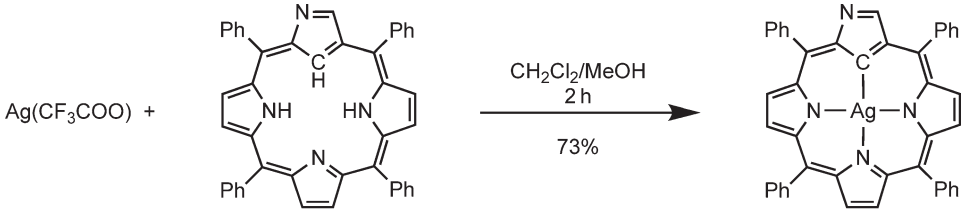

170

Scheme 22

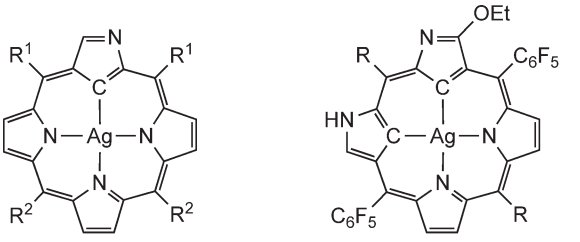

171: $R^1 = R^2 = C_6F_5$
172: R^1 = Ph; R^2 = H

173a: R = C_6F_5
173b: R = 2,6-$C_6H_3Cl_2$
173c: R = 2-$C_6H_4NO_2$
173d: R = 3-$C_6H_4NO_2$
173e: R = 4-$C_6H_4NO_2$

Figure 53 Structure of **171**, **172** and **173a–e**.

Later, extension of the work to the silver(III) mono- and doubly *N*-confused porphyrins with various organic pendants has been achieved by the same group.[227–230] Similarly, the silver(III) centers possessed a slightly distorted square-planar coordination geometry, with short Ag–C bond distances of ca. 2.033(4) Å for **171** and 1.987(8) Å and 2.011(8) Å for **173a** (see Figure 53). Its acid–base, spectroelectrochemical, and photochemical properties were also studied in conjunction with the free base ligands as well as the analogous copper(III) complex.[231–233] It was demonstrated that **173a** could be used as a very efficient singlet oxygen photosensitizer in acetonitrile solution, with a singlet oxygen quantum yield of 0.92.[232,233] Substituted *N*-confused porphyrins at the nitrogen of the "external" pyrrole were achieved by direct alkylation, and subsequent reactions with silver(I) salts gave a series of silver(III) *N*-confused porphyrins **174–178**, as shown in Schemes 23 and 24. The presence of **174** and **175** was identified in solution state only, while **176–178** were isolated as solids (Schemes 23 and 24).[234]

2.04.3.3 Carbaporphyrinoid System

In addition to the *N*-confused porphyrins, carbaporphyrinoids represent another class of ligands in the porphyrin family. In general, they are porphyrin-type compounds with one or more pyrrole units being replaced with carbocyclic moieties. The organosilver chemistry of this class of ligands was started only in 2002 when Lash and co-workers reported the first class of silver(III) carbaporphyrin complexes.[235] By the reaction of silver(I) acetate with the carbaporphyrin ligands in methanol–dichloromethane at room temperature, **179a** and **179b** could be obtained in good yield (Scheme 25).

It is noteworthy to mention that employment of silver(I) trifluoroacetate in place of silver(I) acetate, as in the case of *N*-confused porphyrin, did not give the desired products. This has been attributed to the better basicity of the acetate anion than the trifluoroacetate, which aided the deprotonation of the three interior CH/NH protons at the carbaporphyrin ligand. Besides, it has been noticed that an excessive amount of silver acetate was required for the synthesis. The mechanism of the silver insertion reaction for this type of ligands was proposed, according to what Brückner had proposed for the synthesis of silver(III) *meso*-triarylcorroles.[218,236] The reaction was suggested to occur via a disproportionation reaction, with the supportive observation of silver deposit formation after the reaction.[237]

$$3\mathrm{Ag(I)} \rightarrow \mathrm{Ag(III)} + 2\mathrm{Ag(0)}$$

The crystal structure for **179b** was determined which showed a planar geometry for the silver center and the carbaporphyrin ligand. A small tilt angle of 5.09° for the indene unit relative to the mean macrocyclic plane was determined, and the Ag–C bond length was 2.015(4) Å. Extension of the work to the benzocarba-, benzi-, oxybenzi-, oxynaphthi-, tropi-, and azuliporphyrins was reported.[238–240]

2.04.3.4 *O*-confused Oxaporphyrin System

Modification of the carbaporphyrin ligands could also be made by the interchange of an exocyclic methine group with a heteroatom such as oxygen. Ligands of this type are referred to as *O*-confused oxaporphyrins. Silver(III) complexes

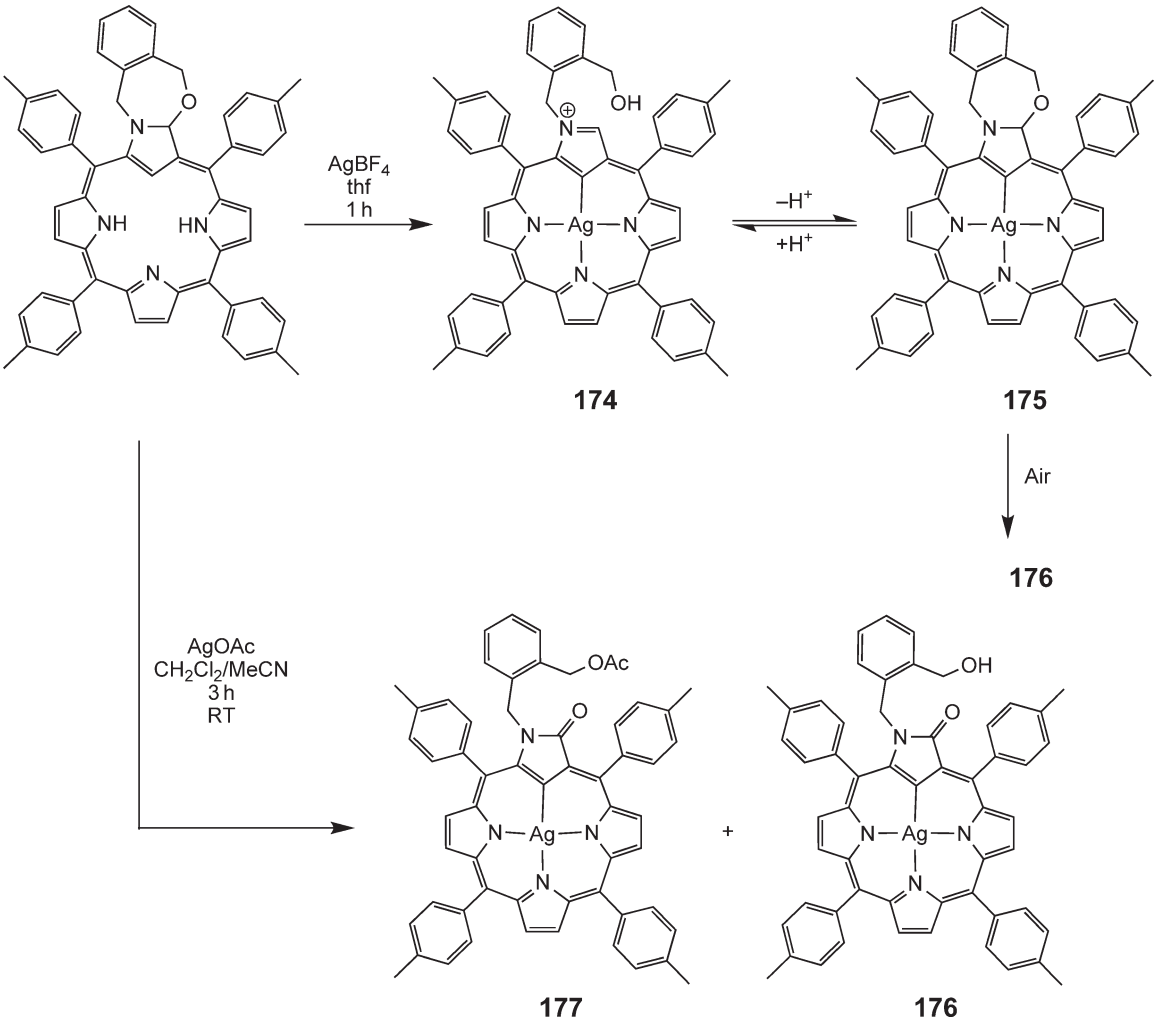

Scheme 23

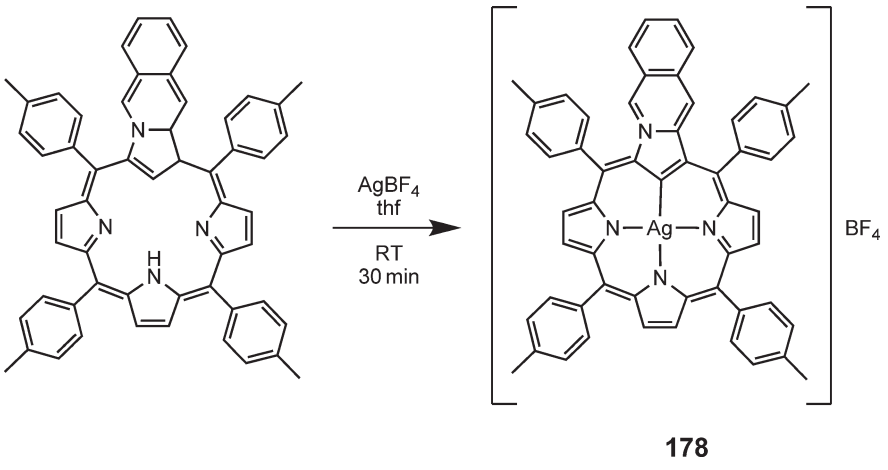

Scheme 24

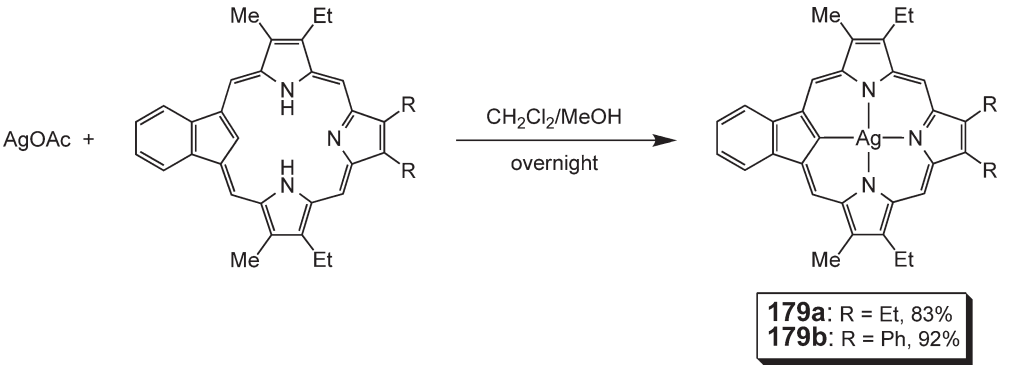

Scheme 25

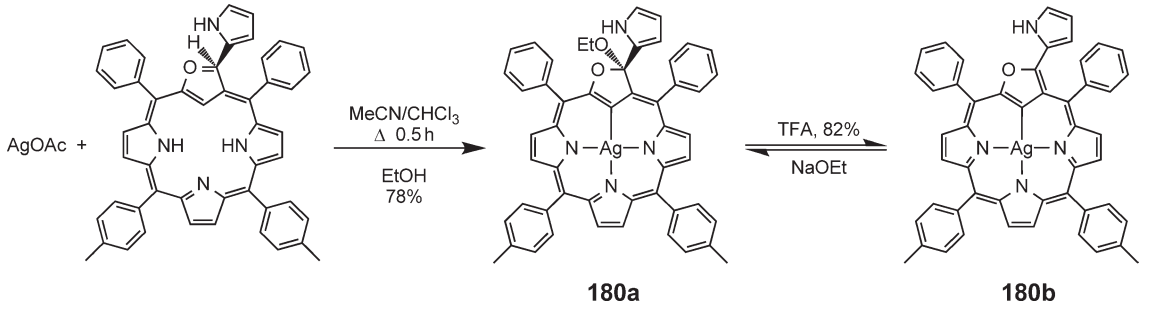

Scheme 26

with this class of ligands were reported by Latos-Grażyński and co-workers.[241] The reaction of silver(I) acetate with the free base ligand in refluxing chloroform–acetonitrile, followed by reaction with ethanol, gave **180a** in 78% yield. The crystal structure of **180a** revealed an Ag–C bond distance of 2.020(7) Å, which was comparable to distances found in other silver(III) carbaporphyrin complexes.[226,235] Interconversion of **180a** and **180b** was achieved by respective addition of trifluoroacetic acid (TFA) and sodium ethoxide (Scheme 26).

References

1. Beverwijk, C. D. M.; Van Der Kerk, G. J. M.; Leusink, A. J.; Noltes, J. G. *Organomet. Chem. Rev. A* **1970**, *5*, 215–280.
2. Schmidbaur, H.; Bayler, A. In *The Chemistry of Organic Derivatives of Gold and Silver*; Patai, S., Rappoport, Z., Eds.; Wiley: Chichester, 1999; pp 211–225.
3. Fackler, J. P.; Liu, C. W. *Sci. Synth.* **2004**, *3*, 663–690.
4. Van Koten, G.; Noltes, J. G. In *Comprehensive Organometallic Chemistry I*; Wilkinson, G., Stone, F. G. A., Abel, E. W., Eds.; Pergamon: Oxford, 1982; Vol. 2, pp 709–763.
5. Van Koten, G.; James, S. L.; Jastrzebski, J. T. B. H. In *Comprehensive Organometallic Chemistry II*; Abel, E. W., Stone, F. G. A., Wilkinson, G., Eds.; Elsevier: Oxford, 1995; Vol. 3, pp 57–133.
6. Semerano, G.; Riccoboni, L. *Ber.* **1941**, *74B*, 1089–1099.
7. Semerano, G.; Riccoboni, L.; Callegari, F. *Ber.* **1941**, *74B*, 1297–1308.
8. Semerano, G.; Riccoboni, L.; Götz, L. *Z. Elektrochem.* **1941**, *47*, 484–486.
9. Semerano, G.; Riccoboni, L. *Z. Physik. Chem.* **1941**, *A189*, 203–218.
10. Tyrra, W.; Naumann, D. J. *Fluorine Chem.* **2004**, *125*, 823–830.
11. Antes, I.; Frenking, G. *Organometallics* **1995**, *14*, 4263–4268.
12. Miller, W. T.; Snider, R. H.; Hummel, R. J. *J. Am. Chem. Soc.* **1969**, *91*, 6532–6534.
13. Oehr, C.; Suhr, H. *Appl. Phys. A* **1989**, *49*, 691–696.
14. Jeffries, P. M.; Wilson, S. R.; Girolami, G. S. *J. Organomet. Chem.* **1993**, *449*, 203–209.
15. Nesmeyanov, A. N.; Sedova, N. N.; Struchkov, Y. T.; Andrianov, V. G.; Stakheeva, E. N.; Sazonova, V. A. *J. Organomet. Chem.* **1978**, *153*, 115–122.
16. Meyer, M. E.; Gambarotta, S.; Floriani, C.; Chiesi-Villa, A.; Guastini, C. *Organometallics* **1989**, *8*, 1067–1079.
17. Tyrra, W. E. *J. Fluorine Chem.* **2001**, *112*, 149–152.

18. Tyrra, W.; Wickleder, M. S. *Z. Anorg. Allg. Chem.* **2002**, *628*, 1841–1847.
19. Leusink, A. J.; van Koten, G.; Noltes, J. G. *J. Organomet. Chem.* **1973**, *56*, 379–390.
20. Edwards, D. A.; Harker, R. M.; Mahon, M. F.; Molloy, K. C. *J. Chem. Soc., Dalton Trans.* **1997**, 3509–3513.
21. Kronenburg, C. M. P.; Jastrzebski, J. T. B. H.; Boersma, J.; Lutz, M.; Spek, A. L.; van Koten, G. *J. Am. Chem. Soc.* **2002**, *124*, 11675–11683.
22. Hwang, C.-S.; Power, P. P. *J. Organomet. Chem.* **1999**, *589*, 234–238.
23. Papasergio, R. I.; Raston, C. L.; White, A. H. *J. Chem. Soc., Chem. Commun.* **1984**, 612–613.
24. van den Ancker, T. R.; Raston, C. L. *J. Organomet. Chem.* **1995**, *500*, 289–297.
25. van den Ancker, T. R.; Bhargava, S. K.; Mohr, F.; Papadopoulos, S.; Raston, C. L.; Skelton, B. W.; White, A. H. *J. Chem. Soc., Dalton Trans.* **2001**, 3069–3072.
26. Naumann, D.; Wessel, W.; Hahn, J.; Tyrra, W. *J. Organomet. Chem.* **1997**, *547*, 79–88.
27. Voelker, H.; Labahn, D.; Bohnen, F. M.; Herbst-Irmer, R.; Roesky, H. W.; Stalke, D.; Edelmann, F. T. *New J. Chem.* **1999**, *23*, 905–909.
28. Belanzoni, P.; Rosi, M.; Sgamellotti, A.; Baerends, E. J.; Floriani, C. *Chem. Phys. Lett.* **1996**, *257*, 41–48.
29. Contel, M.; Jiménez, J.; Jones, P. G.; Laguna, A.; Laguna, M. *J. Chem. Soc., Dalton Trans.* **1994**, 2515–2518.
30. Contel, M.; Garrido, J.; Gimeno, M. C.; Jones, P. G.; Laguna, A.; Laguna, M. *Organometallics* **1996**, *15*, 4939–4943.
31. Bondi, A. *J. Phys. Chem.* **1964**, *68*, 441–451.
32. Fernández, E. J.; Gimeno, M. C.; Laguna, A.; López-de-Luzuriaga, J. M.; Monge, M.; Pyykkö, P.; Sundholm, D. *J. Am. Chem. Soc.* **2000**, *122*, 7287–7293.
33. Laguna, M.; Villacampa, M. D.; Contel, M.; Garrido, J. *Inorg. Chem.* **1998**, *37*, 133–135.
34. Janssen, M. D.; Herres, M.; Spek, A. L.; Grove, D. M.; Lang, H.; van Koten, G. *J. Chem. Soc., Chem. Commun.* **1995**, 925–926.
35. Janssen, M. D.; Köhler, K.; Herres, M.; Dedieu, A.; Smeets, W. J. J.; Spek, A. L.; Grove, D. M.; Lang, H.; van Koten, G. *J. Am. Chem. Soc.* **1996**, *118*, 4817–4829.
36. Lang, H.; Köhler, K.; Rheinwald, G.; Zsolnai, L.; Büchner, M.; Driess, A.; Huttner, G.; Strähle, J. *Organometallics* **1999**, *18*, 598–605.
37. Gimeno, M. C.; Jones, P. G.; Laguna, A.; Villacampa, M. D. *J. Chem. Soc., Dalton Trans.* **1995**, 805–810.
38. Bardají, M.; Laguna, A.; Laguna, M. *J. Organomet. Chem.* **1995**, *496*, 245–248.
39. García, M. P.; Jiménez, M. V.; Lahoz, F. J.; Oro, L. A. *Inorg. Chem.* **1995**, *34*, 2153–2159.
40. Doucette, W. J.; Kim, J.; Kautz, J. A.; Gipson, S. L. *Inorg. Chim. Acta* **2000**, *304*, 237–240.
41. Forniés, J.; Martín, A.; Martín, L. F.; Menjón, B.; Kalamarides, H. A.; Rhodes, L. F.; Day, C. S.; Day, V. W. *Chem. Eur. J.* **2002**, *8*, 4925–4934.
42. Albéniz, A. C.; Espinet, P.; Martín-Ruiz, B. *Chem. Eur. J.* **2001**, *7*, 2481–2489.
43. Albéniz, A. C.; Espinet, P.; López-Cimas, O.; Martín-Ruiz, B. *Chem. Eur. J.* **2005**, *11*, 242–252.
44. Ara, I.; Forniés, J.; Ramos, S.; Tomás, M. *Synth. React. Inorg. Met.-Org. Chem.* **2003**, *33*, 1723–1739.
45. Mendia, A.; Cerrada, E.; Fernandez, E. J.; Laguna, A.; Laguna, M. *J. Organomet. Chem.* **2002**, *663*, 289–296.
46. Naumann, D.; Tyrra, W.; Herrmann, R.; Pantenburg, I.; Wickleder, M. S. *Z. Anorg. Allg. Chem.* **2002**, *628*, 833–842.
47. Codina, A.; Fernández, E. J.; Jones, P. G.; Laguna, A.; López-de-Luzuriaga, J. M.; Monge, M.; Olmos, M. E.; Pérez, J.; Rodriguez, M. A. *J. Am. Chem. Soc.* **2002**, *124*, 6781–6786.
48. Wessel, W.; Tyrra, W.; Naumann, D. *Z. Anorg. Allg. Chem.* **2001**, *627*, 1264–1268.
49. Bunge, S. D.; Boyle, T. J.; Headley, T. J. *Nano Lett.* **2003**, *3*, 901–905.
50. Schönherr, H.-J.; Wanzlick, H.-W. *Angew. Chem., Int. Ed.* **1968**, *7*, 141–142.
51. Öfele, K. *J. Organomet. Chem.* **1968**, *12*, P42–P43.
52. Arduengo, A. J., III; Harlow, R. L.; Kline, M. *J. Am. Chem. Soc.* **1991**, *113*, 361–363.
53. Bourissou, D.; Guerret, O.; Gabbaï, F. P.; Bertrand, G. *Chem. Rev.* **2000**, *100*, 39–91.
54. Weskamp, T.; Böhm, V. P. W.; Herrmann, W. A. *J. Organomet. Chem.* **2000**, *600*, 12–22.
55. Herrmann, W. A. *Angew. Chem., Int. Ed.* **2002**, *41*, 1290–1309.
56. Arnold, P. L. *Heteroatom Chem.* **2002**, *13*, 534–539.
57. Perry, M. C.; Burgess, K. *Tetrahedron: Asymmetry* **2003**, *14*, 951–961.
58. Lin, I. J. B.; Vasam, C. S. *Comments Inorg. Chem.* **2004**, *25*, 75–129.
59. Arduengo, A. J., III; Dias, H. V. R.; Calabrese, J. C.; Davidson, F. *Organometallics* **1993**, *12*, 3405–3409.
60. Guerret, O.; Solé, S.; Gornitzka, H.; Teichert, M.; Trinquier, G.; Bertrand, G. *J. Am. Chem. Soc.* **1997**, *119*, 6668–6669.
61. Guerret, O.; Solé, S.; Gornitzka, H.; Trinquier, G.; Bertrand, G. *J. Organomet. Chem.* **2000**, *600*, 112–117.
62. Fox, M. A.; Mahon, M. F.; Patmore, N. J.; Weller, A. S. *Inorg. Chem.* **2002**, *41*, 4567–4573.
63. Chung, M. C. *Bull. Korean Chem. Soc.* **2002**, *23*, 1160–1162.
64. Chung, M. C. *Bull. Korean Chem. Soc.* **2002**, *23*, 921–923.

65a. Caballero, A.; Díez-Barra, E.; Jalón, F. A.; Merino, S.; Tejeda, J. *J. Organomet. Chem.* **2001**, *617–618*, 395–398.

65b. Caballero, A.; Díez-Barra, E.; Jalón, F. A.; Merino, S.; Tejeda, J. *J. Organomet. Chem.* **2001**, *627*, 263–264.

66. Wang, H. M. J.; Lin, I. J. B. *Organometallics* **1998**, *17*, 972–975.
67. Chianese, A. R.; Li, X.; Janzen, M. C.; Faller, J. W.; Crabtree, R. H. *Organometallics* **2003**, *22*, 1663–1667.
68. Ramnial, T.; Abernethy, C. D.; Spicer, M. D.; McKenzie, I. D.; Gay, I. D.; Clyburne, J. A. C. *Inorg. Chem.* **2003**, *42*, 1391–1393.
69. Sentman, A. C.; Csihony, S.; Waymouth, R. M.; Hedrick, J. L. *J. Org. Chem.* **2005**, *70*, 2391–2393.
70. Lee, K. M.; Wang, H. M. J.; Lin, I. J. B. *J. Chem. Soc., Dalton Trans.* **2002**, 2852–2856.
71. Chen, W.; Liu, F. *J. Organomet. Chem.* **2003**, *673*, 5–12.
72. Boehme, C.; Frenking, G. *Organometallics* **1998**, *17*, 5801–5809.
73. Nemcsok, D.; Wichmann, K.; Frenking, G. *Organometallics* **2004**, *23*, 3640–3646.
74. Lee, C. K.; Lee, K. M.; Lin, I. J. B. *Organometallics* **2002**, *21*, 10–12.
75. Li, D.; Liu, D. *J. Chem. Crystallogr.* **2003**, *33*, 989–991.
76. Liu, Q.-X.; Xu, F.-B.; Li, Q.-S.; Zeng, X.-S.; Leng, X.-B.; Chou, Y. L.; Zhang, Z.-Z. *Organometallics* **2003**, *22*, 309–314.
77. Bildstein, B.; Malaun, M.; Kopacka, H.; Wurst, K.; Mitterböck, M.; Ongania, K.-H.; Opromolla, G.; Zanello, P. *Organometallics* **1999**, *18*, 4325–4336.
78. Pytkowicz, J.; Roland, S.; Mangeney, P. *J. Organomet. Chem.* **2001**, *631*, 157–163.
79. Pytkowicz, J.; Roland, S.; Mangeney, P. *Tetrahedron: Asymmetry* **2001**, *12*, 2087–2089.
80. Alexakis, A.; Winn, C. L.; Guillen, F.; Pytkowicz, J.; Roland, S.; Mangeney, P. *Adv. Synth. Catal.* **2003**, *345*, 345–348.
81. Pytkowicz, J.; Roland, S.; Mangeney, P.; Meyer, G.; Jutand, A. *J. Organomet. Chem.* **2003**, *678*, 166–179.

82. Herrmann, W. A.; Schneider, S. K.; Öfele, K.; Sakamoto, M.; Herdtweck, E. *J. Organomet. Chem.* **2004**, *689*, 2441–2449.
83. Pyykkö, P. *Chem. Rev.* **1997**, *97*, 597–636.
84. Yam, V. W.-W.; Lo, K. K.-W. *Chem. Soc. Rev.* **1999**, *28*, 323–334.
85. Catalano, V. J.; Malwitz, M. A. *Inorg. Chem.* **2003**, *42*, 5483–5485.
86. Catalano, V. J.; Malwitz, M. A.; Etogo, A. O. *Inorg. Chem.* **2004**, *43*, 5714–5724.
87. McGuinness, D. S.; Cavell, K. J. *Organometallics* **2000**, *19*, 741–748.
88. Tulloch, A. A. D.; Danopoulos, A. A.; Winston, S.; Kleinhenz, S.; Eastham, G. *J. Chem. Soc., Dalton Trans.* **2000**, 4499–4506.
89. Coleman, K. S.; Chamberlayne, H. T.; Turberville, S.; Green, M. L. H.; Cowley, A. R. *J. Chem. Soc., Dalton Trans.* **2003**, 2917–2922.
90. Frøseth, M.; Dhindsa, A.; Røise, H.; Tilset, M. *J. Chem. Soc., Dalton Trans.* **2003**, 4516–4524.
91. Bonnet, L. G.; Douthwaite, R. E.; Kariuki, B. M. *Organometallics* **2003**, *22*, 4187–4189.
92. César, V.; Bellemin-Laponnaz, S.; Gade, L. H. *Organometallics* **2002**, *21*, 5204–5208.
93. Kascatan-Nebioglu, A.; Panzner, M. J.; Garrison, J. C.; Tessier, C. A.; Youngs, W. J. *Organometallics* **2004**, *23*, 1928–1931.
94. Larsen, A. O.; Leu, W.; Oberhuber, C. N.; Campbell, J. E.; Hoveyda, A. H. *J. Am. Chem. Soc.* **2004**, *126*, 11130–11131.
95. Van Veldhuizen, J. J.; Campbell, J. E.; Giudici, R. E.; Hoveyda, A. H. *J. Am. Chem. Soc.* **2005**, *127*, 6877–6882.
96. Lee, H. M.; Zeng, J. Y.; Hu, C.-H.; Lee, M.-T. *Inorg. Chem.* **2004**, *43*, 6822–6829.
97. Chiu, P. L.; Lee, H. M. *Organometallics* **2005**, *24*, 1692–1702.
98. Chen, W.; Wu, B.; Matsumoto, K. *J. Organomet. Chem.* **2002**, *654*, 233–236.
99. Chiu, P. L.; Chen, C. Y.; Zeng, J. Y.; Lu, C. Y.; Lee, H. M. *J. Organomet. Chem.* **2005**, *690*, 1682–1687.
100. Wanniarachchi, Y. A.; Khan, M. A.; Slaughter, L. M. *Organometallics* **2004**, *23*, 5881–5884.
101. Hu, X.; Tang, Y.; Gantzel, P.; Meyer, K. *Organometallics* **2003**, *22*, 612–614.
102. Hu, X.; Castro-Rodriguez, I.; Olsen, K.; Meyer, K. *Organometallics* **2004**, *23*, 755–764.
103. Baker, M. V.; Brown, D. H.; Haque, R. A.; Skelton, B. W.; White, A. H. *Dalton Trans.* **2004**, 3756–3764.
104. Nielsen, D. J.; Cavell, K. J.; Skelton, B. W.; White, A. H. *Inorg. Chim. Acta* **2002**, *327*, 116–125.
105. Danopoulos, A. A.; Tulloch, A. A. D.; Winston, S.; Eastham, G.; Hursthouse, M. B. *Dalton Trans.* **2003**, 1009–1015.
106. Simons, R. S.; Custer, P.; Tessier, C. A.; Youngs, W. J. *Organometallics* **2003**, *22*, 1979–1982.
107. Douthwaite, R. E.; Houghton, J.; Kariuki, B. M. *Chem. Commun.* **2004**, 698–699.
108. Garrison, J. C.; Simons, R. S.; Talley, J. M.; Wesdemiotis, C.; Tessier, C. A.; Youngs, W. J. *Organometallics* **2001**, *20*, 1276–1278.
109. Garrison, J. C.; Simons, R. S.; Tessier, C. A.; Youngs, W. J. *J. Organomet. Chem.* **2003**, *673*, 1–4.
110. Garrison, J. C.; Simons, R. S.; Kofron, W. G.; Tessier, C. A.; Youngs, W. J. *Chem. Commun.* **2001**, 1780–1781.
111. Arnold, P. L.; Scarisbrick, A. C.; Blake, A. J.; Wilson, C. *Chem. Commun.* **2001**, 2340–2341.
112. Arnold, P. L.; Scarisbrick, A. C. *Organometallics* **2004**, *23*, 2519–2521.
113. Nielsen, D. J.; Cavell, K. J.; Skelton, B. W.; White, A. H. *Inorg. Chim. Acta* **2003**, *352*, 143–150.
114. Melaiye, A.; Simons, R. S.; Milsted, A.; Pingitore, F.; Wesdemiotis, C.; Tessier, C. A.; Youngs, W. J. *J. Med. Chem.* **2004**, *47*, 973–977.
115. Melaiye, A.; Sun, Z.; Hindi, K.; Milsted, A.; Ely, D.; Reneker, D. H.; Tessier, C. A.; Youngs, W. J. *J. Am. Chem. Soc.* **2005**, *127*, 2285–2291.
116. Perry, M. C.; Cui, X.; Burgess, K. *Tetrahedron: Asymmetry* **2002**, *13*, 1969–1972.
117. Ku, R.-Z.; Huang, J.-C.; Cho, J.-Y.; Kiang, F.-M.; Reddy, K. R.; Chen, Y.-C.; Lee, K.-J.; Lee, J.-H.; Lee, G.-H., Peng, S.-M., *et al. Organometallics* **1999**, *18*, 2145–2154.
118. Julian, R. R.; May, J. A.; Stoltz, B. M.; Beauchamp, J. L. *J. Am. Chem. Soc.* **2003**, *125*, 4478–4486.
119. Perreault, D.; Drouin, M.; Michel, A.; Harvey, P. D. *Inorg. Chem.* **1992**, *31*, 3688–3689.
120. Fortin, D.; Drouin, M.; Turcotte, M.; Harvey, P. D. *J. Am. Chem. Soc.* **1997**, *119*, 531–541.
121. Turcotte, M.; Harvey, P. D. *Inorg. Chem.* **2002**, *41*, 2971–2974.
122. Perreault, D.; Drouin, M.; Michel, A.; Harvey, P. D. *Inorg. Chem.* **1993**, *32*, 1903–1912.
123. Fortin, D.; Drouin, M.; Harvey, P. D.; Herring, F. G.; Summers, D. A.; Thompson, R. C. *Inorg. Chem.* **1999**, *38*, 1253–1260.
124. Fortin, D.; Drouin, M.; Harvey, P. D. *J. Am. Chem. Soc.* **1998**, *120*, 5351–5352.
125. Fortin, D.; Drouin, M.; Harvey, P. D. *Inorg. Chem.* **2000**, *39*, 2758–2769.
126. Fournier, E.; Sicard, S.; Decken, A.; Harvey, P. D. *Inorg. Chem.* **2004**, *43*, 1491–1501.
127. Fournier, É.; Lebrun, F.; Drouin, M.; Decken, A.; Harvey, P. D. *Inorg. Chem.* **2004**, *43*, 3127–3135.
128. Li, M.-X.; Cheung, K.-K.; Mayr, A. *J. Solid State Chem.* **2000**, *152*, 247–252.
129. Benouazzane, M.; Coco, S.; Espinet, P.; Martín-Alvarez, J. M.; Barberá, J. *J. Mater. Chem.* **2002**, *12*, 691–696.
130. Dias, H. V. R.; Jin, W. *J. Am. Chem. Soc.* **1995**, *117*, 11381–11382.
131. Dias, H. V. R.; Wang, Z.; Jin, W. *Inorg. Chem.* **1997**, *36*, 6205–6215.
132. Reger, D. L.; Collins, J. E.; Rheingold, A. L.; Liable-Sands, L. M.; Yap, G. P. A. *Organometallics* **1997**, *16*, 349–353.
133. Effendy; Lobbia, G. G.; Pettinari, C.; Santini, C.; Skelton, B. W.; White, A. H. *Inorg. Chim. Acta* **2000**, *298*, 146–153.
134. Dias, H. V. R.; Jin, W. *Inorg. Chem.* **1996**, *35*, 3687–3694.
135. Dias, H. V. R.; Lu, H.-L.; Gorden, J. D.; Jin, W. *Inorg. Chem.* **1996**, *35*, 2149–2151.
136. Dias, H. V. R.; Singh, S. *Inorg. Chem.* **2004**, *43*, 7396–7402.
137. Dias, H. V. R.; Singh, S. *Inorg. Chem.* **2004**, *43*, 5786–5788.
138. Djordjevic, B.; Schuster, O.; Schmidbaur, H. *Inorg. Chem.* **2005**, *44*, 673–676.
139. Adams, N. G.; Smith, D.; Tichy, M.; Javahery, G.; Twiddy, N. D.; Ferguson, E. E. *J. Chem. Phys.* **1989**, *91*, 4037–4042, and references therein.
140. Hurlburt, P. K.; Anderson, O. P.; Strauss, S. H. *J. Am. Chem. Soc.* **1991**, *113*, 6277–6278.
141. Hurlburt, P. K.; Rack, J. J.; Dec, S. F.; Anderson, O. P.; Strauss, S. H. *Inorg. Chem.* **1993**, *32*, 373–374.
142. Hurlburt, P. K.; Rack, J. J.; Luck, J. S.; Dec, S. F.; Webb, J. D.; Anderson, O. P.; Strauss, S. H. *J. Am. Chem. Soc.* **1994**, *116*, 10003–10014.
143. Strauss, S. H. *J. Chem. Soc., Dalton Trans.* **2000**, 1–6.
144. Lupinetti, A. J.; Jonas, V.; Thiel, W.; Strauss, S. H.; Frenking, G. *Chem. Eur. J.* **1999**, *5*, 2573–2583.
145. Tsumori, N.; Xu, Q.; Hirahara, M.; Tanihata, S.; Souma, Y.; Nishimura, Y.; Kuriyama, N.; Tsubota, S. *Bull. Chem.. Soc. Jpn.* **2002**, *75*, 2257–2268.
146. Xu, Q.; Souma, Y. *Top. Catal.* **1998**, *6*, 17–26.
147. Souma, Y.; Kawasaki, H. *Catal. Today* **1997**, *36*, 91–97.
148. Souma, Y.; Tsumori, N.; Willner, H.; Xu, Q.; Mori, H.; Morisaki, Y. *J. Mol. Catal. A* **2002**, *189*, 67–77.

149. Al-Farhan, K. A.; Abu-Salah, O. M.; Mukhalalati, M.; Jaafar, M. *Acta Cryst.* **1969**, *C51*, 1089–1092.
150. Rais, D.; Yau, J.; Mingos, D. M. P.; Vilar, R.; White, A. J. P.; Williams, D. J. *Angew. Chem., Int. Ed.* **2001**, *40*, 3464–3467.
151. Rais, D.; Mingos, D. M. P.; Vilar, R.; White, A. J. P.; Williams, D. J. *J. Organomet. Chem.* **2002**, *652*, 87–93.
152. Al-Farhan, K. A.; Ja'far, M. H.; Abu-Salah, O. M. *J. Organomet. Chem.* **1999**, *579*, 59–62.
153. Chui, S. S. Y.; Ng, M. F. Y.; Che, C.-M. *Chem. Eur. J.* **2005**, *11*, 1739–1749.
154. Corfield, P. W. R.; Shearer, H. M. M. *Acta Cryst.* **1966**, *20*, 502–508.
155. King, R. B. *J. Chem. Inf. Comput. Sci.* **1994**, *34*, 410–417.
156. Brasse, C.; Raithby, P. R.; Rennie, M.-A.; Russell, C. A.; Steiner, A.; Wright, D. S. *Organometallics* **1996**, *15*, 639–644.
157. Lin, Y.-Y.; Lai, S.-W.; Che, C.-M.; Cheung, K.-K.; Zhou, Z.-Y. *Organometallics* **2002**, *21*, 2275–2282.
158. Wang, C.-F.; Peng, S.-M.; Chan, C.-K.; Che, C.-M. *Polyhedron* **1996**, *15*, 1853–1858.
159. Yam, V. W.-W.; Fung, W. K.-M.; Cheung, K.-K. *Organometallics* **1997**, *16*, 2032–2037.
160. Lo, W.-Y.; Lam, C.-H.; Yam, V. W.-W.; Zhu, N.; Cheung, K.-K.; Fathallah, S.; Messaoudi, S.; Le Guennic, B.; Kahlal, S.; Halet, J.-F. *J. Am. Chem. Soc.* **2004**, *126*, 7300–7310.
161. Yam, V. W.-W.; Fung, W. K.-M.; Cheung, K.-K. *Organometallics* **1998**, *17*, 3293–3298.
162. Díez, J.; Gamasa, M. P.; Gimeno, J.; Aguirre, A.; García-Granda, S. *Organometallics* **1997**, *16*, 3684–3689.
163. Yam, V. W.-W.; Fung, W. K.-M.; Wong, M.-T. *Organometallics* **1997**, *16*, 1772–1778.
164. Yam, V. W.-W.; Fung, W. K.-M.; Cheung, K.-K. *J. Cluster Sci.* **1999**, *10*, 37–69.
165. Yam, V. W.-W.; Fung, W. K.-M.; Cheung, K.-K. *Chem. Commun.* **1997**, 963–964.
166. Yam, V. W.-W.; Lo, W.-Y.; Lam, C.-H.; Fung, W. K.-M.; Wong, K. M.-C.; Lau, V. C.-Y.; Zhu, N. *Coord. Chem. Rev.* **2003**, *245*, 39–47.
167. Yam, V. W.-W.; Lo, W.-Y.; Zhu, N. *Chem. Commun.* **2003**, 2446–2447.
168. Yam, V. W.-W.; Cheng, E. C.-C.; Zhu, N. *New J. Chem.* **2002**, *26*, 279–284.
169. Yam, V. W.-W.; Lam, C.-H.; Fung, W. K.-M.; Cheung, K.-K. *Inorg. Chem.* **2001**, *40*, 3435–3442.
170. Yip, J. H. K.; Wu, J.; Wong, K.-Y.; Yeung, K.-W.; Vittal, J. J. *Organometallics* **2002**, *21*, 1612–1621.
171. Wei, Q.-H.; Zhang, L.-Y.; Shi, L.-X.; Chen, Z.-N. *Inorg. Chem. Commun.* **2004**, *7*, 286–288.
172. Wei, Q.-H.; Yin, G.-Q.; Zhang, L.-Y.; Shi, L.-X.; Mao, Z.-W.; Chen, Z.-N. *Inorg. Chem.* **2004**, *43*, 3484–3491.
173. Wei, Q.-H.; Zhang, L.-Y.; Yin, G.-Q.; Shi, L.-X.; Chen, Z.-N. *J. Am. Chem. Soc.* **2004**, *126*, 9940–9941.
174. Teo, B. K.; Xu, Y. H.; Zhong, B. Y.; He, Y. K.; Chen, H. Y.; Qian, W.; Deng, Y. J.; Zou, Y. H. *Inorg. Chem.* **2001**, *40*, 6794–6801.
175. Davis, R. B.; Scheiber, D. H. *J. Am. Chem. Soc.* **1956**, *78*, 1675–1678, and references therein.
176. Pouwer, R. H.; Williams, C. M.; Raine, A. L.; Harper, J. B. *Org. Lett.* **2005**, *7*, 1323–1325, and references therein.
177. Dikusar, E. A.; Koval'skaya, S. S.; Vashkevich, E. V.; Kozlov, N. G.; Potkin, V. I.; Moiseichuk, K. L. *Russ. J. Gen. Chem.* **1999**, *69*, 1732–1735.
178. Dikusar, E. A.; Kozlov, N. G.; Koval'skaya, S. S.; Popova, L. A.; Moiseichuk, K. L. *Russ. J. Gen. Chem.* **2001**, *71*, 290–293.
179. Dikusar, E. A.; Potkin, V. I.; Vashkevich, E. V.; Kozlov, N. G.; Kaberdin, R. V. *Russ. J. Gen. Chem.* **2004**, *74*, 578–581.
180. Ukhin, L. Y.; Suponitskii, K. Y.; Kartsev, V. G. *Chem. Nat. Compd.* **2003**, *39*, 482–488.
181. Dillinger, S.; Bertus, P.; Pale, P. *Org. Lett.* **2001**, *3*, 1661–1664.
182. Shahi, S. P.; Koide, K. *Angew. Chem., Int. Ed.* **2004**, *43*, 2525–2527.
183. Armand, F.; Albouy, P.-A.; Da Cruz, F.; Normand, M.; Huc, V.; Goron, E. *Langmuir* **2001**, *17*, 3431–3437.
184. Guo, G.-C.; Zhou, G.-D.; Wang, Q.-G.; Mak, T. C. W. *Angew. Chem., Int. Ed.* **1998**, *37*, 630–632.
185. Vogel, A.; Reischauer, C. *Jahresber. Chem.* **1858**, 208.
186a. Liebermann, C. *Justus Liebigs Ann. Chem.* **1865**, *135*, 268.
186b. Liebermann, C.; Damerov, F. *Ber. Dtsch. Chem. Ges.* **1892**, *25*, 1096.
186c. Fackler, J. P., Jr. In *Encyclopedia of Inorganic Chemistry,* King, R. B., Ed.; Wiley, 2005; Vol. VIII, pp 5197–5203.
187. Vestin, R.; Ralf, E. *Acta Chem. Scand.* **1949**, *3*, 101–124.
188. Österlöf, J. *Acta. Cryst.* **1954**, 7, 637.
189. Jin, X.-L.; Zhou, G.-D.; Wu, N.-Z.; Tang, Y.-Q. *Acta Chim. Sinica* **1990**, *48*, 232–236.
190. Guo, G.-C.; Zhou, G.-D.; Mak, T. C. W. *J. Am. Chem. Soc.* **1999**, *121*, 3136–3141.
191. Bruce, M. I.; Low, P. J. *Adv. Organomet. Chem.* **2004**, *50*, 179–444.
192. Guo, G. C.; Wang, Q.-G.; Zhou, G.-D.; Mak, T. C. W. *Chem. Commun.* **1998**, 339–340.
193. Wang, Q.-M.; Mak, T. C. W. *Angew. Chem., Int. Ed.* **2001**, *40*, 1130–1133.
194. Wang, Q.-M.; Mak, T. C. W. *Chem. Eur. J.* **2003**, *9*, 43–50.
195. Zhao, X.-L.; Mak, T. C. W. *Dalton Trans.* **2004**, 3212–3217.
196. Wang, Q.-M.; Mak, T. C. W. *J. Am. Chem. Soc.* **2000**, *122*, 7608–7609.
197. Wang, Q.-M.; Guo, G.-C.; Mak, T. C. W. *J. Organomet. Chem.* **2003**, *670*, 235–242.
198. Zhao, X.-L.; Mak, T. C. W. *Polyhedron* **2005**, *24*, 940–948.
199. Wang, Q.-M.; Guo, G.-C.; Mak, T. C. W. *J. Cluster Sci.* **2002**, *13*, 63–73.
200. Wang, Q.-M.; Mak, T. C. W. *J. Am. Chem. Soc.* **2001**, *123*, 7594–7600.
201. Wang, Q.-M.; Mak, T. C. W. *J. Cluster Sci.* **2001**, *12*, 391–398.
202. Wang, Q.-M.; Mak, T. C. W. *Chem. Commun.* **2001**, 807–808.
203. Wang, Q.-M.; Mak, T. C. W. *Chem. Commun.* **2002**, 2682–2683.
204. Zhao, X.-L.; Wang, Q.-M.; Mak, T. C. W. *Chem. Eur. J.* **2005**, *11*, 2094–2102.
205. Wang, Q.-M.; Lee, H. K.; Mak, T. C. W. *New J. Chem.* **2002**, *26*, 513–515.
206. Wang, Q.-M.; Mak, T. C. W. *J. Am. Chem. Soc.* **2001**, *123*, 1501–1502.
207. Wang, Q.-M.; Mak, T. C. W. *Angew. Chem., Int. Ed.* **2002**, *41*, 4135–4137.
208. Wang, Q.-M.; Mak, T. C. W. *Dalton Trans.* **2003**, 25–27.
209. Kockelmann, W.; Ruschewitz, U. *Angew. Chem. Int. Ed.* **1999**, *38*, 3492–3495.
210. Zhao, L.; Mak, T. C. W. *J. Am. Chem. Soc.* **2004**, *126*, 6852–6853.
211. Zhao, X. L.; Mak, T. C. W. *Organometallics* **2005**, *24*, 4497–4499.
212. Herzberg, G.; Spinks, J. W. T. *Z. Physik* **1934**, *91*, 386–399.
213. Emsley, J. *The Elements*, 2nd Ed. Oxford University Press: Oxford, 1991, p 176.
214. Cremer, U.; Kockelmann, W.; Bertmer, M.; Ruschewitz, U. *Solid State Sci.* **2002**, *4*, 247–253.
215. Offermanns, J.; Ruschewitz, U. *Z. Anorg. Allg. Chem.* **2000**, *626*, 649–654.

216. Lee, J.-H.; Curtis, M. D.; Kampf, J. W. *Macromolecules* **2000**, *33*, 2136–2144.
217. Gimeno, M. C.; Laguna, A. In *Comprehensive Coordination Chemistry II*; McCleverty, J. A., Meyer, T. J., Eds.; Elsevier, 1995; Vol. 6, pp 911–1145.
218. Brückner, C. *J. Chem. Edu.* **2004**, *81*, 1665–1669.
219. Eujen, R.; Hoge, B.; Brauer, D. J. *Inorg. Chem.* **1997**, *36*, 1464–1475.
220. Yang, D.-S.; Bancroft, G. M.; Puddephatt, R. J.; Tse, J. S. *Inorg. Chem.* **1990**, *29*, 2496–2501.
221. Dukat, W.; Naumann, D. *Rev. Chim. Miner.* **1986**, *23*, 589–603.
222. Geiser, U.; Schlueter, J. A.; Williams, J. M.; Naumann, D.; Roy, T. *Acta Cryst. B* **1995**, *51*, 789–797.
223. Geiser, U.; Schlueter, J. A.; Dudek, J. D.; Williams, J. M. *Acta Cryst. C* **1995**, *51*, 1779–1782.
224. Eujen, R.; Hoge, B.; Brauer, D. J. *Inorg. Chem.* **1997**, *36*, 3160–3166.
225. Naumann, D.; Tyrra, W.; Trinius, F.; Wessel, W.; Roy, T. *J. Fluorine Chem.* **2000**, *101*, 131–135.
226. Furuta, H.; Ogawa, T.; Uwatoko, Y.; Araki, K. *Inorg. Chem.* **1999**, *38*, 2676–2682.
227. Furuta, H.; Maeda, H.; Osuka, A. *J. Am. Chem. Soc.* **2000**, *122*, 803–807.
228. Maeda, H.; Osuka, A.; Ishikawa, Y.; Aritome, I.; Hisaeda, Y.; Furuta, H. *Org. Lett.* **2003**, *5*, 1293–1296.
229. Furuta, H.; Morimoto, T.; Osuka, A. *Org. Lett.* **2003**, *5*, 1427–1430.
230. Maeda, H.; Osuka, A.; Furuta, H. *Tetrahedron* **2004**, *60*, 2427–2432.
231. Araki, K.; Winnischofer, H.; Toma, H. E.; Maeda, H.; Osuka, A.; Furuta, H. *Inorg. Chem.* **2001**, *40*, 2020–2025.
232. Araki, K.; Engelmanm, E. M.; Mayer, I.; Toma, H. E.; Baptista, M. S.; Maeda, H.; Osuka, A.; Furuta, H. *Chem. Lett.* **2003**, *32*, 244–245.
233. Engelmann, F. M.; Mayer, I.; Araki, K.; Toma, H. E.; Baptista, M. S.; Maeda, H.; Osuka, A.; Furuta, H. *J. Photochem. Photobiol. A* **2004**, *163*, 403–411.
234. Chmielewski, P. J. *Org. Lett.* **2005**, *7*, 1789–1792.
235. Muckey, M. A.; Szczepura, L. F.; Ferrence, G. M.; Lash, T. D. *Inorg. Chem.* **2002**, *41*, 4840–4842.
236. Brückner, C.; Barta, C. A.; Briñas, R. P.; Bauer, J. A. K. *Inorg. Chem.* **2003**, *42*, 1673–1680.
237. Lash, T. D.; Rasmussen, J. M.; Bergman, K. M.; Colby, D. A. *Org. Lett.* **2004**, *6*, 549–552.
238. Miyake, K.; Lash, T. D. *Chem. Commun.* **2004**, 178–179.
239. Lash, T. D.; Colby, D. A.; Szczepura, L. F. *Inorg. Chem.* **2004**, *43*, 5258–5267.
240. Bergman, K. M.; Ferrence, G. M.; Lash, T. D. *J. Org. Chem.* **2004**, *69*, 7888–7897.
241. Pawlicki, M.; Latos-Grażyński, L. *Chem. Eur. J.* **2003**, *9*, 4650–4660.

2.05
Gold Organometallics

H Schmidbaur and A Schier, Technische Universität München, Garching, Germany

2.05.1 Introduction

This chapter summarizes work published in the general area of organogold chemistry in the period 1994–2005. It complements the accounts presented in COMC (1995) and COMC (1982).[1,2] Results already included in these previous treatises are generally not duplicated in this edition. Only a few general remarks are made as an introduction to each individual chapter, and key references to older work are given where appropriate.

The reader should note that there is a fully comprehensive coverage of organogold chemistry up to the year 1980 in the *Gmelin Handbook of Inorganic Chemistry*.[3] Apart from COMC (1982) and COMC (1995), later reviews are available in *Encyclopedia of Inorganic Chemistry*[4] and in a monograph,[5] as a compilation of preparative procedures in the two leading series oriented at synthetic chemistry,[6,7] and as summaries of theoretical work.[8,9]

An organogold compound is defined as a species which contains at least one gold–carbon bond. The nature of this bond is largely covalent and may vary between the extreme cases of a true σ-bond between the gold atom and a substituent or ligand which is monohapto-*C*-coordinated (η^1), and a π-complexation of an organic molecule which becomes attached to the metal atom in a dihapto-*C*,*C*-coordination (η^2). It should be observed that no higher hapticities have been discovered in any organogold compound: neither in (allyl)gold nor in (arene)gold complexes the hapticity reaches the multihapto-C_n-coordination (η^n) otherwise common in organometallic chemistry of transition metals. It should be remembered that it has long been established that in solution and in the solid state, the (cyclopentadienyl)gold(I) complexes – although fluxional – have their $[C_5H_5]^-$ unit σ-bonded to the gold atom through one carbon atom only.[10] No centered (benzene)gold(I) complex (η^6) is known in the condensed phase.[11]

The "organization" of previous comprehensive accounts of organogold chemistry has followed either the number of Au–C bonds in a molecule, the hapticity of the organic components, the nuclearity of the compounds, and/or the oxidation state of the metal. This rigid order has been found impractical for the treatment of the results to be presented for the period 1994–2005. Reflecting contemporary funding policies, research during this period has lately been much more focused on potential applications of the gold compounds concerned. Because gold(I) compounds have a rigid-rod structure, endeavors into molecular crystal engineering, non-linear optical (NLO) materials, and mesogenic phases have been most common. Moreover, the now well-established aggregation of linearly two-coordinate gold(I) compounds through aurophilic contacts can augment or give rise to photophysical properties, in particular luminescence and phosphorescence. Together, these aspects have led to a specific growth of "alkynyl"- and "isocyanide" gold chemistry, and a combination of both.

By contrast, the development of simple alkyl- or alkenylgold chemistry has slowed down considerably as compared to previous decades, except for the usage of these compounds as precursors to gold catalysts. In this context, "carbene" complexes of gold have continued to attract interest. On the other hand, although the science of gold "clusters, nanoparticles, and surfaces" has been extremely topical, little "organogold" chemistry other than catalysis of reactions of alkenes and alkynes has been relevant to date to these particular areas, where gold–sulfur compounds are dominant.[5]

"Ylide" complexes of gold are unique in that they exhibit an exceptional chemical and thermal stability, which facilitates preparative and structural work very considerably. It was in this class of compounds that a large variety of true organogold(II) and mixed valence organogold(I)/(III) complexes was discovered. These are rare in the remainder of organogold chemistry.

The preference of "soft" gold(I) for carbon as compared to oxygen donors leads to unusual structures, as for example, the *C*-binding[12,13] of the acetylacetonate unit in gold(I) complexes $(Ph_3P)AuCH[C(=O)Me]_2$ and even $[(Ph_3P)Au]_2C[C(=O)Me]_2$, while for "hard" gold(III), standard chelation by the two oxygen atoms of the diketonate group prevails.[14] As in many reactions in gold(I) chemistry, the second step of the *C*-auration of the diketone is strongly influenced by aurophilic bonding between the geminal gold atoms.[9,13] These and related phenomena are well documented for all areas of gold chemistry and therefore not elaborated anywhere in this account.[2,5,8,9,15]

As in previous volumes,[1,2] the solution chemistry of gold "cyanides" as well as the solid-state chemistry of binary and polynary gold "cyanides" and "carbides" have been excluded from this review.

2.05.2 Alkylgold Compounds

"Donor-free compounds" RAu and R_3Au are inherently unstable and no experimental data are available. However, model systems such as CH_3Au and $(CH_3)_3Au$ were the subjects of several early theoretical studies.[2,8] More recent work has considered the stability of the $[CH_3Au]^+$ cations in a $^2A_1$ state (^1S atomic state). Depending on the

theoretical approach, the Au–C distance was calculated to be in the range 2.105–2.125 Å and the Au–C dissociation energy at 45.5 ± 5 kcal mol^{-1}.[16]

"Donor-stabilized compounds" with simple, non-functional alkyl substituents R are known mainly for gold in its standard oxidation states +1 and +3, that is, (L)AuR and $(L)AuR_3$, respectively. For the latter, R may be replaced by halide, pseudohalide, or other anionic or neutral ligands leading to compounds of the general formula $(L)AuR_nX_{3-x}$.

Complexes of the type (L)AuR have been isolated with a large variety of donors L, including predominantly tertiary phosphines and isocyanides. The dinuclear complex $(dppm)(AuMe)_2$ has been prepared by treatment of $(dppm)(AuCl)_2$ with MeLi and structurally characterized.[17] Examples (L)AuR with a carbene ligand L are also known. A simple methyl compound was prepared from the chloride complex with dimethylmagnesium (Equation (1)).[18]

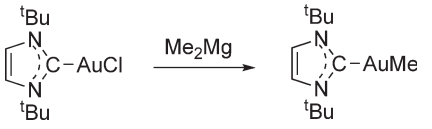

(1)

Compounds (L)AuR have been used as precursor molecules for the *in situ* preparation of the strong nucleophiles $[(L)Au]^+ X^-$ by treatment with strong acids HX ($X = CF_3SO_3$, CF_3CO_2, BF_4, PF_6, SbF_6 etc.; L = tertiary phosphine; R = alkyl) in polar solvents (Equation (2)). The solutions are used as catalysts for the activation of alkenes and alkynes for addition of water, alcohols, and amines (Sections 4 and 10).

$$(L)AuR + HX \rightarrow RH + [(L)Au]^+X^- \tag{2}$$

First examples of complexes of α,ω-digold alkylidenes have been prepared in moderate yields from the corresponding di-Grignard reagents with 2 equiv. of $(Ph_3P)AuBr$ as colorless, crystalline products. The structure of the dinuclear compound with the $–(CH_2)_4–$ spacer has been determined (Equation (3)).[19] Preparative efforts oriented at the synthesis of the analogous ethane, propane, and hexane derivatives were unsuccessful.

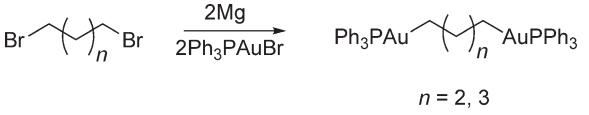

$n = 2, 3$ (3)

Di- and tri-auro-"methane" complexes $(R_3PAu)_nCH_{4-n}$ with $n = 2$, 3 are unknown, but tetraauromethane complexes $(R_3PAu)_4C$ ($n = 4$) with bulky substituents R and a tetrahedral structure have been described.[20] With smaller ligands R_3P, including Ph_3P, these complexes exist in protonated or alkylated forms as cations $[HC(AuPR_3)_4]^+$ and $[R^1C(AuPR_3)_4]^+$ with a square-pyramidal structure. Salts with these cations are obtained from the corresponding polyborylmethanes[21] or trimethylsilyl diazomethanes (Scheme 1).[22] The known penta- and hexaaurated methan(di)ium salts with particularly stable trigonal and octahedral structures, respectively, are byproducts of these reactions.[15,22,23,24]

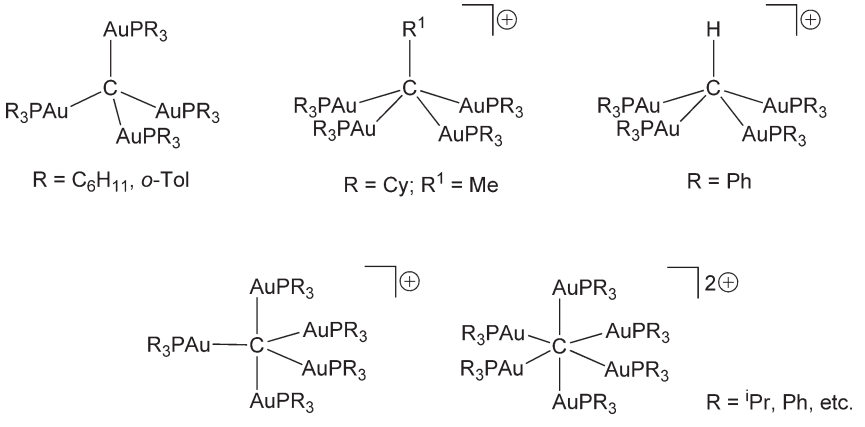

Scheme 1

Quantum-chemical calculations have shown that tetraauromethane complexes are strong nucleophiles (Brønsted bases). The reorganization of the structure upon alkylation or protonation leads to an enormous gain in energy owing to strong aurophilic interactions at the edges of the basal square.[25] The cations $[HC(AuPPh_3)_4]^+$ are aggregated into dimers in the tetrafluoroborate salt through aurophilic bonding between parallel edges of neighboring cations.[22]

Anionic complexes $[R_2Au]^-$ are present in salts with metal or large quaternary cations, but only a few compounds of this type have been isolated.[1,2] Solutions of the lithium salts generated *in situ* are substrates for addition reactions with alkyl halides leading to alkylgold(III) compounds.[26]

Functions $[R_2Au]^-$ are also present in the large family of gold(I) complexes of phosphonium, arsonium, and sulfonium "ylides". Section 2.05.6 is dedicated to this class of complexes, where dinuclear compounds with gold in the oxidation state +2 are also common.

Quasi-phosphonium centers in the β-position to the gold atom are also present in the compounds obtained upon auration of difunctional ligands of the dppm type. Complexation of the phosphorus atoms strongly activates the bridging methylene group of this ligand. Deprotonation is achieved even by a weak base. Subsequent reaction with a gold(I) complex affords the corresponding polynuclear derivatives (Equation (4)).[27,28,29,30] The reaction with an acetylacetonate[31] or an alkynyl complex requires no base.[30] Additional activation by an iodine substituent facilitates the auration as demonstrated for a ruthenium complex (Equation (5)).[32] The facile auration of 1,3-diketones and related sulfones has already been mentioned.[12,13]

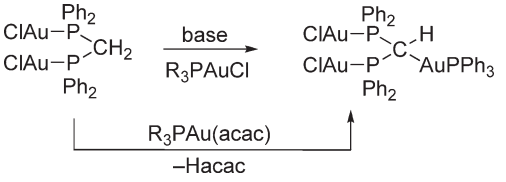

(4)

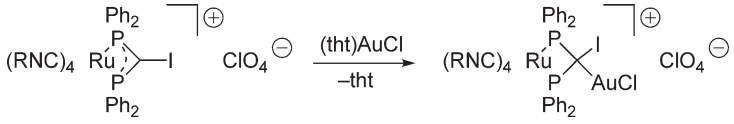

(5)

Donor-stabilized complexes $(L)AuR_3$ can be used for the preparation of derivatives with mixed substitution patterns, mainly of the type $(L)AuR_2R^1$ as demonstrated for R = Me (*trans*), R^1 = *trans*-(Cl)C═CH(Cl), L = Ph_3P, and for R = Me (*cis*), R^1 = –C≡CH, –C≡CMe or –C≡CPh, and L = Me_3P or Ph_3P.[26] For this purpose, one of the Au–C bonds is cleaved by an acid HX to generate compounds *cis*-Me_2XAuL, which can be subjected to metathesis with an organometallic reagent (Equation (6)). The molecular structures of *cis*-$Me_2IAuPMe_3$, *cis*-$Me_2IAuPPh_3$ and *cis*-$Me_2ClAuPPh_3$ have been determined. The 1,2-dichlorovinyl compound has the rare *trans*-Me_2Au configuration,[33] probably owing to steric effects, while the alkynyl derivatives have the conventional *cis*-Me_2Au arrangement.[26]

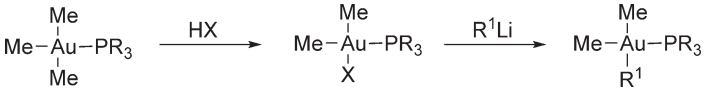

(6)

Substitution of the halogen atom by another tertiary phosphine affords the ionic compounds $[cis\text{-}Me_2Au(PR_3)_2]^+X^-$. The retention of the *cis*-structure has been confirmed for R = Me and X = I and ClO_4.[33]

Dimeric $(Me_2AuCl)_2$ has been used to close the cationic adamantane cage of a bowl-shaped *P*,*N*-donor ligand with a $[cis\text{-}Me_2Au]^+$ unit. The two chlorine atoms are accommodated in the $[cis\text{-}Me_2AuCl_2]^-$ counterion (Equation (7)).[34]

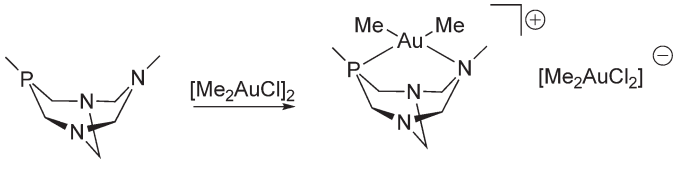

(7)

2.05.3 Alkenylgold Compounds

Subsequent to earlier work on simple σ-alkenylgold complexes,[2,35,36] for example, those of the vinyl type $R_3PAu–CH{=}CH_2$, very few investigations have been dedicated to this class of organogold compounds. Attempts to prepare α,ω-digold alkene complexes were unsuccessful. The reactions between the corresponding dimetallated olefins and R_3PAuX complexes led to elimination of the hydrocarbon.[19] C–C coupling of alkynyl groups in the coordination sphere of platinum centers gave enyne complexes with the en function side-on coordinated to the metal atom.[37]

(1-Alkoxy-vinyl)gold(I) complexes have been obtained from the reaction formulated in Equation (8). The gold atom has been shown to be η^1-bonded to the α-carbon atom.[38]

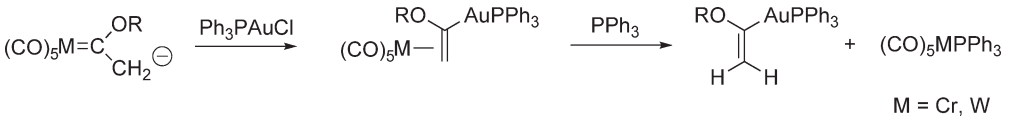

(8)

If certain heterocycles like thiophene are classified as heteroatom-bridged butadienes, then heteroarylgold complexes can be included in the chapter on alkenylgold complexes. The compounds are typically obtained through metallation of the heterocycle using RLi reagents followed by metathesis with $(R_3P)AuX$ complexes. The monoauration can be followed by a geminal diauration, which is preferred over complexation at the heteroatom owing to aurophilic bonding (Equations (9a) and (9b)).[19,39]

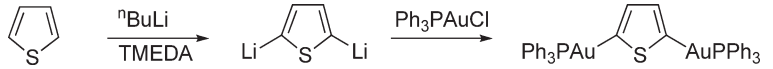

(9a)

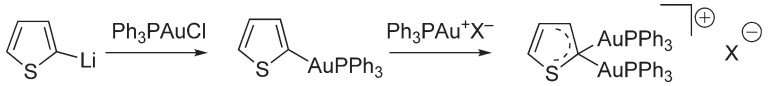

(9b)

2.05.4 Alkynylgold Compounds

Gold(I) alkynyls and their complexes have been an important class of organogold compounds from the very beginning of organogold chemistry.[2] By contrast, the class of gold(III) alkynyls is poorly developed and only a small number of representative compounds is known. Alkynylgold compounds have recently been reviewed, focusing on various aspects of their chemistry.[40–43]

2.05.4.1 Alkynylgold(I) Compounds

2.05.4.1.1 Donor-free alkynylgold(I) compounds $[Au_2C_2]$, $M[AuC_2]$, and $[RC{\equiv}CAu]_n$

"Donor-free alkynyls of gold(I)" of the net composition Au_2C_2 and [RC≡CAu] were among the first organogold compounds to be prepared. It had been observed early on that an explosive precipitate (gold acetylide, fulminating gold, a gold carbide) is formed as acetylene gas C_2H_2 is passed into solutions of a gold salt.[44] Ternary alkali gold carbides $M[AuC_2]$ can be prepared from AuI and C_2H_2 in solutions of the alkali metals M = Li, Na, K in liquid ammonia. The primary products $M[Au(C{\equiv}CH)_2]$ lose C_2H_2 at 110 °C.[45] Oxidation products of alkali gold carbides have also been investigated.[46]

Terminal alkynes RC≡CH were later found to give similar reactions, and several oligomers and polymers $[RC{\equiv}CAu]_n$ have been isolated.[2] Because of their low solubility and the concomitant problems in obtaining single crystals, their structure was in doubt for quite some time until the first crystal structures were determined, showing, for example, that $[^tBuC{\equiv}CAu]_n$, previously formulated as a cyclic tetramer,[47] is in fact a "catena" species consisting of two interconnected cyclic hexamers.[48] In the crystals, the two interpenetrating hexamers are related by a twofold axis. In each hexamer, the gold atoms are in three different types of coordination: two σ-bonds (η^1, terminal) to two neighboring acetylide groups as in an anion $[Au(C{\equiv}C^tBu)_2]^-$, two π-bonds (η^2, side-on) to two acetylide groups, or terminal (η^1) "and" side-on (η^2). One of the six gold atoms of each ring is engaged in aurophilic bonding between the hexamers. Scheme 2 shows one of the interpenetrating rings and the catena principle in a simplified form. The structure of $[^tBuC{\equiv}CAu]_{12}$ may be representative for other RC≡CAu compounds, but there is only a paucity of structural data.

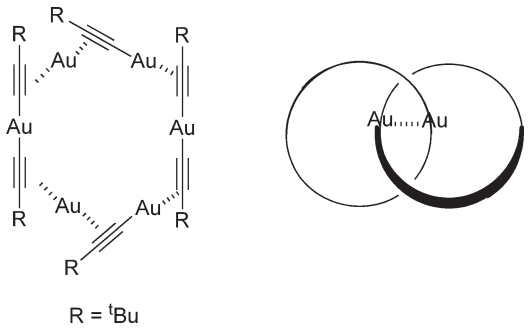

Scheme 2

Donor-free gold(I) alkynyls play an important role as precursors in the synthesis of related complexes. The compounds are generally prepared from the alkyne, a gold(I) compound with ligands L, which are readily displaced, and a base (Equations (10) and (11)).

$$(L)AuX + RC{\equiv}CH + base \rightarrow RC{\equiv}CAu + L + HX\text{–}base \quad (10)$$

$$[AuL_2]^+X^- + RC{\equiv}CH + base \rightarrow RC{\equiv}CAu + 2L + HX\text{–}base \quad (11)$$

Here, L = thioether,[49–51], NH_3;[48] X = acac, halide;[52] base = NEt_3,[53] MeONa, NaOC(O)Me,[50] etc. While the oligomers $[RC{\equiv}CAu]_n$ are generally poorly soluble in common organic solvents, they are readily dissolved upon addition of donor molecules, including tertiary phosphine,[30,50,54,55] isocyanide,[56] carbene,[57] and ylide molecules,[53] or halide anions.[52] Even ammonia will afford a complex $H_3NAuC{\equiv}CPh$, but not $H_3NAuC{\equiv}C^tBu$ (Equation (12)).[48]

$$[RC{\equiv}CAu]_n + nL \rightarrow n(L)AuC{\equiv}CR \quad (12)$$

Here, R = H, alkyl, alkenyl, alkynyl, aryl, heteroaryl, other substituents; L = R_3P, RNC, R_2C, R_3PCH_2, halide, etc.

2.05.4.1.2 Alkynylgold(I) compounds (L)AuC≡CR

A large number of these complexes has been prepared via the above direct route or via other methods (below). The structure features a linear skeleton. With small ligands L, the compounds are generally associated into oligomers or polymers via aurophilic bonding, as recently demonstrated for $Me_3PAuC{\equiv}CPh$.[26]

The 1:1 complexes of alkynylgold compounds (L)AuC≡CR with strong donors L can also be conveniently prepared from the corresponding gold halides (L)AuX (X = Cl, Br, I), an alkyne HC≡CR, and a base. For many representative examples, the reactions with an alkali alkanolate in an alcohol[58] or with triethylamine in dichloromethane are the methods of choice (Equation (13)).[59]

$$(L)AuX + RC{\equiv}CH + base \rightarrow (L)AuC{\equiv}CR + (base)HX \quad (13)$$

R can be an alkyl, trialkylsilyl, alkenyl [60] or (hetero)aryl group.[42,50,58,59,61–63] L may generally represent a tertiary phosphine or an isocyanide, but also a phosphonium ylide $R_3P{=}CHR^1$.[64] The substituent R of the alkynyl group can be varied including a large range of functions. Heteroaryl groups, like pyridyl groups, can be alkylated or used as donors to obtain onium salts or complexes, respectively.[42] Owing to the mild reaction conditions, R may contain sensitive functions such as amino acids,[63] or the ligand L may bear an azo group.[65]

The auration of the alkyne may also be achieved by using a silylalkyne. Desilylation followed by an *in situ* auration converts a compound $RC{\equiv}CSiMe_3$ into the corresponding RC≡C–AuL complex.[66]

Together with silylalkynyl halides, alkynylgold(I) complexes have been used as C–C coupling reagents (Equations (14) and (15)).[67]

$$(R_3P)AuC{\equiv}CR^1 + I\text{–}C{\equiv}C\text{–}SiMe_3 \rightarrow R^1C{\equiv}C\text{–}C{\equiv}C\text{–}SiMe_3 + (R_3P)AuI \quad (14)$$

$$(R_3P)Au(C{\equiv}C)_nSiMe_3 + (dppm)(CO)_7Co_3C\text{–}C{\equiv}C\text{–}I \rightarrow (dppm)(CO)_7Co_3C(C{\equiv}C)_{n+1}SiMe_3 + (R_3P)AuI \quad (15)$$

Another particularly convenient preparative method is the reaction of the corresponding gold(I) acetylacetonate complex with the alkyne, which requires no auxiliary base.[42,68–71] This reaction is also useful for the simple acetylides (L)AuC≡CH.[72] The acetylacetonates can be isolated and introduced as the true reagents, or prepared *in situ* using the corresponding gold(I) halide complex and Tl(acac) (Equations (16) and (17)).[73]

$$(L)Au(acac) + RC{\equiv}CH \rightarrow (L)AuC{\equiv}CR + Hacac \tag{16}$$

$$(L)AuX + Tl(acac) + RC{\equiv}CH \rightarrow (L)AuC{\equiv}CR + TlCl + Hacac \tag{17}$$

Exchange of the ligand L can be executed for complexes with weak donors L′, such as diethylamine, which are readily replaced by, for example, tertiary phosphines.[71] Ligands L can also be transformed into other ligands by a simple addition reaction. Thus, addition of a secondary amine to an (isocyanide)gold-alkynyl to give the (carbene)-gold-alkynyl is a common reaction. With NEt_3, no such addition takes place (Equation (18)).[71]

$$^{t}BuNCAuCl + RC{\equiv}CH + 2NEt_2H \rightarrow RC{\equiv}CAu[C(NEt_2)NH^{t}Bu] + NEt_2H_2^{+}Cl^{-} \tag{18}$$

(L)AuC≡CR complexes can also be obtained by ligand exchange starting from precursors with homoleptic substitution ($PPN^{+} = (Ph_3P)_2N^{+}$; Equation (19)).[71]

$$PPN^{+}[Au(C{\equiv}CH)_2]^{-} + [(R_3P)_2Au]X \rightarrow 2R_3PAuC{\equiv}CH + PPN^{+}X^{-} \tag{19}$$

Selective ligand exchange in complexes with two strongly different donors can be employed for special combinations of ligands, including ylides (Equation (20)).[64]

$$[R_3PCH_2Au(tht)]ClO_4 + RC{\equiv}CH + KOH \rightarrow R_3PCH_2AuC{\equiv}CR + KClO_4 + H_2O + tht \tag{20}$$

Finally, the reaction of (L)AuX complexes with metallated alkynes in an inert solvent and at low temperature is a particularly safe pathway to complexes with more delicate components (X = halogen; M = alkali metal; Equation (21)).[74,75]

$$(L)AuX + RC{\equiv}CM \rightarrow (L)AuC{\equiv}CR + MX \tag{21}$$

The same arsenal of preparative methods has been applied successfully for the corresponding dinuclear derivatives of ethyne HC≡CH and dialkynes HC≡C–X–C≡CH, where X can be virtually any spacer unit.[50,52,54,55,57,61,62,71,76–83] As mentioned in the introduction to this chapter, ethyne is readily converted into polymeric explosive "AuC≡CAu" and its complexes (L)AuC≡CAu(L), of which the families with $L = R_3P$[84] and L = RNC are particularly large (Chapter 7). With the unit X in (L)AuC≡CXC≡CAu(L) being an alkylidene spacer, flexible complexes are obtained, while with alkenylidene, alkynylidene, or arylidene units,[57] rigid molecules (L)AuC≡CXC≡CAu(L) are generated. Specific examples are presented below in the context with the structural patterns of extended systems.

With the alkynyl functionality greater than two, "starbust" type complexes are obtained, as derived, for example, from 1,3,5-trialkynylbenzenes [85] or -triazines,[86] 1,1,2,2-tetraalkynylethenes,[85] or bis(1,2-dialkynyl)phenylene-bridged crown ethers[87] or calixarenes.[88,89]

Compounds (L)AuC≡CR can appear as ligands in the coordination sphere of transition metals. The interaction may be fluxional with metal–metal contacts M–Au and the alkyne coordinated side-on (η^2, dihapto) to the gold atom. Typical examples are (cp)(CO)(NO)W[$Ph_3PAuC{\equiv}C^{t}Bu$][90] and $Fe_3(CO)_9[R_3PAuC{\equiv}C^{t}Bu]$, with R = Ph, ^{i}Pr, for which several isomers have been observed in solution.[91]

$[(Ph_3P)Au]^{+}$ units were also found to be attached side-on to complexes with $[(CO)_5ReC{\equiv}CRe(CO)_5]$ units. These adducts may undergo ligand redistribution to give the homoleptic ions.[92]

Addition of $[(R_3P)Au]^{+}$ cations to di(phenylethynyl)platinum(II) complexes leads to C–C coupling, affording 1,4-diphenylbutadiyne and 1-phenyl-1-[(triphenylphosphine)gold]-butenynyl as ligands coordinated to the platinum atom (Scheme 3).[37] $(C_6F_5)_2Pt(CO)(thf)$ undergoes addition of $Ph_3PAuC{\equiv}C^{t}Bu/Ph$ molecules with elimination of the thf ligand to give the *trans*- or *cis*-bis(pentafluorophenyl)(^{t}butyl/phenyl-ethynyl)(carbonyl)platinum complexes, respectively, with the $[(R_3P)Au]$ parts coordinated side-on to the triple bond.[93]

Lithiation of the complex $[(cp)(CO)_2W]_2(HC{\equiv}CPh)$ with its tetrahedral W_2C_2 core unit followed by treatment with $(Ph_3P)AuCl$ gives the corresponding cluster with the hydrogen atom replaced by the $Au(PPh_3)$ group. A diaurated complex is obtained with $(dppm)(AuCl)_2$.[94,95]

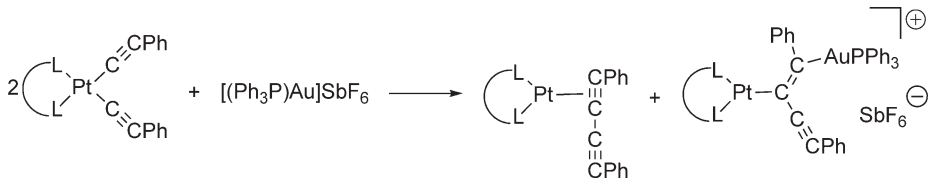

Scheme 3

CuCl has been shown to form a 1 : 1 adduct with $(Ph_3P)AuC{\equiv}CFc$ (Fc = ferrocenyl), which has a dimeric structure with a square $(CuCl)_2$ core unit of which each Cu atom is coordinated side-on to a triple bond of the substrate. A similar *2 : 2* aggregate is formed with CuBr and $(Ph_3P)AuC{\equiv}CAu(PPh_3)$.[66]

2.05.4.1.3 Compounds with di(alkynyl)gold(I) anions $[Au(C{\equiv}CR)_2]^-$

Salts with di(alkynyl)aurate(I) anions are very common reagents for the preparation of other gold(I) complexes. A large number of examples with R taken from all sorts of organic functionalities have been prepared and characterized, mainly in a search for new classes with potentially useful photophysical properties (below).

The most convenient pathway to this important class of compounds is the reaction of alkynes $RC{\equiv}CH$ with salts of the bis(acetylacetonato)gold anion.[71] This reaction leads to almost any type of target compounds, including those with R = H, alkyl, alkenyl, alkynyl, aryl, heteroaryl, etc. (Q = metal or quaternary or PPN cation; Equation (22)).

$$Q[Au(acac)_2] + 2RC{\equiv}CH \rightarrow Q[Au(C{\equiv}CR)_2] + 2acacH \qquad (22)$$

Among the products of pertinent work, there are the simple ethynyl compounds $Q[Au(C{\equiv}CH)_2]$[72] as well as the derivatives $Q[Au(C{\equiv}CR)_2]$ with R = ^{t}Bu, $SiMe_3$, CH_2Cl, CH_2Br, and CH_2OH,[71] or $C{\equiv}CH$ [96] and $C{\equiv}CR^1$, where R^1 may represent an organometallic group such as $W(CO)_3(C_5H_5)$ or Pt(dppe) (dppe = 1,2-bis(diphenylphosphino)ethane).[96] The group of compounds with aralkynyl substituents $Q[Au(C{\equiv}CR)_2]$ (R = aryl) is particularly large and includes examples with R = Ph, $C{\equiv}C$–Ph, or *p*-C_6H_4–$C{\equiv}C$–Ph,[96] *p*-C_6H_4–X with X = NO_2, *p*-C_6H_4–$CH{=}CH$–C_6H_4–NO_2-4, *p*-C_6H_4–$C{\equiv}C$–C_6H_4–NO_2-4, etc.,[97] X = NH_2,[98] and X = CN.[81]

Di(ethynyl)benzenes have been attached to a common gold(I) center through one of the two ethynyl groups each to give anions the structure of which can be further extended via the remaining free ethynyl functions.[52] The two alkynyl groups at the gold center may also be terminated by organometallic functions as in a case with $[Cu_3(dppm)_3I]$ end groups.[96]

Heteroaryl groups are present in the 4-pyridyl-ethynyl compounds[81,99,100] and their extended variants with $C{\equiv}C$–C_6H_4–$C{\equiv}C$–pyr-4 ligands.[81,99] These compounds can be quaternized with MeI or coordinated to a metal complex at their terminal pyridyl functions to give species addressed as molecular rods or molecular wires.[81,99] Similar reactions were carried out with 3-phenanthrolinyl-ethynyl complexes,[62] and special examples are also known with R based on calixarenes.[51]

Di(ethynyl)gold moieties can be used as bridging units between transition metals as demonstrated for square-grid complexes with Pt(dppe) acceptor components.[96]

The complex $[(Me_3P)_2Ag]^+[Au(C{\equiv}CPh)_2]^-$ was found to lose PMe_3 on standing at room temperature to give the product $[(Me_3P)_2Ag]^+[Ag_2Au_3(C{\equiv}CPh)_6]^-$. The anion has approximately D_{3h}-symmetry with a trigonal-bipyramidal Ag_2Au_3 core unit and the phenylethynyl groups π-coordinated to the silver atoms. There is significant metallophilic (Ag/Au) bonding as confirmed by theoretical calculations (Scheme 4).[101] Anionic clusters of the type $[M_2M'_3(C{\equiv}CR)_6]^-$ with M/M′ various combinations of coinage metals have been described previously.[43,102]

2.05.4.1.4 Compounds with complex alkynylgold(I) anions $[RC{\equiv}CAuX]^-$

Mixed-ligand anions $[RC{\equiv}CAuX]^-$ are rare in organogold chemistry. Selected examples have been obtained from reactions of $[RC{\equiv}CAu]_n$ oligomers with halides Q^+X^-, from $Q[Au(acac)_2]$ salts with alkynes, followed by acids HX in the molar ratio 1 : 1 : 1, and from complexes (tht)AuCl (tht = tetrahydrothiophene) or $[(Ph_3P)_2C]AuCl$ with an alkyne and a base (1 : 1 : 1). Known examples of products include salts $Q^+[HC{\equiv}CAuCl/Br]^-$[72] and $[(Ph_3P)_2CH]^+[PhC{\equiv}CAuCl]^-$.[52,53] Anions with mixed alkynyl/aryl substituents are present in $PPN^+[C_6F_5AuC{\equiv}CH]^-$ or $[2,4,6\text{-}(O_2N)_3C_6H_2AuC{\equiv}CH]^-$, obtained from $PPN^+[ArAuCl]^-$ and Tl(acac), followed

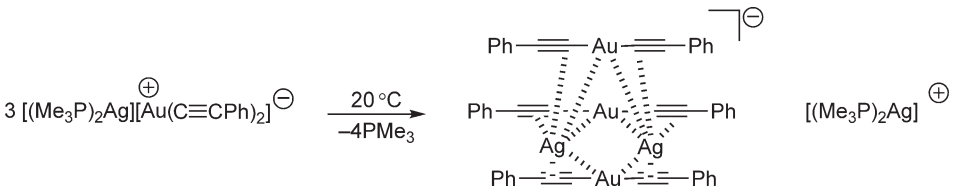

Scheme 4

by reaction with C_2H_2.[73] The compounds can be used as substrates for further conversions into other (organo)gold compounds.

2.05.4.1.5 Selected alkynylgold(I) compounds with photoemissive properties

Owing to their "rigid-molecular-rod" -type structure and the electronic communication between polarizable ligands across the metal center, complemented by intermolecular metallophilic interactions, alkynylgold(I) compounds are expected to show intrinsic physical properties which are of interest in diverse fields of application, including in particular photoluminescence (phosphorescence),[42] NLO effects,[103] mesogenic behavior,[104] and design and construction of multidimensional frameworks. A large collection of systems has been investigated in this context.[41]

Scheme 5 shows a group of alkynylgold(I) complexes for which the studies focused on the UV–VIS electronic absorption and emission properties. Most of these compounds are of the type [(L)AuC≡CR], for which the methods of synthesis have been summarized above. The products were found to show phosphorescence in various polymorphs and crystal forms of solvates. Although there are no metallophilic interactions discernible in the crystal between most of the monomers due to the steric effect of the large tertiary phosphines, there is nevertheless strong excitonic coupling based on other weak interactions, which depend on the organization of the molecules in the crystal.[105,106]

For the compounds in Scheme 6, the intrinsic emissions of the aralkyne groups were shown to be "illuminated" ("switched on") by coupling to the $AuPR_3$ centers. The S_0–T_1/S_1–T_1 energy separations (between 2.0 and 0.8 eV) are clearly tunable by adjusting the substituents and ligands of the complexes.[82] The effects are particularly pronounced with substrates containing an oligothiophene backbone, for which aurophilic contacts as well as π–π-stacking and hydrogen bonding modify the intermolecular interactions.[107]

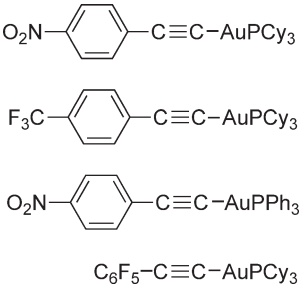

Scheme 5

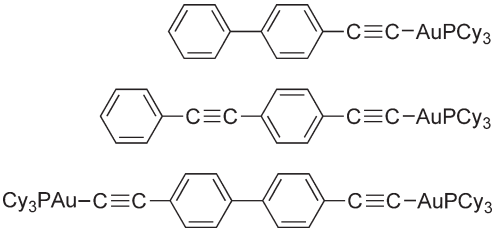

Scheme 6

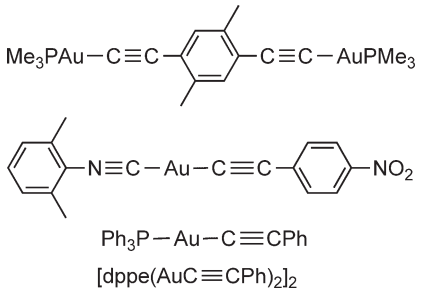

Scheme 7

Scheme 7 gives examples with reduced steric effects of the auxiliary ligand L. The electronic emission of these molecules is strongly influenced by metallophilic bonding or π–π-stacking.[76] The tetranuclear dimer $[(dppe)(AuC{\equiv}CPh)_2]_2$ with Au···Au separations of 3.153 Å has a long-lived emissive $^3(\pi$–$\pi^*)$ excited state.[106,108] $PhC{\equiv}CAuPPh_3$ has electron-transfer properties toward the methyl viologen system.[108] Trinuclear complexes of the type $[(P\text{–}P)_2Au_3(C{\equiv}CR)_2]^+X^-$ with P–P = dppe or bis(diphenylphospino)ferrocene (dppf) with strong aurophilic bonding have pronounced photoemissive properties.[106] The complex $(dppm)(AuC{\equiv}C^tBu)_2$ undergoes transformation into a tetranuclear compound by auration of the bridging CH_2 group of the dppm ligand. The product $(^tBuC{\equiv}CAuPPh_2)_2CHAu(Ph_2PCH_2PPh_2)AuC{\equiv}C^tBu$ has been fully characterized.[30]

Scheme 8 gives species with extended [109] or "starbust" -type structures, which are strongly luminescent even with the large ligand L = PCy_3.[85] The diphenylfluorene derivative shows a remarkable heavy atom effect on the intersystem crossing rate.[78]

Similar findings were obtained with the combinations of selected ditertiary phosphines and mono- or difunctional alkynes.[71]

Compounds presented in Scheme 9 have provided evidence for the influence of the otherwise rarely investigated *p*-anilino-ethynyl group and a variety of auxiliary ligands on the luminescence, NLO, and mesogenic properties of this type of complexes.[98]

Scheme 10 features the phenanthrolinyl unit as a substituent to the ethynyl groups in three different compositions. Strong room-temperature $^3(\pi$–$\pi^*)$ phosphorescence is observed. It appears that gold(I) coordination enables spin-orbit coupling and facilitates triplet emission.[62,110] In the corresponding rhenium complexes (with a facial structure), there is an intramolecular charge transfer Au(I)–Re(I) giving rise to modified emission (luminescence scaffolding).[77] Tricationic ruthenium complexes of bis(phenanthrolinylethyl)gold(I) anions have been prepared with $[(bipy)_2Ru]^{2+}$ building blocks. Salts with quaternary counterions show intense emission at 620 nm upon irradiation at 360 nm.[110]

Compounds shown in Scheme 11 are based on the fluorene system with different "spacer units" connecting the two benzene rings. The unit X in the 9-position strongly influences the optical properties of these alkynylgold(I) emitters. Complementary electrochemical studies have been carried out for the fluorenone species.[79,80]

Scheme 12 introduces systems with organometallic end groups at the alkynyl part.[41,95]

The (alkenyl–ethynyl)gold(I) complexes shown in Scheme 13 were prepared with mono- and ditertiary phosphine ligands and used as substrates for the coordination of coinage metal cations. The products are strongly luminescent.[60]

Scheme 14 demonstrates the usage of diaryl(ethynyl)phosphines for the design of strongly luminescent dinuclear complexes. The corresponding pentafluorophenyl compounds (X = C_6F_5) have also been prepared. When the reactions of $Ph_2PC{\equiv}CH$ are carried out with tris(pentafluorophenyl)gold(III) complexes, addition of alcohol to the ethynyl group occurs as a side-reaction.[111]

Related work is dedicated to compounds with (L)AuC≡C–functions attached to crown ether and cryptand-type units, following the idea that the luminescence properties of the chromophores will be influenced by complexation of cations in the polyether groups.[87] Scheme 15 presents two examples of the "devices" probed in these highly successful studies.

The investigations have been extended to include calixarenes as core units bearing both (L)AuC≡C– and crown ether functions (Scheme 16).[88,89] Some of these examples show high Na/K selectivity.[89] If the gold atoms are introduced with weak auxiliary ligands L, two calixarene cores may become bridged by C≡C–Au–C≡C units to give tetranuclear complexes.[51]

Quaternary salts as shown in Scheme 17 with terminal cyano or 4-pyridyl functions become strongly photoluminescent when acidified in dichloromethane solution or quaternized with methyl iodide.[81]

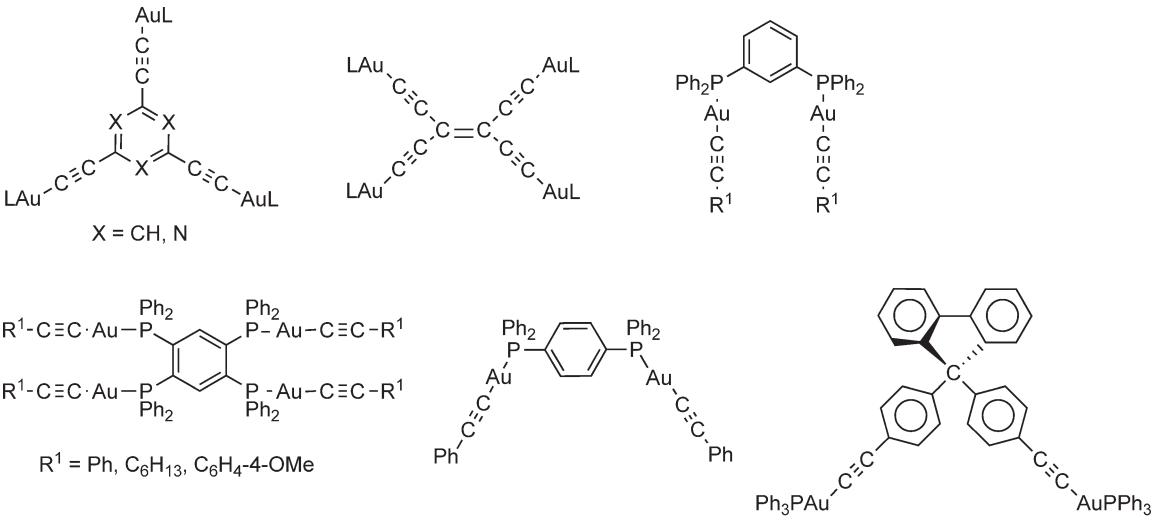

$LAuC{\equiv}CR^1$

Donor components L

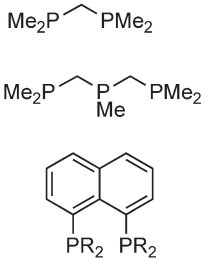

Alkynyl components

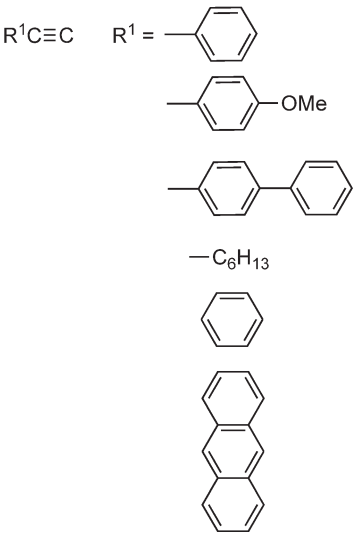

Scheme 8

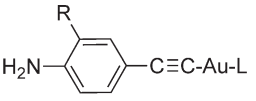

L = PPh_3, $P(C_6H_4\text{-}4\text{-}OMe)_3$, $P(C_6H_4\text{-}4\text{-}F)_3$, $P(C_6H_4\text{-}3\text{-}Me)_3$, C≡N

R = H, Me

Scheme 9

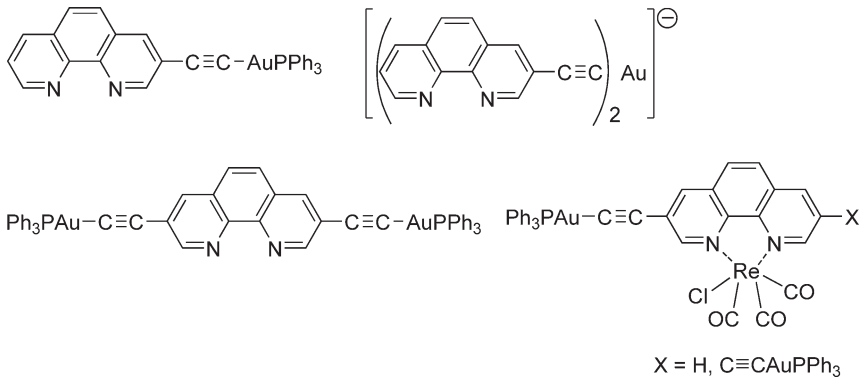

Scheme 10

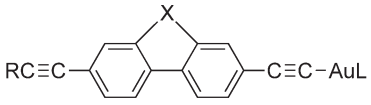

L = PMe_3, PPh_3

R = H, $(C_5H_4)Fe(C_5H_5)$ [Fc], $AuPPh_3$

X = CH_2, $C(CN)_2$, $C(C_6H_{13})_2$, $CH(C_6H_4$-4-Fc), C=O

Scheme 11

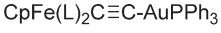

L = PPh_3, PMe_3; $(L)_2$ = dppe

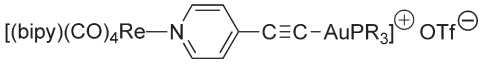

bipy = bipyridyl, di(^{t}Bu)bipyridyl; R = Ph, *p*-To

Scheme 12

2.05.4.1.6 Alkynylgold(I) compounds with NLO properties

Numerous compounds of the types (L)AuC≡CR and $Q^+[Au(C{\equiv}C{-}R)_2]^-$ were investigated for their properties as NLO materials. Some of the examples were found to have the largest cubic optical non-linearity for monomeric organometallics.[103] Examples are given in Scheme 18. For all of these compounds, the quadratic/cubic hyperpolarizability (linear optical and quadratic NLO response) have been determined. The studies were complemented by cyclovoltammetric measurements.[58,59,103,112–117]

2.05.4.1.7 Alkynylgold(I) compounds with chain and framework structures

Owing to the rigid-rod-type structure, alkynylgold(I) complexes can be used as building units for multidimensional systems. Typical examples are one-dimensional polymers of the general formula $[{-}Au{-}C{\equiv}N{-}C_6H_4{-}4{-}C{\equiv}C{-}]_n$ prepared from $ClAu{-}C{\equiv}N{-}C_6H_4{-}4{-}C{\equiv}CH$ and a base. The phenylene unit may be substituted.[56] Extended systems with linear or angular units – or combinations thereof – have been obtained with substituted 1,3-diethynylbenzenes,[52,55,57] 1,4-diethynylbenzenes,[57] and 3,5-diethynylpyridines,[61] or nona-1,8-diyne[71] and 1,2- and 1,3-di(1-prop-1-ynoxy)benzene[49] using the versatile acetylacetonate method or other standard procedures. A large variety of

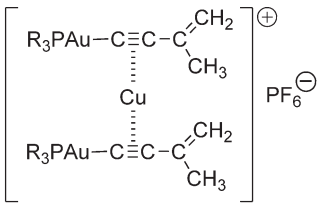

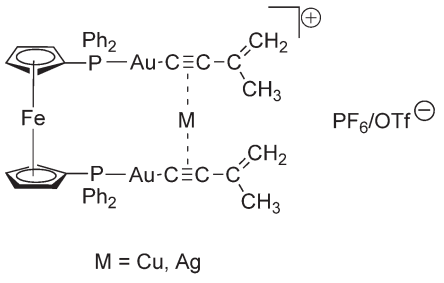

Scheme 13

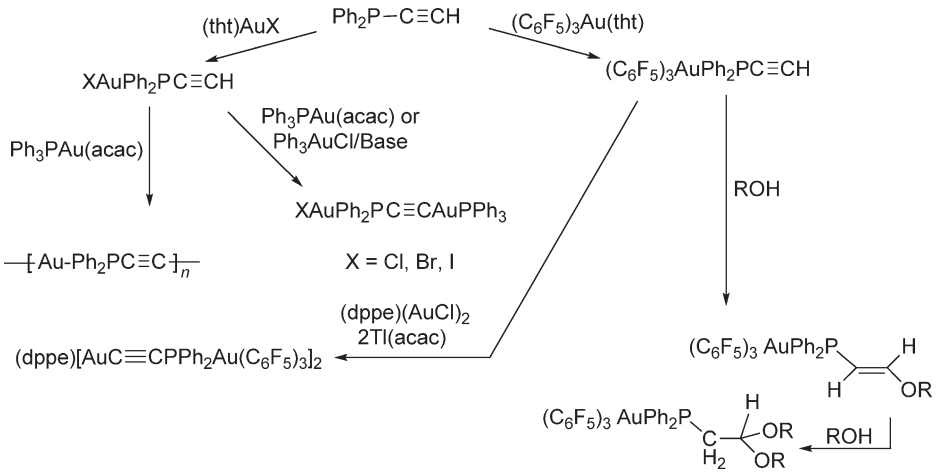

Scheme 14

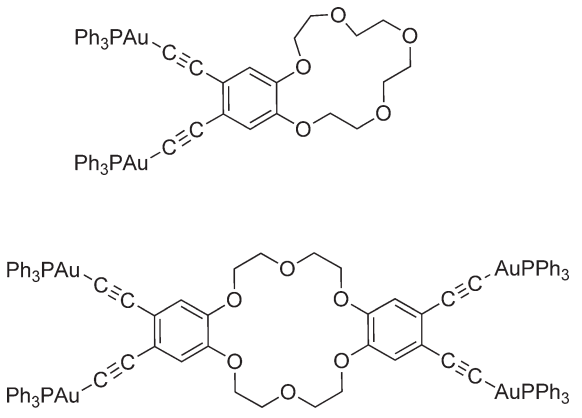

Scheme 15

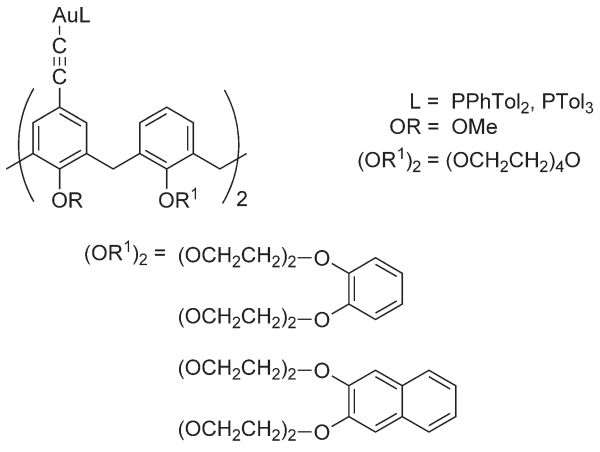

Scheme 16

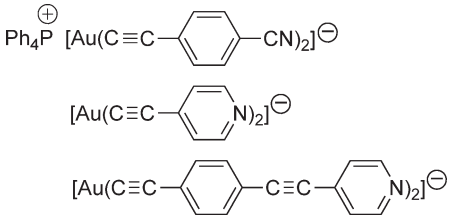

Scheme 17

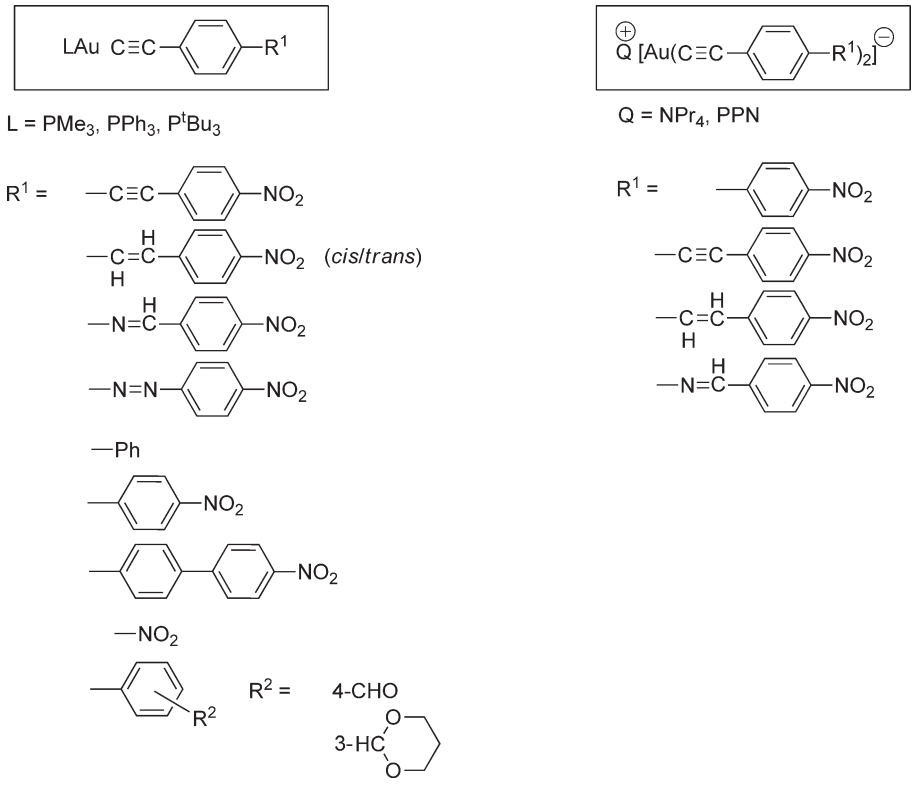

Scheme 18

auxiliary ligands was employed (tertiary phosphines, isocyanides, carbenes), including dppm, 1,4-diisocyano-2,3,5,6-tetramethyl-benzene,[50,55] 4,4′-diisocyano-diphenyl- and 2,2-di(4-isocyano-phenyl)propane.[50] Many of these materials are photoluminescent (e.g., Ref: 49), but there is no clear dependence of the emissive properties on structural details including the presence or absence of aurophilic interactions.

2.05.4.1.8 Alkynylgold(I) compounds with catena structures

Cyclic alkynylgold(I) compounds were shown to be particularly susceptible to spontaneous formation of catena structures, that is, of interpenetrating ring assemblies.[48] In very detailed studies, it has been demonstrated that there are delicate equilibria relating monocyclic monomers and dimers with the catena-bicyclic species in solutions, out of which either the catenanes or the other forms may be crystallized.[118] Model systems are shown in Scheme 19.[54] Depending on the nature of the "hinge" group X and the "spacer" group Z, the system may adopt different configurations, including monocyclic monomers, monocyclic dimers, higher oligomers (mainly hexamers), and catena dimers. In all cases investigated to date, aurophilic bonding contributes to the stability of the catena forms, and facilitates the transition from one oligomeric form to the other.[119]

2.05.4.2 Alkynylgold(III) Compounds

Only a very few alkynylgold(III) compounds have been reported. The earliest examples were complexes with mixed substitution patterns, such as $(RC{\equiv}C)R^1{}_2Au(L)$, where $R/R^1 = \text{alkyl}$ and $L = PR_3$.[26] Subsequent work has shown that compounds of the type $(RC{\equiv}C)_3Au(L)$ are accessible only with carefully selected combinations of ligands L and substituents R. For most combinations, the syntheses fail owing to rapid reductive elimination of dialkynyls (Equations (23) and (24)).[120]

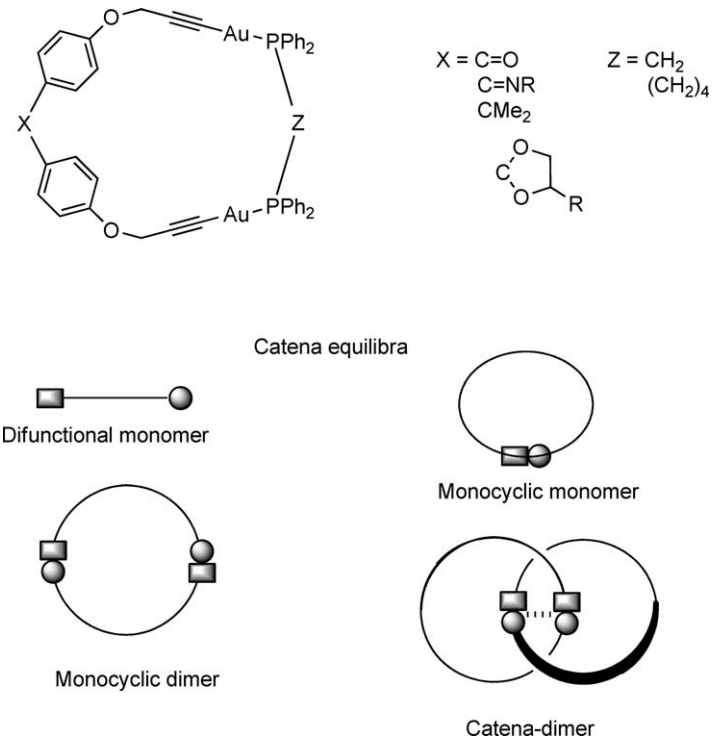

Scheme 19

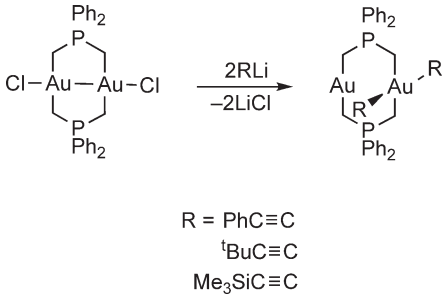

Scheme 20

$$(L)Au(C{\equiv}CR)_3 \rightarrow (L)AuC{\equiv}CR + RC{\equiv}C{-}C{\equiv}CR \quad (23)$$

$$[Au(C{\equiv}CR)_4]^- \rightarrow RC{\equiv}C{-}C{\equiv}CR + [Au(C{\equiv}CPh)_2]^- \quad (24)$$

The preparation and structural characterization were successful for the complexes $(L)Au(C{\equiv}C)_3$, with $L = PMe_3$ or Me_2PhPCH_2 and R = Ph. The two compounds are colorless and diamagnetic, and have the expected square-planar configuration of the gold(III) center.[120]

Salts with the homoleptic $[Au(C{\equiv}CR)_4]^-$ anion have been obtained in only one case (R = Ph), with $[^nBu_4N]^+$ as the counterion. The synthesis from $(Me_3P)Au(C{\equiv}CPh)_3$ and $PhC{\equiv}CLi$ followed by precipitation with $^nBu_4N^+Br^-$ from thf requires carefully controlled conditions. It is accompanied by reductive elimination of diphenyldiacetylene to give $[^nBu_4N]^+[Au(C{\equiv}CPh)_2]^-$ as the byproduct. The crystal structure of the colorless, diamagnetic mixed-anion salt $2[^nBu_4N]^+[Au(C{\equiv}CPh)_2]^-[Au(C{\equiv}CPh)_4]^-$ has been determined. The anions are linear and square planar, respectively.[120]

A mixed alkynyl/arylgold(III) complex, derived from 3-[(2-methyl-2-phenyl)ethyl]-biypridyl, has been prepared via orthometallation of the phenyl group. The compound has a square-planar gold(III) center in a C_2N_2 coordination.[121] A dinuclear mixed valence Au(I)/Au(III) cyclic ylide complex has been obtained by a ligand redistribution occurring upon treatment of the dinuclear gold(II) complex with 2 equiv. of $RC{\equiv}CLi$ (Scheme 20).[122]

2.05.4.3 Addition Reactions of Alkynes Catalyzed by Gold Complexes

A large variety of gold complexes were found to catalyze the addition of nucleophiles to alkynes. This subject has been reviewed.[123–125] Both internal and terminal alkynes undergo this reaction, as demonstrated for the addition of alcohols to 3-hex-yne[126] or of water to phenylacetylene.[127] For the former, $[(R_3P)Au]^+X^-$ salts are most efficient as catalysts. These are generated *in situ* from the alkyls $(R_3P)AuMe$ in dichloromethane upon treatment with strong acid HX ($X = CF_3CO_2^-$, $CF_3SO_3^-$, RSO_3^-, etc.) and in the presence of a co-catalyst (generally a Lewis acid like BF_3).[128] For the latter, arylgold(III) complexes were found to be most effective.[127]

If the nucleophilic and the alkyne functions are located at the ends of the same substrate, cyclizations are induced by the gold catalysts to produce both carbo- and heterocycles. For these reactions, $AuCl_3$ (in MeCN) is the catalyst of choice, while $(Ph_3P)AuCl$ is inactive.[129–131] By contrast, α,ω-enynes are cyclized, using $[(R_3P)Au]X$ catalysts obtained from $(Ph_3P)AuCl$ and $AgBF_4$ or $AgSbF_6$.[132] The cyclization of enol ethers with alkynes shown in Equation (25) is catalyzed by $AuCl_3$ in methanol. The energy profile for the proposed reaction mechanism has been studied by theoretical calculations.[133]

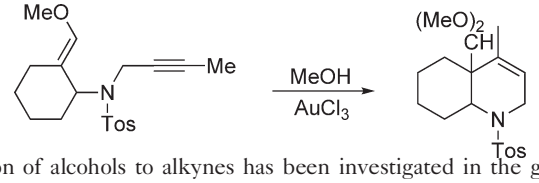

(25)

The gold(I)-catalyzed addition of alcohols to alkynes has been investigated in the gas phase by mass spectrometry techniques. While in the condensed phase, an efficient coupling to the corresponding enol ethers has been observed, in the

gas phase, kinetic and entropic restrictions are too large to permit bond formation in strictly bimolecular collisions mediated by Au^+ and $[(Me_3P)Au]^+$ at thermal energies. Complementary theoretical studies (DFT) of the system Au^+/C_2H_2/MeOH corroborated the experimental findings, for which a mechanistic model has been designed. According to these results, solvent-assisted hydrogen migration or protonation/deprotonation sequences play a major role in the condensed phase.[125] These calculations were preceded by studies of the interaction of olefins with gold(I) cations in the gas phase.[134]

Alkenylation of arenes has been achieved in hydroarylation reactions using both gold(I) and gold(III) catalysts. Thus, 1,3,5-trimethylbenzene (mesitylene) was converted into the (1-phenyl-)ethenyl derivative (Equation (26)) with catalysts produced from $AuCl_3$ and AgX ($X = CF_3SO_3$, BF_4, SbF_6, ClO_4) or from $(R_3P)AuCl$ and AgX in nitromethane. A cluster compound, $Au_9Ag_{11}Cl_{28}$, of unknown structure was isolated from the reaction of $AuCl_3$ with $AgOSO_2CF_3$ in nitromethane.[135]

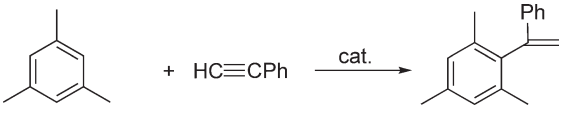

(26)

Cyclotrimerization of arylacetylene was observed in the reaction of $[PhC{\equiv}CAg]_n$ with $[(dppm)_2Au_2(MeCN)_2]^{2+}[BF_4^-]_2$ in dichloromethane. The products form an Au_5Ag_9 cluster containing 1,2,3-triphenylarene units aurated in the 4,5,6-positions.[136]

2.05.5 Arylgold Compounds

"Ligand-unsupported" arylgold(I) compounds are known only as oligomers $[ArAu]_n$ with highly substituted aryl groups Ar, that provide efficient steric shielding to the metal atoms which form a cyclic core unit with strong aurophilic bonding. One carbon atom of each aryl groups forms a μ^2-bridge between two metal atoms, and each metal atom is a μ^2-bridge between two aryl groups ($Ar = 2,4,6\text{-}Me_3C_6H_2$).[137] The monomeric unit (ArAu) with $Ar = 2,4,6\text{-}(CF_3)_3C_6H_2$ has been trapped in a pincer-type molecule $(cp)_2Ti(C{\equiv}CSiMe_3)_2$.[138] Triarylgold(III) compounds (Ar_3Au) with donor-free aryl groups have not been isolated.

"Ligand-supported" compounds (L)AuAr and $(L)AuAr_3$ are known with a large variety of simple or substituted aryl groups Ar and neutral donors L. L may be substituted by an anionic ligand X^- to give anions $[ArAuX]^-$ and $[Ar_3AuX]^-$, respectively. With X = Ar, the homoleptic anions $[Ar_2Au]^-$ and $[Ar_4Au]^-$ are obtained, complemented by mixed species $[Ar_nAuX_{4-n}]^-$. Representatives of all these classes of molecules and anions have been documented in the early literature,[2,139–141] but some of the analytical, spectroscopic, and structural data were provided only in the period which is covered in the present account.

2.05.5.1 Arylgold(I) Complexes

The most straightforward synthesis of compounds (L)AuAr uses the metathesis of (L)AuX precursors with aryllithium reagents, as, for example, executed for the preparation of $(Ph_3P)AuPh$. The crystal structure of this benchmark complex has been determined. The linear coordination geometry is as expected. No aurophilic contacts are discernible in the crystal packing. Short Au···Au contacts are observed, however, in the dinuclear compound $(dppm)(AuPh)_2$ with an intramolecular intermetallic distance of 3.154(1) Å. This complex shows a UV–VIS absorption at 290–300 nm and is luminescent in fluid solution at room temperature.[17]

1,4-Diaurated phenylenes have been prepared by dilithiation of 1,4-dibromo-2,5-dimethyl-benzene followed by treatment with 2 equiv. of $(Ph_3P)AuCl$. A similar procedure gives the 4,4′-diaurated diphenyl. In an analogous way, 9,10-dilithio-anthracene yields the 9,10-diaurated arene. The structures have all been confirmed by X-ray crystallography (Scheme 21).[39] Alkali tetraphenylborates can also be employed as phenylating agents.[142]

Complexes with the more labile tht ligand can be employed for the preparation of a large number of derivatives. Compounds (tht)AuAr, obtained from ArLi and (tht)AuCl, are readily converted into complexes (L)AuAr with $L = PPh_3$, P(*o*-Tol)$_3$, 2,5-dimethylpyridine (lutidine), and MeCN. With 2,2′-bipyridyl, the dinuclear complexes $(bipy)(AuAr)_2$ are obtained. With halide anions X^-, salts of the type $[ArAuX]^-$ are accessible (X = Cl, Br, I). The salts with homoleptic anions $[AuAr_2]^-$ have been synthesized from salts $NR_4^+[AuBr_2]^-$ and 2 equiv. of ArLi (R = Et, ^{n}Bu). Treatment of these products with $AgBF_4$, followed by 4-methyl-pyridine, affords $[(4\text{-Me-py})_2Ag]^+[AuAr_2]^-$. Oxidative addition of halogen X_2 (X = Cl, Br, I) to salts with the above anions gives rise to products with the corresponding anionic arylgold(III) species, for example, $NR_4^+[ArAuX_3]^-$ or *trans*-$NR_4^+[Ar_2AuX_2]^-$, respectively. The aryl group used in this comprehensive study was 2,4,6-tris(trifluoromethyl)phenyl.[143]

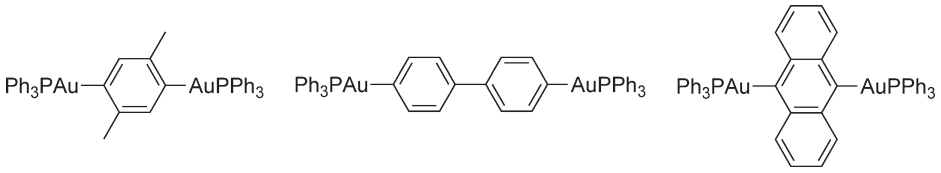

Scheme 21

Compound (tht)AuC_6F_5, as well as (tht)$Au(C_6F_5)_3$, react with 2-amino-thiazoline to give the ring *N*-coordinated adducts of this heterocycle. By contrast, the reaction with $(Ph_3P)Au(acac)$ leads to ring cleavage, producing the dinuclear complex of a 2-cyanamido-ethylthiolate (Equation (27)).[144]

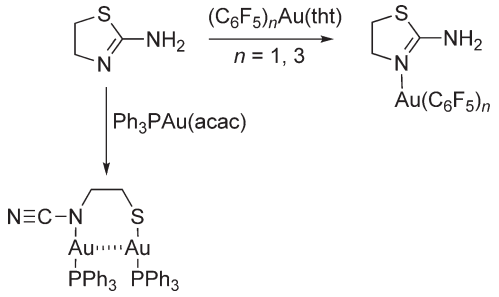

(27)

The reaction of (tht)AuC_6F_5 with the diazonium compound Ph_2CN_2 is also very complex and yields an adduct of a hydrazone, probably via the carbene Ph_2C: as an intermediate (Equation (28)).[145]

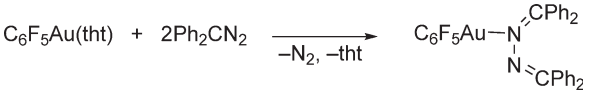

(28)

Salts of the type $PPN^+[C_6F_5AuCl]^-$ can be converted into the acetylacetonate $PPN^+[C_6F_5Au(acac)]^-$, and finally into the mixed aryl(ethynyl)gold(I) complex using Tl(acac) and C_2H_2, respectively. The same sequence applies to the 2,4,6-trinitro-phenyl-(picryl) and 2-nitro-phenyl-gold complexes.[73]

Treatment of (tht)AuC_6F_5 with 1-methyl-imidazol-2-yl-lithium gives an ionic product which can be converted into the neutral carbene complex upon *N*-methylation with MeI (Equation (29)).[146]

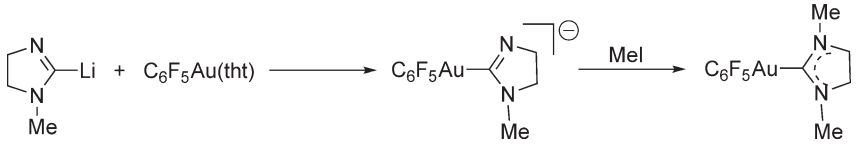

(29)

The reaction of (tht)AuC_6F_5 with a difunctional aminophosphine gives high yields of the dinuclear arylgold(I) complex. The counterparts in gold(III) chemistry have been prepared in the same way using (tht)$Au(C_6F_5)_3$. The same pattern was observed with the disulfide of this ligand in the reactions with (tht)$Au(C_6F_5)_3$ and $[(C_6F_5)_2Au(OEt_2)_2]ClO_4$ (Scheme 22).[147]

Compound (tht)AuC_6F_5 undergoes random aryl exchange with pentafluorophenylpalladium(II) complexes, while the 3,5-dichloro-2,4,6-trifluorophenylgold complex specifically catalyzes the *trans–cis* isomerization of $[Ar_2Pd(tht)_2]$. The reaction appears to follow an associative mechanism.[148]

Arylation of gold(I) complexes can also be accomplished using arylbismuth reagents. Tris(2-dimethylaminomethyl-phenyl)bismuth reacts with $(Me_2S)AuCl$ to give a cyclic dinuclear product (Scheme 23). With Ph_3Bi, the primary product $PhAuPPh_3$ is further aurated to produce the cationic species $\{\mu\text{-}Ph[Au(PPh_3)]_2\}^+$ as the tetrafluoroborate.[149] There is precedent for this type of phenyl bridging, with prototypes being structurally confirmed.[150,151]

Salts with the anion $[(C_6X_5)_2Au]^-$ with X = F, Cl have been found to trap coinage metal and neighboring main group metal cations (like Tl^+) to give mixed metal aggregates with short metallophilic contacts. Examples in case are $\{Tl_2[Au(C_6Cl_5)_2]_2(Me_2CO)\}$[152] and $\{Cu[Au(C_6F_5)_2](MeCN)(C_4N_2H_4)\}$,[153] where acetone, acetonitrile, and pyrimidine can be auxiliary ligands. The products are strongly photoluminescent with variations depending on the

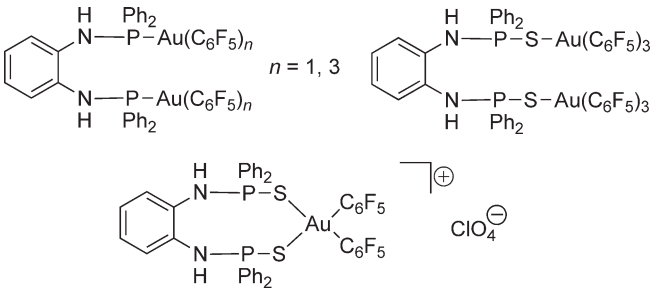

Scheme 22

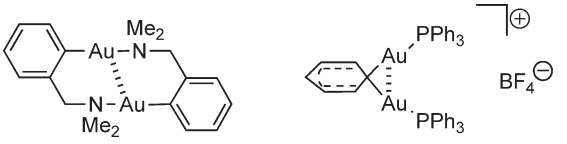

Scheme 23

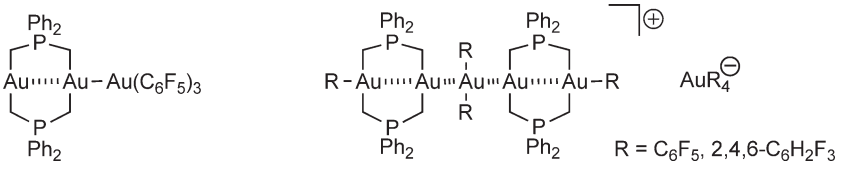

Scheme 24

combinations of metals, stoichiometry, and the nature of the auxiliary ligands.[154] A discussion of their unprecedented structures is not within the scope of this review.

Unusual aurophilic bonding between gold in different oxidation states appears to be responsible for the adduct formation between $(C_6F_5)_3Au$ and cyclic ylide complexes with gold in the oxidation state +1 and +2 and in related compounds with an ionic structure (Scheme 24).[155–157]

2-Diphenylphosphino-arylgold(I) compounds form cyclic dimers, which can be oxidized with halogen or other agents X_2 to give the dinuclear gold(II) complexes with a transannular Au–Au bond. These products undergo rearrangements leading to mixed valence Au(I)/Au(III) complexes or to oxidative C–C coupling. The course of the rearrangement depends strongly on the substitution pattern of the aryl group and on the nature of X. In the orthomethylated cases (with X = Cl, Br, I, $PhCO_2$, C_6F_5), one gold atom of the product appears in a terminally bonded AuX unit while the other one has become integrated in a four-membered ring.[158] The metamethylated isomers or the unsubstituted compound are converted into the 2,2′-bis(diphenylphosphino)diphenyl complexes,[159] while with dithiocarbamate, the product features an *S*,*S*-chelated gold(III) center (Scheme 25).[160]

2.05.5.2 Arylgold(III) Complexes

Direct access to arylgold(III) compounds is given by the auration of aromatic hydrocarbons with anhydrous $AuCl_3$ in an inert solvent like hexane (with evolution of HCl). Benzene, toluene, the three isomeric xylenes, mesitylene, cumulene, anisol, and chlorobenzene have been converted into products of the type $ArAuCl_2$ which were isolated as the 2,6-dimethyl-pyridine (lutidine) complexes. The reactions are regioselective with the incoming $AuCl_2$ substituent directed into the activated positions of the ring following established rules for electrophilic aromatic substitution (Equation (30)).[161]

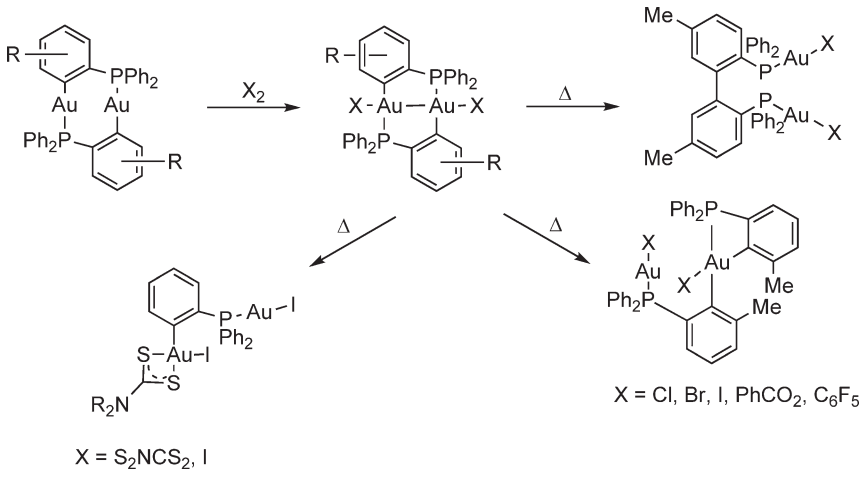

Scheme 25

$$ArH + AuCl_3 \xrightarrow[-HCl]{} [ArAuCl_2] \xrightarrow{L} ArAuCl_2(L) \qquad (30)$$

An alternative preparative pathway is based on the arylation of salts with the anion $[AuCl_4]^-$with organometallic reagents. Organomercurials Ar_2Hg thus afford salts with the anions $[ArAuCl_3]^-$ as the primary products from which the complexes $ArAuCl_2(L)$ can be produced upon treatment with a donor ligand $L = PR_3$, etc. The mild reaction conditions allow the introduction of functional aryl groups such as azoaryls in a first or second arylation step.With a donor function available in one of the aryl groups, intramolecular complexation (chelation) leads to neutral complex molecules (Scheme 26).[162]

With a Schiff base present in the organomercurial, this chelation affords complexes which can be transformed into a large number of derivatives. With a stronger donor like $L = PPh_3$, the chelation is abandoned. Substitution of Cl^- by ClO_4^- using $AgClO_4$ in acetone leads to auration of the solvent (Scheme 27).[163] Ketones of this type were subsequently converted into Schiff bases with aniline, their chelation abandoned by offering PPh_3 or dppe, and their Cl^- substituted by CN^-, OAc^-, or I^-. Treatment with $AgClO_4$ leads to coordination of the keto oxygen atom to the gold(III) center.[164]

Anions $[Ar_2AuCl_2]^-$ have been generated using organomercurials with $Ar = 2\text{-}O_2N\text{–}C_6H_4$, $2\text{-}F_3C\text{–}C_6H_4$. Their reaction with Tl(acac) affords the chelated acetylacetonate complexes, but upon treatment with Ph_3P, the acac ligand becomes *C*-monodentate. Metathesis with sodium phenolate followed by hydrolysis gives the dimeric diarylgold(III) hydroxide, which was structurally characterized as the etherate (Scheme 28).[165] Further arylation of the anions $[Ar_2AuCl_2]^-$ with azoaryl- and 2-dimethylamino-methyl-aryl-mercury compounds give cyclic triarylgold(III) complexes (Scheme 29).[163]

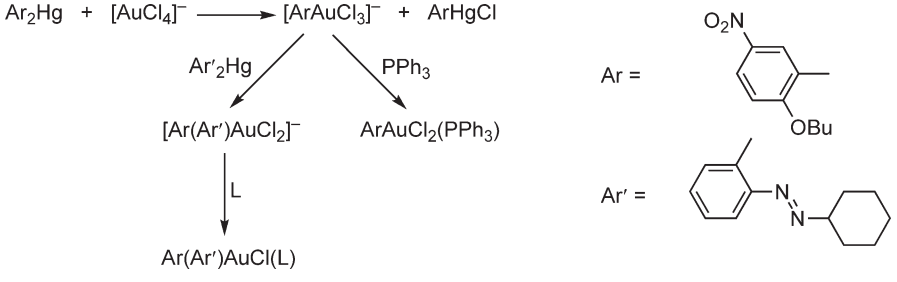

Scheme 26

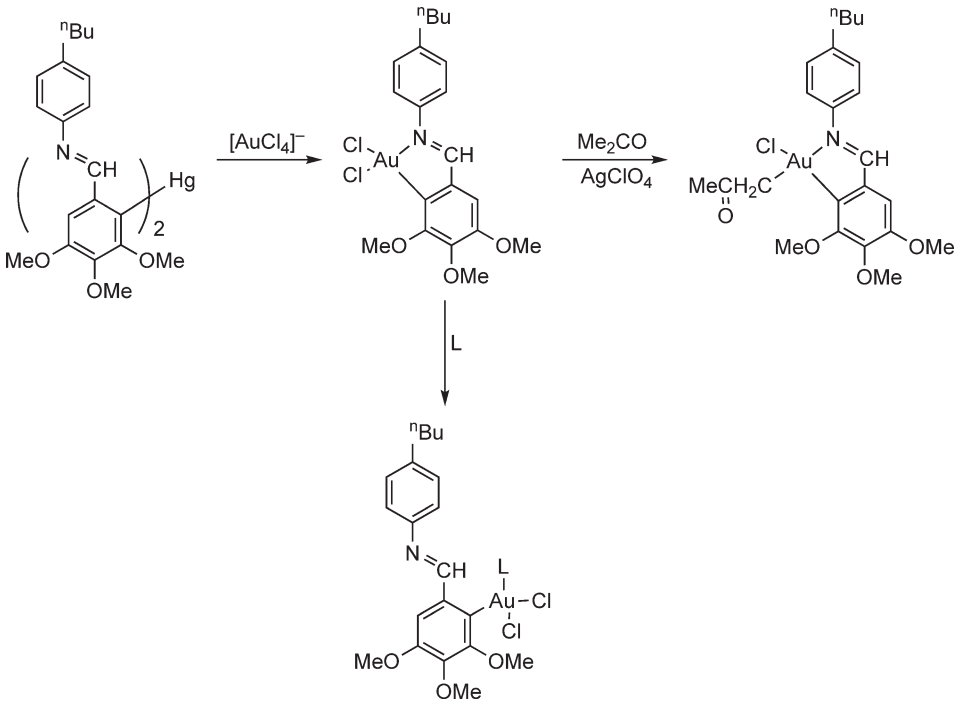

Scheme 27

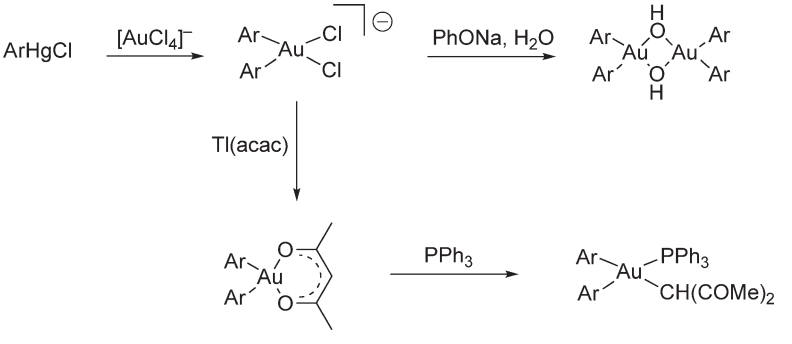

Scheme 28

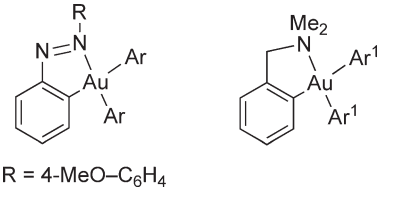

Scheme 29

Compound (tht)Au(C_6F_5)$_3$ reacts readily with a variety of tertiary phosphines to give the corresponding complexes as demonstrated, for example, for diphenyl(ethynyl)phosphine. The coordination of the *P*-center activates the ethynyl triple bond for the two-step addition of alcohols. The ethynyl group can further be aurated to give extended systems with gold in two different oxyidation states (Equation (31)).[70]

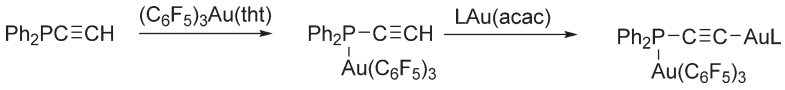

(31)

A diorganogold(III) complex with the aryl substituent attached to a bipyridyl ligand was found to undergo unexpected reductive elimination of the hydrocarbon upon treatment with Ph_3P which involves C–C coupling (Equation (32)).[121]

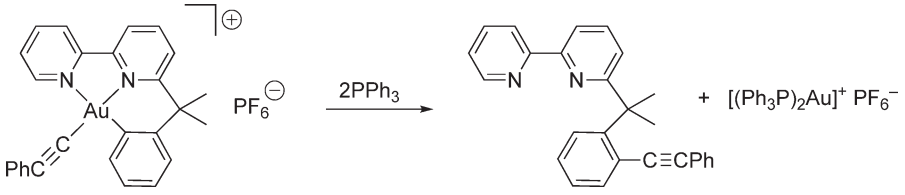

(32)

2.05.6 Ylide Complexes of Gold

This section is dedicated to organogold compounds in which the carbanionic center of an onium ylide is attached as a σ-donor to the gold atom in any of its common oxidation states (Au(I), Au(II), Au(III)). In the majority of complexes, the ligands are phosphonium or (oxo)sulfonium ylides with tetracoordinate, positively charged P or S atoms. Since the mid-1970s, ylide complexes of gold have attracted considerable interest owing to the inherent stability of their Au–C bonds, which renders these compounds readily available. The compounds are convenient model compounds for the study of substitution, oxidation, and reduction reactions, and many other conversions of organogold compounds. In COMC (1982) and COMC (1995),[1,2] large chapters have already been dedicated to this chemistry (covering the literature to 1993), the contents of which are not reconsidered here. The field is still growing rapidly, and in the period 1993–2005, significant advances have again been made. Several reviews have appeared in which the chemistry has been included, at least in part.[5,6,7,29,166,167,168]

2.05.6.1 Ylide Complexes of Gold(I)

Phosphonium ylides, which can be written in the two familiar canonical forms, are available with a wide variety of substituents both at the phosphorus and at the carbon atoms (Scheme 30). In gold complexes, without any exceptions, they function as two-electron donors, as proposed by the dipolar form to give discrete Au–C σ-bonds (η^1, monohapto). No side-on, π-coordination (η^2), as might be expected out of the ylene form, has been observed to date.

Bis-ylides (Scheme 31) may function as four-electron donors and become geminally diaurated. The donor capacity of ylides is generally higher than that of most other ligands, and even powerful donors like tertiary phosphines can thus be readily replaced by non-stabilized ylides. Ylides may therefore be used as auxiliary ligands which are retained, while other components of the coordination sphere are subject to substitution.

Scheme 30

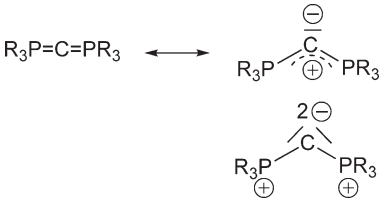

Scheme 31

Scheme 32

Sulfonium and oxosulfonium ylides or mixed phosphonium/sulfonium ylides are equally potent σ-donors for gold(I) and gold(III) centers (Scheme 32).[1,2,166,168]

Formulas of phosphonium/sulfonium ylide complexes should be written with onium charges at the P or S atoms and negative charges at the metal atom, but for the sake of convenience and clarity, these charges are omitted.

The excellent donor properties of ylides are amply reflected in many of the early prototypes of this chemistry,[2,166] but they are also obvious from some of the more recent studies, for example, of complexes [(ylide)Au(tht)]$^+ClO_4^-$, where (ylide) can be $Ph_3P{=}CH_2$, $MePh_2P{=}CH_2$, $Me_2PhP{=}CH_2$, $Ph_3P{=}CHPh$, or $Ph_3As{=}CH_2$. The (tht) ligand can be replaced selectively by nucleophiles L/X^-, such as tertiary phosphines, arsines and stibines, pyridine and phenanthroline, alkynyl, and tetra(carbonyl)cobaltate to give compounds [(ylide)Au(L)]$^+ClO_4^-$ or (ylide)AuX.[169] (Carbene)gold(I) acetylacetonates react directly with phosphonium or sulfoxonium salts to give acetylacetone and mixed carbene/ylide complexes such as {$(Et_2N)(^tBuNH)C$]Au[$CH_2S(O)Me_2$]}$^+ClO_4^-$.[170]

Substrates with two labile substituents such as (tht)AuCl can be converted into ylide complexes in two steps. An example of this type is the product $[(Ph_3PCH_2)_2Au]^+ClO_4^-$ obtained upon the reaction with two ylides, followed by anion exchange. The cation with its linear CH_2–Au–CH_2 core unit crystallizes with the tetracyanochinodimethane anion as a green crystalline product.[171]

Even the less reactive ylides with substituents reducing their nucleophilic character undergo smooth reactions as demonstrated with $Ph_3P{=}CH{-}CH_2{-}C{\equiv}N$ and $Ph_3P{=}CH{-}C{\equiv}N$[172] or $Ph_3P{=}CH{-}SO_2$-*p*-Tol.[173] The products can be obtained from the free ylides or from the corresponding phosphonium salts using an auxiliary base: with (Ph_3P)Au(acac), $[Ph_3PCH_2CN]^+ClO_4^-$ can be converted into the dinuclear cation. In this "acac" method, the acetylacetonate anions act as the auxiliary base for the double deprotonation of the phosphonium cation. The primary product may even accept a third $[(Ph_3P)Au]^+$ unit at the cyano group (Scheme 33).[172] $Ph_3P{=}CHSO_2$-*p*-Tol is the ligand in the mononuclear complex molecule $Ph_3PCH(AuCl)SO_2$-*p*-Tol and in the dinuclear salt $[(Ph_3PCHSO_2$-*p*-Tol$)_2Au]^+SO_3CF_3^-$, with its central HC–Au–CH unit featuring two carbon centers of chirality.[173]

$[Ph_3PCH_2PPh_3]^{2+}2X^-$ can similarly be converted into dinuclear complexes (Scheme 34).[173] $[MePh_2P{=}CH{-}PPh_2Me]^+SO_3CF_3^-$ reacts with (tht)AuX, where X = Cl or C_6F_5, to give salts with the central carbon atom of the cation monoaurated. This carbon atom is conventionally tetracoordinated as demonstrated by structure analysis.[174] The fully phenylated bis-ylide $Ph_3P{=}C{=}PPh_3$ is only monoaurated in $(Ph_3P)_2C$–Au–C≡C–C_6H_4–4-NO_2 prepared from equimolar quantities of the components.[173]

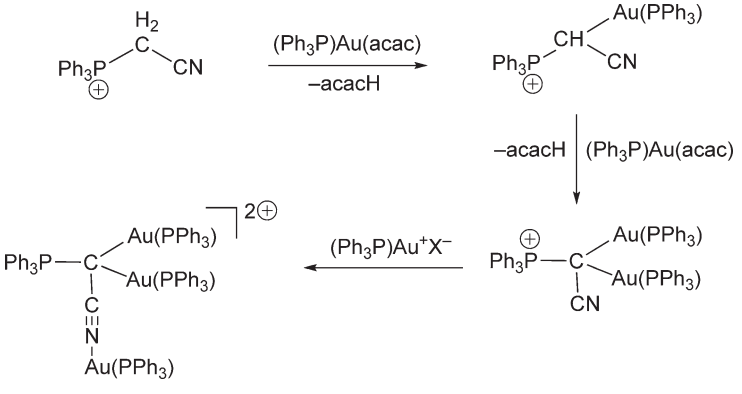

Scheme 33

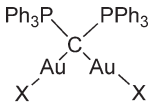

X = Cl, C_6F_5

Scheme 34

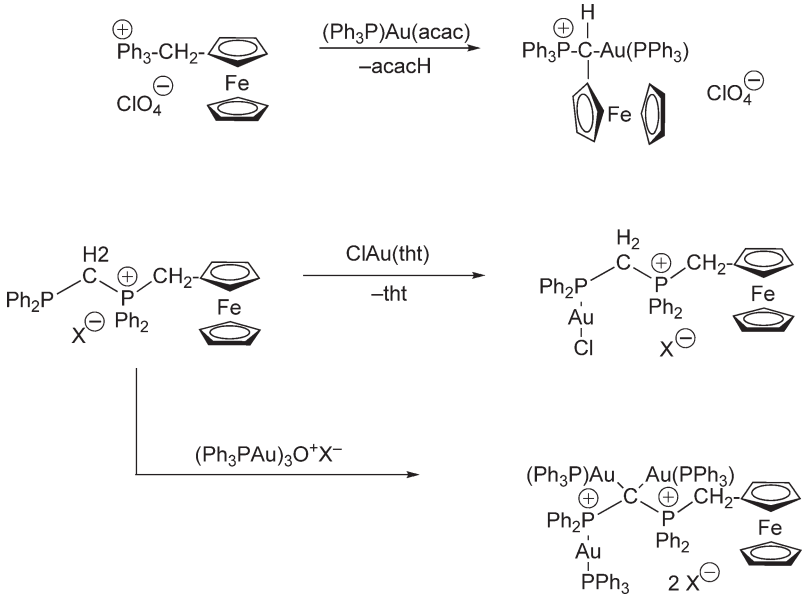

Scheme 35

Similar results were obtained with ferrocenylmethyl phosphonium salts $[FcCH_2PPh_3]^+ClO_4^-$: treatment with $(Ph_3P)Au(acac)$ affords $[(Ph_3P)Au–CH(PPh_3)Fc]^+ClO_4^-$. The corresponding extended substrate derived from dppm gives both a *P*-monoaurated and a *C*,*C*-diaurated product (Scheme 35).[28] The ligand dppm dihapto-coordinated to a gold(III) center has C–H-acidic methylene protons and may be considered an ylide analog. This is borne out by the facile diauration with $(Ph_3P)Au(acac)$.[28]

It is interesting to note that an ylide bearing a potential β-diketonate functionality is aurated regioselectively at the ylidic carbanion, as proved for the product obtained from $Ph_3P{=}CHC(O)CH_2COOEt$ and (tht)AuCl. A complex $[(ylide)_2Au]^+ClO_4^-$ was also generated with this ylide.[175] [(2-Thiazolylcarbonyl)methylene]triphenylphosphorane has also been employed as a ligand. It was transferred from a niobium complex.[176] Chiral *N*,*N*′-diaryl-α-naphthamidinium-*N*-1,2,3,4-tetra(methoxycarbonyl)cyclopentadien-5-yl ylides have also been introduced as ligands to gold(I). This is an exceptional case in which the onium charge is delocalized over an amidinium unit, which is to be considered in a different context.[177]

Regarding structure and bonding of mononuclear ylide complexes of gold, as investigated by analytical, spectroscopic, and theoretical methods in solution and in the solid state, it has been found that the fundamental configuration follows conventional rules.[28,174] In the solid, however, there are distinct non-conventional intra- and intermolecular aurophilic interactions, manifested by sub-van der Waals contacts of gold atoms. These interactions determine certain conformations[178] and specific modes of aggregation.[173] This aggregation may be accompanied by photoluminescence phenomena, but the origin of these physical effects is not always clear. Intermolecular aurophilic contacts are absent if steric crowding prevents the mutual approach to reach Au···Au distances less than 3.5 Å, and if contributions from other intermolecular forces are dominant, which is particularly common for compounds with hydrogen-bonding capabilities.

One of the most remarkable recent extensions of the chemistry of aurated ylides was the multiauration of dimethyl(oxo)sulfonium methylide using trimethyl(oxo)sulfonium salts and $(Ph_3P)Au(acac)$ in different

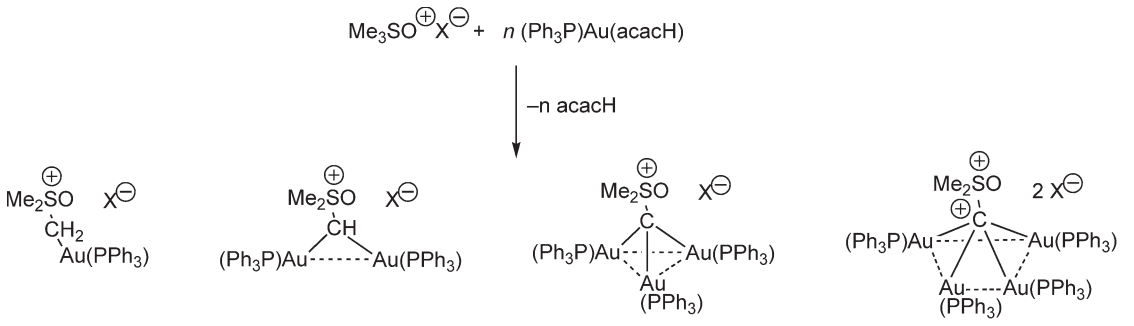

Scheme 36

stoichiometries.[179] The ylidic carbon atom was found to accept up to four gold atoms without cleavage of an S–C bond (Schemes 1 and 36).

This is an important parallel to the analogous process first discovered for phosphorus ylides in the late 1980s,[166] and extended to simple hydrocarbons in the mid-1990s.[15] Note that carbon is again found to become hypercoordinate in a square-pyramidal geometry (Scheme 37).

Ylides with onium centers bearing two or more carbon atoms with acidic hydrogen atoms can be polyaurated at the carbanionic groups generated upon deprotonation.[2,166] Thus, phosphonium salts with cations such as $[Me_4P]^+$ or $[Ph_2PMe_2]^+$ can be metallated, for example, with alkyllithium reagents, at two different carbon atoms to give phosphonium bis-methylide anions $[Me_2P(CH_2)_2]^-$ and $[Ph_2P(CH_2)_2]^-$, respectively, which can form open-chain or cyclic gold(I) complexes (Scheme 38).[2,3,7,168]

These were found to have a particularly rich coordination chemistry, because the close proximity of the two gold atoms leads to significant transannular aurophilic interactions, facilitating, for example, the stoichiometric oxidation to compounds with a transannular Au–Au bond with the metal atoms in the rare Au(II) state (Scheme 39).[2,166,168]

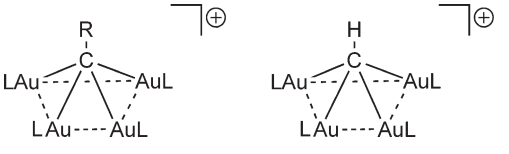

Scheme 37

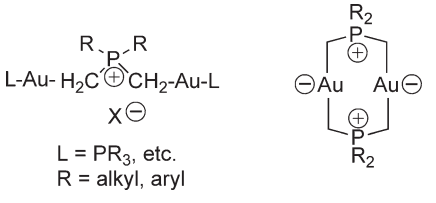

Scheme 38

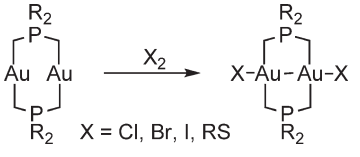

Scheme 39

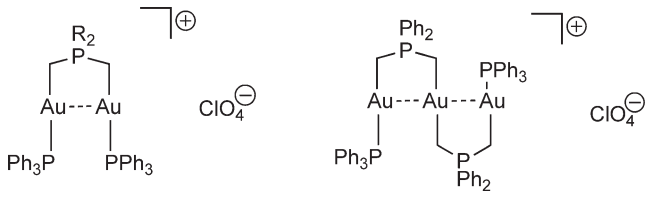

Scheme 40

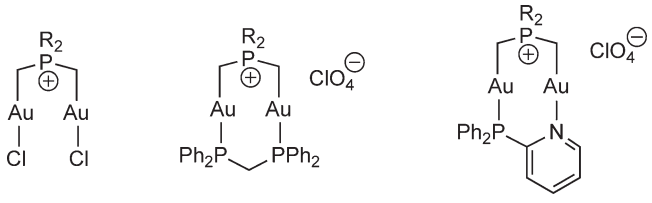

Scheme 41

Elegant investigations have subsequently been dedicated to the preparation and separation of *cis*- and *trans*-isomers of compounds, with different substituents at each phosphorus atom. The products were converted into their adducts with SO_2, and oxidized to the Au(II) dithiocarbamates using thiuram disulfides. In NMR experiments, it has been demonstrated that these compounds undergo ligand exchange through ring opening and closing, for which rate constants have been determined. For this process, a mechanism has been proposed which is supported by the observation that the exchange is suppressed by base.[180]

Investigations of the ligand-exchange reactions have shown cases of irreversible ring opening. Thus, treatment of the cyclic ylide complexes with $[(Ph_3P)_2Au]^+ClO_4^-$ or $[(Ph_3P)Au]^+ClO_4^-$ yields products with open-chain di- or trinuclear cations (Scheme 40), whereas with $[PPN]^+[AuCl_2]^-$, products with dinuclear anions are formed.[29,178] These were found to react with 2 equiv. of $AgClO_4$ in the presence of dppm or 2-pyridyl-diphenylphosphine to give mixed-ligand cyclic systems (Scheme 41). Two cyclic systems with different bridging ligands may again undergo facile exchange in solution. This was exploited with various dialkylcarbamate ligands.[181]

Ring opening of the ylide aurocycles can also be accomplished using a strong mineral acid. Thus, treatment with perchloric acid in the presence of Ph_3P or dppe gives an open-chain product or a new heterocycle, respectively (Equation (33)).[182] The latter was found to crystallize with TCNQ. The nature of these green or brown adducts, which exhibit variations in their stoichiometry and may show interesting electrical conductivity, is not yet fully explored.[171] Red or black compounds with similar properties were obtained by reacting a series of other polysulfur heterocycles directly with $NaAuCl_4$ in methanol containing sodium methanolate.[183]

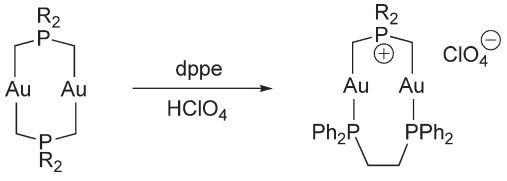

(33)

Cyclic dinuclear ylide complexes have also been prepared with sulfur ylides. The reactions of $(dppm)(AuCl)_2$ or $(dppe)(AuCl)_2$ with trimethylsulfoxonium tetrafluoroborate and base under phase-transfer conditions gave the products shown in Scheme 42. Auration of the dppm ligand leads to the byproducts.[27]

"Structure and bonding" in cyclic ylide complexes have been studied extensively in earlier experimental and theoretical work.[2] There is general agreement that transannular aurophilic bonding has a significant influence on the stability and reactivity of this family of compounds. There is also evidence for "inter"-molecular aurophilic bonding between these auracycles, but the number of examples is still limited (Scheme 43).[27,155–157,181]

The stereochemistry and dynamics were investigated by spectroscopic and structural techniques yielding a consistent picture of the general constitutional and conformational pattern, which is best described as based on the chair- or (less frequently) tub-form[184] of a folded six-membered ring with two opposite edges extended by the

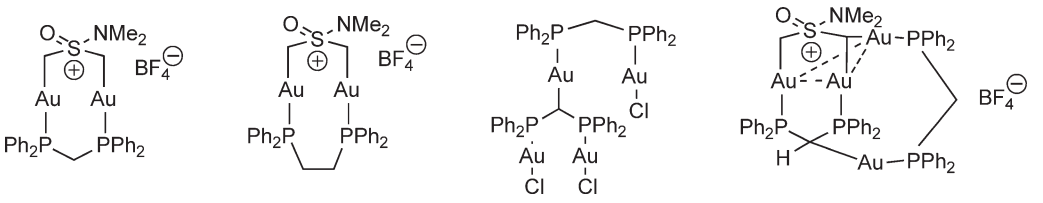

Scheme 42

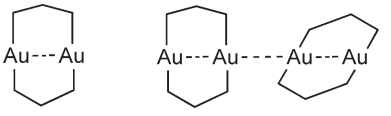

Scheme 43

Scheme 44

insertion of linearly two-coordinate gold atoms (Scheme 44). Theoretical studies have been extended to compounds with mixed ligands employing HF and MP2 calculations with LANL2DZ basis sets.[185]

2.05.6.2 Ylide Complexes of Gold(II)

Cyclic ylide complexes are readily oxidized not only by aggressive reagents like elemental halogens but also by milder oxidants like disulfides, or even mercaptanes in the presence of molecular oxygen, as shown for a reaction with pyridine-2-thiol in air (Equation (34)).[182] A similar reaction is known to take place with thiuramdidulfides.[2,180]

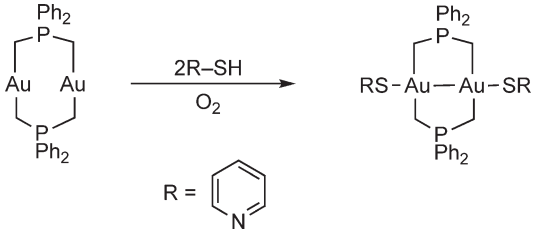

(34)

The preparation of chlorine derivatives is carried out in a more convenient way using $PhICl_2$ instead of Cl_2 gas, as demonstrated for the mixed-ligand auracycles with R = Me, Et (Equation (35)).[184]

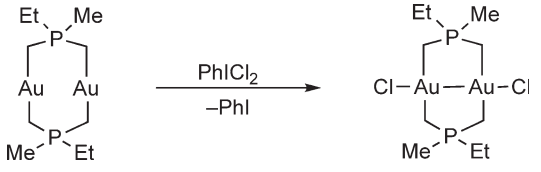

(35)

The chloride or, generally, halide ligands X in compounds shown in Scheme 39 can readily be replaced by other anionic or neutral ligands. Treatment with $AgClO_4$ in the presence of donors L like R_3P, tht, or even H_2O leads to

stable complexes, several of which have been crystallized (Equation (36)).[186,187] Direct displacement of Cl by organic groups using organometallic reagents is also straightforward in standard cases.[187]

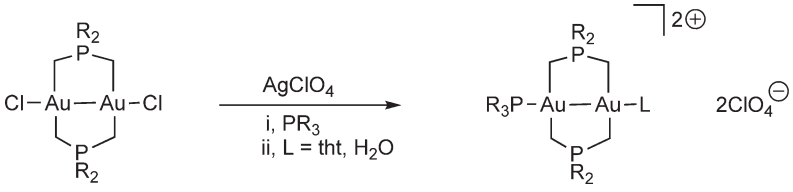

(36)

However, recent experiments have shown that the substitution may take a different course and lead to Au(I)/Au(III) mixed-valent compounds. This is not only true upon methylation, as demonstrated in very early studies,[168] but also upon introduction of alkynyl substituents. The reaction with 2 equiv. of R–C≡CH/KOH or R–C≡C–Li gives compounds with a linearly two-coordinate gold(I) and a square-planar four-coordinated gold(III) center in the same ring. Upon reaction with $AgClO_4$ in the presence of tht, followed by alkali chloride, the original substrate is recovered. This is an excellent example for the reversibility of the site exchange of ligands between metal centers with the equilibrium strongly depending on the nature of the substituents (Equation (37)).[188]

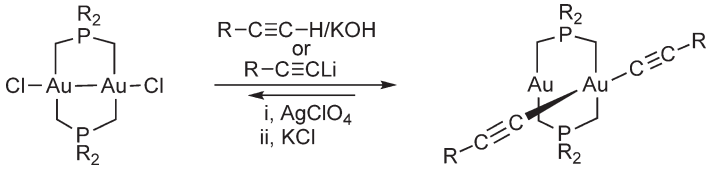

(37)

An intriguing observation was made by Uson *et al.* in 1991 while following the reaction of a cyclic ylide complex with $(C_6F_5)_3Au$, which leads to a 1 : 1 adduct with the triarylgold acceptor attached to one of the two ring gold atoms.[156,157] The product is a rare case of unsupported Au(I)–Au(III) donor/acceptor bonding, which is even less readily explained by conventional concepts than the more abundant aurophilic bonding between two or more gold(I) centers. Similar observations have been made in reactions summarized in Scheme 24. Some of the products again feature this new type of Au–Au bonding, which requires further theoretical investigation.[155]

Structure and bonding in the (diamagnetic) ylide complexes of gold(II) were studied very thoroughly by analytical, spectroscopic, structural, and theoretical techniques shortly after their discovery.[2,168] The principles of configuration and conformation of the eight-membered ring with its transannular gold–gold bond are the same as in the gold(I) precursors compounds (Schemes 39, 44). There is general agreement that this transannular Au–Au bond must be taken as a true two-center/two-electron σ-bond, comparable, for example, to the Hg–Hg bond in dinuclear mercury(I) compounds. Recent Raman investigations have confirmed this picture for the series with X = Cl, Br, I. There is a convincing correlation between Au–Au distances, as determined by X-ray diffraction and Au–Au stretching frequencies (Scheme 45).[189,190]

2.05.6.3 Ylide Complexes of Gold(III)

Oxidative addition of 2 moles of halogen to the cyclic ylide gold(I) complexes leads to the corresponding gold(III) complexes, which can appear in several different configurations originating from the *cis*- and *trans*-orientation of the halogen atoms at each gold atom.[168] Subsequent studies have extended this work to species with substituents other than halogen. This work has focused on diphenyldithiophosphinates and diphenyl(thio)phosphonium methylides. Owing to the lower oxidative power of these pseudohalogen ligands, the gold(III) compounds undergo facile elimination of the corresponding disulfides to give dinuclear gold(II) compounds with the transannular Au–Au bond (Scheme 46).[191]

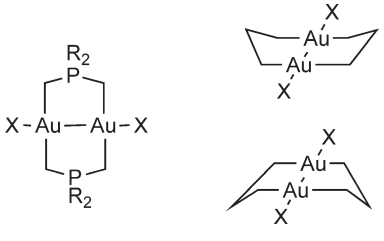

Scheme 45

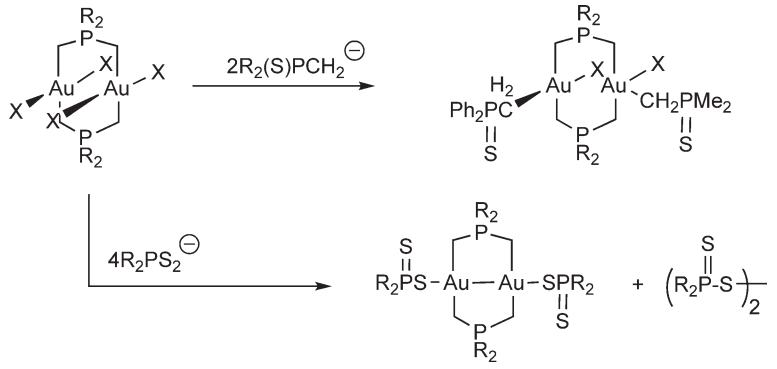

Scheme 46

Oxidative addition of dihalomethanes CH_2X_2 to cyclic gold(I) ylide compounds yields bicyclic compounds with a methylene bridge between two gold(III) centers.[2] The two halogens can also be replaced by diphenyldithiophosphinate groups to give products which are kinetically stable toward reductive elimination (Equation (38)).[191]

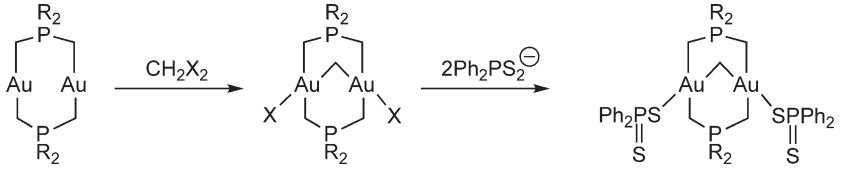

(38)

2.05.7 Isocyanide Complexes of Gold

Isocyanides RNC have been employed extensively as ligands for gold cations, and gold(I) complexes of the types (RNC)AuX and $[(RNC)_2Au]^+X^-$ in particular are legion. As for alkynylgold compounds (Section 4), research activities in this area have several quite obvious reasons, as follows.

(i) Attachment of rod-like isocyanide ligands to linearly two-coordinate gold(I) centers leads to long, largely unidimensional molecular or cationic complexes with electrically di- or multipolar characteristics. These species therefore are promising candidates for components of NLO materials.

(ii) The molecules or cations may further become aligned both in solution and in the solid state, giving rise not only to crystalline solids but also to partially ordered liquids and smectic or nematic phases.

(iii) The rod-like structures with small molecular diameters facilitate intermolecular actions of the van der Waals or dispersion type, including the intriguing aurophilic interactions,[192–197] which attract unrelenting interest because they are assumed to be responsible for the photoluminescence properties observed for most of the complexes.[198]

(iv) Isocyanide complexes of gold(I) are often the key synthons for the preparation of the corresponding carbene complexes (Section 8).

(v) (RNC)AuX and $[(RNC)_2Au]^+X^-$ complexes are readily obtained from the most common reagents like $(Me_2S)AuCl$, (tht)AuCl, (CO)AuCl, (RCN)AuX, $[(RCN)_2Au]^+X^-$, (L)Au(acac), and $M^+[Au(acac)_2]^-$ by substitution reactions with 1 or 2 equiv. of the isocyanide, respectively (Equation (39)).

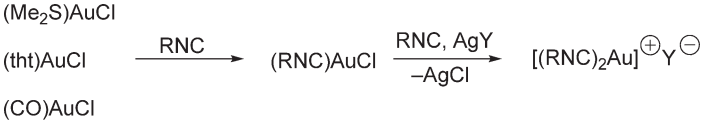

(39)

Y = BF_4, F_3CSO_3, ClO_4; R = alkyl, aryl; tht = C_4H_8S

These reactions show that isocyanides are powerful ligands for gold(I) which are able to replace most of the other ligands.

Most gold(I) isocyanide complexes are colorless, crystalline materials, stable in air at room temperature, and soluble in common organic solvents. The compounds have been generally well characterized by IR/Raman and NMR spectroscopy, and crystal structures have been determined for almost a 100 examples. From the spectroscopic and structural data, it has been concluded that gold(I) isocyanides are strong σ-donors and poor π-acceptors.

Only very few gold(III) isocyanide complexes have been prepared. Following an early synthesis of $(RNC)AuCl_3$ complexes,[199] the $(RNC)AuBr_3$ analogs have been synthesized much later by oxidative addition of Br_2 to the corresponding (RNC)AuBr complexes.[200] No triodides are known. Reactions of $K[AuCl_4]$ with isocyanides were shown to lead to reduction of gold(III) to gold(I) and dealkylation of the isocyanide to form (isocyanide)gold cyanides.[201]

In the present account, the standard preparations and analytical procedures employed for certain groups of compounds are not recapitulated. The reader is rather directed to the more special properties of the complexes. Many of the simple compounds of isocyanides RNC with R = Me, Et, ^{n}Pro, iPro, Ph, etc. were published in the early literature.[2,3,5] Almost all of the later work is dedicated to complexes of ligands with R groups of a specific shape or functionality which allow an influence on the molecular properties or the association modes.

Although the molecular structures of most complexes are generally very simple, with linear chains of atoms R–N≡C–Au–X or [R–N≡C–Au–C≡N–R] as the fundamental motif of bonding, the crystals show many variations of molecular packing. These cover the whole range from monomers entertaining only van der Waals contacts, to oligomers or chain-like aggregates with the components at short distance suggesting strong aurophilic bonding or other interactions at intermediate distances. A demonstration of many of these packing patterns would need large space not available in this account. The original work should be consulted for details.

2.05.7.1 Mono(isocyanide)gold(I) Complexes

Several gold(I) halide and pseudohalide complexes with alkyl- and arylisocyanide compounds were prepared via standard routes and structurally characterized in the 1990s.[2,3,6,7] One of the more comprehensive studies included (MeNC)AuX (X = Cl, I), (^{t}BuNC)AuX (X = Cl, Br, I), (PhNC)AuX (X = Cl, Br (two modifications), I, SCN), (MesNC)AuCl, and [MeOC(O)CH_2NC]AuX with X = Cl, Br, I, SCN (Mes = mesityl, 2,4,6-$Me_3C_6H_2$).[192] Most of the compounds are aggregated into chains via aurophilic contacts, but dimers are also observed, for example, (MesNC)AuI and [MeOC(O)CH_2NC]AuI, and even sheets, as for [MeOC(O)CH_2NC]AuCl/Br. In the latter, each gold atom is surrounded by three other gold atoms from neighboring molecules. All compounds are at least weakly photoluminescent.[192,202]

Some of the intermolecular Au···Au contacts in (RNC)AuX aggregates are exceedingly long, for example, in the "dimer" [(^{t}BuNC)AuI]$_2$, and therefore *ab initio* calculations (MP2 level) were carried out to clarify the bonding situation for parallel head-to-tail and crossed dimers (Scheme 47). The energy balance for the conformations was found to be very delicate and not dominated solely by aurophilic interactions of the electron correlation type. Long-ranging quadrupole–quadrupole as well as dipole-induced dipole interactions also play a major role.[202]

The chain structure of (^{t}BuNC)AuCl was reconsidered in the context with studies of the dimeric complex [(*p*-Cl-C_6H_4-SO_2-CH_2-NC)AuCl]$_2$. While the former has a long Au···Au contact of as much as 3.695 Å,[192] indicating at the best very weak aurophilic bonding, the complex with an isocyanide with a sulfone group is tightly aggregated with a short contact of only 3.0634(4) Å, and yet the latter – counter-intuitively – has a higher-energy Au-centered phosphorescence than the former. This result has been explained by a different extent of excited-state distortions in dimers versus extended chains.[193] Similar results were obtained in MP2 and DF calculations of a group of other R(NC)AuX compounds. Experiments had shown that intermolecular Au···Au interactions are needed in order to

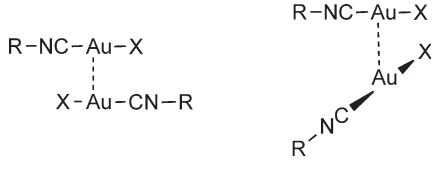

Scheme 47

observe Au-based luminescence. Compounds associated as chains of antiparallel molecules have similar luminescence properties with an orange-red phosphorescence and a very large Stokes shift (ca. 20,000 cm^{-1}), originating from a ground-state structure with very large Au···Au separations. It is suggested that these distances shrink in the excited states. Crossed dimers show blue-green emissions with smaller Stokes shifts despite having shorter Au···Au distances.[203]

The three (cyclohexylisocyanide)gold(I) halides ($C_6H_{11}NC$)AuX (X = Cl, Br, I) are all aggregated into chains, with neighboring molecules in head-to-tail arrangements. In the pleated chains, the Au···Au contacts vary from small to large alterations of Au···Au bond lengths, such that the series may be taken as a sequence of dimers only. The differences have been ascribed to steric effects, but there may also be other contributions as with the (^{t}BuNC)AuX compounds. All three compounds are colorless solids, which display a strong orange luminescence with a strikingly large Stoke's shift. The diffuse reflectance spectra show a three-band pattern in the 200–330 nm range.[194]

(Alkylisocyanide)gold(I) halides with long alkyl chains form crystalline rotator phases with distinct transformation temperatures from the crystalline to the rotator phase, and from the rotator to the isotropic liquid phase. A series of complexes ($C_nH_{2n+1}NC$)AuCl with $n = 7$–11 was investigated. In the crystalline form, the molecules are associated via aurophilic contacts which resemble the hydrogen bonds in the alcohols $C_nH_{2n+1}OH$ where the organization of the molecules is determined by hydrogen bonding and where rotator phases have already been identified in previous studies. In both cases, the rotator phase behavior – the concerted thermal expansion of the hydrocarbon chains – is based on a similar cross-section area of the hydrocarbon chains attached to the functional AuCl (aurophilicity) and OH units (hydrogen bonding), respectively, which are known to be associated with similar energetics.[204]

The conversion of the ($C_nH_{2n+1}NC$)AuCl chlorides into the corresponding thiophenolates ($C_nH_{2n+1}NC$)AuSPh by metathesis (using NaSPh in methanol) leads to unstable products which lose isocyanide upon standing at room temperature. The *n*-pentyl and *n*-heptyl intermediates, (*n*-$C_5H_{11}NC$)AuSPh and (*n*-$C_7H_{15}NC$)AuSPh, could be isolated and their structure determined. The intermolecular contacts are not strictly of the aurophilic type but show an intermediate situation with almost equidistant intermolecular Au···Au and Au···S contacts, which may be indicative of the mechanism of the decomposition reaction which affords luminescent gold(I) thiophenolate $[AuSPh]_n$.[205]

In a search for liquid crystalline phases, a series of (*p*-alkoxy-phenyl)isocyanide complexes was prepared from (Me_2S)AuCl and the corresponding ligands RNC, where R = $C_nH_{2n+1}O$-C_6H_4 with $n = 2$–12 (in even numbers).[206] The chlorides were converted into the bromides and iodides in metathesis reactions using KBr/KI. Mesogenic behavior was found for most of the new materials with transition temperatures in the range from ca. 95 to 160 °C. In most cases, smectic phases A were observed between the crystalline and the isotropic states.[207,208]

This work was extended to include acetylides (alkynyls) of the type (RNC)Au-C≡C-C_6H_4-*p*-C_nH_{2n+1}, with $n = 6$–12 (even numbers), and R as above. The compounds were prepared from (tht)AuCl and the alkynes *p*-HC≡C-C_6H_4-C_nH_{2n+1} in aqueous acetone with soda as a weak base. The resulting insoluble, polymeric alkynylgold(I) complexes were dissolved in an organic solvent by adding equivalent quantities of the isocyanides. All products show distinct transitions from a crystalline to a smectic A phase and finally to the isotropic melts.[206]

Related compounds with alkynyl groups bearing a different series of substituents were obtained from (^{t}BuNC)AuCl and the alkynes *p*-X-C_6H_4–C≡CH, where X ≡ NO_2–, *p*-NO_2-C_6H_4, *p*-NO_2-C_6H_4–CH≡CH–. The materials were studied for their potential mesogenic, NLO, and luminescence behavior, and for this purpose converted into the corresponding carbene complexes by addition of Et_2NH.[209]

Even more extended rod-like molecules were prepared with isocyanide ligands in which two *para*-substituted aryl groups are separated by a carboxylate spacer and both the terminal and the inner arene bear a long-chain alkoxy group (Scheme 48). The compounds were prepared from (Me_2S)AuCl and the corresponding ligand L. The mesogenic properties vary with the chain length of the alkoxy groups ($m = 1$–6; $n = 8$–12). On heating, the crystalline phases are first transformed into either nematic or smectic (C or A) phases, and finally into isotropic liquids.[210]

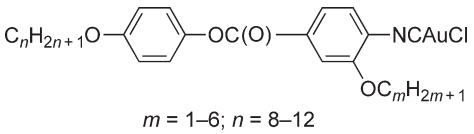

m = 1–6; *n* = 8–12

Scheme 48

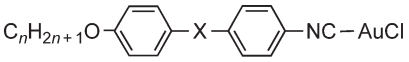

n = 9–12; X = –C(O)O–, –C≡C–, –CH_2CH_2–

Scheme 49

Similar work was carried out with ligands featuring different flexible or rigid spacers (X = –C(O)O–, –C≡C–, –CH_2–CH_2–) and terminal alkoxy groups where n = 9–12. These compounds and the carbene complexes derived therefrom by addition of alcohols also show mesogenic properties (Scheme 49).[211,212]

The combination of isocyanide and alkynyl ligands at a gold(I) center was further probed with phenylene dialkynes having different substitution patterns. The durol-type dialkyne was converted into the dinuclear gold(I) complex with ^{t}BuNC molecules as the terminal ligands, and the 1,3-diethynyl-benzene into the related complexes. L represents ^{t}BuNC or 2,6-$Me_2C_6H_3NC$, and the arene was employed with or without methyl substituents R. The ^{t}BuNC complexes were converted into the corresponding carbene complexes by addition of $NHEt_2$ (Scheme 50).[213]

3,5-Diethynyl-pyridine was reacted with 2 equiv. of (Me_2S)AuCl to give a gold alkynyl as an insoluble coordination polymer of unknown structure. This product could be dissolved in organic solvents with ^{t}BuNC to afford the bis(isocyanide) complex with an angular structure (Scheme 50).[214]

The first polynuclear structures with gold(I) centers coordinated to isocyanide and alkynyl groups were prepared through a novel exchange of alkynyl ligands. This special route became necessary, because the coupling of certain complexes proved elusive (Equation (40)): AuCl complexes of isocyanides with terminal alkynyl groups are subject to decomposition upon treatment with a variety of auxiliary bases.

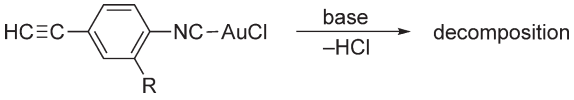

(40)

Polymers of the composition –[-Au-CN-C_6H_4-C≡C-]$_n$– were therefore obtained from (isocyanide)gold(I) alkynyls with a terminal isocyanide function at the arene group. With a sufficiently different donor strength of the two alkynyl groups, elimination of the independent alkyne ligand is accomplished (Equation (41)).[215,216] The first structure of a mononuclear compound of this series, (XyNC)AuC≡C-C_6H_4-4-NO_2, has been determined (Xy = 2,6-$Me_2C_6H_3$–),

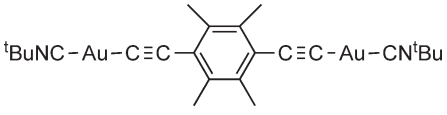

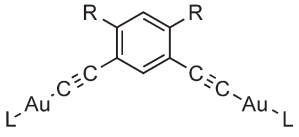

R = H, Me; L = ^{t}BuNC, 2,6-$Me_2C_6H_3NC$

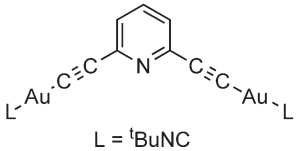

L = ^{t}BuNC

Scheme 50

and the UV–VIS absorption and emission characteristics of the family of complexes have been explored. EHMO quantum-chemical calculations were carried out for the model compounds (HNC)AuC≡CH and (PhNC)AuC≡CPh, and the results served for a preliminary assignment of the emission processes.[217]

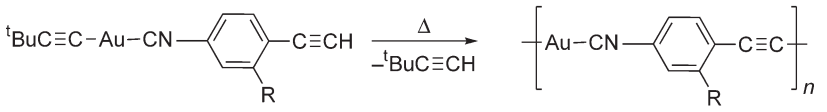

(41)

R = H, Me

Even larger, conjugated systems were synthesized by employing both difunctional isocyanides and difunctional alkynes. In all the cases, the components have structural rigidity, which lends rigid-rod character to the complexes prepared from them. Many of the complexes are associated via intermolecular aurophilic contacts, which appear to have a distinct influence on the photophysical behavior, but are as yet not a necessary condition for luminescence (Scheme 51).[196]

Polymeric (isocyanide)gold(I) aryls ("gold oligo-phenylene-ethynylene-isonitriles") were tested as electrical conductors at metal–molecule–metal junctions (π-conjugated molecular wires), but the preparation, structure, and properties of the materials were not fully disclosed (Scheme 52).[218]

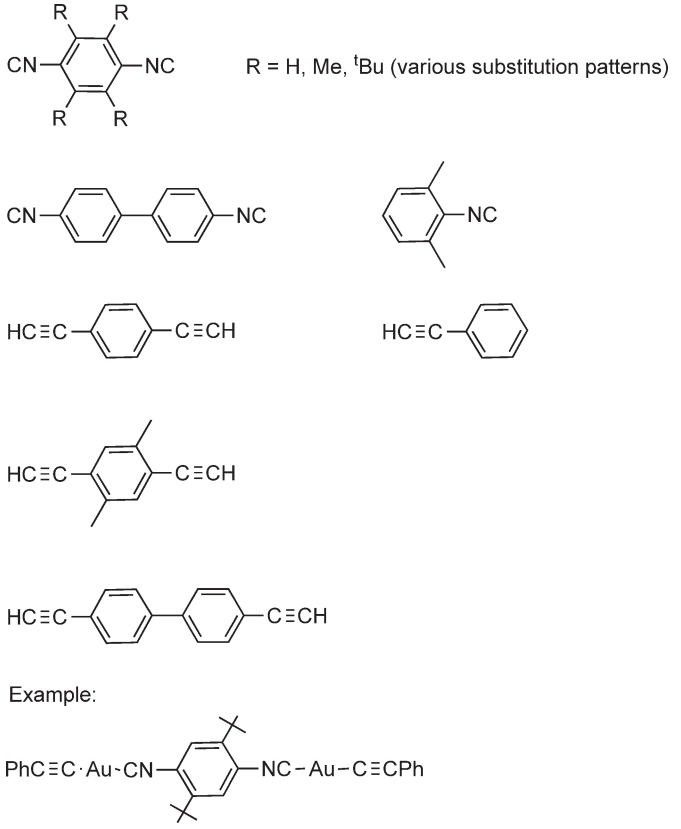

Scheme 51

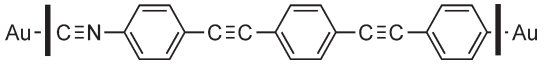

Scheme 52

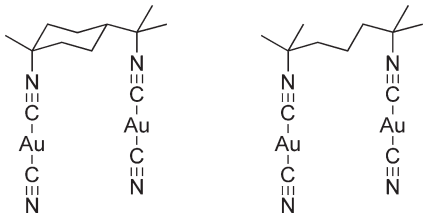

Scheme 53

(Isocyanide)gold(I) "cyanides" (RNC)AuCN are of special structural interest because these complexes represent almost perfect rigid-rod molecules with minimum molecular cross-sections. The fascinating sheet structure of (MeNC)AuCN with a two-dimensional array of gold atoms in close proximity was studied already in the 1970s.[219] A more detailed investigation of a larger family of compounds has shown that a variety of structural motifs arises as the substituent R is expanded (R = ^{i}Pro, ^{n}Bu, ^{t}Bu, Cy). Dimers, tetramers, chains, double chains, combinations of oligomers in chains, and layers/sheets are encountered, all of which have intimate Au···Au contacts and show similar UV–VIS absorption spectra. However, the luminescence properties are very different, indicating that both the ground-state and excited-state structures play a role in the emissive properties.[197]

It should be noted that the preparation of complexes (RNC)AuCN can be carried out via very special routes. Thus AuCN reacts with MeI to give (MeNC)AuCN. This reaction involves an interesting *N*-alkylation of an Au(I)-bound cyanide group.[219] Other (RNC)AuCN complexes were obtained from the reaction of K[$AuCl_4$] with the isocyanide in methanol. Examples are the compounds (L)$Au_2(CN)_2$ with L = 1,8-diisocyano-*p*-menthane or 2,5-diisocyano-2,5-dimethyl-hexane. The reactions proceed with a dealkylation of an isocyanide in the coordination sphere of a gold(III) center to produce free cyanide (Scheme 53).[201]

(^{t}BuNC)AuCl was shown to be inserted into bis(pentamethylcyclopentadienyl)silicon to give the bis(pentamethyl-cyclopentadienyl)chlorosilyl-gold(I) complex of the isocyanide (Equation (42)).[220]

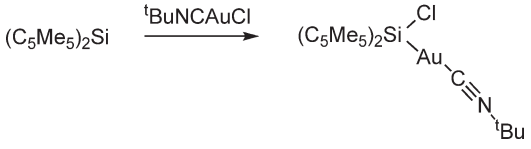

(42)

2.05.7.2 Bis(isocyanide)gold(I) Complexes

Owing to the good ligand properties of isocyanides for complexation of gold(I), complexes of the type $[(RNC)_2Au]^+X^-$ are readily available through a variety of synthetic routes. One new approach is the substitution of organic nitriles. The reaction is carried out in acetonitrile and gives quantitative yields (Equation (43)).[221]

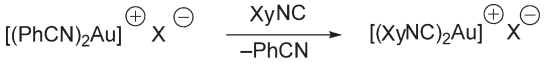

(43)

X = BF_4; Xy = 2,6-$Me_2C_6H_3$

A more conventional pathway uses the halide complexes (RNC)AuX which are reacted with 1 equiv. of the isocyanide, preferentially in the presence of a silver salt ($AgSO_3CF_3$, $AgBF_4$) for removal of the halide X as AgX (Equation (44)).[222]

(44)

X = Cl, Br, I; Y = BF_4, F_3CSO_3, ClO_4

Complexes with R = Me, Ph, Mes have been isolated and fully characterized including structural studies. As judged from the Au···Au distances, the aurophilic interactions between the cations are at best very weak.[222] Salts with the cations $[(CyNC)_2Au]^+$ and $[(^{t}BuNC)_2Au]^+$ and the $[(C_6H_4S_2)_2Au]^-$ anion were obtained in the reaction of the (RNC)AuCl complexes with dithiocatechol 1,2-$C_6H_4(SH)_2$.[223] The reaction of this dithiol with 2 equiv. each of

(CyNC)AuCl and MeONa in methanol yields a tetranuclear compound $[(C_6H_4S_2)Au(CNCy)]_2Au_2$ and a mixed [(isocyanide)(carbene)Au]$^+$Cl$^-$ complex. Both products are associated into chains with alternating components through aurophilic contacts (Equation (45)).[224]

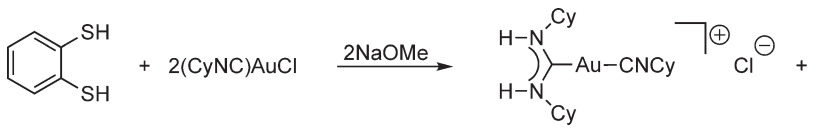

(45)

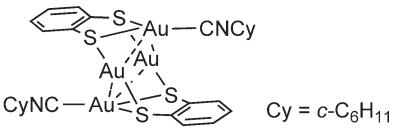

The vibrational spectra of the compounds $[(MeNC)_2Au]BF_4$, $[(PhNC)_2Au]ClO_4$, and $[(p\text{-TolNC})_2Au]BF_4$ have been studied and the Au–C stretching frequencies assigned at 330/334, 350/342/351, and 348/350 cm^{-1}, respectively (IR/Raman).[225]

2.05.7.3 (Isocyanide)gold(III) Complexes

Two complexes $(RNC)AuCl_3$ with R = Ph, *p*-Tol have been reported in the older literature.[199] The compounds were obtained as yellow solids from the reaction of $HAuCl_4$ with the isocyanides in ethanol. Mixed complexes of the type $(RNC)AuX_n(C_6F_5)_{3-n}$ with certain combinations of $n = 0$–3, X = Cl, Br, I, and R = ^{t}Bu, Cy, Ph, *p*-Tol have also been documented from earlier work.[226–228]

Compounds (RNC)AuI with R = Me, Cy, ^{t}Bu are not oxidized by iodine. The products are polyiodides with the homoleptic isocyanide complex cations, for example, $[(CyNC)_2Au]^+I_5^-$ or $[(^tBuNC)_2Au]^+[AuI_2]^-$ I_2. By contrast, complexes (RNC)AuBr react with bromine to give the corresponding $(RNC)AuBr_3$ compounds (R = Me, Cy, ^{t}Bu). Compound $(^tBuNC)AuBr_3$ has been crystallized and its structure determined (Equation (46)).[200]

(46)

Pentafluorophenylgold(I) complexes of the type $[p\text{-R-}(C_6H_4)_m\text{-NC})]AuC_6F_5$ were found to add iodine to give the $(p\text{-R-}C_6H_4\text{-NC})AuI_2(C_6F_5)$ compounds with $m = 1$, 2 and R = $C_nH_{2n+1}O$ ($n = 2$–12 (even numbers)). Contrary to the gold(I) analogs, the products do not exhibit mesogenic properties.[229]

2.05.8 Carbene and Carbeniate Complexes of Gold

Carbenes form stable complexes with many metals in the periodic table of the elements, and gold is no exception. In fact, the chemistry of this class of organogold compounds for some time has been one of the fastest growing subdisciplines. While the corresponding chapters were still short in previous accounts,[1,2] the inventory for this review is now particularly rich and diverse.[230] As for other classes of carbene complexes, this upsurge is based on expectations for potential applications in various fields such as NLO materials, liquid crystalline phases, and catalysis. Where applicable, this is indicated for each of the entries in this chapter.

Carbenes are defined as molecular species with formally divalent and two-coordinate carbon atoms bearing various substituents X and Y and a lone pair of electrons. While the simple representatives are of low stability (such as $:CH_2$) and may only appear as short-lived reaction intermediates or in adducts with electron donors, some cyclic systems can be readily isolated. This is particularly true for many of the *N*-heterocyclic carbenes (NHCs), which are now widely applied as ligands to metals ("Wanzlick–Arduengo carbenes"). Such carbenes based on imidazol and benzimidazol have become the working horses in this branch of organogold chemistry (Scheme 54).

Early work focused on compounds with open-chain carbenes generally synthesized in the coordination sphere of the gold atom, for example, by addition of amines or alcohols to isocyanide ligands in the corresponding gold complexes. Subsequent synthetic approaches have relied on the *in situ* deprotonation of onium salt precursors by a

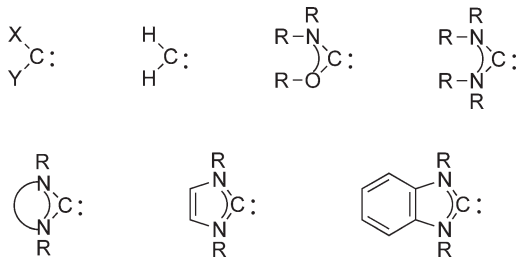

Scheme 54

strong base either prior to the addition of the gold substrate or in its presence, while others have exploited the carbene transfer route from one metal to the other. Both strategies are better suited for the more stable cyclic carbenes.

2.05.8.1 Gas-phase Studies of (Carbene)gold Complexes

The role of the most simple carbene, methylene :CH_2, as a ligand to gold cations and clusters and mixed metal cluster cations (with platinum) was investigated in experimental (Fourier transform ion-cyclotron resonance mass spectrometry, with isotopic labeling) and quantum-chemical studies. Gas-phase cationic species $AuCH_2^+$, $Au_2CH_2^+$, or $Pt_mAu_nCH_2^+$, which may play an important role in gold-catalyzed reactions, such as the C–N coupling of methane and ammonia, were considered.[231–235] The dinuclear complex $PtAuCH_2^+$ was found to mediate best the C–N bond coupling reaction to afford the aminocarbene complex, whereas larger clusters mainly yield carbide species.

The nature of the carbene-to-gold bonds in heterocyclic carbene complexes was studied by quantum chemical calculations at the BP86 level of theory using an energy decomposition analysis[236] and MP2 and DFT methods.[237–239] Unsubstituted imidazol-2-ylidene was chosen as the model ligand. From the results, it has been concluded that the Au–C interaction is largely electrostatic in nature, with only ca. 35% covalent interaction (20% π-backbonding) both for (carbene)AuX (X = Cl, Br, I) and $[(carbene)_2Au]^+$ species. Calculated geometries for the complexes are in good agreement with experimental values for complexes with *N*-substituted ligands. A comparison has shown that the Au–C dissociation energies are highest for gold as compared to the corresponding silver and copper complexes. Structures with coplanar carbene ligands are not significantly favored over the structures with the ligand planes perpendicular.[236,237]

Hypothetical (carbene)gold(I) structures of intermediates and reaction coordinates have been calculated (B3LYP/6-31G and LAN2DZ levels) for $(H_3P)Au^+$-catalyzed cyclization reactions of terminal enynes. The endocyclic skeletal rearrangement reactions were found to proceed exclusively via cyclopropylcarbene complexes.[240]

2.05.8.2 Non-cyclic Carbenes as Ligands to Gold Atoms

Regarding "mono(carbene)gold(I) complexes," the classical route of preparation of gold(I) carbene complexes – the addition of amines to isocyanides – was successfully applied to several series of (carbene)gold(I) alkynyls, including particularly interesting multifunctional gold(I) alkynyls. (*t*-Butylisocyanide)gold(I) chloride can first be converted into the alkynyl complex with the alkyne and an auxiliary base, and the intermediates can be subjected to the addition of a secondary amine (Scheme 55). Alternatively, the isocyanide complex may first be converted into the carbene complex by addition of the amine and then reacted with thallium acetylacetonate.[241]

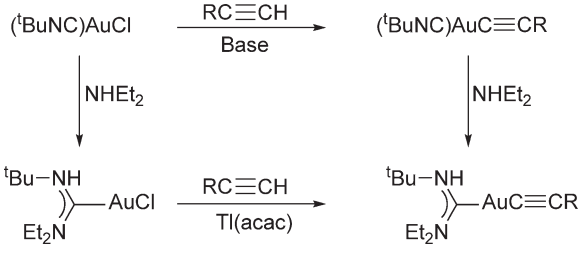

Scheme 55

Dinuclear (^{t}butylisocyanide)(aralkynyl)gold complexes (aralkynyl = 1,3- and 1,4-di(ethynyl)phenyl) were also found to undergo rapid addition of diethylamine to give the corresponding carbene complexes, which can be used as building blocks for one- or two-dimensional systems.[242] The same group of compounds is accessible from preformed (carbene)gold(I)(acac) complexes which react with the aralkynes with liberation of acacH.

Thiols like pyridine-2-thiol yield (carbene)gold thiolates, and onium salts give cationic (carbene)gold ylide complexes, isolated and characterized as the perchlorates.[170] The reaction of dithiocatechol with (cyclohexylisocyanide)gold chloride affords a carbene complex $[(CyNC)AuC(NHCy)_2]^+Cl^-$, which co-crystallizes with a neutral tetranuclear complex $[(CyNCAu)_2Au_2(S_2C_6H_4)_2]$.[224]

The addition of amines to multinuclear (isocyanide)gold complexes was also applied to polyfunctional substrates such as the aminoglycoside neomycine B. This compound can be transformed into the hexa(isocyanide), the terminal functions of which are readily attached to six gold atoms upon reaction with $(Me_2S)AuCl$. Subsequent addition of $^tBuNH_2$ or $PhNH_2$ affords the corresponding carbene complexes.[243]

It has been established previously that the addition of alcohols to (isocyanide)gold(I) complexes produces the imino(alkoxy)carbene complexes in high yields and with a wide variety of substituents attached both to the nitrogen and oxygen atoms. This reaction has been applied for the production of the first (carbene)gold(I) complexes which form mesophases (liquid crystals). For this purpose, aryl isocyanides with spacers between at least two arenes and with long-chain substituents in the periphery were first attached to gold(I) centers by reaction with $(Me_2S)AuCl$, followed by the addition of an alcohol which produces the (aminoaryl)(alkoxy)carbene complexes (Scheme 56). The addition of alkylamines or alkylidene diamines affords the corresponding mono- or dinuclear bis(amino)carbene complexes, respectively.[244] The products may have different stereochemistry regarding the conformation of the substituents at the carbene carbon atom (*E*/*Z*), which influences the range of the liquid crystalline behavior. For several substitution patterns, enantiotopic smectic A phases were observed.[245]

Monocarbene complexes of gold(I) are generated in a variety of carbene-transfer reactions from other transition metals. These include the reactions of (diaminocarbene) or alkyl(amino)carbene tungstenpentacarbonyl complexes with $(Me_2S)AuCl$[246] or directly with $HAuCl_4$, respectively.[247] In the latter reaction, (carbene)gold(III) complexes are also formed, as already shown in previous reports.[248] From a dicarbonyl(tripyrazolylborato)molybdenum arsenylcarbyne complex, a (carbene)gold(I) complex $(Me_2N)_2CAuCl$ was produced upon reaction with $(CO)AuCl$.[249]

Anionic alkoxy Fischer-type carbene complexes were shown to react with $(Ph_3P)AuCl$ to give a unique vinyl ether complex, which is bound in a quasi-η^1 fashion to the Cr/Mo centers. Upon treatment with triphenylphosphine, the gold-vinyl ether ligand can be liberated and isolated. This reaction thus gives access for the first time to aurated vinyl ethers (Scheme 57).[38]

"Cationic bis(carbene)gold(I) complexes" have been known for several decades,[1,2] but their interesting photophysical properties as related to details of solid-state and solution structures have been studied much more recently. It has been shown that aggregation of the cations via aurophilic contacts appears to be the basis for intense photoluminescence in most cases where simple diaminocarbenes are present as ligands. Thus, in the solvent-free or acetone-solvated crystalline phases of bis[bis(methylamino)carbene]gold(I) hexafluorophosphate, the cations are stacked with short Au···Au contacts in specific conformations supported by hydrogen bonding, and luminescence is observed in both cases. Frozen solutions (liquid nitrogen) are also luminescent, and the color is different in

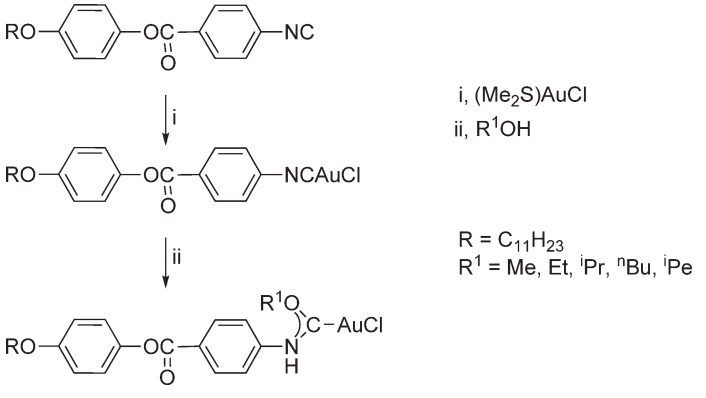

Scheme 56

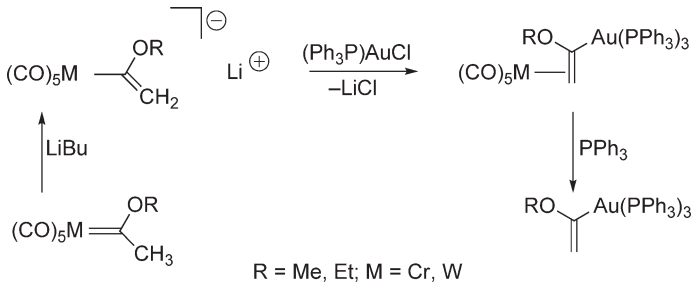

Scheme 57

different solvents. However, the solutions are non-luminescent at room temperature. The bis[dimethylamino(methylamino)-carbene]gold(I) salt with the same anion has a structure with isolated cations in the crystal, and no luminescence is discernible in the solid or solution state (Scheme 58).[250]

Similar observations were made with bis[alkoxy(alkylamino)carbene]gold complexes, which are prepared by ring opening of trinuclear precursors with trifluoromethanesulfonic (triflic) acid. Through anion metathesis, several crystalline forms were obtained, the structures of which were determined. The triflate salt has a chain of cations in the crystal, while the chloroform solvate of a *p*-benzoquinolate contains only monomeric cations. In the solvent-free crystals, dimers are present (Scheme 59).[251]

In the crystal, most trinuclear carbeniate complexes are known to be stacked with close aurophilic interactions, and organic π-acids can be intercalated into these stacks.[252] Similar intercalation takes place with the cations of simple silver and thallium(I) salts. The cations become attached to form polymetallic core units through metallophilic bonding.[253] With the trinuclear silver pyrazolates, both metal and ligand exchange have been observed to give new stacks of trinuclear units.[254]

The adsorption or inclusion of solvent molecules may lead to spectacular optical phenomena, as observed for the trinuclear crystalline gold(I) carbeniate complex $[Au(N(Me)=C(OMe)]_3$.[24,255]

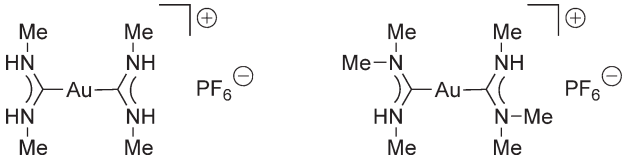

Scheme 58

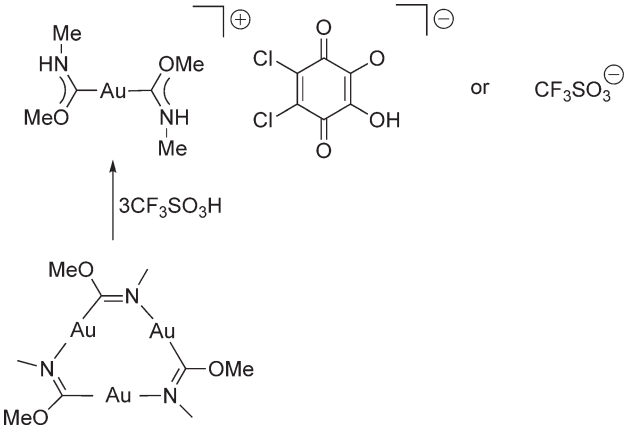

Scheme 59

2.05.8.3 Cyclic Carbenes as Ligands to Gold Atoms

Heterocyclic carbenes have been applied as ligands to gold(I) and gold(III) with a wide variety of heteroatoms and substitution patterns.[256,257] Gold(I) forms 1 : 1 and 1 : 2 complexes with a linear coordination geometry, while at gold(III) centers, carbenes appear only in combination with other ligands in a square-planar array.

The most common ligands are those derived from imidazole and benzimidazol (Scheme 54), followed by the (benz)thiazols. The free Wanzlick–Arduengo carbenes can be isolated and employed for the synthesis of the complexes, but often it is more convenient to prepare the carbenes *in situ* from the dimers or the corresponding onium salts, or to use carbene-transfer reactions.[256–259]

A whole series of (imidazol-2-ylidene)gold(I) complexes with the "1 : 1 stoichiometry" has been prepared from the readily available silver chloride adducts, which upon reaction with $(Me_2S)AuCl$, followed by chloride metathesis, give the complexes shown in Scheme 60.

More than half of the members of this family have been structurally characterized and the Au–C distances correlated with the donor ability of the *trans*-substituent X/Me. A similar correlation was established for the chemical shifts of ^{13}C resonances in the NMR spectra. According to these results, the *trans*-influence of the carbene ligand appears to be comparable to that of triphenylphosphite $P(OPh)_3$. Owing to the bulkiness of the ^{t}Bu substituents, the complexes are not aggregated in the crystals. By contrast, the corresponding methyl-substituted compounds are aggregated to form chains via aurophilic contacts and are photoluminescent.[18]

The synthesis of the analogous (benzimidazol-2-ylidene)gold(I) complexes follows the same preparative routes. The chlorides are generally the key compounds, which are readily converted into the bromides or iodides (using metathesis), the thiolates (using a thiol and a base), or the acetylides (using the alkyne and a base). Most of these compounds are photoluminescent. The structure of the chloride with the *N*,*N*′-dimethylated ligand has been determined and shows a dimer with aurophilic contacts, while for the *N*,*N*′-diethyl homolog, the oligomerization is based on π–π stacking. Treatment of the (carbene)AuCl compounds with K_2CO_3 affords the $[(carbene)_2Au]^+$ salts.[259]

(*N*,*N*′-dialkyl-"benz"-imidazol-ylidene)gold(I) bromides were also prepared from the silver complexes upon reaction with $(Me_2S)AuCl$ in a 1 : 1 ratio, while the di(carbene)gold(I) cations result from the same reaction in the 2 : 1 ratio. The compound with R = Et and with PF_6^- as the counterion has been structurally characterized.[258] In related studies, the imidazol-2-ylidene ligands were also transferred to the gold center from the pentacarbonyltungsten complexes upon reaction with $(Me_2S)AuCl$. Allyl, benzyl, and 4-pentenyl groups served as *N*-substituents.[247,248]

Compounds of the same type are accessible by reaction of 1-methyl-imidazol-2-yl lithium with components XAu(tht) (X = CN, C_6F_5). Treatment of the complex salts thus obtained as intermediates with strong methylating agents affords the carbene complexes (Scheme 61).[257,260]

Note that this reaction can also be used for the preparation of complexes with mixed substituents if the alkylating agent has a different group. Such complexes have also been generated by ring cleavage of trinuclear complexes, for example, with acyl halides (Equation (47)).[261]

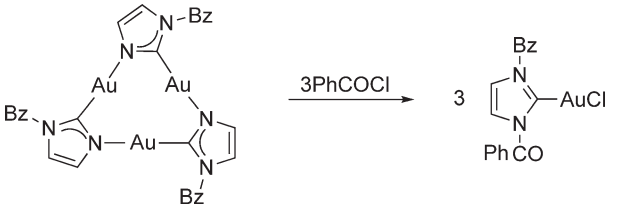

(47)

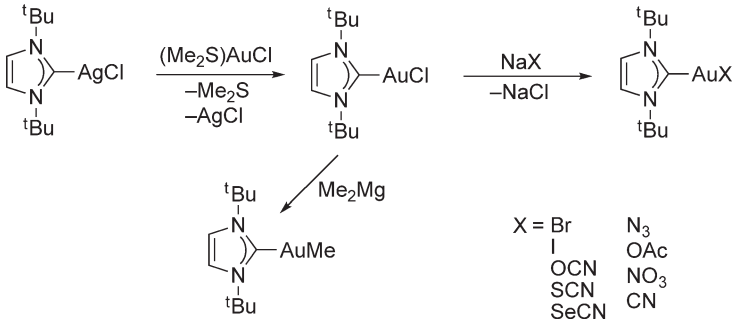

Scheme 60

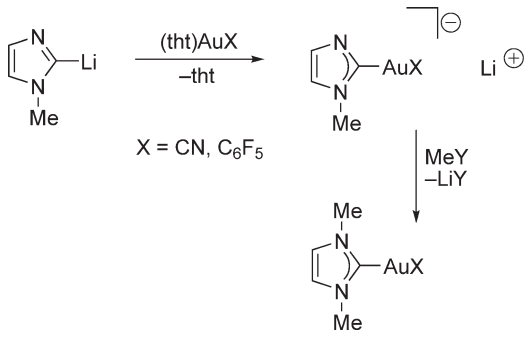

Scheme 61

Note that the addition of halogens or other strongly oxidizing agents to the triauracycle leads to oxidative addition at the gold atoms.[262,263] The oxidation states of the metal atoms in the addition, oxidation, or cleavage products have been confirmed, that is, by ^{179}Au Mössbauer spectroscopy.[145] Mononuclear imidazol-2-ylidene complexes with two different *N*-substituents have been prepared and employed as catalysts for the addition of water to 3-hexyne with Lewis acids as co-catalysts (Scheme 62).[264]

Carbenes with extremely complex substituents R have also been trapped by gold(I) complexes, as exemplified by compounds in Schemes 63[265a,265b] and 64.[265]

Two major routes give access to (thiazol-2-ylidene)gold(I) complexes with 1 : 1 stoichiometry. The corresponding thiazolium salts react with base in the presence of gold(I) precursors to give the products in high yield. Alternatively, the corresponding carbeniate complexes can be *N*-protonated or *N*-alkylated to afford compounds of this series (Scheme 65).[257,266]

It is noteworthy that both types of reactions can also be applied to prepare (carbene)gold(III) compounds: *N*-alkylthiazolium salts react with $HAuCl_4$ or $NaAuCl_4$, followed by the addition of base, to give (thiazol-2-ylidene)gold(III)

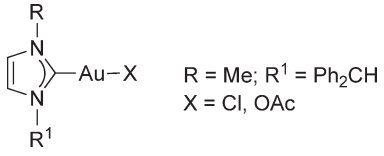

Scheme 62

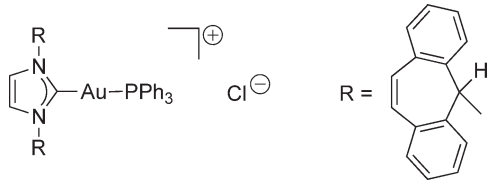

Scheme 63

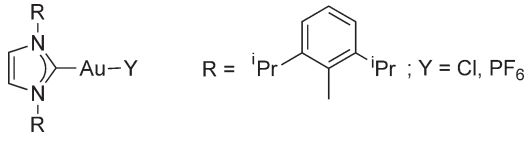

Scheme 64

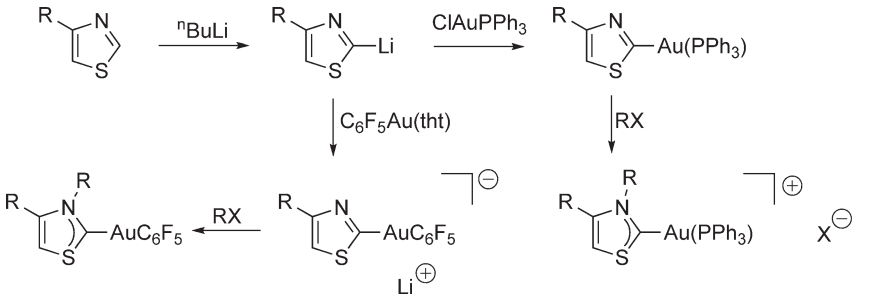

Scheme 65

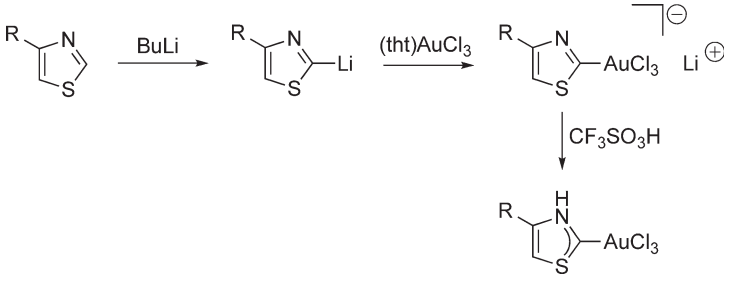

Scheme 66

complexes (Equation (48)), and lithiated thiazol reacts with (tht)$AuCl_3$, followed by 1 equiv. of acid to give the same product (Scheme 66).[257,267]

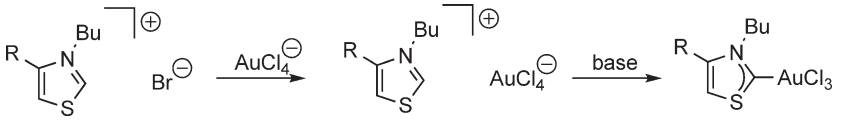

(48)

2-Lithiated thiazols react with $(Ph_3P)AuCl$ to a neutral gold(I) thiazolate, which upon alkylation is transformed into the cationic carbene complex, while the reaction with (tht)AuC_6F_5 followed by alkylation leads to the neutral complex (Scheme 65).[260]

One Au–C bond in bis(thiazol-2-ylidene)gold(I) cations is cleaved in the reaction with elemental iodine to give the corresponding (carbene)AuI complex and a 2-iodo-thiazolium salt, while chlorine and bromine oxidize the gold center to the gold(III) state.[267]

2-Lithiated pyridine reacts with (tht)AuCl in the molar ratio 1 : 1 to give a poorly soluble oligomeric gold complex $(C_6H_4NAu)_n$, which dissolves upon addition of equivalent quantities of HCl (or methyl trifluoromethylsulfonate), affording 2-chlorogold-substituted pyridinium betaines which have also been formulated as carbene complexes. With a 2 : 1 molar ratio of reagents, the di(carbene)/di(pyridyl) complexes are obtained (Scheme 67). The di(pyridinium)aurate(I) chloride was isolated as a crystalline dihydrate.[268]

2-Oxazolinyl-thien-5-yl- and 2-oxazolinyl-thien-3-yl-lithium react with (tht)AuCl to produce the corresponding gold(I) complexes as a dimer and a trimer, respectively. Mononuclear compounds are obtained with (tht)AuC_6F_5 and $(Ph_3P)AuCl$ (Scheme 68).[269]

The synthetic principles underlying the preparation of the 1 : 1 carbene complexes (above) are also applicable to "products with a 2 : 1 ligand/metal ratio". The carbene components may be introduced as free carbenes or their dimers,[270] or generated *in situ* from the onium salts.[254,256,271,272] A second major pathway uses anionic heterocycles (carbeniates) which can be *N*-protonated or *N*-alkylated in the coordination sphere of the gold atom.[147,254,256,260,273] In standard cases, metallation of the heterocycles was carried out with alkyllithium or -magnesium reagents, but lithium dimethylaurate(I) has also been employed, making the reaction a one-step process.[256]

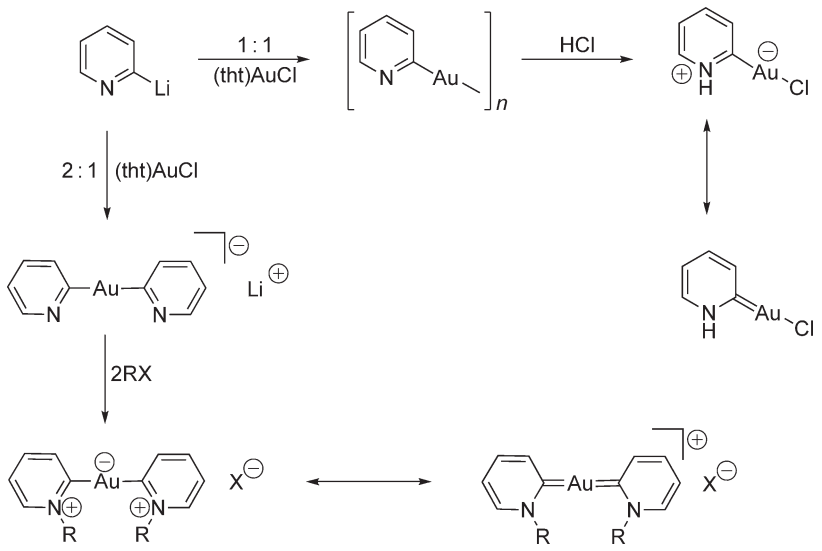

Scheme 67

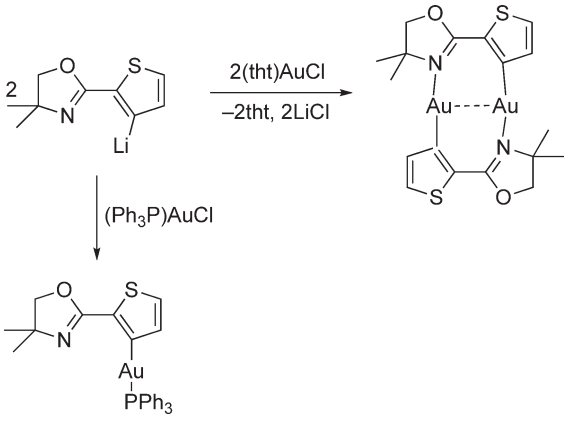

Scheme 68

These methods have been applied mainly to imidazol-, benzimidazol-, thiazol-, and benzthiazol-based carbenes,[255,274,275] but there are also examples with triazols and tetrazoles.[274] In the following, a few representative examples are presented which illustrate the strategies. The complex with a carbazol ligand shows strong luminescence (Scheme 69).[272]

Bis[*N*,*N*′-di(2-pyridyl)- and -di(2-pyridyl-methyl)-imidazol-2-ylidene]aurate(I) tetrafluoroborates have been prepared from the analogous silver(I) complexes on reaction with (tht)AuCl and their structures determined. The configuration of the cations with sterically well-protected two-coordinate gold centers shows no anomalies. However, fascinating structures are found for the adducts with silver tetrafluoroborate obtained as acetonitrile

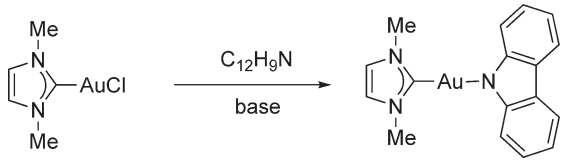

Scheme 69

solvates. The cationic portion of the 2-pyridyl-substituted compound is a one-dimensional array of the components associated via intra- and intercationic Au···Ag interactions, while that of the 2-pyridyl-methyl homolog forms helical strings based on similar metallophilic contacts. In both cases, the silver atoms are coordinated by the pyridine substituents and solvent molecules and entertain short, sub-van der Waals distances to the gold atoms. Crystals of the compounds are strongly luminescent (Equation (49)).[276]

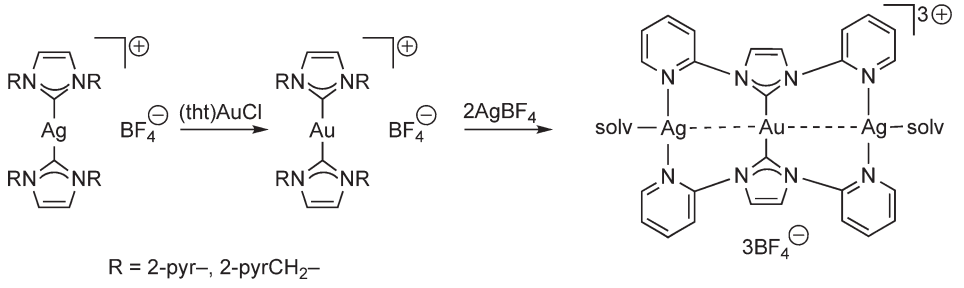

(49)

In an effort to prepare mesogenic phases based on di(carbene)gold(I) complex salts, $(Me_2S)AuCl$ was treated with *N*,*N*′-dialkyl-benzimidazolium bromides in a phase-transfer catalytic (PTC) system. Bilayered liquid crystals were obtained for samples with long-chain substituents $R = C_nH_{2n+1}$, $n = 12$, 14, 16. The transition temperatures for the mesophases are in the ranges 100–150 °C (Equation (50)).[271] The same type of cations with gold and silver centers was isolated with $[AgBr_2]^-$ or $[PF_6]^-$ counterions, but only the homometallic silver/silver complex with $R = C_{14}H_{29}$ and the dibromoargentate anion showed mesogenic properties.[258,277]

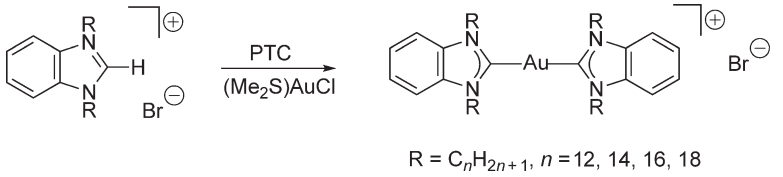

(50)

Di(*N*,*N*′-dimethyl- and -diethyl-benzimidazol-2-ylidene)gold(I) hexafluorophosphates are photoluminescent in the crystalline state. Metathesis produces an equally luminescent bis(1,2-dicyano-ethene-1,2-ditholato)aurate(III).[272]

Selected mono- and di(*N*,*N*′-diorganyl-imidazol-2-ylidene)gold(I) complexes have been investigated for their antibacterial activity. Positive effects against *Staphylococcus* and *Enterococcus* bacteria, *Escheria coli*, and *Pseudomona aeruginosa* were encountered in particular with the *N*-substituents being mesityl or benzyl (Equation (51)).[278]

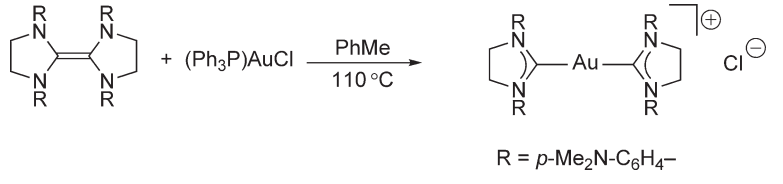

(51)

N,*N*′-di(*p*-dimethylamino-benzyl) derivatives of di(imidazolidinylidene)gold(I) salts were polymerized into polyimides by condensation with arene-tetracarboxylic anhydrides. The products are tough, but flexible, and have high glass transition temperatures and high thermal stability. Yellow films of the materials are transparent above 365 nm.[279]

"Oxidation" of di(carbene)gold(I) salts has been investigated for several families of compounds. Both imidazol-2-ylidene and thiazol-2-ylidene complexes were found to undergo oxidative addition of chlorine and bromine to give the gold(III) complexes with a square-planar configuration and with the two carbene ligands in *trans*-position (Equation (52)). The structure of the example with X = Cl, Y = NMe, R^1 = Me has been determined. With iodine, Au–C cleavage to give the (carbene)AuI complexes and 2-iodo-imidazolium or -thiazolium salts has been observed.[237,267] The gold oxidation states have been confirmed by ^{179}Au Mössbauer spectroscopy.[263] Electrochemical reduction of the di(carbene)dihalogold(III) salts in acetonitrile with tetrabutylammonium perchlorate as the auxiliary conductant leads back to the gold(I) complexes. No gold(II) intermediate has been observed.[273] DF

quantum-chemical calculations were performed for the gold(I) and gold(III) complexes, and the results compared to the structures determined by X-ray diffraction.[237]

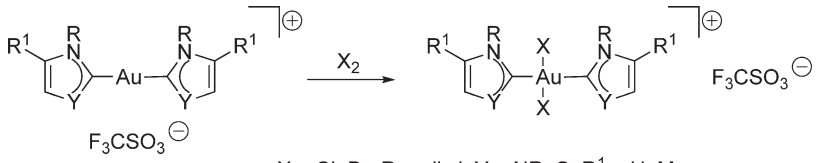

(52)

X = Cl, Br; R = alkyl; Y = NR, S; R^1 = H, Me

Homoleptic gold(III) complexes with four carbeniate ligands based on *C*-bound tetrazoles were revisited. Four equiv. of an isocyanide were added to an alkali tetra(azido)aurate(III). During the addition, the deep red azido complexes are decolorized and thermally stable compounds are obtained. The products are not yet true carbene complexes, but with strong acid, monoprotonated compounds are generated, in which at least one ligand is proposed to have carbene character. From the IR spectra, it has been concluded that a strong N–H···N hydrogen bond links two adjacent ligands (Equation (53)).[274]

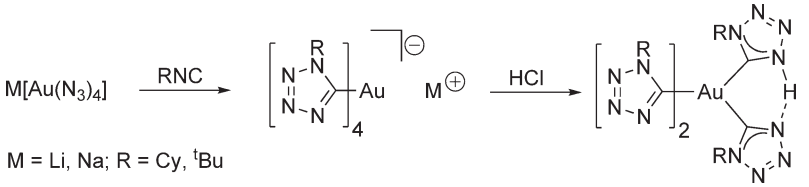

(53)

M = Li, Na; R = Cy, ^{t}Bu

A series of dipodal carbene ligands has been designed and introduced into gold chemistry, aiming at optimized catalytic and pharmaceutical performance of selected complexes of this metal. The donor functions were based on imidazol-2-ylidene units which are bridged either by short methylene, large-span *ortho*- and *meta*-xylylidene, or naphthalene-2,3-dimethylidene spacers. Owing to the configurational restraints, no chelation of gold(I) is possible and metal-bridging is the preferred mode of complexation. With the larger spacers, not only open-chain but also macrocyclic complexes of the cyclophane type are possible. If the spacer is derived from 2,6-dimethylpyridine, one or two additional donor functions are available (Scheme 70).[280]

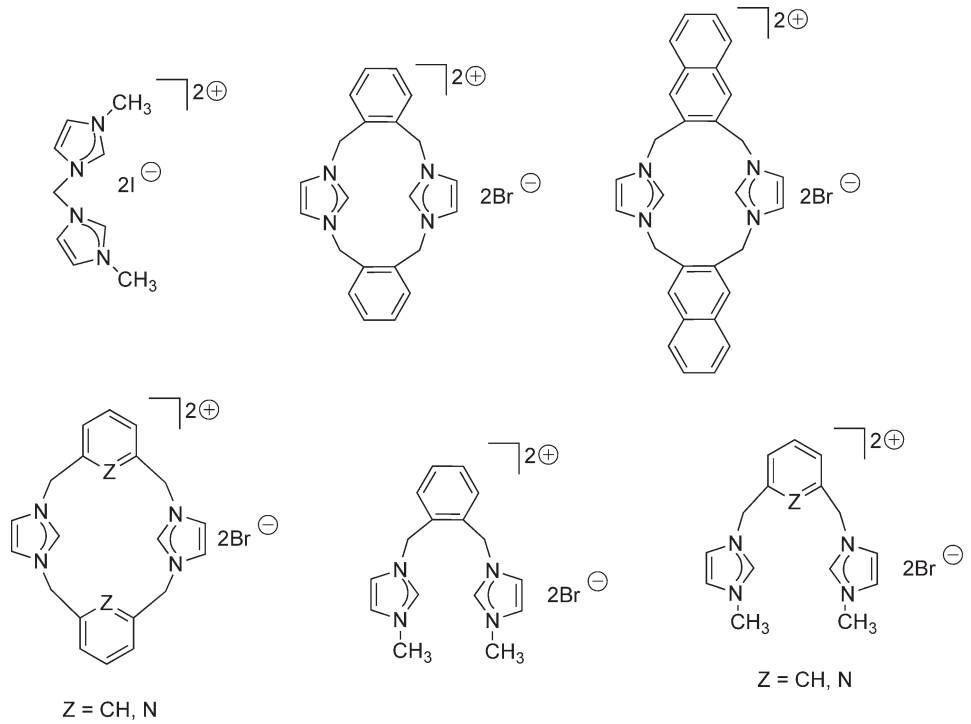

Z = CH, N

Z = CH, N

Scheme 70

The reactions of the corresponding diimidazolium salts with $(Me_2S)AuCl$ in dimethylformamide require the presence of an alkali carboxylate as a mild base. (Application of a strong base like NaH or ^tBuOK led to intractable mixtures.) The products thus prepared were all found to be based on dinuclear dications $[(dicarbene)_2Au_2]^{2+}$ with non-coordinating chloride or bromide anions. No case of mononuclear, crown ether-type coordination was encountered. In the dications, two linear C–Au–C units are running parallel, allowing for transannular aurophilic bonding and photoluminescent properties in favorable cases (Scheme 71). The cyclophane-type complexes are rigid in solution, while the others are fluxional as demonstrated by NMR studies. The extra pyridine donor functions are not employed for coordination.[280]

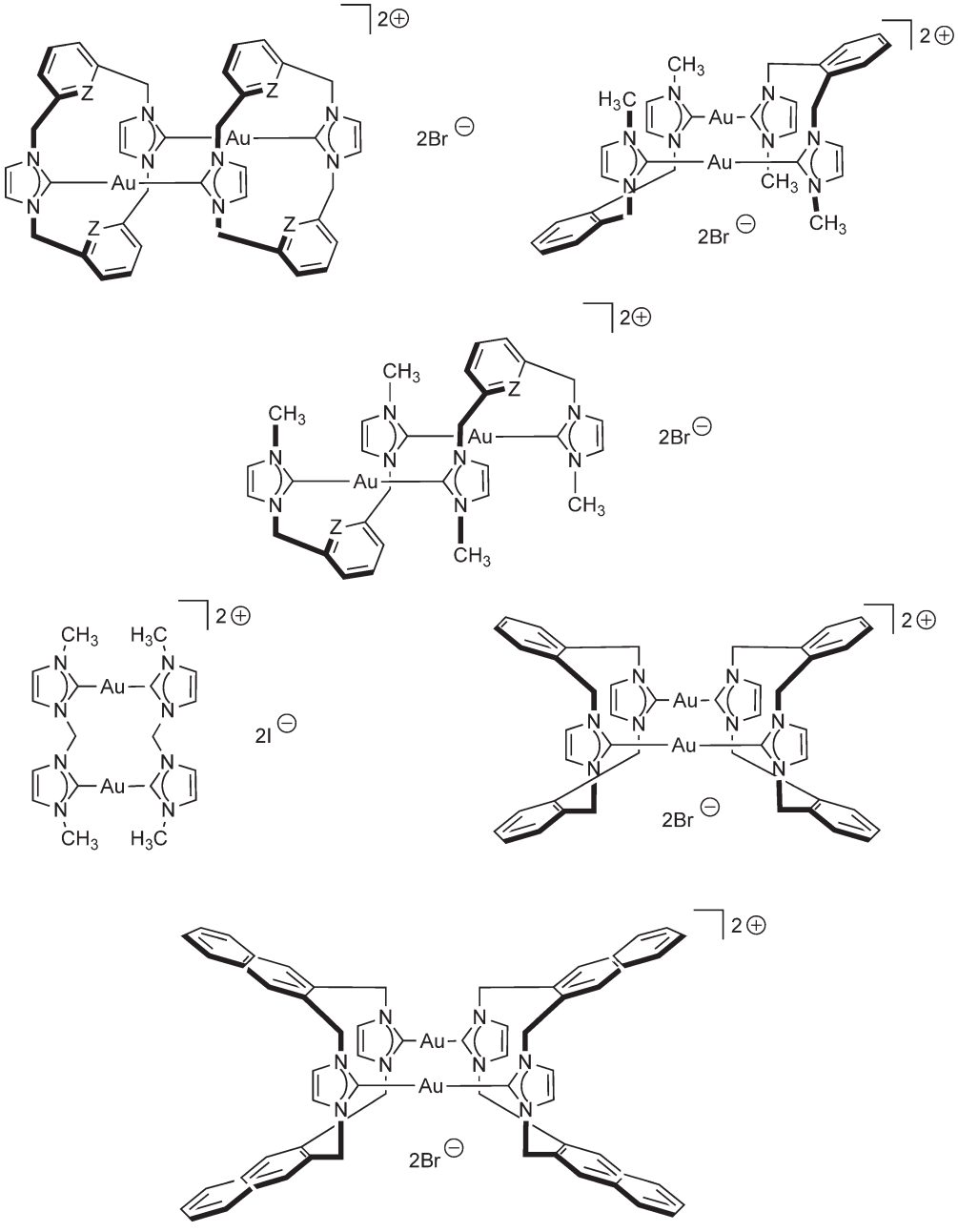

Scheme 71

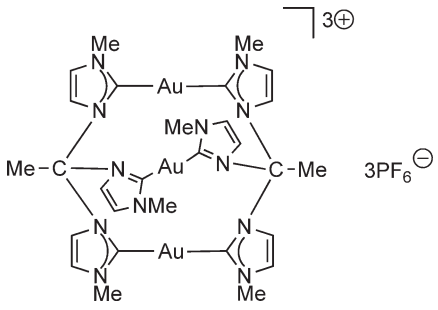

Scheme 72

Some of the compounds have been evaluated for their ability to induce mitochondrial membrane permeabilization, which is believed to play a fundamental role in the regulation of programmed cell apoptosis. The effects observed are not in line with a conventional model of action related to the accumulation of the lipophilic compounds in the cell, and further studies are necessary.[281]

Gold(I) complexes with dipodal di(imidazol-2-ylene) ligands were obtained with borato-bridged carbenes. These anionic ligands with a BH_2 bridge between the N atoms of two imidazol rings (Equation (54)) are isoelectronic with the neutral CH_2-bridged ligands (Scheme 71). Accordingly, the reaction of their lithium salts with $(Ph_3P)AuCl$ affords neutral dinuclear complexes with transannular aurophilic interactions across the macrocycle. Note that the tertiary phosphine is readily replaced by the powerful carbene ligand.[282]

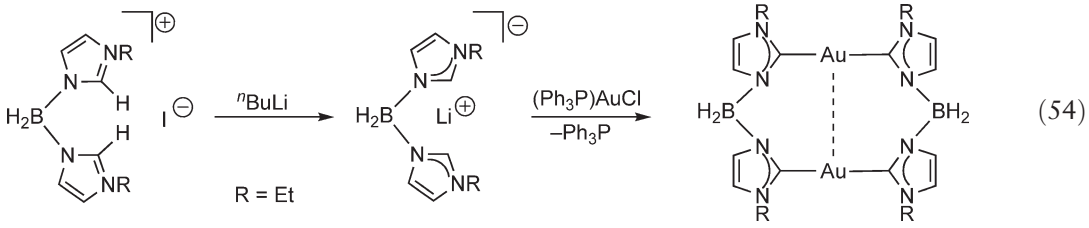

(54)

A related tripodal carbene ligand with an MeC bridgehead was used to form trinuclear gold(I) complexes: 1,1,1-tris(3-methylimidazol-1-yl-2-ylidene)ethane (TIMEMe, Scheme 72). For its synthesis, a tris-imidazolium salt precursor upon reaction with Ag_2O and a base was first converted into the trisilver salt, which then afforded the gold(I) complex on treatment with $(Me_2S)AuCl$. The product crystallized as the hexafluorophosphate $[(TIMEMe)_2Au_3](PF_6)_3$. The trication with three linear C–Au–C linkages between the carbon atoms of two different ligands has D_3-symmetry. The results of DF calculations indicate that the Au–C bond has significant π-contributions complementing the conventional σ-donor interaction.[238]

2.05.9 Carbonyl Complexes of Gold

Gold forms only a small family of carbonyl complexes, that is, compounds with carbon monoxide as a ligand. It was noted already at the beginning of the twentieth century that "binary" gold carbonyls $Au_m(CO)_n$ are not stable at room temperature.[3] Species of this type have later been observed under low-temperature matrix conditions and considered in theoretical calculations,[2] but all gold carbonyl complexes known to date which can be handled under standard conditions are "ternary" compounds, that is, compounds with a third component other than gold and carbon monoxide. In addition to the classical examples prepared in the 1920s, Au(CO)Cl and Au(CO)Br, subsequent work has demonstrated the existence of a few other 1 : 1 complexes such as a tetrachloroaurate(III) $Au(CO)ClAuCl_3$, a fluorosulfate $Au(CO)OSO_2F$, and a tris(pyrazolyl)borate $Au(CO)\{HB[3,5\text{-}(F_3C)_2C_3N_2H]_3\}$. In addition, the first 1 : 2 complexes have been isolated and fully characterized, in which the cation $[Au(CO)_2]^+$ is associated with non-polarizable counterions like $[Sb_2F_{11}]^-$ and $[UF_6]^-$, and there are also the first reports of applications of these (carbonyl)gold complexes in catalysis. Most of this experimental work was complemented by state-of-the-art quantum chemical studies.

The "chemistry of carbonyl derivatives of gold and related organometallics" was last reviewed in 1997, and the work covered by this article[283] and more recent additions are outlined in more detail below.

2.05.9.1 Theoretical Studies

The elusive nature of binary gold carbonyls – known only from earlier matrix-isolation studies and from CO adsorbed on surfaces of bulk gold – has prompted quantum-chemical studies of the hypothetical species $Au(CO)_n$ with $n = 1, 2, 3$.[284,285] Two independent investigations (on the HF and *ab initio* level, MP2, CCSD(T)) have consistently shown that the complexation of one CO molecule to one gold atom in the gas phase leads to a bent species with an Au–C≡O angle of 151°. However, this calculated $^2Au_1$ ground state (C_s-symmetry) is only 2 kJ lower in energy than the linear form. The bonding is based mainly on weak dispersion forces as an electron correlation effect, which give an Au–CO dissociation energy of ca. 30 kJ mol^{-1}. There is very little charge transfer from the metal atom to the ligand. The neutral, binary 1 : 2 ($D_{\infty h}$-symmetry) and 1 : 3 (D_{3h}-symmetry) complexes show similar energy characteristics.

The affinity of gold cations Au^+ to CO is much higher. Theoretical studies have confirmed the results of gas-phase ligand exchange experiments (followed by mass spectrometry).[286–288] The linear $[Au(CO)]^+$ cation ($C_{\infty v}$-symmetry) has calculated Au–CO dissociation energies in the range from 44.1 to as much as 59.5 kcal mol^{-1}, depending on details of the relativistic/quasi-relativistic method chosen for the quantum-chemical approach. On the MP2-TZ2P+f level of theory, the Au–C distance was found to be 1.91 Å long and the Au–CO dissociation energy 50.1 kcal mol^{-1}. An experimental value is available for the Au–C bond distance in (CO)AuCl, which is 1.93(2) Å,[289] in good agreement with the calculations. Ion/molecule reactions employing the bracketing technique in ion cyclotron resonance mass spectrometric studies[290] lead to an affinity sequence $C_6F_6 < H_2O < CO < C_2H_4 < C_6H_6 < NH_3$ for Au^+ cations.

Neutral and charged gold carbonyl species have also been observed on gold field emitter tips upon interaction with CO gas at room temperature in the presence of high electrostatic fields. The adsorbed complexes and the desorption pathways were identified using time-of-flight mass spectroscopy. [(CO)Au] species are more abundant than $[Au(CO)_2]$ species. The product distribution was rationalized by DF calculations of the electronic structure of the complexes.[291]

The reactions of the gold anion Au^- and of the di- and triatomic gold cluster monoanions Au_2^- and Au_3^- with CO were studied in a radio-frequency octopole ion trap experiment at cryogenic temperatures. Au^- shows no affinity for CO, but the two cluster anions absorb up to two CO molecules. Particular stability has been ascribed to $[Au_3(CO)_2]^-$, for which the binding energy has been estimated from thermolysis rate coefficients.[292]

DF calculations were carried out on CO complexes of small neutral, cationic, and anionic gold clusters Au_n with $n = 1$–6. The η^1-coordination mode (terminal *C*-coordination) was found to be the most favorable one irrespective of the charge of the cluster, and cluster planarity is more stable for the bare clusters and their carbonyls. As expected, adsorption energies are greatest for the cationic clusters, and decrease with size. Instead, the adsorption energies of the anions increase with the size of the cluster reaching a local maximum for $[Au_5(CO)]^-$, in agreement with experiments.[293]

CO desorption from photoexcited free (carbonyl)gold clusters has been studied by photoelectron spectroscopy. For the particular example $[Au_2(CO)]^-$, the unimolecular desorption threshold has been approximated by statistical calculations using the experimentally determined rate constants.[294]

2.05.9.2 Mono(carbonyl)gold(I) Compounds

The most simple preparative method for (CO)AuX compounds is the reaction of commercial $HAuCl_4$(aq.) or anhydrous $AuCl_3$ with CO in thionyl chloride. This reaction proceeds via the intermediates $(CO)AuClAuCl_3$ and $[Au_2(AuCl_4)_2]$ and finally affords high yields of (CO)AuCl (Ref: 283, and references therein). With suitable precautions, the corresponding bromide (CO)AuBr can be obtained from $AuBr_3$ and CO. Owing to the lability of $COBr_2$, it is necessary to remove the bromine with an unsaturated hydrocarbon. The direct synthesis from AuBr and CO is also possible.[283] Very few successful substitution reactions of (CO)AuCl to give other (CO)AuX compounds have been reported. In most cases, CO is replaced by the incoming ligand. This is also true for strained and unstrained olefins.[283,290]

The fluorosulfate $(CO)AuOSO_2F$ has been prepared by thermolysis of $[Au(CO)_2]^+OSO_2F^-$,[295,296] and isolated as a colorless solid. The carbonyl group shows an unusually high ν(CO) stretching frequency at 2,198 cm^{-1}, and the ^{13}C NMR spectrum has a resonance at 174 ppm.[297] In HSO_3F solution, both parameters show solvation effects, suggesting dissociation into solvated $[Au(CO)]^+$ cations (Scheme 73).

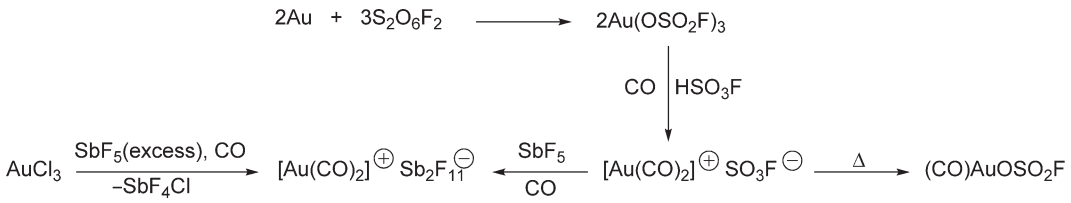

Scheme 73

Solutions containing the $[Au(CO)]^+$ cation are also obtained by treatment of commercial gold(III) oxide Au_2O_3 with concentrated sulfuric acid in a CO atmosphere. Depending on the reaction conditions, both $[Au(CO)]^+$ and $[Au(CO)_2]^+$ are present in these solutions as demonstrated by IR and NMR spectroscopy. The solution catalyzes the carbonylation of terminal olefins and a mechanism has been proposed for the process (Equation (55)).[298,299] This chemistry has been reviewed in a larger context.[300]

$$Au_2O_3 \xrightarrow[CO]{H_2SO_4} [Au(CO)]^{\oplus}_{solv} \xrightarrow{CO} [Au(CO)_2]^{\oplus}_{solv} \qquad (55)$$

A (carbonyl)gold(I) tri(pyrazolyl)borate was prepared via two routes. The first one started from the tetrabutylammonium tri(pyrazolyl)borate which was reacted with Au(CO)Cl, while the second one used the corresponding silver(tetrahydrofuran) complex as a reactant for Au(CO)Cl. Both reactions must be carried out in a CO atmosphere to avoid decomposition. The structure of the product (colorless crystals) has been determined by X-ray diffraction methods. The gold atom is in a quasi-tetrahedral environment with a terminal CO ligand on the threefold axis of the approximate molecular C_{3v}-symmetry. The Au–C bond length is short at 1.862(9) Å. The ν(CO) stretching frequency is 2,144 cm^{-1} for the crystals and 2,125 cm^{-1} for solutions in cyclohexane, where $\delta(^{13}C)$ for the NMR signal of the CO ligand appears at 172.6 ppm. This compound is the first and only gold(I) carbonyl with a tetrahedrally coordinated gold atom (Equation (56)).[301]

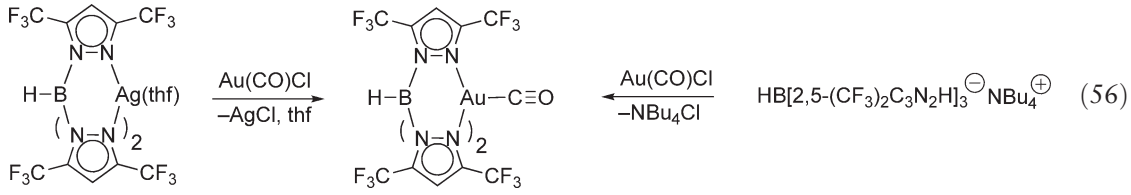

(56)

2.05.9.3 Di(carbonyl)gold(I) Compounds

Solutions containing the $[Au(CO)_2]^+$ cation were first obtained upon dissolving $Au(OSO_2F)_3$ in $HOSO_2F$ in a CO atmosphere (Scheme 73). The cation was identified by a complete analysis of the vibrational spectra including all isotope combinations,[296] followed in later work by NMR spectroscopic studies.[297] The ν(CO) bands of the cation with $D_{\infty h}$-symmetry appear in the IR spectrum at 2,251, 2,211, and 2,174 cm^{-1}, complemented by a Raman line at 2,254 cm^{-1}, [296,297] and the ^{13}C resonance appears at 162 ppm.[297] Both sets of data are significantly different from those of the $[Au(CO)]^+$ cation. According to a temperature-dependent NMR study, rapid CO exchange between the two cations occurs in solution at room temperature.

A colorless, crystalline compound $[Au(CO)_2]^+[Sb_2F_{11}]^-$ was prepared by treatment of $(CO)AuOSO_2F$ with SbF_5 in a CO atmosphere. This product is stable to 100 °C.[297] In a more convenient synthesis, it is also available from $AuCl_3$ and SbF_5 under CO gas,[295] with phosgene and SbF_4Cl as the byproducts (Scheme 73).

The hexafluorouranate(V) with the formula $[Au(CO)_2]^+[UF_6]^-$ was obtained by dissolving gold powder in liquid anhydrous HF containing UF_6 in a CO atmosphere. The crystalline product is stable at room temperature but decomposes on warming above ca. 50 °C. Two decomposition pathways were observed which afford either Au metal, CO gas, and a residue of UF_6, or Au metal, a mixture of CO and COF_2 gas, and a residue of UF_5. The compound was

$$^{n}Bu_4N^{+}[(CO)_5WC(O)Ph]^{-} + Ph_3PAuCl \longrightarrow Ph_3PAuC(O)Ph + {}^{n}Bu_4N^{+}[(CO)_5WCl]^{-}$$

Scheme 74

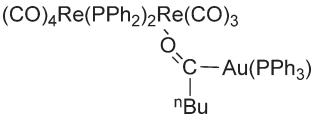

Scheme 75

identified by analytical data and by the vibrational spectra which are closely analogous to those of the other known salts with the $[Au(CO)_2]^{+}$ cation (Equation (57)).[302]

$$Au + UF_6 \xrightarrow[HF_{liq}]{CO} [Au(CO)_2]^{\oplus}[UF_6]^{\ominus} \xrightarrow{\Delta} \begin{matrix} (a)\ Au + 2CO + UF_6 \\ (b)\ 2Au + CO + COF_2 + 2UF_5 \end{matrix} \qquad (57)$$

Salts with the $[Au(CO)_2]^{+}$ cation have been proposed to be important intermediates in the transport of gold in hydrothermal fluids. Gold deposits may accumulate through formation and decomposition of (carbonyl)gold salts under geochemically relevant conditions, similar to the mechanism advanced with salts based on the $[Au(SH)_2]^{-}$ anion.[303]

"Acyl"-gold compounds with the function Au–C(O)–R may appear under the "carbonyl complex" heading, although in the taxonomy of the present chapter, these compounds could also be covered elsewhere. No insertion of CO into the Au–C bond of an organogold compound has been reported. Only a single example of the type LAu(C═O)R is known in the non-coordinated state. This was prepared from tetra-*n*-butylammonium benzoylpentacarbonyltungstate and Ph_3PAuCl with a quaternary ammonium salt as the byproduct. The molecule has Au–C and C═O distances of 2.085(5) and 1.200(7) Å. The sum of the angles at the carbonyl carbon atom is close to 360°, indicating planarity and thus sp^2-hybridization (Scheme 74). With $Li[(CO)_5WC(═O)Ph]$, only an adduct of the acylgold complex is obtained.[304]

Treatment of $Re_2(CO)_8(PPh_2)_2$ with $^{n}BuLi$ followed by Ph_3PAuCl was found to afford a yellow complex $(CO)_4Re(PPh_2)_2Re(CO)_3[Ph_3PAu(C═O)^{t}Bu]$ (70% yield) in which the acylgold complex unit is attached to one of the Re atoms via its carbonyl oxygen atom (Scheme 75).[305]

2.05.10 π-Complexes of Alkenes, Alkynes, and Arenes with Gold Compounds

It has been known from the earliest observations in gold chemistry that olefins form very weak π-complexes with gold in any of its oxidation states.[1–3] Therefore, only a very few stable complexes of this type have been isolated. However, unstable π-complexes of olefins with gold compounds are believed to be important intermediates or transient species in gold-catalyzed reactions of unsaturated organic compounds.[122–125,131,286–288,307–312]

2.05.10.1 Alkenes

In crystals of the complex of AuCl with a strained ligand system such as dibenzocyclopheptatrienylphosphine, there is no evidence for significant π-complexation. By contrast, the corresponding copper(I) and silver(I) complexes clearly show η^2-coordination of the metal atoms to the C═C bond (Scheme 76).[313]

By contrast, *endo*-dicyclopentadiene forms a stable crystalline 1 : 1 complex with AuCl, which is a dimer in the solid state with short aurophilic contacts. The Au–C distances are 2.20(1) and 2.16(1) Å (Scheme 77).[314]

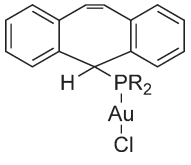

Scheme 76

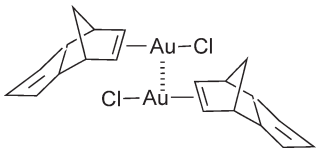

Scheme 77

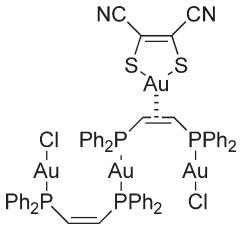

Scheme 78

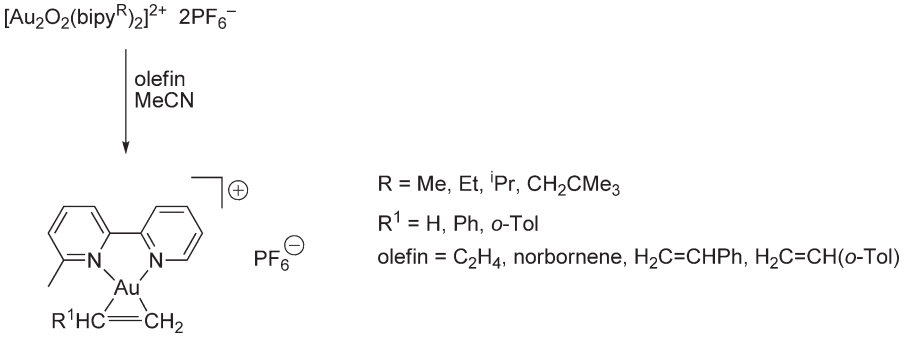

Scheme 79

all-(*Z*)-Tribenzo[12]annulene is transformed into the isomeric [4+2]-cycloadduct upon reaction with AuCl in dichloromethane. No AuCl complex could be isolated. With copper(I) and silver(I) salts, stable π-complexes are obtained.[315]

π-Complexes of olefins with gold(III) compounds are rare. Coordination of *cis*-bis(diphenylphosphine)ethane by 2 equiv. of AuCl sufficiently activates the C═C bond to make it an efficient donor toward cationic (1,2-dicyano-1,2-dithiolate)gold(III) units (Scheme 78).[316]

The cationic dinuclear oxo-gold(III) complexes of substituted bipyridyls react with olefins to give the stable coordination compounds shown in Scheme 79. The reactions are often incomplete, produce many byproducts, and give low yields of the olefin complexes.[317]

The coordination of ethene to Au^+ cations in the gas phase has been investigated by mass spectrometry techniques[309] with special consideration dedicated to H/D isotope effects.[308] Regarding the quality of the bonding of C_2H_4 to the coinage metal cations M^+, the bond energy varies discontinuously with Au^+ being most strongly bound (Au/Cu/Ag), while the equilibrium isotope effects show a continuous behavior (Cu/Ag/Au).[308] The results are in excellent agreement with theoretical calculations.[131,308–310] $[C_2H_4Au]^+$ is best described as an auracyclopropylium cation, while the bonding in the corresponding silver and gold species has an increasing electrostatic character.[308] The geometry of free ethylene is most strongly distorted by the coordination to Au^+ with the dihedral angle of the H_2C═C units reduced from 180° to 163.2°, but to 169.8° for Ag^+ and 167.9° for Cu^+.[310,312]

2.05.10.2 Alkynes

In general, gold cations Au^+ and their adducts with auxiliary ligands $[LAu]^+$, as well as gold(I) halides AuX, form only weak π-complexes with alkynes. Stable compounds have been isolated only with special combinations of components, but unstable species may nevertheless play an important role in gold chemistry as short-lived intermediates or transient species.

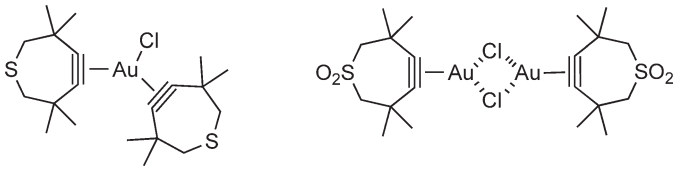

Scheme 80

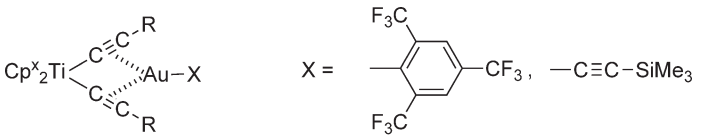

$Cp^x = C_5H_4SiMe_3$

R = $SiMe_3$, ^{t}Bu

Scheme 81

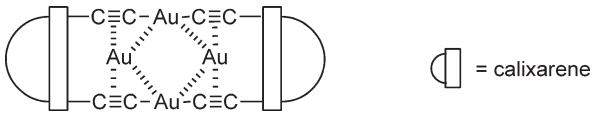

Scheme 82

Strained cyclic alkynes are the most powerful olefinic π-donors for gold(I) centers. This has been demonstrated for the cycloheptynes shown in Scheme 80. The Au–C distances are in the range from 2.050 to 2.100 Å.[318] There is also evidence for the coordination of AuCl to $Me_3Si–C{\equiv}C–SiMe_3$, but no details are available.[319]

Bis-π-coordination has been realized in tweezers-type dialkynyltitanium complexes, as shown in Scheme 81.[74,92,93,141,320,321] Theoretical calculations were carried out for the model system $[Cl_2Ti(C{\equiv}CH)_2]MMe$ with M = Cu, Ag, Au. It has been shown that the gold complex has the lowest stability in the series.[321]

Cations Au^+ have been embedded between parallel –C≡C–Au–C≡C– units connecting two calixarenes (Scheme 82). The symmetrical side-on coordination is slightly distorted to allow for aurophilic bonding.[51]

2.05.10.3 Arenes

There is no experimental evidence for π-complexation of arenes to gold centers in the condensed phase. Quantum-chemical calculations were carried out on various levels of theory for 1 : 1 and 2 : 1 complexes of benzene and substituted benzenes with Au^+ in the gas phase. For all model systems investigated, it has been predicted that an η^1-coordination to a single carbon atom is the ground state of the cation (C_s-symmetry for $[(C_6H_6)Au]^+$ and C_{2h}-symmetry for $[(C_6H_6)_2Au]^+$).[11,322,323] Similar results were obtained for hexafluorobenzene, for which a coordination to one of the fluorine atoms is comparable in energy. All aggregates are expected to be fluxional, similar to protonated arenes.[324,325]

References

1. Puddephatt, R. J. *Comprehensive Organometallic Chemistry I*; Wilkinson, G., Stone, F. G. A., Abel, E. W., Eds.; Pergamon: Oxford, 1982; Vol. 2, p 765.
2. Grohmann, A.; Schmidbaur, H. *Comprehensive Organometallic Chemistry II*; Abel, E. W., Stone, F. G. A., Wilkinson, G., Eds.; Elsevier: Oxford, 1995; Vol. 2, pp 1–56.

3. Schmidbaur, H. *Gmelin Handbook of Inorganic Chemistry, Organogold Compounds*; Springer: Berlin, 1980.
4. Schmidbaur, H. *Encyclopedia of Inorganic Chemistry*; Wiley: Chichester, 1994, p 1226.
5. Schmidbaur, H., Ed. *Gold - Progress in Chemistry, Biochemistry and Technology*; Wiley: Chichester, 1999.
6. Schmidbaur, H.; Schier, A. *Science of Synthesis, Hoeben–Weyl Methods of Molecular Transformations*; O'Neil, I., Ed.; Thieme: Stuttgart, 2003; Vol. 3, p 691.
7. Schmidbaur, H.; Grohmann, A.; Olmos, M. E.; Schier, A. *The Chemistry of Organic Derivatives of Gold and Silver*; Patai, S., Rapoport, Z., Eds.; Wiley: Chichester, 1999; pp 227–312.
8. Pyykkö, P. *Angew. Chem., Int. Ed.* **2004**, *43*, 4412–4453.
9. Schmidbaur, H.; Cronje, S.; Djordjevic, B.; Schuster, O. *Chem. Phys.* **2005**, *311*, 151.
10. Werner, H.; Otto, H.; Ngo-Khac, T.; Burschka, C. *J. Organomet. Chem.* **1984**, *262*, 123.
11. Dargel, T. K.; Hertwig, R. H.; Koch, W. *Mol. Phys.* **1999**, *96*, 583.
12. Gibson, D.; Johnson, B. F. G.; Lewis, J. *J. Chem.* Soc. A **1970**, 367.
13. Djordjevic, B.; Porter, K. A.; Nogai, S.; Schier, A.; Schmidbaur, H. *Organometallics* **2003**, *22*, 5336.
14. Glass, G. E.; Tobias, R. S. *J. Organomet. Chem.* **1968**, *15*, 481.
15. Schmidbaur, H. *Chem. Soc. Rev.* **1995**, *24*, 391.
16. Holthausen, M. C.; Heinemann, C.; Cornehl, H. H.; Koch, W.; Schwarz, H. *J. Phys. Chem.* **1995**, *102*, 4931–4941.
17. Hong, X.; Cheung, K.-K.; Cuo, C.-X.; Che, C.-M. *J. Chem. Soc., Dalton Trans.* **1994**, 1867–1871.
18. Baker, M. V.; Barnard, P. J.; Brayshaw, S. K.; Hickey, J. L.; Skelton, B. W.; White, A. H. *Dalton Trans.* **2005**, 37–43.
19. Porter, K. A.; Schier, A.; Schmidbaur, H. In *Perspectives in Organometallic Chemistry*; Screttas, C. G., Steele, B. R., Eds.; RSC: Special Publication No. 287, Cambridge, 2003; pp 74–85.
20. Steigelmann, O.; Schmidbaur, H. *Z. Naturforsch. Teil B* **1992**, *47*, 1721.
21. Steigelmann, O.; Bissinger, P.; Schmidbaur, H. *Z. Naturforsch. Teil B* **1993**, *48*, 72.
22. Schmidbaur, H.; Gabbai, F. P.; Schier, A.; Riede, J. *Organometallics* **1995**, *14*, 4969.
23. Schmidbaur, H.; Porter, K. A. In *Carbocation Chemistry*; Olah, G. A., Prakash, G. K. S., Eds.; Wiley: Hoboken, 2004; pp 291–308.
24. Schmidbaur, H. *Gold Bull.* **2000**, *33*, 3.
25. Pyykkö, P.; Tamm, T. *Organometallics* **1998**, *17*, 4842–4852.
26. Schuster, O.; Liau, R.-Y.; Schier, A.; Schmidbaur, H. *Inorg, Chim. Acta* **2005**, *358*, 1429.
27. Feng, D.-F.; Shaw, S.; Liu, C. W.; Lin, I. J. B.; Wen, Y.-S.; Liu, L.-K. *Organometallics* **1997**, *16*, 901–909.
28. Barranco, E. M.; Gimeno, M. C.; Laguna, A. *Inorg. Chim. Acta* **1999**, *291*, 60–65.
29. Laguna, A.; Laguna, M.; Gimeno, M. C.; Fernandez, E. J.; Jimenez, J.; Bardaji, M.; Lopez-de-Luzuriaga, J. M.; Jones, P. G. In *Chemistry of the Copper and Zinc Triads*; Welch, A. J., Chapman, S. K., Eds.; Royal Society of Chemistry: Cambridge, 1993, pp 168–171 (Spec. Publ. Nr. 131).
30. Payne, N. C.; Ramachandran, R.; Puddephat, R. J. *Can. J. Chem.* **1995**, *73*, 6–11.
31. Vicente, J.; Chicote, M. T. *Coord. Chem. Rev.* **1999**, *193–195*, 1143–1161.
32. Ruiz, J.; Mosquera, M. E. G.; Garcia, G.; Patron, E.; Riera, V.; Garcia-Granda, S.; Van der Maelen, F. *Angew. Chem., Int. Ed. Engl.* **2003**, *42*, 4767–4771.
33. Schuster, O.; Schmidbaur, H. *Z. Naturforsch.* **2006**, *61b*, 1–5.
34. Assmann, B.; Angermaier, K.; Paul, M.; Riede, J. *Chem. Ber.* **1995**, *128*, 891–900.
35. Nesmeyanov, A. N.; Perevalova, E. G.; Grandberg, K. I.; Lemenovskii, K. I. *Izv. Akad. Nauk., Ser. Khim.* **1974**, 1124.
36. Nesmeyanov, A. N.; Perevalova, E. G.; Ovchinnikov, M. V.; Snakin, Y. Y.; Grandberg, K. I. *Izv. Akad. Nauk., Ser. Khim.* **1978**, 1925.
37. Ursini, C. V.; Dias, G. H. M.; Horner, M.; Bortoluzzi, A. J.; Morigaki, M. K. *Polyhedron* **2000**, *19*, 2261–2268.
38. Raubenheimer, H. G.; Esterhuysen, M. W.; Timoshkin, A.; Chen, Y.; Frenking, G. *Organometallics* **2002**, *21*, 3173–3181.
39. Porter, K. A.; Schier, A.; Schmidbaur, H. *Organometallics* **2003**, *22*, 4922–4927.
40. Yam, V. W.-W.; Kam-Wing Lo, K.; Man-Chung Wong, K. *J. Organomet. Chem.* **1999**, *578*, 3–30.
41. Cheung, K.-L.; Yip, S.-K.; Yam, V. W.-W. *J. Organomet. Chem.* **2004**, *689*, 4451–4462.
42. Vicente, J.; Chicote, M.-T.; Abrisqueta, M. D.; Gonzales-Herrero, P.; Guerro, R. *Gold Bull.* **1998**, *31*, 83–87.
43. Abu-Salah, O. M. *J. Organomet. Chem.* **1998**, *565*, 211.
44. Matthews, J. A.; Waters, L. L. *J. Am. Chem. Soc.* **1900**, *22*, 108.
45. Offermanns, J.; Ruschewitz, U.; Kneip, C. *Z. Allg. Anorg. Chem.* **2000**, *626*, 649–654.
46. Schrandt, O.; Müller-Buschbaum, H. *J. Alloys Compd.* **1994**, *206*, 259–262.
47. Coates, G. E.; Parkin, C. *J. Chem. Soc.* **1962**, 3220–3226.
48. Mingos, D. M. P.; Yau, J.; Menzer, S.; Williams, D. J. *Angew. Chem., Int. Ed.* **1995**, *34*, 1894–1896.
49. Hunks, W. J.; MacDonald, M.-A.; Jennings, M. C.; Puddephatt, R. J. *Organometallics* **2000**, *19*, 5036–5070.
50. Irwin, M. I.; Jia, G.; Payne, N. C.; Puddephatt, R. J. *Organometallics* **1996**, *15*, 51–57.
51. Yip, S.-K.; Cheng, E. C.-C.; Yuan, L.-H.; Zhu, N.; Yam, V. W.-W. *Angew. Chem., Int. Ed.* **2004**, *43*, 4954–4957.
52. Vicente, J.; Chicote, M.-T.; Abrisqueta, M. D.; Alvarez-Falcon, M. M. *J. Organomet. Chem.* **2002**, *663*, 40–45.
53. Vicente, J.; Singhai, A. R.; Jones, P. G. *Organometallics* **2002**, *21*, 5887–5900.
54. McArdle, C. P.; Jennings, M. C.; Vittal, J. J.; Puddephatt, R. J. *Chem. Eur.* **2001**, *7*, 3572–3583.
55. MacDonald, M.-A.; Puddephatt, R. J.; Yap, G. P. A. *Organometallics* **2000**, *19*, 2194–2199.
56. Jia, G.; Puddephatt, R. J.; Vittal, J. J.; Payne, N. C. *Organometallics* **1993**, *12*, 263–265.
57. Vicente, J.; Chicote, M.-T.; Alvarez-Falcon, M. M.; Abrisqueta, M.-D.; Hernandez, F. J.; Jones, P. G. *Inorg. Chim. Acta* **2003**, *347*, 67–74.
58. Whittall, I. R.; Humphrey, M. G.; Houbrechts, S.; Persoons, A.; Hockless, D. C. R. *Organometallics* **1996**, *15*, 5738–5745.
59. Hurst, S. K.; Cifuentes, M. P.; McDonagh, A. M.; Humphrey, M. G.; Samic, M.; Luther-Davis, B.; Asselberghs, I.; Persoons, A. *J. Organomet. Chem.* **2002**, *642*, 259–267.
60. Yam, V. W.-W.; Cheung, K.-L.; Cheng, E. C.-C.; Zhu, N.; Cheung, K.-K. *Dalton Trans.* **2003**, 1830–1835.
61. Vicente, J.; Chicote, M.-T.; Alvarez-Falcon, M. M.; Bautista, D. *Organometallics* **2004**, *23*, 5707–5712.
62. Yamamoto, Y.; Shiotsuka, M.; Okuno, S.; Onaka, S. *Chem. Lett.* **2004**, *33*, 210–211.
63. Kayser, B.; Altman, J.; Nöth, H.; Knizek, J.; Beck, W. *Eur. J. Chem.* **1998**, 1791–1798.
64. Aguirre, C. J.; Gimeno, M. C.; Laguna, A.; Laguna, M.; Lopez de Luzuriaga, J. M.; Puente, F. *Inorg. Chim. Acta.* **1993**, *208*, 31–36.
65. Alder, M. J.; Flower, K. R.; Pritchard, R. G. *J. Organomet. Chem.* **2001**, *629*, 153–159.
66. Lang, H.; Koecher, S.; Back, S.; Rheinwald, G.; van Koten, G. *Organometallics* **2001**, *20*, 1968–1972.

67. Antonova, A. B.; Bruce, M. I.; Ellis, B. G.; Gaudio, M.; Humphrey, P. A.; Jevric, M.; Melino, G.; Nicholson, B. K.; Perkins, G. J.; Skelton, B. W.; Stapleton, B.; White, A. H.; Zaitseva, N. N. *Chem. Commun.* **2004**, 960–961.
68. Vicente, J.; Chicote, M.-T. *Coord. Chem. Rev.* **1999**, *193–195*, 1143–1161.
69. Vicente, J.; Chicote, M.-T.; Abrisqueta, M.-D. *Dalton Trans.* **1995**, 497.
70. Bardaji, M.; Laguna, A.; Jones, P. G. *Organometallics* **2001**, *20*, 3906–3912.
71. Vicente, J.; Chicote, M.-T.; Abrisqueta, M.-D.; Jones, P. G. *Organometallics* **1997**, *16*, 5628–5636.
72. Vicente, J.; Chicote, M.-T.; Abrisqueta, M.-D. *J. Chem. Soc., Dalton Trans.* **1995**, 497–498.
73. Vicente, J.; Chicote, M.-T.; Abrisqueta, M.-D.; Jones, P. G. *Organometallics* **2000**, *19*, 2629–2632.
74. Koehler, K.; Silverio, S. J.; Hyla-Kryspin, I.; Gleiter, R.; Zsolnai, L.; Driess, A.; Huttner, G.; Lang, H. *Organometallics* **1997**, *16*, 4970–4979.
75. Bruce, M. I.; Horn, E.; Matisons, J. G.; Snow, M. R. *Aust. J. Chem.* **1984**, *37*, 1163.
76. Irwin, M. J.; Vittal, J. J.; Puddephatt, R. J. *Organometallics* **1997**, *16*, 3541–3547.
77. Yamamoto, Y.; Shiotsuka, M.; Onaka, S. *J. Organomet. Chem.* **2004**, *689*, 2905–2911.
78. Wong, W.-Y.; Liu, L.; Poon, S.-Y.; Choi, K.-H.; Cheah, K.-W.; Shi, J.-X. *Macromolecules* **2004**, *37*, 4496–4504.
79. Wong, W.-Y.; Ho, K.-Y.; Choi, K.-H. *J. Organomet. Chem.* **2003**, *670*, 17–26.
80. Wong, W.-Y.; Choi, K.-H.; Lu, G.-L.; Shi, J.-X.; Lai, P.-Y.; Chan, S.-M.; Lin, Z. *Organometallics* **2001**, *20*, 5446–5454.
81. Ferrer, M.; Rodriguez, L.; Rossell, O.; Pina, F.; Lima, J. C.; Bardia, M. F.; Solans, X. *J. Organomet. Chem.* **2003**, *678*, 82–89.
82. Chao, H.-L.; Lu, W.; Li, Y.; Chan, M. C. W.; Che, C.-M.; Cheung, K.-K.; Zhu, N. *J. Amer. Chem. Soc.* **2002**, *124*, 14696–14706.
83. Yam, V. W.-W.; Choi, S. W.-K. *J. Chem. Soc., Dalton Trans.* **1996**, 4227–4232.
84. Liau, R.-Y.; Schier, A.; Schmidbaur, H. *Organometallics* **2003**, *22*, 3199–3204.
85. Lu, W.; Zhu, N.; Che, C.-M. *J. Organomet. Chem.* **2003**, *670*, 11–16.
86. Hu, Q. Y.; Lu, W. X.; Tang, H. D.; Sung, H. H. Y.; Wen, T. B.; Williams, I. D.; Wong, G. K. L.; Lin, Z.; Jia, G. *Organometallics* **2005**, *24*, 3966–3973.
87. Lu, X.-X.; Li, C.-K.; Cheng, E. C.-C.; Zhu, N.; Yam, V. W.-W. *Inorg. Chem.* **2004**, *43*, 2225–2227.
88. Yam, V. W.-W.; Cheung, K.-L.; Yuan, L.-H.; Wong, K. M.-C.; Cheung, K.-K. *Chem. Commun.* **2000**, 1513–1514.
89. Yam, V. W.-W.; Yip, S.-K.; Yuan, L.-H.; Cheung, K.-L.; Zhu, N.; Cheung, K.-K. *Organometallics* **2003**, *22*, 2630–2637.
90. Ipaktschi, J.; Munz, F. *Organometallics.* **2002**, *21*, 977–981.
91. Delgado, E.; Donnadieu, B.; Garcia, M. E.; Garcia, S.; Zuiz, M. A.; Zamora, F. *Organometallics* **2002**, *21*, 780–782.
92. Mihan, S.; Sünkel, K.; Beck, W. *Chem. Eur. J.* **1999**, *5*, 745–753.
93. Berenguer, J. R.; Fornies, J.; Lalinde, E.; Martinez, F.; Urriolabeita, E.; Welch, A. J. *J. Chem. Soc., Dalton Trans.* **1994**, 1291–1299.
94. Ferrer, M.; Rossell, O.; Seco, M.; Pellinghelli, M. A.; Tiripicchio, A. *Organometallics* **1995**, *14*, 57–62.
95. Gamase, M. P.; Gimeno, J.; Godefroy, I.; Lastra, E.; Martin-Vaca, B. M.; Garcia-Granda, S.; Gutierrez-Rodriguez, A. *J. Chem. Soc., Dalton Trans.* **1995**, 1901–1906.
96. Bruce, M. I.; Hall, B. C.; Skelton, B. W.; Smith, M. E.; White, A. H. *J. Chem. Soc., Dalton Trans.* **2002**, 995–1001.
97. Vicente, J.; Chicote, M.-T.; Abrisqueta, M. D.; Ramirez de Arellano, M. C.; Jones, P. G.; Humphrey, M. G.; Cifuentes, M. P.; Samoc, M.; Luther-Davies, B. *Organometallics* **2000**, *19*, 2968–2974.
98. Hogarth, G.; Alvarez-Falcon, M. M. *Inorg. Chim. Acta* **2005**, *358*, 1386–1392.
99. Ferrer, M.; Rodriguez, L.; Rossell, O.; Lima, J. C.; Gomez-Sal, P.; Martin, A. *Organometallics* **2004**, *23*, 5096–5099.
100. Ferrer, M.; Rodriguez, L.; Rossell, O.; Pina, F.; Lima, J. C.; Bardia, M. F.; Solans, X. *J. Organomet. Chem.* **2004**, *689*, 270.
101. Schuster, O.; Monkowius, U.; Schmidbaur, H.; Ray, R. S.; Krüger, S.; Rösch, N. *Organometallics* **2005**, *25*, 1004–1011.
102. Hussain, M. S.; Ul-haque, M.; Abu-Salah, O. M. *J. Cluster. Sci.* **1996**, *7*, 167.
103. Whittal, I. R.; Humphrey, M. G.; Hockless, D. C. *Aust. J. Chem.* **1997**, *50*, 991–998.
104. Kaharu, T.; Ishil, R.; Adachi, T.; Yoshida, T.; Takahashi, S. *J. Mater. Chem.* **1995**, *5*, 687–692.
105. Lu, W.; Zhu, N.; Che, C.-M *J. Amer. Chem. Soc.* **2003**, *125*, 16081–16088.
106. Yam, V. W.-W.; Cheung, K.-L.; Yip, S.-K.; Cheung, K.-K. *J. Organomet. Chem.* **2003**, *681*, 196–209.
107. Li, P.; Ahrens, B.; Choi, K.-H.; Muhammad, S.; Raithby, P. R.; Wilson, P. J.; Wong, W.-Y. *Cryst. Eng. Comm.* **2002**, *4*, 405–412.
108. Li, D.; Hong, X.; Che, C.-M.; Lo, W. C.; Peng, S. M. *Dalton Trans.* **1993**, 2929–2932.
109. Yam, V. W.-W.; Choi, S. W.-K.; Cheung, K.-K. *Organometallics* **1996**, *15*, 1734–1739.
110. Shiotsuka, M.; Yamamoto, Y.; Okuno, S.; Kitou, M.; Nozaki, K.; Onaka, S. *Chem. Commun.* **2002**, 590–591.
111. Bardaji, M.; Jones, P. G.; Laguna, A. *J. Chem. Soc., Dalton Trans* **2002**, 3624–3629.
112. Whittal, I. R.; Cifuentes, M. P.; Humphrey, M. G.; Luther-Davies, B.; Samoc, M.; Houbrechts, S.; Persoons, A.; Heath, G. A.; Bogsanyi, D. *Organometallics* **1997**, *16*, 2631–2637.
113. Hurst, S. K.; Lucas, N. T.; Cifuentes, M. P.; Humphrey, M. G.; Samoc, M.; Luther-Davies, B.; Asselberghs, I.; Van Boxel, R.; Persoons, A. *J. Organomet. Chem.* **2001**, *633*, 114–124.
114. McDonagh, A. M.; Lucas, N. T.; Nigel, T.; Cifuentes, M. P.; Humphrey, M. G.; Houbrechts, S.; Persoons, A. *J. Organomet. Chem.* **2000**, *605*, 193–201.
115. Whittall, I. R.; Humphrey, M. G.; Samoc, M.; Luther-Davies, B. *Angew. Chem., Int. Ed.* **1997**, *36*, 370–371.
116. Houbrechts, S.; Boutton, C.; Clays, K.; Persoons, A.; Whittall, I. R.; Naulty, R. H.; Cifuentes, M. P.; Humphrey, M. G. *J. Nonlinear Opt. Phys. Chem.* **1998**, *7*, 113–120.
117. Houbrechts, S.; Wada, T.; Sasabe, H.; Morrall, J. P. L.; Whitall, I. R.; McDonagh, A. M.; Humphrey, M. G.; Persoons, A. *MCLC S&T, Sect. B: Nonlinear Opt.* **1999**, *22*, 165–168.
118. Puddephatt, R. J. *Coord. Chem. Rev.* **2001**, *216*, 313.
119. Mohr, F.; Eisler, D. J.; McArdle, C. P.; Christopher, P.; Atieh, K.; Jennings, M. C.; Puddephatt, R. J. *J. Organomet. Chem* **2003**, *670*, 27–36.
120. Schuster, O.; Schmidbaur, H. *Organometallics* **2005**, *24*, 2289–2296.
121. Cinellu, M. A.; Minghetti, G.; Pinna, M. V.; Stoccoro, S.; Zucca, A.; Manassero, M. *J. Chem. Soc., Dalton Trans.* **1999**, 2823–2831.
122. Mendez, L. A.; Jimenez, J.; Cerrada, E.; Mohr, F.; Laguna, M. *J. Amer. Chem. Soc.* **2005**, *127*, 852–853.
123. Hashmi, A. S. K. *Angew. Chem., Int. Ed.* **2005**, *98*.
124. Schilling, G. *GIT Laborfachz.* **2003**, *47*, 621.
125. Roithova, J.; Hrusak, J.; Schröder, D.; Schwarz, H. *Inorg. Chim. Acta* **2005**, *358*, 4287–4292.
126. Teles, J. H.; Brode, S.; Chabanas, M. *Angew. Chem., Int. Ed.* **1998**, *37*, 1415–1418.
127. Casado, R.; Contel, M.; Laguna, M.; Romero, P.; Sanz, S. *J. Amer. Chem. Soc.* **2003**, *125*, 11925–11935.

128. Roembke, P.; Schmidbaur, H.; Cronje, S.; Raubenheimer, H. G. *J. Mol. Catal.* **2004**, *212*, 35–42.
129. Nevado, C.; Cardenas, D. J.; Echavarren, A. M. *Chem. Eur. J.* **2003**, *9*, 2627–2635.
130. Müller, T. E. *Tetrahedron Lett.* **1998**, *39*, 5961–5962.
131. Hashmi, A. S. K.; Rudolph, M.; Weyrauch, J. P.; Wölfle, M.; Frey, W.; Bats, J. W. *Angew. Chem., Int. Ed.* **2005**, *44*, 2798.
132. Nieto-Oberhuber, C.; Munoz, M. P.; Bunuel, E.; Nevado, C.; Cardenas, D. J.; Echavarren, A. M. *Angew. Chem., Int. Ed. Engl.* **2004**, *43*, 2402–2406.
133. Nevado, C.; Cardenas, D. J.; Echavarren, A. M. *Chem. Eur. J.* **2003**, *9*, 2627–2635.
134. Hrusak, J.; Schröder, D.; Koch, R. H.; Schwerdtfeger, P.; Schwarz, H. *Organometallics* **1995**, *14*, 1284.
135. Reetz, M. T.; Sommer, K. *Eur. J. Org. Chem.* **2003**, 3485–3496.
136. Wei, Q.-H.; Zhang, L.-Y.; Yin, G.-Q.; Shi, L.-X.; Chen, Z.-N. *J. Amer. Chem. Soc.* **2004**, *126*, 9940–9941.
137. Gambarotta, S.; Floriani, C.; Chiesi-Villa, A.; Guastino, C. *Chem. Commun.* **1983**, 1304.
138. Lang, H.; Koehler, K.; Zsolnai, L. *Chem. Commun.* **1996**, 2043–2044.
139. Uson, R.; Laguna, A. *Coord. Chem. Rev.* **1986**, *70*, 1.
140. Laguna, A.; Gimeno, M. C. *Trends Organomet. Chem.* **1994**, *1*, 231.
141. Contel, M.; Jimenez, J.; Jones, P. G.; Laguna, A.; Laguna, M. *J. Chem. Soc., Dalton Trans.* **1994**, 2515.
142. Sladek, A.; Hofreiter, S.; Paul, M.; Schmidbaur, H. *J. Organomet. Chem.* **1995**, *501*, 47.
143. Espinet, P.; Martin-Barrios, S.; Villafane, F.; Jones, P. G.; Fischer, A. K. *Organometallics* **2000**, *19*, 290–295.
144. Bardaji, M.; Laguna, A.; Perez, M. R.; Jones, P. G. *Organometallics* **2002**, *21*, 1877–1881.
145. Bordoni, S.; Busetto, L.; Cassani, M. C.; Albano, V. G.; Sabatino, P. *Inorg. Chim. Acta* **1994**, *222*, 267–273.
146. Raubenheimer, H. G.; Lindeque, L.; Cronje, S. *J. Organomet. Chem.* **1996**, *511*, 177–184.
147. Bella, P. A.; Crespo, O.; Fernandez, E. J.; Fischer, A. K.; Jones, P. G.; Laguna, A.; Lopez-de-Luzuriaga, J. M.; Monge, M. *J. Chem. Soc., Dalton Trans.* **1999**, 4009–4017.
148. Cassado, A. L.; Espinet, P. *Organometallics* **1998**, *17*, 3677–3683.
149. Schuster, O.; Schier, A.; Schmidbaur, H. *Organometallics* **2003**, *22*, 4079–4083.
150. Schmidbaur, H.; Inoguchi, Y. *Chem. Ber.* **1980**, *113*, 1646.
151. Baukova, T. V.; Kuz'mina, C. G.; Oleinikova, N. A.; Lemenovskii, D. A.; Blumenfeld, A. L. *J. Organomet. Chem.* **1997**, *530*, 27.
152. Fernandez, E. J.; Lopez-de-Luzuriaga, J. M.; Monge, M.; Olmos, M. E.; Perez, J. *J. Amer. Chem. Soc.* **2002**, *124*, 5942–5943.
153. Fernandez, E. J.; Laguna, A.; Lopez-de-Luzuriaga, J. M.; Monge, M.; Olmos, M. E. *Inorg. Chem.* **2005**, *44*, 1163–1165.
154. Fernandez, E. J.; Lopez-de-Luzuriaga, J. M.; Monge, M.; Montiel, M.; Olmos, M. E.; Perez, J.; Laguna, A.; Mendizabal, F.; Mohamed, A. A.; Fackler, J. P., Jr., *Inorg. Chem. Acta* **2004**, *43*, 3573–3581.
155. Laguna, A.; Laguna, M.; Jimenez, J.; Lahoz, F. J.; Olmos, E. *Organometallics* **1994**, *13*, 253–257.
156. Uson, R.; Laguna, A.; Tarton, M. T.; Jones, P. G. *Chem. Commun.* **1988**, 740.
157. Uson, R.; Laguna, A.; Jimenez, J.; Jones, P. G. *Angew. Chem., Int. Ed.* **1991**, *30*, 198.
158. Bhargava, S. K.; Mohr, F.; Bennett, M. A.; Welling, L. L.; Willis, A. C. *Inorg. Chem.* **2001**, *40*, 4271.
159. Bhargava, S. K.; Mohr, F.; Bennett, M. A.; Welling, L. L.; Willis, A. C. *Organometallics* **2000**, *19*, 5628.
160. Bennett, M. A.; Bhargava, S. K.; Mohr, F.; Welling, L. L.; Willis, A. C. *Aust. J. Chem.* **2002**, *55*, 267–270.
161. Fuchita, Y.; Utsunomija, Y.; Yasutake, M. *J. Chem. Soc., Dalton Trans.* **2001**, 2330–2334.
162. Vicente, J.; Bermudez, M. D.; Carrion, F. J.; Jones, P. G. *Chem. Ber.* **1996**, *129*, 1395–1399.
163. Vicente, J.; Bermudez, M. D.; Carrion, F. J.; Jones, P. G. *Chem. Ber.* **1996**, *129*, 1301–1306.
164. Vicente, J.; Bermudez, M. D.; Carrello, M.-P.; Jones, P. G. *J. Organomet. Chem.* **1993**, *456*, 305–312.
165. Vicente, J.; Bermudez, M. D.; Carrion, F. J.; Jones, P. G. *J. Organomet. Chem.* **1996**, *508*, 53–57.
166. Schmidbaur, H. *Angew. Chem. Int. Ed.* **1983**, *22*, 907.
167. Vicente, J.; Chicote, M. T.; Abrisqueta, M. D.; Gonzales-Herrero, P.; Guerrero, R. *Gold Bull.* **1998**, *31*, 126–130.
168. Fackler, J. P., Jr., *Inorg. Chem.* **2002**, *41*, 1–72.
169. Aguirre, C. J.; Gimeno, M. C.; Laguna, A.; Laguna, M.; Lopez -de-Luzuriaga, J. M.; Puente, F. *Inorg. Chim. Acta* **1993**, *208*, 31–36.
170. Vicente, J.; Chicote, M.-T.; Abrisqueta, M. D.; Alvarez-Falcon, M. M.; Ramirez de Arellano, M. C.; Jones, P. G. *Organometallics* **2003**, *22*, 4327–4333.
171. Cerrada, E.; Gimeno, M. C.; Laguna, A.; Orera, V.; Jones, P. G. *J. Organomet. Chem.* **1996**, *506*, 203–210.
172. Vicente, J.; Chicote, M. T.; Lagunas, M.-C. *Helv. Chim. Acta* **1999**, *82*, 1202–1210.
173. Vicente, J.; Singhal, A. R.; Jones, P. G. *Organometallics* **2002**, *21*, 5887–5900.
174. Romeo, I.; Bardaji, M.; Gimeno, M. C.; Laguna, M. *Polyhedron* **2000**, *19*, 1837–1841.
175. Carbo, M.; Falvello, L. R.; Navarro, R.; Soler, T.; Urriolabeitia, E. P. *Eur. J. Inorg. Chem.* **2004**, *11*, 2338–2347.
176. Antinola, A.; Carrilo-Hermosilla, F.; Diez-Barra, E.; Fernandez-Baeza, J.; Lara-Sanchez, A.; Otero, A.; Tejeda, J. *J. Organomet. Chem.* **1998**, *570*, 97–105.
177. Dushenko, G. A.; Mikhailov, I. E.; Kompan, O. E.; Zschunke, A.; Reck, G.; Schulz, B.; Mugge, C.; Minkin, V. I. *Mendeleev Commun.* **1997**, *4*, 127–129.
178. Cerrada, E.; Gimeno, M. C.; Jimenez, J.; Laguna, A.; Laguna, M.; Jones, P. G. *Organometallics* **1994**, *13*, 1470–1475.
179. Vicente, J.; Chicote, M. T.; Guerriero, R.; Jones, P. G. *J. Amer. Chem. Soc.* **1996**, *118*, 699–700.
180. Heinrich, D. D.; Staples, R. J.; Fackler, J. P., Jr. *Inorg. Chim. Acta* **1995**, *229*, 61–75.
181. Bardaji, M.; Connelly, N. G.; Gimeno, M. C.; Jimenez, J.; Jones, P. G.; Laguna, A.; Laguna, M. *J. Chem. Soc., Dalton Trans.* **1994**, 1163–1167.
182. Bardaji, M.; Cerrada, E.; Jones, P. G.; Laguna, A.; Laguna, M. *J. Chem. Soc., Dalton Trans.* **1997**, 2263–2266.
183. Nakano, M.; Kuroda, A.; Matsubayashi, G. *Inorg. Chim. Acta* **1997**, *254*, 189–193.
184. Van Zyl, W. E.; Lopez-De-Luzuriaga, J. M.; Fackler, J. P., Jr.; Staples, R. J. *Can. J. Chem.* **2001**, *79*, 896–903.
185. Guo, C.-X.; Chan, C.-K.; Che, C.-M. *Chem. Res. Chinese Univ.* **1997**, *13*, 138–145.
186. Gimeno, M. C.; Jimenez, J.; Laguna, A.; Laguna, M.; Jones, P. G.; Parish, R. V. *J. Organomet. Chem.* **1994**, *481*, 37–44.
187. Bardaji, M.; Blasco, A.; Jimenez, J.; Jones, P. G.; Laguna, A.; Laguna, M.; Merchan, F. *Inorg. Chim. Acta* **1994**, *223*, 55–61.
188. Mendez, L. A.; Jimenez, J.; Cerrada, E.; Mohr, F.; Laguna, M. *J. Amer. Chem. Soc.* **2005**, *127*, 852–853.
189. Carlson, T. F.; Fackler, J. P., Jr. *J. Organomet. Chem.* **2000**, *596*, 237–241.
190. Clark, R. J. H.; Tocher, J. H.; Fackler, J. P., Jr.; Neira, R.; Murray, H. H.; Knochel, H. J. *J. Organomet. Chem.* **1986**, *303*, 437.
191. Neitling, D. C.; Staples, R. J.; Fackler, J. P., Jr. *Inorg. Chim. Acta* **1997**, *263*, 35–48.

192. Schneider, W.; Angermaier, K.; Sladek, A.; Schmidbaur, H. *Z. Naturforsch.* **1996**, *51B*, 790.
193. Elbjeirami, O.; Omary, M. A.; Stender, M.; Balch, A. L. *Dalton Trans.* **2004**, 3173–3175.
194. White-Morris, R. L.; Olmstead, M. M.; Balch, A. L.; Elbjeirami, O.; Omary, M. A. *Inorg. Chem.* **2003**, *42*, 6741–6748.
195. Pathaneni, S. S.; Desiraju, G. R. *J. Chem. Soc., Dalton Trans.* **1993**, 319.
196. Irwin, M. J.; Jia, G.; Payne, N. C.; Puddephatt, R. J. *Organometallics* **1996**, *15*, 51.
197. White-Morris, R. L.; Stender, M.; Tinti, D. S.; Balch, A. L. *Inorg. Chem.* **2003**, *42*, 3237.
198. Yam, V. W. W.; Lo, K. K. W. *Chem. Soc. Rev.* **1999**, *28*, 323.
199. Sacco, A.; Freni, M. *Gazz. Chim. Ital.* **1956**, *86*, 195.
200. Schneider, D.; Schuster, O.; Schmidbaur, H. *Organometallics* **2005**, *24*, 3547–3551.
201. Che, C.-M.; Wong, W. T.; Lai, T. F.; Kwing, H.-L. *Inorg. Chim. Acta* **1992**, *197*, 177.
202. Liau, R.-Y.; Mathieson, T.; Schier, A.; Berger, R. J. F.; Runeberg, N.; Schmidbaur, H. *Z. Naturforsch.* **2002**, *57B*, 881.
203. Gonser, M. W.; Elbjeirami, O.; Cundari, T. R.; Omary, M. A. Abstracts of papers, *227th ACS National Meeting*, Anaheim, Ca, USA, March 28–April 1, 2004.
204. Bachman, R. E.; Fioritto, M. S.; Fetics, S. K.; Cocker, T. M. *J. Amer. Chem. Soc.* **2001**, *123*, 5376–5377.
205. Bachman, R. E.; Bodolsky-Bettis, S. A.; Glennon, S. C.; Sirchio, S. A. *J. Amer. Chem. Soc.* **2000**, *122*, 7146–7147.
206. Coco, S.; Espinet, P.; Falagan, S.; Martin-Alvarez, J. M. *New J. Chem.* **1995**, *19*, 959–964.
207. Alejos, P.; Coco, S.; Espinet, P. *New J. Chem.* **1995**, *19*, 799–805.
208. Benouazzane, M.; Coco, S.; Espinet, P.; Martin-Alvarez, J. M. *J. Mater. Chem.* **1995**, *5*, 441–445.
209. Vicente, J.; Chicote, M.-T.; Abrisqueta, M.-D.; Ramirez de Arellano, M. C.; Jones, P. G.; Humphrey, M. G.; Cifuente, M. P.; Samoc, M.; Luther-Davies, B. *Organometallics* **2000**, *19*, 2968–2974.
210. Kaharu, T.; Ishii, R.; Takahashi, S. *J. Chem. Soc., Chem. Commun.* **1994**, 1349–1350.
211. Zhang, S.-W.; Ishii, R.; Takahashi, S. *Organometallics* **1997**, *16*, 20–26.
212. Kaharu, T.; Ishii, R.; Adachi, T.; Yoshida, T.; Takahashi, S. *J. Mater. Chem.* **1995**, *5*, 687–692.
213. Vicente, J.; Chicote, M.-T.; Alvarez-Falcon, M. M.; Abrisqueta, M.-D.; Hernandez, F. J.; Jones, P. G. *Inorg. Chim. Acta* **2003**, *347*, 67–74.
214. Vicente, J.; Chicote, M.-T.; Alvarez-Falcon, M. M.; Bautista, D. *Organometallics* **2004**, *23*, 5707–5712.
215. Jia, G.; Puddephatt, R. J.; Vittal, J. J.; Payne, N. C. *Organometallics* **1993**, *12*, 263.
216. Jia, G.; Payne, N. C.; Vittal, J. J.; Puddephatt, R. J. *Organometallics* **1993**, *12*, 4771.
217. Irwin, M. J.; Vittal, J. J.; Puddephatt, R. J. *Organometallics* **1997**, *16*, 3541.
218. Kushmerick, J. G.; Naciri, J.; Yang, J. C.; Shashidhar, R. *Nano Letters* **2003**, *3*, 897–900.
219. Esperas, S. *Acta Chem. Scand.* **1976**, *A30*, 527.
220. Theil, M.; Jutzi, P.; Neumann, B.; Stammler, A.; Stammler, H.-G. *J. Organomet. Chem.* **2002**, *662*, 34–42.
221. Yau, J.; Mingos, D. M. P. *J. Chem. Soc., Dalton Trans.* **1997**, 1103–1111.
222. Schneider, W.; Sladek, A.; Bauer, A.; Angermaier, K.; Schmidbaur, H. *Z. Naturforsch.* **1997**, *52B*, 53.
223. Ehlich, H.; Schier, A.; Schmidbaur, H. *Z. Naturforsch.* **2002**, *57B*, 890.
224. Ehlich, H.; Schier, A.; Schmidbaur, H. *Organometallics* **2002**, *21*, 2400.
225. Bruni, S.; Bandini, A. L.; Cariati, F.; Speroni, F. *Inorg. Chim. Acta* **1993**, *203*, 127–128.
226. Uson, R.; Laguna, A.; Vicente, J.; Garcia, J.; Bergareche, B.; Brun, P. *Inorg. Chim. Acta* **1978**, *28*, 237.
227. Uson, R.; Laguna, A.; Bergareche, B. *J. Organomet. Chem.* **1980**, *184*, 411.
228. Uson, R.; Laguna, A.; Laguna, M.; Fernandez, E.; Jones, P. G.; Sheldrick, G. M. *J. Chem. Soc., Dalton Trans.* **1982**, 1971.
229. Bayon, R.; Coco, S.; Espinet, P.; Fernandez-Mayrdomo, C.; Martin-Alvarez, J. M. *Inorg. Chem.* **1997**, *36*, 2329.
230. Raubenheimer, H.; Cronje, S. In *Gold - Progress in Chemistry, Biochemistry and Technology*; Schmidbaur, H., Ed.; Wiley: Chichester, 1999; pp 557–632.
231. Koszinowski, K.; Schroeder, D.; Schwarz, H. *Organometallics* **2004**, *23*, 1132–1139.
232. Aschi, M.; Brönstrup, M.; Diefenbach, M.; Harvey, J. N.; Schröder, D.; Schwarz, H. *Angew. Chem., Int. Ed.* **1998**, *37*, 829.
233. Diefenbach, M.; Brönstrup, M.; Aschi, M.; Schröder, D.; Schwarz, H. *J. Amer. Chem. Soc.* **1999**, *121*, 10614.
234. Koszinowski, K.; Schröder, D.; Schwarz, H. *Angew. Chem., Int. Ed.* **2004**, *43*, 121–124.
235. Koszinowski, K.; Schröder, D.; Schwarz, H. *J. Amer. Chem. Soc.* **2003**, *125*, 3676–3677.
236. Nemcsok, D.; Wichmann, K.; Frenking, G. *Organometallics* **2004**, *23*, 3640–3648.
237. Raubenheimer, H. G.; Olivier, P. J.; Lindeque, L.; Desmet, M.; Hrusak, J.; Kruger, G. J. *J. Organomet. Chem.* **1997**, *544*, 91–100.
238. Hu, X.; Castro-Rodriguez, I.; Olsen, K.; Meyer, K. *Organometallics* **2004**, *23*, 755–764.
239. Boehme, C.; Frenking, G. *Organometallics* **1998**, *17*, 5801–5809.
240. Nieto-Oberhuber, C.; Munoz, M. P.; Bunuel, E.; Nevado, C.; Cardenas, D. J.; Echavarren, A. M. *Angew. Chem., Int. Ed.* **2004**, *43*, 2402–2406.
241. Vicente, J.; Chicote, M.-T.; Abrisqueta, M.-D.; Jones, P. G. *Organometallics* **1997**, *16*, 5628–5636.
242. Vicente, J.; Chicote, M. T.; Alvarez-Falcon, M. M.; Abrisqueta, M.-D.; Hernandez, F. J.; Jones, P. G. *Inorg. Chim. Acta* **2003**, *347*, 67–74.
243. Krawielitzki, S.; Beck, W. *Chem. Ber. Recl.* **1997**, *130*, 1654–1662.
244. Zhang, S. W.; Ishil, R.; Takahashi, S. *Organometallics* **1997**, *16*, 20–26.
245. Ishii, R.; Kahru, T.; Pirio, N.; Zhang, S.-W.; Takahashi, S. *J. Chem. Soc., Chem. Commun.* **1995**, 1215–1216.
246. Ku, R.-Z.; Peng, S.-M.; Liu, S.-T. *Book of Abstracts, 216th ACS National Meeting*, ACS: Washington, D.C., 2005.
247. Ku, R.-Z.; Huang, J.-C.; Cho, J.-Y.; Kiang, F.-M.; Reddy, K. R.; Chen, Y.-C.; Lee, K.-J.; Lee, J.-H.; Lee, G.-H.; Peng, S.-M.; Liu, S.-T. *Organometallics* **1999**, *18*, 2145–2154.
248. Bonati, F.; Burini, A.; Pietroni, B. R. *J. Organomet. Chem.* **1989**, *375*, 147.
249. Weber, L.; Dembeck, G.; Loenneke, P.; Stammler, H.-G.; Neumann, B. *Organometallics* **2001**, *20*, 2288–2293.
250. White-Morris, R. L.; Olmstead, M. M.; Jiang, F.; Tinti, D. S.; Balch, A. L. *J. Amer. Chem. Soc.* **2002**, *124*, 2327–2336.
251. Jiang, F.; Olmstead, M. M.; Balch, A. L. *Dalton Trans.* **2000**, *22*, 4098–4103.
252. Olmstead, M. M.; Jiang, F.; Attar, S.; Balch, A. L. *J. Amer. Chem. Soc.* **2001**, *123*, 3260–3267.
253. Burini, A.; Mohamed, A. A.; Fackler, J. P., Jr. *Comments Inorg. Chem.* **2003**, *24*, 253.
254. Mohamed, A. A.; Burini, A.; Fackler, J. P., Jr. *J. Amer. Chem. Soc.* **2005**, *127*, 5012–5013.
255. Vickery, J. C.; Olmstead, M. M.; Fung, E. Y.; Balch, A. L. *Angew. Chem. Int. Ed.* **1997**, *36*, 1179.

256. Raubenheimer, H. G.; Cronje, S. *J. Organomet. Chem.* **2001**, *617–618*, 170–181.
257. Deetlefs, M.; Raubenheimer, H. G.; Esterhuysen, M. W. *Catalysis Today* **2002**, *72*, 29–41.
258. Wang, H. M. J.; Lin, I. J. B. *Organometallics* **1998**, *17*, 972–975.
259. Wang, H. M. J.; Chen, C. Y. L.; Lin, I. J. B. *Organometallics* **1999**, *18*, 1216–1223.
260. Raubenheimer, H. G.; Scott, F.; Kruger, G. J.; Toerien, J. G.; Otte, R.; van Zyl, W.; Taljaard, I.; Olivier, P.; Linford, L. *J. Chem. Soc., Dalton Trans.* **1994**, 2091–2097.
261. Bovio, B.; Burini, A.; Pietroni, B. R. *J. Organomet. Chem.* **1993**, *452*, 287–291.
262. Bonati, F.; Burini, A.; Pietroni, B. R. *J. Organomet. Chem.* **1991**, *408*, 271.
263. Bovio, B.; Calogero, S. S.; Wagner, F. E.; Burini, A.; Pietroni, B. R. *J. Organomet. Chem.* **1994**, *470*, 275–283.
264. Schneider, S. K.; Herrmann, W. A.; Herdtweck, E. *Z. Anorg. Allg. Chem.* **2003**, *629*, 2363–2370.
265a. Boehler, C.; Stein, D.; Donati, N.; Grützmacher, H. *New J. Chem.* **2002**, *26*, 1291–1295.
265b. de Fremono, P.; Scott, N. M.; Stevens, E. D.; Nolan, S. P. Abstracts of Papers, *228th ACS National Meeting*, Philadelphia, PA, USA, August 22–26, 2004.
266. Raubenheimer, H. G.; Scott, F.; Roos, N.; Otte, R. *J. Chem. Soc., Chem. Commun.* **1990**, 1722.
267. Raubenheimer, H. G.; Olivier, P. J.; Lindeque, L.; Desmet, M.; Hrusak, J.; Kruger, G. J. *J. Organomet. Chem.* **1997**, *544*, 91–100.
268. Raubenheimer, H. G.; Toerien, J. G.; Kruger, G. J.; Otte, R.; van Zyl, W.; Olivier, P. *J. Organomet. Chem.* **1994**, *466*, 291–295.
269. Desmet, M.; Raubenheimer, H. G.; Kruger, G. J. *Organometallics* **1997**, *16*, 3324–3332.
270. Seckin, T.; Koytepe, S.; Ozdemir, I.; Cetinkaya, B. *J. Inorg. Organomet. Polym.* **2003**, *13*, 9–20.
271. Lee, K. M.; Lee, C. K.; Lin, I. J. B. *Angew. Chem., Int. Ed.* **1997**, *36*, 1850–1852.
272. Wang, H. M. J.; Vasam, C. S.; Tsai, T. Y. R.; Chen, S.-H. A. H. H.; Lin, I. J. B. *Organometallics* **2005**, *24*, 486–493.
273. Kuhlkamp, P.; Raubenheimer, H. G.; Field, J. S.; Desmet, M. *J. Organomet. Chem.* **1998**, *552*, 69–74.
274. Wehlan, M.; Thiel, R.; Fuchs, J.; Beck, W.; Fehlhammer, W. P. *J. Organomet. Chem.* **2000**, *613*, 159–169.
275. Raubenheimer, H. G.; Otte, R.; Cronje, S. In *Chemistry of the Copper and Zinc Triads*; Welch, A. J., Chapman, S. K., Eds.; Royal Society of Chemistry, 1993; (Spec. Publ. Nr. 133), pp 172–175.
276. Catalano, V. J.; Malwitz, M. A.; Etogo, A. O. *Inorg. Chem.* **2004**, *43*, 5714–5724.
277. Lee, C. K.; Lee, K. M.; Lin, I. J. B. *Organometallics* **2002**, *21*, 10–12.
278. Oezdemir, I.; Denizci, A.; Oetztuerk, H. T.; Cetinkaya, B. *Appl. Organomet. Chem.* **2004**, *18*, 318–322.
279. Seckin, T.; Koytepe, S.; Oezdemir, I.; Cetinkaya, B. *J. Inorg. Organomet. Polym.* **2003**, *13*, 9–20.
280. Barnard, P. J.; Baker, M. V.; Berners-Price, S. J.; Skelton, B. W.; White, A. H. *Dalton Trans.* **2004**, 1038–1047.
281. Barnard, P. J.; Baker, M. V.; Berners-Price, S. J.; Day, D. A. *J. Inorg. Biochem.* **2004**, *98*, 1642–1647.
282. Frankel, R.; Kniczek, J.; Ponikwar, W.; Nöth, H.; Polborn, K.; Fehlhammer, W. P. *Inorg. Chim. Acta.* **2001**, *312*, 23–39.
283. Dell'Amico, D. B.; Calderazzo, F. *Gold Bull.* **1997**, *30*, 21–24.
284. Mendizabal, F. *Organometallics* **2001**, *20*, 261–265.
285. Schwerdtfeger, P.; Bowmaker, G. A. *J. Chem. Phys.* **1994**, *100*, 4487.
286. Schröder, D.; Hrušák, J.; Hertwig, R. H.; Koch, W.; Schwerdtfeger, P.; Schwarz, H. *Organometallics* **1995**, *14*, 312–316.
287. Veldkamp, A.; Frenking, G. *Organometallics* **1993**, *12*, 4613.
288. Hrušák, J.; Schröder, D.; Schwarz, H. *Chem. Phys. Lett.* **1994**, *225*, 416.
289. Jones, P. G. *Z. Naturforsch.* **1982**, *37b*, 823.
290. Antes, I.; Frenking, G. *Organometallics* **1995**, *14*, 4263.
291. Chau, T.-D.; Visart de Bocarme, T.; Kruse, N.; Wang, R. L. C.; Kreuzer, H. J. *J. Chem. Phys.* **2003**, *119*, 12605–12610.
292. Hagen, J.; Soccaciu, L. D.; Heiz, U.; Bernhardt, T.; Woeste, L. *Eur. Phys. Jour. D* **2003**, *24*, 327–330.
293. Wu, X.; Senapati, L.; Nayak, S. K.; Selloni, A.; Hajaligol, M. *J. Chem. Phys.* **2002**, *117*, 4010–4015.
294. Luttgens, G.; Pontius, N.; Bechthold, P. S.; Neeb, M.; Eberhardt, W. *Phys. Rev. Lett.* **2002**, *88*, 076102/1–076102/4.
295. Wang, C.; Siu, S. C.; Hwang, G.; Bach, C.; Bley, B.; Bodenbinder, M.; Willner, H.; Aubke, F. *Can. J. Chem.* **1996**, *74*, 1952–1958.
296. Willner, H.; Aubke, F. *Inorg. Chem.* **1990**, *29*, 2195.
297. Willner, H.; Schaebs, J.; Hwang, G.; Mistry, F.; Jones, R.; Trotter, J.; Aubke, F. *J. Amer. Chem. Soc.* **1992**, *114*, 8972.
298. Xu, Q.; Imamura, Y.; Fujiwara, M.; Souma, Y. *J. Org. Chem.* **1997**, *62*, 1594–1598.
299. Xu, Q.; Souma, Y. *Stud. Surf. Sci. Cat.* **2003**, *145*, 215–218.
300. Souma, Y. *Shokubai* **1996**, *38*, 218–223.
301. Diaz, H. V. R.; Jin, W. *Inorg. Chem.* **1996**, *35*, 3687.
302. Adelheim, M.; Bader, W.; Höhn, E. G.; Jacob, E. *Chem. Ber.* **1991**, *124*, 1559.
303. Wang, T. *Dizhi Zhaokuang Luncong* **1998**, *13*, 82–84.
304. Raubenheimer, H. G.; Esterhuysen, M. W.; Esterhuysen, C. *Inorg. Chim. Acta* **2005**, i. pr.
305. Haupt, J.-J.; Petters, D.; Flörke, U. *J. Organomet. Chem.* **1998**, *553*, 497–501.
306. Schwarz, H. *Angew. Chem., Int. Ed.* **2003**, *42*, 4442–4454.
307. Hashmi, A. S. K. *Gold Bull.* **2004**, *37*, 51.
308. Schröder, D.; Wesendrup, R.; Hertwig, R. H.; Dargel, T. K.; Grauel, H.; Koch, W.; Bender, B. R.; Schwarz, H. *Organometallics* **2000**, *19*, 2608–2615.
309. Hertwig, R. H.; Koch, W.; Schröder, D.; Schwarz, H.; Hrusak, J.; Schwerdtfeger, P. *J. Phys. Chem.* **1996**, *100*, 12253.
310. Hertwig, R. H.; Hrusak, J.; Schröder, D.; Koch, W.; Schwarz, H. *Chem. Phys. Lett.* **1995**, *236*, 194.
311. Schröder, D.; Hrusak, J.; Hertwig, R. H.; Koch, W.; Schwerdtfeger, P.; Schwarz, H. *Organometallics* **1997**, *14*, 312.
312. Schröder, D.; Schwarz, H.; Pyykkö, P. *Inorg. Chem.* **1998**, *37*, 624.
313. Thomaier, J.; Boulmaaz, S.; Schonberg, H.; Ruegger, H.; Currao, A.; Grützmacher, H.; Hillebrecht, H.; Pritzkow, H. *New J. Chem.* **1998**, *22*, 947–958.
314. Hakansson, M.; Eriksson, H.; Jagner, S. *J. Organomet. Chem.* **2000**, *602*, 133–136.
315. Yoshida, T.; Kuwatani, Y.; Hara, K.; Yoshida, M.; Matsuyama, H.; Iyoda, M.; Nagase, S. *Tetrahedron Lett.* **2001**, *42*, 53–56.
316. Davila, R. M.; Staples, R. J.; Fackler, J. P., Jr. *Organometallics* **1994**, *13*, 418–420.
317. Cinellu, M. A.; Minghetti, G.; Stoccoro, S.; Zucca, A.; Manassero, M. *Chem. Commun.* **2004**, 1618–1619.
318. Schulte, P.; Behrens, U. *Chem. Commun.* **1998**, 1633–1634.
319. Mezailles, N.; Ricard, L.; Mathey, F.; Le Floch, P. *Eur. J. Inorg. Chem.* **1999**, 2233–2241.

320. Lang, H.; Rheinwald, G. *J. Prakt. Chem.* **1999**, *341*, 1–19.
321. Kovacs, A.; Frenking, G. *Organometallics* **1999**, *18*, 887–894.
322. Schröder, D.; Diefenbach, M.; Schwarz, H.; Schier, A.; Schmidbaur, H. In *Relativistic Effects in Heavy-element Chemistry and Physics*; Hess, B. A., Ed.; Wiley: Chichester, 2002; pp 245–258.
323. Schröder, D.; Brown, R.; Schwerdtfeger, P.; Schwarz, H. *Int. J. Mass Spectrom.* **2000**, *132*, 73.
324. Diefenbach, M.; Schwarz, H. *Electronic Encyclopedia of Computational Chemistry*; Rague-Schleyer, P. v., Ed.; Wiley: Chichester, 2004; pp 1–21.
325. Schröder, D.; Schwarz, H.; Hrusak, J.; Pyykkö, P. *Inorg. Chem.* **1998**, *37*, 624–632.

2.06
Zinc Organometallics

L Stahl and I P Smoliakova, University of North Dakota, Grand Forks, ND, USA

2.06.1 General Introduction

2.06.1.1 Background

The organometallic chemistry of zinc began with the syntheses of ethylzinc iodide and diethylzinc by Frankland in 1848,[1] making organozinc chemistry one of the oldest topics of organometallic chemistry. Despite its early beginnings, organozinc chemistry did not reach the prominence of organolithium and organomagnesium chemistry, mainly because of the much lower reactivity of organozinc compounds. For the better part of the twentieth century, the chemistry of zinc compounds with direct zinc–carbon bonds was limited largely to specialized applications, such as the Reformatsky reaction and the Simmons–Smith reagent.

The low reactivity of organozinc compounds, once considered a major impediment, has now become one of their greatest assets. Thus, their extreme functional-group tolerance has made organozinc compounds important nucleophiles in multistep organic syntheses. Due to its unmatched versatility, the organic chemistry of zinc compounds has undergone a spectacular growth since the publication of COMC (1995), and there is no sign that this trend will be abating soon.

In addition to their versatility, organozinc compounds also possess practical advantages over the much more reactive organolithium and organoaluminum reagents in organic synthesis. Thus, organozinc compounds, with the exception of $ZnMe_2$ and $ZnEt_2$ in their neat forms, are easy to handle, and because of their low toxicity they are also easy to dispose.

Inorganic and organometallic chemists have for many years valued diorganozinc compounds as selective alkylating agents and metallating agents. Because $ZnMe_2$ and $ZnEt_2$ are commercially available, they have become the metallating agent of choice when exploring the coordination chemistry of new ligands. Zinc moieties can be introduced as both monovalent (ZnR^+) and divalent (Zn^{2+}) ions, which makes them suitable for a variety of ligands. Unlike conventional metallating agents, which are largely main group compounds, the incorporation of organozinc species provides a realistic example of how a ligand will bind transition metals. The absence of a paramagnetism, combined with the one-step introduction of the metal into the ligand, allow for a rapid screening of zinc complexes by NMR spectroscopic methods.

Beyond these fundamental aspects, the great versatility of organozinc compounds can also be seen in the important roles they play in commercial applications. Organozinc complexes have been shown to be excellent catalysts and pre-catalysts for the polymerization of esters and the co-polymerization of epoxides and carbon dioxide; they are also co-catalysts in polyolefin catalysis.

Most semi-conducting zinc compounds, such as the chalcogenides ZnS and ZnSe, are made from simple organozinc compounds and volatile sources of chalcogens, such as H_2S and H_2Se. Because of the enormous economic importance of these solid-state materials, these MOCVD processes are among the major consumers of organozinc compounds.

2.06.1.2 Scope

This chapter is broadly divided into the inorganic chemistry of organozinc compounds, which comprises Sections 2.06.2–2.06.15, and the organic chemistry of organozinc compounds (Section 2.06.16), which deals with applications of these reagents in organic synthesis.

The inorganic section is organized by structure, rather than function, making it easier for the reader to both find relevant topics and to assimilate the information. Following a brief review of some fundamental aspects of elemental zinc, its chemistry, and its place in the periodic table, the organometallic chemistry of zinc is covered in a systematic fashion.

Section 2.06.3 deals with fundamental spectroscopic and computational studies of short-lived organozinc species that are rarely covered in reviews of this kind. The most important classes of organozinc reagents, namely diorganozinc compounds, organozinc halides, and the neutral donor adducts of both, are reviewed in the Sections 2.06.4–2.06.6. Zinc carbenoids, particularly the Simmons–Smith reagent and related compounds, and the more recent heterocarbene adducts of organozinc compounds are treated together in Section 2.06.7. Charged organozinc species, namely organozinc cations and organozincates, are discussed in this order in Sections 2.06.8 and 2.06.9.

Starting with Section 2.06.10, heteroatom-substituted organozinc compounds are introduced, beginning with organozinc amides and organozinc compounds bearing heavier groups 15 donor ligands and ending with organozinc hydrides and organozinc borohydrides in Section 2.06.14. The organozinc chemistry of compounds with direct metal–metal bonds, including the first molecular compound of zinc(I), decamethyldizincocene, concludes the inorganic portion of this chapter.

The second part of this chapter is devoted to the use of organozinc compounds in organic synthesis and is organized by functional groups. This part begins with addition reactions of organozinc reagents to carbonyl compounds, followed by nucleophilic and radical reactions with enones. Catalyzed and uncatalyzed reactions of organozinc compounds with carboxylic acid derivatives are covered next. Reactions of organozinc compounds with imines, nitrones, and related functional groups are discussed in Section 2.06.16.5. An entire Section, 2.06.16.6, is devoted to the ever-important cyclopropanation of olefins with halomethylzinc reagents. A variety of transition metal-catalyzed reactions, such as the copper-catalyzed allylic alkylations and metal-catalyzed cross-coupling reactions conclude the chapter.

Because of the separation of this chapter into fundamental synthetic and structural aspects of organozinc compounds and the applications of these compounds in organic synthesis, many topics are treated twice, but with decidedly different emphases. By way of example, the important organozinc alkoxides are covered first in the inorganometallic section, where the emphasis is on their syntheses, structures, and applications other than in organic synthesis. Later, in Section 2.06.16.2, the uses of such compounds as chiral catalysts in asymmetric addition reactions are discussed.

The organization of the material in this chapter is naturally subjective, and certain topics could equally well have been discussed in another section or in a different order. For example, the Simmons–Smith reagent is both an alkylzinc iodide and a carbenoid, and because both sections exist in this chapter, it is discussed under the more specific heading of zinc carbenoids.

A large number of all citations to organozinc compounds deal with the use of these compounds as precursors for solid-state materials, particularly for MOCVD applications. The latter area has become so interdisciplinary and grown to such an extent that the editors of this edition considered it prudent to devote an entire volume (Volume 12) to the use of organometallic compounds in materials chemistry. While the syntheses and structures of potential organozinc precursors for such applications will be treated in this chapter, the detailed aspects of the conversion of organozinc compounds to solid-state materials are the topic of Volume 12.

In this edition, one of the most obvious changes is the separation of the organometallic chemistry of zinc from that of cadmium. This change was made necessary by the ever-increasing number of publications for both elements and the need to keep the amount of material manageable. Even with this focus on only one element the current chapter cannot be an all-inclusive coverage of organozinc chemistry.

The selection of topics is naturally subjective and reflects the authors' biases, but it is hoped that this chapter provides a balanced coverage of modern organozinc chemistry, without omitting any major area completely. Of the thousands of citations to organozinc compounds during the reviewed period, not all are considered in this chapter. The authors have focused exclusively on material that was published in the peer-reviewed literature, and for this reason, conference proceedings and patents are not included. To provide a seamless coverage from COMC (1995), the literature has been reviewed from late 1993 through the first half of 2005, although older references are cited where appropriate.

2.06.2 Zinc and Its Place in the Periodic Table

2.06.2.1 The Element

Zinc is a bluish-white, lustrous metal which tarnishes in air. It is present in the earth's crust as sulfide (sphalerite), carbonate, or silicate ores, to the extent of only 78 ppm, making it the 23rd most abundant element.[2] The metal is obtained from its ores by roasting and subsequent reduction with coke or by electrolysis. Approximately 8.36 million metric tons of zinc were produced worldwide in 2002; of this amount, two-thirds were from ores, while one-third was obtained from recycled zinc.[3] The ease of mining and refining of the ore and the subsequent low price of the metal (ca. \$ 1.2 kg^{-1} in 1998)[3] have made zinc the third most popular non-ferrous metal (after aluminum and copper).[3]

Most of the zinc produced is used as metal, mainly for the galvanization of auto bodies and of other iron and steel structures.[4] Zinc alloys are also popular as structural materials, for example, for the construction of roofs and the fabrication of die cast auto parts. Zinc has a long history as an anodic battery component (Daniell's cell), and the introduction of zinc-air batteries with run times of more than 12 h promises that zinc will continue to play a major role in future battery technologies.[5] Approximately one-quarter of the zinc produced is used in compounds, mainly as zinc oxide, which is an additive in automobile tires and an important paint pigment. Simple diorganozinc compounds have become important source materials in the electronics industry, where they are used for the deposition of group 12/16 and group 12/15 semi-conducting materials.

Zinc is an essential element and of considerable biological importance, being present in the human body to the extent of 2 to 3 grams.[6] More than three hundred zinc-containing enzymes have been identified, of which carboxypeptidase, alcohol dehydrogenase, superoxide dismutase, DNA and RNA polymerases, and thermolysin are among the most important.[7] Zinc is also present in structural proteins, such as the "zinc fingers," which play an important role in DNA binding proteins.[8]

2.06.2.2 Zinc's Place in the Periodic Table

Zinc is the first element in group 12 and thus a *d*-block element. Despite its unambiguous position in the periodic table, there is still some division of opinion on whether zinc and its group 12 congeners, cadmium and mercury, are main group or transition metals. That zinc is often considered a main group metal by transition metal chemists, but a transition metal by main group chemists suggests that it does not quite fit either category.

Whether zinc is a main-group or transition metal depends, of course, on one's definition of transition metal and main-group metal. Those who classify zinc as a main-group metal cite its (almost) exclusive oxidation number of +2 in compounds (but see Section 2.06.15.2) and the absence of a partially filled *d*-shell in the metal and its compounds. Those who classify zinc as a transition metal usually note its much greater effective nuclear charge, polarizing power and its limited, but well defined, coordination chemistry.

Perhaps it is best to consider zinc as a privileged element, in that it partakes of chemical characteristics of both main group and transition metals. It may be this versatility of zinc which is its greatest asset, and which is responsible for the increasing popularity of the element and its organometallic compounds.

2.06.2.3 The Atomic and Chemical Properties of Zinc

Selected atomic properties of zinc, together with those of the related elements magnesium, copper, and cadmium, are summarized in Table 1. Zinc has five isotopes, ^{64}Zn (48.9%), ^{66}Zn (27.8%), ^{67}Zn (4.1%), ^{68}Zn (18.6%), and ^{70}Zn (0.6%). Only one of these, namely ^{67}Zn, has a nuclear spin ($I = 5/2$ and $\mu = 0.87524$), and one, ^{65}Zn, is radioactive with a half-life of 244 days.

Although zinc is formally a *d*-block element, some of its chemical properties are similar to those of the alkaline earth metals, especially those of magnesium. This is mainly due to zinc's exclusive exhibition of the +2 oxidation state in all its compounds and its appreciable electropositive character. With a standard potential of −0.763 V, zinc is considerably more electropositive than copper and cadmium.

As a consequence of its closed-shell electron configuration, zinc has a negative electron affinity, that is, the removal of an electron from Zn^- is exothermic. The electronegativity of zinc (1.588 PU) is intermediate between those of the alkaline earth metals and the first row transition metals and remarkably similar to that of beryllium (1.57 PU).

The zinc +2 ion, with its six-coordinate radius of 0.74 Å, is almost identical in size to both the magnesium (0.72) and the copper (0.73) ions, but zinc is much more polarizing than the alkaline earth metal and consequently has a well-defined, albeit limited, coordination chemistry. In keeping with the much lower hardness of Zn^{2+} ($\eta = 10.88$ eV) versus Mg^{2+} (32.55 eV),[9] zinc has a much greater affinity for softer ligands than magnesium, a fact that is also reflected in the natural occurrence of zinc as sulfide ores.

2.06.2.4 Structure and Bonding

In inorganic compounds, where zinc is almost invariably present in its divalent form, the common coordination numbers for zinc are 4 through 6. Systematic crystal structure analyses and computational studies on zinc complexes have shown that zinc's preference for octahedral over tetrahedral coordination is not nearly as pronounced as that of magnesium. The energy penalty for changes in coordination from 6 to 5 or from 6 to 4 is also much lower for zinc than for magnesium, and this may explain zinc's role in catalytic enzymes where coordinative flexibility is crucial.[10] Because of zinc's filled 3*d* shell, there are no ligand field effects and four-coordinate zinc is always tetrahedral, unless a rigid multidentate ligand imposes a planar coordination geometry.

In organozinc compounds, whether neutral or charged, zinc never exceeds coordination number 4, and in cases where this rule appears to be violated the additional bonds are invariably not fully developed. With its closed-shell

Table 1 Selected atomic and physical data for zinc and related elements

Element	*Magnesium*	*Copper*	*Zinc*	*Cadmium*	*References*
Atomic number, atomic mass	12, 24.305	29, 63.546	30, 65.38	48, 112.41	
Electron configuration	[Ne]$3s^2$	[Ar]$4s^1 3d^{10}$	[Ar]$4s^2 3d^{10}$	[Kr]$5s^2 4d^{10}$	
Electronegativity, χ based on CE (PU) Pauling's value	1.293, 1.31	1.85, 1.90	1.588, 1.65	1.521, 1.69	430[a],431[a]
Covalent radius (Å)	1.36	1.17	1.25	1.48	432
Ionic radius, M^{2+} (Å) (C.N.)	0.57(4), 0.72(6)	0.57(4), 0.73(6)	0.60(4), 0.74(6)	0.78(4), 0.95(6)	433
Van der Waals radius (Å), in RM-type molecules	2.45	2.30	2.25	2.32	434
First ionization potential (kJ mol^{-1})	737.53	745.25	906.09	867.7	435
Second ionization potential (kJ mol^{-1})	1450.27	1957.69	1732.88	1630.99	435
Third ionization potential (kJ mol^{-1})	7732.33	3553.55	3830.47	3615.30	435
Electron affinity (kJ mol^{-1})	−39	118.5	−58	−68	436
E° (M^{2+}/M), V	−2.375	0.340	−0.763	−0.404	437
Chemical hardness, M (η), eV	3.90	3.25	4.94	4.66	438
Chemical hardness, M^{2+} (η), eV	32.55	8.27	10.88	10.29	438

[a]Values are given in Pauling units and are based on configuration energies.

$1s^2 2s^2 2p^6 3s^2 3p^6 4s^2 3d^{10}$ electron configuration, zinc must be promoted to a $4s^1 4p^1$ configuration to form two covalent bonds. This *sp* hybridization scheme limits neutral, two-coordinate organozinc compounds to linear molecules of the type ZnR_2 or RZnX, in which zinc uses two $4sp$ hybrid orbitals to bind both ligands. Numerous high-quality computational studies have shown (see Section 2.06.4.7), however, that at least in diorganozinc compounds only the 4*s* orbitals are appreciably involved in bonding, with little or no participation from the 3*d* and 4*p* orbitals.

Additional bonds are thus donor bonds, and to accept electron pairs from neutral and anionic ligands, zinc uses the two remaining 4*p* orbitals to form sp^2 and sp^3 hybrids. In the absence of steric effects, discrete, homoleptic, anionic tri- and tetraorganozinc compounds (zincates) have almost always ideal trigonal-planar and tetrahedral geometries, respectively.

2.06.3 Spectroscopic and Computational Studies of Stable and Short-Lived Organozinc Species

Quantum chemical *ab initio* calculations for the 2*s* and 2*p* core level binding energies of isolated zinc atoms, small clusters and small, zinc-containing molecules, showed negligible energy shifts for dimethyl- and diethylzinc.[11] A significant lowering of the energies of these orbitals was observed when strong donor molecules were present, as in $[Zn(NH_3)_2Me_2]$, $[Zn(Py)_2Me_2]$, and $[Zn(Py)_2(CF_3)_2]$ (Py = pyridine). This information is useful, among others, for the interpretation of organozinc compounds adsorbed on surfaces. Thus, diethylzinc adsorbs on cold (90 K) Rh(111) surfaces as a molecule while it decomposes at higher temperatures (765 K) with the formation of metallic zinc.[12]

Electron-transfer (ET) reactions are important processes in chemistry, biochemistry, and physics. Using *ab initio* calculations on the ET element V_{ab}, of bimetallic model systems of the type [Zn–Zn] and [Zn–L–Zn], L = O, S, CH_2, and C_2, J. Calzado and F. Sanz showed that electronic coupling in the bridged systems was significantly larger.[13] This suggests that the through-bond, rather than the through-space, mechanism is the most important contributor. There is also an exponential dependence of these couplings on the distance between the metal centers and on the nature of the bridging group.

In the course of *ab initio* studies on the bonding in diatomic zinc compounds, Boldyerev and Simon determined the electronic ground state, the equilibrium bond length, the vibrational frequencies, and the dissociation energies of ZnC.[14] At all levels of theory (B3LYP, MP2, and QCISD), $^3\Sigma^-$ was the ground state. The calculated bond length (1.992 Å) at the QCSID/6-311++G(*d*, *f*) suggests substantial chemical, rather than van der Waals, bonding. The significant charge transfer from zinc to carbon caused a charge buildup of 0.66 electrons on C and a concomitant dipole moment of 2.77 D. The harmonic frequency ($\omega = 482\,cm^{-1}$) and the dissociation energy (0.932 eV, 89.9 kJ mol^{-1}) were also determined.

The unstable zinc carbene, $ZnCH_2$, is a prototype for organozinc compounds and an intermediate in the Clemmensen reduction and other organic transformations involving zinc.[15] The bonding in $ZnCH_2$ was studied by *ab initio* Hartree–Fock methods, and some of the results are outlined in Figure 1. Depending on whether the methylene group is in its triplet ($^3B_1$) or singlet ($^1A'$) form when it interacts with the zinc atom, two states are obtained for $ZnCH_2$, namely **A** and **B**. In the ground state **A**, the single bond between methylene and zinc is formed by the pairing of one of the $4sp_z$ electrons of zinc and the one electron in the sp_σ orbital of CH_2, while two electrons remain non-bonding. In the higher energy (49.0 kJ mol^{-1}) singlet state **B**, the zinc atom donates an electron pair from its 4*s* orbital into the empty sp^3 orbital on CH_2.[16] In both bond descriptions, the zinc–carbon interaction is a single bond with dissociation energies of 120.5 kJ mol^{-1} for **A** and 155.6 kJ mol^{-1} for **B**. The zinc–carbon bond lengths of **A** (1.9847 Å), **B** (1.8871 Å), and of the monocation $ZnCH_2^+$ (1.8666 Å) were also calculated. Photolysis of $ZnCH_2$ generates the carbynezinc hydride HZnCH, which is 100 kJ mol^{-1} less stable than **A**, and has a triplet $^3\Sigma^-$ ground state. Its zinc–carbon single bond was calculated to be 1.864 Å long.

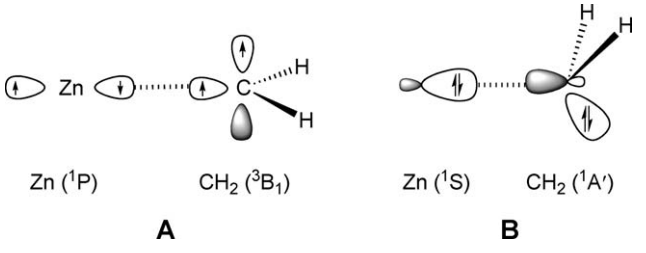

Figure 1 Bonding interaction between Zn(^{1}P) and CH_2 ($^3B_1$) (**A**) and Zn(^{1}S) and CH_2 ($^1A'$) (**B**).

In MALDI-TOF-MS, a technique that is used to determine the molecular weight distribution of polymers, the polymeric molecules are ionized by the attachment of transition metal ions.[17] A theoretical study showed that the complexation energies of Zn^{2+} range from 281.1 kJ mol^{-1} for methane to 691.8 kJ mol^{-1} for dodecane. These values are ca. three times higher than those for Cu^{+} and Co^{+} and ca. five times higher than those for Zn^{+}. Divalent zinc in form of the monocyclopentadienyl complex $CpZn^{+}$ has a substantially lower complexation energy (only 86.3 kJ mol^{-1}) with methane.

Alkylzinc radicals are both model systems for metal–ligand interactions in organometallic chemistry and intermediates in the decomposition of dialkylzincs in their thermal decomposition to zinc film depositions for optical and electronic devices. Pooley and Ellis analyzed laser-induced fluorescence spectra (LIF) of ZnMe and ZnEt, generated from DC discharge fragmentation of the appropriate dialkylzinc compounds, and assigned the molecular vibrations.[18] For ethylzinc, which has C_s symmetry in its 2A″ground state, the ground-state vibrational frequencies for the Zn–C stretch and the Zn–C–C bend were shown to be 387 and 180 cm^{-1}, respectively.

ESR studies of methylzinc radicals in a solid neon matrix found the expected 1 : 3 : 3 : 1 quartet for the $^{12}CH_3Zn$ radicals.[19] The spectra of the isotopomers $^{13}CH_3Zn$, $^{13}CD_3Zn$, $^{12}CH_3{}^{67}Zn$, and $^{12}CH_3{}^{67}Zn$ were also recorded, and $^{12}CH_3{}^{67}Zn$ ($I = 5/2$) exhibited the expected widely spaced sextet of quartets. The magnetic parameters of these species and of ZnH were determined and compared to those obtained from theoretical studies.

Two photoionization techniques, namely resonance-enhanced multiphoton ionization (REMPI) and zero kinetic energy (ZEKE) photolectron spectra, of the methyl- and ethylzinc radicals allowed the vibrational frequencies of the first excited states of the radicals and of the corresponding cations to be obtained.[20,21] These techniques provide spectra of much higher resolution than conventional photoelectron spectroscopy (PES) spectra, which is important for the closely spaced spectral lines of organometallic species. Analyses of these spectra revealed that the Zn–C bonds shorten and their force constants increase upon removal of the electron, a finding that is consistent with the previously determined bond dissociation energies for the radical ZnMe (79.6 kJ mol^{-1}) and the cation $ZnMe^{+}$ (297.5 kJ mol^{-1}).[22] Because the ionization energy of the ZnMe radical (7.273 eV, 701.7 kJ mol^{-1}) is less than that of the zinc atom (9.394 eV, 906.5 kJ mol^{-1}), it is assumed that the electron is removed from an antibonding orbital. The authors used the spectroscopic data to construct "experimental" MO diagrams for both ZnMe and $ZnMe_2$ and to predict the qualitative changes for the bonding in ZnR_2 molecules.

Using quantum chemical *ab initio* calculations, Fang and Grieman assigned the main features of the electronic spectra of $ZnMe_2$ and $ZnMe_2{}^{+}$.[23] The Zn–C bond length for the ground state of $ZnMe_2$ was calculated to be 1.9891 Å, while the Zn–C bond length for the ground and excited states of $ZnMe_2{}^{+}$ were calculated to be 2.0971 and 2.1214 Å, respectively.

2.06.4 Diorganozinc Compounds

2.06.4.1 Introduction

Diorganozincs are the most important organozinc compounds, because of their extensive use in both uncatalyzed and catalyzed asymmetric organic transformations. While these compounds were once limited to simple alkyl or aryl substituents, numerous recent innovations now allow the synthesis of diorganozinc compounds bearing almost any conceivable functionalized organic group. In organometallic chemistry, diorganozinc compounds are used as mild metallating and selective alkylating agents.

The simplest diorganozinc compounds, $ZnMe_2$ and $ZnEt_2$, are commercially available from many vendors. All other diorganozinc compounds can be synthesized by one or more of the following synthetic methods, which are detailed in Figure 2:

(i) Metathesis reaction from zinc halides and alkali or alkaline earth metal organometallics.
(ii) Transmetallation from diorganomercury compounds.
(iii) Protonolysis of an organozinc or an amidozinc compound with acidic hydrocarbons.
(iv) Disproportionation of organozinc halides (Schlenk equilibrium).
(v) Iodine–zinc exchange.
(vi) Boron–zinc exchange.
(vii) Nickel-catalyzed hydrozincation.
(viii) Substrate-specific reactions.

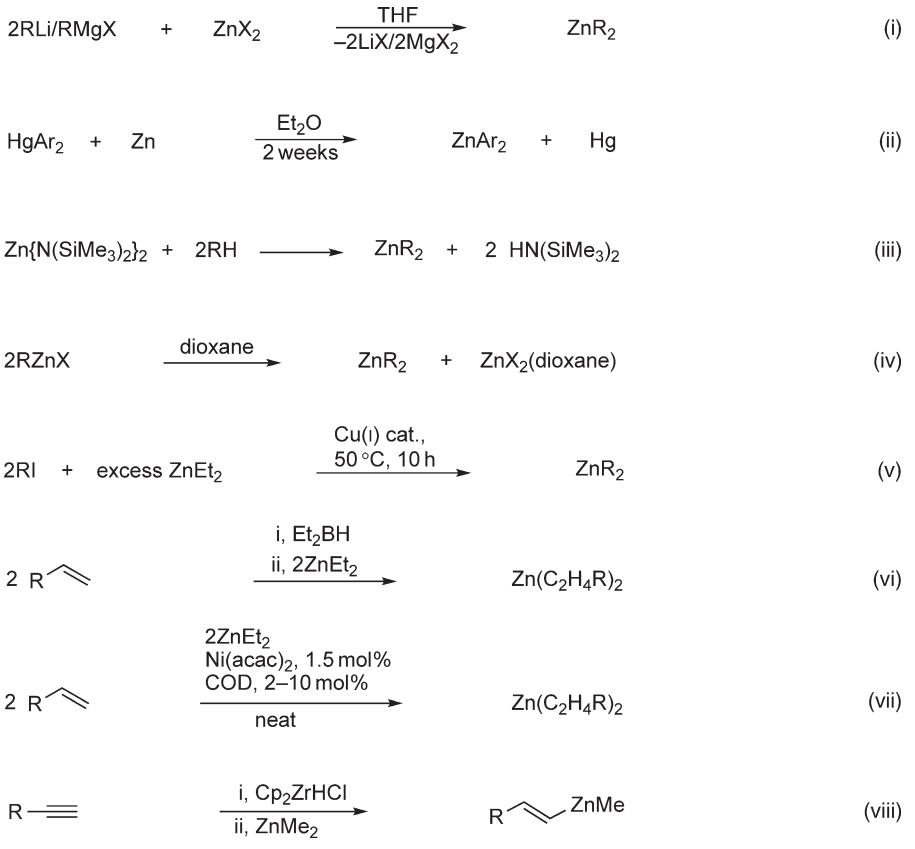

Figure 2

The first four of these reactions have been known for many years and are used routinely for the preparation of diorganozinc compounds with non-functionalized R groups. The by far most common of these is the transmetallation of zinc halides with alkali or alkaline earth organometallics (i). Reaction (ii), the exchange reaction of zinc with organomercury compounds, has limited scope, but it is useful when the product must be rigorously halide free. Because the reaction is heterogeneous, it often takes weeks to go to completion, and the toxicity of the organomercury compounds poses a serious health hazard. Reaction (iii), the protonolysis of a zinc amide, works well for acidic hydrocarbons, such as cyclopentadienes or alkynes. Because organozinc halides are in equilibrium with the respective diorganozinc compounds and the zinc halides, the diorganozinc species can be obtained either by precipitating the zinc dihalides with 1,4-dioxane, reaction (iv), or by distilling off the diorganozinc if it is sufficiently volatile.

Reactions (v)–(viii) constitute modern organic methods for the synthesis of diorganozinc compounds with functionalized R groups. In reaction (v), which is catalyzed by Cu(I) salts and proceeds by a radical mechanism, a primary alkyl iodide reacts in neat $ZnEt_2$ at ca. 50 °C to furnish the diorganozinc compound. Secondary alkyl iodides also react under these conditions, but only with $Zn(Pr^i)_2$, which is not commercially available and must be prepared *in situ*. Monosubstituted alkenes can be converted to the corresponding diorganozinc compounds either by boron–zinc exchange (vi), in which the alkene is first treated with diethylborane and then with diethylzinc, or by the nickel-catalyzed hydrozincation of olefins (vii). Finally, routes involving special organic substrates, such as the synthesis of diisoalkylzincs from monosubstituted alkenes via an organozirconium catalyst (viii), have also been developed.

2.06.4.2 Homoleptic Dialkylzinc Compounds

Bis(trimethylsilylmethyl)zinc **1** is synthesized by the addition of 2 equiv. of trimethylsilylmethylmagnesium bromide to anhydrous zinc bromide, as shown in Scheme 1.

After removal of $MgBr_2$ by filtration, bis(trimethylsilylmethyl)zinc **1** can be distilled at 41 °C and 0.1 torr.[24]

1

Scheme 1

The utility of the iodine–zinc exchange for the synthesis of diorganozincs having functionalized organic groups is demonstrated by the synthesis of bis(5-pivaloxypentyl)zinc **2** from diethylzinc and 5-iodopentylpivalate.[25]

Iodine–zinc exchange has also been used for the preparation of perfluorodiorganozinc compounds. CF_3I was known to react with $ZnEt_2$ to give $Zn(CF_3)_2$, but for the higher homologs only mixtures of R_fZnI and $Zn(R_f)_2$ (R_f = perfluorinated alkyl group) are obtained.[26] It was recently shown, Scheme 3, that primary and secondary perfluoroalkyl iodides (R_fI) react cleanly with $ZnEt_2$ in a non-donor solvent, such as hexane, to furnish the corresponding bis(perfluoroalkyl)zinc compounds, provided Lewis bases (L = CH_3CN, THF, and DMSO) are present.[27] The reaction time must be carefully monitored to obtain clean products, which are invariably isolated as Lewis base adducts.

Functionalized olefins may be converted to the corresponding diorganozinc compounds via hydroboration and subsequent boron–zinc exchange, as shown in Scheme 4.[28]

For internal olefins, the hydroboration step is slower, taking days rather than hours, and in this case the boron–zinc exchange requires the use of $Zn(Pr^i)_2$ (Scheme 5). The reaction is stereospecific, provided that the diisopropylzinc is metal halide free.[29,30]

Because of its stereospecificity, this boron–zinc exchange reaction has also been investigated theoretically.[31] A density functional study at the B3PW91 level investigated the mechanism of the alkyl group transfer from boron to zinc and sought possible intermediates along the reaction coordinate. In the methyl exchange between BMe_3 and $ZnMe_2$, a four-membered Me–Zn–Me–B ring and a trigonal-bipyramidal $MeZn–BMe_4$ moiety with a direct zinc–boron bond were identified as intermediates. All three equatorial methyl groups on boron have strong interactions with the zinc center, and this feature, together with the hypervalent carbon atoms in the four-membered ring, preserves the configuration of the chiral carbon atoms upon transfer from boron to zinc.

Scheme 2

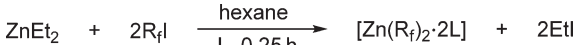

3

Scheme 3

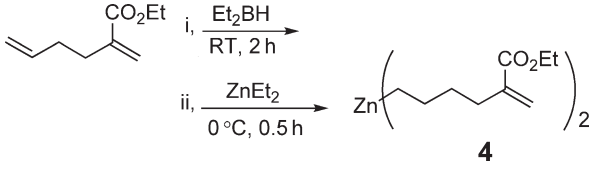

4

Scheme 4

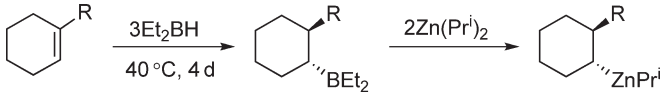

Scheme 5

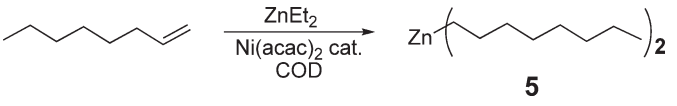

5

Scheme 6

A more convenient, but less general, synthesis of diorganozincs from olefins is the nickel-catalyzed hydrozincation, shown in Scheme 6. The yields (40–63%) are independent of the amount of diethylzinc added, but dependent on the nature of the olefin. For allylic and homoallylic alcohols and amines, yields as high as 85–95% are possible.[32,33]

Highly efficient syntheses of both hetero- and homoleptic diorganozinc compounds, such as **6** and **7**, were achieved by the UV ($\lambda \geq 280$ nm) irradiation of mixtures of functionalized organoiodides and diethyl- or diisopropylzinc (Scheme 7).[34] Irradiation with ultraviolet light avoids the use of a large excess of diethylzinc, which often furnishes homoleptic diorganozincs rather than the desired heteroleptic ones. Reaction times rarely exceed 2 h and conversions from 55 to 95% were commonly achieved.

Negishi *et al*. reported the regioselective synthesis of diisoalkyl derivatives from monosubstituted alkenes in yields ranging from 58–95%, Scheme 8, from the *in situ* prepared ethylene complex $Cp_2Zr(C_2H_4)$.[35] The zirconocene–ethylene complex presumably undergoes alkene insertion to furnish a zirconacyclopentane which further reacts with diethylzinc to yield the diisoalkylzinc compound.

An unusual diorganozinc compound consisting of an eight-membered ring of alternating zinc and carbon atoms **9** was obtained as shown in Scheme 9.[36] The bulky alkyl ligand (2-pyridyl)$C(SiMe_3)_2$ was first transferred to antimony via transmetallation from a lithium salt, and this was followed by a chlorotrimethylsilane elimination. The reaction of the organoantimony chloride with diethylzinc then gave **9**.

As shown in Figure 3, the Lewis-basic pyridyl groups form donor bonds with the Lewis-acidic zinc to yield an S_4-symmetric polycyclic compound. The pyramidalized zinc atoms are three coordinate, being surrounded by two relatively long Zn–C bonds (2.032(7) Å) and one short Zn–N donor bond (2.031(5) Å).

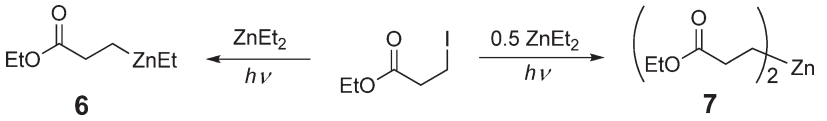

6 7

Scheme 7

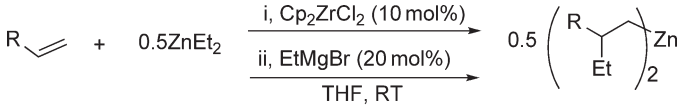

8

Scheme 8

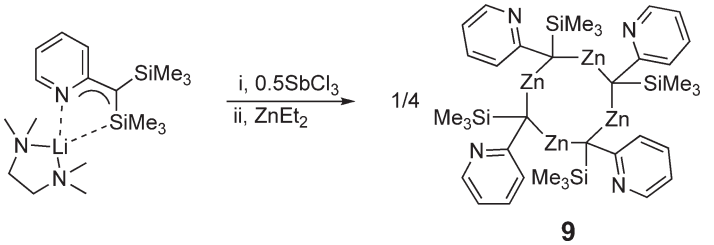

9

Scheme 9

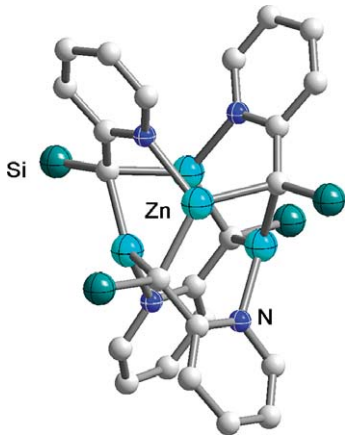

Figure 3 Solid-state structure and partial labeling scheme of tetrameric $[(2\text{-pyridyl})CSiMe_3Zn]_4$ **9**. The trimethylsilyl groups have been truncated to the silicon atoms. Here and in all following figures the hydrogen atoms are not shown, and the carbon atoms are not labeled.

2.06.4.3 Homoleptic Diarylzinc Compounds

Despite the extensive history of organozinc chemistry, the first solid-state structure of a Lewis base-free diorganozinc compound with σ-bound ligands, namely diphenylzinc, was not reported until 1990.[37] Diphenylzinc was synthesized by the transmetallation of diphenylmercury with metallic zinc (Scheme 10) and, after multiple sublimations, obtained halide free in 67% yield.

In the solid state, **10** (Figure 4) consists of dimeric $[PhZn(\mu\text{-}Ph)_2ZnPh]$ units, each zinc atom being surrounded in a distorted trigonal-planar fashion by two bridging and one terminal phenyl group. The bridging and terminal phenyl groups are almost orthogonal to each other. The zinc–carbon bonds of the terminal phenyl groups (1.946(5) Å) are slightly shorter than those of the bridging phenyl groups (2.011(5) Å), while the zinc–carbon bonds connecting the two $ZnPh_2$ moieties (2.404(4) Å) are considerably longer.

$$HgPh_2 + Zn \xrightarrow[2\,\text{weeks}]{Et_2O} \underset{\mathbf{10}}{ZnPh_2} + Hg$$

Scheme 10

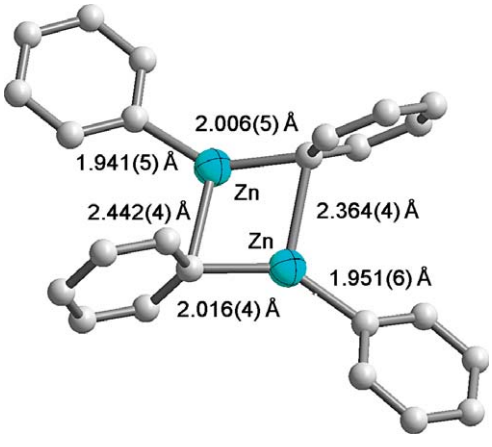

Figure 4 Solid-state structure, partial labeling scheme and selected bond lengths of dimeric $ZnPh_2$ **10**.

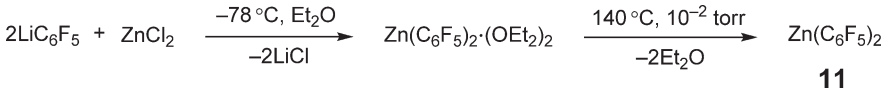

Scheme 11

The addition of a diethyl ether solution of $ZnCl_2$ to *in situ* prepared LiC_6F_5 (Scheme 11) yielded initially an oily product, which was identified as a mixture of $Zn(C_6F_5)_2$ and its diethyl etherate, namely $[Zn(C_6F_5)_2(OEt_2)_2]$.[38] After multiple vacuum distillations, ether-free $Zn(C_6F_5)_2$ **11** was obtained as a free-flowing powder.

In contrast to $ZnPh_2$, **11** consists of monomeric, linear $[Zn(C_6F_5)_2]$ units in which both perfluorophenyl substituents form a dihedral angle of 76.7(2)°. The zinc–carbon bonds are 1.928(4) Å long, on average, and thus substantially shorter than those of the previously reported $[Zn(C_6F_5)_2(THF)_2]$,[39] which has isometric zinc–carbon bonds of 2.003(3) Å lengths.

Edelmann *et al.* reported $Zn\{2,4,6\text{-}(CF_3)_3C_6H_2\}_2$ **12** from zinc chloride and $2,4,6\text{-}(CF_3)_3C_6H_2Li$, according to Scheme 12.[40] The solid-state structure of **12** consists of discrete $Zn\{2,4,6\text{-}(CF_3)_3C_6H_2\}_2$ units, with a dihedral angle of 67° between both aryl planes. The equidistant Zn–C bonds (1.949(3) Å) are not quite linear, enclosing a C–Zn–C bond angle of 170.0(1)°.

The synthesis and structure of the related $Zn(p\text{-}CF_3C_6H_4)_2$ **13** from $p\text{-}CF_3C_6H_4Li$ and zinc chloride were reported recently.[41] In the solid-state, Figure 5, the compound is linear (C–Zn–C = 178.50(9)°) and has symmetrical Zn–C bonds with bond lengths of 1.932(2) Å. The two aromatic rings form a dihedral angle of 56°, and there are weak interactions between the hydrogen atoms of one ring and the π-cloud of a neighboring aromatic ring. Dimesitylzinc **14** was obtained by the unconventional protonolysis of a cyclic methylzinc boroxide with dimesitylborinic acid, as shown in Scheme 13.[42] The monomeric molecules have crystallographic inversion symmetry and are thus both strictly linear and perfectly coplanar. This coplanarity is in stark contrast to the ring conformations of the diphenylzinc compounds discussed above, and it may reflect crystal packing forces as steric repulsion of the methyl groups would argue against it.

The solid-state structure of **14**, which is shown in Figure 6, revealed zinc–carbon bonds (1.9422(19) Å) that are, somewhat unexpectedly, of the same length as those in $Zn\{2,4,6\text{-}(CF_3)_3C_6H_2\}_2$, despite the decidedly different electronic properties of the ligands.

Scheme 12

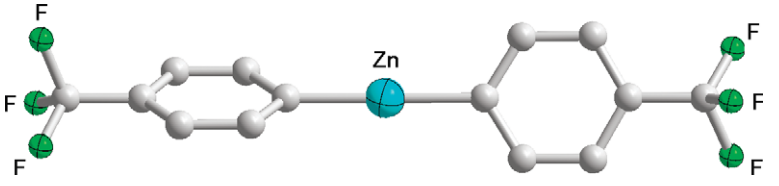

Figure 5 Solid-state structure and partial labeling scheme of $Zn(p\text{-}CF_3C_6H_4)_2$ **13** Dimesitylzinc **14** was obtained by the unconventional protonolysis of a cyclic.

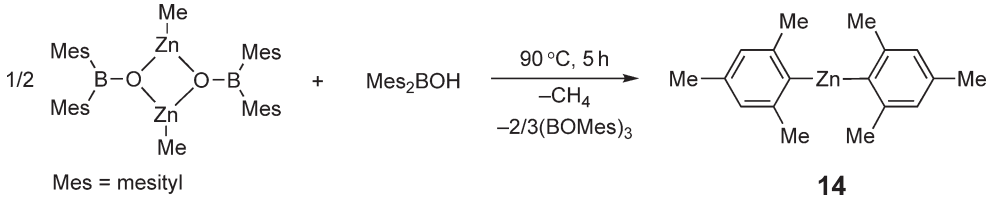

Scheme 13

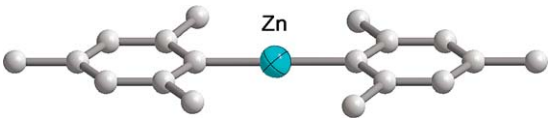

Figure 6 Solid-state structure and partial labeling scheme of $Zn\{2,4,6\text{-}(CH_3)_3C_6H_2\}_2$ **14**.

2.06.4.4 Heteroleptic Diorganozinc Compounds

Heteroleptic diorganozincs compounds, that is, compounds of the type $R–Zn–R^1$, have a tendency to exchange organic substituents and to disproportionate, unless special precautions are taken. Disproportionation can be prevented either by the incorporation of very bulky organic groups or by blocking the empty orbitals with neutral donor ligands. While heteroleptic diorganozinc compounds were for many years mainly of theoretical interest, they have become exceedingly useful in organic synthesis. The often large excess of diorganozincs necessary in organic transformations is a serious problem for reagents bearing valuable R groups. An elegant solution to this problem is the use of heteroleptic diorganozincs bearing both a readily available non-transferable ligand, such as $(Me_3Si)_3C$, and the functionalized organic group to be transferred.

Westerhausen and co-workers synthesized (Scheme 14) stable heteroleptic diorganozinc compounds by treating lithium organo(halo)zincates and organozinc halides with alkyl- or aryllithium reagents.[43] Solid-state structures of Lewis base-free heteroleptic dialkylzincs, such as **15** (Figure 7), are still relatively rare. The almost-linear (176.2(2)°) molecule has slightly asymmetric zinc–carbon bonds. As expected, the Zn–C bond to the bulkier tris(trimethylsilyl)methyl groups is somewhat longer (1.971(3) Å) than that of the bis(trimethylsilyl)methyl group (1.946(4) Å).

The bulky tris(trimethylsilyl)methyl, bis(trimethylsilyl)methyl, and trimethylsilylmethyl groups are popular non-transferable alkyl groups because their dialkylzinc derivatives show little or no tendency to disproportionate. General routes to heteroleptic dialkylzincs bearing these ligands are the alkylation of organozinc halides or, for *in situ* reactions, the comproportionation of the appropriate diorganozinc compounds. Scheme 15 shows that for diorganozinc compounds bearing the smallest of these ligands, namely $Me_3SiCH_2Zn(n\text{-Pent})$ **16**, some disproportionation of the heteroleptic dialkylzincs does occur.[24]

$$Li[\{(Me_3Si)_3C\}_2Zn_2Cl_3]_2\cdot 2THF\cdot OEt_2 + 2LiCH(SiMe_3)_2 \xrightarrow[-3LiCl,\ -Et_2O,\ -THF]{} 2(Me_3Si)_3CZnCH(SiMe_3)_2$$

15

Scheme 14

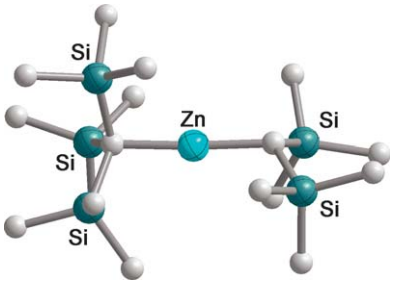

Figure 7 Solid-state structure and partial labeling scheme of $(Me_3Si)_3CZnCH(SiMe_2)_2$ **15**.

$$0.9Zn(n\text{-Pent})_2 + 0.9Zn(CH_2SiMe_3)_2 \underset{}{\overset{THF}{\rightleftharpoons}} 1.8Me_3SiCH_2Zn(n\text{-Pent})$$

16

Scheme 15

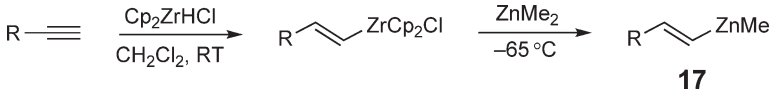

17

Scheme 16

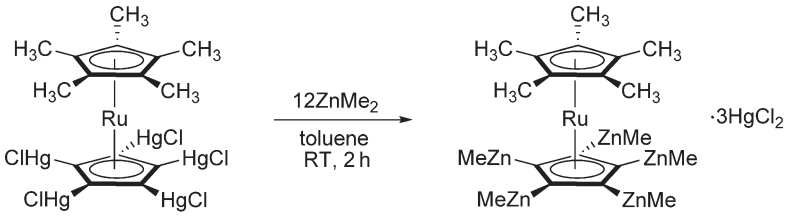

18

Scheme 17

As Scheme 16 shows, vinyl(methyl)zinc compounds **17** were obtained from the hydrozirconation of terminal alkynes with Cp_2ZrHCl, followed by treatment with dimethylzinc. The initially formed vinyl zirconium complex undergoes rapid transmetallation with $ZnMe_2$ to yield the product.[44]

An unusual series of heteroleptic diorganozinc compounds in which one of the organic groups is a ruthenocenyl moiety was reported by Seneviratne and Winter.[45] The treatment of penta(chloromercurio)pentamethylruthenocene with excess dimethylzinc gave penta(methylzinco)pentamethylruthenocene **18** (Scheme 17). Although the product, which precipitated with 3 equiv. of mercuric chloride, could not be characterized by X-ray techniques, its chemical derivatization allowed an unambiguous structure assignment. Thus, treatment of $[(Me_5C_5)Ru\{C_5(MeZn)_5\}]$ with water, iodine, or dimethylsulfide furnished $[(Me_5C_5)Ru(C_5H_5)]$, $[(Me_5C_5)Ru(C_5I_5)]$, and $[(Me_5C_5)Ru\{C_5(SMe)_5\}]$, respectively. Decakis(methylzinco)ruthenocene, synthesized in a similar manner as **18**, afforded, upon treatment with water and bromine, ruthenocene and decabromoruthenocene, respectively.

2.06.4.5 Diorganozinc Compound Bearing π-Bound Ligands

Although diorganozinc compounds with π-bound ligands were synthesized a century after the seminal work by Frankland on dialkylzincs,[1] the structural chemistry of these compounds is more mature than that of homoleptic organozinc compounds with σ-bound ligands. Organozinc compounds with π-bound ligands are limited to cyclopentadienyl rings, the most common being the bis(cyclopentadienyl)zinc compounds known as zincocenes.[46] Common to all zincocenes is their lack of a symmetrical, or metallocene, structure. Thus, the prototype zincocene, $Zn(Cp)_2$ **19**, whose solid-state structure is shown in Figure 8, is a polymeric compound, in which each zinc ion is surrounded by three η^2-bound cyclopentadienyl rings. Two of these ligands are bridging and one is terminal, and the zinc–carbon bond lengths span the wide range from 2.04(3) to 2.48(6) Å.

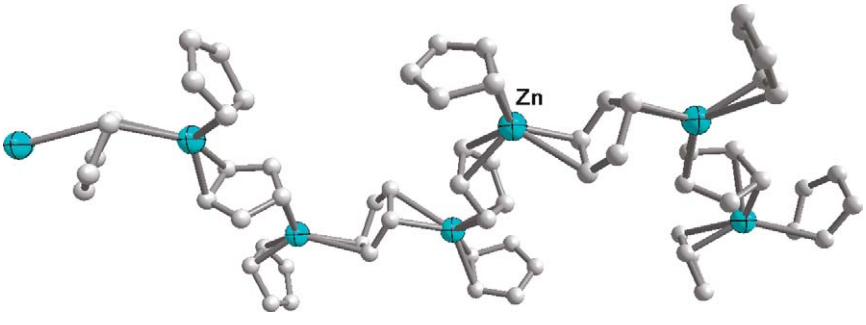

Figure 8 Solid-state structure and partial labeling scheme of a section of polymeric $Zn(C_5H_5)_2$ **19**.

Substituted zincocenes are monomeric, but even these monomeric compounds have slipped sandwich structures, featuring one η^5-and one η^1-cyclopentadienyl group. The η^5-Cp rings often exhibit a wide range of Zn–C distances, which makes a definitive assignment of their hapticity difficult. The η^1-Cp rings, in turn, show a peculiar perpendicular arrangement between the zinc–carbon bond and the cyclopentadienyl plane, which suggests that the interaction is an $\eta^1(\pi)$-bond, rather than the common $\eta^1(\sigma)$-bond in which the carbon atom is sp^3 hybridized. With its $[Ar]4s^23d^{10}$ electron configuration, zinc can only form two covalent bonds. The bonding in zincocenes is thus often intermediate between covalent and ionic with the formation of both σ- and π-bonds between metal and ligand. This mixture of σ- and π-bonding in zincocenes, which has been termed "peripheral,"[47] is not static, however, and fluxional molecules are almost always observed. Slipped sandwich structures were found in both gas-phase electron diffraction studies and solid-state X-ray studies of decamethylzincocene $Zn(C_5Me_5)_2$[48,49] and of the phenyl-substituted analog $Zn(C_5Me_4Ph)_2$ **20**, whose structure is shown in Figure 9.

Bis[(tris(isopropyl)cyclopentadienyl)]zinc ($Zn\{C_5(Pr^i)_3H_2\}_2$, **21**) and bis[(tetrakis(isopropyl)cyclopentadienyl)]zinc ($Zn\{C_5(Pr^i)_4H\}_2$, **22**) were synthesized from the respective potassium cyclopentadienides and zinc iodide as shown in Scheme 18.[50] The same slipped sandwich compounds were also isolated from zinc-reduced VCl_3 solutions when they were treated with these alkali metal cyclopentadienides at room temperature.[51] The outcomes of these reactions suggest that zincocenes are likely intermediates in the syntheses of transition metal metallocenes, in which the metal halides have been pre-reduced with zinc. The solid-state structure of $Zn\{C_5(Pr^i)_4H\}_2$ is shown in Figure 10. The sole

Figure 9 Solid-state structure and partial labeling scheme of $Zn(C_5Me_4Ph)_2$ **20**.

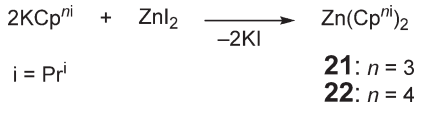

Scheme 18

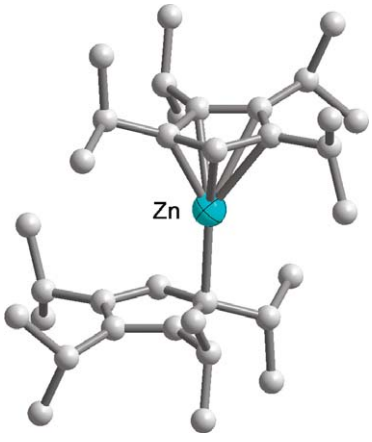

Figure 10 Solid-state structure and partial labeling scheme of $Zn\{C_5(Pr^i)_4H)\}_2$ **22**.

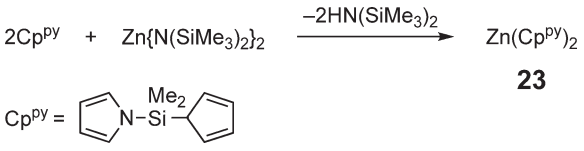

Scheme 19

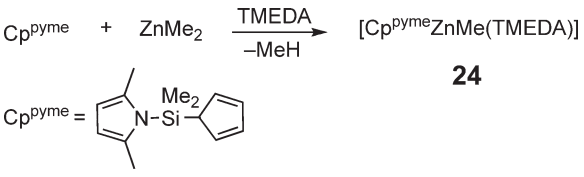

Scheme 20

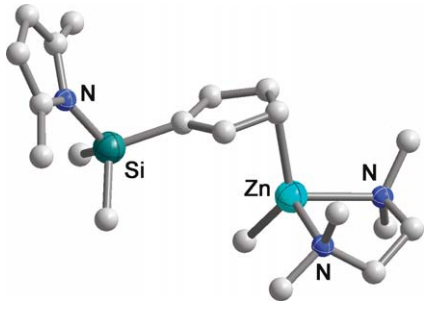

Figure 11 Solid-state structure and partial labeling scheme of **24**.

Zn–C bond of the monohapto ring is 2.223(4) Å long, while the zinc–carbon bonds of the η^5-bound Cp ring span the wide range 1.991(4)–2.514(3) Å. The short contact is the shortest Zn–C bond yet observed for a π-bound ring, while the long contact is barely a bond at all. The asymmetry of **22** is maintained in solution.

The reaction of 2 equiv. of a pyrrole-substituted cyclopentadiene with $Zn[N(SiMe_3)_2]_2$ (Scheme 19) afforded the dicyclopentadienylzinc complex **23**.[52] A solid-state structure of this compound was not obtained, but room-temperature ^{1}H NMR spectroscopic studies showed two equivalent cyclopentadienyl groups, whose signals broadened on cooling.

Dimethyl- and diethylzinc reacted with dimethylpyrrole- and mesityl-substituted cyclopentadiene ligands to give monocyclopentadienyl(methyl)zinc and -ethyl(zinc) compounds. These products then formed, Scheme 20, crystalline adducts with tetramethylethylenediamine (TMEDA) such as **24**, whose solid-state structure is shown in Figure 11.

The zinc atom is pseudo-tetrahedrally surrounded by the cyclopentadienyl and methyl groups and the chelating TMEDA ligand, while the dimethylpyrrole pendant is not coordinated to the metal. The zinc–methyl bond (1.985(2) Å) and the $\eta^1(\pi)$-bound cyclopentadienyl ligand (2.185(2) Å) are both slightly elongated, possibly due to the steric crowding about zinc.

2.06.4.6 Chemical and Physical Properties of Diorganozinc Compounds

Diorganozinc compounds are colorless liquids or low-melting solids that are very soluble in all conventional organic solvents. Although diorganozinc compounds, with few exceptions, are monomeric in solution, short-lived dimeric species, similar to **10**, must be present in solution, because of the exchange of organic substituents in heteroleptic diorganozinc compounds. Diorganozinc compounds are more reactive than organozinc halides, but less reactive than tri- and tetraorganozincates. They are readily hydrolyzed by water, with the formation of zinc hydroxide

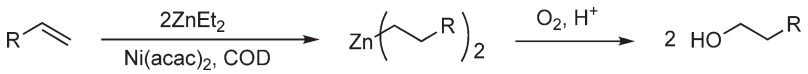

Scheme 21

and the corresponding organic groups. The lower dialkylzincs, especially dimethylzinc and diethylzinc, react vigorously and sometimes explosively with oxygen.

The reactivity of diorganozincs with oxygen can be exploited for the synthesis of alcohols. Like many main-group alkyls, dialkylzincs react with oxygen with the initial formation of alkyl peroxides (Zn–O–O–R) which then interact with an additional equivalent of dialkylzinc to produce zinc alkoxides.[53] Hydrolysis of these alkoxides gives the corresponding alcohols in good yields. In general, however, this is not an efficient synthetic route to alcohols because the metal alkyls are normally made from alkyl halides, which in turn are derived from the alcohols. For organozinc compounds synthesized from alkenes, however, such as the hydrozincation shown in Scheme 21, the alcohols are useful products.

2.06.4.7 Structural Studies of Diorganozinc Compounds Bearing σ-Bound Ligands

Although simple diorganozinc compounds with σ-bound ligands constitute the oldest class of organozinc compounds, prior to 1990, the only solid-state structural information on such species was the citation of a single crystal X-ray analysis of $ZnEt_2$, with a Zn–C bond length of 1.923 Å.[54] Full X-ray structural data on diorganozinc compounds were not available until 1990, when Markies *et al*. reported the solid-state structure of diphenylzinc.[37]

The geometry of the C–Zn–C backbone and the Zn–C bond lengths of $ZnMe_2$ (1.929(4) Å) had been determined by rotational Raman spectroscopy in 1960.[55] PES and *ab initio* studies on $ZnMe_2$ appeared in 1977 and a gas-phase electron diffraction (GED) study of $ZnMe_2$, $ZnEt_2$, and $Zn(Pr^n)_2$ was published in 1982.[56] *Ab initio* MO calculations reproduced the structural parameters of $ZnMe_2$ well and suggested that the Zn–C bonds are pure σ-bonds and that the *d*-orbitals of zinc are not significantly involved in the bonding.

The past decade has seen an increase in the number of physical and computational studies on the structures and thermodynamics of diorganozinc compounds. Equilibrium geometries of $ZnMe_2$ and $ZnPh_2$ (MP2/I) and their bond dissociation energies (MP2) have been calculated.[57] For $ZnMe_2$ and $ZnPh_2$, these investigations yielded Zn–C bond lengths of 1.925 and 1.914 Å, respectively, in very good agreement with experimental data. These calculations also predicted monomeric $ZnPh_2$ to have D_{2d} symmetry with orthogonal phenyl rings, as is typically found for the solid-state structures of many of the diarylzinc compounds that have since been characterized. The natural bond orbital (NBO) analysis of $ZnMe_2$ and $ZnPh_2$ suggests that the fairly ionic Zn–C bonds have a formal bond order of 1/2.

An extensive study involving gas electron diffraction (GED), PES, and density-functional calculations (DFT) of seven homoleptic dialkyzinc compounds has greatly increased the available structural and thermodynamic parameters on these compounds.[58] The calculated and experimentally determined bond lengths, molecular symmetries, enthalpies of formation, mean Zn–C bond rupture enthalpies of $ZnMe_2$, $ZnEt_2$, $Zn(Pr^i)_2$, $Zn(Pr^n)_2$, $Zn(Bu^t)_2$, Zn(*neo*-Pent)$_2$, and $Zn(Me_3SiCH_2)_2$ are collected in Tables 2 and 3. Because non-bonded ligand–ligand interactions are negligible in these two-coordinate compounds, the geometric and thermodynamic differences can be attributed entirely to electronic factors.

Table 2 Structural data of selected dialkylzinc compounds from gas electron diffraction (GED) and computational (DFT) studies

Compound	*Symmetry*	*GED(Zn–C)* (Å)	*C–Zn–C* (°)	*Symmetry*	*DFT(Zn–C)* (Å)	*C–Zn–C* (°)
$ZnMe_2$	D_3	1.930(2)[56]	180.0	D_3	1.945[58]	180.0
$ZnEt_2$	C_2	1.950(2)[56]	180.0	C_2	1.960[58]	180.0
$Zn(Pr^n)_2$	C_2	1.952(3)[56]	180.0	C_2	1.960[58]	180.0
$Zn(Pr^i)_2$	C_2	1.961(3)[58]	178.0(7)	C_2	1.975[58]	179.9
$Zn(Bu^t)_2$	D_3	1.974(3)[58]	180.0	D_3	1.988[58]	180.0
Zn(*neo*-Pent)$_2$	C_2	1.960(3)[58]	180(2)	C_2	1.963[58]	179.4
$Zn(CH_2SiMe_3)_2$	C_2	1.935(6)[58]	172(4)	C_2	1.948[58]	179.9

Table 3 Selected thermodynamic data of some diorganozinc compounds

Compound	*Experimental* ΔH_f° (kJ mol^{-1})	*Estimated* ΔH_f° (kJ mol^{-1})	*Estimated mean Zn–C bond rupture enthalpies* (kJ mol^{-1})
$ZnMe_2$	53(1)[439]		186(2)
$ZnEt_2$	56(4)[439]	57(8)[58]	157(4), 156(8)[58]
$Zn(Pr^n)_2$	17(23)[439]	10(8)[58]	157(12), 159(8)[58]
$Zn(Pr^i)_2$		32(8)[58]	132(8)
$Zn(Bu^t)_2$		−17(8)[58]	116(8)
Zn(*neo*-Pent)$_2$	−123(17)[440]	−117(8)[58]	157(17)[440], 162(8)[58]
$Zn(CH_2SiMe_3)_2$	−355(21)[440]	−306(8)[58]	195(21)[440], 179(8)[58]

From Table 2, it may be seen that the experimentally determined metal–ligand bonds of dialkylzinc compounds fall into the relatively narrow range of 1.930(3)–1.974(3) Å. The zinc–carbon bonds, which increase linearly with the number of methyl groups on the α-carbon, have the following order: $ZnMe_2 \approx Zn(CH_2SiMe_3)_2 < ZnEt_2 \approx Zn(Pr^n)_2 \approx Zn(neo\text{-Pent})_2 < Zn(Pr^i)_2 < Zn(Bu^t)_2$. Substituents on the β-carbon obviously have a much smaller effect on bond length than those on the α-carbon, and replacing a β-carbon with a silicon atom shortens the zinc–carbon bond.

Experimental and estimated thermodynamic data of homoleptic dialkylzinc compounds are listed in Table 3. Like many organometallic compounds, the lower dialkylzincs have a positive enthalpy of formation, and only the incorporation of silicon atoms in the β-position imparts significant thermodynamic stability. The mean Zn–C bond rupture enthalpies, all of which are quite low, follow a similar trend as the bond lengths in these compounds. Thus, the presence of methyl substituents in the α-position weakens the zinc–carbon bonds, while silyl substituents strengthen them.

2.06.4.8 Structural Studies of Diorganozinc Compounds Bearing π-Bound Ligands

Table 4 lists zinc–carbon bond lengths for selected zincocenes, as determined by GED and X-ray crystallography. With the exception of bis(cyclopentadienyl)zinc, which is polymeric, all compounds are monomers and have slipped sandwich structures. The zinc–carbon bonds of the η^1-cyclopentadienyl ligands, which span the comparatively narrow range of 2.04(6)–2.094(3) Å, are ca. 0.1 Å longer than those of zinc–alkyl bonds. Not unexpectedly, the zinc–carbon bonds of the η^5-bound cyclopentadienyl ligands span a wide range (2.0 to 2.5 Å), the upper limit being somewhat subjective; here, the authors have chosen a contact of 2.5 Å as a cutoff for a proper bond.

Because of their unusual structure and bonding, the spectroscopic and physical properties of zincocenes remain a topic of active investigation. Solid- and solution-phase IR- and Raman-spectroscopic studies were used to probe the bonding in $ZnCp_2$ at ambient and low (20 K) temperatures. Based on the well-separated ligand-centered and metal–ligand vibrations, a slipped sandwich structure was proposed. Crystals of zincocene undergo a phase transition on cooling to 20 K.[59]

Ab initio (HF) calculations and second-order many-body perturbation theory (MBPT(2)) were used to obtain information on the structures and energies of ZnCp and $ZnCp_2$.[60] In the ground state of ZnCp, the unpaired electron resides in an *s*-like orbital on zinc, and the bonding is essentially that of a Zn^+ ion coordinated to a cyclopentadienide ligand. The dissociation energy of ZnCp to Zn and Cp was calculated to be 158.6 and 132.2 kJ mol^{-1}, using MBPT(2) and spin-projected MBPT(2), respectively, while the corresponding values for the dissociation of $ZnCp_2$ to ZnCp and Zn were 296.2 and 266.9 kJ mol^{-1}, respectively.

Table 4 Structure types and Zn–C bond lengths of some homoleptic zincocenes

Compound	*Structure type*	*Zn–C bond length* η^1*-Cp* (Å)	*Zn–C bond lengths* η^5*-Cp* (Å)	*References*
$Zn(C_5Me_5)_2$	slipped sandwich	disordered, X-ray	disordered	48
$Zn(C_5Me_5)_2$	slipped sandwich	2.04(6) GED	2.28(2)	441
$Zn(C_5H_4SiMe_3)_2$	slipped sandwich	2.07(10) GED	2.26(3)	441
$Zn(C_5Me_4Ph)_2$	slipped sandwich	2.094(3) X-ray	2.093(3)–2.299(3)	48
$Zn[C_5(Pr^i)_4H]_2$	slipped sandwich	2.055(3) X-ray	1.991(4)–2.514(3)	50
$Zn(C_5H_5)_2$	polymer, three η^2–Cp ligands per Zn		2.04(3)–2.48(6)	46

2.06.4.9 Diorganozinc Compounds as Alkylating Agents

Diorganozinc compounds are selective alkylating agents for the synthesis of alkyl- or aryl-substituted transition metal compounds. This selectivity is partially due to the fact that only one of the two organic groups is transferred, leading to the formation of organozinc halides, which are even less reactive than the diorganozinc compounds themselves. Overalkylation is thus rarely a problem, and group 5 metal halides, in particular, have been successfully monoalkylated with diorganozinc compounds.

The relatively low reactivity of diorganozinc compounds is demonstrated by the fact that even the addition of 2 or 3 equiv. of $ZnPh_2$ to $[NbCl_2\{N(SiMe_3)_2\}_2]$ gave only the monophenyl product $[NbCl\{N(SiMe_3)_2\}_2Ph]$.[61]

Fox *et al.* dialkylated a tantalum(aryloxo)(amido) trichloride with 2 equiv. diethylzinc to furnish the corresponding diethyltantalum complex **25**, as shown in Scheme 22.[62]

Even the addition of 4 equiv. of dimethylzinc to a bis(dicarbollide)tantalum dichloride, Scheme 23, produced only the monomethyl complex **26** in an isolated yield of 75%.[63] In these reactions, the oxidation state of the transition metal and the steric bulk of its ligands obviously play a role in the degree of alkylation.

2.06.4.10 Well-defined Diorganozinc Compounds in Polyolefin Catalysis

Zinc compounds have recently been used as pre-catalysts for the polymerization of lactides and the co-polymerization of epoxides and carbon dioxide (see Sections 2.06.8–2.06.12). The active catalysts in these reactions are not organozinc compounds, but their protonolyzed products. A few well-defined organozinc compounds, however, have been used as co-catalysts and chain-transfer reagents in the transition metal-catalyzed polymerization of olefins.

The addition of a large excess of bis(ω-alkenyl)zinc compounds to the $TiCl_3$-catalyzed polymerization of propene resulted in an increased polymer yield, but a reduction in the molecular weights of the polymers.[64] This suggests that the diorganozinc compounds are both co-catalysts and chain-transfer agents in this polymerization. The catalyst activity decreased in the order bis(3-butenyl)zinc < bis(7-octenyl)zinc < chlorodiethylaluminum. Bis(7-octenyl)zinc was co-polymerized with propene to afford hexylzinc side chains, whose zinc–carbon moieties were converted to vinyl groups by the addition of allyl bromide.

The transition metal-catalyzed polymerization of olefins yields high molecular weight polymers as the result of the successive insertion of monomer into the metal–carbon bond of the growing polymer chain. This chain growth is

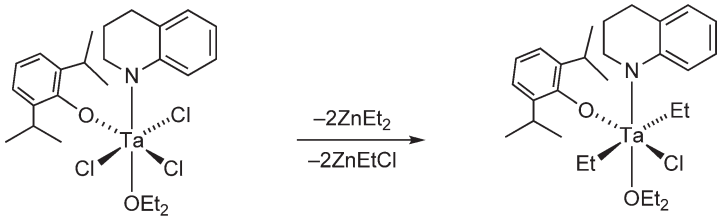

25

Scheme 22

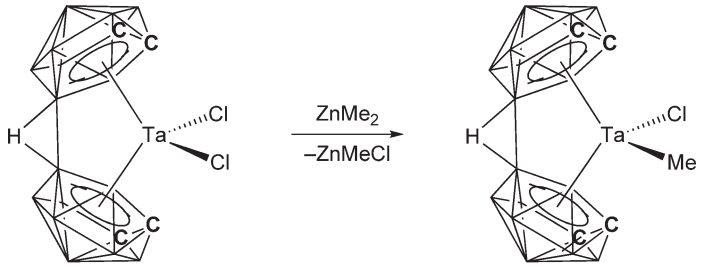

26

Scheme 23

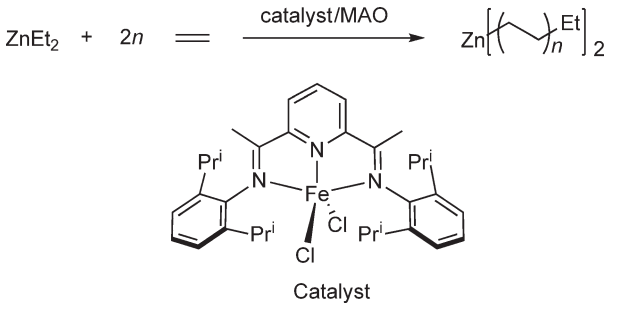

Scheme 24

limited by chain-transfer processes, one of which is the chain transfer to the $AlMe_3$ present in the MAO co-catalyst. Gibson and co-workers reported the first case of a chain transfer to diethylzinc in the bis(imino)pyridineiron-catalyzed polymerization of ethene. Addition of 500 equiv. of $ZnEt_2$ to the catalytic system, Scheme 24, caused a significant reduction in the molecular weight from ca. 192,000 to 800, accompanied by a substantially decreased polydispersity from 19.2 to 1.1.[65,66] These observations led the authors to conclude that the long-chain dialkylzinc compounds were formed by the iron-catalyzed chain growth on zinc. After hydrolysis or chain displacement from zinc by $Ni(acac)_2$ linear alkanes or α-olefins, respectively, were obtained, which exhibited the technologically-desirable Poisson distribution.

2.06.5 Organozinc Halides

2.06.5.1 Introduction

Organozinc halides share with diorganozinc compounds the distinction of being the oldest organozinc compounds. While organozinc halides were for many years limited to iodides, the discoveries of various forms of activated zinc and the introduction of homogeneous routes have now made most organozinc bromides, and even organozinc chlorides accessible. Their comparatively low reactivity once limited the use of organozinc halides in organic synthesis, but transition metal catalysts have greatly expanded the scope of these reagents.

Most organic halides, with the exception of organic fluorides, can be converted to the corresponding organozinc halides by one of the following methods:

- oxidative addition of an organic halide to activated zinc,
- reaction of a zinc halide with organolithium or Grignard reagents,
- comproportionation of a diorganozinc compound and a zinc dihalide, and/or
- TM-catalyzed reaction between a diorganozinc or organozinc halide and an organic halide.

2.06.5.2 Organozinc Halides by the Oxidative Addition of Organohalides to Zinc

Metallic zinc is typically covered with a zinc oxide layer that must be removed before the metal can engage in an oxidative addition reaction with organic halides. This activation can be done in one of several ways.

Zinc/copper couple (Zn/Cu), produced by the treatment of zinc with HCl, followed by the addition of copper(II) sulfate, has been known since the seminal work of Simmons and Smith.[67] A less reactive form of activated zinc, but one that is sufficiently active for most applications, is produced by the treatment of the metal with 1,2-dibromoethane, followed by Me_3SiCl.[68] The most reactive form of activated zinc, the so-called Rieke zinc (Zn^*), is finely divided metallic zinc produced by the homogenous reduction of zinc halides in THF.[69]

It was also Guijarro and Rieke who investigated the rates and mechanisms of organic bromides with Rieke zinc.[70,71] They discovered that the oxidative addition of the organic bromide to zinc proceeds by a one-electron transfer as the rate-limiting step. The rate of the reaction, which is first order in organic bromide, shows a strong dependence on the structure of the organic bromide. The relative rates of these substrates span approximately five orders of magnitude, with the reactivity trend being allyl, benzyl > tertiary > secondary > primary > aryl > vinyl. This rate dependence on the organic structure can be used to selectively insert zinc into only one of the several

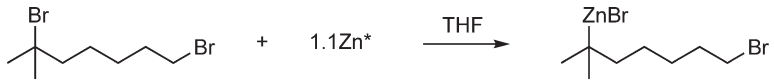

27

Scheme 25

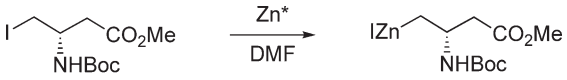

28

Scheme 26

carbon–bromine bonds. Thus, 1,6-dibromo-6-methylheptane reacted with 1.1 equiv. of Rieke zinc (Scheme 25) with the oxidative addition of the tertiary, but not the primary, carbon–bromine bond to zinc.

In a related study, Rieke and Guijarro studied the configurational stability of the zinc–carbon bond in 2-butylzinc bromide and (1-phenylprop-2-yl)zinc bromide, using a bis(oxazoline) as a chiral resolving agent.[72] From their data, the authors determined the $\Delta G^{\ddagger}$ of inversion at the secondary carbon of (1-phenylprop-2-yl)zinc bromide to be 113.8 kJ mol^{-1}.

The general utility of the oxidative addition of functionalized organic halides to zinc was demonstrated by the formation of organozinc iodides **28** from protected β- and γ-amino acids (Scheme 26).[73] The organozinc iodides prepared in this manner were neither sufficiently stable nor sufficiently reactive in THF, but excellent yields were obtained in more polar aprotic solvents, such as DMF and DMSO.

2.06.5.3 Organozinc Halides by Transmetallations

The combination of equimolar amounts of tris(trimethylsilyl)methyllithium and zinc bromide in a THF/diethyl ether mixture, Scheme 27, furnished tris(trimethylsilyl)methylzinc bromide, as a lithium bromide/ether adduct.[43] The compound, which may also be formulated as a lithium alkyldibromozincate, showed no ligand redistribution reactions. It is monomeric in solution and can be treated with 1 equiv. of an organolithium reagent to afford heteroleptic diorganozinc compounds.

2.06.5.4 Organozinc Halides by Transition Metal-catalyzed Reactions

Nickel and palladium complexes catalyze the conversion of alkyl iodides to alkylzinc iodides **30** with added diethylzinc (Scheme 28).[74] Thus, for example, 1-iodooctane was converted at room temperature to *n*-octylzinc iodide after treatment with 2 equiv. of diethylzinc in the presence of 1.5 mol% of a palladium bis(phosphine) complex.

A nickel-catalyzed conversion of primary alkyl iodides in neat diethylzinc, Scheme 29, was reported by Vettel *et al.*[33] Although many nickel(II) complexes are suitable catalysts for this reaction, the best results were obtained with

29

Scheme 27

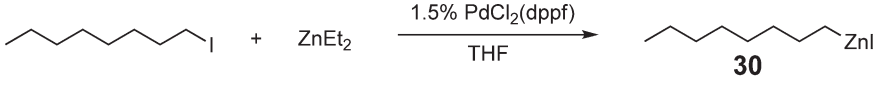

30

dppf = 1,1′-bis(diphenylphosphino)-ferrocene

Scheme 28

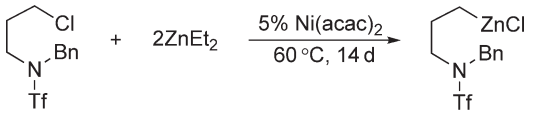

31

Scheme 29

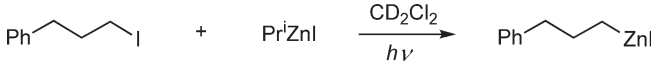

32

Scheme 30

$Ni(acac)_2$ at 55 °C. Primary alkyl chlorides also undergo this reaction, but at much lower rates than iodides, the reaction taking days rather than hours.

Charette *et al.* converted both primary and secondary alkyl iodides to the corresponding alkylzinc iodides, using either ethylzinc iodide or isopropylzinc iodide.[34] The reactions, for example, Scheme 30, which were performed in UV-irradiated ($\lambda \geq 280$ nm) chloroform solutions, gave conversions as high as 88% in less than 4 h.

2.06.5.5 Neutral Adducts of Organozinc Halides

Unless they bear very bulky substituents, organozinc halides exist in solution and the solid state as dimers, trimers, and higher aggregates (see COMC (1982), Section 16.1.3.3). Ethylzinc chloride was isolated in monomeric form, as its TMEDA adduct, from an ill-defined transformation involving an organoantimony dichloride compound and diethylzinc in the presence of TMEDA (see Scheme 9).[36] The solid-state structure of this pseudo-tetrahedral organozinc compound is shown in Figure 12. The molecule has crystallographic *m*-symmetry, the mirror plane passing through the zinc and chlorine atoms and the ethyl group. The Zn–Cl (2.270(3) Å) and Zn–Et (1.942(13) Å) bonds have normal lengths.

2.06.6 Neutral Adducts of Diorganozinc Compounds

2.06.6.1 Introduction

Diorganozinc compounds are not very Lewis acidic and do not stongly bind monodentate, neutral group 16 donor ligands. Ether adducts of ZnR_2, for example, are fluxional in solution, and their NMR spectra show averaged signals of free and coordinated diorganozinc species.

Neutral adducts of diorganozinc compounds are important precursors in MOCVD applications, where the Lewis bases may either serve as purifying agents and/or as reagents. Lewis base adducts of diorganozincs, especially those having chiral ancillary ligands, are becoming increasingly important in catalysis. With some donor ligands, diazabutadienes being the most important, diorganozinc compounds are non-innocent and ultimately form organozinc amides and as such are covered in Section 2.06.10.7.

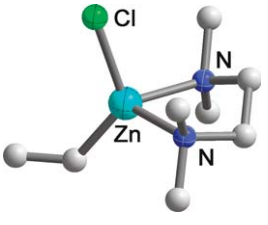

Figure 12 Solid-state structure and partial labeling scheme of [EtZnCl(TMEDA)].

2.06.6.2 Diorganozinc Compounds Bearing Monodentate Donor Ligands

Group 12/16 compounds are semi-conductors that can be deposited as thin films by MOCVD. Dimethylzinc, for example, reacts with hydrogen sulfide and hydrogen selenide to produce zinc sulfide and zinc selenide, respectively. To gain a better understanding of the adducts that precede the protonolysis of $ZnMe_2$ by group 15 and group 16 element hydrides, dimethylzinc was co-deposited with NH_3, PH_3, AsH_3, H_2O, H_2S, and H_2Se in an argon matrix.[75] The antisymmetric IR stretch of $ZnMe_2$ appears as a triplet at 614.3, 616.7, and 619.6 cm^{-1} as the result of the three major isotopes of zinc, which correlates well with the vapor-phase band at 613 cm^{-1}. Adduct formation was indicated most strongly by the antisymmetric Me–Zn–Me stretch which shifted by 8 to 34 cm^{-1}, correlating well with both the proton affinities of the hydrides and adduct strengths. For some of the non-metal hydrides both 1 : 1 and 1 : 2 adducts were observed, with ammonia being shown to interact most strongly with dimethylzinc.

The molecular structure and binding energies of the hypothetical dimethylzinc–hydrogen selenide adduct ($Me_2Zn{\cdot}SeH_2$) were studied with *ab initio* and DFT methods.[76] Both molecules showed minimal perturbations upon adduct formation, in agreement with a very weak binding energy of ca. −13 kJ mol^{-1} (B3LYP/6-311+G(2*d*,*p*) level) at room temperature, suggesting that the monoadduct is unlikely to be a stable gas-phase species. A potential di-adduct, $Me_2Zn{\cdot}(SeH_2)_2$, is even less stable (by ca. 80 kJ mol^{-1}) with respect to the precursors.

Cyclic thioethers $S(CH_2)_n$, $n = 3$, 4, form 1 : 1 adducts with diphenylzinc that have similar dimeric structures as diphenylzinc,[77] as shown for $[Ph_2ZnS(CH_2)_4]_2$ in Figure 13. The zinc–sulfur bond is quite long, 2.5025(5) Å, and the bridging phenyl groups form two decidedly unsymmetrical Zn–C bonds (2.114(2) and 2.261(2) Å), which are substantially longer than the bonds to the terminal phenyl groups (1.983(2) Å).

Dialkylzinc compounds have a tendency to form colored, and sometimes paramagnetic, adducts with π-acceptor ligands. The potentially bridging nitrogen donor pyrazine (and 4,4′-bipyridine) formed dinuclear complexes, Scheme 31, while the chelating 2,2′- bipyridine formed mononuclear adducts with diisopropylzinc.[78] In the bis(diisopropylzinc)·pyrazine adduct **33**, the presence of an unpaired electron was detected, but the resolution of the ESR spectra was insufficient for an unambiguous structural assignment.

Diethylzinc forms a colorless monoadduct with 1,4-diazabicyclo[2,2,2]octane (dabco) **34** and an orange-colored bis-adduct with acridine.[79] The mono-dabco adduct, Figure 14, crystallizes in the form of infinite zigzag chains, in which each diethylzinc moiety bridges two dabco units. The coordination environment about zinc is distorted tetrahedral, with Zn–C and Zn–N bonds ranging from 1.93(3) to 2.10(2) Å and from 2.24(2) to 2.37(2) Å, respectively.

The sequential treatment of tris(*tert*-butylimido)sulfonate with methyllithium and dimethylzinc (Scheme 32) produced an unusual dimethylzinc adduct of lithium-*S*-methyl-tri(*tert*-butylimido)sulfonate **35**, shown in Figure 15.[80] Here, two imido–nitrogen atoms chelate the lithium ion, while the third one functions as a neutral

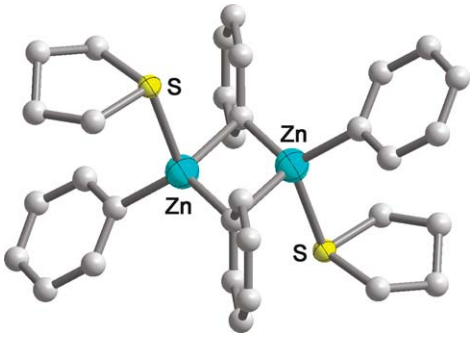

Figure 13 Solid-state structure and partial labeling scheme of $[Ph_2ZnS(CH_2)_4]_2$.

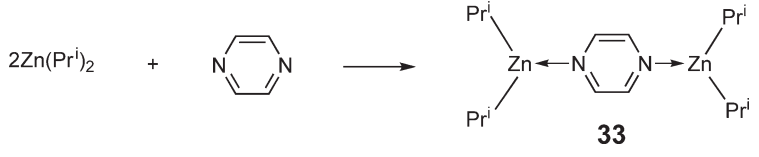

33

Scheme 31

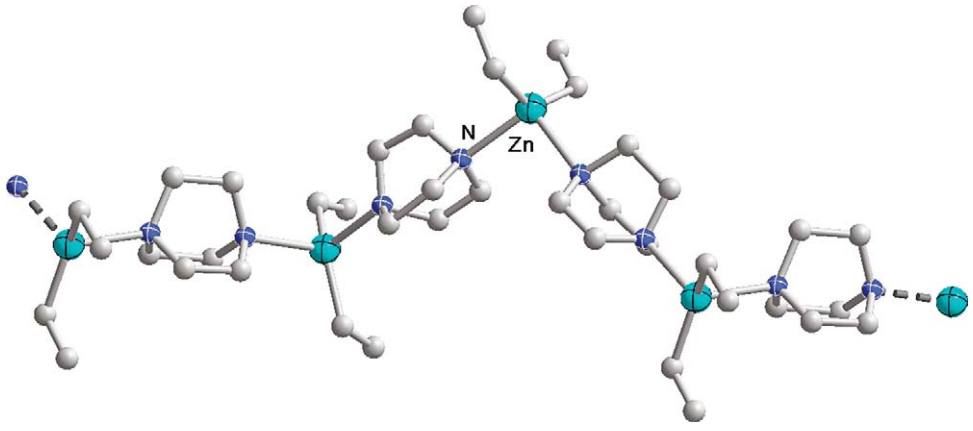

Figure 14 Solid-state structure and partial labeling scheme of polymeric [Et_2Zn(dabco)] **34**.

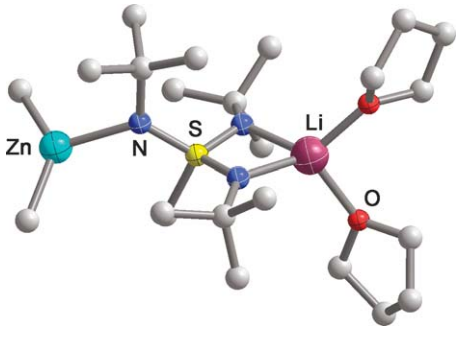

Figure 15 Solid-state structure and partial labeling scheme of [$(THF)_2$Li{$NBu^t)_3$SMe}$ZnMe_2$] **35**.

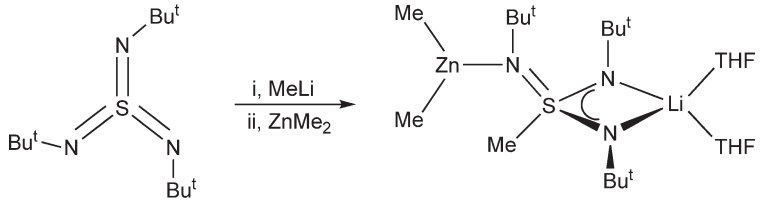

35

Scheme 32

donor to a dimethylzinc moiety. The N–Zn donor bond (2.1374(17) Å) of the sp^2-hybridized nitrogen atom is shorter than those in diorganozinc adducts with aliphatic bidentate nitrogen donors, such as **37**.

2.06.6.3 Diorganozinc Compounds Bearing Bidentate Donor Ligands

The single crystal X-ray structures of the simple adducts Et_2Zn(TMEDA) and Me_2Zn(2,2′-bipy) were reported.[36,81] The zinc–carbon (2.17(2) Å) and zinc–nitrogen (2.294(5) Å) bonds of Et_2Zn(TMEDA) are substantially longer than those of Me_2Zn(2,2′-bipy), which are 2.056(5) and 2.116(9) Å long, respectively.

Westerhausen and co-workers developed synthetic routes for heteroleptic diorganozinc compounds that rely on either the steric bulk of the organic substituents or on Lewis basicity to prevent disproportionation.[82,83] The chelating TMEDA prevented even heteroleptic diorganozinc compounds bearing small methyl groups from disproportionating (Scheme 33).

$$[(TMEDA)Zn(Cl)CH(SiMe_3)Ph] + MeLi \xrightarrow[-LiCl]{} [(TMEDA)Zn(CH_3)CH(SiMe_3)Ph]$$

36

Scheme 33

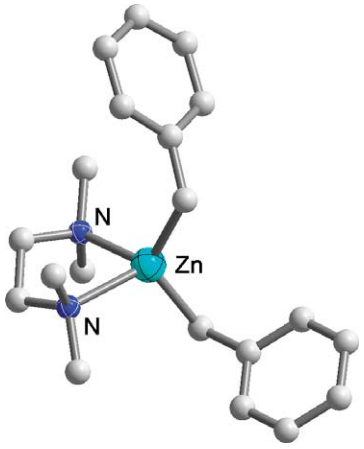

Figure 16 Solid-state structure and partial labeling scheme of $[(C_6H_5CH_2)_2Zn(TMEDA)]$ **37**.

The authors observed a linear relationship between the C–Zn–C bond angles and Zn–N bond lengths of these neutral donor adducts of diorganozincs. The larger the C–Zn–C bond angle, the longer the zinc–nitrogen bond, and this trend is essentially independent of the electronic and steric properties of the organic groups.

The reactions of a benzylzinc chloride TMEDA adduct with either benzyllithium or benzyl(trimethylsilyl)lithium TMEDA adduct yielded both homoleptic dibenzylzinc (**37**, Figure 16) and heteroleptic monobenzylzinc compounds as TMEDA adducts. The heteroleptic diorganozinc compounds do not disproportionate as long as TMEDA is present, but removal of the chelating nitrogen ligand in the gas phase does cause disproportionation.

Although tertiary amine adducts of dialkylzincs are used extensively in MOCVD applications, structural data on such adducts are still relatively rare. The combination of dimethylzinc with the polynitrogen macrocycles 1,4,8,11-tetramethyl-1,4,8,11-tetraazacyclotetradecane and 1,4,7,10,13,16-hexamethyl-1,4,7,10,13,16-hexaazacyclooctadecane afforded the corresponding bis(dimethylzinc) adducts as colorless, crystalline solids.[84] The solid-state structure of the centrosymmetric dimethylzinc adduct of hexaazacyclooctadecane **38** shows (Figure 17) that the coordination environment about zinc is distorted tetrahedral, with bond angles that range from about 80° to 138°. The zinc–nitrogen and zinc–carbon bonds are much more constant, however, ranging from 2.282(3) to 2.331(2) Å and from 2.000(3) to 2.032(6) Å, respectively. In contrast to the sparteine adduct of dimethylzinc, both complexes liberate dimethylzinc when heated to 90–120 °C *in vacuo*.

Non-luminescent, octahedral Ru(II) complexes bearing two 4,4′-di(*tert*-butyl)bipyridine and one bibenzimidazole ligand become luminescent upon coordination of diethylzinc to the bibenzimidazole **39**, as shown in Scheme 34.[85]

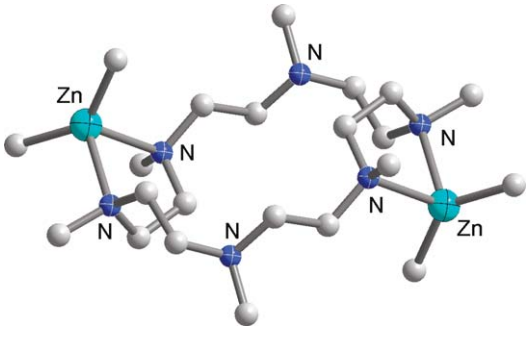

Figure 17 Solid-state structure and partial labeling scheme of the di-adduct $[(Me_2Zn)_2(MeN)_6(C_2H_4)_6]$ **38**.

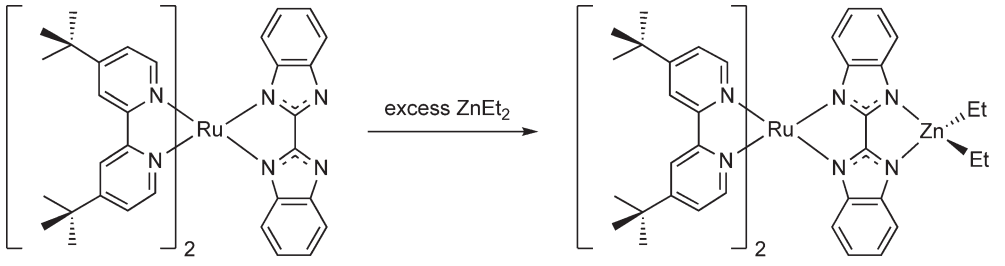

39

Scheme 34

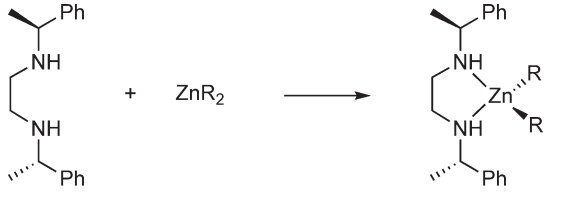

40: R = Me
41: R = Et

Scheme 35

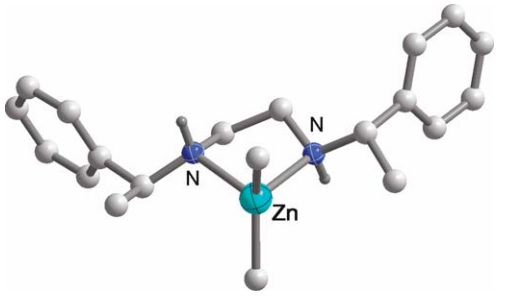

Figure 18 Solid-state structure and partial labeling scheme of [Me_2Zn·(*S*,*S*)-ebpe] **40**.

Wave length and intensity of the emission depend on the concentration and the ligands of the coordinated zinc species. The authors suggest that a reverse influence, namely the tuning of the zinc–ethyl bond by the ruthenium complex, may also be possible.

Acetophenone was reduced enantioselectively in yields of over 90% and with enantiomeric excesses (ee's) of up to 88% by poly(methylhydrosiloxane) in the presence of catalytic amounts of chiral dialkylzinc complexes. The reactions are ligand accelerated, because the chiral ligands (*S*,*S*)- (or *R*,*R*)-*N*,*N*′-ethylenebis(1-phenylethylamine), synthesized as shown in Scheme 35 and here abbreviated as (*S*,*S*)-ebpe and (*R*,*R*)-ebpe, are present in sub-stoichiometric quantities with respect to the dialkylzinc catalysts.[86] The solid-state structure of the C_2-symmetric Me_2Zn·(*S*,*S*)-ebpe **40**, which is shown in Figure 18, revealed slightly elongated zinc–carbon bonds (2.007(4) Å) and zinc–nitrogen (2.230(3) Å) donor bonds.

2.06.6.4 Crown Ether Clathrates of Diorganozinc Compounds

In the late 1980s, the groups of Richey and Bickelhaupt reported rotaxanes in which linear diorganozinc compounds appear to have been threaded though the "holes" of crown ethers.[87,88] Single crystal X-ray analyses proved that these

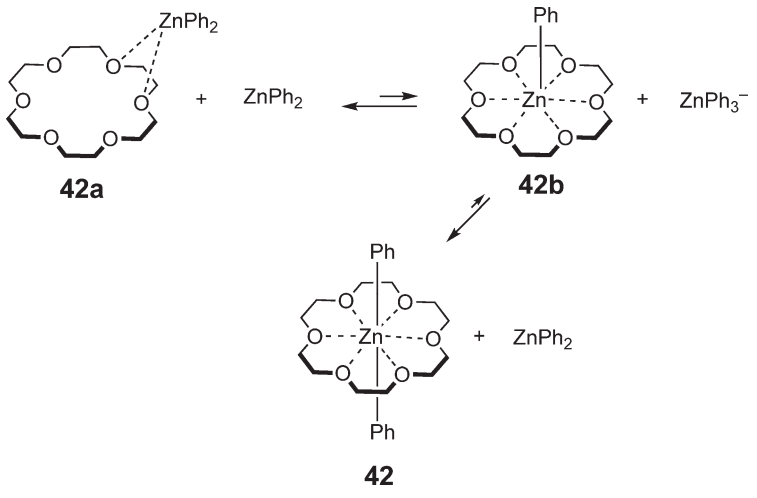

Scheme 36

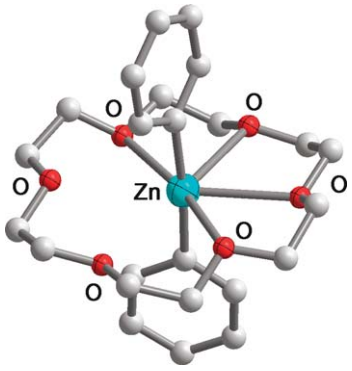

Figure 19 Solid-state structure and partial labeling scheme of Ph_2Zn(18-crown-6) **42**.

compounds are rotaxanes in the solid state, and the very simple NMR spectra of these compounds suggested that these symmetric structures also persist in solution.

The mechanism of rotaxane formation is still under investigation, since these molecules cannot be formed by the simple passage of the linear molecule through the hole in the crown ether, as the opening is much too small. For Ar_2Zn(18-crown-6), Ar = phenyl **42** and *p*-tolyl **43**, it was shown that a peripheral crown ether complex **42a** (Scheme 36) forms rapidly, and that a second molecule of the diorganozinc abstracts an organic ligand from this complex to yield a crown ether chelated organozinc cation and a triorganozincate **42b**.[89] In a final step, the organozincate transfers one of the organic groups to the opposite side of the crown ether to complete the rotaxane structure **42**. Because rotaxanes are stable indefinitely in the absence of free diorganozincs, the "dethreading" of rotaxanes presumably occurs by the reverse of this mechanism.

Diorganozinc compounds do not form rotaxanes with 15-crown-5 and its nitrogen analogs, but the nitrogen macrocycles do initiate the disproportionation of diorganozincs to organozinc cations and zincate anions. The X-ray structure analysis of the essentially air stable Ph_2Zn(18-crown-6) (Figure 19) revealed equidistant Zn–C bonds (1.981(3) and 1.988(3) Å) that are, contrary to the parameters in the free diorganozinc compounds, longer than those in the diethyl analog (1.957(5) Å).[90] The zinc–oxygen distances, which range from 2.674(3) to 3.024(3) Å, are too long to be true bonds, suggesting that these rotaxanes are clathrates rather than adducts.

A ferrocenyl-based aldimine chelated dimethylzinc with its imino and oxygen atom to produce the tetrahedral dimethylzinc complex **44**. Both zinc–carbon bonds are equidistant (1.974(2) Å) and the zinc–oxygen donor bond (2.381(2) Å) is substantially longer than the zinc–nitrogen counterpart (2.213(2) Å) (Scheme 37).[91]

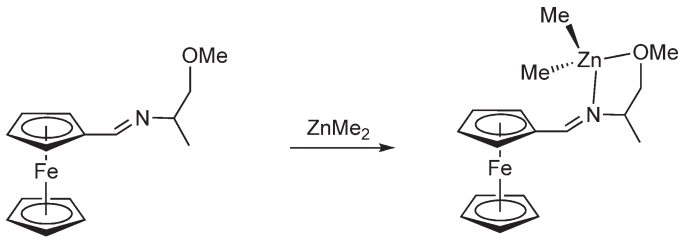

44

Scheme 37

2.06.7 Zinc Carbenoids and Zinc Heterocarbene Adducts

2.06.7.1 The Simmons–Smith Reagent and Related Carbenoid Compounds

Few organozinc compounds match the general synthetic versatility of the Simmons–Smith reagent, which has been used for decades for the stereospecific cyclopropanation of olefins. The classical Simmons–Smith reagent, ICH_2ZnI, and the related Furukawa ($EtZnCH_2I$) and Wittig ($Zn(CH_2I)_2$) reagents are generally referred to as zinc carbenoids, because they react with the transfer of a carbene moiety, even though the compounds themselves are organozinc iodides or diorganozinc compounds. Despite the maturity of these reactions, there is still an ongoing debate as to the true nature of these compounds, both in solution and the solid state, in addition to the mechanism of the cyclopropanation.

Charette and Marcoux used low-temperature ^{13}C NMR spectroscopic techniques to unambiguously characterize iodomethylzinc complexes of chiral diethers in solution.[92] They also showed that the Schlenk equilibrium for the Simmon–Smith reagent (Scheme 38) lies predominantly on the ICH_2ZnI side, and that the reagent is not a mixture of $Zn(CH_2I)_2$ and ZnI_2, as had been suggested. In notable contrast, however, Furukawa's reagent ($EtZnCH_2I$) is in equilibrium with $ZnEt_2$ and $Zn(CH_2I)_2$.

Charette *et al*. also reported single crystal X-ray structures of two crown ether complexes of the Simmons–Smith reagent, namely [ICH_2ZnI·18-crown-6] **45** and [ICH_2ZnI·benzo-18-crown-6] **46**.[93] The solid-state structure of **45** is shown in Figure 20. Similar to the structure of diorganozinc rotaxanes (Section 2.06.6.4), the zinc atom is associated with only three oxygen atoms, and even these contacts, ranging from 2.34(1) to 2.60(1) Å, are longer than conventional zinc–oxygen donor bonds.

Isolable and storable bis(halomethyl)zinc adducts of 2,2′-bipyridine and 2,2′-biquinoline (biquin) formed upon mixing bis(halomethyl)zinc reagents and the chelating nitrogen donor ligands.[94] Single crystal X-ray analyses were performed on the 2,2′-biquinoline complexes of $Zn(CH_2I)_2$ (Denmark's reagent) and of $Zn(CH_2Cl)_2$, namely [$(ClCH_2)_2Zn$·biquin] **46** and [$(ICH_2)_2Zn$·biquin] **47**. The solid-state structure of **46**, shown in Figure 21, revealed

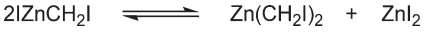

Scheme 38

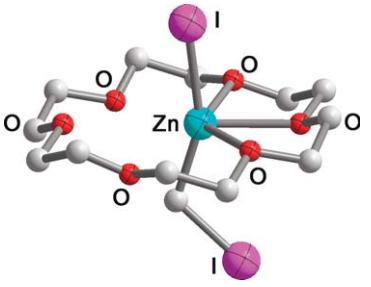

Figure 20 Solid-state structure and partial labeling scheme of [ICH_2ZnI·18-crown-6] **45**.

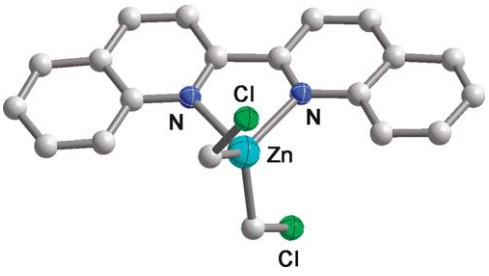

Figure 21 Solid-state structure and partial labeling scheme of $[(ClCH_2)_2Zn{\cdot}biquin]$ **46**.

a pseudo-tetrahedral metal atom, featuring slightly asymmetrical zinc–carbon (2.013(5) and 2.054(6) Å) and zinc–nitrogen (2.117(4) and 2.137(4) Å) bonds. Both, the structure and the bond parameters for **47**, are similar.

Bernardi and co-workers investigated the mechanism of the Simmons–Smith reaction theoretically at the DFT (B3LYP) level of theory, using $ClCH_2ZnCl$ as a model system.[95] Of the two available reaction channels (addition and insertion), the former process was found to have the lower activation energy (107.7 vs. 150.7 kJ mol^{-1}), and this result correlates well with the exclusive cyclopropanation over the competing insertion reaction.

In a related DFT study, the hypothetical zinc carbene CH_2ZnCl_2 was compared to its carbenoid isomer, $ClCH_2ZnCl$, and the latter structure was shown to be 107.5 kJ mol^{-1} more stable than the former. The zinc carbene structure, by contrast, is only a transition state, which connects two equivalent carbenoids.[96]

A density functional study (B3LYP level) probed the mechanism of zinc insertion into CH_2I_2 to form the Simmons–Smith reagent and the subsequent cyclopropanation of ethylene.[97] The energy of activation of the zinc insertion into the carbon–iodine bond of CH_2I_2 to generate the C_s-symmetric ICH_2ZnI is 123.4 kJ mol^{-1}, and the reaction was determined to be exothermic by 152.3 kJ mol^{-1}. The reaction of ICH_2ZnI with CH_2CH_2 has a barrier of 85.8 kJ mol^{-1} and is exothermic by 119.2 kJ mol^{-1}. An alternative mechanism of cyclopropanation via the intermediate CH_2ZnI was also studied. The ease of cyclopropanation by carbenoid species was found to depend on the electrophilicity of the methylene carbon, steric bulk, nature of the leaving group, and the reaction mechanism.

2.06.7.2 Adducts of *N*-Heterocyclic Carbenes

In contrast to the Simmons–Smith reagent and similar carbenoids, which are reactive and therefore difficult to characterize, adducts of the *N*-heterocyclic 1,3-diorganylimidazol-2-ylidenes are remarkably stable. The first *N*-heterocyclic carbene complex of zinc, namely the 1,3-di(1-adamantyl)imidazol-2-ylidene diethylzinc complex **48*** (Figure 22), was reported by Arduengo *et al.* in 1993.[98] Because of the general utility of these *N*-heterocyclic

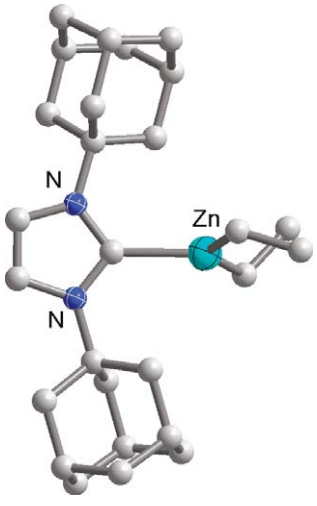

Figure 22 Solid-state structure and partial labeling scheme of **48**.

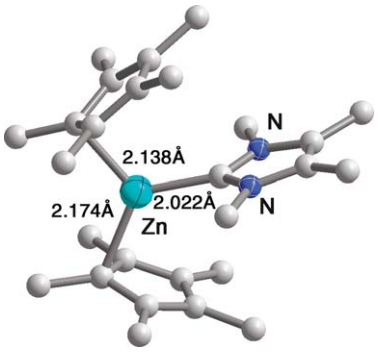

Figure 23 Solid-state structure, partial labeling scheme and selected bond lengths of [$(Cp^*)_2$Zn(1,3,4,5-tetramethylimidazol-2-ylidene)] **49**.

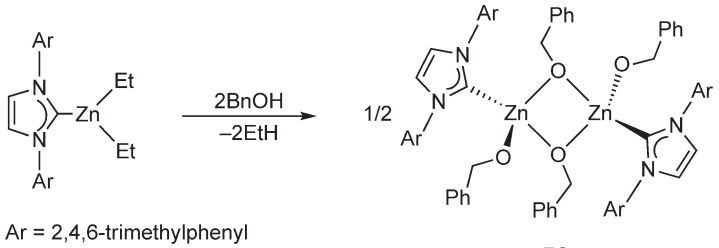

Scheme 39

carbenes as ancillary ligands in many catalytic processes, there has been an increase in reports on such heterocarbene adducts of zinc.

Bis(pentamethylclopentadienyl)zincocene, $Zn(Cp^*)_2$ ($Cp^* = C_5Me_5$), reacted with 1 equiv. of 1,3,4,5-tetramethylimidazol-2-ylidene to give the monocarbene complex $(Cp^*)_2$Zn(1,3,4,5-tetramethylimidazol-2-ylidene) **49**, whose structure is shown in Figure 23.[99] In contrast to the slipped sandwich structure of decamethylzincocene, here both pentamethylcyclopentadienyl groups are η^1-bound to the pseudo-trigonal planar zinc atom. The ^{13}C NMR signal of the carbene carbon appears substantially upfield (175.4 ppm) to that of the free ligand (213.7 ppm).

Jensen *et al.* reported the stereoselective polymerization of D,L-lactide with dibenzyloxidezinc(2,4,6-trimetylphenyimidazol-2-ylidene), which was synthesized as shown in Scheme 39.[100] Surprisingly, a mixture of the heterocarbene and benzyl alcohol was a better catalyst for polylactide formation than the zinc complex, and unlike **50** the mixture produced heterotactically enriched polylactide.

Because of the success of zinc-based catalysts in the ring-opening polymerization (ROP) of oxiranes and lactides, Wang *et al.* synthesized a series of heterocarbene-supported zinc complexes, as shown in Scheme 40.[101] Both **51** and **52** feature pseudo-tetrahedral zinc atoms which are coordinated by a 1,3-dimesitylimidazol-2-ylidene, THF, and either two chloride or triflate ligands. The zinc–carbon bonds for **51** and **52** are 2.036(2) and 1.996(3) Å long, respectively, the latter bond being the shortest recorded zinc–heterocarbene bond to date. The compounds showed no activity for the polymerization of propylene oxide, but **52** did polymerize cyclohexene oxide. The replacement of the trifluorosulfonate groups with chloride and carboxylates allowed the co-polymerization of cyclohexene oxide with carbon dioxide.

2.06.8 Organozinc Cations

2.06.8.1 Introduction

Organozinc cations are compounds of the type RZn^+, but the true structure of these charged species is more complex than indicated by this simple formula. Thus, the zinc atom is never one coordinate, but it is always associated with additional ligands or solvent molecules. These cations are therefore more accurately represented as $[RZn(L)]^+$. Truly

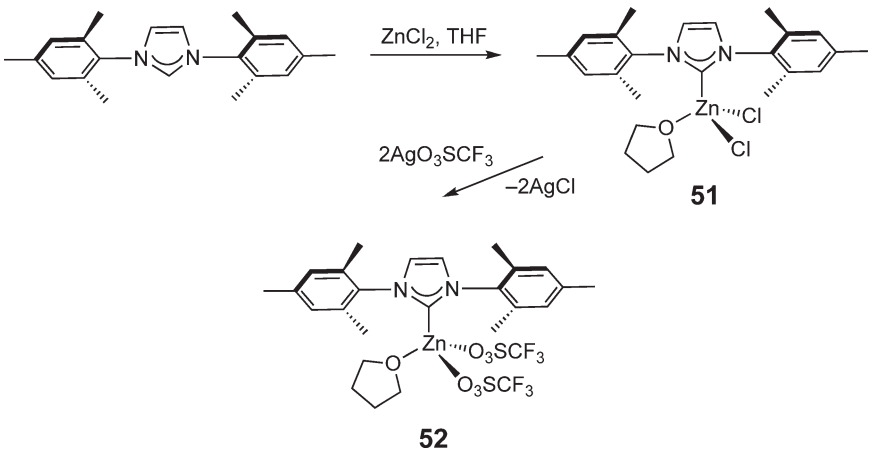

Scheme 40

isolated cations exist in solution, and especially in the solid state, only in the presence of special, non-coordinating anions. Despite the relative weakness of zinc–carbon bonds and the amphoteric nature of zinc, zinc cations do not form spontaneously by the disproportionation of diorganozinc species, but they must be generated by one of three synthetic methods:

- protonolysis of diorganozinc compounds,
- Lewis acid-induced abstraction of R or X groups from ZnR_2 or RZnX, and/or
- macrocycle-induced disproportionations of diorganozinc compounds.

Interest in organozinc cations increased substantially when they were shown to be excellent catalysts for the polymerization of esters and epoxides.

2.06.8.2 Organozinc Cations from the Protonolysis of Diorganozinc Compounds

Diazabutadiene adducts of diorganozinc compounds, for example, [ZnR_2(Bu^{t}N═CHCH═NBu^t)], undergo alkyl-transfer reactions from zinc to the chelating ligand. Wissing *et al.* hypothesized that these reactions proceed with the intermediacy of organozinc cations and investigated the charged species in some detail.[81] The insoluble, white [MeZn(Bu^{t}N═CHCH═NBu^t)][OTf] **53** was generated (Scheme 41) by combining ether solutions of the dimethylzinc diazabutadiene adduct [Me_2Zn(Bu^{t}N═CHCH═NBu^t)] and of trifluoromethanesulfonic acid (HOTf).

A Hartree–Fock geometry optimization suggested that, in solution, the zinc atom of **53** has a planar coordination environment. In the solid state, shown in Figure 24, however, the zinc atom is tetrahedral, with a short zinc–oxygen contact of 2.089(4) Å that indicates a significant bonding interaction. The zinc–methyl (1.958(6) Å) and zinc–nitrogen (2.093(4) Å) bonds have normal lengths.

N,*N*′,*N*″-trialkylated 1,3,5-triazacyclohexanes (R_3TAC) have been used extensively as ligands for homogeneous transition metal catalysts.[102,103] The protonolysis of diethylzinc by the addition of protonated *N*,*N*′,*N*″-alkylated

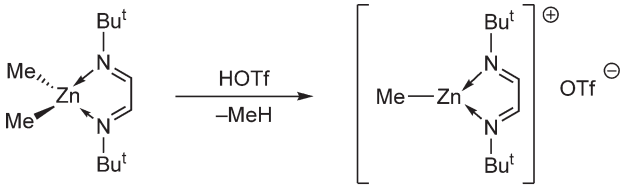

Scheme 41

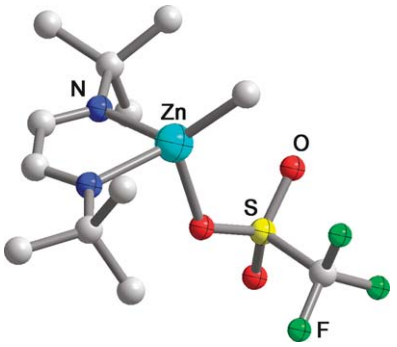

Figure 24 Solid-state structure and partial labeling scheme of [MeZn(Bu^{t}N═CHCH═NBu^t)][OTf] **53**.

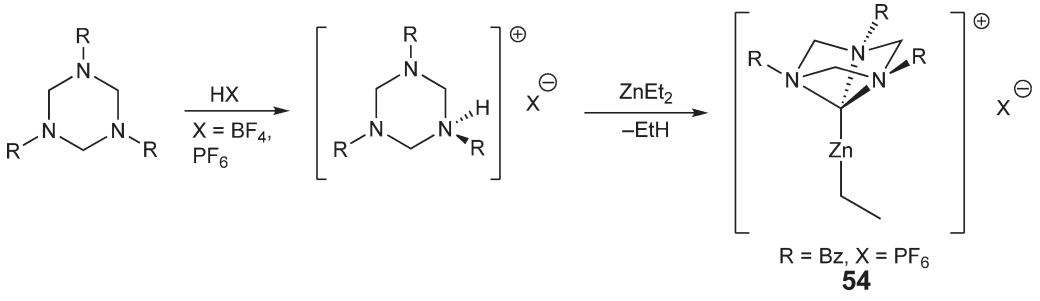

Scheme 42

1,3,5-triazacyclohexanes, Scheme 42, afforded moisture sensitive ethylzinc salts, in which the organozinc moiety is η^3-chelated by the R_3TAC (R = Me, benzyl (Bz), *p*-fluorobenzyl, Pr^i) ligands.

A crystal suitable for X-ray diffraction was obtained for R = benzyl and X = PF_6 **54**, and the solid-state structure for the cation of this compound is shown in Figure 25.

The complex has crystallographic *m*-symmetry, the mirror plane bisecting the unique benzyl group, the nitrogen atom to which it is attached, and the ethylzinc moiety. The pseudo-tetrahedral zinc atom has a short (1.930(4) Å) zinc–ethyl bond, but comparatively long (2.230(2) Å) nitrogen–zinc donor bonds.

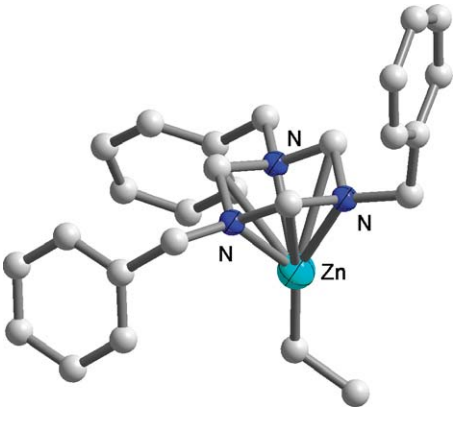

Figure 25 Solid-state structure and partial labeling scheme of the cation of **54**.

2.06.8.3 Catalytically Active Cationic Organozinc Complexes

Cationic diorganoaluminum species with non-coordinating anions are activators in the high-temperature polymerization of olefins, while mixtures of $AlEt_3/B(C_6F_5)_3$ also show moderate activity for the polymerization of ethylene. Neutral magnesium, calcium, and zinc compounds, in turn, have been used as catalysts for the polymerization of esters and epoxides.

Bochmann and co-workers have explored organozinc cations, which had not previously been investigated, for their role as catalysts in these polymerizations.[104,105] Upon mixing dimethyl- or diethylzinc with $B(C_6F_5)_3$ in toluene, a rapid exchange of the alkyl and pentafluorophenyl group occurred to afford $[Zn(C_6F_5)_2{\cdot}\text{toluene}]$. In toluene–ether solvent mixtures, however, the same starting materials reacted with alkyl group transfer to give the organozinc salts $[RZn(OEt_2)_3][RB(C_6F_5)_3]$, which feature non-coordinating alkyltris(pentafluorophenyl)borate ions in solution.

Treatment of $ZnEt_2$ with $[Ph_3C][B(C_6F_5)_4]$ led to β-hydride abstraction and the formation of ethene and $Zn(C_6F_5)_2$. The addition of $[H(OEt_2)_2][B(C_6F_5)_4]$ to homoleptic dialkylzinc compounds generated quantitatively the corresponding monoalkylzinc cations as tris(diethylether) adducts (Scheme 43).

These salts are soluble in diethyl ether and dichloromethane, but relatively insoluble in petroleum ether. The ethylzinc complex **55b** was investigated by single crystal X-ray techniques, and the structure of the cation is shown in Figure 26.

The zinc atom has almost ideal tetrahedral coordination geometry, with bond angles ranging from 115.37(10)° to 123.60(9)°. The zinc–carbon bond (1.964(3) Å) has a similar length as in the neutral $[MeZn(OBu^t)]_4$ tetramer,[106] in which zinc is also tetrahedrally surrounded by one alkyl group and three oxygen atoms.

Hannant *et al.* also reported the synthesis (Scheme 44) of cationic zinc complexes bearing bulky diazabutadiene ligands.[107] ^{19}F NMR spectroscopy showed that the borate anions of these compounds are non-coordinating in

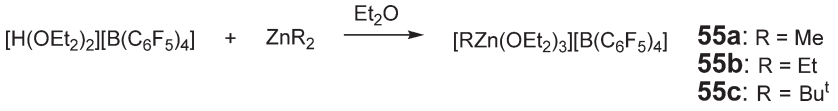

Scheme 43

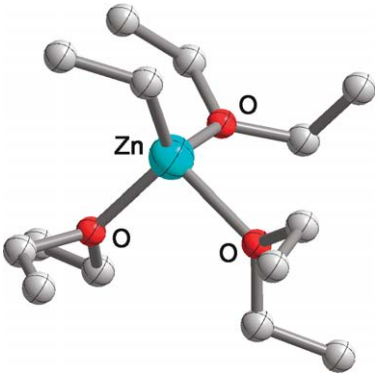

Figure 26 Solid-state structure and partial labeling scheme for the cation of $[EtZn(OEt_2)_3][B(C_6F_5)_4]$ **55b**.

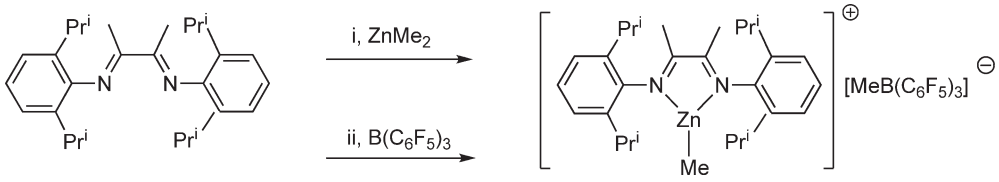

56

Scheme 44

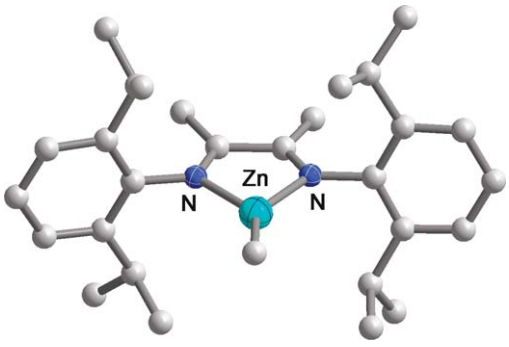

Figure 27 Solid-state structure and partial labeling scheme for the cation of **56**.

solution, and a single crystal X-ray analysis confirmed that this is also true in the solid state. The cationic diazabutadienezincmethyl complex **56** is the first zinc cation, featuring a trigonal-planar metal, coordinated by a neutral ligand (Figure 27).

The zinc–methyl bond (1.914(4) Å) is the shortest zinc–carbon bond reported to date, while the zinc–nitrogen bonds (2.040(2) Å) are slightly longer than those in neutral, three-coordinate zinc diketiminato complexes (Figure 48).

Cationic complexes, such as **55** and **56**, catalyze the polymerization of propylene oxide, cyclohexene oxide, and of ε-caprolactone with substantially higher activities than neutral zinc complexes.

2.06.8.4 Cationic Organozinc Complexes Bearing Macrocyclic Ligands

In the presence of polydentate ligands, some diorganozinc compounds disproportionate to the corresponding organozincate and the organozinc cation, the latter being chelated by the polydentate ligand. Because diorganozinc compounds do not form cations as readily as the corresponding magnesium compounds, cation formation is often promoted by the addition of Lewis acids, such as AlR_3, or by the incorporation of better leaving groups, such as halides or aryloxides.

Thus, in the presence of macrocycles, trialkylaluminum and even diorganozinc compounds have been used as alkide and halide abstractors to generate macrocycle-chelated organozinc cations (Scheme 45).[108,109]

Cyclopentadienyl(ethyl)zinc disproportionates in the presence of crown ethers, cryptands, as well as cyclic and acyclic tri- and tetraaza ligands to the ethylzinc cation and the ethyldicyclopentadienylzincate $[EtZnCp_2]^-$, which exist in solution as contact ion pairs. To generate cationic species of the type $[EtZn(L)]^+$ (L = macrocycle) with truly non-coordinating anions, Richey and co-workers used 1,2,3,4-tetraphenylcyclopentadiene. Equilibrium mixtures were obtained when adding a second macrocyclic ligand, L^*, to solutions of $[RZn(L)]^+$ (Scheme 46). The rate of exchange of L^* with the cations is fast, with half-lives ranging from minutes to hours.

$$ZnR_2 + AlR_3 \xrightarrow{\text{macrocycle}} [RZn(\text{macrocycle})]^+ + [AlR_4]^-$$

$$RZnX + ZnR_2 \xrightarrow{\text{macrocycle}} [RZn(\text{macrocycle})]^+ + [R_2ZnX]^-$$

X = halide, aryloxide

Scheme 45

$$[RZn(\text{macrocycle})]^+ + \text{macrocycle}^* \rightleftharpoons [RZn(\text{macrocycle}^*)]^+ + \text{macrocycle}$$

Scheme 46

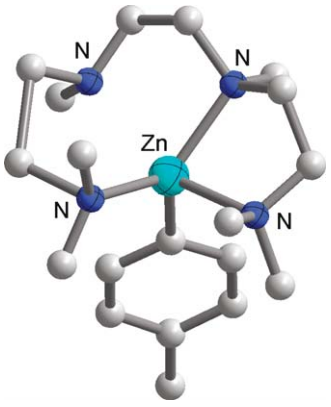

Figure 28 Solid-state structure and partial labeling scheme for the cation of [*p*-tolZn(N_4)] [Ph_4C_5H] **57**.

The equilibrium constants, obtained by NMR spectroscopic methods, showed a strong dependence on both the macrocycles and the diorganozinc compounds. Polydentate nitrogen donor ligands, particularly triazacyclononanes, form much stronger complexes than cryptands and crown ethers.

A single crystal X-ray analysis on [*p*-tolZn(N_4)]$^+$ [Ph_4C_5H]$^-$ (N_4 = 1,1,4,7,10,10-hexamethyl-1,4,7,10-tetraazadecane) **57**, shown in Figure 28, revealed that despite the relative compactness and flexibility of the acyclic ligand, only three of the four nitrogen atoms are coordinated to zinc.[110] Together with the *para*-tolyl group, the tetraazadecane creates a highly distorted tetrahedral coordination geometry about the metal, with a long zinc–carbon bond (2.01(1) Å) and nitrogen–zinc dative bonds that range from 2.13(1) to 2.35(1) Å.

2.06.9 Organozincates

2.06.9.1 Introduction

Organozincates are compounds of the general formulas M[ZnR_3] and M_2[ZnR_4], where M is an alkali or alkaline earth metal and R is an organic group, or occasionally a non-metal or a group bound through a non-metal. Organozincates are almost as old as organozinc chemistry itself,[111] but the first X-ray structural characterization of an organozincate, namely that of Li_2[$ZnMe_4$], Figure 29, was not reported until 1968.[112,113] In this compound, the zinc atoms are surrounded in a slightly distorted tetrahedral fashion by elongated Zn–C bonds (2.07 Å).

Organozincates can be divided into two broad groups, namely triorganozincates, [ZnR_3]$^-$, having three-coordinate, trigonal-planar zincate ions, and tetraorganozincates [ZnR_4]$^{2-}$, having four-coordinate, tetrahedral zincate ions. Heteroleptic zincates, of the formulas [ZnR_2R^1]$^-$ or [ZnR_3R^1]$^{2-}$, where $R \neq R^1$, are also quite common. Organozincates may also be classified by the interaction between the cation and anions, as isolated or contact ion pairs.

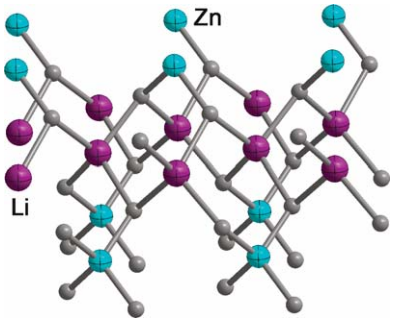

Figure 29 The solid-state structure of Li_2[$ZnMe_4$]. The grey spheres represent the methyl groups.

Organozincates are most commonly prepared by the addition of organolithium or Grignard reagents to ZnX_2 or ZnR_2. A less direct synthesis of organozincates is the disproportionation of diorganozinc compounds to organozinc cations and organozincates in the presence of macrocyclic ligands. The chemistry of zincates was recently reviewed by Wheatley *et al*., as part of a more extensive treatise on the chemistry of group 12 and 13 metal "ate" complexes.[114]

2.06.9.2 Homoleptic Triorganozincates

The reaction of dibenzylmagnesium with dibenzylzinc in THF in a 1 : 2 ratio, Scheme 47, afforded quantitatively the tribenzylzincate $[Mg(THF)_6][Zn(CH_2Ph)_3]_2$ **58**, which exists in the solid state in the form of isolated hexakis(tetrahydrofuran)magnesium cations and trigonal-planar tribenzylzincate ions, the latter being shown in Figure 30.[115] The colorless, air sensitive salt is stable at room temperature under a nitrogen atmosphere.

The coordination geometry about zinc is perfectly planar with an angle sum of 360°. The Zn–C bonds range from 2.032(2) to 2.058(2) Å.

The first structurally characterized triarylzincate $[Li(TMEDA)_2][Zn\{2,4,6\text{-}(Pr^i)_3C_6H_2\}_3]$ **59** was a byproduct of the lithiation of $VCl_3(THF)_3$ with $Li(2,4,6\text{-}(Pr^i)_3C_6H_2)_3$, in which the vanadium compound had been pre-reduced with metallic zinc.[116] In the solid state, the compound consists of isolated, tetrahedrally coordinated lithium ions and trigonal-planar tris(tris(isopropyl)phenyl)zincate ions. The Zn–C bonds are equidistant (2.039(7) Å), but the C–Zn–C bond angles are variable, ranging from 112.2(3)° to 125.4(3)°.

The analogous triphenylzincate **60** and trimesitylzincate **61** were obtained by the treatment of zinc bromide bis(tetrahydrofuranate) with the respective Grignard reagents, as outlined in Scheme 48.[117]

Both compounds consist of discrete magnesium-containing cations and zincate anions in the solid state, the zinc atoms being surrounded in a trigonal-planar fashion by the aryl substituents. In the bulky trimesityl complex, these rings form large dihedral angles of ca. 67° with the coordination plane, while for the sterically less encumbered **60** the phenyl rings lie almost in the coordination plane, giving the anion a disc-like appearance.

The homoleptic tris[bis(trimethylsilyl)amido]zincate $[Na(12\text{-crown-}4)_2]$ $[Zn\{N(SiMe_3)_2\}_3]$ reacted with phenylacetylene (Scheme 49) to yield $[Na(12\text{-crown-}4)_2]_2$ $[Zn(CCPh)_3(THF)][Zn(CCPh)_3]$ **62**.[118]

$$Mg(CH_2Ph)_2(THF)_2 + 2Zn(CH_2Ph)_2 \longrightarrow [Mg(THF)_6]\,[Zn(CH_2Ph)_3]_2$$

58

Scheme 47

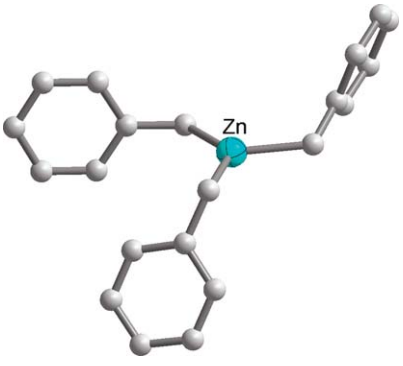

Figure 30 Solid-state structure and partial labeling scheme for the $[Zn(CH_2Ph)_3]^-$ anion of **58**.

$$3ArMgBr + ZnBr_2(THF)_2 \xrightarrow[-MgBr_2]{} [MgBr(THF)_5]\,[ZnAr_3]$$

60: Ar = phenyl
61: Ar = mesityl

Scheme 48

$$2[Na(12\text{-crown-}4)_2][Zn\{N(SiMe_3)_2\}_3] + 6HCCPh \longrightarrow \underset{\mathbf{62a}}{[Na(12\text{-crown-}4)_2]_2[Zn(CCPh)_3]} \quad \underset{\mathbf{62b}}{[Zn(CCPh)_3(THF)]}$$

Scheme 49

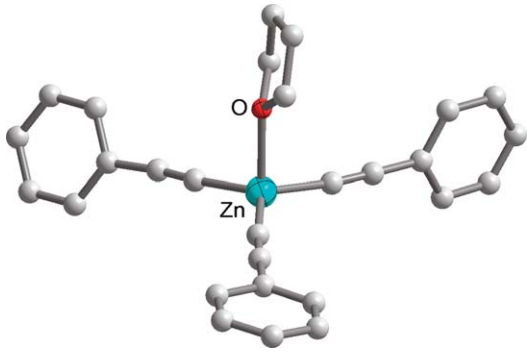

Figure 31 The solid-state structure and partial labeling scheme of $[Zn(CCPh)_3(THF)]^-$ **62b**.

In **62**, two zincate ions of different composition, namely $[Zn(CCPh)_3]^-$ **62a** and its THF adduct $[Zn(CCPh)_3(THF)]^-$ **62b**, co-crystallized (Figure 31). Both, the coordination of only one zincate ion with THF and the trigonal-pyramidal structure of **62b**, show that the interaction between zinc and the THF molecule in **62b** must be weak. The zinc–carbon bonds in **62a** and **62b** are 1.967(7) and 2.003(5) Å long, respectively.

2.06.9.3 Homoleptic Tetraorganozincates

Ternary acetylides of the composition $M[M'(C_2)_n]$, M = alkali metal, M′ = transition metal, are solid-state compounds, which depending upon their composition may exhibit either insulator or semi-conductor behavior.

The reaction of alkali metal hydrogenacetylides with the corresponding tetracyanozincates (Scheme 50) gave the potassium- and rubidium tetrakis(hydrogenacetylido)zincates. The solid-state structure of the rubidium analog **64** was determined from Rietveld-refined X-ray powder data and shown to be isomorphous with that of the previously reported potassium salt $K_2[Zn(C_2H)_4]$.[119] These alkali metal zincates have structures that are similar to those of scheelite ($CaWO_3$) and anatase (TiO_2). The highly symmetrical anion of **64** and selected bond lengths are shown in Figure 32.

$$4MC_2H + M_2[Zn(CN)_4] \xrightarrow{NH_3(l)} \{M_2[Zn(C_2H)_4]\cdot nNH_3\} + 4MCN \quad \begin{matrix}\mathbf{63}\text{: M = K; } n = 2\\ \mathbf{64}\text{: M = Rb; } n = 0\end{matrix}$$

Scheme 50

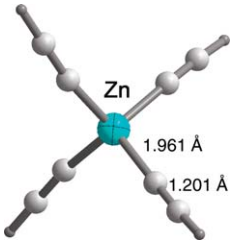

Figure 32 Solid-state structure and partial labeling scheme of $[Zn(C_2H)_4]^{2-}$ **64**.

$$[Zn\{N(SiMe_3)_2\}_2] + 4Li(CCPh) \xrightarrow[tmeda]{toluene} [\{Li(tmeda)\}_2Zn(CCPh)_4 + 2Li\{N(SiMe_3)_2\}]$$

65

Scheme 51

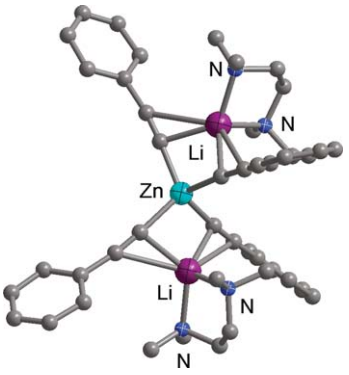

Figure 33 The solid-state structure and partial labeling scheme of $[\{Li(TMEDA)\}_2Zn(CCPh)_4]$ **65**.

When the potassium derivative was allowed to stand in ammonia, single crystals of the diammoniate $\{K_2[Zn(C_2H)_4]\cdot 2NH_3\}$**63** separated.[120] A low-temperature, single crystal X-ray analysis of **63** showed it to consist of tetrahedral $[Zn(C_2H)_4]^{2-}$ ions, which feature almost linear Zn–C–C units. The zinc–carbon bonds (2.053(3) Å) are slightly longer than those in **64**, while the carbon–carbon bonds are identical (1.203(4) Å) in length.

Four equivalents of lithium phenylacetylide reacted with bis{bis(trimethylsilyl)amido}zinc (Scheme 51) to form the ion-paired dilithiotetra(phenylacetylido)zincate **65**, whose structure is shown in Figure 33.[121] The zinc–carbon bonds (2.05 Å) are somewhat longer than those observed in the tri(phenylacetylido)zincate **62a**, due to the increase in both the coordination number and the negative charge on the ion. Each lithium ion is associated with the zincate ion through coordination to two of the triple bonds.

Using an anionic arylamine with a pendent dimethylaminomethyl group in the *ortho*-position, Rijnberg *et al.* synthesized the lithium triarylzincate **66**, which crystallized as a contact ion pair (Scheme 52).[122]

The zinc atom is coordinated by three phenyl groups, and displays mean Zn–C bond lengths of 2.049(2) Å, and a relatively long Zn–N donor bond (2.340(3) Å).

A much more symmetrical zincate, namely $[Li_2Zn(o\text{-}C_6H_4CH_2NMe_2)_4]$ **67**, Figure 34, was obtained by the same workers when 2 equiv. of $Li(o\text{-}C_6H_4CH_2NMe_2)$ were allowed to interact with $Zn(o\text{-}C_6H_4CH_2NMe_2)_2$. In this contact ion pair, the zinc atom is tetrahedrally surrounded by four phenyl rings, while the lithium ions are coordinated by two *ipso*-carbon atoms of two phenyl groups and two amino groups.

The zinc–phenyl bonds (2.139(4) Å) of this almost perfectly tetrahedral zincate are substantially longer than those in $ZnPh_2$ (1.979(4) Å).

Treatment of zinc dichloride with various 1,4-dilithiobutanes gave the corresponding contact ion pair dilithio bis(1,4-dibutanediyl)zincates as ether and TMEDA adducts.[123] Figure 35 shows the solid-state structure of the

$$Li(o\text{-}C_6H_4CH_2NMe_2) + Zn(o\text{-}C_6H_4CH_2NMe_2)_2 \xrightarrow{THF}$$

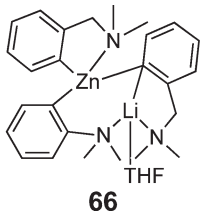

66

Scheme 52

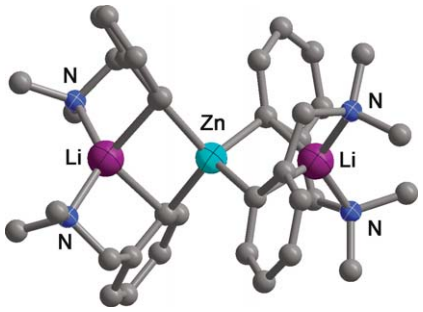

Figure 34 The solid-state structure and partial labeling scheme of $[Li_2Zn(o\text{-}C_6H_4CH_2NMe_2)]$ **67**.

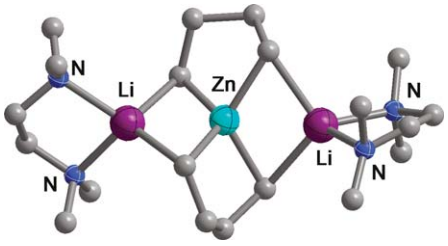

Figure 35 Solid-state structure and partial labeling scheme of $[Li(TMEDA)]_2[Zn(CH_2CH_2CH_2CH_2)_2]$.

trispirocyclic $[Li(TMEDA)]_2[Zn(CH_2CH_2CH_2CH_2)_2]$ with its distorted tetrahedrally coordinated zinc atom. The mean zinc–carbon and lithium–carbon bond lengths are 2.119(4) and 2.295(8) Å, respectively.

2.06.9.4 Heteroleptic Triorganozincates

The reaction of diorganozincs bearing bulky trimethylsilyl-substituted methyl groups and methyl- or phenyllithium in the presence of the 1,3,5-trimethyl-1,3,5-triazacyclohexane (TACH), Scheme 53, afforded the corresponding lithium zincates as poorly soluble ion pairs.[124]

The solid-state structure of **68c**, Figure 36, shows that the zinc atom is surrounded in a trigonal-planar fashion by one methyl group and two 2,4,6-trisilacyclohexyl ligands, of which one has a chair conformation, while the other one has a boat conformation.

If the nucleophile R^1 is replaced with bis(trimethylsilyl)amide, Scheme 54, a much more soluble lithium zincate **69** is isolated as a contact ion pair. A further increase in the steric bulk of either the organic substituents of the diorganozinc or of the nucleophile gave equilibria from which no organozincates could be isolated.

The reactions of methyllithium with the TMEDA adduct of trimethylsilyl(benzyl)zinc chloride or of lithium trimethylsilylbenzyl with zinc dichloride yielded, in the presence of excess TMEDA, compounds of the type $[Li(TMEDA)_2][Me_{3-n}Zn(CHSiMe_3Ph)_n]$, $n = 1$–3.[125] All of these zincates are solvent-separated ion pairs with trigonal-planar zincate ions. The larger the organic group on zinc, the more thermally stable and less reactive the organozincates. Thus, $[Li(TMEDA)_2]$ $[Me_2Zn(CHSiMe_3Ph)]$ decomposes at 35 °C, while $[Li(TMEDA)_2][Zn(CHSiMe_3Ph)_3]$ melts at 202 °C.

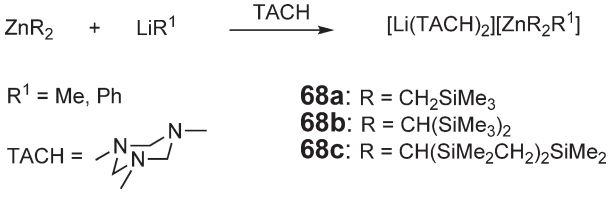

Scheme 53

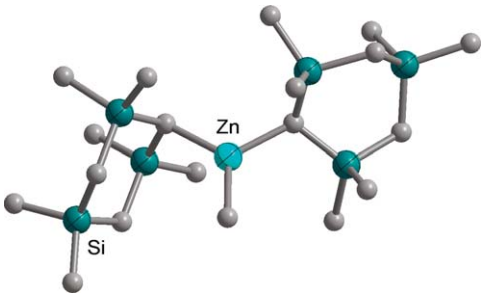

Figure 36 The solid-state structure and partial labeling scheme of $[MeZn\{CH(SiMe_2CH_2)_2SiMe_2\}_2]^-$ **68c**.

$$Zn(CH_2SiMe_3)_2 + LiN(SiMe_3)_2 \xrightarrow{TACH} [Li(TACH)Zn(CH_2SiMe_3)_2{\cdot}N(SiMe_3)_2]$$
69

Scheme 54

$$2HN(SiMe_3)_2 + Bu^nLi + ZnMe_2 \xrightarrow[-Bu^nH]{-MeH} [Li\{N(SiMe_3)_2\}_2ZnMe]_n$$
70

Scheme 55

Mixtures of hexamethyldisilazane, *n*-butyllithium, and dimethylzinc reacted, Scheme 55, with the formation of a lithium zincate **70**. In the solid state, Figure 37, **70** consists of four-membered, C_2-symmetric LiN_2Zn rings, which form a polymeric structure through bridging methyl groups from zinc to lithium.[126]

Many 1,4-diazabutadiene adducts of dialkylzinc compounds show unusual reactivities (see also Section 2.06.10.7), such as the intramolecular electron transfer from zinc to the chelating ligand and the subsequent dimerization of these radicals.[127] In solution, the carbon–carbon coupled dimer $[MeZn(Bu^tN{=}CHCH{=}NBu^t)_2ZnMe]$ **71** is in equilibrium with its radical monomers (Scheme 56). Addition of potassium to a THF solution of the dimer produced cleanly **72**, the first heteroleptic alkyldiamidozincate.

The solid-state structure of **72** (Figure 38) consists of a polymer of alternating THF-solvated potassium cations and diamidomethylzincate anions. The alternating zincate ions, which are rotated by about 180° with respect to each other, sandwich the potassium ions. Each potassium ion is η^2-coordinated to one methyldiamidozincate and η^4-coordinated to the other. The zinc–methyl and zinc–nitrogen bonds of the zincate ion are 1.954(5) and 1.989(8) Å, respectively.

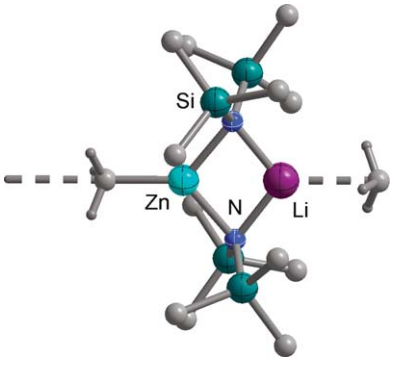

Figure 37 A section of the solid-state structure and partial labeling scheme of polymeric $[Li\{N(SiMe_3)_2\}_2ZnMe]$ **70**.

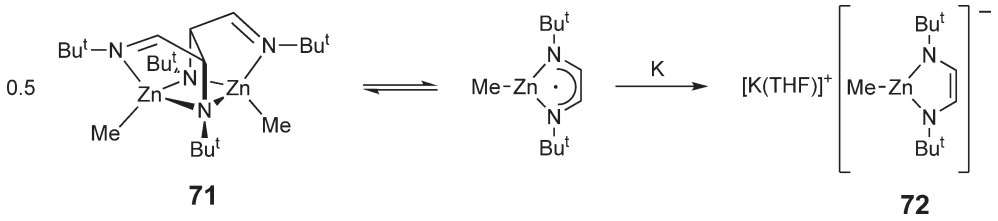

Scheme 56

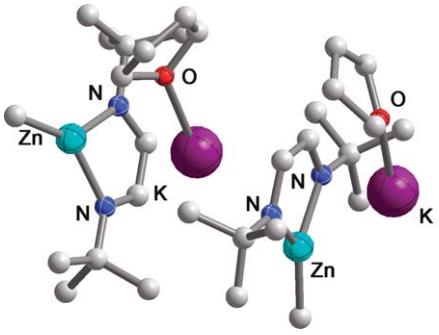

Figure 38 Solid-state structure and partial labeling scheme of two repeat units of **72**.

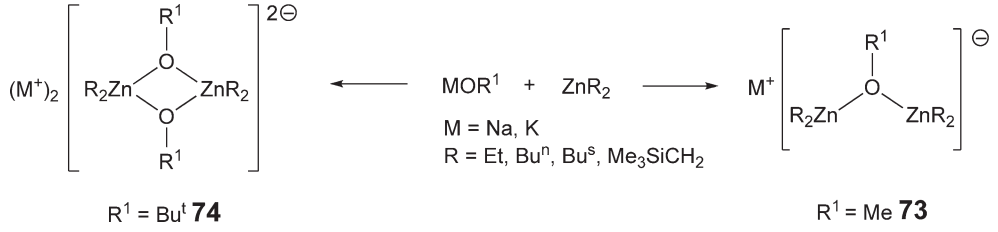

Scheme 57

Addition of insoluble NaOMe and KOMe to benzene solutions of ZnR_2, Scheme 57, gave soluble 1 : 2 zincates of the composition $M[(R_2Zn)_2OMe]$ **73** (M = Na, K; R = Et, Bu^n, Bu^s, Me_3SiCH_2).[128] By contrast, combining dialkylzincs with benzene-soluble $KOBu^t$ produces the dianionic zincate **74**.

2.06.9.5 Heteroleptic Tetraorganozincates

Anionic organometallic compounds are often significantly more reactive than their neutral precursors. Triorganozincates, $[ZnR_3]^-$, for example, are much better nucleophiles than diorganozinc compounds or organozinc halides, the order of reactivity being $[ZnR_3]^- > ZnR_2 > RZnX$. It is therefore reasonable to assume that tetrasubstituted dianionic zincates are more reactive than the monoanionic triorganozincates.

Although the existence and structures of tetraorganozincates in the solid state are now well established, the reactivity patterns of these compounds in organic synthesis are still largely unknown. Homoleptic and heteroleptic tetrasubstituted dianionic zincates of the type $[ZnR_3X]$, X = Me, CN, SCN, were prepared as shown in Scheme 58

Scheme 58

$$Li[ZnMe_3] + LiMe \rightleftharpoons Li_2[ZnMe_4]$$

Scheme 59

and tested for their effectiveness in the intermolecular opening of epoxides, bromine–zinc exchange of bromobenzenes, tellurium–zinc exchange of 2-pyridinyltellurium compounds, and the intramolecular Michael addition, among others.[129,130] In most cases, these dianionic zincates were more reactive than the trimethylzincates or brought about transformations that were not possible with trisubstituted zincates.

Based on these remarkable results by Uchiyama *et al*., Mobley and Berger investigated the existence of tetrazincates in solution by NMR spectroscopic methods.[131] Using fully ^{13}C-labeled organic substituents, the authors detected carbon–carbon couplings over two bonds, allowing them to determine the number of chemically equivalent methyl groups on the zinc atom. Addition of $^{13}CH_3Li$ to $Li[Zn(^{13}CH_3)_3]$ affords a mixture of three products, Scheme 59, which consists mainly of $^{13}CH_3Li$ and $Li[Zn(^{13}CH_3)_3]$, and a small amount of the tetramethylzincate $Li_2[Zn(^{13}CH_3)_4]$. The authors attribute the reluctance of trimethylzincate to accept a second methide group to coulombic repulsion, and conclude that $[ZnMe_4]^{2-}$ is likely thermodynamically unstable in solution despite its obvious stability in the solid state.

2.06.9.6 Computational Studies on Organozincates

Mori *et al*. conducted DFT studies on $ZnMe_2$, $[ZnMe_3]^-$, and $[ZnMe_4]^{2-}$ to understand the reactivity patterns of these important nucleophiles in organic synthesis.[132] At the B3LYP/631 level, the zinc–carbon bonds of $ZnMe_2$ and $[ZnMe_4]^{2-}$ were calculated to be 1.93 and 2.22 Å long, respectively, in good agreement with previous experimental and computational studies. According to an NBO analysis, the zinc–carbon bonds of $ZnMe_2$ consist of 76% carbon electrons and 23% zinc electrons. The carbon 2*p* orbitals, whose energy levels increase from −6.55 eV, −1.08 eV, and 5.09 eV, for $ZnMe_2$, $[ZnMe_3]^-$, and $[ZnMe_4]^{2-}$, respectively, are always the HOMOs. The 3*d* orbitals of zinc follow the same trend, ranging from −13.03 to −12.95 eV for $ZnMe_2$, −7.46 to −7.38 eV for $[ZnMe_3]^-$, and −0.19 to 0.15 eV for $[ZnMe_4]^{2-}$. These values suggest that organozincates, in contrast to organocuprates, behave as alkyl-centered nucleophiles.

2.06.10 Organozinc Amides

2.06.10.1 Introduction

Organozinc amides, which were once mainly of academic interest, have become one of the most actively investigated classes of organozinc compounds, because of their utility in catalysis and their role as model compounds for zinc-containing enzymes. Although bulky, monodentate amines still find applications in organozinc chemistry; the most commonly used ligands in this area are purpose-specific chelating amides with two or more donor atoms. Zinc seems to have an inherent preference for the coordination of nitrogen over oxygen, as reflected in the comparatively much shorter Z–N bonds.

2.06.10.2 Organozinc Compounds Bearing Monodentate Amides

Primary amines of varying steric bulk (aniline, 2,4,6-trimethylaniline, 2,6-diisopropylaniline, and *tert*-butylamine) reacted with $ZnEt_2$ or $Zn(CH_2SiMe_3)_2$ to yield the corresponding organozincamido complexes as dimeric, trimeric, and tetrameric rings or polycycles.[133,134] The solid-state structure of $\{EtZnN(H)Bu^t\}_3$ **75**, which adopts a chair conformation, is shown in Figure 39.

Depending on the reaction conditions, either one or both of the amino hydrogens can be removed in these reactions, and occasionally more unusual products, such as the tetranuclear ethylzinc/ethoxyzinc/2,6-diisopropylphenylamido complex **76**, Figure 40, were isolated.

Malik and O'Brien synthesized compounds of the type $RZnN(R^1)_2$ (R = Me, Et, and R^1 = Et, Pr^i, Bu^i, Me_3Si; R = Np, Bu^i, and R^1 = Et, Pr^i and Bu^i) because their high vapor pressures (5–6 torr at 0 °C) make them suitable precursors for MOCVD applications.[135]

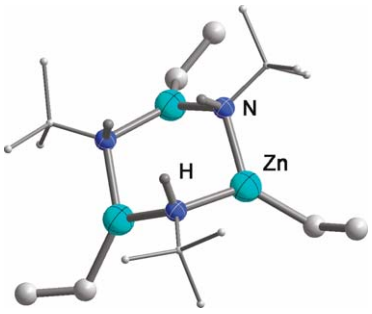

Figure 39 The solid-state structure and partial labeling scheme of $\{EtZnN(H)Bu^t\}_3$ **75**.

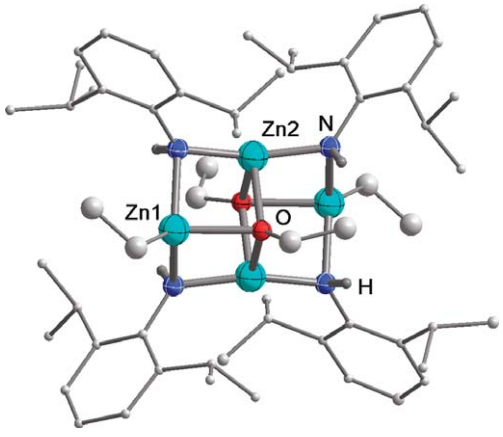

Figure 40 Solid-state structure and partial labeling scheme of **76**.

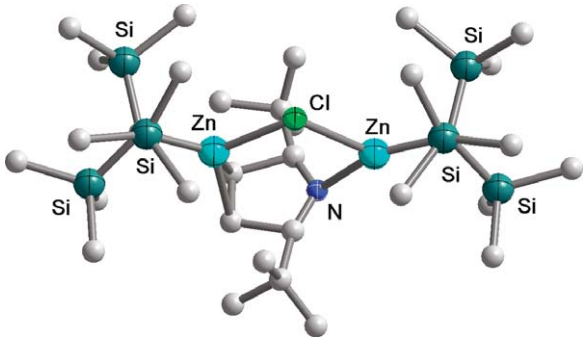

Figure 41 Solid-state structure and partial labeling scheme of **77**.

The reaction of tris(trimethylsilyl)methylzinc chloride with lithium 2,5-di(*tert*-butyl)pyrrolide afforded [bis{tris(trimethylsilyl)methylzinc}(μ-chloride){μ-2,5-di(*tert*-butyl)pyrrolide}] **77**, irrespective of the stoichiometry of the reagents. The solid-state structure of this organozinc amide/chloride, Figure 41, shows that the chloride and the pyrrolide ligands bridge both zinc atoms, the latter ligand doing so in a κ-*N*, κ^2-*C* fashion.[136]

2.06.10.3 Organozinc Compounds Bearing Chelating Amido/Amino Ligands

The monoprotic, chelating secondary/tertiary amines *N*,*N*,*N*′-trimethylethylenediamine and -propylenediamine reacted with $ZnMe_2$ and $ZnEt_2$ to produce alkylzincamido/amines.[137] These compounds have the general formulas $[RZnMeN(CH_2)_nNMe_2]_2$, R = Me, Et; $n = 2$, 3, and crystallize as dimers with the formation of a central $(Zn–N)_2$ ring.

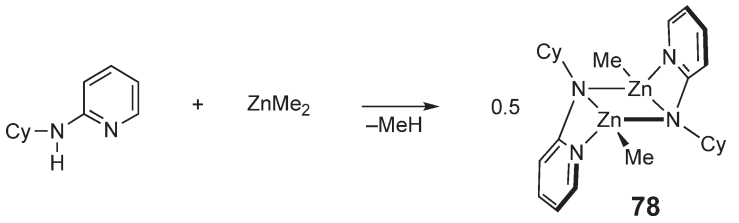

Scheme 60

Various secondary amines with internal nitrogen donors, namely *N*-2-pyridylaniline, *N*-2-pyridylcyclohexylamine, and 1,3,4,6,7,8-hexahydro-2*H*-pyrimido[1,2-*a*]pyrimidine, reacted with $ZnMe_2$ to give dimeric or trimeric methylzincamido compounds.[138] Thus, as shown in Scheme 60, dimeric $[MeZn\{CyN(2\text{-}C_5H_4N)\}]_2$ **78** formed when *N*-2-pyridylcyclohexylamine was treated with dimethylzinc. Metallation of the guanidine $Me_2NC(NPr^i)(HNPr^i)$ with $ZnMe_2$ (Scheme 61) gave the guanidinate complex $Me_2NC(NPr^i)_2ZnMe$ **79**, which crystallizes as a bowl-shaped dimer with crystallographically imposed C_2-symmetry and an almost perfectly planar, central $(Zn–N)_2$ ring.[139]

Chakraborty and Chen reported the syntheses and structures of organzinc compounds bearing chiral *trans*-1,2-$(HNSiMe_3)_2$-cyclohexanediyl ligands for the stereoselective polymerization of methacrylates. Depending upon the reaction conditions, Scheme 62, either the fully deprotonated trimeric bis(amido)methylzinc complex **80**, or a dimeric amido(amino)methylzinc complex **81** were isolated.[140]

The zincation of *N*-(2-diphenylphosphinophenyl)-2,6-diisopropylaniline with $ZnEt_2$, Scheme 63, afforded an ethylzinc complex bearing a chelating amidophosphine ligand **82**.[141] The compound features a three-coordinate zinc atom with zinc–nitrogen (1.911(4) Å) and zinc–carbon (1.956(5) Å) bonds of average lengths, but the zinc–phosphorus (2.4450(14) Å) donor bond is quite long. Upon treating hexakis(aminocyclohexyl)cyclotriphosphazene with excess diethylzinc, Scheme 64, Lawson *et al.* obtained hexakis{amidocyclohexyl(ethylzinc)}cyclotriphosphazene **83**.[142] The analogous cyclotetraphosphazene $P_4N_4(NHCy)_8$, by contrast, lost only six of its eight ionizable protons, yielding again a hexakis(ethylzinc) derivative, namely $[(EtZn)_6P_4N_4(NCy)_6(NHCy)_2]$.

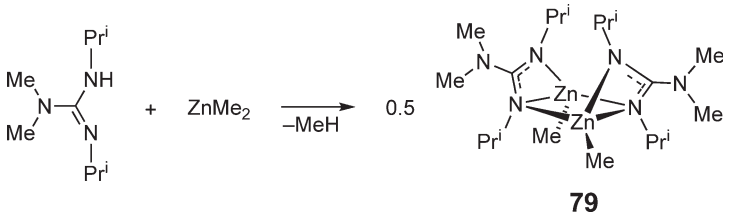

Scheme 61

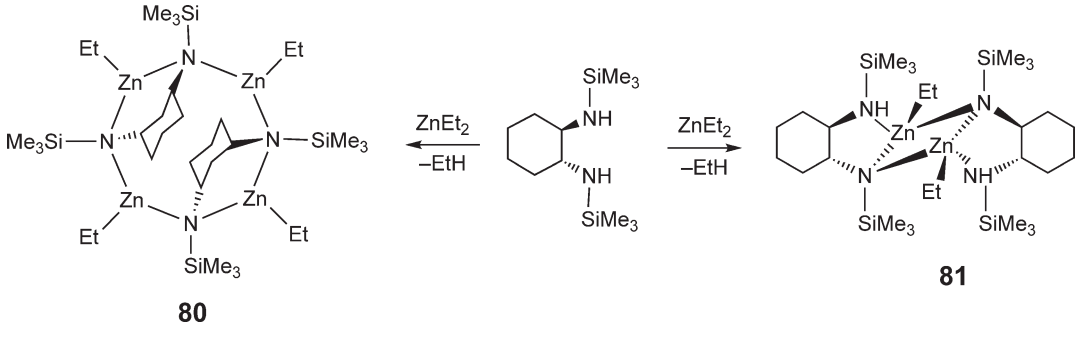

Scheme 62

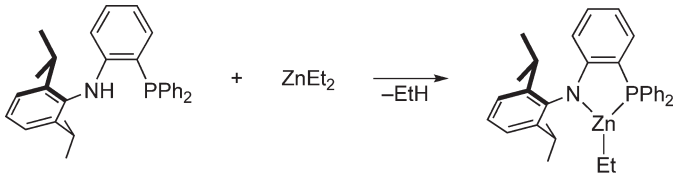

82

Scheme 63

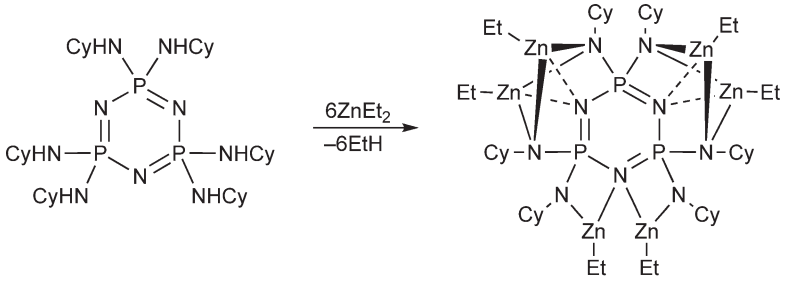

83

Scheme 64

Figure 42 is a view of **83** perpendicular to the non-crystallgraphic C_2-axis, which contains the unique phosphorus atom (P1) and interconverts the two equivalent phosphorus atoms (P2). The ^{31}P NMR spectrum, consisting of one doublet and one triplet in a 2 : 1 ratio, confirms that this structure is maintained in solution.

An attempted synthesis, Scheme 65, of a heterozincate from dimethylzinc and bis{(2-pyridyl)methyl}lithium gave instead the dimeric [bis{(2-pyridyl)methyl}methylzinc] complex **84**, shown in Figure 43.[143] The intermolecular zinc–carbon bond to the bridging carbon atoms is remarkably short (2.269(3) Å), while the zinc–methyl bond is slightly elongated (1.974(3) Å).

Wirringa *et al*. obtained an unusual 1,3-diaza-2-phosphaallyl(methylzinc) complex (Figure 44, **85**), featuring a two-coordinate phosphorus atom, from the deprotonation of a bulky amino(imino)phosphine with dimethylzinc.[144]

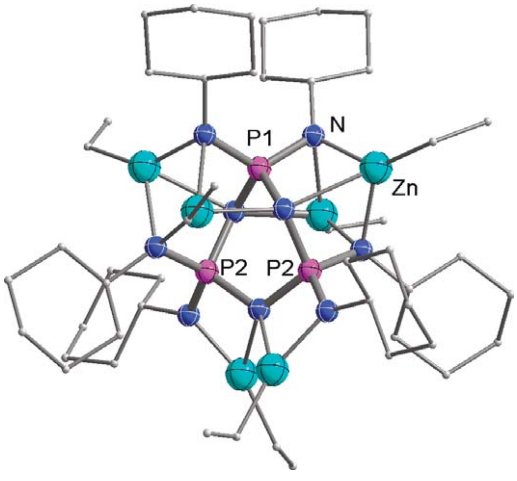

Figure 42 Solid-state structure and partial labeling scheme of **83**.

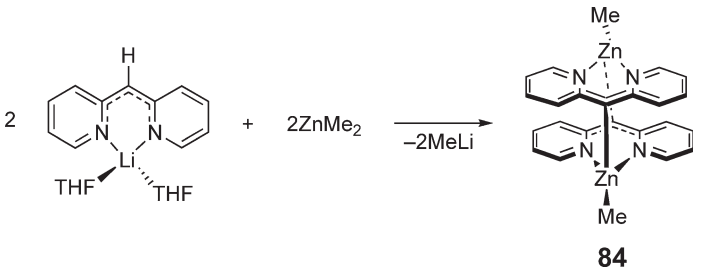

84

Scheme 65

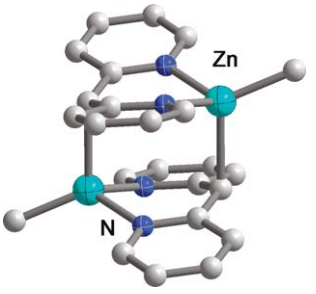

Figure 43 Solid-state structure and partial labeling scheme of **84**.

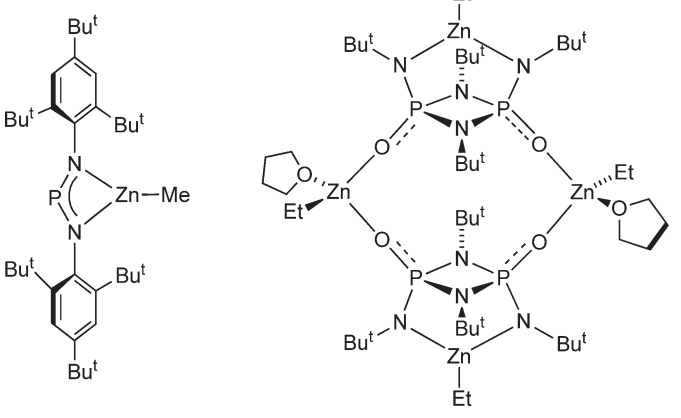

85 **87**

Figure 44

By contrast, the addition of 2 equiv. of $ZnMe_2$, Scheme 66, to the cyclodiarsazane *cis*-[Cy(H)NAs(μ-NCy)$_2$AsN(H)Cy] did not deprotonate the arsenic compound. The reaction proceeded instead with the transfer of the methyl group from zinc to arsenic and the rupture of the (As–N)$_2$ ring.[145]

A structurally similar cyclodiphosph(v)azane, however, was deprotonated with diethylzinc to provide the tetranuclear [{(O═PNBu^t)$_2$(μ-NBu^t)$_2$ZnEt}(ZnEt·THF)]$_2$ (Figure 44, **87**).[146] This dimer contains ethylzinc moieties in two chemically distinct environments, as seen in Figure 45, namely a three-coordinate, trigonal-planar ethylzinc group, chelated by both amido nitrogen atoms, and a four-coordinate, tetrahedral ethylzinc moiety that is coordinated by three oxygen atoms.

Secondary carboxylic amides of the type PhC(O)NR(H) were rapidly deprotonated with dimethylzinc to furnish mainly tetrameric and hexameric mono(methylzinc) derivatives.[147]

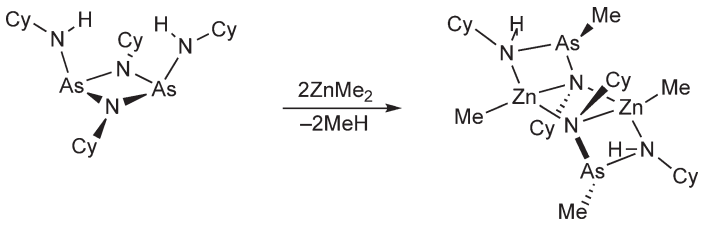

86

Scheme 66

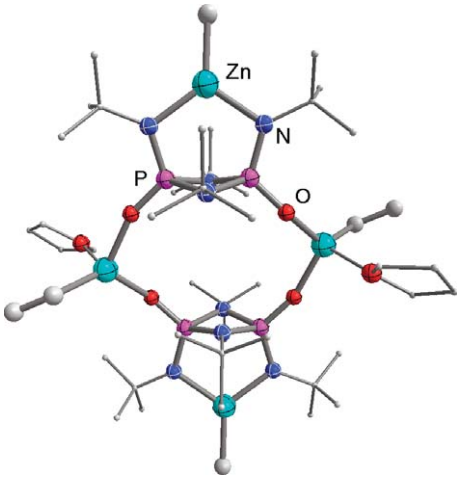

Figure 45 Solid-state structure and partial labeling scheme of **87**.

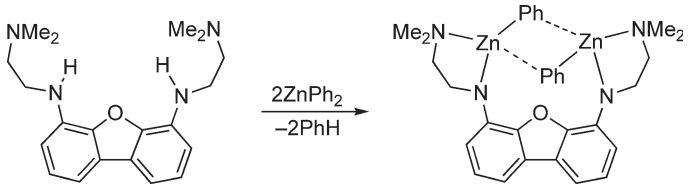

88

Scheme 67

A bis(secondary/tertiary) ligand reacted with diphenylzinc to afford the bis(phenylzinc) complex **88** (Scheme 67).[148] The unusual reactivity of this dinuclear species was demonstrated by its interactions with trimethylphosphine oxide and *N*,*N*-dimethylacetamide. In both cases, the products contained eight-membered rings incorporating both zinc atoms; the structure of the bis(trimethylphosphine oxide) product is shown in Figure 46.

2.06.10.4 Organozinc Compounds Bearing Chelating Diimines

Blackmore *et al.* investigated the organozinc chemistry of bulky 2,6-bis(α-iminoalkyl)pyridines, which had proved to be outstanding ligands for late transition metal polyolefin catalysts. Both dimethyl- and diethylzinc formed adducts with these tridentate ligands.[149] While the dimethylzinc adduct is stable, the diethylzinc analog, with its weaker Zn–C bond (see Section 2.06.4.7), reacted with ethyl transfer to the aromatic nitrogen atom, Scheme 68, to yield the stable *N*-alkylated complex **89**, Figure 47. Treatment of **89** with $B(C_6F_5)_3$ in dichloromethane gave a cationic complex, which

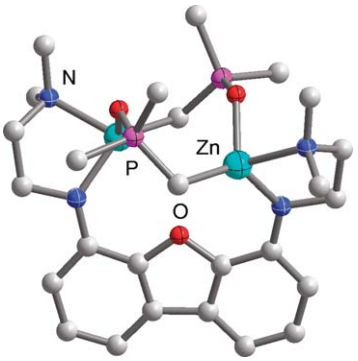

Figure 46 Solid-state structure and partial labeling scheme of $[(PhNC_2H_4NMe_2)ZnCH_2Me_2PO]_2$.

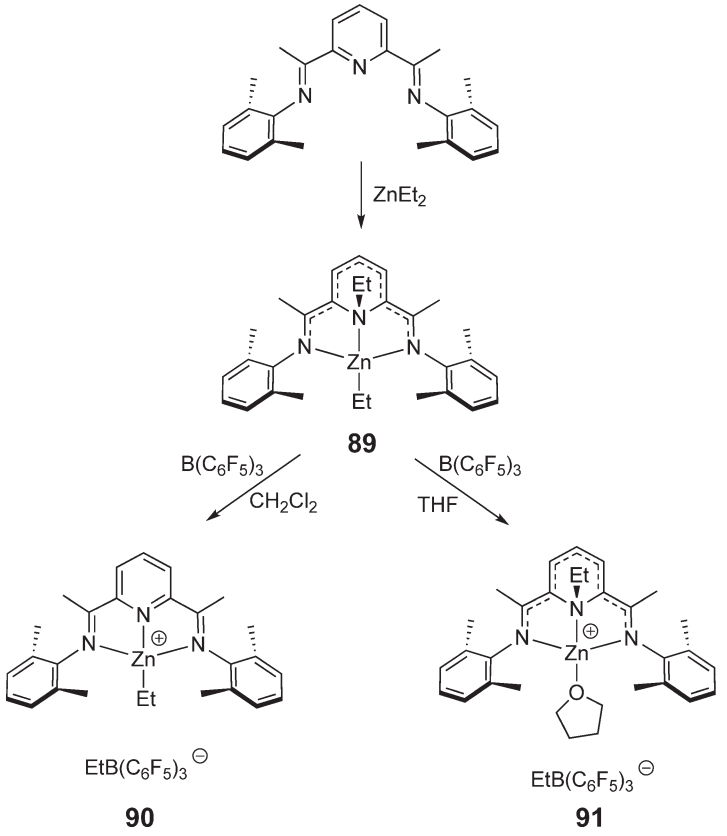

Scheme 68

then underwent ethyl group transfer from nitrogen to zinc **90**. In THF, by contrast, the strong coordination of the cyclic ether to zinc prevented such a transfer, affording **91** instead.

2.06.10.5 Organozinc Compounds Bearing Chelating Diiminates

Organozinc diiminates of various ligand platforms (particularly β-diketiminates (BDIs)) have been used extensively in catalysis, especially for the polymerizations of lactides and epoxides and the co-polymerization of epoxides with carbon dioxide.

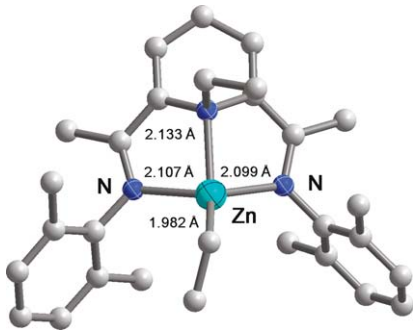

Figure 47 Solid-state structure, partial labeling scheme and selected bond lengths of **89**.

Moore *et al.* have systematically investigated the influence of these ligands' steric bulk on the catalytic activities of their zinc complexes.[150] The (BDI)zinc alkyl complexes are polymerization catalysts in their own rights, but they serve mainly as precursors for catalytically active β-diiminatozinc alkoxides and acetates. The ethylzinc β-diiminate **93** formed almost quantitatively upon treatment of the β-diketimine with diethylzinc (Scheme 69).[151] The analogous methylzinc **92** and phenylzinc **94** derivatives were reported almost simultaneously by Prust *et al.*[152] As the single crystal X-ray analysis of **93**, Figure 48, shows, these organozinc diketiminate complexes feature almost perfectly planar, six-membered rings in the solid state.

Exposure of **93** to dry oxygen furnished the corresponding ethyl peroxide complex, which is highly active for the expoxidation of enones, and crystallizes dimeric with bridging Zn–O bonds.[153]

The introduction of cyano groups in the 3-position of diketimiminate ligands greatly increased the crystallinity of their complexes (Figure 49, **95**), due to the formation of one-dimensional coordination polymers. A new β-oxo-δ-diimine ligand, in turn, allowed the synthesis of a bimetallic organozinc complex **96**, by the same methods that had been used for the syntheses of the mononuclear species **92–94**.[154]

Dove *et al.* designed and synthesized unsymmetrically substituted β-diketimininate ligands **97**, bearing bulky diisopropylphenyl and Lewis-basic anisyl groups for the purpose of lowering the Lewis acidity of their zinc complexes.[155] In both solution phase and the solid state, however, the oxygen atom does not seem to interact sufficiently with the zinc atom to have a noticeable effect on the Lewis acidity of the metal center.

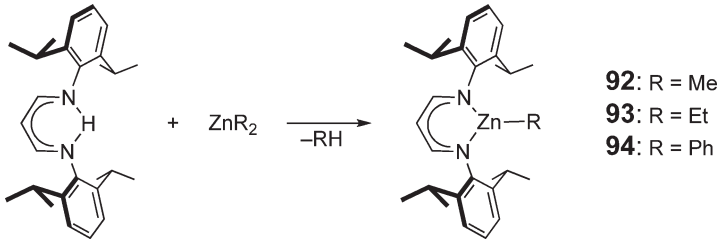

Scheme 69

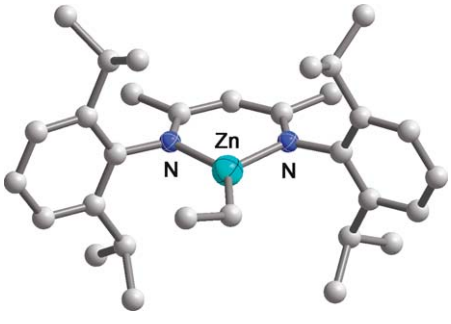

Figure 48 Solid-state structure and partial labeling scheme of **93**.

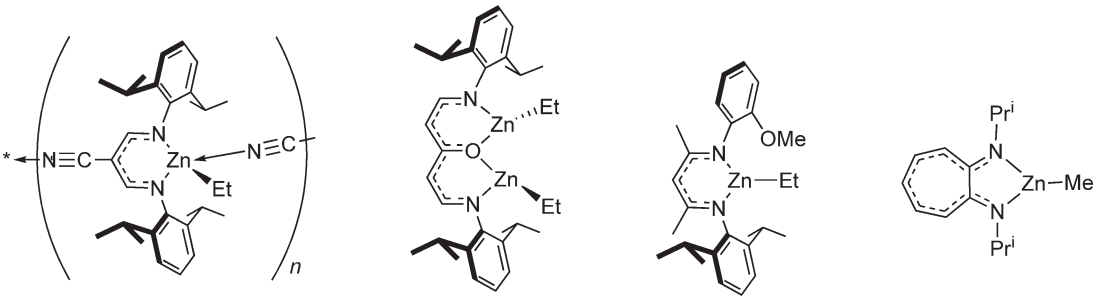

Figure 49

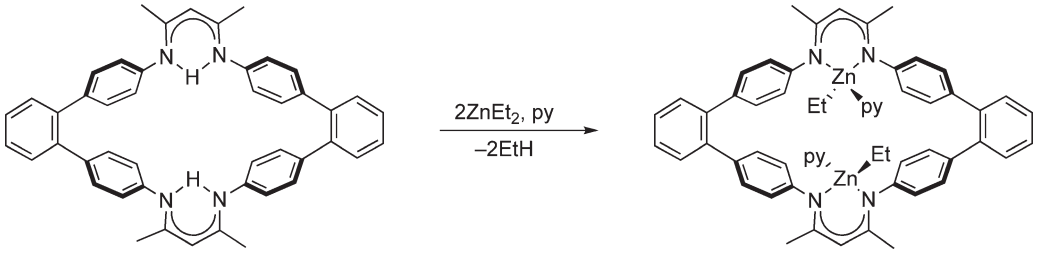

Scheme 70

Lee *et al*. incorporated two diketimine units into macrocycles that are large enough to allow the synthesis of dinuclear, rather than mononuclear, species. Treatment of these ligands, Scheme 70, with 2 equiv. of zinc in pyridine yielded the dinuclear bis(ethylzinc) complex **98**, featuring two proximal, co-facial ethylzinc centers.[156] The zinc–carbon (1.949(9) Å) and zinc–nitrogen (2.022(6) Å) bonds to the ligand have average lengths, while the donor bond from pyridine (2.267(8) Å) is expectedly longer.

A similar approach, but using a somewhat smaller and acyclic bis(aminotroponimine) ligand, Scheme 71, afforded the bis(organozinc) complexes **99** and **100**. Due to the structural flexibility of the ligand, the diorganozinc complexes adopted an "open" conformation with spatially remote trigonal-planar zinc centers. The analogous mono(aminotroponimine) yielded, on treatment with dimethylzinc, the mononuclear methylzinc compound **101**, shown in Figure 49.[157,158]

Although bis(iminophosphorano)methanides are structurally similar to BDIs, these phosphorus-containing ligands yield metallacycles with much more flexible backbones than diketiminates, a feature that is mainly due to the incomplete delocalization of the ligands' π-electrons. Thus, dimethylzinc deprotonated $H_2C(Ph_2P{=}NSiMe_3)_2$ (Scheme 72) to afford the methylzinc complex **102**, which adopted a boat conformation. This trigonal-planar zinc complex, in turn, reacted with adamantyl isocyanate to form a tetrahedral methylzinc complex **103**, bearing a new tripodal *N,N,N*-ligand, as shown in Figure 50.[159]

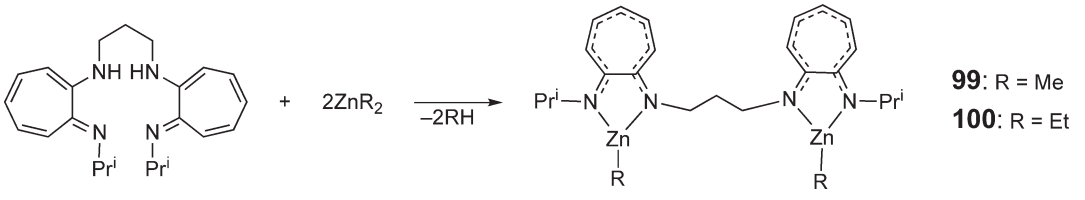

Scheme 71

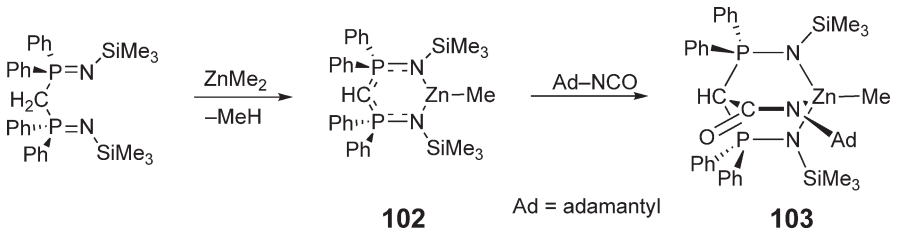

Scheme 72

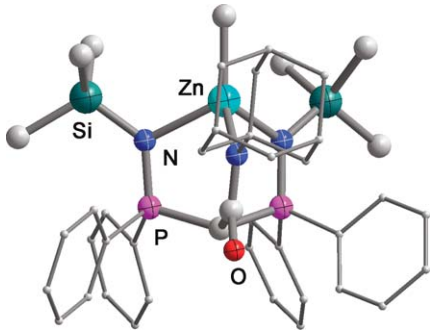

Figure 50 Solid-state structure and partial labeling scheme of **103**.

Hill and Hitchcock reported a methylzinc complex similar to **102**, but one bearing bulky *N*-aryl groups, for the stereoselective polymerization of lactides.[160]

2.06.10.6 Organozinc Compounds Bearing Pyrazolylborates and Related Bi- and Tridentate Ligands

The monoanionic, tridentate nitrogen donor tris(pyrazolyl)borate, Tp, has a long history of providing stable tetrahedral coordination environments for metals of varying sizes and oxidation states. The organozinc chemistry of tris(pyrazolyl)borates and similar ligands is currently focused on the role of such compounds as model systems for the active site in zinc enzymes and as precursors for catalysts that are useful in ring-opening polymerization reactions.

Consequently, many reports on pyrazolylborate–zinc compounds have dealt with the modification of the classical tris(pyrazolyl)borate design to better mimic specific enzyme sites,[161] or to improve the performance parameters of organozinc catalysts for the polymerization of cyclic esters. This was done by:

- changing the substituents on the pyrazolyl groups,
- replacing one or more of the pyrazolyl groups with hydrogen or donor functionalities, and
- synthesizing tridentate, boron-free ligands that are structurally similar to tris(pyrazolyl)borates.

Treatment of $ZnMe_2$ with the thallium salt of a bis(pyrazolyl)hydroborate gave the methylzinc complex [BpZnMe] **104** in which zinc is three coordinate.[162] This complex reacted with paraformaldehyde, Scheme 73, with the direct insertion of the CH_2O moiety into the B–H bond to produce the methylzinc complex **105** (Figure 51), in which zinc is tetrahedrally surrounded by the methyl group and the newly formed *N,N,O*-ligand.[163]

Silver and thallium salts of pyrazolylborates provide cleaner routes to metal complexes of these ligands than alkali metal derivatives. The silver complex $[HB\{3,5\text{-}Pz(CF_3)_2\}_3]Ag(THF)$, for example, reacted with diethylzinc to afford $[HB\{3,5\text{-}(CF_3)_2Pz\}_3]ZnEt$ **106**, shown in Figure 52, as the sole product.[164]

For applications in ring-opening catalysis of chiral lactides, pyrazolylborates have been suitably modified to yield chiral zinc complexes. An example of such a chiral pre-catalyst is the highly sterically encumbered tris(indazolyl)borate methylzinc complex **107**, introduced by Chisholm *et al.*, whose C_3-symmetric structure is shown in Figure 53.[165]

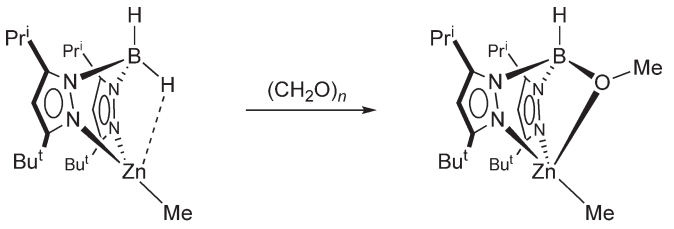

104 **105**

Scheme 73

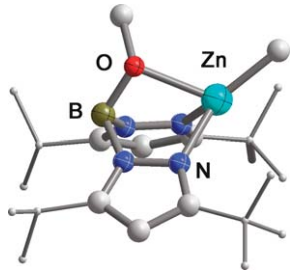

Figure 51 Solid-state structure and partial labeling scheme of 105.

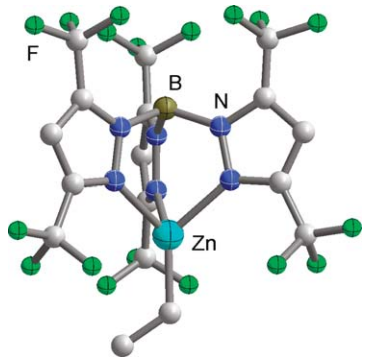

Figure 52 Solid-state structure and partial labeling scheme of **106**.

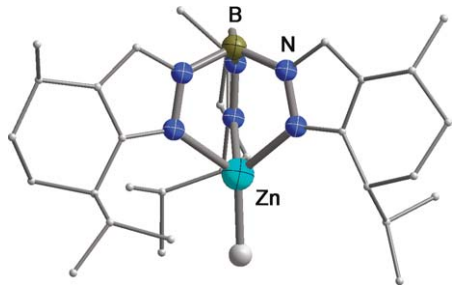

Figure 53 Solid-state structure and partial labeling scheme of **107**.

2.06.10.7 Organozinc Compounds Bearing 1,4-Diazabutadienes and Related Ligands

N,N′-disubstituted 1,4-diaza-1,3-butadienes (DAB) react with diorganozinc compounds to give colored adducts of the type $[R_2Zn\{R^1NC(H)C(H)NR^1\}]$ (**108**, Scheme 74).[166–169] These adducts are thermally stable at room temperature for $ZnMe_2$ and $Zn(CH_2SiMe_3)_2$, but they are unstable for all other diorganozinc compounds. Depending upon the substituents on zinc and on the diazabutadiene ligands, a variety of amido(imino)organozinc compounds were formed (see also Section 2.06.9.4).

Such reactions are initiated by a single electron transfer from the dialkylzinc moiety to the diazabutadiene ligand to afford radical pairs **109**, which collapse by the regioselective transfer of the organic radical to the nitrogen **110** or carbon **111** atoms of the diazabutadiene moiety. If the alkyl radical escapes from the organozinc radical, the latter dimerizes reversibly to **112** via the formation of a very long yet credible carbon–carbon bond.

In their outcomes, similar, but mechanistically different, coupling reactions were observed in the zincation of (*tert*-butyldimethylsilyl)(2-pyridinemethyl)amine (Scheme 75), which produced methylzinc(*tert*-butyldimethylsilyl)(2-pyridylmethyl)amide **113**. Thermolysis of **113**, or its treatment with one additional equivalent of dimethylzinc, yielded the C–C coupled dimer [1,2-bis(*tert*-butyldimethylsilylamido)-1,2-dipyridylethane]bis(methylzinc) **114**.[170]

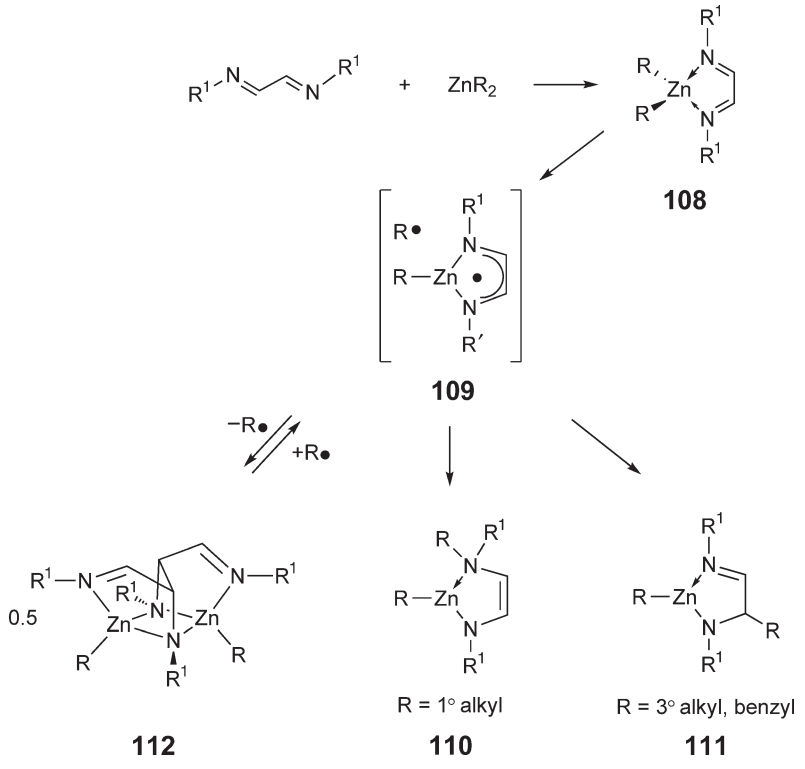

Scheme 74

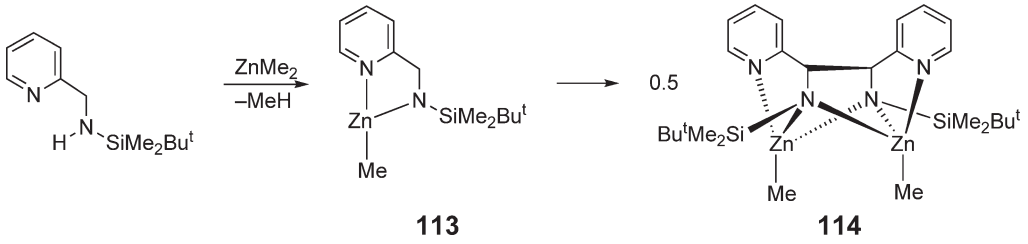

Scheme 75

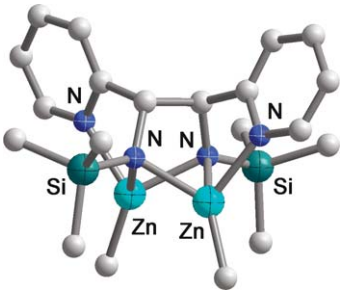

Figure 54 Solid-state structure and partial labeling scheme of **114**.

Figure 54 shows the solid-state structure of C_2-symmetric **114**, which crystallizes as a racemate of *S*,*S* and *R*,*R* isomers. The perspective view emphasizes the coupled ligand backbone and the tetrahedral coordination of both zinc atoms by three nitrogen atoms and one methyl group. The zinc–nitrogen bonds range in length from 2.088(2) to 2.157(2) Å, while the zinc–methyl bonds are 1.964(3) Å long.

The outcome of the reaction shown in Scheme 75 depends strongly on the nature of the metal and of the aromatic ring, but not on the steric bulk of the amine substituent.[171] Thus, dibutylmagnesium metallates the ligand without coupling, and the absence of ligand coupling was also noted when the pyridyl group was replaced with a phenyl ring. When this dinuclear zinc complex was treated with triisopropylsilylphosphine and arsine, the zinc methyl bond was cleaved and trinuclear zinc complexes **115** were formed.[172]

Protonolysis of **114** with acetamide yielded the free ligand in racemic form, namely as (1*S*,2*S*)- and (1*R*,2*R*)-1,2-dipyridyl-1,2-bis{(*tert*-butyldimethylsilyl)amino}ethane.[173]

The deprotonation of 2-pyridylmethylamine with dimethylzinc, Scheme 76, afforded methylzinc-2-pyridylmethylamide **116**, which crystallizes as a trimer, but exists in solution in a dimer–trimer equilibrium. A dinuclear zinc complex bearing a diamino(tetrapyridyl) ligand **117**, which must have been formed in a complex sequence of reactions, was isolated in low yield from a THF solution of **116**.[174]

A ligand similar to that in **116**, bis(2-pyridylmethyl)amine, reacted with diethylzinc as shown in Scheme 77 to form, after intramolecular rearrangements, the dinuclear complex **118**, which is the formal derivative of a *cis*-1,2-dipyridylimidoethene.[175]

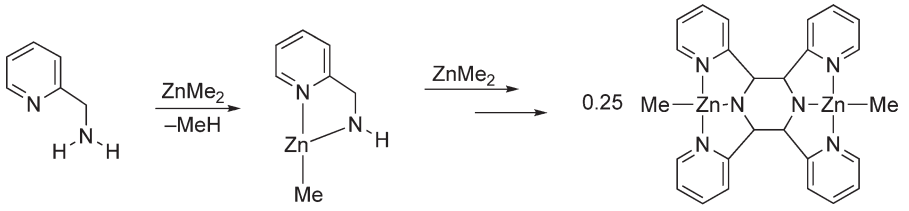

Scheme 76

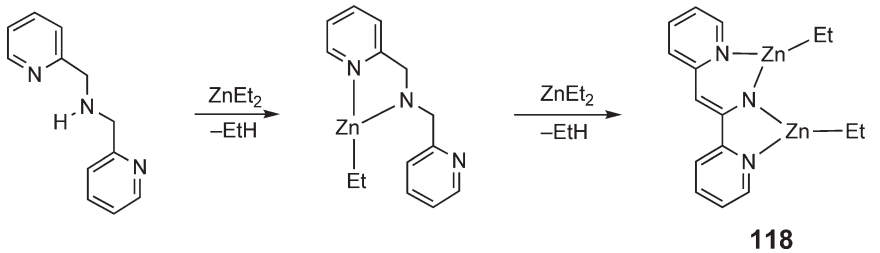

Scheme 77

2.06.10.8 Organozinc Amide/Phosphorus Ylides and Organozinc Iminophosphoranes

Methylenetriphenylphosphorane reacted with $Zn\{N(SiMe_3)_2\}_2$ in a multistep reaction (Scheme 78) to furnish initially the 1,3-dizincatacyclobutane **119**, featuring two three-coordinate zinc atoms, and finally the α-zincated phosphorus ylide **120**.[176]

When the trimethylphosphoraneiminatozinc bromide heterocube $[ZnBr(NPMe_3)]_4$ was treated with MeLi,[177] Bu^nLi,[177] Me_3SiC_2Li, and Me_3SiC_4Li,[178] the corresponding alkyl- and alkynylzinc heterocubanes $[ZnR(NPMe_3)]_4$ (R = Me, Bu^n, C_2SiMe, **121**, and C_4SiMe) were obtained (Scheme 79). The solid-state structure of **121** is shown in Figure 55.

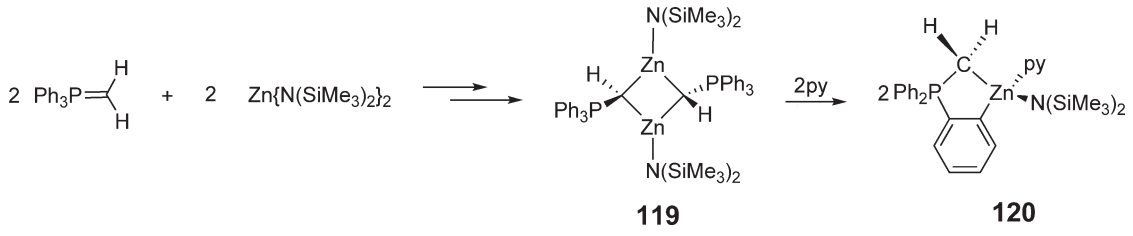

Scheme 78

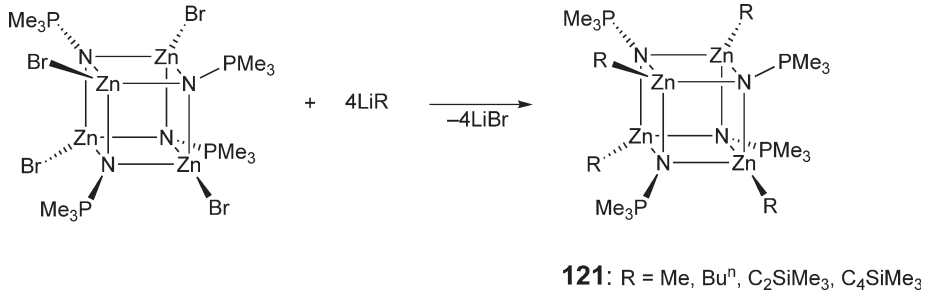

Scheme 79

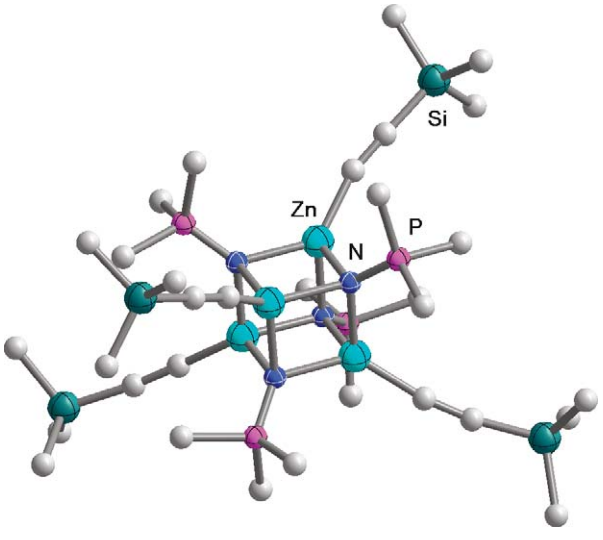

Figure 55 Solid-state structure and partial labeling scheme of **121**.

2.06.11 Organozinc Compounds Bearing Heavier Group 15 Donor Ligands

There were significantly fewer reports on organozinc compounds bearing ligands with heavier group 15 donors than those on organozinc amides. This is mainly due to the weakness of the zinc–pnictide bonds, which rules out the use of Zn–E moieties in functional molecules. The instability of these bonds, however, has been exploited for the synthesis of zinc–pnictide materials.

Organozinc phosphides have been investigated because they are precursors for binary and ternary phosphides, such as Zn_3P_2 or $ZnSnP_2$, which have applications as semi-conductors, infrared detectors, and light-emitting diodes. A variety of dialkylzincs (R = Me, Et, Pr^i, Bu^t, Bu^n, CH_2SiMe_3) reacted with $HE(SiMe_3)_2$, E = P, As, Scheme 80, to furnish the alkylzincphosphido or -arsenido heterocycles of the composition $[RZnE(SiMe_3)_2]_n$, $n = 2$, 3, the trimeric phosphorus analog of which is shown in Figure 56.[179] Depending upon the steric bulk of the organic zinc substituents, these species are dimeric or trimeric in solution, occasionally exhibiting dimer–trimer equilibria. For sufficiently bulky organic substituents on zinc, even monomeric compounds are accessible. Thus, $(Me_3Si)_3CZnCl$ reacted with $LiP(SiMe_3)_2$ to yield $(Me_3Si)_3CZnP(SiMe_3)_2$, whose monomeric solution structure was supported by cryoscopic measurements.[180] All compounds have limited thermal stability, decomposing in solution within days and in the solid state within weeks when kept at room temperature.

Because of the additional reactivity introduced by the second hydrogen atom, organozincphosphido and arsenido complexes of primary phosphines and arsines are quite rare. The sequential addition of $ZnMe_2$ and $Sb(NMe_2)_3$ to H_2PBu^t, Scheme 81, did not afford the targeted heterobimetallic $[\{Sb(PBu^t)_3\}(ZnMe)_3]_n$, but produced instead the zinc phosphide dimethylamine adduct $[MeZn(PBu^t)\cdot HNMe_2]_3$ **122**.[181] This trimeric heterocycle, which is the first organozinc compound of a primary phosphide, adopts the half-boat structure shown in Figure 57.

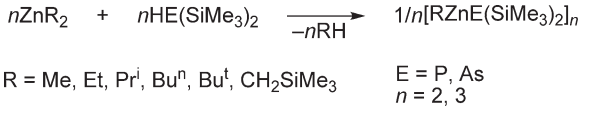

Scheme 80

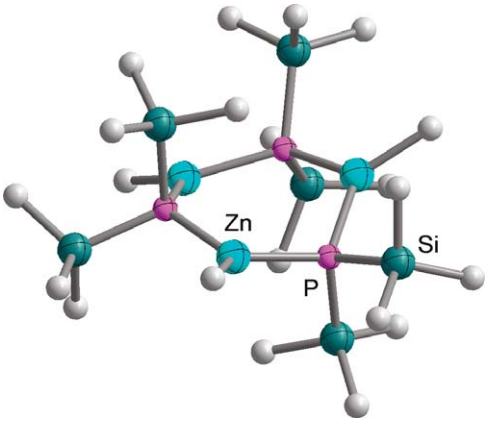

Figure 56 Solid-state structure and partial labeling scheme of $[MeZnP(SiMe_3)_2]_3$.

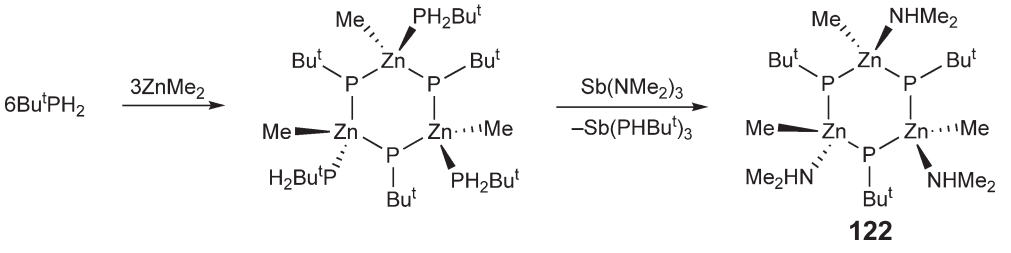

Scheme 81

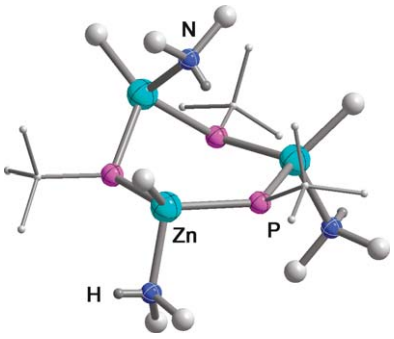

Figure 57 Solid-state structure and partial labeling scheme of $[MeZn(PBu^t)\cdot HNMe_2]_3$ **122**.

2.06.12 Organozinc Compounds Bearing Alkoxides, Siloxides, Boryloxides, Complex Oxides, and Related Ligands

2.06.12.1 Organozinc Compounds Bearing Simple Alkoxides and Related Monodentate Oxygen Donors

Because of their ease of crystallization, alkylzinc alkoxides are often isolated as decomposition products in reactions involving organozinc compounds. The methylzinc lithium *tert*-butoxide heterocubes $[\{(THF)LiOBu^t\}_2(MeZnOBu^t)_2]$[182] (Figure 58, **123**) and $[(LiOBu^t)(MeZnOBu^t)_3]$[183] **124** were isolated as hydrolysis products from reactions involving amines, amidines, *tert*-butyllithium, and dimethylzinc.

Heterobimetallic clusters (Figure 58, **125** and **126**) with solvent-dependent structures were also obtained upon mixing alkali metal *tert*-butoxides and –trimethylsiloxides in THF, TMEDA, and toluene.[184] The common occurrence of heterocubes shows that there is a strong driving force for the formation of heterocubic structures in organozinc alkoxides. Solvent effects are important, however, as demonstrated by the formation of *seco*-diheterocubic compounds in TMEDA.

Protonolysis of diarylzinc compounds of the type $ZnAr_2$ (Ar = *p*-CF_3-C_6H_4, C_6F_5, 2,4,6-Me-C_6H_2) by the sterically encumbered alcohol $(Pr^i)_2CHOH$ furnished di- and trinuclear arylzinc alkoxides of the general formula $[(Ar)_a(Zn)_b(OR)_c]$, $a = 2$; $b = 2$, 3; $c = 2$, 4.[41] The solid-state structure of the trinuclear complex $[(C_6F_5)Zn\{\mu\text{-}(Pr^i)_2CHO\}_2Zn\{\mu\text{-}(Pr^i)_2CHO\}_2Zn(C_6F_5)]$ **127** is shown in Figure 59. The zinc–carbon bonds in these compounds are isometric (1.943(2) Å), while the zinc–oxygen bonds range from 1.911(1) to 1.955(1) Å. None of these complexes is active for the homopolymerization of propylene oxide or its co-polymerization with CO_2, suggesting that terminal alkoxides are necessary to initiate and propagate the polymerization process.

Iodomethylzinc alkoxides are likely intermediates in the Simmons–Smith cyclopropanation of prochiral allylic alcohols. The methanolysis of $ZnEt_2$ furnished MeOZnEt, which reacted with CH_2I_2 to yield iodomethylzinc methoxide.[185] The product is isolated in the form of the centrosymmetric, corner-sharing diheterocubane $[(MeO)_8Zn_7(CH_2I)_6]$ **128**, whose structure is shown in Figure 60.

Related halomethylzinc alkoxides, which are monomeric in solution, were studied for their effectiveness in cyclopropanation reactions. The Lewis acid-catalyzed reaction is the only reaction pathway at low temperature and

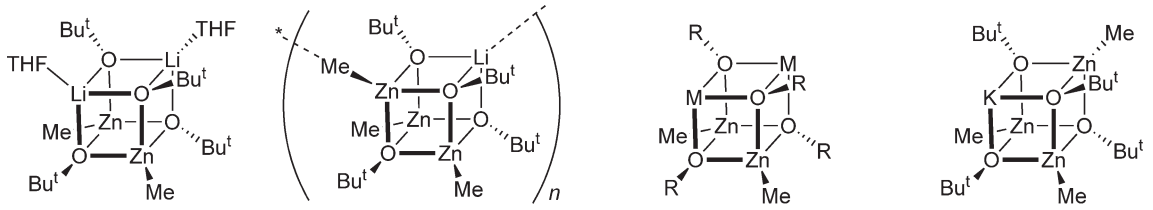

Figure 58

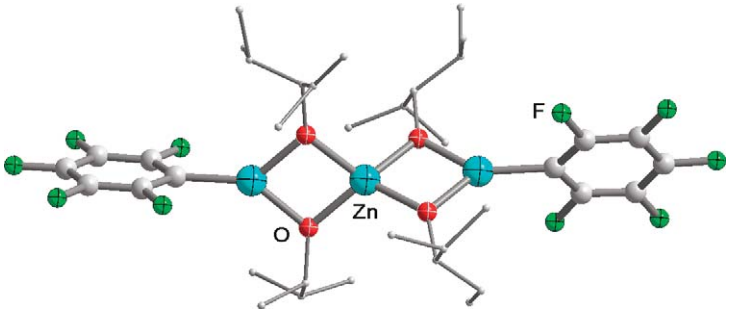

Figure 59 Solid-state structure and partial labeling scheme of **127**.

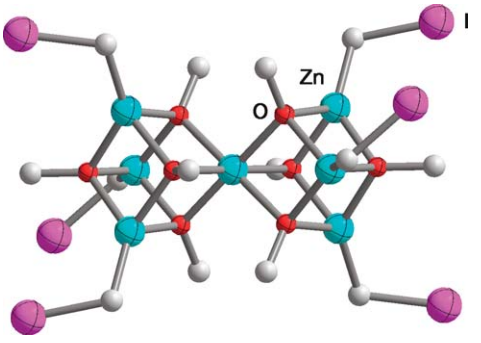

Figure 60 Solid-state structure and partial labeling scheme of **128**.

the predominant mechanism at higher temperatures. The halomethylzinc alkoxides of 4-methoxybenzyl alcohol were structurally characterized and shown to be heterocubes of the composition $[XCH_2ZnOCH_2C_6H_4p\text{-}OMe]_4$, X = Cl, I.[186]

Diorganoboryloxides, R_2BO^-, bearing bulky organic substituents are quasi-alkoxide ligands for main group and transition metals. Because of the π-acceptor properties of boron, these anions are weaker π-donors than alkoxides, and this is reflected in their structural chemistry. Diethylzinc reacted with the borinic anhydride $(9\text{-BBN})_2O$, Scheme 82, to afford the alkylzincboryloxide $[EtZnO(9\text{-BBN})]_4$ **129**, which also crystallizes in heterocubic form.[187]

By contrast, the sterically bulkier dimesitylborinic acid reacted with diethylzinc with the formation of the dimer **130**, Figure 61, which was cleaved by the addition of bipyridine to give a monomeric bipyridine adduct.[188] An analogous four-membered ring compound was obtained from the protonolysis of $ZnMe_2$ with dimesitylborinic acid. To probe the electronic effects of the boryloxide ligands in these compounds, dimethylzinc was also treated with dimesitylmethanol to afford an analogous boron-free dimeric alkoxide.[189]

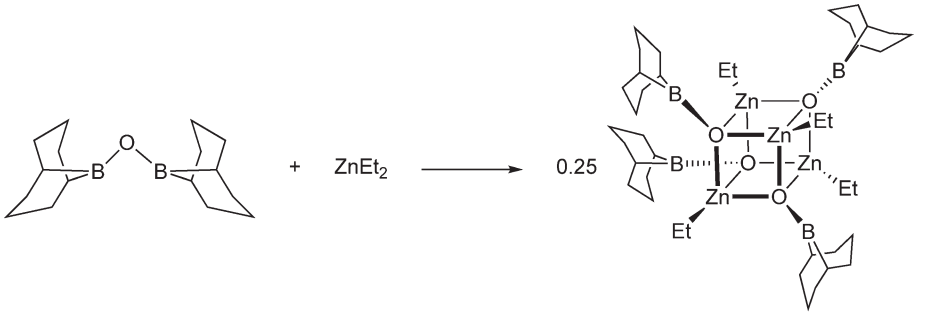

129

Scheme 82

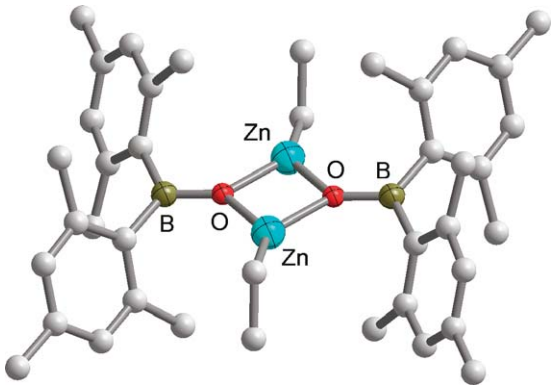

Figure 61 Solid-state structure and partial labeling scheme of **130**.

2.06.12.2 Organozinc Compounds Bearing Siloxides and Phosphonates

The controlled protonolysis of dialkylzincs with triorganosilanols and diorganodisilanols (Scheme 83),[190,191] yielded, depending upon the steric bulk of the dialkylzincs and the silanols, four-membered rings, spirocycles **131**, polycyclic compounds, and heterocubes **132**.

Predictably, alkyltrisilanols react with dialkylzincs to yield larger aggregates, such as **133**, which are much more inorganic in nature than those formed by mono- and disilanols (Scheme 84). Often these zinc siloxanes are without direct zinc–carbon bonds and resemble the silicates for which they serve as model compounds.[192] The specific structures of these products depend heavily on the substituents of the silanetriols and diorganozincs, as well as the reaction stoichiometries.[193]

Organophosphonates are isoelectronic with organotrisiloxides. Like zinc siloxides and zinc siloxanes, zinc phosphonates are actively investigated as porous materials, for applications in catalysis, as molecular sieves, and for electronic devices. Dimethyl- and diethylzinc reacted with *tert*-butylphosphonic acid in THF solution to furnish,

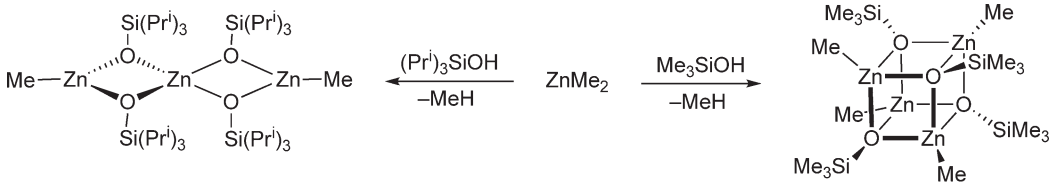

131 **132**

Scheme 83

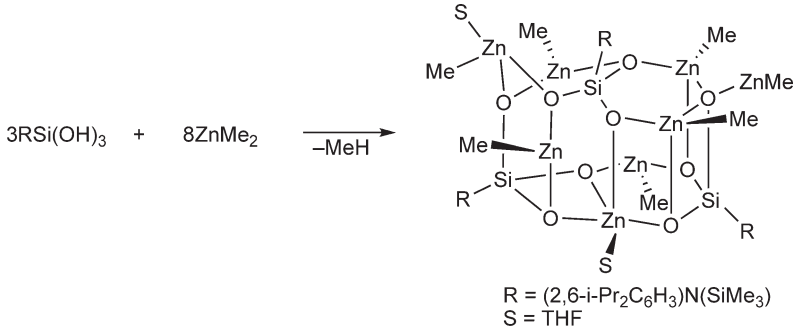

133

Scheme 84

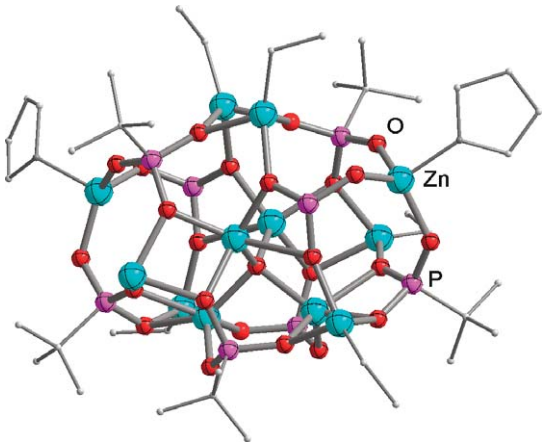

Figure 62 Solid-state structure and partial labeling scheme of **134**. Some of the organic substituents have been omitted to improve clarity.

depending upon the ratio of diorganozinc compound to acid and the organic substituents on zinc, organozinc phosphonates of widely differing nuclearity and structures. Thus, the dodecanuclear organozinc phosphonate $[Zn_2(THF)_2(EtZn)_6Zn_4(\mu_4\text{-}O)(Bu^tPO_3)_8]$ **134**, Figure 62, was isolated if the ratio of $ZnEt_2$ to *tert*-butylphosphonic acid was 1.5 : 1,[194] whereas if the ratio. $ZnMe_2$ to $Bu^tRP(O)(OH)_2$ ratio was 2 : 1, then a much more open tetranuclear organozinc phosphonate was produced.[195]

2.06.12.3 Organozinc Alkoxides Derived From Diols, Triols, and Related Compounds

Chisholm *et al.* synthesized organozinc compounds with bulky biphenolates as catalysts for the ring-opening polymerization of lactides.[196] The protonolysis of diethyzinc by the biphenols, in the presence of diisopropylmethanol, afforded the polycyclic, trimetallic zinc–di(ethylzinc) pre-catalyst **135**, which polymerizes *rac*-lactide to polylactide, enriched in *isi*- and *sis*-tetrads (Scheme 85).

The interactions of dimethyl- and diethylzinc with bulky tris(hydroxyphenyl)methanes, Scheme 86, yielded, depending on the reaction conditions, a variety of alkylzinc alkoxides, featuring two-, three-, and four-coordinate zinc centers. These polynuclear compounds (Figure 63 shows the trinuclear ethylzinc derivative **136**) are relatively poor catalysts for the co-polymerization of cyclohexene oxide and carbon dioxide.[197]

The mono- and dinuclear ethylzinc complexes **137** and **138**, respectively, were obtained when a 1,3-dimethylether *p*-Bu^t-calix[4]arene was treated with one and two equivalents of diethylzinc (Scheme 87).[198] Excess $[ZnEt_2(tmeda)]$, in turn, reacted with this calixarene to furnish a pentanuclear dicalixarene. The syntheses and structures of related diorganozinc calixarenes, featuring both identical and non-identical organozinc moieties, were reported recently.[199] The solid-state structure of the bis(ethylzinc)-1,3-dibenzylether-*p*-Bu^t-calix[4]arene **139**, which bears a close resemblance to **138**, is shown in Figure 64.

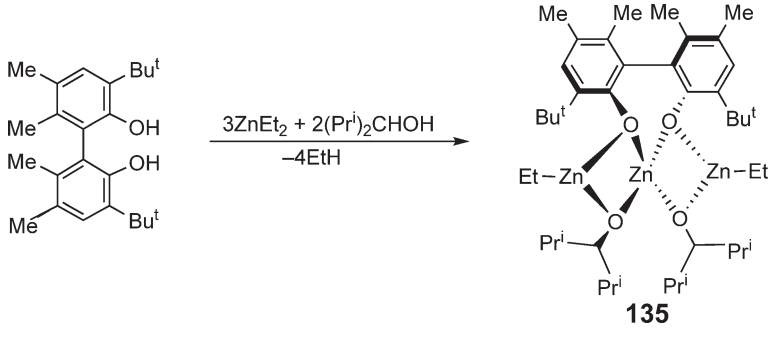

Scheme 85

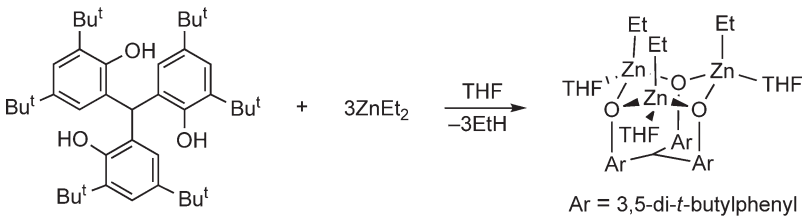

136

Scheme 86

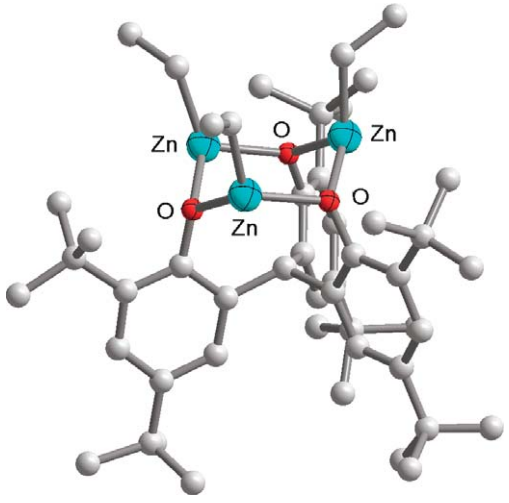

Figure 63 Solid-state structure and partial labeling scheme of **136**.

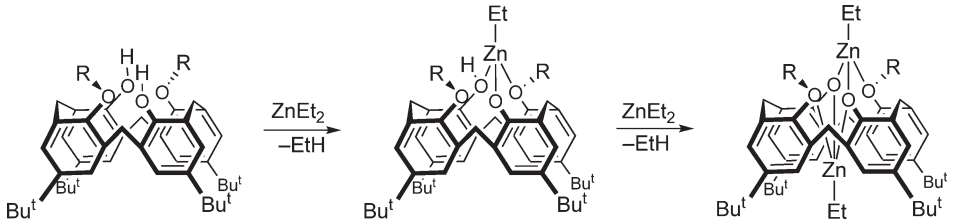

137 138

Scheme 87

Acetylacetone was deprotonated with diethylzinc in toluene to afford $[EtZn(acac)]_2$ (Figure 65, **140**) which crystallized in dimeric form. The quality of the X-ray data was too low to obtain reliable bond parameters, but the coordination environment about zinc is distorted tetrahedral, with two intramolecular and one intermolecular Zn–O bond.[200]

Various diorganozinc compounds (ZnR_2; R = Me, Et, Pr, Pr^i, Bu^t, Ph) reacted with *o*-quinones by two mechanisms, namely (i) a single-electron transfer from ZnR_2 to the quinone to yield, after hydrolysis, alkyl(phenyl)oxyphenols, and (ii) a polar 1,2- and 1,4-addition of ZnR_2 similar to those of conjugated ketones.[201] Diorganozinc compounds with low ionization potentials favor a polar mechanism.

2.06.12.4 Organozinc Carbamates and Organozinc Thiocarbamates

Organozinc carbamates are typically made by the CO_2 insertion into the Zn–N bonds of organozinc amides, Scheme 88, and isolated as oligomers.[202] Occasionally, alkylzinc carbamates are obtained that are "rich" in carbamate

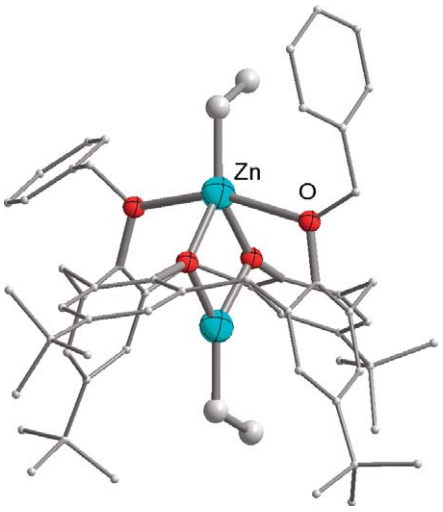

Figure 64 Solid-state structure and partial labeling scheme of **139**.

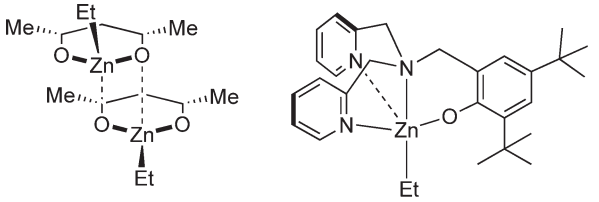

140 **151**

Figure 65

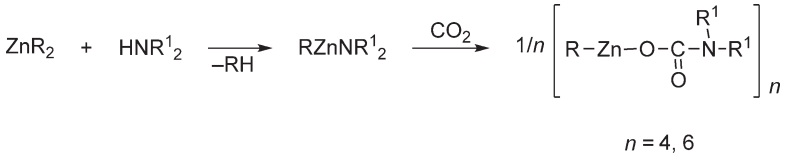

Scheme 88

moieties, for example, $[Zn_4Me_2(O_2CNEt_2)_6]$ (**141**, Figure 66), due to the presence of zinc dicarbamates ($Zn(O_2CNR_2)_2$, which were formed by the complete protonolysis of ZnR_2 with excess secondary amine.[204]

These carbamate-rich species can be converted to conventional alkylzinc carbamates by treatment with excess dialkylzinc. Donor solvents force the dissociation of the alkylzinc carbamate aggregates to give complexes of lower nuclearity. For example, pyridine converts the tetrameric $[MeZn(O_2CNPr^i)_2]_4$ to the dimeric $[MeZn\{O_2CN(Pr^i)_2\}(py)]_2$ **142**, shown in Figure 67.[204]

The monothiocarbamato complex $[Et_4Zn(OSCNEt_2)_2(NEt_2)_2]$ was obtained by bubbling COS through an *in situ* prepared $Zn(NEt_2)_2$ solution.[205] Here, the tetranuclear aggregate was low in thiocarbamate and rich in bis(diethylamido)zinc, due to the incomplete insertion of COS.

2.06.12.5 Organozinc Compounds Bearing Aminoalkoxides

The ethylzinc compound **143**, created from a bulky diaminophenol by treatment with $ZnEt_2$, as shown in Scheme 89, was synthesized for the purpose of creating a well-defined zinc catalyst for the polymerization of lactides.[206]

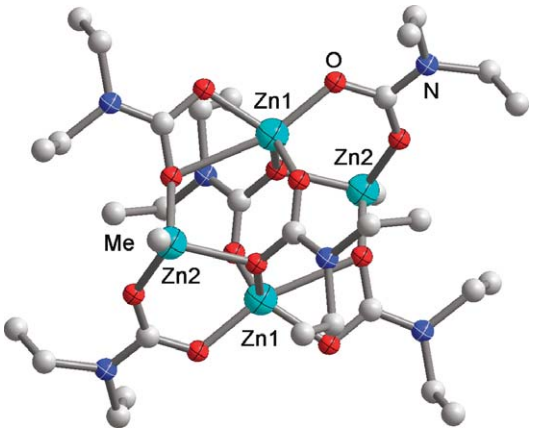

Figure 66 Solid-state structure and partial labeling scheme of **141**.

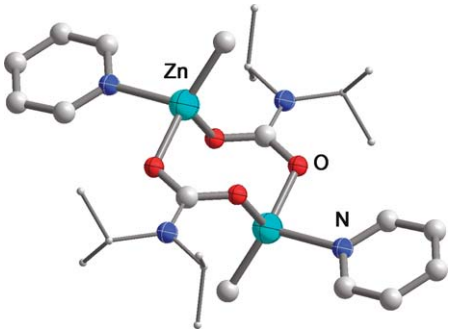

Figure 67 Solid-state structure and partial labeling scheme of **142**.

The coordination geometry about zinc is pseudo-tetrahedral with long zinc–nitrogen (av. 2.139(3) Å), zinc–carbon (1.997(4) Å), and zinc–oxygen (1.956(2) Å) bonds.

The alkylation of prochiral aldehydes to chiral alcohols is catalyzed by monomeric, chiral β-aminoalkoxide-complexed zincalkyls, which exhibit strong chiral amplification effects. In other words, the catalysts produce chiral products in much greater excess than expected based on the ee of the catalyst. It was shown that in scalemic mixtures, that is, mixtures with unequal amounts of both enantiomers, of alkylzinc derivatives of (2*S*)- and (2*R*)-3-*exo*-(dimethylamino)isoborneol three species exist in solution, namely the homochiral (*S,S*)-**144** and (*R,R*)-**144** dimers, and the heterochiral (*S,R*)-**144** dimer (Scheme 90).[207] Because the dissociation constants for the homochiral dimers ($K_d = 3 \times 10^{-2}$) are larger than those for the heterochiral dimer ($K_d = 1 \times 10^{-5}$), the former are much more dissociated into their catalytically active monomers, allowing only the catalytic activity of the largely dissociated homochiral dimers to be expressed.[209] Consequently, catalyst mixtures having a 20% ee of one isomer can produce chiral alcohols with ee's as high as 88%. The solid-state structure of the heterochiral (*S,R*)-**144** dimer, Figure 68, shows the reduced steric repulsion, which is responsible for its lower dissociation constant.

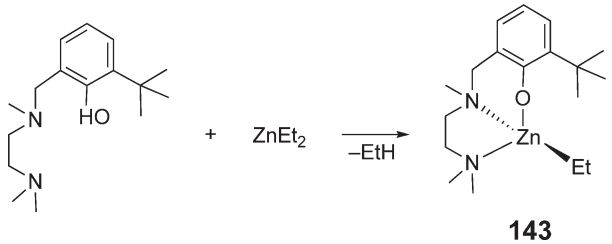

143

Scheme 89

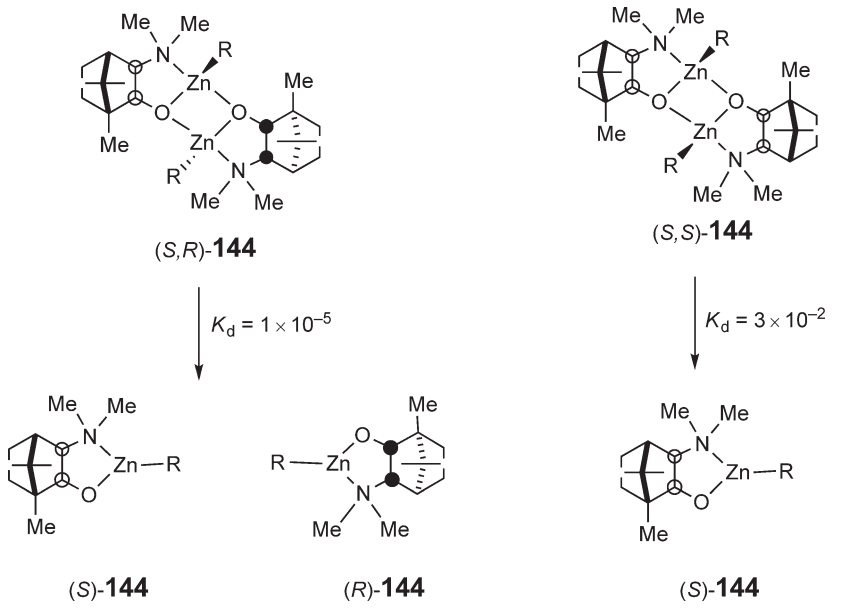

Scheme 90

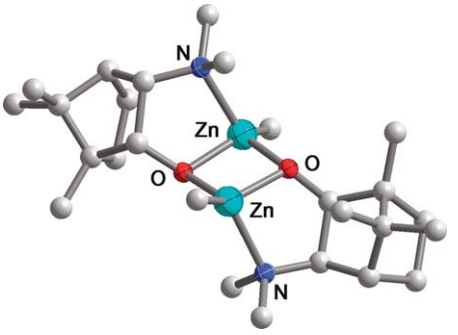

Figure 68 Solid-state structure and partial labeling scheme of the heterochiral dimer (*S,R*)-**144**.

In a related study involving structurally similar chiral methylzinc anisyl fencholates, both chiral amplification and depletion were observed in the catalytic alkylations of benzaldehyde.[209] Thus, methylzinc anisyl fencholates, bearing sterically small substituents in the *ortho*-position of the anisyl group, crystallized preferentially as homochiral dimers, as shown for the methyl-substituted anisyl group in Scheme 91. Because of the greater stability of the homochiral dimers, scalemic mixtures of both enantiomers of the ligand showed a chiral depletion of the benzyl alcohol.

By constrast, the methylzinc complexes bearing the sterically more encumbered anisyl fencholates with *tert*-butyl and trimethylsilyl substituents dimerized preferentially in the heterochiral form, resulting in the more common chiral amplification effects observed for classical dimethylaminoisoborneol systems.

Figure 69 shows the solid-state structure of the thermodynamically more stable homochiral dimer (*R,R*)-**145**,[210] which features a highly puckered central $(Zn–O)_2$ ring with almost isometric Zn–O bond lengths.

Chiral methylzinc aminoalkoxides **146a–c** were obtained from the reaction of $ZnMe_2$ with aminoalcohols, having chiral centers in their carbon backbones (Scheme 92).[211] The methylzinc aminoalkoxides crystallize dimeric and trimeric with the formation of intermolecular zinc–oxygen bonds and creation of additional chiral centers.

A chiral ethylzinc aminoalkoxide **147**, synthesized by the addition of $ZnEt_2$ to (*S*)-diphenyl(pyrrolidin-2-yl)methanol, Scheme 93,[212] catalyzes the asymmetric co-polymerization of cyclohexene oxide with CO_2 in almost quantitative yield and with an ee of 49%. This value is somewhat lower than that obtained by the same authors from the *in situ* generated monomeric form of the catalyst, which furnished product with an ee of 70%.[213]

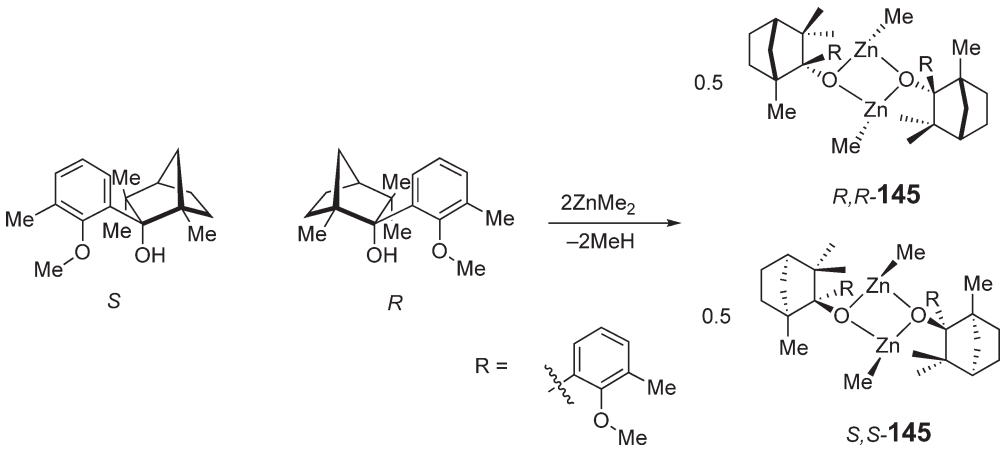

Scheme 91

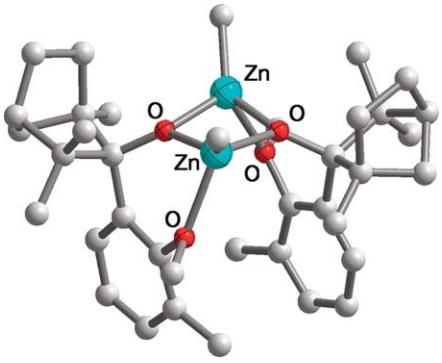

Figure 69 Solid-state structure and partial labeling scheme of the homochiral dimer *R,R*-**145**.

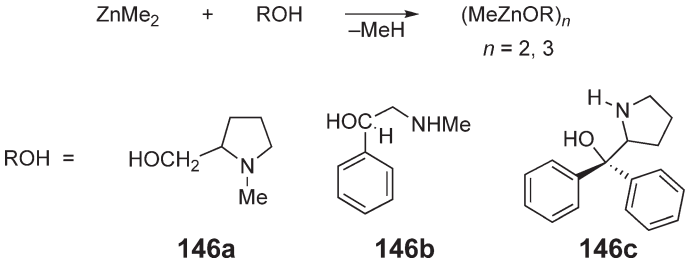

Scheme 92

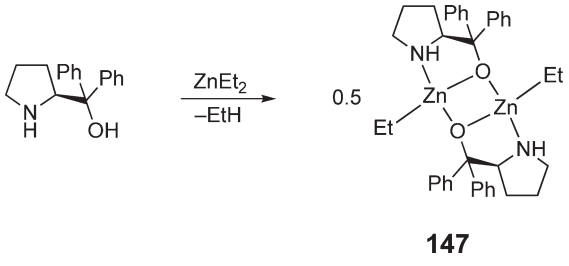

Scheme 93

2.06.12.6 Organozinc Alkoxides Bearing Chelating Mixed Donor Ligands

Enantiomerically pure and racemic β-carbonyl sulfoximes were treated with diethylzinc to afford the corresponding ethylzinc enolates **148a–c** in both racemic and optically active forms (Scheme 94).[214] Despite their rather similar solution structures, these complexes exhibited markedly different solid-state structures and reactivities with electrophiles.

The seemingly straightforward protonolysis of $ZnMe_2$ with 2-(methylthio)ethanol in CH_2Cl_2 (Scheme 95) afforded $[MeZn(\mu_3\text{-}OCH_2CH_2SMe)Zn(\mu\text{-}Cl)Me]_2$ **149**.[215] The presence of both methyl and chloride substituents on zinc suggests that the solvent (CH_2Cl_2) is involved in the reaction, which should call into question the use of dichloromethane as solvent in the Simmons–Smith reaction.

Another functionalized alcohol, namely 2-aziridineethanol (azol), reacted with diethylzinc to yield almost quantitatively the ethylzinc alkoxide EtZn(azol), which is trimeric in solution.[216] The introduction of dry dioxygen into solutions of EtZn(azol) gave the peroxoethylzinc alkoxide EtOOZn(azol), which co-crystallized with EtZn(azol) in a 1 : 1 ratio as a face-sharing di-*seco*-heterocube **150** (Figure 70).

The two chemically different zinc atoms show decidedly different coordination environments. Thus, the "inorganic" zinc atom (Zn1) has an octahedral environment and is surrounded by four oxygen and two nitrogen atoms, while the "organometallic" zinc atom (Zn2) is in the pseudo-tetrahedral environment of one ethyl group and three oxygen atoms.

Trösch and Vahrenkamp reported a bis(2-picolyl)(2-hydroxy-3,5-di-*tert*butylbenzyl)amine ethylzinc complex **151** (Figure 65) as a model compound for the active site of zinc enzymes.[217]

Despite the importance of organozinc catalysts bearing β-aminoalkoxides in asymmetric catalysis, there has been no comprehensive computational screening of suitable monoprotic and aprotic bidentate chelating ligands for this

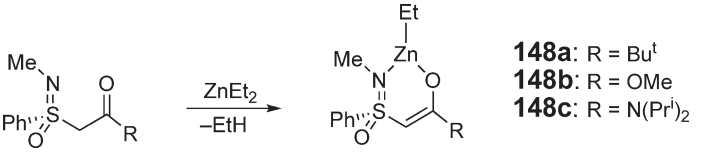

Scheme 94

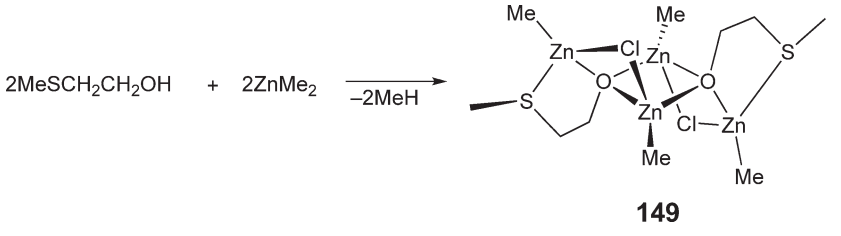

Scheme 95

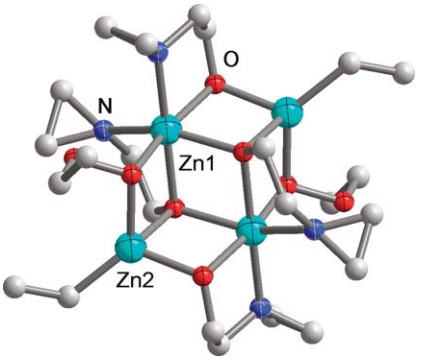

Figure 70 Solid-state structure and partial labeling scheme of **150**.

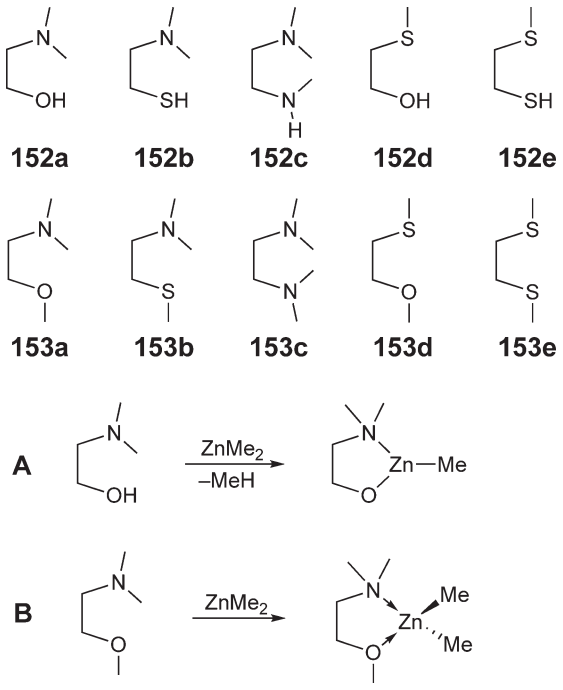

Scheme 96

reaction. A study at the HF and B3LYP levels of theory sought to discover the variations in energies and structures that occur when the ligands **152a–e** and **153a–e** react with dimethylzinc (Scheme 96).[218] Not unexpectedly the enthalpies of formation for the methylzinc complexes derived from protic ligands **152a–e** (A) are almost one order of magnitude larger (-84 to $-126\,kJ\,mol^{-1}$) than those obtained for the dimethylzinc adducts of the neutral ligands **153a–e** (-8 to $-38\,kJ\,mol^{-1}$). The absolute values of the enthalpies of formation for reaction A decrease in the order NS > SS > NO > NN > OO, while for reaction B the order is NN > NO > NS > OO > SS. Given the importance of aminoalcohols as ligands in the stereospecific alkylation of aldehydes, the position of the NO ligands appears to be too low. It is not surprising, however, that only the **152** ZnMe complexes are capable of coordinating a second equivalent of $ZnMe_2$ exothermically, a feature that is essential for the successful alkylation of aldehydes.

2.06.13 Organozinc Compounds Bearing Heavier Group 16 Donor Ligands

2.06.13.1 Introduction

Reports on the organozinc chemistry with heavier group 16 donor ligands for the reviewed period were limited to sulfur donors. As with the organozinc chemistry of anionic oxygen donors, three themes dominate this area of research, namely the use of organozinc compounds:

- as model systems for zinc enzymes,
- as precursors for new zinc chalcogenides, and
- as enantioselective catalysts in organic transformations.

2.06.13.2 Organozinc Compounds Bearing Heavier Group 16 Donor Ligands as Model Systems for Enzymes

In most zinc enzymes, the metal is tetrahedrally coordinated by either nitrogen atoms alone or by a combination of nitrogen and oxygen atoms. To model zinc enzymes having the much rarer S-donor environments, a number of approaches have been pursued. The most direct routes to such ligands involve the replacement of one or more

pyrazolyl substituents of a tris(pyrazolyl)borate with 2-mercapto-1-methylimidazolyl groups. Kimblin *et al.* synthesized both bis and tris(2-mercapto-1-methylpyrazolyl)borates; the synthesis of the former ligand and of its methylzinc complex **154** are shown in Scheme 97.[219,220] Mixed pyrazolylborate complexes, bearing both S-donor and N-donor pyrazolyl groups, such as bis(mercaptopyrazolyl)pyrazolylhydroborato methylzinc **156**, whose solid-state structure is shown in Figure 71, have also been reported.[221]

A more substantial departure from the classical pyrazolylborate motif is the replacement of two pyrazolyl moities with *tert*-butylthiomethyl groups, a substitution which creates *N,S,S*-donor ligands. Thus, metallation of $PhB(Pz)(CH_2SBu^t)_2$ with dimethylzinc furnished the monomethylzinc complex **157** (Figure 72).[222]

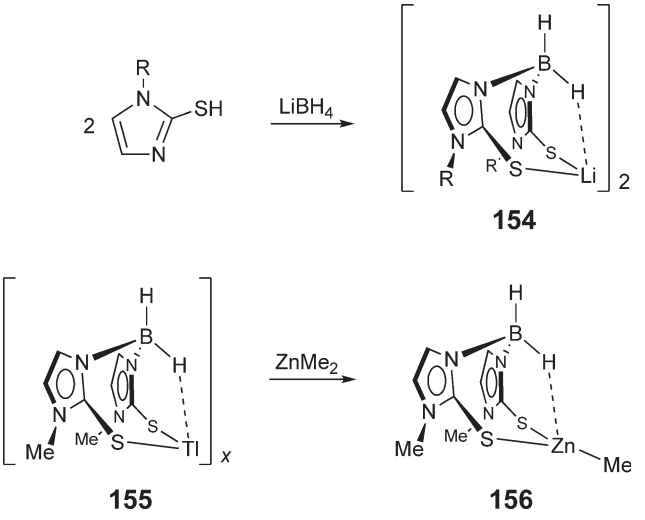

Scheme 97

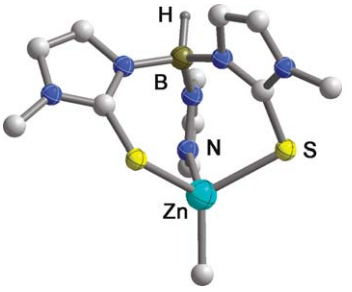

Figure 71 Solid-state structure and partial labeling scheme of **156**.

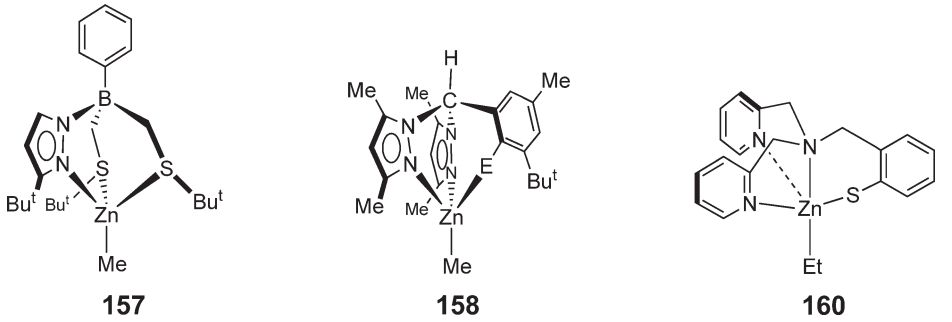

Figure 72

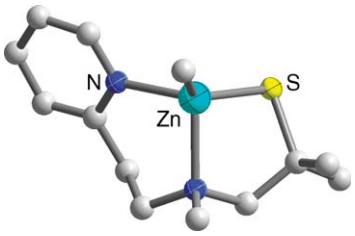

Figure 73 Solid-state structure and partial labeling scheme of **159**.

Hammes and Carrano reported heteroscorpionate ligands that provide *N,N,O* or *N,N,S*-coordination environments by dispensing entirely with the boron atom.[223] By connecting two pyrazolyl units and a phenyl group, bearing either an OH or an SH substituent, with a CH moiety they created neutral ligands that are structurally similar to tris(pyrazolyl)borates. The negative charge of the ligand is introduced by the deprotonation of the OH (or SH) group with $ZnMe_2$, as shown for the SH-substituted ligand in complex **158**.

Chang *et al.* synthesized a 2-methyl-1-[methyl-(2-pyridin-2-yl-ethyl)amino]propane-2-thiol, which when treated with dimethylzinc gave the methylzinc complex **159** (Figure 73).[224] A somewhat similar ethylzinc complex **160**, supported by the boron-free ligand 2-mercaptobenzyl-bis-(2-pyridylmethyl)amine, proved chemically unstable.[225]

2.06.13.3 Organozinc Compounds Bearing Heavier Group 16 Donor Ligands as Material Precursors

Diethylzinc reacted with 1 equiv. of sulfur in toluene to furnish a colorless crystalline compound with the empirical formula EtZnSEt **161**, whose structure was revealed by single crystal X-ray analysis as that shown in Figure 74.[226]

The ethylzinc ethylthiolate cluster consists of an ethyl-studded $(ZnS)_9$ core, having a wurtzite structure, which is capped with an ethylthiolate group on one end and an ethylzinc moiety on the other. All zinc and sulfur atoms are four coordinate, and the Zn–S bonds range from 2.40(1) to 2.49(1) Å. On heating (700 °C), this cluster decomposed to cubic zinc blende (sphalerite), proving that the structures of molecular precursors do not dictate the structure of the product in the thermolytic synthesis of solid-state materials.

Treatment of the known pentameric $[MeZnSBu^t]_5$ with pyridine and 1,3,5-trimethylhexhydro-1,3,5-triazine produced dinuclear zinc adducts of the type $[\{MeZnSBu^t\}_2L]_2$, L = pyridine, 1,3,5-trimethylhexhydro-1,3,5-triazine **162**, whose solid-state structures were determined.[227] The perspective view of **162**, shown in Figure 75, emphasizes the highly puckered central four-membered $(ZnS)_2$ ring and the tetrahedral environment of the zinc atoms. In the course of these studies, the solid-state structure of $[MeZnSBu^t]_5$ was also reinvestigated.

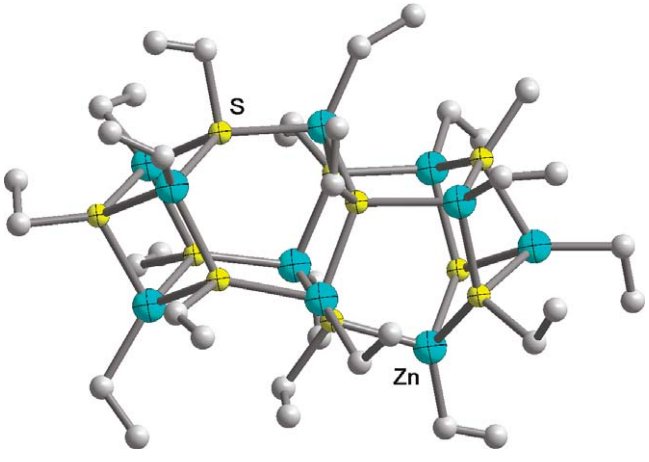

Figure 74 Solid-state structure and partial labeling scheme of **161**.

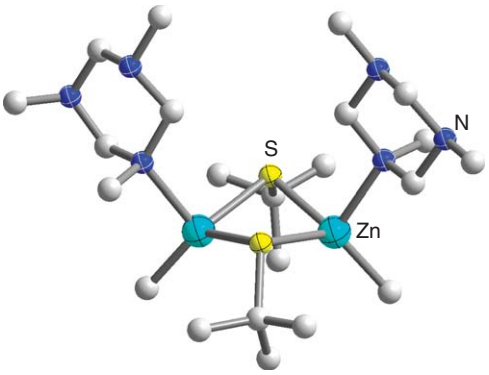

Figure 75 Solid-state structure and partial labeling scheme of **162**.

2.06.13.4 Organozinc Compounds Bearing Heavier Group 16 Donor Ligands in Catalysis

Rijnberg *et al*. reported chiral aminoarenethiols as inexpensive and easily modifiable chiral ligands for the enantioselective alkylation of prochiral aldehydes and ketones (Scheme 98).[228] The alkylzinc complexes were synthesized either by protonolysis of dialkylzinc reagents with the thiols or by the treatment of alkylzinc chloride with the trimethylsilyl-substituted ligands. Methyl- and ethylzinc complexes of these ligands, for example, **163**, reacted in 1,2-addition reactions with benzaldehyde to furnish the corresponding benzyl alcohols with very high ee's and in high yields.

2.06.14 Organozinc Hydrides and Organozinc Borohydrides

2.06.14.1 Introduction

Despite the fact that organozinc hydrides are the conceptually simplest monoorganozinc compounds of the type RZnX, organozinc compounds bearing only hydrogen are short-lived species that have only been observed spectroscopically. All stable organozinc hydrides are, in fact, organozinc compounds of polyhydride ligands.

Methylzinc hydride was formed by the insertion of excited zinc atoms, in their $^3P_1$ state, into the C–H bond of methane in an argon matrix.[229] The MeZnH product was characterized on the basis of its infrared spectrum and determined to be a linear molecule with C_{3v} symmetry. The band at 1866.1 cm^{-1} is due the Zn–H stretch, while the band at 565.5 cm^{-1} was assigned to the Zn–C stretching vibration. Additional bands for isotopically labeled species were also reported.

2.06.14.2 Organozinc Borohydrides

Downs *et al*. reported the synthesis of methylzinc tetrahydridoborate **164** by the two routes shown in Scheme 99.[230] The compound is an extremely moisture and oxygen sensitive, colorless, polycrystalline solid, whose solid-state structure was determined by X-ray analysis. Figure 76 shows that **164** consists of helical polymers of alternating methylzinc and tetrahydridoborate ions. The zinc atom is formally pentacoordinate, making this one of the few organozinc compounds with five-coordinate zinc atom.

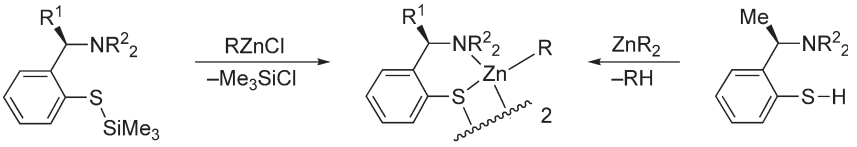

R = Me, Et

163

Scheme 98

$$2ZnMe_2 + B_2H_6 \longrightarrow BMe_3 + MeZnBH_4 + ZnH_2$$

164

$$MeZnCl + LiBH_4 \longrightarrow MeZnBH_4 + LiCl$$

164

Scheme 99

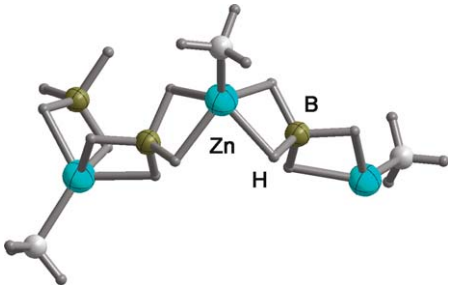

Figure 76 Solid-state structure and partial labeling scheme of a portion of polymeric **164**.

$$3ZnMe_2 + B_4H_{10} \longrightarrow [(ZnMe)_2B_3H_7]_2$$

165

Scheme 100

In a related study tetraborane(10), B_4H_{10}, was treated, Scheme 100, with a threefold excess of dimethylzinc to produce not the expected $MeZnB_3H_8$, but the dimeric, tetranuclear $[(ZnMe)_2B_3H_7]_2$ **165**.[231] The solid-state structure of **165** (Figure 77) shows that Zn1 has a similar coordination geometry as that in **164**, being in an approximately square-pyramidal coordination geometry of four hydrogens from two B_3H_8 moieties and one methyl group. The second zinc atom is approximately trigonal planar and coordinated by its methyl group and two boron atoms of one B_3H_8 moiety. This second methylzinc group has an exceedingly short zinc–carbon bond (1.919(15) Å), while the methyl–zinc bond of the five-coordinate zinc atom Zn1 (1.949(14) Å) has average length.

Because of the rarity of five-coordinate zinc, McKee conducted computational studies at the DFT/ECP level on two methylzinc hydridoborates, namely the dimeric $[(MeZn)_2B_3H_7]_2$ discussed above, and dimeric $[MeZnBH_4]_2$, whose cation was detected in mass spectra.[232] In both cases, the dimerization of these species from their hypothetical monomers was calculated to be exothermic, namely by 42.7 kJ mol^{-1} for $[MeZnBH_4]_2$ and by 27.2 kJ mol^{-1} for $[(MeZn)_2B_3H_7]_2$.

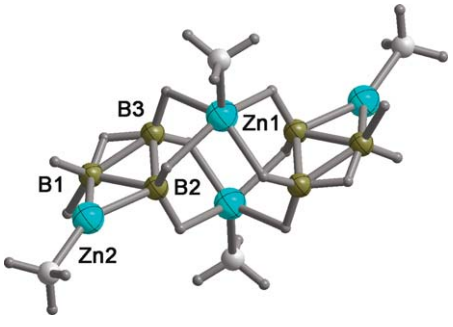

Figure 77 Solid-state structure and partial labeling scheme of **165**.

2.06.15 Organozinc Compounds with Metal–Metal Bonds

2.06.15.1 Introduction

Of the three group 12 metals, only mercury has a well-developed chemistry with the metal in the +1 oxidation state, while cadmium and zinc, respectively, exhibit this oxidation state either exceedingly seldom or not at all. This increase in the stability of the lower oxidation state as one descends the group is characteristic of main group metals, but not of transition metals.

The report by Resa *et al.* on a hydrocarbon-soluble, molecular compound of monovalent zinc, namely decamethyldizincocene, therefore caused considerable excitement among inorganic and organometallic chemists alike.[233] Organozinc compounds with direct zinc–transition metal bonds have also been reported recently, and this area of organozinc chemistry with direct metal–metal bonds will undoubtedly witness considerable growth in the near future.

2.06.15.2 Organozinc Compounds with a Direct Zinc–Zinc Bond: The First Molecular Compound of Zinc(I)

One of the most convenient synthetic pathways to heteroleptic diorganozinc compounds is the comproportionation of two homoleptic diorganozinc species (see Section 2.06.4.4). The attempted synthesis of pentamethylcyclopentadienyl(ethyl)zinc **167** by combining $Zn(\eta^5\text{-}C_5Me_5)_2$ and $ZnEt_2$ at room temperature, Scheme 101, yielded mixtures of the targeted half-sandwich compound and decamethyldizincocene.[233] When the reaction was repeated at −10 °C in diethyl ether, decamethyldizincocene **166** was obtained as the only product in yields of 45%. Subsequently, an improved synthesis of **166**, by mixing $K(C_5Me_5)$, $ZnCl_2$, and KH in a 2 : 1 : 1 ratio in THF (−20 °C), produced **166** in yields of 60–80%.[234] Decamethyldizincocene is a colorless, crystalline solid that is very soluble in most organic solvents and exceedingly sensitive to oxygen and moisture, spontaneously inflaming in air even in the solid state.

Because of the unusual nature of this molecule—it is the first molecular zinc(I) compound—it was thoroughly chemically and structurally characterized. Low-temperature X-ray structures with both molybdenum and copper radiation led to identical results (Figure 78). The structure of $(\eta^5\text{-}C_5Me_5)Zn\text{–}Zn(\eta^5\text{-}C_5Me_5)$ consists of two eclipsed $(\eta^5\text{-}C_5Me_5)Zn$ units connected by a direct zinc–zinc (2.305(3) Å) bond, which is substantially shorter than the sum of the covalent radii of two zinc atoms (2.50 Å). The presence of bridging hydrides was discounted by the high resolution mass spectral data and by protonolysis.

The solid-state structure of **166** shows that the pentamethylcyclopentadienyl ligands are symmetrically bound to the zinc atoms in a pentahapto fashion, with isometric Zn–C bonds, ranging from 2.27 to 2.30 Å.

The high symmetry of decamethyldizincocene is also reflected in its simple NMR spectra. Thus, the ^1H NMR spectrum exhibited one singlet at $\delta = 2.02$ ppm, while two singlets at 10.0 and 108.5 ppm were observed in the ^{13}C NMR spectrum.

del Rio *et al.* used density functional studies (B3LYP) to investigate the structure and bonding of this decamethyldizincocene.[234] Of three conceivable structures, namely $(\eta^5\text{-}C_5Me_5)Zn\text{–}Zn(\eta^5\text{-}C_5Me_5)$ **166a**, $(\eta^3\text{-}C_5Me_5)Zn\text{–}Zn(\eta^3\text{-}C_5Me_5)$ **166b**, and $(\eta^5\text{-}C_5Me_5)Zn\text{–}Zn(\eta^1\text{-}C_5Me_5)$ **166c**, the pseudo bis(allylic) structure **166b** was the true minimum. The energies differ by only 0.4 kJ mol^{-1}, however, suggesting that it is best to use $(\eta^5\text{-}C_5Me_5)Zn\text{–}Zn(\eta^5\text{-}C_5Me_5)$ to describe the structure of **166**. The zinc–zinc bond length was calculated to be 2.331 Å, which matches the experimentally observed value exactly. The zinc–zinc bond, which is formed almost exclusively (96%)

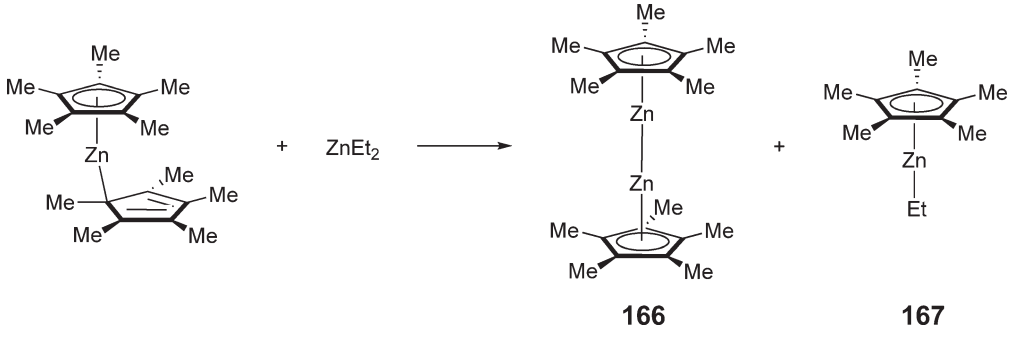

Scheme 101

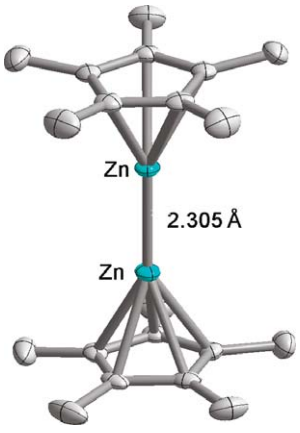

Figure 78 Solid-state structure and partial labeling scheme of decamethyldizincocene **166**.

by the overlap of the 4*s* orbitals of both metal atoms, with minimal contributions from the 4*p* orbitals, has a bond dissociation energy of 277.4 kJ mol^{-1}.

Xie *et al.* performed DFT studies on the unsubstituted CpZn–ZnCp, using both the B3LYP and BP86 methods, and obtained zinc–zinc bonds of 2.336 and 2.315 Å, respectively, in good agreement with the experimental results.[235] The geometry-optimized molecule has an eclipsed conformation (D_{5h}), but the staggered D_{5d} conformation is of almost identical energy. These computational studies show that the zinc–zinc bond has almost pure *s*-character ($sp^{0.03}d^{0.01}$) and predict that the decomposition of decamethyldizincocene to decamethylzincocene and zinc is endothermic by ca. 351 kJ mol^{-1}. Furthermore, the potential hydride-bridged dimer CpZn(μ-H)$_2$ZnCp was determined to be unstable with respect to dissociation to its CpZnH monomers.

The report of the first zinc compound with a Zn–Zn core elicited a number of critical comments on the structure and bonding of decamethyldizincocene, and the interpretation of the results.[236,237] None of the authors of these commentaries questioned the data or their interpretation. Parkin, however, has pointed out that the formal oxidation state of +1 for zinc in this compound is merely due to the convention that metals are assigned an oxidation state of 0 when they form bonds with like atoms.[237] If the conventional definition of valence, namely "the capacity of atoms to form bonds to other atoms" is used, then the zinc atoms in decamethyldizincocene are not monovalent, but divalent. The synthesis of a paramagnetic organozinc compound in which zinc uses only one of its two 4*s* electrons will remain an interesting challenge to many synthetic organometallic chemists.

2.06.15.3 Organozinc Compounds with a Direct Zinc–Metal Bond

The triruthenium pentahydride cluster [{(η^5-C$_5$Me$_5$)Ru}$_3$(μ-H)$_3$(μ_3-H)$_2$] reacted with exactly 1 equiv. of diethylzinc, Scheme 102, with the elimination of ethane and the formation of [{(η^5-C$_5$Me$_5$)Ru}$_3$(μ-H)$_3$(μ_3-ZnEt)(μ_3-H)] **168** in

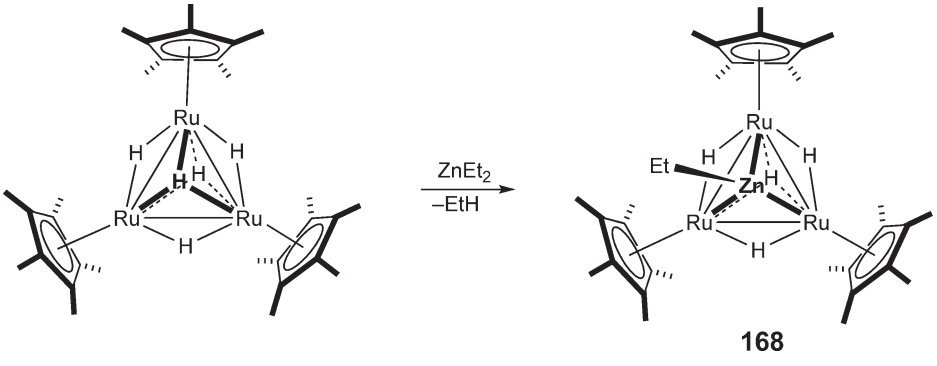

168

Scheme 102

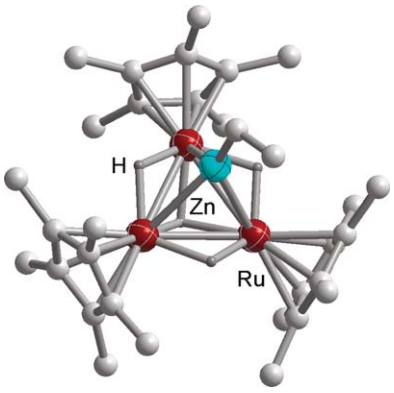

Figure 79 Solid-state structure and partial labeling scheme of **168**.

which the ethylzinc moiety caps one of the triangular faces.[238] A bicapped cluster, namely $[\{(\eta^5\text{-}C_5Me_5)Ru\}_3(\mu\text{-}H)_3(\mu_3\text{-}ZnEt)_2]$, was isolated when excess diethylzinc was added.

The solid-state structure of **168**, Figure 79, confirms the very high symmetry of the molecule. The zinc–ruthenium bonds are 2.66 Å long on average, and thus considerably longer than the sum of the covalent radii of these metals.

2.06.16 The Application of Organozinc Compounds in Organic Synthesis

2.06.16.1 Introduction

The application of organozinc compounds in organic synthesis has experienced a renaissance during the last decade, for which there are three major reasons. First, compared to the more common organomagnesium and organolithium reagents, organozinc compounds are compatible with many functional groups; therefore, zinc derivatives are more chemoselective and can be used in transformations of polyfunctional compounds.[239] Second, during recent years, organozinc compounds of diverse structure, including functionalized and enantiomerically enriched forms, have become available through new synthetic methods.[32,33,68,240–245] Third, organozinc reagents undergo transmetallation with some metals, such as Cu, Ni, Pd, Ti, and others.[246] Upon transmetallation, new species with novel properties are formed. For this reason, when organozinc compounds are used with promoters containing another metal, their reactivity pattern may change quite dramatically. Numerous transformations based on Cu-, Ni-, Pd-, Ti-, Zr-, Co-, Mn-, and Fe-catalyzed reactions of organozinc derivatives with organic compounds have been reported.[68,246] The potential of such transformations is so enormous that one can easily predict that this field of study will continue to grow.

Because of the enormous volume of information regarding the use of organozinc derivatives in organic chemistry, this survey is focused only on recent major trends in this area. Valuable information about preparation methods of major types of organozinc compounds and their reactions can be found in two recent books[246,247] and reviews.[68,114,248,249] There have been a number of reviews devoted to specific applications of organozinc reagents in synthesis; references will be provided in the corresponding sections of this chapter.

2.06.16.2 Addition of Organozinc Reagents to Aldehydes, Ketones, and α-Ketoesters

2.06.16.2.1 Chiral ligands used in addition reactions of diorganozincs with aldehydes

Perhaps the most investigated reaction of organozinc compounds is their addition to the carbonyl group of aldehydes. A broad range of simple and functionalized diorganozincs and a great variety of aldehydes have been studied in this transformation. The reaction furnishes chiral secondary alcohols, which are essential building blocks in the synthesis of natural products and other important compounds. Recent studies of this transformation have been devoted to its asymmetric catalytic versions (Scheme 103).

In the reported enantioselective additions of dialkylzincs and diphenylzinc to aldehydes, a great variety of structurally different ligands with different kinds of chirality have been used. A very detailed account of major developments in this area up to the year of 2001 can be found in a review of L. Pu and H.-B. Yu.[250] The majority of

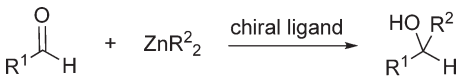

Scheme 103

chiral inductors used in these reactions are *N,O*-ligands, including oxazoline derivatives with planar and central chirality[251,252] [(R_p,*S*)-**169** and (R_p,*S*)-**170**] substituted ethylenediamines[253] [e.g., (1*R*,1′*R*,2′*S*)-**171**], amino alcohols with a sulfamido group[254] [e.g., (*S*,*R*)-**172**], amino alcohols with central chirality[255,256] (e.g., **173** and **174**), binaphthyl-based axially chiral amino acids[257] **175a–f**, [2.2]paracyclophane derivatives[258] [e.g., (S_p,*S*)-**176a**], and aziridino alcohols[259] (**178–181**, Figure 80). As a rule, these ligands provided very good or excellent

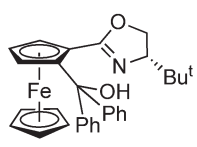

(R_p,*S*)-**169**

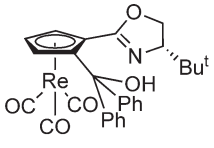

(R_p,*S*)-**170**

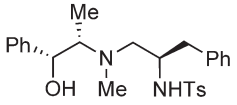

(1*R*,1′*R*, 2′*S*)-**171**

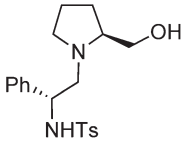

(*S*,*R*)-**172**

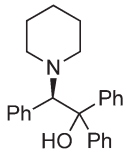

173

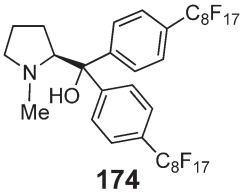

174

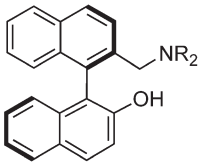

175a–f

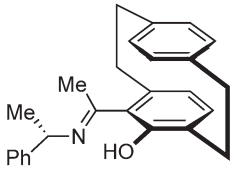

(S_p,*S*)-**176a**

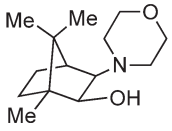

177

R = Me, Bu, Bn, $(CH_2)_4$, $(CH_2)_5$, $(CH_2)_2O(CH_2)_2$

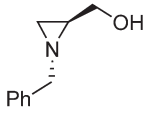

178

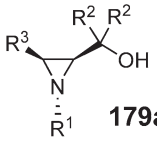

179a–j

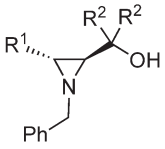

180a–c

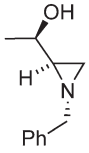

181

179a: R^1 = $PhCH_2$; R^2 = H; R^3 = Me
179b: R^1 = $PhCH_2$; R^2 = R^3 = Me
179c: R^1 = $PhCH_2$; R^2 = Ph, R^3 = Me
179d: R^1 = Ph_3C; R^2 = H, R^3 = Me
179e: R^1 = R^2 = H; R^3 = Me
179f: R^1 = R^3 = Me; R^2 = H
179g: R^1 = Bu^n; R^2 = H; R^3 = Me
179h: R^1 = Pr^i; R^2 = H; R^3 = Me
179i: R^1 = $PhCH_2$; R^2 = H; R^3 = Ph
179j: R^1 = $PhCH_2$; R^2 = Me; R^3 = Ph

180a: R^1 = Me; R^2 = H
180b: R^1 = Me; R^2 = Et
180c: R^1 = Ph; R^2 = H

Figure 80 N,O-Ligands used without an additional metal promoter in reactions of diorganozincs with aldehydes.

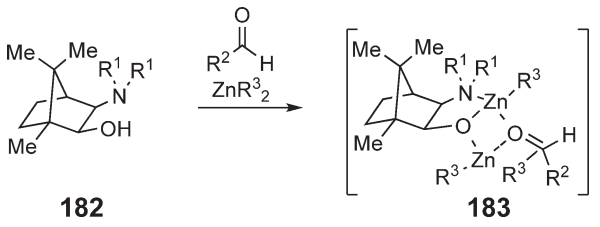

182 183

Scheme 104

enantioselectivities for a wide range of aromatic and aliphatic aldehydes and diverse zinc organometallics. It is important to emphasize that these *N,O*-ligands have been used without any additional metal promoters.

The mechanism of the reactions catalyzed by *N,O*-ligands is believed to be well understood and includes the formation of a complex **183** containing two zinc atoms, a chiral ligand (e.g., **182**), and an aldehyde in a ratio of 2 : 1 : 1 (Scheme 104).[250,260,261]

Another group of reactions of diorganozincs with carbonyl compounds requires not only a chiral ligand, but an additional metal promoter, usually $Ti(OPr^i)_4$. Enantiopure compounds used in such transformations during the last decade include, but are not limited to, ditriflamides[262,263] (e.g., **184**), camphorsulfonamide derivatives[263–268] (e.g., **185**), 1,3-dioxalane-based dialcohols[269] (the so-called TADDOL derivatives, e.g., **186a** and **186b**), binaphthol[263] (BINOL, **187**) and a variety of its derivatives[270] (e.g., **188**,[271] Figure 81). An excellent survey of organozinc reactions with aldehydes catalyzed by BINOLate–Ti(IV) complexes can be found in a paper by Walsh and co-workers.[270]

A variety of different combinations of chiral ligands and $Ti(OPr^i)_4$ provided good to excellent levels of enantioselectivity. The mechanism of the Ti(IV)-promoted reactions appears to be completely different from that of additions catalyzed by *N,O*-ligands. Balsells *et al.* found that in the reactions using $MeTi(OPr^i)_3$ as the only source of the alkyl group, the enantioselectivities were the same as in those employing $ZnMe_2$ along with a catalyst. This significant finding suggested that the zinc atom was not actively involved in the addition step intermediate; it was the Ti atom that was transferring the alkyl group to the carbonyl moiety. Based on their meticulous mechanistic study, the authors proposed the structure of the intermediate containing two Ti atoms (**189**, Figure 82).[270]

2.06.16.2.2 Use of mixed diorganozinc reagents ZnR^1R^2

Usually, only symmetrical diorganozincs, ZnR_2, are used in additions to the carbonyl group. In these reactions, only one group R is transferred to the carbonyl moiety. An interesting approach for employing mixed diorganozincs, ZnR^1R^2, was proposed by Knochel and co-workers.[262,272] They found that $RZnCH_2SiMe_3$, obtained from ZnR_2 and

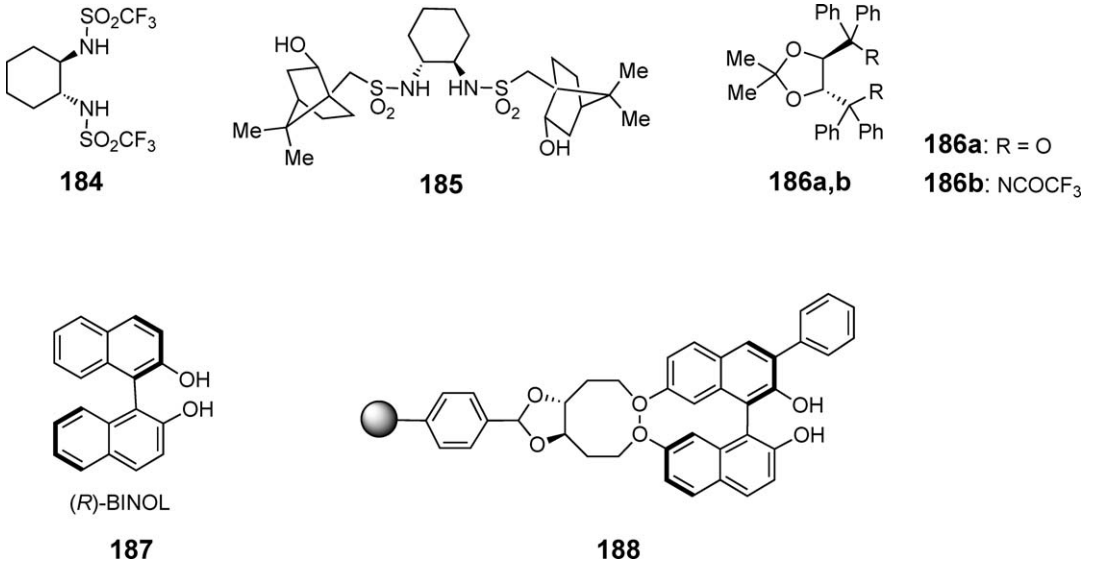

184 185 186a,b

186a: R = O
186b: $NCOCF_3$

187 188

Figure 81 Examples of chiral ligands used in addition reactions of diorganozincs with carbonyl compounds promoted by Ti(IV).

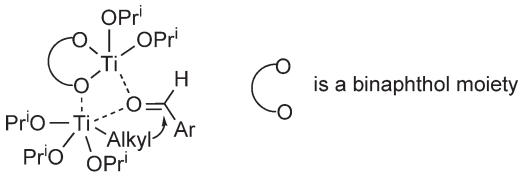

189

Figure 82

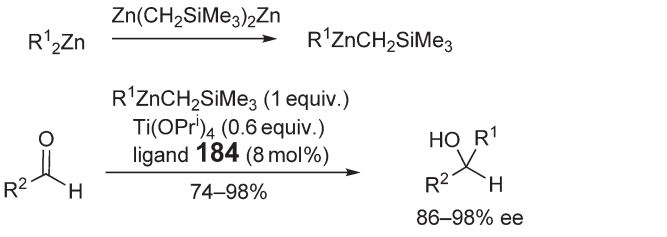

R^1 = Et, C_5H_9, Cl(CH$_2$)$_4$, PivO(CH$_2$)$_3$, PivO(CH$_2$)$_4$, PivO(CH$_2$)$_5$, AcO(CH$_2$)$_5$
R^2 = alkyl or aryl group

Scheme 105

Zn(Me$_3$SiCH$_2$)$_2$, is capable of reacting with aromatic and aliphatic aldehydes by transferring only the R group to the carbonyl substrate. These mixed reagents are less reactive than the corresponding diorganozincs; therefore, catalysts are necessary in reactions of RZnCH$_2$SiMe$_3$ with aldehydes. An asymmetric version of this transformation was studied using (1*R*,2*R*)-1,2-bis(trifluoromethanesulfonamido)cyclohexane (**184**, Figure 81). The reported enantioselectivities were very high for all the organometallic reagents screened, including MeZnCH$_2$SiMe$_3$ (Scheme 105).[262]

Mixed alkylarylzincs have been used by the Bolm group for the arylation of carbonyl compounds. They reported that a 1 : 2 mixture of ZnPh$_2$/ZnEt$_2$ provided higher enantioselectivities than ZnPh$_2$ alone when reactions of aromatic aldehydes were catalyzed by ferrocenyl and rhenium-tricarbonyl oxazolines (**169** and **170**, respectively, see Figure 80).[251,252,273] It has been reasonably suggested that ZnEtPh is formed in an equilibrium with ZnPh$_2$ and ZnEt$_2$. Remarkably, no product of the ethyl group transfer was detected. Bolm and Rudolph also accomplished the addition of an aryl group to aromatic aldehydes using a mixture of ArB(OH)$_2$ and ZnEt$_2$.[274] For example, reactions of substituted benzaldehydes with a mixture of PhB(OH)$_2$ and ZnEt$_2$ in the presence of a chiral ligand **169** afforded the corresponding diaryl methanols in high yields (79–95%) and very high levels of enantioselectivity.

2.06.16.2.3 Asymmetric amplification in autocatalytic additions of diisopropylzinc to some aldehydes

While investigating the reaction of ZnPr$^i_2$ with pyrimidine-5-carboxaldehyde **190**, the Soai group made the important discovery that these two compounds reacted in the presence of a catalytic amount of (*S*)-2-methyl-1-(5-pyrimidyl)propan-1-ol **191** of a low enantiomeric purity (as low as 2%) to furnish the same alcohol as the addition product with ee's up to 89% (Scheme 106). This most remarkable finding was the first case of asymmetric amplification in autocatalytic reactions.[275]

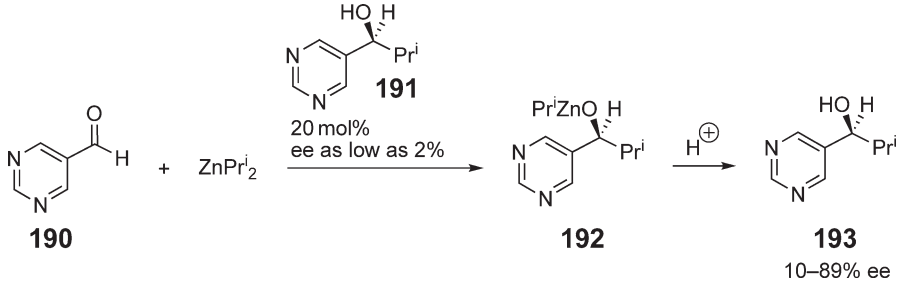

Scheme 106

Later, the same group reported amplifications of ee in asymmetric additions of $ZnPr^i_2$ to quinoline-3-, pyridine-3-, and substituted pyrimidine-5-carbaldehydes catalyzed by the corresponding quinolyl,[276] pyridyl,[277] and pyrimidyl[278–280] alcohols, respectively. One of the best catalysts turned out to be 1-(2-*tert*-butylethynyl-5-pyrimidyl)-2-methyl-1-propanol: a sample of this compound of a very low enantiomeric purity (0.00005%) replicated itself providing the final product with ee above 99.5%.[278] It is interesting that asymmetric autocatalysis works only with $ZnPr^i_2$ implying that steric requirements in these reactions are likely to be very important. It has also been suggested that the observed amplification of products' ee's is facilitated by selective precipitation of species of lower ee in the course of reactions.[281] A detailed account of asymmetric amplification in autocatalytic additions of $ZnPr^i_2$ can be found in two reviews of Soai and co-workers.[282,283] Their spectacular results have inspired other research groups to carry out additional investigation of this phenomenon.[261,281,284]

2.06.16.2.4 Use of ionic liquids

One of the important new directions in the study of addition reactions of organozinc compounds to aldehydes is the use of ionic liquids. Usually, application of these compounds in reactions with common organometallic reagents has a serious problem: ionic solvents are usually reactive toward them, particularly Grignard and organolithium derivatives. It has been recently reported that carbonyl compounds react with allylzinc bromide formed *in situ* from allyl bromide and zinc in the ionic liquid 3-butyl-1-methylimidazolium tetrafluoroborate, [bmim][BF_4].[285] Another important finding is that the more reactive $ZnEt_2$ alkylates aldehydes in a number of ionic liquids at room temperature.[286] The best yields (up to 96%) were obtained in *N*-butylpyridinium tetrafluoroborate, [bpy][BF_4] (Scheme 107).

Additions of the Reformatsky-type reagents to aldehydes can also proceed in ionic solvents (Scheme 108).[287] Three ionic liquids have been tested: 8-ethyl-1,8-diazbicyclo[5,4,0]-7-undecenium trifluoromethanesulfonate ([EtDBU][OTf]), [bmim][BF_4], and [bmim][PF_6]. The reactions in the first solvent provided higher yields of alcohols **194** (up to 93%), although results obtained for two other ionic liquids were also comparable with those reported for conventional solvents.

The same authors have also reported the application of green solvents in additions of terminal alkynes to aldehydes in the presence of $Zn(OTf)_2$ and 1,8-diazabicyclo[5,4,0]-7-undecene (DBU, Scheme 109).[287] The reactions proceeded very slowly, but afforded desirable alcohols **195** in moderate to good yields.

Overall, green solvents appear to be a valuable alternative to conventional solvents in addition reactions of diverse organozinc reagents to aldehydes.

2.06.16.2.5 Addition of diorganozinc reagents to ketones

Reactions of organometallic derivatives with ketones, which are less electrophilic than aldehydes, usually require an equimolar amount of a chiral ligand. The first catalytic enantioselective addition of an organometallic reagent, namely $ZnPh_2$, to dialkyl and aryl alkyl ketones was reported in 1998 by Dosa and Fu (Scheme 110).[288] The procedure

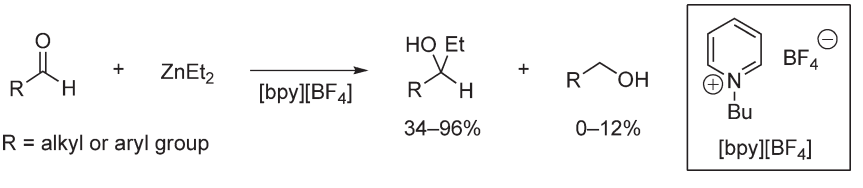

Scheme 107

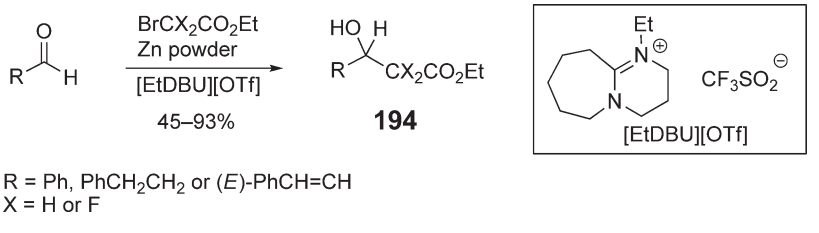

Scheme 108

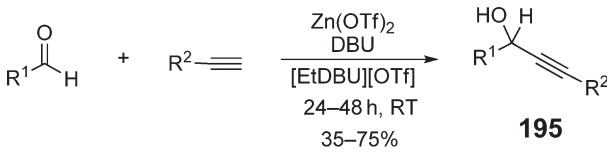

R^1 = Ph, 4-PhC_6H_4, 4-$NO_2C_6H_4$, PhCH=CH
R^2 = Ph, C_4H_9, C_6H_{13}

Scheme 109

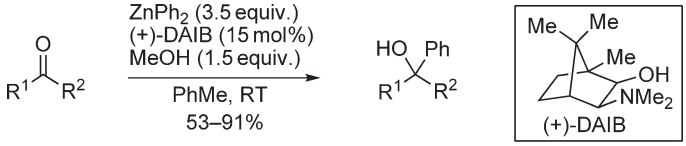

R^1 = alkyl or aryl group
R^2 = Me, Et

Scheme 110

required the use of 3-*exo*-(dimethylamino)isoborneol (DAIB) and methanol. The latter reacted with $ZnPh_2$ to furnish a methoxyzinc derivative with the increased Lewis acidity of the zinc atom.[289] The application of the α-hydrogen-free $ZnPh_2$ instead of dialkylzincs prevented carbonyl substrate reduction.

The same year, Ramón and Yus published data on the enantioselective addition of dialkylzinc to ketones in the presence of a stoichiometric amount of $Ti(OPr^i)_4$ and a catalytic amount (20 mol%) of a sulfonamide chiral inductor.[263,264] The observed enantioselectivity depended on the size of the chiral ligand used and was highest for camphor-derived monosulfonamides. This research was followed by studies focused on the design of other sulfonamide ligands.[265,267,268,290,291] Thus far, the best results have been achieved for additions of dialkylzincs to various ketones using $Ti(OPr^i)_4$ and ligand **185** (Figure 81, Scheme 111).[265,267,268]

The study of alkynylation of methyl ketones using a terminal alkyne, $ZnMe_2$, and a salen derivative **196** as a chirality inductor provided a new method for the preparation of α-hydroxyacetylenes (**197**, Scheme 112).[292]

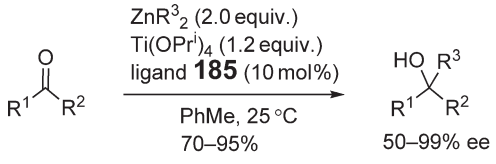

R^1 = Me, Et, CH_2Br
R^2 = Ph, 4-MeC_6H_4, 4-$CF_3C_6H_4$, 2-Nf, (*E*)-PhCH=CH, PhC≡C
R^3 = Me, Et

Scheme 111

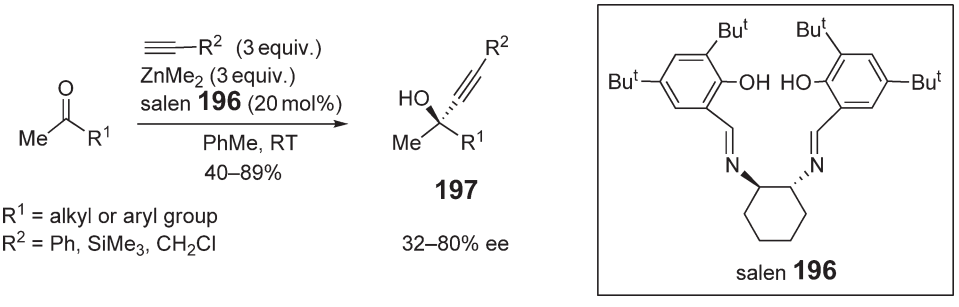

R^1 = alkyl or aryl group
R^2 = Ph, $SiMe_3$, CH_2Cl

Scheme 112

The method suggests using 20 mol% of the ligand which, due to the presence of both Lewis-acidic and Lewis-basic sites, is capable of activating both the ketone and the nucleophile. A linear correlation between the ee of the catalyst and that of the product was established, suggesting that only one molecule of the salen ligand is involved in the enantiodifferentiating step.

2.06.16.2.6 Addition of diorganozinc reagents to α-ketoesters

Enantioselective alkylation and alkynylation of α-ketoesters using organozincs have been recently studied by research groups of Kozlowski and Jiang. The Kozlowski group tested several salen complexes as chiral catalysts with $ZnEt_2$ as an alkylating agent (Scheme 113).[293,294] The method provided the corresponding α-hydroxyesters **199** in high yields and moderate selectivity with the best results obtained for the $Ti(OPr^i)_2$–salen complex **198**.

In the study of the Jiang group,[295] the amino alcohol **200** was employed as a catalyst, and $Zn(OTf)_2$ and a terminal alkyne were brought together to generate a Zn-containing alkynylating reagent (Scheme 114). This system afforded α-hydroxyesters **201** with ee's up to 94% and, in general, in high yield.

2.06.16.2.7 Reactions of organozincates with carbonyl compounds

Reactions of organozincates with aldehydes and ketones were thoroughly investigated by Richey and co-workers (Scheme 115).[296,297] In contrast to dialkylzincs, which do not give addition products with ketones and even aldehydes in non-coordinating solvents, Et_3ZnLi in toluene reacted with aldehydes and ketones to furnish desirable secondary and tertiary alcohols, respectively, in 94–99% yield. Potassium and sodium analogs gave lower yields of addition products, particularly with methyl ketones. Attempts using zincates of composition Et_2ZnX, X = *tert*-BuOK, *tert*-BuOLi, or Bu_4NBr, were less successful: Et_2Zn(*tert*-BuOK) reacted with benzaldehyde and benzophenone only, two other zincates were even less reactive and gave addition products with benzaldehyde only. The authors thoroughly studied the kinetics for Et_3ZnLi additions and reported the Hammet plot for the reactions with substituted acetophenones.

A theoretical study of the reaction mechanism for addition of organozincate complexes to aldehydes was recently performed using density functional theory.[298] It has been suggested that the addition takes place through formation of a four-centered transition state and, therefore, it can be considered a typical nucleophilic reaction.

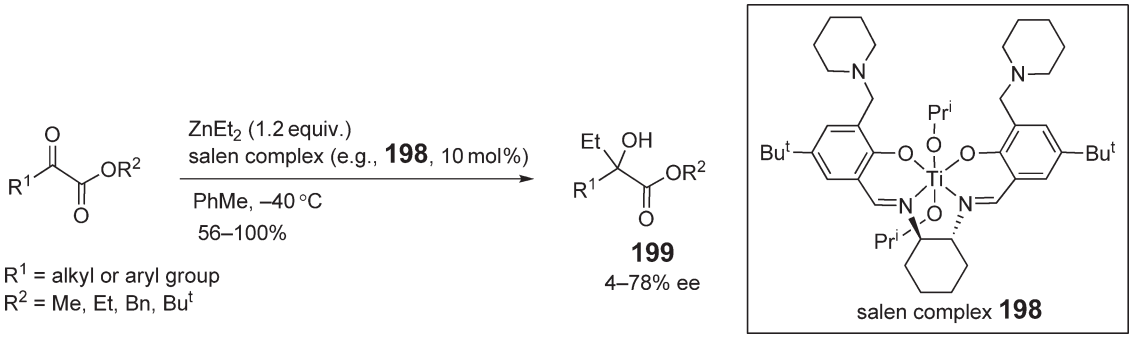

Scheme 113

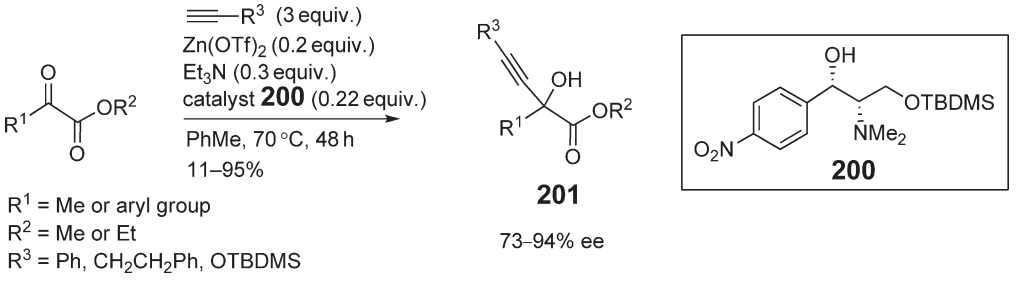

Scheme 114

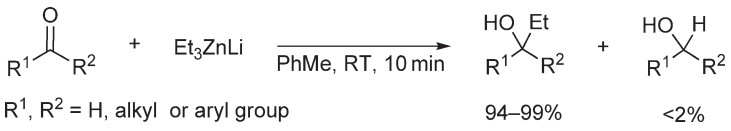

Scheme 115

2.06.16.3 Reactions of Organozinc Reagents with Enones

2.06.16.3.1 Nucleophilic additions

Conjugate additions of organozincs to enones and other Michael acceptors are usually carried out either in the presence of copper salts[68] or an appropriate Lewis acid, such as TMSI or $BF_3{\cdot}OEt_2$.[299] In 1996, the group of Knochel reported that the use of *N*-methylpyrrolidinone (NMP) as a co-solvent allowed successful copper-free conjugate additions of primary and secondary diorganozincs to a number of Michael acceptors (Scheme 116).[300] Reactions of enones and α,β-unsaturated nitriles still required the use of 1 equiv. of Me_3SiCl as a promoter. Mixed reagents $RZnCH_2SiMe_3$ (see Section 2.06.16.2.2.) also provided high yields of the products in similar reactions.[272] Treatment of cyclohexenone with alkylzinc iodides instead of diorganozinc reagents in the presence of Me_3SiI led to the corresponding products in much lower yield.[300]

Enantioselective additions of dialkylzincs and diphenylzinc to enones and related compounds were accomplished using catalytic amounts of Cu salts and optically active ligands, including biphenol-based phosphoramidites[301–304] and pyridine phosphites,[305,306] binaphthalene-derived phosphates[307] and oxazoline phosphites,[308] binaphthyl-thiophosphoramides,[309] binaphthylselenophosphoramides,[309] thiophosphoramides,[310] and aminophosphine oxazolines.[311] For example, both cyclic and acyclic enones gave high yields and ee's up to 98% when reacted with $ZnEt_2$ in the presence of a copper(I) salt and binaphthylthiophosphoramide **204** (Scheme 117).[309] Biphenol-based phosphoramidites **205** have been found to be an excellent choice for addition reactions of $ZnEt_2$ to both enones and α-nitroalkenes (Scheme 117).[302]

In most of the recently reported conjugate additions of organozinc reagents, enantiopure ligands were used in combination with copper salts, such as $Cu(OTf)_2$[303,304,311,312] $Cu(CH_3CN)_4BF_4$,[305–307,309] $Cu(CH_3CN)_4ClO_4$,[309,310] or copper(I) 2-thiophenecarboxylate,[302] although Ni-catalyzed reactions of this type have been described as well.[313–315] Recently, well-defined optically active copper-containing complexes, namely copper(I) aminoarenethiolates **206** (Figure 83), were investigated in conjugate addition reactions of diethylzinc, as well as Grignard reagents.[316] This interesting study shed some light on possible structures of the intermediates.

The presence of Cu(I) or Cu(II) salts in the aforementioned reactions is critical. It is believed that organozinc reagents undergo transmetallation with copper species to yield more reactive complexes.[301] A proposed[301] catalytic cycle (Scheme 118) suggests that the alkyl group transferred to the enone from the copper metal in a bimetallic intermediate **207**.

A recently disclosed transformation describes an interesting oxovanadium(V)-induced vicinal dialkylation of cyclic enones by dialkylzincs.[317] The method is based on the previous finding of the same authors that oxidation of

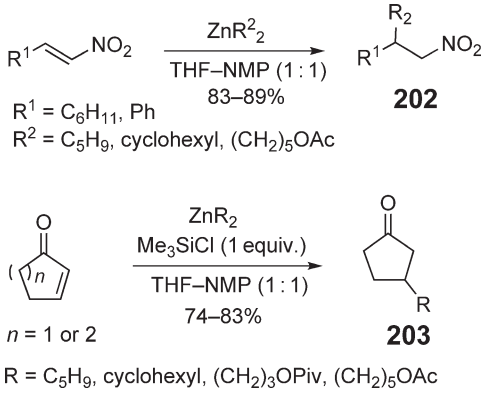

Scheme 116

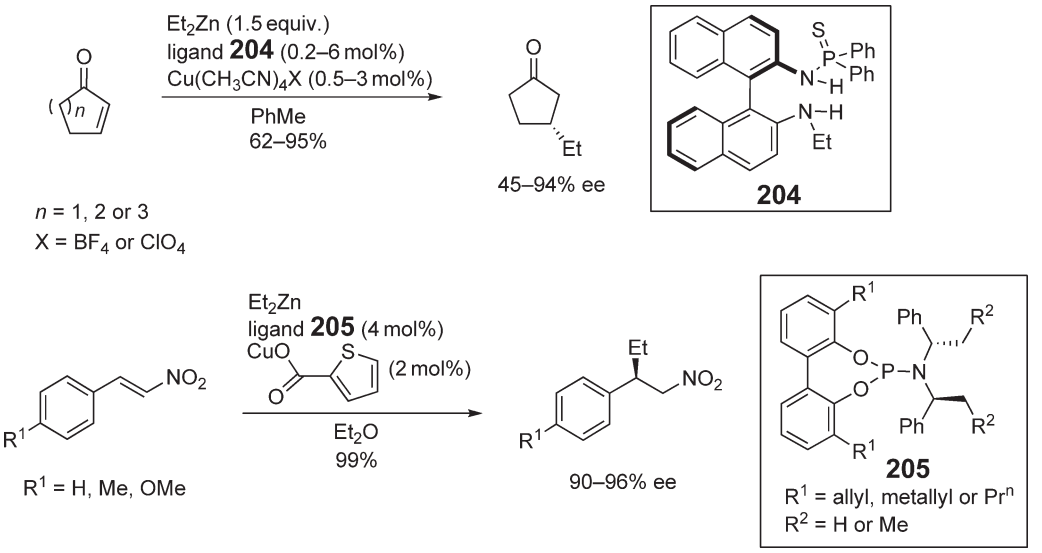

Scheme 117

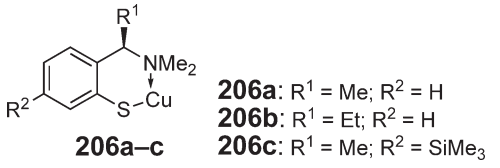

Figure 83 Examples of well-defined Cu-containing enantiopure complexes used in conjugate addition reactions with diethylzinc.[82]

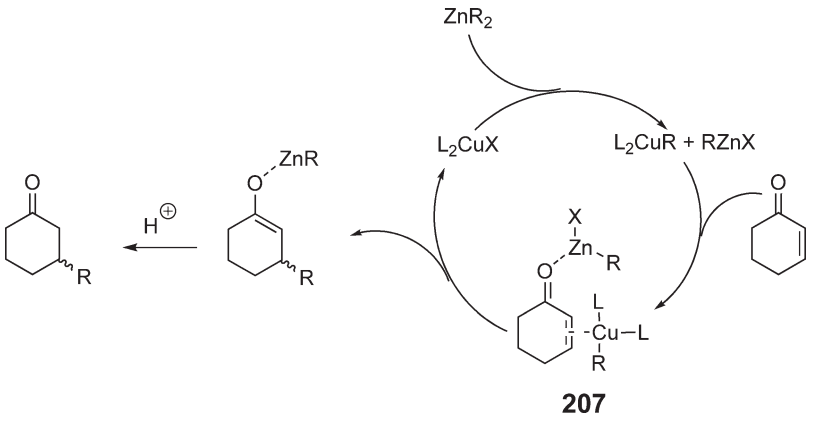

Scheme 118

alkylarylzincs and arylalkylzincates with $VO(OEt)Cl_2$ results in ligand coupling.[318] The vicinal dialkylation of α,β-unsaturated ketones occurs through several steps: (i) activation of the enone by an oxovanadium species, for example, $VO(OEt)Cl_2$, (ii) conjugate addition of dialkylzinc to the activated enone **208**, and (iii) oxidative coupling of the organic fragment in Zn-containing intermediate **209** (Scheme 119). This methodology has also been applied to lithium trialkylzincates; isolated yields were in the range of 38–72%.[317] It is worth mentioning that $Me_2BuZnLi$ dialkylated cyclohexenone regioselectively furnishing 2-methyl-3-butylcyclohexanone in 51% yield.

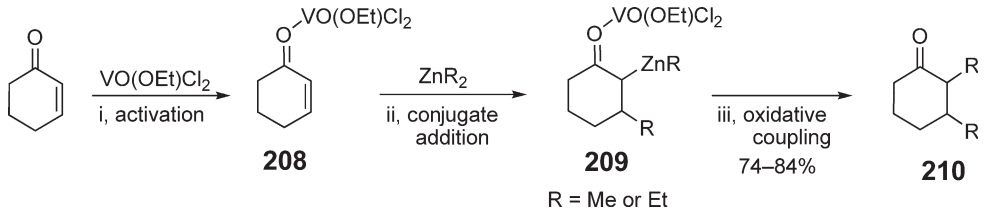

Scheme 119

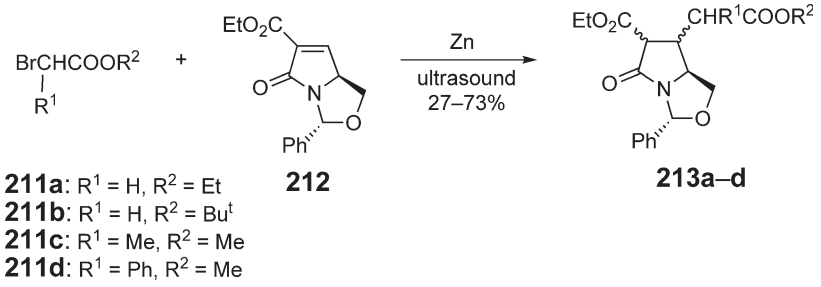

Scheme 120

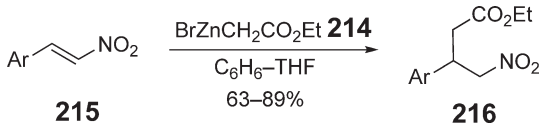

Scheme 121

It is well known that Reformatsky reagents can react with conjugate carbonyl compounds. During the last decade, more complex Michael acceptors have been tested in the addition reactions with these organozinc compounds. In particular, it has been demonstrated that the Reformatsky reagents prepared from bromides **211a–d** are capable of alkylating α,β-unsaturated lactam **212** under mild conditions to form desirable compounds **213a–d** in satisfactory yields (Scheme 120).[319]

Reformatsky reagent **214** also reacted with α-nitrostyrenes **215** to form the corresponding 1,4-addition products **216** in good yields (Scheme 121).[320] The optimal conditions for the reaction were determined to be 48 h at 60 °C. A 3 : 1 mixture of C_6H_6–THF gave better yields than THF alone, although the latter is the most common solvent for this type of reaction.

2.06.16.3.2 Diethylzinc-mediated radical additions to enones

Recently Bertrand *et al.* discovered that $ZnEt_2$ is capable of initiating radical additions to enones. When air was introduced to the reaction mixture, containing cyclohexenone, $ZnEt_2$, and isopropyl or *tert*-butyl iodide, the corresponding 3-alkyl-substituted cycloxenones **217a** and **217b** were formed (Scheme 122).[321] It is apparent that additional studies of this transformation are necessary.

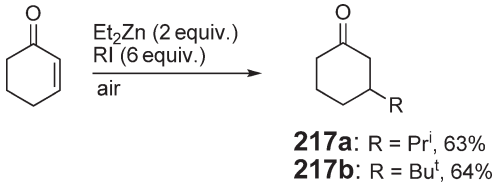

Scheme 122

2.06.16.4 Reactions of Organozinc Reagents with Acyl Halides, Anhydrides, and Other Carboxylic Acid Derivatives

2.06.16.4.1 Catalyzed reactions

Dialkylzinc and diphenylzinc are capable of reacting with acyl halides and related derivatives in the presence of suitable catalysts. For example, $ZnMe_2$ and $ZnEt_2$ reacted with a number of structurally different acyl chlorides in the presence of excess $AlCl_3$ to afford the corresponding ketones in very high yields (Scheme 123).[322]

A unique nickel-catalyzed alkylative monofunctionalization of cyclic anhydrides using dialkylzinc and diphenylzinc provided γ- or β-keto acids (Scheme 124).[323] This reaction also required the use of $Ni(cod)_2$ or $Ni(acac)_2$ and a bidentate ligand. As it was observed by Knochel in the reactions of dialkylzinc with alkyl iodides (*vide infra*), addition of an electron-deficient alkene,[324] for example, 4-fluoromethylstyrene, accelerated the rate of the reaction and increased the yield of the desired products. The alkylzinc reagents BuZnBr and $EtO_2CCH_2CH_2ZnBr$ also reacted with anhydrides, although the yields were lower.

Recently, the Rovis group reported acylation of dialkylzinc and diphenylzinc reagents by acyl fluorides, chlorides, anhydrides, and thioesters in the presence of air sensitive $Ni(cod)_2$ or air stable $Ni(acac)_2$ and a bidentate ligand, such as (2-diphenylphosphinoethyl)pyridine (pyphos; Scheme 125).[325] It is noteworthy that epimerizable stereocenters tolerated the conditions used.

Thioesters **219**, which can be obtained in one step from carboxylic acids, have been found to be suitable substrates for preparation of ketones **220** using alkyl- and arylzinc iodides (Scheme 126).[326] The preferred method used $PdCl_2(PPh_3)_2$ as a catalyst and provided the corresponding ketones in high yields. The value of the protocol is its remarkable chemoselectivity: a number of functional groups—such as the carbonyl group, amino group, ester, sulfide, α-acetate, and aromatic bromide and chloride—do not react with RZnI under the conditions used. Attempts using $ZnEt_2$ instead of EtZnI were unsuccessful: only the corresponding aldehydes, the products of reduction, were

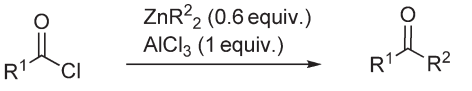

R^1 = aryl or alkyl group
R^2 = Me or Et

Scheme 123

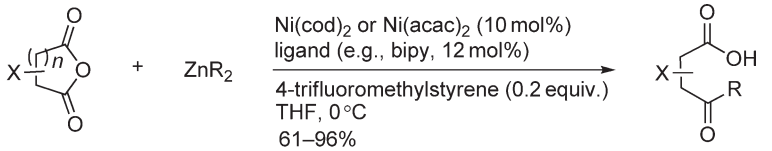

n = 0, 1
X = one or more alkyl substituents
R = Me, Et, Ph

Scheme 124

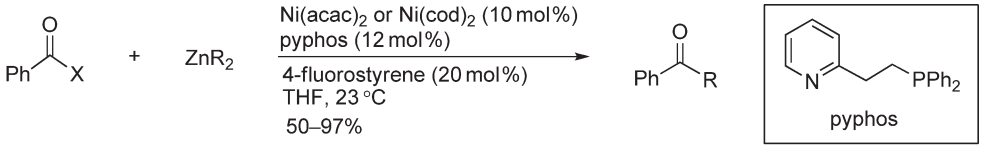

X = F, Cl, CN, SEt, $PhCO_2$, OPh, O-2-Py, S-2-Py
R = Me, Et, Pr^i, $EtO_2CCH_2CH_2$

Scheme 125

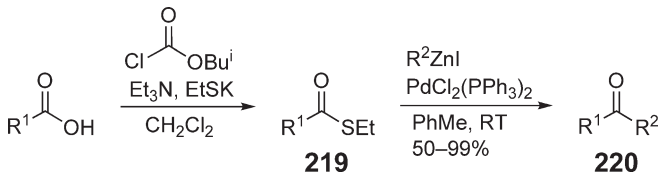

Scheme 126

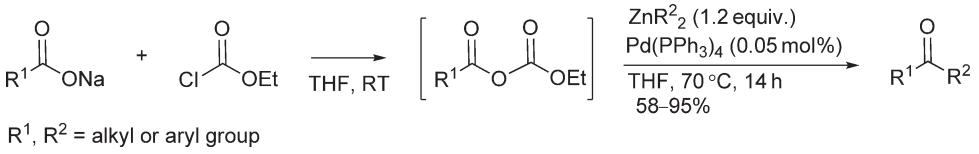

Scheme 127

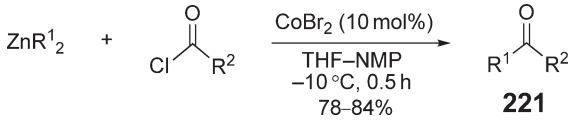

Scheme 128

detected. In a recent variation of this method, dodecanethiol esters derived from odorless dodecanethiol showed a very similar reactivity pattern toward EtZnI; therefore, the use of the modified procedure has a definite practical advantage.[327]

Another Pd-catalyzed reaction of aryl- and alkylzinc halides used carboxylic anhydrides as starting organic compounds (Scheme 127).[328] One of the advantages of this method is that anhydrides can be synthesized *in situ* from the corresponding sodium salts of carboxylic acids and ethyl chloroformate. The scope of the method includes aliphatic and aromatic anhydrides, phenyl-, ethyl-, isopropyl-, and *n*-butylzinc iodides.

In 1996, Reddy and Knochel disclosed that diorganozinc reagents can be acylated by acid chlorides in the presence of 10 mol% $CoBr_2$ using a 1 : 1 mixture of THF–NMP as solvent.[329] The reactions were complete in 30 min at −10 °C and afforded 78–84% yield of the corresponding ketones (**221**, Scheme 128). The same reactions were also carried out using $FeCl_3$ as a catalyst.[329] These transformations also provided high yields of the products (74–82%), but required longer reaction times.

2.06.16.4.2 Uncatalyzed reactions

Reactions of allylzinc halides with carbon nucleophiles are rare examples of uncatalyzed transformations of organozinc compounds. Allylzinc bromide, formed *in situ*, reacted with a number of structurally diverse acyl chlorides furnishing the corresponding ketones **222** in high yields (Scheme 129).[330] No isomerization to the corresponding α,β-unsaturated ketones was observed under the conditions used (RT, 5 min–6 h).

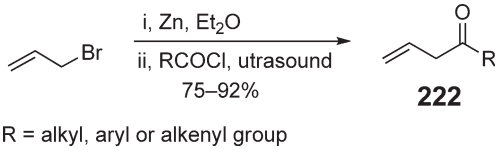

Scheme 129

2.06.16.5 Reactions of Organozinc Reagents with Imines and Other C═N Bond-containing Compounds

2.06.16.5.1 Nucleophilic addition of diorganozincs to imines

One of the significant achievements in synthetic chemistry during the last decade is the development of methodologies for asymmetric additions of organometallic derivatives, particularly dialkylzincs, to imine derivatives. Thus far, the following types of imines have been successfully alkylated by diorganozinc reagents: *N*-(*p*-methoxyphenyl)imines[331,332] (**223a** and **223b**), *N*-sulfonylimines[333] (**224a** and **224b**), *N*-acylimines[334,335] (**225a** and **225b**), and *N*-phosphinoylimines[336–344] (**226a** and **226b**, Figure 84).

Reactions of *N*-(*p*-methoxyphenyl)imines **223a** and **223b** with diorganozincs result in the formation of chiral arylalkyl secondary amines **227**, Scheme 130). Upon alkylation of three other types of imines **224b–226b**, valuable amine precursors are obtained, which can be transformed in one step to the corresponding primary amines with a chiral center in the α-position.

The majority of the studied imines **223b–226b** were synthesized from primary amines, such as benzylamine and its *p*-substituted derivatives. It is noteworthy that an attempt using an *N*-phosphinoylimine obtained from secondary α-methylbenzylamine failed.[337] Aliphatic imines have also been screened in the alkylations with diorganozinc reagents, although not as thoroughly as their aromatic analogs.[331,338] A major drawback in working with alkylimines is the difficulty in obtaining them in pure form and in high yields. To circumvent this problem, aliphatic *o*-anisidyl imines **223a** were prepared *in situ*, followed by alkylation with $ZnEt_2$ (Scheme 131). This procedure allowed preparation of the desirable alkylarylamines **228** in 57–98% yield and with excellent enantioselectivity.[331]

Results of a similar "*in situ*" approach have recently been reported for the asymmetric addition of diethylzinc to *N*-phosphinoylalkylimines **226a**. The Charette group has shown that compounds **226a**, formed *in situ* from the corresponding *p*-toluenesulfinyl adducts **230**, undergo enantioselective catalytic alkylation with $ZnEt_2$ with 90–97% ee (Scheme 132).[338] Adduct **230** can be readily obtained from the corresponding amines, diphenylphosphinic amide and *p*-toluenesulfinic acid.[338]

Bräuse and co-workers, who were interested in alkylation and acylation of *N*-acylimines **225b**, have also used an "*in situ*" approach in their studies.[334,335] *N*-Formyl and *N*-acetylimines, formed *in situ*, reacted with dialkylzincs[335] or diphenylzinc[334] affording amine precursors in excellent yields. The report[334] of the Bräuse group appears to be the only account of enantioselective arylation of imine derivatives by organozinc reagents. Similarly to the aforementioned arylation of aldehydes,[251] it has been found that a mixed zinc reagent formed *in situ* from $ZnPh_2$ and $ZnEt_2$ reacts with imine derivatives furnishing only phenylated products **233**. It is noteworthy that deprotection of the *N*-formylamine **233** proceeded in quantitative yield (Scheme 133).[334]

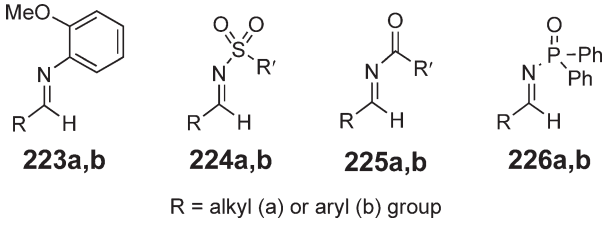

Figure 84 Imine derivatives alkylated by diorganozinc reagents.

Scheme 130

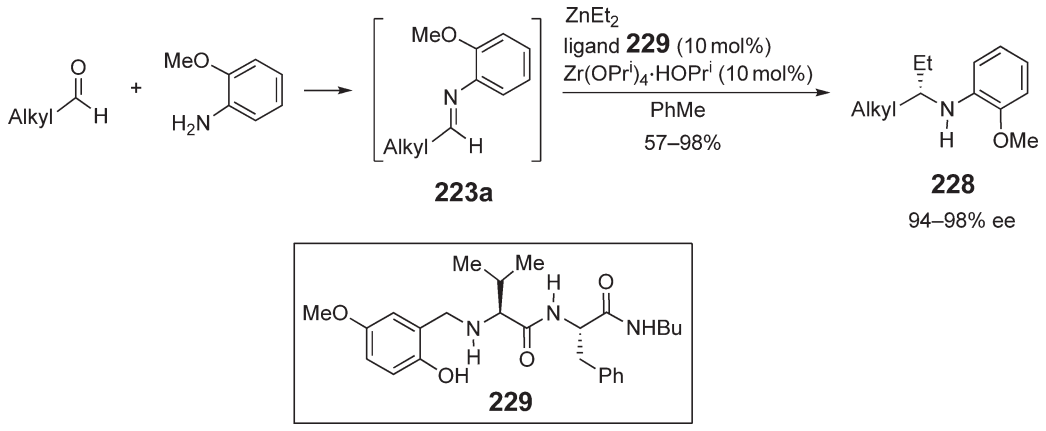

Scheme 131

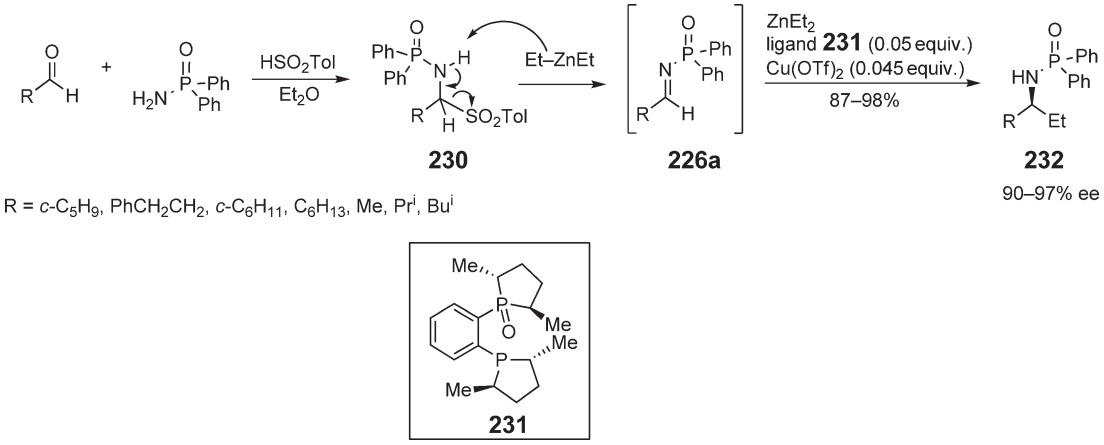

Scheme 132

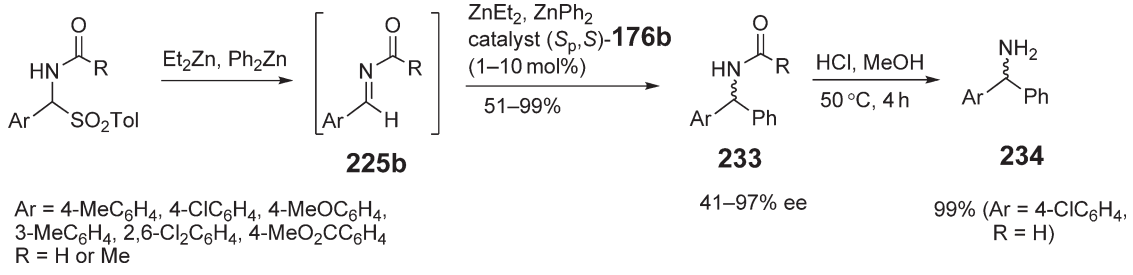

Scheme 133

A great variety of chiral inductors have been tested in imine alkylations by diorganozincs (Figure 85). In earlier studies, these reactions were promoted by stoichiometric amounts of a chiral ligand (e.g., **179i** and **179j**,[337] **235**,[341,342] and **236**,[336] see Figures 80 and 85). More recent reports describe applications of catalytic amounts of a chiral ligand used in a combination with catalytic amounts of Zr(IV) or Cu(II) salts. The majority of reported chiral catalysts belong to one of the following types of compounds: phospines (e.g., **237**)[339] and diphosphines **238–241**,[333,339] imino alcohols **169**,[334] **170**,[334] **176a** and **176b**,[335] **242**,[344] **243**,[344] and **244**[334]), phosphoramidites **245**,[339] amino phosphines **246a** and **246b**,[333,339] and peptide-based ligands (**247**[331,332] and **248**,[332] Figures 80 and 85).

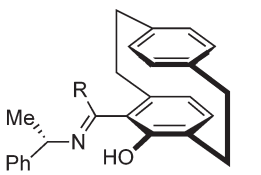

(S_p,S)-**176a,b**

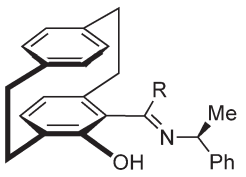

(R_p,S)-**176a,b**

176a: R = Me
176b: R = Ph

235a: R^1 = Me; R^2 = H
235b: R^1 = Et; R^2 = H
235c: R^1 = Pr^i; R^2 = H
235d: R^1 = $PhCH_2$; R^2 = H
235e: R^1 = $PhCH_2$; R^2 = Me
235f: R^1 = $PhCH_2$; R^2 = Pr^i
235g: R^1 = $PhCH_2$; R^2 = Ph

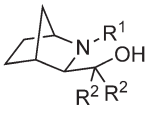

235a–g

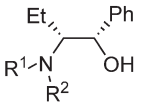

236a,b

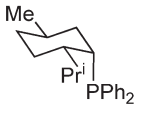

237

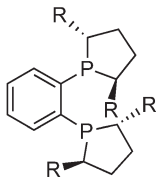

238a–c

238a: R = Me
238b: R = Et
238c: R = Pr^i

R^1 = R^2 = Bu
R^1, R^2 = $CH_2CH_2OCH_2CH_2$

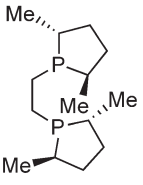

239

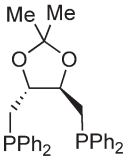

240

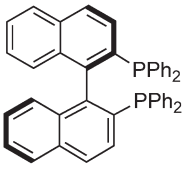

241

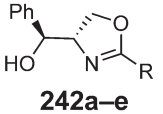

242a–e

242a: R = Ph
242b: R = Pr^i
242c: R = Nf
242d: R = Bn
242e: R = CH_2Nf

242f: R^1 = 2-Br
242g: R^1 = 4-Br
242h: R^1 = 2-Me
242i: R^1 = 3-Me
242j: R^1 = 4-Me
242k: R^1 = 4-MeO

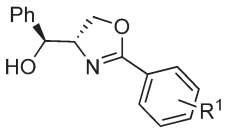

242f–k

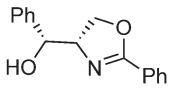

242l

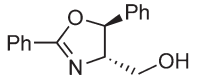

243

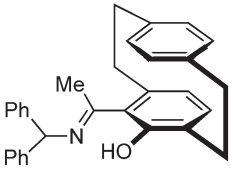

(S_p)-**244**

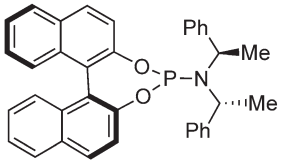

245

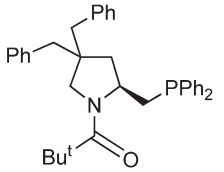

246a,b

246a: R = H
246b: R = $PhCH_2$

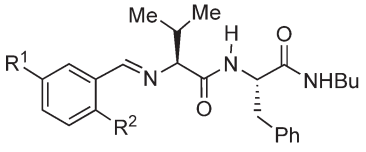

247a–d

247a: R^1 = OMe; R^2 = OH
247b: R^1 = NMe_2; R^2 = OH
247c: R^1 =H; R^2 = OH
247d: R^1 = H; R^2 = PPh_2

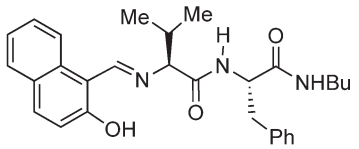

248

Figure 85 Examples of chiral ligands used for the alkylation and arylation of imines by diorganozinc reagents.

Recently, Dahmen and Bräuse[335] reported asymmetric dialkylzinc addition to imines in the presence of optically active ligands without an additional metal involved. Alkylation of *N*-acylimines, which were generated *in situ* from *N*-(*tert*-butyloxycarbonyl)-α-(*p*-tolylsulfonyl)benzylamines, was catalyzed by optically active [2.2]paracyclophane-based ketimine *N,O*-ligands **176a** and **176b** (Figure 85) with both planar and central chirality.

A highly creative method for $ZnMe_2$-mediated addition reactions of alkenylzirconocenes to aldimines was recently proposed by the Wipf group.[345,346] The protocol includes a three-step sequence: (i) alkyne hydrozirconation, (ii) transmetallation using $ZnMe_2$, and (iii) aldimine **226a** addition to the intermediate vinylic zinc derivative **250** (Scheme 134). Interestingly, one more step can be added to this sequence: when CH_2Cl_2 or CH_2I_2 are used in step (iii), cyclopropanation of the allylic amides **251** takes place in high yield.[345,347] The methodology shown in Scheme 134 was also applied by the same group to asymmetric vinylation of aldehydes using enantiopure *N,O*- and *N,S*-ligands as chiral inductors.[346,348]

2.06.16.5.2 Reactions of allyl- and benzylzinc halides with polymer-supported imines

During the past decade, the main focus of studies related to the well-known[349] $CeCl_3$- or $SnCl_2$-catalyzed reactions of allylzinc and benzylzinc halides with imines was the application of polymer-supported chiral imines.[350,351] An example of such reactions is shown in Scheme 135.[350] It should be noted that attempts using arylzinc reagents in these reactions failed.[351]

2.06.16.5.3 Nucleophilic addition of zinc-containing reagents to nitrones

Nitrones have a more reactive C═N bond toward nucleophilic addition compared to imines. In spite of this fact, there have been only a limited number of studies on the nucleophilic addition reactions of nitrones, particularly organometallic reagents.[352–355] During the last decade, research related to reactions of nitrones with zinc-containing reagents was essentially focused on (i) dialkylzinc-assisted alkynylations[356–358] and vinylations[359] of nitrones, (ii) catalytic asymmetric nucleophilic additions to the C═N bond,[360–364] and (iii) nitrone allylations by allylzinc halides.[365,366]

The catalytic generation of alkynylzinc derivatives **254** from terminal alkynes was performed using either a mixture of $Zn(OTf)_2$ and Pr^i_2NEt (method A)[357,358] or $ZnEt_2$ (method B).[356] The Zn-containing intermediates **254** reacted with nitrones, affording the corresponding *N*-propargyl hydroxylamines **255** in good or excellent yields (Scheme 136). Both protocols allow application of terminal alkynes with an additional functional group, such as a C═C bond (method A and B), CN bond (B), trimethylsilyl ether (A), trimethylsilyl group (A and B), ester (B), acetal (B), *tert*-butyl ether (B), or alkyl chloride (B).

A recently reported vinylation of nitrones was accomplished by using $ZnMe_2$ and vinylboronic esters of pinacol **256**. The optimal conditions for the addition were 3.5 h at 60 °C in DMF. Yields of the products, *N*-allylic hydroxyamines **257**, varied significantly from 14% to 92% (Scheme 137).[359]

An important, but not extensively explored, research area is the asymmetric addition of organozinc reagents to nitrones. During the last decade, there have been only a few publications in this field. In 1993, the group of Ukaji and Inomata discovered that 3,4-dihydroisoquinoline *N*-oxide **258a** can be alkylated by $ZnMe_2$ or $ZnEt_2$ in the presence of a catalytic amount of bromomagnesium (2*S*,3*R*)-4-dimethylamino-1,2-diphenyl-3-methyl-2-butoxide **259** in 33–66% ee.[367] In the next study, they slightly expanded the scope of substrates and reported 78% ee for nitrone **258c**.[361] Addition of 0.3 equiv. bromomagnesium triphenylmethoxide was shown to be essential for attaining this level of enantioselectivity. Higher values of ee (up to 95%) were reported when nitrones were slowly added to a mixture of dialkylzinc and dicyclopentyl (*R,R*)-tartrate (**260**, Scheme 138).[360,362,364]

Asymmetric additions of Reformatsky-type reagents to nitrones **258a** and **258b** have also been reported (Scheme 139).[368] The reagents were prepared *in situ* from $ZnEt_2$ and the corresponding iodoacetic acid ester. Diisopropyl (*R,R*)-tartrate **262** was employed as a chiral inductor. Enantioselectivities varied significantly; the best results were obtained at 0 °C when a nitrone was added to the reaction mixture over a 2 h period.

Similarly to other allylic organometallic reagents,[354] allylzinc bromide and substituted allylic derivatives are capable of reacting with nitrones.[365,366] As in other reactions of allylzinc halides, they were prepared *in situ* from the corresponding allylic halide and zinc powder. The addition step occurred with complete regioselectivity for crotyl **264b** and prenyl **264c** derivatives (Scheme 140). It is noteworthy that the reactions proceeded faster and with reversed *syn*/*anti*-diastereoselectivity when they were carried out in the presence of Et_2AlCl. Yields of the isolated products varied significantly and depended on the order of reagent addition.

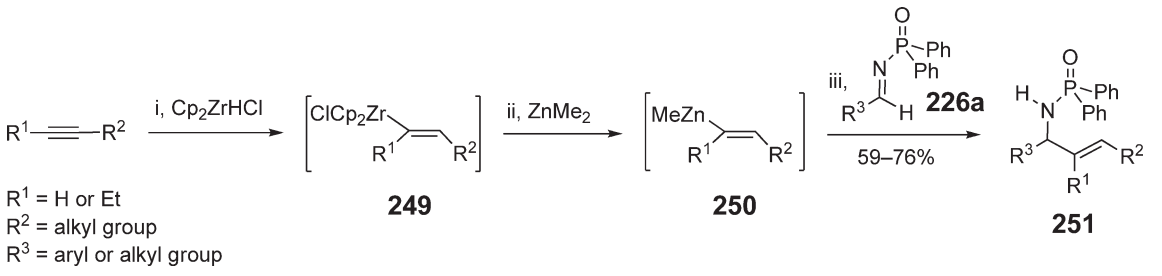

Scheme 134

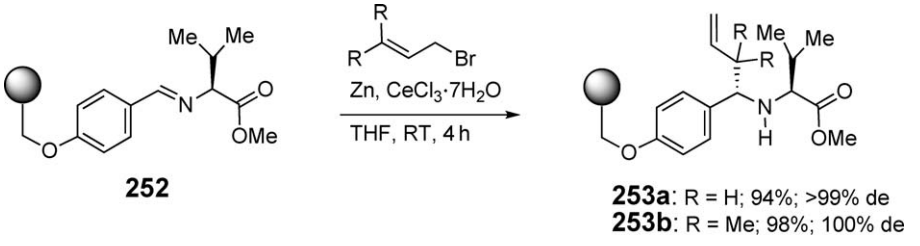

Scheme 135

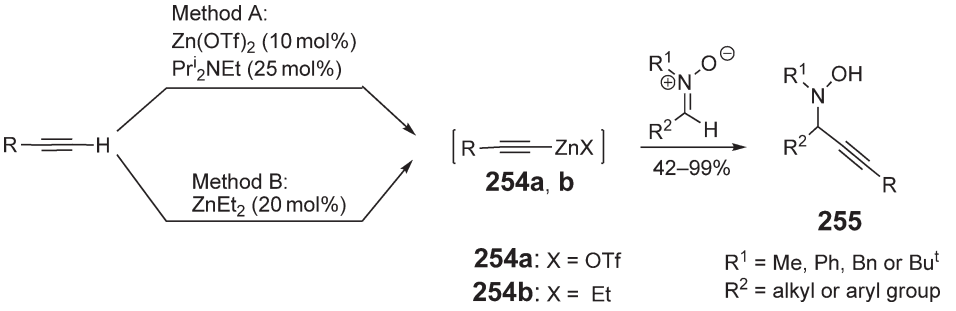

Scheme 136

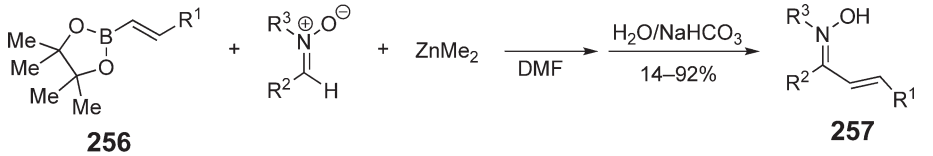

Scheme 137

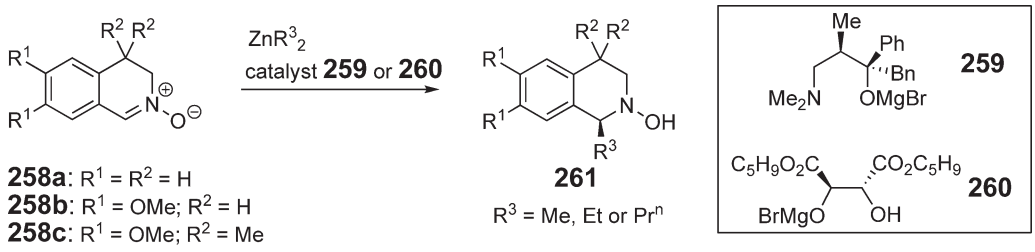

Scheme 138

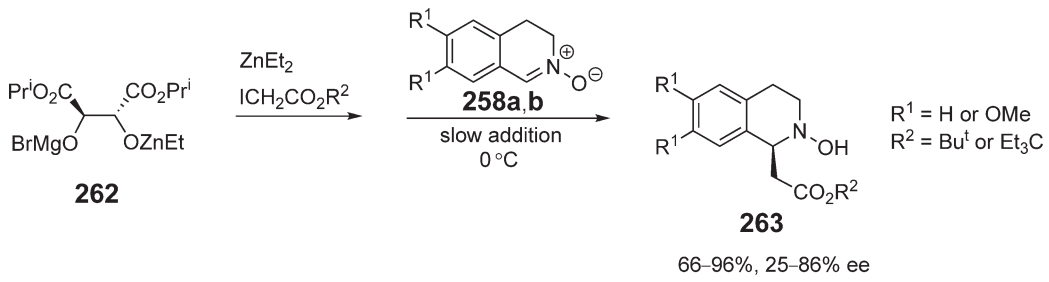

Scheme 139

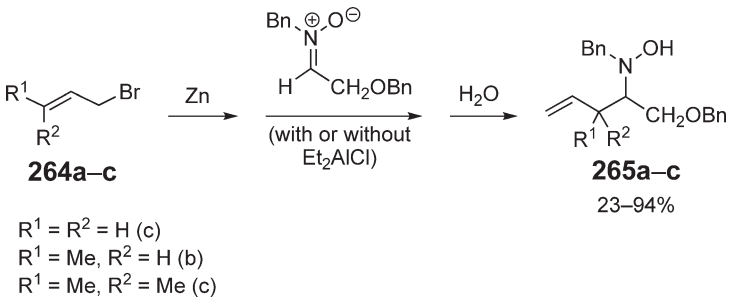

Scheme 140

2.06.16.5.4 Nucleophilic addition of zinc organometallic reagents to other C═N bond-containing compounds

During the last decade, there has been little research done in the field of nucleophilic additions of organozincs to C═N bond-containing compounds, except for imines and nitrones. A rare exception is the paper by Hanessian and Yang, which described zinc-mediated allylations of glyoxylic ester oximes and Oppolzer's (1*S*)-(−)-2,10-camphorsultam analog **266** in aqueous media (Scheme 141).[369] The reactions proceeded in very high yields, with complete regioselectivity and, in the case of optically active substrates, with very high diastereoselectivity. The addition products **267** were converted to valuable optically active α-amino acids **268** in two steps.

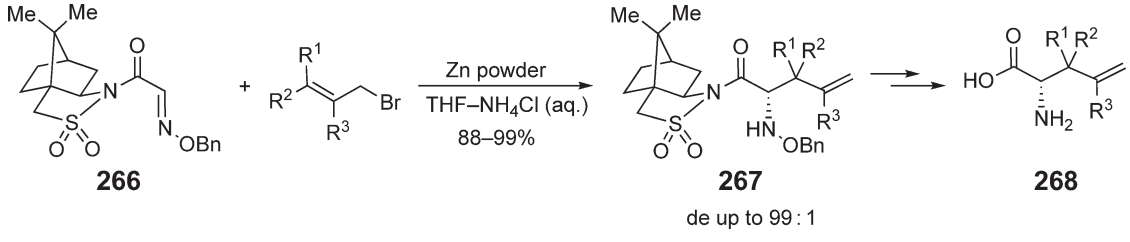

Scheme 141

2.06.16.5.5 Radical additions to imines, nitrones, and related compounds

It has been known for more than a decade that organozinc compounds can participate in radical reactions, particularly in Pd- or Ni-catalyzed intramolecular cyclizations[370,371] and cyclopropanation.[372] However, only recently has it been shown that, in the presence of oxygen, $ZnEt_2$ and $ZnMe_2$ can promote radical additions to the C═N bond.[321,373–379] Dialkylzincs participate in these reactions as the initiators and the chain-transfer reagents. Among the different types of the C═N bond-containing compounds tested in radical reactions with $ZnEt_2$, oxime ethers,[380,381] particularly glyoxylic oxime ether,[382–384] seem to be the best radical acceptors.

In earlier studies of ZnR_2-mediated radical additions to the C═N bond-containing substrates, alkyl iodides were employed as reagents. For example, Bertrand *et al.* investigated radical and nucleophilic additions of alkyl iodides to glyoxylate imines (e.g., **269**) in the presence of $ZnEt_2$.[321,375] If the reaction mixture contained oxygen, due to the radical additions, secondary amines **270** were the major, if not the only, products. When the mixture was degassed, the amount of the alternative product **271** increased significantly (Scheme 142). Similar findings were reported for the $ZnEt_2$-initiated radical additions of isopropyl and *tert*-butyl iodide to glyoxylic oxime ethers, hydrazones, or imines.[321]

The $ZnEt_2$-initiated radical additions to glyoxylic[384] and other[374] oxime ethers, including those anchored to a polymer (e.g., **272**), yielded valuable precursors for α-amino acids (Scheme 143).

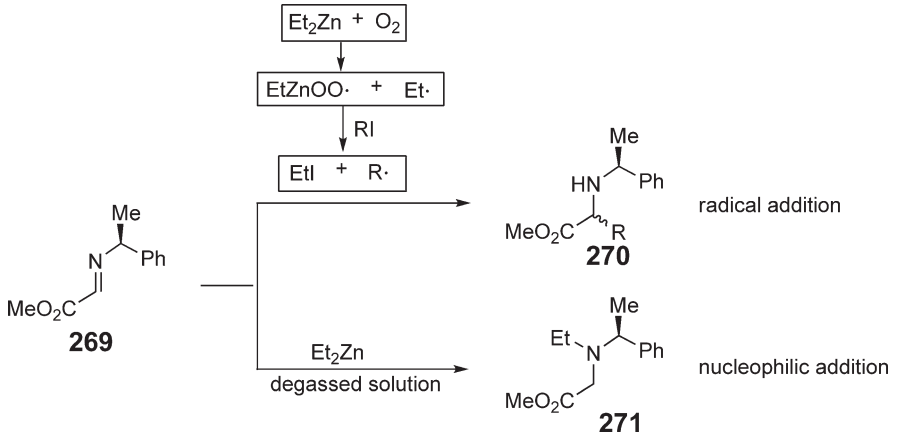

Scheme 142

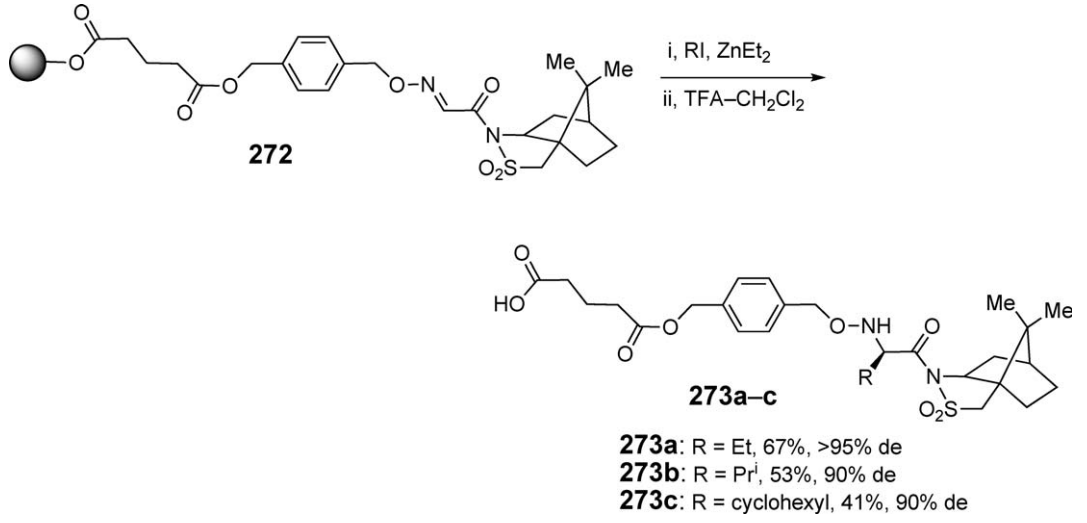

Scheme 143

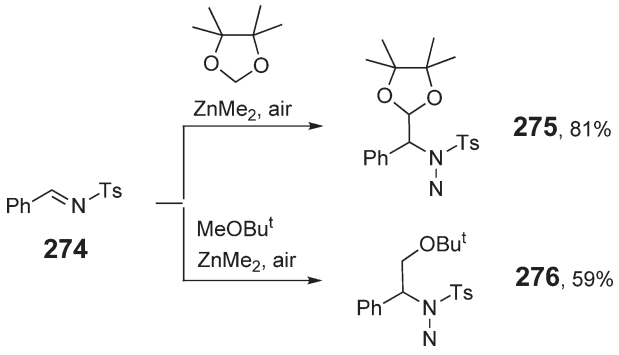

Scheme 144

More recently, the group of Tomioka reported the $ZnMe_2$-mediated additions of ethers and related oxygen-containing compounds to simple[378] and *N*-tosyl-substituted[377,379] **274** imines (Scheme 144). Attempts to render these transformations asymmetric, unfortunately, had little success.[379]

Other examples of ZnR_2-initiated radical additions to C═N bond-containing compounds can be found in a recent review by Miyabe *et al.*[373] Overall, radical additions to imines and related derivatives may be considered as a valuable alternative to nucleophilic additions, particularly for the introduction of secondary and tertiary alkyl groups. In general, organozinc-mediated radical reactions are a new and significant direction with great potential.[382,385]

2.06.16.6 Halomethylzinc-mediated Cyclopropanation Reactions

During the last decade, a number of new methods for regioselective, diastereoselective, or enantioselective cyclopropanations using Zn-containing reagents have been reported. A very detailed survey of recent (up to the year 2003) developments in the area of cyclopropanation reactions, particularly using zinc-containing reagents, was recently published by Lebel *et al.*[386]

In Simmons–Smith-like additions, a number of different halomethylzinc reagents of general structure $XZnCH_2Y$ can be employed. Recently, the group of Shi reported the preparation and application of a set of new reagents of the general structure $RXZnCH_2I$.[387,388] The major advantage of using them is that their reactivity can be finely tuned by changing the R group. Among the tested compounds of the structure RXH, the best cyclopropanation results were obtained for the derivatives of carboxylic acids with strongly electron-withdrawing substituents in the α-position, such as trifluoroacetic acid (Scheme 145).

The Shi group has also investigated asymmetric cyclopropanations using R^*OZnCH_2I obtained from the corresponding optically active alcohols R^*OH. Reactions of R^*OZnCH_2I turned out to be slow, and the addition of a Lewis acid was necessary to facilitate the cyclopropanation step. Unfortunately, the conversions were far from complete even with the Lewis acid, and the observed enantioselectivities were low. In one of the best experiments, *trans*-β-methylstyrene was cyclopropanated by R^*OZnCH_2I, yielding the corresponding product with 51% ee; no absolute configuration of compound **278** was assigned (Scheme 146).

Fournier and Charette proposed a new *gem*-dizinc carbenoid, IZnCHIZnI **279**, for alkene cyclopropanation.[389] They reported that EtZnI reacted with $CHCl_3$ to form unstable **279**, which was capable of reacting with the Bn-protected allylic alcohols **280a–c**. The final step of the reaction sequence was quenching the Zn-containing intermediate **281a–c** with an electrophile (Scheme 147).

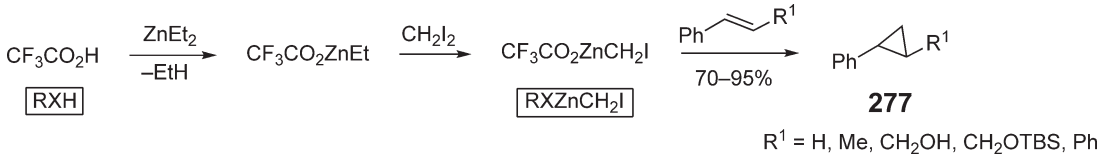

Scheme 145

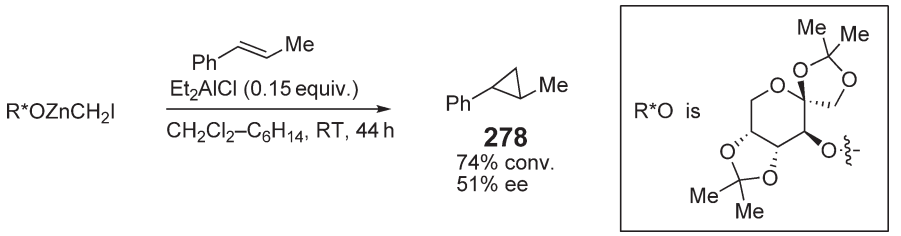

Scheme 146

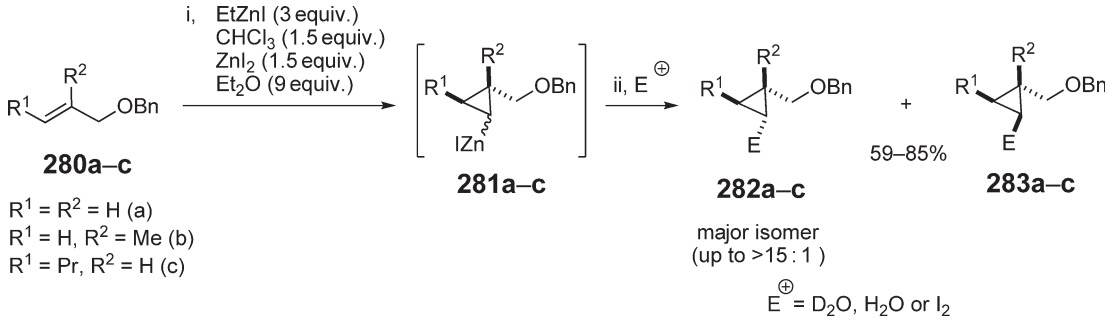

Scheme 147

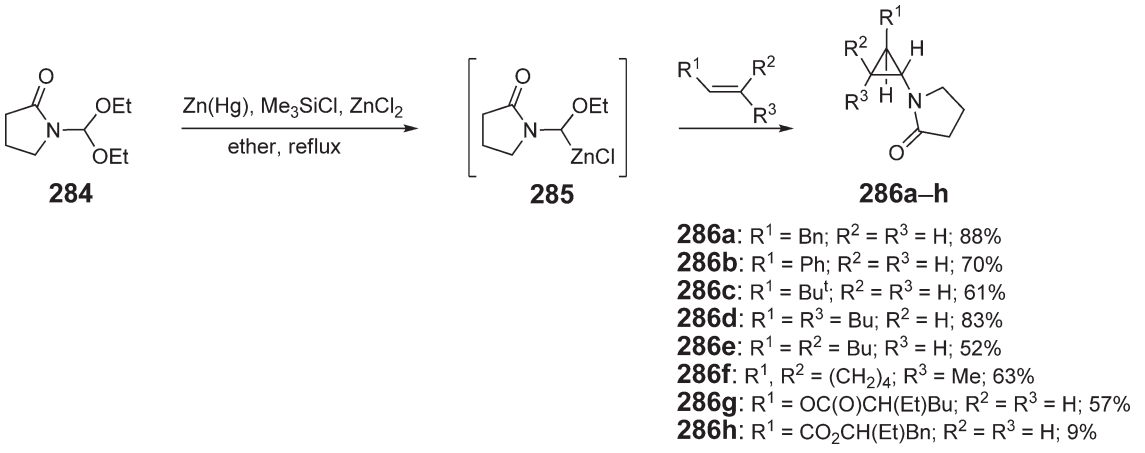

Scheme 148

The preparation of an unusual organozinc carbenoid **285** from amide **284** has been recently reported.[390] The carbenoid **285** was used in amidocyclopropanation reactions of diverse alkenes (Scheme 148).[390] Unfortunately, experiments employing other amides yielded the corresponding products in low yields.

2.06.16.7 Copper-catalyzed Asymmetric Allylic Alkylations with Alkylzinc Reagents

Asymmetric allylic substitution reactions have been studied for many years because they provide valuable chiral compounds. Regardless of the alkylating agent used, there are two major goals in these reactions: (i) to minimize the amount of S_N2 products, and (ii) to maximize the enantiomeric purity of the S_N2' products. Various approaches have been investigated to achieve these goals. Recently, the efforts of several research groups have been focused on the

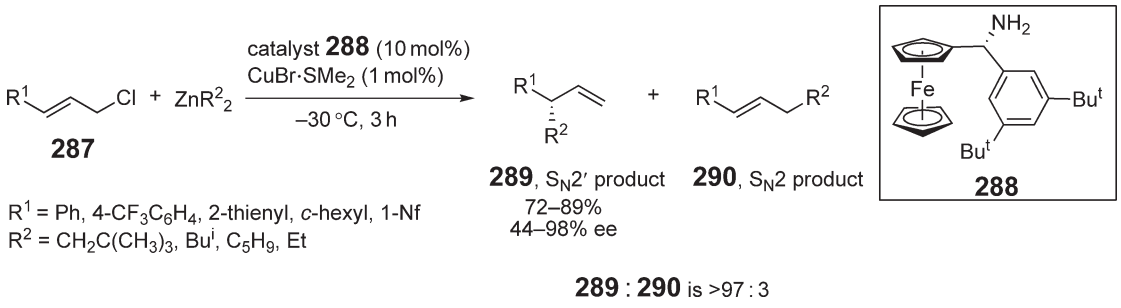

Scheme 149

use of organozinc compounds as alkylating reagents in copper-catalyzed catalytic allylic substitutions and the search for efficient chiral inductors for such systems.

In 1999, Dübner and Knochel reported a significant breakthrough: reactions of allylic chlorides **287** with dialkylzincs in the presence of CuBr·Me_2S and optically active ferrocenylamines provided the S_N2' products **289** with high regioselectivity (up to >99 : 1) and 37–87% ee.[391] These results were obtained only for bulky organozinc reagents: dineopentylzinc, dimyrtanylzinc, $Zn(CH_2SiMe_3)_2$, and $Zn(CH_2SiPhMe_2)_2$. Another shortcoming of this method was the requirement of a very low temperature of −90 °C for the reactions. Later, they modified the ligand; this allowed even higher enantioselectivities to be achieved at −30 °C (Scheme 149).[392] However, the enantioselectivity problem for non-bulky alkyl groups was not solved.

The results of the Knochel group inspired others to continue the search for more efficient catalysts. Feringa with co-workers investigated the use of chiral phosphoramidites as chiral ligands in the reactions of similar allylic substrates. They achieved an 85 : 15 ratio of S_N2' : S_N2 products and 77% ee using $ZnEt_2$.[393] Related phosphorimidides have also been studied by the group of Alexakis.[394] They reported ee's up to 96% for similar reactions catalyzed by copper(I) thiophen-2-carboxylate. It is noteworthy that chiral *spiro*-phosphoramidite and phosphite ligands tested in reactions with cinnamyl halides gave only moderate levels of enantioselectivity.[395] Substitution reactions of cinnamyl phosphate and related compounds in the presence of the sulfamido group-containing Schiff bases and their derivatives were studied by the Gennary group.[396–398] They reported good to excellent (up to 100 : 0) ratios for S_N2' : S_N2 products, but low levels of enantioselectivity for chiral products. The best result of 40% ee was reached in the transformation shown in Scheme 150.[396]

The idea of Hoveyda with co-workers to employ their peptide ligands (e.g., **295**) as chiral inductors in allylic substitutions with dialkylzincs turned out to be very rewarding.[399–401] As a result of meticulous screening of numerous optically active ligands, copper salts, and substrates under various conditions, they achieved excellent results for aliphatic alkenes. Particularly, allylic substitution products with tertiary **297** and quaternary **299** carbon centers were obtained regioselectively and with 78–96% ee (Scheme 151).[401]

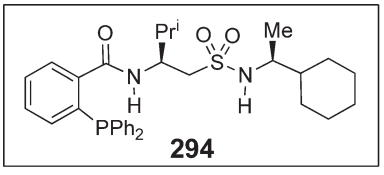

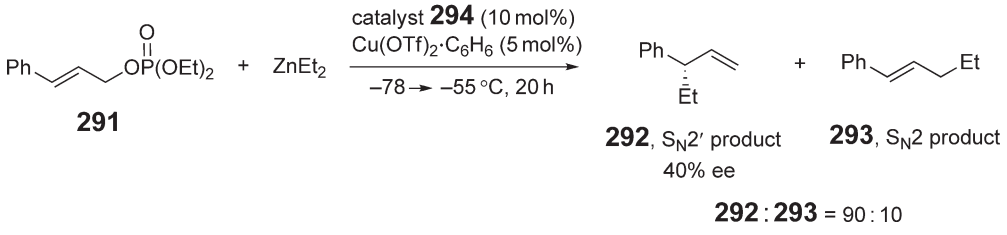

Scheme 150

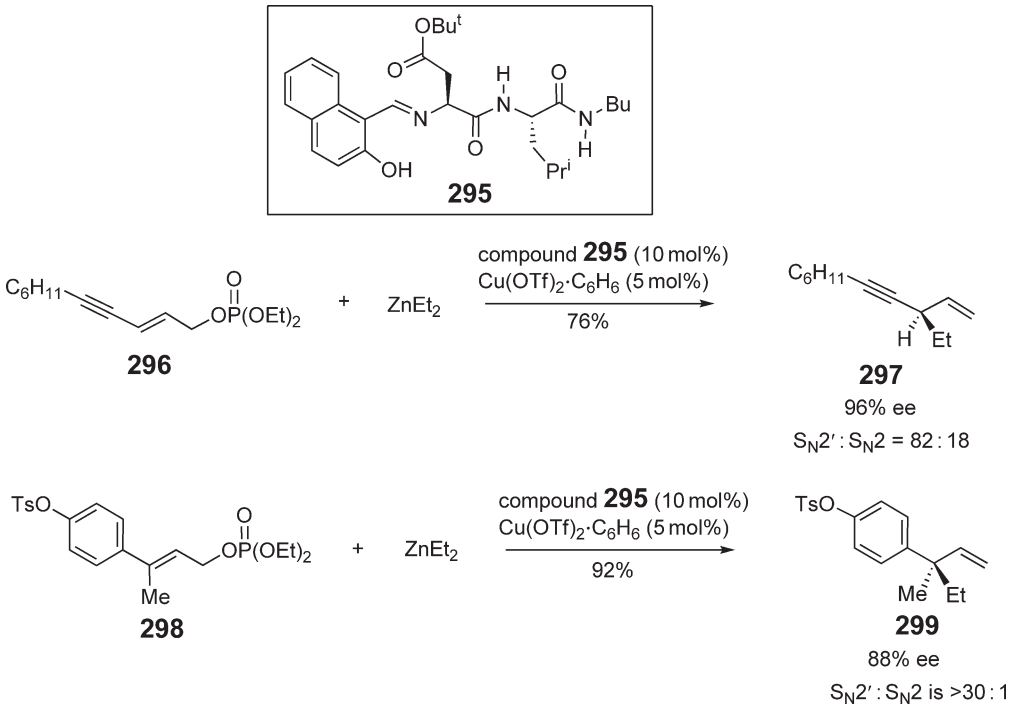

Scheme 151

Hoveyda and co-workers also tested optically active *N*-heterocyclic carbenes and their silver complexes in copper-catalyzed reactions of allylic phosphates with dialkylzincs.[402] The ratios of $S_N2' : S_N2$ products were higher than 98 : 2 and the ee varied from 34% to 98%.

It is noteworthy that $ZnEt_2$ has been used as a base in enantioselective allylic substitutions. A remarkable increase in ee was observed when $ZnEt_2$ was used instead of KH, NaH, LiH, LDA, or BuLi in the Pd-catalyzed alkylations of allylic acetates by enolates of malonic esters and related compounds.[403] In contrast, application of $ZnEt_2$ was not as very effective as in similar iridium-catalyzed allylic alkylations.[404]

2.06.16.8 Reactions of Organozinc Reagents with Alkyl, Aryl, and Alkenyl Halides

2.06.16.8.1 Metal-catalyzed cross-coupling reactions between organozinc derivatives and alkyl halides

Development of new methodologies for formation of carbon–carbon bonds has been one of the major tasks in organic chemistry. Obviously, organometallic compounds, particularly zinc derivatives, have found great use in such reactions. During the past several years, there have been several significant reports of nickel- and palladium-catalyzed reactions of dialkylzincs and alkylzinc halides with alkyl halides of diverse structure. A detailed account of most of these studies can be found in a recent review by Knochel *et al.*[246]

In 1996, the Knochel group reported their observations that primary alkyl iodides with a C=C bond and three or four carbons between the halogen and the (sp^2)C atom **300** reacted with dialkylzincs to form alkene **301** (Scheme 152).[405] The reaction took place in the presence of a catalytic amount of $Ni(acac)_2$.

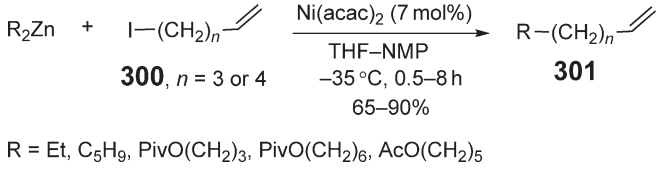

Scheme 152

All alkyl halides used in the couplings were primary, although some of them were branched or had an ester functionality. Some of the dialkylzincs had a functional group without affecting the outcome of the reaction. For example, organozinc derivative **302** with a silyl enol ether group reacted with alkyl iodide **303**, affording the desired product **304** in 65% yield (Scheme 153).

The presence of a remote C═C double bond in the alkyl halide was critical: saturated analogs underwent nickel-catalyzed halogen–zinc exchange.[248] It has been suggested that the double bond coordinates to the nickel atom. As a π-acceptor, the C═C bond removes some electron density from the metal, thus facilitating the reductive coupling (Scheme 154).[246]

The next achievement of the group of Knochel was a successful coupling of dialkylzincs with alkyl iodides, containing functional groups other than a C═C bond.[324,406] They found that the introduction of certain additives, such as *m*-trifluoromethylstyrene or acetophenone, increased the reaction rate and the yield of desired coupling products.

Primary and secondary alkylzinc iodides and benzylic zinc halides also undergo Ni-catalyzed reactions with various primary alkyl iodides and bromides.[407–409] According to the procedure by Knochel and co-workers, the transformations with alkylzinc iodides, which are less reactive than the corresponding dialkylzincs, require the presence of two additives: Bu_4NI and 4-fluorostyrene (Scheme 155).[407,408]

An alternative protocol for treating alkylzinc bromides with primary and secondary alkyl bromides and iodides was described by Zhou and Fu.[409] In the study, a combination of $Ni(cod)_2$ and a chiral oxazoline ligand **306** was used as a catalytic system providing 62–88% yield of product **307**; *N,N*-dimethylacetamide (DMA) was the reaction solvent (Scheme 156).

Arylzinc bromides are also capable of reacting with functionalized primary alkyl iodides in the presence of $Ni(acac)_2$.[410] The couplings readily occurred in the presence of an equimolar amount of 4-trifluoromethylstyrene at −15 °C.

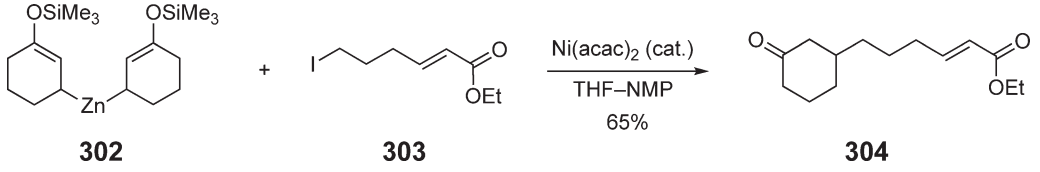

Scheme 153

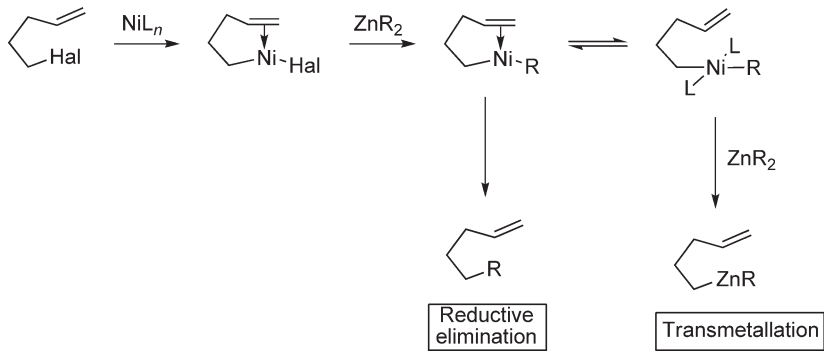

Scheme 154

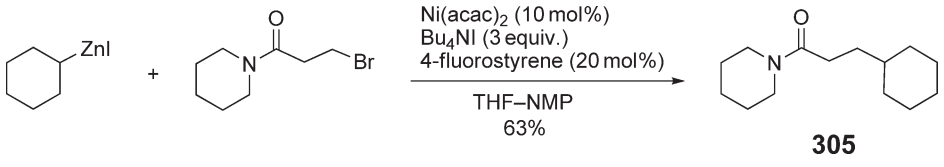

Scheme 155

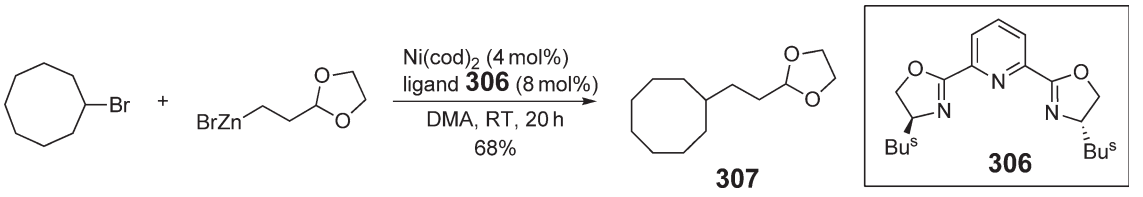

Scheme 156

One of the most recent developments in the field of Ni-catalyzed reactions of alkyl halides with organozinc derivatives is a study of Terao *et al.*[411] They reported the use of three additives in the couplings: 1,3-butadiene, *N,N*-bis(penta-2,4-dienyl)benzylamine **308a**, and 2,2-bis(penta-2,4-dienyl)malonic acid dimethyl ester **308b**. Addition of tetraene **308b** to the reaction mixtures significantly increased the product yields (Scheme 157). The remarkable effect of these additives was explained by the formation of the bis-π-allylic complex **309** as the key intermediate (Scheme 158).

When Knochel and his co-workers attempted to use $[PdCl_2(CH_3CN)_2]$ and related palladium(II) complexes as catalysts in the reactions of dialkylzincs with alkyl iodides, they observed the formation of the halogen–zinc exchange[405] or cyclization[406] products only. A recent paper of Zhou and Fu demonstrated that palladium complexes can also be used in the coupling reactions of alkylzinc bromides with alkyl iodides, bromides, chlorides, and

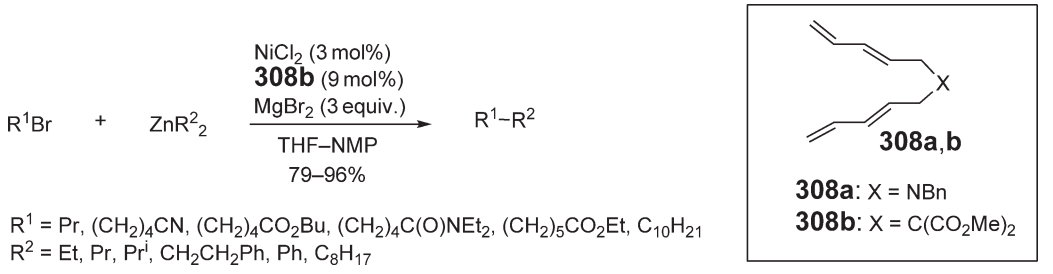

Scheme 157

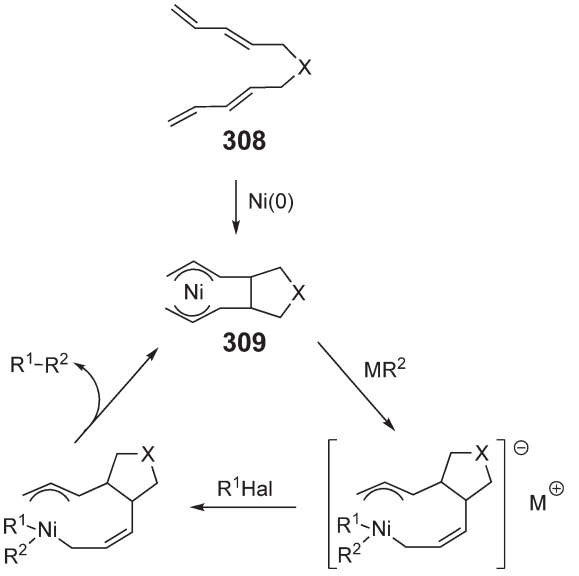

Scheme 158

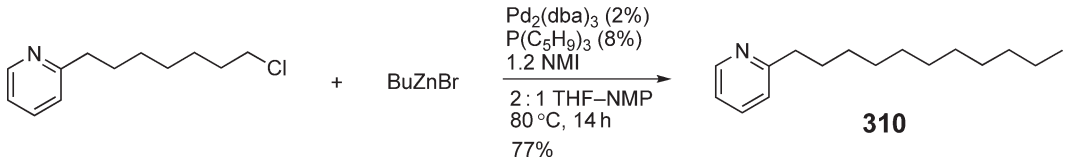

Scheme 159

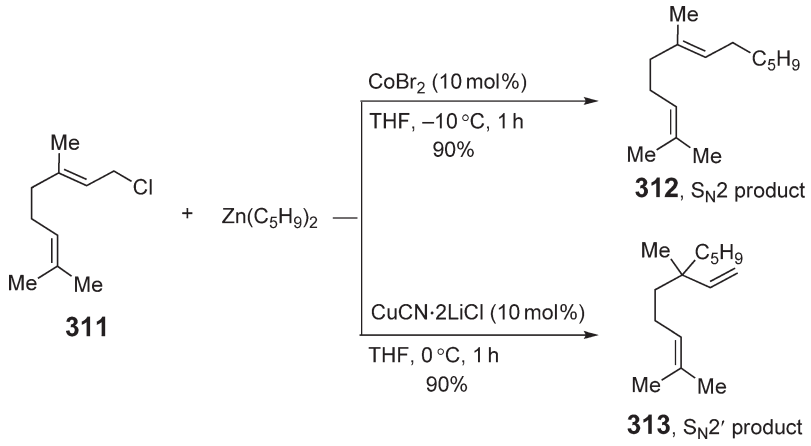

Scheme 160

tosylates.[412] They developed a unique catalytic system, containing 2% $Pd_2(dba)_3$ and 8% tricyclopentylphosphine, which provided high yields of desirable coupling products (e.g., **310**, Scheme 159). Addition of *N*-methylimidazole (NMI) to the reaction mixture was shown to be essential as well. It is remarkable that this system worked equally well for chlorides, bromides, iodides, and tosylates. Three types of organozinc derivatives gave excellent results: alkyl-, alkenyl-, and arylzinc halides. It was also shown that instead of air sensitive tricyclopentylphosphine (PR_3), its air stable salt $[HPR_3]BF_4$ can be used as a component of the catalytic system.[412,413]

The Knochel group has reported that dialkylzincs and alkylzinc iodides react with allylic chlorides and phosphates in the presence of $CoBr_2$ to form compounds with a new C–C bond.[329] For example, geranyl chloride **311** reacted with dipentylzinc to give the S_N2 product **312** in 90% yield (Scheme 160). Surprisingly, when $CoBr_2$ was replaced with CuCN·2LiCl in the same reaction, the S_N2' product **313** was isolated in the same yield. As expected, allylations of alkylzinc iodides required longer reaction times than those of diorganozincs.

2.06.16.8.2 Metal-catalyzed cross-coupling reactions of organozinc derivatives with aryl and vinyl halides

2.06.16.8.2.(i) Application of Reformatsky reagents

Reactions of the Reformatsky reagents with aryl and vinyl halides have been known for some time (see references 10–15 in the paper of Hama *et al.*[414]). Studies in this field were concentrated on synthesis of target compounds using this transformation and on the development of new catalysts to increase the generally modest yields of coupling products. For example, Cantin *et al.* reported a reaction of the vinylic iodide **314** with the Reformatsky reagent, prepared *in situ* from ethyl α-bromoacetate and zinc (Scheme 161).[415] The coupling required the application of

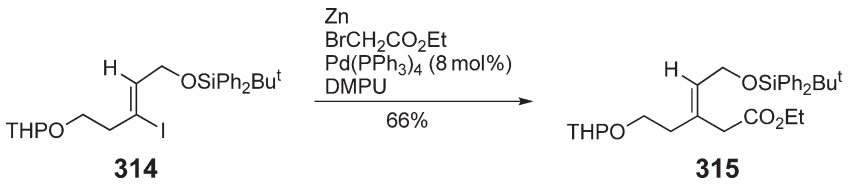

Scheme 161

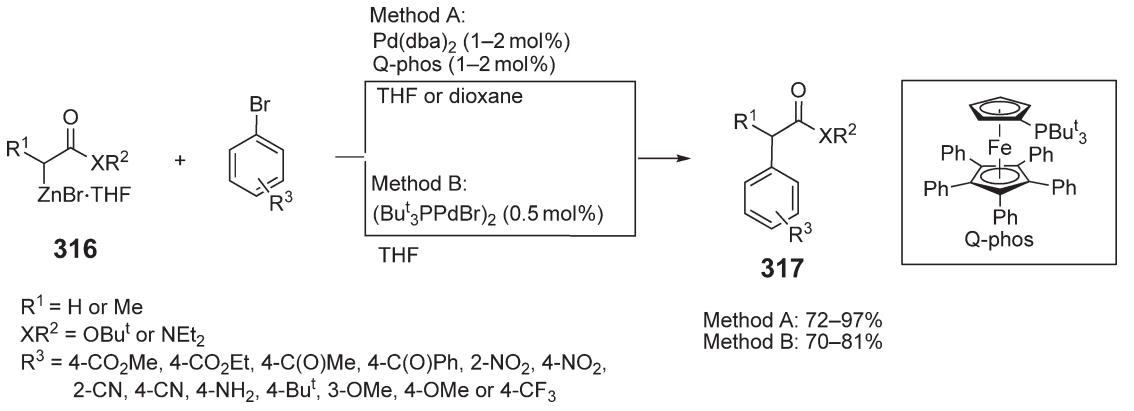

Scheme 162

$Pd(PPh_3)_4$ and *N*,*N*′-dimethyl-*N*,*N*′-propylene urea (DMPU). The product of this reaction **315** was a key intermediate in the synthesis of (*Z*)-olefinic RNA containing adenine and thymine as bases.

Recently, the group of Hartwig published their study of the palladium-catalyzed coupling of aryl bromides with structurally diverse Reformatsky reagents **316**.[414] The latter compounds were synthesized from *N*,*N*′-diethyl amides or *tert*-butyl esters of acetic and propionic acids. The authors reported two catalytic systems for the coupling. In the first method, a combination of $Pd(dba)_2$ and a bulky phosphine (Q-phos) was applied, affording α-arylated esters and amides **317** in excellent isolated yields (Scheme 162). In the second, less general method, the dimeric Pd(I) complex $(Bu^t_3PPdBr)_2$ was used (Scheme 162). Then, Hartwig demonstrated that the same products can be synthesized from the corresponding silyl ketene acetals or ketenimides and aryl bromides in the presence of 0.5 equiv. ZnF_2, 1% $Pd(dba)_2$, and 2% $P(Bu^t)_3$.[414,416]

Most recently, Bentz and co-workers established that the Pd-catalyzed α-arylation of esters and amides, using Reformatsky reagents and the corresponding aryl bromides, can be successfully performed under microwave conditions.[417] The reported yields are somewhat lower than those reported by Hartwig;[414] however, this approach does not require the use of Q-phos and can be considered as valuable alternative for α-arylation.

2.06.16.8.2.(ii) Reactions of alkylzinc halides with aryl and vinyl halides

As in the case of Negishi coupling reactions of alkyl halides with organozinc halides, the latter compounds undergo reactions with aryl halides in the presence of palladium or nickel catalysts. In 1996, the group of Knochel reported reaction conditions for arylation of aryl iodides and aryl triflates by arylzinc bromides in the presence of $Pd(dba)_2$ and a phosphine.[418] For the reactions of aryl triflates, higher yields were obtained for 1,1-bis(diphenylphosphino)ferrocene (dppf); tri-*o*-furylphosphine (tfp) provided better results for aryl iodides (Scheme 163). Later, the same group showed that aryl triflates can be replaced by the corresponding nonaflates, $ArOSO_2(CF_2)_3CF_3$, which are readily available and can be purified using flash chromatography.[419]

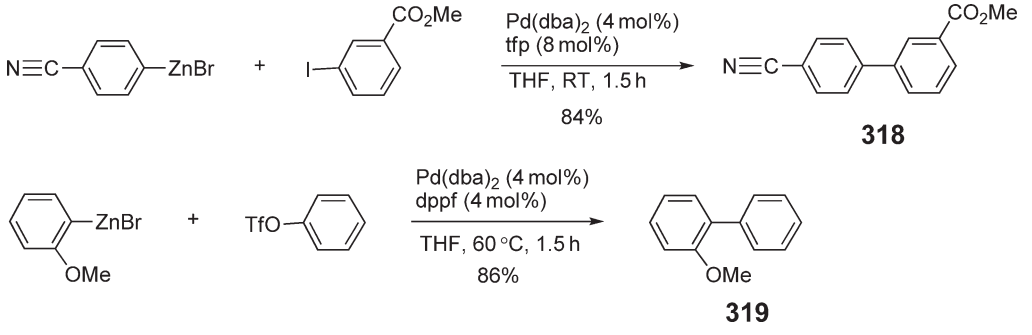

Scheme 163

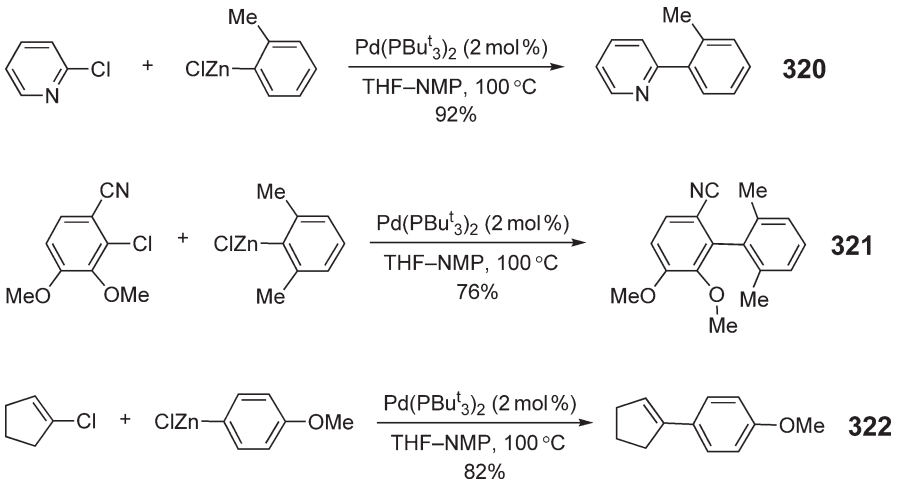

Scheme 164

A general method for the Pd-catalyzed cross-couplings of alkyl- and arylzinc chlorides with aryl, heteroaryl, and vinyl chlorides was reported by Dai and Fu.[420] They determined that the commercially available and air stable complex Pd(PBu$^t_3$)$_2$ catalyzed these reactions leading to the formation of an (sp^2)C–(sp^2)C bond (Scheme 164). Remarkably, bulky biaryls with two, three, or even four *ortho*-substituents (e.g., **323**) were obtained in very high yields (76–96%).

During the last decade, it has also been shown that reactions of substituted aryl chlorides with simple and functionalized alkylzinc iodides can be catalyzed by either a soluble Ni(0) source[421] (prepared from $NiCl_2$, PPh_3, and *n*-BuLi) or Ni(0) on charcoal.[422] The latter, heterogeneous reaction, has the advantage of a simplified workup. In both types of Ni(0)-catalyzed Negishi couplings, the products were isolated in very high yields (73–96% and 66–91%, respectively).

2.06.16.9 Miscellaneous Reactions of Organozinc Reagents

2.06.16.9.1 Catalytic reactions of alkylzinc halides with α-chloroketones

Alkylzinc halides generated *in situ* by transmetallation of Grignard reagents with $ZnCl_2$ reacted with cyclic and acyclic α-chloroketones in the presence of $Cu(acac)_2$ or CuCl to form α-alkylketones in 45–96% yield. It appears that the presence of magnesium is essential: cyclopentylzinc chloride obtained from the corresponding alkyl halide and zinc provided no desirable product. Attempts using $ZnPr^i_2$ and the Mg-free organozinc derivative, generated *in situ* from $ZnCl_2$ and *n*-C_4H_9Li, were unsuccessful as well. Interestingly, alkylation of the optically active chloride (*S*)-**323** occurred with inversion of configuration (Scheme 165).[423] It is noteworthy that in a related recent study, α-chloroketones were alkylated by organotin enolates in the presence of a catalytic amount of $ZnCl_2$.[424]

Recently, a new method for synthesis of tertiary amines **326** from *N*,*N*-dialkyl *O*-benzoyl hydroxylamines **325** was proposed.[425] The protocol is based on the copper-catalyzed reaction of hydroxylamines **325** with dialkyl- and diarylzinc reagents (Scheme 166). It is noteworthy that alkyl- and phenylzinc halides also reacted with compounds **325**, however, yields were significantly lower than those for ZnR_2 (18–29% vs. 69–98%).

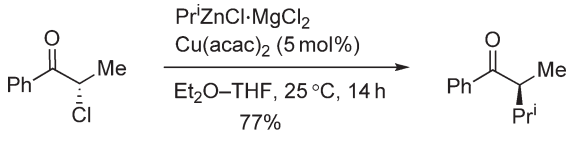

(*S*)-**323**
95% ee

(*S*)-**324**
95% ee

Scheme 165

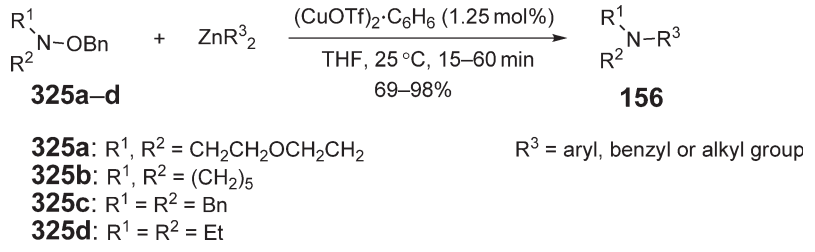

Scheme 166

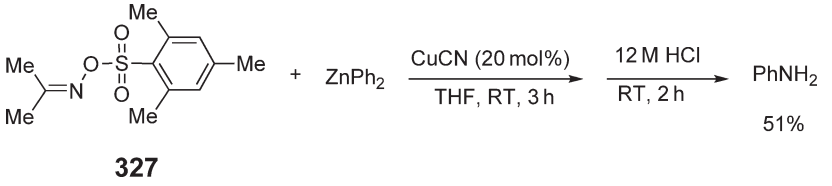

Scheme 167

A similar but less useful amination reaction was reported by the Erdik group.[426,427] They found that diarylzincs and trialrylzincates reacted with acetone *O*-(2,4,6-trimethylphenylsulfonyl)oxime **327** and *O*-methylhydroxylamine in the presence of CuCN. The products of this reaction were hydrolyzed to afford the corresponding primary amines in modest yield (Scheme 167).

2.06.16.9.2 Application of organozinc complexes as catalysts

Zinc-containing compounds have also been used as catalyst. Recently, Trost *et al.* reported asymmetric aldol reactions of methyl ynones **331** with pyruvaldehyde ketals **330** in the presence of a dinuclear zinc catalyst **329** generated from $ZnEt_2$ and a pentadentate *O*,*N*,*O*,*N*,*O*-ligand (**328**, Scheme 168).[428] This reaction is a unique case of enantioselective autoinduction with product incorporation into the catalyst and a reversal of the absolute configuration.

Another recent example is the asymmetric Mannich-type reaction of hydroxyketones using a $ZnEt_2$–BINOL complex as a catalyst.[429] The complex provided superior enantioselectivity and had a very high turnover number.

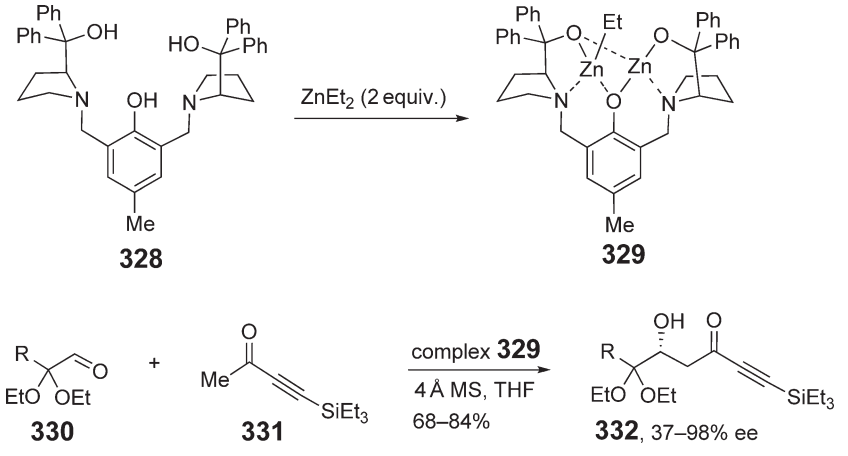

Scheme 168

References

1. Kolbe, H; Frankland, E. *Ann.* **1848**, *65*, 288.
2. Greenwood, N. N.; Earnshaw, A. *Chemistry of the Elements*, 2nd ed.; Butterworth-Heinemann: Oxford, 1997.
3. USGS http://minerals.usgs.gov.
4. AMERICAN Zinc ASSOCIATION http://www.zinc.org.
5. PAUL SCHERRER INSTITUT http://ecl.web.psi.ch.
6. Cotton, F. A.; Wilkinson, G.; Murillo, C. A.; Bochmann, M. *Advanced Inorganic Chemistry*, 6th ed.; Wiley-Interscience: New York, 1999; pp 598–629.
7. Prasad, A. S. *Biochemistry of Zinc*; Plenum Press: New York, 1993.
8. Vallee, B. L.; Auld, D. S *Faraday Discuss.* **1992**, *93*, 47–68.
9. Pearson, R. G. *Chemical Hardness*; Wiley-VCH: Weinheim, 1997.
10. Bock, C. W.; Kaufman Katz, A.; Glusker, J. P. *J. Am. Chem. Soc.* **1995**, *117*, 3754–3756.
11. Rößler, N.; Staemmler, V. *Phys. Chem. Chem. Phys.* **2003**, *5*, 3580–3586.
12. Kovacs, I.; Iost, N; Solymosi, F. *J. Chem. Phys.* **1994**, *101*, 4236–4247.
13. Jiménez Calzado, C.; Fernández Sanz, J. *J. Mol Struct. (Theochem)* **1997**, *390*, 61–65.
14. Boldyrev, A. I.; Simons, J. *Mol. Phys.* **1997**, *92*, 365–379.
15. San Miguel, M. A.; Márques, A.; Fernández Sanz, J. *J. Am. Chem. Soc.* **1996**, *118*, 429–436.
16. San Miguel, M. A.; Márquez, A.; Fernández Sanz, J. *J. Phys. Chem.* **1996**, *100*, 1600–1604.
17. Ehlers, A. W.; de Koster, C. G.; Meier, R. J.; Lammertsma, K. *J. Phys. Chem.* **2001**, *105*, 8691–8695.
18. Pooley, S. J.; Ellis, A. M. *J. Mol. Spectrosc.* **1997**, *185*, 48–53.
19. McKinley, A. J.; Karakyriakos, E.; Knight, L. B., Jr.; Babb, R.; Williams, A. *J. Phys. Chem. A* **2000**, *104*, 3528–3526.
20. Barckholtz, T. A.; Powers, D. E.; Miller, T. A.; Bursten, B. E. *J. Am. Chem. Soc.* **1999**, *121*, 2576–2584.
21. Pushkarsky, M. B.; Stakhursky, V. L.; Miller, T. A. *J. Phys. Chem. A.* **2000**, *104*, 9184–9190.
22. Georgiadis, R.; Armentrout, P. B. *J. Am. Chem. Soc.* **1986**, *108*, 2119–2126.
23. Fang, E. E.; Grieman, F. J. *Main Group Met. Chem.* **1994**, *17*, 447–452.
24. Berger, S.; Langer, F.; Lutz, C.; Knochel, P.; Mobley, T. A.; Reddy, C. K. *Angew. Chem., Int. Ed. Engl.* **1997**, *36*, 1496–1498.
25. Eisenberg, C.; Knochel, P. *J. Org. Chem.* **1994**, *59*, 3760–3761.
26. Lange, H.; Naumann, D. *J. Fluorine Chem.* **1984**, *26*, 435–444.
27. Naumann, D.; Schorn, C.; Tyrra, W. *Z. Anorg. Allg. Chem.* **1999**, *625*, 827–830.
28. Schwink, L.; Knochel, P. *Tetrahedron Lett.* **1994**, *35*, 9007–9010.
29. Micouin, L.; Oestreich, M.; Knochel, P. *Angew. Chem., Int. Ed.* **1997**, *36*, 245–246.
30. Boudier, A.; Darcel, C.; Flachsmann, F.; Micouin, L.; Oestreich, M.; Knochel, P. *Chem. Eur. J.* **2000**, *6*, 2748–2761.
31. Hupe, E.; Knochel, P.; Szabó, K. J. *Organometallics* **2002**, *21*, 2203–2207.
32. Vettel, S.; Vaupel, A.; Knochel, P. *Tetrahedron Lett.* **1995**, *36*, 1023–1026.
33. Vettel, S.; Vaupel, A.; Knochel, P. *J. Org. Chem.* **1996**, *61*, 7473–7481.
34. Charette, A. B.; Beauchemin, A.; Marcoux, J.-F. *J. Am. Chem. Soc.* **1998**, *120*, 5114–5115.
35. Gagneur, S.; Montchamp, J.-L.; Negishi, E.-I. *Organometallics* **2000**, *19*, 2417–2419.
36. Andrews, P. C.; Raston, C. L.; Skelton, B. W.; White, A. H. *Organometallics* **1998**, *17*, 799–782.
37. Markies, P. R.; Schat, G.; Akkerman, O. S.; Bickelhaupt. *Organometallics* **1990**, *9*, 2243–2247.
38. Sun, Y.; Piers, W. E.; Parvez, M. *Can. J. Chem.* **1998**, *76*, 513–517.
39. Weidenbruch, M.; Herrndorf, M.; Schäfer, A.; Pohl, S.; Saak, W. *J. Organomet. Chem.* **1989**, *361*, 139–145.
40. Brooker, S.; Bertel, N.; Stalke, D.; Noltemeyer, M.; Roesky, H. W.; Sheldrick, G. M.; Edelmann, F. T. *Organometallics* **1992**, *11*, 192–195.
41. Chisholm, M. H.; Gallucci, J. C.; Yin, H.; Zhen, H. *Inorg. Chem.* **2005**, *44*, 4777–4785.
42. Cole, S. C.; Coles, M. P.; Hitchcock, P. B. *Dalton Trans.* **2003**, 3663–3664.
43. Westerhausen, M.; Rademacher, B.; Schwarz, W.; Weidlein, J. *J. Organomet. Chem.* **1994**, *469*, 135–149.
44. Wipf, P.; Xu, W. *Tetrahedron Lett.* **1994**, *35*, 5197–5200.
45. Seneviratne, K. N.; Winter, C. H. *Organometallics* **1997**, *16*, 2498–2499.
46. Budzelaar, P. H. M.; Boersma, J.; van der Kerk, G. J. M.; Spek, A. L.; Duisenberg, A. J. M. *J. Organomet. Chem.* **1985**, *281*, 123–130.
47. Beattie, J. K.; Nugent, K. W. *Inorg. Chim. Acta* **1992**, *198–200*, 309–318.
48. Fischer, B.; Wijkens, P.; Boersma, J.; van Koten, G.; Smeets, W. J. J.; Spek, A. L.; Budzelaar, P. H. M. *J. Organomet. Chem.* **1989**, *376*, 223–233.
49. Blom, R.; Boersma, J.; Budzelaar, P. H. M.; Fischer, B.; Haaland, A.; Volden, H. V.; Weidlein, J. *Acta Chem. Scand.* **1986**, *A40*, 113–120.
50. Burkey, D. J.; Hanusa, T. P. *J. Organomet. Chem.* **1996**, *512*, 165–173.
51. Overby, J. S.; Jayaratne, K. C.; Schoell, N. J.; Hanusa, T. P. *Organometallics* **1999**, *18*, 1663–1668.
52. Walker, D. A.; Woodman, T. J.; Schormann, M.; Hughes, D. L.; Bochmann, M. *Organometallics* **2003**, *22*, 797–803.
53. Klement, I.; Lütjens, H.; Knochel, P. *Tetrahedron* **1997**, *53*, 9135–9144.
54. Rundle, R. E. *Survey of Progress in Chemistry*; Scott, F. A., Ed.; Academic: New York, 1963; vol. 1, p 95.
55. Rao, K. S.; Stoicheff, B. P.; Turner, R. *Can. J. Phys.* **1960**, *38*, 1516–1520.
56. Almenningen, A.; Helgaker, T. U.; Haarland, A.; Samdal, S. *Acta Chem. Scand.* **1982**, *A36*, 159–166.
57. Antes, I.; Frenking, G. *Organometallics* **1995**, *14*, 4263–4268.
58. Haarland, A.; Green, J. C.; McGrady, G. S.; Downs, A. J.; Gullo, E.; Lyall, M. J.; Timberlake, J.; Tutukin, A. V.; Volden, H. V.; Østby, K.-A. *Dalton Trans.* **2003**, 4356–4366.
59. Garkusha, O. G.; Lokshin, B. V.; Borisov, G. K. *J. Organomet. Chem.* **1998**, *553*, 59–65.
60. Zakrzewski, V. G.; Ortiz, J. V. *J. Phys. Chem.* **1994**, *98*, 13198–13202.
61. Bott, S. G.; Hoffman, D. M.; Rangarajan, S. P. *J. Chem. Soc., Dalton Trans.* **1996**, 1979–1982.
62. Fox, P. A.; Gray, S. D.; Bruck, M. A.; Wigley, D. E. *Inorg. Chem.* **1996**, *35*, 6027–6036.
63. Su, Y.-X.; Reck, C. E.; Guzei, I. A.; Jordan, R. F. *Organometallics* **2000**, *19*, 4858–4861.
64. Shiono, T.; Kurosawa, H.; Soga, K. *Macromolecules* **1995**, *28*, 437–443.
65. Britovsek, G. J. P.; Cohen, S. A.; Gibson, V. C.; Maddox, P. J.; van Meurs, M. *Angew. Chem., Int. Ed.* **2002**, *41*, 489–491.

66. Britovsek, G. J. P.; Cohen, S. A.; Gibson, V. C.; Maddox, P. J.; van Meurs, M. *J. Am. Chem. Soc.* **2004**, *124*, 10701–10712.
67. Smith, R. D.; Simmons, H. E. *Org. Synth.* **1947**, *41*, 72–75.
68. Knochel, P.; Singer, R. D. *Chem. Rev.* **1993**, *93*, 2117–2188.
69. Rieke, R. D. *Acc. Chem. Res.* **1977**, *10*, 301–306.
70. Guijarro, A.; Rieke, R. D. *Angew. Chem., Int. Ed.* **1998**, *37*, 1679–1681.
71. Guijarro, A.; Rosenberg, D. M.; Rieke, R. D. *J. Am. Chem. Soc.* **1999**, *121*, 4155–4167.
72. Guijarro, A.; Rieke, R. D. *Angew. Chem., Int. Ed.* **2000**, *39*, 1475–1479.
73. Dexter, C. S.; Jackson, R. F. W. *Chem. Commun.* **1998**, 75–76.
74. Stadtmüller, H.; Lentz, R.; Tucker, C. E.; Stüdemann, T.; Dörner, W.; Knochel, P. *J. Am. Chem. Soc.* **1993**, *115*, 7027–7028.
75. Bai, H.; Ault, B. S. *J. Phys. Chem.* **1994**, *98*, 6082–6088.
76. Maung, N. *Thechem.* **1998**, *434*, 255–264.
77. Dickson, R. S.; Fallon, G. D.; Zhang, Q.-Q. J. *Chem. Soc., Dalton Trans.* **2000**, 1973–1974.
78. Hasenzahl, S.; Kaim, W.; Stahl, T. *Inorg. Chim. Acta* **1994**, *225*, 23–34.
79. Huang, X.; Sun, H.; Wang, X.; Liu, Y. J.; You, X.; Sun, X. *Main Group Met. Chem.* **1996**, *19*, 161–165.
80. Walfort, B.; Leedham, A. P.; Russell, C. A.; Stalke, D. *Inorg. Chem.* **2001**, *40*, 5668–5674.
81. Wissing, E.; Kaupp, M.; Boersma, J.; Spek, A. L.; van Koten, G. *Organometallics* **1994**, *13*, 2349–2356.
82. Westerhausen, M.; Wieneke, M.; Schwarz, W. *J. Organomet. Chem.* **1996**, *522*, 137–146.
83. Westerhausen, M.; Wieneke, M.; Rademacher, B. B.; Schwarz, W. *Chem. Ber.* **1997**, *130*, 1499–1505.
84. Coward, K. M.; Jones, A. C.; Steiner, A.; Bickley, J. F.; Smith, L. M.; Pemble, M. E. *J. Chem. Soc., Dalton Trans.* **2000**, 3480–3482.
85. Rau, S.; Büttner, T.; Temme, C.; Ruben, M.; Görls, H.; Walther, D.; Duati, M.; Fanni, S.; Vos, J. G. *Inorg. Chem.* **2000**, *39*, 1621–1624.
86. Mimoun, H.; de Saint Laumer, J. Y.; Giannini, L.; Scopelliti, R.; Floriani, C. *J. Am. Chem. Soc.* **1999**, *121*, 6158–6166.
87. Pajerski, A. D.; BergStresser, G. L.; Parvez, M.; Richey, H. G., Jr. *J. Am. Chem. Soc.* **1988**, *110*, 4844–4845.
88. Markies, P. R.; Nomoto, T.; Akkerman, O. S; Bickelhaupt, F. *J. Am. Chem. Soc.* **1988**, *110*, 4845–4846.
89. Chubb, J. E.; Richey, H. G., Jr., *Organometallics* **1998**, *17*, 3204–3209.
90. Fabicon, R. M.; Parvez, M.; Richey, H. G., Jr. *Organometallics* **1999**, *18*, 5163–5169.
91. Hecht, E. A. *Z. Anorg. Allg. Chem.* **2001**, *627*, 2351–2358.
92. Charette, A. B.; Marcoux, J.-F. *J. Am. Chem. Soc.* **1996**, *118*, 4539–4549.
93. Charette, A. B.; Marcoux, J.-F.; Bélanger-Gariépy, F. *J. Am. Chem. Soc.* **1996**, *118*, 6792–6793.
94. Charette, A. B.; Marcoux, J.-F.; Molinaro, C.; Beauchemin, A.; Brochu, C.; Isabel, É *J. Am. Chem. Soc.* **2000**, *122*, 4508–4509.
95. Bernardi, F.; Bottoni, A.; Miscione, G. P. *J. Am. Chem. Soc.* **1997**, *119*, 12300–12305.
96. Bernardi, F.; Bottoni, A.; Miscione, G. P. *Organometallics* **2000**, *19*, 5529–5532.
97. Fang, W.-H.; Phillips, D. L.; Wang, D.-Q.; Li, Y.-L. *J. Org. Chem.* **2000**, *67*, 154–160.
98. Arduengo, A. J., III; Rasika Dias, H. V.; Davidson, F.; Harlow, R. L. *J. Organomet. Chem.* **1993**, *462*, 13–18.
99. Arduengo, A. J., III; Davidson, F.; Krafczyk, R.; Marshall, W. J.; Tamm, M. *Organometallics* **1998**, *17*, 3375–3382.
100. Jensen, T. R.; Breyfogle, L. E.; Hillmyer, M. A.; Tolman, W. B. *Chem. Commun.* **2004**, 2504–2505.
101. Wang, D.; Wurst, K.; Buchmeiser, M. R. *J. Organomet. Chem.* **2004**, *689*, 2123–2130.
102. Haufe, M.; Köhn, R. D.; Weimann, R.; Seifert, G.; Zeigan, D. *J. Organomet. Chem.* **1996**, *520*, 121–129.
103. Haufe, M.; Köhn, R. D.; Kociok-Köhn, G.; Filippou, A. C. *Inorg. Chem. Commun.* **1998**, *1*, 263–266.
104. Walker, D. A.; Woodman, T. J.; Hughes, D. L.; Bochmann, M. *Organometallics* **2001**, *20*, 3772–3776.
105. Sarazin, Y.; Schormann, M.; Bochmann, M. *Organometallics* **2004**, *23*, 3296–3302.
106. Herrmann, W. A.; Bogdanovich, S.; Behm, J.; Denk, M. *J. Organomet. Chem.* **1992**, *430*, C33–C38.
107. Hannant, M. D.; Schormann, M.; Bochmann, M. *J. Chem. Soc., Dalton Trans.* **2002**, 4071–4073.
108. Tang, H.; Parvez, M.; Richey, H. G., Jr. *Organometallics* **1996**, *15*, 4891–4893.
109. Fabicon, R. M.; Richey, H. G., Jr., *Organometallics* **2001**, *20*, 4018–4023.
110. Tang, H.; Parvez, M.; Richey, H. G., Jr. *Organometallics* **2000**, *19*, 4810–4819.
111. Wanklyn, J. A. *Proc. R. Soc. London* **1857**, *9*, 341–345.
112. Alsdorf, H. Dissertation, University of Hamburg, Hamburg, 1969.
113. Weiss, E.; Wolfrum, R. *Chem. Ber.* **1968**, *101*, 35–40.
114. Linton, D. J.; Schooler, P.; Wheatley, A. E. H. *Coord. Chem. Rev.* **2001**, *223*, 53–115.
115. Rijnberg, E.; Jastrzebski, J. T. B. H.; Boersma, J.; Kooijman, H.; Spek, A. L.; van Koten, G. *J. Organomet. Chem.* **1997**, *541*, 181–185.
116. Thiele, K.; Görls, H.; Seidel, W. *Z. Anorg. Allg. Chem.* **1998**, *624*, 555–556.
117. Krieger, M.; Geiseler, G.; Harms, K.; Merle, J.; Massa, W.; Dehnicke, K. *Z. Anorg. Allg. Chem.* **1998**, *624*, 1387–1388.
118. Putzer, M. A.; Neumüller, B.; Dehnicke, K. *Z. Anorg. Allg. Chem.* **1997**, *623*, 539–544.
119. Cremer, U.; Pantenburg, I.; Ruschewitz, U. *Inorg. Chem.* **2003**, *42*, 7716–7718.
120. Cremer, U.; Ruschewitz, U. *Z. Anorg. Allg. Chem.* **2004**, *630*, 337–343.
121. Edwards, A. J.; Fallaize, A.; Raithby, P. R.; Rennie, M.-A.; Steiner, A.; Verhorevoort, K. L.; Wright, D. S. *J. Chem. Soc., Dalton Trans.* **1996**, 133–137.
122. Rijnberg, E.; Jastrzebski, J. T. B. H.; Boersma, J.; Kooijman, H.; Veldman, N.; Spek, A. L.; van Koten, G. *Organometallics* **1997**, *16*, 2239–2245.
123. Fröhlich, H.-O.; Kosan, B.; Undeutsch, B; Görls, H. *J. Organomet. Chem.* **1994**, *472*, 1–13.
124. Westerhausen, M.; Rademacher, B.; Schwarz, W.; Henkel, S. *Z. Naturforsch.* **1994**, *49b*, 199–210.
125. Westerhausen, M.; Wieneke, M.; Ponikwar, W.; Nöth, H.; Schwarz, W. *Organometallics* **1998**, *17*, 1438–1441.
126. Forbes, G. C.; Kennedy, A. R.; Mulvey, R. E.; Rowlings, R. B.; Clegg, W.; Liddle, S. T.; Wilson, C. C. *Chem. Commun.* **2000**, 1759–1760.
127. Rijnberg, E.; Boersma, J.; Jastrzebski, J. T. B. H.; Larkin, M. T.; Spek, A. L.; van Koten, G. *J. Chem. Soc., Chem. Commun.* **1995**, 1839–1840.
128. Fabicon, R. M.; Richey, H. G., Jr. *J. Chem. Soc., Dalton Trans.* **2001**, 783–788.
129. Uchiyama, M.; Kameda, M.; Mishima, O.; Yokoyama, N.; Koike, M.; Kondo, Y.; Sakamoto, T. *J. Am. Chem. Soc.* **1996**, *118*, 8733–8734.
130. Uchiyama, M.; Kameda, M.; Mishima, O.; Yokoyama, N.; Koike, M.; Kondo, Y.; Sakamoto, T. *J. Am. Chem. Soc.* **1998**, *120*, 4934–4946.
131. Mobley, T. A.; Berger, S. *Angew. Chem., Int. Ed.* **1999**, *38*, 3070–3072.
132. Mori, S.; Hirai, A.; Nakamura, M.; Nakamura, E. *Tetrahedron* **2000**, *56*, 2805–2809.
133. Olmstead, M. M.; Grigsby, W. J.; Chacon, D. R.; Hascall, T.; Power, P. P. *Inorg. Chim. Acta* **1996**, *251*, 273–284.

134. Westerhausen, M.; Bollwein, T.; Pfitzner, A.; Nilges, T.; Deiseroth, H.-J. *Inorg. Chim. Acta* **2001**, *312*, 239–244.
135. Azad Malik, M.; O'Brien, P. *Polyhedron* **1997**, *16*, 3593–3599.
136. Westerhausen, M.; Wieneke, M.; Nöth, H.; Seifert, T.; Pfitzner, A.; Schwarz, W.; Schwarz, O.; Weidlein, J. *Eur. J. Inorg. Chem.* **1998**, 1175–1182.
137. Malik, M. A.; O'Brien, P.; Motevalli, M.; Jones, A. C. *Inorg. Chem.* **1997**, *36*, 5076–5081.
138. Birch, S. J.; Boss, S. R.; Cole, S. C.; Coles, M. P.; Haigh, R.; Hitchcock, P. B.; Wheatley, A. E. H. *Dalton Trans.* **2004**, 3568–3574.
139. Coles, M. P.; Hitchcock, P. B. *Eur. J. Inorg. Chem.* **2004**, 2662–2672.
140. Chakraborty, D.; Chen, E. Y.-X. *Organometallics* **2003**, *22*, 769–774.
141. Liang, L.-C.; Lee, W.-Y.; Hung, C.-H. *Inorg. Chem.* **2003**, *42*, 5471–5473.
142. Lawson, G. T.; Jacob, C.; Steiner, A. *Eur. J. Inorg. Chem.* **1999**, 1881–1887.
143. Gornitzka, H.; Hemmert, C.; Bertrand, G.; Peiffer, M.; Stalke, D. *Organometallics* **2000**, *19*, 112–114.
144. Wirringa, U.; Voelker, H.; Roesky, H. W.; Shermolovich, Y.; Markovski, L.; Usón, I.; Noltemeyer, M.; Schmidt, H.-G. *J. Chem. Soc., Dalton Trans.* **1995**, 1951–1956.
145. Bond, A. D.; Hopkins, A. D.; Rothenberger, A.; Wolf, R.; Woods, A. D.; Wright, D. S. *Organometallics* **2001**, *20*, 4454–4456.
146. Lief, G. R.; Moser, D. F.; Stahl, L.; Staples, R. J. *J. Organomet. Chem.* **2004**, *689*, 1110–1121.
147. Boss, S. R.; Haigh, R.; Linton, D. J.; Schooler, P.; Shields, G. P.; Wheatley, A. E. H. *Dalton Trans.* **2003**, 1001–1008.
148. Hlavinka, M. L.; Hagadorn, J. R. *Organometallics* **2005**, *34*, 4116–4118.
149. Blackmore, I. J.; Gibson, V. C.; Hitchcock, P. B.; Rees, C. W.; Williams, D. J.; White, A. J. P. *J. Am. Chem. Soc.* **2005**, *127*, 6012–6020.
150. Moore, D. R.; Cheng, M.; Lobkovsky, E. B.; Coates, G. W. *J. Am. Chem. Soc.* **2003**, *125*, 11911–11924.
151. Cheng, M.; Moore, D. R.; Reczek, J. J.; Chamberlain, B. M.; Lobkovsky, E. B.; Coates, G. W. *J. Am. Chem. Soc.* **2001**, *123*, 8738–8749.
152. Prust, J.; Stasch, A.; Zheng, W.; Roesky, H. W.; Alexopoulos, E.; Usón, I.; Böhler, D.; Schuchardt, T. *Organometallics* **2001**, *20*, 3825–3828.
153. Lewiński, J.; Ochal, Z.; Bojarksi, E.; Tratkiewicz, E.; Justyniak, I.; Lipkowski, J. *Angew. Chem., Int. Ed.* **2003**, *42*, 4643–4646.
154. Allen, S. D.; Moore, D. R.; Lobkovsky, E. B.; Coates, G. W. *J. Organomet. Chem.* **2003**, *683*, 137–148.
155. Dove, A. P.; Gibson, V. C.; Marshall, E. L.; White, A. J. P.; Williams, D. J. *Dalton Trans.* **2004**, 570–578.
156. Lee, S. Y.; Na, S. J.; Kwon, H. Y.; Lee, B. Y.; Kang, S. O. *Organometallics* **2004**, *23*, 5382–5385.
157. Gamer, M. T.; Roesky, P. W. *Eur. J. Inorg. Chem.* **2003**, 2145–2148.
158. Herrmann, J.-S.; Luinstra, G. A.; Roesky, P. W. *J. Organomet. Chem.* **2004**, *689*, 2720–2725.
159. Kasani, A.; McDonald, R.; Cavell, R. G. *Organometallics* **1999**, *18*, 3775–3777.
160. Hill, M. S.; Hitchcock, P. B. *J. Chem. Soc., Dalton Trans.* **2002**, 4694–4702.
161. Kisko, J. L.; Fillebeen, T.; Hascall, T.; Parkin, G. *J. Organomet. Chem.* **2000**, *596*, 22–26.
162. Dowling, C. M.; Parkin, G. *Polyhedron* **2001**, *20*, 285–289.
163. Dowling, C.; Parkin, G. *Polyhedron* **1996**, *15*, 2463–2465.
164. Rasika Dias, H. V.; Jin, W. *Inorg. Chem.* **2003**, *42*, 5034–5036.
165. Chisholm, M. H.; Eilerts, N. W.; Huffman, J. C.; Iyer, S. S.; Pacold, M.; Phomphrai, K. *J. Am. Chem. Soc.* **2000**, *122*, 11845–11854.
166. Wissing, E.; van Gorp, K.; Boersma, J.; van Koten, G. *Inorg. Chim. Acta* **1994**, *220*, 55–61.
167. Wissing, E.; van der Linden, S.; Rijnberg, E.; Boersma, J.; Smeets, W. J. J.; Spek, A. L.; van Koten, G. *Organometallics* **1994**, *13*, 2602–2608.
168. Wissing, E.; Rijnberg, E.; van der Schaaf, P. A.; van Gorp, K.; Boersma, J.; van Koten, G. *Organometallics* **1994**, *13*, 2609–2615.
169. Rijnberg, E.; Boersma, J.; Jastrzebski, J. T. B. H.; Lakin, M. T.; Spek, A. L.; van Koten, G. *Organometallics* **1997**, *16*, 3158–3164.
170. Westerhausen, M.; Bollwein, T.; Makropoulos, N.; Rotter, T. M.; Habereder, T.; Suter, M.; Nöth, N. *Eur. J. Inor. Chem.* **2001**, 851–857.
171. Westerhausen, M.; Bollwein, T.; Makropoulos, N.; Schneiderbauer, S.; Suter, M.; Nöth, N.; Mayer, P.; Piotrowski, H.; Polborn, K.; Pfitzner, A. *Eur. J. Inor. Chem.* **2002**, 389–404.
172. Westerhausen, M.; Bollwein, T.; Warchhold, M.; Nöth, N. *Z. Anorg. Allg. Chem.* **2001**, *627*, 1141–1145.
173. Westerhausen, M.; Bollwein, T.; Karaghiosoff, K.; Schneiderbauer, S.; Vogt, M.; Nöth, N. *Organometallics* **2002**, *21*, 906–911.
174. Westerhausen, M.; Bollwein, T.; Mayer, P.; Piotrowski, H. *Z. Anorg. Allg. Chem.* **2002**, *628*, 1425–1432.
175. Westerhausen, M.; Kneifel, A. N.; Kalisch, A. *Angew. Chem., Int. Ed.* **2005**, *44*, 96–98.
176. Steiner, M.; Grützmacher, H.; Pritzkow, H.; Zsolnai, L. *Chem. Commun.* **1998**, 285–286.
177. Krieger, M.; Gould, R. O.; Harms, K.; Parsons, S.; Dehnicke, K. *Chem. Ber.* **1996**, *129*, 1621–1625.
178. Krieger, M.; Gould, R. O.; Neumüller, B.; Harms, K.; Dehnicke, K. *Z. Anorg. Allg. Chem.* **1998**, *624*, 1434–1442.
179. Rademacher, B.; Schwarz, W.; Westerhausen, M. *Z. Anorg. Allg. Chem.* **1995**, 287–300.
180. Rademacher, B.; Schwarz, W.; Westerhausen, M. *Z. Anorg. Allg. Chem.* **1995**, 1439–1446.
181. Bashall, A.; Cole, J. M.; García, F.; Primo, A.; Rothenberger, A.; McPartlin, M.; Wright, D. S. *Inorg. Chim. Acta* **2003**, *354*, 41–48.
182. Davies, R. P.; Linton, D. J.; Schooler, P.; Snaith, R.; Wheatley, A. E. H. *Chem. Eur. J.* **2001**, 7, 3696–3704.
183. Bond, A. D.; Linton, D. J.; Schooler, P.; Wheatley, A. E. H. *J. Chem. Soc., Dalton Trans.* **2001**, 3173–3178.
184. Merz, K.; Hu, H.-M.; Rell, S.; Driess, M. *Eur. J. Inorg. Chem.* **2003**, 51–53.
185. Charette, A. B.; Beauchemin, A.; Francoeur, S.; Bélanger-Gariépy, F.; Enright, G. D. *Chem. Comm.* **2002**, 466–467.
186. Charette, A. B.; Molinaro, C.; Brochu, C. *J. Am. Chem. Soc.* **2001**, *123*, 12610–12167.
187. Luliński, S.; Madura, I.; Serwatowski, J. Zachara. *J. Inorg. Chem.* **1999**, *38*, 4937–4941.
188. Anulewicz-Ostrowska, R.; Luliński, S.; Pindelska, E.; Serwatowski, J. *Inorg. Chem.* **2002**, *41*, 2525–2528.
189. Cole, S. C.; Coles, M. P.; Hitchcock, P. B. *Organometallics* **2004**, *23*, 5159–5168.
190. Driess, M.; Merz, K.; Rell, S. *Eur. J. Inor. Chem.* **2000**, 2517–2522.
191. Merz, K.; Block, S.; Schoenen, R.; Driess, M. *Dalton Trans.* **2003**, 3365–3369.
192. Anantharaman, G.; Roesky, H. W.; Schmidt, H.-G.; Noltemeyer, M.; Pinkas, J. *Inorg. Chem.* **2003**, *42*, 970–973.
193. Anantharaman, G.; Chandasekhar, V.; Nehete, U. N.; Roesky, H. W.; Vidovic, D.; Magull, J. *Organometallics* **2004**, *23*, 2251–2256.
194. Yang, Y.; Pinkas, J.; Noltemeyer, M.; Schmidt, H.-G.; Roesky, H. W. *Angew. Chem. Int. Ed.* **1999**, *38*, 664–665.
195. Anantharaman, G.; Chandasekhar, V.; Walawalkar, M. G.; Roesky, H. W.; Vidovic, D.; Magull, J.; Noltemeyer, M. *Dalton Trans.* **2004**, 1271–1275.
196. Chisholm, M. H.; Lin, C.-C.; Gallucci, J. C.; Ko, B.-T. *Dalton Trans.* **2003**, 406–412.
197. Dinger, M. B.; Scott, M. J. *Inorg. Chem.* **2001**, *40*, 1029–1036.
198. Gardiner, M. G.; Lawrence, S. M.; Raston, C. L.; Skelton, B. W.; White, A. H. *Chem. Commun.* **1996**, 2491–2492.
199. Bukhaltsev, E.; Goldberg, I.; Vigalok, A. *Organometallics* **2004**, *23*, 4540–4543.

200. Walther, D.; Döhler, T.; Theyssen, N.; Görls, H. *Eur. J. Inorg. Chem.* **2001**, 2049–2060.
201. Abakumov, G. A.; Cherkasov, V. K.; Abakumova, L. G.; Nevodchikov, V. I.; Druzhkov, N. O.; Makarenko, N. P.; Kursky, J. A. *J. Organomet. Chem.* **1995**, *491*, 127–133.
202. Abrahams, I.; Azad Malik, M.; Motevalli, M.; O'Brien, P. *J. Chem. Soc., Dalton Trans.* **1995**, 1043–1046.
203. Azad Malik, M.; O'Brien, P. *Inor. Chim. Acta* **1998**, *274*, 239–242.
204. Tang, Y. T.; Kassel, W. S.; Zakharov, L. N.; Rheingold, A. L.; Kemp, R. A. *Inorg. Chem.* **2005**, *44*, 359–364.
205. Chunggaze, M.; Azad Malik, M.; O'Brien, P.; White, A. J. P.; Williams, D. J. *J. Chem. Soc., Dalton Trans.* **1998**, 3839–3844.
206. Williams, C. K.; Breyfogle, L. E.; Choi, S. K.; Nam, W.; Young, V. G., Jr.,; Hillmyer, M. A.; Tolman, W. B. *J. Am. Chem. Soc.* **2003**, *125*, 11350–11359.
207. Kitamura, M.; Suga, S.; Niwa, M.; Noyori, R. *J. Am. Chem. Soc.* **1995**, *117*, 4832–4842.
208. Kitamura, M.; Suga, S.; Niwa, M.; Noyori, R.; Zhai, Z.-X.; Suga, H. *J. Phys. Chem.* **1994**, *98*, 12776–12781.
209. Goldfuss, B.; Khan, S. I.; Houk, K. N. *Organometallics* **1999**, *18*, 2927–2929.
210. Steigelmann, M.; Nisar, Y.; Rominger, F.; Goldfuss, B. *Chem. Eur. J.* **2002**, *8*, 5211–5218.
211. Hecht, E. *Z. Anorg. Allg. Chem.* **2000**, *626*, 2223–2227.
212. Nakano, K.; Nozaki, K.; Hiyama, T. *J. Am. Chem. Soc.* **2003**, *125*, 5501–5510.
213. Nozaki, K.; Nakano, K.; Hiyama, T. *J. Am. Chem. Soc.* **1999**, *121*, 11008–11010.
214. Bolm, C.; Müller, J.; Zehnder, M.; Neuburger, M. A. *Chem. Eur. J.* **1995**, *1*, 312–317.
215. Lewiński, J.; Marcianiak, W.; Ochal, Z.; Lipkowski, J.; Justyniak, I. *Eur. J. Inorg. Chem.* **2003**, 2753–2755.
216. Lewiński, J.; Marcianiak, W.; Lipkowski, J.; Justyniak, I. *J. Am. Chem. Soc.* **2003**, *125*, 12698–12699.
217. Trösch, A.; Vahrenkamp, H. *Inorg. Chem.* **2001**, *40*, 2305–2311.
218. Weston, J. *Organometallics* **2001**, *20*, 713–720.
219. Kimblin, C.; Bridgewater, B. M; Hascall, T.; Parkin, G. *J. Chem. Soc., Dalton Trans.* **2000**, 891–897.
220. Kimblin, C.; Bridgewater, B. M; Hascall, T.; Parkin, G. *J. Chem. Soc., Dalton Trans.* **2000**, 1267–1274.
221. Melnick, J. G.; Docrat, A.; Parkin, G. *Chem. Commun.* **2004**, 2870–2871.
222. Chiou, S.-J.; Innocent, J.; Riordan, C. G.; Lam, K.-C.; Liable-Sands, L.; Rheingold, A. L. *Inorg. Chem.* **2000**, *39*, 4347–4353.
223. Hammes, B. S.; Carrano, C. J. *Inorg. Chem.* **1999**, *38*, 4593–4600.
224. Chang, S.; Sommer, R. D.; Rheingold, A. L.; Goldberg, D. P. *Chem. Commun.* **2001**, 2396–2397.
225. Trösch, A.; Vahrenkamp, H. *Z. Anorg. Allg. Chem.* **2001**, *627*, 2523–2527.
226. Zeng, D.; Hampden-Smith, M. J.; Duesler, E. N. *Inorg. Chem.* **1994**, *33*, 5376–5377.
227. Azad Malik, M.; Motevalli, M.; Walsh, J. R.; O'Brien, P.; Jones, A. C. *J. Mater. Chem.* **1995**, *5*, 731–736.
228. Rijnberg, E.; Hovestad, N. J.; Kleij, A. W.; Jastrzebski, J. T. B. H.; Boersma, J.; Janssen, M. D.; Spek, A. L.; van Koten, G. *Organometallics* **1997**, *16*, 2847–2857.
229. Greene, T. M.; Andrews, L.; Downs, A. J. *J. Am. Chem. Soc.* **1995**, *117*, 8180–8187.
230. Aldridge, S.; Blake, A. J.; Downs, A. J.; Parsons, S.; Pulham, C. R. *J. Chem. Soc., Dalton Trans.* **1996**, 853–859.
231. Aldridge, S.; Blake, A. J.; Downs, A. J.; Parsons, S. *J. Chem. Soc., Chem. Commun.* **1995**, 1363–1364.
232. McKee, M. L. *Chem. Phys. Lett.* **1997**, *280*, 273–279.
233. Resa, I.; Carmona, E.; Guttierez-Puebla, E.; Monge, A. *Science* **2004**, *305*, 1136–1138.
234. del Río, D.; Galindo, A.; Resa, I.; Carmona, E. *Angew. Chem., Int. Ed.* **2005**, *44*, 1244–1247.
235. Xie, Y.; Schaeffer, H. F. III; King, R. B. *J. Am. Chem. Soc.* **2005**, *127*, 2818–2819.
236. Schnepf, A.; Himmel, H.-J. *Angew. Chem., Int. Ed.* **2005**, *44*, 2–4.
237. Parkin, G. *Science* **2004**, *305*, 1117–1118.
238. Ohashi, M.; Matsubara, K.; Iizuka, T.; Suzuki, H. *Angew. Chem., Int. Ed.* **2003**, *42*, 937–939.
239. Knochel, P.; Hupe, E.; Houte, H. *Act. Chim.* **2003**, 12–16.
240. Langer, F.; Devasagayaraj, A.; Chavant, P. Y.; Knochel, P. *Synlett* **1994**, 410–412.
241. Langer, F.; Schwink, L.; Devasagayaraj, A.; Chavant, P.-Y.; Knochel, P. *J. Org. Chem.* **1996**, *61*, 8229–8243.
242. Micouin, L.; Knochel, P. *Synlett* **1997**, 327–328.
243. Hupe, E.; Knochel, P. *Org. Lett.* **2001**, *3*, 127–130.
244. Hupe, E.; Calaza, M. I.; Knochel, P. *Chem. Eur. J.* **2003**, *9*, 2789–2796.
245. Klement, I.; Knochel, P.; Chau, K.; Cahiez, G. *Tetrahedron Lett.* **1994**, *35*, 1177–1180.
246. Knochel, P.; Calaza, M. I.; Hupe, E. In *Metal-catalyzed Cross-coupling Reactions*, 2nd ed.; de Meijere, A., Diederich, F., Eds.; Wiley: Weinheim, 2004; Vol. 2, pp 619–670.
247. Knochel, P., Jones, P., Eds.; *Organozinc Reagents: A Practical Approach*; Oxford University Press: New York, 1999.
248. Knochel, P. *Synlett* **1995**, 393–403.
249. Knochel, P.; Perea, J. J. A.; Jones, P. *Tetrahedron* **1998**, *54*, 8275–8319.
250. Pu, L.; Yu, H.-B. *Chem. Rev.* **2001**, *101*, 757–824.
251. Bolm, C.; Hermanns, N.; Hildebrand, J. P.; Muniz, K. *Angew. Chem., Int. Ed.* **2000**, *39*, 3465–3467.
252. Bolm, C.; Kesselgruber, M.; Hermanns, N.; Hildebrand, J. P.; Raabe, G. *Angew. Chem., Int. Ed.* **2001**, *40*, 1488–1490.
253. Sprout, C. M.; Richmond, M. L.; Seto, C. T. *J. Org. Chem.* **2004**, *69*, 6666–6673.
254. Mao, J.; Wan, B.; Wang, R.; Wu, F.; Lu, S. *J. Org. Chem.* **2004**, *69*, 9123–9127.
255. Fontes, M.; Verdaguer, X.; Sola, L.; Pericas, M. A.; Riera, A. *J. Org. Chem.* **2004**, *69*, 2532–2543.
256. Nugent, W. A. *Chem. Commun. (Cambridge)* **1999**, 1369–1370.
257. Ko, D.-H.; Kim, K. H.; Ha, D.-C. *Org. Lett.* **2002**, *4*, 3759–3762.
258. Bräse, S.; Dahmen, S.; Hoefener, S.; Lauterwasser, F.; Kreis, M.; Ziegert, R. E. *Synlett* **2004**, 2647–2669.
259. Tanner, D.; Korno, H. T.; Guijarro, D.; Andersson, P. G. *Tetrahedron* **1998**, *54*, 14213–14232.
260. Kitamura, M.; Okada, S.; Suga, S.; Noyori, R. *J. Amer. Chem. Soc.* **1989**, *111*, 4028–4036.
261. Gridnev, I. D.; Brown, J. M. *Proc. Natl. Acad. Sci. USA* **2004**, *101*, 5727–5731.
262. Lutz, C.; Knochel, P. *J. Org. Chem.* **1997**, *62*, 7895–7898.
263. Ramón, D. J.; Yus, M. *Tetrahedron* **1998**, *54*, 5651–5666.
264. Ramón, D. J.; Yus, M. *Tetrahedron Lett.* **1998**, *39*, 1239–1242.
265. Jeon, S.-J.; Li, H.; Garcia, C.; LaRochelle, L. K.; Walsh, P. J. *J. Org. Chem.* **2005**, *70*, 448–455.

266. Yus, M.; Ramón, D. J.; Prieto, O. *Eur. J. Org. Chem.* **2003**, 2745–2748.
267. García, C.; LaRochelle, L. K.; Walsh, P. J. *J. Amer. Chem. Soc.* **2002**, *124*, 10970–10971.
268. Yus, M.; Ramón, D. J.; Prieto, O. *Tetrahedron: Asymmetry* **2002**, *13*, 2291–2293.
269. Seebach, D.; Beck, A. L.; Heckel, A. *Angew. Chem., Int. Ed.* **2001**, *40*, 92–138.
270. Balsells, J.; Davis, T. J.; Carroll, P.; Walsh, P. J. *J. Amer. Chem. Soc.* **2002**, *124*, 10336–10348.
271. Lipshutz, B. H. *Tetrahedron Lett.* **2000**, *41*, 9515–9521.
272. Berger, S.; Langer, F.; Lutz, C.; Knochel, P.; Mobley, T. A.; Reddy, C. K. *Angew. Chem., Int. Ed.* **1997**, *36*, 1496–1498.
273. Bolm, C.; Muñiz, K. *Chem. Commun. (Cambridge)* **1999**, 1295–1296.
274. Bolm, C.; Rudolph, J. *J. Amer. Chem. Soc.* **2002**, *124*, 14850–14851.
275. Soai, K.; Shibata, T.; Morioka, H.; Choji, K. *Nature* **1995**, *378*, 767–768.
276. Shibata, T.; Choji, K.; Hayase, T.; Aizu, Y.; Soai, K. *Chem. Commun. (Cambridge)* **1996**, 1235–1236.
277. Soai, K.; Sato, I. *Chirality* **2001**, *14*, 548–554.
278. Sato, I.; Urabe, H.; Ishiguro, S.; Shibata, T.; Soai, K. *Angew. Chem., Int. Ed.* **2003**, *42*, 315–317.
279. Shibata, T.; Morioka, H.; Hayase, T.; Choji, K.; Soai, K. *J. Amer. Chem. Soc.* **1996**, *118*, 471–472.
280. Shibata, T.; Yonekubo, S.; Soai, K. *Angew. Chem., Int. Ed.* **1999**, *38*, 659–661.
281. Bueno, F. G.; Iwamura, H.; Blackmond, D. C. *Angew. Chem., Int. Ed.* **2004**, *43*, 2099–2103.
282. Soai, K.; Shibata, T.; Sato, I. *Bull. Chem. Soc. Jpn.* **2004**, *77*, 1063–1073.
283. Soai, K.; Sato, I. *Chirality* **2002**, *14*, 548–554.
284. Gridnev, I. D.; Serafimov, J. M.; Quiney, H.; Brown, J. M. *Org. Biomol. Chem.* **2003**, *1*, 3811–3819.
285. Law, M. C.; Wong, K.-Y.; Chan, T. H. *Green Chem.* **2002**, *4*, 161–164.
286. Law, M. C.; Wong, K.-Y.; Chan, T. H. *Green Chem.* **2004**, *6*, 241–244.
287. Kitazume, T.; Kasai, K. *Green Chem.* **2001**, *3*, 30–32.
288. Dosa, P. I.; Fu, G. C. *J. Amer. Chem. Soc.* **1998**, *120*, 445–446.
289. Ramón, D. J.; Yus, M. *Angew. Chem., Int. Ed.* **2004**, *43*, 284–287.
290. Yus, M.; Ramón, D. J.; Prieto, O. *Tetrahedron: Asymmetry* **2002**, *13*, 1573–1579.
291. Yus, M.; Ramón, D. J.; Prieto, O. *Tetrahedron: Asymmetry* **2003**, *14*, 1103–1114.
292. Cozzi, P. G.; Locatelli, M. *Lett. Org. Chem.* **2004**, *1*, 208–211.
293. DiMauro, E. F.; Kozlowski, M. C. *J. Amer. Chem. Soc.* **2002**, *124*, 12668–12669.
294. DiMauro, E. F.; Kozlowski, M. C. *Org. Lett.* **2002**, *4*, 3781–3784.
295. Jiang, B.; Chen, Z.; Tang, X. *Org. Lett.* **2002**, *4*, 3451–3453.
296. Musser, C. A.; Richey, H. G., Jr., *J. Org. Chem.* **2000**, *65*, 7750–7756.
297. Maclin, K. M.; Richey, H. G., Jr., *J. Org. Chem.* **2002**, *67*, 4602–4604.
298. Uchiyama, M.; Nakamura, S.; Ohwada, T.; Nakamura, M.; Nakamura, E. *J. Amer. Chem. Soc.* **2004**, *126*, 10897–10903.
299. Hanson, M. V.; Rieke, R. D. *J. Amer. Chem. Soc.* **1995**, *117*, 10775–10776.
300. Reddy, C. K.; Devasagayaraj, A.; Knochel, P. *Tetrahedron Lett.* **1996**, *37*, 4495–4498.
301. Feringa, B. L. *Acc. Chem. Res.* **2000**, *33*, 346–353.
302. Alexakis, A.; Polet, D.; Rosset, S.; March, S. *J. Org. Chem.* **2004**, *69*, 5660–5667.
303. Urbaneja, L. M.; Alexakis, A.; Krause, N. *Tetrahedron Lett.* **2002**, *43*, 7887–7890.
304. Arnold, L. A.; Naasz, R.; Minnaard, A. J.; Feringa, B. L. *J. Org. Chem.* **2002**, *67*, 7244–7254.
305. Hu, Y.; Liang, X.; Wang, J.; Zheng, Z.; Hu, X. *Tetrahedron: Asymmetry* **2003**, *14*, 3907–3915.
306. Liang, Y.; Gao, S.; Wan, H.; Hu, Y.; Chen, H.; Zheng, Z.; Hu, X. *Tetrahedron: Asymmetry* **2003**, *14*, 3211–3217.
307. Scafato, P.; Cunsolo, G.; Labano, S.; Rosini, C. *Tetrahedron* **2004**, *60*, 8801–8806.
308. Knöbel, A. K. H.; Escher, I. H.; Pfaltz, A. *Synlett* **1997**, 1429–1431.
309. Shi, M.; Wang, C.-J.; Zhang, W. *Chem. Eur. J.* **2004**, *10*, 5507–5516.
310. Shi, M.; Zhang, W. *Tetrahedron: Asymmetry* **2004**, *15*, 167–176.
311. Blanc, C.; Agbossou-Niedercorn, F. *Tetrahedron: Asymmetry* **2004**, *15*, 757–761.
312. Mandoli, A.; Calamante, M.; Feringa, B. L.; Salvadori, P. *Tetrahedron: Asymmetry* **2003**, *14*, 3647–3650.
313. Montgomery, J.; Chevliakov, M. V.; Brielmann, H. L. *Tetrahedron* **1997**, *53*, 16449–16462.
314. Savchenko, A. V.; Montgomery, J. *J. Org. Chem.* **1996**, *61*, 1562–1563.
315. De Vries, A. H. M.; Imbos, R.; Feringa, B. L. *Tetrahedron: Asymmetry* **1997**, *8*, 1467–1473.
316. Arink, A. M.; Braam, T. W.; Keeris, R.; Jastrzebski, J. T. B. H.; Benhaim, C.; Rosset, S.; Alexakis, A.; van Koten, G. *Org. Lett.* **2004**, *6*, 1959–1962.
317. Hirao, T.; Takada, T.; Sakurai, H. *Org. Lett.* **2000**, *2*, 3659–3661.
318. Hirao, T.; Takada, T.; Ogawa, A. *J. Org. Chem.* **2000**, *65*, 1511–1515.
319. Dyer, J.; Keeling, S.; Moloney, M. G. *Tetrahedron Lett.* **1996**, *37*, 4573–4576.
320. Menicagli, R.; Samaritani, S. *Tetrahedron* **1996**, *52*, 1425–1432.
321. Bertrand, M. P.; Feray, L.; Nouguier, R.; Perfetti, P. *J. Org. Chem.* **1999**, *64*, 9189–9193.
322. Arisawa, M.; Torisawa, Y.; Kawahara, M.; Yamanaka, M.; Nishida, A.; Nakagawa, M. *J. Org. Chem.* **1997**, *62*, 4327–4329.
323. Bercot, E. A.; Rovis, T. *J. Amer. Chem. Soc.* **2002**, *124*, 174–175.
324. Giovannini, R.; Stüdemann, T.; Dussin, G.; Knochel, P. *Angew. Chem., Int. Ed.* **1998**, *37*, 2387–2389.
325. Zhang, Y.; Rovis, T. *J. Amer. Chem. Soc.* **2004**, *126*, 15964–15965.
326. Tokuyama, H.; Yokoshima, S.; Yamashita, T.; Fukuyama, T. *Tetrahedron Lett.* **1998**, *39*, 3189–3192.
327. Miyazaki, T.; Han-ya, Y.; Tokuyama, H.; Fukuyama, T. *Synlett* **2004**, 477–480.
328. Wang, D.; Zhang, Z. *Org. Lett.* **2003**, *5*, 4645–4648.
329. Reddy, C. K.; Knochel, P. *Angew. Chem., Int. Ed.* **1996**, *35*, 1700–1701.
330. Ranu, B. C.; Majee, A.; Das, A. R. *Tetrahedron Lett.* **1996**, *37*, 1109–1112.
331. Porter, J. R.; Traverse, J. F.; Hoveyda, A. H.; Snapper, M. L. *J. Amer. Chem. Soc.* **2001**, *123*, 10409–10410.
332. Porter, J. R.; Traverse, J. F.; Hoveyda, A. H.; Snapper, M. L. *J. Amer. Chem. Soc.* **2001**, *123*, 984–985.
333. Fujihara, H.; Nagai, K.; Tomioka, K. *J. Amer. Chem. Soc.* **2000**, *122*, 12055–12056.
334. Hermanns, N.; Dahmen, S.; Bolm, C.; Bräuse, S. *Angew. Chem., Int. Ed.* **2002**, *41*, 3692–3694.

335. Dahmen, S.; Bräuse, S. *J. Amer. Chem. Soc.* **2002**, *124*, 5940–5941.
336. Soai, K.; Hatanaka, T.; Miyazawa, T. *J. Chem. Soc., Chem. Commun.* **1992**, 1097–1098.
337. Andersson, P. G.; Guijarro, D.; Tanner, D. *J. Org. Chem.* **1997**, *62*, 7364–7375.
338. Côté, A.; Boezio, A. A.; Charette, A. B. *Proc. Natl. Acad. Sci. USA* **2004**, *101*, 5405–5410.
339. Boezio, A. A.; Charette, A. B. *J. Amer. Chem. Soc.* **2003**, *125*, 1692–1693.
340. Côté, A.; Boezio, A. A.; Charette, A. B. *Angew. Chem., Int. Ed.* **2004**, *43*, 6525–6528.
341. Pinho, P.; Andersson, P. G. *Tetrahedron* **2001**, *57*, 1615–1618.
342. Guijarro, D.; Pinho, P.; Andersson, P. G. *J. Org. Chem.* **1998**, *63*, 2530–2535.
343. Boezio, A. A.; Pytkowicz, J.; Cote, A.; Charette, A. B. *J. Amer. Chem. Soc.* **2003**, *125*, 14260–14261.
344. Zhang, X.-M.; Zhang, H.-L.; Lin, W.-Q.; Gong, L.-Z.; Mi, A.-Q.; Cui, X.; Jiang, Y.-Z.; Yu, K.-B. *J. Org. Chem.* **2003**, *68*, 4322–4329.
345. Wipf, P.; Kendall, C.; Stephenson, C. R. J. *J. Amer. Chem. Soc.* **2003**, *125*, 761–768.
346. Wipf, P.; Kendall, C. *Angew. Chem., Int. Ed.* **2002**, *8*, 1778–1784.
347. Wipf, P.; Kendall, C. *Org. Lett.* **2001**, *3*, 2773–2776.
348. Wipf, P.; Ribe, S. *J. Org. Chem.* **1998**, *63*, 6454–6455.
349. Dembélé, Y. A.; Belaud, C.; Villiéras, J. *Tetrahedron: Asymmetry* **1992**, *3*, 511–514.
350. Itsuno, S.; El-Shehawy, A. A.; Abdelaal, M. Y.; Ito, K. *New J. Chem.* **1998**, 775–777.
351. Wu, G.; Cai, Z.-W.; Bednarz, M. S.; Kocy, O. R.; Gavai, A. V.; Godfrey, J. D., Jr.; Washburn, W. N.; Poss, M. A.; Sher, P. M. *J. Comb. Chem.* **2005**, *7*, 99–108.
352. Enders, D.; Reinhold, U. *Tetrahedron: Asymmetry* **1997**, *8*, 1895–1946.
353. Merino, P.; Franco, S.; Merchan, F. L.; Tejero, T. *Synlett* **2000**, 442–454.
354. Lombardo, M.; Trombini, C. *Synthesis* **2000**, 759–774.
355. Merino, P.; Franco, S.; Merchan, F. L.; Tejero, T. *Recent Res. Dev. Synth. Org. Chem.* **1998**, *1*, 109–121.
356. Pinet, S.; Pandya, S. U.; Chavant, P. Y.; Ayling, A.; Vallee, Y. *Org. Lett.* **2002**, *4*, 1463–1466.
357. Frantz, D. E.; Fässler, R.; Carreira, E. M. *J. Amer. Chem. Soc.* **1999**, *121*, 11245–11246.
358. Frantz, D. E.; Fässler, R.; Tomooka, C. S.; Carreira, E. M. *Acc. Chem. Res.* **2000**, *33*, 373–381.
359. Pandya, S. U.; Pinet, S.; Chavant, P. Y.; Vallee, Y. *Eur. J. Org. Chem.* **2003**, 3621–3627.
360. Ukaji, Y.; Shimizu, Y.; Kenmoku, Y.; Ahmed, A.; Inomata, K. *Bull. Chem. Soc. Jpn* **2000**, *73*, 447–452.
361. Ukaji, Y.; Kenmoku, Y.; Inomata, K. *Tetrahedron: Asymmetry* **1996**, *7*, 53–56.
362. Ukaji, Y.; Shimizu, Y.; Kenmoku, Y.; Ahme, A.; Inomata, K. *Chem. Lett.* **1997**, 59–60.
363. Inomata, K.; Ukaji, Y. *Rev. Heteroatom Chem.* **1998**, *18*, 119–140.
364. Ukaji, Y.; Inomata, K. *Synlett* **2003**, 1075–1087.
365. Fiumana, A.; Lombardo, M.; Trombini, C. *J. Org. Chem.* **1997**, *62*, 5623–5626.
366. Dondoni, A.; Franco, S.; Junquera, F.; Merchán, F. L.; Merino, P.; Tejero, T.; Bertolasi, V. *Chem. Eur. J.* **1995**, 505–520.
367. Ukaji, Y.; Hatanaka, T.; Ahmed, A.; Inomata, K. *Chem. Lett.* **1993**, 1313–1316.
368. Ukaji, Y.; Yoshida, Y.; Inomata, K. *Tetrahedron: Asymmetry* **2000**, *11*, 733–736.
369. Hanessian, S.; Yang, R.-Y. *Tetrahedron Lett.* **1996**, *37*, 5273–5276.
370. Stadtmüller, H.; Vaupel, A.; Tucker, C. E.; Stüdemann, T.; Knochel, P. *Chem. Eur. J.* **1996**, *2*, 1204–1220.
371. Stadtmüller, H.; Knochel, P. *Synlett* **1995**, 463–464.
372. Rousseau, G.; Slougui, N. *J. Amer. Chem. Soc.* **1984**, *106*, 7283–7285.
373. Miyabe, H.; Ueda, M.; Naito, T. *Synlett* **2004**, 1140–1157.
374. Miyabe, H.; Konishi, C.; Naito, T. *Org. Lett.* **2000**, *2*, 1443–1445.
375. Bertrand, M. P.; Feray, L.; Nouguier, R.; Perfetti, P. *Synlett* **1999**, 1148–1150.
376. Bertrand, M. P.; Coantic, S.; Feray, L.; Nouguier, R.; Perfetti, P. *Tetrahedron* **2000**, *56*, 3951–3961.
377. Yamada, K.-i.; Fujihara, H.; Yamamoto, Y.; Miwa, Y.; Taga, T.; Tomioka, K. *Org. Lett.* **2002**, *4*, 3509–3511.
378. Yamada, K.-i.; Yamamoto, Y.; Tomioka, K. *Org. Lett.* **2003**, 1797–1799.
379. Yamada, K.-i.; Yamamoto, Y.; Miwa, Y.; Maekawa, M.; Tomioka, K. *J. Org. Chem.* **2004**, *69*, 1531–1534.
380. Miyabe, H.; Konishi, C.; Naito, T. *Chem. Pharm. Bull.* **2003**, *51*, 540–544.
381. Miyabe, H.; Nishimura, A.; Fujishima, Y.; Naito, T. *Tetrahedron* **2003**, *59*, 1901–1907.
382. Ueda, M.; Miyabe, H.; Sugino, H.; Naito, T. *Org. Biomol. Chem.* **2005**, *3*, 1124–1128.
383. Ueda, M.; Miyabe, H.; Nishimura, A.; Sugino, H.; Naito, T. *Tetrahedron: Asymmetry* **2003**, *14*, 2857–2859.
384. Miyabe, H.; Ushiro, C.; Ueda, M.; Yamakawa, K.; Naito, T. *J. Org. Chem.* **2000**, *65*, 176–185.
385. Bazin, S.; Feray, L.; Vanthuyne, N.; Bertrand, M. P. *Tetrahedron* **2005**, *61*, 4261–4274.
386. Lebel, H.; Marcoux, J.-F.; Molinaro, A. B.; Charette, A. B. *Chem. Rev.* **2003**, *103*, 977–1050.
387. Lorenz, J. C.; Long, J.; Yang, Z.; Xue, S.; Xie, Y.; Shi, Y. *J. Org. Chem.* **2004**, *69*, 327–334.
388. Yang, Z.; Lorenz, J. C.; Shi, Y. *Tetrahedron Lett.* **1998**, *39*, 8621–8624.
389. Fournier, J.-F.; Charette, A. B. *Eur. J. Org. Chem.* **2004**, *2004*, 1401–1404.
390. Begis, G.; Cladingboel, D.; Motherwell, W. B. *Chem. Commun. (Cambridge)* **2003**, 2656–2657.
391. Dübner, F.; Knochel, P. *Angew. Chem., Int. Ed.* **1999**, *38*, 379–381.
392. Dübner, F.; Knochel, P. *Tetrahedron Lett.* **2000**, *41*, 9233–9237.
393. Malda, H.; van Zijl, A. W.; Arnold, L. A.; Feringa, B. L. *Org. Lett.* **2001**, *3*, 1169–1171.
394. Tissot-Croset, K.; Polet, D.; Alexakis, A. *Angew. Chem., Int. Ed.* **2004**, *43*, 2426–2428.
395. Shi, W.-J.; Wang, L.-X.; Fu, Y.; Zhu, S.-F.; Zhou, Q.-L. *Tetrahedron: Asymmetry* **2003**, *14*, 3867–3872.
396. Ongeri, S.; Piarulli, U.; Roux, M.; Monti, C.; Gennari, C. *Helv. Chim. Acta* **2002**, *85*, 3388–3399.
397. Piarulli, U.; Daubos, P.; Claverie, C.; Roux, M.; Gennari, C. *Angew. Chem., Int. Ed.* **2003**, *42*, 234–236.
398. Piarulli, U.; Daubos, P.; Claverie, C.; Monti, C.; Gennari, C. *Eur. J. Org. Chem.* **2005**, 895–906.
399. Luchaco-Cullis, C. A.; Mizutani, H.; Murphy, K. E.; Hoveyda, A. H. *Angew. Chem., Int. Ed.* **2001**, *40*, 1456–1459.
400. Murphy, K. E.; Hoveyda, A. H. *J. Amer. Chem. Soc.* **2003**, *125*, 4690–4691.
401. Kacprzynski, M. A.; Hoveyda, A. H. *J. Amer. Chem. Soc.* **2004**, *126*, 10676–10681.
402. Larsen, A. O.; Leu, W.; Oberhuber, C. N.; Campbell, J. E.; Hoveyda, A. H. *J. Amer. Chem. Soc.* **2004**, *126*, 11130–11131.
403. Fuji, K.; Kinoshita, N.; Tanaka, K. *Chem. Commun. (Cambridge)* **1999**, 1895–1896.

404. Kinoshita, N.; Marx, K. H.; Tanaka, K.; Tsubaki, K.; Kawabata, T.; Yoshikai, N.; Nakamura, E.; Fuji, K. *J. Org. Chem.* **2004**, *69*, 7960–7964.
405. Devasagayaraj, A.; Stüdemann, T.; Knochel, P. *Angew. Chem., Int. Ed.* **1995**, *34*, 2723–2725.
406. Giovannini, R.; Stuedemann, T.; Devasagayaraj, A.; Dussin, G.; Knochel, P. *J. Org. Chem.* **1999**, *64*, 3544–3553.
407. Piber, M.; Jensen, A. E.; Rottländer, M.; Knochel, P. *Org. Lett.* **1999**, *1*, 1323–1326.
408. Jensen, A. E.; Knochel, P. *J. Org. Chem.* **2002**, *67*, 79–85.
409. Zhou, J.; Fu, G. C. *J. Amer. Chem. Soc.* **2003**, *2003*, 14726–14727.
410. Giovannini, R.; Knochel, P. *J. Amer. Chem. Soc.* **1998**, *120*, 11186–11187.
411. Terao, J.; Todo, H.; Watanabe, H.; Ikumi, A.; Kambe, N. *Angew. Chem., Int. Ed.* **2004**, *43*, 6180–6182.
412. Zhou, J.; Fu, G. C. *J. Amer. Chem. Soc.* **2003**, *125*, 12527–12530.
413. Netherton, M. R.; Fu, G. C. *Org. Lett.* **2001**, *3*, 4295–4298.
414. Hama, T.; Liu, X.; Culkin, D. A.; Hartwig, J. F. *J. Amer. Chem. Soc.* **2003**, *125*, 11176–11177.
415. Cantin, M.; Schutz, R.; Leumann, C. J. *Tetrahedron Lett.* **1997**, *38*, 4211–4214.
416. Liu, X.; Hartwig, J. F. *J. Amer. Chem. Soc.* **2004**, *126*, 5182–5191.
417. Bentz, E.; Moloney, M. G.; Westaway, S. M. *Tetrahedron Lett.* **2004**, *45*, 7395–7397.
418. Rottländer, M.; Palmer, N.; Knochel, P. *Synlett* **1996**, 573–575.
419. Rottländer, M.; Knochel, P. *J. Org. Chem.* **1998**, *63*, 203–208.
420. Dai, C.; Fu, G. C. *J. Amer. Chem. Soc.* **2001**, *2001*, 2719–2724.
421. Lipshutz, B. H.; Blomgren, P. A.; Kim, S.-K. *Tetrahedron Lett.* **1999**, *40*, 197–200.
422. Lipshutz, B. H.; Blomgren, P. A. *J. Amer. Chem. Soc.* **1999**, *121*, 5819–5820.
423. Malosh, C. F.; Ready, J. M. *J. Amer. Chem. Soc.* **2004**, *126*, 10240–10241.
424. Yasuda, M.; Tsuji, S.; Shigeyoshi, Y.; Baba, A. *J. Amer. Chem. Soc.* **2002**, *124*, 7440–7447.
425. Berman, A. M.; Johnson, J. S. *J. Amer. Chem. Soc.* **2004**, *126*, 5680–5681.
426. Erdik, E.; Daskapan, T. *Synth. Commun.* **1999**, *29*, 3989–3997.
427. Erdik, E.; Daskapan, T. *J. Chem. Soc., Perkin Trans. 1* **1999**, 3139–3142.
428. Trost, B. M.; Fettes, A.; Shireman, B. T. *J. Amer. Chem. Soc.* **2004**, *126*, 2660–2661.
429. Matsunaga, S.; Yoshida, T.; Morimoto, H.; Kumagai, N.; Shibasaki, M. *J. Amer. Chem. Soc.* **2004**, *126*, 8777–8785.
430. Values are given in Pauling units and are based on configuration energies, as reported in: Mann, J. B.; Meek, T. L.; Allen, L. C. *J. Am. Chem. Soc.* **2000**, *122*, 2780–2783.
431. Mann, J. B.; Meek, T. L.; Knight, E. F.; Capitani, J. F.; Allen, L. C. *J. Am. Chem. Soc.* **2000**, *122*, 5132–5137.
432. Sanderson, R. T. *Inorganic Chemistry*; Reinhold: New York, 1967.
433. Shannon, R. D. *Acta Cryst.* **1976**, *A32*, 751–767.
434. Batsanov, S. S. *J. Mol. Struct. (THEOCHEM)* **1999**, *468*, 151–159.
435. Moore, C. E. Ionization potentials and ionization limits; Natl. Stand. Ref. Data Ser. (U.S. Natl. Bur. Stand.); NSRDS-NBS, 1970, *34*
436. Hotop, H.; Lineberger, W. C. *J. Phys. Chem. Ref. Data* **1985**, *14*, 731.
437. Bard, A. J., Parsons, R., and Jordan, J., Eds. *Standard Potentials in Aqueous Solution*; Marcel Dekker: New York, 1985.
438. Pearson, R. G. *Inorg. Chem.* **1988**, *27*, 734–740.
439. Affefy, H. Y.; Liebermann, J. F.; Stein, S. E. *Neutral Thermochemical Data*, in NIST Chemistry WebBook, NIST Standard Reference Database Number 69 – July 2001 Release, Mallard, W. G.; Lindstrom, P. J., National Institute of Science and Technology, (http://webbook.nist.gov).
440. Gümrükçüoglü, I. E.; Jeffery, J.; Lappert, M. F.; Pedley, J. B; Rai, A. K. *J. Organomet. Chem.* **1988**, *341*, 53–62.
441. Bloom, R.; Boersma, J.; Budzelaar, P. H. M.; Fischer, B.; Haaland, A.; Volden, H. V.; Weidlein, J. *Acta. Chem. Scand.* **1986**, *A40*, 113–120.

2.07
Mercury and Cadmium Organometallics

F P Gabbaï Melaimi, C N Burress, M-A Melaimi, and T J Taylor, Texas A&M University, College Station, TX, USA

2.07.1 Mercury

2.07.1.1 Introduction

Despite their toxicity, organomercury derivatives continue to be widely used by academic chemists. The sustained popularity of this class of organometallic compounds stems from their unique abilities to mediate organic transformations. These derivatives are also useful starting materials for the synthesis of a broad range of organometallic compounds. While these chemical facets came to light several decades ago, the chemistry of organomercury compounds has recently experienced notable developments.

Some of these developments have come with the discovery that organomercurials can display significant Lewis acidity when substituted by electron-withdrawing groups. Taking into account the air and water stability of organomercurials, these discoveries have fueled a great deal of research directed toward the synthesis of

polyfunctional organomercurials as Lewis-acidic hosts for neutral and anionic substrates. Other exciting developments in organomercury chemistry have resulted from the unusual properties that mercury displays as a heavy atom. For example, theoretical calculations suggest that metallophilic interactions should occur in the chemistry of organomercurials such as $(HgMe_2)_2$ which is predicted to form a perpendicular dimer with an Hg(II)···Hg(II) bond of 3.41 Å.[1] The occurrence of metallophilic contacts in mercury compounds, which has now been experimentally confirmed,[2–4] originates from the dispersion forces magnified by relativistic effects. These relativistic effects are also responsible for the inherent softness of mercury(II) cations and their ability to engage in dispersive interactions with polarizable substrates such as arenes or other polynuclear complexes.

While it is our intent to be comprehensive in our treatment of the topic, space limitation forces us to restrict our coverage to selected examples which will hopefully allow the reader to capture the most important aspects of current organomercury chemistry. Although the material used to write this chapter has been extracted from original research reports that have appeared in the last 10 years, we would like to direct the reader to a series of recent reviews which deal with some aspects of organomercury chemistry.[5–25]

2.07.1.2 Formation of the Mercury–Carbon Bond

2.07.1.2.1 Metathesis reactions

Metathesis reactions continue to be extensively employed in the synthesis of organomercury compounds. While most reactions involve the use of organolithium or Grignard reagents, other organometallic compounds are sometimes used as starting materials.

2.07.1.2.1.(i) Alkylmercury compounds

Owing to their synthetic utility, novel alkylmercury derivatives continue to be prepared often. Recent examples include a series of mercurated methoxy- and dimethylaminoalkyl derivatives **1–4** which have been synthesized from the corresponding Grignard reagents and further alkylated by reaction with Bu^tLi.[26] Interestingly, the resulting dialkylmercury derivatives react with Bu^tLi to afford $Bu^t{}_2Hg$ and the lithiated methoxy- and dimethylaminoalkyl derivatives. Analogous synthetic procedures have been employed for the synthesis of $[(Ph(CH_2)_2)_2Hg]$ and $[(Ph(CH_2)_3)_2Hg]$.[27] Grignard reagents have also been used for the synthesis of 1,4-butanediylbis(bromomercury) **5** and 1,6-hexanediylbis(bromomercury) **6** which were isolated in moderate yields.[28] These derivatives are poorly soluble in most organic solvents including DMSO but cleanly react with indium(I) halides to afford the corresponding α,ω-alkanediylbis(dibromoindium) compounds. Less common routes to the synthesis of alkylmercury derivatives involve the use of organozirconium(IV) species as starting materials. For example, the cyclopropylcarbinylmercury chloride **7** was obtained by treatment of the corresponding bis(cyclopentadienide)zirconium methoxide complex with $HgCl_2$ (Equation (1)).[29]

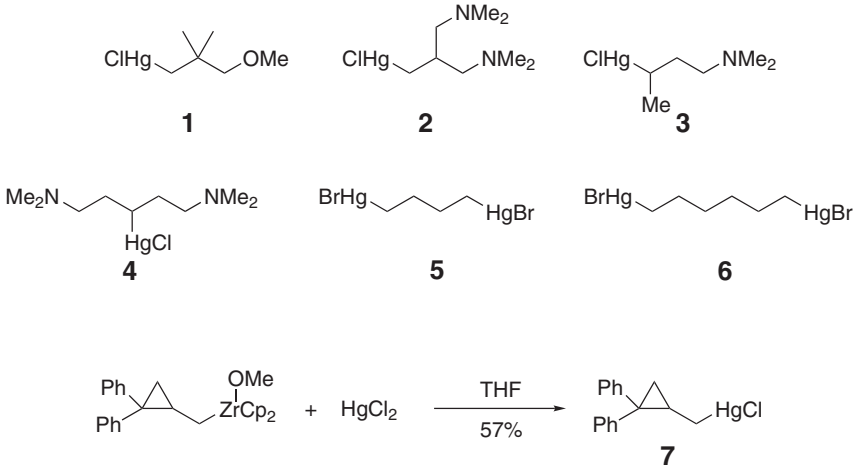

Organolithium reagents stabilized by α-silyl groups have been recently used for the synthesis of mononuclear derivatives such as compounds **8**, **9** which the bulky $(PhMe_2Si)_3C$ and $(Me_3Si)_3C$ as ligands directly attached to the mercury center.[30] Other examples include the dialkylmercury products shown in Equations (2) and (3).[31,32]

In the solid state, the pyridine nitrogen atom of compound **10** forms secondary interactions with the mercury center. Intramolecular coordination of the nitrogen atom is, however, not observed in derivative **11** in which N → Si π-bonding possibly monopolizes the nitrogen lone pair.

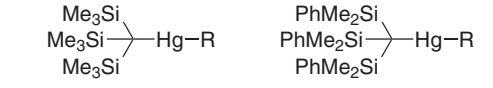

R = Me, Pr^i, Bu, Bu^t, Ph R = Me, Bu, CH_2Ph, Ph

8 **9**

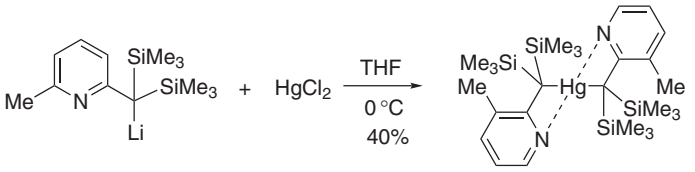

10 (2)

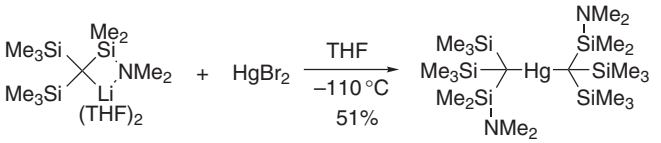

11 (3)

Similar strategies have been adopted for the introduction of dicarbanionic ligands in both mononuclear and dinuclear organomercury derivatives. The lithium salts of the $[(Me_3Si)_2CSiMe_2CH_2CH_2SiMe_2C(SiMe_3)_2]^{2-}$ and $[1,3\text{-}C_6H_4(CH(SiMe_3)]^{2-}$ dianions can be converted into organomercury derivatives **12** (Equation (4)) and **13** (Equation (5)), respectively, by reaction with the appropriate mercury salts.[33,34] In the case of **13**, the reaction is stereoselective and only affords the *meso*-derivative, which possibly results from an anion template effect. The non-silylated analog of **13**, namely α,α'-*m*-xylenediylbis(mercury chloride) **14**, has been recently prepared from the corresponding di-Grignard reagent (Equation (6)).[35] In the solid state, derivative **14** forms an intricate three-dimensional(3-D) network in which the individual molecules are connected by secondary Hg-Cl interactions.

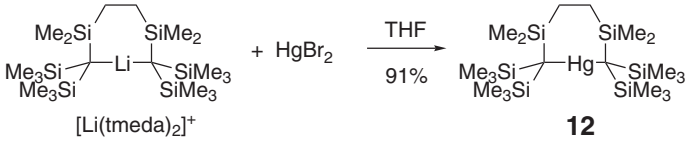

12 (4)

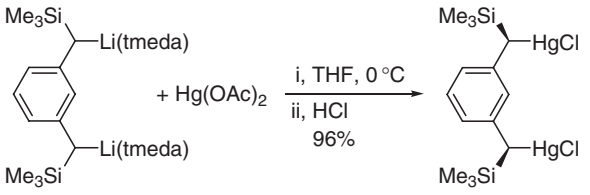

13 (5)

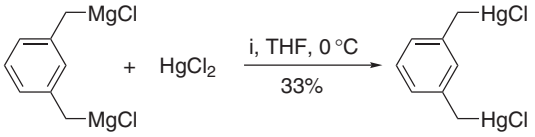

(6)

14

Bis(thiomethyl)mercury derivatives **15** and **16** have been prepared by reaction of the corresponding lithium reagents with $HgCl_2$ (Equation (7)).[36] In a similar way, deprotonation of the coordinated bis(diphenylphosphino)-methane (DPPM) ligand in $[Cr(CO)_4(Ph_2PCH_2PPh_2)]$ with Bu^nLi followed by reaction with MeHgCl affords the phosphinomethylmercury complex **17** (Equation (8)).[37] A crystal structure of this derivative confirmed ligation of the mercury atom to the central carbon atom of the DPPM ligand.

$$[Li_2(CH_2SR)_2(tmeda)_2] + HgCl_2 \xrightarrow[-78\,^\circ C]{THF} Hg(CH_2SR)_2$$

15: R = Me (75%)
16: R = Ph (96%)

(7)

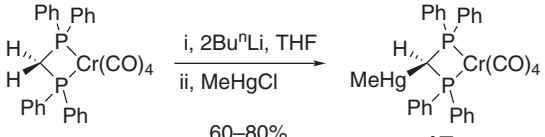

(8)

17

Reaction of $LiC_5Me_4(SiMe_2Bu^t)$ with $HgCl_2$ affords either $[\{Hg(\eta^1\text{-}C_5Me_4(SiMe_2Bu^t))Cl\}_4]$ **18** or $[Hg(\eta^1\text{-}C_5Me_4(SiMe_2Bu^t))_2]$ **19** depending on the stoichiometry of the reagents.[38] These two compounds have been fully characterized, and their crystal structure determined. While previous mercury–cyclopentadienide complexes were shown to have fluxional structures, solution and solid-state studies indicate that these two derivatives are non-fluxional with the mercury atom bound to the silylated carbon atom.

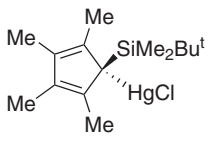

18

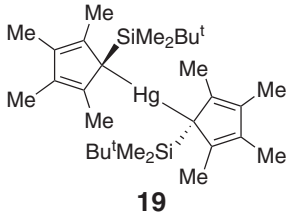

19

2.07.1.2.1.(ii) Arylmercury compounds

A broad range of novel arylmercury derivatives have been prepared from the corresponding lithium compounds. In addition to simple fluorinated arylmercury compounds such as $(2\text{-}FC_6H_4)HgCl$, $(2,6\text{-}F_2C_6H_3)HgCl$,[39] 9-(chloromercurio)anthracene,[40] and $(2\text{-}Me_2N(CH_2)_2OC_6H_4)_2Hg$,[41] this synthetic approach has also been used for the preparation of polymercurated derivatives. For instance, the di-Grignard reagent of 1-bromo-2-(2-bromoethyl)benzene reacts with $HgCl_2$ in THF to afford 1-(bromomercurio)-2-[2-(bromomercurio)ethyl]benzene (Scheme 1).[42]

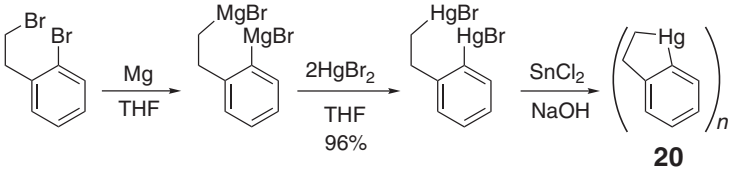

20

Scheme 1

Reduction of the latter with $SnCl_2$ leads to the formation of 1-mercuraindane **20**, which exists as an equilibrating mixture of dimers and trimers. 9,10-Bis(chloromercurio)anthracene, which is obtained from the corresponding dilithium reagent in THF, constitutes another example of a recently prepared dinuclear mercury compound.[40] Remarkably, the triple lithiation of 1,3,5-tribromobenzene with 7 equiv. of lithium 4,4′-*t*-butylbiphenyl, afforded 1,3,5-$C_6H_3(HgBr)_3$ **21** as the main product (Equation (9)).[43] The chloride analog, 1,3,5-$C_6H_3(HgCl)_3$ **22**, has also been prepared by reaction of 1,3,5-$C_6H_3(SnMe_3)_3$ with $HgBr_2$ in Et_2O/THF at low temperature (Equation (10)).[44] The identity of these poorly soluble derivatives was confirmed by ^1H NMR in d_6-DMSO as well as by X-ray analysis in the case of the chloro-complex **22**.

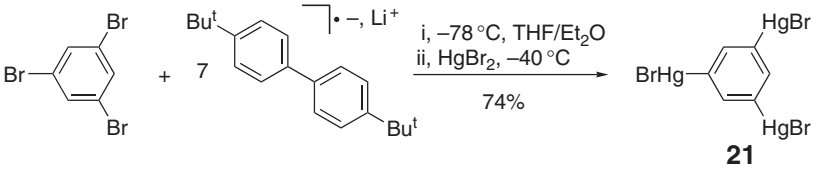

21 (9)

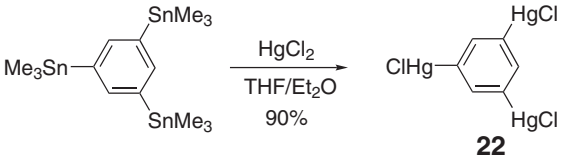

22 (10)

Organolithium derivatives have also proved useful for the synthesis of mercury derivatives featuring functionalized aryl rings. For example, dilithiation of benzylalcohol in the presence of tmeda followed by reaction with $HgCl_2$ and aqueous work-up afforded Hg[$C_6H_4(CH_2OH)$]Cl **23** (Equation (11)),[45] which, in the presence of pyridinium chlorochromate, is oxidized to afford the corresponding mercurated benzaldehyde. The diorganomercurial **24**, prepared from the Grignard reagent, can be converted into the corresponding dialdehyde **25** by deprotection of the acetal with *p*-toluenesulfonic acid (Scheme 2).[46] The latter is converted into a diimine by reaction with arylamines such as 4-$MeC_6H_4NH_2$.

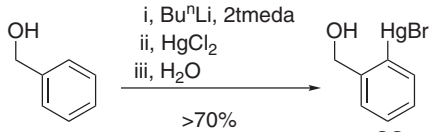

23 (11)

Similarly, dilithiation of 2-(4-bromophenoxy)ethanol in the presence of magnesium 2-ethoxyethoxide followed by reaction with 0.5 equiv. of $HgCl_2$ afforded the corresponding diarylmercury compound 4-($HO(CH_2)_2O$)-$C_6H_4)_2Hg$ **26** whose crystal structure has been determined (Equation (12)).[47] In addition to these alcohol and ether derivatives, thio- and phosphinoaryl mercury compounds have also been prepared. Thus, the dilithium salt

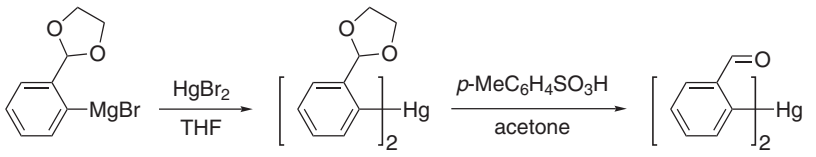

24 **25**

Scheme 2

[2-Li(SLi)C_6H_4] reacts with $HgCl_2$ to afford polymeric [(2-C_6H_4S)Hg]$_n$ **27** as an insoluble, colorless solid (Equation (13)).[48] The diaryl complex [Hg(2-$C_6H_4PPh_2$)$_2$] **28**, prepared from the corresponding lithium reagent, serves as a starting material for mixed metal–mercury cyclometallated complexes (Equation (14)).[49] A similar approach has been adopted for the preparation of [Hg(2,6-$C_6H_3(NMe_2)_2$)$_2$] **29** (Equation (15)), an amino derivative which features intramolecular coordination of the nitrogen atom to the mercury center in the solid state.[50] Finally, it is worth mentioning a new synthesis for bis(3-pyridyl)mercury, which has been recently obtained by reaction of $HgBr_2$ with 3-pyridylmagnesium chloride.[51] Former syntheses of these organomercurials involved direct mercuration of pyridine.

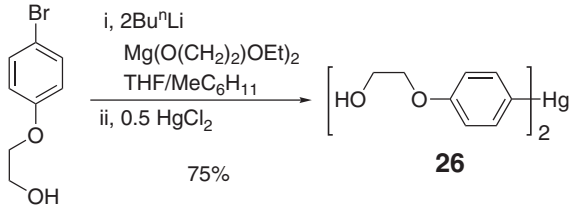

(12)

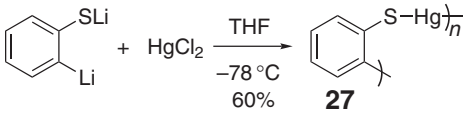

(13)

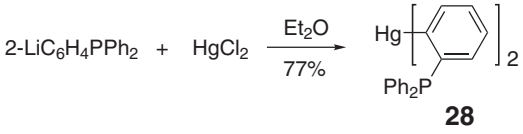

(14)

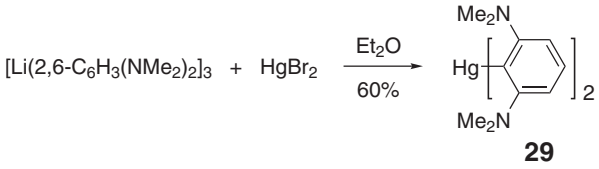

(15)

Aryl derivatives of the heavier group 6 derivatives can also serve for the synthesis of arylmercury compounds.[52] For instance, treatment of the diaryltellurium complex **30** with $HgCl_2$ leads to the formation of a coordination complex which undergoes a slow dismutation reaction to afford the arylmercury chloride derivative **31** and the corresponding tellurium species (Scheme 3).[53]

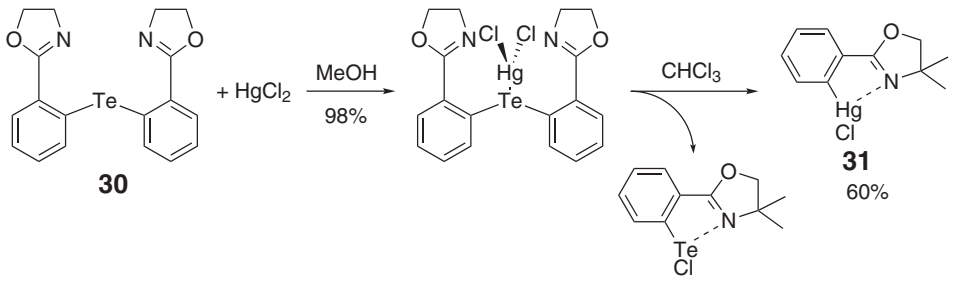

Scheme 3

Macrocyclic complexes containing arylmercury moieties have also been investigated. For instance, lithiation of (1,3-phenylene)-16-crown-5 and (2-bromo-1,3-phenylene)-19-crown-6 followed by reaction with 0.5 equiv. $HgBr_2$ affords bis[(1,3-phenylene-16-crown-5)-2-yl]mercury **32** and bis[(1,3-phenylene-19-crown-6)-2-yl]mercury **33**, respectively.[54,55] The reaction leading to **33** also affords isolable quantities of (2-bromomercurio-1,3-phenylene)-19-crown-6.[55] Organolithium reagents have also been used for the synthesis of macrocyclic complexes containing a mercury atom directly incorporated in the ring. For example, the mercuracycle **34** was obtained by lithiation of the corresponding dibromide followed by treatment with $HgBr_2$.[56]

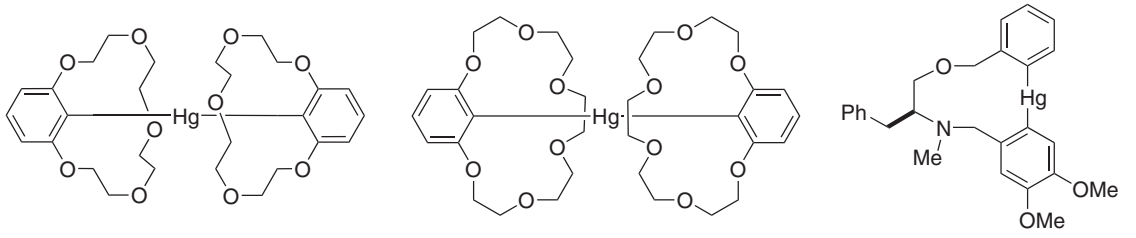

32 **33** **34**

2.07.1.2.1.(iii) Alkenylmercury species

A remarkable series of vinylmercury hydride **35–37** derivatives have been recently synthesized from the Grignard reagents and $HgCl_2$ followed by reaction with Bu^n_3SnH.[57] The stability of these hydrides has allowed for their characterization by NMR spectroscopy. Fluorinated vinylmercury complexes have also been investigated. For example, high yields of $Hg(CF{=}CF_2)_2$ **38** have been obtained by the low-temperature reaction of 2 equiv. of $Li(CF{=}CF_2)$ and $HgCl_2$.[58] In the solid state, molecules of this air stable organomercurial adopt a planar structure and interact with one another by secondary Hg–F interactions. In the gas phase, however, electron diffraction studies confirm that there is free rotation about the Hg–C bonds. Using a less conventional approach, the cyclohexadienyl derivative **39** has been obtained by a ligand-exchange reaction involving a silylated starting material and $HgCl_2$ (Equation (16)).[59] This reaction, however, necessitates the use of NH_4F, which probably facilitates displacement of the silyl group.

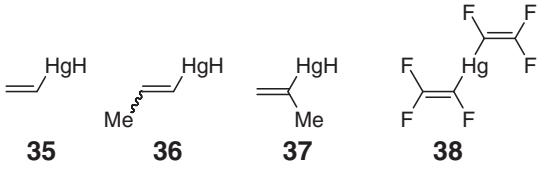

35 **36** **37** **38**

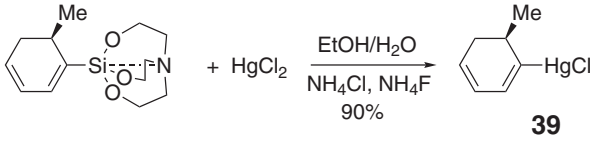

39 (16)

Methylene-ylene-phosphoranes possess acidic C–H groups, which can be readily deprotonated using organolithium reagents. Thus, reaction of **40** with $HgCl_2$ affords the diorganomercury compound **41** whose structure has been determined (Equation (17)).[60a] Related phosphorus(III) mercury derivatives such as **42** have been obtained by reaction of the (phosphaalkenyl)lithium carbenoid (*Z*)-[(2,4,6-$Bu^t_3C_6H_2$)P=CClLi] with 1 equiv. of $HgCl_2$ in THF at −110 °C (Equation (18)).[60b]

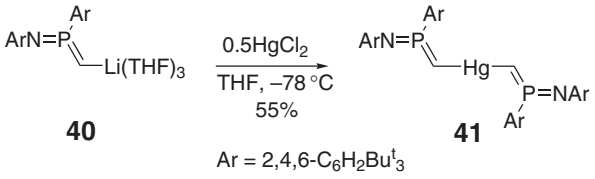

(17)

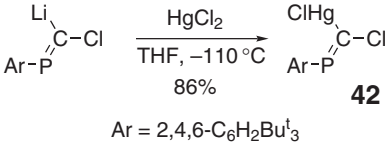

(18)

Deprotonation of the nitronyl nitroxide **43** with $LiN(Pr^i)_2$ occurs at the C_2 position and affords a solution containing the corresponding organolithium derivatives. The latter reacts with $Hg(OAc)_2$ to yield a rare example of a C_2-metallated nitronyl nitroxide **44** (Equation (19)). In the solid state, this paramagnetic derivative forms tetramers in which the individual molecules interact via secondary Hg–O interactions involving the N–O oxygen atoms.[61] Additionally, derivative **45** has been successfully synthesized from the corresponding lithium salt and $HgCl_2$.[62]

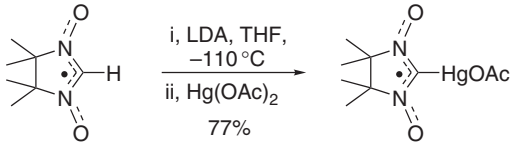

(19)

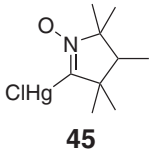

2.07.1.2.1.(iv) Alkynylmercury derivatives

Organolithium reagents have also been employed for the synthesis of novel bis(alkynyl)mercury derivatives. These include $Hg(C{\equiv}CCF_3)_2$[63] and **46–48**,[64] which have been synthesized along with the bis(alkynyl)aurate analogs. Bis(alkynyl)mercury species such as **49** can also be obtained by reaction of monosubstituted alkynes with $K_2[HgI_4]$ in basic aqueous solutions.[65,66]

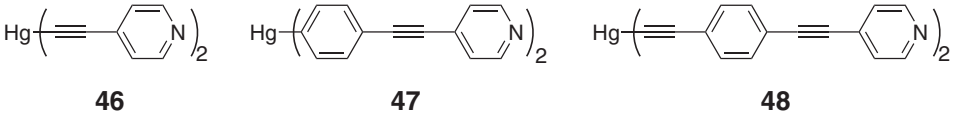

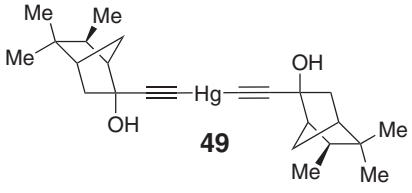

In addition to these examples, several polynuclear mercury alkynyl derivatives have been prepared. Examples of such derivatives include compounds **50–56** which have been obtained by reaction of the MeHgCl with the primary alkyne in basic methanolic conditions.[67,68] The phenyl analogs have also been isolated. Most of these compounds have been characterized by FTIR, NMR, and FABMS, and in the case of **51–53** by single crystal X-ray diffraction.

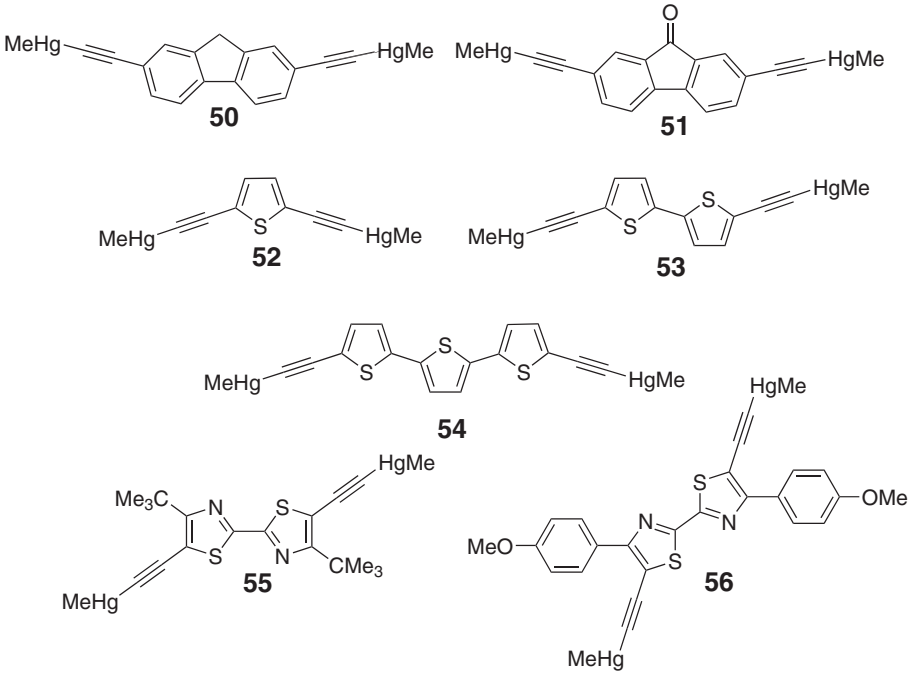

Formation of these dinuclear mercury derivatives is accompanied by a red shift of the absorbance of the bis(alkynyl) backbone. For example, conversion of 2,7-bis(alkynyl)fluorene into the corresponding bis(methylmercury) derivative **50** leads to a shift of the main absorption band of the bis(alkynyl) backbone from 505 to 567 nm. Similar results have been obtained for **51–56**.[67,68]

In the absence of capping ligands, polymeric alkynylmercury derivatives can be readily prepared. Polymer **57** is formed by reaction of $HgCl_2$ with 9,9-bis(4-ethynylphenyl)-fluorene in a basic methanolic solution. This polymer, whose average molecular weight (M_w) is only 8,900, shows a strong triplet emission of the organic chromophore enhanced by the presence of the mercury heavy atom.[69]

2.07.1.2.1.(v) Carborane–mercury derivatives

A series of alkyl-substituted macrocycles featuring mercury atoms connected by *closo*-carborane units has been recently synthesized. Examples of such macrocycles include the hexamethyl derivative **58** and the hexadecamethyl derivative **59** whose alkyl-substituted carborane backbones impart improved solubility in hydrocarbon solvents.[70,71] While **58** was synthesized from *closo*-9,12-Me_2-1,2-Li_2-1,2-$C_2B_{10}H_8$ and $Hg(OAc)_2$, compound **59** was obtained as a

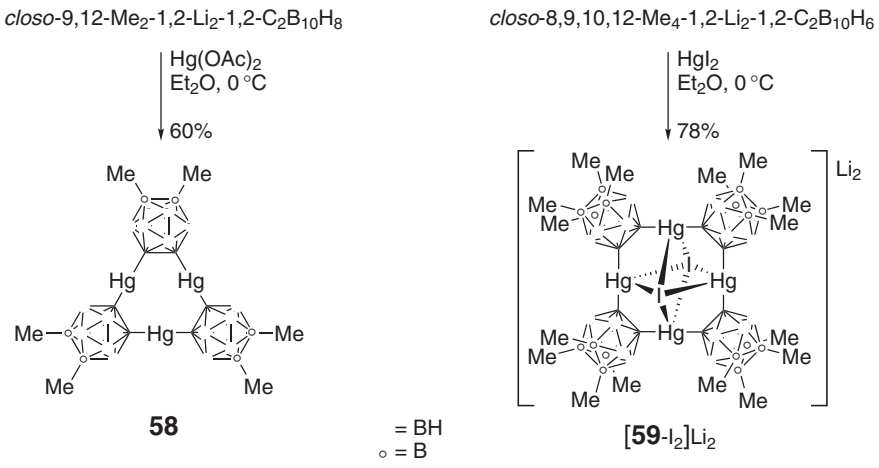

Scheme 4

diiodide complex from *closo*-8,9,10,12-Me_4-1,2-Li_2-1,2-$C_2B_{10}H_6$ and HgI_2 (Scheme 4). In order to shed light on the possible templating role of the halide anion, the use of a phenyl-substituted carborane cage has also been considered. Reaction of *closo*-3-Ph-1,2-Li_2-1,2-$C_2B_{10}H_9$ with $HgCl_2$ affords the chloride adduct of the tetranuclear mercury derivative as a mixture of isomers which differ by the respective orientation of the phenyl groups.[72] The same reaction with HgI_2 yields only one isomer with an "up–down–up–down" orientation of the phenyl groups (Equation (20)). Formation of this single isomer, which was isolated as the iodide adduct **60**, shows that the halide is present in the product-determining transition state. The large iodide leads to a conformation where both the iodide–phenyl and phenyl–phenyl steric repulsions are minimized, whereas the smaller chloride anion provides little steric bias in the orientation of the phenyl group.

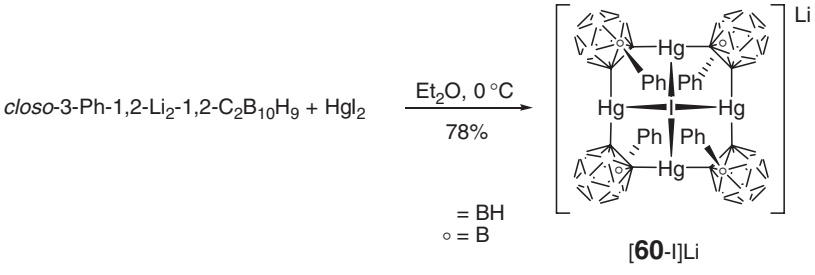

(20)

2.07.1.2.2 Mercuration of organic substrates possessing acidic C–H groups

Organic compounds such as terminal alkynes can undergo direct mercuration using various mercury salts. For instance, alkyne **61** has been shown to react with $Hg(OAc)_2$ to form the symmetrical bis-alkyl-mercury complex **62** (Equation (21)).[73]

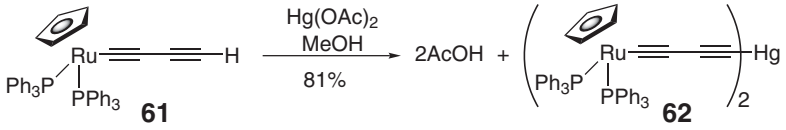

(21)

The mercuration of phosphonium derivatives has also been observed. The methylene group of the dimeric palladium complex **63** substituted by a carbonyl and a phosphonium functionality is readily mercurated upon reaction with $Hg(OAc)_2$ to afford complex **64** (Equation (22)).[74] Further studies demonstrated that the presence of a triphenylphosphonium group alone is sufficient to promote proton–mercury exchange. For example, the reaction of

benzyltriphenylphosphonium **65** with $Hg(OAc)_2$ or $Hg(OCOCF_3)$ in hot ethanol yields compounds **66** and **67**, respectively (Scheme 5).[75] This reaction most likely proceeds via formation of a phosphorus ylide intermediate. A similar mechanism has been proposed for the conversion of the phosphonium derivatives **68a–c** into the mercury derivatives **69a–c** (Scheme 6).[76]

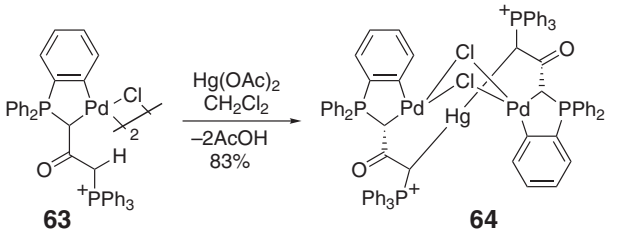

(22)

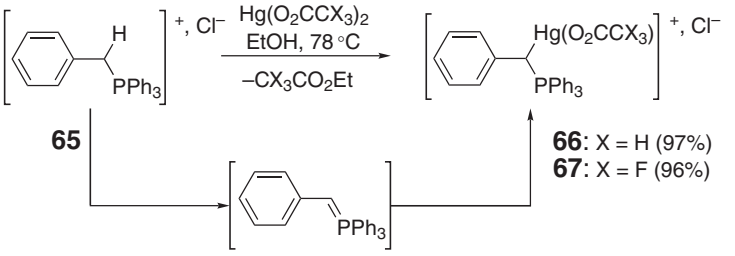

Scheme 5

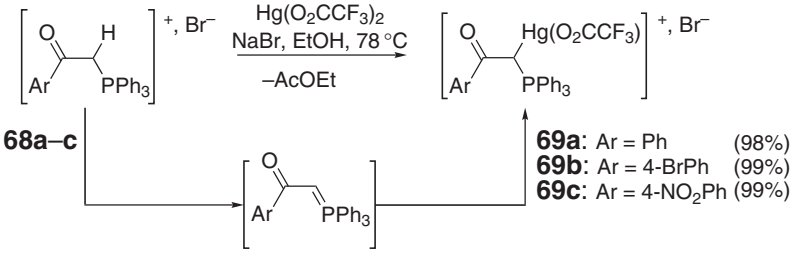

Scheme 6

The reaction of dimethylimidazolium chloride with $Hg(OAc)_2$ under slightly basic conditions gives the homoleptic bis(carbene) mercury complex **70** (Equation (23)).[77] The reaction proceeds through deprotonation of the imidazolium followed by the coordination of the carbene to the mercury atom. This approach is quite general and has been applied to a variety of other complexes[78–80] including **71** which features a chelating bis(carbene) ligand (Equation (24)).[81] Interestingly, the bis(tosylate) imidazolium salt of the bidentate carbene ligand present in **71** forms an ionic liquid which has been successfully employed to extract mercury salts from aqueous media.

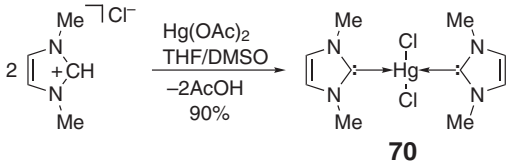

(23)

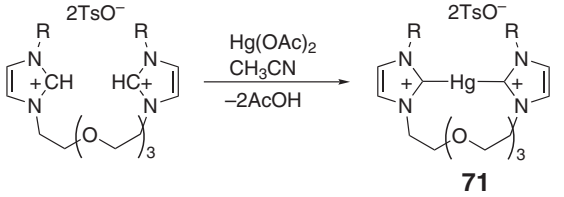

(24)

2.07.1.2.3 Mercuration of aromatic substrates

Mercuration reactions provide a convenient approach to a broad range of arylmercury derivatives.[82,83] This approach has been applied to a number of substrates, including phenols, indoles, phenylpyridines, and *N*-arylamides.[83] The products of these reactions as well as their conditions are summarized in Table 1.[84–91] Other examples of such reactions include the mercuration of 2-(2′-naphthyl)pyridine (Equation (25))[92] and terephthaldehyde (Equation (26))[93] with $Hg(OCOCF_3)_2$ and $Hg(ClO_4)_2$, which afford **72** and **73**, respectively.

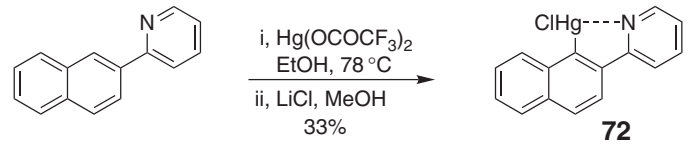

(25)

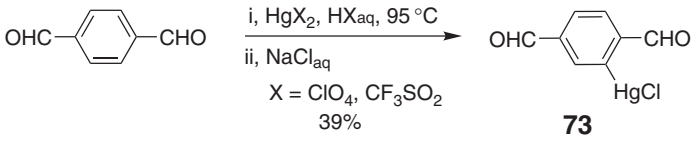

(26)

Table 1 Selected examples of mercuration reactions involving aromatic substrates

Starting material	*Conditions*	*Product*	*Yields (%)*	*References*
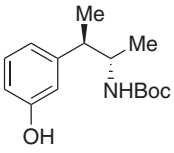	$Hg(OAc)_2$ MeOH	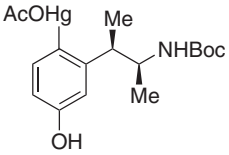	27	83
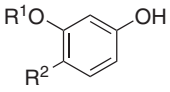	i, $Hg(OAc)_2$ MeOH ii, LiCl	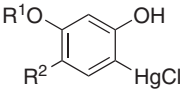	R^1 R^2 OMe OBn 80 OBn OMe 85 OBn OBn 80	84
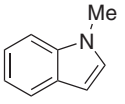	i, 2 $Hg(OAc)_2$ EtOH, Et_2O ii, LiCl, MeOH, 70%	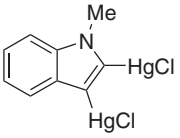	92	85
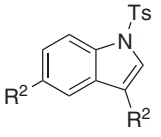	i, $Hg(OAc)_2$ AcOH, $HClO_4$ ii, NaCl	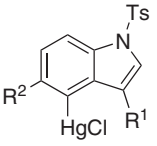	R^1 R^2 Br H 83 CHO H 85 CO_2Me H 71 Me H 76	86
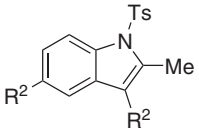	i, $Hg(OAc)_2$ AcOH, $HClO_4$ ii, NaCl	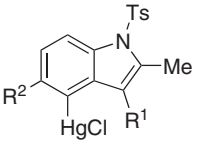	Me H 74 Br OMe 49	86

(*Continued*)

Table 1 (Continued)

Starting material	*Conditions*	*Product*	*Yields (%)*	*References*
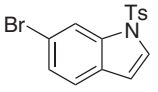	$Hg(OAc)_2$ AcOH, $HClO_4$ H_2O	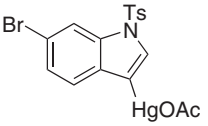	97	87
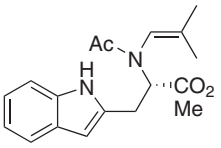	i, $Hg(OAc)_2$ AcOH/$HClO_4$ H_2O ii, NaCl	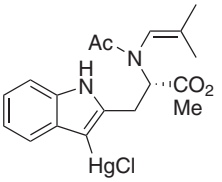	45	88
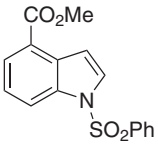	i, $Hg(OAc)_2$ AcOH, $HClO_4$ ii, NaCl	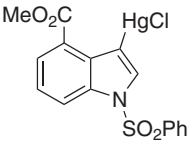	99	89
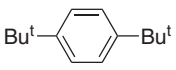	i, 2 $Hg(O_2CCF_3)_2$ 210 °C ii, NaCl, H_2O	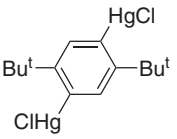	96	90
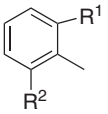	i, $Hg(OAc)_2$ AcOH, 110 °C ii, LiCl/H_2O	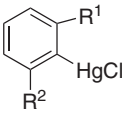	R^1 R^2 $CONH_2$ H 17 CONHEt H 21 $CONEt_2$ $CONEt_2$ 10	91

Since the regioselectivity of mercuration reactions is often hard to control, recent efforts have focused on the use of Lewis-basic substituents whose role is to direct the approach of the mercuric ion to a specific position. Reaction of the diazo derivative **74** with $Hg(OAc)_2$ leads to mercuration of the naphthalene moiety in the 8-position rather than mercuration of the electron-rich imidazole carbon atoms.[94] Presumably, the diazo–imidazole bidentate moiety coordinates to the mercuric cation, thereby directing substitution at the naphthalene 8-position (Equation (27)).

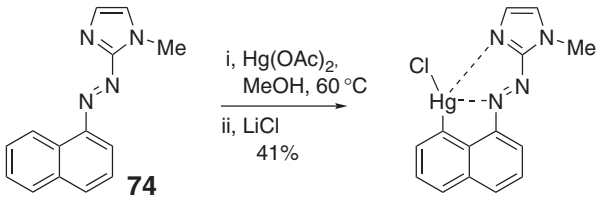

(27)

The arene groups in (η^6-arene)tricarbonylchromium complexes are typically electron poor and display poor reactivity toward electrophiles. In the case of mercuration reactions, this lack of reactivity can be overcome by attachment of Lewis-basic substituents to the arene ring. For example, in the case of **75a–c**, the presence of a pyridyl, oxazolyl, or methyl-*N*,*N*-dimethylamino group promotes *ortho*-mercuration, leading to the formation of the bimetallic complexes **76a–c** (Equation (28)).[95–97]

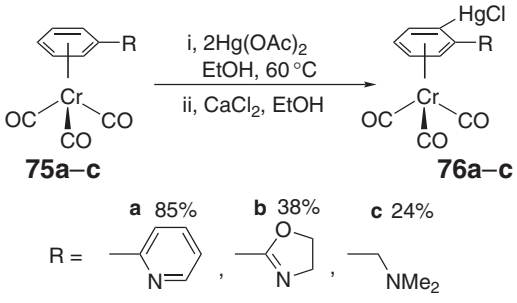

(28)

Iminophosphoranes of the type $Ph_3P{=}NAr$ typically react with HgX_2 (X = Cl, Br, I) to afford the corresponding coordination complexes $Ph_3P{=}NAr(HgX_2)$.[98] In the case of **77**, reaction with $Hg(OAc)_2$ in THF under reflux follows a different course and yields the organomercury species **78** indicating that the iminophosphorane moiety acts as an *ortho*-directing substituent (Equation (29)).[99]

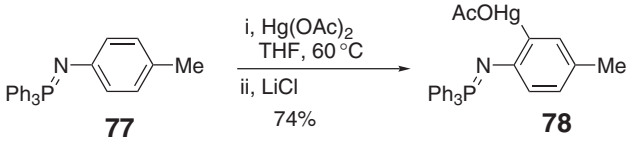

(29)

Aromatic heterocycles can also be mercurated. For example, *N*-acetylpyrrole and *N*-phenylsulfonylpyrrole react with $HgCl_2$/NaOAc to form the monomercurated products **79** and **80**, respectively (Equations (30) and (31)). The amide or sulfonamide group provides an oxygen donor atom that coordinates with the incoming mercuric ion, ultimately directing mercuration at the 2-position.[100]

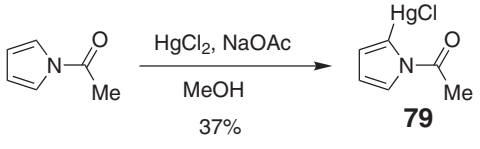

(30)

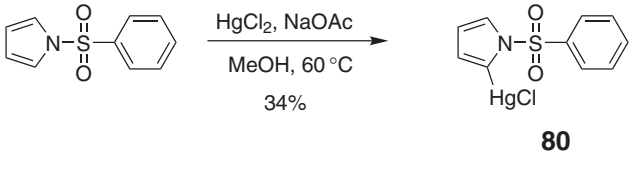

(31)

Thiophenes **81a** and **81b**, which bear carboxylic acid functionalities, have been mercurated using a variety of mercury salts, including $Hg(OAc)_2$ and $Hg(OCOCF_3)_2$. When $Hg(OAc)_2$ is employed, these reactions afford a mixture of monomercurated **82a** and **82b** and dimercurated products **83a** and **83b** (Equation (32)).[101] Dimercuration is also observed when 3,4-ethylenedioxythiophene **84** is treated with $Hg(OAc)_2$ to form **85** (Equation (33)).[102]

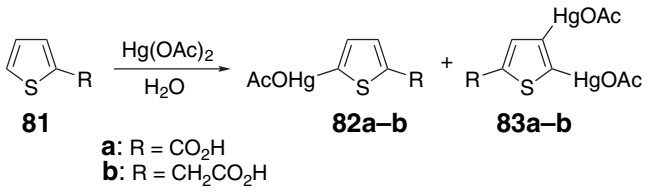

(32)

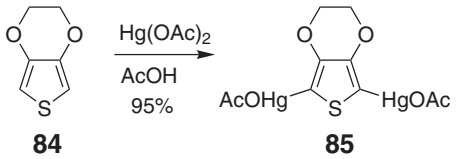

(33)

2.07.1.2.4 Mercuration of metallocenes and sandwich complexes

Although the mercuration of ferrocene has been reported for many years, only recently has the mechanism of this reaction been elucidated. Recent studies indicate that the soft mercuric cation undergoes complexation to the Lewis-basic iron center prior to mercuration. This event is followed by the rate-limiting *endo*-attack of the cyclopentadienyl ring and subsequent product formation (Scheme 7).[103]

The mercuration of ferrocenylimines with $Hg(OAc)_2$ has been studied.[104–106] Mercuration occurs selectively at the α-position relative to the imine group to afford compounds **86a–i** (Scheme 8).[107,108] The regioselectivity of these reactions points to the directing role of the Lewis-basic imine functionality. Similar factors probably play a role in the formation of the ferrocenylketone and ferrocenylaldehyde derivatives **87a–f** and **87g–j**, respectively.[109] These derivatives readily react with amines to afford the corresponding imines (Scheme 9). Presumably, the Lewis-acidic mercury center of the monomercurated ferrocenylketones and ferrocenylaldehydes activates the carbonyl functionality toward nucleophilic attack by the amine.

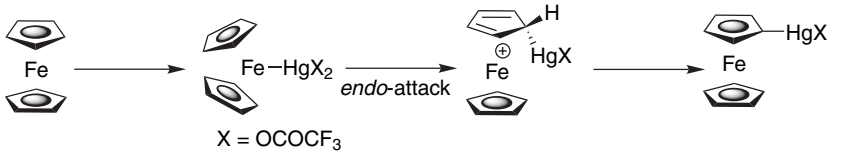

Scheme 7

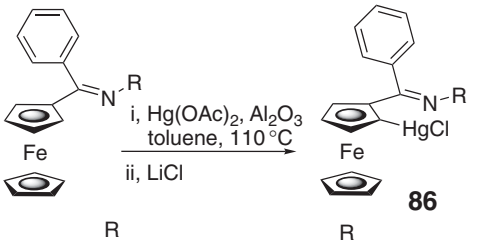

R		R	
a: *o*-BrC_6H_4	23%	**f**: *p*-BrC_6H_4	30%
b: *p*-MeC_6H_4	44%	**g**: *m*-ClC_6H_4	30%
c: *p*-$MeOC_6H_4$	39%	**h**: *m*-BrC_6H_4	23%
d: C_6H_5	44%	**i**: *o*-ClC_6H_4	6%
e: *p*-ClC_6H_4	44%		

Scheme 8

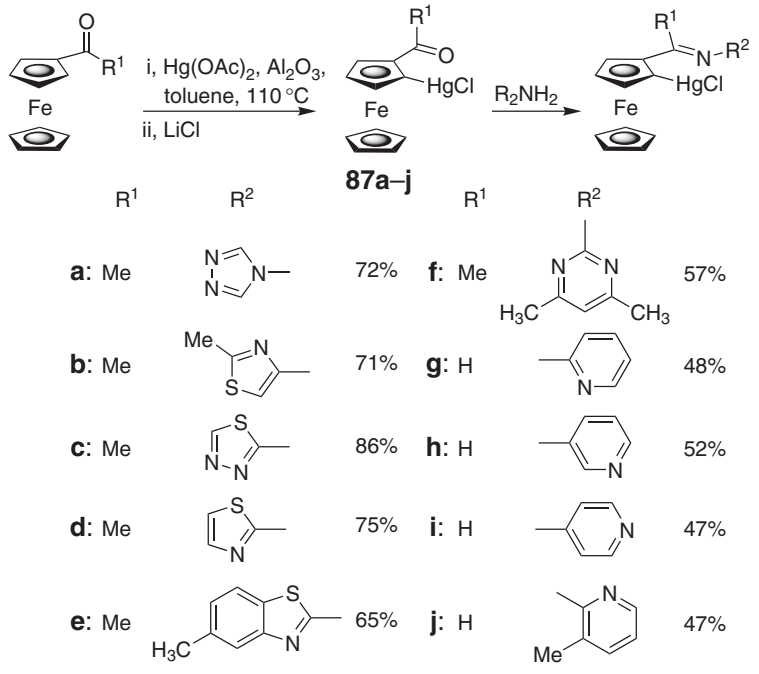

Scheme 9

As recently reported, the decamercuration of ferrocene, which typically employs $Hg(OAc)_2$ or $Hg(OCOCF_3)_2$ as reagents, can be conveniently carried out with $Hg(OCOCCl_3)_2$ and affords decachloromercurioferrocene in quantative yield after treatment with NaCl.[110] Decamercuration is also observed when osmocene is allowed to react with $Hg(OAc)_2$.[111] Recent studies indicate that the permercuration of substituted ferrocenes is not always straightforward. For example, the reaction of 1,1′-dimethylferrocene with excess $Hg(OAc)_2$ followed by treatment of the reaction products with $CuCl_2$ affords a mixture of the octa-, hepta-, and hexachlorinated dimethylferrocene derivatives in a 22 : 74 : 4 ratio (Scheme 10).[112] The low solubility of the polymercurated derivatives is most likely responsible for the difficulties associated with permercuration.

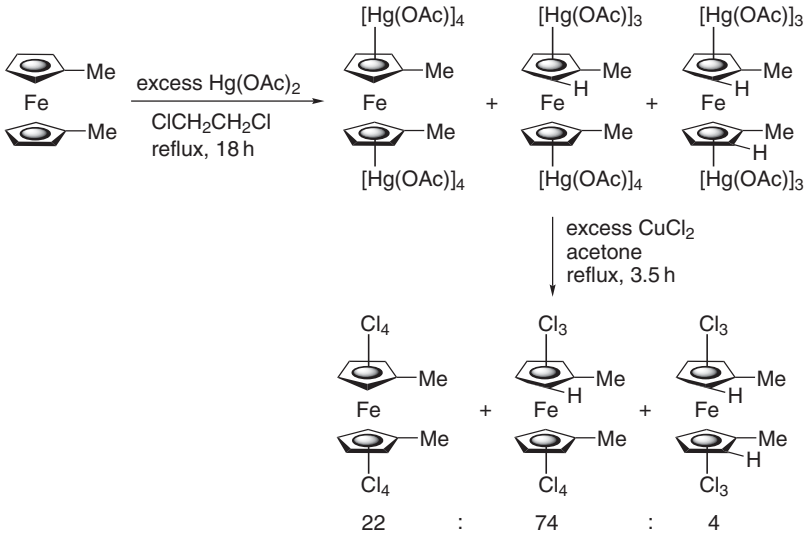

Scheme 10

Polymercuration of (cyclobutadiene)cyclopentadienylcobalt complexes has also been reported. Upon reaction with $Hg(OAc)_2$, complexes **88a–c** afford a mixture of products containing one to five mercury atoms. Higher yields of the pentamercurials **89a–c** were obtained when $Hg(OCOCF_3)_2$ was employed (Equation (34)).[113]

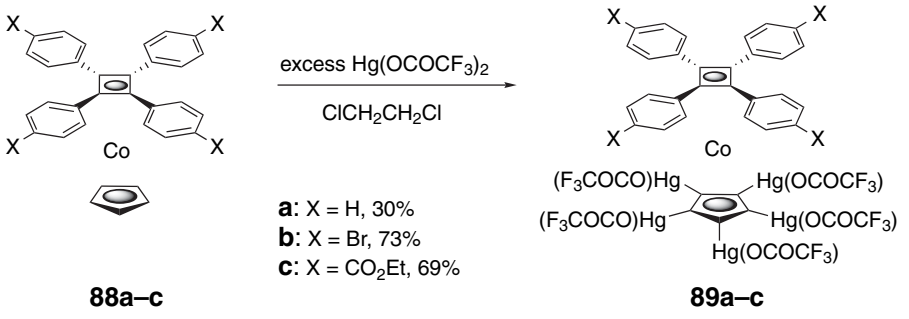

88a–c **89a–c** (34)

2.07.1.2.5 Solvomercuration of alkenes

2.07.1.2.5.(i) Intermolecular solvomercuration of alkenes

The solvomercuration of alkenes has been exhaustively studied and is now well understood. The mechanism of this reaction proceeds through two steps: coordination of the mercuric ion to the alkene to form a fluxional cationic intermediate and subsequent nucleophilic *anti*-attack. Charge stabilization of the cationic intermediate constitutes one of the factors dictating the regioselectivity of the reaction (Scheme 11).

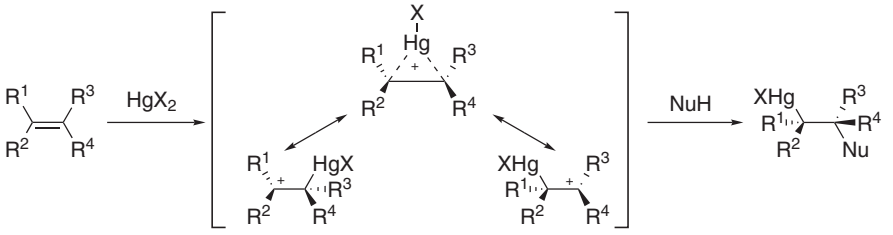

Scheme 11

For asymmetric alkenes such as **90**, the diastereoselectivity of the initial mercuration directs the stereochemistry in the final product. The presence of a coordinating ether group in **90** increases the selectivity as illustrated in Equation (35).[114] The coordination of the mercury by the oxygen of the OTBDPS functionality tends to favor the *syn*-diastereomer **91** over the *anti*-diastereomer **92**.[115]

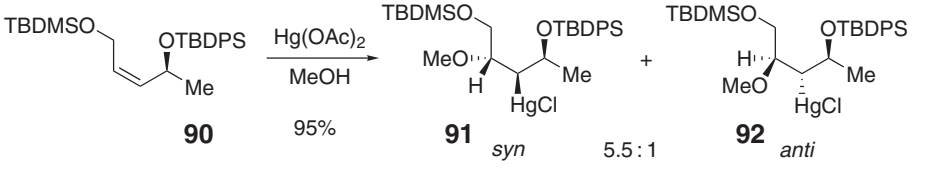

90 **91** *syn* **92** *anti* (35)

Unlike the oxymercuration of acyclic olefins, oxymercuration of bicyclic olefins often gives *syn*-addition products. Norbornenes **93**, for example, show exclusive *exo*-oxymercuration. In this reaction, the ratio between the isomers depends on the nature of the *exo*-substituent (R^1) and *endo*-substituent (R^2) (Equation (36)). The presence of electron-withdrawing *exo*-substituents always leads to a much greater selectivity in favor of **94a–d** over **95a–d**.[116,117] As indicated by extensive theoretical calculations, the charge distribution in the transition states governs the selectivity of these reactions.[118]

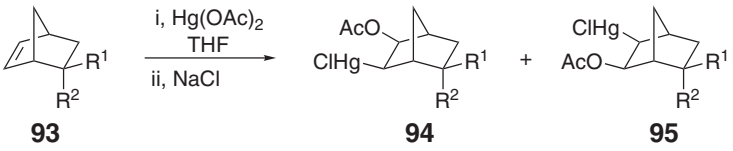

93 **94** **95**

(36)

Entry	R^1	R^2	*Yields* (%)	*Ratio* **94** : **95**
a	OTBS	H	83	12 : 1
b	H	OTBS	69	4 : 1
c	OBn	H	58	9 : 1
d	H	OBn	36	6 : 1

2.07.1.2.5.(ii) Intramolecular solvomercuration of alkenes

For intramolecular solvomercuration reactions, the regioselectivity is usually affected by the size of the resulting cycle, with the formation of a five-membered ring (as in **96**) being favored over formation of a six-membered ring (as in **97**; Scheme 12). Additionally, stabilization of the carbocationic intermediate will also influence the regioselectivity of the subsequent nucleophilic attack. In some cases, both factors oppose one another to form a mixture of products. This is, for example, the case in the oxymercuration of *para*-substituted styrenes **98a** and **98b** which give rise to mixtures of the 6-*endo* and 5-*exo* attack products **99a** and **99b**, and **100a** and **100b**. In the case of **98c**, the presence of an electron-donating *para*-methoxy group greatly stabilizes the formation of a carbocation α from the phenyl group leading to the exclusive formation of **100c** (Scheme 13).[119]

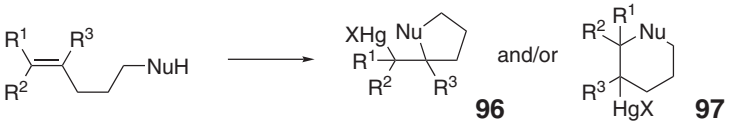

96 **97**

Scheme 12

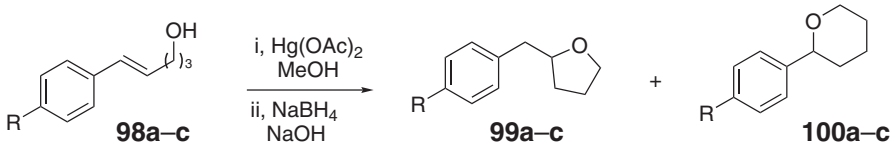

98a–c **99a–c** **100a–c**

a	H	52	48
b	Me	47	53
c	MeO	~	100

Scheme 13

The high selectivity of these reactions has been employed in the synthesis of highly substituted products,[120–124] such as **101** (Equation (37)).[125,126] The diastereoselectivity of the reaction leading to **101** originates from the chelation-controlled approach of the mercury(II) cations as well as from conformational constraints about the central six-membered ring. Homochiral auxiliary ligands can also be used to control the enantioselectivity of this type of reactions. For example, the bisoxazoline ligand **102** gives good ee in the intramolecular solvomercuration reaction leading to **103** (Equation (38)).[127]

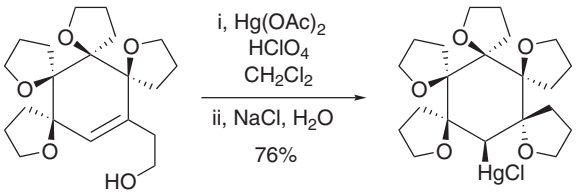

101 (37)

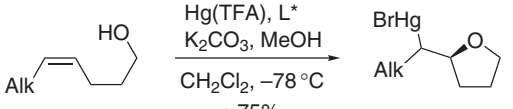

103
>86% ee (38)

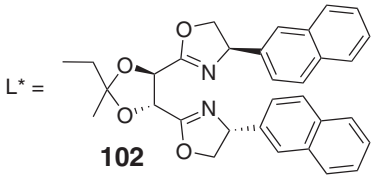

102

In another variant of such reactions, the hemi-acetal **104**, generated *in situ* by reaction of the corresponding allylic alcohol with acetaldehyde, undergoes cyclization in the presence of HgClOAc to afford the mercurated acetal **105**.[128] Under these conditions, the reaction leads to the *syn*-product with a high selectivity (dr > 10 : 1; Scheme 14). The same strategy has been applied iteratively for the stereoselective synthesis of natural products containing 1,3,5,7,9-pentaether chains.[129]

Ring-closing reactions promoted by mercuric salts are valuable transformations which find an increasing use in the total synthesis of various natural products.[130–140] Several examples of solvomercurations demonstrating the applicability of these transformations to the synthesis of natural product precursors are presented in Table 2. Piperidines (entry a), [141] pyrans (entries b–d), [142–144] and furans (entries e, f)[145,146] have been obtained in good yields and diastereoselectivity. These derivatives serve as starting materials for various natural products and can be demercurated under reducing conditions.[147]

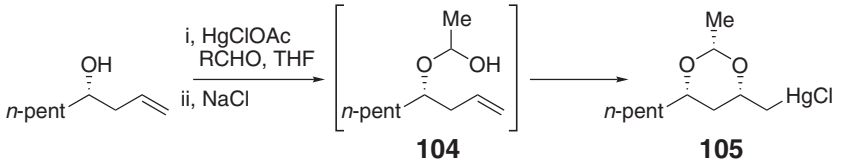

104 **105**

Scheme 14

2.07.1.2.6 Solvomercuration of alkynes

2.07.1.2.6.(i) Intermolecular solvomercuration of alkynes

A series of studies assessing substituent effects on the acetoxymercuration of diarylethynes have been reported.[148] With substrates such as **106a–d**,[149,150] acetoxymercuration yields **107a–d** and **108a–d** as mixtures of regioisomers (Equation (39)). Electrophilic attack of the alkyne by the mercuric ion is the rate-determining step. Accordingly, in the presence of electron-donating substituents, the reaction rates typically increase.

Table 2 Selected examples of intramolecular solvomercuration of alkenes

Entry	*Starting material*	*Reagent*	*Product*	*References*
a	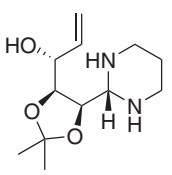	$Hg(OAc)_2$, CH_3CN, 88%	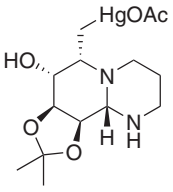	141
b	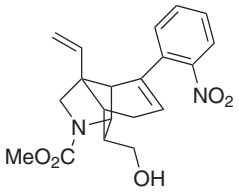	i, $Hg(OAc)_2$, CH_2Cl_2; ii, NaCl, 43%	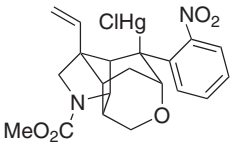	142
c	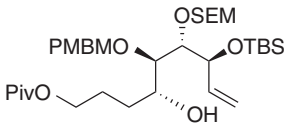	i, $Hg(OAc)_2$, THF; ii, KCl, 96%	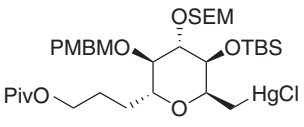	144
d	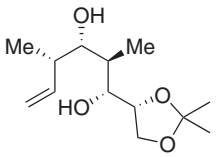	i, $Hg(OAc)_2$, C_6D_6; ii, brine, 87%	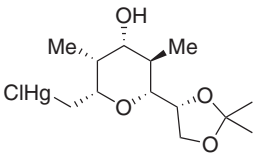	145
e	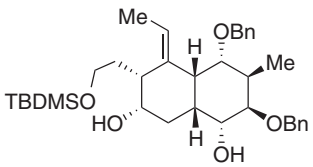	i, $Hg(OTf)_2$, HgO, THF; ii, NaCl, 44%	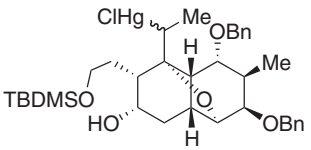	146
f	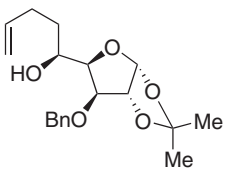	$HgCl_2$, H_2O, 90%	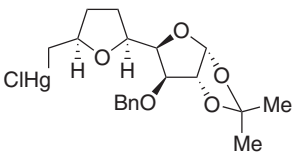	147

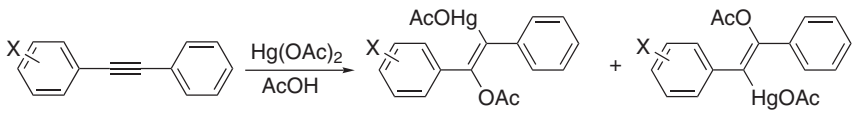

106a–d	**X**	**107a–d**	**108a–d**
a	4-OMe	100%	~
b	3-OMe	50%	50%
c	4-Cl	14%	86%
d	4-NO2	~	100%

(39)

In most cases, it has been proposed that the cationic intermediate resulting from electrophilic attack by the mercuric ion is, in fact, a mercurinium species **109** in which the mercury cation is unsymmetrically coordinated to the two alkynyl carbon atoms. Hence, these reactions typically afford Markovnikov products. In the presence of excess $Hg(OAc)_2$, nucleophilic attack of the mercurinium intermediate is intermolecular and occurs in an *anti*-fashion leading to the (*E*)-isomer. When no excess of $Hg(OAc)_2$ is present, nucleophilic attack of the mercurinium intermediate is intramolecular and occurs in a *syn*-fashion leading to the (*Z*)-isomer.[151]

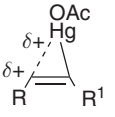

109

As illustrated by the conversion of **110** to **111** (Equation (40)), the acetoxymercuration of aryltrimethylsilylalkynes proceeds through addition of the mercury moiety α from the silicon atom.[152] The regioselectivity of this reaction, which is not influenced by the nitrophenyl substituent, can be rationalized by invoking an unsymmetrical mercurinium species with a great deal of positive charge at the silicon–β-carbon atom stabilized by the $SiMe_3$ group. For aryl(hydroxmethyl)ethynes[151,153] such as **112**, the Lewis-basic hydroxyl group directs the mercury to the alkynyl carbon atom bound to the hydroxymethyl functionality leading to **113** (Equation (41)).

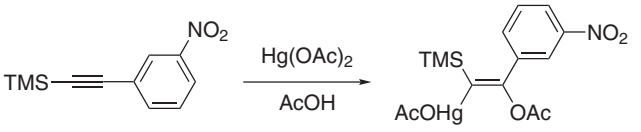

110 **111** (40)

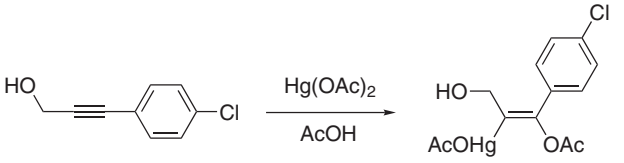

112 **113** (41)

2.07.1.2.6.(ii) Intramolecular solvomercuration of alkynes

When the alkynyl substrate possesses a nucleophilic functionality, intramolecular solvomercuration reactions can sometimes be observed. These reactions, which result in the formation of a heterocycle, have been used in the total synthesis of natural products. For example, reaction of **114** with $Hg(OAc)_2$ affords the benzofuran derivative **115**, which is an important intermediate for the synthesis of various neolignans (Equation (42)).[154,155]

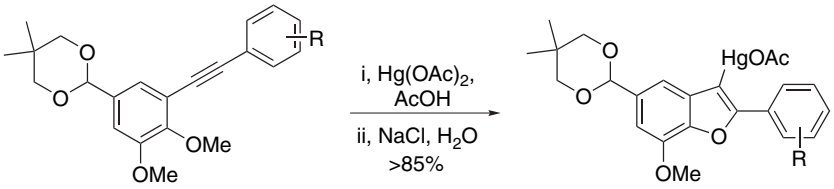

114 **115** (42)

In another example, $Hg(OTf)_2$ has been used for the stereoselective ring expansion of **116** to **117** with excellent stereospecificity for the (*Z*)-isomer (Equation (43)).[156] Carbomercuration reactions have also been observed for derivatives such as **118**, which possesses both an allylic silane as well as an alkynyl functionality. For **118**, the reaction affords the 5-*exo*-ring compound **119** as the (*Z*)-isomer. Formation of the (*E*)-isomer is disfavored because the bulk of the TMS group precludes an *anti*-attack (Equation (44)).[157]

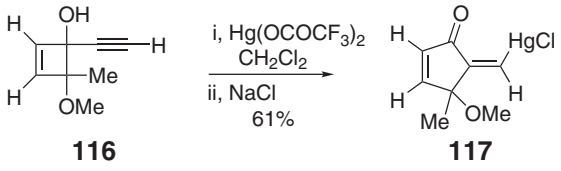

(43)

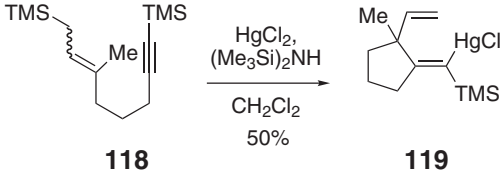

(44)

2.07.1.2.7 Ring-opening solvomercuration of cyclopropanes

The ring opening of cyclopropanes promoted by mercury salts has been used extensively in total synthesis. The initial approach of the mercury to the less-hindered carbon atom of the cyclopropane ring and the stabilization of the positive charge are the key factors governing the regio- and stereoselectivity of these reactions. These characteristics are observed in the reactions of **120**[158–161] with $Hg(OAc)_2$, $Hg(OCOCF_3)_2$, or $Hg(NO_3)_2$ (Scheme 15). The rate of the reaction increases as the electrophilicity of the reagent increases, with the nitrate salt reacting the fastest. When $Hg(OAc)_2$ or $Hg(OCOCF_3)_2$ are employed, the intermediate formed by coordination of the mercury to the methylene group of the cyclopropane ring undergoes nucleophilic attack by a methanol molecule to afford the *syn*/*anti*-products **121**. When $Hg(NO_3)_2$ is used, the nitrate anion acts as the nucleophile leading to the formation of **122**.

The stability of the cationic intermediate formed in these reactions often dictates the regioselectivity. A recent example illustrating this principle is shown in Scheme 16.[162] The high stereoselectivity observed in the conversion of **123** to **124** suggests a concerted mechanism in which the cleavage of the cyclopropane C–C bond is synchronous with the nucleophilic attack (Scheme 16). By contrast, the bis(cyclopropane) derivative **125** undergoes solvomercuration to afford **126** with a low diastereomeric excess (9% de). The cationic center resulting from the addition of the mercury fragment is stabilized by the neighboring α-cyclopropane ring. This excessive stabilization results in a loss of selectivity of the ensuing nucleophilic addition leading to a mixture of both epimers.

The alkoxycyclopropane–methylsilane **127** reacts with $Hg(NO_3)_2$ to afford the allylic mercury derivative **128** (path A, Scheme 17). The ability of the silyl group to promote positive charge development at the β-carbon atom is responsible for this regioselectivity. This effect can be largely countered by the introduction of phenyl groups as in **129**. The electron-donating properties of these substituents favor positive charge development at the γ-carbon atom, leading to formation of the substituted furan derivative **130** (path B).[163,164]

Internal cyclopropane ring-opening reactions have also been developed using hydroxyl-substituted cyclopropanes. A typical example of this strategy comes from the reaction of the polycylic alcohol **131**, which reacts quantitatively with $Hg(OAc)_2$ to yield the acetal **132** (Equation (45)).[165] Carbonate moieties can also be used as internal nucleophiles as, for example, in the case of **133**, which affords **134** in a 60% yield upon reaction with $Hg(OCOCF_3)$ (Equation (46)).[166]

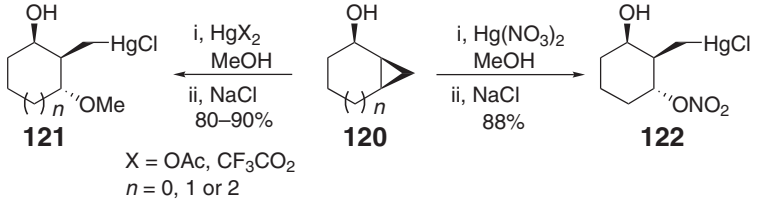

Scheme 15

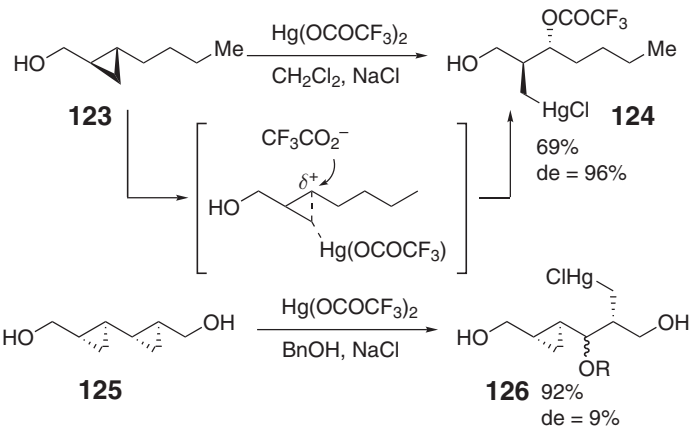

Scheme 16

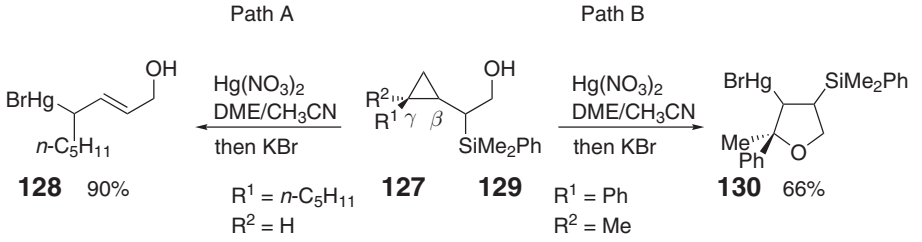

Scheme 17

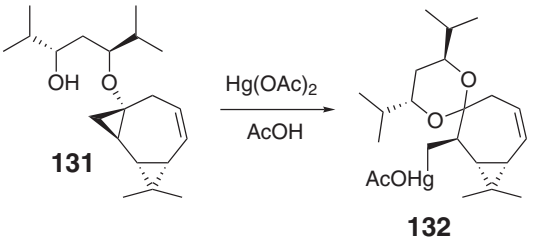

(45)

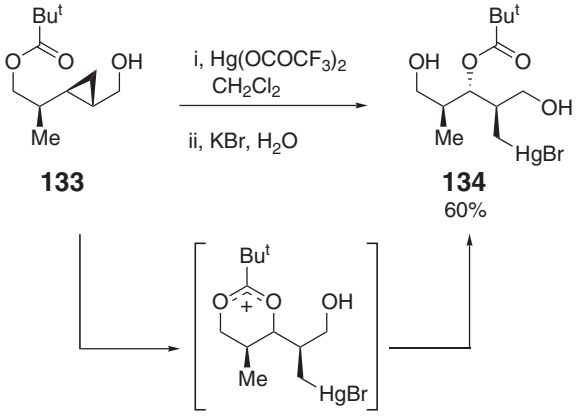

(46)

These intramolecular reactions can be carried out under mild conditions and are typically very selective. These characteristics make them ideally suited in the synthesis of natural products such as zincophorin (Equation (47)).[167] In this synthesis, a key step is the intramolecular hydroxymercuration of **135** which results in the formation of the pyran moiety of **136** with good selectivity (85% yield, 86% de).

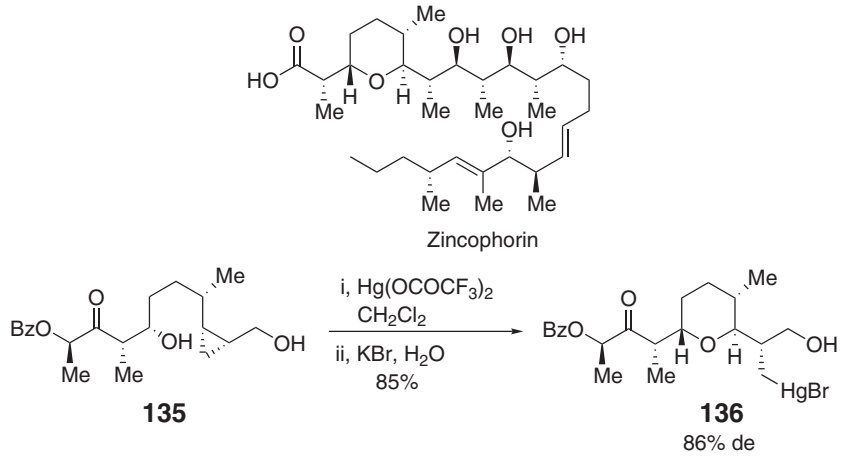

(47)

2.07.1.3 Important Transformations Involving Organomercury Derivatives

2.07.1.3.1 C–H activation

Complexes of general formula $[Hg(\eta^2\text{-arene})_2\text{-}(MCl_4)_2]$ (M = Al or Ga), which have been recently synthesized, promote fast hydrogen/deuterium (H/D) exchange in a variety of aromatic substrates.[168,169] For example, the bis(toluene) adduct $[Hg(\eta^2\text{-toluene})_2\text{-}(GaCl_4)_2]$ promotes the H/D exchange reaction of naphthalene with C_6D_6 (Equation (48)).[170] In the early stages of the reaction, rapid arene exchange occurs leading to the formation of $[Hg(naphthalene)_2\text{-}(GaCl_4)_2]$ as the dominant species. Kinetic studies suggest that this bis(naphthalene) complex acts as a strong Brönsted acid which protonates C_6D_6. Recombination of the resulting $[C_6D_6H]^+$ with the naphthylmercury species allows for the H/D exchange reaction to occur. This type of reaction has also been applied to the H/D exchange reaction of C_6D_6 with C_6H_5Et, *ortho*-$C_6H_4Me_2$, and 1,2,3-$C_6H_3Me_3$.[171]

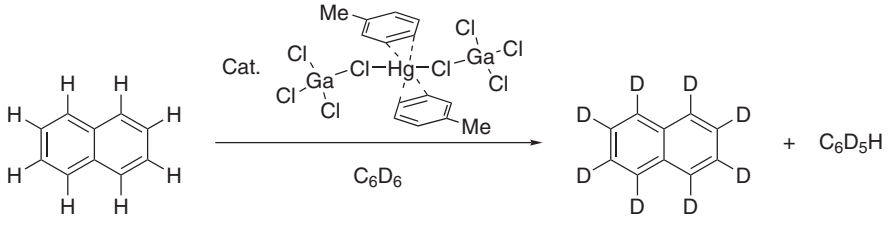

(48)

In 1993, Periana reported a method for the catalytic oxidation of methane. This reaction, which is catalyzed by Hg^{2+} ions in concentrated H_2SO_4, affords CH_3OSO_3H, water, and SO_2 according to the catalytic cycle presented in Scheme 18.[172] The key step of this catalytic reaction is an electrophilic substitution reaction in which the $[Hg(OSO_3H)]^+$ ion reacts with methane to displace a proton and to form CH_3HgOSO_3H. Recent computational work carried out on the activation of methane by the model cation $[HgF]^+$ suggests the formation of a methane complex ($[HgF]^+$–CH_4, Figure 1) where the two components are held together by ion-induced dipole interactions as well as a donor–acceptor interaction involving the C–H σ-bonds of methane and the electron-deficient mercury center.[173] The binding energy of this complex was calculated to be $-23.3\,kcal\,mol^{-1}$, indicating that these interactions are substantial.

2.07.1.3.2 Synthesis of organometallic derivatives

2.07.1.3.2.(i) Ligand-exchange reactions

Owing to the thermodynamic weakness of the Hg–C bond, organomercurials can serve to transfer organic ligands to both main group and transition metal centers. Such reactions have recently been used for the preparation of

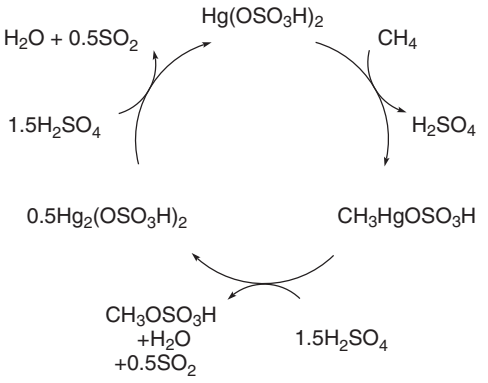

Scheme 18

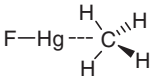

Figure 1 Representation of the calculated structure of $[HgF]^{+}$–CH_4.

polyfunctional boranes. For example, the fluorinated trimercury derivative **137** reacts with BBr_3 to afford **138** (Equation (49)).[174] In a similar fashion, the 1,1′-bis(chloromercurio)ferrocene **139** reacts with $(C_6F_5)_2BCl$ to yield **140** (Equation (50)).[175,176] The same strategy has been applied to the synthesis of aluminum derivatives such as **141** (Equation (51)).[85]

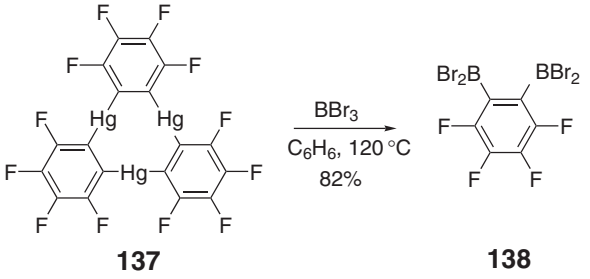

(49)

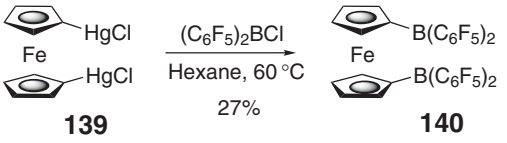

(50)

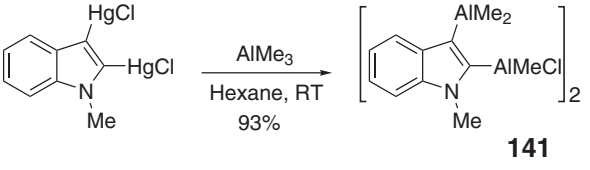

(51)

Other remarkable examples showcasing the synthetic potential of this approach concern the preparation of decamagnesiated and decazincated ferrocene derivatives from the corresponding decakis(chloromercurio)ferrocene complex **142** (Scheme 19).[177,178]

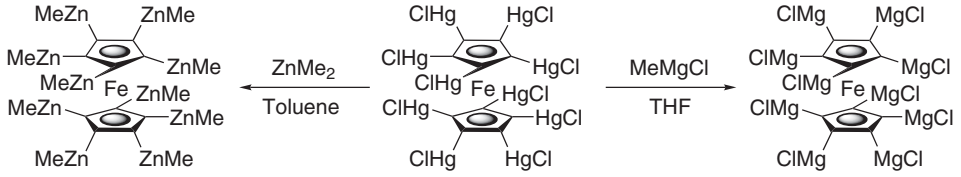

142

Scheme 19

Arylmercury compounds are also often used as starting materials for the synthesis of palladium(II) complexes. These reactions, whose reagents and products are compiled in Table 3, typically involve the use of chloromercurio derivatives with palladium chloride complexes (entries a–d). [93,95,179–181] Similar procedures have been applied to the synthesis of ruthenium(II) and gold(III) complexes (entries e and f).[181,182]

2.07.1.3.2.(ii) Transmetallation reactions

The transmetallation reaction of organomercurials with metallic or low-valent main group compounds provides a convenient entry into the chemistry of various organo-main-group derivatives.[14] Typically, such reactions proceed smoothly and yield mercury metal as a sole byproduct, which greatly facilitates the isolation of the products. This synthetic methodology has been recently applied to the synthesis of *ortho*-phenylene zinc which could be obtained from trimeric *ortho*-phenylene mercury **143** and elemental zinc in THF (Equation (52)). In solution, this zinc derivative exists as a trimer but crystallizes as a dimer **144** with two molecules of THF coordinated to each zinc center.[183] In a similar way, the 1-mercuraindane **20** reacts with elemental magnesium to afford 1-magnesaindane **145**, which is dimeric in THF at room temperature (Equation (53)).[42] Thiomethylmagnesium derivatives such as $Mg(CH_2SMe)Cl$ have also been prepared from elemental magnesium and the corresponding bis(thiomethyl)mercury complex.[184]

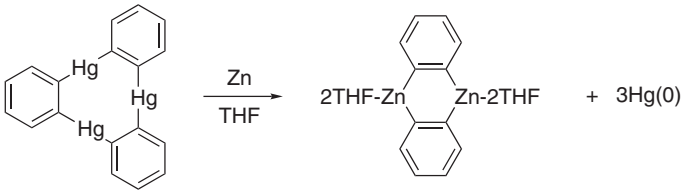

143 **144** (52)

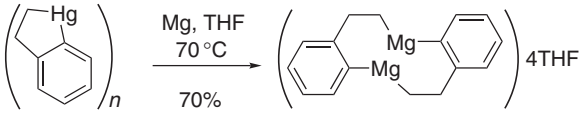

20 **145** (53)

Analogous approaches have been used for the synthesis of dinuclear indium complexes. The transmetallation reactions of compounds **5** and **6** with 2 equiv. of InBr in THF yield 1,4-butanediyl- **146**, and 1,6-hexanediylbis[bis(THF)indiumdibromide] **147**, respectively, which have been isolated in moderate yields (Equation (54)).[28] Similarly, α,α'-*meta*-xylenediylbis(mercurychloride) **14** reacts cleanly with InCl to afford α,α'-*meta*-xylenediylbis(indiumdichloride) as a tetrakis(THF) adduct (**148**; Equation (55)). This type of reaction has also been shown to occur with *ortho*-phenylene mercury complexes. For example, trimeric *ortho*-phenylene mercury **143** and its fluorinated analog **137** react with InBr to afford the corresponding 9,10-dihydro-9,10-diindaanthracene derivatives **149** and **150** (Scheme 20).[185,186] More complex reactions have been observed when InCl is used instead of InBr. In this case, the reaction affords a heteronuclear trifunctional complex that contains one mercury and two indium atoms (**151**; Scheme 20).[187] An incomplete transmetallation has also been observed in the reaction of 1,8-bis(bromomercurio)naphthalene with InBr, which affords the mercuraindacycle **152** in which the mercury and indium centers are only separated by about 3 Å (Equation (56)).[188] Comparable transmetallation reactions have also been used for the synthesis of aryllanthanide derivatives.[10]

Table 3 Transmetallation reactions involving aromatic organomercury derivatives as starting materials

Entry	*Organomercury starting material*	*Reagents and conditions*	*Product*	*Yield (%)*	*References*
a	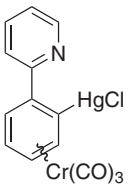	i, $PdCl_2(MeCN)_2$ Acetone −20 °C ii, Pyridine	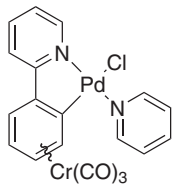	58	95
b	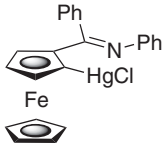	Li_2PdCl_4 CH_2Cl_2/MeOH	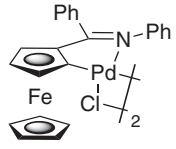	75	179
c	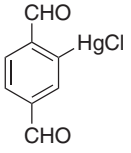	$Pd_2Cl_2(PPH_3)_2$ $[Me_4N]Cl$ Acetone Reflux	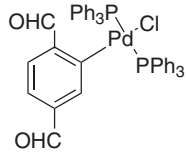	64	93
d	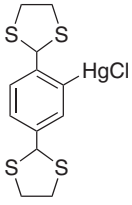	$PdCl_2(PPh_3)_2$ $[Me_4N]Cl$ Acetone/dioxane 0 % °C	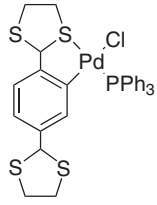	64	180
e	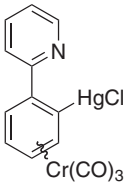	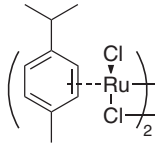 Acetone 0 °C	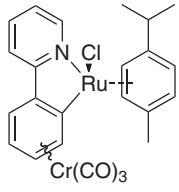	70	181
f	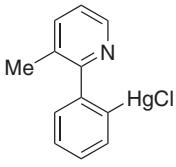	$Na[AuCl_4]\cdot 2H_2O$ MeCN	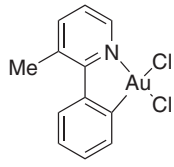	60	182

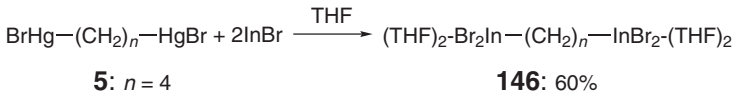

5: $n = 4$
6: $n = 6$

146: 60%
147: 46%

(54)

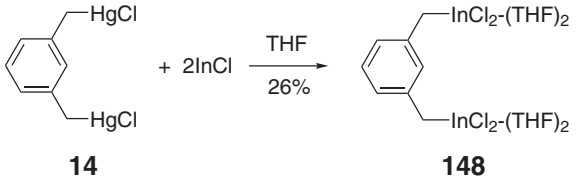

14 **148** (55)

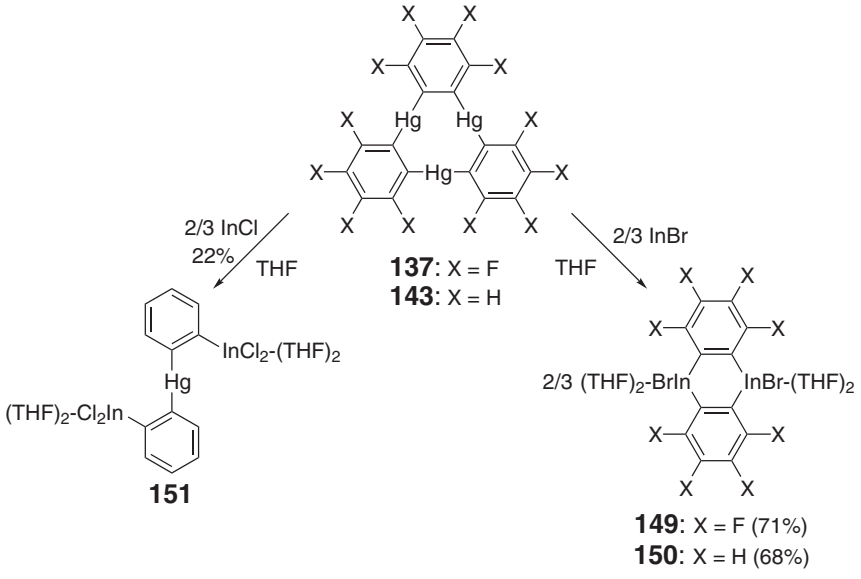

Scheme 20

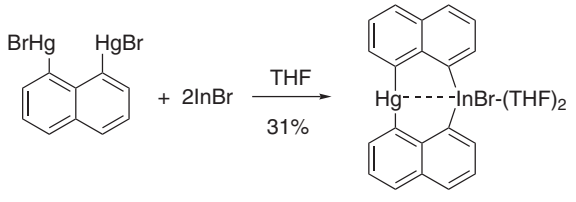

152 (56)

2.07.1.4 Structures of Organomercury Compounds

2.07.1.4.1 Mercury carbene and carbonyl complexes

Extensive characterization of the first two thermally stable mercury carbonyls has been performed. Compounds $[Hg(CO)_2][Sb_2F_{11}]_2$ and $[Hg_2(CO)_2][Sb_2F_{11}]_2$ have been analyzed by ^{13}C MAS-NMR, Raman, and IR spectra, and, in the case of $[Hg(CO)_2][Sb_2F_{11}]_2$, X-ray crystallography (Figure 2).[189,190] The dication $[Hg(CO)_2]^{2+}$ is linear, and the mercury center engages in secondary interactions with fluorine atoms of the $[Sb_2F_{11}]^-$ counteranions. The mercury carbonyl Hg–C bond of 2.08 Å has mostly σ-character, as confirmed by the high ν_{CO} of 2279.5 and 2247.5 cm^{-1} for the $[Hg(CO)_2][Sb_2F_{11}]_2$ and $[Hg_2(CO)_2][Sb_2F_{11}]_2$, respectively. This conclusion is in agreement with recent theoretical work.[191]

Linear coordination complexes are also observed with carbenes rather than carbonyl ligands. However, recent structural work carried out on bis(carbene) complexes indicates that coordination of the counteranion can lead to significant deviation of the $C_{carbene}$–Hg–$C_{carbene}$ angle from linearity. In **70**, for example, the two chloride anions are

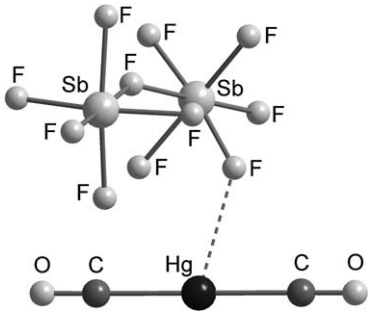

Figure 2 Structure of $[Hg(CO)_2]^{2+}$ with one of the $[Sb_2F_{11}]^-$ counteranions.

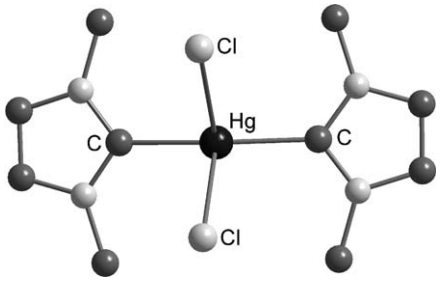

Figure 3 Structure of **70**. Hydrogen atoms omitted for clarity.

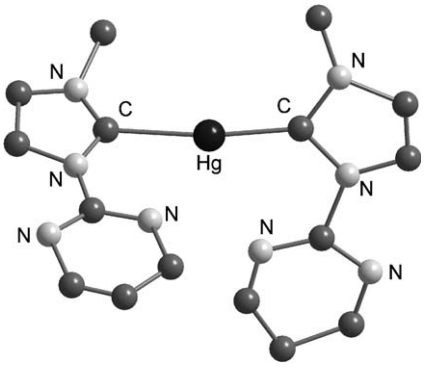

Figure 4 Structure of **153**. Hydrogen atoms omitted for clarity.

bound to the mercury centers via Hg–Cl bonds of 2.83 Å, which results in a bending of the $C_{carbene}$–Hg–$C_{carbene}$ angle (161.4°; Figure 3).[77] A smaller distortion, induced by intramolecular secondary Hg–N interactions, is observed in the bis[1-methyl-3-pyrimidylimidazol-2-ylidene] mercury complex **153** ($C_{carbene}$–Hg–$C_{carbene}$ angle = 172°; Figure 4).[80]

2.07.1.4.2 Mercury π-complexes with alkene and alkyne ligands

The centrosymmetrical complex **154**, formed by interaction of the quinolyl ligand with $HgCl_2$, features intramolecular coordination of one of the cyclopentadiene C=C bonds to the mercury center. The resulting Hg–C(sp^2) distances of 2.81 and 2.88 Å are longer than typical Hg–C σ-bonds but remain much shorter than the sum of the van der Waals radii. This dihapto interaction does not result in a significant lengthening of the coordinated C=C

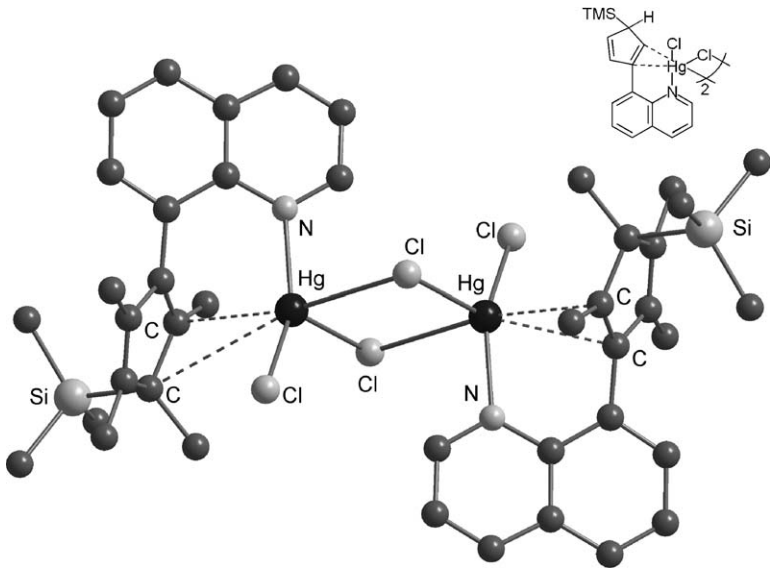

Figure 5 Structure of **154**. Hydrogen atoms omitted for clarity.

bond[192] (Figure 5). Shorter Hg–C distances are observed in the dicationic complex **155** formed by reaction of $HgBr_2$ with tmtaa(Ni). In this complex, the mercury interacts with the central carbon of the β-diiminate fragment to form an Hg–C bond of 2.256 Å (Figure 6).[193]

The reaction of tetraethynylplatinum derivatives with mercury dihalide in acetone affords complexes **156** and **157** in which the mercury centers are coordinated to two neighboring mercury alkynyl functionalities.[194,195] In turn, each alkynyl functionality interacts with the mercury center in an η^2-fashion. For complexes **156** and **157**, the resulting Hg–C_{sp} bonds, which range from 2.41 to 2.77 Å, are longer than typical Hg–C σ-bonds but shorter that those observed in **154**. In **156**, the greater flexibility of the structure allows for the formation of shorter Hg–C(sp) bonds than in **157** (av. Hg–C(sp) = 2.52 Å for **156** and 2.64 Å for **157**). The formation of such complexes is not limited to the case of

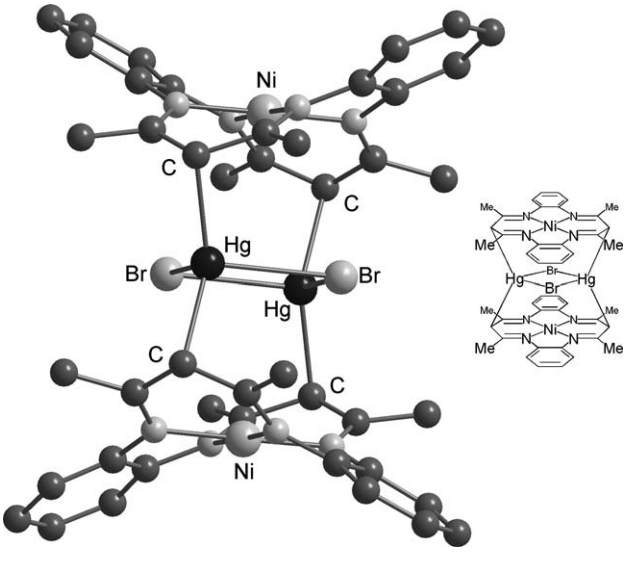

Figure 6 Structure of **155**. Hydrogen atoms omitted for clarity.

tetraethynylplatinum complexes and is also observed for $(\eta^5\text{-}C_5H_5SiMe_3)_2Ti(C{\equiv}CPh)_2$ which forms complex **158** upon reaction with $Hg(CN)_2$.[196] Weak intramolecular secondary Hg–C interactions exceeding 3.3 Å have been observed in the solid state of various mercury acetylides,[197] including $Hg(C{\equiv}CTMS)_2$ and $Hg(C{\equiv}CPh)_2$.[198]

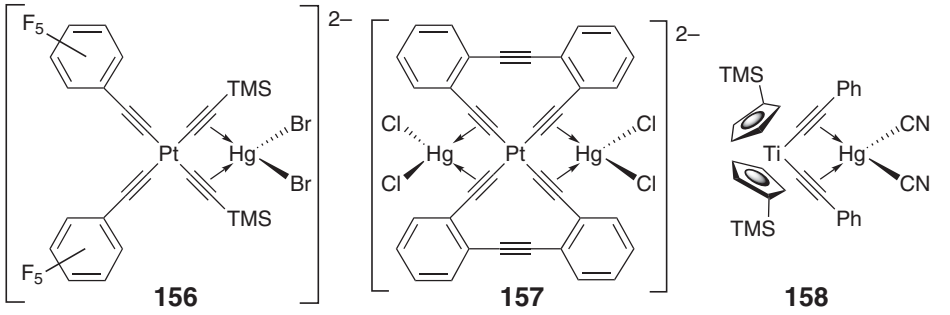

2.07.1.4.3 Mercury π-complexes with aromatic ligands

In a continuation of earlier studies on $[Hg_2(1,3,5\text{-}Me_3C_6H_3)_2]\text{-}(AlCl_4)_2$,[199] Kloo and co-workers have recently studied the $Hg_2Cl_2/GaCl_3$/benzene system using Raman spectroscopy and liquid X-ray scattering. Their data, complemented by DFT calculations, are in agreement with the existence of an $Hg_2(C_6H_6)_2^{2+}$ complex with the benzene ligand coordinated in an $\eta^1/quasi\text{-}\eta^3$-fashion along the Hg–Hg bond (Figure 7).[200]

In addition to $[Hg(\eta^2\text{-toluene})_2\text{-}(GaCl_4)_2]$,[168] other mercury–arene complexes of general formula $[Hg(\eta^2\text{-arene})_2\text{-}(AlCl_4)_2]$ have been prepared.[169] These include the bis(toluene), bis(*o*-xylene), and bis(1,2,3-trimethylbenzene) complexes **159**, **160**, and **161**, respectively, whose structures have all been determined (Figure 8). While the arene in **159** and **161** is coordinated in an asymmetrical η^2-fashion, the η^2-1,2,3-trimethylbenzene ligands of **160** form two nearly equal Hg–C bonds of 2.45 and 2.46 Å. DFT calculations show that the Hg–arene interactions are mostly ionic.

Longer Hg–π interactions are observed in the *para-t*-butylcalix[4]arene mercury complex **162**. The mercury atom forms primary bonds with the two sulfur atoms and engages in weaker secondary interactions with two arene rings of the calixarene whose centroids sit at 3.07–3.11 Å from the metal center.[201]

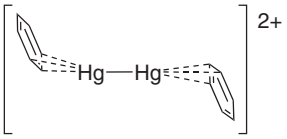

Figure 7 Representation of the calculated structure of $Hg_2(C_6H_6)_2^{2+}$.

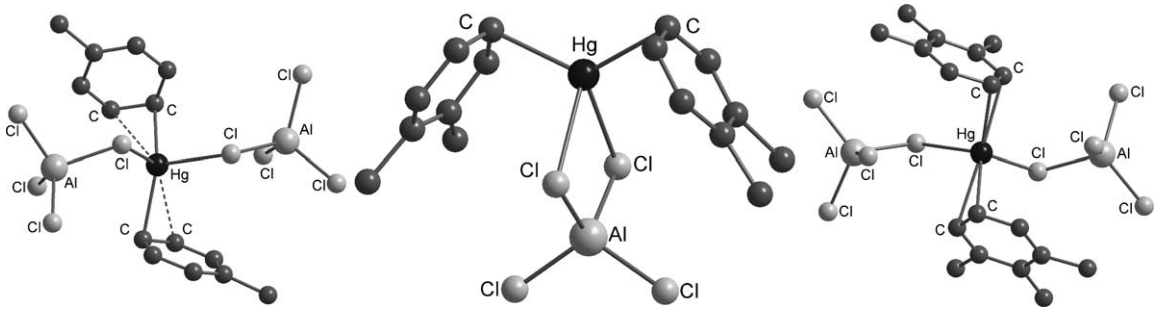

Figure 8 Molecular structure of **159** (left), **160** (middle), and **161** (right). Hydrogen atoms omitted for clarity.

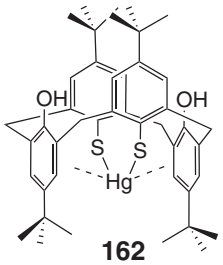

162

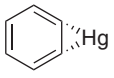

Figure 9 Representation of the calculated structure of the exciplex ^{3}[Hg(η^2-arene)].

In an effort to characterize the species formed in vapors containing mercury and arenes upon irradiation with UV light, the formation of exciplexes between excited mercury atoms and arenes has been investigated theoretically. For benzene, these investigations suggest the formation of an exciplex involving the Hg atom in the $^3P_1$ state and an η^2-bound molecule of benzene. This loose complex (^{3}[Hg(η^2-arene)] Figure 9) with estimated Hg–C bonds of 2.36 Å allows for transfer of the triplet excited state to the arene. In the case of alkyl-substituted benzenes, population of the triplet states triggers a number of subsequent reactions including C–C bond scissions.[202,203]

2.07.1.5 Organomercurials as Lewis Acids

2.07.1.5.1 Anion complexation

In the presence of electron-withdrawing substituents, organomercurials, which do not typically exhibit any significant Lewis-acidity, form adducts with a number of neutral and anionic Lewis-basic substrates. Bis(trifluoromethyl)-mercury **163** is a good example of such a Lewis-acidic organomercurial. It complexes fluoride, bromide, iodide, and thiocyanate to afford anionic complexes whose structures have been determined. The fluoride complex [(**163**–μ_2-F)$_2$]$^{2-}$ (Figure 10), formed by the reaction of TASF with **163**, adopts a dimeric structure, with the fluoride bridging the mercury atoms.[204] Dinuclear anionic complexes [(**163**–μ_2-X)$_2$]$^{2-}$ (X = Br, I, SCN) are also formed when **163** is allowed to react with [MePPh$_3$]Br, [MePPh$_3$]I, and [(18-C-6)-K][SCN].[205] In all cases, the bonds formed between the anions and the mercury centers are greater than typical covalent interactions but remain well within the sum of the van der Waals radii (Table 4). Anion binding to the mercury center also leads to a detectable deviation of the C–Hg–C angle from linearity (Table 4).

For bromide and iodide, the nature of the countercation influences the structure of the anionic complex. In fact, when the [(18-C-6)-K]Br and [(18-C-6)-K]I salts are used, the anionic complexes ([**163**–X]$^-$, X = Br, I) remain mononuclear and adopt a T-shaped structure (Figure 11). In both cases, the Hg–X bonds are shorter than those observed in the corresponding dinuclear complexes in agreement with the terminal location of the anion. The reaction of bis(pentafluoro)phenylmercury **164** with [(18-C-6)-K]Br and [(18-C-6)-K]I also afford T-shaped complexes [**164**–Br] and [**164**–I]. The Hg–Br (2.93 Å) and Hg–I (3.12 Å) bonds found in these complexes are longer than those observed in [**163**–Br]$^-$ and [**163**–I]$^-$ indicating that **164** is a weaker Lewis acid than **163**.[206]

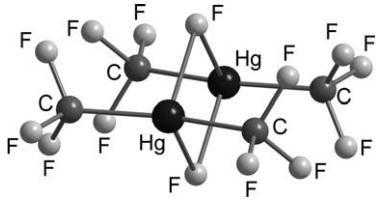

Figure 10 Structure of [**163**-μ_2-F]$_2^{2-}$.

Table 4 Important geometrical parameters in the structures of the halide complexes of **163** and **164**

Complex	*X*	*F*	*Br*	*I*	*SCN*
$[(\mathbf{163}\text{–}\mu_2\text{-X})_2]^{2-}$	Hg–X [Å]	2.39; 2.41	2.97; 3.00	3.17; 3.19	2.99; 3.01
	C–Hg–C [°]	162.1	164.6	162.8	166.1
$[\mathbf{163}\text{–X}]^-$	Hg–X [Å]		2.85	3.01	
	C–Hg–C [°]		165.0	161.4	

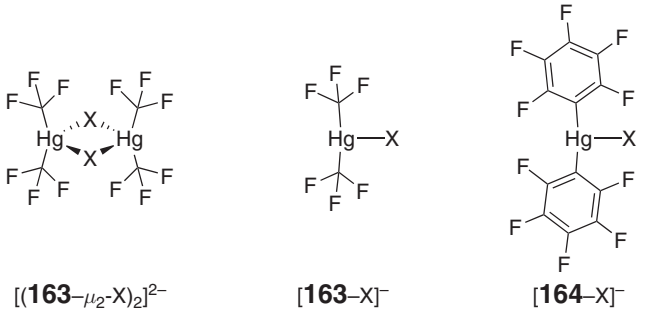

$[(\mathbf{163}\text{–}\mu_2\text{-X})_2]^{2-}$ $[\mathbf{163}\text{–X}]^-$ $[\mathbf{164}\text{–X}]^-$

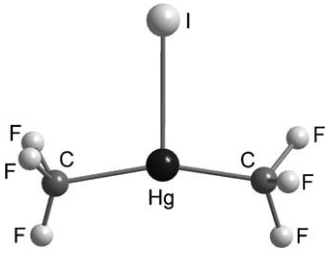

Figure 11 Structure of $[\mathbf{163}\text{–I}]^-$.

Electron-withdrawing substituents have also been used to enhance the Lewis acidity of polyfunctional organomercurials. Trimeric perfluoro-*ortho*-phenylene mercury **137** has been extensively studied as an anion acceptor. While $[\mathbf{137}\text{–Cl}]^-$, $[\mathbf{137}\text{–Br}]^-$, and $[\mathbf{137}\text{–I}]^-$ have been previously isolated,[207] recent ESI mass spectrometric studies suggest the gas-phase formation of stable 2 : 1 complexes ($[\mathbf{137}_2\text{–X}]^-$, X = F, Cl, Br, I), in which the halide is sandwiched by two molecules of **137**.[208] Related anionic sandwich complexes[209] have been obtained by reaction of $[B_{10}H_{10}]^{2-}$ or $[B_{12}H_{12}]^{2-}$ with **137**.[210] Structural characterization of $[\mathbf{137}_2\text{–}[B_{10}H_{10}]]^{2-}$ and $[\mathbf{137}_2\text{–}[B_{12}H_{12}]]^{2-}$ indicates the presence of multiple H–Hg bridges ranging from 2.5 to 2.8 Å. The hexacyanoferrate anion sandwich complex $[\mathbf{137}_2\text{–}[Fe(CN)_6]]^{3-}$ has also been isolated (Figure 12).[211] The cohesion of this sandwich results from multiple Hg–N interactions whose length (2.72–2.91 Å) is well within the sum of the van der Waals radii of mercury and nitrogen.

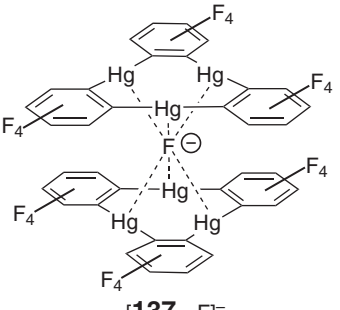

$[\mathbf{137}_2\text{–F}]^-$

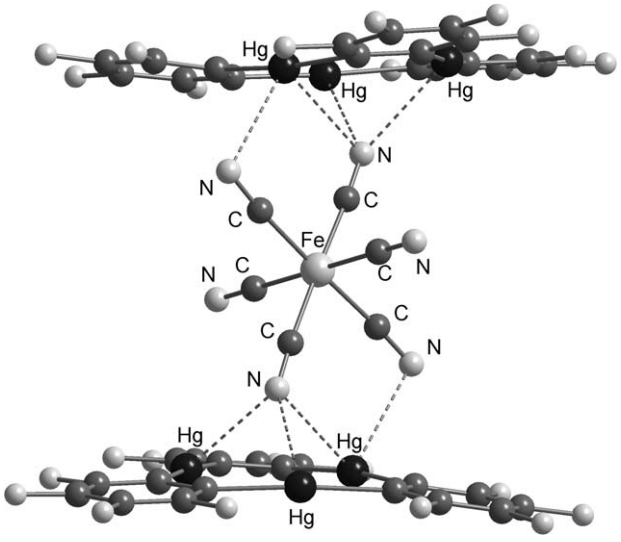

Figure 12 Structure of [**137**$_2$– $[Fe(CN)_6]]^{3-}$.

Reaction of **137** with $[NBu_4][SCN]$ leads to formation of the anionic complex [**137**–SCN]$^-$, which adopts a multi-decker structure with the anion sandwiched between successive molecules of **137** (Figure 13).[212] The sulfur atoms of the SCN^- ion in [**137**–SCN]$^-$ interacts unsymmetrically with the mercury atoms of the neighboring molecules of **137** forming four short Hg–S bonds that range from 3.06(1) to 3.36(1) Å and two long bonds of 3.74(1) and 3.87(1) Å. While the longer Hg–S bonds approach the limit for the involvement of dative interactions, the shorter ones are comparable to those observed in [**163**–SCN]$^-$.

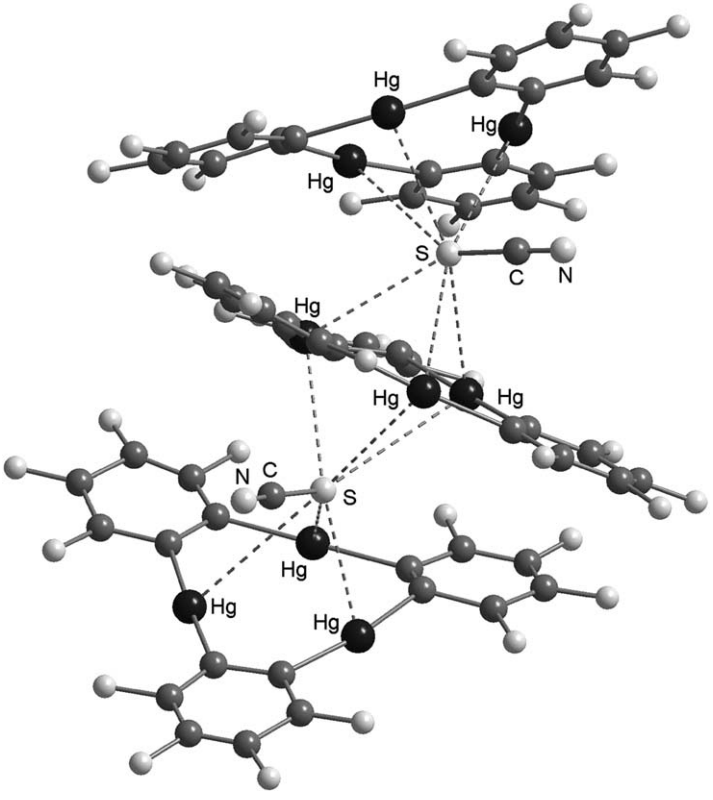

Figure 13 Portion of a stack in the structure of [**137**–SCN]$^-$.

Due to the electron-withdrawing properties of the carborane cage, the mercury centers of mercuracarborands have increased Lewis acidity, thereby making these species effective hosts for anions.[11,12] Recent studies indicate that trinuclear mercuracarborands such as **58** react with PPNCl, $MePPh_3Br$, and LiI to afford sandwich complexes ($[\mathbf{58}_2\text{–Cl}]^-$, $[\mathbf{58}_2\text{–Br}]^-$, and $[\mathbf{58}_2\text{–I}]^-$, respectively) in which the halide anion interacts with all neighboring mercury centers in an octahedral fashion (Figure 14).[213,214] The structures of these complexes have been determined by X-ray analysis and their existence in solution has been confirmed by ^{199}Hg NMR. In the solid, the Hg–X distances all exceed 3 Å (Hg–Cl = 3.15–3.18 Å, Hg–Br = 3.07–3.39, Hg–I = 3.25–3.27 Å). The formation of these complexes is proposed to arise from the overlap of the halide-filled *p*-orbitals with a set of empty 6*p*-orbitals from the mercury atoms.

Another remarkable example of a mercuracarborand halide adduct has been obtained by reaction of the octamethyl tetranuclear derivative **165** with $[NMe_4]F$. This reaction affords complex $[\mathbf{165}\text{–F}]^-$ in which the fluoride is coordinated to the four mercury centers in an approximate square-planar arrangement (Equation (57)). The Hg–F distances, which range from 2.56 to 2.65 Å, are slightly longer than those found in $[\mathbf{163}\text{–}\mu_2\text{-F}]^{2-}$. The ^{199}Hg NMR resonance of the complex indicates coupling to the fluorine atom with $^1J_{Hg-F} = 698$ Hz.[215]

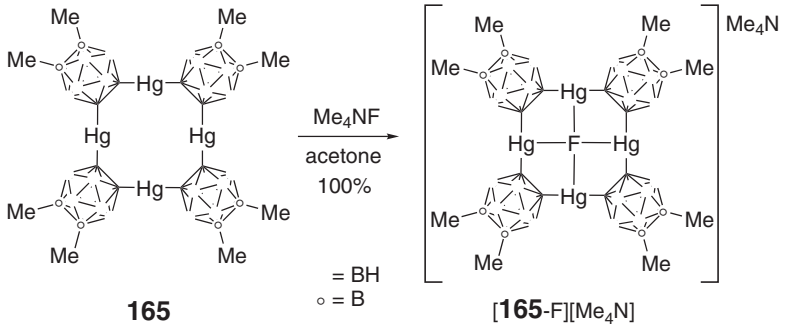

(57)

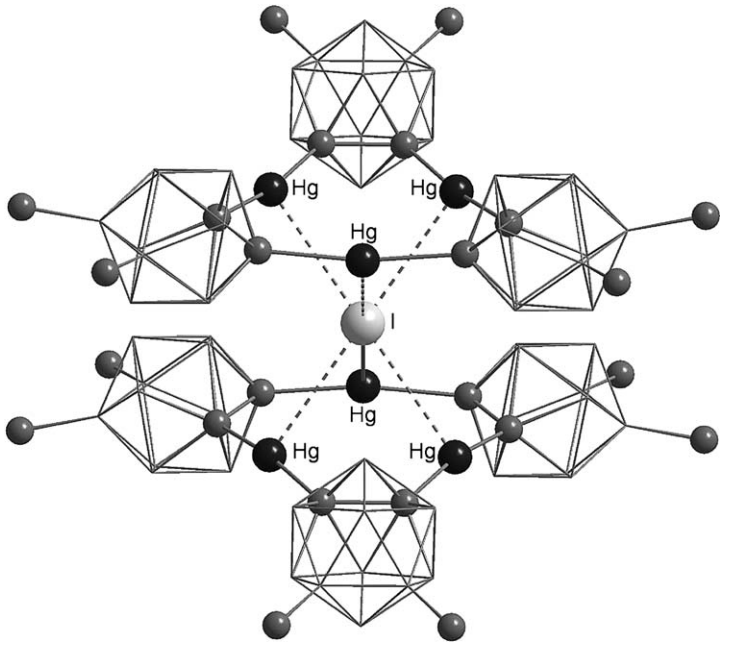

Figure 14 Structure of $[\mathbf{58}_2\text{–I}]^-$. Boron and hydrogen atoms omitted for clarity.

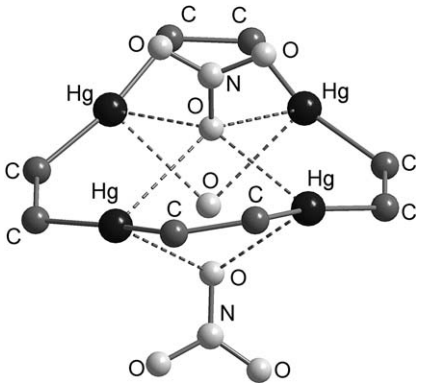

Figure 15 Structure of [**166**–$(NO_3)_2(H_2O)]^{2-}$. Carborane cages have been omitted for clarity.

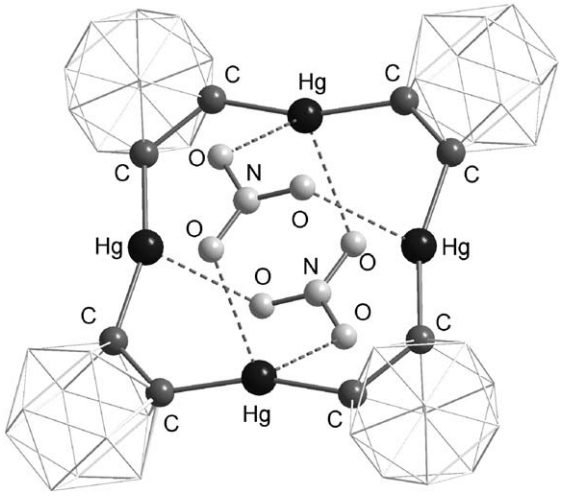

Figure 16 Structure of [**166**–$(NO_3)_2]^{2-}$. Boron and hydrogen atoms omitted for clarity.

The reaction of the tetranuclear mercuracarborand **166** with 2 or 3 equiv. of KNO_3/18-C-6 in acetone affords two different nitrate complexes namely [**166**–$(NO_3)_2(H_2O)]^{2-}$ and [**166**–$(NO_3)_2]^{2-}$ (Figures 15 and 16). In both cases, the nitrate anions are ligated to the mercury centers by Hg–O interactions ranging from 2.60 to 3.08 Å. In [**166**–$(NO_3)_2]^{2-}$, the two anions coordinate with all four mercury atoms in a face-on trihapto fashion from either side of the plane.[216]

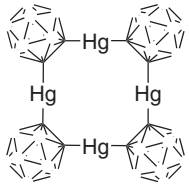

166 • = BH

2.07.1.5.2 Complexation of neutral derivatives

Polynuclear organomercurials featuring proximal mercury centers have often been considered as multidentate Lewis acids. This research area has witnessed some noteworthy developments which will be summarized in the following sections.

2.07.1.5.2.(i) *ortho*-Phenylene mercury complexes

With the multiple activation of organic substrates by polydentate Lewis acids as an ultimate goal, a number of studies have centered on the isolation of complexes in which the basic site of an organic guest molecule interacts simultaneously with the mercury centers of polynuclear organomercurials. For example, 1,2-bis(trifluoroacetatomercurio)-3,4,5,6-tetrahexylbenzene **167** complexes diethylformamide (DEF) in CH_2Cl_2 to form a 1 : 1 complex [**167**–DEF], which is significantly more stable than complexes formed between DEF and non-chelating mercury Lewis acids.[217] Crystallographic evidence for higher coordination numbers has been obtained in the case of the tetradentate dicationic Lewis acid **168** which crystallizes from DEF to form a [**168**–(μ_4-DEF)$_2$] (Figure 17).[218]

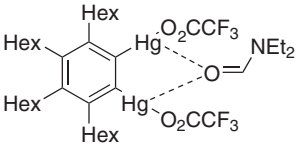

[**167**–DEF]

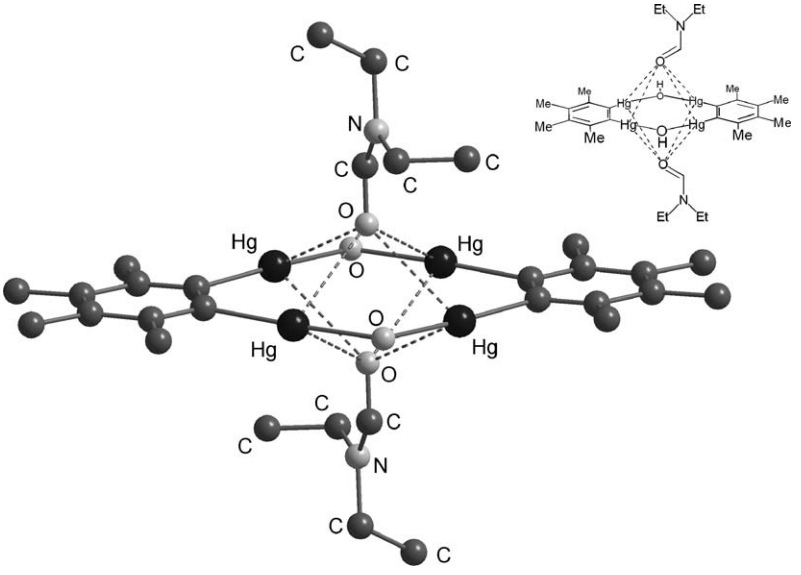

Figure 17 Structure of [**168**·(μ_4-DEF)]. Hydrogen atoms omitted for clarity.

As mentioned earlier, the use of electron-withdrawing backbones in polydentate organomercurials has received a great deal of attention. As a result, the coordination chemistry of a number of polynuclear organomercurials with fluorinated backbones has been investigated. 1,2-Bis(chloromercurio)tetrafluorobenzene (**169**) is a prototypical example of such fluorinated organomercurials. It interacts with a number of organic substrates including acetone, DMF, propylene oxide, THF, and acetonitrile.[219–221] The resulting complexes have 1 : 1 stoichiometry with the electron-rich heteroatom coordinated to both mercury centers (Table 5). The length of the bond formed between the mercury centers and the heteroatom is consistent with the presence of secondary interactions. For example, in [**169**-μ_2-acetone], the Hg–O bonds (2.679(13) and 2.776(14) Å) are shorter than the sum of the van der Waals radii of oxygen and mercury (3.2 Å) (Figure 18).[219] Aldehydes are too weakly basic to form chelate complexes with bidentate organomercurials. In fact, acetaldehyde does not form any adducts with **169**, and the complex [**169**–benzaldehyde] only shows terminal ligation of the carbonyl functionality to one of the mercury atoms.[221] Similar results have been obtained with 1,2-bis (cyanomercurio)tetrafluorobenzene.[222] Complexes of 2 : 1 stoichiometry have also been observed with dimethyl methylphosphonate[223] and DMSO[224] as substrates. In the latter case, molecules of [**169**-(μ_2-DMSO)$_2$] form a microporous structure in which the individual components are held by Hg–Cl and π–π interactions. This structure features large channels that are filled by solvate DMSO molecules. The formation of adducts also occurs with fluorinated monofunctional organomercurials such as chloromercurio–pentafluorobenzene (**170**), which complexes both DMF and DMSO (Figure 19).[225] The DMSO adduct has a T-shaped structure, with an Hg–O bond of 2.542(4) Å.

Table 5 Structures of the adducts formed by **169** with organic substrates

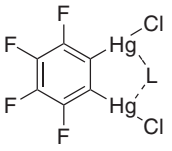

169.μ_2-L

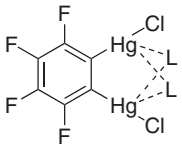

169.(μ_2-L)$_2$

L	*References*	*L*	*References*
	221	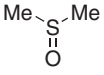	224
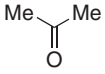	219	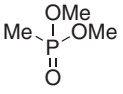	223
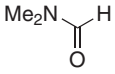	219		
	221		
	220		

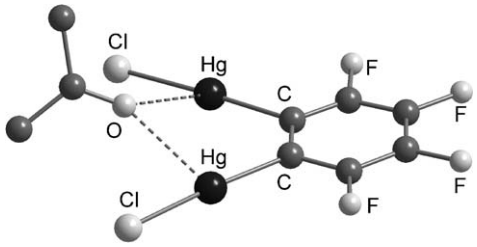

Figure 18 Structure of [**169**·μ_2-acetone]. Hydrogen atoms omitted for clarity.

Comparable results have been obtained with trimeric perfluoro-*ortho*-phenylene mercury **137**.[8,13,226] This derivative exhibits a rich coordination chemistry toward neutral electron-rich substrates, including organic carbonyls,[227,228] amides,[229–231] nitriles,[230,232] phosphoramides,[231] and sulfoxides,[231] with which it usually forms discrete [**137**–μ_3-L], [**137**–(μ_3-L)$_2$], and [**137**–(μ_3-L)$_2$(L)] complexes (Table 6). In all the complexes, the electron-rich terminus of the triply bridging ligands interacts with the three mercury atoms of **137** via secondary interactions. In the [**137**–(μ_3-L)$_2$] complexes, two molecules of the donor are coordinated to the mercury centers of **137** on either side of the molecular plane. A similar situation is encountered in [**137**–(μ_3-L)$_2$(L)] where an additional ligand is terminally ligated to one of the mercury centers. The [**137**–μ_3-acetone] and [**137**–(μ_3-acetonitrile)$_2$] are representative examples of [**137**–μ_3-L] and [**137**–(μ_3-L)$_2$] adducts, respectively.[228,232] The carbonyl oxygen atom of the acetone in [**137**–μ_3-acetone] is simultaneously bound to the three mercury centers of **137** (Figure 20).[228] The resulting Hg–O distances of 2.810(12)–2.983(12) Å indicate the presence of secondary interactions. Further inspection of the structure shows that the trinuclear mercury(II) complex [**137**–μ_3-acetone] forms co-facial dimers which are held by two mercuriophilic

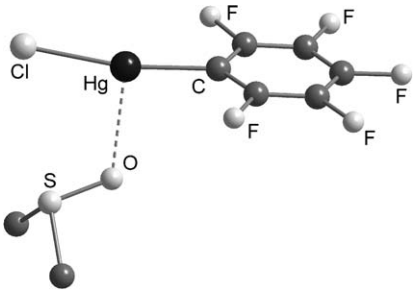

Figure 19 Structure of [**170**·DMSO]. Hydrogen atoms omitted for clarity.

Table 6 Structures of the adducts formed by **137** with organic substrates

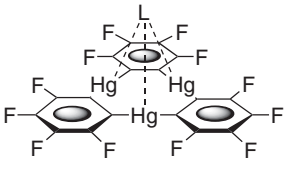

137.μ_3-L

L	*References*
Pr^n–C≡N	230
CH_2=C(H)–C≡N	232
Me–C(=O)–H	227
Me–C(=O)–Me	228
Ph–C(=O)–Ph	227

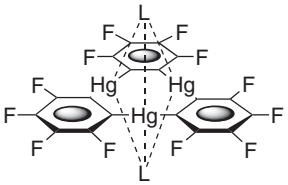

137.(μ_3-L)$_2$

L	*References*
Me–C≡N	232
Ph–C(=O)–Me	227
Me_2N–C(=O)–H	229,231
Me_2N–C(=O)–Me	230
$(Me_2N)_2P(=O)NMe_2$	231

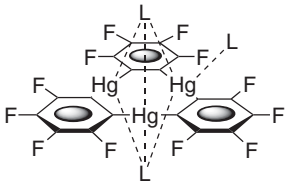

137.(μ_3-L)$_2$(L)

L	*References*
Me–C(=O)–Me	227
Me–C(=O)–O–Et	231
Me–S(=O)–Me	231

interactions of 3.51 Å. In [**137**-(μ_3-acetonitirile)$_2$], the nitrogen atoms of the two acetonitrile molecules cap each face of the trinuclear mercury complex and are held by Hg–N secondary interactions of 2.93 and 2.99 Å (Figure 21).[232]

Interaction of **137** with dimethyl sulfide in 1,2-dichloroethane leads to the formation of the polymeric adduct [**137**–μ_6-Me_2S]$_n$, which features sandwiched dimethyl sulfide molecules (Figure 22).[233] The sulfur atom of the latter interacts simultaneously with the mercury centers of two neighboring molecules of **137** and thereby achieves hexacoordination.

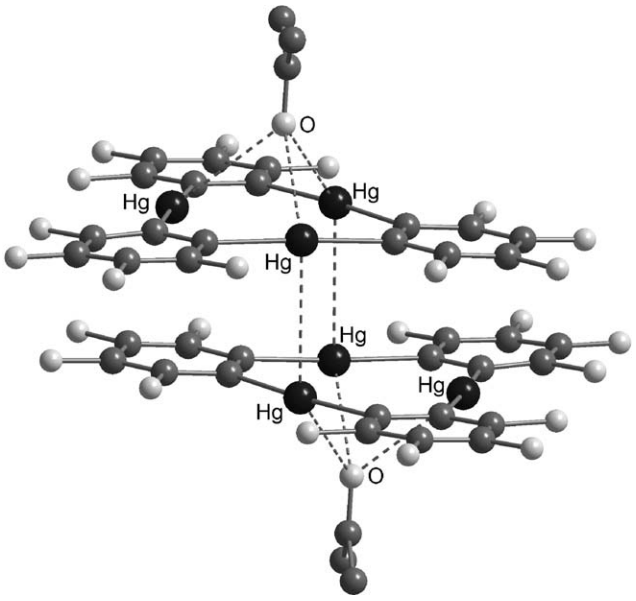

Figure 20 Structure of [**137**-μ_3-acetone]. Hydrogen atoms omitted for clarity.

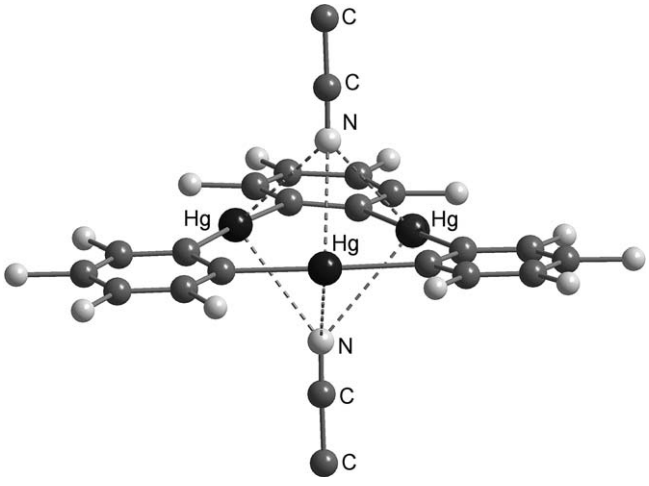

Figure 21 Structure of [**137**-(μ_3-acetonitrile)$_2$]. Hydrogen atoms omitted for clarity.

2.07.1.5.2.(ii) Mercuracarborands

The electron-withdrawing properties of the *ortho*-carborane cages impart substantial Lewis acidity to the mercury centers of mercuracarborands. While these macrocyclic organomercurials readily complex anionic guests, a number of adducts involving neutral donors have also been obtained. For instance, the hexamethylated mercuracarborand **58** has been isolated as a tris(acetonitrile) adduct (Figure 23).[70] One of the acetonitrile ligands bridges the three mercury atoms with which it forms secondary interactions similar to those observed in [**137**–(μ_3-acetonitrile)$_2$].[232] The other two acetonitrile molecules are terminally ligated to two of the mercury centers. Mercuracarborand **58** also forms a water adduct in which the oxygen atom is triply coordinated to the mercury centers.[234] In the crystal, two molecules of this adduct sandwich a benzene molecule which is held by four O–H$\cdots\pi$ hydrogen bonds (Figure 24). The formation of this unusual aggregate is made possible by the triple coordination of the water molecule which increases

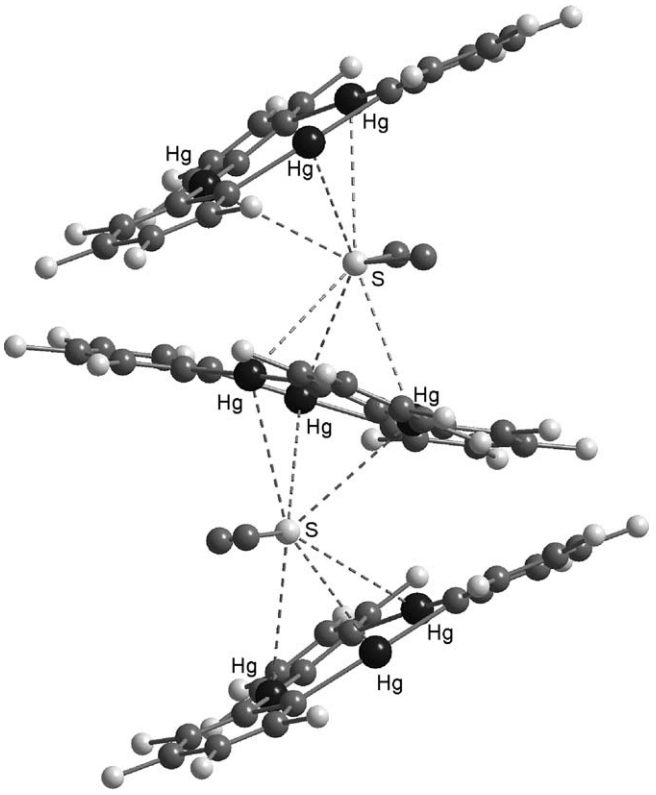

Figure 22 Portion of a stack observed in the structure of [**137**-μ_6-Me_2S]$_n$. Hydrogen atoms omitted for clarity.

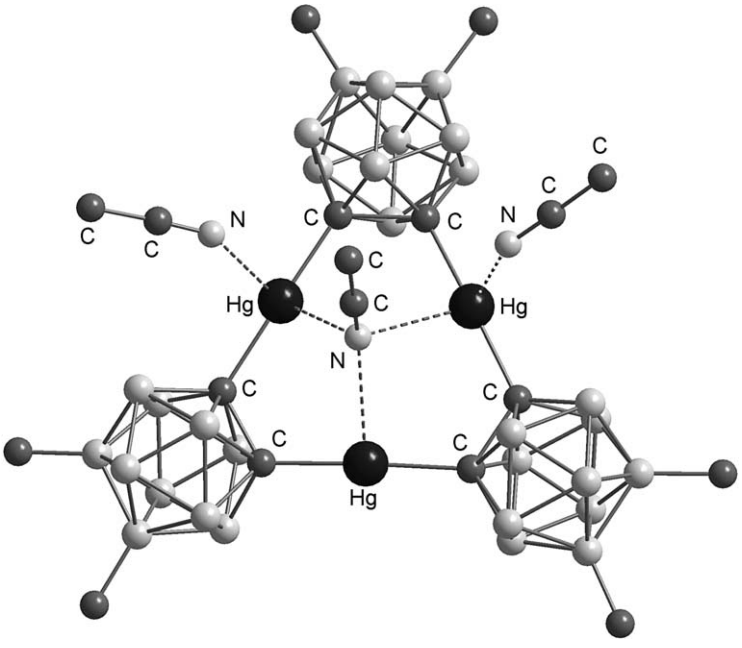

Figure 23 Structure of the tris(acetonitrile) adduct of **58**. Hydrogen atoms omitted for clarity.

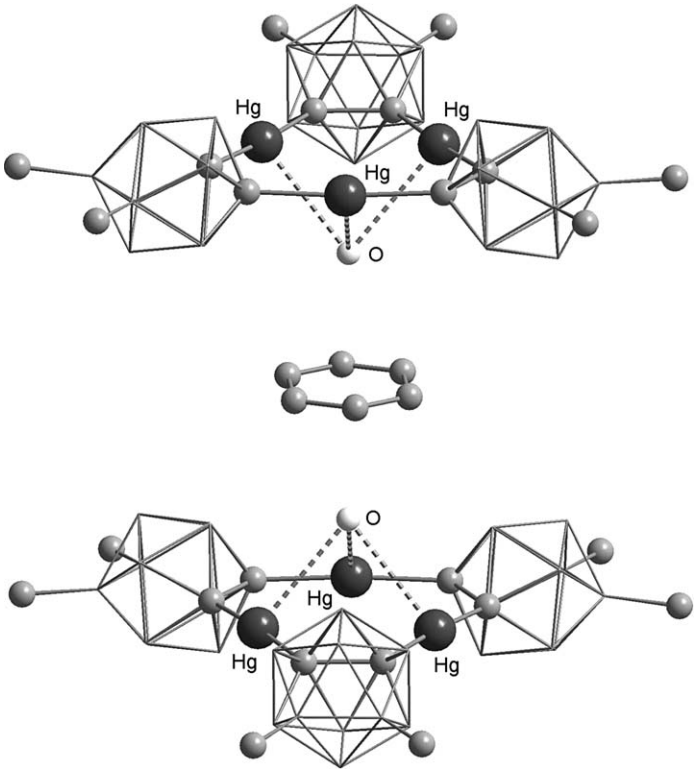

Figure 24 Structure of [**58**–$(OH_2)_2$-C_6H_6]. Boron and hydrogen atoms omitted for clarity.

its acidity and ability to engage in strong hydrogen bonding interactions. Finally, the dinuclear derivative **171** has been isolated as an ethanol adduct with the oxygen atom chelated between the two mercury centers.[72]

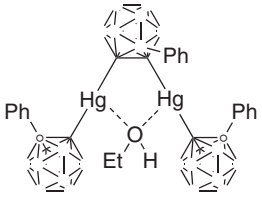

171-EtOH = BH
∘ = B

2.07.1.5.3 Supramolecular self-assembly

Polyfunctional organomercurials have emerged as useful building blocks for the construction of supramolecular species. Compound **137**, for instance, was shown to complex benzene, yielding extended binary stacks where the two components alternate (Figure 25).[235] These stacks are rather compact (centroid distance of 3.24 Å), so that secondary π-interactions occur between the benzene molecule and the mercury centers. Each of the six C–C bonds of the benzene molecule interacts with one of the six mercury centers of the two juxtaposed molecules of **137**. As a result, the benzene is hexacoordinated in a μ_6-η^2:η^2:η^2:η^2:η^2:η^2 fashion. The strength of the Hg–C interactions must be relatively weak as no change could be detected in the C–C bond lengths of the aromatic substrate. As indicated by wideline deuterium NMR, the sandwiched benzene molecules undergo an in-plane 60° reorientation with an activation energy of 52 ± 4 kJ mol^{-1}.[13] The magnitude of this activation energy suggests the presence of directional interactions between the mercury atoms of **137** and the benzene molecules.

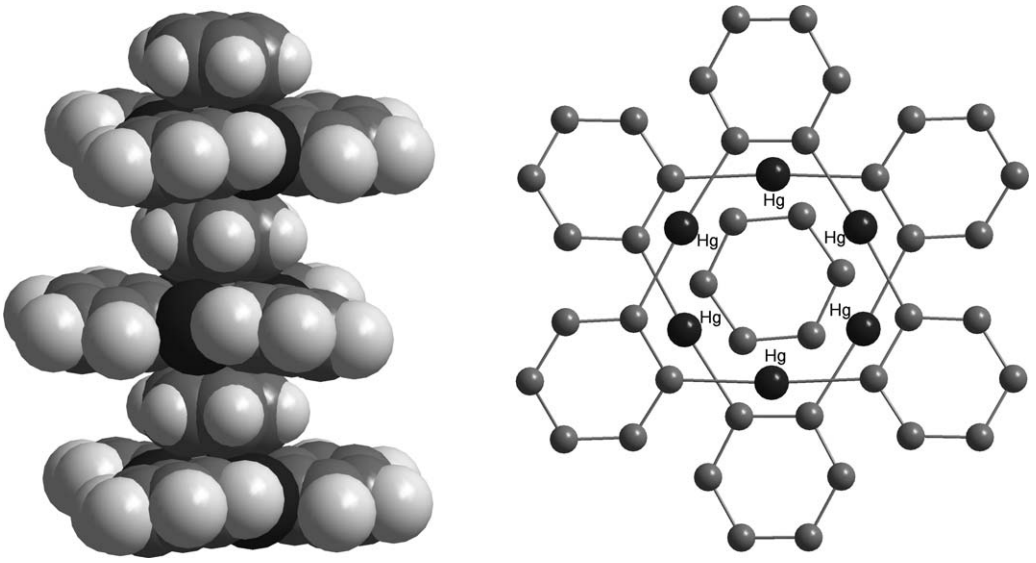

Figure 25 Left: Side view of a portion of a stack in the structure of [**137**-benzene]. Right: Top view showing the sandwiched benzene molecule in [**137**-benzene]. Fluorine and hydrogen atoms omitted for clarity.

In order to assess how the bulk of the arene influences the structure of such stacked assemblies, the adducts of **137** with toluene, *o*-, *m*-, and *p*-xylenes, and mesitylene have been synthesized and structurally characterized.[236] These adducts tend to form extended binary stacks similar to those found in [**137**–benzene]. The substituted benzene molecules adopt an apparently random orientation with respect to the trinuclear core of **137**, thus suggesting that the binding might be largely dispersive and electrostatic. The interaction of **137** with larger aromatic substrates such as biphenyl, naphthalene, pyrene, and triphenylene has also been investigated.[237,238] The structure of the resulting adducts consists of extended stacks where eclipsed molecules of **137** alternate with the aromatic substrate (Figure 26). These complexes all have short Hg–C contacts in the 3.2–3.4 Å range, reflecting the presence of secondary polyhapto-π interactions occurring between the electron-rich aromatic molecules and the acidic mercury centers. Recent investigations also indicate that **137** complexes to the π-face of heteroatom-containing substrates such as tetrathiafulvalene (TTF).[239]

The biphenyl, naphthalene, pyrene, and triphenylene adducts display intense room-temperature phosphorescence.[237,238] These observations indicate the occurrence of a mercury heavy atom effect, which promotes

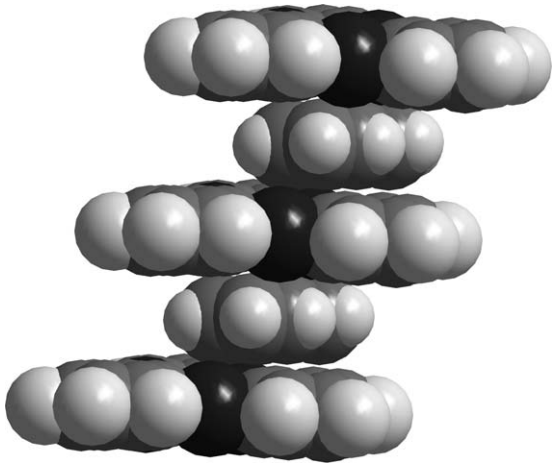

Figure 26 Space-filling representation of a portion of a stack observed in the structure of [**137**–$C_{10}H_8$].

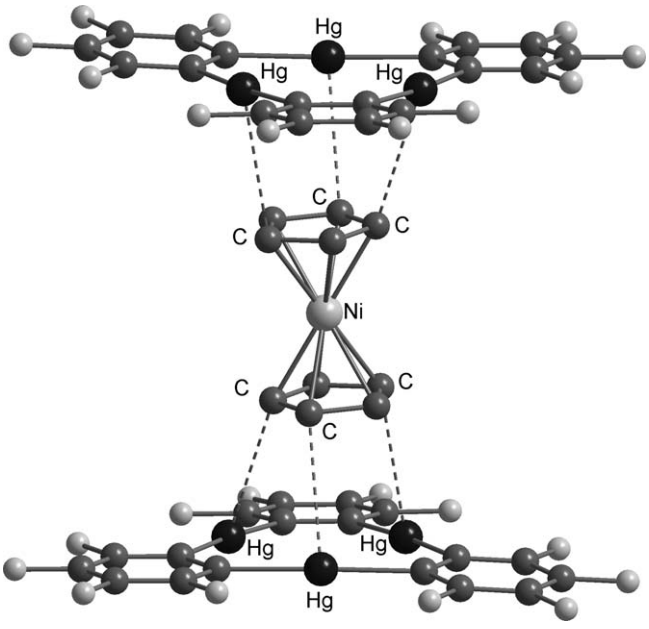

Figure 27 Structure of [**137**–$NiCp_2$]. Hydrogen atoms omitted for clarity.

population of the T_1 state of the aromatic chromophore. Time-resolved measurements indicate excited-state lifetimes ranging from 0.3 to 1 ms. These phosphorescence lifetimes are much shorter than those of the free arenes (~seconds) providing further support of heavy atom effects.

Simple mixing of **137** with ferrocene or nickelocene results in the formation of supramolecular electrophilic double sandwiches, in which each cyclopentadienide ring of the metallocene is capped by a molecule of **137**. The shortest Hg–C distance ranges (3.20–3.24 Å) indicate that the carbon atoms of the cyclopentadine (Cp) rings are in close contact with the mercury centers (Figure 27). Unlike pure nickelocene, which is air sensitive and displays a green color, the nickelocene-based double sandwich is a dark red solid. The unusual color of this complex results from an increase in the intensity of the formally spin-forbidden $^3A_{2g} \rightarrow {}^1E_{1g}$ transition, once again indicating the occurrence of a mercury heavy atom effect.[240]

2.07.2 Cadmium

2.07.2.1 Introduction

The organometallic chemistry of cadmium remains much less developed than that of mercury. This certainly results from the limited number of applications involving organocadmium compounds in organic and organometallic chemistry. Nonetheless, organocadmium compounds, and especially $CdMe_2$, have become important reagents for the synthesis of cadmium chalcogenide films and nanoparticles. Since this field of research is somewhat peripheral to classical organometallic chemistry, the use of organocadmium compounds as precursors for cadmium chalcogenide phases will not be covered in this chapter.

2.07.2.2 Formation of the Cadmium–Carbon Bond

Efforts to improve the efficient synthesis of organocadmium complexes by reaction of elemental cadmium with alkyl halides have been reported. Recent studies show that the presence of catalytic amounts of CuI and BuMgI in the reaction of alkyliodides with cadmium metal allows for the formation of **172a–c** in high yield and high purity (Equation (58)).[241]

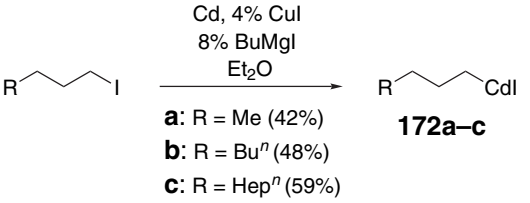

(58)

The metathesis reaction of organolithium reagents with cadmium halides remains the most popular method for the synthesis of organocadmium derivatives. Recent examples illustrating the usefulness of this synthetic method include the alkylcadmium derivatives **173–178**.[242–244] Arylcadmium compounds have been prepared using the same method.[31] For instance, reaction of 2-$LiC_6H_4CH_2NEt_2$ **179** with $CdCl_2$ leads to the symmetrical compound **180**. The structure of these compounds reveals that the cadmium atom is coordinated by the nitrogen atom of the amino group (Equation (59)). Arylcadmium species can also be obtained by decarboxylation of arylcarboxylate salts, as illustrated by the conversion of **181** to **182** presented in Equation (60).[245]

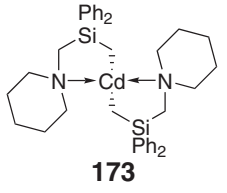

173

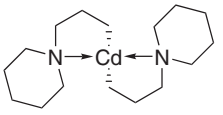

174

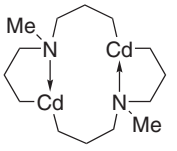

175

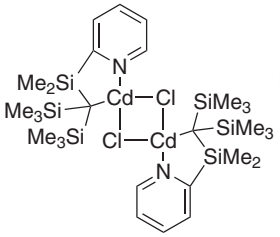

176

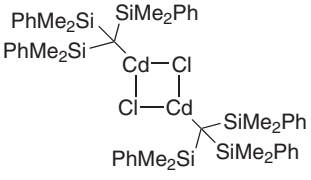

177

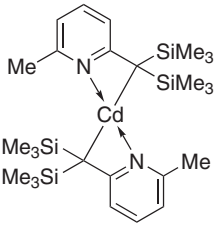

178

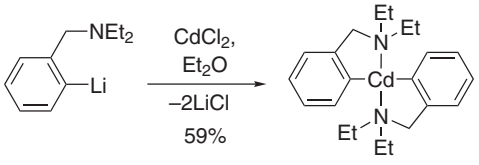

179 **180**

(59)

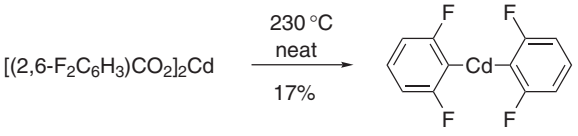

181 **182**

(60)

Aromatic electrophilic substitution has also been used in the synthesis of arylcadmium species. In a recent example, aniline was shown to undergo electrophilic metallation upon treatment with $Cd(OCOCF_3)_2$, yielding the *para*-substituted cadmium derivative **183** (Equation (61)).[246]

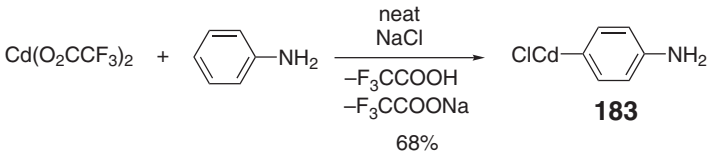

(61)

Additionally, $Cd(OCOCF_3)_2$ reacts with methyl-substituted quinolium perchlorate salts **184** in basic media to afford the organocadmium compound **185** (Scheme 21).[247]

The metathesis reaction of fluorinated alkyl iodides with reagents such as $CdMe_2$ is a well-established procedure for the synthesis of fluoroalkyl cadmium derivatives. A recent application of this method has allowed for the synthesis of compound **186**, as shown in Scheme 22.[248] This reaction is accompanied by formation of **187**, which results from the insertion of the difluorocarbene in the methyl–cadmium bond. Presumably, the difluorocarbene is generated by a radicalar process involving HCF_2I and $CdMe_2$.

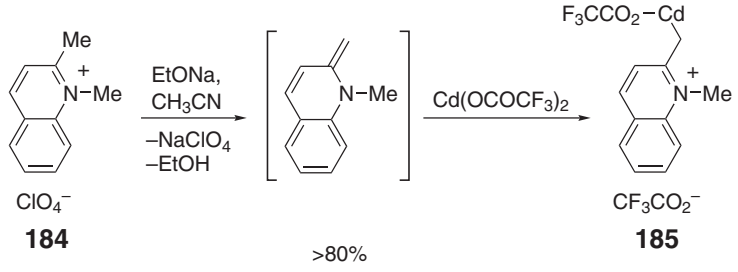

Scheme 21

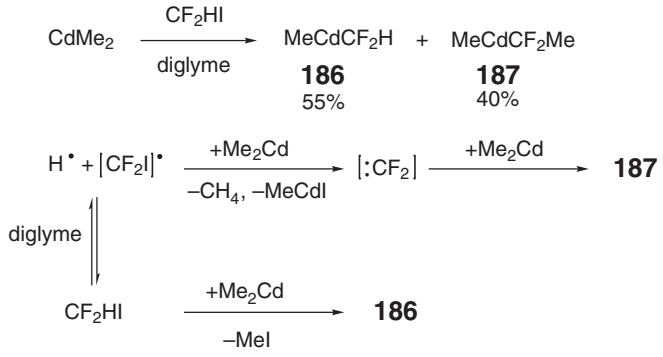

Scheme 22

2.07.2.3 Structures of Organocadmium Compounds

Carbene adducts of dimethylcadmium **188–190** have been obtained by simple addition of $CdMe_2$ to the corresponding carbene at room temperature.[249] All the three adducts have similar structures. In the case of **190**, the $C_{carbene}$–Cd bond of 2.33 Å is 0.15 Å longer than the C_{methyl}–Cd bonds of 2.18 Å (Figure 28). As a result, the cadmium atom is in a distorted trigonal-planar environment with a C_{methyl}–Cd–C_{methyl} angle of 136°.

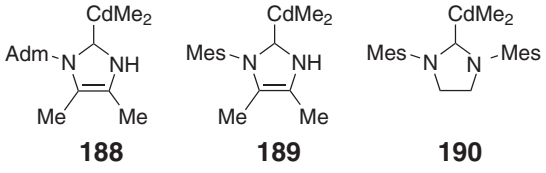

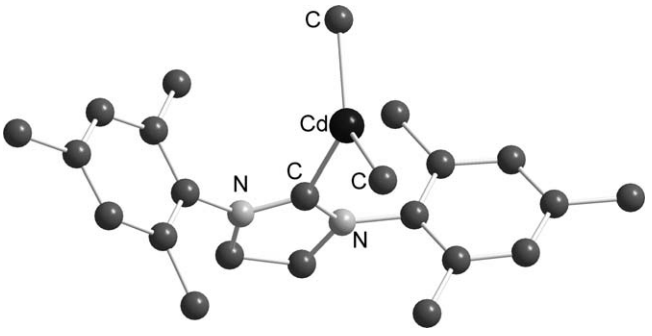

Figure 28 Structure of **190**. Hydrogen atoms omitted for clarity.

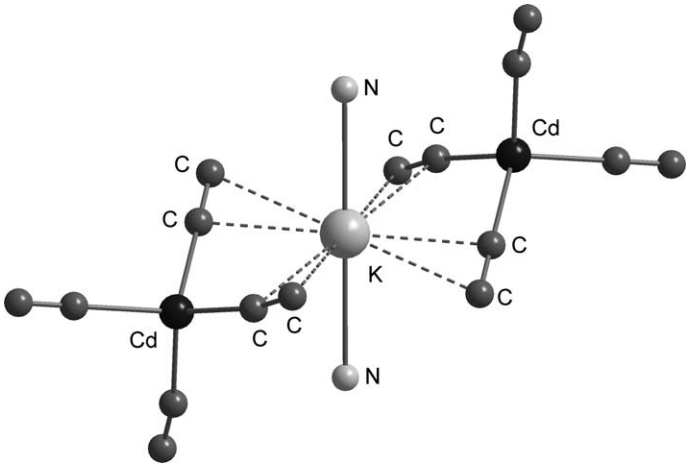

Figure 29 Structure of Compound **191**. Hydrogen atoms omitted for clarity.

A novel cadmate complex has been formed by the reaction of $Cd(NH_2)_2$ with KC≡CH in the presence of acetylene in liquid ammonia.[250] The potassium salt, $K_2Cd(CCH)_4$-$2NH_3$ **191**, has been structurally characterized. The cadmium center is tetrahedrally coordinated to four acetylide units with which it forms Cd–C bonds of 2.23–2.25 Å (Figure 29). The acetylide ligands are π-coordinated to two crystallographically distinct potassium ions whose coordination sphere is completed by two ammonia molecules.

The reaction of $CdCl_2$ with $(NBu_4)_2[Pt(C{\equiv}CPh)_4]$ leads to the formation of a dianionic tetranuclear complex **192**, in which two $[Pt(C{\equiv}CPh)_4]^{2-}$ units are connected by two $[ClCd]^+$ units as shown in Figure 30.[251] The cadmium atoms are π-coordinated to the C_α atoms of the four acetylide ligands with which they form Cd–C bonds of 2.46 and 2.60 Å. The short distances between the platinum and cadmium atoms of 2.96 Å also argue for the presence of a Pt–Cd bonding interaction. The same reaction affords a trinuclear complex **193**, in which two $CdCl_2$ units are π-coordinated to two *cis*-alkynyl ligands of the platinum complex (Figure 31). As indicated by the relatively short Cd–C bonds (2.40–2.67 Å), the alkynyl functionality interacts with the cadmium centers in an η^2-fashion. The luminescence properties of these compounds were also studied, and compound **192** exhibited metal–metal-based charge-transfer bands, whereas metal-to-ligand charge-transfer bands were observed in compound **193**.

Unusual arene–cadmium π-complexes have been recently prepared and structurally characterized. For example, the *meta*-benziporphyrin complex **194**, which can be obtained by reaction of the free base with $CdCl_2$, possesses a cadmium atom that is bound to the *meta*-phenylene unit of the ligand in an apparent η^1-fashion (Figure 32). The resulting Cd–C distance of 2.71 Å is shorter than the sum of the van der Waals radii.[252] Despite this relatively short contact, DFT calculations and AIM analysis point to the weakness of the interaction. Comparable weak arene–cadmium π-interactions are also observed in the *para*-benziporphyrin cadmium chloride complex **195**.[253]

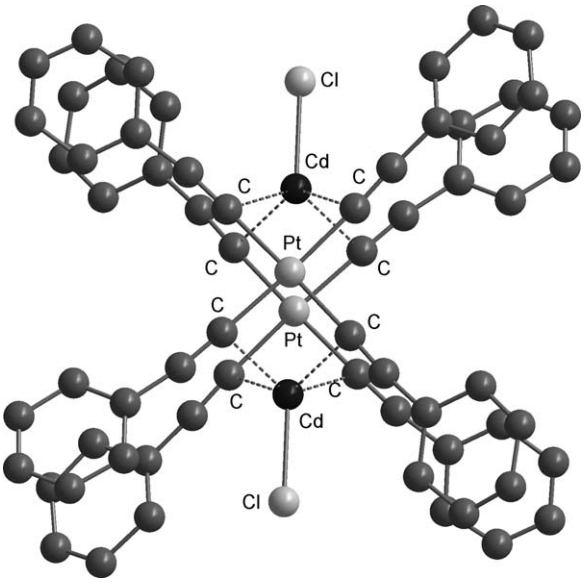

Figure 30 Structure of compound **192**. Only one orientation of each disordered phenyl group is represented. Hydrogen atoms omitted for clarity.

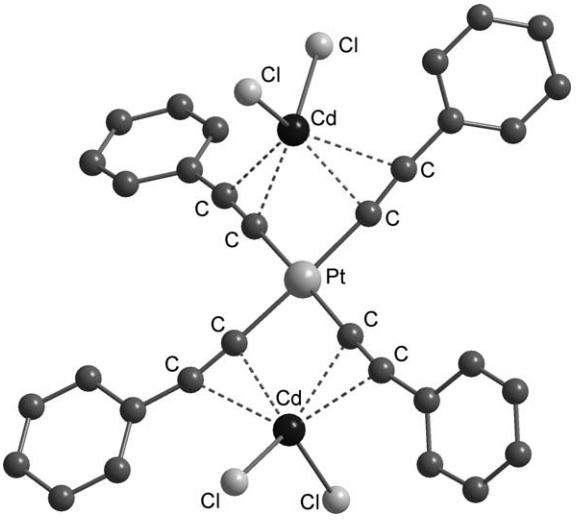

Figure 31 Structure of compound **193**. Hydrogen atoms omitted for clarity.

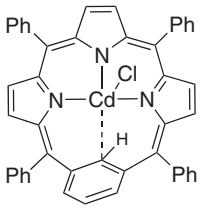

194

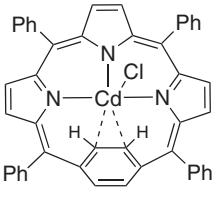

195

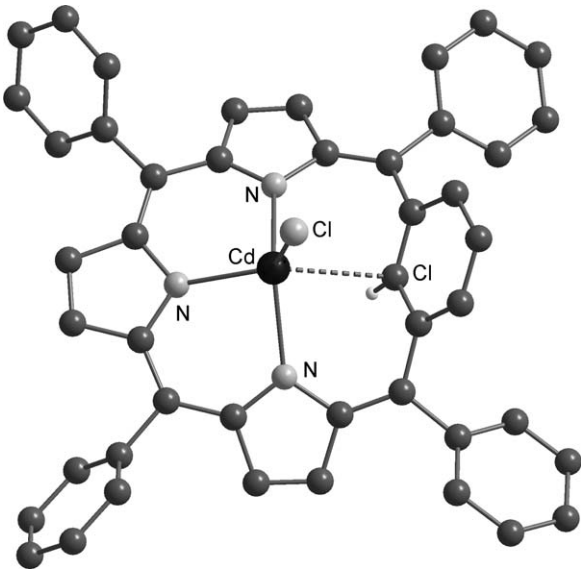

Figure 32 Structure of compound **194**. The hydrogen atom at the 2-position of the *meta*-phenylene ring is shown; other hydrogen atoms are omitted for clarity.

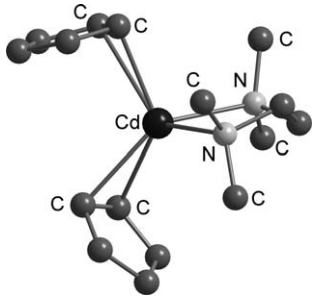

Figure 33 Structure of compound **196**. Hydrogen atoms omitted for clarity.

The first complex exhibiting π-coordination of a Cp ligand to a Cd(II) center in the solid state, namely, [Cp_2Cd-tmeda] **196**, has been recently isolated and structurally characterized (Figure 33).[254] Both Cp rings interact with the cadmium center in an η^2-fashion with Cd–C distances ranging from 2.34 to 2.74 Å.

The reaction of dabco (1,4-diazobicyclo[2.2.2]octane) with Me_2Cd yields a 1 : 1 adduct **197**, which adopts a linear polymeric structure (Figure 34).[255] The cadmium atom is coordinated by two dabco units and two methyl carbon atoms giving rise to a distorted tetrahedral environment. Finally, the organocadmium adduct **198** (Figure 35) has been isolated from the reaction of Me_2Cd with $Cd[(SeP\text{-}i\text{-}Pr_2)_2N]_2$.[256] The solid-state structure consists of dimeric units where each methylcadmium unit is coordinated to three selenium atoms. The geometry about the cadmium center is tetrahedral with a Cd–C distance of 2.16 Å, which is comparable to that observed in other cadmium alkyl complexes.

2.07.2.4 Important Transformations Involving Organocadmium Derivatives

2.07.2.4.1 Metathesis reactions

Organocadmium species are useful reagents for the transfer of fluorinated alkyl or aryl groups to other main group or transition metal centers. Most of the recent cases illustrating this property involve the use of $Cd(CF_3)_2$ and $Cd(C_6F_5)_2$

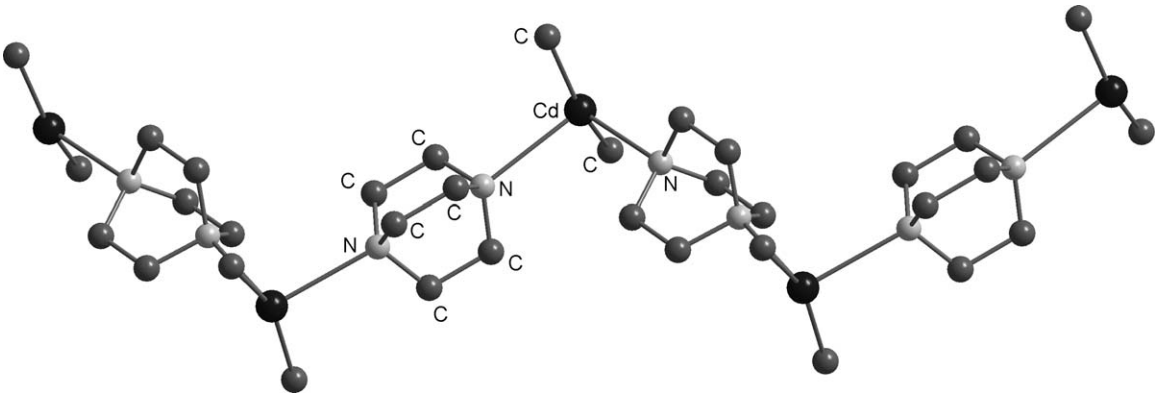

Figure 34 Extended structure of **197**. Hydrogen atoms omitted for clarity.

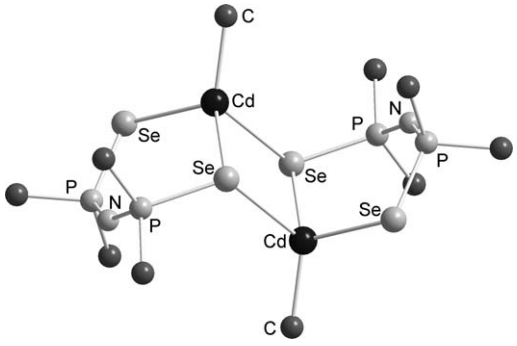

Figure 35 Structure of **198**. Alkyl chains are reduced to the first carbon atom for clarity. Hydrogen atoms omitted for clarity.

as trifluoromethyl and pentafluorophenyl group-transfer reagents, respectively. In all cases, the final product is obtained via a metathesis reaction involving the organocadmium species and main group or metal halide reagents. Recent examples demonstrating the potential of this synthetic approach are compiled in Table 7.[257–270]

2.07.2.4.2 Generation of difluorocarbene

The reaction of donor-free $Cd(CF_3)_2$ with PF_5 in a 2 : 1 ratio results in the formation of $(CF_3)_3PF_2$ in 80% yield. This reaction does not proceed via metathesis but involves the generation of difluorocarbene that subsequently inserts in the P–F bonds of PF_5 (Equation (62)).[271] The same general strategy has been used for the cyclopropanation of a variety of alkenes and alkynes including cyclohexene, *cis*-stilbene, and tolane (Scheme 23).[272] Finally, the difluorocarbene generated in this fashion can insert in the metal–chlorine bond of Me_3SnCl and $AsCl_3$[272] as well as in the copper–carbon bond of C_6F_5Cu.[273]

$$2PF_5 + 3Cd(CF_3)_2 \xrightarrow[80\%]{\substack{CHCl_3\\ -40\,^{\circ}C}} (CF_3)_3PF_2 \qquad (62)$$

Table 7 Metathesis reactions involving fluorinated organocadmium derivatives as reagents

Starting material	*Reagent and conditions*	*Yield (%)*	*Product*	*References*
$InCl_3$	$Cd(C_6F_5)_2$ MeCN, −30 °C	43	$In(C_6F_5)_3$	257,258
$In(C_6F_5)_3$	i, $Cd(C_6F_5)_2$MeCN ii, PPNCL	12	$[PPN][In(C_6F_5)_4]$	257,258
Ph_3GeCl	$Cd(CF_3)_2$–glyme $CHCl_3$	72	Ph_3GeCF_3	259
Ph_3SnCl	$Cd(CF_3)_2$–glyme $CHCl_3$	80	Ph_3SnCF_3	259
Ph_3PbBr	$Cd(CF_3)_2$–glyme THF	81	Ph_3PbCF_3	259
$PhPb(OAc)_3$	$Cd(CF_3)_2$–glyme THF	64	$PhPb(OAc)(CF_3)_2$	259
$Bu^n{}_3SnCl$	$C_6F_{13}CdX$ (X=1 or C_6F_{13}) DMF	81	$Bu^n{}_3SnC_6F_{13}$	260
$SbCl_3$	$Cd(CF_3)_2$–2MeCN MeCN 20 °C	90	$Sb(CF_3)_3$	261
BrF_3	$Cd(C_6F_5)_2$ CH_2Cl_2/MeCN <0 °C		$C_6F_5BrF_2$	262
IF_3	$Cd(C_6F_5)_2$ CH_2Cl_2/MeCN −78 °C	97	$C_6F_5IF_2$	263
C_6F_5XeF	$Cd(C_6F_5)_2$ CH_2Cl_2, −78 °C	75	$Xe(C_6F_5)_2$	264,265
CuI	$Cd(C_2F_5)_2$–2MeCN PPCNl CH_2Cl_2, −50 °C		$[PPN][Cu(C_6F_5)_2]^-$	266
$[Ag(CN)_2]^-$	$Cd(CF_3)_2$–diglyme DMF		$[Ag(CF_3(CN)_2]^-$	267
$K[Ag(CN)_2]$	$Cd(CF_2H_2$-tetraglyme DMF, 0 °C	20	$[Ag(CF_2H)(CN)_2]^-$	268
$(RPF_2)AuCl$ (R = NEt_2, NMe_2, Ph, Cp)	$Cd(CF_3)_2$–DME CH_2Cl_2 −40 °C	35–37	$(RPF_2)Au(CF_3)$	269
$M(CO)_5Br$ (M = Mn, Re)	$Cd(R_f)_2$, $AgBF_4$ CH_2Cl_2 $R_f = C_nF_{2n+1}$ (n = 1–4,6), C_6F_5		$M(CO)_5Rf$	270

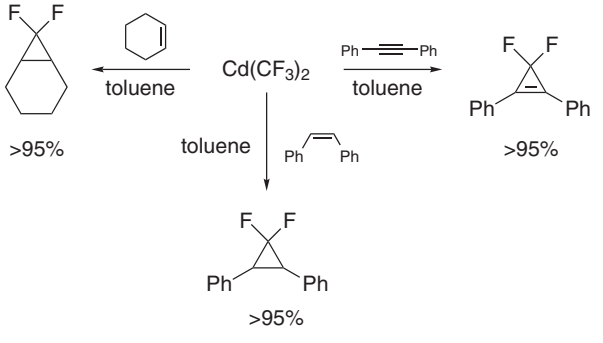

Scheme 23

Acknowledgments

The authors would like to thank the National Science Foundation, the Petroleum Research Fund, and the Welch Foundation for financial support while writing this chapter.

References

1. Pyykkö, P.; Straka, M. *Phys. Chem. Chem. Phys.* **2000**, *2*, 2489–2493 and references therein.
2. Burini, A.; Fackler, J. P., Jr.; Galassi, R.; Grant, T. A.; Omary, M. A.; Rawashdeh-Omary, M. A.; Pietroni, B. R.; Staples, R. J. *J. Am. Chem. Soc.* **2000**, *122*, 11264–11265.
3. Pickett, N. L.; Just, O.; VanDerveer, D. G.; Rees, J. S. *Acta Crystallogr., Sect. C: Cryst. Struct. Commun.* **2000**, *C56*, 412–413.
4. Zamora, F.; Sabat, M.; Janik, M.; Siethoff, C.; Lippert, B. *Chem. Commun.* **1997**, 485–486.
5. Mingos, D. M. P.; Vilar, R.; Rais, D. *J. Organomet. Chem.* **2002**, *641*, 126–133.
6. Wuest, J. D. *Acc. Chem. Res.* **1999**, *32*, 81–89.
7. Vaugeois, J.; Simard, M.; Wuest, J. D. *Coord. Chem. Rev.* **1995**, *145*, 55–73.
8. Shur, V. B.; Tikhonova, I. A. *Russ. Chem. Bull.* **2003**, *52*, 2539–2554.
9. Kitching, W.; Glenn, M. *Science of Synthesis* **2004**, *3*, 133–303.
10. Deacon, G. B.; Forsyth, C. M.; Nickel, S. *J. Organomet. Chem.* **2002**, *647*, 50–60.
11. Wedge, T. J.; Hawthorne, M. F. *Coord. Chem. Rev.* **2003**, *240*, 111–128.
12. Hawthorne, M. F.; Zheng, Z. *Acc. Chem. Res.* **1997**, *30*, 267–276.
13. Haneline, M. R.; Taylor, R. E.; Gabbaï, F. P. *Chem. Eur. J.* **2003**, *9*, 5189–5193.
14. Bickelhaupt, F. *Chem. Soc. Rev.* **1999**, *28*, 17–23.
15. Meyer, C.; Blanchard, N.; Deffosseux, M.; Cossy, J. *Acc. Chem. Res.* **2003**, *36*, 766–772.
16. Shannon, I. J. *Annu. Rep. Prog. Chem., Sect. A: Inorg. Chem.* **2004**, *100*, 141–150.
17. Malito, J. *Annu. Rep. Prog. Chem., Sect. A: Inorg. Chem.* **2003**, *99*, 125–138.
18. Malito, J. *Annu. Rep. Prog. Chem., Sect. A: Inorg. Chem.* **2002**, *98*, 115–128.
19. Malito, J. *Annu. Rep. Prog. Chem., Sect. A: Inorg. Chem.* **2001**, *97*, 117–131.
20. Malito, J. *Annu. Rep. Prog. Chem., Sect. A: Inorg. Chem.* **2000**, *96*, 147–159.
21. Malito, J. *Annu. Rep. Prog. Chem., Sect. A: Inorg. Chem.* **1999**, *95*, 93–104.
22. Gorrell, I. B. *Annu. Rep. Prog. Chem., Sect. A: Inorg. Chem.* **1998**, *94*, 137–148.
23. Gorrell, I. B. *Annu. Rep. Prog. Chem., Sect. A: Inorg. Chem.* **1997**, *93*, 117–127.
24. Gorrell, I. B. *Annu. Rep. Prog. Chem., Sect. A: Inorg. Chem.* **1996**, *92*, 113–125.
25. Gorrell, I. B. *Annu. Rep. Prog. Chem., Sect. A: Inorg. Chem.* **1995**, *91*, 115–129.
26. Moene, W.; Vos, M.; Schakel, M.; De Kanter, F. J. J.; Schmitz, R. F.; Klumpp, G. W. *Chem. Eur. J.* **2000**, *6*, 225–236.
27. Spaniel, T.; Schmidt, H.; Wagner, C.; Merzweiler, K.; Steinborn, D. *Eur. J. Inorg. Chem.* **2002**, 2868–2877.
28. Tschinkl, M.; Schier, A.; Riede, J.; Schmidt, E.; Gabbaï, F. P. *Organometallics* **1997**, *16*, 4759–4761.
29. Vasse, J.-L.; Szymoniak, J. *Tetrahedron Lett.* **2004**, *45*, 6449–6451.
30. Al-Juaid, S. S.; Eaborn, C.; Lickiss, P. D.; Smith, J. D.; Tavakkoli, K.; Webb, A. D. *J. Organomet. Chem.* **1996**, *510*, 143–151.
31. van den Ancker, T. R.; Engelhardt, L. M.; Henderson, M. J.; Jacobsen, G. E.; Raston, C. L.; Skelton, B. W.; White, A. H. *J. Organomet. Chem.* **2004**, *689*, 1991–1999.
32. Al-Juaid, S. S.; Eaborn, C.; El-Hamruni, S. M.; Hitchcock, P. B.; Smith, J. D. *Organometallics* **1999**, *18*, 45–52.
33. Eaborn, C.; Lu, Z.-R.; Hitchcock, P. B.; Smith, J. D. *Organometallics* **1996**, *15*, 1651–1655.
34. Tschinkl, M.; Schier, A.; Riede, J.; Mehltretter, G.; Gabbaï, F. P. *Organometallics* **1998**, *17*, 2921–2923.
35. Tschinkl, M.; Schier, A.; Riede, J.; Gabbaï, F. P. *Inorg. Chem.* **1997**, *36*, 5706–5711.
36. Steinborn, D.; Ruffer, T.; Bruhn, C.; Heinemann, F. W. *Polyhedron* **1998**, *17*, 3275–3280.
37. Hutton, A. T.; Wewers, F. P. *J. Organomet. Chem.* **1995**, *492*, C14–C16.
38. Hitchcock, P. B.; Keates, J. M.; Lawless, G. A. *J. Am. Chem. Soc.* **1998**, *120*, 599–600.
39. Layeghi, H.; Tyrra, W.; Naumann, D. *Z. Anorg. Allg. Chem.* **1998**, *624*, 1601–1610.
40. Tschinkl, M.; Bachman, R. E.; Gabbaï, F. P. *J. Organomet. Chem.* **1999**, *582*, 40–44.
41. Salteris, C. S.; Kostas, I. D.; Micha-Screttas, M.; Heropoulos, G. A.; Screttas, C. G.; Terzis, A. *Main Group Met. Chem.* **1999**, *22*, 427–434.
42. Goedheijt, M. S.; Nijbacker, T.; Horton, A. D.; de Kanter, F. J. J.; Akkerman, O. S.; Bickelhaupt, F. *Eur. J. Inorg. Chem.* **2003**, 638–643.
43. Rot, N.; Bickelhaupt, F. *Organometallics* **1997**, *16*, 5027–5031.
44. Rot, N.; De Kanter, F. J. J.; Bickelhaupt, F.; Smeets, W. J. J.; Spek, A. L. *J. Organomet. Chem.* **2000**, *593–594*, 369–379.
45. Rickard, C. E. F.; Roper, W. R.; Tutone, F.; Woodgate, S. D.; Wright, L. J. *J. Organomet. Chem.* **2001**, *619*, 293–298.
46. Flower, K. R.; Howard, V. J.; Naguthney, S.; Pritchard, R. G.; Warren, J. E.; McGown, A. T. *Inorg. Chem.* **2002**, *41*, 1907–1912.
47. Salteris, C. S.; Kostas, I. D.; Micha-Screttas, M.; Steele, B. R.; Heropoulos, G. A.; Screttas, C. G.; Terzis, A. *J. Organomet. Chem.* **1999**, *590*, 63–70.
48. Cera, M.; Cerrada, E.; Laguna, M.; Mata, J. A.; Teruel, H. *Organometallics* **2002**, *21*, 121–126.
49. Bennett, M. A.; Contel, M.; Hockless, D. C. R.; Welling, L. L.; Willis, A. C. *Inorg. Chem.* **2002**, *41*, 844–855.
50. Cornu, D.; Hitchcock, P. B.; Lappert, M. F.; Uiterweerd, P. G. H. *Polyhedron* **2002**, *21*, 635–640.
51. Trecourt, F.; Breton, G.; Bonnet, V.; Mongin, F.; Marsais, F.; Queguiner, G. *Tetrahedron* **2000**, *56*, 1349–1360.
52. Naumann, D.; Tyrra, W.; Hermannn, R.; Pantenburg, I.; Wickleder, M. S. *Z. Anorg. Allg. Chem.* **2002**, *628*, 833–842.
53. Apte, S. D.; Zade, S. S.; Singh, H. B.; Butcher, R. J. *Organometallics* **2003**, *22*, 5473–5477.
54. Kostas, I. D.; Gruter, G.-J. M.; Akkerman, O. S.; Bickelhaupt, F.; Kooijman, H.; Smeets, W. J. J.; Spek, A. L. *Organometallics* **1996**, *15*, 4450–4458.
55. Kostas, I. D.; Akkerman, O. S.; Bickelhaupt, F.; Veldman, N.; Spek, A. L. *J. Organomet. Chem.* **1999**, *572*, 93–104.
56. Spring, D. R.; Krishnan, S.; Blackwell, H. E.; Schreiber, S. L. *J. Am. Chem. Soc.* **2002**, *124*, 1354–1363.

57. Guillemin, J.-C.; Bellec, N.; Szetsi, S. K.; Nyulaszi, L.; Veszpremi, T. *Inorg. Chem.* **1996**, *35*, 6586–6591.
58. Banger, K. K.; Brisdon, A. K.; Brain, P. T.; Parsons, S.; Rankin, D. W. H.; Robertson, H. E.; Smart, B. A.; Buehl, M. *Inorg. Chem.* **1999**, *38*, 5894–5900.
59. Lee, S. S.; Lee, I. S.; Chung, Y. K. *Organometallics* **1996**, *15*, 5428–5431.
60a. Baumgartner, T.; Schinkels, B.; Gudat, D.; Nieger, M.; Niecke, E. *J. Am. Chem. Soc.* **1997**, *119*, 12410–12411.
60b. van der Sluis, M.; Wit, J. B. M.; Bickelhaupt, F. *Organometallics* **1996**, *15*, 174–180.
61. Weiss, R.; Kraut, N.; Hampel, F. *J. Organomet. Chem.* **2001**, *617–618*, 473–482.
62. Voinov, M. A.; Grigor′ev, I. A. *Tetrahedron Lett.* **2002**, *43*, 2445–2447.
63. Brisdon, A. K.; Crossley, I. R. *Chem. Commun.* **2002**, 2420–2421.
64. Ferrer, M.; Rodriguez, L.; Rossell, O.; Pina, F.; Lima, J. C.; Bardia, M. F.; Solans, X. *J. Organomet. Chem.* **2003**, *678*, 82–89.
65. Dikasur, E. A.; Koval'skaya, S. S.; Vashkevich, E. V.; Kozlov, N. G.; Potkin, V. I.; Moiseichuk, K. L. *Russ. J. Gen. Chem.* **1999**, *69*, 1732–1735.
66. Dikasur, E. A.; Kozlov, N. G.; Koval'skaya, S. S.; Popova, L. A.; Moiseichuk, K. L. *Russ. J. Gen. Chem.* **2001**, *71*, 290–293.
67. Wong, W.; Choi, K.; Lu, G.; Shi, J.; Lai, P.; Chan, S. *Organometallics* **2001**, *20*, 5446–5454.
68. Wong, W.; Choi, K.; Lu, G. *Organometallics* **2002**, *21*, 4475–4481.
69. Wong, W.; Liu, L.; Poon, S.; Choi, K.; Cheah, K.; Shi, J. *Macromolecules* **2004**, *37*, 4496–4504.
70. Zinn, A. A.; Zheng, Z.; Knobler, C. B.; Hawthorne, M. F. *J. Am. Chem. Soc.* **1996**, *118*, 70–74.
71. Zheng, Z.; Knobler, C. B.; Mortimer, M. D.; Kong, G.; Hawthorne, M. F. *Inorg. Chem.* **1996**, *35*, 1235–1243.
72. Zheng, Z.; Knobler, C. B.; Hawthorne, M. F. *J. Am. Chem. Soc.* **1995**, *117*, 5105–5106.
73. Bruce, M. I.; Halet, J.-F.; Le Guennic, B.; Skelton, B. W.; Smith, M. E.; White, A. H. *Inorg. Chim. Acta* **2003**, *350*, 175–181.
74. Falvello, L. R.; Fernández, S.; Navarro, R.; Urriolabeitia, E. P. *Inorg. Chem.* **1999**, *38*, 2455–2463.
75. Nevstruev, A. N.; Moskalenko, A. I.; Boev, V. I.; Polennikov, V. V. *Russ. J. Org. Chem.* **2002**, *38*, 1542–1544.
76. Nevstruev, A. N.; Moskalenko, A. I.; Boev, V. I.; Porokhnya, S. N. *Russ. J. Gen. Chem.* **2004**, *74*, 530–535.
77. Arduengo, J. A., III; Harlow, R. L.; Marshall, W. J.; Prakasha, T. K. *Heteroatom Chem.* **1996**, *7*, 421–426.
78. Bildstein, B.; Malaun, M.; Kopacha, H.; Ongania, K.-H.; Wurst, K. *J. Organomet. Chem.* **1998**, *552*, 45–61.
79. Bildstein, B.; Malaun, M.; Kopacha, H.; Ongania, K.-H.; Wurst, K. *J. Organomet. Chem.* **1999**, *572*, 177–187.
80. Lee, K.-M.; Chen, J. C. C.; Lin, I. J. B. *J. Organomet. Chem.* **2001**, *617–618*, 364–375.
81. Hobrey, J. D.; Visser, A. E.; Spear, S. K.; Reichert, M.; Swatloski, R. P.; Broker, G. A.; Rogers, R. D. *Green Chem.* **2003**, *5*, 129–135.
82. Davies, A.; Ng, K. M. *J. Chem. Soc., Perkin Trans. 2* **1998**, 2599–2608 and references therein.
83. Langer, O.; Dölle, F.; Valette, H.; Halldin, C.; Vaufrey, F.; Fuseau, C.; Coulon, C.; Ottaviani, M.; Nagren, K., Bottlaender, M., *et al. Bioorg. Med. Chem.* **2001**, *9*, 677–694.
84. da Silva, A. J. M; Melo, P. A.; Silva, N. M. V.; Brito, F. V.; Buarque, C. D.; de Souza, D. V.; Rodrigues, V. P.; Pocas, E. S. C.; Noel, F., Albuquerque, E. X., *et al. Biorg. Med. Chem. Lett.* **2001**, *11*, 283–286.
85. Reck, C. E.; Bretschneider-Hurley, A.; Heeg, M. J.; Winter, C. H. *Organometallics* **1998**, *17*, 2906–2911.
86. Brown, M. A.; Kerr, M. A. *Tetrahedron Lett.* **2001**, *42*, 983–985.
87. Garg, N. K.; Sarpong, R.; Stoltz, B. M. *J. Am. Chem. Soc.* **2002**, *124*, 13179–13184.
88. Baran, P. S.; Corey, E. J. *J. Am. Chem. Soc.*, **2002**, *124*, 7904–7905.
89. Mann, J.; Barbey, S. *Tetrahedron* **1995**, *51*, 12763–12774.
90. Reck, C. E.; Winter, C. H. *Organometallics* **1997**, *16*, 4493–4496.
91. Bonnardel, P. A.; Paris, R. V. *J. Organomet. Chem.* **1996**, *515*, 221–232.
92. Ford, A.; Sinn, E.; Woodward, S. *J. Organomet. Chem.* **1995**, *493*, 215–220.
93. Vicente, J.; Abad, J.; Rink, B.; Herandez, F.; Ramirez de Arellano, M. C. *Organometallics* **1997**, *16*, 5269–5282.
94. Dinda, J.; Bag, K.; Sinha, C.; Mostafa, G.; Lu, T. H. *Polyhedron* **2003**, *22*, 1367–1376.
95. Berger, A.; de Cian, A.; Djukic, J. P.; Fischer, J.; Pfeffer, M. *Organometallics* **2001**, *20*, 3230–3240.
96. Berger, A.; Djukic, J. P.; Pfeffer, M. *Organometallics* **2003**, *22*, 5243–5260.
97. Berger, A.; Djukic, J. P.; Pfeffer, M.; de Cian, A.; Kyritsakas-Gruber, N.; Lacour, J.; Vial, L. *Chem. Commun.* **2003**, 658–659.
98. Braun, T. P.; Gutsch, P. A.; Zimmer, H. *Z. Naturforsch. B* **1999**, *54*, 858–862.
99. Vicente, J.; Abad, J.; Clemente, R.; Lopez-Serrano, J.; Ramirez de Arellano, M. C.; Jones, P. G.; Bautista, D. *Organometallics* **2003**, *22*, 4248–4259.
100. Clark, G. R.; Ng, M. M. P.; Roper, W. R.; Wright, L. J. *J. Organomet. Chem.* **1995**, *491*, 219–229.
101. Popović, Z.; Soldin, Z.; Plavec, J.; Vikić-Topić, D. *App. Organomet. Chem.* **2000**, *14*, 598–603.
102. Meng, H.; Perepichka, D. F.; Bendikov, M.; Wudl, F.; Pan, G. Z.; Yu, W.; Dong, W.; Brown, S. *J. Am. Chem. Soc.* **2003**, *125*, 15151–15162.
103. Cunningham, A. F. *Organometallics* **1997**, *16*, 1114–1122.
104. Huo, S. Q.; Zhu, Y. J.; Wu, J. *J. Organomet. Chem.*, **1995**, *490*, 243–247.
105. Wu, Y.; Cui, X.; Zhou, N.; Song, M.; Yun, H.; Du, C.; Zhu, Y. *Tetrahedron: Asymmetry* **2000**, *11*, 4877–4883.
106. Hou, X.; Cui, X.; Song, M.; Hao, X.; Wu, Y. *Polyhedron* **2003**, *22*, 1249–1253.
107. Wu, Y. J.; Ciu, X. L.; Liu, Y. H.; Yuan, H. Z.; Mao, X. A. *J. Organomet. Chem.* **1997**, *543*, 63–70.
108. Cui, X. L.; Wu, Y. J.; Zou, D. P.; He, C. H.; Chai, J. J. *Polyhedron* **1999**, *18*, 1023–1027.
109. Lin, K.; Song, M.; Zhu, Y.; Wu, Y. *J. Organomet. Chem.* **2002**, *660*, 139–144.
110. Neto, A. F.; Borges, A. D. L.; Campos, I. P. A.; Miller, J. *Synth. React. Inorg. Met. Org. Chem.* **1997**, *27*, 1543–1551.
111. Kur, S. A.; Rheingold, A. L.; Winter, C. H. *Inorg. Chem.* **1995**, *34*, 414–416.
112. Kur, S. A.; Winter, C. H. *J. Organomet. Chem.* **1996**, *512*, 39–44.
113. Harrison, R. M.; Brotin, T.; Noll, B. C.; Michl, J. *Organometallics* **1997**, *16*, 3401–3412.
114. Cormick, R.; Löfstedt, J.; Perlmutter, P.; Westman, G. *Tetrahedron Lett.* **1997**, *38*, 2737–2740.
115. Cormick, R.; Perlmutter, P.; Selajarern, W.; Zang, H. *Tetrahedron Lett.* **2000**, *41*, 3713–3716.
116. Mayo, P.; Poirier, M.; Rainey, J.; Tam, W. *Tetrahedron Lett.* **1999**, *40*, 7727–7730.
117. Mayo, P.; Tam, W. *Tetrahedron* **2002**, *58*, 9513–9525.
118. Mayo, P.; Orlova, G.; Goddard, J. D.; Tam, W. *J. Org. Chem.* **2001**, *66*, 5182–5191.
119. Senda, Y.; Kanto, H.; Itoh, H. *J. Chem. Soc., Perkin Trans. 2* **1997**, *2*, 1143–1146.
120. Andrey, O.; Glanzmann, C.; Landais, Y.; Parra-Rapado, L. *Tetrahedron* **1997**, *53*, 2835–2854.
121. Hayes, P.; Suthers, B. D.; Kitching, W. *Tetrahedron Lett.* **2000**, *41*, 6175–6179.

122. Enierga, G.; Hockless, D. C. R.; Perlmutter, P.; Rose, M.; Sjöberg, S.; Wong, K. *Tetrahedron Lett.* **1998**, *39*, 2813–2814.
123. Marcotte, S.; D'Hooge, F.; Ramadas, S.; Feasson, C.; Pannecoucke, X.; Quirion, J.-C. *Tetrahedron Lett.* **2001**, *42*, 5879–5882.
124. Paolucci, C.; Venturelli, F.; Fava, A. *Tetrahedron Lett.* **1995**, *36*, 8127–8128.
125. Paquette, L. A.; Bolin, D. G.; Stepanian, M.; Branan, B. M.; Mallavadhani, U. V.; Tae, J.; Eisenberg, S. W. E.; Rogers, R. D. *J. Am. Chem. Soc.* **1998**, *120*, 11603–11615.
126. Paquette, L. A.; Stepanian, M.; Branan, B. M.; Edmondson, S. D.; Bauer, C. B.; Rogers, R. D. *J. Am. Chem. Soc.* **1996**, *118*, 4504–4505.
127. Ho Kang, S.; Kim, M. *J. Am. Chem. Soc.* **2003**, *123*, 4684–4685.
128. Sarraf, S. T.; Leighton, J. L. *Org. Lett.* **2000**, *2*, 403–405.
129. Sarraf, S. T.; Leighton, J. L. *Org. Lett.* **2000**, *2*, 3205–3208.
130. Parker, K. A.; Resnick, L *J. Org. Chem.* **1995**, *60*, 5726–5728.
131. Cipolla, L.; Lay, L.; Nicotra, F.; Panza, L; Russo, G. *Chem. Commun.* **1995**, 1993–1994.
132. Paterson, I.; Smith, J. D.; Ward, R. A. *Tetrahedron* **1995**, *51*, 9413–9436.
133. Matzanke, N.; Gregg, R. J.; Weinreb, S. M. *J. Org. Chem.* **1997**, *62*, 1920–1921.
134. Pakulski, Z.; Zamojski, A. *Tetrahedron* **1997**, *53*, 3723–3728.
135. Ruddock, P. L.; Williams, D. J.; Reese, P. B. *Steroids* **1998**, *63*, 650–664.
136. Beyersbergen van Henegouwen, W. G.; Fieseler, R. M.; Rutjes, F. P. J. T.; Hiemstra, H. *Angew. Chem., Int. Ed.* **1999**, *38*, 2214–2217.
137. Liu, T.-Z.; Li, J.-M.; Isobe, M. *Tetrahedron* **2000**, *56*, 10209–10219.
138. Hornberger, K. R.; Hamblett, C. L.; Leighton, J. L. *J. Am. Chem. Soc.* **2000**, *122*, 12894–12895.
139. Dreher, S. D.; Hornberger, K. R.; Sarraf, S. T.; Leighton, J. L. *Org. Lett.* **2000**, *2*, 3197–3199.
140. Dreher, S. D.; Leighton, J. L. *J. Am. Chem. Soc.* **2001**, *123*, 341–342.
141. Berges, D. A.; Fan, J.; Liu, N.; Dalley, N. K. *Terahedron* **2001**, *57*, 9915–9924.
142. Fay, W. N.; Hong, L.; Danishefsky, S. J. *J. Am. Chem. Soc.* **2002**, *124*, 9812–9824.
143. Yokoshima, S.; Tokuyama, H.; Fukuyama, T. *Angew. Chem., Int. Ed.* **2000**, *39*, 4073–4075.
144. Dankwardt, J. W.; Dankwardt, S. M.; Schlessinger, R. H. *Tetrahedron Lett.* **1998**, *39*, 4979–4982.
145. Liu, B.; Zhou, W.-S. *Tetrahedron Lett.* **2003**, *44*, 4933–4935.
146. Gössinger, E.; Schwartz, A.; Sereinig, N. *Terahedron* **2001**, *57*, 3045–3061.
147. Gurjar, M. K.; Mohapatra, S.; Phalgune, U. D.; Puranik, V. G.; Mohapatra, D. K. *Tetrahedron Lett.* **2004**, *45*, 7899–7902.
148. Ballico, E.; Cerichelli, G.; Fossa, S.; Floris, B.; Giordano, F. *Main Group Met. Chem.* **1997**, *20*, 301–312.
149. Ballico, E.; Floris, B. *Main Group Met. Chem.* **1998**, *21*, 527–542.
150. DiVona, M. L.; Floris, B.; Licoccia, S. *Magn. Reson. Chem.* **1998**, *36*, 797–800.
151. Berra, A.; DiVona, M. L.; Floris, B.; Licoccia, S. *Appl. Organometal. Chem.* **2000**, *14*, 565–569.
152. Floris, B.; Toppi, L. *Main Group Met. Chem.* **1999**, *22*, 209–216.
153. Berra, A.; Bietti, M.; Floris, B. *Main Group Met. Chem.* **2000**, *23*, 149–161.
154. Kao, C.; Chern, J. *Tetrahedron Lett.* **2001**, *42*, 1111–1113.
155. Kao, C.; Chern, J. *J. Org. Chem.* **2002**, *67*, 6772–6787.
156. Liebeskind, L. S.; Bombrun, A. *J. Org. Chem.* **1994**, *59*, 1149–1159.
157. Huang, H.; Forsyth, C. J. *J. Org. Chem.* **1997**, *62*, 8595–8599.
158. Kočovský, P.; Grech, J. M.; Mitchell, W. L. *J. Org. Chem.*, **1995**, *60*, 1482–1483.
159. Kočovský, P.; Grech, J. M.; Mitchell, W. L. *Tetrahedron Lett.* **1996**, *37*, 1125–1128.
160. Kočovský, P.; Dunn, V.; Gogoll, A.; Langer, V. *J. Org. Chem.* **1999**, *64*, 101–119.
161. Vasin, V. A.; Semenov, A. V.; Razin, V. V. *Russ. J. Org. Chem.* **2004**, *40*, 653–658.
162. Barrett, G. M.; Tam, W. *J. Org. Chem.* **1997**, *62*, 4653–4664.
163. Landais, Y.; Parra-Rapado, L. *Tetrahedron Lett.* **1996**, *37*, 1209–1212.
164. Landais, Y.; Parra-Rapado, L. *Eur. J. Org. Chem.* **2000**, 401–418.
165. Tei, T.; Sugimura, T.; Katagiri, T.; Tai, A.; Okuyama, T. *Tetrahedron: Asymmetry* **2001**, *12*, 2727–2730.
166. Cossy, J.; Blanchard, N.; Meyer, C. *Org. Lett.* **2001**, *3*, 2567–2569.
167. Cossy, J.; Blanchard, N.; Defosseux, M.; Meyer, C. *Angew. Chem., Int. Ed.* **2002**, *41*, 2144–2146.
168. Borovik, A. S.; Bott, S. G.; Barron, A. R. *Angew. Chem., Int. Ed.* **2000**, *39*, 4117–4118.
169. Borovik, A. S.; Bott, S. G.; Barron, A. R. *J. Am. Chem. Soc.* **2001**, *123*, 11219–11228.
170. Branch, C. S.; Barron, A. R. *J. Am. Chem. Soc.* **2002**, *124*, 14156–14161.
171. Borovik, A. S.; Barron, A. R. *J. Am. Chem. Soc.* **2002**, *124*, 3743–3748.
172. Horsley, J. A.; Vanderveken, D. J.; Periana, R. A. *Catal. Today* **1995**, *23*, 333–339.
173. Periana, R. A.; Taube, D. J.; Evitt, E. R.; Loffler, D. G.; Wentrcek, P. R.; Voss, G.; Masuda, T. *Science* **1993**, *259*, 340–343.
174. Williams, V. C.; Piers, W. E.; Clegg, W.; Elsegood, M. R. J.; Collins, S.; Marder, T. B. *J. Am. Chem. Soc.* **1999**, *121*, 3244–3245.
175. Carpenter, B. E.; Piers, W. E.; McDonald, R. *Can. J. Chem.* **2001**, *79*, 291–295.
176. Carpenter, B. E.; Piers, W. E.; Parvez, M.; Yap, G. P. A.; Rettig, S. J. *Can. J. Chem.* **2001**, *79*, 857–867.
177. Seneviratne, K. N.; Bretschneider-Hurley, A.; Winter, C. H. *J. Am. Chem. Soc.* **1996**, *118*, 5506–5507.
178. Seneviratne, K. N.; Winter, C. H. *Organometallics* **1997**, *16*, 2498–2499.
179. Wu, Y. J.; Liu, Y. H.; Ding, K. L.; Yuan, H. Z.; Mao, X. A. *J. Organomet. Chem.* **1995**, *505*, 37–42.
180. Vicente, J.; Abad, J.-A.; Hernandez-Mata, F. S.; Rink, B.; Jones, P. G.; Ramirez de Arellano, M. C. *Organometallics* **2004**, *23*, 1292–1304.
181. Djukic, J.-P.; Berger, A.; Duquenne, M.; Pfeffer, M.; de Cian, A.; Kyritsakas-Gruber, N.; Vachon, J.; Lacour, J. *Organometallics* **2004**, *23*, 5757–5767.
182. Parish, R. V.; Wright, J. P.; Pritchard, R. G. *J. Organomet. Chem.* **2000**, *596*, 165–176.
183. Goedheijt, M. S.; Nijbacker, T.; Akkerman, O. S.; Bickelhaupt, F.; Veldman, N.; Spek, A. L. *Angew. Chem., Int. Ed. Engl.* **1996**, *35*, 1550–1552.
184. Rueffer, T.; Bruhn, C.; Steinborn, D. *Z. Anorg. Allg. Chem.* **2001**, *627*, 2408–2412.
185. Tschinkl, M.; Schier, A.; Riede, J.; Gabbaï, F. P. *Inorg. Chem.* **1998**, *37*, 5097–5101.
186. Gabbaï, F. P.; Schier, A.; Riede, J.; Schichl, D. *Organometallics* **1996**, *15*, 4119–4121.
187. Gabbaï, F. P.; Schier, A.; Riede, J. *Chem. Commun.* **1996**, 1121–1122.
188. Gabbaï, F. P.; Schier, A.; Riede, J.; Sladek, A.; Goerlitzer, H. W. *Inorg. Chem.* **1997**, *36*, 5694–5698.

189. Aubke, F. *J. Fluorine Chem.* **1995**, *72*, 195–201.
190. Bodenbinder, M.; Balzer-Jöllenbeck, G.; Willner, H.; Batchelor, R. J.; Einstein, F. W. B.; Wang, C.; Aubke, F. *Inorg. Chem.* **1996**, *35*, 82–92.
191. Lupinetti, A. J.; Jonas, V.; Thiel, W.; Strauss, S. H.; Frenking, G. *Chem. Eur. J.* **1999**, *5*, 2573–2583.
192. Enders, M.; Ludwig, G.; Pritzkow, H. *Eur. J. Inorg. Chem.* **2002**, 539–542.
193. Kajiwara, T.; Murao, R.; Ito, T. *J. Chem. Soc., Dalton Trans.* **1997**, 2537–2538.
194. Berenguer, J. R.; Fornies, J.; Lalinde, E.; Martin, A.; Moreno, M. T. *J. Chem. Soc., Dalton Trans.* **1994**, 3343–3348.
195. Zhang, D.; McConville, D. B.; Tessier, C. A.; Youngs, W. J. *Organometallics* **1997**, *16*, 824–825.
196. Frosch, W.; del Villar, A.; Lang, H. *J. Organomet. Chem.* **2000**, *602*, 91–96.
197. Wong, W.; Lu, G.; Liu, L.; Shi, J.; Lin, Z. *Eur. J. Inorg. Chem.* **2004**, 2066–2077.
198. Faville, S. J.; Henderson, W.; Mathieson, T. J.; Nicholson, B. K. *J. Organomet. Chem.* **1999**, *580*, 363–369.
199. Frank, W.; Dincher, B. *Z. Naturforsch. B* **1987**, *42*, 828–834.
200. Ulvenlund, S.; Rosdahl, J.; Fischer, A.; Schwerdtfeger, P.; Kloo, L. *Eur. J. Inorg. Chem.* **1999**, 633–642.
201. Delaigue, X.; Hosseini, M. W.; Kyritsakas, N.; De Cian, A.; Fischer, J. *Chem. Commun.* **1995**, 609–610.
202. Fowley, L. A.; Lee, J. C.; Crabtree, R. H.; Siegbahn, P. E. M. *J. Organomet. Chem.* **1995**, *504*, 57–67.
203. Fowley, L. A.; Lee, J. C.; Crabtree, R. H. *Organometallics* **1996**, *15*, 1157–1165.
204. Viets, D.; Lork, E.; Watson, P. G.; Mews, R. *Angew. Chem., Int. Ed.* **1997**, *36*, 623–624.
205. Naumann, D.; Schulz, F.; Pantenburg, I.; Tyrra, W. *Z. Anorg. Allg. Chem.* **2004**, *630*, 529–534.
206. Schulz, F.; Pantenburg, I.; Naumann, D. *Z. Anorg. Allg. Chem.* **2003**, *629*, 2312–2316.
207. Shur, V. B.; Tikhonova, I. A.; Yanovskii, A. I.; Struchkov, Yu. T.; Petrovskii, P. V.; Panov, S. Yu.; Furin, G. G.; Vol'pin, M. E. *J. Organomet. Chem.* **1991**, *418*, C29–C32.
208. Koomen, J. M.; Lucas, J. E.; Haneline, M. R.; King, J. D. B.; Gabbaï, F. P.; Russell, D. H. *Int. J. Mass Spectrom.* **2003**, *225*, 225–231.
209. Saitkulova, L. N.; Bakhmutova, E. V.; Shubina, E. S; Tikhonova, I. A.; Furin, G. G.; Bakhmutov, V. I.; Gambaryan, N. P.; Chistyakov, A. L.; Stankevich, I. V., Shur, V. B., *et al. J. Organomet. Chem.* **1999**, *585*, 201–210.
210. Shubina, E. S.; Tikhonova, I. A.; Bakhmutova, E. V.; Dolgushin, F. M.; Antipin, M. Y.; Bakhmutov, V. I.; Sivaev, I. B.; Teplitskaya, L. N.; Chizhevsky, I. T., Pisareva, I. V., *et al. Chem. Eur. J.* **2001**, *7*, 3783–3790.
211. Tikhonova, I. A.; Dolgushin, F. M.; Tugashov, K. I.; Ellert, O. G.; Novotortsev, V. M.; Furin, G. G.; Antipin, M. Y.; Shur, V. B. *J. Organomet. Chem.* **2004**, *689*, 82–87.
212. Tikhonova, I. A.; Dolgushin, F. M.; Yanovsky, A. I.; Struchkov, Y. T.; Gavrilova, A. N.; Saitkulova, L. N.; Shubina, E. S.; Epstein, L. M.; Furin, G. G.; Shur, V. B. *J. Organomet. Chem.* **1996**, *508*, 271–273.
213. Lee, H.; Diaz, M.; Knobler, C. B.; Hawthorne, M. F. *Angew. Chem., Int. Ed.* **2000**, *39*, 776–778.
214. Lee, H.; Knobler, C. B.; Hawthorne, M. F. *J. Am. Chem. Soc.* **2001**, *123*, 8543–8549.
215. Bayer, M. J.; Jalisatgi, S. S.; Smart, B.; Herzog, A.; Knobler, C. B.; Hawthorne, M. F. *Angew. Chem., Int. Ed.* **2004**, *43*, 1854–1857.
216. Zinn, A. A.; Knobler, C. B.; Harwell, D. E.; Hawthorne, M. F. *Inorg. Chem.* **1999**, *38*, 2227–2230.
217. Vaugeois, J.; Wuest, J. D. *J. Am. Chem. Soc.* **1998**, *120*, 13016–13022.
218. Vaugeois, J.; Simard, M.; Wuest, J. D. *Organometallics* **1998**, *17*, 1215–1219.
219. Tschinkl, M.; Schier, A.; Riede, J.; Gabbaï, F. P. *Organometallics* **1999**, *18*, 1747–1753.
220. Tschinkl, M.; Gabbaï, F. P. *J. Chem. Crystallogr.* **2003**, *33*, 595–598.
221. Beckwith, J. D.; Tschinkl, M.; Picot, A.; Tsunoda, M.; Bachman, R.; Gabbaï, F. P. *Organometallics* **2001**, *20*, 3169–3174.
222. King, J. B.; Gabbaï, F. P. *Organometallics* **2003**, *22*, 1275–1280.
223. Tschinkl, M.; Bachman, R. E.; Gabbaï, F. P. *Organometallics* **2000**, *19*, 2633–2636.
224. Tschinkl, M.; Schier, A.; Riede, J.; Gabbaï, F. P. *Angew. Chem., Int. Ed.* **1999**, *38*, 3547–3549.
225. Tschinkl, M.; Schier, A.; Riede, J.; Gabbaï, F. P. *Organometallics* **1999**, *18*, 2040–2042.
226. Haneline, M. R.; Gabbaï, F. P. *Z. Naturforsch. B: Chem. Sci.* **2004**, *59*, 1483–1487.
227. King, J. B.; Tsunoda, M.; Gabbaï, F. P. *Organometallics* **2002**, *21*, 4201–4205.
228. King, J. B.; Haneline, M. R.; Tsunoda, M.; Gabbaï, F. P. *J. Am. Chem. Soc.* **2002**, *124*, 9350–9351.
229. Baldamus, J.; Deacon, G. B.; Hey-Hawkins, E.; Junk, P. C.; Martin, C. *Aust. J. Chem.* **2002**, *55*, 195–198.
230. Tikhonova, I. A.; Dolgushin, F. M.; Tugashov, K. I.; Petrovskii, P. V.; Furin, G. G.; Shur, V. B. *Russ. Chem. Bull.* **2001**, *50*, 1673–1678.
231. Tikhonova, I. A.; Dolgushin, F. M.; Tugashov, K. I.; Petrovskii, P. V.; Furin, G. G.; Shur, V. B. *J. Organomet. Chem.* **2002**, *654*, 123–131.
232. Tikhonova, I. A.; Dolgushin, F. M.; Yanovsky, A. I.; Starikova, Z. A.; Petrovskii, P. V.; Furin, G. G.; Shur, V. B. *J. Organomet. Chem.* **2000**, *613*, 60–67.
233. Tsunoda, M.; Gabbaï, F. P. *J. Am. Chem. Soc.* **2003**, *125*, 10492–10493.
234. Lee, H.; Knobler, C. B.; Hawthorne, M. F. *Angew. Chem., Int. Ed.* **2001**, *40*, 3058–3060.
235. Tsunoda, M.; Gabbaï, F. P. *J. Am. Chem. Soc.* **2000**, *122*, 8335–8336.
236. Haneline, M. R.; King, J. B.; Gabbaï, F. P. *J. Chem. Soc., Dalton Trans.* **2003**, *13*, 2686–2690.
237. Omary, M. A.; Kassab, R. M.; Haneline, M. R.; Elbjeirami, O.; Gabbaï, F. P. *Inorg. Chem.* **2003**, *42*, 2176–2178.
238. Haneline, M. R.; Tsunoda, M.; Gabbaï, F. P *J. Am. Chem. Soc.* **2002**, *124*, 3737–3742.
239. Haneline, M. R.; Gabbaï, F. P. *C. R. Chimie* **2004**, *7*, 871–876.
240. Haneline, M. R.; Gabbaï, F. P. *Angew.Chem., Int. Ed. Engl.* **2004**, *43*, 5471–5474.
241. Eremeev, I. V.; Danov, S. M.; Skudin, A. G.; Sakhipov, V. R. *Russ. J. Gen. Chem.* **2003**, *73*, 556–559.
242. Schumann, H.; Freitag, S.; Girgsdies, F.; Hemling, H.; Kociok–Köhn, G. *Eur. J. Inorg. Chem.* **1998**, 245–252.
243. Strohmann, C.; Schildbach, D. *Acta Cryst.* **2002**, *C58*, m447–m449.
244. Eaborn, C.; Hill, M. S.; Hitchcock, P. B.; Smith, J. D. *J. Chem. Soc., Dalton Trans.* **2002**, 2467–2472.
245. Padelidakis, V.; Tyrra, W.; Conrad, F.; Naumann, D. *J. Fluorine Chem.* **1998**, *91*, 219–220.
246. Boev, V. I.; Denisov, S. P.; Moskalenko, A. I.; Stamova, L. G.; Gulin, A. V. *Russian J. Gen. Chem.* **2000**, *70*, 1812–1813.
247. Denisov, S. P.; Moskalenko, A. I.; Boev, V. I.; Stamova, L. G.; Gulin, A. V. *Russ. J. Gen. Chem.* **2001**, *71*, 1070–1075.
248. Eujen, R.; Hoge, B.; Brauer, D. J. *J. Organomet. Chem.* **1996**, *519*, 7–20.
249. Arduengo, A. J.; Goerlich, J. R.; Davidson, F.; Marshall, W. J. *Z. Naturforsch. B.* **1999**, *54*, 1350–1356.
250. Cremer, U.; Pantenburg, I.; Ruschewitz, U. *Inorg. Chem.* **2003**, *42*, 7716–7718.
251. Charmant, J.; Falvello, L.; Forniés, J.; Gómez, J.; Lalinde, E.; Moreno, M.; Orpen, A.; Rueda, A. *Chem. Commun.* **1999**, 2045–2046.
252. Stępień, M.; Latos-Grażuyński, L.; Szterenberg, L.; Panek, J.; Latajka, Z. *J. Am. Chem. Soc.* **2004**, *126*, 4566–4580.

253. Stępień, M.; Latos–Grażuyński, L. *J. Am. Chem. Soc.* **2002**, *124*, 3838–3839.
254. Barr, D.; Edwards, A.; Raithby, P.; Rennie, M.; Verhorevoort, K.; Wright, D. *J. Organomet. Chem.* **1995**, *493*, 175–179.
255. Wang, X.; Sun, H.; Sun, X.; You, X. *Acta Cryst.* **1995**, *C51*, 1754–1756.
256. Afzaal, M.; Crouch, D.; Malik, M.; Motevalli, M.; O'Brien, P.; Park, J. *J. Mater. Chem.* **2003**, *13*, 639–640.
257. Choi, Z.-H.; Tyrra, W.; Adam, A. *Z. Anorg. Allg. Chem.* **1999**, *625*, 1287–1292.
258. Choi, Z.-H. *J. Korean Chem. Soc.* **1999**, *43*, 52–57.
259. Galiotos, J. K.; Morrison, J. A. *Organometallics* **2000**, *19*, 2603–2607.
260. Burton, D. J.; Jairaj, V. *J. Fluorine Chem.* **2004**, *125*, 673–680.
261. Grobe, J.; Golla, W.; Van, D. L.; Krebs, B.; Laege, M. *Organometallics* **1998**, *17*, 5717–5720.
262. Frohn, H. J.; Giesen, M.; Welting, D.; Henkel, G. *Eur. J. Solid State Inorg. Chem.* **1996**, *33*, 841–853.
263. Frohn, H. J.; Schrinner, K. *Z. Anorg. Allg. Chem.* **1997**, *623*, 1847–1849.
264. Frohn, H.-J.; Theissen, M. *Angew. Chem., Int. Ed.* **2000**, *39*, 4591–4593.
265. Frohn, H.-J.; Theissen, M. *J. Fluorine Chem.* **2004**, *125*, 981–988.
266. Naumann, D.; Roy, T.; Caeners, B.; Hutten, D.; Tebbe, K.-F.; Gilles, T. *Z. Anorg. Allg. Chem.* **2000**, *626*, 999–1003.
267. Eujen, R.; Hoge, B.; Brauer, D. J. *Inorg. Chem.* **1997**, *36*, 1464–1475.
268. Eujen, R.; Hoge, B.; Brauer, D. J. *Inorg. Chem.* **1997**, *36*, 3160–3166.
269. Graefe, A.; Kruck, T. *J. Organomet. Chem.* **1996**, *506*, 31–35.
270. Naumann, D.; Kaiser, M. *Z. Anorg. Allg. Chem.* **1995**, *621*, 812–816.
271. Eujen, R.; Haiges, R. *Z. Naturforsch. B: Chem. Sci.* **1998**, *53*, 1455–1460.
272. Eujen, R.; Hoge, B. *J. Organomet. Chem.* **1995**, *503*, C51–C54.
273. Yang, Z. Y.; Burton, D. J. *J. Fluorine Chem.* **2000**, *102*, 89–103.